A *Drosophila melanogaster* Model to Evaluate Environmental and Genetic Strategies for Altering Circadian Dysfunction and Neurotoxicity in Huntington's Disease

A thesis submitted in partial fulfilment
of the requirements for the degree of

Doctor of Philosophy

By

Pavitra Prakash

To the

Evolutionary and Organismal Biology Unit

Jawaharlal Nehru Centre for Advanced Scientific Research

Jakkur, Bengaluru – 560 064, India

May 2023

Declaration

I hereby declare that the thesis titled "***A Drosophila melanogaster Model to Evaluate Environmental and Genetic Strategies for Altering Circadian Dysfunction and Neurotoxicity in Huntington's Disease***", submitted towards the partial fulfilment of the PhD degree is the result of investigations carried out by me at the Evolutionary and Organismal Biology Unit of the Jawaharlal Nehru Centre for Advanced Scientific Research, Bengaluru, India, under the supervision of Prof. Sheeba Vasu. The work incorporated in this thesis has not been submitted for any other degree elsewhere.

In keeping with reporting scientific observations, this study has taken due care to acknowledge and cite other investigators' work. Any omission that may have occurred due to oversight or misjudgment is regretted.

Pavitra Prakash

Bengaluru, India

18th May 2023

Chronobiology and Behavioural Neurogenetics Laboratory
Neuroscience Unit, Jawaharlal Nehru Centre for Advanced Scientific Research
P.O. Box. 6436, Jakkur, Bangalore - 560 064, INDIA

CERTIFICATE

This is to certify that the work described in this thesis titled, "***A Drosophila melanogaster Model to Evaluate Environmental and Genetic Strategies for Altering Circadian Dysfunction and Neurotoxicity in Huntington's Disease***", submitted towards the partial fulfilment of the PhD degree, is the result of investigations carried out by **Ms Pavitra Prakash** in the Evolutionary and Organismal Biology Unit of the Jawaharlal Nehru Centre for Advanced Scientific Research, Bengaluru, India, under my supervision. The results presented in this thesis have not previously formed the basis for awarding any other diploma, degree, or fellowship.

Sincerely,

Sheeba Vasu

18th May 2023

sheeba@jncasr.ac.in; sheebavasu@gmail.com; Ph: 91-080-22082987

Synopsis

Circadian Disruptions in Huntington's Disease Modelled in *Drosophila melanogaster*

The prevalence of devastating age-related diseases such as neurodegenerative diseases is rising with a growing elderly population worldwide, drastically affecting the quality of life in the affected persons and their caregivers (Wyss-Coray, 2016; Gitler et al., 2017; Lassonde, 2017; Bejot and Yaffe, 2019). There is a pressing need for studies to understand these diseases better and to develop therapeutic strategies. **Neurodegenerative diseases** (NDs) are a wide range of **brain-related conditions** where a specific set of neurons become dysfunctional or even degenerate. Some of the well-known NDs include Parkinson's disease, Alzheimer's disease, Huntington's disease, and Amyotrophic Lateral Sclerosis. **Huntington's Disease** (HD) is inherited and caused by a mutation in the gene coding for Huntingtin (HTT) protein. The mutation is the expansion of repeats of the CAG codon in the Huntingtin gene (*htt*) beyond a threshold of 35-40 CAG repeats. The resulting mutant Huntingtin protein has expanded repeats (>35-40) of the amino acid Glutamine (Q), often called polyQ repeats, thus categorising HD as a polyQ disease. Typical HD symptoms include motor defects such as involuntary uncoordinated jerky movements, cognitive defects like problems in emotion recognition and attention, and psychiatric difficulties such as aggression and depression, all affecting the quality and duration of life (Gusella and MacDonald, 2006; Bates et al., 2015). Despite varying clinical manifestations, HD shares several notable features with other NDs. These include a typical middle-aged disease onset that affects specific brain regions or neuronal groups despite widespread protein expression, progressive neuronal degeneration, accumulation of protein aggregates, **motor, cognitive and psychological disturbances**, and worsening symptoms with age. Like several other NDs, HD thus takes a massive toll on patients and their caregivers (Taylor and Bramble, 1997; Happe et al., 2002; Mills et al., 2009). Despite decades of research, **treatments delaying HD onset or slowing its progression have yet to meet much success at the clinical level**. Moreover, though mechanisms of disrupted protein homeostasis, oxidative stress and synaptic toxicity are common among NDs (Dugger and Dickson, 2017; Gan et al., 2018; Ruffini et al., 2020), a clear understanding of HD pathogenesis, basis for differential neuronal susceptibility, the role of

aggregation in toxicity, and an overarching view on time-course and sequence of molecular and cellular events, remain elusive.

Recently, circadian and sleep impairments in ND have been gaining attention. Since many patients show circadian and sleep abnormalities before the more well-known symptoms and disease manifestations, these are now considered prodromal symptoms of NDs (Arnulf et al., 2008; Soneson et al., 2010; Goodman et al., 2011; Morton et al., 2014; Lebreton et al., 2015; Bellosta Diago et al., 2017). The neurons in the brain regions controlling circadian behaviour, such as the hypothalamus, specifically the Supra Chiasmatic Nucleus, are vulnerable targets of HD (Fifel and Videnovic, 2020). Circadian dysfunctions also disrupt neuronal homeostasis and worsen neurological symptoms, creating a feed-forward loop (Hastings and Goedert, 2013; Musiek, 2015). Moreover, improving circadian functions alleviates neurodegenerative processes, implying a reciprocal interaction of the two networks, providing unusual interventional opportunities (Hood and Amir, 2017a; Leng et al., 2019; Carter et al., 2021; Voysey et al., 2021a). Given the vulnerability of the circadian system to HD, circadian disruptions aggravating HD and their amenability to moderation, **I was interested in studying the impact of HD on circadian rhythms, uncovering suppressors of circadian dysfunction and disease-modifying strategies,** and improving our understanding of HD pathogenesis **using *Drosophila melanogaster* due to its well-established repertoire of circadian behaviours and underlying neuronal network as well as genetic and molecular players.**

Drosophila melanogaster is extensively used as a model organism in studying NDs. It offers several advantages such as ease of use, short generation time and life cycle, cost-effectiveness, and availability of genetic, molecular, and physiological tools to introduce and study the effect of human genes. *Drosophila,* commonly called the fruit fly or the vinegar fly, also has homologs for 75% of the human disease genes, shares fundamental cellular and signalling pathways with humans, has a relatively simple nervous system and exhibits complex behaviours (Reiter et al., 2001a; McGurk et al., 2015; Rosas-Arellano et al., 2018). Many physiological processes and behaviours show circadian rhythms, which repeat every ~24 hours, even without external time cues. Some examples are sleep-wake cycles, rhythms in hormonal levels and metabolites. The core molecular clock comprises a transcriptional/translational feedback loop (TTFL) in flies, with Clock, Cycle, Period (PER), and Timeless proteins being the primary players (Tataroglu and Emery, 2015; Young, 2018). The circadian neuronal circuit in the *Drosophila* brain consists of

~150 neurons, each exhibiting self-sustained rhythms in clock protein levels, also called molecular clock oscillations (Nitabach and Taghert, 2008; King and Sehgal, 2020). This neuronal circuit controls a robust, reproducible, easily assayable, well-characterised rhythmic behaviour, the locomotor activity/rest rhythms (Tataroglu and Emery, 2014). Of these neurons, ~ 8-9 pairs of ventrolateral neurons (LNv) express a neuropeptide, the Pigment dispersing Factor (PDF). There are two types of LNv- the small LNv (sLNv) and the large LNv (lLNv), with each brain hemisphere having 4-5 of each type. PDF and sLNv are critical for maintaining locomotor activity rhythms under constant dark conditions (DD) (without external time cues or free-running conditions) (Renn et al., 1999; Grima et al., 2004a; Stoleru et al., 2004; Shafer and Taghert, 2009).

A region of the human Huntingtin gene containing exon1 with expanded Q repeats (**expanded HTT** or expHTT) is **targeted to the PDF expressing LNv of *Drosophila*** to study its effect on circadian functions and characterise HD-induced neurodegenerative phenotypes in these flies. Parallelly, the neurodegenerative expHTT is used to compromise the LNv to understand their contribution to circadian behaviour. Targeting the critical pacemaker neurons offers an advantage over the widely used pan-neuronal approach. Such a restricted expression system makes assessing associated events at the neuronal and circuit level and precisely controlled functional output at the behavioural level possible. Studying the effect of a neurodegenerative protein at multiple levels, each functionally and specifically related, aids in precise inferences and testing the robustness and efficacy of disease-modifying strategies at many levels.

The thesis is structured into seven chapters. The Material and Methods section describes each chapter's experimental setup, conditions, methodology, analyses, and statistical tests. The experiments combine neurogenetic, behavioural, immunocytochemical and imaging techniques to address most questions. *pdf>Q128* is the fly line of focus, expressing expHTT having 128 Q repeats (HTT-Q128) in the PDF-expressing LNv (PDF^+ LNv). *pdf>Q128* (HD flies) is compared with all the appropriate controls: the non-expanded HTT expressing line *pdf>Q0* (without Q repeats) and the parental controls *Q128* and *pdfGal*. Below is a brief outline of each chapter's broad objectives, findings, and conclusions.

Synopsis

Chapter 1 is a detailed introduction to HD, its epidemiology, genetic basis, HTT protein structure, modifications and function, the role of aggregation and polyQ expansion in HD toxicity, and the pathogenic mechanisms underlying HD with a focus on disturbances in protein homeostasis, some of the prevalent therapeutic approaches to HD, basics of mammalian and *Drosophila* circadian biology, *Drosophila* as a model for HD, the crosstalk between the circadian and the neurodegenerative systems, the need to study such interactions and the objectives of this study.

Chapter 2 addresses the first objective of my research: **establishing and characterising the HD-induced circadian alterations** and the associated neurodegenerative phenotypes **in a *Drosophila* model**. Expressing expHTT in LNv of *Drosophila* disrupts their circadian locomotor activity rhythms in DD, rendering most of the flies arrhythmic and a few rhythmic flies with weak rhythms of ~24h period. At the neuronal level, *pdf>Q128* flies show a PDF loss only from the sLNv soma while persisting in its dorsal axonal projections and the lLNv. The molecular clock protein PER is also lost from sLNv and diminishes in lLNv. The expHTT mostly appears as inclusions (speckled clumped appearance), in contrast to the even, cell-wide distribution or diffuse appearance of the un-expanded version, HTT-Q0. In flies expressing different lengths of polyQ expansions of expHTT in the LNv, behavioural arrhythmia demonstrates a polyQ-length-dependent deterioration: the longer the Q repeat, the earlier the age of arrhythmia initiation. The arrhythmicity, loss of PDF and aggregation worsen as the flies age. **The *Drosophila* circadian HD model recapitulates several key HD features** such as selective neuronal dysfunction, expHTT inclusions, **circadian disruptions**, progressive decline of phenotypes and a polyQ-length-dependent worsening of symptoms. Locomotor activity rhythms of these flies are unaffected under light-dark (LD) conditions. Their sleep levels, sleep quality and lifespan are unaffected.

The findings further improve our comprehension of the function of the neuropeptide PDF in the sLNv in maintaining activity rhythms in DD. I also report a unique finding that PDF is present in the dorsal projections (DP) of sLNv, and its levels in the DP continue to oscillate under DD, even in the absence of PER and PDF in the cell bodies. The oscillations in PDF levels in DP are also functional, as their downstream target neurons show synchronised PER oscillations. Several studies report an association of arrhythmic activity with loss of oscillations in PDF levels in the

sLNv DP but intact sLNv molecular oscillations, strengthening the conclusion that PDF oscillations are critical for behavioural rhythms (Nitabach et al., 2006; Fernández et al., 2007a; Depetris-Chauvin et al., 2011; Gunawardhana and Hardin, 2017). However, in this study, PDF oscillations are uncoupled from behavioural rhythms (Prakash et al., 2017). Despite PDF oscillations in sLNv DP and synchronous PER oscillations in the downstream circadian neuronal subsets, the activity rhythms in DD are arrhythmic, highlighting the insufficiency of these oscillations in activity rhythm sustenance in the absence of PER in the sLNv. Thus, the maintenance of free-running activity rhythms by sLNv is not limited to its output via oscillations in PDF levels.

Chapter 3 assesses the **role of the environmental factor light in modifying expHTT-induced circadian neurodegenerative phenotypes**. Providing circadian bolstering cyclic time cues during development, like high-intensity LD cycles or multiple time cues that change gradually (semi-natural conditions), did not alter the breakdown of activity rhythms of *pdf>Q128* adults in DD or their entrainment to LD. However, varying the light regimes affect the cellular phenotypes of *pdf>Q128*: the circadian-disrupting regime of the continuous presence of light or **constant light (LL) aggravating neurodegenerative features**. At the same time, LD is intermediate toxic, and DD (absence of light) is relatively less toxic. LL accelerates the loss of PDF from sLNv soma and promotes expHTT inclusions more than the other two regimes. These findings provide strong evidence for constant light and light/dark cycles amplifying neurodegenerative phenotypes, suggesting light negatively impacts neurodegenerative outcomes. They also highlight the significance of environmental regimens in ND progression and the need to integrate circadian hygiene, such as lighting conditions, in treating NDs.

Chapter 4 looks at the role of **temperature in modifying expHTT-induced circadian dysfunction and neurotoxicity**. It addresses the potential for environmental interventions like temperature, which influences circadian and neurodegenerative networks as a therapeutic avenue for neurodegenerative diseases. It establishes two temperature-dependent mechanisms that target different life stages as regimes that impede HD circadian neurodegenerative phenotypes. HD flies in both temperature regimes display a delay in the behavioural rhythm breakdown and loss of circadian neuropeptide PDF from the sLNv to different extents. In both regimes, the temperatures experienced as adults determine early-age rhythm rescue. The first regime,

development-specific temperature cycles, restores low-amplitude sLNv molecular clock oscillations but does not alter the expHTT inclusion load. The rescue of early-age activity rhythms is inhibited by light during development. The second regime, **adult-restricted upshift to warm temperatures**, does not restore sLNv clock oscillations but decreases expHTT inclusion load. Its rescue of early-age activity rhythms has little interference from light during development or clock disruptions during development. At the same time, Hsp70 plays a role in the regime's rhythm execution. This regime enhances activity consolidation over an extended duration and is more neuroprotective. Hence, the findings support **temperature-based environmental treatments as effective suppressors of circadian neurodegenerative phenotypes** and prospective therapeutic regimens for NDs.

Chapter 5 describes a screen of **genetic modifiers of cellular toxicity in HD for their ability to suppress expHTT-induced circadian behavioural arrhythmia**. From a host of cellular neurotoxic modifier proteins of HD, two proteins of the **Heat Shock Protein** (Hsp) family, **Hsp40 and HSP70**, emerge as **promising suppressors** of behavioural arrhythmicity in the initial screen. Co-expression of Hsp40 (a co-chaperone of the central chaperone HSP70) with expHTT in the LNv substantially prolongs rhythmicity, rescues PER oscillations in the sLNv of young flies and prevents PDF loss from sLNv soma. It also reduces expHTT inclusion load accompanied by the appearance of a novel form of expHTT, oval and spot-like, present as a single spot per LNv. The nature of this Spot expHTT, its localisation, and its constituents warrant investigation. Co-expression of expHTT with HSP70 in the LNv also rescues early-age arrhythmicity without recovering PDF or PER in the sLNv or modifying expHTT aggregation. Thus, from this study, **Hsp40 emerges as a potent mitigator of expHTT-induced circadian neurogenerative phenotypes** in *Drosophila* (Prakash et al., 2022). Hsps are well-established suppressors of cellular neurodegenerative features (Duncan et al., 2015a; Hipp et al., 2019a; Sinnige et al., 2020). However, this is the **first report on the role of Hsp in suppressing circadian dysfunction** associated with a neurodegenerative disease like HD. This circadian rescue was at the neuronal and behavioural levels of the sLNv pacemaker's core clock and its neuronal output and the behavioural rhythms in a relatively sustained fashion. These results also suggest that proteostasis perturbations underlie circadian disruptions associated with HD. The interaction of ND-induced circadian defects and proteostasis is relatively unexplored, and my study sets encouraging precedence.

Chapter 6 briefly investigates the role of *Drosophila* Huntingtin (dhtt) in HD circadian dysfunction and the protein context of the polyQ expansion in disrupting activity rhythms. Several specific questions were asked, and the findings are briefly stated here. *dhtt* is not essential for free-running *Drosophila* activity rhythms, nor does dHtt overexpression protect *pdf>Q128* flies from becoming arrhythmic. The effects of the cellular and protein contexts of the polyQ expansion on the free-running activity rhythms are examined by expressing full-length HTT, only the expanded polyQ peptide or the polyQ expanded MJD protein (causing the Machado Joseph Disease or Spinocerebellar Ataxia-3) in the LNv, and in the latter two cases, also in a larger group of circadian neurons. While the full-length HTT did not affect the activity rhythms, expression of expanded polyQ in a broad group of circadian neurons weakens the rhythms, and that of expanded MJD led to arrhythmia. These non-consistent effects of the expanded polyQ proteins in the circadian context and how they differ from the pathophysiology reported on targeting other cellular groups **emphasise the critical role that protein contexts**, such as flanking sequences and protein length, and **the cellular contexts**, respectively, **play in mediating expanded-polyQ's toxicity**.

Chapter 7 provides a summary of the salient findings of this study and the conclusions thereof. It also establishes an overarching model of modifiers of circadian dysfunction and neurotoxicity, showing various trajectories towards neuroprotection and circadian rehabilitation. The critical take-home is that **for mitigating HD-induced neurotoxicity at the behavioural level, Hsp40-overexpression > adult-restricted-warm-temperatures > development-specific-temperature-cycles > HSP70-overexpression**. This descending order of suppression of neurotoxicity follows the extent of cellular rescue by the intervening regimens. Hsp40 improves circadian parameters at the behavioural, neuronal, and molecular levels and decreases the cellular inclusion load, whereas HSP70 only improves the behavioural rhythms. At the same time, the temperature regimes confer intermedial rescue. This chapter also outlines possible future questions that can be addressed, both immediate and long-term, and draws attention to the need for and scope of research in related fields.

In summary, this study characterises a *Drosophila* circadian model of HD that enumerates several crucial characteristics. The circadian disruptions observed here, such as arrhythmic activity/rest patterns and disruptions of sLNv pacemakers' molecular clock and output function, mirror similar

features found in mammalian models and patients of HD. This system also efficiently screens for environmental and genetic modifiers, with the potential for conducting pharmacological screens. A screen for different light conditions shows that lighting conditions worsen neurodegenerative features, emphasising the need for good circadian hygiene, particularly under compromised neuronal health. The study uncovers a previously unrecognised benefit of warm temperatures and temperature cycles in enhancing circadian functions and neurodegenerative phenotypes in HD flies, two distinct underlying mechanisms of delayed neurotoxicity, and promising potential for incorporating passive heat therapy or body warming into ND treatments. Established neuroprotectors Hsp40 and HSP70 are found to suppress circadian dysfunction, with Hsp40 providing sustained benefits to neuronal health, circadian markers, outputs, and rhythmic function. Two independent studies show the involvement of Hsps in evoking circadian rhythmicity, thus establishing **Hsps as nodal protein targets for circadian rehabilitation and neuroprotection**. These results also suggest the involvement of mechanisms maintaining cellular proteostasis in the sustenance of circadian rhythms, particularly under disease conditions that challenge proteostasis. In several instances during this study, the neuronal dysfunction is associated with increased inclusion load, strongly suggesting that the expHTT inclusions are indicators of toxicity. It also establishes the dispensability of endogenous *Drosophila* Huntingtin for free-running circadian rhythms. Further, the findings espouse consideration of the protein and cellular contexts while inferring the toxicity related to expanded polyQs.

The various deterrents of HD-induced toxicity and their underlying physiological mechanisms discerned in this study broaden our understanding of the interactions between the circadian and the neurodegenerative axes and the effects of the external environment and cellular proteostasis on them. Crucially, they illustrate that **various non-mutually exclusive pathways exist for circadian neuroprotection**. The outcome of this study using the robust and versatile *Drosophila melanogaster* is a springboard for testing in clinically relevant models and a paradigm to explore new therapeutic avenues that will benefit not only our understanding of HD but also of other NDs, particularly in the circadian context, and inform advances to improve the quality of life in HD patients and carers.

Dedication

This thesis is dedicated to "***The Evolution of Me***"

The Girl I have been,

The Woman I have become,

and

The limitless potential for who I can be!

Acknowledgements

An African proverb says, "*It takes a village to raise a child!"*. A worldwide community has helped me get to the finishing line.

First and foremost, I thank my research advisor, Prof. Sheeba Vasu, for being incredibly patient and supportive, for her faith in me, and for helping me troubleshoot and focus on the immediate next steps in the face of setbacks without dwelling. She also has provided a safe space for me to find my way, even if that sometimes took a while. I thank the late Prof. Vijay Kumar Sharma for his guidance and advice. I have constantly remembered his question, "*Why should we care?*" He also urged me to dive deep into the subject instead of wading in the shallow waters. I took both these statements to heart and, at times, pushed myself so deep into the subject that getting out was a challenge. Nevertheless, thank you, sir, for making me care and invest in the problem.

I thank the Council of Scientific & Industrial Research (CSIR), India, for the research fellowship and the Jawaharlal Nehru Centre for Advanced Scientific Research (JNCASR), Bengaluru, India, for the intramural funding.

I thank Prof. Amitabh Joshi for his coursework on Statistics, which has helped me with data analysis. Seeing him in his elements during presentations, his articulation, keen sense of observation and interesting take on things has been a learning experience. I thank Prof. TNC Vidya for her excellent course on Animal Behaviour involving discussions and thought experiments, which have helped me form a hypothesis-testing template and approach a problem from different angles. I thank the late Prof. K.S. Krishnan for his input during the formative years of my PhD with his simple but critical questions, inquisitiveness and infectious enthusiasm towards research. I thank Prof. Ravi Manjithaya for being a supportive GSAC member. Discussing the interface of protein homeostasis, autophagy, and HD with him helped me refine my research questions. I also thank Prof. Maneesha Inamdaar and Prof. Hemalatha Balaram for their valuable suggestions during poster sessions. I thank Prof. Sutirth Dey for his sound advice on navigating the academic landscape and Dr. María Fernanda Ceriani for clarifying specific findings from her lab. I am grateful to Acharya sir, Jayashree ma'am, and Prasanna sir for their constant support and encouragement throughout my PhD journey.

I thank many members of the scientific community world-over for sharing fly resources and reagents. Foremost, Prof. Troy Littleton, MIT, for the HTT fly lines. Prof. Charlotte-Helfrich Förster, JMU Würzburg and Prof. Todd Holmes, UC Irvine, for comments on the manuscripts. Profs Michael Rosbash, Brandeis University; Lawrence Marsh, UC Irvine; Paul Hardin, Texas A&M; Michael Nitabach, Yale University; Jeffrey C Hall, Brandeis University; Jae Park, Vanderbilt University; Florence Maschat, Université de Montpellier; Norbert Perrimon, Harvard Medical School; Nobuyuki Nukina, RIKEN, for fly lines and antibodies. I thank Profs KS Narayan and MRS Rao, JNCASR Central Imaging facility, particularly Suma and Sunil Kumar, Vasu, Deboshree, Rohan and Simi, NCBS-CCAMP, Prof. H. Krishnamurthy and Raksha for their assistance with confocal microscopy. I thank the Bloomington and Vienna *Drosophila* Stock

Centres for the fly lines and PubMed and NCBI for easing my navigation through research-related literature.

I am grateful to the ever-present and helpful Rajanna and Muniraju, whose impeccable work ethic has inspired me. Their cheerful company with Kannada songs playing in the background made mundane cooking days fun! I thank colleagues from EBL and ABL for having helped me through gruelling coursework and assignments and keeping me company at odd hours. Thank you, Snigdho, Joy, Soundarya, Dhananjay, Kanika, Sajith, Miraj, Avani, Srikant, and Neha from EBL, and Hansraj and Mihir from ABL. Keerti and Nandini have been fun friends to hang out with on campus. I thank friends from TSU, EMU and MBGU - Sarada, Priyanka, Meha, Ponnu, PP, Rajesh, Jose, Vicky, Sankalp, Deepthi, SaiKishan, Aarati, Vijay J, and Arpit, who made my stay at JNC enjoyable.

I was fortunate to have an inspiring set of mentors from CBL in Shahnaz, Pankaj bhai, Koustubh, and Nisha and an inquisitive set of peers in Nikhil, Vishwanath, and Anuj. Other lab members, Vinodh, Pawan, Reshmi, Archana, Arghya, Poojashri, Abhilash, Manishi, Chitrang and Arijit, provided inputs during the Clock-club. Intense discussions during lab meets have helped me formulate and refine research questions, troubleshoot and overcome roadblocks and compile a cohesive narrative for my work. Thanks to Abhilash for help with statistics and MATLAB and Anuj and Manishi for remotely connecting me to the lab computer.

I want to thank R & D assistants Basha for helping me at the start of HD experiments and Enakshi for helping with cooks and food changes. Thanks to Revathi and Sushma for their super-efficient help through massive locomotor setups, dissections, sample processing, and food cooks. I would not have managed those crazy dissection days without you two! I have had the opportunity to work with some fantastic and very driven short-term students, particularly Sindhuja, G Priya, Arpit and Aishwarya Nambiar, whose enthusiasm and hard work have helped and inspired me to do some exciting and intense experiments that have provided excellent results. Pawas, Aditi, Femi, and Danita added colour during the summers. Joydeep, Manswini, Anjali, Goirik, and Pritha worked with me on some of the HD experiments, and Shambhavi and Ratna made for interesting late-night conversations.

Priya has been a great mentor, initiating me into the world of fly pushing, a good friend and a warm and caring presence during my PhD life. I speak for the entirety of the old BNL when I say that Priya kept us in line and instilled some crazy standards for cleanliness and experimental rigour. It has been a pleasure to share lab space with Antara, a fine research companion whose booming laugh and kickass attitude kept things interesting! Payel has been a good friend and a great labmate to work with, always bringing a lot of positivity and cheer to the lab. I thank her for her help with food cooks, stock maintenance and through some problematic locomotor set-ups in the dark. Thanks to my three biggest cheerleaders, Aisha, Sheetal and Viveka, over the years! Aisha has been highly supportive, always positive and pumped up. Discussions with her on temperature sensation in flies and comments on the temperature chapter have been constructive. Sheetal and her PJs grew on me! Her knack for cutting into the heart of the matter

and unique perspective has given me much research insight. Her encouragement and support kept me going, especially when the going was tough. Vinky, I have so much to say! For now, I thank you from the bottom of my heart for always being one call away, no matter what. Thank you for being you!

I thank Aishwarya Iyer for discussing the *Drosophila* circadian clock network and generously sharing food vials. I thank Rutvij for his extensive help with statistics and MATLAB. His pointed questions and discussions have raised the bar and aided me in articulation. I have had intense and exciting discussions on HD with Ankit, and I thank him for his assistance with some of the Hsp experiments and pertinent questions on the manuscript. I also thank other lab members, Roshan, Pragya, Mansi, and Surajit, for their helpful suggestions during the work presentation.

I am thankful to the JNCASR community, the academic, administrative, accounts and purchase, the technical, the security, the medical, the hostel, and the housekeeping staff for their help in small and big ways that have made my stay and work at JNC comfortable and smooth.

I am immensely indebted and grateful to my therapist, Shilpa, for pulling me out, holding my hand, sitting with me, and helping me find my wings and fly.

I eagerly looked forward to dinner outings with Mamta, Mugdha and Dhanno, which have been great stressbusters filled with laughter and joy. Chitra has been a good listener, a great friend and a constant companion in this journey. KD, Renu, KC bhai, Bhavna and Ashwini have supported me at different points in my journey with their kind words. Asha Vinitha have been emphatic supporters with their warm acceptance, gentle nudges and immense enthusiasm. Meetings with Deepu are like a homecoming: welcoming, with no expectations and rejuvenating.

I am grateful to my immediate and far-off family for their prayers and for learning not to ask uncomfortable questions like, “When are you finishing your PhD?” Thanks to Attais-Attimbers, Chittis-Chittapas, Periammas-Periappas, Chinpatis-Chintaatas, Maamas-Maamis, Aunties-Uncles, Akkas-Annas, Thangis-Tammas, Chechis-Chettans and the Kutti Shaitans. I am grateful to my grandparents for their love and support. My Taata, bless his soul, would be happy to know I have finally moved from writing Chapter 2 to finishing the thesis. My Paati has been a great source of joy, warmth and unconditional love. My parents, Appa and Amma, have been very patient and supportive every step of the way! I cannot express my gratitude in words. You gave me the space when I asked for it and the comfort and amenities needed to accomplish long hours of uninterrupted writing. I am grateful to Amma for proofreading my thesis and the end-note referencing and linking. Anu and Jom, my boat companions, I have you as you have me. You will get there very soon! Thank you, Navaneeth, my best takeaway from JNCASR, for being my bedrock of support every step of the way. I thank my amazing in-laws and the whole of the acquired family for their unwavering faith and support. Durga Amma and Geetechi, N’s angels, have become my angels, too! I thank my second family at Mana Jardin, Roopa, Ganesh, Aunty, Uncle and Chinnu for their company and encouragement. I am grateful to Ranjani Aunty, Soumitra Uncle, Deeda, Anu, Mahesh, Vivaan and Suniyettan for making difficult days better with homecooked food and great company.

Acknowledgements

I thank friends in Stockholm, Verena, Angelina, Sardar, Malin, Sheila, and Maria, for making my life comfortable in small but significant ways and trainers Lars, Helen and Jan, for motivating me to be physically fit and supporting me in that journey. I am grateful to Keren, Urban and family for making my stay in Åkersberga extraordinarily comfortable and memorable. I thank Silvian for encouraging me and helping me show up to write every day. Srikanth, Vivek, Vipin, Akshay, Madhu, Daani and Croor were good friends who made weekends lively! My special thanks to Sumesh for providing workspace at IITM to facilitate my thesis writing and Sriram, Pandu, Remya, and Ravi for making my Chennai stint fruitful. I thank friends at Mohali and Ropar, Shweta, Inaya, Mohit, Aunty, Uncle, Ruchi, Kapil, Pari, Adi and Devranjan for providing me with a haven away from home. I thank the housekeeping assistants who kept the wheels running: Jyoti, Sridevi, Bindu, Chandrakanta, Kamalesh, Fatima, Shobha, Sara, Renu, Lokesh, Rajesh and the late Moin.

Workouts at Cult Fit in Bengaluru and Friskiss and Svettis in Åkersberga have been great mood uplifters and helped channel my frustration and redefine my relationship with health and physical fitness. I am happy to have had retail therapy via Myntra, Ajio, Flipkart and Amazon! I am thankful for the emotional support and comfort indulgences that have been constant background companions across massive data analysis and thought processes. These include Kindle, Amazon Music, Spotify, Wynk Music, Youtube, Audible, Netflix, Amazon Prime, Hotstar, and TV series like Hercule Poirot, Midsomer Murders, Vera, McDonald and Doyd, Miss Fisher's Murder Mysteries, Foyle's War, The Inspector Lynley Mysteries, Professor T, The Monk, The Mentalist, Bones, Strike, Hinterland, Shetland, Blue Bloods, Criminal UK, Miss Scarlet and the Duke, Elementary, The Closer, Castle, The Doctor Blake Mysteries, and Murdoch Mysteries!

Last but not least, I thank the two anonymous reviewers of my thesis. I apologise in advance for its length. Writing this thesis has been a journey of self-discovery, a labour of hardship and love, many years in the making. It has been my only avenue to document many ideas and work through some turbulences. I thank you in advance for taking the time and having the patience to go through this humungous piece of work. I truly appreciate your efforts and feedback. Furthermore, for anyone whom I have inadvertently missed out, my apologies. You have my gratitude for your aid in achieving this feat!

List of publications

1. **Prakash P, Nambiar A, Sheeba V**. "Oscillating PDF in termini of circadian pacemaker neurons and synchronous molecular clocks in downstream neurons are not sufficient for sustenance of activity rhythms in constant darkness". **PLoS One**. 2017 May 30;12(5):e0175073.

   https://doi.org/10.1371/journal.pone.0175073

   Author Contributions - Conceptualisation: PP, VS. Formal analysis: PP, AN. Funding acquisition: VS Investigation: PP, AN, VS. Methodology: PP, VS. Project administration: VS. Resources: VS. Supervision: VS. Writing – original draft: PP.

   This article has been reused and forms a part of Chapter 2 under the CC BY 4.0 license of PLoS One.

2. **Prakash P, Pradhan AK, Sheeba V**. "Hsp40 overexpression in pacemaker neurons delays circadian dysfunction in a *Drosophila* model of Huntington's disease". **Dis Model Mech**. 2022 Jun 1;15(6):dmm049447.

   https://doi.org/10.1242/dmm.049447

   Author Contributions - Conceptualisation: PP, VS. Methodology: PP, VS. Validation: PP. Formal analysis: PP, AKP. Investigation: PP, AKP. Resources: VS. Writing - original draft: PP. Writing - review & editing: PP, AKP, VS. Visualization: PP. Supervision: VS. Project administration: VS. Funding acquisition: VS.

   This article has been reused and forms a part of Chapter 5 under the CC-BY license of Dis Model Mech.

The **underline** indicates the first authorship.

Table of Contents

List of Figures and Tables

List of Figures and Tables

List of Figures and Tables

List of Figures and Tables

List of Figures and Tables

List of frequently appearing abbreviations

Abbreviation	Full Form
aa	Amino acid
Aβ	Amyloid beta
AC(s)	Anterior Cell(s)
AD	Alzheimer's Disease
ADP	Adenosine Diphosphate
AI	Anticipation Index
ALAN	Artificaial Light at Night
ALIS	Aggresome-like Induced Structures
APOD	Age-associated Protein Deposit
APP	Amyloid Precursor Protein
Arr	Arrhythmic
ASPS	Advanced Sleep Phase Syndrome
ASO(s)	Antisense Oligonucleotide(s)
ATP	Adenosine Triphosphate
ATX	Ataxin
a.u	Arbitrary units
AVP	Arginine Vasopressin
AW(s)	Age window(s)
BACHD	Bacterial Artificial Chromosome (BAC)-mediated transgenic HD mice model expressing full-length human mutant HTT
BAG	Bcl-2 Associated Athanogene
BBB	Blood-brain Barrier
BDNF	Brain-derived Neurotrophic Factor
BH	Benjamini-Hochberg
BMAL1	Brain and Muscle ARNTL (Aryl hydrocarbon Receptor Nuclear Translocator–Like) 1
BTR	Body Temperature Rhythm
CAGs	Cytosine Adenine Guanine(repeats)
cAMP	Cyclic Adenosine Monophosphate
CASA	Chaperone-assisted Selective Autophagy

Abbreviation	Full Form
CBP	cAMP Response Element (CRE) Binding Protein
CBT(s)	Cognitive Behavioural Therapy(ies)
CCG(s)	Clock-controlled Gene(s)
CCT	Chaperonin-containing TCP-1
CFTR	Cystic Fibrosis Transmembrane Conductance Regulator
CHIP	C-terminal Hsp70-interacting Protein, a E3 ubiquitin ligase
CK1	Casein Kinase 1
CK1δ	Casein Kinase 1 delta
clk	CLOCK gene
CLK	CLOCK protein
CLOCK	Circadian Locomotor Output Cycle Kaput
CMA	Chaperone-Mediated Autophagy
CNN	Circadian Neuronal Network
CNS	Central Nervous System
CP	Contralateral Projections
CRD(s)	Circadian Rhythm Disruption(s)
CSF	Cerebrospinal Fluid
CIRBP(s)	Cold-induced RNA Binding Protein(s)
CRE	cAMP Response Element Binding
CRY	Cryptochrome protein
CSP	Cysteine String Protein
CT	Circadian Time
C-T	C-Terminal
cwo	CLOCKWORK ORANGE gene
CWO	CLOCKWORK ORANGE protein
cyc	CYCLE gene
CYC	CYCLE protein
DA	Dopamine
DBT	Doubletime

Abbreviation	Full Form	Abbreviation	Full Form
DD	Constant Darkness	**HIP**	Huntingtin Interacting Protein
Df	Deficiency	**HOP**	Hsp70/Hsp90 Organizing Protein
dhtt	*Drosophila* huntingtin gene	**HSE**	Heat Shock Elements
dhtt	*Drosophila* huntingtin protein	**HSD**	Honest Significant Difference
Diff	Diffuse	**Hsf1**	Heat Shock Factor 1
DN(s)	Dorsal Neuron(s)	**Hsp(s)**	Heat Shock Protein (s)
DN1(s)	Dorsal Neuron(s) 1	**HSR**	Heat Shock Response
DN1a(s)	Dorsal Neuron(s) 1 anterior	***Htt***	Huntingtin gene
DN1p(s)	Dorsal Neuron(s) 1 posterior	**HTT**	Huntingtin protein
DN2(s)	Dorsal Neuron(s) 2	***hHTT***	Human huntingtin gene (usually denoted as *HTT*)
DN3(s)	Dorsal Neuron(s) 3	**hHTT**	Human huntingtin protein (usually denoted as HTT)
DNA	Deoxyribonucleic acid	**HTTex1**	HTTexon1
DP	Dorsal Projections	**GPi**	Internal Globus Pallidus
DRPLA	Dentatorubral-pallidoluysian Atrophy	**IB(s)**	Inclusion Body(ies)
DSPS	Delayed Sleep Phase Syndrome	**Inc**	Inclusion(s)
E	Evening	**INQ**	Intranuclear Quality Control Compartment
E-activity	Evening Activity	**IPOD**	Insoluble Protein Deposit
E-peak	Evening Peak	**ipRGC(s)**	Intrinsically Photosensitive Retinal Ganglion Cell(s)
E-AI	Evening Anticipation Index	**JDP**	J-domain Containing Proteins
E-box	Enhancer Box	**JHD**	Juvenile HD
EGP	External Globus Pallidus	**JUNQ**	Juxta Nuclear Quality Control Compartment
ER	Endoplasmic Reticulum	**kb**	kilobases
expHTT	expanded Huntingtin (refers to HTT ≥40 polyQ repeats)	**KDa**	Kilo Dalton
FDR	False Discovery Rate	**LAMP-2A**	Lysosome-associated Membrane Protein 2A
GABA	Gamma (γ)-Amino Butyric Acid	**LC3**	Microtubule-associated protein 1A/1B-Light Chain 3
GOF	Gain-of-Function	**LD**	Light/dark cycles
HA	Heat Acclimation	**LL**	Constant Light
HAP1	Huntingtin-Associated Protein 1	**lLNv(s)**	Large Ventral-Lateral Neuron(s)
HD	Huntington's Disease	**LLPS**	Liquid-liquid Phase Separation
HDCRG	Huntington's Disease Collaborative Research Group	**LN(s)**	Lateral Neuron(s)
HDAC	Histone Deacetylase	**LNd(s)**	Dorsal Lateral Neuron(s)
HEAT	Huntingtin, Elongation factor 3, regulatory A subunit of phosphoprotein phosphatase, TOR1	**LNv(s)**	Ventral Lateral Neuron(s)
Hip	Hsc70-Interacting Protein	**LOF**	Loss-of-Function

Abbreviation	Full Form
LPN(s)	Lateral Posterior Neuron(s)
M	Morning
M-activity	Morning Activity
M-peak	Morning Peak
M-AI	Morning Anticipation Index
MB	Mushroom Body
MC	Motor Centres
MHC	Major Histocompatibility Complex
mHTT	Mutant Huntingtin
miRNA	MicroRNA
MJD	Machado-Joseph Disease
MMP	Matrix Metalloproteinase
MPP11	M-phase Phosphoprotein 11
MPTP	1-methyl-4-phenyl-1,2,3,6-tetrahydropyridine, a drug that causes selective destruction of dopaminergic neurons
MSGN(s)	Medium Siny GABAergic Neuron(s)
MSN(s)	Medium Spiny Neuron(s)
MTOC	Microtubule Organizing Centre
N17	The first 17 amino acids of HTT protein at its N-terminal
N-T	N-Terminal
NA	Not Applicable
NAC	Nascent Polypeptide-associated Complex
NBD	Nucleotide Binding Domain
NBR1	Neighbour of BRCA1 Gene 1
nd	Not different
ND or NDs	Neurogenerative Disease(s)
NEF(s)	Nucleotide Exchange Factor(s)
NES	Nuclear Export Signal
NF-κb	Nuclear Factor Kappa b
NLS	Nuclear Localisation Signal
NMDA	N-methyl-D-aspartate
NMDAR(s)	NMDA Receptor(s), a receptor for the excitatory neurotransmitter glutamate
NS	Not Significant
NTA	Not Available
NuMA	Nuclear Mitotic Apparatus protein
p53	tumour suppressor protein 53
PD	Parkinson's Disease
pdf	Pigment Dispersing Factor gene
PDF	Pigment Dispersing Factor peptide
PDFR	Pigment Dispersing Factor Receptor
pdp1	Par domain protein 1 gene
PDP1	Par domain protein 1 protein
per	PERIOD gene
PER	PERIOD protein
PEST	Proline, Glutamic Acid, Serine, Threonine
PGC1α	Peroxisome proliferator-activated receptor gamma coactivator 1-alpha, a transcriptional coactivator
PI	Pars Intercerebralis
piRNA	Piwi-interacting RNA
PN	Proteostatic Network
PNs	Projection Neurons
POIC	PDF Oscillation Independent Component
polyP	poly Proline
polyQ(s)	poly Glutamine(s)
PQC	Protein Quality Control
PP	Protein Phosphatases
PRD	Proline-Rich Domain
PTM(s)	Post-Translational Modification(s)
Q	Glutamine
QBP1	polyQ-Binding Peptide 1
QC	Quality Control

List of Abbreviations

Abbreviation	Full Form	Abbreviation	Full Form
'*r*'	The magnitude of the radial vector of a circular plot representing the extent of activity consolidation	**sRNA**	Small regulatory RNA
R6/2	A transgenic mice model of HD expressing the N-terminal portion (exon 1) of the mutated human HTT gene (145Qs) under human gene promoter elements	**SOD**	Superoxide Dismutase
RAC	Ribosome Associated Chaperones	**STN**	Subthalamic Nucleus
REST/NRSF	RE1-silencing transcription factor (also known as neuronal restrictive silencing factor)	**TBP**	TATA Binding Protein
Rhes	Ras homolog enriched in the striatum	**TC**	Thermophase/cryophase cycles (temperature cycles)
Rhy	Rhythmic	**TF(s)**	Transcription Factor(s)
RNA	Ribonucleic acid	***tim***	TIMELESS gene
RNAi	RNA interference	**TIM**	TIMELESS protein
ROS	Reactive Oxygen Species	**TNT(s)F**	Tunnelling Nanotube(s)
S2 cells	Schneider 2 cells	**TPR**	Temperature Preference Rhythm
SAD	Seasonal Affective Disorder	**TRF**	Time-restricted Feeding
SBD	Substrate Binding Domain	**TRiC**	T-complex protein-1 (TCP-1) Ring Complex
SBMA	Spinal and Bulbar Muscular Atrophy	**TrkB**	Tropomyosin Receptor Kinase B
SCA	Spinocerebellar Ataxia	**TTFL(s)**	Transcriptional/Translational Feedback Loop(s)
SCN	Suprachiasmatic Nucleus	**UAS**	Upstream Activating Sequences
SCRD(s)	Sleep and Circadian Rhythm Disruption(s)	**Ub**	Ubiquitin
SD	Standard Deviation	**UPR**	Unfolded Protein Response
SDS	Sodium Dodecyl Sulfate	**UPS**	Ubiquitin Proteasomal System
SGG	Shaggy	**VIP**	Vasoactive Intestinal Peptide
SH3	Src homology region 3	***vri***	VRILLE gene
siRNA	small interfering RNA	**VRI**	VRILLE protein
sLNv(s)	Small Ventral Lateral Neuron(s)	**WT**	Wildtype
SNc	Substantia Nigra pars Compacta	**ZT**	Zeitgeber Time
SP1	Specific Protein 1		

Glossary of circadian terms

Rhythms: Events that occur repeatedly in the same order at fixed intervals.

Period: The time to complete one event cycle or between two subsequent events.

Amplitude: The magnitude of change from the mean within a cycle between a rhythm's peak or trough and its mean value.

Biological Rhythms: Rhythms in behaviour and physiological processes in living organisms observed across taxa. The rhythms can be categorised based on the time-interval between subsequent events into ultradian (high frequency, repeating many times in a day; e.g. heart rate, blinking), circatidal (~12.4h, with the tide, the activity of certain crab species), circadian (~24h, e.g., sleep-wake cycles), infradian (>24h) like circalunar rhythms (~28d, e.g. menstrual cycle) and circannual (~365d, e.g. seasonal cycles, hibernation, many reproductive cycles and bird migrations).

Chronobiology: The study of biological rhythms, both endogenously and exogenously driven.

Circadian rhythms: Latin 'circa'= about, 'dies or diem or dian'=a day; 'circadian'=about a day. For biological rhythms to be called circadian rhythms, they must fulfil a few criteria (Pittendrigh, 1954; Pittendrigh, 1960; Kidd et al., 2015). The rhythms must be **endogenous**, i.e., internally generated. They must have a periodicity of ~24h (not precisely 24h), persisting without any external time cues (**self-sustained free-running rhythms with a period of ~24h**). The intrinsic period of these rhythms should not change within a range of physiological temperature values (**temperature-compensated**) or with changing nutrition status (**nutrition-compensated**). These rhythms must synchronise to external cycles of a time cue (like light, temperature, and food availability) by maintaining a stable phase relationship (**entrainment to external time cues**).

Free-running conditions: Absence of any perceivable external time cues or constant conditions. E.g. Constant darkness (DD) and constant temperatures (25 °C), Constant light (LL) and constant temperatures (25 °C).

Free-running rhythms: Circadian rhythms under constant conditions. The period thus exhibited is referred to as the free-running period.

Activity rhythms: Circadian rhythms in the locomotor activity of *Drosophila* are made of periodic bouts of activity and rest, such that the time interval between the initiation (or completion) of two subsequent activity bouts is about 24h.

Circadian Time (**CT**): Time as defined by the period of the endogenous cycle under constant darkness; circadian day = time taken for one complete cycle. For example, for day-active animals, CT0 is the time of activity onset, and for night-active animals, CT12 is the time of activity onset.

Subjective day/night: Time under constant conditions (e.g.DD or LL) corresponding to the previously exposed zeitgeber cycle, like light/dark cycles.

Phase: A recognisable part of the cycle identified by the specific time at which it occurs in a cycle (e.g. within each cycle: acrophase, the peak of the event; bathyphase, nadir or trough of the event; onset, the start of the event; offset, end of the event); its stage in the cycle relative to that of the external time.

Zeitgeber: German for 'time-giver'. External time cues like light, temperature, and humidity

Entrainment: Synchronisation of circadian rhythms to zeitgebers such that

i) There is a period matching between the synchronised rhythm and the zeitgeber cycle.

ii) A stable phase relationship is established between the synchronised rhythm and the zeitgeber.

iii) Post-removal of the zeitgeber (i.e., moving into constant conditions), the synchronised rhythm starts free running from the entrainment phase established with the zeitgeber.

Masking-Acute response of an organism to an external time cue without the involvement of the endogenous circadian clocks.

Zeitgeber Time (**ZT**): Time defined relative to a zeitgeber cycle like the light-dark cycle. For example, under 12h:12h LD, ZT0 is lights-on time, ZT1 is one hour after lights-ON, ZT12 is light-OFF time and so on.

LD25: **Light/Dark cycle**. A 24h cycle of 12h of light and 12h of darkness at 25 °C.

M-activity: Referring to locomotor activity around lights-ON in an LD cycle

E-activity: Referring to locomotor activity around lights-OFF in an LD cycle

M-peak: Phase of the peak of activity with reference to the time of lights-ON in an LD cycle.

E-peak: Phase of the peak of activity with reference to the time of lights-off in an LD cycle

TC: **Thermophase/Cryophase cycle**. A 24-hour (h) cycle of 12h of warm and 12h of cool temperatures in constant darkness can be perceived as day and night, respectively. In this study, a TC of 12h:12h 29°C:21°C has been used.

Phase-relationship: The phase/stage of an endogenous cycle relative to external time or a phase/stage in the Zeitgeber cycle. Also known as the phase of entrainment, it is the difference between the phase of endogenous rhythm and the phase of the zeitgeber (Pittendrigh and Daan, 1976). E.g. The timing of activity onset relative to lights-ON: if activity onset coincides with lights-ON, then the onset of the rhythm is in-phase with the light cycle; if their timings do not coincide, then they are out-of-phase by a magnitude of the difference in their timing: if the difference is negative, i.e. onset phase happens before light-on, then the phase of the endogenous cycle is advanced concerning the zeitgeber, whereas if the difference is positive, i.e. onset phase occurs after light-on, then there is a phase delay.

Photoperiod: The day length or time duration of light in an LD cycle. Photoperiod in a 12h:12h LD is 12h, in a 14h:10h LD is 14h, and in a 13h:13h LD is 13h.

Anticipatory activity: The gradual increase in activity exhibited by organisms before a time cue is expected to be present. This clock-controlled anticipatory activity is often used to distinguish a circadian behaviour from a mere behavioural response to an external stimulus.

Actogram: Graphical representation of the circadian activity/rest cycle over several cycles with time-of-day on the *x*-axis and each consecutive cycle/day on the *y*-axis. In this study, the actograms are double plotted with the *x*-axis extending over forty-eight hours or two days.

Periodogram: A method to identify significant frequencies or dominant periods of a time series**.**

Robustness of rhythm: A measure of how consistently the rhythm maintains the most predominant periodicity daily (over at least seven days for activity rhythms). It measures the strength or the power of the oscillator/rhythm for a periodicity, i.e. how stably it can maintain a specific periodicity daily against perturbations. It is typically the value of the periodogram peak above the 1% significant threshold of the chi-square analysis.

Coupling involves signalling between multiple oscillators to establish stable phase and period relationships.

Damping: Decline in the amplitude of the circadian cycle.

Chronotype: An individual's natural inclination or preferred time of being active or asleep.

CHAPTER 1

Introduction

1.1 HUNTINGTON'S DISEASE

Huntington's disease is an autosomal dominantly inherited disease characterised by progressive uncontrolled dance-like movements termed chorea, psychiatric impairments, and cognitive decline (Gusella and MacDonald, 1995). In 1872, Dr George Huntington provided the classical description of HD, then known as Huntington's chorea, highlighting its hereditary nature, psychiatric and cognitive symptoms and typical middle-age onset (Huntington, 1872). Before this, several post-mortem studies pointed out neurodegeneration in specific brain regions: areas of basal ganglia of which the striatum is severely affected, the thalamus and the cerebral cortex (Stier, 1903; Jelgersma, 1908; Rüb et al., 2015). In 1983, DNA samples from a community of people living around the Lake Maracaibo region of Venezuela, a high-density area of HD gene carriers, helped assign the genetic basis of HD (Gusella et al., 1983). However, it was only in 1993 that the human Huntingtin gene (*Htt* or *IT15*) was identified (HDCRG, 1993). The mutant *Htt* was found with a tract of expanded repeats (>35 units) of the trinucleotide Cytosine-Guanine-Adenine (CAG) (HDCRG, 1993). The translated mutant Huntingtin protein (HTT) has an expanded tract (>35) of the amino acid Glutamine (Q) in its N-terminal (Aronin et al., 1995; Persichetti et al., 1995; Sharp et al., 1995; Trottier et al., 1995). HD belongs to a family of CAG triplet expansion or polyQ expansion diseases, where repeat expansions are found in the coding regions (Reiner et al., 2011; Stoyas and La Spada, 2018b). These diseases share standard features such as a polyQ threshold for pathogenicity, a direct relationship of repeat number with severity, an inverse relationship with age-of-onset and a typical middle-age onset (Paulson, 2018; Podvin et al., 2019). The progression of polyQ diseases is similar to that of other neurodegenerative diseases (NDs), such as Parkinson's disease (PD) and Alzheimer's disease (AD), with symptoms getting worse over time, differential degeneration in distinct brain areas, abnormal protein processing, the formation of protein aggregates, cell-autonomous toxic effects, a reduction in the quality of life, and a shorter life span (Skovronsky et al., 2006). Other polyQ diseases are Spinal and Bulbar Muscular Atrophy (SBMA or Kennedy's disease), Dentatorubral-pallidoluysian atrophy (DRPLA or Haw River syndrome), and six types of spinocerebellar ataxia: SCA1, SCA2, SCA3 (Machado Joseph disease), SCA6, SCA7 and SCA17 (Orr and Zoghbi, 2007). The proteins' functions and the polyQ tracts' position in them vary. A summary of the polyQ family of diseases is provided in Table 1.1.

Table 1. 1 A brief overview of PolyQ Diseases.

Disease	Protein affected	Normal CAG repeats	Expanded CAG repeats	Function	Brain region(s) affected	Main clinical features
Spinal and bulbar muscular atrophy (SBMA) or Kennedy's disease	Androgen Receptor	<34	38–70	Hormone-dependent transcription factor	Anterior horn and bulbar neurons, dorsal root ganglion	Motor weakness, bulbar symptoms, tremors, gynecomastia, hypogonadism
Huntington's disease (HD)	Huntingtin	6–35	40–250	Scaffold protein associated with autophagy, signalling, transport, transcription	Striatum and cortex	Severe movement abnormalities, chorea, dystonia, cognitive decline, psychiatric features
Dentatorubral-pallidoluysian atrophy (DRPLA)	Atrophin-1	6–35	48–93	Transcription cofactor	Cerebellum, brainstem, cerebral cortex, basal ganglia, Luys' body	Ataxia, myoclonus epilepsy, chorea, dementia
Spinocerebellar ataxia type 1 (SCA1)	Ataxin-1	6–35	>39	Transcription cofactor	Cerebellar Purkinje cells, dentate nucleus, brain stem	Ataxia, bulbar symptoms, spasticity, polyneuropathy, cognitive impairment
Spinocerebellar ataxia type 2 (SCA2)	Ataxin-2	14–31	37-270	RNA-binding protein implicated in RNA homeostasis	Cerebellar Purkinje cells, brain stem, frontotemporal lobes	Ataxia, slow saccades, decreased reflexes, polyneuropathy, parkinsonism
Spinocerebellar ataxia type 3 (SCA3)	Ataxin-3	12–44	~60–87	Deubiquitinase	Cerebellar dentate neurons, basal ganglia, brain stem, spinal cord	Ataxia, severe spasticity, polyneuropathy, parkinsonism, diplopia, dystonia
Spinocerebellar ataxia type 6 (SCA6)	Ataxin-6 or $CACNA1_A$	≤18	20–33	Calcium channel subunit/transcription factor	Cerebellar Purkinje and granule cells, dentate nucleus, inferior olive	Ataxia, dysarthria, nystagmus, tremors
Spinocerebellar ataxia type 7 (SCA7)	Ataxin-7	7–27	37–460	Component of SAGA acetyltransferase complex, role in transcription	Cerebellum, brain stem, macula, visual cortex	Ataxia, retinal degeneration, ophthalmoplegia, cardiac involvement in infantile variant

A tabulation of the family of polyQ expansion diseases caused by the expansion of CAG repeats, highlighting the affected protein, possible functions, brain areas, and clinical symptoms. All the diseases are autosomal dominantly inherited, except for SBMA, which displays X-linked inheritance (Gatchel and Zoghbi, 2005; Takahashi et al., 2010; Paulson, 2018; Stoyas and La Spada, 2018b; Bunting et al., 2022).

1.1.1 HD genetics

The human *Htt* gene is located on chromosome 4p16.3, spans >200kb, contains 67 exons, and the CAG repeats are located at its 5'end (HDCRG, 1993; Ambrose et al., 1994). The CAG repeat is polymorphic with the wild-type gene carrying 10–35 CAG repeats, a mean value of ~18 repeats across the population (Snell et al., 1993). The HD mutation is autosomal dominant, with a mutation on either allele leading to disease phenotypes. Units of 36-39 CAG in the *Htt* gene are considered to be of reduced penetrance in the form of developing symptoms at later ages or may never become symptomatic, and ≥40 CAG to have full-penetrance (HDCRG, 1993; Rubinsztein et al., 1996; McNeil et al., 1997). Longer stretches of CAG repeats are strongly correlated with an earlier age of disease onset and less strongly with an increased disease severity (Andrew et al., 1993; Duyao et al., 1993; Snell et al., 1993; Illarioshkin et al., 1994; Brandt et al., 1996; Ravina et al., 2008; Rosenblatt et al., 2012). HD onset is typically in middle age, around 35-50 years, with a disease duration of 15-20 years (Novak and Tabrizi, 2010; Ross and Tabrizi, 2011). The most common HD alleles bear 40-50 CAGs (Finkbeiner, 2011). The number of repeats accounts for about 60% of the variation in age at onset, while the remainder is determined by genetic, epigenetic and environmental factors (Wexler et al., 2004; Imarisio et al., 2008; Barbé and Finkbeiner, 2022; Jurcau, 2022). Larger repeats (>60) lead to onset before 20 years of age, termed juvenile HD and occur predominantly when the disease gene is transmitted from the father (Nance and Myers, 2001). However, the disease duration, i.e. the period between motor onset and death, does not seem to depend on the CAG repeat length (Keum et al., 2016). According to reports, pneumonia, heart disease, infections, and suicide are the leading causes of death in HD patients (Lanska et al., 1988a; Sørensen and Fenger, 1992; Rodrigues et al., 2017; Solberg et al., 2018). In *Htt*, CAG repeats of >27 units are unstable and susceptible to gametic repeat expansion (MacDonald et al., 1993; Kremer et al., 1995; McMurray, 2010), leading to genetic anticipation, where subsequent generations are increasingly susceptible to expansion in the repeat number and disease severity and earlier age-of-onset, especially when paternally inherited (Duyao et al., 1993; Telenius et al., 1993; Trottier et al., 1994; Wheeler et al., 1999; Semaka et al., 2006). The

expanded CAG repeats are somatically unstable, the repeat length progressively increasing with time, and the tissue-specificity of this somatic instability could be contributing to the tissue specificity of the disease (Telenius et al., 1994; De Rooij et al., 1995; Wheeler et al., 1999; Kennedy and Shelbourne, 2000; Kennedy et al., 2003; Shelbourne et al., 2007a; Gonitel et al., 2008; Jimenez-Sanchez et al., 2017). Most HD patients have a family history, but the sporadic onset of HD with no prior family history has also been reported (Myers et al., 1993; Davis et al., 1994; Dürr et al., 1995; Almqvist et al., 2001). These cases are typically caused by intermediate-length alleles (27-35 CAG repeats) (ACMG/ASHG, 1998), usually on the paternal side, that are at risk of expanding during meiosis into a disease-causing range in the next generation (Goldberg et al., 1993; Semaka et al., 2006; Semaka et al., 2013). The frequency of intermediate alleles in the general population ranges from 1% to 3.9% (Semaka et al., 2006) and has important implications for predictive genetic counselling. Though people with intermediate alleles are mainly asymptomatic, one study suggests they exhibit behavioural phenotypes (Killoran et al., 2013).

Individuals with the HD mutation who are homozygous and heterozygous have similar ages at which symptoms first appear, but homozygotes advance the disease more severely than heterozygotes (Georgiou et al., 1999; Alonso et al., 2002; Squitieri et al., 2003; Anca et al., 2004). With varied clinical symptoms and occasionally different dates of onset, HD monozygotic twins are discordant, providing evidence that somatic instability, prenatal or postnatal environmental variables, and epigenetic factors all affect the phenotypic manifestation of HD (Georgiou et al., 1999; Anca et al., 2004; Friedman et al., 2005; Gómez-Esteban et al., 2007).

1.1.2 Epidemiology

The prevalence of HD is approximately 5.70 per 100,000 in North America, Europe, and Australia and is more significant than in Asia, which is approximately 0.40 per 100,000 (Pringsheim et al., 2012). The difference in HTT haplotypes explains this geographically, with the high-risk haplo-variants A1 and A2 relatively enriched in the European cohorts. Also, the average CAG tract length of healthy individuals in Europe (18.4 ± 3.7 CAG) is higher than that of Asian and African

populations (~16 CAG) (Squitieri et al., 1994; Warby et al., 2009). One study from India indicates healthy individuals with 16.8 ± 2.08 CAG and HD patients with 41-56 CAG (Pramanik et al., 2000). However, a study sampling an Indian population shows normal individuals with a mean CAG repeat size of 18.3, symptomatic individuals with 40-50 CAG repeats, and high-risk haplotype A, closer to the European population (Moily et al., 2014).

1.1.3 Clinical features of HD

Individuals with HD can become symptomatic at any time, before which they have no obvious detectable symptoms, and symptoms progressively worsen with age (Kremer, 2002; Bates et al., 2014). Several changes in the brain are known to occur decades before disease manifestation (this phase is often referred to as the "prodrome" of HD). They can be attributed to altered development and early neurodegeneration (Paulsen, 2010; Kerschbamer and Biagioli, 2015). Manifestation of HD occurs when individuals exhibit characteristic motor symptoms chorea (involuntary dance-like movements of extremities and facial twitches), dystonia (repetitive muscle contractions resulting in uncontrollable movements and abnormal fixed postures) and slowness in movement (bradykinesia) (Roos, 2010; Ross and Tabrizi, 2011). Over time, posture, gait and balance get affected, and the inability to initiate voluntary movements (akinesia) and rigidity affect the ability to perform everyday tasks, disabling the individual functionally. Gradually, talking and swallowing becomes difficult and, at later stages, result in choking. The psychiatric and cognitive impairments often precede motor decline by several years but may be subtle, making differential diagnosis difficult (Marder et al., 2000; Novak and Tabrizi, 2011; Paulson, 2018). Psychiatric symptoms include depression, suicidal tendencies, apathy, low self-esteem, guilt and anxiety, irritability, obsessive-compulsive behaviour and, at later stages, paranoia, psychosis, and hypo-sexuality (Roos, 2010; Novak and Tabrizi, 2011). Cognitive impairments involve a decline in executive functions: difficulty in concentration, planning, organization, multi-tasking and making mental adjustments, loss of psychomotor functions, and learning and memory loss that can develop into dementia (Roos, 2010; Novak and Tabrizi, 2011). Sleep and circadian rhythm disturbances often precede motor symptoms and are detailed in a

future section. Metabolic and endocrine disturbances are prevalent, with weight loss being a prominent pre-diagnostic hallmark. HD patients in advanced stages depend on caregivers but can comprehend language and recognize people. Most HD patients die from complications accompanying the disease, such as aspiration pneumonia, cardiovascular diseases, choking, infection, or nutritional deficiencies (Lanska et al., 1988a; Lanska et al., 1988b).

Most clinical features of Huntington's disease can be attributed to widespread central nervous system degeneration and prominently in basal ganglia's striatal area (affected nuclei: caudate nucleus and putamen) (Fig1.1) (Cepeda et al., 2007; Reiner et al., 2011). The basal ganglia are a neuronal circuit regulating voluntary movement, and its inputs are essential for the cortex to exert proper motor control. The central input centre of the basal ganglia is the striatum, comprising the caudate nucleus and putamen. Depending on the striatal input to the cortex, the cortex can be stimulated to increase motor activity or inhibited to decrease motor activity (Fig 1.2a). Neurodegeneration of the striatal medium spiny GABA neurons is a characteristic of HD that contributes to cortical over-stimulation and chorea (Fig 1.2b).

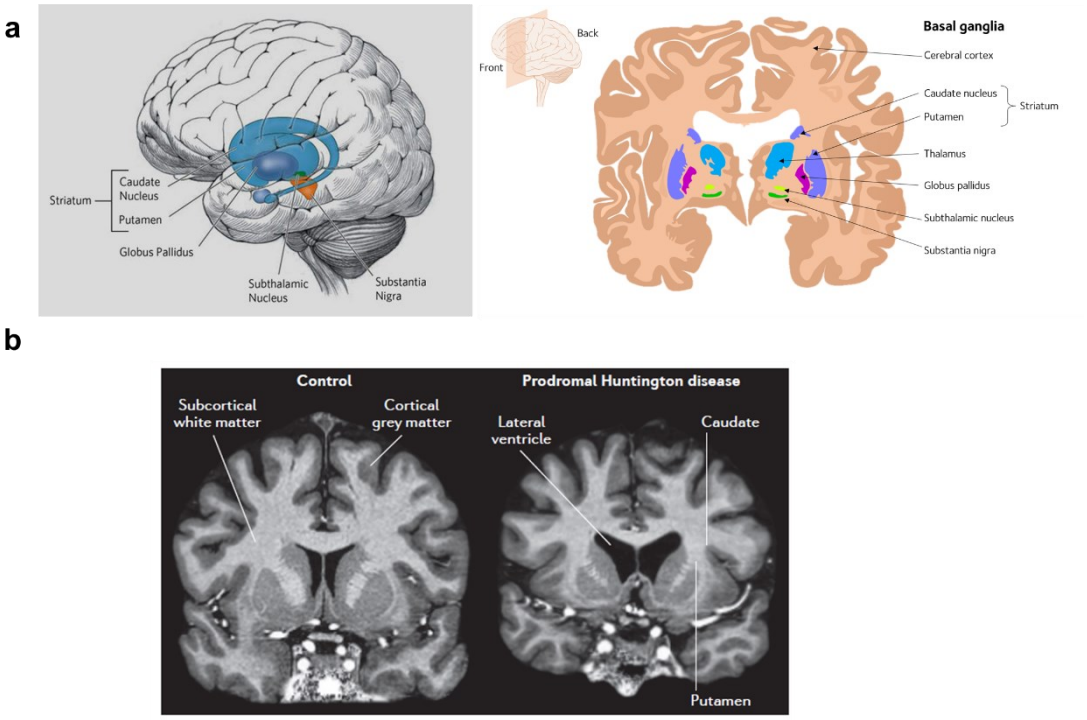

Fig 1. 1 The brain areas that are primarily affected and undergo neurodegeneration in HD. Basal Ganglia (striatum or caudate-putamen and globus pallidus) of the brain and related nuclei (subthalamic nucleus, substantia nigra) are viewed via a sagittal section (left) and a coronal section (right). (b) Striatal area in a healthy brain (left) and an HD brain showcasing neurodegeneration (right). Image sources: (Watson and Breedlove, 2012) (a, left), modified from https://en.wikipedia.org/wiki/Basal_ganglia#/media/File:Basal_ganglia_circuits.svg and https://brainmadesimple.com/basal-ganglia-structure/ (a right) and (Bates et al., 2015) (b).

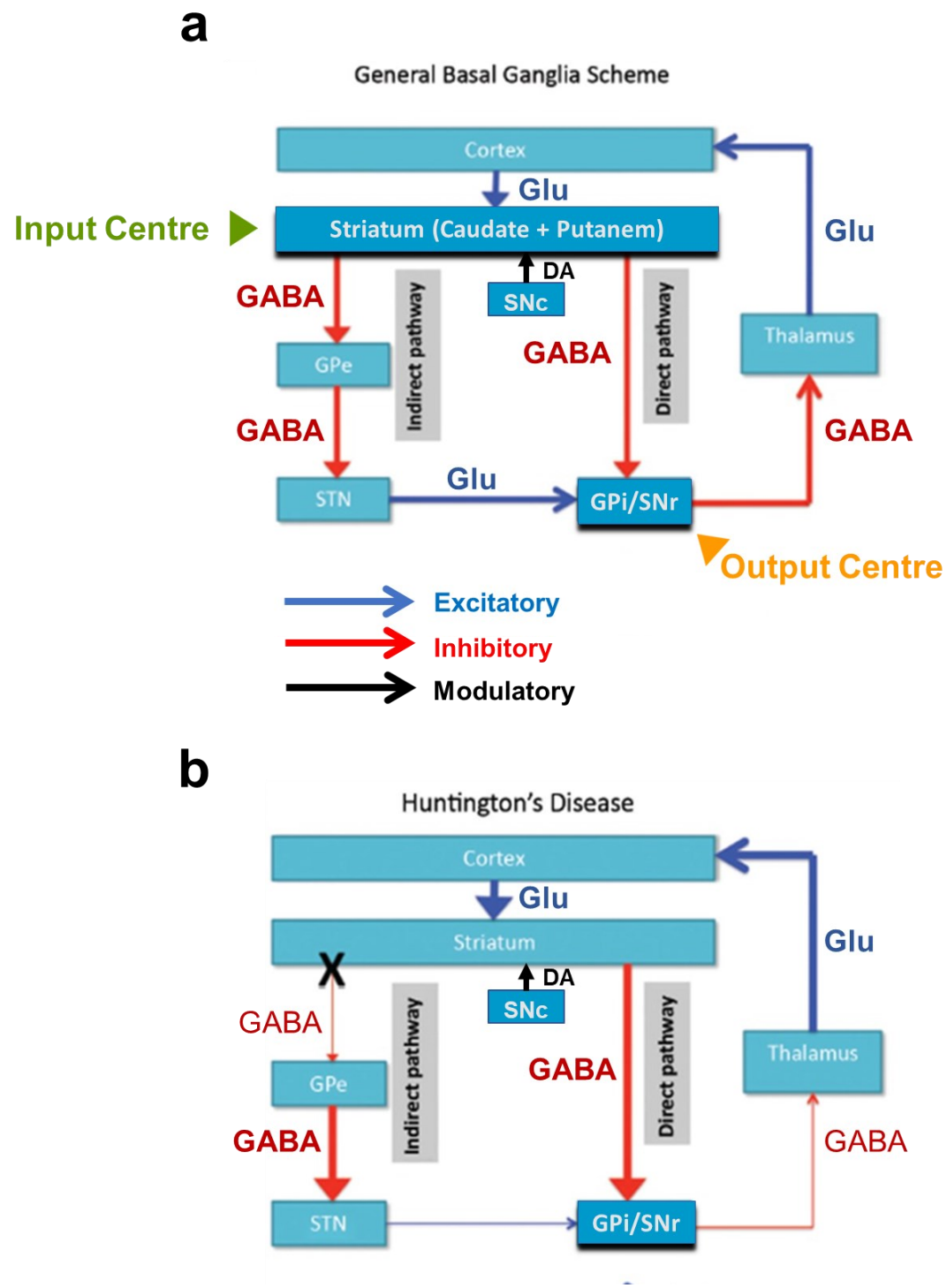

Fig 1. 2 Basal ganglia's regulation of the motor cortex via direct and indirect pathways.
(a) Striatum, the input centre of the basal ganglia, receives excitatory glutaminergic (Glu) innervation from the cerebral cortex and specific thalamic nuclei and dopaminergic (DA) innervations from substantia nigra pars compacta (SNc). 90% of striatal neurons are inhibitory medium-spiny GABAergic neurons (MSGNs). The output centre of the basal ganglia comprises the internal globus pallidus (GPi) and substantia nigra pars reticulate (SNr). The default action of the basal ganglia output on the cortex is inhibitory, turning down the motor activity (GPi/SNr's GABAergic inhibition of the thalamus inhibits the cortical excitation by thalamic glutamate).

Striatal information can reach the output centre GPi/SNr through two pathways with opposing outcomes. In the direct pathway, striatal GABAergic inhibition of the GPi/SNr prevents the default route and eventually activates the cortex, increasing motor activity. In the indirect pathway, striatal GABAergic inhibition of the external globus pallidus (GPe) prevents GPe's GABAergic inhibition of the subthalamic nucleus (STN), ensuring glutaminergic activation of the GPi/SNr, promoting the default pathway of cortical inhibition and lowering the motor activity. (b) In HD, the striatal GABAergic MSNs in the indirect pathway are more dramatically affected than those in the direct pathway, decreasing their inhibitory control over the motor cortex and increasing motor activity that correlates with chorea, which often dominates the early course of HD. At later stages, slowness of movement can be attributed to the direct pathway also getting affected, leading to lowered motor cortex activation (Figure modified from (Kalkhoven et al., 2014)).

Marked neuronal loss and shrinkage are also seen in deep layers of the cerebral cortex. Other areas less affected include other areas of basal ganglia (globus pallidus, ventral pallidum, substantia nigra, subthalamic nucleus, nucleus accumbens), subcortical white matter, specific hypothalamic nuclei, certain areas of the hippocampus, amygdala, thalamus, parietal lobe, cerebellum and brain stem, with varying degrees of atrophy (shrinkage or wasting) and neuronal loss (Rosas et al., 2003; Walker, 2007; Reiner et al., 2011; Bates et al., 2014). Along with neuronal loss and shrinkage, widespread gliosis is prominent in HD with activated microglia and neuroinflammation across the brain (Reiner et al., 2011; Bates et al., 2014). Some features of HD, such as impaired metabolic, endocrine, and immune functions, skeletal-muscle wasting, weight loss, cardiac failure, testicular atrophy and osteoporosis, could be mediated by expanded HTT in the peripheral tissues (van der Burg et al., 2009).

1.1.4 Huntingtin protein

1.1.4.1 Expression pattern

The *Htt* gene encodes a large 348KDa soluble Huntingtin protein made of 3144 amino acids that are expressed throughout the human body over the entire lifetime with the highest concentration in the CNS neurons and testis (Hoogeveen et al., 1993; Li et al., 1993; Strong et al., 1993; Landwehrmeyer et al., 1995; Sharp et al., 1995; Trottier et al., 1995; Tartari et al., 2008). *Htt* gene transcription gives two mRNA transcripts differing in the size of their 3' untranslated region as a result of differential 3' polyadenylation, of which the larger transcript (~13.7kb) is predominantly found in adult and foetal brains and the smaller fragment (~10.3kb) is more widely

distributed (Lin et al., 1993; Romo et al., 2018). Though rare, alternate HTT mRNA splice variants are also found giving rise to HTT isoforms (Hughes et al., 2014; Ruzo et al., 2015), uncovering potential for functional and regulatory diversity.

Within the brain, HTT is widely expressed in both neurons and glia, with neuronal expression predominating; there are regional differences in expression patterns and levels, but they do not correspond to areas of selective vulnerability (Li et al., 1993; Strong et al., 1993; Landwehrmeyer et al., 1995; Sharp et al., 1995; Fusco et al., 1999). In neurons, HTT is enriched in cell bodies, dendrites and axons and is also found at synapses associated with vesicular structures (DiFiglia et al., 1995; Gutekunst et al., 1995; Sharp et al., 1995; Trottier et al., 1995; Velier et al., 1998; Hoffner et al., 2002; Li et al., 2003). Sub-cellularly, HTT is mostly cytoplasmic and is associated with the cytoskeleton, membranous organelle and vesicles, and plasma membrane (DiFiglia et al., 1995; Gutekunst et al., 1995; Sharp et al., 1995; Trottier et al., 1995; Velier et al., 1998; Kegel et al., 2005) but also shows nuclear localisation (Hoogeveen et al., 1993; Sapp et al., 1997; Kegel et al., 2002). HTT subcellular localization is dynamic, and its conformation changes depending on its localization (Ko et al., 2001). The levels and pattern of HTT expression between pre-symptomatic HD patients, symptomatic HD patients and non-HD individuals are comparable, suggesting that HD mutation does not lead to altered protein expression levels or patterns (Li et al., 1993; Aronin et al., 1995; Landwehrmeyer et al., 1995; Schilling et al., 1995) However, expanded HTT accumulates as inclusions in the nucleus and cytoplasm of neurons (DiFiglia et al., 1997; Sapp et al., 1997; Gutekunst et al., 1998), which is detailed in a later section.

1.1.4.2 Structure and evolution of Huntingtin

Pictorial representations of the HTT protein are shown in Fig 1.3. The polyQ stretch in HTT is preceded by 17 amino acids (aa) and followed by a proline-rich domain (~40aa, henceforth PRD) (HDCRG, 1993). The first 17aa of HTT (N-terminal to the polyQ, and henceforth N17) are conserved among vertebrates (Tartari et al., 2008) and carry a nuclear export signal (NES) (Maiuri et al., 2013; Zheng et al., 2013). It can undergo post-translational modifications like acetylation, sumoylation and ubiquitination at three Lysine residues and phosphorylation at two

Serines and these impact the sub-cellular localisation, function, proteolytic cleavage, degradation and clearance of HTT and the ability of pathogenic HTT to aggregate and cause cellular toxicity (Steffan et al., 2004; Thompson et al., 2009; Zheng et al., 2013). The ~40 residue Proline-Rich Domain (PRD) (C-terminal to the polyQ) is polymorphic in humans, poorly conserved across species and found only in mammals, suggesting a recent HTT evolution (Harjes and Wanker, 2003; Tartari et al., 2008). Through the PRD, HTT can interact with several proteins that contain Src homology region 3 (SH3) or tryptophan (WW) domains (Harjes and Wanker, 2003; Gao et al., 2006). PRD also has roles in HTT aggregation (Dehay and Bertolotti, 2006) and turnover (Southwell et al., 2008). Since the pathogenic mutation of polyQ is in exon 1, the rest of the protein from the other 66 exons is not well studied. About 16 HEAT repeats (Huntingtin, Elongation factor 3, Regulatory, a subunit of phosphoprotein phosphatase, TOR1), a sequence of ~40 amino acids found multiple times in a protein, are found in HTT, organised into four clusters along the length of HTT, are relatively conserved across species, and are thought to be necessary for protein-protein interactions, intracellular transport and chromosomal segregation (Andrade and Bork, 1995; Neuwald and Hirano, 2000; Tartari et al., 2008; Palidwor et al., 2009). Several proteins that interact with HTT via the HEAT-repeat region include HTT-interacting protein (HIP) 1, HIP14 and HTT-associated protein (HAP) 1 (Harjes and Wanker, 2003). HEAT repeats promote intra-molecular interactions and provide flexibility to adapt around 100 structurally distinct conformations (Seong et al., 2010; Saudou and Humbert, 2016); inter-HTT interactions result in self-assembly and homodimerisation. Interspersed between HEAT repeats are proteolysis-susceptible PEST sequences (Proline, Glutamic Acid, Serine, Threonine-rich) (Warby et al., 2008). A nuclear localisation signal (NLS) is found in the N-terminal of HTT and might help in its nuclear entry via facilitated diffusion (Desmond et al., 2012). A highly conserved NES is also found at the C-terminal of HTT and is essential for nucleo-cytoplasmic shuttling (Xia et al., 2003). The biophysical characterisation of a full-length HTT structure suggests an elongated superhelical solenoid with a diameter of ~200 Å (Li et al., 2006).

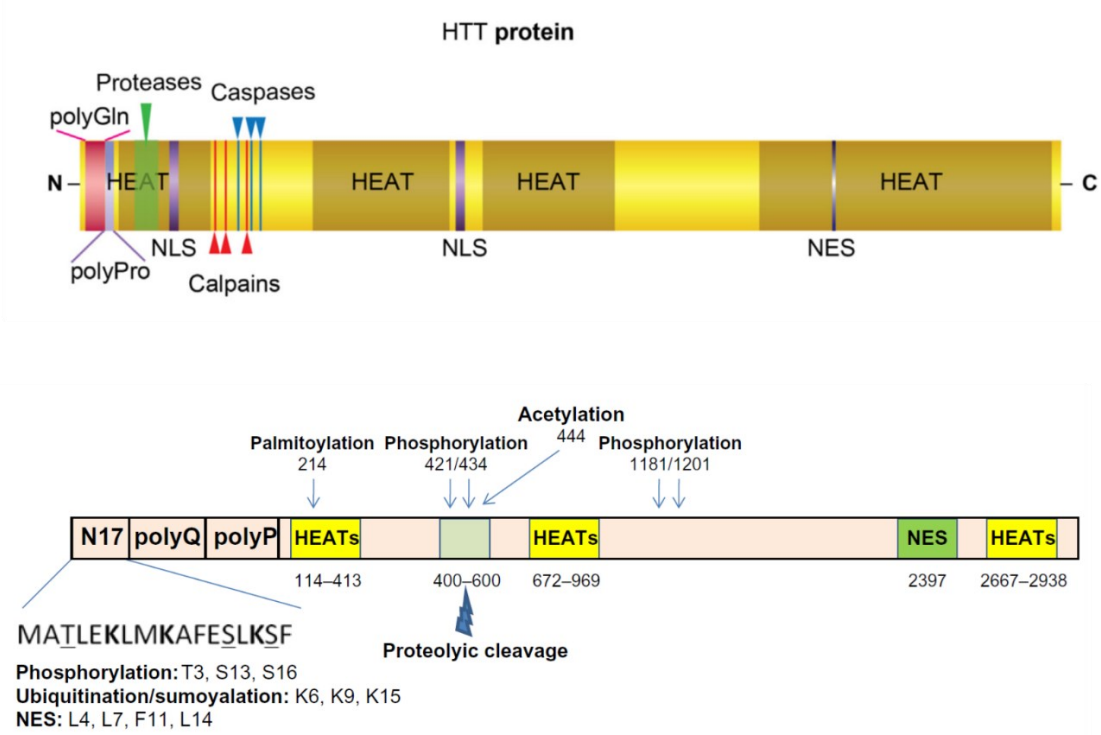

Fig 1. 3 Schematics of the HTT protein.

A full-length HTT protein showing the various domains, including the seventeen amino acids at the N-terminal (N17), the polyQ or polyGln stretch, the poly proline (polyP) or the proline-rich domain (PRD), and the HEAT repeats. Some of the proteolysis sites, the NLS and NES regions (top) and post-translational modification sites (bottom) are also shown. (Figure Sources Top (Déglon, 2017); Bottom (Zheng and Diamond, 2012)).

1.1.4.3 Post-translational modifications of Huntingtin

Post-translational modifications (PTMs) of HTT play a critical role in HD pathogenesis. Most of these modifications have been studied for pathogenic HTT. They alter HTT's intra-cellular localisation and transport, function, stability, degradation, ability to aggregate, toxicity and interactions with other proteins (Saudou and Humbert, 2016). For example, polyQ expansion in HTT leads to dysregulated HTT PTMs (and that of other associated effector proteins), altering function (for HTT, both loss-of-function, LOF and gain-of-function, GOF) and perturbing cellular homeostasis (HD-induced PTM disruptions of effector proteins and its effects on cellular physiology are reviewed in (Lontay et al., 2020)).

HTT undergoes phosphorylation at several Ser residues and some Tyr and Thr residues along the length of the protein (by kinases like Akt, ERK1, IKK, Cdk5 and Nemo-like kinase (NLK) and dephosphorylated by Ser/Thr phosphatases PP1 and PP2A), ubiquitination (by ubiquitin ligase E2-25K and E3ligases like Ube3a, Skp1-Cul1-F-box, Parkin, and CHIP (C terminal Hsp70 interacting protein)) and sumoylation at three N-terminal Lys residues (by E3 ligase Rhes (Ras homolog enriched in the striatum)), palmitoylation at an N-terminal Cys residue (by palmitoyl transferases HIP14 and HIP14L) and acetylation at a few Lys residues towards the N-terminal end (cAMP Response Element Binding Protein or CBP is the acetyltransferase and histone deacetylase 1 or HDAC1 the deacetylase) (Ehrnhoefer et al., 2011; Schulte and Littleton, 2011; Saudou and Humbert, 2016; Lontay et al., 2020). These PTMs have variable disease consequences: phosphorylation, acetylation, ubiquitination, and palmitoylation of expHTT are all generally neuroprotective, whereas SUMOylation is detrimental; phosphorylation decreases expHTT aggregation, and acetylation decreased fibril formation (Ehrnhoefer et al., 2011; Lontay et al., 2020; Schaffert and Carter, 2020; Johnson et al., 2022). HTT phosphorylation is critical for BDNF vesicular transport and targets HTT to proteasomal turnover, and a decline in phosphorylation is linked to excitotoxicity (Colin et al., 2008; Thompson et al., 2009; Metzler et al., 2010; Jiang et al., 2020). Acetylation targets HTT to autosomal degradation (Jeong et al., 2009) and ubiquitination to degradation via proteasome and chaperone-assisted selective autophagy (Kalchman et al., 1996; Bjørkøy et al., 2005; Jana and Nukina, 2005). Palmitoylation

is vital for its normal trafficking to Golgi and folding (Yanai et al., 2006), SUMOylation is associated with its nuclear entry and transcriptional disruption (Steffan et al., 2004), and myristoylation of wildtype (WT) HTT at Gly553 promotes autophagosome formation (Martin et al., 2014).

***Proteolysis of Huntingtin*:** HTT undergoes proteolysis at multiple sites defined by PEST domains (Warby et al., 2008) by multiple proteases such as caspases, calpain, cathepsins, endopeptidases and matrix metalloproteinase 10 (MMP 10) (Ehrnhoefer et al., 2011; Saudou and Humbert, 2016; van der Bent et al., 2022). Both wild-type and expanded HTT are substrates for proteolytic cleavage *in vitro*, but expHTT is subjected to selective proteolysis by many proteases and preferentially cleaved (Goldberg et al., 1996; Lunkes and Mandel, 1998; Wellington et al., 1998; Landles et al., 2010; Kim et al., 2021a). In HD, there is an increase in protease activity and proteolysis of expHTT leads to a critical pathogenic event: generation and cytoplasmic accumulation of toxic N-terminal (N-T) fragments containing the expanded polyQ stretch, their translocation into the nucleus, followed by nuclear accumulation and toxicity (Benn et al., 2005; Graham et al., 2006; Wang et al., 2008; Ghosh and Tabrizi, 2018a; van der Bent et al., 2022). HTT fragments with normal-length polyQ mainly localise at the cytoplasm without forming aggregates or inducing toxicity (Xu and Wu, 2015). However, studies suggest that nuclear localisation is not a prerequisite for toxicity (Hackam et al., 1999; Trushina et al., 2003). HTT fragments containing expanded polyQ show an inverse relation with fragment length: the shorter the HTTexon1 (HTTex1) fragment, the higher its aggregation propensity (level and rate), amyloid seeding ability, the likelihood of nuclear translocation and toxicity (Barbaro et al., 2015). Toxic C-terminal non-polyQ fragments generated upon both WT and expHTT proteolysis disrupt dynamin-1 activity, leading to ER stress and cell death (El-Daher et al., 2015). This finding and the lack of evidence for cleavage of WT HTT in healthy individuals suggests that proteolysis of WT HTT can lead to its loss-of-function (Saudou and Humbert, 2016; Caterino et al., 2018). On the other hand, proteolysis of expHTT leads to gain-of-toxic functions like interfering with transcription, autophagy, and ER homeostasis (Saudou and Humbert, 2016). The incomplete

splicing also generates the pathogenic N-T fragments and premature polyadenylation of *expHTTexon1* RNA, translating to a short toxic protein (Sathasivam et al., 2013; Neueder et al., 2017). expHTT RNA fragments also sequester splicing components, dysregulating splicing mechanisms (Lin et al., 2016; Schilling et al., 2019).

1.1.4.4 HTT partners

Both WT and expHTT interact with a plethora of proteins (the recent count is ~3000 proteins) involved in diverse cellular activities, including gene expression (transcription, RNA processing, epigenetic regulation, translation), protein stability, activity, localisation, and interactions (PTMs, proteases), signal transduction, proteostasis (protein folding, proteasomal and autophagic degradation pathways), mitochondrial function, Ca^{2+} signalling and bioenergetics, cellular dynamics (cytoskeletal network, vesicular trafficking and endocytosis), synaptic transmission, metabolism, stress response and cell death (Kaltenbach et al., 2007; Culver et al., 2012; Shirasaki et al., 2012; Tourette et al., 2014; Yao et al., 2014; Greco et al., 2022; Podvin et al., 2022). PolyQ expansion in HTT leads to alterations in protein-protein interactions involving HTT, resulting in various functional consequences contributing to disease physiology (Ratovitski et al., 2012; Wanker et al., 2019; Podvin et al., 2022). The wide interactome of HTT is consistent with its scaffolding function owing to its large size, stability and the presence of protein-interaction domains like PRD and HEAT, serving as a hub that tethers various molecules into a large protein assembly to coordinate cellular processes (Saudou and Humbert, 2016). The dynamics of HTT interactome are influenced by several factors, including the polyQ expansion and length, HTT protein length, HTT proteolysis, PTMs and fragment length, conformer type, subcellular localisation, cell/tissue/neuron type, brain region, and age; many of these are differently altered in HD contributing to cellular dysfunction (Shirasaki et al., 2012; Sap et al., 2021; Greco et al., 2022; Kennedy et al., 2022; Seefelder et al., 2022; Xu et al., 2023). The HTT interactome is now curated in a web-based platform called HTT-OMNI (HTT OMics and Network Integration) (Kennedy et al., 2022), and the proteomic profiling in HD models and patients is also extensively reviewed (Seeley and Kegel-Gleason, 2021).

1.2 HUNTINGTIN: FROM FUNCTION TO DYSFUNCTION AND NEW "TOXIC" FUNCTIONS

1.2.1 Huntington's disease: GOF or LOF

HD is a dominantly inherited disease, and three mechanisms by which expanded polyQ affects HTT and causes pathogenicity have been proposed: (1) Haploinsufficiency—a single copy of WT gene produces insufficient protein leading to HD symptoms (2) A dominant negative effect leading to loss-of-function (LOF) of WT protein: the mutant HTT prevents the functioning of the WT protein, especially when acting as a multimer (3) Toxic gain-of-function (GOF) by mutant HTT. Haploinsufficiency cannot explain the disease as a patient with only one functional *Htt* did not develop HD (Ambrose et al., 1994). Many studies support the GOF hypothesis, but evidence for LOF of WT HTT contributing to HD is also gaining traction (Cattaneo et al., 2005; Bates et al., 2014). Though rare, HD homozygotes exhibit disease progression that is more severe than heterozygotes (Squitieri et al., 2003). Like other triplet-repeat-expansion diseases, HD is not a true-dominant disease, and GOF only explains some disease features (Reiner et al., 2011).

1.2.2 LOF in HD: Native functions of HTT

The loss of WT HTT contributing to HD is evident from the involvement of HTT in multiple cellular functions, as briefly discussed below (reviewed in (Schulte and Littleton, 2011; Saudou and Humbert, 2016; Liu and Zeitlin, 2017)). Further, over-expression of WT HTT improves neuronal survival under specific stresses; in an HD background, increasing WT HTT expression alleviates some HD effects while decreasing the WT levels exacerbates them (Cattaneo et al., 2005).

***Embryonic development, neurogenesis, and cell division*:** Developmental impairments due to WT HTT's LOF are critical to HD pathogenesis (Mehler et al., 2019). Huntingtin is essential for embryonic development as huntingtin-knockout mice (*Hdh–/–*) die before gastrulation (Duyao et al., 1995; Nasir et al., 1995; Zeitlin et al., 1995; Dragatsis et al., 1998). *Hdh+/–* heterozygote

mice usually develop but, as adults, show neuronal, behavioural, and cognitive deficits, suggesting a role for WT HTT as adults (Duyao et al., 1995; Nasir et al., 1995; Zeitlin et al., 1995). HTT and its levels are also critical for neuronal development, where it has a region-specific differential role (White et al., 1997; Dragatsis et al., 2000; Auerbach et al., 2001; Reiner et al., 2003). Given normal development in HD, mutant HTT seems to retain WT functions during development (Wexler et al., 1987; Myers et al., 1989; Leavitt et al., 2001; Van Raamsdonk et al., 2005). HTT, associated with centrioles of dividing cells, is crucial for mitosis and, as a result, for neuronal differentiation and determining neural progenitor fate (Godin et al., 2010; Godin and Humbert, 2011). Many studies support WT LOF during development as a significant contributor to HD pathology in adults and lend credence to recognising HD as a neurodevelopmental disorder (Arteaga-Bracho et al., 2016; Mehler et al., 2019).

BDNF: The striatum depends on a brain-derived neurotrophic factor (BDNF) for its development, function and survival, and its supply is from cortical neuronal efferents (Altar et al., 1997; Baquet et al., 2004; Liot et al., 2013; Baydyuk and Xu, 2014). WT HTT promotes BDNF mRNA transcription in cortical neurons (Zuccato et al., 2001; Zuccato et al., 2003), transport of BDNF vesicles along microtubules (Gauthier et al., 2004) and retrograde transport of BDNF receptor TrkB (tropomyosin receptor kinase B) along striatal dendrites (Cohen et al., 2011; Liot et al., 2013).

In ciliogenesis: HTT is important for the transport of PCM1 (pericentriolar material 1) to centrosomes in mediating ciliogenesis (Keryer et al., 2011; Haremaki et al., 2015).

In axonal transport- HTT is a scaffolding protein essential for cellular trafficking (Jimenez-Sanchez et al., 2017; Gatto et al., 2020), as discussed below.

***Vesicular and organelle trafficking*:** HTT helps in the microtubule-based transport of organelles and vesicles containing a variety of cargo in both anterograde and retrograde directions (Li et al., 1995; Block-Galarza et al., 1997; Engelender et al., 1997; Li et al., 1999; McGuire et al., 2006; Caviston et al., 2007). The cargo includes synaptic precursor, v-SNARE VAMP7 protein, BDNF, amyloid precursor protein (APP), GABA-receptor, TrkA and organelles, including lysosomes,

autophagosomes, endosomes and mitochondria (Schulte and Littleton, 2011; Saudou and Humbert, 2016). HTT also scaffolds GAPDH (Glyceraldehyde 3-phosphate dehydrogenase) onto vesicles, which is crucial for the local energy supply via vesicular glycolysis to transport fast-moving vesicles within axons (Zala et al., 2013b). HTT is also implicated in the transport of vesicles from ER to Golgi (Brandstaetter et al., 2014).

***Endocytosis, vesicle recycling, and endosomal trafficking*:** HTT is involved in clathrin-mediated endocytosis in association with HIP1 and HIP12 (Sittler et al., 1998; Rao et al., 2001; Waelter et al., 2001), vesicle recycling in association with Rab11 (Li et al., 2008b; Power et al., 2012; Elias et al., 2015), F-actin-based endosomal trafficking in association with HAP40 and Rab5 (Pal et al., 2006).

***Transcription and post-transcriptional gene regulation*:** HTT functions as a transcription regulator in association with transcriptional factors like CBP and the tumour suppressor protein 53 (p53) (Steffan et al., 2000), the nuclear factor-kB (NF-kB) (Takano and Gusella, 2002), activators like CA150 (Holbert et al., 2001) and repressors like REST/NRSF (Repressor element-1 silencing transcription factor/ Neuron-restrictive silencer factor) (Zuccato et al., 2003). It regulates gene expression of various cellular pathways and modulates transcription during early embryogenesis and of nuclear receptors (Zuccato et al., 2003; Futter et al., 2009; Seong et al., 2010). HTT also participates in post-transcriptional modifications like Processing body (P-body) formation, RNA transport, and RNA translation via its association with Argonaut 2 (Ago2) and RNA binding proteins (Savas et al., 2008; Culver et al., 2012).

***Synaptogenesis and synaptic plasticity*:** HTT is essential for developing excitatory synapses (McKinstry et al., 2014) and long-term-learning-related synaptic plasticity (Choi et al., 2014).

***Cell signalling*:** HTT interacts with proteins of signal transduction cascades (Liu et al., 1997b; Saudou and Humbert, 2016).

***Cell stress response and cell death*:** HTT is anti-apoptotic by blocking the activation of caspase-3, caspase-8 and caspase-9 and the formation of the apoptosome (Rigamonti et al., 2000;

Rigamonti et al., 2001; Gervais et al., 2002), acts as a ROS sensor (DiGiovanni et al., 2016) and mediates cellular stress response (Munsie and Truant, 2012; Nath et al., 2015).

***Selective macroautophagy*:** HTT has LC3-interacting repeats (LIRs) and serves as a scaffold for various autophagic proteins (Ochaba et al., 2014). It contributes to cargo recognition, loading of ubiquitinylated proteins into autophagosomes and initiation of selective macroautophagy via interactions with the cargo adaptor p62 and the autophagy initiation kinase ULK1 (Unc-51 like kinase-1) (Rui et al., 2015). In association with HAP1, it facilitates autophagosome transport to the lysosome, thereby helping in the degradation of autophagosome content and retrograde transport of autophagosomes (Wong and Holzbaur, 2014). Normal-length polyQ domain interacts with Beclin-1, an autophagy initiator and prevents its proteasomal degradation, promoting autophagy (Ashkenazi et al., 2017).

***DNA damage repair*:** HTT localises at sites of DNA damage in the nucleus and participates in base excision repair (Maiuri et al., 2017).

Given the physiological significance of WT HTT in various cellular processes, treatments that reduce activity or levels of HTT need to be specific to expHTT. Such therapies also need to consider unintended neurological and developmental consequences as expHTT suffices to fulfil the developmental roles of WT HTT (see above). Reducing WT HTT makes CNS more sensitive to the neurotoxic effects of expHTT (Auerbach et al., 2001). These studies also highlight the confounding physiological effects of the therapeutic elimination of Huntingtin in HD patients. Thus, treatment strategies should not only aim to suppress the toxic effects of expHTT but also improve the activity of WT HTT.

1.2.3 GOF in HD: Toxic non-native interactions of the mutant protein

The polyQ expansion in the HTT endows it with new toxic functions often unrelated to normal HTT function and are critical for HD pathogenesis (Broadley and Hartl, 2009; Zuccato and Cattaneo, 2009; Finkbeiner, 2011). This newly gained cytotoxicity of mutant HTT protein modifies both HTT function and that of its interacting partners, harming cellular health and integrity through its aberrant intra-protein and inter-protein interactions (homotypic and heterotypic) (Wanker et al., 2019). Some structural and physiological consequences of polyQ expansion in HTT, the resulting aggregation and their role in the gain-of-function toxicity are discussed below.

1.2.3.1 Expanded HTT conformation and aggregation

Full-length WT HTT in complex with HAP40 was revealed via cryo-electron microscopy to be predominantly a folded α-helical protein. This conformationally flexible multivalent hub is stabilised by binding with its interacting protein partners (Guo et al., 2018b).

***Heterogeneity in expHTT conformation and aggregation*:** expHTT is found in many conformationally distinct forms *in vivo* and *in vitro*: monomers, oligomers, proto-fibrils, and fibrils of full-length expHTT and a variety of truncated N-terminal (N-T) species (Wanker et al., 2019). The polyQ containing N-T fragment is a highly flexible and intrinsically disordered peptide (Kim et al., 2009; Giorgini, 2013; Baias et al., 2017). The N-T expHTT species self-associate, assembling into higher-order structures like spherical oligomers or amyloid fibrils *in vitro* and *in vivo* that are broadly referred to as aggregates (Sathasivam et al., 2010; Sahoo et al., 2016; Wagner et al., 2018). This complex self-association landscape of N-T expHTT involves distinct aggregation pathways featuring many intermediate species that can interconvert and differ in their neurotoxicity and lifetimes (Nekooki-Machida et al., 2009; André et al., 2013; Boatz et al., 2020). The repertoire of HTTex1 species includes monomers, dimers and tetramers (Sahoo et al., 2016), spherical oligomers (Poirier et al., 2002), isolated nanofibrils (Sahl et al., 2016; Sahoo et al., 2016), clusters of mature fibrils (Scherzinger et al., 1997) and fibril-rich inclusions

(DiFiglia et al., 1997; Bäuerlein et al., 2017). Structural and conformer polymorphism of the same primary structure is a common feature of amyloidogenic proteins (Tycko, 2015).

Oligomers are typically small protein aggregates (1-15nm) with globular morphology; they can also be aggregates wide-ranging in size (small multimers (dimers, trimers to decamers) to large structures of >100 proteins) and shape (non-fibrillar and proto-fibrillar species) (Adegbuyiro et al., 2017; Hipp et al., 2019b). The **expHTT fibrils** are long rod-like filamentous, amyloid-like structures (Boatz et al., 2020) (Fig 1.4). expHTT fibrils derived from artificial systems comprise a tightly packed, rigid and dehydrated core of polyQ regions in anti-parallel β-sheet arrangement flanked by N-T and C-T domains (Fig 1.4b) (Sharma et al., 2005; Sivanandam et al., 2011; Hoop et al., 2016; Wagner et al., 2018; Boatz et al., 2020) that are themselves polymorphic (Tycko, 2015; Caulkins et al., 2018). In contrast, the misfolded N-T monomers and oligomers likely assume random coil or α-helical conformation *in vivo* with polyQ tracts exposed on the surface (Kang et al., 2017; Wagner et al., 2018; Kotler et al., 2019). In the aggregation mechanism, in addition to the on-pathway wherein expHTT intermediates lead directly to fibril formation, there are also **off-pathway expHTT aggregates** like **annular aggregates** (ring-shaped aggregates made of oligomers or protofibrils) and **amorphous aggregates** (non-filamentous globular aggregates, granular in appearance, rich in β structure, lacking long-range order and larger than oligomers) that do not lead to fibril formation (Adegbuyiro et al., 2017). **Inclusion bodies (IBs)** are typically large (several microns in size), insoluble, mostly spherical protein deposits of accumulated aggregated material (fibrils, amorphous aggregates, and other species) that are easily visible by light microscopy (Adegbuyiro et al., 2017; Bäuerlein et al., 2020). IBs of expHTT from primary mouse neurons and HeLa cells are mostly made up of amyloid fibrils (Bäuerlein et al., 2017). In contrast, those from *S. cerevisiae* are also amorphous (Gruber et al., 2018). These distinct structural and morphological features confer distinct biochemical properties and interaction profiles to insoluble expHTT fibrils and IBs compared to soluble expHTT oligomers, monomers, and other reactive intermediate species (Wanker et al., 2019).

Various factors influence the nature and conformation of expHTT intermediates and aggregates, the kinetics and outcome of the aggregation pathway, conformer stability and toxic potential. These include the sample preparation method, environmental factors like pH and temperature, mechanical factors like shear and agitation, specific solvents and surfaces, presence of membranes, polyQ length and concentration, the cell models used, *in vitro vs. in vivo* models and the cellular context (intra- or extra-cellular, cell-type, subcellular localisation and compartmentalisation), the presence of other polyQ-containing proteins, intrinsically disordered proteins and seeding-competent species, and the HTT interactome (Kampinga and Bergink, 2016; Adegbuyiro et al., 2017; Bäuerlein et al., 2020; Boatz et al., 2020; Riguet et al., 2021).

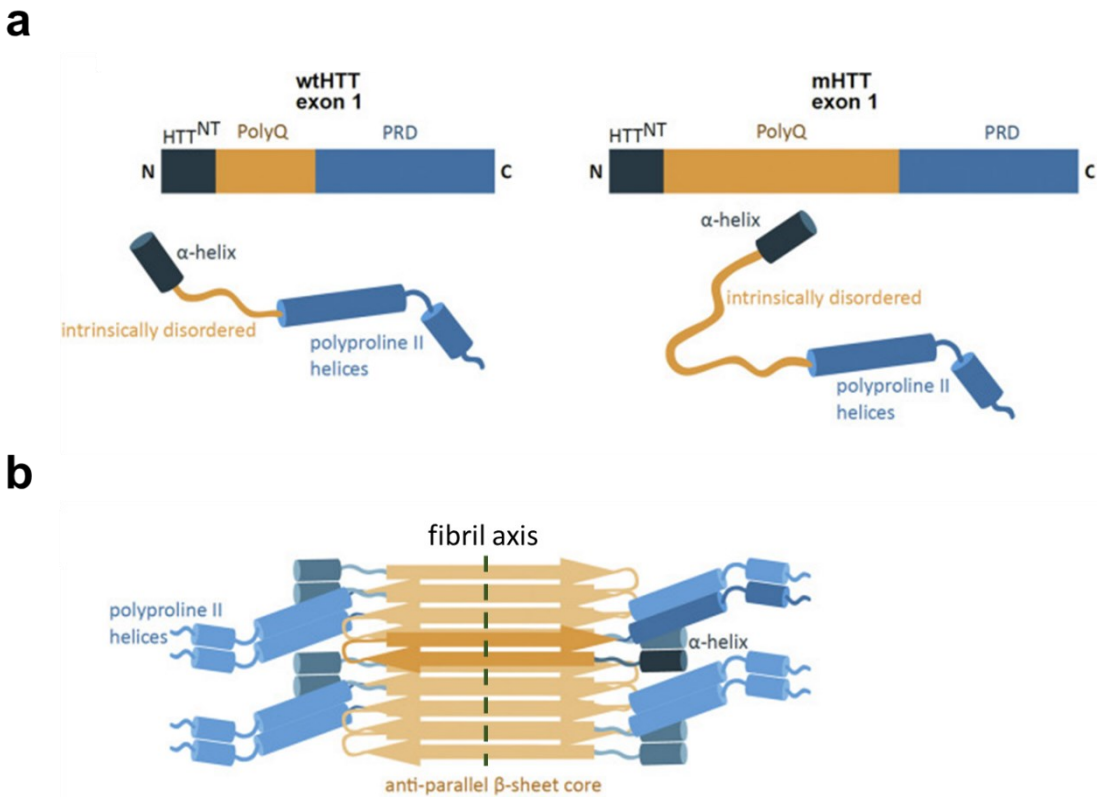

Fig 1. 4 Structures of HTTexon 1 and expHTTexon1 fibril.
(a) Schematic of primary (top) and secondary structure (bottom) of HTTexon1 of WT HTT (left) and mutated HTT with the expanded polyQ (right) showing the N17aa, polyQ domain and proline-rich domain (PRD). (b) Mutant HTT (mHTT) exon 1 HTT fibril architecture. Amyloid fibrils are characterized by cross-β-sheet architecture in which anti-parallel β-sheet structures run perpendicular to the long fibril axis (Chiti and Dobson, 2017) and flanking HTT-NT (dark blue) and PRD domains (blue) overhang at the sides of the fibril. A single monomer is highlighted in darker colours (figure from (Jarosińska and Rüdiger, 2021)).

***From N-T expHTT fragments to fibrils*:** A nucleated growth mechanism has been proposed for the conversion of N-T expHTT fragments into fibrils: an initial rate-limiting step of spontaneous but rare and slow primary nucleation event (lag phase) followed by an exponential elongation or growth phase (log phase) (Arndt et al., 2015; Wagner et al., 2018; Wanker et al., 2019; Wetzel, 2020). Two competing events can mediate the initial nucleation. The first is a complex two-step nucleation pathway involving the formation of **oligomeric intermediates** (dimers, tetramers and α-helix-rich oligomers) undergoing an energetically unfavourable **conformational change** to a stable β-sheet structure, followed by the formation of **aggregation-competent nuclei** *de novo* (new non-fibrillar or fibrillar oligomers). The second is an inefficient, albeit simple classical nucleation pathway of formation of a thermodynamically unfavourable **monomeric** amyloid **nucleus** by re-arranging a soluble monomer (intramolecular transition from random coil to random coil to β-sheet), a concentration-dependent event. The slow nucleation event is then followed by the rapid growth of the fibril nuclei by recruiting new monomers to form large, highly stable β-sheet-rich structures with a fibrillary morphology. There is little clarity on the exact nature of expHTT conformers initiating the aggregation pathway (monomers or small oligomers) and those functioning as "nuclei" (monomers, small oligomers, small metastable oligomers, large stable oligomers). The lag phase can be bypassed by pre-existing "nuclei", such as fibril fragments and preformed fibrils bound by free monomers or multimers promoting elongation (Chiti and Dobson, 2017). In addition, the elongating expHTT fibril can induce a fast secondary nucleation event: nucleated fibril branching, i.e., growth of new branches from the surface of existing fibrils and formation of highly complex fibrillary aggregates with multiple ends (Wagner et al., 2018). Branched fibrils seem unique to expHTT aggregation, not observed in other aggregate-prone NDs.

The polyQ domain in monomeric HTT seems conformationally disordered and compact, irrespective of its length (Hoffner and Djian, 2014). It can transiently adopt different conformations: random coil, extended loop, α-helix (near the N-terminal domain), or a β-sheet (in expHTT aggregates) (Kim et al., 2009; Boatz et al., 2020; Urbanek et al., 2020). Its aggregation kinetics and final morphology are influenced by its flanking sequences: the preceding

amphipathic α-helical N-terminal 17 amino acids (N17) promotes whereas the following C-terminally located PRD decreases the propensity of expHTT aggregation (Bhattacharyya et al., 2006; Thakur et al., 2009; Crick et al., 2013; Shen et al., 2016). A simple model for expHTT aggregation initiated by the spontaneous homotypic interaction of multiple N17 domains resulting in the formation of α-helix rich oligomers that bring polyQ stretches from different fragments into proximity, enhancing polyQ-polyQ interactions, facilitating the coil-to-β sheet transition, constituting the lag phase, has been proposed (Arndt et al., 2015; Caterino et al., 2018; Wanker et al., 2019; Jarosińska and Rüdiger, 2021).

1.2.3.2 The toxic species in HD: small soluble oligomers *vs.* large insoluble aggregates

The first issue with this question is the lack of clear definitions for each category and classification regarding which entities fall into which category based on size, composition, or visibility. Secondly, this issue primarily arises from the vast spectrum of expHTT conformers. Third, the various expHTT aggregate conformers *in vivo* are likely heterogenic or made of more than one conformer type and a mix of soluble and insoluble species (Sahl et al., 2012; Duim et al., 2014). However, suppose one were to assume that broadly, two classes of expHTT forms exist *in vivo*: the relatively more minor, soluble, oligomeric class and the more prominent, insoluble inclusions. Their differential contribution to HD toxicity is highly variable and under intense debate, as detailed below.

Large insoluble aggregates in HD: Are they toxic or protective? There is evidence for both scenarios. Given the sheer size of inclusions they physically block intracellular functions like axonal transport; trap proteins with glutamine-rich domains and intrinsically disordered regions and critical cellular proteins: components of the degradation and protein quality control systems (chaperones, proteins, ubiquitin and 26S proteasome components, thereby interfering with cellular proteostasis), neuronal proteins, RNA-binding proteins, and WT HTT (secondary LOF), TFs (CBP, TBP, SP1) (transcriptional deregulation); distort chromatin; interact with organelles and cellular membranes: interact with ER, trap ER vesicles, disrupt ER morphology and

dynamics, inducing ER stress, disrupt nuclear envelope, nucleocytoplasmic transport and activate neuronal cell cycle, permeabilize lipid vesicles and disrupt membrane lipid bilayer integrity, alter Ca^{2+} homeostasis, deregulate mitochondrial respiration and morphology; show prion-like features of transmitting between cells: infecting naive cells that do not express expHTT or show aggregation, provide neighbouring cells with aggregation-competent seeds to nucleate aggregation of WT HTT and other polyQ containing proteins (cross-seeding) (Chen et al., 2001; Nucifora et al., 2001; Suhr et al., 2001; Waelter et al., 2001; Gunawardena et al., 2003; Lee et al., 2004; Pieri et al., 2012; Burke et al., 2013b; Costanzo et al., 2013; Liu et al., 2015a; Wear et al., 2015; Kim et al., 2016; Li et al., 2016; Woerner et al., 2016; Bäuerlein et al., 2017; Gasset-Rosa et al., 2017; Hosp et al., 2017; Isas et al., 2017; Trajkovic et al., 2017; Ast et al., 2018; Drombosky et al., 2018; Masnata et al., 2019; Sameni et al., 2020; Wetzel, 2020; Riguet et al., 2021). On the other hand, there is evidence that expHTT inclusions do not correlate with toxicity; soluble oligomeric species are the toxic species in HD and their sequestration into larger aggregates (fibrillar and amorphous) and IB formation, a protective mechanism to minimise the toxic effects of soluble expHTT conformers (oligomers and even monomers) by reducing their surface-to-volume ratio and shielding reactive surfaces (Saudou et al., 1998; Gutekunst et al., 1999; Kuemmerle et al., 1999; Arrasate et al., 2004; Bodner et al., 2006; Diaz-Hernandez et al., 2006; Nagai et al., 2007; Takahashi et al., 2008; Miller et al., 2010a; Sun et al., 2015; Branco-Santos et al., 2017; Ramdzan et al., 2017). Toxic effects of soluble oligomers include perturbation of critical cellular processes by interacting with about 800 different proteins involved in energy metabolism and mitochondrial function, protein and vesicle trafficking, RNA processing, ribosome biogenesis and transcription, dampened CREB signalling, increased ROS, induction of ER stress and apoptosis (Schaffar et al., 2004; Leitman et al., 2013; Kim et al., 2016; Moily et al., 2017; Ramdzan et al., 2017). So, even though the formation of large insoluble cellular deposits might start as a protective mechanism, cells with IBs enter quiescence that transiently prolongs survival, but, in the long run, these deposits sequester other crucial proteins, disrupting cellular homeostasis and cellular functionality, becoming detrimental (Ramdzan et al., 2017; Soares et al., 2019). One possible way around this debate is to look at the process of aggregation as an effort

by the cell to restore proteostasis during which various intermediate species and aggregate forms of expHTT are generated, and their differential toxicity is incidental, depending on the context. It is evident from the above studies that both the soluble and insoluble and the small oligomeric and the larger inclusion species are all disease-relevant, contributing to neurotoxicity, depending on the age, disease stage, presence of modifying factors and cellular prowess.

1.2.3.3 How does polyQ expansion render HTT toxic?

Polymerised polyQ adopts a β-sheet enriched structure in multimeric aggregates. However, it is unclear whether the transition to β-sheet conformation happens first, followed by polyQ polymerization or whether oligomerization of the polyQ leads to conformational change (Hoffner and Djian, 2015). There are conflicting reports about the effect of polyQ expansion on the secondary structure of expHTT: some studies show no significant structural differences between monomeric WT HTT and expHTT (Chen et al., 2001; Klein et al., 2007; Warner et al., 2017; Newcombe et al., 2018; Huang et al., 2021); whereas others support a polyQ-length-dependent change in monomeric conformation of expHTT (e.g. extended conformation to collapsed state and compaction or random-coil to α-helical state or formation of stable intramolecular β-hairpins or rich in amyloid-like structures) (Nagai et al., 2007; Walters and Murphy, 2009; Kar et al., 2011; Peters-Libeu et al., 2012; Kar et al., 2013; Perevozchikova et al., 2014; Monsellier et al., 2015; Daldin et al., 2017; Bravo-Arredondo et al., 2018). The former group of studies suggest an increase in the overall size and surface area of the globular polyQ domain accompanying the polyQ expansion, increasing the binding sites and promoting non-native and toxic gain-of-function interactions, ultimately triggering HTTex1 aggregation. Despite the differences, the consensus from different studies is that polyQ expansion favours HTTex1 aggregation. polyQ expansion can increase aggregation probability by affecting the kinetics and flux of nucleation-growth polymerization in many ways: decreasing the size of the critical nucleus and (or) the protein concentration required to trigger fibril assembly, enhancing the generation of spherical oligomers and the rate of nucleation of the amyloid and elongation of the nuclei and fibrils (Bhattacharyya et al., 2006; Rossetti et al., 2008; Thakur et al., 2009; Monsellier et al., 2015;

Sahoo et al., 2016; Caterino et al., 2018; Drombosky et al., 2018; Pandey et al., 2018; Silva et al., 2018). Other effects of the elongation of the polyQ tract in HTT ex1 are increasing its β-sheet propensity (Kang et al., 2017; Priya and Gromiha, 2019) and polyQ compactness, thereby reducing polyQ's conformational flexibility and reducing N17-PRD's interactions (Caron et al., 2013; Kang et al., 2017; Bravo-Arredondo et al., 2018), reducing solubility (Fiumara et al., 2010), altering its PTMs (Warby et al., 2005; Yanai et al., 2006), proteolytic cleavage (El-Daher et al., 2015), and interactions with lipid membranes (Burke et al., 2013a).

1.2.3.4 Aggregates under the spotlight in this study- the expHTT "inclusions."

In literature, a wide variety of expHTT conformers have been termed as 'aggregates' inconsistently and often ambiguously (irrespective of their solubility, order and stability, shape, ultrastructure- granular *vs* fibrillar, type of bonding, polymerisation and interactions), not excluding small, soluble, oligomeric aggregates, large oligomers, amorphous conformations, amyloids and large insoluble IBs (Finkbeiner, 2011; Adegbuyiro et al., 2017; Bäuerlein et al., 2020), thereby creating much confusion regarding the nature of aggregates and their role in HD pathology. In this study, the clumped puncta-like structures of expHTT visible via light microscopy are the aggregates species of focus, and they are referred to as "inclusions" (Inc). Moreover, the non-punctate, evenly distributed appearance of intracellular HTT is referred to as "diffuse" (Diff). As suggested by Finkbeiner et al. (2011) (Finkbeiner, 2011), naming the cellular deposits visualized via light microscopy as inclusions is inclusive as there are no assumptions regarding their polymeric state (monomers, dimers, or oligomers), their ultrastructure (fibrillar or amorphous aggregates) or their solubility (SDS- soluble or -insoluble).

1.2.3.5 Pathological mechanisms underlying HD

A diverse range of mutually non-exclusive molecular and cellular pathways underlie HD pathology, destabilizing the transcriptome, epigenome, proteome and metabolome. Many of these interact and feed-forward onto one another, creating a complex network of pathophysiological events. This section details some critical molecular, cellular, and neuronal impairments attributed to HD (Fig 1.5). Given their focal importance in this study, I have emphasised impaired proteostasis and the role of molecular chaperones in HD in greater detail.

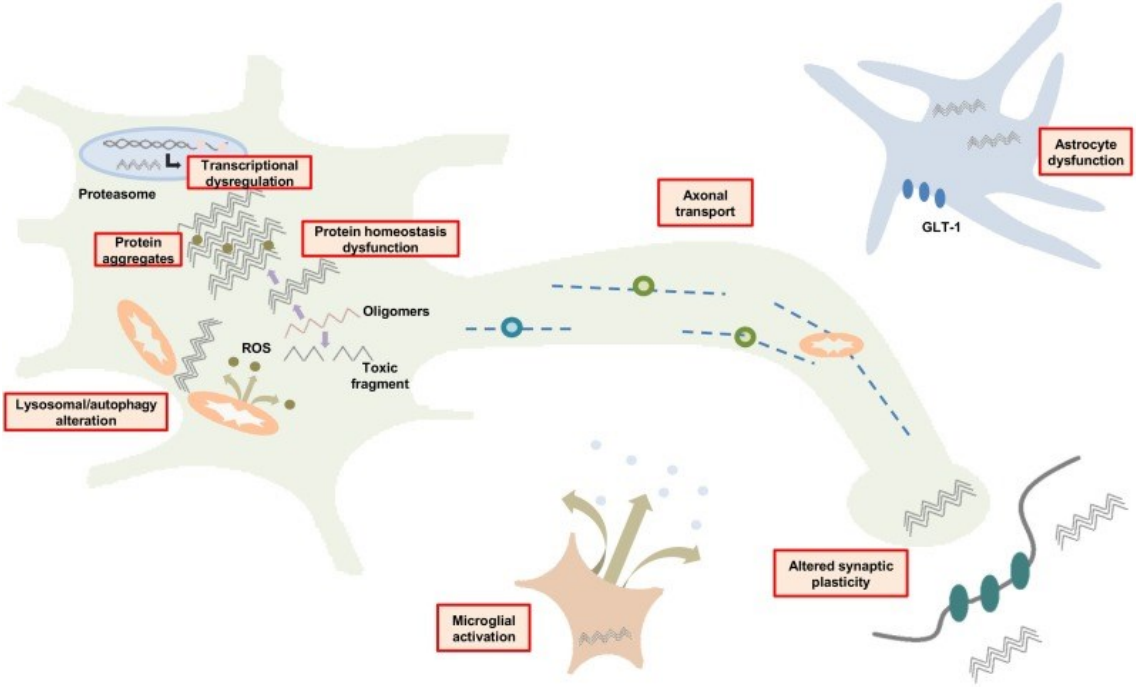

Fig 1. 5 A schematic showing some of the neuropathological mechanisms in HD.
These and several other mechanisms are discussed in the text (Figure from (Gatto et al., 2020)).

***Axonal transport, neurotransmission, and synaptic activity deficits*:** Neuronal and synaptic defects are early pathological occurrences in HD (Jimenez-Sanchez et al., 2017; Smith-Dijak et al., 2019). These include deficits in basal synaptic transmission, intrinsic excitability, processes modulating synaptic strength, and neuronal dysfunction and death due to loss of trophic support and excitotoxicity. There is transcriptional deregulation and altered synthesis, transport, release, activity and signalling of neurotransmitters like dopamine (DA), glutamate, acetylcholine, serotonin, GABA, and adenosine and their receptors and synaptic proteins like post-synaptic

density 95 (PSD-95), cysteine-string protein (CSP), complexin II, synapsin I, adaptor protein 2 (AP-2) and HAP1 (Zuccato and Cattaneo, 2014; Tyebji and Hannan, 2017; Smith-Dijak et al., 2019). Loss of WT HTT function in mediating exocytosis and endocytosis also contributes to altered synaptic activity (Zuccato et al., 2010). expHTT causes axonal transport defects in the transport of proteins and organelles along axons either by aggregates physically blocking axons (Li et al., 2001; Lee et al., 2004) or sequestering motor proteins or due to loss of WT HTT function (Gunawardena et al., 2003; Trushina et al., 2004). Neurotrophins like BDNF, which promote neuronal survival and are essential for synaptic plasticity, are decreased in HD brains, partly due to loss of WT-HTT function, as previously described. However, expHTT also contributes to defective BDNF signalling, altering the promotor-specificity of BDNF transcription and indirectly by affecting the activity of TFs, impairing HAP1 function, and reducing microtubule-mediated BDNF vesicle delivery, causing an imbalance in levels of BDNF receptors, namely, the pro-survival TrkB and pro-apoptotic and pro-inflammatory $p75^{NTR}$ and impairing astrocytic BDNF release (Zuccato and Cattaneo, 2014; Tyebji and Hannan, 2017; Gatto et al., 2020; Barron et al., 2021). Altered dopamine signalling contributes to motor disturbances in HD, ROS formation and inhibition of autophagy (Kim et al., 2021a).

***Excitotoxicity*:** Excitotoxicity is neuronal cell death resulting from continued stimulation and excessive activation of glutamate receptors due to excess extracellular glutamate (Labbadia and Morimoto, 2013). Glutamate excitotoxicity in HD is observed in striatal postsynaptic neurons that receive glutaminergic input from the cortex and thalamus and is mediated through their NMDA (N-methyl-D-aspartate) receptors (NMDARs), causing calcium influx into cells (Pérez-Navarro et al., 2006; Raymond et al., 2011; Reiner and Deng, 2018). It leads to sustained neuronal membrane depolarization, Ca^{2+} overload, and mitochondrial energy failure, triggering apoptotic pathways (Arundine and Tymianski, 2003). Factors contributing to striatal glutamate excitotoxicity in HD include altered glutamate release, impaired glutamate clearance from the synaptic cleft, downregulation of the glutamate transporter GLT1, impaired uptake of striatal glutamate by glial cells, increased sensitivity of NMDARs to glutamate by expHTT-induced

tyrosine phosphorylation, increased NMDAR's activity and stability, disrupted NMDAR recycling, and reduced expression of the anti-apoptotic synaptic NMDAR (Zuccato et al., 2010; Jurcau, 2022).

***Transcriptional dysregulation*:** Like WT HTT's function as a transcriptional regulator, expHTT also interacts with several TFs like CREB, Sp1, NF-κB, RES, p53, the TATA-binding protein (TBP) and coactivators like CBP, PGC-1α, but the interactions are often non-native, altering their transcriptional activity, promoter accessibility and recruitment of RNA polymerase II, eventually leading to a transcriptional failure (Seredenina and Luthi-Carter, 2012; Valor, 2015; Xiang et al., 2018). Also, many of these factors get sequestered in polyQ aggregates, leading to their depletion and transcriptional dysregulation. For example, expHTT inhibits CREB phosphorylation and acetyltransferase activity of CBP and sequesters them in aggregates, impairing cAMP-dependent signalling and downstream target gene expression (Steffan et al., 2001; Li et al., 2008b; Moily et al., 2017; Xiang et al., 2018). Thus, expHTT affects the expression of a vast network of genes involved in the development, neurogenesis, synaptic transmission, cell signalling, organelle biogenesis, immune, inflammation and stress response, metabolism, epigenetic modifications, proteostasis, cell growth, proliferation, and survival (Luthi-Carter et al., 2000; Luthi-Carter et al., 2002; Sipione et al., 2002; Choi et al., 2009; Seredenina and Luthi-Carter, 2012; Valor, 2015).

***Epigenetic imbalance*:** Various epigenetic alterations are observed in HD, including modifications to histone ubiquitylation and phosphorylation (Valor and Guiretti, 2014). Altered histone acetylation is well characterized in HD. It is mainly restricted to specific gene loci (Igarashi et al., 2003; Sadri-Vakili et al., 2007; McFarland et al., 2012; Valor et al., 2013; Guiretti et al., 2016) and HDAC inhibitors, including sirtuin1 (Sirt1), a non-classical inhibitor, improve HD phenotype in animal models (Steffan et al., 2001; Chuang et al., 2009; Jiang et al., 2011). DNA methylation patterns are altered at the promoter, proximal, and distal regulatory regions (Ng et al., 2013; Villar-Menéndez et al., 2013; Wang et al., 2013). Histone methylation marks, namely H3K4me3, a mark of active promoters and H3K9me2 and H3K27me3, a heterochromatin mark, are differentially altered in the striatum of HD mice (Ryu et al., 2006; Vashishtha et al., 2013;

Biagioli et al., 2015). These epigenetic changes in HD have been attributed to decreased HAT activity of CBP and the deregulation of histone methylation enzymes (Francelle et al., 2017).

***Deregulation of non-coding RNAs*:** Both short non-coding RNAs (sncRNAs) like microRNAs (miRNAs) and piwi-interacting RNAs (Johnson et al., 2008; Maciotta et al., 2013; Dubois et al., 2021) and long non-coding RNAs (lncRNAs) like taurine upregulated gene 1 (TUG1) and maternally expressed 3 (MEG3) (Johnson, 2012; Dong and Cong, 2021), that regulate gene expression epigenetically, mRNA stability, splicing and translational induction, the levels and cellular localisation of RNA and protein pool (Salta and De Strooper, 2017), are dysregulated in HD.

***Mitochondrial dysfunction*:** Neurons have a high energy demand, depend on the mitochondrial oxidative phosphorylation to meet them, and require mitochondrial trafficking from cell soma to neuronal outgrowths, regulated by intracellular Ca^{2+} levels (Sheng, 2017). Mitochondria are essential for regulating calcium homeostasis and the related secondary messenger signalling. Also, being producers of reactive oxygen species (ROS), mitochondria are sources and targets of oxidative stress. expHTT disrupts mitochondrial morphology, membrane potential, permeability, and fission-fusion dynamics in favour of fission, calcium-buffering capacity, energy metabolism and trafficking and damaged mitochondrial clearance by mitophagy. Mechanisms of expHTT-induced alterations include altered transcription of peroxisome proliferator-activated receptor-γ coactivator 1α (PGC1α), a key regulator of energy metabolism and mitochondrial biogenesis and inhibition of mitochondrial protein import complex TIM23 (Franco-Iborra et al., 2018; Zheng et al., 2018; Jurcau, 2022). The overall HD effects on the mitochondria are manifold: 1) increased ROS production and oxidative damage (Fão and Rego, 2021) and triggering neuroinflammation (Kumar and Ratan, 2016); 2) Ca^{2+} handling defects; 3) ATP depletion, cellular energy deficits and impediment of core cellular activities; all of which can trigger the sustained opening of mitochondrial permeability transition pore (mPTP), along with expHTT interaction with the mitochondrial outer membrane, leading to mitochondrial swelling, lowering of mitochondrial membrane potential, the release of Cytochrome c and activation of caspase-dependent and -

independent apoptosis pathways and neuronal death (Labbadia and Morimoto, 2013; Carmo et al., 2018; Zheng et al., 2018; Fão and Rego, 2021; Jurcau and Jurcau, 2022).

***Oxidative stress*:** Neurons are particularly vulnerable to oxidative damage given their high metabolic rate, increased oxygen consumption and free radical generation, enrichment of fatty acids prone to peroxidation and transition metals that catalyse the formation of reactive species, lower ROS scavenging capacity and antioxidants, and poor regeneration ability (Franco-Iborra et al., 2018). In HD, there is evidence for oxidative stress: oxidative damage of proteins, lipids, polysaccharides, and nucleic acids, mitochondrial tricarboxylic acid (TCA) cycle and electron transport chain (ETC) deficits and augmented NOX (nicotinamide adenine dinucleotide phosphate (NADPH) oxidase), a ROS generating enzyme in the plasma membrane, alterations in activity of antioxidant enzymes like peroxiredoxins, glutathione peroxidases, superoxide dismutase 2 (SOD2) and catalase and decreased levels of antioxidants like reduced glutathione (GSH) and peroxiredoxin 1 (Prx1), oxidation of critical metabolic enzymes like aconitase and ATP synthase, reducing their activity and leading to bioenergetic deficit, dysregulation of iron and copper homeostasis leading to their accumulation (Fox et al., 2007; Muller and Leavitt, 2014) and benefits from treatments with antioxidants like α-Lipoic acid, flavonoids, L-ascorbic acid and coenzyme Q10 (Browne and Beal, 2006; Muller and Leavitt, 2014; Franco-Iborra et al., 2018; Zheng et al., 2018; Paul and Snyder, 2019; Fão and Rego, 2021).

Impairments in Ca^{2+} homeostasis: Ca^{2+} is a critical cellular secondary messenger, and its concentrations are crucial in the CNS for growth, differentiation, survival, gene expression, neural activity, neurotransmission, and synaptic plasticity. expHTT alters cellular Ca^{2+} homeostasis in several ways (reviewed in (Giacomello et al., 2013; Kolobkova et al., 2017; Mackay et al., 2018; Pchitskaya et al., 2018; Ureshino et al., 2019)) causing a persistent ER Ca^{2+} leak by influencing Ca^{2+} efflux channels on the ER, namely, the inositol-1,4,5-triphosphate receptor (IP3R) and the ryanodine receptor (RyR), thus, depleting Ca^{2+} in ER that also enhances neuronal store-operated Ca^{2+} entry (SOCE) pathway; directly hyperactivates store-operated Ca^{2+} channel (SOCC) in the plasma membrane responsible for Ca^{2+} influx; enhances expression of extrasynaptic NMDAR;

causes transcriptional deregulation of Ca^{2+} handling proteins; interacts and alters association with calcium-binding proteins like calmodulin and calretinin. All the above increase cytosolic Ca^{2+} concentrations, increase Ca^{2+} uptake by mitochondria, overloading mitochondria and collapsing its membrane potential (also via direct association of expHTT with mitochondria), opening MPTP, and activating apoptosis. ExpHTT also activates Ca^{2+}-dependent caspase, calpain, and calcium-signalling disturbance in transcriptions and cell signalling. However, some studies also show defects in the Ca^{2+} uptake capacity of mitochondria and, thus, lower Ca^{2+} in mitochondria (Panov et al., 2002; Brustovetsky, 2016).

***Metabolic disruptions*:** Energy metabolism deficits in HD are seen both in the brain and peripheral tissues; they include alteration of glucose homeostasis, decrease in its uptake and metabolism, decreases in expression of glucose transporters, increase in lactate levels, decrease in the ATP/ADP ratio, defects in TCA enzymes, decrease in mitochondrial number, size and function, repression of PGC-1α, a key regulator of energy metabolism, dysregulation of deacetylase SIRT1 that impairs the metabolic stress factor DAF-16/FOXO3a and progressive weight loss and muscle wasting, despite increased caloric intake (Mochel and Haller, 2011; Carmo et al., 2018; Illarioshkin et al., 2018). In addition, there are impairments in cholesterol and fatty acid synthesis, urea cycle, amino acid, purine and neurotransmitter metabolism and gut-brain homeostasis (Singh and Agrawal, 2022).

***Glial dysfunction*:** expHTT-induced downregulation of Kir4.1 expression results in a decreased membrane potential and conductance, thus altering astrocyte sensitivity to neuro mediators and pH, reduction of excitatory amino acid transporter 2 (EAAT), leading to impaired glutamate clearance by astrocytes, and oligodendroglia myelination defects (Gatto et al., 2020; Wilton and Stevens, 2020; Jurcau and Jurcau, 2022).

***Neuroinflammation*:** CNS neuroinflammation and peripheral inflammatory response have been documented in HD (reviewed in (Jimenez-Sanchez et al., 2017; Palpagama et al., 2019; Gatto et al., 2020; Gómez-Jaramillo et al., 2022; Jurcau, 2022)). These include activation of microglia (the resident immune cells of the CNS) and reactive astrocytosis, leading to decreased

antioxidants and increased brain pro-oxidants. There are also changes in the levels of proinflammatory mediators like cytokines, chemokines, c-reactive protein, and matrix metalloproteins (MMPs) in the cerebrospinal fluid (CSF) and plasma and BBB damage by inflammatory blood cells. Many of these responses are also induced by altered interactions between expHTT and BDNF, expHTT-induced neuronal oxidative stress, transcriptional dysregulation of TFs like HSF1, myeloid lineage-determining factors, and NF-κB mediated inflammatory response. Other aberrant microglial signalling pathways are the kynurenine pathway, the main pathway for nicotinamide adenine dinucleotide formation and the cannabinoid receptor pathway.

***Cell-to-cell transmission of expHTT*:** A newly uncovered mechanism of pathophysiology in NDs is a cell-to-cell transmission of pathogenic proteins like tau or α-synuclein leading to interneuronal spreading of misfolded proteins to various brain regions (Brettschneider et al., 2015; Jucker and Walker, 2018). Several mechanisms for inter-neuronal propagation of aggregates have been proposed, including exosomes, exophagy, receptor-mediated endocytosis, direct penetration via plasma membrane, and finally, through tunnelling nanotubes (TNTs), long actin-rich membrane bridges directly connecting cells' cytoplasm (Lim and Lee, 2017; Davis et al., 2018; Donnelly et al., 2022). Compelling evidence supports the idea that prion-like spreading of expHTT is prevalent in HD (reviewed in (Donnelly et al., 2022)). A few examples are the unidirectional pre- to postsynaptic spread of expHTT aggregates from R6/2 cortex to wild-type MSNs in the striatum (Pecho-Vrieseling et al., 2014), the spread of fluorescently labelled expHTT aggregates from a specific set of neurons to the entire brain in *Drosophila* leading to non–cell-autonomous neurodegeneration via soluble NSF attachment protein receptor (SNARE)-mediated fusion events (Babcock and Ganetzky, 2015), trans-synaptic transfer of expHTT aggregates in *Drosophila* olfactory system with a brief visit to glial cytoplasm and requiring the glial scavenger receptor Draper (Donnelly et al., 2020) and very recently, a Rhes GTPase induced biogenesis of TNT-like cellular protrusions ("Rhes tunnels") that transport Rhes-positive cargoes including

expHTT between neurons in culture and intact mouse brain (Sharma and Subramaniam, 2019; Ramírez-Jarquín et al., 2022).

Other pathological mechanisms: These include disrupted nuclear pore complex, which is critical for nucleocytoplasmic transport of proteins and other molecules (Gasset-Rosa et al., 2017; Grima et al., 2017), disturbed purinergic signalling (Wiprich and Bonan, 2021), CAG repeat instability and somatic expansion, impairment of DNA repair pathways (Ghosh and Tabrizi, 2018a), accumulation of four homopolymeric expansion proteins (polyAla, polySer, polyLeu, and polyCys) synthesised via the sense and antisense repeat-associated non-ATG (RAN) translation (Bañez-Coronel et al., 2015) and crosstalk with other aggregate-prone proteins like α-Synuclein and tau isoforms (Jimenez-Sanchez et al., 2017).

1.3 PROTEOSTASIS IN ND

Protein homeostasis or proteostasis refers to the optimal maintenance of the proteome to help organisms respond to constantly changing internal and external demands by regulating the concentration, shape, location and interactions of individual proteins while balancing cellular protein biogenesis and degradation (Balch et al., 2008; Balchin et al., 2016; Yerbury et al., 2016; Fernández-Fernández and Valpuesta, 2018). Proteostasis involves mechanisms regulating protein synthesis, preventing aberrant protein interactions, and optimising protein folding, trafficking, activation, degradation, and clearance (Labbadia and Morimoto, 2015; Sweeney et al., 2017). The proteostasis network (PN) comprises protein folding chaperones, Ubiquitin-proteasomal system (UPS), autophagy pathways, stress-response pathways such as HSR (Heat Shock Response), UPR (Unfolded Protein Response) in the ER and mitochondria, various associated signalling pathways, and compartmentalisation of misfolded proteins into specific regions of the cell (Bouchecareilh and Balch, 2011; Labbadia and Morimoto, 2015; Yerbury et al., 2016). Any condition that overwhelms the proteostasis system can be considered stressful and involves environmental and physiological stressors. Proteostasis stressors include temperature (heat-stress or hypothermia), UV light, osmotic changes, heavy metal pollutants, exposure to toxins, bacterial infections, starvation, errors in transcription, translation or PTMs (post-translational modifications), hypoxia, metabolic defects, oxidative stress, mutations, acute global misfolding and ageing (Akerfelt et al., 2010; Ali et al., 2010; Kampinga and Bergink, 2016; Klaips et al., 2018; Shacham et al., 2019). In NDs like HD and other polyQ diseases, protein misfolding and accumulation of mutant protein as soluble intermediates, aggregates, and inclusion bodies significantly burden the cellular protein homeostasis systems. Additionally, with advancing age, there is an overall decline in proteostasis machinery, including the molecular chaperone network, and this further overwhelms the cellular machinery (Hipp et al., 2014; Labbadia and Morimoto, 2015; Gorenberg and Chandra, 2017; Koyuncu et al., 2017). The aggregates and IBs also physically trap proteasomal components and engage with the chaperone machinery, depleting their availability and further compounding the proteotoxic stress (Hipp et al., 2014; Yerbury et al., 2016; Sweeney et al., 2017; Hipp et al.,

2019b). The increased aggregation and decreased proteostasis capacity amplify the protein misfolding toxicity by feeding onto one another, leading to a mutually exacerbating self-propagating cycle, resulting in proteostasis collapse and cell death (Hipp et al., 2014; Labbadia and Morimoto, 2015; Sweeney et al., 2017; Hipp et al., 2019b). Additionally, when cells are under chronic stress, as in the case of ND, they go into a maladaptive stress response, wherein sustained HSR activation leads to a general protein folding deficiency and cells become refractive to additional stressors (Roth et al., 2014; Klaips et al., 2018; Hipp et al., 2019b).

1.3.1 Molecular chaperones in proteostasis

Molecular chaperones (Hsps or Heat shock proteins) are critical in maintaining cellular proteostasis (Hartl et al., 2011; Kim et al., 2013). Many are constitutive, and some are upregulated under stress conditions (Ali et al., 2010). Hsps participate in a range of housekeeping and stress-induced protein folding, trafficking, and quality control activities (Kim et al., 2013; Smith et al., 2015; Balchin et al., 2016; Ciechanover and Kwon, 2017; Nillegoda et al., 2018; Zarouchlioti et al., 2018). Hsps provide hydrophobic cover to nascent polypeptides, prevent non-native interactions within the polypeptide and with other proteins, assist in their *de novo* folding, assembly and intracellular localisation, translocation of organellar and secretory proteins across membranes, and modulate the activation of regulatory proteins (Hartl and Hayer-Hartl, 2009; Kim et al., 2013; Mannini and Chiti, 2017; Nillegoda et al., 2018). Under conditions of stress, they prevent aberrant aggregation of proteins, are integral to disaggregation mechanisms, unfold misfolded proteins, provide optimal conditions for their refolding, and target terminally misfolded proteins for degradation (Hartl and Hayer-Hartl, 2009; Kim et al., 2013; Radons, 2016; Zarouchlioti et al., 2018).

Upon proteotoxic stress, the well-conserved heat shock response (HSR) is activated in cells by the activation of the constitutively expressed Hsf1 (Heat Shock Factor 1) (Akerfelt et al., 2010; Anckar and Sistonen, 2011; Neef et al., 2011; Labbadia and Morimoto, 2015). Under proteotoxic conditions, an increase in protein misfolding promotes the dissociation of the Hsp90 complex from HSF1, thereby, the removal of Hsp90-mediated repression on Hsf1, leading to the

conversion of inactive monomers of Hsf1 into DNA-binding active trimers, that upon nuclear translocation, bind to HSEs (heat shock elements) upstream of Hsp genes and initiate their transcription. Downstream products of HSR activation, like molecular chaperones Hsp90, Hsp70 and Hsp40, negatively regulate the HSF-1 activation pathway, thereby modulating the duration and intensity of the HSR per cellular needs. HSR and UPR work to restore cellular proteostasis by decreasing protein synthesis and increasing the production and activation of PN components such as chaperones (Zarouchlioti et al., 2018; Shacham et al., 2019).

Molecular chaperone families are named according to the molecular weight of their members. These include the Hsp27 (HspB or small Hsps or sHsps), Hsp40 (DnaJ or JDP), Hsp60 (HspD or chaperonins), Hsp70 (HspA), Hsp90 (HspC), Hsp110 (HspH) (Kampinga and Bergink, 2016; Reis et al., 2016). Among the mammalian chaperones, Hsp70 and Hsp90 are the central effectors of proteostasis, acting in association with the Hsp40 co-chaperones as part of a multi-protein complex (Reis et al., 2016). Hsp70, Hsp90 and chaperonins are involved in *de novo* protein folding and refolding through multiple ATP-dependent cycles of folding and release (Hartl and Hayer-Hartl, 2009; Mattoo and Goloubinoff, 2014; Brehme and Voisine, 2016b).

1.3.2 Hsps in HD

Hsps play a central role in the management of neurodegenerative diseases like HD. They aid by modifying aggregation and exerting aggregation-independent effects such as preventing apoptosis and inflammatory response. The levels of ATP-dependent Hsps and their capacity to aid proteostasis reduce with age, contributing to the middle-age onset of HD and other NDs (Taylor and Dillin, 2011; Brehme et al., 2014a; Yerbury et al., 2016; Hipp et al., 2019b; Margulis et al., 2020). Some of these effects and the role of Hsps in neuroprotection are discussed in Chapter 5. HTT is an Hsp system client and, like many other polyQ proteins, is bound by components of chaperone machinery such as Hsp40 and Hsp70 (Cummings et al., 1998; Chai et al., 1999; Jana, 2000; Muchowski et al., 2000; Kim et al., 2002; Shimura et al., 2004b; Wyttenbach, 2004b; Dedmon et al., 2005; Muchowski and Wacker, 2005; Scior et al., 2018). I discuss a few examples of the usefulness of Hsps in ameliorating HD pathogenicity below.

In a cellular model of HD, overexpression of Hsp40 or Hsp70 suppresses aggregation and cell death, with co-expression of the two being the most effective (Jana, 2000). In another cellular HD model, Hsp40 overexpression inhibits HTT aggregation and independently suppresses cell death by inhibiting the activation of caspase-3 and caspase-9 (Zhou et al., 2001). Overexpression of Hsp40 or Hsp70, or both improves many neurodegenerative phenotypes in *Drosophila* polyQ and HD models, including rescuing external eye and retinal degeneration, neurotoxicity, and cell death, enhancing motor performance and survival, suppressing aggregation, and increasing detergent-soluble polyQ (Jana, 2000; Kazemi-Esfarjani and Benzer, 2000; Ghosh and Feany, 2004; Iijima-Ando et al., 2005; Fayazi et al., 2006b; Branco et al., 2008; Liévens et al., 2008). Overexpression of Hsp40 improves neurological performance, decreases mutant HTT aggregate load, increases its solubility, and these effects were dependent on Hsp40-ubiquitin interaction and cooperation with Hsp70 in the R6/2 mouse model of HD (Labbadia et al., 2012). Overexpression of the Hsp40 DNAJB6 in R6/2 mice decreases aggregation, delays motor symptoms and enhances survival (Kakkar et al., 2016). However, overexpression of Hsp70 in R6/2 mice has mixed effects. One study shows a delay in expanded HTT aggregation without affecting disease phenotypes (Hay, 2004), while another shows an effect on disease progression without affecting aggregation (Hansson et al., 2003). Deleting Hsp70 in the same mouse model worsens physical, behavioural, and neurological symptoms and increases inclusion body size without affecting fibrillar aggregates (Wacker et al., 2009).

Over-expression of the co-chaperone and ubiquitin ligase CHIP (E3 ubiquitin ligase C-terminal Hsp70-interacting protein) promotes ubiquitination and degradation of expHTT, suppresses aggregation, cell death and neurotoxicity in cell culture, primary neurons, and a zebra fish HD model (Jana et al., 2005; Miller et al., 2005). HD mice haplo-sufficient for CHIP have accelerated HD progression (Miller et al., 2005). BAG-1 (BAG for Bcl-2 associated athanogene), a NEF (Nucleotide exchange factor), associates with HTT and protects against cell death in an HD cellular model (Jana and Nukina, 2005) and reduces mutant HTT aggregates and enhances its clearance via proteasome in cells and protects against photoreceptor loss in a *Drosophila* HD model (Sroka et al., 2009).

Full-length HTT proteins, both expanded and wild-type, are Hsp90 clients, and upon Hsp90 inhibition, mHTT is degraded by the proteasome without HSR induction (Baldo et al., 2012).

Other studies show that upon Hsp90 inhibition, heat shock response is initiated via HSF activation, and the mHTT aggregation and toxicity are ameliorated in HD cellular, fly and mouse models (Sittler et al., 2001; Herbst and Wanker, 2007; Fujikake et al., 2008; Labbadia et al., 2011). By binding to N-terminal fragments of HTT, engaging the deubiquitinase USP19 (ubiquitin-specific protease 19) that deubiquitinates mHTT, promoting its accumulation and aggregation, Hsp90 prevents mHTT's proteasomal degradation (He et al., 2017).

TRiC, a CCT-based chaperonin complex, inhibits an amyloidogenic switch, reduces SDS-insoluble aggregates, and rescues cellular toxicity in yeast and mammalian cells (Behrends et al., 2006; Tam et al., 2006; Tam et al., 2009). CCT-based chaperonins decrease expHTT aggregation possibly via a cap and contain a mechanism (i.e. capping expHTT fibrillar ends and encapsulating oligomers), thus inhibiting fibril growth and containing reactive oligomers (Shahmoradian et al., 2013; Darrow et al., 2015). Treating HD mice with CCT1 and CCT3 decreased expHTT levels by promoting proteasomal degradation, improving BDNF axonal transport, and rescuing striatal neuronal atrophy (Zhao et al., 2016a). A recent study in *Drosophila* shows that some of the CCT's neuroprotective effects could stem from its requirement in autophagosomal degradation (Pavel et al., 2016).

sHSPs such as αB-crystallin (ABC) or HspB5 are down-regulated in HD mice (Zabel et al., 2002; Hay, 2004; Oliveira et al., 2016). In cell culture, ROS is reduced without affecting HTT aggregates by overexpressing HspB1 (Hsp27) (Wyttenbach et al., 2002). In contrast, SDS-insoluble aggregates are reduced (Carra et al., 2008), and aggregates are cleared via macroautophagy in a BAG-3-dependent manner by overexpressing HspB8 (Hsp22) (Carra et al., 2008). In *Drosophila*, expanded polyQ-induced aggregation and compound eye degeneration are prevented by overexpressing HSPB5 (ABC) and HSPB7 (cvHSP) (Vos et al., 2010; Tue et al., 2012), which in BACHD mice (bacterial artificial chromosome (BAC)-mediated transgenic HD), improves motor, cognitive and neurological features, and delays HD onset and progression non-cell-autonomously (Oliveira et al., 2016). In *Drosophila*, dHsp110 is a potent suppressor of HTT aggregation and neurodegeneration (Zhang et al., 2010c).

1.3.3 Protein degradation mechanisms in HD

Both the UPS and autophagy pathways are involved in the clearance of expHTT: their downregulation promotes aggregation and toxicity, whereas their enhancement promotes expHTT clearance and ameliorates aggregation and toxicity (Sarkar and Rubinsztein, 2008; Li et al., 2010; Juenemann et al., 2013; Rai et al., 2019). HTT is ubiquitinated (Kalchman et al., 1996; Jana et al., 2005; Jana and Nukina, 2005); however, the ability of UPS to degrade N-terminal fragments containing polyQ expansions was controversial: some studies showing UPS's inability to degrade them (Holmberg et al., 2004; Venkatraman et al., 2004; Raspe et al., 2009) versus others showing their degradation by UPS (Michalik and Van Broeckhoven, 2004; Juenemann et al., 2013). The resolution came from studies showing efficient degradation of polyQ containing N-terminal fragments by the UPS, provided expHTT forms are relatively unfolded, soluble, in a non-aggregated state or as incipient aggregates that can be dissociated by the chaperone system (Verhoef et al., 2002; Hipp et al., 2014). However, this pathway gets compromised throughout HD, accumulating insoluble Ubiquitin-containing aggregates (Sieradzan et al., 1999; Waelter et al., 2001; Mitra et al., 2009; Li et al., 2010). Proteasomal saturation, age-dependent proteasomal decline, accumulation of larger protein aggregates, and insoluble inclusions shift the expHTT clearance load towards autophagic degradation (Hipp et al., 2014; Martin et al., 2015). Later studies suggest the involvement of both systems in expHTT clearance depending on the expHTT form, solubility, length of N-terminal HTT, protein context, cellular location (lack of autophagy in the nucleus and presence of nuclear E3-ligase), age and disease-stage and slower clearance of expHTT in the axons than cell body and that of aggregated expHTT than diffuse versions (Iwata et al., 2005; Li et al., 2010; Juenemann et al., 2013; Tsvetkov et al., 2013; Zhao et al., 2016b).

Chaperones in protein degradation: The chaperone system is also responsible for determining whether misfolded and aggregated proteins will undergo another cycle of unfolding/refolding/disaggregation or be directed towards degradation on a case-by-case basis, often referred to as the triage decision (Esser et al., 2004; Sharma et al., 2010; Fernández-Fernández and Valpuesta, 2018; Mogk et al., 2018). The Hsp70 promotes ubiquitination and degradation of terminally misfolded proteins via its interactions with the co-chaperone CHIP (an E3 ubiquitin ligase). The proteasome coupling factor BAG1 (having a ubiquitin-like domain) interacts with the 26S proteasome, a pathway referred to as Chaperone-assisted Proteasomal Degradation (CAP) (Lüders et al., 2000; Alberti et al., 2003; Kettern et al., 2010; Behl, 2011). CHIP targets many polyQ proteins, including HTT, for proteasomal degradation and ameliorates neurodegenerative phenotypes (Jana and Nukina, 2005; Miller et al., 2005; Al-Ramahi et al., 2006; Adachi et al., 2007; Choi et al., 2007; Morishima et al., 2008; Williams et al., 2009). A pathway activated upon proteotoxic stress that couples the Hsp70-Hsp110-based disaggregase complex with the 26S proteasome via Ubiquilin-2 (UBQLN2) that colocalises with aggregated HTT and facilitates its clearance has been described (Hjerpe et al., 2016).

***Impairment of ubiquitin-proteasomal system*:** In HD, there are contradictory reports: an impaired UPS (Bence et al., 2001; Jana et al., 2001; Waelter et al., 2001; Venkatraman et al., 2004; Bennett et al., 2005) and a functionally competent UPS (Bowman et al., 2005; Bett et al., 2006; Tydlacka et al., 2008; Maynard et al., 2009; Schipper-Krom et al., 2014). This contradiction has been addressed by the finding that UPS impairment is transient, and its function recovers, coinciding with the formation of inclusion bodies (Mitra et al., 2009; Ortega et al., 2010). Probable causes for impaired proteasomal activity in HD are the sequestration of UPS components in inclusions and the arrest of proteasome due to its interaction with aggregation-resistant forms of expHTT (Jimenez-Sanchez et al., 2017; Harding and Tong, 2018b). Reduced proteasomal activity is now considered a secondary effect of expHTT aggregation, not a cause. It reflects the inability of cells to maintain protein homeostasis: the disruption of protein-folding-homeostasis by diffuse misfolded expHTT and by chaperone sequestration into aggregates, resulting in a diversion of

cellular proteins to the UPS, competing for the limited capacity of 26S and overloading the UPS with an excess of other misfolded and (or) ubiquitinated substrate proteins (Hipp et al., 2012a; Bersuker et al., 2016). It is now suggested that proteasomes are not irreversibly sequestered in expHTT aggregates; they are recruited to inclusions dynamically and reversibly without affecting their activity (Schipper-Krom et al., 2014).

***Autophagy defects*:** Lysosome-mediated macroautophagy (MA) plays a critical role in aggregate clearance and clears both soluble and aggregated forms of expHTT (Ravikumar et al., 2002; Qin et al., 2003; Croce and Yamamoto, 2019). WT HTT is an autophagy scaffold involved in cargo recognition, autophagy initiation and promotion (Ochaba et al., 2014; Wong and Holzbaur, 2014; Rui et al., 2015; Ashkenazi et al., 2017). Defective autophagy in HD is attributed to expHTT-mediated effects of inefficient recognition and loading of the cytosolic cargo, particularly organelles, into autophagosomes (Martinez-Vicente et al., 2010), inhibition of Beclin-1 regulated starvation-induced autophagy by either sequestering Beclin-1 in inclusions or by suppressing the inhibitor of Beclin-1 inactivator (Mealer et al., 2014). The increase in autophagosomes largely devoid of cargo in HD is attributed to expHTT-induced defective cargo loading (Ravikumar et al., 2004; Martinez-Vicente et al., 2010).

***The fate of misfolded or aggregated proteins*:** Chaperones also target proteins to autophagic degradation via Chaperone-Mediated Autophagy (CMA) and Chaperone-assisted Selective Autophagy (CASA or BAG-3 mediated selective Macroautophagy, also known as Aggrephagy) (Behl, 2011; Kaushik and Cuervo, 2012; Qi and Zhang, 2014). CMA is mediated by the recognition of Hsc70 (HspA8) substrates and certain cochaperones and its association with the lysosomal LAMP-2A receptor (Lysosome-associated membrane protein 2A) (Behl, 2011). CMA is mediated by the recognition of Hsc70 (HspA8) substrates and certain cochaperones and its association with the lysosomal LAMP-2A receptor (Lysosome-associated membrane protein 2A) (Behl, 2011). CASA involves the recognition of ubiquitinated moieties on aggregate-prone proteins and aggresomes by the ubiquitin-binding autophagic cargo receptors such as p62/SQSTM1 (sequestosome 1) and NBR1 (neighbour of BRCA1 gene 1), in complex with HSc70, HspB8 and co-chaperone BAG3 and recruitment into the LC3-II containing double-

membraned autophagosome (Lamark and Johansen, 2012; Stürner and Behl, 2017; Jacomin and Nezis, 2019). CMA and CASA are involved in the clearance of aggregate-prone expHTT (Carra et al., 2005; Carra et al., 2008; Fuchs et al., 2009; Thompson et al., 2009; Bauer et al., 2010; Koga et al., 2011; Qi et al., 2012; Qi and Zhang, 2014). Recently unresolved or terminally aggregates, under certain situations, were shown to be ejected from the cell into the extracellular space via large membrane–surrounded vesicles called exophers in a lysosome-dependent manner in *Caenorhabditis elegans* (Melentijevic et al., 2017).

Hsps also promote the active sequestration of aggregated proteins and that of small oligomeric reactive species, localising their toxicity and their conversion into larger, relatively benign aggregates or deposits (Behrends et al., 2006; Sontag et al., 2014; Mannini and Chiti, 2017; Sontag et al., 2017; Tittelmeier et al., 2020a) (discussed in Chapter 5).

Disaggregases typically utilise ATP hydrolysis energy for unfolding and solubilising large protein aggregates (Mattoo and Goloubinoff, 2014; Sousa and Lafer, 2019). The mammalian disaggregase machinery comprises a tri-chaperone system of Hsp70 (either HspA1/Hsp70 or HspA8/Hsc70, hHsc70 having superior efficiency) in association with Hsp40 (A and B classes) and Hsp110 (HspH1-3), a NEF (Shorter, 2011; Rampelt et al., 2012; Mattoo and Goloubinoff, 2014; Duncan et al., 2015a; Gao et al., 2015; Nillegoda and Bukau, 2015; Nillegoda et al., 2018; Scior et al., 2018; Mayer and Gierasch, 2019). Through their synergistic action, this versatile disaggregase is known to solubilise both disordered amorphous aggregates and ordered aggregates such as amyloids (Shorter, 2011; Rampelt et al., 2012; Gao et al., 2015; Mogk et al., 2018; Nillegoda et al., 2018; Scior et al., 2018; Sousa and Lafer, 2019; Wentink et al., 2020). Concerning HTT, a recent study in cell culture and a *C elegans* model shows that the disaggregase comprising of HSC70 (Hsp-1), DNAJB1(DNJ-13) and Hsp110 (Apg2), in the presence of ATP, suppresses HTTExon1Q48 amyloid fibril formation and reverses its aggregation and nearly completely disaggregates the HTTExon1Q75 fibrils (Scior et al., 2018). In *Drosophila*, the finding of a dHsp110 protein named HSC70cb (human APG-2), interacting with DnaJ-1 (human DNAJB1) to suppress polyQ toxicity and HD-induced eye degeneration, hints at a disaggregate-like property (Kuo et al., 2013b).

1.4 DIFFERENTIAL VULNERABILITY IN HD

Most neurodegenerative diseases exhibit differential neuronal vulnerability: a particular set of neurons or brain regions are more susceptible to disease-protein-mediated toxicity, dysfunction and cell death than others despite the widespread expression of the protein across the brain (Fu et al., 2018). In HD, the striatal and, to a lesser extent, the cortical neurons, particularly medium spiny GABAergic striatal projection neurons (75% of primate striatal neurons), show greater sensitivity to expHTT-mediated toxic effects (Morigaki and Goto, 2017). Within the striatum are regional and temporal differences in the extent of projection neuron loss (Rüb et al., 2015). Even within the MSNs, differential vulnerability depends on the projection targets, neurochemical content, and receptor. Those in the indirect pathway are more vulnerable than those in the direct pathway (Han et al., 2010; Fu et al., 2018). There is no evidence of a significantly high expression of WT or expanded HTT in the regions most affected (Li et al., 1993; Gutekunst et al., 1995; Ide et al., 1995). However, expanded polyQ tract lengths are longer in the striatum than in the cortex (Kennedy et al., 2003; Shelbourne et al., 2007a). The physiological basis for this selectivity is a subject of ongoing research. It relates to the differences in intrinsic biochemistry, anatomy, and connectivity of the neurons, preferentially pre-disposing them to disease protein toxicity. A common theme of selectively vulnerable neuronal populations across several NDs is a narrowly constrained and tightly controlled firing property highly dependent on calcium trafficking and signalling (Roselli and Caroni, 2015). Probable mechanisms contributing to differential neuronal susceptibility in ND are the neuronal proteostasis machinery, i.e., chaperones, protein clearance pathways and their ability to care for misfolded and aggregated proteins, genetic variability in the disease-protein expression and the propagation property of aggregate-prone proteins (Fu et al., 2018). Since striatal neurons depend on cortical BDNF for their function and survival, expHTT-induced reduction in BDNF contributes to striatal vulnerability (Zuccato and Cattaneo, 2014). A few specific examples are reduction of neurotrophic inputs to striatum in the form of BDNF, reduction in the metabolic activator PGC-1α (PPAR gamma coactivator 1alpha) in the striatal MSNs and dysregulation of neuroprotective factors in striatum like the striatum-enriched guanine

nucleotide-binding protein Rhes; glutamate excitotoxicity via striatum-enriched NR2 subunit (NR2B) of NMDAR that enhances the NMDA channel permeability, alters the pro-survival synaptic NMDAR and pro-apoptotic extra synaptic NMDAR, and increases sensitivity of MSN to metabotropic and ionotropic glutamate receptor agonists; high energy demand of the MSNs to maintain hyperpolarized state and low levels of free radical scavenger enzymes (SOD1 and SOD2), rendering them more susceptible to mitochondrial dysfunction; age-dependent reduction in calcium-binding proteins like calbindin, thus, altering Ca^{2+} homeostasis; lower UPS activity and autophagic capacity of neurons in the striatum than the cortex, insufficient activation of Hsps and the HSR in the striatum, reducing the capacity of MSNs in tolerating proteostasis stressors; MSNs' higher propensity for somatic expansion (Kovalenko et al., 2012) and contributions from proteins selectively enriched in striatal neurons like STEP (striatal-enriched protein tyrosine phosphatase) and PDE10A (phosphodiesterase 10A) (reviewed in (Margulis and Finkbeiner, 2014; Morigaki and Goto, 2017; Sala et al., 2017; Fu et al., 2018; Creus-Muncunill and Ehrlich, 2019)). Non-cell-autonomous and circuit-based mechanisms in HD and the role of non-neuronal cells are now being investigated to explain the differential vulnerability in HD (Creus-Muncunill and Ehrlich, 2019).

1.5 PROGRESS IN HD THERAPY: FROM THE LAB TO THE CLINIC

Genetic, small molecular, and pharmacological interventions targeting a wide variety of cellular pathways across various cellular and animal models with the potential for altering Huntington's disease progression have been reported (reviewed in (Jimenez-Sanchez et al., 2017; Dickey and La Spada, 2018; Ghosh and Tabrizi, 2018a; Kim et al., 2021a; Jurcau and Jurcau, 2022)). Large-scale screens have uncovered many therapeutic candidates *in vitro* and *in vivo* (reviewed in (Calamini et al., 2013; Lenz et al., 2013; Lewis and Smith, 2016; Krench and Littleton, 2017; Costa and Maciel, 2022)). In this section, I briefly discuss disease-modifying treatments under clinical trials, potential pre-clinical candidates interfering with expHTT aggregation and treatments providing symptomatic relief. Currently, most existing treatments provide symptomatic relief, and no approved disease-modifying treatments exist (Tabrizi et al., 2019). However, research on neuroprotective therapies to prevent disease onset and halt or slow the disease progression is limited but promising (Palaiogeorgou et al., 2023).

1.5.1 expHTT-lowering therapies

One promising avenue currently undergoing clinical trials is the expHTT-lowering therapies, either by reducing synthesis or enhancing degradation. These could be DNA-targeting, RNA-targeting, or protein-targeting.

DNA-targeted approaches: These directly target the DNA of the HTT gene by using a protein-coding sequence encapsulated in a viral vector that transduces cells upon intracranial injection to produce a functional, non-native therapeutic protein (reviewed in (Wild and Tabrizi, 2017)). These have the potential to ameliorate all aspects of HD. Zinc finger proteins (**ZFPs**)- have a Zn finger array that can bind specific DNA sequences and a functional domain that acts on the DNA to cleave or regulate gene expression (Klug, 2010). Zinc finger transcription factors (ZFTRs) have been developed that suppress expHTT explicitly (Garriga-Canut et al., 2012; Zeitler et al., 2014) and are now in the pre-clinical stages of testing (TAK-686 and ZF-KOX1) (Ferguson et al., 2022). Clustered, regularly interspaced short palindromic repeats (CRISPR) associated system 9

(Cas9) combined with a synthetic guide RNA (gRNA) generates a construct that can cut DNA with high precision at any chosen site and can be used for targeted genome editing. The potential for **CRISPR/Cas9** in HD is tantalising: shortening CAG length in expanded alleles to regular length, inactivating mutant allele by inserting a missense mutation or stop codon and upregulating the WT allele (Cox et al., 2015). It has been successfully used in cell and animal models to inactivate selectively and permanently the mutant *HTT* (Shin et al., 2016; Yang et al., 2017). Further testing in large animal models is required for these strategies before clinical testing in HD patients.

RNA-targeted approaches: This approach involves reducing the translation of *HTT* mRNA using antisense oligonucleotides (ASOs), RNAi agents, or small-molecule-like splicing modulators, and show symptomatic and molecular and neuronal improvements (reviewed in (Wild and Tabrizi, 2017; Tabrizi et al., 2022)). ASOs are synthetic single-stranded DNA molecules that bind pre-mRNA in the nucleus, targeting them for degradation by RNase H. Two clinical trials have been completed with ASOs for HD, the Ionis/Roche ASO program (HTT_{RX} / RG6042) and the Wave Life Sciences program (WVE120101 and WVE-120102) (Barker et al., 2020; Tabrizi et al., 2022). A third trial with WVE-003 is underway. Both the completed trials report a lack of target engagement and expHTT lowering in the CSF (Kingwell, 2021). Current ASOs, thus, suffer from the lack of animal models with the relevant SNPs and target engagement, off-target inflammatory effects, and sufficient expHTT lowering in target structures like the caudate and putamen nuclei. In contrast, allele-specific ASOs targeting CAGs have off-target effects of binding to other RNAs with CAGs (Tabrizi et al., 2022).

RNAi involves double-stranded RNAs like short interfering RNA (siRNA), short hairpin RNA (shRNA) or microRNA (miRNA) acting on mature, spliced, cytosolic mRNA, targeting them for degradation by the RNA-induced silencing complex (RISC). RNAi methods show promise and are under development (e.g. AMT-130 miRNA is in Phase I clinical trials) but suffer from delivery and distribution challenges in the brain. Work is also underway to identify small molecular agents that lower expHTT levels through selective modulation of mRNA splicing, are brain penetrant, and can be orally administered (Bhattacharyya et al., 2021). Branaplam

(LMI070), a splicing modulator, decreases WT and expHTT (Keller et al., 2022), but a Phase 2 trial was halted due to it causing nerve damage. Another candidate under Phase 2 clinical trials is the PTC518.

***Protein-targeted approaches*:** expHTT clearance is achieved by upregulating its ubiquitination and proteasomal degradation or macroautophagy via genetic and pharmacological methods (reviewed in (Harding and Tong, 2018b; Barker et al., 2020; Jarosińska and Rüdiger, 2021; Kim et al., 2021a)). The UPS can be exploited to target specific substrates for degradation via proteolysis targeting chimaeras (PROTACs) and has been demonstrated successfully to degrade expHTT in cell lines (Sakamoto et al., 2001; Tomoshige et al., 2017). Trim-Away, an antibody-based recognition of HTT by cytosolic antibody receptor TRIM21, is also an E3 ubiquitin ligase (Clift et al., 2017). Autophagic inducers that have shown promise in cell and animal models and have potential for clinical trials include Felodipine, an L-type calcium channel blocker that induces mTOR-independent autophagy (Siddiqi et al., 2019), and autophagosome-tethering compounds (ATTEC). These molecular glues interact with expHTT and LC3 (Li et al., 2019b) and can cross the BBB. Induction of expHTT degradation via chaperone-mediated autophagy by engineering a fusion protein containing polyQ-binding peptide 1 (QBP1) and HSC70-binding motif and amelioration of HD symptoms has been demonstrated in mice model (Bauer et al., 2010).

Though adeno-associated viral (AAV) vectors are the most used delivery method, they are single-shot vectors, not allowing for repeated administration or dosage correction. They also elicit immune responses, and their tissue distribution is variable. Some of the challenges facing HTT lowering therapies are allele-selective lowering to expHTT alone, delivery of disease-modifiers directly into the brain and to specific CNS targets, lowering toxicity, penetration and distribution of AAV-delivered agents into the CNS, optimising dosage, the degree of HTT lowering, the disease stage of intervention and the long-term effects of HTT-lowering treatments in HD patients (Barker et al., 2020; Tabrizi et al., 2022).

1.5.2 DNA repair modifiers

Genome-wide studies on HD patients have uncovered DNA repair proteins as the primary modifier of HD progression, for example, *Fan1*. This nuclease is protective and a component of a mismatch repair pathway like MSH3 that drives CAG expansion (Moss et al., 2017; Lee et al., 2019; Iyer and Pluciennik, 2021; Wheeler, 2021). Their potential in HD therapeutics is being explored. An ASO TTX-3360 that reduces mRNA for DNA damage proteins has finished pre-clinical trials (Wiggins and Feigin, 2021).

1.5.3 Cell replacement therapy

Cell therapy is the restoration of degenerated neurons using stem cells procured from normal developing foetal striatum or induced pluripotent stem cell-derived neuronal stem cells, mesenchymal stem cells, or autologous stem cells, with future potential for clinical translation (Björklund and Parmar, 2020; Ferguson et al., 2022). They also improve regeneration capacity and provide pro-survival factors. Clinical trials with long-term intravenous injections of stem cells are ongoing.

1.5.4 expHTT-interfering therapies

Antibody-based therapies: These either directly interact with expHTT, interrupting its downstream pathology or target specific proteins promoting HD pathogenesis (reviewed in (Ferguson et al., 2022)). For example, an intrabody INT41 targeting the PRD, the proline-rich region (PRR) on the carboxyl (3′) side of the polyglutamine expansion interfering with expHTT-mediated cellular pathogenesis (Amaro and Henderson, 2016), is under pre-clinical trials. ANX005, a monoclonal antibody specific to C1q, inhibiting activation of the classical complement cascade, is under Phase 2 clinical trials.

***Other small molecule therapies*:** Examples of small molecular drugs undergoing clinical trials are pridopidine (formerly ACR16), a sigma-1 receptor agonist increasing BDNF production and a dopamine stabilizer affecting striatal pathways contributing to motor deficits, Sage-718, an NMDA receptor antagonist, resveratrol, a naturally occurring antioxidant and P110 that improves

mitochondrial health ((Ferguson et al., 2022), from https://hdsa.org/hd-research/therapies-in-pipeline/# and ClinicalTrials.gov that provide a listing of HD therapies in various stages of basic, pre-clinical and clinical stages).

1.5.5 Anti-aggregation strategies

This strategy targets the various expHTT conformers like monomers, oligomers and soluble and insoluble aggregates by altering the kinetics and flux of the aggregation pathway either by preventing the formation of a "toxic" conformer (e.g. by increasing the energy barrier of the polyQ transition to β-sheet) or destabilisation them and converting them into benign forms or stabilization of a "benign" conformer (e.g. by Hsps) or directing terminally misfolded conformers to degradation (see above: protein-targeted approaches) (reviewed in (Denis et al., 2019; Minakawa and Nagai, 2021; Chopra et al., 2022; van der Bent et al., 2022)). Examples of inhibitors of polyQ and expHTT aggregation are intrabodies like C4 scFv (first single-chain Fv; targeting N17) and rAAV6-INT41 (targeting the PRD), peptides like QBP1 (prevents toxic β-sheet conformation transition of the polyQ monomers), small chemical molecules like methylene blue, curcumin, arginine, GLYN122, trehalose, actinomycin D, Geldanamycin, cyclohexanol, a few of which are molecular chaperone modifiers and single-stranded oligonucleotide aptamers.

1.5.6 Therapies providing symptomatic relief

The commonly prescribed medications for HD offer only symptomatic relief: reduce chorea (e.g. tetrabenazine and deutetrabenazine that reversibly inhibits VMAT2 (Vesicular Monoamine Transporter 2) and deplete central monoamines like dopamine, anti-glutamatergic like amantadine and riluzole), improve behavioural symptoms (e.g. atypical anti-psychotic drugs lolanzapine and like risperidone that are monoaminergic receptor inhibitors), reduce depression (e.g. antidepressants that are generally serotonin reuptake inhibitors (SSRIs) like citalopram and fluoxetine) and stabilise mood (e.g. anticonvulsants like sodium valproate and carbamazepine that have myriad effects including downregulation of excitatory neurotransmitters and upregulation of inhibitory ones) (reviewed in (Dash and Mestre, 2020; Ferguson et al., 2022)). However, these

are replete with side effects like weight gain, sexual dysfunction, dizziness, gastrointestinal disturbances, depression, insomnia, and skin conditions.

Non-pharmacological, non-invasive lifestyle adaptations in HD management include physical therapy, exercise and walking, balance aids for impaired balance and gait, speech therapy and electronic communication devices for speech impairments, diet modifications, and liquid food supplements for patients having eating difficulties and suffering from malnutrition, and regular constant psychological counselling (Ghosh and Tabrizi, 2018b; Ferguson et al., 2022). Likewise, **interventions to provide relief from sleep and circadian disruptions in HD are an active area of research**. **Screening for strategies to alleviate circadian impairments associated with HD** and understanding their mode of action **using a *Drosophila* model of HD is at the crux of this study.**

1.6 CIRCADIAN RHYTHMS

This study focuses on circadian rhythms, their disruptions in Huntington's Disease and investigating strategies to improve them. Humans exhibit circadian rhythms, patterns of daily repeatability (~24h periodicity) that are generated by endogenous timekeepers, in almost every aspect of their physiology, behaviour and performance: rhythms in core body temperature, cortisol, urine volume, activity, the timing of sleep/wake, REM sleep, memory processes, alertness, cognition, executive functions, reaction time, mood, reward and hunger (Hastings et al., 2007; Benca et al., 2009; Valdez et al., 2012; Broussard et al., 2017a; Logan and McClung, 2019; Yalçin et al., 2022).

1.6.1 Basics of a circadian system

A circadian system is primarily made up of three major components: (a) an input pathway to transmit environmental signals to the self-sustained circadian oscillator, (b) the endogenous circadian oscillator/ pacemaker itself, and (c) output pathways by which the circadian pacemaker exerts its rhythmic influence on the biochemistry, physiology, and behaviour of an organism (Fig 1.6). The core circadian molecular oscillators are often interlocked transcriptional/translational feedback loops (TTFLs) comprising positive and negative elements, wherein transcriptional activators initiate transcription, followed by the translation of transcriptional repressors that inhibit their transcription by binding to and inactivating their transcriptional activators.

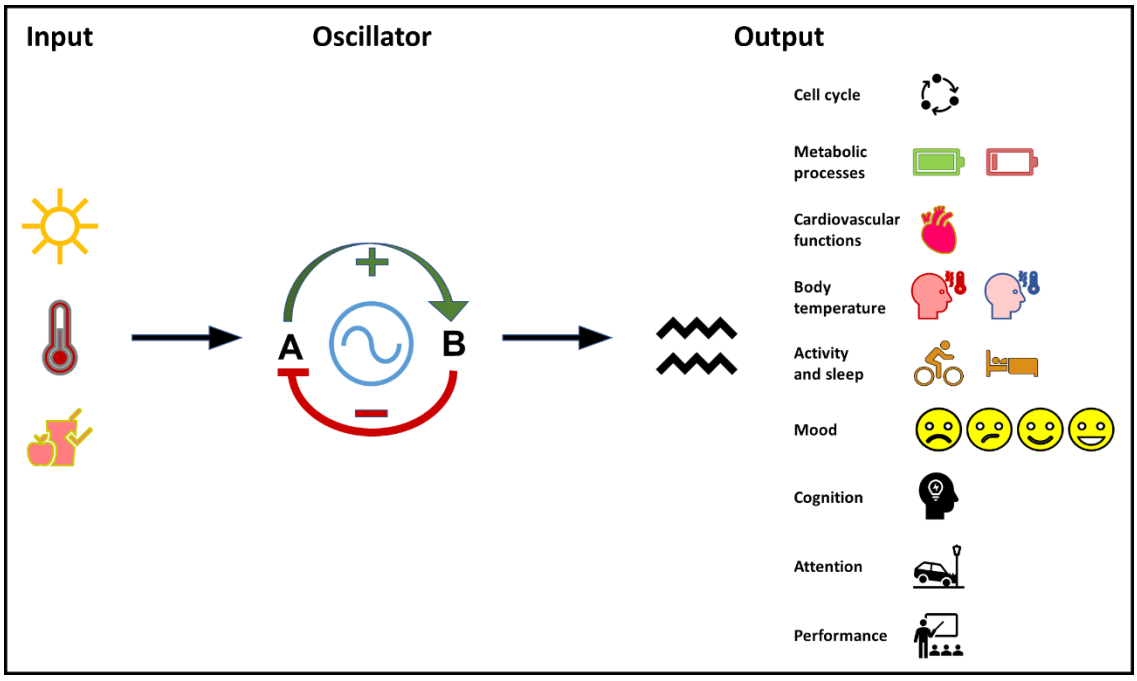

Fig 1. 6 Basic module of a circadian system.
The fundamental components of a circadian system are an input, a self-sustained oscillator, and an output. In its simplest form, the molecular clockwork is an autoregulatory feedback loop. An input could be various factors such as light, temperature, food and social interactions that act as zeitgebers, enabling the circadian clock to synchronize with the environmental cycles. Output signals relay time information from the core clock to the rest of the organism. Output pathways can be described at multiple levels: rhythmic gene expression downstream of the central oscillator, anatomic outputs/transmitter outputs of the pacemaker cells and organismal output in terms of temporally organized behaviour and physiology.

1.6.2 Relevance of circadian clocks

Circadian rhythms are governed by internal molecular clocks (self-sustained transcriptional/ translational feedback loops) that influence various physiological outputs, translating to rhythms in physiology and behaviour. Circadian clocks help organisms adapt to daily cycles in environmental factors like light, temperature, and humidity and cycles in other external factors like food and mate availability and avoidance of predators and harsh conditions. Anticipating and scheduling various biological processes at favourable times of the day following external changes increases the organism's chances of survival and mating, thereby its fitness, thus conferring an external adaptive advantage of exhibiting circadian rhythmicity (Vaze et al., 2014; Schibler et al., 2015; Nikhil and Sharma, 2017; Patke et al., 2020). Circadian clocks help maintain internal synchrony, coordinating the various rhythms within the body (internal rhythms) for temporal

order, conferring an intrinsic advantage to organismal health. This clock also ensures the temporal separation of chemically incompatible pathways and restricts the duration of potentially harmful pathways to only the time of requirement (Schibler et al., 2015). Organisms with dysfunctional clocks show fitness disadvantages like reduced lifespan and fertility (Allemand et al., 1973; Schaffer et al., 1998; Beaver et al., 2002; Green et al., 2002; Kumar et al., 2005). There are also several studies demonstrating the advantage of circadian resonance, i.e., when the endogenous period matches that of the environment (von Saint Paul and Aschoff, 1978; Klarsfeld and Rouyer, 1998; Ouyang et al., 1998; Woelfle et al., 2004; Dodd et al., 2005; Emerson et al., 2008; Lone et al., 2010; Horn et al., 2019). The critical significance of circadian clocks and rhythms in organismal health span becomes very evident considering the negative impact of situations that cause circadian clock disruptions. Disruptions can result from clock gene mutations such as advanced and delayed sleep phase syndrome (ASPS and DSPS), environmental difficulties such as transmeridian travel (jet lag) or short days (Seasonal Affective Disorder, SAD), occupational difficulties such as shift work, modern lifestyles such as aberrant lighting conditions (light-emitting electronic devices, ALAN- artificial light at night), irregular meal timings, neurodegenerative diseases such as AD, PD, and HD, and ageing (Evans and Davidson, 2013; Potter et al., 2016). These disruptions adversely affect the health and well-being of an individual, increasing the risk and incidence of metabolic (e.g. obesity, diabetes), cardiovascular, gastrointestinal, reproductive, endocrinal, psychiatric disorders, cancer and addiction and impacting day-to-day functioning by impairing cognition and physical performance (Evans and Davidson, 2013; Logan et al., 2014; Khan et al., 2018; Patke et al., 2020; Yalçin et al., 2022; Verma et al., 2023).

1.7 MAMMALIAN CIRCADIAN SYSTEM

1.7.1 Mammalian molecular clockwork

The primary molecular clock comprises TTFLs (reviewed in (Reppert and Weaver, 2002; Mohawk et al., 2012; Mendoza-Viveros et al., 2017; Takahashi, 2017; Hastings et al., 2019), described in the next section for *Drosophila*. The central components of the mammalian molecular clockwork are transcriptional activators CLOCK (circadian locomotor output cycle kaput), and BMAL1 (brain and muscle ARNTL 1 (aryl hydrocarbon receptor nuclear translocator–like), and transcriptional repressors Period (PER1, PER2 and PER3) and Cryptochrome (CRY1 and CRY2). Additional feedback loops positively regulated by CLOCK:/BMAL1 and negatively by PER1, PER2, CRY1, and CRY2 influence circadian oscillations' period, phase, and amplitude. These components include the transcriptional repressors retinoic acid-related orphan nuclear receptor Rev-erbα/β and E4BP4 (or Nuclear Factor, Interleukin 3 Regulated NFIL3) and the transcriptional activators RAR-related orphan receptor Rorα/β and the D-site albumin promoter binding protein Dbp.

1.7.2 Mammalian central clock: The Suprachiasmatic Nucleus

The site of the master circadian pacemaker in mammals is the Suprachiasmatic Nucleus (SCN), a bilateral cluster of 20,000 neurons on either side of the third ventricle, atop the optic chiasm, located in the anterior hypothalamus (reviewed in (Mohawk and Takahashi, 2011; Hastings et al., 2018)). Individual neurons of the SCN are each autonomous cell clocks exhibiting molecular clock oscillations, firing rate and gene expression rhythms, and oscillatory transcriptional networks (Lowrey and Takahashi, 2004; Ueda et al., 2005). SCN neurons are distinctive in that they exhibit circadian rhythms in firing patterns, are the first to be synchronised by external light/dark cycles, have network-wide topologically organised coupling mechanisms via intra-network interactions that allow SCN neurons to be synchronised in complete darkness, are buffers against genetic and environmental perturbations, and are the direct recipients of light information (light inducing SCN neuronal firing) (Herzog, 2007; Welsh et al., 2010; Evans, 2016). The spontaneous firing rate cycle, the key SCN output driving circadian rhythmicity, is higher during

the day in diurnal and nocturnal mammals, encoding solar time (Bano-Otalora et al., 2021). The SCN organisation is shown in Fig 1.7.

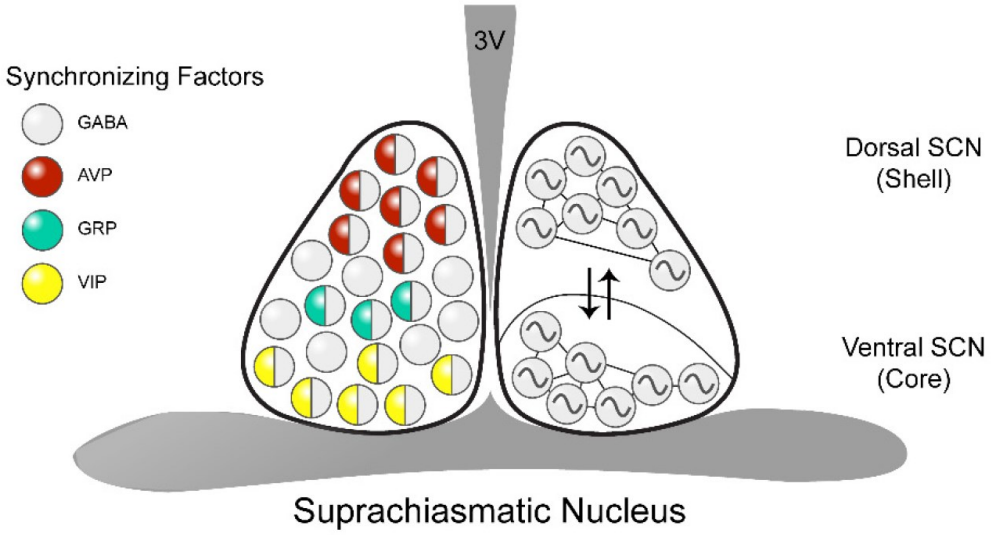

Fig 1. 7 Organisation of the SCN.
The SCN is subdivided into a dorsomedial shell and a ventrolateral core. Shell is primarily the zone of Arginine vasopressin (AVP) neurons and a few calretinin-containing (CAR) neurons. The core is the zone of Vasoactive intestinal polypeptide (VIP) and Gastrin releasing peptide (GRP) neurons. About 30% of the SCN terminals contain GABA, and glutamate is an additional SCN transmitter. These SCN neurons, with their respective neurotransmitters and diffusible signals, communicate between the different SCN regions. They also convey circadian and external time information like light/dark signals to hypothalamic target structures (figure from (Hegazi et al., 2019)).

Photoentrainment of the SCN: The SCN is thought to be the sole receiver of light information for photic entrainment of the entirety of the mammalian system. It receives light information from the visual photoreceptors. Also, it receives non-visual photic signals via innervation by melanopsin expressing intrinsically photosensitive retinal ganglion cells (ipRGCs) that make up the retinohypothalamic tract (RHT) and are essential for photoentrainment and light-mediated phase setting of the SCN and its output rhythms (reviewed in (Welsh et al., 2010; Hughes et al., 2014; Ashton et al., 2022)).

Effect of temperature: In mice, the SCN itself is resistant to temperature resetting, an emergent property of SCN neuronal network coupling, but cells and tissues outside the SCN and the

peripheral clocks can be synchronized by temperature as temperature cycles or heat pulses (Brown et al., 2002; Buhr et al., 2010; Tamaru et al., 2011; Saini et al., 2012). However, rat SCN is temperature sensitive, phase shifted by temperature and entrained by it (Ruby et al., 1999; Herzog and Huckfeldt, 2003). Core body temperature shows daily clock-controlled cycling, synchronising peripheral clocks (Brown et al., 2002; Schibler, 2009). Temperature effects on the circadian rhythms involve HSF1 and cold-induced RNA binding proteins (CIRBPs), reset peripheral clocks via transcriptional, post-transcriptional and translational mechanisms (Reinke et al., 2008; Tamaru et al., 2011; Morf et al., 2012; Liu et al., 2013; Schneider et al., 2014; Ki et al., 2015).

Coupling within the SCN: Isolated SCN neurons are weaker and less reliable oscillators (Webb AB et al., 2008; Webb et al., 2009), and dispersed SCN neurons exhibit a range of circadian periods and phase heterogeneity (Welsh et al., 1995; Honma et al., 1998; Honma et al., 2004; Evans et al., 2011). Coupling of SCN neurons via network interactions results in more precise, higher amplitude SCN neuronal rhythms that are robust against perturbations, including resetting by temperature and retain function even in the face of dysfunctional molecular clocks (Nakamura et al., 2002; Herzog et al., 2004; Liu et al., 2007; Abraham et al., 2010; Buhr et al., 2010; Ko et al., 2010; Evans et al., 2012). SCN inter-cellular communication enables network-level synchronization of the period by establishing unique and stable phase relationships (though oscillators can peak at different times and can exhibit a distribution of phase relationships) that are coordinated as a population providing network rhythmicity which is integral to SCN functioning in maintaining tissue-level rhythms and strong outputs to downstream tissues (Aton and Herzog, 2005; Ciarleglio et al., 2009; Welsh et al., 2010; Herzog et al., 2015; Evans, 2016; Michel and Meijer, 2020). VIP and its receptor VPAC2 are essential for intercellular coupling within the SCN (Aton and Herzog, 2005; Brown et al., 2007; Hughes et al., 2008).

SCN neuronal outputs: The well-known SCN neuronal outputs are Arginine vasopressin (AVP), Gamma amino butyric acid (GABA), glutamate, Vasoactive Intestinal Peptide (VIP) and melatonin. VIP and its receptor VPAC2 share molecular and functional similarities with that of

the *Drosophila* circadian output neuropeptide, the Pigment Dispersing Factor (PDF) and its receptor PDFR, respectively, like synchronising neuronal clocks and mediating light entrainment (Aton et al., 2005; Vosko et al., 2007; Frenkel and Ceriani, 2011; Talsma et al., 2012). Another significant circadian output is melatonin, a precisely timed hormonal message of darkness, whose synthesis and release are under SCN control (Moore and Klein, 1974) and a faithful reflection of dawn and dusk signals from the SCN, with melatonin peaking at night (Stehle et al., 2001).

1.7.3 Peripheral oscillators

Besides the SCN, autonomous circadian rhythms are present in every tissue of the body; the extra-SCN brain clocks and clocks in other parts of the body are referred to as "peripheral clocks" (Balsalobre et al., 1998; Yamazaki et al., 2000; Yoo et al., 2004). In mammals, most peripheral oscillators are considered slave oscillators to the master clock SCN as they depend on the SCN for phase coordination between cells in tissue via humoral and neuronal signals (Dibner et al., 2010; Lowrey and Takahashi, 2011; Mohawk et al., 2012). Though the peripheral clocks show autonomous cell oscillations and their rhythm generation is SCN-independent, they are not intrinsically photosensitive and depend on the SCN for rhythm maintenance (coordination and synchronization) and light information (Hastings et al., 2003), but are temperature-sensitive and can be synchronised by temperature (Brown et al., 2002) and food (Damiola et al., 2000; Stokkan et al., 2001).

1.8 *DROSOPHILA* CIRCADIAN SYSTEM

The *Drosophila melanogaster* circadian system is well-established and extensively studied and shares several genetic, organisational and functional similarities with the mammalian system (see 1.10). Individual rhythms in behaviour, like those in locomotion, feeding, egg-laying, courting, and temperature preference, as well as populational rhythms of eclosion that gate the emergence of adults from pupa to specified times of the day, are all displayed by the *Drosophila.*

1.8.1 The *Drosophila* molecular clock

The *Drosophila melanogaster* circadian molecular clock, in its most basic form, comprises an interlocked transcriptional-translational feedback loop (reviewed in (Hardin, 2006; Benito et al., 2007; Hardin, 2011; Peschel and Helfrich-Förster, 2011; Tataroglu and Emery, 2015; Helfrich-Förster, 2017; Patke et al., 2020)). The core clock proteins are Period (PER), Timeless (TIM), CLOCK (CLK) and CYCLE (CLK) and the molecular clockwork constituting the feedback loop is explained in Fig 1.8. The timing of this feedback loop determines the speed and amplitude of the clock and is finely regulated by posttranscriptional modifications. These regulate clock protein dimerization, nuclear translocation, and degradation/stabilization that incorporate time delays into the loop; a ~6-8h delay between the *per*/*tim* mRNA peaks and the PER/TIM protein peaks is critical for the functioning of the main negative feedback loop. *per* and *tim* mRNAs peak at late-evening / early- or mid-night, whereas the PER TIM proteins peak late-night / pre-dawn. For instance, phosphorylation of PER and TIM by the Shaggy (SGG) kinase and PER further by Casein kinase 2 (CK2) and Doubletime (DBT) allows the nuclear translocation of the PER/TIM/DBT, their binding to and inhibition of CLK/CYC dimer's DNA binding, thereby repressing their transcription. Post degradation of TIM, phosphorylation of PER by DBT leads to PER proteasomal degradation. A slower dimerization of PER/TIM or downregulating kinases CK2 or SGG delays the nuclear entry of PER and slows down molecular rhythms, resulting in an extended period (Gekakis et al., 1995; Ko et al., 2010; Chiu et al., 2011; Yu et al., 2011).

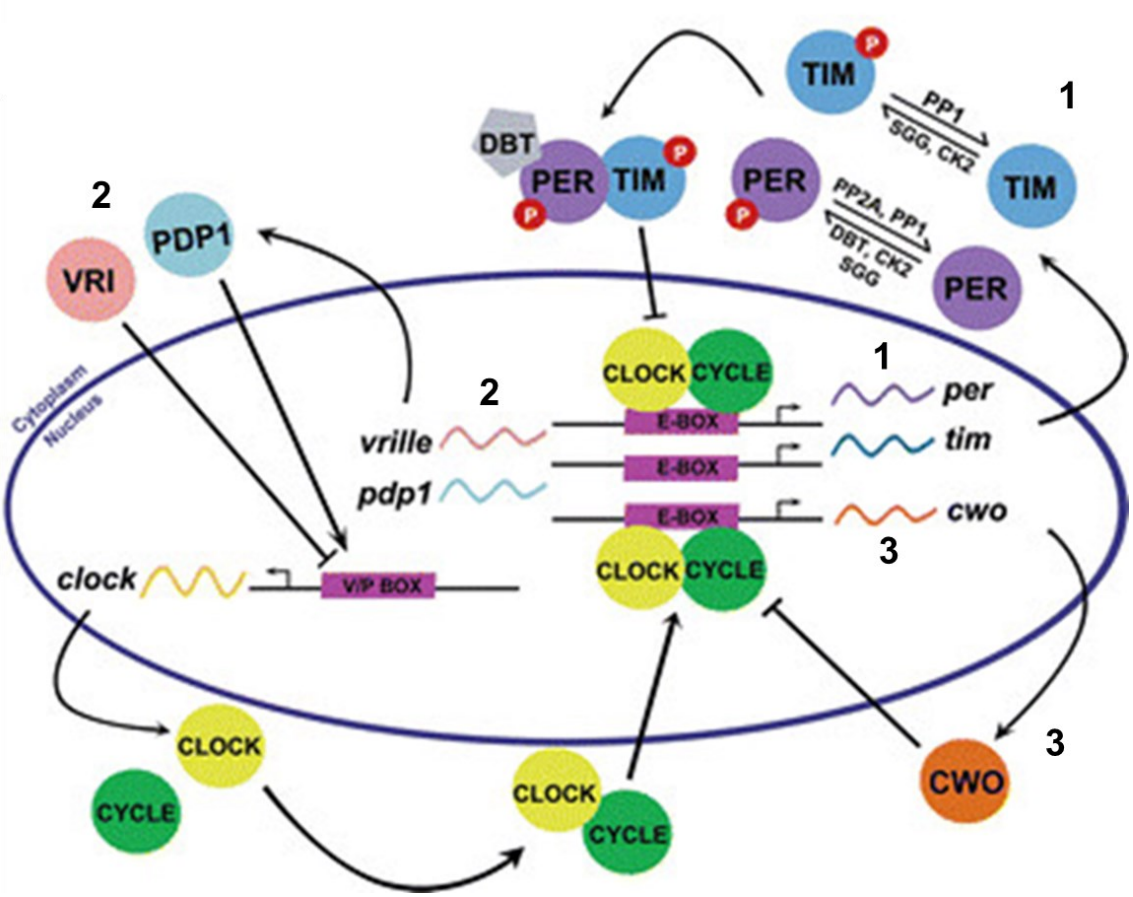

Fig 1. 8 A conceptual schematic of the Drosophila molecular clock.
1) The positive circadian clock regulators CLK and CYC dimerise and bind upstream *per* and *tim* genes to E-boxes, activating their transcription. Translation and accumulation of the negative regulators PER and TIM in the cytoplasm follow. Dimerization of PER and TIM prevents PER degradation, stabilizing it and allowing the complex to translocate to the nucleus; dimers bind to the CLC/CYC complex, dissociating them from E-boxes and inhibiting *per/tim* transcription and that of other genes with E-boxes, thus, completing one cycle. Once PER and TIM levels go down, CLK/CYC can reactivate *per* and *tim* transcription and start another transcription cycle. Kinases like DBT, SGG and CK2 and phosphatases like PP1 and PP2 regulate the phosphorylation states of PER and TIM, determining their stability, levels, and cellular localization. 2) The secondary loop is initiated again by CLK/CYC binding to E-boxes of *vrille* (*vri*) and *par domain protein 1 epsilon* (*pdp1ε*), activating their transcription. VRI accumulates first, translocates to the nucleus, and represses *clk* transcription by binding to VRI-/PDP1-boxes on the *clk* promoter. In contrast, PDP1ε accumulates later, moves into the nucleus four hours after VRI and activates *clk* transcription, thus leading to CLK oscillation and reinforcing the primary feedback loop. 3) In the third feedback loop, CLK-CYC via the E-box activates the transcription of CLOCKWORK ORANGE (CWO), which upon translation into the transcriptional inhibitor CWO translocates into the nucleus, competitively binds to the E-box, and inhibits CLK-CYC-activated transcriptions, independently reinforcing the primary negative loop of transcriptional inhibition by the PER/TIM/DBT complex (figure from (Mendoza-Viveros et al., 2017)).

1.8.2 The *Drosophila* circadian neuronal circuit

One easily measurable and robust behavioural rhythm exhibited by *Drosophila* is rhythms in their locomotor activity/rest patterns. Under 12h light: 12h dark cycles (LD), *Drosophila melanogaster* exhibits a bimodal pattern of locomotor activity, with a morning bout close to lights-ON (M-activity) and an evening bout close to lights-OFF (E-activity) and relative inactivity in the middle of the day and night (Frenkel and Ceriani, 2011). This rhythm persists with a circadian period (~ 24h) even under constant darkness (DD). This timed activity/rest is evoked by a neuronal network in the adult fly central nervous system made of about 150 specialised clock neurons (~75 per brain hemisphere), often referred to as pacemakers, each characterised by the presence of self-sustained cell-autonomous molecular clock (Sheeba et al., 2008b). The *Drosophila* circadian neuronal network (CNN), modulating various aspects of activity rhythms, are divided into subgroups grossly based on their anatomical location, as shown in Fig 1.9a.

This study's target circadian neuronal groups are the PDF-expressing ventrolateral neurons or the LNvs: the small LNvs and the large LNvs (Fig 1.9b). PDF from the LNv is a circadian output neuropeptide. For the behavioural rhythmicity of flies in DD, functional clocks in PDF^{+} LNv, specifically, the sLNv and PDF, are critical (Grima et al., 2004; Stoleru et al., 2004; Renn et al., 1999). The roles of LNv and PDF in evoking free-running activity rhythms and in light entrainment are discussed in Chapter 2. Furthermore, PER is considered the marker for functional molecular clocks. This study's circadian behavioural output is the adult activity/rest rhythm primarily under free-running conditions of constant darkness (DD) at constant temperatures.

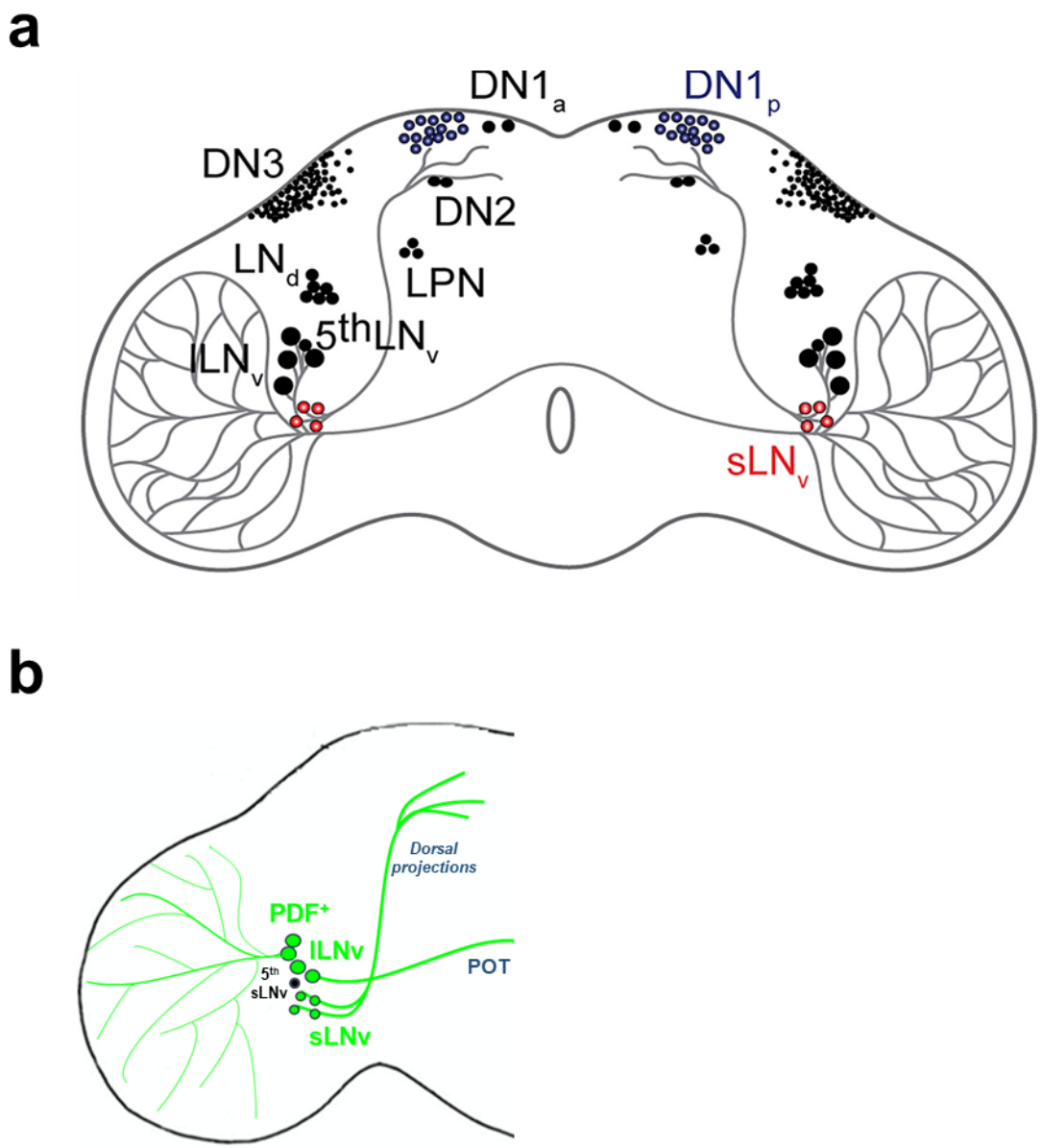

Fig 1. 9 A schematic of the Drosophila circadian neuronal network.

(a) The *Drosophila* circadian neurons are divided into subgroups based on anatomical location. In the lateral protocerebrum are the Lateral Neurons (LNs): nine ventral lateral neurons (LNvs), six dorsal lateral neurons (LNds) and three Lateral Posterior Neurons (LPNs) in each hemisphere. In the dorsal protocerebrum are the Dorsal Neurons (DNs): 2 DN1as, 15 DN1ps, 2 DN2s and 35-40 DN3s (Shafer et al., 2006; Hermann-Luibl and Helfrich-Forster, 2015). Based on their size, the LNvs are divided into small LNv (sLNv) and large LNv (lLNv) (Figure from (Jeong et al., 2022). (b) Out of the LNs, 8 LNv per hemisphere: about 4 small LNv (sLNv) and 4-5 large LNv (lLNv) express the neuropeptide **Pigment Dispersing Factor** (PDF in green) (Helfrich-Förster, 1995). The sLNv send axonal projections towards the dorsal protocerebrum, and the lLNv axons run via the posterior optic tract (POT) to the contralateral side. The 5th sLNv (black) does not express PDF.

.

1.8.3 *Drosophila* clock entrainment

Drosophila circadian clocks can be entrained by both light and temperature. Their relative strengths of entrainment are context-dependent, with light being the stronger zeitgeber in many scenarios (Miyasako et al., 2007; Yoshii et al., 2010; Harper et al., 2016) (discussed in Chapter 4).

1.8.3.1 Light entrainment

Under 12h:12h LD, PER and TIM proteins peak at midnight; light pulse at early-night delays their accumulation and the phase of the circadian oscillation, whereas light pulse later at night hastens the loss of PER and TIM, advancing the clock phase (Marrus et al., 1996). *Drosophila* circadian clocks perceive light via different photopigments (rhodopsin family and cryptochrome) in photoreceptive organs (the compound eyes, ocelli, and the Hoffbauer-Buchner eyelets and clock neurons) (Yoshii et al., 2015; Helfrich-Förster, 2020). Unlike mammalian CRY, *Drosophila* CRY is a blue-light cellular photoreceptor, central to light resetting of the molecular clock (Emery et al., 1998; Stanewsky et al., 1998; Emery et al., 2000b). It is present in many clock neuronal groups (CRY^- are primarily the DN1ps, DN2s, DN3s, LPNs and 3 LNds) (Benito et al., 2008; Yoshii et al., 2008), rendering them intrinsically photosensitive. A light-mediated conformational change in CRY facilitates its binding to TIM and recruiting the E3 ubiquitin ligase JETLAG, facilitating TIM degradation, preventing PER-TIM dimerisation, and exposing PER to destabilising phosphorylation, followed by its proteasomal degradation, thus resetting the circadian pacemaker (Ceriani et al., 1999; Busza et al., 2004; Koh et al., 2006; Peschel et al., 2009) (reviewed in (Foley and Emery, 2020)).

1.8.3.2 Temperature entrainment

After light, the temperature is the next strongest zeitgeber for fly clocks. Entrainment of activity rhythms to temperature cycles requires functional molecular clocks, particularly *clk and cyc* (Yoshii et al., 2002; Yoshii et al., 2005). Rectangular temperature cycles not only entrain the activity rhythms (M- and E-activity peaks exhibited) and circadian molecular clocks under DD but also LL that otherwise renders flies arrhythmic (Tomioka et al., 1998a; Tomioka et al., 1998b;

Yoshii et al., 2002; Glaser and Stanewsky, 2005; Yoshii et al., 2007; Currie et al., 2009). Most clock neurons, unlike their intrinsic light-sensitivity, rely on temperature inputs from thermosensors in peripheral organs like the aristae on the antennae and the chordotonal organs as well as in other brain neurons like the Anterior Cells (ACs) (Hamada et al., 2008; Sehadova et al., 2009; Lee et al., 2013; Chen et al., 2015b; Roessingh et al., 2015; Das et al., 2016; Tang et al., 2017; Chen et al., 2018; Yadlapalli et al., 2018). The CRY^{-} LPNs and DNs show greater temperature sensitivity and are more prominent in temperature entrainment (Busza et al., 2007) (Yoshii et al., 2005; Miyasako et al., 2007; Yoshii et al., 2010), as discussed in Chapter 4.

1.8.4 The *Drosophila* circadian neuronal network: Hierarchical or plastic with bidirectional coupling?

A simplistic dual-oscillator model elegantly explains the activity/rest rhythms of *Drosophila* under LD: two mutually coupled clocks, the M-oscillators comprising of the PDF^+ LNv, specifically the sLNvs (and likely a few DN1ps) governing the M-activity and the E-oscillators made of the three CRY^+ LNd and the 5^{th} sLNv (and likely some DN1ps) controlling the E-activity (Grima et al., 2004b; Stoleru et al., 2004; Rieger et al., 2006; Zhang et al., 2010c; Yoshii et al., 2012; Chatterjee et al., 2018b). Also, in DD, the dual-oscillator model predicts a hierarchical order. The M-oscillators or the sLNvs have been considered the central pacemaker and the dominant oscillators governing the period of other oscillators. However, later work challenges this dual-oscillator hierarchical model and supports a distributed network model comprising multiple oscillators coordinated via network interactions (Stoleru et al., 2005; Dissel et al., 2014; Guo et al., 2014; Yao and Shafer, 2014; Beckwith and Ceriani, 2015a; Delventhal et al., 2019; Schlichting et al., 2019d; Jaumouillé et al., 2021). The coupling rules governing various pacemaker interactions and their relative roles in shaping different aspects of the rhythm changes are context-dependent: changing with the environmental conditions like lighting conditions, photoperiod, light intensity, temperature, abrupt *vs* gradual changes, the waveform of change, the complexity of multiple zeitgebers, laboratory conditions *vs* natural settings and genetic backgrounds like interrupted PDF signalling, sLNv functioning and the presence of CRY (e.g. refer (Yoshii et al., 2012; Beckwith and Ceriani, 2015b; Chatterjee et al., 2018b; Schlichting et al., 2019d)). Thus, the organisation of the clock neuronal network is plastic with multiple independent neuronal oscillators, each capable of orchestrating activity bouts, but orchestrating the entirety of behavioural rhythms is an emergent property of the network (Yoshii et al., 2012; Yao and Shafer, 2014; Yao et al., 2016). The behavioural rhythms result from bidirectional interaction between neuronal oscillators, network coupling, and the resulting network output. Such an organisation also provides space and time for fine-tuning the network responses to changing environments and contributes to network resilience. Indeed, the emerging idea is to view the CNN as comprised of neuronal feedback loops analogous to the genetic feedback loops of the molecular clock (Ahmad et al., 2021).

1.8.5 Communication of *Drosophila* circadian signals: Neurotransmitters and Neuropeptides

Though LNvs are the central pacemakers and PDF is considered the primary peptidergic neuronal clock output, eliciting rhythmic locomotor activity requires coupling and coordination of the entire clock network. The coupling involves several other neuropeptides and neurotransmitters (Beckwith and Ceriani, 2015b). **Neuropeptides** involved in communicating circadian signals are Ion Transport Peptide (ITP), Neuropeptide F (NPF), short NPF (sNPF), CCHamide 1, CNMamide, FMRFamide, IPNamide, SIFamide, DH31, DH44, Allostatin A and C (Ast-A and Ast-C), Leucokinin, Hugin-Pyrokinin, *Drosophila* Insulin-like peptides (DILPs), DTk (*Drosophila* Tachykinin) and buricon, (Ahmad et al., 2021; Nässel and Zandawala, 2022; Reinhard et al., 2022). **Neurotransmitters** of the clock network include glycine, serotonin, glutamate, acetylcholine, GABA, dopamine and octapamine (Muraro et al., 2013; Hegazi et al., 2019).

1.8.6 *Drosophila* clock output at multiple levels

Circadian regulation occurs at multiple levels, giving rise to different rhythmic outputs of the circadian neuronal network. Examples include rhythms in intracellular Ca^{2+} levels, neuronal electrical activity (LNv, DN1), membrane excitability, sodium and potassium ion conductance, timed neurotransmitter release, structural plasticity like sLNv axonal terminal remodelling (number of arbours, branching, volume, synaptic contacts) and sensitivity to PDF and dopamine (Cao and Nitabach, 2008; Fernández et al., 2008; Sheeba et al., 2008b; Gorostiza et al., 2014; Flourakis et al., 2015; Petsakou et al., 2015; Klose et al., 2016; Liang et al., 2016; King and Sehgal, 2020). In addition, temporal information is coded through the rhythmic transcription of clock-controlled genes (CCGs) like *takeout*, *lark* and *narrow abdomen*, among others, that elicit physiological rhythms (King and Sehgal, 2020). The mechanisms by which time information is conveyed from the **circadian circuit to the output centres** (non-clock neurons) to mediate behavioural and physiological rhythms are now emerging. Three neuronal populations have been identified in the pars intercerebralis, a key output centre: Dh44 (+) (Diuretic Hormone 44) neurons; SIFa (+) neurons; and Dilp2 (+) (*Drosophila* insulin-like peptide 2) neurons, the latter only involved in rhythmic feeding and metabolism (Cavanaugh et al., 2014; Barber et al., 2016; King et al., 2017; Bai et al., 2018; Barber et al., 2021). sLNv directly communicates with (Lk+)- neurons (that project onto regions of locomotor control) and the PI output centres via DN1s (Cavey et al., 2016).

1.9 PARALLELS BETWEEN *DROSOPHILA* AND MAMMALIAN CLOCKS

From the discussion detailed above, one can see several parallels between the *Drosophila* and mammalian circadian systems in terms of the conservation of clock genes, molecular clockwork, common motifs of circadian neuronal organization, and mechanisms of temporal regulation of physiology and behaviour. They share the core TTFLs, post-transcriptional and -translational mechanisms, their effect on clock protein stability, localization and partner associations, and orchestration of time delays that are integral to the feedback loop and regulation of the period, amplitude, and phase of circadian oscillations. At the level of the circadian clock neuronal network, in both flies and mammals, they are organized into a multi-oscillatory distributed network, and overt rhythms are an emergent property of the oscillator coupling and interactions within the network, thus also providing various checkpoints for regulation in response to environmental signals and internal demands. They also share similarities in the neuropeptide and neurotransmitters involved, exhibiting functional conservation and rhythms in electrical activity, neuronal plasticity, structural complexity and receptor sensitivity and their crucial role in fine-tuning the clock network. Light can entrain both oscillators using different underlying mechanisms, though only the *Drosophila* clock neurons (central and peripheral) are intrinsically photosensitive. The *Drosophila* CNN can be entrained by temperature, but the SCN resists it. Both systems possess cell-autonomous peripheral oscillators, but mammalian peripheral clocks depend more on their central pacemaker SCN than those of the *Drosophila*. Moreover, regarding the functional significance of circadian clocks across taxa, clock gene mutations and circadian rhythm disruptions (CRD) by genetic, experimental, or extrinsic means have fitness costs and detrimental consequences to health. Thus, many open questions on the reciprocal relationship between circadian health and neuronal- and organismal- health, the consequences of circadian breakdown and interventions to alter them can be addressed in *Drosophila*.

1.10 *DROSOPHILA* AS A MODEL ORGANISM FOR NEURODEGENERATION

Drosophila melanogaster is a well-established genetic model system to carry out a variety of studies. Fundamental cellular processes are very similar between humans and flies, like regulating gene expression, cell cycle, cell signalling, synaptic transmission, membrane trafficking and cell death (Rubin et al., 2000; Ambegaokar et al., 2010; Hirth, 2010). Also, many genes, gene pathways and signalling pathways are conserved between humans and flies (Adams et al., 2000; Rubin et al., 2000). Adult flies (brain at ~$8 \times 107\ \mu m^3$) have relatively simple nervous systems (100,000 neurons) (compared to some 86 billion in humans), enabling study at single-neuronal level, and yet exhibit complex behaviours such as olfaction, courtship, mating, locomotion, circadian behaviours, navigation, learning and memory, addiction, and proprioception (Bier, 2005; Simpson, 2009). Human and *D. melanogaster* nervous systems are also structurally and physiologically similar: organisation, constituents like neurons and glia, neurotransmitters, and the presence of a blood-brain barrier (BBB) (Tello et al., 2022). Flies are easy to grow, maintain and work with, have short generation time and lifespan, produce many offspring, possess minimal genetic redundancy, and fly pushing is relatively cost-effective. *Drosophila* is a powerful research system with a constantly growing and evolving repertoire of genetic tools to intervene and study changes at every level of biological organisation, in space (tissue/cell-specific) and time (at every life stage), to carry out large scale screens (genetic/pharmacological/environmental), study behaviour, map neural circuits and understand the relationship between genes, circuits, and behaviour, to carry out rigorous assays to reliably score various disease phenotypes including those of neurodegeneration at all organisational levels (e.g. neuronal inclusions, cell death assays, brain vacuolisation, neuronal morphology and activity, network outputs like neuropeptide release, synaptic plasticity and communication, behavioural assays of locomotor and cognitive performance, lifespan, ROS levels etc) (Venken et al., 2011; Lenz et al., 2013; Ugur et al., 2016; Martín and Alcorta, 2017; Guo et al., 2019; Luan et al., 2020; Schaffert and Carter, 2020; Tello et al., 2022). Approximately 75% of human genes associated with diseases have a *Drosophila* ortholog (Reiter et al., 2001a; Bier, 2005). All of these make *Drosophila* an excellent model to study many human diseases, including neurological

diseases, screen for enhancers or suppressors of disease outcomes, identify various mechanisms underlying disease progression, test their roles in the pathogenic process, identify potential therapeutic targets, and test potential environmental and pharmacologic agents of modification (Rezaval, 2015; Şentürk and Bellen, 2018). *The Bloomington Drosophila Stock Centre* has curated *Drosophila* models for a wide-ranging human neurodegenerative disease.

Huntington's disease is exceptionally well suited to be modelled in *Drosophila* because the triggering event, i.e. mutation in a single gene *htt* involving a trinucleotide repeat expansion, has been identified. Evidence that expanded polyglutamine itself drives the neurodegenerative process from transgenic mice and cell culture studies (Ikeda et al., 1996; Mangiarini et al., 1996; Ordway et al., 1997; Paulson et al., 1997) led to the development of the *Drosophila* models of HD that use various lengths of human HTT containing the polyQ tract, often the truncated hHTT versions (Bolus et al., 2020).

1.10.1 *Drosophila* models of HD

Drosophila HD models express different lengths of the expanded human *HTT* gene. Exon 1: First 142aa (hHTT Q75 and Q120) (Jackson et al., 1998), first 90aa (hHTTQ93) (Steffan et al., 2001), hHTT Q48 and Q152 (Doumanis et al., 2009), hHTT Q46, Q72 and Q103 (Zhang et al., 2010b) and first 88aa (hHTTQ96) (Weiss et al., 2012); longer exon fragments: first 171aa (hHTTQ138) (Mugat et al., 2008), first 336aa (hHTTQ128) (Kaltenbach et al., 2007; Branco et al., 2008), first 548aa (hHTTQ128) (Lee et al., 2004) and 12-exons or first 588aa (hHTTQ138) (Weiss et al., 2012); the entire protein coding sequence ($hHTT^{FL}Q128$) (Romero et al., 2008). The transgenes are typically targeted to be expressed in the compound eye, central nervous system, motor neurons, mushroom bodies, neuromuscular junction, or glia. The commonly used neurodegenerative readouts in flies typically include external eye phenotype (ommatidial structure, size and pigmentation), retinal and photoreceptor degeneration (number of intact rhabdomeres), neuron numbers, brain vascularisation and cell death, neuroanatomical/morphological and neurophysiological changes, alterations in circadian rhythms, tests for motor abilities like climbing or flying or larval mobility, assessing cognitive performance via learning and memory paradigms like olfactory learning and courtship

conditioning, polyQ aggregation and lifespan (Green and Giorgini, 2012; McGurk et al., 2015; Rosas-Arellano et al., 2018). These have helped capture different aspects of HD, as discussed below.

The early *Drosophila* models of HD revealed striking similarities with mouse models. In the first *Drosophila* model of HD, expression of N-terminal fragments of hHTT with 75 and 120 glutamine residues resulted in a polyQ-length-dependent age-of-onset and severity of neurodegeneration in the photoreceptor neurons of the compound eye and progressive worsening of neurodegeneration and nuclear accumulation of expHTT inclusions with age (Jackson et al., 1998). Deletion of the tumour suppressor gene *p53* suppressed neurodegeneration (Bae et al., 2005). Expression of expanded hHTTex1 Q93 in flies led to progressive neurodegeneration and reduced their lifespan, which improved upon pharmacological and genetic inhibition of HDAC (Steffan et al., 2001). Expression of the first 548 aa of the human HTT protein, which encompasses the highest stretch of homology between the *Drosophila* and human HTT proteins with an expanded PolyQ tract of 128 repeats (HTT-Q128), resulted in the rough eye phenotype, widespread defects in membrane excitability and brain activity, lowered locomotor speed of third instar larvae, motor defects in flies and decreased survival (Lee et al., 2004). expHTT aggregates were observed in the cytoplasm and processes of neurons, which were dependent on the time, cellular and protein contexts. In the first full-length (FL) *Drosophila* HD model, expressing HTTFL-Q128 in motor neurons leads to progressive neurodegeneration, reduced lifespan, and impaired motor performance (Romero et al., 2008). Expression of nuclear-targeted expHTT (hHTT-Q152(NLS)) in the peripheral nervous system of larvae showed neuronal dysfunction without cell death, where dendrite morphology, nerve activity and locomotion were altered (Nishimura et al., 2010). Glial expression of expHTT is also toxic and leads to locomotor defects, aggregation and lifespan reduction in flies (Liévens et al., 2008; Tamura et al., 2009). Thus, *Drosophila* models have replicated many of the pathogenic processes of HD, such as a dominant gain-of-function neurotoxicity, dependence of age-of-onset and severity on repeat length, decline in longevity, progressive neurodegeneration, visible protein aggregates and deficits in motor function and cognitive performance, despite gross anatomical and genomic differences between

humans and fruit flies (reviewed in (Chan et al., 2002; Marsh and Thompson, 2004; Xu et al., 2015; Rosas-Arellano et al., 2018; Bolus et al., 2020).

HD studies in *Drosophila* have revealed essential principles regarding the pathophysiological mechanisms of HD. For example, axonal transport defects in HD were established in flies as a result of motor protein titration, aggregation, vesicle stalling and sequestration of other expanded polyglutamine proteins by the cytoplasmic aggregates (Gunawardena et al., 2003; Lee et al., 2004; Sinadinos et al., 2009). Defective Histone deacetylation and transcription dysregulation contribute to HD, which is rescued by the overexpression of *Drosophila* CREB-binding protein (CBP) (Taylor et al., 2003b). Post-translational modifications like SUMOylation of exon 1 expHTT exacerbated neurodegeneration, whereas ubiquitination attenuated it (Steffan et al., 2004). The role of autophagy in HD has been shown using flies lacking a key apoptosis regulator, Dark (*Drosophila* Apaf-1 related killer), that neutralised polyQ pathogenesis (Sang et al., 2005). Using rapamycin (an inhibitor of mTOR), the roles of macroautophagy in the clearance of expHTT aggregates and mitochondria and reduction of apoptosis in the protection against HD were demonstrated in flies (Ravikumar et al., 2004; Ravikumar et al., 2006). From an initial yeast screen of HTT partners, HD suppression studies in flies first revealed the involvement of the SNARE complex and, thus, alterations in synaptic transmission in HD pathology (Kaltenbach et al., 2007). Work with the full-length HTT brought to light the mechanisms during early stages of HD, elevated presynaptic Ca^{2+} levels and increased neurotransmission and in the absence of nuclear accumulation of expHTT and a novel role for HTT in synaptic function (Romero et al., 2008).

Glial cell dysfunction in HD was demonstrated in *Drosophila,* where glia expression of expHTT decreases dEAAT1 transcription and antagonises the epidermal growth factor receptor (EGFR) signalling pathway at an upstream step between EGFR and ERK (EGFR-Ras-extracellular signal-regulated kinase) activation (Lievens et al., 2005). The ability of expHTT to activate distinct pathways of toxicity in the brain neurons (AKT kinase-insensitive) and retinal photoreceptors and glia (AKT kinase-sensitive) was shown in flies (Liévens et al., 2008). Further, evidence that glial cells expressing expHTT have a developmental and a non-cell autonomous effect on neurons was shown in flies (Tamura et al., 2009).

HTT's native functions have been evaluated by downregulating endogenous *Drosophila* Htt (Zhang et al., 2009), showing a role for HTT in fast axonal transport (Gunawardena et al., 2003). Loss of function of WT HTT contributing to HD has been demonstrated by exacerbations on reducing WT dHtt (Mugat et al., 2008; Zhang et al., 2009) or improvements in HD flies on overexpressing WT HTT either dHtt or hHTT548aa (Mugat et al., 2008) or P42, a 23aa long hHTT peptide (Arribat et al., 2013).

Both aggregated and soluble forms of expHTT were shown to contribute to toxicity using an RFP-tagged hHTTQ138 fly line (Weiss et al., 2012). The *Drosophila* model of cardiac amyloidosis captures expHTT-induced cardiomyopathy (Melkani et al., 2013). *Drosophila* HD models have helped elucidate the role of metal ions like copper in HD progression (Xiao et al., 2013). A study comparing the relative toxicities of different naturally occurring HTT fragments in *Drosophila* revealed that the exon 1 fragment was highly toxic (Barbaro et al., 2015). Transcellular spreading of HTT aggregates was shown in the *Drosophila* brain (Babcock and Ganetzky, 2015). expHTT was shown to interfere with endosomal recycling, elevate BMP signalling in the nerve terminals of flies and trigger excessive synaptic connections (Akbergenova and Littleton, 2017). A recent study implicates immune dysregulation in the blood cells of HD flies (Lin et al., 2019b).

Fly studies have been pivotal in discovering novel pathways of neuropathology and establishing suppressors of HD toxicity *in vivo* or intact animal models with potential as treatment options. These include, HDAC inhibitors (Steffan et al., 2001; Pallos et al., 2008), tissue transglutaminase inhibition (covalently cross-linking proteins) (Karpuj et al., 2002; Bortvedt et al., 2010; McConoughey et al., 2010), polyQ binding protein 1 (QBP1) (a peptide inhibitor) (Nagai et al., 2003), lithium via the Wnt/Wg pathway by inhibiting a glycogen synthase kinase-3 (GSK3β/shaggy) (Berger et al., 2005), engineered C4 single-chain Fv (sFv) antibodies (intrabodies) (Wolfgang et al., 2005), combinatorial drug treatments (Agrawal et al., 2005; Bortvedt et al., 2010), green tea flavonoid epigallocatechin-3-gallate (a copper chelator and aggregation inhibitor) (Ehrnhoefer et al., 2006), the endocytic and signal transduction scaffold Intersectin (ITSN) (activates JNK-MAPK pathway) (Scappini et al., 2007), molecular chaperones and the heat shock response upregulation (Liévens et al., 2008; McLear et al., 2008; Sroka et al.,

2009; Vos et al., 2010; Kuo et al., 2013b; Maheshwari et al., 2014; Sajjad et al., 2014), downregulation of hsrω (large non-coding regulatory RNAs) (Mallik and Lakhotia, 2009), glial enhancement of mitochondrial uncoupling proteins (UCPs) (Besson et al., 2010), Puromycin-sensitive aminopeptidase (PSA) (a cytosolic polyQ-sequence-digesting enzyme) (Menzies et al., 2010), neuroprotective metabolite kynurenic acid (KYNA) (a modulator of cholinergic and glutamatergic neurotransmission) relative to the neurotoxic metabolite 3-hydroxykynurenine (3-HK) (Campesan et al., 2011), Meclizine, a silencer of oxidative metabolism (Gohil et al., 2011), methylene blue (modulator of amyloidogenic aggregation) (Sontag et al., 2012), Pcaf (a histone acetyltransferases and part of a DNA repair complex) (Bodai et al., 2012), Rab GTPases (intracellular membrane trafficking regulators): Rab5 (Ravikumar et al., 2008), Rab11 (Steinert et al., 2012), Rab8 (Delfino et al., 2020), the antioxidant enzymes Glutathione peroxidase (GPx) (Mason et al., 2013) and superoxide dismutase (Melkani et al., 2013), curcumin (a phytochemical with anti-oxidant, -inflammatory and -fibrilogenic properties) (Chongtham and Agrawal, 2016), human c-myc (a proto oncogene) (Raj and Sarkar, 2017), the deubiquitinase Usp12 (a neuronal autophagy inducer) (Aron et al., 2018), Glutamine Synthetase 1 (GS1) (favours autophagy) (Vernizzi et al., 2020), and improving mitochondrial respiration via E3 ubiquitin ligase Parkin, NADH-quinone oxidoreductase 1 (Ndi1) or alternative oxidase (AOX) (Campesan et al., 2023). Using flies, the ease and speed of carrying out large-scale suppressor and enhancer screens of genes, RNAis, small molecules, chemicals, pharmacological agents, and natural compounds and validating potential candidates to suppress expHTT toxicity have revealed HTT interacting partners, potential drug targets and a host of mitigators of HD. Some of the promising reveals have been overexpression of the *Drosophila* homolog of human myeloid leukemia factor 1 (dMLF1) (Kazemi-Esfarjani, 2002), C2-8 (a small-molecule inhibitor of aggregation)(Zhang et al., 2005), HTT partners which are proteins involved in synaptic transmission, cytoskeletal organization and biogenesis, proteolysis, and regulation of transcription or translation (Kaltenbach et al., 2007), rotenone and 2,4-dinitrophenol (small molecule metabolic inhibitors of mitochondrial and glycolytic function) (Varma et al., 2007), genes involved in heat shock response, UPS, TFs, RNA metabolism, signal transduction, and apoptosis (Branco et al., 2008) autophagy enhancers (Williams et al., 2008), genes related to nuclear transport, nucleotide

processes, and signalling (Doumanis et al., 2009), genes of protein biogenesis, cytoskeleton/protein trafficking, chaperone family, nonsense-mediated mRNA decay, and kinases and phosphatases (Zhang et al., 2010b), inhibition of matrix metalloproteinases (Miller et al., 2010b), Inhibition of lkb1 (a tumour suppressor and a negatively regulating kinase of the mTOR/Insulin pathway) and drugs like Camptothecin and OH-Camptothecin (DNA Topoisomerase 1 inhibitors), and 18β-Glycyrrhetinic acid and Carbenoxolone (a mTOR inhibitor through PI3K/AKT) (Schulte et al., 2011), EVP4593 (a small molecule inhibitor of NF-κB signalling and store-operated calcium entry pathway) (Wu et al., 2011), inhibition of RRAS signalling (Miller et al., 2012), negative regulator of ubiquitin-like protein 1 (NUB1) that reduces HTT abundance (Lu et al., 2013), inhibition of glutaminyl cyclase (QPCT) (Jimenez-Sanchez et al., 2015), chlorzoxazone (reduces excitatory neurotransmission, anti-inflammatory) and deferoxamine (an iron chelating agent with antioxidant properties) (Smalley et al., 2016), 10O5, 8F20, AN1 and AN2 (autophagosome-tethering or expHTT-LC3 linker compounds that interact with both LC3 and expHTT to bring about allele-selective reduction of expHTT levels) (Li et al., 2019b) and glial depletion of dCBP (ortholog of CBP/Cp300 transcription co-activators) (Martin et al., 2021).

As discussed, several underlying pathophysiological mechanisms of HD are also exhibited in *Drosophila* HD models, suggesting evolutionarily conserved disease processes (Krench and Littleton, 2017; Rosas-Arellano et al., 2018; Costa and Maciel, 2022). The findings in *Drosophila* have improved our understanding of the cellular, molecular, and genetic mechanisms underlying disease progression. *Drosophila* has also served as a powerful platform to test for disease modifiers and develop therapeutic strategies and drugs to delay, arrest, or, in the future, even reverse disease processes of human NDs. The structural and physiological similarities between *Drosophila* and the vertebrate nervous system also confer greater translatability of therapeutic effects. The strength and usefulness of *Drosophila* as a model to study circadian dysfunction associated with ND are detailed in the next section.

1.11 RELATIONSHIP BETWEEN CIRCADIAN HEALTH AND NEURODEGENERATION

1.11.1 Circadian and sleep disturbances in HD

Circadian and sleep impairments are common in neurodegenerative diseases. They are prodromal in many NDs and are independent predictive markers for ND onset (Leng et al., 2019; Park and Colwell, 2019; Lananna and Musiek, 2020). Circadian abnormalities in ND are often in the direction of dampening, i.e. with a reduction in the amplitude rather than a phase change (Voysey et al., 2021a).

A physiological basis for sleep and circadian abnormalities in HD is the disruption of the hypothalamus, the seat of the SCN and sleep/wake-gating orexin neurons (Kassubek et al., 2004; Aziz et al., 2007; Politis et al., 2008; Petersén and Gabery, 2012). In post-mortem HD patient samples, the VIP and AVP immunoreactive neurons are diminished in the SCN (van Wamelen et al., 2013). In HD patients, the hypothalamic neuropeptide populations of orexin, vasopressin, and oxytocin are also reduced (Aziz et al., 2008; Gabery et al., 2010).

Signs of HD-associated sleep and circadian disturbances include delayed sleep phase, increased latency in sleep onset, nocturnal awakenings, increased nocturnal activity, fragmented nighttime sleep, abnormal motor activity during nocturnal sleep, decreased slow-wave sleep, suppressed REM sleep, insomnia, decreased total sleep time and efficiency, early waking time, increased daytime sleepiness and decreased daytime activity levels, increased ratio of nighttime to daytime activity, elevated daily cortisol levels and delayed or suppressed melatonin peak, lowered plasma melatonin, as gathered from HD animal models and a few from HD patients (Morton et al., 2005; Alders et al., 2009; Aziz et al., 2009b; Videnovic et al., 2009; Goodman and Barker, 2010; Morton, 2013; Kalliolia et al., 2014; Piano et al., 2015; Hood and Amir, 2017b; Herzog-Krzywoszanska and Krzywoszanski, 2019; Zhang et al., 2019; Voysey et al., 2021a). Some of these are present years before the disease manifests, though not readily apparent to the patients and worsens on approaching manifest disease onset (Arnulf et al., 2008; Goodman et al., 2011; Lazar et al., 2015). Thus, circadian and sleep disturbances can independently predict NDs (Hood

and Amir, 2017b). In HD patients, sleep impairments correlate with depression and poor cognition (Aziz et al., 2010). Poor consolidation of activity rest rhythms, disruption in sleep rhythm and decline in sleep quality dramatically impact the quality of life and are a significant reason for the admission of individuals to care homes (Pollak and Perlick, 1991; Bianchetti et al., 1995; Barone et al., 2009).

Rodent models of HD recapitulate most of these findings and show progressive sleep and circadian abnormalities with age and disease severity under free-running and LD conditions (Morton et al., 2005; Kantor et al., 2013). The findings also highlight the effect of HD on nearly all aspects of the mammalian circadian organisation: the input, molecular oscillators, and the output, and it affects both central and peripheral rhythms (Fifel and Videnovic, 2020; Colwell, 2021) as detailed below. In R6/2 mice models, the circadian output neuropeptide VIP's immunostaining, its mRNA, and the mRNA of its receptor VPAC2 are reduced in the SCN (Fahrenkrug et al., 2007). Rhythms in molecular clock genes' *bmal1* and *per2* mRNAs are impaired in the SCN, motor cortex, striatum, and peripheral tissues (Morton et al., 2005; Pallier et al., 2007; Maywood et al., 2010). Behaviourally, there is a progressive breakdown of free-running activity rhythms, an increase in daytime activity, a decline in night activity, and a mirroring of disrupted day/night activity patterns seen in HD patients (Morton et al., 2005; Kudo et al., 2011). Sleep and electroencephalogram (EEG) disturbances are apparent at the presymptomatic stage of HD in these mice (Kantor et al., 2013). However, the SCN electrophysiological output and rhythms in circadian gene expression in organotypic SCN slices assayed *in vitro* are not altered, suggesting that the brain circuits efferent and afferent to the SCN are affected without compromising the core SCN clockwork (Pallier et al., 2007).

In contrast, other mice models of HD (BACHD and Q175) show a dampened spontaneous firing activity of SCN neurons, loss of rhythms in SCN resting membrane potential and a defective SCN neuronal output seen as an enhancement in BK currents (big-conductance Ca^{2+} activated K^{+} currents) (Kudo et al., 2011; Kuljis et al., 2018; Smarr et al., 2019). Activity rhythm amplitude of BACHD mice declines with age, their sensitivity to the phase-shifting effects of light reduces, and rhythms in body temperature and heart rate are disrupted without alterations to PER2

expression in SCN (Kudo et al., 2011; Fisher et al., 2016). These mice also have long-period activity rhythms, entraining to 12h:12h LD without visual impairments (Oakeshott et al., 2011). Q175 HD mice display age- and dose-dependent decline in the circadian wheel running rhythms, evidenced by a decrease in the power of rhythms in DD, in the precision of the daily onset of activity and activity levels under LD and DD, and poor sleep quality and levels (Loh et al., 2013). They also have dampened rhythms in heart rate and core body temperature, deficits in SCN neuronal output and a breakdown of phase coherence between various ultradian rhythms, a sign of internal desynchrony (Smarr et al., 2019).

HD mice models also have dysfunctional ipRGC and attenuated pupillary light response, contributing to circadian entrainment defects (Ouk et al., 2017). Retinal dysfunction and degeneration (Helmlinger, 2002; Batcha et al., 2012), downregulation in the expression of melanopsin and cone opsin (Ouk et al., 2016; Lin et al., 2019a), and impairment in photic synchronisation to phase delays (Ouk et al., 2019), contribute to defects in photic entrainment of HD mice.

The circadian disturbances are not restricted to the brain; peripheral tissues like the liver have a loss of rhythms of key clock-controlled metabolic outputs mainly due to altered feeding patterns and inputs from central clocks in the SCN (Maywood et al., 2010). There is also systemic circadian desynchrony as evidenced by disrupted rhythms in cortisol, melatonin, and body temperature (Aziz et al., 2009b; Aziz et al., 2009c; Kudo et al., 2011; Fisher et al., 2013; Adamczak-Ratajczak et al., 2017; Raupach et al., 2020).

Overall evidence, therefore, is indicative of a strong SCN pathophysiology in HD. HD circadian pathology is not restricted to the central clocks. It also affects peripheral clocks and rhythms, disrupting circadian rhythms at the input, oscillator, and output levels under both free-running conditions of DD and entraining conditions of LD.

1.11.1.1 Circadian disturbances in *Drosophila* models of ND

Drosophila melanogaster models of HD recapitulate many of the HD circadian features. Expression of eGFP-tagged HTTQ103 in LNv decreases rhythm robustness and PDF^{+} sLNv

numbers and suppresses PER levels in LNv (Xu et al., 2019b). Expressing HTT-ex1Q93 pan-neuronally abolished rhythms in CYC, PER, and TIM mRNA levels (Khyati et al., 2021) and expressing it in the LNv neurons results in behavioural arrhythmicity and reduction in PDF (Mason et al., 2013; Delfino et al., 2020). PER-driven expression of HTT-ex1Q120 leads to altered clock transcript rhythms (Faragó et al., 2019). These flies also show sleep deficits, such as reduced and fragmented daily sleep, leading to overall hyperactivity and increased sleep-onset latency. On the pan-neuronal expression of the full-length HTT, nighttime sleep is fragmented and reduced, activity is elevated, sleep latency is increased, daytime sleep is increased, activity is reduced, and longevity is diminished. These are reversed upon the reduction of PKA signalling (Gonzales and Yin, 2010; Gonzales et al., 2016).

Fly models of other neurodegenerative diseases like AD and PD also show circadian and sleep distress, mirroring the disease features. AD flies are arrhythmic in DD, have difficulty re-synchronising to phase-shifted LD, and their evening anticipation index diminishes (Chen et al., 2014). In flies with increased cleavage of endogenous Amyloid Precursor Protein cleavage (by dBACE overexpression), free-running activity rhythms are disrupted in aged flies, PER oscillations in LNs dampened, and their median lifespan is reduced (Blake et al., 2015). Expression of human Tau mutant (TauE14) in *Drosophila* LNv disrupts free-running rhythms, leading to a loss of PDF^{+} sLNv dorsal projections (DP) and mitochondria from the sLNv DP (Zhang et al., 2022). Expression of the 0N4R isoform of tau in the TIM neurons leads to weak rhythms and a reduction of rhythmic flies, elevates lLNv spontaneous firing rate, increases activity levels and sleep latency and reduces sleep levels and quality (Buhl et al., 2019). Flies expressing Aβ42 have reduced daytime and nighttime sleep, fragmentation, and abnormal sLNv dorsal arborisations (Tabuchi et al., 2015b; Song et al., 2017). *Drosophila Tau* deficient flies show circadian and sleep alterations such as loss of M-anticipation in LD, increased daytime activity levels, decreased daytime sleep, and sleep fragmentation at night (Arnes et al., 2019). They also have fewer sLNv axonal crosses at ZT2 compared to the control. Sleep patterns are altered in flies with knock-in of hTau without affecting circadian locomotor rhythms (Cassar et al., 2020). The sLNv axonal arborisation pattern and their oscillations are modified in these flies.

Flies carrying the hTau^{V337M} mutation show sleep disturbances, locomotor defects, neuronal degeneration and loss of daily fluctuation in sLNv projection patterns, but their rhythmicity is unaffected (Cassar et al., 2020).

Drosophila mutants of mitochondrial ligase MUL1 and PARKIN that are models for PD show an increase in ROS levels, decrease in antioxidant SOD1, reduced survival, increase in daytime activity levels, changes in clock mRNA oscillations and reduction in autophagy protein ATG5 in the LNv (Doktór et al., 2019). Many *PINK1* mutant flies are arrhythmic or have weak rhythms, and their lLNv electrophysiology is altered (Julienne et al., 2017). PD fly models also exhibit sleep deficits and a loss of morning anticipation as the flies age (Gajula Balija et al., 2011).

Flies expressing expMJD in the TIM^{+} neurons are arrhythmic in DD and show decreased mRNA levels of nearly all clock genes, loss of PER protein in the heads, decreased number of PDF^{+} sLNv and reduced lifespan (Kadener et al., 2006). GMR-driven expression of CHMP2B, associated with frontotemporal dementia (FTD) and amyotrophic lateral sclerosis (ALS), disrupts circadian rhythms in eclosion, shortens the period of activity rhythms, and reduces mRNA levels of TIM (Lee et al., 2019). In a *Drosophila* model of Fragile X Syndrome (FXS), *dfmr1* mutants have arrhythmic activity and weak eclosion rhythms (Dockendorff et al., 2002; Morales et al., 2002). While the oscillations of the molecular clock or in the PDF levels in the sLNv DP are unaffected, CREB oscillations are dampened, and sLNv DP arborisations are misrouted and are more extensive.

Thus, like their mammalian counterparts, fly models of NDs, including HD, capture the ND-associated molecular, physiological, and behavioural circadian and sleep defects at all levels of circadian organization in both DD and LD. These reports provide a sound basis for using a fly circadian model to understand the circadian disturbances associated with HD, test for ways and means to alleviate them and investigate the relationship between the circadian and the neurodegenerative axes.

1.11.2 Influence of circadian and sleep axes on neurodegeneration

There is proof for a feedforward influence of circadian and sleep disruptions on neurodegeneration, implicating them in the aetiology of NDs (Carter et al., 2021; Voysey et al., 2021a). Consequently, interactions of the circadian and neurodegenerative axes are bi-directional (Lananna and Musiek, 2020; Carter et al., 2021). Circadian health is intricately linked to neuropathology and possibly involves pathways of neuronal proteostasis, immune and inflammatory responses, oxidative stress response, synaptic homeostasis, and neuronal metabolism (Leng et al., 2019; Lananna and Musiek, 2020; Colwell, 2021). Circadian clocks affect the phase and amplitude of peak (or trough) and the period (effective duration) of most physiological processes at the cellular, tissue, organ, systems, and organism levels. It is not surprising that circadian disturbances are often not the primary cause but rather a consequence of ND; their impairment in NDs adds to the pathophysiology and hastens and worsens disease progression.

NDs, like HDs involving aggregation-prone proteins, suffer from disrupted cellular proteostasis. The proteome and physiology are under circadian regulation, allowing circadian health to mitigate or aggravate neurodegenerative processes (Hastings and Goedert, 2013). These circadian influences could occur at protein syntheses and processing stages, such as transcription, translation, protein folding, PTMs, activation and protein clearance via UPS and autophagy. A few examples are the daily rhythms in the expression of pro-survival or pro-death factors, aggregate-prone proteins, and metabolic states, thereby determining the susceptibility of certain daily phases to aggregation, mitochondrial dysfunction, or apoptosis (Hastings and Goedert, 2013; Colwell, 2021). For example, sleep helps in the clearance of misfolded proteins via the regulation of glymphatic flow (Nedergaard and Goldman, 2020), and sleep deprivation leads to amyloid-β (Aβ) accumulation (Shokri-Kojori et al., 2018). The circadian system modulates the expression and levels of redox sensors and antioxidants, affecting the cell's redox state, response, and pre-disposition to oxidative stress (Kondratova and Kondratov, 2012; Giebultowicz, 2018; Lananna and Musiek, 2020). Clock genes such as *Bmal1* are suggested to regulate antioxidant response (Lee et al., 2013). Among other potential links between circadian clocks and

neurodegeneration are the darkness hormone melatonin, a potent antioxidant enriched in the brain and CSF (Reiter et al., 2001b), the inflammatory response, mitochondrial function, and DNA damage repair (Kondratova and Kondratov, 2012; Lananna and Musiek, 2020; Carter et al., 2021; Wang and Li, 2021).

Much evidence provides traction for the impingement of the circadian axis in neuropathology. Functional circadian clocks help manage ageing-related homeostatic challenges and offer neuroprotection during ageing. Overexpression of clock genes in ageing flies or PDF in PDF^{+} LNv slows the age-related deterioration of activity rhythms (Koh et al., 2006; Umezaki et al., 2012). Overexpression of CRY in clock neurons of flies improves the robustness of activity rhythms in DD, extends their lifespan and reduces oxidative damage (Rakshit and Giebultowicz, 2013). Also, neuronal expression of some of the clock genes improves the survival of older flies and modifies resistance to stresses like hyperthermia, oxidation, starvation, and constant light (Solovev et al., 2019). WT *Drosophila* with rhythmic locomotor activity has significantly extended lifespans than arrhythmic ones (Kumar et al., 2005).

Conversely, circadian disruptions compromise neuronal health and further aggravate age-related symptoms. per^{01} flies post-exposure to oxidative stress show a higher mortality rate, more significant accumulation of oxidatively damaged proteins and lipids, and compromised vertical climbing ability than age-matched WT flies (Krishnan et al., 2009). Clock mutant flies the arrhythmic per^{01}, or the short period (16h) per^{T} (that experience chronic jet lag, with a daily 8-h delay), show reduced longevity and startle-induced locomotion with age (a measure of age-related locomotor impairment), with the later having a more severe effect than the former, suggesting that chronic jet lag is more detrimental than arrhythmicity to ageing flies (Vaccaro et al., 2016). Non-native light conditions (20:4) that disrupt circadian rhythms in mice impact their neuronal health, leading to cognitive difficulties (Karatsoreos et al., 2011). Similarly, in hamsters, chronic "jet lag" disrupting circadian rhythms leads to decreased cognitive performance and neurogenesis in the Hippocampus (Gibson et al., 2010; Kott et al., 2012). Epidemiological studies show an association between dampened circadian activity rhythms or sleep fragmentation in cognitively healthy people with an increased risk of developing dementia (Tranah et al., 2011; Lim et al.,

2013). Also, a study in HD patients shows a correlation between sleep disturbances and coexistent anxiety and depression (Jha et al., 2019).

1.11.2.1 Clock gene mutations associated with ND

There is evidence for the involvement of clock genes in protection against neuropathology. Circadian clock disruption via *per* deletion aggravates oxidative stress and decreases the lifespan of *Drosophila* (Krishnan et al., 2008; Krishnan et al., 2009). Age-related dampening of circadian rhythms in flies is associated with decreased levels of *Cry*, the light-responsive clock regulator, and CRY overexpression, which improves rhythmicity (Rakshit and Giebultowicz, 2013). Also, *Bmal1* knockout mice develop astrogliosis independent of SCN and systemic circadian function (Musiek et al., 2013). A direct link between clock genes, circadian control and the aetiology of neurodegenerative diseases is also present. SNPs in *Bmal1* and *per1* increase the predisposition to PD (Chen et al., 2013; Chen et al., 2015b; Gu et al., 2015). Further, the expression of ND causative genes such as *presenilin-2*, *a-synuclein*, *γ-synuclein* and *dTau* are under clock control (Esler and Wolfe, 2001; Panda et al., 2002; Bélanger et al., 2006; Arnes et al., 2019). A recent study finds an association between human CRY1 variants and attention deficit/hyperactivity disorder (ADHD) (Onat et al., 2020).

1.11.2.2 Circadian and sleep disruptions worsen ND

Circadian disruptions negatively impact neuronal and organismal health and worsen neurodegenerative symptoms. These become evident with both circadian-disrupting environments and in the case of clock gene mutations across animal models. In *Drosophila*, altering the duration of light: dark cycles from 12h:12h to 10h:10h reduces mHTT-induces PDF loss from sLNv and mHTT aggregation, and this protection under altered LD is lost in per^{S} mutants, demonstrating that the timing of LD cycles affect mHTT-induced neurodegeneration and involves clock genes (Xu et al., 2019b). Rats exposed to 90 days of continuous bright light show a decrease in TH-positive neurons in the substantia nigra (SN) region, and a reduction of dopamine levels, sensitising them to PD (Romeo et al., 2013). Mice pre-exposed to circadian disruption due to an extended photo phase (LD of 20h:4h) on exposure to PD-inducing MPTP

have exacerbated motor and cognitive deficits, dopaminergic neuronal loss and neuroinflammation (Lauretti et al., 2017b). In AD fly models, alterations of sleep/wake behaviour via exposure to dim light at night or via mechanical or genetic sleep deprivations increase brain vacuole numbers, a sign of neurodegeneration (Kim et al., 2018), induces short-term memory defects (Seugnet et al., 2009) or increases brain Aβ burden and augments the AβArctic-induced increase in neuronal excitability and LNv synaptic morphology (Tabuchi et al., 2015b).

Similarly, in AD mice, sleep deprivation increases Aβ in brain interstitial fluid and Aβ plaque formation, whereas enhancing sleep by blocking wakefulness-promoter Orexin's receptor decreases plaque formation (Kang et al., 2009). Chronic sleep deprivation disrupts circadian gene expression in the SCN and accelerates AD pathology in mice (Niu et al., 2022). Long-term exposure of sub-pathological Aβ rats to LL accelerates aggregation of exogenous Aβ42 (Sharma and Goyal, 2020b). Such correlations are also found in humans. A single night of sleep deprivation increases the Aβ burden in the human brain (Shokri-Kojori et al., 2018), and symptomatic HD patients with sleep problems have more severe neuropsychiatric symptoms (Baker et al., 2016).

HD mice in a *Bmal1* hemizygous background and AD mice with *Bmal1* knockout show exacerbated neurodegeneration, astrocyte activation and altered gene expression, respectively (Musiek et al., 2013; McKee et al., 2022). Deletion of *Bmal1* globally in the brain accelerates amyloid plaque accumulation, while local deletion promotes fibrillar plaque deposition (Kress et al., 2018). Clock mutations in the background of a neurodegeneration-prone mutation (such as *sniffer* or *swiss cheese*) compromise longevity and aggravate neurodegeneration in *Drosophila* (Krishnan et al., 2012). In contrast, in one study, clock gene mutation improves neuropathology, wherein expHTT expression in the LNv of Clk^{Jrk} heterozygotes enhances PDF^{+} sLNv numbers and eliminates expHTT aggregates (Xu et al., 2019a).

1.11.2.3 Cases where circadian disruptions do not appear to affect ND

In a few cases, circadian alterations did not affect some neurodegenerative symptoms. AD flies with deficient clocks (per^0 background) are like those with intact clocks in their climbing ability, neurodegeneration, and longevity (Long et al., 2014a). R6/2 mice treated with bright light and time-restricted voluntary exercise show delay in activity rhythm breakdown and improved synchronisation to LD but not lifespan (Cuesta et al., 2014).

1.11.2.4 Circadian reinforcement improves ND

Bolstering circadian rhythms via environmental, genetic, or pharmacological interventions delays or mitigates neurogenerative symptoms.

***Environmental*:** In R6/2 mice with altered oscillations of peripheral metabolic outputs, a scheduled feeding cycle restores behavioural rhythms and liver metabolic gene expression (Maywood et al., 2010). Time-restricted feeding (TRF) in two HD mice models improves circadian rhythms in behaviour, sleep deficits, autonomic nervous system dysfunction, and motor and cognitive symptoms, alters the phase of PER2::LUC rhythms and restores levels of striatal HD markers comparable to WT (Wang et al., 2018; Whittaker et al., 2018). TRF and treatment with glucagon-like peptide-1 (GLP-1), a metabolic signal to the SCN on feeding, improves various circadian rhythms, metabolic homeostasis, cognitive performance and hypothalamic clock gene expression and reduces ND pathology like Aβ deposits in AD mice (Dong et al., 2022). Repeated phase shifts ameliorate the activity rhythms breakdown in the LD of R6/2 mice (Wood et al., 2013). Blue light therapy in mice HD models (BACHD and Q175) improves activity rhythm defects and motor performance and alters HD markers in the striatum and cortex (Wang et al., 2017). Prolonged daylight exposure (16:8 LD) also improves the survival and rhythm strength of R6/2 mice (Ouk et al., 2017). Sleep Restriction Therapy (SRT), a modality of Cognitive Behavioural Therapy (CBT) for insomnia (CBT-I), is a behavioural intervention that compresses sleep opportunity to match it more closely to sleep ability, leading to enhanced sleep drive (Miller et al., 2014). SRT (via compressing the dark period of LD, i.e. 14:10 LD) reverses

sleep impairments due to Aβ and extends lifespan in flies (Belfer et al., 2021). Bright light therapy improves sleep and helps with depressive symptoms in AD and PD patients (van Wamelen et al., 2015; Liu et al., 2020). Flies affected by glioblastoma-induced neurodegeneration are arrhythmic primarily, and the few rhythmic ones have long period rhythms; exposing them to a 14h:14h LD cycle improves their rhythmicity, lifespan and reduces glioblastoma growth and neurotoxicity (Jarabo et al., 2022).

Exercise: Environmental enrichment and physical exercise have been beneficial in alleviating some of the HD symptoms in HD mice and patients (Carter et al., 2000; Sullivan et al., 2001; Trembath et al., 2010; Wood et al., 2010; Aungier et al., 2012a; Busse et al., 2013; Khalil et al., 2013; Skillings et al., 2014). Aβ42-expressing flies subjected to exercise as locomotor activity via a rotating tube device, "swing boat", for 30 min a day for 12 days lowers nighttime sleep fragmentation and improves nighttime sleep levels and median survival time (Berlandi et al., 2017).

***Social Cues*:** Vehicle-treated R6/2 mice housed together have alterations in their sleep-wake cycle and improvements in cognitive function, suggesting that social settings aid circadian rehabilitation (Pallier et al., 2007). Similarly, housing circadian disrupted HD sheep with a healthy sheep flock improves the HD flock's circadian behaviour, suggesting social cues' influence on circadian abnormalities (Maywood et al., 2010).

***Pharmacological*:** Treatment with either a sleep-promoting or a wake-promoting drug improves cognitive decline and apathy in R6/2 mice while combining the two works best (Pallier et al., 2007; Pallier and Morton, 2009). The sleep-promoting drug also reverses the dysregulated expression of *mPer2* in the SCN (Pallier et al., 2007). Improving sleep via Orexin receptor antagonist mitigates cognitive defects in R6/1 mice (Cabanas et al., 2019). Melatonin, a hormone secreted by the pineal gland that is signalling darkness, delays HD onset, prolongs the lifespan of R6/2 mice, and mediates the neuroprotective effect via the MT1 receptor (Wang et al., 2011). Melatonin is also neuroprotective as its depletion leads to mitochondrial ROS damage and elevates inflammatory response, while its prescription to R6/2 mice reduces inflammation

(Jauhari et al., 2020). In a *Drosophila* HD model, treatment with curcumin, a polyphenol contained in turmeric that activates BMAL1 and melatonin, restores circadian gene expression, activity and eclosion rhythms, and climbing ability (Khyati et al., 2021). Treatment with a REV-ERB (a nuclear receptor and a mammalian circadian clock component) agonist SR9009 reverses cognitive decline and improves synaptic function in an AD mice model (Roby et al., 2019). In AD fly models, pharmacological induction of sleep reverses age-dependent cognitive impairments (McBride et al., 2010; Dissel et al., 2015), memory defects, synaptic deficits, and disrupted cAMP signalling in clock neurons (Dissel et al., 2017).

Genetic: Enhancing sleep genetically by conditionally activating Fan-shaped Body neurons in Aβ expressing flies decreases Aβ burden (Tabuchi et al., 2015b). In an Amyotrophic Lateral Sclerosis fly model, overexpression of *shaggy* (a circadian kinase and the fly homolog of glycogen synthase kinase 3) in the LNv neurons partially improves activity rhythms in DD (Xu et al., 2019a).

1.12 A NEED TO STUDY CIRCADIAN-NEURODEGENERATIVE INTERACTIONS IN HD

From the descriptions above, it is evident that there is a reciprocal relationship between circadian health and neurodegenerative diseases, creating a feed-forward loop where the worsening of one exacerbates the other while improving one enhances the other. This avenue of circadian influence on neurodegenerative aspects is an emerging field. Furthermore, there is limited data on the circadian influence on HD progression, especially regarding environmental influence. Also, investigating the interacting pathways and molecular players involved in and affecting both the circadian and neurological axes has been predominantly studied in a unidirectional manner. There is a pressing need to take an unbiased and integrative approach to examine these interactions under disease conditions to uncover the molecular players and pathways that can serve as potential interfacial/nodal therapeutic targets. Such an approach also serves as a step towards integrating chronotherapy with the more conventional neuropathological treatments, complementing them and improving treatment efficacy. Further, chronobiological therapies are relatively inexpensive, easy to incorporate into the everyday lifestyle and will benefit both the patients and their caregivers.

1.13 OBJECTIVES OF MY STUDY

Given the bi-directional nature of influence and interactions between the circadian and neurodegeneration axes, I set out to characterize the circadian disturbances at both the behavioural and neuronal levels associated with expressing expanded Huntingtin (expHTT) in the PDF expressing LNv subset of *Drosophila* circadian neurons under free-running conditions (DD) and entraining conditions (LD) (Chapter 2). Once the circadian neurodegenerative features were established, I focused on uncovering potential environmental and genetic strategies to alleviate HD-induced circadian behavioural impairments and the associated neuropathology. The rationale for using environmental interventions is that they can directly influence the circadian system and also affect neurodegeneration. They are relatively non-invasive and inexpensive and can be tested directly in clinically relevant mammalian and non-human primate models and adopted into lifestyle with a little effort. Genetic interventions directly uncover genes that affect both the chronobiological and neurological aspects, provide mechanistic insights regarding pathways involved and their interactions and contribute towards integrating chronotherapy into neuromedicine.

The tissue-specific targeting of expHTT to the LNv was achieved using the GAL4-UAS system (Brand and Perrimon, 1993) (Fig 1.10).

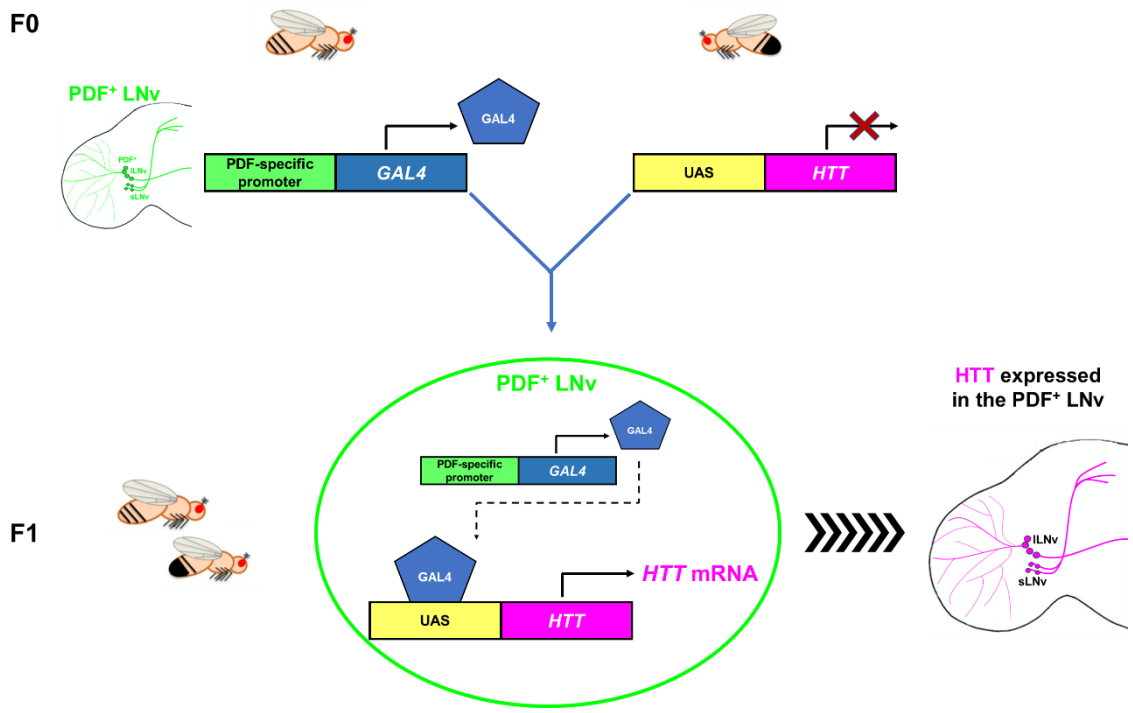

Fig 1. 10 The Drosophila GAL4-UAS system.
The basis of this system is that transcriptional activation of the target gene (*HTT* in this example) fused to an upstream activating sequence (UAS) is achieved when the yeast transcriptional activator *GAL4* binds the *UAS* sequences. Tissue-specificity is ensured by fusing the *GAL4* gene with a tissue-specific promoter, the PDF-specific promoter in this study (henceforth, the *driver* line). A cross between the parental lines (F0), namely, the *pdfGal4 driver* line and the *UAS* line carrying the *HTT* gene (top), yielded progeny (F1) that express *Gal4* in the PDF$^+$ LNv neurons, which binds to the UAS sites upstream of the *HTT* gene and activates its transcription, eventually resulting in HTT expression in the PDF$^+$ LNv (bottom). The gene of interest can be hHTT-polyQ with no Q repeats (Q0) or expanded repeats of 128Qs (Q128).

First, the expHTT-expressing flies were exposed to various light regimes to test the effect of environmental treatments on HD phenotypes. Of particular interest was the effect of the circadian-disrupting regime of constant light on HD-induced circadian dysfunction and neurotoxicity (Chapter 3). The subsequent chapter investigated the impact of circadian-bolstering environments like temperature cycles and other temperature-based regimes that could potentially affect expHTT levels and serve as mild stressors on expHTT-induced circadian behavioural outcomes and neurotoxicity (Chapter 4). I then screened the known cellular neurotoxic modulators of HD to discover those that could specifically modify the circadian behavioural defects of HD flies (Chapter 5). I also looked at the circadian behaviour of *Drosophila* on expressing the full-length expanded HTT or only the expanded polyQ peptide or expanded

Ataxin-3 to test the effects of the protein context flanking the polyQs on the circadian disturbance in NDs and investigated the role of *Drosophila* Huntingtin (*dhtt*) in circadian rhythms and expHTT-induced loss of circadian rhythms (Chapter 6). Throughout this study, I also try to decipher the role of expHTT inclusions in neurotoxicity.

Throughout this study, two categories of inferences have been made. The first is regarding the impact of expHTT on the circadian system at the behavioural and neuronal levels and ways to modify those effects. The second is using the neurodegenerative expHTT to disrupt circadian neuronal functioning and better understand the LNv circuit contribution to rhythmic activity/rest behaviour and CNN communication. The central emphasis of this study is on the former category to improve our understanding of the neurodegenerative processes, including circadian disruptions underlying HD, with conclusions regarding the latter discussed as and when they arise.

CHAPTER 2

Characterisation of a *Drosophila* Circadian Model of Huntington's Disease

Work from this chapter has been published as "Prakash P, Nambiar A, Sheeba V. Oscillating PDF in termini of circadian pacemaker neurons and synchronous molecular clocks in downstream neurons are not sufficient for sustenance of activity rhythms in constant darkness. PLoS One. 2017 May 30;12(5):e0175073."

https://doi.org/10.1371/journal.pone.0175073

2.1 INTRODUCTION

2.1.1 A need for a *Drosophila* circadian model of HD

Circadian and sleep disturbances are one of the hallmarks and early symptoms of HD (Morton, 2013; Herzog-Krzywoszanska and Krzywoszanski, 2019). Recent studies show that neurodegenerative diseases like HD disrupt circadian rhythms, impact neurodegenerative outcomes, and hasten disease progression (Hastings and Goedert, 2013; Musiek, 2015). Interventions that improve circadian rhythms suppress neurogenerative symptoms, and those leading to circadian dysfunction worsen the symptoms (Musiek, 2015; Hood and Amir, 2017b; Giebultowicz, 2018; Leng et al., 2019; Voysey et al., 2021a). I was keen on understanding such systemic interactions and studying HD's impact on circadian rhythms and vice-versa. To do so, I chose the versatile model organism *Drosophila melanogaster,* which has a well-studied circadian neuronal network (CNN) that controls circadian rhythms in physiology and behaviour. Notably, circadian neurons are known targets of neurodegenerative proteins such as expanded Huntingtin (expHTT), as evidenced by loss of molecular clock rhythms, lowered levels of clock outputs, impairment of the mammalian central clock SCN and circadian and sleep disturbances observed in HD models (Morton et al., 2005; Maywood et al., 2010; Kudo et al., 2011; Fifel and Videnovic, 2020).

Most *Drosophila* models of HD target a large group of neurons in the eye or the brain that are not specifically responsible for controlling behavioural readouts such as flying or climbing. Many such behaviours are often not directly functionally associated with the neuronal groups targeted. Also, in many studies targeting a larger neuronal group, the disease modifiers have only been tested for their ability to modify the cellular toxicity of HD and their impact on disease outcomes at the organismal level, such as behaviour, is unknown. The circadian neuronal circuit of the fly, a well-characterised group of neurons known to control a robust and reproducible behavioural output such as the locomotor activity rhythms, helps overcome some of these limitations. The circadian model/framework provides a handle on the neuronal and circuit-function-dependent output levels, i.e., the behavioural levels and readouts of the core clock, neuronal and behavioural

outputs. Thus, it allows for an organismal study to assess the time course and sequence of pathophysiological events and test the efficacy of disease-modifying strategies at multiple levels: the clock's neuronal function (molecular clock and neuronal output) and functionally associated behavioural output, which is also a consequence of the CNN interactions. In the recent past, targeting the fly circadian system for neurodegenerative studies has become popular (Kadener et al., 2006; Sheeba et al., 2010; Chen et al., 2014; Blake et al., 2015; Means et al., 2015; Tabuchi et al., 2015a; Song et al., 2016; Julienne et al., 2017; Buhl et al., 2019; Farago et al., 2019; Xu et al., 2019a).

2.1.2 The *Drosophila* circadian neuronal circuit: A HD model

The circadian neuropeptide Pigment Dispersing Factor (PDF) expressed in the LNv (4 small LNv (sLNv) and 4-5 large LNv (lLNv)) controls rhythmic locomotor activity in DD (Helfrich-Förster, 1995; Renn et al., 1999). sLNv are crucial for behavioural rhythmicity in DD (Grima et al., 2004a; Stoleru et al., 2004). In the *Drosophila* model, the expression of human Huntingtin was targeted to this small group (~8 pairs) of PDF^{+} LNv. Readouts of circadian cellular function and locomotor activity/rest behavioural rhythms helped characterise the effects of expanded HTT (expHTT) expression in the LNv over time.

The current approach helps in drawing two sets of inferences. One is the effect of expHTT on neuronal function in general, with a spotlight on circadian neuronal function, insights into the time course of HD pathogenesis and its impact on circadian rhythms at both the cellular and behavioural levels. The other uses expHTT as a neurodegenerative tool to perturb the LNv subset of the CNN to refine our understanding of LNvs' relative contributions in modulating *Drosophila* activity rhythms. In the current chapter, with the help of the same set of experimental results, I draw inferences regarding how the circadian system is perturbed in HD (see 2.1.3) and on the control of circadian activity rhythms by the LNvs (see 2.1.4 and 2.1.5).

2.1.3 Circadian dysfunction in flies expressing expHTT in the LNv

The first aspect addressed is HD's circadian disruptions and other neurodegenerative features. The specific questions addressed are how expressing expHTT in the LNv of *Drosophila* affects behavioural activity rhythms and sleep in DD (Sections 2.3.1). How are the neuronal circadian markers of the LNv, such as the neuropeptide PDF and core molecular clock protein PER, affected (Sections 2.3.2 and 2.3.5)? Do the behavioural rhythms in DD show a polyQ-length-dependent breakdown (Section 2.3.3)? Is there any evidence for sLNv apoptosis (Section 2.3.4)? Does the expression of expHTT in the LNv alter activity rhythms and sleep in LD (Section 2.3.6)? Do prior light cues influence their entraining ability (Section 2.3.7), and does expHTT expression in the LNv affect the fly lifespan (Section 2.3.9)?

The key findings addressing the above questions are briefly stated here. Upon expressing expHTT, namely HTT-Q128 in the LNv, flies showed an evident circadian dysfunction at both the neuronal and behavioural levels. These flies exhibit disrupted free-running circadian locomotor activity rhythms and loss of clock output neuropeptide PDF from the sLNv soma and molecular clock protein PER and its oscillations in the LNv. They also exhibited some of HD's critical characteristic neurodegenerative features, such as a polyQ length-dependent age-of-onset of arrhythmicity, expHTT inclusions in the LNv, and a selective susceptibility of sLNv to expHTT with loss of PDF from its soma. At the same time, PDF in sLNv axonal arbours and lLNv were not affected. However, the results for cellular dysfunction *vs.* cell death were inconclusive. The activity rest rhythms of these flies showed entrainment to LD without disruptions in sleep levels or quality. Eliminating light cues before LD exposure did not affect the entrainment of activity rhythms of these flies to LD. expHTT expression in the LNv did not affect fly survivorship.

2.1.4 The role of PDF in the sLNv in sustaining activity rhythms

Functional circadian clocks in the LNv, specifically the small LNv, are necessary and sufficient for behavioural rhythmicity in DD (Grima et al., 2004a; Stoleru et al., 2004). Flies lacking PDF

are similar to flies lacking LNv: mostly arrhythmic, and the few weakly rhythmic flies have a short period (Renn et al., 1999). PDF receptor (PDFR) mutants phenocopy pdf^{01} and PDF acting via PDFR on LNv and other circadian neurons is sufficient to rescue rhythmicity (Hyun et al., 2005; Lear et al., 2005; Mertens et al., 2005; Lear et al., 2009). PDF in the sLNv dorsal projections (DP) accumulates rhythmically and is possibly secreted rhythmically (Park et al., 2000). In the absence of external time cues, PDF acts as a coupling signal that synchronises the molecular clocks among circadian neurons to bring about coherent locomotor activity rhythms (Park et al., 2000; Peng et al., 2003; Lin et al., 2004; Stoleru et al., 2005; Nitabach et al., 2006; Fernández et al., 2007b; Wu et al., 2008a; Wu et al., 2008b; Sheeba et al., 2008c). Without PDF, molecular oscillations in the sLNv subgroup dampen and become asynchronous in DD. Furthermore, oscillations in other circadian neurons (LNd, DN1 and DN2) become decoupled from sLNv and run with a short period reflected as weak, short-period activity rhythms (Renn et al., 1999; Peng et al., 2003; Lin et al., 2004; Fernández et al., 2007b; Sheeba et al., 2008c). Additional studies suggest complex functions for PDF: drive molecular rhythms in some neuronal groups, synchronise molecular oscillations among certain circadian neuronal groups and shorten or lengthen periods in other neuronal groups (Stoleru et al., 2005; Yoshii et al., 2009; Yao and Shafer, 2014; Beckwith and Ceriani, 2015b). Studies show that loss of behavioural rhythmicity occurs with disruption of PDF oscillations in sLNv DP, suggesting that PDF oscillations are necessary for activity rhythms in DD (Nitabach et al., 2006; Fernández et al., 2007b; Depetris-Chauvin et al., 2011). In the above studies, the molecular clock in the sLNv is intact, and the output, i.e. PDF oscillations, are affected. However, it is unclear whether, upon disruption of the sLNv molecular clock, PDF oscillation in sLNv DP and its downstream synchronising functions are affected. Also, it is unknown whether, in the absence of PDF in sLNv soma, oscillating PDF in sLNv DP can sustain rhythmic activity. Therefore, I set out to assess the role of the sLNv circadian molecular clock and PDF in modulating locomotor activity rhythms in DD and ask whether the function of PDF is mainly via its oscillations in the sLNv DP.

Under LD, flies without PDF or lacking PDF expressing LNv or with downregulated PDF do not have a morning (M) peak and have an advanced phase of the evening (E) peak (Renn et al., 1999;

Shafer and Taghert, 2009). PDF downregulation in the lLNv alone did not affect activity rhythms under LD, showing that sLNv PDF is sufficient for M-activity (Shafer and Taghert, 2009). However, whether sLNv PDF is necessary for M-anticipation is unclear. Previous studies did not achieve a complete PDF loss, specifically from sLNv soma and DP (Shafer and Taghert, 2009; Sheeba et al., 2010). I established such a phenotype using a combination of genetic and environmental strategies. There is a complete loss of PDF selectively from the sLNv (both in soma and DP), and this allowed me to test the necessity of sLNv PDF for M-anticipation.

2.1.5 A refined understanding of the role of PDF and sLNv in modulating activity rhythms

The study's second objective was to explore the role of LNv, especially sLNv and PDF, in driving activity rhythms with the help of expHTT, which disrupts the LNv function. The critical questions raised are the following: (a) whether the sustenance of free-running rhythms by sLNv in DD is limited to its output as oscillations in PDF levels in its DP and downstream synchrony of molecular oscillations in the PDF^- neurons (Section 2.3.5), (b) the role of the LNv molecular clock probed via PER oscillations in driving these rhythms (Section 2.3.5), and (c) the role of the sLNv PDF and PER in the entrainment of activity rhythms to LD cycles, particularly the M-anticipation (Sections 2.3.8 and 2.3.9).

Expressing expHTT in the LNv enabled selective PDF loss from sLNv soma without affecting PDF in the lLNv. Such flies helped assess the role of sLNv PDF and its oscillations in the dorsal projections in driving activity rhythms in DD. Despite lacking PDF and PER in the sLNv soma, these flies showed PDF oscillations in the sLNv DP and synchronous PER oscillations in the downstream circadian neurons and, yet, were behaviourally arrhythmic in DD. These results suggest that PDF oscillations in the sLNv DP are insufficient to sustain activity rhythms in DD. Results also allude to an additional component in the sLNv for the free-running activity rhythm sustenance: independent of the PDF oscillations in the sLNv DP and possibly dependent on the PDF in the sLNv soma and PER-driven molecular clock of the sLNv.

Under LD, flies completely lacking PDF from the sLNv exhibited M-peak with anticipation to lights-ON and correctly phased E-peak, showing unambiguously that sLNv PDF is not necessary for M-anticipation. PDF in the lLNv is sufficient for this behaviour. Additionally, the finding that activity rhythms entrain to LD with a clear M-peak even when PER is undetectable in the sLNv demonstrates that PER-driven clocks in the sLNv are unnecessary for the M-peak.

2.2 MATERIALS AND METHODS

2.2.1 Fly lines

Transgenic fly lines with the coding region for the first 548 amino acids of the *Htt* gene containing either non-expanded form without polyQ repeats (*w;+;UAS-HTT-Q0A;+*) or an expanded tract of 128 glutamine (Q) repeats (*w;UAS-HTT-Q128C;+*) were a gift from Troy Littleton, Massachusetts Institute of Technology (Lee et al., 2004). Transgenic fly lines with Exon1 coding for 81 amino acids of the *Htt* gene containing either a non-expanded form with 20 Q-repeats (*w;UAS-HTT-Q20;+*) or expanded forms with intermediate Q-repeats of 50 (*w;+;UAS-HTT-Q50*) or with higher Q-repeats of 93 (*w;+;UAS-HTT-Q93*) was a gift from J Lawrence Marsh, UC Irvine.

In a previous study that used the above fly lines, the genetic background was *yw* and even controls *yw/Q0*, *yw/Q128* and *pdfGal4/Q0* exhibit relatively poor rhythmicity - ranging from about 60 to 70% (Sheeba et al., 2010). For this study, the flies were backcrossed onto a w^{1118} background for over seven generations to negate the possible genetic background influences. Males of *UAS-HTT* were crossed either with females of w^{1118}*;pdfGal4;+* to obtain flies that expressed non-expanded or expanded form of Huntingtin in the PDF neurons (*pdf>Q0* or *pdf>Q128*) or with females of w^{1118}*;+;+* (BL 5905) to obtain UAS controls (*Q0* and *Q128*). *pdfGal* denotes the Gal4 control, and w^{1118} serves as the background control. Similarly, the *pdf>Q20*, *pdf>Q50* and *pdf>Q93* lines were made. For co-expression of HTT-Q and PDF in the LNv neurons, *ywpdfGal4;UAS-PDF:+* were crossed with *UAS-HTT-Q* lines to obtain *pdf>Q0,PDF* and *pdf>Q128,PDF*. *UAS-pdf* was a gift from Paul Hardin, Texas A& M University (Renn et al., 1999). For co-expression of HTT-Q and myrGFP in the LNv, w^{1118}*;+;pdfGal4* females were crossed with *w;UAS-HTT;UAS-myr-GFP* males (*pdf>Q0,GFP* and *pdf>Q128,GFP*). For co-expression of HTT-Q and Apoliner in the LNv, w^{1118}*;+;pdfGal4* females were crossed with *w;UAS-HTT-Q;UAS-Apoliner* (*pdf>Q0,Apo* and *pdf>Q128,Apo*). The *UAS* lines were *myrGFP* (BL32200) and *Apoliner* (BL32123). Unless specified otherwise, all fly lines and crosses were maintained on a standard cornmeal medium under 12:12h LD cycles at 25˚C. Subsequently, activity was recorded in specific light regimes from post-eclosion age day 3 (3d, henceforth age is denoted in this format) to capture changes from an early age.

2.2.2 Behavioural assays

Virgin male flies (age 1-2d-old) were housed individually in glass tubes (length 6.5 cm, diameter 7 mm), with one end having corn food (0.25 ml) and a seal of paraffin wax and the other end plugged with cotton. Their activity rhythms were recorded using the TriKinetics DAM system (TriKinetics, Waltham, MA). The assays were carried out at 25°C in incubators (Sanyo MIR-154 and Percival DR36VL). Data were collected every 5 min in most cases; in the LL experiment, the data were collected every 1 min; for the dim LD and phase shift experiments, glass tubes of 5mm diameter were used. For the LL experiment, flies were transferred into tubes with fresh food at ages 9 and 23. Raw time series data obtained during DD have been analysed with the CLOCKLAB software (Actimetrics, Wilmette, IL) Chi-square periodogram with a cut-off of p = 0.01 (Pfeiffenberger et al., 2010).

The rhythm characteristics were quantified over three 7d age windows (AWs) comprising AW1 (age 3d-9d early window), AW2 (age 10d-16d middle window) and AW3 (age 17d-23d late window) to track progressive changes. The amplitude of the periodogram over the 1% cut-off was used to measure the rhythm robustness. A fly was considered rhythmic if the periodogram amplitude was above the cut-off, and this was further confirmed with a visual inspection of the actogram. The following steps were carried out to determine the extent of daily activity consolidation '*r*'. 24h activity/rest time series data binned every 1h were converted into a polar coordinate system of a circle made of 24 points. The 24 equidistant points around the circle represented the time of the day and the related activity at each of those 24 time points. Each such point on the circle was resolved into their Cartesian x and y coordinates by multiplying that time's sine and cosine values with activity counts in that hour, thus assigning an activity level to each of the 1h bin time points. A vector sum of the resolved x and y coordinates normalised by total daily activity provided the X and Y vectors for daily activity distribution. The resultant of these two vectors is '*r'* (radius of the unit circle). This radial distance '*r*' from the centre indicates the extent of activity consolidation. Due to the multiplication of sine and cosine values for each time point with the activity at that time, a rhythmic fly with consolidated activity is expected to have a higher

magnitude of '*r*'. In contrast, an arrhythmic fly with daily dispersed activity has a lower '*r*' because the activity is multiplied by all the time points in a day. Daily '*r*' was averaged across flies.

The daily activity counts were calculated by averaging 15 min binned raw data across flies over 24h. The mean activity profiles for LD were plotted by averaging 15min activity counts over 7d for an individual and then averaging across flies. The measures for morning and evening anticipation, the anticipation indices (AI), were quantified by a previously reported method as the ratio of activity counts 3h before dark/light or light/dark transitions to the activity count 6h before that transition (Harrisingh et al., 2007). Mean normalised activity profiles are plotted by averaging 15min binned individual fly raw activity over 5d, normalized by the individual's total activity, and averaged across flies. Sleep was analysed using the PySolo software described previously (Gilestro and Cirelli, 2009), with data collected every minute.

2.2.2.1 Statistical analysis

The proportion of rhythmic to arrhythmic flies between genotypes for each AW was compared using an mxn Fisher's Exact contingency test followed by multiple 2x2 Fisher's tests. The *p*-values were corrected for False Discovery Rate (FDR, FDR set at 5%) using the Benjamin-Hochberg procedure. For comparison of rhythmicities of a genotype across AWs, the Cochran Q test followed by pairwise McNemar's test and Bonferroni corrections were carried out. With multiple independent experiments (as in Fig 2.1), a repeated-measures ANOVA was carried out on arcsine square-root transformed proportions of rhythmicity with genotype as the categorical factor, followed by post-hoc with Tukey's HSD test. For comparisons of genotypes or of AWs (or age) in terms of period, rhythm robustness, '*r*', activity levels, anticipation indices, and sleep, the data sets (or transformed data sets) were analysed for ANOVA assumptions of normality and variance homogeneity using Shapiro-Wilk test and Levene's test respectively. A repeated-measures ANOVA was carried out if these two assumptions and the assumption of sphericity were satisfied (using Mauchly's Sphericity test), followed by Tukey's HSD or Unequal N Tukey's

HSD post-hoc tests, depending upon the data set. Suppose even one of the conditions was not met. Then, instead of a repeated-measures ANOVA, the data sets comparing genotypes for an AW (or age) were suitably transformed to test for assumptions of one-way ANOVA. Where the data set was normally distributed, and their variances were found homogenous, a one-way ANOVA was done, followed by post-hoc testing with Tukey's HSD or Unequal N Tukey's HSD. If the datasets were normally distributed but did not satisfy the assumption of variance homogeneity, the Welch ANOVA followed by Games-Howell tests were carried out. Where the data sets were not normally distributed despite transformations, the non-parametric Kruskal-Wallis test followed by multiple comparisons of mean ranks (corrected for the number of comparisons) was carried out. Friedman's test, followed by pairwise Wilcoxon tests with Bonferroni corrections, was applied to compare a genotype between AWs. To compare a genotype between ages (e.g. with *r*-value, daily activity and sleep levels), Friedman's test for repeated measures followed by post-hoc tests with the Conover and Benjamini-Hochberg methods were used. For Benjamini-Hochberg, FDR was set at 5%. Two-way factorial ANOVA followed by Unequal N Tukey's HSD was conducted to compare genotypes and regimes in an AW (Fig 2.14c-f). Specifically, for between-genotype-comparisons for an AW (or an age), the Kruskal-Wallis test for the period (Figs 2.1e and 2.4e) and '*r*' (Figs 2.1c and 2.4c), an ANOVA (Fig 2.1d) or the Welch's ANOVA (Fig 2.4d) for rhythm robustness, a repeated measures ANOVA (Fig 2.1f) or the Welch's ANOVA for activity levels (Fig 2.4f), the Welch's ANOVA for daily sleep in DD (Fig 2.1g), a one-way ANOVA for daytime sleep, nighttime sleep and daily sleep in LD (Fig 2.9g), a one-way ANOVA for daytime activity, nighttime activity and daily activity levels (Figs 2.9c-d and 2.11d), a Kruskal-Wallis test for day and night activity (Fig 2.10c-d), a one-way ANOVA for morning and evening anticipation indices (Figs 2.9e-f, 2.10e-f, 2.11e) and a Kruskal-Wallis test for morning anticipation index (Fig 2.11e) were carried out.

Statistical analyses were mainly executed using STATISTICA™ 7.0 (StatSoftInc, 2004) and R (RCoreTeam, 2013). Welch's ANOVA was performed using a Microsoft Excel template from http://www.biostathandbook.com/onewayanova.html (McDonald, 2014), McNemar's test

using SciStatCalc (SciStatCalc) and Friedman's test followed by the Conover test for '*r*', activity and sleep levels using ASTATSA (ASTATSA).

2.2.3 Immunocytochemistry and image analysis

A previously described immunocytochemical method was used (Sheeba et al., 2008c). Adult fly brains were dissected in ice-cold 1X PBS at specified ages, fixed with 4% paraformaldehyde at room temperature (RT) for 30 minutes. 10% horse serum in 0.5% PBT was used as a blocking solution. For co-staining with anti-HTT, samples were incubated with blocking-solution for 1h at RT, 6h at 4°C and primary antibody for 48h at 4°C. For co-staining with anti-PER and anti-PDF, samples were incubated with blocking solution for 1h at RT, overnight at 4°C and primary antibody for 48h at 4°C. For single staining with anti-PDF, the samples were incubated with blocking solution for 1h at RT and with primary antibody for 24h at 4°C. Incubation with secondary antibodies was for 24h at 4°C. Post-immunostaining, whole brains were mounted on slides using 70% glycerol in 1XPBS.

Primary antibodies used were anti-Huntingtin Mouse (1:500) (Millipore MAB2166) along with anti-PDF Rabbit (1:30,000) (a gift from Michael Nitabach, Yale University) and anti-GFP Chicken (1:1000) (Sigma-Aldrich G6539), anti-PER Rabbit (1:20,000) (a gift from Jeffrey C Hall, Brandeis University) with anti-PDF Mouse (1:5000) (DSHB PDF C7). Secondary antibodies Alexa Fluor (Invitrogen) (1:3000) anti-rabbit488, anti-rabbit546, anti-mouse546, anti-mouse633 and anti-chicken488 were used.

pdf>Q128 flies were grouped into rhythmic (Rhy) or arrhythmic (Arr) categories based on the method described above to ascertain the status of PDF and were sampled on alternate days for dissection at CT2-4 following the previous LD. Since most *pdf>Q128* flies are arrhythmic, few rhythmic flies were available for dissection at ages 7d and 15d.

For PDF oscillations in the sLNv DP, *pdf>Q128* and *Q128* flies were dissected at age 9d at CT2-3 (CT2), CT6-7 (CT6), CT10-11 (CT10), CT14-15 (CT14), CT18-19 (CT18) and CT22-23 (CT22) in DD (7d in DD) or ZT2-3 (ZT2) and ZT11-12 (ZT11) in LD and stained with anti-PDF rabbit (1:30,000). For PER oscillations, 9d-old *pdf>Q128* and *pdf>Q0* were dissected at CT23-

24 (CT23), CT5-6 (CT5), CT11-12 (CT11), CT17-18 (CT17) or ZT23-24 (ZT23), ZT5-6 (ZT5), ZT11-12 (ZT11), ZT17-18 (ZT17). These samples were co-stained with anti-PDF to enable the identification of the LNvs. A change in PER intensity across time points was considered a circadian oscillation when intensity at a time point is statistically different from its neighbouring time points on either side.

For detecting PDF in the sLNv DP in flies reared in constant light (LL), a higher concentration of anti-PDF rabbit (1:10,000) was used to detect very low PDF levels. In many flies expressing expHTT in the LNv, PDF was not detected in the sLNv soma, although it could be present at extremely low levels. However, despite increasing antibody concentrations thrice the usual levels, PDF was not detected in the sLNv soma of most *pdf>Q128* flies (section 2.3.5), suggesting that PDF in sLNv soma is possibly negligibly small or altogether eliminated. In contrast to PDF in sLNv soma, PDF was readily detected in sLNv DP and lLNv. A higher concentration of anti-PER Rabbit (1:5000) was also used to detect low levels of PER in *pdf>Q128*.

2.2.3.1 Image acquisition and analysis

The samples were viewed under a Zeiss Axio Observer Z1 epifluorescence microscope using the 63X/oil1.4 objective. PDF^+ LNv were counted, and the presence of DP was noted. Images were captured as a *z*-stack of 1µm interval using the 40X/oil1.3 objective, keeping the lamp intensity and exposure time constant across samples to quantify PDF intensity in the sLNv DP. NIH imaging software ImageJ (Schneider et al., 2012) was used on maximum intensity projection images to quantify PDF intensity in the DP by subtracting the DP intensity from an area-matched background by an analyser blind to the genotype and time point. At least three independent experiments per light regime with two-time points corresponding to the peak and trough were carried out to confirm oscillations of PDF in sLNv DP of *pdf>Q128*.

For quantification of PER intensity, images were captured as described above. The PER intensity for a cell at its sharpest *z*-plane was obtained, and the mean PER intensity of that group was subtracted from an equal area of average background intensity in the vicinity using image J (Sheeba et al., 2008c). At ZT11, as no or negligible PER signal was observed in both genotypes, PER intensity was assigned a low value of 0.001. In DD, when PER signal was not detected above the background on quantification, PER intensity was set to 0.001. In DD, when an LNv was observed with PDF staining but no corresponding signal over the background in PER, the PER intensity for those LNv was assigned a value of 0.001. The standard deviation (SD) for PER intensity was calculated for each hemisphere. The mean SD across hemispheres was compared between genotypes for each time point to determine the extent of synchrony within a neuronal group (Zhang et al., 2010a). Confocal *z*-stacks were captured using Zeiss LSM700, LSM 880 and Olympus FV1000 for representative images. To aid the visualisation of DNs, they have been uniformly imaged at a higher laser power and PMT gain than the LNs.

2.2.3.2 Statistical analysis

A two-way ANOVA was performed with genotype and age or regime and age as fixed factors for cell numbers. For PDF and PER staining intensity, a two-way factorial ANOVA was carried out with genotype and time as the fixed factors. Post hoc multiple comparisons were conducted using

Tukey's Honest Significant Difference test at α = 0.05. The Kolmogorov-Smirnov test was done for cell number distributions at $\alpha = 0.05$.

2.2.3 Lifespan assay

Lifespan assay was carried out in flies of *yw* background. Ten replicate vials containing ten 2d-old virgin males were set up for each genotype. The vials were placed horizontally in DD at 25°C, and every day at nearly the same time, the vials were examined, and any dead flies were noted under a safe red light. Flies were transferred into fresh food vials once every three days in DD. Survivorship curves for each genotype were plotted following the flies' death. The mean lifespan per vial was calculated and averaged over vials. A one-way ANOVA with genotype as the fixed factor was carried out for statistical analysis of mean lifespan, followed by post hoc comparisons using Tukey's Honest Significance test at α = 0.05.

OriginPro 8 (Origin(Pro)), Sigma Plots 11.0 (SigmaPlot), and Adobe InDesign 3.0 (AdobeIndesignCS) were used for making figures.

2.3 RESULTS

2.3.1 Expression of expHTT in the LNv abolishes free-running rhythms

A previous study showed that expression of expHTT (HTT-Q128) in the PDF expressing LNv (henceforth denoted as PDF^{+} LNv) results in the flies showing arrhythmic locomotor activity in constant darkness as early as 3d, with a selective loss of PDF-only from the sLNv (Sheeba et al., 2008b; Sheeba et al., 2010). However, in that study, the rhythmicity of control flies was low (Sheeba et al., 2010); therefore, I backcrossed the flies to reduce background effects. These *pdf>Q128* flies were arrhythmic from the first day in DD (Fig 2.1a top-centre), whereas all controls were rhythmic (Fig 1a), and the percentage of rhythmic *pdf>Q128* flies was significantly lower than controls across AWs (Fig 2.1b). Thus, in a w^{1118} background, despite the controls exhibiting close to 90-100% rhythmicity across age, HTT-Q128 expressing flies were mostly arrhythmic in DD with no rhythm improvement even after sufficient time, concordant with the previous study (Sheeba et al., 2010). Also, arrhythmicity set in as early as age 3d, immediately upon placing the flies in DD (Fig 2.1a). Together with the previous study where flies received 4d of LD before entry into DD (Sheeba et al., 2010), these results suggest that the duration of LD post-eclosion and before the DD are not critical in determining the day of arrhythmicity onset. To obtain a more detailed temporal resolution of change in rhythm features (daily, as opposed to 7d AWs), I estimated '*r*', an indicator of the consolidation of daily activity. *pdf>Q128* flies showed poor daily activity consolidation '*r*' than controls for most of the time of activity recording, beginning at age 6d, up to 19d, (at which time, controls also started to show a reduction in *r*) (Fig 2.1c). A small fraction of *pdf>Q128* flies was weakly rhythmic, as evidenced by very low values for robustness, and exhibited close to 24h periods (Figs 2.1d and 2.1e). Flies expressing the non-expanded form HTT-Q0 (*pdf>Q0*) showed robust rhythms comparable to *pdfGal* and w^{1118} (Fig 2.1d) with a consistently long period, which is partly reflective of the long period of the genetic background of its parent, the driver *pdfGal4* (Fig 2.1e). The *UAS* control *Q128* showed relatively less robust rhythms than other controls in AW2, though not as poor as *pdf>Q128* flies (Fig 2.1d).

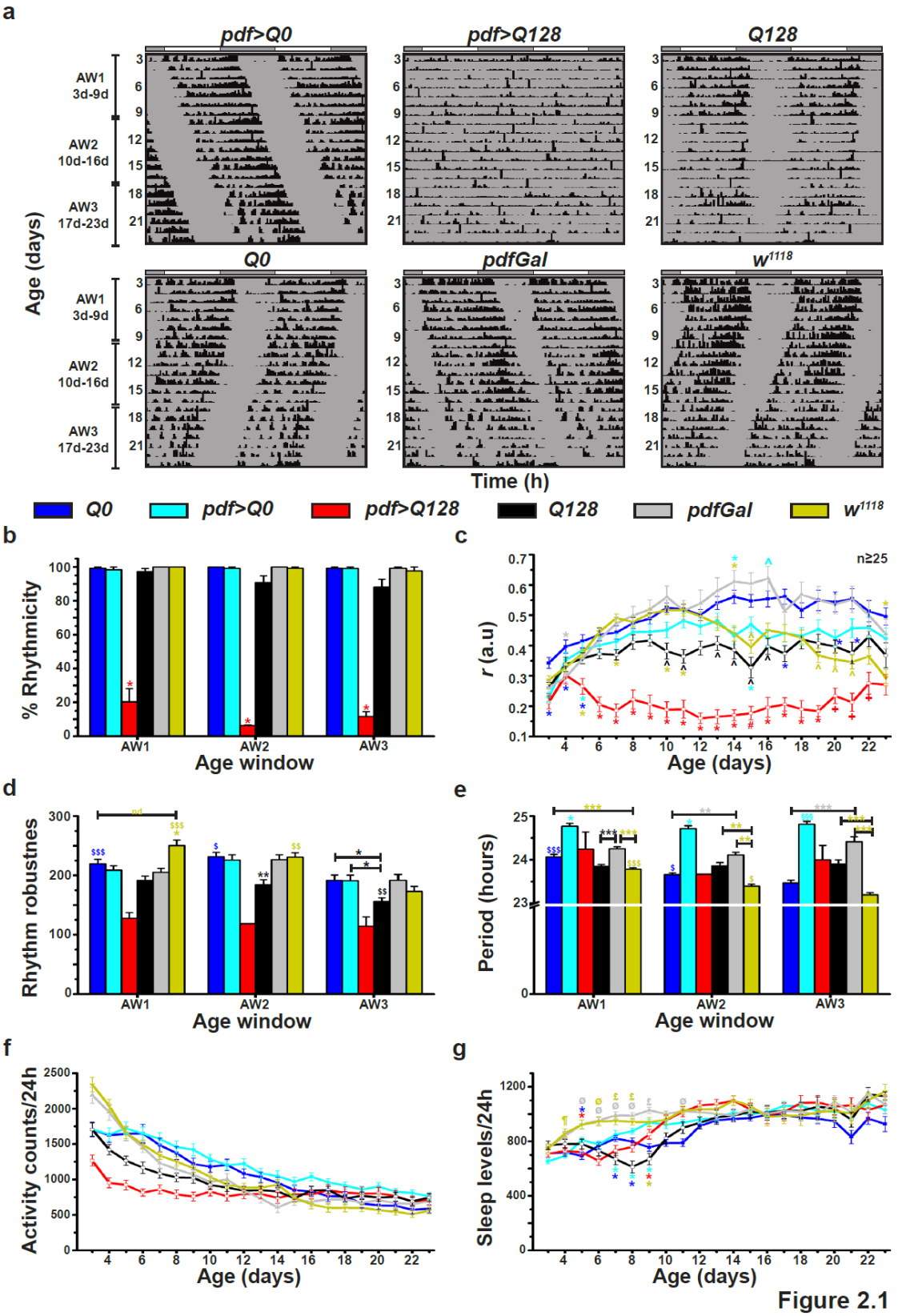

Fig 2. 1 Flies expressing expHTT in the LNv exhibit a loss of locomotor activity/rest behavioural rhythms in constant darkness.

(a) Representative double plotted, normalized actograms (*x*-axis = 48h) for *pdf>Q0*, *pdf>Q128*, *Q128*, *Q0*, *pdfGal* and w^{1118} depicting activity data for >21days in DD (age 3d-23d on *y*-axis).

The 21d activity data is divided into three 7d age windows (AWs), namely AW1 (3d-9d), AW2 (10d-16d) and AW3 (17d-23d), as depicted on the left side to capture progressive changes. The white and grey bars above actograms represent light and dark phases of the previous LD. (b) The percentage of rhythmic flies averaged over four independent experiments is plotted across three AWs. *pdf>Q128* has significantly poor rhythmicity compared to other genotypes (* $p<0.001$). (c) Mean '*r*' per day across age. Symbols indicate statistically significant differences at $p<0.05$: specific colour * indicates a difference of that coloured genotype from the genotype nearest which the * is placed or is indicative of difference from all other genotypes in cases where a coloured * is placed near the same coloured genotype, coloured # indicates a difference of that specific-coloured genotype from all other genotypes except *Q128*, coloured ^ indicates a difference of that specific-coloured genotype from *Q0* and *pdfGal*, coloured + indicates a difference of that specific-coloured genotype from all genotypes except w^{1118}. n≥25 indicates that at least 25 flies remained alive for all genotypes up to age 23d. (d) Mean robustness of rhythmic flies across age. In AW1, w^{1118} has significantly more robust rhythms than other genotypes (* $p<0.05$). In AW2, *Q128* has relatively less robust rhythms than other genotypes (** $p<0.01$). *pdf>Q128* was not considered for statistical tests, as few were rhythmic. nd, not different. (e) Mean free-running period across AWs. Symbols indicate statistically significant differences (* $p<0.05$, ** $p<0.01$ and *** $p<0.001$). *pdf>Q0* has a longer period than other genotypes (cyan * $p<0.05$) in AW1 and AW2 and from all genotypes except *pdfGal* in AW3 (cyan §§§ $p<0.001$). *pdf>Q128* was not considered for statistical tests, as few were rhythmic. (f) Mean daily activity counts across age. (g) Mean daily sleep levels across ages. Symbols indicate statistically significant differences, as described in (c). Additionally, ¶ indicates difference from *pdf>Q0*, *pdf>Q128* and *Q0*, £ difference from *pdf>Q128*, *Q0*, and Q128, and ø difference from *pdf>Q0*, *pdf>Q128*, *Q0*, and *Q128*. Across all panels, coloured $ indicates a difference between AWs for that genotype ($ $p<0.05$, $$.$p<0.01$and $$$ $p<0.001$), and error bars are SEM.

The *pdfGal4* driver, in addition to driving expression in the PDF$^+$ small and large LNv of the *Drosophila* brain, also targets four large and two small abdominal neurons in the ventral nerve cord (Ab-PDF) (Helfrich-Forster, 1997). The Ab-PDF neurons do not express the molecular clock genes, are unaffected by PDF neurons in the Ventral nerve Cord (or abdominal PDF or Ab-PDF neurons) do not express the molecular clock genes, are unaffected by Clk^{Jrk} and cyc^{01} mutations and PDF from these neurons are not necessary for circadian activity rhythms in *Drosophila* (Park et al., 2000; Shafer and Taghert, 2009; Nassel and Winther, 2010). However, PDF in the Ab-PDF neurons modulates the period of the molecular clocks in the oenocytes (peripheral tissues that produce pheromones) and their oenocyte's physiological output (Krupp et al., 2013). Since the circadian behaviour readout used in my study is the circadian locomotor activity rhythms, for which the PDF from the abdominal ganglia is dispensable, the effects of expressing expHTT using *pdfGal4* on the activity rhythms are primarily attributed to their effect on the PDF$^+$ LNvs in the fly brain.

Arrhythmicity and poorly consolidated activity are often associated with changes in activity levels *per se*. Even though young *pdf>Q128* flies showed relatively low activity levels, they were not statistically different from controls (Fig 2.1f). Given that HD causes sleep disturbances, upon examination of sleep levels in these flies, young flies of *pdf>Q128* had lowered daily sleep levels than *pdfGal* & *w1118*, but so was the case with *pdf>Q0*, *Q0*, and *Q128* (Fig 2.1g). *pdf>Q128* flies had fragmented sleep with lower bout length and higher bout number than most controls except *Q128* (not shown), which is likely a genetic background effect. In summary, flies expressing expHTT in PDF neurons have poorly consolidated activity/rest rhythms evidenced by arrhythmicity, while their sleep is not compromised.

2.3.2 expHTT expression in LNv led to selective loss of PDF from the sLNv soma, while PDF presence in dorsal projections is unaffected

I then asked whether the weak rhythms of rhythmic *pdf>Q128* flies corresponded to having a significantly greater number of PDF^+ sLNv than their arrhythmic counterparts. A previous report suggests that a single LNv is sufficient to elicit rhythmicity in DD if the LNv terminals reach the superior protocerebrum (Helfrich-Förster, 1998). Across age, *pdf>Q128* flies (Rhy and Arr) had significantly fewer PDF^+ sLNv soma (Figs 2.2a and 2.2b top). The frequency distribution of the PDF^+ sLNv soma showed a left skew towards 0, significantly different from the right-skewed distribution of *pdf>Q0* across age (Fig 2.3a Fig left). In contrast, the PDF^+ lLNv soma numbers and distributions were comparable between genotypes (Figs 2.2a and 2.2b bottom, Fig 2.3a right). Consistent with reported results (Sheeba et al., 2008b; Sheeba et al., 2010), most *pdf>Q128* flies showed loss of PDF from the sLNv soma (Fig 2.2a). Interestingly, in *pdf>Q128* flies, the number (Fig 2b top, blue *vs* red bars) and frequency distribution (Fig 2.3a) of PDF^+ sLNv soma between rhythmic and arrhythmic individuals were not different at ages 7d and 15d. Notably, rhythmic and arrhythmic *pdf>Q128* flies had PDF in their sLNv DP (Fig 2.2a). Pooling weakly rhythmic flies of ages 7d and 15d, about 71% of flies (10/14 brain samples) did not have detectable PDF in the sLNv soma. Still, they had PDF in their DP (Fig 2.2a centre), suggesting that their residual rhythmicity might stem from PDF in the DP or non-sLNv mechanisms. In a tiny proportion of arrhythmic flies (10/73), at least one PDF^+ sLNv soma was detectable until age 15d (Figs 2.2a third column and 2.3a). However, regardless of PDF absence from the sLNv soma, these

arrhythmic flies exhibited PDF in their sLNv DPs (Fig 2.2a third, fourth columns), revealing that the presence of PDF$^+$ sLNv with intact DP does not ensure rhythmicity. These findings show that for most *pdf>Q128* flies, weakening or breakdown of activity rhythms is associated with PDF loss from sLNv soma, while PDF is present in their sLNv DPs and lLNvs.

In both rhythmic and arrhythmic flies of *pdf>Q128*, the inclusion form (Inc) of expHTT was found in the LNv, whereas HTT in the LNv of control *pdf>Q0* was completely diffuse in appearance (Fig 2.1a second-row).

Since very few *pdf>Q128* flies had PDF$^+$ sLNv soma and when present, their numbers were significantly small, I did not quantify the PDF levels or cellular distribution in these cells. In a separate experiment, at the centre of AW1 (age 5d-6d), when a sufficiently high number of flies would likely have at least one PDF$^+$ sLNv, I found no difference between PDF levels in the soma of sLNv or lLNv between *pdf>Q128* and *pdf>Q0* (Fig 2.3b). To overcome PDF depletion by expHTT, PDF was co-expressed with HTT-Q128 in the LNv (*pdf>Q128,PDF*). However, such flies were arrhythmic, like *pdf>Q128*, and their percentage rhythmicities were significantly lower than controls (Figs 2.3c and 2.3d).

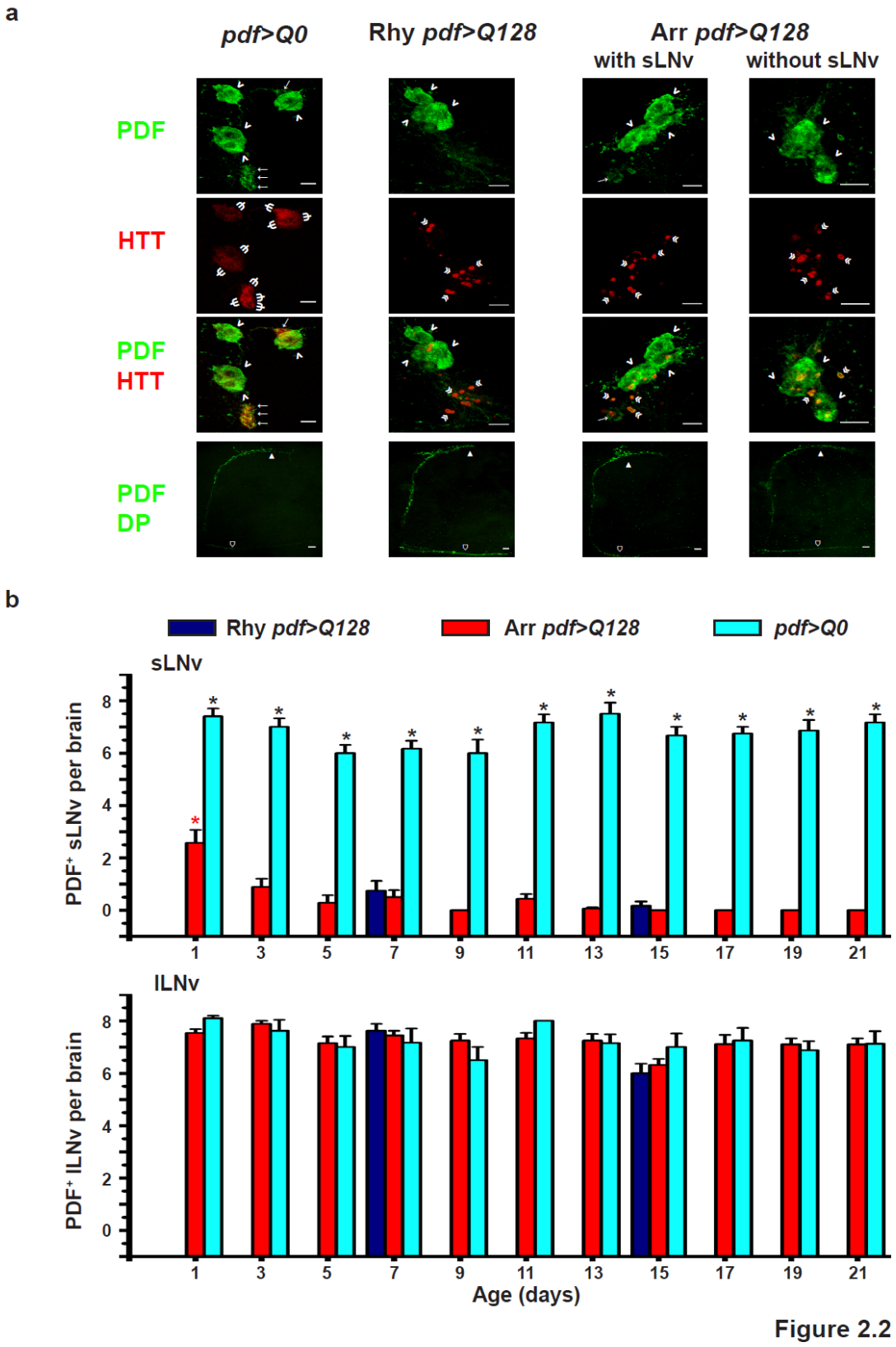

Fig 2. 2 Behaviourally rhythmic and arrhythmic pdf>Q128 flies mostly lack PDF in their sLNv soma, which is present in their DP.

Representative images of adult brains of rhythmic *pdf>Q0* (age 11d), rhythmic *pdf>Q128* (age 7d) and arrhythmic *pdf>Q128* (age 11d) stained for PDF(green) and HTT (red) showing sLNv soma (→ arrows), lLNv soma (> arrowheads), sLNv dorsal projections (▲ triangles), lLNv contralateral projections (⌂ house), diffuse HTT staining (Ψ psi) and inclusions of expHTT (« double arrowheads). Examples of arrhythmic *pdf>Q128* with one sLNv soma (third column) and no sLNv (fourth column) are shown. Scale bars are 10 µm. (b) Top: Average number of PDF^+ sLNv soma per brain for rhythmic *pdf>Q0* flies and arrhythmic *pdf>Q128* flies across age and for rhythmic *pdf>Q128* at ages 9d and 15d. Symbols indicate statistically significant differences: * (black) between *pdf>Q128* and *pdf>Q0* for each age (p<0.0001), * (red) between *pdf>Q128* at age 1d from both rhythmic and arrhythmic *pdf>Q128* at other ages (p<0.001). Bottom: Average number of PDF^+ lLNv soma per brain plotted as in top panel. n= 6-10 whole brains/genotype/age. Across all panels, error bars are SEM.

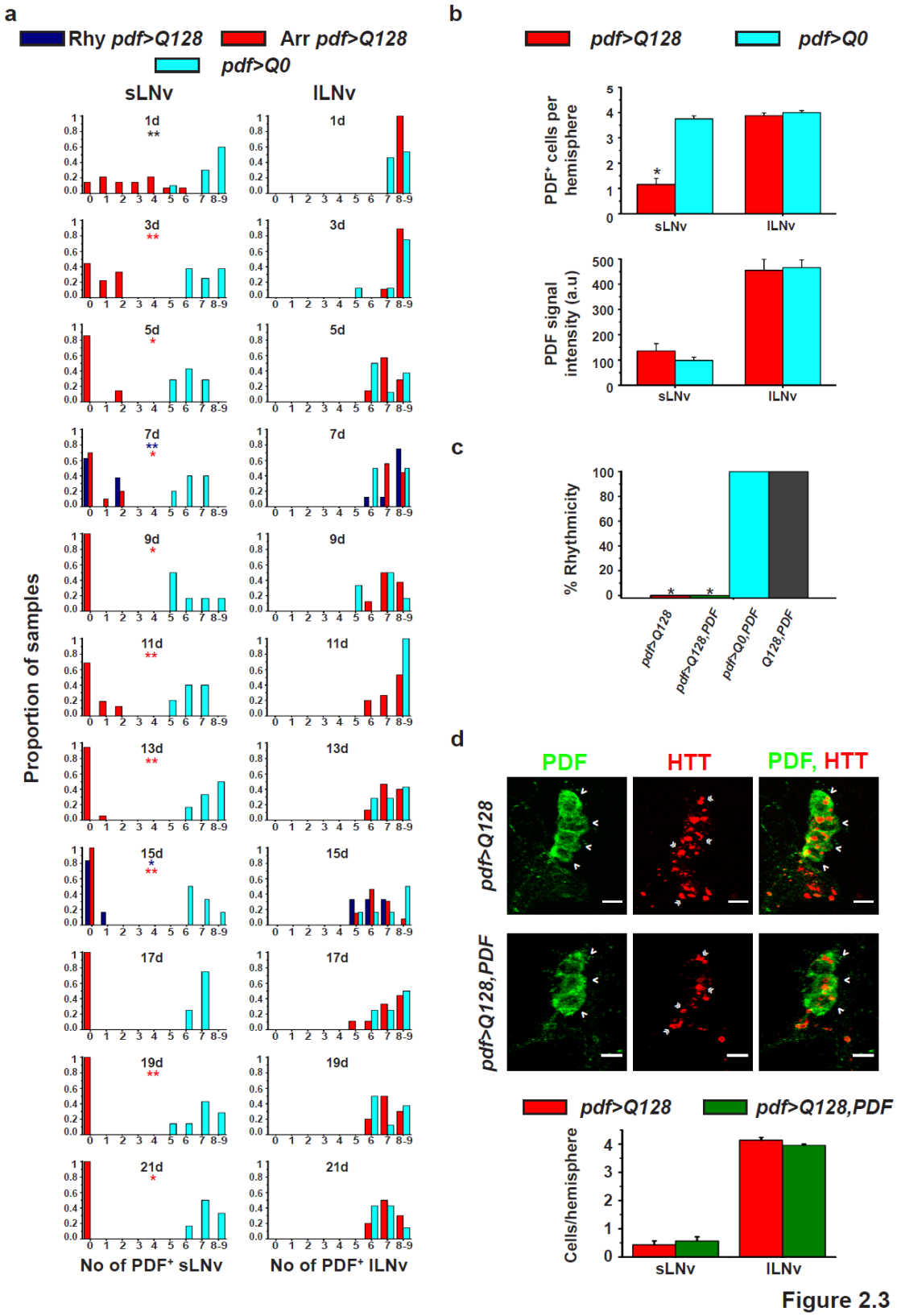

Figure 2.3

Fig 2. 3 Rhythmic and arrhythmic pdf>Q128 flies show a similar distribution of PDF⁺ sLNv soma. (a) Frequency distribution of the proportion of brain samples with 0 or more PDF⁺ soma (sLNv or lLNv) at each age is plotted for rhythmic *pdf>Q0* and rhythmic and arrhythmic *pdf>Q128*. The distribution of *pdf>Q0* is significantly different from rhythmic *pdf>Q128* (blue *) and

arrhythmic *pdf>Q128* (red *). * $p<0.005$ and *** $p<0.001$. (b) Mean LNv soma numbers (top) and signal intensity of PDF in them (bottom) for *pdf>Q128* and *pdf>Q0* for 6d-old flies under LD. * indicates a difference between genotypes at $p<0.0001$. a.u, arbitrary units. (c) The percentage rhythmicity of flies is plotted where *indicates a significant difference at $p<0.0001$ from the controls with near 100% rhythmicity. (d) Top: Representative images of 9d-old brains of *pdf>Q128* and *pdf>Q128,PDF* stained for PDF (green) and HTT (red) showing lLNv soma (> arrowheads) and inclusions of expHTT (« double arrowheads). Scale bars are 10 µm. Bottom: Mean number of PDF^+ sLNv and lLNv soma per hemisphere for the two genotypes. Mostly, no PDF^+ sLNv soma are detectable in both genotypes. Across panels, error bars are SEM.

2.3.3 Arrhythmicity in free-running rhythms shows a polyQ-length dependence

polyQ diseases show a polyQ-length-dependent increase in severity and a decrease in the age of symptom onset (Finkbeiner, 2011). Given the extreme phenotype with HTT-Q128, using a different set of polyQ-HTT lines, I asked if the arrhythmicity in activity rhythms shows a polyQ-length dependence. An intermediate-length polyQ HTT (HTT-Q50) and a longer-length polyQ HTT (HTT-Q93) were the expHTT lines, for which HTT-Q20 served as the non-expanded control. *pdf>Q93* was arrhythmic from age 3d (Fig 2.4a top), as is also evident from the significantly lower percentage of flies that were rhythmic compared to controls in AW1 (Fig 2.4b) and their relatively poor daily activity consolidation '*r*' (Fig 2.4c). The few rhythmic flies in AW1 had low rhythm robustness that differed significantly from other controls (Fig 2.4d). In AW2 and AW3, a more significant percentage of *pdf>Q93* flies became rhythmic compared to AW1 yet had poorer rhythmicity than controls but not *pdf>Q50* (Fig 2.4b), and these were weak rhythms compared to their relevant non-expanded controls (Fig 2.4d). All flies with the intermediate expansion *pdf>Q50* were rhythmic in AW1 but became progressively arrhythmic (Fig 2.4a top), with percentage rhythmicity falling significantly in AW3 compared to earlier AWs (Fig 2.4b). In AW2 and AW3, *pdf>Q50* had significantly fewer rhythmic flies than most controls (Fig 2.4b). The onset of arrhythmicity occurred between ages 14d-16d (second half of AW2). However, this fall in rhythmicity with time did not reflect in their '*r*', as around 13d, *pdf>Q50* was different only from *pdfGal* (Fig 2.4c, see plum-coloured * placed near the *pdfGal* curve in grey) and at 15d, from *pdf>Q20* (Fig 2.4c, see cyan-coloured * placed near the *pdf>Q50* curve in plum). A noticeable lack of difference in '*r*' for *pdf>Q50* from controls could be because the *r*' of most genotypes begins to fall around the middle age of the recording. The robustness of

rhythmic *pdf>Q50* flies was lower than its *non-expanded* and *UAS* controls but not the *driver* control in AW2 (Fig 2.4d). Both *pdf>Q20* and *pdf>Q50* had more extended periods than other genotypes in AW1 and AW2 (Fig 2.4e). *pdf>Q93* had lower activity levels than most other genotypes in early ages (up to 7d) but not different than *pdfGal*, which had low activity levels for most of the run (Fig 2.4f). In summary, a longer expanded polyQ led to an early and immediate arrhythmicity onset and reduced rhythm robustness. In contrast, with a shorter expanded polyQ, arrhythmicity is delayed, and rhythm robustness is affected to a lesser degree. These observations highlight a dependence of the age-of-onset of rhythm disturbance and the magnitude of rhythm disturbance on the polyQ-length.

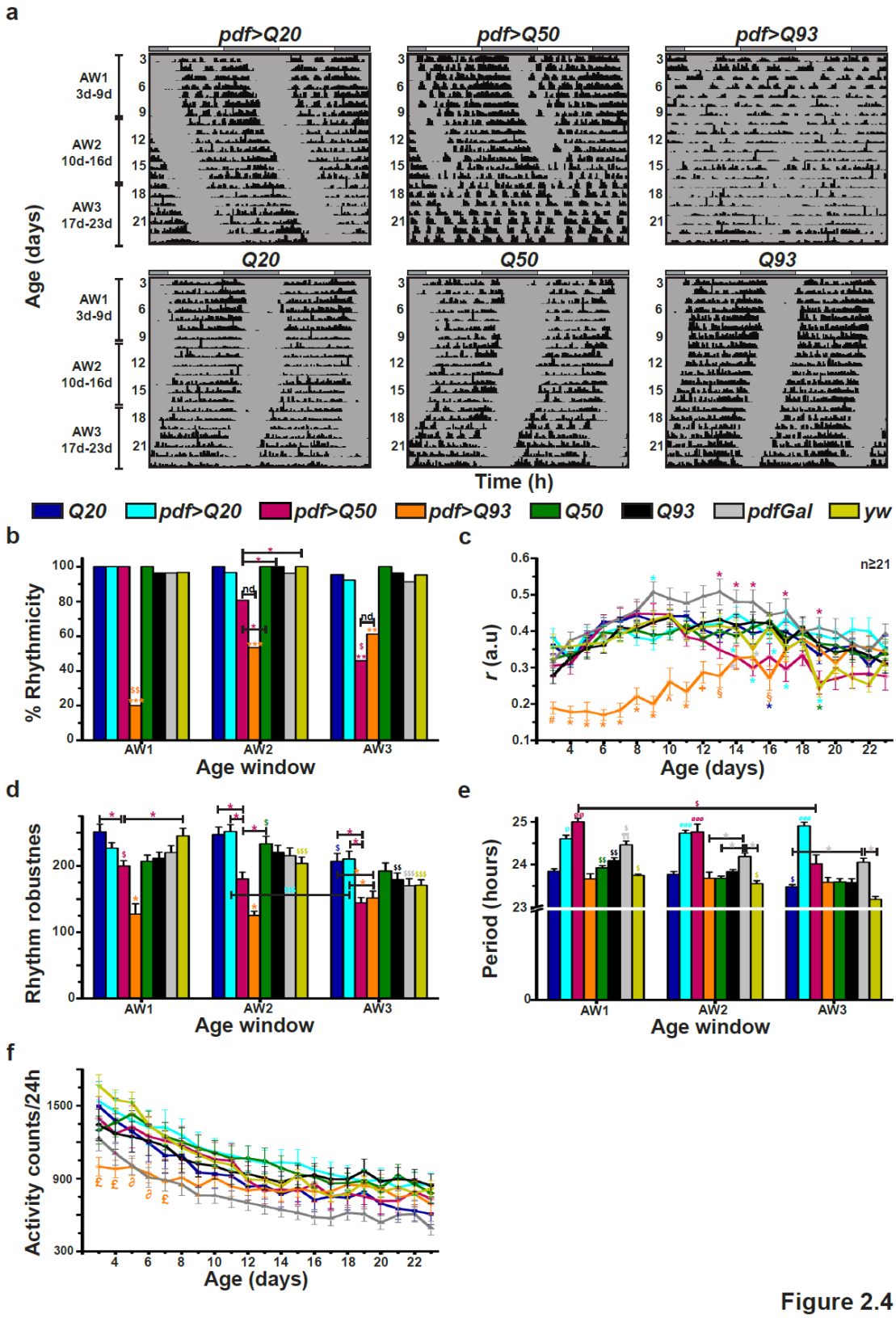

Figure 2.4

Fig 2. 4 Expression of expHTT with an intermediate-length-polyQ leads to a delay in arrhythmicity in DD.

(a) Representative double plotted, normalized actograms for *pdf>Q20*, *pdf>Q50*, *pdf>Q93*, *Q20*, *Q50* and *Q93* w^{1118} depicting activity data for >21days in DD (age 3d-23d on the *y*-axis). All other details

are like Fig 2.1a. (b) The percentage of rhythmic flies is plotted across three AWs. Coloured * indicates a significant difference between the specific-coloured genotype and all other genotypes or indicated genotype(s). nd, not different. (c) Mean '*r*' per day across age. Symbols indicate statistically significant differences at $p<0.05$: specific colour * between that coloured genotype from the genotype nearest which the * is placed or * coloured genotype from all other genotypes in cases where a coloured * is placed near the same coloured genotype, coloured # of that specific-coloured genotype from other genotypes except *pdf>Q50* and *Q93*, coloured § of that specific-coloured genotype from other genotypes excepting *pdf>Q20* and *Q20*, coloured ^ of that specific-coloured genotype from other genotypes excepting *pdf>Q20* and *Q50* and coloured + of that specific-coloured genotype from other genotypes excepting *pdf>Q50* and *Q50*. n≥21 indicates that at least 21 flies remained alive for all genotypes up to age 23d. (d) Mean robustness of rhythmic flies across age. Coloured * indicates a significant difference between the specific-coloured genotype and all other genotypes or indicated genotype(s). (e) Mean free-running period across AWs. Coloured symbols indicate statistically significant differences of the specific-coloured genotype: * - from indicated genotypes, ¶ - from *pdf>Q93*, *Q20*, *Q50* and w^{1118} and ø - from other genotypes excepting *pdf>Q20* and *pdfGal*. (f) Mean daily activity counts across age. Coloured symbols indicate statistically significant differences of the specific-coloured genotype: £ - from all genotypes excepting *pdfGal*, and ø - from other genotypes excepting *pdf>Q93* and *pdfGal*. Across panels, statistically significant differences are indicated at $p<0.05$ (single symbol), $p<0.1$(double symbol) and $p<0.001$ (triple symbol); coloured $ denotes differences between AWs for that genotype and error bars are SEM.

2.3.4 GFP loss from sLNv soma mirrors PDF loss from sLNv soma in expHTT-expressing flies

I then wanted to distinguish whether PDF loss from sLNv soma is due to the neuropeptide PDF loss or if the sLNv is altogether lost. In a prior study using *pdf>Q128,NacBach-CD8::GFP*, neither PDF nor GFP were detected in sLNv (Sheeba et al., 2008b). Here, I used the *10X-UAS myrGFP*, a *Drosophila* codon-optimised, myristoylated membrane GFP, having greater signal strength when expressed using a basal promoter, thus enhancing GFP and enabling detection (Pfeiffer et al., 2012). Using *pdf>Q128;myrGFP*, GFP was not detected in sLNv soma, and this mirrored PDF loss from sLNv soma (Fig 2.5a) in terms of mean numbers (Fig 2.5b) and frequency distribution at ages 0d and 9d (Fig 2.5c), suggesting compromised cell integrity. However, PDF and GFP are detected in the sLNv dorsal terminals, indicating that the neurons are likely present.

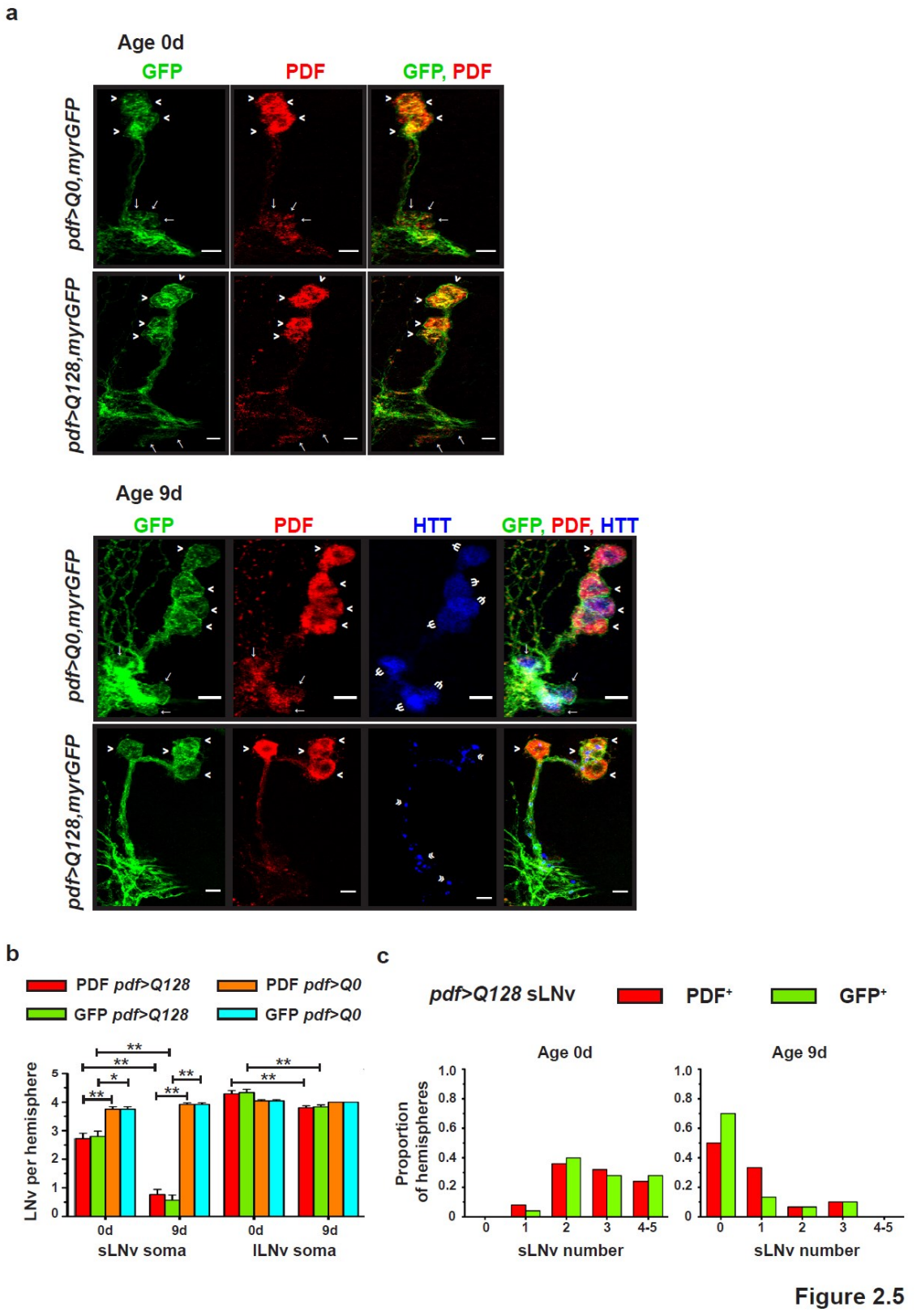

Figure 2.5

Fig 2. 5 expHTT-expressing flies show selective loss of GFP from the sLNv soma.

(a) Representative images of adult brains of *pdf>Q0,myrGFP* and *pdf>Q128,myrGFP* at age 0d (top) stained for GFP (green) and PDF (red) and at age 9d (bottom) stained for GFP (green), PDF (red) and HTT (blue). Images show showing sLNv soma (→ arrows), lLNv soma (> arrowheads), diffuse HTT staining (Ψ psi) and inclusions of expHTT (« double arrowheads).

Scale bars are 10 µm. (b) The average number of PDF^+ or GFP^+ LNv soma per hemisphere in *pdf>Q128,myrGFP* and *pdf>Q0,myrGFP* at ages 0d and 9d. Symbols indicate statistically significant differences: * at $p<0.001$ and ** at $p<0.0001$. Error bars are SEM. (c) Frequency distribution of the proportion of hemispheres with 0 to 5 PDF^+ or GFP^+ sLNv soma at age 0d (left) and 9d (right). n= 20-24 hemispheres/genotype/age. Across all panels, error bars are SEM.

Apoliner is a genetically encoded fluorescence-based caspase sensor. A membrane-tagged RFP is linked to a nuclear-localised signal (NLS) tagged eGFP via a sensitive linker caspase activation (Bardet et al., 2008). The linker comprises DIAP1 (a caspase inhibitor known as the *Drosophila* inhibitor of apoptosis protein 1), cleaving upon apoptosis induction by effector caspases, leading to its degradation. Upon caspase activation, the linker is cleaved, allowing the NLS-eGFP to translocate to the nucleus, enabling the detection of spatially distinct fluorescence signals: RFP on the membrane and GFP in the nucleus (Bardet et al., 2008). Since in *pdf>Q128*, PDF from the sLNv soma is lost, the dissection of freshly eclosed flies allows for detecting a few PDF^+ sLNv, allowing a window to capture apoptosis induction via caspase activation. In *pdf>Q128,Apo* at age 0d, PDF, if detected in the sLNv soma (in blue) was primarily cytoplasmic. For both GFP and RFP, a similar staining pattern emerged comparable to GFP and RFP in *pdf>Q0* (Fig 2.6 top and centre). At a later age of 9d, in *pdf>Q128,Apo* neither PDF^+ sLNv nor GFP or RFP stained sLNv soma were detected, while in the lLNv, RFP and GFP were present and similar to PDF in cellular distribution (Fig 2.6 bottom). Using a static measurement such as GFP-RFP-based *Apoliner*, when PDF was detected in sLNv soma at an early age, I do not find any evidence for apoptosis in the form of nuclear GFP. At a later age, PDF and Apoliner markers were undetectable. Events leading to apoptosis of sLNv soma are probably fast and transient and, therefore, cannot be captured through such snapshot measurements. Thus, the results are inconclusive as to whether the disappearance of PDF from sLNv amounts to an apoptotic cell death.

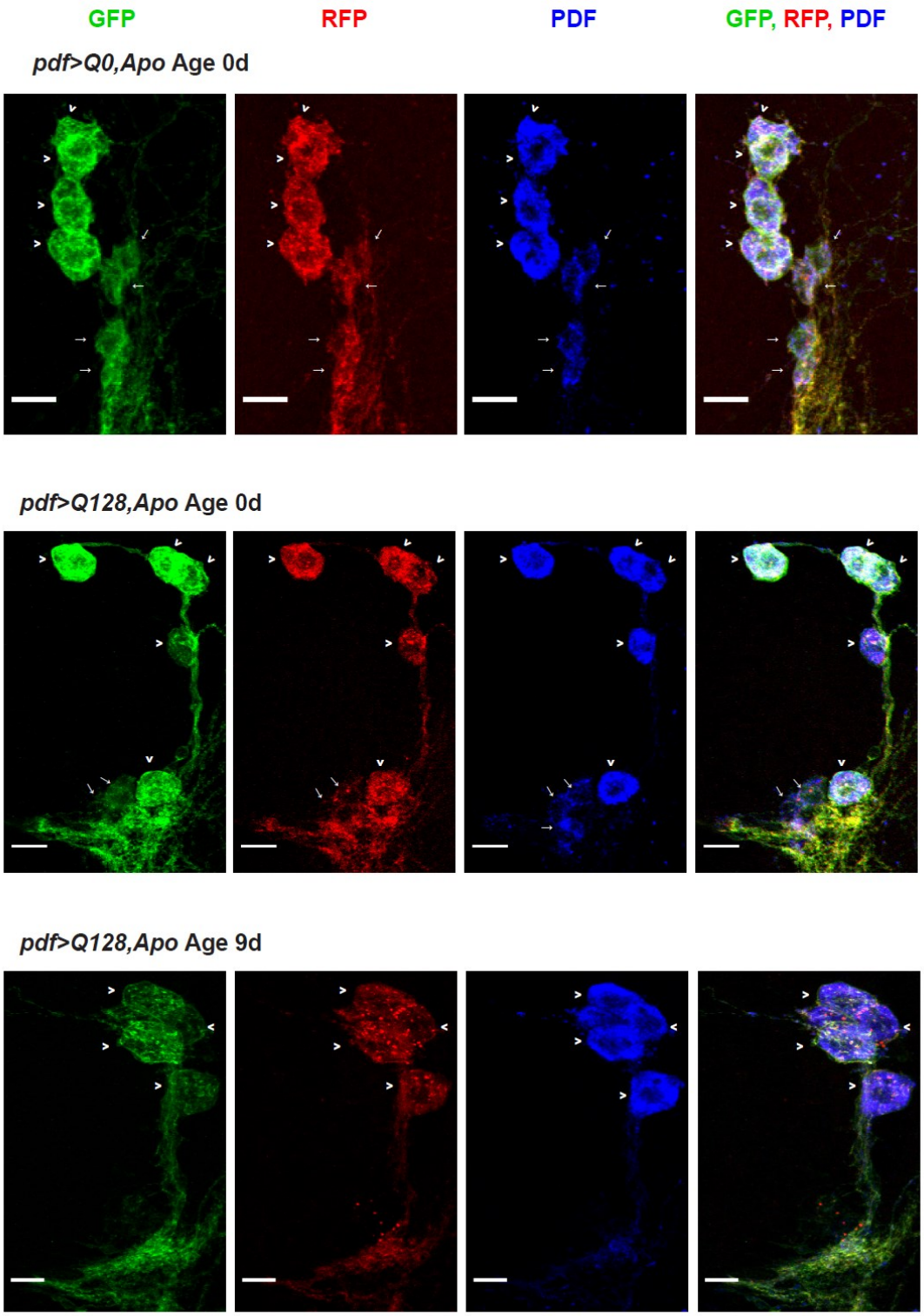

Figure 2.6

Fig 2. 6 expHTT-expressing flies show a loss of Apoliner-GFP and RFP from the sLNv soma. Representative images of adult brains of *pdf>Q0,Apo* (top) and *pdf>Q128,Apo* (centre) at age 0d and *pdf>Q128,Apo* (bottom) at age 9d stained for GFP (green), RFP (red) and PDF (blue). Images show sLNv soma (arrows) and lLNv soma (arrowheads). Scale bars are 10 µm. n= 20 hemispheres/genotype/age.

2.3.5 Loss of PER from the sLNv and persistence of PDF oscillations in the sLNv dorsal projections accompanied by synchronous PER oscillations in the PDF$^-$ circadian neurons in HD flies in DD

Flies expressing expHTT are behaviourally arrhythmic in DD, and PDF is not detectable in the soma of sLNv, although detectable in their DP (Fig 2.2). Previous studies using different approaches have suggested that oscillations in PDF levels in the sLNv DP are crucial for synchronising the molecular oscillations between various circadian neuronal groups in DD (Lin et al., 2004; Nitabach et al., 2006; Wu et al., 2008b; Yoshii et al., 2009). To assess whether PDF detected in the sLNv DP of *pdf>Q128* flies oscillates, I examined the brains of 9d-old adult flies reared under LD and transferred into DD at age 2d. *pdf>Q128* showed oscillation in the PDF levels in their sLNv DP with intensity at CT2 significantly higher than CT6-CT18 (Fig 2.7a). PDF levels in sLNv DP of control *Q128* oscillated, with intensity at CT2 significantly greater than CT14-CT22 (Fig 2.7a). The PDF peak at CT2 of *pdf>Q128* and *Q128* were in-phase. However, the rise and fall of PDF levels in *pdf>Q128* was earlier than *Q128* (Fig 2.7a), suggesting a short period oscillation in PDF levels of *pdf>Q128*. Across most time points, PDF levels in *pdf>Q128* were higher than *Q128*, but the peak-to-trough difference was qualitatively comparable. Thus, *pdf>Q128* in DD exhibit a significant oscillation in PDF levels in the sLNv DP.

Oscillating PDF levels in the sLNv DP are not direct measurements of rhythmic secretion. However, the functional consequence of such a secretion would be to synchronise molecular oscillations among circadian neurons. Hence, I assessed the oscillations of PER levels in different circadian neuronal subsets. In *pdf>Q128*, PER mainly was not detected in the sLNv soma (Figs 2.7b left and 2.8a centre), and frequency distribution of PER$^+$ sLNv soma showed that most hemispheres had no PER$^+$ sLNv soma, which is significantly different from the distribution of *pdf>Q0* (Fig 2.8a left). Pooling across time points, the percentage of hemispheres having sLNv soma stained by neither PER nor PDF was 83.3%; by both PER and PDF, it was 7.7%; by only the PDF, it was 5.9%, and by only PER, it was 3.1%. The number and distribution of PER$^+$ sLNv soma resembled that of PDF$^+$ sLNv soma (Fig 2.8a centre, right). In controls, PER in the sLNv

oscillated with a trough at CT11 and a peak at CT23 (Figs 2.7b right and 2.7c top-left). The very few PER$^+$ sLNv detected in *pdf>Q128* had intensities lower than that of control at CT23, CT5 and CT17 (Figs 2.7b and 2.8d top-left). Despite increasing antibody concentrations four-fold, PER$^+$ sLNv were mainly undetectable in *pdf>Q128* (Fig 2.8b). Thus, expHTT expression in the LNv results in a loss of detectable PER from the sLNv soma.

Only half of the PDF$^+$ lLNv soma of *pdf>Q128* were PER$^+$ (Fig 2.8c). In *pdf>Q0*, lLNv soma, PER showed dampened oscillations of very low amplitude (Figs 2.7b right and 2.7c top-centre). PER in the lLNv soma of *pdf>Q128* did not oscillate and had significantly lower intensity than *pdf>Q0* across time points (Figs 2.7b and 2.7c top-centre). Thus, in *pdf>Q128* flies, although PDF levels in the lLNv soma and the PDF$^+$ lLNv numbers are unaffected (Fig 2.2 and 2.3b), there is a significant reduction of PER levels in the lLNv soma.

Like its control, 5th sLNv of *pdf>Q128* showed a trough in PER oscillations at CT11 (Figs 2.7b and 2.7c top-right), and its amplitude was mostly comparable and in phase with its controls. In LNd of *pdf>Q128*, like controls, PER showed a prominent oscillation with a trough at CT11 (Figs 2.7b and 2.7c bottom-left), and its levels were similar to *pdf>Q0*. DN1s of *pdf>Q0* and *pdf>Q128* showed a comparable amplitude of PER oscillations with a trough at CT11 (Figs 2.7b and 2.7c bottom-centre). *pdf>Q128* and *pdf>Q0* showed PER oscillations in the DN2 with a trough at CT23 (Fig 2.7c bottom-right). Interestingly, the trough phase of PER intensity within each neuronal group in *pdf>Q128* were similar to their counterparts in *pdf>Q0* at CT11 (Fig 2.8d). Strikingly, in *pdf>Q128*, even in the absence of PDF in the sLNv soma, the PER intensity oscillations in the 5th sLNv, LNd, and DN1 (hereafter referred to as the PDF$^-$ neurons) were in phase. PER intensity in the DN2 showed a trough at CT23 in both the genotypes, which was phase-advanced compared to other neuronal groups. A previous study made a similar observation (Veleri et al., 2003). Further, as a measure of within-group synchrony, for the LNd and DN1 neuronal groups, the standard deviation of PER intensity per hemisphere was estimated. This measure for *pdf>Q128* was not higher than controls for most time points (Table 2.1), suggesting that within-group synchrony is unaffected. This synchrony in PER level oscillations between

PDF$^-$ neurons is indirect evidence that rhythmic PDF accumulation in the sLNv DP of *pdf>Q128* flies is functional and perhaps indicative of rhythmic PDF secretion.

In summary, the expression of expHTT in the LNv reduces PER levels to below the detection limit in the sLNv. PER being a central clock component, this amounts to disrupting the free-running molecular clocks in the sLNv. In the lLNv, there is a significant reduction in PER levels. However, since PER oscillations in the lLNv dampen in DD of even wild-type flies and are not essential for circadian activity rhythms in DD (Shafer et al., 2002; Grima et al., 2004a; Lin et al., 2004), the breakdown of rhythmic activity is most likely due to an sLNv circadian dysfunction. The persistence of PDF oscillations in the sLNv DP and synchronous molecular oscillations in the PDF$^-$ neurons in these arrhythmic flies suggest that these oscillations are insufficient for DD activity rhythms. The continuance of oscillations in PDF levels in the sLNv DP, even in the absence of detectable PER in the sLNv soma, suggests that these oscillations are not dependent on somal PER-driven molecular clocks. Overall, in *pdf>Q128* flies, the circadian pacemaker function of the sLNv that maintains behavioural rhythmicity in DD is abolished. This sLNv dysfunction is independent of PDF oscillations in its DP and downstream synchrony of molecular oscillations between other circadian neurons. These results provide evidence for decoupling the oscillations in the PDF levels in the sLNv DP from the free-running behavioural activity rhythms. Thus, these results challenge the notion that the sLNv evokes self-sustained activity rhythms in DD via oscillations of PDF levels in its DP.

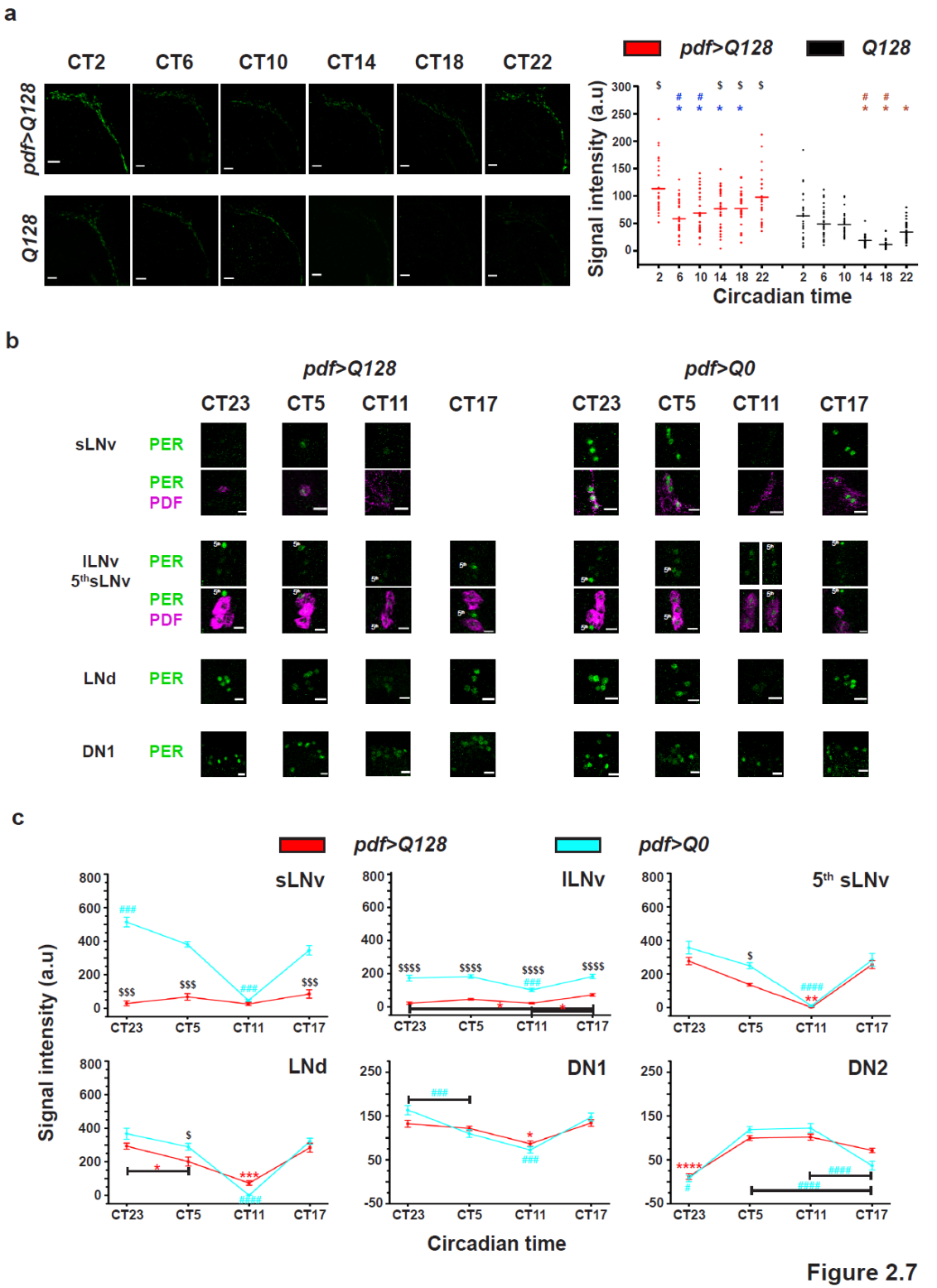

Figure 2.7

Fig 2. 7 Oscillations of PDF levels in the sLNv dorsal termini persist despite a loss of PDF in their soma.

(a) Left: Representative images of 9d-old adult brains showing PDF (green) in the sLNv dorsal projections (DP) at six time points in DD for *pdf>Q128* and *Q128*. Scale bars are 10 µm. Right: Quantifying the PDF intensity in the sLNv DP across time points for both the genotypes, where each circle represents individual hemisphere values and the horizontal line depicts the mean value. Symbols indicate statistically significant differences: * (blue) of CT2 from CT6-CT18 for *pdf>Q128*

at $p<0.01$, # (blue) of CT22 from CT6-CT10 for *pdf>Q128* at $p<0.05$, * (brown) of CT2 from CT14-CT22 for *Q128* at $p<0.05$, # (brown) of CT6-CT10 from CT14-CT18 for *Q128* at $p<0.05$ and $ (black) between *pdf>Q128* and *Q128* at indicated time points at $p<0.0001$. n≥26 hemispheres/genotype/time point. (b) Representative images of 9d-old adult brains stained for PER (green) in the different circadian neuronal groups at four-time points in DD for *pdf>Q128* and *pdf>Q0*. Its co-staining with PDF (magenta) identifies the LNv soma. At CT17, there is no representative image for sLNv in *pdf>Q128*. Scale bars are 10 µm. (c) Quantification of PER intensity across time points in the different circadian neuronal groups for *pdf>Q128* and *pdf>Q0* in DD. Very few *pdf>Q128* flies had detectable PDF$^+$ and PER$^+$ sLNv soma. Symbols indicate statistically significant differences: * (red) between time points for *pdf>Q128*, # (blue) between time points for *pdf>Q0* and $ between genotypes within a time point with single symbol $p<0.05$, double symbols $p<0.01$, triple symbols $p<0.001$and quadruple symbols $p<0.0001$. n=16-20 hemispheres/genotype/time point. Across all panels, error bars are SEM.

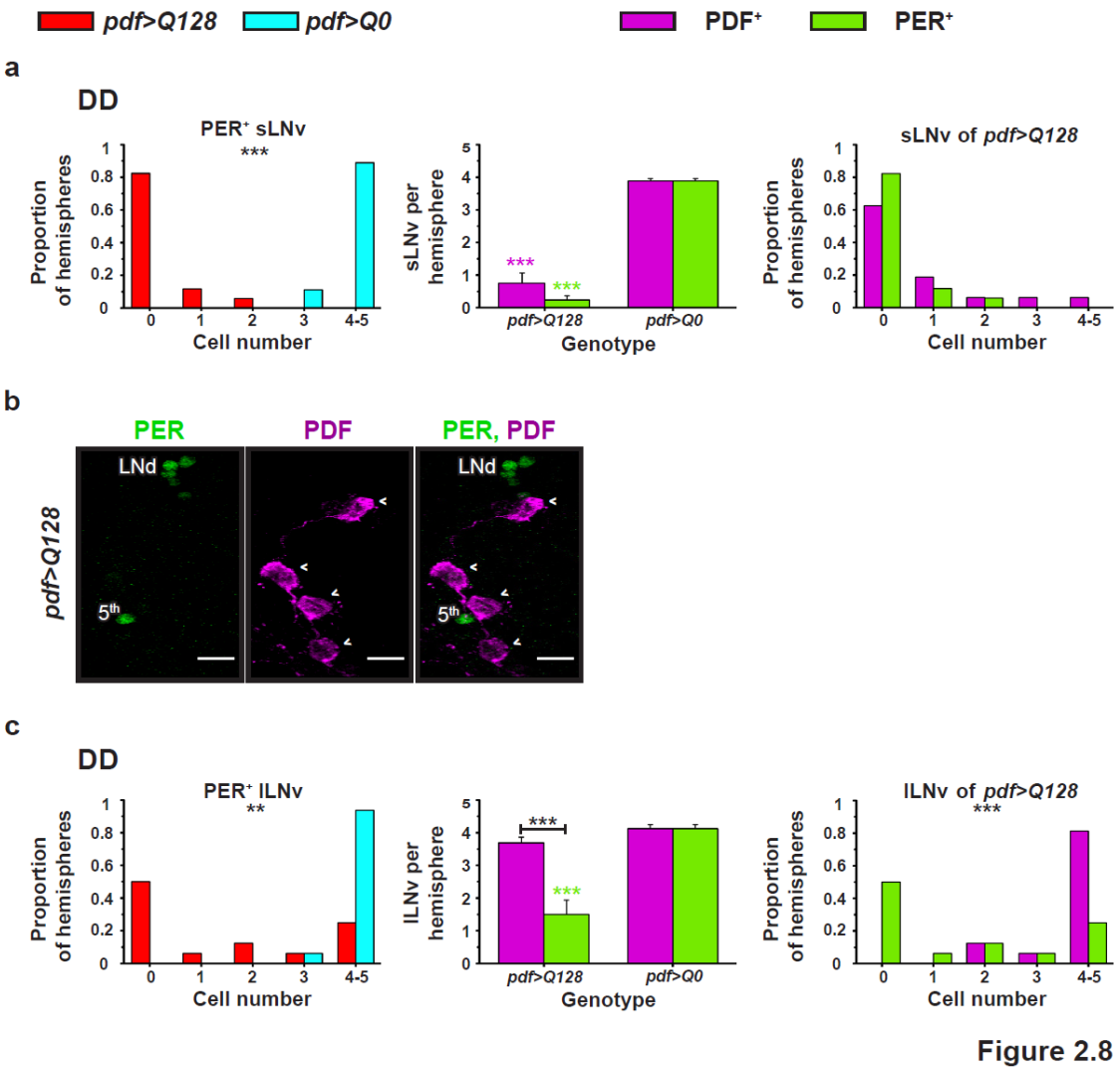

Figure 2.8

Fig 2. 8 expHTT-expressing flies show a loss of sLNv PER and a reduction in lLNv PER under DD.

(a) sLNv soma in 9d-old flies in DD at CT23. Left: Frequency distribution of the proportion of hemispheres with 0 to 5 PER$^+$ sLNv soma in *pdf>Q128* and *pdf>Q0*. *** indicate significantly

differing distributions at $p<0.001$. Centre: Mean number of PDF$^+$ or PER$^+$ sLNv soma in *pdf>Q128* and *pdf>Q0* in DD. *** indicate statistically significant differences between genotypes at $p<0.001$: in magenta for PDF$^+$ sLNv and green for PER$^+$ sLNv. Right: Frequency distribution of the proportion of hemispheres staining 0 to 5 sLNv soma that is PDF$^+$ or PER$^+$ for *pdf>Q128* flies. (b) Representative images of 9d-old brains of *pdf>Q128* stained for PER (green) and PDF (magenta) illustrating a lack of PER from LNv even upon increasing the antibody concentration four-fold. Scale bars are 10 µm. (c) For lLNv soma. All other details are the same as above. Left: ** indicates significantly different distributions at $p<0.005$. Centre: *** (in black) difference in numbers of lLNv soma that are PDF$^+$ and PER$^+$ at $p<0.001$. Right: *** indicates that the two distributions differ significantly at $p<0.001$. Across all panels, error bars are SEM.

Table 2.1 The extent of variation in PER intensity within a neuronal group in expHTT-expressing flies is not greater than that of controls.

	pdf>Q0	***pdf>Q128***
LNd		
CT23	102.81±28.21	132.15±16.6**
CT5	80.6±7.44	116.91±9.26**
CT11	34.41±8.73***	0
CT17	113.45±12.9	124.26±10.69
DN1		
CT23	79.93±7.13	99.98±9.08*
CT5	58.85±3.04	55.97±3.77
CT11	40.58±3.73	44.76±3.46
CT17	56.38±5.81	57.93±3.4

The table shows the within-neuronal group mean ± standard deviation in PER intensity for LNd and DN1 across time points in DD for *pdf>Q128* and its control *pdf>Q0*. The standard deviation within LNd for *pdf>Q128* is significantly lower than that of control at CT23 and CT5 and higher only at CT11 when PER is undetectable in *pdf>Q0*. The standard deviation within DN1s for *pdf>Q128* is significantly lower than *pdf>Q0* at CT23. *$p<0.05$, **$p<0.01$, ***$p<0.001$.

2.3.6 Expression of expHTT in the LNv does not alter the activity rhythms or sleep of flies under LD

Previous studies show that flies expressing expanded HTT-Q128 in the LNv neurons, though arrhythmic in DD, were similar to controls under 12:12h LD cycles with light phase intensity as high as 1000-2500 lux (Sheeba et al., 2010). At high light intensities, acute photic inhibition or stimulation (Refinetti, 2015) could prevent the detection of subtle differences in activity profiles. So, to detect nuanced differences, flies were maintained under low-contrast-LD regimes as adults (moderate-LD: light phase intensity of 100 lux and dim-LD: light phase intensity of 3-8 lux). *pdf>Q128* flies, like their controls, were rhythmic throughout the recording in both LDs (moderate and dim); however, this behavioural rhythmicity of *pdf>Q128* did not persist in DD (Figs 2.9a and 2.10a top). In both regimes, the activity profiles of *pdf>Q128* were like its controls (Figs 2.9b and 2.10b) *pdf>Q0* (left), *Q128* (centre) and *pdfGal* (right) across AWs with appropriately phased morning and evening peaks and relative inactivity at mid-day (Figs 2.9b and 2.10b). In moderate-LD, *pdf>Q128* flies exhibited activity counts and anticipation indices comparable to controls across age (Figs 2.9c-f). In dim-LD, daytime and nighttime activity levels and E-anticipation of *pdf>Q128* were similar to most controls (Figs 2.10c, 2.10d and 2.10f). The M-anticipation index of *pdf>Q128* was comparable to that of *pdf>Q0* and *Q128* in AW1 (Fig 2.10e). Although AW2's M-anticipation of *pdf>Q128* was significantly lower than most controls, it was not different from its *UAS* control *Q128* (Fig 2.10e).

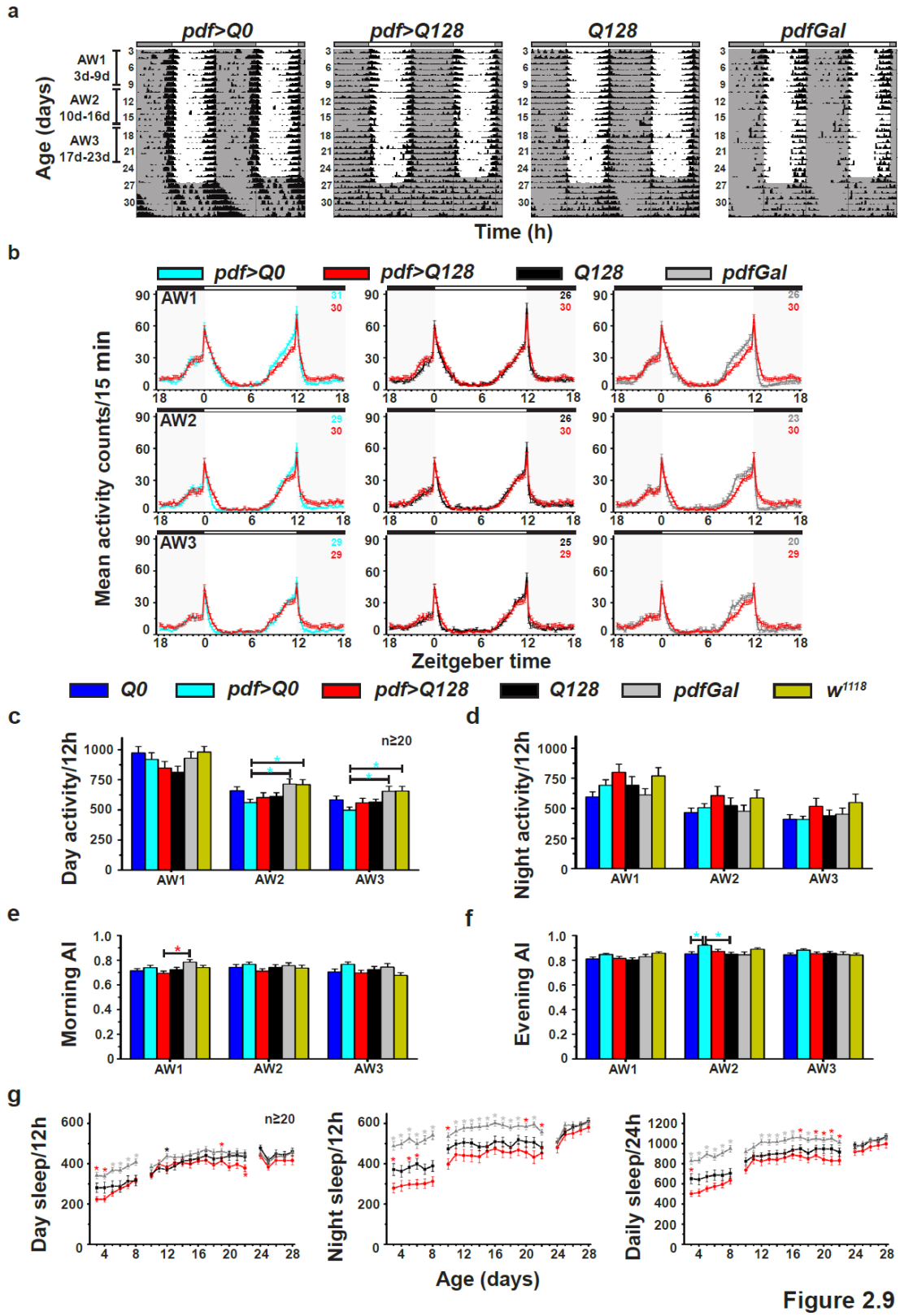

Fig 2. 9 Flies expressing expHTT in the LNv do not show altered activity rhythms under moderate-LD.

(a) Representative double plotted, normalized actograms for *pdf>Q128* and its controls under LD (~100 lux) for 25d (age 3d-27d) followed by DD. The grey-shaded regions represent the dark phase, and the unshaded regions represent the light phase of LD. All other details are like Fig 1a.

(b) The activity counts per 15min are plotted against zeitgeber time for *pdf>Q128* in comparison with either *pdf>Q0* (left) or *Q128* (centre) or *pdfGal* (right) for AW1 (top), AW2 (centre) and AW3 (bottom). The grey-shaded regions and black horizontal bars above represent the dark phase, and the unshaded region and white horizontal bars above represent the light phase of the LD. The coloured numbers at the top right of each panel are the sample size for each genotype. (c-f) Mean daytime activity counts per 12h (c), mean nighttime activity counts per 12h (d), morning anticipation index (e) and evening anticipation index (f) are plotted against AWs with *. Across panels, error bars are SEM. (g) Mean daytime sleep per 12h (left), mean nighttime sleep per 12h (centre) and mean daily sleep per 24h (right) across age for *pdf>Q128*, *Q128* and *pdfGal*. Coloured * indicates statistically significant differences at $p<0.05$: of that coloured genotype from the genotype nearest which the * is placed or * of that coloured genotype from all other genotypes where a coloured * is placed near the same-coloured genotype. Sleep levels on 9d and 23d are not plotted since flies were transferred to fresh tubes and disturbed on those days.

HD patients and mice have poor sleep quality and levels, especially at night, and increased daytime sleep (Hood and Amir, 2017b). *Drosophila* HD models also exhibit sleep deficits (Gonzales and Yin, 2010; Gonzales et al., 2016; Farago et al., 2019). Upon investigating the effect of expressing expHTT in the LNv on the sleep in *pdf>Q128* flies, both *pdf>Q128* and *Q128* had significantly higher sleep levels (daytime, nighttime and daily) than *pdfGal* (Fig 2.9g). *pdf>Q128* had significantly more insufficient sleep than both controls for very few ages (daytime-22d, nighttime-3d, 5d and 7d and daily-3d) (Fig 2.9g), suggesting that lowered sleep levels of *pdf>Q128* might be due to background effects. Overall, the expression of expHTT on LNv did not impact sleep levels in LD.

I also addressed the question of whether flies expressing expHTT in the LNv re-entrain to a phase-shifted LD cycle. *pdf>Q128,* experiencing a 9h advance in lights-ON, shifted their activity in phase to the new LD almost immediately, like the controls (Fig 2.10a, bottom). Thus, loss of PDF from the sLNv soma did not alter the activity rhythms of flies even under low-contrast-LD and phase-shifted-LD. Hence, PDF in the sLNv soma is not required to entrain activity rhythms or modulate the clocks' sensitivity to light. The conclusion that the entraining ability of *pdf>Q128* flies to LD is not affected is based on their control-like M and E anticipations and phasing and not on the phase-of-onset of free-running rhythms following LD, given that these flies are arrhythmic immediately upon entry into DD (Figs 2.9a and 2.10a). In concordance with the previous study (Sheeba et al., 2010), the presented results suggest that PDF in the sLNv soma is not critical for M-anticipation. However, PDF in the sLNv dorsal projections could be mediating effects of the sLNv PDF in LD.

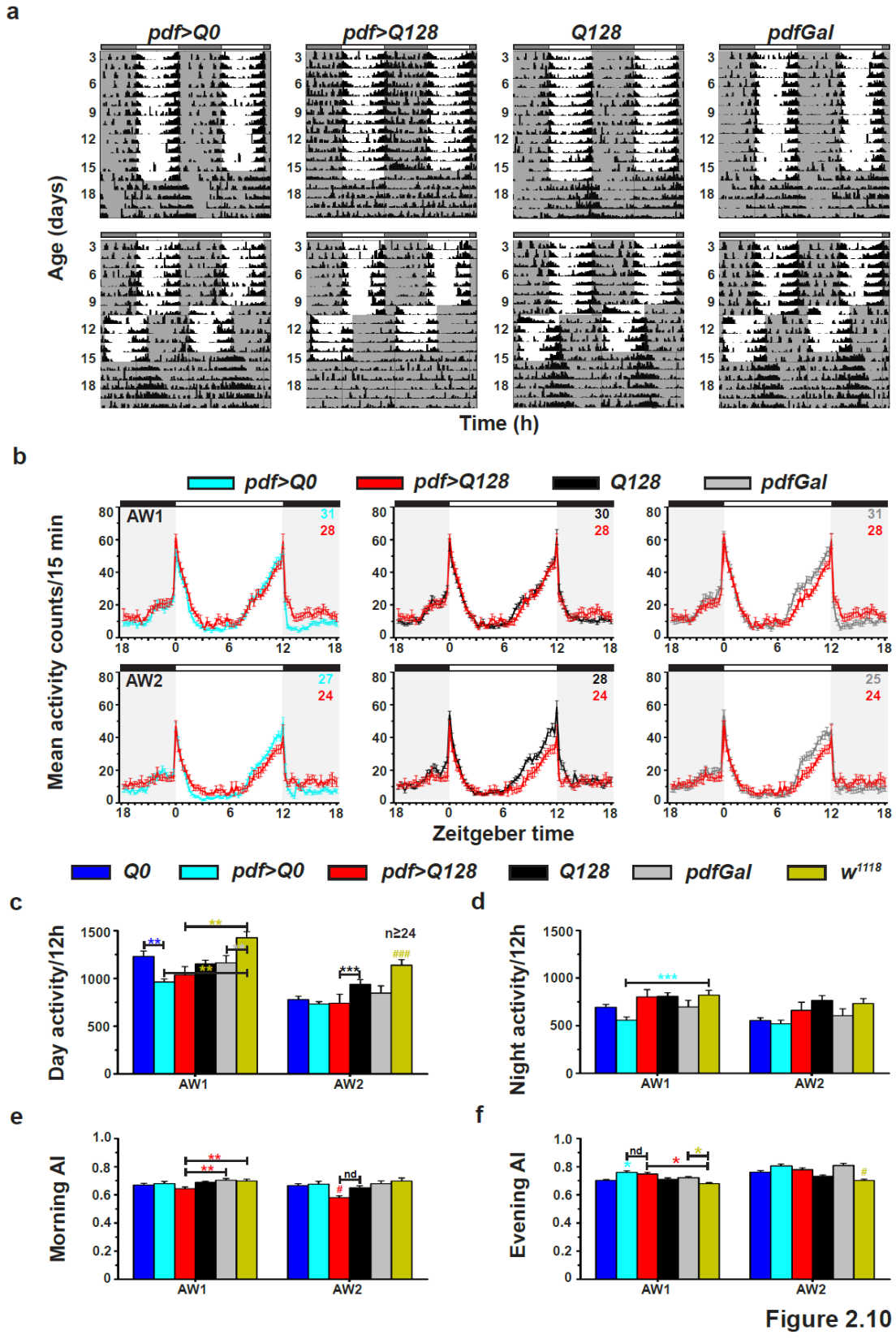

Figure 2.10

Fig 2. 10 Flies expressing expHTT in the LNv do not show altered behaviour under very low-intensity-LD.

(a) Representative double-plotted, normalized actograms for *pdf>Q128* and its controls are plotted. Top: flies are in 12h:12h dim-LD (3-5 lux) for 14d (age 3d-16d), followed by which they are in DD.

Bottom: flies are in 8d of 12h:12h dim-LD (age 3d-10d), followed by a 9h phase-advanced-LD for 5d (age 11d-15d), followed by DD. All other details are like Fig 9a. (b) Mean activity counts per 15 minutes for *pdf>Q128* in comparison with either *pdf>Q0* (left) or *Q128* (centre) or *pdfGal* (right) for AW1 (top) and AW2 (bottom). All other details are like Fig 9b. (c-f) Mean daytime activity counts per 12h (c), mean nighttime activity counts per 12h (d), morning-anticipation index (e), and evening anticipation index (f) are plotted against AWs. Coloured * indicates a significant difference between the specific-coloured genotype and all other genotypes or indicated genotype(s) and coloured # of that genotype from other genotypes except *Q128*. nd, not different. Across panels, statistically significant differences are indicated at $p<0.05$ (single symbol), $p<0.1$(double symbol), and $p<0.001$ (triple symbol), and error bars are SEM.

2.3.7 Prior exposure to arrhythmic conditions does not alter the ability of expHTT-expressing flies to show M-anticipation

The ability of adult *pdf>Q128* flies to show anticipation and appropriately phased M and E peaks even after PDF loss from the sLNv soma could be due to their history of prior exposure to rhythmic conditions of LD. Flies were reared under LD, recorded as adults for 7d in DD, which renders them arrhythmic and then recorded in LD for 8d (light intensity about 220 lux), followed by DD, to rule out such rhythmic-light-history effects. This regime is named DD-LD-DD, signifying the experimental conditions. A control group of age-matched flies was simultaneously recorded in DD throughout the experimental duration and designated DD. In AW1 (age 3d-9d), as expected, *pdf>Q128* flies of both DD and DD-LD-DD were arrhythmic with significantly lower % rhythmicity compared to controls and were not different from each other (Figs 2.11a and 2.11b left). In AW2 (age 10d-16d), *pdf*>Q128 of DD remained arrhythmic (Figs 2.11a top and 2.11b centre). In AW2, *pdf>Q128* flies of DD-LD-DD under light/dark cycles exhibited a profile similar in shape to *Q128* (Fig 2.11c centre) but different from *pdf>Q0* and *pdfGal* (Fig 2.11c left and right). The difference in profiles partly reflects the daytime and daily activity levels of *pdf>Q128* being significantly lower than *pdfGal* (Fig 2.11d). The M-anticipation of both *pdf>Q128* and *Q128* were lower than other genotypes but not different from one another (Fig 2.11e). The E-anticipation of *pdf>Q128* was lower than other genotypes (though well above AI of 0.5) and of *Q128* lower than *pdfGal* (Fig 2.11e). Given that the E-anticipation is under the control of E cells (LNd and PDF$^-$ 5th sLNv), which the *pdfGAl4* driver does not target, the lowered anticipation of *pdf>Q128* could be due to a combination of *UAS* background and environmental

effects. Thus, prior exposure to arrhythmic conditions of DD leads to a difference in daily activity levels and E-anticipation of *pdf>Q128* from its controls but not in M-anticipation. In AW3, *pdf>Q128* from DD and DD-LD-DD were arrhythmic in DD, whereas their controls free-ran from the LD phase (Figs 2.11a and 2.11b right). In conclusion, the persistence of M-anticipation in *pdf>Q128* flies even upon loss of PDF from the sLNv soma is not due to the initial light conditions.

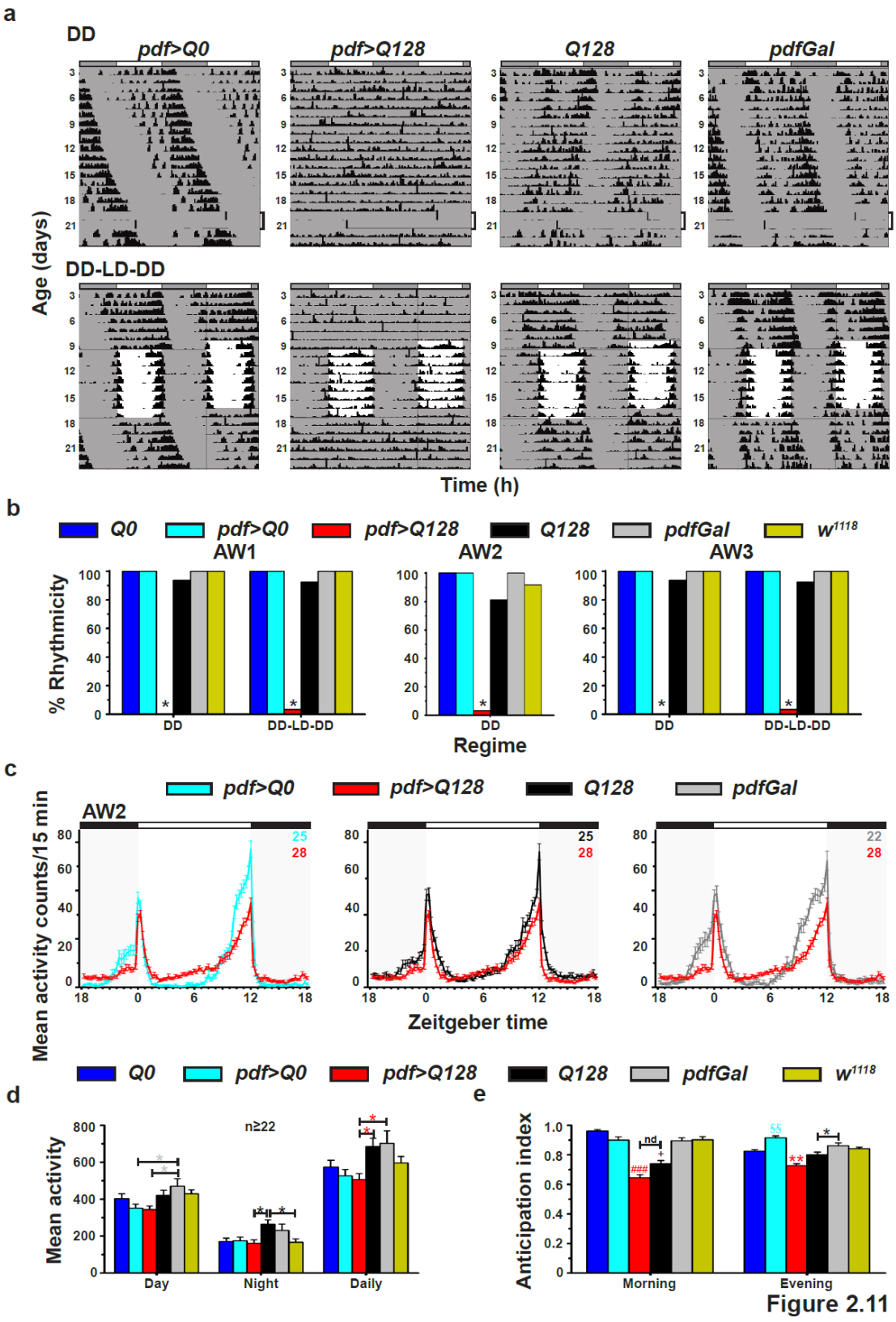

Figure 2.11

Fig 2. 11 expHTT-expressing flies entrain to LD despite experiencing arrhythmic conditions as adults.

(a) Representative double-plotted, normalized actograms for *pdf>Q0*, *pdf>Q128*, *Q128* and *pdfGal* in two regimes. Top: flies are in DD throughout and designated DD. Gaps in actograms around day 20 (indicated) are due to a technical glitch during the recordings. All other details are like Fig 2.1a.

Bottom: flies in DD for 7 days (age 3d-9d), followed by LD for 8 days (age 10d-17d), followed by DD again for 7 days (age 18-14d) and hence designated DD-LD-DD. All other details are similar to Fig 2.9a. (b) The percentage of rhythmic flies is plotted against the regimes for AW1, AW2 and AW3. * indicates a significant difference of *pdf>Q128* from controls at $p<0.0001$ in AW1 and AW2 and $p<0.05$ in AW3. (c-d) Mean activity counts (±SEM) over 12h (daytime or nighttime) and 24h (daily) are plotted. * indicates a significant difference at $p<0.05$. (e-f) Mean anticipation indices for morning and evening transitions are plotted. # indicates a significant difference of *pdf>Q128* from all genotypes except *Q128* at $p<0.001$. $^{+}$ indicates a significant difference of *Q128* from controls at $p<0.001$. Coloured * indicates a significant difference between the specific-coloured genotype and all other genotypes or indicated genotype(s), coloured # of that genotype from other genotypes excepting *Q128* and coloured § of that genotype from other genotypes excepting *pdfGal*. Across panels, error bars are SEM. Across panels, statistically significant differences are indicated at $p<0.05$ (single symbol), $p<0.1$(double symbol), and $p<0.001$ (triple symbol), and error bars are SEM.

2.3.8 Circadian molecular clock in the sLNv is not necessary for entrainment to LD

PDF is critical for anticipating dark-light transition (M-anticipation) (Renn et al., 1999). A previous study showed that flies expressing expHTT and lacking PDF in the sLNv soma exhibit M-anticipation under high-intensity-LD (1000-2500 lux) (Sheeba et al., 2010). The present study demonstrates that these flies show M-anticipation even under low-intensity-LD (100 lux) (Fig 2.9). Moreover, *pdf>Q128,* like its control *Q128,* shows prominent oscillation in the PDF levels in the sLNv DP: intensity at ZT2 is significantly higher than ZT11 (Fig 2.12). The circadian molecular oscillations in the sLNv of *pdf>Q128* flies under LD cycles were tested to understand their role in entrainment via PER staining. On average, fewer PER^{+} sLNv somas were found in *pdf>Q128* compared to *pdf>Q0* (Figs 2.13a and 2.13b left), and their mean numbers and distribution closely corresponded with those of PDF^{+} sLNv soma of *pdf>Q128* (Fig 2.13b centre and right). The few PER^{+} sLNv somas detected in *pdf>Q128* had significantly reduced intensities at ZT23 and ZT5 than *pdf>Q0,* which showed clear oscillations of PER in the sLNv (Figs 2.13a and 2.13d top left). Thus, even in the presence of cyclic light cues, PER is mainly undetected in the sLNv soma, suggesting a pronounced impairment of the PER-driven molecular clock in the sLNv of expHTT-expressing flies.

PER and PDF in the lLNv soma of *pdf>Q128* were comparable in numbers and distribution to the lLNv PER and PDF in *pdf>Q0*, respectively (Fig 2.13a and 2.13c). In these neurons, PER showed an apparent oscillation with a trough at ZT11 under LD (Figs 2.13a left and 2.13d top-centre), although they were of low amplitude compared to *pdf>Q0*, which showed robust PER

oscillations (Figs 2.13a and 2.13d top centre). In *pdf>Q128*, even in the absence of PDF and PER in the sLNv soma, PER levels oscillated in phase across neuronal groups and with controls, with a trough at ZT11 (Figs 2.13a and 2.13d). Thus, despite the loss of PDF and PER from the sLNv soma under LD, there is a rhythmic PDF accumulation in the sLNv DP and persistence of M-anticipation. The photic entrainment of activity rhythms of flies lacking PER oscillations in the sLNv suggests that the sLNv molecular clock is not essential for this phenomenon.

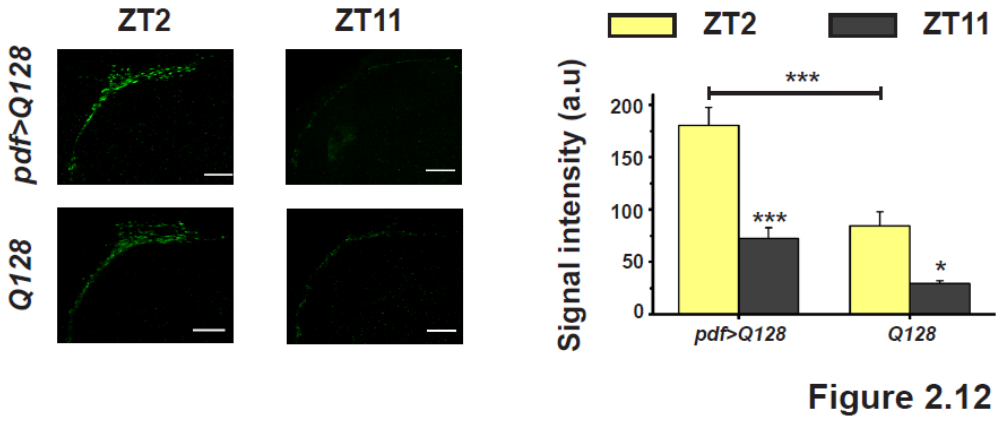

Fig 2. 12 Flies expressing expHTT show the PDF levels oscillating in their sLNv DP under LD.
(a) Left: Representative images of adult brains showing PDF (green) in the sLNv DP at two time points under LD for *pdf>Q128* and *Q128*. Scale bars are 20 µm. Right: The quantification of PDF intensity in the sLNv DP across time points where both genotypes show a diurnal oscillation. * $p<0.05$, ** $p<0.01$, *** $p<0.0001$. n=18-24 hemispheres/genotype/time point.

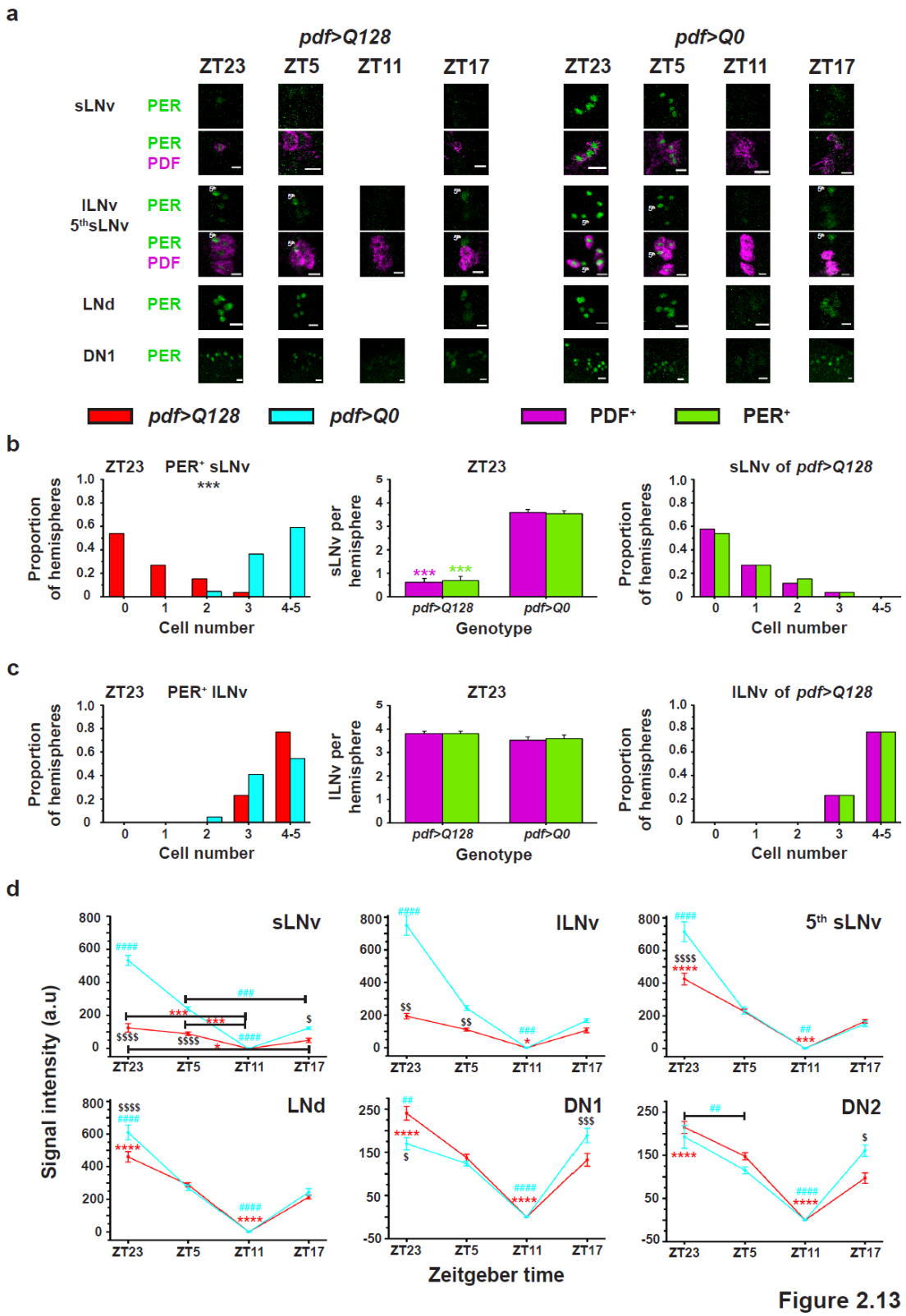

Figure 2.13

Fig 2. 13 Flies expressing expHTT show loss of PER from the sLNv and dampened oscillations of PER in the lLNv under LD.

a) Representative images of 9d adult brains stained for PER (green) in different circadian neuronal groups at four time points in LD for *pdf>Q128* and *pdf>Q0*. PDF (magenta) is co-stained to identify LNv soma. At ZT11, PER levels were deficient and not visible in most samples.

There are no representative images for PER in sLNv and LNd of *pdf>Q128* at ZT11. Scale bars are 10 µm. (b) sLNv soma in 6d-old flies in LD at ZT23. Left: Frequency distribution of the proportion of hemispheres with 0 to 5 PER^+ sLNv soma in *pdf>Q128* and *pdf>Q0.* *** indicate significantly differing distributions at $p<0.001$. Centre: Mean number of PDF^+ or PER^+ sLNv soma in *pdf>Q128* and *pdf>Q0* in DD. *** indicate statistically significant differences between genotypes at $p<0.001$: in magenta for PDF^+ sLNv soma and green for PER^+ sLNv soma. Right: Frequency distribution of the proportion of hemispheres staining 0 to 5 sLNv soma that is PDF^+ or PER^+ for *pdf>Q128* flies. (c) For lLNv. All other details are the same as above. (d) Quantifying PER intensity across time points in various circadian neuronal groups for 9d-old *pdf>Q128* and *pdf>Q0* under LD. All other details are the same as in Fig.8d. The error bars are SEM across all panels.

2.3.9 PDF in the sLNv is not necessary for morning anticipation under LD

The *pdf>Q128* flies retain their ability to exhibit M-anticipation without PDF in the sLNv soma. The entrainability of *pdf>Q128* could be due to the conveyance of time information from the sLNv to the rest of the circuit by oscillating PDF levels in its dorsal projections or a PDF-independent light-dependent process. Other experiments revealed that *pdf>Q128* flies raised and maintained in constant light (LL), over time (age 23d), show a loss of PDF from the sLNv DP also, whereas their age-matched *pdf>Q0* controls remain unaffected (Chapter 3, Fig 3.9e). This regime (LL) generated flies lacking PDF in the sLNv termini and aided in determining the necessity of PDF cycling in projections for M-anticipation under LD. One group of flies were in LL (about 200 lux) during development, and their activity was recorded as adults in LL up to 23d, followed by LD for 10d, followed by DD (denoted by the superscript LL-LD, Fig 2.14a top-left). In the control regime, flies were reared and recorded under LD for 33d followed by DD (denoted by the superscript LD-LD, Fig 2.14a bottom-left). In *pdf*>$Q128^{LL-LD}$ flies, no PDF^+ sLNv soma was detectable at age 23d and 28d, similar to *pdf*>$Q128^{LD-LD}$ (Figs 2.15a and 2.15b top-left), and PDF^+ lLNv soma numbers were comparable between regimes (Figs 2.15a and 2.15b top-right). *pdf>*$Q128^{LL-LD}$ flies showed PDF presence in sLNv DP in all samples at age 9d (Figs 2.15a top-left and 2.15b bottom-left). However, by 23d of age, PDF in the sLNv DP was lost in ~ 80% of the hemispheres while still present in all *pdf>*$Q128^{LD-LD}$ flies till 28d (Figs 2.15a and 2.15b bottom-left). In both regimes, PDF was present in lLNv contralateral projections across age (Figs 2.15a and 2.15b bottom-right). In *pdf>*$Q128^{LL-LD}$ at age 28d, the PDF was undetectable in the sLNv DP of most flies even after experiencing 5d of LD (Fig 2.15b bottom-left). The behavioural

analysis focused on this 5d age window of 24d-28d (AW4) to address the necessity of PDF in the sLNv DP for M-anticipation. In AW4, *pdf>Q128*$^{LL\text{-}LD}$ and *pdf>Q128*$^{LD\text{-}LD}$ exhibited activity profiles like their respective within-regime controls (Fig 2.14a right). The LD profile of *pdf>Q128*$^{LL\text{-}LD}$ (where PDF is absent in the sLNv DP) was also like that of *pdf>Q128*$^{LD\text{-}LD}$ (where PDF is present in the sLNv DP) with similarly phased morning and evening peaks and gradual build-up of activity before the dark/light and light/dark transitions (Fig 2.14b left). The morning and evening AIs of *pdf>Q128*$^{LL\text{-}LD}$ were not different from *pdf>Q128*$^{LD\text{-}LD}$ or *Q128* and *pdfGal* in the LL-LD regime (Fig 2.14c and d). In LL-LD, the daytime activity levels of the three genotypes were similar (Fig 2.14e), while the nighttime activity of *pdf>Q128* was lower than its controls (Fig 2.14f). In conclusion, M-anticipation does not require oscillating PDF in the sLNv DP, since even in the absence of PDF in sLNv DP (*pdf>Q128*$^{LL\text{-}LD}$), flies entrain to LD as well as controls (Fig 2.14b-d). As *pdf>Q128*$^{LL\text{-}LD}$ flies in LL-LD lack PDF in the sLNv (soma and DP), these results demonstrate that PDF in the sLNv is dispensable for M-anticipation, so long as PDF is present in the lLNv.

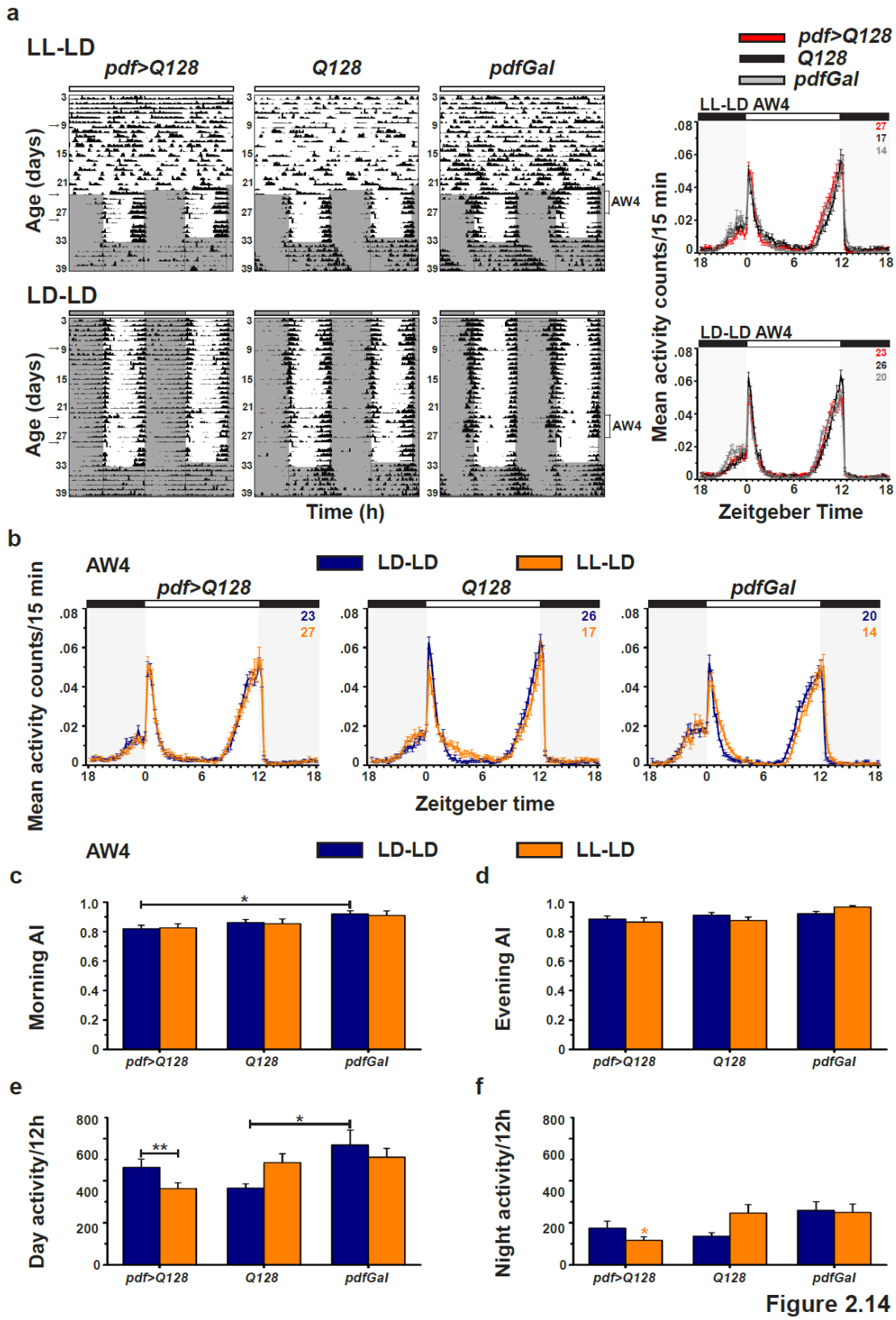

Fig 2. 14 Flies without PDF in their sLNv exhibit morning and evening anticipation.

a) Left: Representative double-plotted, normalised actograms for *pdf>Q128*, *Q128* and *pdfGal* in LL-LD (top) and LD-LD (bottom). The horizontal unshaded bar on top in LL-LD depicts the developmental regime LL. All other details are like Fig 9a. In LL-LD and LD-LD, AW4 (age 24d-28d) is indicated. The gap in the actograms is due to an interruption of the recording. Arrows at ages 9d, 23d and 28d indicate the ages at which dissections were carried out. Right: Mean normalized activity counts per 15 min comparing *pdf>Q128*, *Q128* and *pdfGal* in LL-AW4 (top) and under LD-AW4 (bottom). All other details are similar to Fig 9b. (b) Mean normalized activity counts per 15 min comparing LL-LD with LD-LD for each genotype in AW4. All other details are like Fig 9b. (c-f) Morning anticipation index (c), evening anticipation index (d), mean daytime activity counts per 12h (e) and mean nighttime activity counts per 12h (f) are plotted for all three genotypes in both regimes. * indicates significant difference at * at $p<0.05$ and ** at $p<0.01$. Across all panels, error bars are SEM.

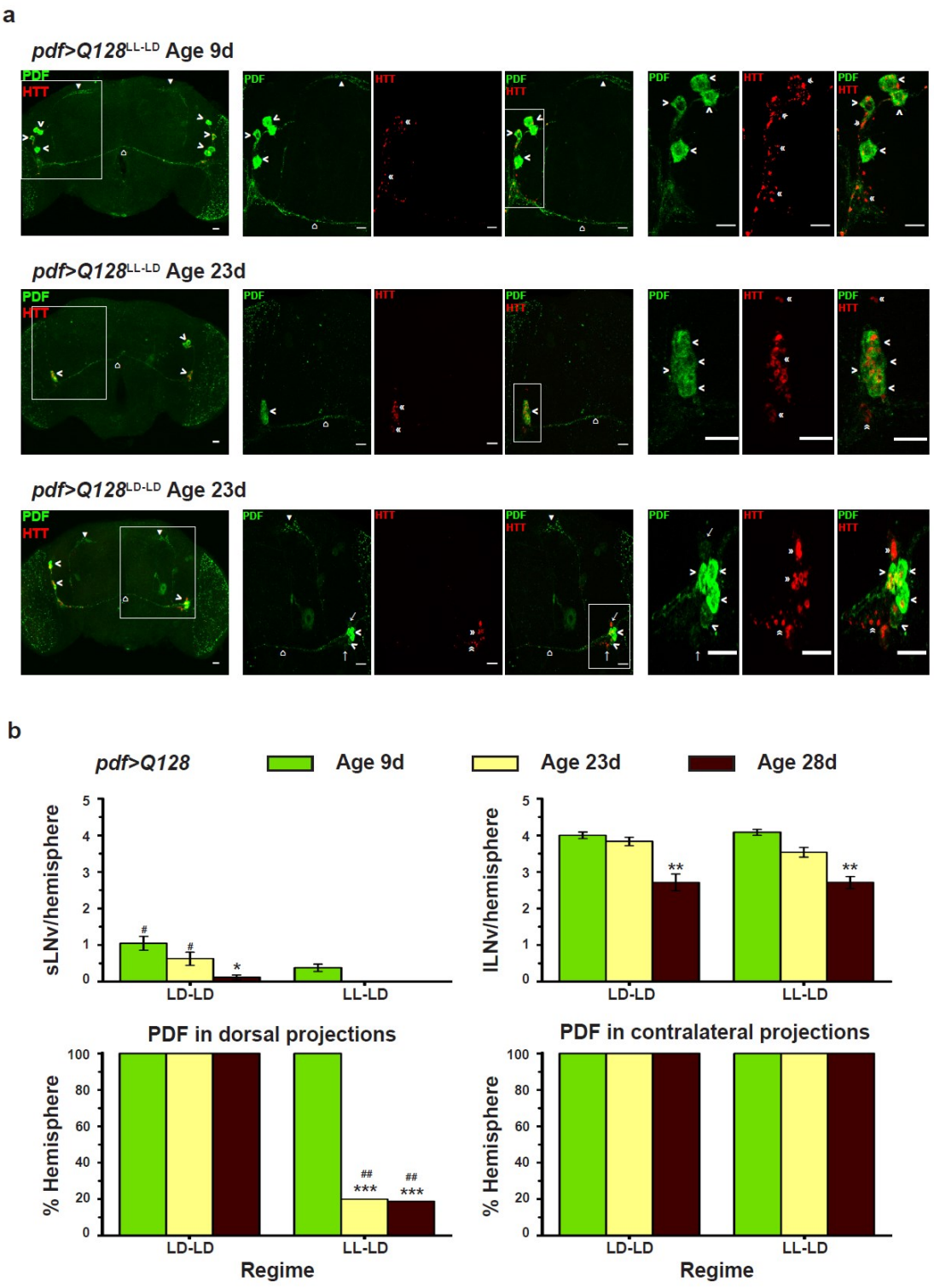

Figure 2.15

Fig 2. 15 expHTT-expressing flies in LL show a loss of PDF from the sLNv soma and DP.
(a) Representative images of adult brains of *pdf>Q128* stained for PDF (green) and HTT (red) showing sLNv soma (→ arrows), lLNv soma (> arrowheads), sLNv dorsal projections (▲ triangles), lLNv contralateral projections (⌂ house), diffuse HTT staining (Ψ psi) and inclusions of expHTT (« double arrowheads) for LL (age 9d top, age 23d centre) and LD (age 23d bottom).

Scale bars are 20 µm. Marked rectangles in each panel set are enlarged in the next panel. (b) Top left: The mean number of sLNv soma per hemisphere in both regimes across age. At age 28d, flies in the LL regime post age 23d have experienced 5d of LD. Symbols indicate statistically significant differences: * of LD-LD 28d from LD-LD 23d at $p<0.01$, # between regimes at specified age at $p<0.001$. Top right: Mean lLNv soma per hemisphere in both regimes across age. ** indicate significant differences of age 28d from earlier ages in both regimes at $p<0.001$. Bottom left: Percentage of hemispheres with PDF in sLNv DP for both regimes across age. Symbols indicate statistically significant differences: *** of 28d in LL-LD from earlier ages at $p<0.0001$ and ## between regimes at denoted ages at $p<0.0001$. Bottom right: Percentage of hemispheres with PDF in lLNv CP is plotted for both regimes across age. For all dissections, n=20-24 hemispheres/genotype/age/regime. Across panels, error bars are SEM.

2.3.10 expHTT expression in the LNv does not affect the lifespan of flies

The expression of neurodegenerative proteins reduces lifespan in animal models (Lu and Vogel, 2009). So, I asked whether expHTT expression in the 8 pairs of LNv circadian neurons affects the lifespan of these flies. The survivorship curves of expanded *pdf>polyQ* (where Q>35) were comparable to their relevant controls (Fig 15a left and b left). The mean lifespan of expHTT-expressing flies was not lower than their appropriate controls (*pdf>Q128* from *pdf>Q0*, *Q128 and yw*; *pdf>Q50* and *pdf>Q93* from *pdf>Q20*, *Q50*, *Q93, pdfGal and yw*) (Fig 15a right and b right). Thus, the expression of expHTT in the LNv circadian neurons does not affect the fly's lifespan.

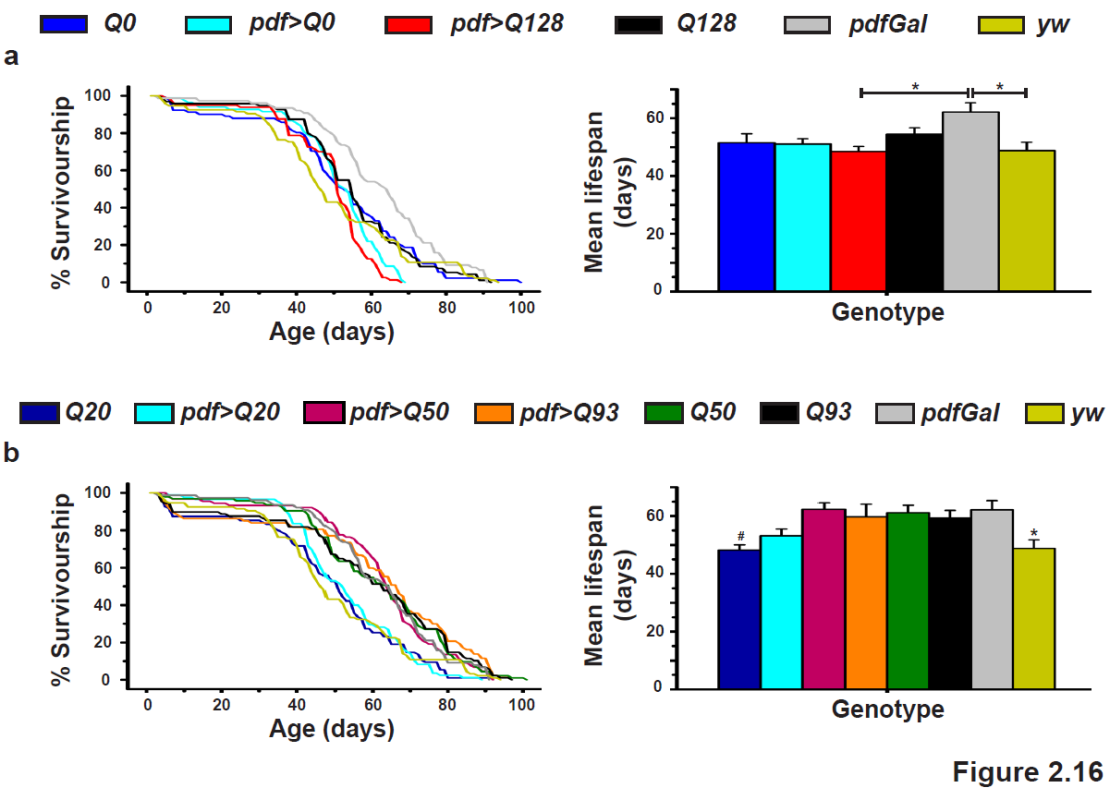

Figure 2.16

Fig 2. 16 Mean lifespans of flies expressing expHTT in their LNvs are unaffected.

(a) Left: Survivorship curves for *pdf>Q128* and its controls. Right: Mean lifespan of *pdf>Q128* and its controls with * indicating significant differences at $p<0.05$. (b) Left: Survivorship curves for *pdf>Q93*, *pdf>Q50* and their relevant controls. Right: Mean lifespan of *pdf>Q93*, *pdf>Q50* and their relevant controls. Symbols indicate significant differences: * of *yw* from *pdf>Q50* and *pdfGal* at $p<0.05$ and # of *Q20* from *pdf>Q50*, *Q50* and *pdfGal* at $p<0.05$. Across all panels, error bars are SEM.

2.4 DISCUSSION

2.4.1 Circadian model of HD

Flies expressing expHTT are arrhythmic in constant darkness and show associated loss of PDF and PER from sLNv soma. The onset of arrhythmicity is polyQ-length-dependent, with long polyQ stretches like *pdf>Q93* and *pdf>Q128* becoming arrhythmic from an early age, evident immediately upon introduction in DD. In contrast, intermediate stretches, i.e. *pdf>Q50,* become arrhythmic later. Upon introducing flies in DD, the immediate arrhythmicity of *pdf>Q128* does not alter when maintained for a longer duration in LD before the DD. Expression of expHTT in LNv also results in inclusions of expHTT in both sLNv and lLNv, characterised in detail in Chapter 3. Despite the expression of HTT-Q128 in both sLNv and lLNv, PDF is lost selectively only from the sLNv soma while being present in the sLNv DP and the lLNv under both DD and LD. Thus, the circadian model of HD shows features characteristic of HD, such as the polyQ-length-dependent onset of arrhythmicity, presence of HTT inclusions and selective susceptibility of a cell group. The lifespan of expHTT-expressing flies is not affected, which is not surprising, given that few neurons (~ 16) are targeted.

Expression of expHTT in the LNv affects sLNv soma where PDF and PER are lost, whereas sLNv DP seems unaffected in its structure and the persistence of oscillations in PDF levels. Using immunocytochemical methods, PDF and PER were undetectable in the sLNv soma. One could argue that expHTT in the sLNv soma is merely preventing the detection of these proteins using the said method, and the proteins may still be present. However, even RFP that gets detected without antibodies is undetectable in the sLNv soma of these flies. Another argument against expHTT preventing protein detection is that the sLNv DP and lLNv also show the presence of expHTT. However, these regions stain for antibodies against PDF and are detectable with GFP and RFP. The crucial evidence that PER and PDF reduction occurs *in vivo* in the sLNv soma is the physiological consequence of their absence, that being behavioural arrhythmicity in DD of *pdf>Q128* flies, a clear reflection of sLNv circadian dysfunction. The loss of membrane GFP from sLNv soma (Fig 5) and spillover of HTT inclusions into the vicinity of sLNv soma suggest

cellular stress in the sLNv soma. However, from observations with Apoliner, I cannot conclude whether sLNv undergoes apoptosis. The transition from PDF in sLNv soma to no PDF is likely very rapid and transient, preventing capturing any apoptotic events using snapshot quantifications. Continuous live-cell monitoring might help resolve this issue. A previous study describes a similar encounter with the TUNEL assay's inability to capture apoptotic events in these flies (Sheeba et al., 2010). PDF in projections of sLNv also suggests that the sLNv may be present, though dysfunctional. In the absence of a functional cell body, the continued PDF presence in the projections of sLNv and its cycling in DP is intriguing. Thus, with the limited set of markers used, any conclusion regarding cell apoptosis in the early ages is elusive. However, there is clear evidence for neuronal dysfunction in young HD flies based on the loss of cellular clock markers from the sLNv soma and its functional consequence of behavioural arrhythmicity in DD. The observation that the sLNv dorsal projections stain with PDF and GFP indicates that the neurons are likely present. Moreover, a recent study from the lab on similar HD flies shows the presence of Hsp70-stained sLNv even in the absence of PDF staining in the sLNv (nearly three sLNv per hemisphere at 1d and at least one sLNv per hemisphere at 18d) up to the age of 18d (their numbers reduced compared to 1d old flies) (Sharma et al., 2023), suggesting that the sLNv are present, in young flies. As the flies age, cell death is more likely, as is also supported by the reduction in Hsp70-stained sLNv with age (Sharma et al., 2023).

Expression of HTT-Q128 in the LNv leads to a loss of PER from the LNv. Even in a mouse model of HD (*R6/2*), core clock gene expression in the Supra Chiasmatic Nucleus is attenuated and does not oscillate (Morton et al., 2005; Maywood et al., 2010). In a circadian fly model of another polyQ disorder, the Machado Joseph Disease, loss of PER from the pacemaker neurons was reported (Kadener et al., 2006). Another *Drosophila* model of HD expressing HTT-Q103GFP in the LNv shows a significant reduction of PER in the LNv (Xu et al., 2019a). Wild-type human Huntingtin is involved in various stages of gene expression such as transcription, transport of mRNAs and translation (Kumar et al., 2014). expHTT has been implicated in transcriptional dysregulation either by sequestering critical players of the transcriptional machinery, epigenetic modifications of chromatin, or directly binding to DNA (Kumar et al.,

2014). Loss of PER from LNv could result from HTT-Q128-induced transcriptional dysregulation, leading to downregulation of circadian gene expression.

Expression of HTT-Q128 in the LNv leads to a loss of the critical circadian output neuropeptide PDF from sLNv soma, reflected as a significant decrease in PDF^+ sLNv soma numbers. Vasoactive Intestinal Peptide (VIP), one of the mammalian clock outputs, shares molecular and functional similarities with the *Drosophila* PDF (Aton et al., 2005; Vosko et al., 2007; Frenkel and Ceriani, 2011; Talsma et al., 2012). There is a reduction in the number of VIP immunoreactive neurons in the SCN of HD patients, in the mRNA levels of VIP, its receptor VPAC2 and VIP peptide levels in the SCN of R6/2 mice (Fahrenkrug et al., 2007; van Wamelen et al., 2013). Several factors modulate PDF levels, and expHTT could potentially lower PDF levels by interfering with any of these modulators. The canonical central clock protein CLOCK (CLK), negatively regulated by the PER/TIM complex, is a transcriptional repressor of *pdf* in adult flies (Mezan et al., 2016). In *pdf>Q128* flies, reduction in PER could acutely derepress or activate CLK, thereby suppressing PDF expression. Support for this hypothesis comes from a recent study in which Clk^{Jrk} suppressed the loss of PDF from sLNv in *pdf>Q128* flies, whereas Clk^{Jrk} in a per^{01} background did not suppress as much (Xu et al., 2019a). Chromatin remodelling protein DOM-A (*Drosophila* SWI2/SNF2 protein DOMINO) affects PDF at the transcriptional level (LNv-specific DOM-A downregulation only affects sLNv PDF levels, PDF^+ sLNv soma numbers and length of the sLNv DP) (Liu et al., 2019b) and VRI at the post-transcriptional level (Gunawardhana and Hardin, 2017). PDF levels are also positively regulated by the PDF neuropeptide itself through activation of PDFR in the LNv via the CGNA channel (cyclic-nucleotide-gated channel ion channel subunit A), influenced by the activity of the LNv and negatively controlled by transcription factor Strike or SR and by Matrix Metalloprotease 1 or MMP1 (only in the sLNv DP) (Depetris-Chauvin et al., 2014; Mezan et al., 2016; Herrero et al., 2020).

Despite the expression of HTT-Q128 in the LNv subsets, PDF is selectively lost from sLNv soma, while PDF in lLNv is unaffected. Other studies report such susceptibility of the sLNv: in a Machado Joseph disease model (Kadener et al., 2006), in an HD model, upon the expression of

HTT-Q103GFP in LNv, only PDF^{+} sLNv numbers diminish (Xu et al., 2019a), and upon neuronal reduction of *Drosophila enabled*, an actin polymerase involved in axonal pathfinding (Rezaval et al., 2008). Other reports show a specific effect on PDF levels in the sLNv, but not the lLNv, in a primarily circadian context. These include a near absence of PDF mRNA and protein only in the sLNv of Clk^{Jrk} and cyc^{02} flies (Blau and Young, 1999; Park et al., 2000), the elimination of PDF from sLNv DP, but not from other projections or lLNv upon developmental knockdown of LAR phosphatase (Agrawal and Hardin, 2016) or on the expression of TauE14 in the LNv (Zhang et al., 2021b), PDF levels affected only in sLNv soma and DP upon *vri* inactivation (Gunawardhana and Hardin, 2017), and PDF affected only in the sLNv upon depletion of Domino-A (Liu et al., 2019b).

In contrast to lLNv PDF, PER levels in lLNv show a significant reduction. PER in lLNv is barely detectable in DD and shows dampened oscillations under LD. Nonetheless, PER oscillations in the lLNv dampen in wild-type flies in DD and are not essential for circadian activity rhythms in DD (Shafer et al., 2002; Grima et al., 2004a; Lin et al., 2004). So, the circadian behavioural arrhythmicity reflects the sLNv dysfunction, and the sLNv are selectively susceptible to expHTT. The selective vulnerability of neuronal subsets is a hallmark of HD (Han et al., 2010). The specific vulnerability of sLNv to HTT-Q128 could be due to several unique cellular factors, including its early development, size, variable gene expression pattern and enrichment of neurotoxic factors or (and) impoverishment of neuroprotective factors. An explanation for only the loss of sLNv PDF is that it is non-amidated, whereas lLNv PDF is amidated and has a greater half-life (Helfrich-Förster, 2009). Also, regarding function, lLNv seems to be relatively protected from HTT-Q128 as their firing pattern and frequency are unaffected (Sheeba et al., 2008b). In support, sleep levels seem primarily unaltered. A recent study from the lab shows that the LNv (both s and l) of controls *pdf>Q0* do not stain with antibodies against Hsp70, suggesting that they are relatively unstressed (Sharma et al., 2023). Further, the number of lLNv positive for Hsp70 is fewer than that of sLNv, suggesting that the large neurons are more resistant to stress.

Observing PDF loss only from the sLNv soma alone while being detected in DP is unique. So far, in models of neurological disorders, selectivity for soma has not been reported; in many cases,

axonal degeneration precedes soma loss (Han et al., 2010; Lingor et al., 2012). Even in fly models, expression of neurodegenerative proteins in *Drosophila* circadian neurons results in a decline of PDF signals in sLNv DP or abnormal sLNv axonal arborisation, while PDF in soma is unaffected (Leyssen et al., 2005; Chen et al., 2014; Okray et al., 2015; Song et al., 2016). A recent study expressing phosphomimetic mutant TauE14 in the LNv also shows a contrasting effect on the sLNv than observed here while showing disruption of free-running activity rhythms (Zhang et al., 2022). A selective abolishment of PDF only from the sLNv DP (GFP present, but reduced in intensity), a modest reduction of PDF levels in the sLNv soma and of GFP^+ DP area (a marker of sLNv axonal morphology), but no effect on the number of GFP-labeled sLNv or lLNv soma was seen. These were accompanied by a complete loss of mitochondria from the sLNv DP, with a concomitant increase in its soma, indicating that defects in the transport and localisation of neuropeptides and mitochondria from soma to axons can contribute to such unique and selective neuronal phenotypes associated with NDs. These findings also suggest that neuronal groups are differentially sensitive to neurodegenerative proteins, and the differences in gene expression between sLNv and lLNv can underlie some of this (Kula-Eversole et al., 2010).

A possible explanation for the detrimental effect of expHTT on the sLNv soma over axonal termini is the differential distribution of HTT-Q128 inclusions. The inclusions are numerous in sLNv soma or the region where sLNv soma are likely to be found and fewer and far apart in the axons, possibly accounting for relative protection of axonal PDF from HTT-Q128 during the experimental timescale. The slow diffusion of expanded proteins in the cells could also contribute to this differential distribution. Also, the PDF in sLNv DP could linger around longer due to a sustained local translation or slower degradation/clearance rates of its mRNA.

Upon providing light/dark cycles, the *pdf>Q128* flies are rhythmic in LD and exhibit control-like anticipation to dark/light and light/dark transitions and M and E peak phases. However, the rhythmicity in LD does not sustain on shifting them to DD, where arrhythmicity sets in immediately. Therefore, distinguishing true entrainment from masking under LD in these flies is not straightforward. Nevertheless, *pdf>Q128* flies show control-like- circadian profiles in dim-LD and a quick shift in activity to a phase-shifted LD. Under LD, they also exhibit in-phase

molecular clock protein oscillations between circadian neuronal groups and controls. A previous study showed that the anticipation of these flies is not different from controls across photoperiods (Potdar and Sheeba, 2012). Collating all the above evidence, I conclude that *pdf>Q128* flies entrain to light/dark cycles. Unlike flies expressing $A\beta_{42}$arc pan-neuronally that do not re-synchronise to a phase-shifted LD (Chen et al., 2014) or BAC HD mice that take longer to re-synchronise than wildtype (Kudo et al., 2011), *pdf>Q128* flies showed control-like re-entrainment. This result suggests that the sensitivity of HD flies to phase-shifting effects of light is intact and further supports the conclusion that the entrainability of these flies to LD is unaffected.

2.4.2 Role of the sLNv in mediating free-running activity rhythms

Most weakly rhythmic and arrhythmic *pdf>Q128* flies show loss of PDF from the sLNv soma while it is present in the sLNv DP and the lLNv, suggesting that predominantly, PDF in sLNv soma is critical for robust rhythms. The presence of non-zero sLNv (at least one) with control levels of PDF and intact DP is not always associated with behavioural rhythmicity. This observation contrasts *disco* mutants, where a single LNv with intact DP was sufficient for a fly to be rhythmic (Helfrich-Förster, 1998). Unlike *disco* mutants where the sLNv, when present with DP, are functional like wildtype on the expression of expHTT, despite PDF presence in sLNv, other functional components of sLNv are likely to be compromised. The present study thus reveals that cellular features of PDF distribution, overall sLNv health and functionality, rather than mere PDF presence, are vital in determining rhythmicity. Also, evidence from studies suggests that PDF in the LNv is not entirely essential for activity rhythms, as about 50% of PDF mutants remain weakly rhythmic (Wulbeck et al., 2008; Shafer and Taghert, 2009; Yoshii et al., 2009; King et al., 2017). sLNv are glycinergic, and glycine receptors in DN1ps are essential for modulating the power of activity rhythms, providing an alternative to the PDF-centric rhythm maintenance effects of sLNv (Frenkel et al., 2017).

Flies can be behavioural arrhythmic in DD despite maintaining oscillations in PDF levels in sLNv projections. It thus challenges the central role attributed to oscillations in PDF levels in the sLNv

DP as the primary output of the sLNv for rhythmic free-running locomotor activity. Prior studies with genetic manipulations affecting sLNv functions resulted in the loss of behavioural rhythmicity in DD and an associated loss or altered phasing of PDF oscillations in their DP (Renn et al., 1999; Nitabach et al., 2002; Nitabach et al., 2006; Fernández et al., 2007b; Wu et al., 2008a; Wu et al., 2008b; Depetris-Chauvin et al., 2011; Gunawardhana and Hardin, 2017). Only the PDF oscillations were often affected with the sLNv molecular clock intact (Nitabach et al., 2006; Fernández et al., 2007b; Wu et al., 2008b; Gunawardhana and Hardin, 2017), suggesting that PDF is a critical sLNv output. Thus, in DD, rhythmic PDF accumulation and perhaps secretion have been considered the primary functional outcome of sLNv, leading to rhythmic behaviour. Researchers attribute the short-period rhythms seen in pdf^{01}, hyperactivated LNv in the absence of PDF or LNv-silenced flies to the short period clocks of LNd and DN due to the lack of reset signal in the form of rhythmic PDF (Lin et al., 2004; Wu et al., 2008b; Sheeba et al., 2008c).

From immunocytochemical measurements, it is clear that PDF levels oscillate in the sLNv DP of behaviourally arrhythmic flies in DD. However, this is not direct evidence for rhythmic PDF secretion. Previous studies have shown that in the absence of PDF (Lin et al., 2004; Yoshii et al., 2009) or PDFR (Lear et al., 2005; Zhang et al., 2010a), there is a loss of synchrony among the rest of the circadian neuronal circuit. In light of these studies, the finding of synchronous PER oscillations in the PDF$^-$clock neurons shown here provides indirect evidence for rhythmic PDF release from the sLNv DP and its downstream synchronising effects on the non-LNv neurons. Direct measurements of PDF release, as demonstrated at the larval neuromuscular junction (Levitan et al., 2007), may confirm this phenomenon. Additionally, the few weakly rhythmic flies had a period close to 24h, indicating that oscillating PDF in sLNv DP functions by synchronising the PDF$^-$neuronal oscillators to run with nearly 24 periods. However, this PDF-oscillation-dependent resetting does not seem sufficient for behavioural rhythmicity. Despite rhythmically accumulating PDF in the sLNv DP and likely rhythmic secretion, synchronised molecular oscillations between PDF$^-$ neurons, the locomotor activity remains arrhythmic in DD.

These results suggest that sLNv function in the sustenance of activity rhythms depends not only on PDF oscillations in its DP but also on additional mechanisms independent of oscillating PDF.

Two recent studies support this hypothesis. Unc5 expressing LNv showed a loss of sLNv DP, but the flies remained rhythmic in DD with an unaltered period (Fernandez et al., 2020). CLKΔ expression and PER downregulation knockdown in the LNv impaired rhythms in PDF levels in sLNv DP but did not lead to immediate locomotor arrhythmicity in DD (Jaumouille et al., 2021). Another study indicates that the time-of-day-dependent effects of PDF in gating the molecular clock responses to PDF might not depend on rhythms in the PDF levels but rather on intracellular timing mechanisms (Sabado et al., 2017). In previous studies, loss of oscillations in the PDF levels in the sLNv DP accompanied the breakdown of behavioural rhythms, with the sLNv molecular oscillations essentially remaining unaffected (Nitabach et al., 2006; Fernández et al., 2007b; Depetris-Chauvin et al., 2011; Gunawardhana and Hardin, 2017). In the current study, PDF levels oscillate in the sLNv DP, while the associated locomotor activity behaviour remains arrhythmic, and the molecular clock protein PER is lost from the sLNv. In other words, PDF oscillations in sLNv DP are necessary, but in the absence of functional sLNv clocks, they are insufficient for behavioural rhythmicity. Presented here is evidence for the first time that oscillating PDF in the sLNv DP and synchronous molecular clocks in PDF^- neurons need not translate to rhythmic locomotor activity. The prior studies' strong association of behavioural rhythmicity with PDF oscillations in sLNv DP led to an implicit assumption of causality without invoking an additional component in sLNv. In *pdf>Q128*, uncoupling the PDF oscillations in the sLNv DP from the behavioural rhythms has opened up possibilities for other mechanisms in the sLNv mediating rhythmic behaviour under DD. I refer to such mechanisms as the PDF-oscillation-independent component (POIC). I propose that both components of the sLNv function: oscillations of PDF in the DP acting as a synchronising agent of molecular oscillations in PDF^- neurons and POIC are critical for coherent and robust activity rhythms in DD (Fig 2.17 left).

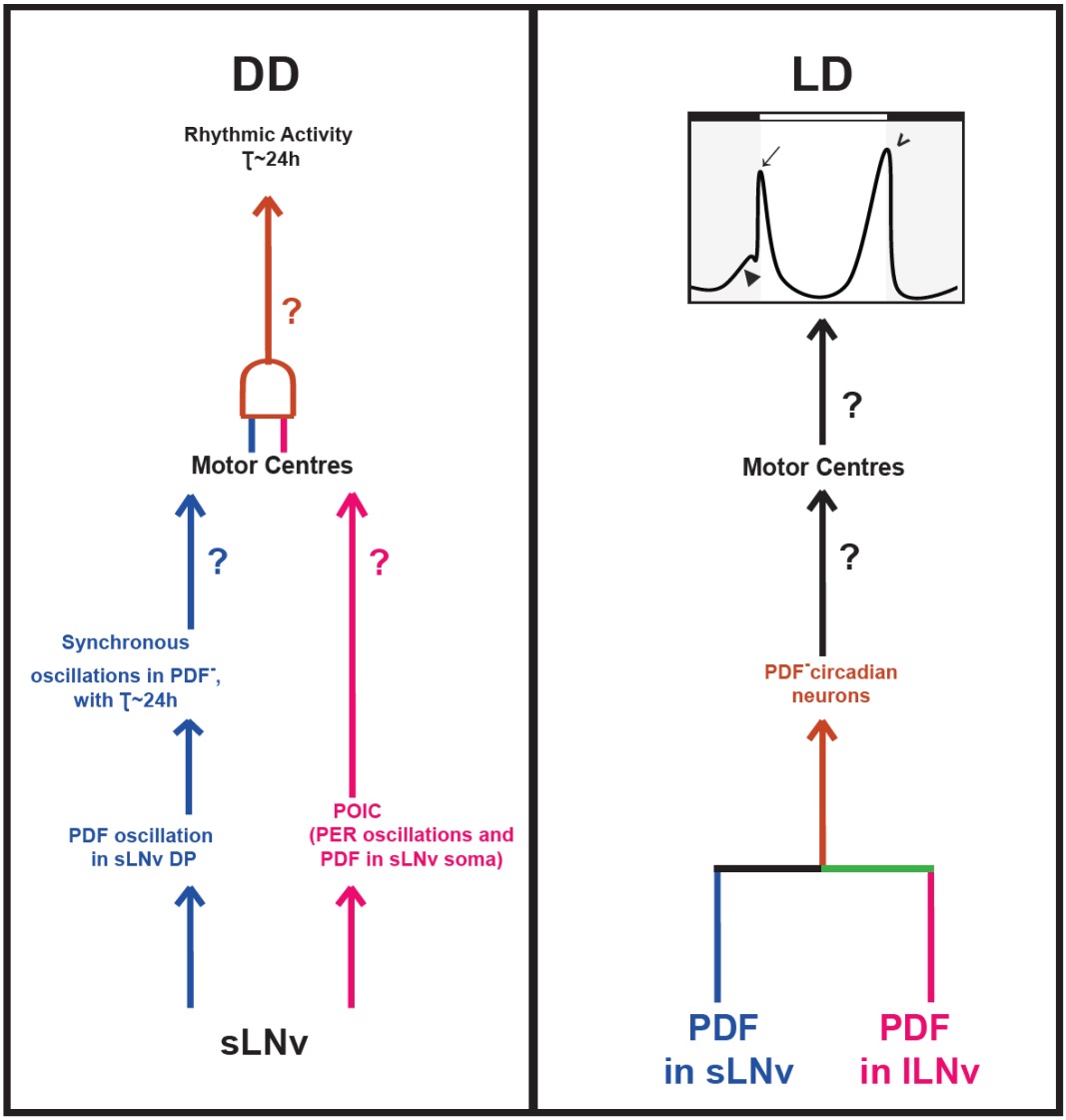

Figure 2.17

Fig 2. 17 Model for LNv-mediated sustenance of activity rhythms in DD and modulation of temporal activity profiles under LD.

Left: (blue) Previous studies have suggested that sLNv sustains rhythmic activity in DD via rhythmic accumulation and likely secretion of PDF from its DP, synchronising the molecular clocks between the PDF⁻ circadian neuronal groups and setting their period to near 24h (Lin et al., 2004; Nitabach et al., 2006; Fernández et al., 2007b; Wu et al., 2008b) and the latter possibly communicating time information to motor centres (MC) (Cavanaugh et al., 2014; King et al., 2017). I propose an additional component (magenta) to control rhythmicity by sLNv, the POIC (PDF-Oscillation-Independent Component), possibly involving PDF in the sLNv soma and molecular clocks in the sLNv. Both inputs seem necessary (brown) for near 24h activity rhythms in DD. Right: Previous studies have shown that, under LD, LNv PDF is critical for the M-peak (arrow), the M-anticipation (triangle) and the E-peak phasing (arrow-head), and that the sLNv PDF is sufficient (Shafer and Taghert, 2009) (blue). This study shows that the lLNv PDF is also sufficient (magenta) for this behaviour. Communication from the LNv to the PDF⁻ neurons via PDFR can bring about this behaviour (Lear et al., 2009) (brown).

One study provides a means for direct synaptic communication of the lLNv with the LNd (Schlichting et al., 2016) (green). Therefore, I propose that PDF inputs from either the sLNv or the lLNv to PDF$^-$ neurons are sufficient. The latter communicates to MC via yet unknown mechanisms to shape the activity profiles under LD.

2.4.2.1 PDF-oscillation-independent component (POIC)

In *pdf>Q128*, behavioural arrhythmicity is associated with losing both PER-dependent molecular clocks and PDF in the sLNv soma. Thus, both seem likely to be integral components of the POIC. There is some indirect evidence for the presence of POIC in the sLNv. The sufficiency of PER expression in the sLNv in a *per^0* background rescuing behavioural arrhythmicity in DD and molecular oscillations in sLNv is well established (Grima et al., 2004a; Cusumano et al., 2009; Seluzicki et al., 2014). Activity rhythm rescue in *per^0* by restoring PER oscillations in the sLNv happens via a direct effect of PDF through PDFR on the TIM levels in PDF$^-$circadian neurons (Seluzicki et al., 2014). However, this behavioural rhythm rescue did not involve restoring molecular clocks in the PDF$^-$ neurons, suggesting a role for sLNv in sustaining free-running activity rhythms without molecular clocks in the PDF$^-$ circadian neurons. The rescue is dependent on the sLNv molecular clock and directly mediated by PDF but independent of PDF oscillations in the DP and synchronous molecular clocks in the PDF$^-$ neurons (Seluzicki et al., 2014). Two recent studies show that near-complete knockdown of PER or TIM in the LNv using CRISPR, with functioning molecular clocks in the rest of the circadian neuronal circuit, did not cause significant loss of rhythmicity in DD or affect the period but reduced the rhythm strength (Delventhal et al., 2019; Schlichting et al., 2019a). Thus, they question the necessity of circadian molecular oscillations in the sLNv to sustain free-running rhythms. Other studies show that in the absence of PDF in the sLNv DP, PDF presence in the sLNv soma, and functional clocks in the sLNv cannot induce behavioural rhythmicity in DD (Agrawal and Hardin, 2016; Zhang et al., 2021b). Thus, it appears that the POIC alone cannot sustain rhythmicity. Support for a combination of clock, circadian output, and neuronal communication from the sLNv for free-running locomotor activity rhythms comes from recent studies. In the absence of functional clocks in the non-LNv circadian neurons or activity-dependent communication between them,

functioning sLNv alone cannot bring out rhythmic activity behaviour (Bulthuis et al., 2019). Further, the maintenance of activity rhythms by the sLNv requires both the clocks in sLNv and neural communication to act additively (Jaumouille et al., 2021). Thus, POIC, in the absence of communication with and between downstream neurons and synchronised clocks in the downstream neurons, would be insufficient in mediating activity rhythms.

A parallel pathway in mediating time-of-day-dependent communication from the sLNv to its target neurons, independent of timed release of PDF, comes from a study that shows that the sensitivity of sLNv to PDF is cyclic and PDFR and a small GTPase, RalA modulate this rhythmic responsiveness (Klose et al., 2016). The circadian role of sLNv is not limited to oscillating PDF. sLNv functional outputs occur in the form of rhythmic changes in electrical activity, structural plasticity (such as axonal morphology and pre-synaptic active sites) and the number of contacts between sLNv and their partners, all of these contributing to behavioural rhythmicity (Muraro et al., 2013; Depetris-Chauvin et al., 2014; Gorostiza et al., 2014; Herrero et al., 2020). The oscillations in the sLNv axonal remodelling are clock-controlled, dependent on PDF from both sLNv and lLNv and sensitive to the amplitude of PDF oscillation in sLNv DP (Fernandez et al., 2008; Depetris-Chauvin et al., 2014; Herrero et al., 2017; Herrero et al., 2020).

There is also evidence for PDF-independent rhythms. About half of the pdf^{01} flies retain weak rhythmicity (Wulbeck et al., 2008; Shafer and Taghert, 2009; Yoshii et al., 2009; King et al., 2017) and hyper-activating LNv in a pdf^{01} background results in short-period free-running rhythms (Sheeba et al., 2008c). sLNv are also glycinergic and glycine-responsive DN1p influence the power of activity rhythms (Frenkel et al., 2017).

POIC could potentially convey information from sLNv to motor centres to drive rhythmic behaviour in DD (Fig 6 left). An early hypothesis was that sLNv directly modulates pre-motor centres to bring about rhythmic behaviour (Lin et al., 2004). sLNv arbours form synaptic contacts in a time-of-day-dependent manner with specific clusters of mushroom body and neurons of Pars Intercerebralis (PI), a locomotor centre shown to control rhythmic activity behaviour (Cavanaugh et al., 2014; Gorostiza et al., 2014; King et al., 2017). Such time-dependent contacts could potentially involve POIC. LNvs access motor centres in the ellipsoid body directly via PDF and

indirectly via intervening dopaminergic neurons (Liang et al., 2019). sLNv modulates Leukokinin neurons, and Leukokinin neuronal communication with its receptor neurons is a critical output circuit for rhythmic locomotor activity in DD (Cavey et al., 2016). sLNv can also indirectly communicate with motor centres via its synaptic arbours with DN1p, which in turn synapse with a subset of PI neurons that are critical for rhythmic behaviour in DD (Zhang et al., 2010a; Cavanaugh et al., 2014; Seluzicki et al., 2014; King et al., 2017). A recent study shows that flies without sLNv DP exhibited unaltered activity rhythms in DD, indicating long-distance action of PDF-dependent sLNv circadian output onto brain regions like dorsal protocerebrum or accessory medulla serving as sites for circadian output (Fernandez et al., 2020). Another recent study showed that the mushroom body, a proposed integration centre for multiple behaviours, has active functional contacts from sLNv (Gorostiza et al., 2014; Pirez et al., 2019). However, its role as an output centre for modulating locomotor activity rhythms is debatable (Helfrich-Förster et al., 2002; Mabuchi et al., 2016).

2.4.3 Role of the sLNv in modulating activity rhythms under LD

A previous report showed a reduction in M-anticipation on partial reduction of PDF (63%) only in sLNv soma, but control-like M-anticipation upon nearly complete removal of PDF from sLNv soma and DP and incomplete reduction (44%) in lLNv (Shafer and Taghert, 2009). Further, flies lacking PDF from sLNv soma (Sheeba et al., 2010) or flies lacking PDF only from the sLNv DP (Agrawal and Hardin, 2016) still show M-anticipation to LD. My study uses a combination of genetic and environmental strategies to establish a phenotype with a specific and complete loss of PDF from the sLNv (soma and DP). Under such conditions, M-peak, M-anticipation, and E-peak phases are unaffected in LD, showing that PDF from the sLNv is unnecessary for LD activity rhythms. In a previous study, PDF down-regulation in both subsets resulted in altered activity rhythms in LD, while rhythms were unaffected upon down-regulation only in the lLNv (Shafer and Taghert, 2009). Therefore, I conclude that PDF from either the sLNv or the lLNv is sufficient for M-peak and M-anticipation (Fig 2.17 right). In *pdf>Q128* flies, despite losing PDF from

sLNv, PDF from lLNv can bring about M-anticipation. A recent study demonstrates synaptic connections between the lLNv and the LNd and provides a possible direct communication to modulate LD behaviour (Schlichting et al., 2016). PDF from the lLNvs seems responsible for circadian adaptation to long photoperiods (Schlichting et al., 2019c). My findings strongly show that cyclic secretion of PDF from sLNv is dispensable for LD behaviour. This conclusion is in agreement with other reports that the DN1ps requires PDF for the morning activity, but the PDF need not be cyclic for entrainment to LD (Kula et al., 2006; Choi et al., 2012; Chatterjee et al., 2018a). In conclusion, PDF from the sLNv is not required for M-anticipation under LD if PDF is available from the lLNv.

PDF is essential for the early development of the sLNv circuit (Gorostiza and Ceriani, 2013). In the present study, loss of PDF in the sLNv soma is evident from an early age, and at a later age of 23d, a complete loss of sLNv PDF is evident. Given the presence of PDF in the sLNv during development and at younger ages of adulthood in these flies, one cannot rule out the role played by sLNv PDF in establishing and maintaining circadian neuronal circuits contributing to the entrainment of activity rhythms to LD. A possible scenario is that after the establishment and maturation of the circuits, the PDF in sLNv is dispensable for LD behaviour. A recent study highlights the developmental necessity of PDF for activity rhythms in LD. The authors show that the downregulation of DOM-A in the circadian neurons developmentally compromises sLNv (Liu et al., 2019b). It brings down PDF^{+} sLNv numbers and PDF levels and shortens the sLNv DP, resulting in a loss of the M-anticipation (Liu et al., 2019b). However, this study targeted a broad group of circadian neurons, resulting in a circuit-wide reduction of PER and TIM.

Rescue of PER in the sLNv of per^{0} flies was sufficient for M-activity and anticipation in LD, suggesting that for M-anticipation, functional clocks in sLNv are essential (Cusumano et al., 2009). However, rescuing PER in PDF^{-} neurons was also sufficient for M-anticipation (Stoleru et al., 2004), suggesting that PER in LNv is unnecessary for M-activity in the presence of functioning clocks in the PDF^{-} neurons. However, the authors hypothesised this rescue to occur via recovery of the PDF output function of LNv (Stoleru et al., 2004). In the present study, in LD, flies showing loss of PER in the LNv, synchronised PER oscillations in the PDF^{-} neurons,

and a complete loss of PDF from the sLNv continue to display morning anticipation. These results prove that M-anticipation persistence in flies without functional LNv PER-driven clocks can occur without recovering the sLNv PDF output function, contrary to suggestions in the previous report (Stoleru et al., 2004). In conclusion, PER-driven molecular clocks in the sLNv are unnecessary when functional clocks are present in the non-LNv neurons for activity rhythms in LD. Two recent studies strengthen this conclusion. Adult-restricted PER downregulation in the LNv, which abolishes rhythms of PER in the LNv and that of PDF levels in the sLNv DP, did not blunt morning anticipation, but eliminating CLK in the LNv did (Jaumouille et al., 2021). CRISPR-mediated near complete knockdown of PER or TIM in the LNv did not affect activity rhythms in LD (though PER knockdown reduced M-AI, M-AI was >1; TIM knockdown flies also lacked PER) (Delventhal et al., 2019). The study suggests that clocks in either LN group (LNv or LNd) are sufficient for this behaviour and that circadian neurons act in a distributed network, compensating for the loss of the molecular clock in specific subsets (Delventhal et al., 2019).

2.4.4 Clocks controlling PDF oscillations in the sLNv dorsal projections

Intriguingly, oscillations in PDF levels persist in the sLNv DP despite the loss of PER, a critical molecular clock component and PDF from the sLNv soma. Given the functional consequence of these oscillations, evidenced by synchronous oscillations in PER levels between PDF^- neurons, these oscillations indicate rhythmic PDF secretion. expHTT is known to block axonal transport (Lee et al., 2004). In *pdf>Q128,* the oscillations in PDF levels at sLNv axonal termini suggest that axonal transport in these flies is not impaired, or if impaired, does not disrupt PDF oscillations in the sLNv.

The oscillations in PDF levels in the sLNv DP persist in the absence of PDF in the sLNv soma (Fig 2.7) or upon increasing PDF levels higher than usual in the LNv (Helfrich-Förster et al., 2000). These observations suggest that the cyclic accumulation of PDF in sLNv terminals does not depend on PDF levels in the sLNv. However, recent studies show that oscillations in PDF levels at the sLNv DP require PDF in the sLNv, PDFR in the LNv, the electrical activity of the

LNv and the responsiveness of PDFR to PDF mediated via CNGA channels (Depetris-Chauvin et al., 2014; Herrero et al., 2020). In the *pdf>Q128* flies, the role of electrical activity and PDFR in mediating oscillations of PDF levels warrants exploration. Another possibility is that lLNv PDF, which is not affected by expHTT, could drive PDF oscillations in the sLNv DP; however, the downregulation of lLNv PDF did not affect PDF oscillations (Herrero et al., 2020).

In *per* and *tim* null mutants, PDF mRNA shows oscillations in the soma of sLNv, but PDF peptide oscillations in the sLNv DP are lost, suggesting post-transcriptional clock control of PDF (Park and Hall, 1998; Park et al., 2000). On the ectopic expression of PDF, rhythmic accumulation occurs only in projections of pacemaker sLNv but not in non-circadian neurons, providing further evidence for clock control of PDF rhythms (Helfrich-Förster et al., 2000). This posttranscriptional circadian regulation of PDF could occur at the level of peptide processing, axonal transport to terminals, accumulation or secretion (Helfrich-Förster et al., 2000; Park et al., 2000). Another study shows that flies with downregulated PER or TIM in the LNv or expressing CYC^{DN} in the LNv have PDF oscillations intact but at significantly dampened levels compared to controls, suggesting a role for molecular clocks in the LNv in modulating PDF level oscillations (Herrero et al., 2017). In another study, the downregulation of PER in the LNv or adult-specific elimination of CLK in the LNv reduced PDF in the sLNv DP and abolished oscillation in its levels (Jaumouille et al., 2021). In expHTT-expressing flies, PER is nearly undetectable in the sLNv soma, suggesting a loss of PER from the sLNv. PER could be present below detection levels but at such low levels, unlikely to oscillate and likely amount to a robust PER-driven molecular clock loss. Under DD, PER oscillations are lost even in the lLNv; therefore, lLNv PER is unlikely to contribute to PDF oscillations in sLNv DP.

The results of continued PDF oscillations in the sLNv DP in the absence of PER in the sLNv soma in DD suggest that PER-independent clock mechanisms in the sLNv mediate these oscillations. Other clock proteins involved in the second feedback loop, such as Vrille and PDP1, could oscillate, inducing PDF oscillations in the sLNv DP. VRI (Vrille), a crucial molecular clock component and part of another analogous interlocked loop operating in *Drosophila*, is activated by CLK-CYC and is required for PDF expression (Gunawardhana and Hardin, 2017). *vri*

inactivation abolishes PDF from the sLNv DP and lowers PDF levels in the sLNv soma (Gunawardhana and Hardin, 2017). CLK is known to repress *pdf* transcription, and MMP1, a direct target of CLK (Kadener et al., 2007), suppresses PDF levels only in the sLNv DP (by cleaving PDF and inhibiting its activity) and possibly its release (Depetris-Chauvin et al., 2014). MMP1 levels are critical for maintaining oscillations in PDF levels at the sLNv DP (Depetris-Chauvin et al., 2014). However, given the loss of PER from the sLNv and possible acute CLK activation in the present study, the continued PDF oscillations in sLNv DP suggest subtle effects on the MMP1 levels that are not significant enough to disrupt PDF levels in the sLNv DP or their oscillations.

Though clocks in the glia are essential for the circadian structural plasticity of the sLNv terminals (Damulewicz et al., 2022a), they do not mediate PDF oscillations in the sLNv DP (Herrero et al., 2017). An alternative to PER-driven clocks is rhythms of oxidation-reduction of peroxiredoxins that persist in *Drosophila* circadian clock mutants, albeit with an altered phase (Edgar et al., 2012). A recent study prompted an exploration of alternatives to conventional molecular clocks (Rey et al., 2018). *Drosophila* Schneider 2 (S2) cells that lack canonical clock-protein-based transcriptional feedback loops and oscillations in secondary loop components exhibit widespread daily oscillations in many genes, especially metabolic transcripts (Rey et al., 2018). The current work provides evidence for the independence of PDF oscillations in the sLNv DP from PER-driven clocks in the sLNv, evoking a need to investigate alternate sources driving these oscillations in the critical pacemaker neurons. Therefore, the lack of molecular clockwork is compensated if the M-oscillator can produce synaptic and peptidergic outputs.

Conversely, the lack of neural transmission from the M-oscillator can be overcome if their internal clocks are functional. In support of these conclusions, later studies suggest that while the clock in the LNv might be dispensable for rhythmicity, the LNv cell bodies are not (Schlichting et al., 2019a). Moreover, there is the likelihood that other pacemakers like the LNds can drive the rhythmicity of PDF and other sLNv outputs (Schlichting et al., 2019c), and interneuronal communication might compensate for the loss of molecular clocks in any given subset (Bulthuis et al., 2019; Ahmad et al., 2021).

CHAPTER 3

Effects of Light Regimes on the Circadian Dysfunction and Neurotoxicity in HD flies

3.1 INTRODUCTION

Circadian and sleep disturbances are widespread in patients suffering from HD and other neurodegenerative diseases and are recapitulated in animal models (Morton, 2013; Fifel and Videnovic, 2020; Voysey et al., 2021a). Disturbances in melatonin rhythm, nocturnal awakenings and daytime sleepiness in HD patients and arrhythmic circadian activity rhythms with disruptions of clock gene oscillations and attenuated spontaneous electrical activity in neurons of the central clock of mice, the Supra Chiasmatic Nucleus (SCN) have been reported (Morton et al., 2005; Pallier et al., 2007; Aziz et al., 2009a; Kudo et al., 2011; Hood and Amir, 2017b) Arrhythmic circadian activity rhythms with molecular clock disruptions in central pacemakers LNv (Sheeba et al., 2008a; Prakash et al., 2017) and disturbed sleep phenotypes (Gonzales and Yin, 2010) are shown in *Drosophila* models of HD. Thus far, most studies focus on the effect of neurological diseases on circadian rhythms and sleep functions (Hastings and Goedert, 2013; Musiek, 2015). However, an important question is whether circadian rhythms impact neurodegenerative outcomes, specifically, whether strengthening rhythms suppress neurodegenerative phenotypes or disrupting rhythms exacerbates them.

There is substantial evidence for the essentiality of a functioning circadian clock on overall organismal health (Kondratova and Kondratov, 2012; Videnovic and Zee, 2015; West and Bechtold, 2015). Emerging evidence suggests that circadian and sleep dysfunction might themselves contribute to neurodegenerative phenotypes (Leng et al., 2019; Lananna and Musiek, 2020; Carter et al., 2021) and is bolstered by observations that such disturbances appear early during disease progression (Arnulf et al., 2008; Soneson et al., 2010; Goodman et al., 2011; Morton et al., 2014; Lebreton et al., 2015; Bellosta Diago et al., 2017) and mutations in core clock genes accelerate neuropathology in ND models of *Drosophila* and mice (Krishnan et al., 2012; Musiek et al., 2013). Environmental conditions resulting in circadian rhythm disruption, such as chronic jet lag, light exposure at night, non-native light/dark cycles (LD) and constant light (LL), are also detrimental to health (Cho, 2001; Karatsoreos et al., 2011; Cho et al., 2015; Lucassen et al., 2016; Vaccaro et al., 2016; Lauretti et al., 2017a; Falcon et al., 2020). Furthermore, restoring circadian rhythmicity by pharmacological, behavioural, or environmental interventions improves several symptoms in a mouse model of HD (Pallier et al., 2007; Pallier and Morton, 2009;

Maywood et al., 2010; Skillings et al., 2014; Ouk et al., 2017). With an increase in exposure to artificial light at night, irregular sleep timings and poor circadian hygiene, minimal exposure to bright light during the day, shift work and jet lag, the effects of environmental light on the progression of NDs is a public health concern (Fonken and Nelson, 2011; Blume et al., 2019; Rumanova et al., 2020; Fernandez, 2022). Hence, I asked whether environmental regimes that modify circadian rhythms also affect the neurodegenerative phenotypes of the previously described *Drosophila* HD model (Chapter 2) (Sheeba et al., 2008a; Prakash et al., 2017). I examined environmental regimes' impact on behavioural arrhythmicity and cellular features in this fly model.

Under seminatural conditions (SN) where multiple environmental cues change gradually, specific clock mutant flies show activity/rest patterns like wild type (Menegazzi et al., 2012a; Vanin et al., 2012; De et al., 2013). A similar observation was also made with $Per2^{BRDM1}$ mice (Daan et al., 2011). Therefore, SN was considered a rhythm-bolstering environment. Under constant light (LL), constant CRY activation leads to constitutive degradation of TIM in clock neurons, disruption of the molecular clockwork and behavioural arrhythmicity in *Drosophila* (Konopka et al., 1989; Price et al., 1995; Lee et al., 1996; Marrus et al., 1996; Myers et al., 1996; Emery et al., 2000a). Therefore, LL was considered a clock-disrupting environment. Flies expressing expanded Huntingtin (expHTT) (HTT-Q128) in their central pacemaker ventral lateral neurons (LNv) are behaviourally arrhythmic under constant darkness (DD) (Chapter 2) (Sheeba et al., 2008a; Prakash et al., 2017). I asked whether clock-enhancing environments attenuate this arrhythmicity. Since the HD flies are behaviourally arrhythmic from day 1 in DD, they were subjected to different environmental regimes in the pre-adult stages. Their activity rhythms were assayed as adults in DD25. *Drosophila* circadian neurons already have functional clocks during pre-adult stages and are light-responsive (Sehgal et al., 1992; Helfrich-Forster, 1997; Kaneko et al., 1997a; Helfrich-Forster et al., 2007; Vallone et al., 2007; Liu et al., 2015b). Pre-adult light exposure entrains the adult circadian clock (Sehgal et al., 1992; Vallone et al., 2007), and pre-adult light regimes can modify the circadian period of adults (Sheeba et al., 2002). At the cellular level, flies expressing expHTT in the LNv lack the circadian output neuropeptide Pigment Dispersing Factor (PDF) and core clock protein Period (PER) in the small LNv (sLNv) soma

(Chapter 2) (Sheeba et al., 2008a; Prakash et al., 2017). expHTT also forms inclusions, and their role in the pathophysiology is varied but is often associated with neurotoxicity (Finkbeiner, 2011; Margulis et al., 2013). So, I asked whether circadian-rhythm-disrupting environments like LL exacerbate expHTT-induced cellular phenotypes by comparing flies under LL with those under LD and DD.

The effect of various environments during pre-adult stages on adult activity rhythms in DD (section 3.3.1) and LD (section 3.3.2) are described. Then, the effect of light regimes on cellular phenotypes of PDF in the LNv soma (section 3.3.3), expHTT forms and inclusions (section 3.3.4) and the relation between inclusions and PDF^{+} sLNv numbers (section 3.3.5) are described.

Here is a summary of the results from the above experiments. *pdf>Q128* flies experiencing pre-adult entraining conditions of LD or SN have arrhythmic activity from the first day of DD, like their counterparts under aperiodic DD or LL. These findings show the inability of rhythm-bolstering environments of LD or SN during development to suppress expHTT-induced adult behavioural arrhythmicity. Across regimes, there is an escalation of the cellular neurodegenerative phenotypes in *pdf>Q128* flies, i.e., loss of PDF from sLNv soma and expHTT inclusions with age, a characteristic of HD. Also, increased expHTT inclusions are associated with the increased PDF loss from the sLNv, suggesting that inclusions are markers for neurotoxicity. Notably, expHTT-expressing flies under LL have accelerated neurodegenerative cellular phenotypes: young flies in LL had a more significant PDF loss from sLNv soma and higher expHTT inclusions than DD and LD. Older *pdf>Q128* flies in LL also lost PDF from sLNv dorsal projections, unlike DD and LD. Thus, the continuous presence of light aggravates the neurodegenerative phenotypes. Interestingly, *pdf>Q128* flies under rhythmic light also had a pronounced PDF loss from sLNv soma than DD. Young *pdf>Q128* flies in LD flies also showed a predominance of expHTT inclusions in LNv and more expHTT inclusions than in DD. The absence of light, i.e. DD, seems to be the least neurotoxic, suggesting a negative effect of light on expHTT-induced phenotypes. In summary, this study supports the importance of circadian hygiene, such as lighting conditions, in impacting neurodegenerative outcomes.

3.2 MATERIALS AND METHODS

3.2.1 Fly lines

Transgenic fly lines used are described in Chapter 2 (section 2.2.1). All fly lines and crosses were maintained on a standard cornmeal medium at 25°C.

3.2.2 Behavioural assays

Flies were placed under four different environmental conditions through development up to 2d adults. Three of the four regimes had constant temperatures of 25°C with either constant darkness (DD) or constant light (LL, 150lux) or cyclic light cues with 12h: 12h Light: Darkness (LD, 150lux). The fourth was seminatural conditions (SN), gradually changing light, temperature, and humidity as strong zeitgebers. SN in Bangalore (12.97° N, 77.59° E), India, during mid-July 2013, had day-light for 12h 30min and night for 11h 30min, sunrise at 6.15 am, sunset at 6.45 pm, mean light $_{daytime}$ ~190 lux, mean temp $_{daytime}$ 23.6 °, mean temp $_{nighttime}$ 21.7°C, mean humidity$_{daytime}$ 79.9%, mean humidity$_{nighttime}$ 85.6%, mean light$_{max}$490lux, mean temp$_{max}$25.9°C, mean temp $_{min}$ 20.8°C, mean humidity$_{max}$90.5% and humidity $_{min}$ 70.3%. More details of the SN enclosure are previously described (Prabhakaran and Sheeba, 2013). Subsequently, activity was recorded in specific light regimes (DD or LD) from post-eclosion age 3d. As described in Chapter 2 (section 2.2.2), behavioural assays were carried out and analysed. For flies reared in DD, LD and LL, for most genotypes, ≥ 25 flies survived up to age 23d under DD recording, and ≥ 28 flies survived up to age 23d under LD recording. *pdfGal* reared in LD and recorded in DD had n= 17 after 16d. SN-reared flies recorded in DD or LD, across genotypes, n ≥ 20 up to 16d, post which n ≥ 10.

3.2.2.1 Statistical analysis

Most *pdf>Q128* flies across AWs and regimes were arrhythmic, and their rhythm robustness and period were not considered for statistical tests. Each data set (untransformed or transformed) was tested for normality using Shapiro-Wilk's test and variance homogeneity using Levene's test. Mauchly's sphericity test was carried out before performing a repeated measures ANOVA. A one-way ANOVA followed by Unequal N HSD was used for comparing rhythm robustness

between genotypes across age windows (AWs) within a regime. A repeated-measures ANOVA followed by Unequal N HSD was used only for SN to DD. The rhythm robustness comparisons between AWs for a genotype for the other regimes used Friedman's test, followed by the Wilcoxon test with a Bonferroni correction applied to the pair-wise *p*-values. The data comparing rhythm period and activity consolidation '*r*' was not normally distributed. Comparing genotypes for an AW or age was done using the Kruskal-Wallis test of ranks, followed by multiple comparisons of mean ranks. For the SN to DD regime, '*r*' between genotypes was compared using Welch's ANOVA on transformed data followed by the Games-Howell test. Friedman's test for repeated measures was used to compare period and activity consolidation '*r*' between AWs or ages for a genotype. Then Wilcoxon matched-pairs tests (or Conover Test for '*r*') with Bonferroni correction (or Benjamini-Hochberg (BH) procedure to decrease the False Discovery Rate (FDR) for '*r*'; FDR set at 5%) on the pair-wise *p*-values were used. An mxn Fisher's Exact test, followed by multiple 2x2 Fisher's Exact tests with BH procedure on all relevant comparisons, were used (using R) to compare the proportion of rhythmicity between genotypes for an AW for a regime. Cochran Q test on the dichotomous variable rhythmicity (rhythmic and arrhythmic categories) was used to compare the proportion of rhythmic flies between AWs for a genotype in a regime, followed by multiple 2x2 McNemar's tests on the dependent samples and BH procedure on all relevant comparisons. Kruskal-Wallis tests followed by multiple comparisons of mean ranks were used for between-regime comparisons of '*r*' for a genotype for each age. A 4x2 Fisher's exact test, followed by multiple 2x2 tests and BH procedure, were used to compare the proportion of rhythmic flies between regimes for a genotype at an AW.

A one-way ANOVA (on untransformed or transformed data) followed by Tukey's HSD (Unequal N HSD for SN to LD) was used to compare daytime or nighttime activity between genotypes for an AW within a regime. Only for the LD to LD regime, nighttime activity between genotypes was compared using Welch's ANOVA on transformed data followed by the Games-Howell test. For comparing morning AI or evening AI between genotypes for an AW in a regime, the Kruskal-Wallis test of ranks followed by multiple comparisons of mean ranks was used. For AW comparisons within a genotype for a regime of daytime and nighttime activities and morning and

evening AIs, Friedman's test followed by the Wilcoxon test with BH procedure was used. The between-regime comparisons of the LD rhythm feature for a genotype for each AW were carried out using one-way ANOVA followed by Unequal N HSD. For evening AI, Kruskal-Wallis tests of ranks followed by multiple comparisons of mean ranks were used. For morning AI of *Q128*, repeated measures ANOVAs, followed by unequal N HSD tests, were used. Other details are described previously in Chapter 2 (section 2.2.2.1).

3.2.3 Immunocytochemistry and image analysis

The fly crosses were placed in the three different regimes: DD, LD (~200 lux) or LL (~200 lux) and remained in the same regime as adults. Dissections were carried out at the following ages: third instar larvae (L3) and adults aged 1d, 7d, 16d and 23d. Immunocytochemistry was carried out as described in Chapter 2 (section 2.2.3). Primary antibodies used were anti-Huntingtin Mouse (1:500) (Millipore MAB2166) along with anti-PDF Rabbit (1:30,000) (a gift from Michael Nitabach, Yale University). Secondary antibodies Alexa fluors (Invitrogen) (1:3000) anti-rabbit488 and anti-mouse546 were used.

3.2.3.1 Image acquisition and analysis

PDF^+ LNv were counted, and the presence of DP was noted by viewing samples under a Zeiss Axio Observer Z1 epifluorescence microscope using the 63X/oil 1.4 objectives. To quantify expHTT inclusions, images were captured as a *z*-stack of 1µm interval using the 40X/oil 1.3 objectives, keeping the lamp intensity and exposure time constant across samples. Confocal *z*-stacks were captured using Zeiss LSM700, LSM 880 or Olympus FV1000 for representative images.

3.2.3.1.1 Categorisation and quantification of expHTT forms

The expHTT forms in each LNv soma were classified based on their appearance under the light microscope as follows: a uniform diffuse fluorescence distribution of expHTT (Diff), puncta-like shiny speckled focal fluorescence distribution of varying sizes were referred to as inclusions (Inc) and a polymorphic fluorescence distribution of diffuse expHTT with a few puncta-like inclusions

(Diff+Inc). There was also PDF$^+$ LNv soma without expHTT fluorescence (No HTT). First, the number of PDF$^+$ sLNv and lLNv soma with and without expHTT staining was noted for each hemisphere. Then, among those stained for expHTT, the sLNv and lLNv soma numbers having different expHTT forms were noted for each hemisphere.

Two sets of information are gathered from labelling expHTT types per LNv. One is at the level of cells, namely, the proportion of sLNvs or lLNvs with different forms of expHTT within each hemisphere. This comparison (intra-hemisphere) shows the within-hemisphere variation in expHTT distribution in LNvs. Since our experimental replicates were at the level of hemispheres and not cells, the within-hemisphere diversity is only qualitative information. The second set of information is at the level of hemispheres. Depending on the most predominant expHTT form found in sLNv (or lLNv) within a hemisphere, each hemisphere was allotted into one of three categories. The categorisation of each hemisphere (inter-hemisphere) based on the predominant expHTT form in the LNv (sLNv or lLNv) was as follows: predominantly diffuse distribution (Diff) or an equal distribution of diffused and inclusions (Diff+Inc) or predominantly inclusions (Inc). This hemisphere-level categorisation is at the experimental replicates level, enabling qualitative statistical analysis. Such inter-hemisphere categorisation allows comparisons between genotypes and ages of the relative proportions of hemispheres enriched in one form of expHTT in sLNv or lLNv relative to another form of expHTT.

3.2.3.1.2 Quantification of expHTT inclusions

The expHTT inclusion number and size were quantified using ImageJ. Maximum intensity projection images were converted to 8-bit images, their backgrounds subtracted (rolling ball radius of 10 pixels), unsharp mask filter applied (radius of 1 pixel, mask weight of 0.7), further processed to sharpen the image, find edges and then an intermodes threshold was applied. The area in the vicinity of the LNv was then outlined, and the analyse particles tool with size specification of 1 to infinity (in μ) was used to obtain measures of inclusion number and the size of inclusions for each hemisphere. The area of inclusion spread is approximately a product of inclusion number and size. A lower limit of 1μ was set for size to avoid false positives and background specks. The proportion of different-sized HTT inclusions (grouped as 1-2μ, 2-3μ, 3-

4µ, 4-5µ, 5-6µ and >6µ) was calculated for each hemisphere and averaged across multiple hemispheres.

Like how expHTT forms in the LNv were categorised at two levels of within-hemisphere and between-hemispheres (with each hemisphere representing the predominant expHTT form in LNv), the inclusion sizes were also categorised. Within-hemisphere categorisation fell in the size ranges of <2µ, >2-<3µ, >3-<4µ, >4-<5µ, >5-<6µ and >6µ. For designating each hemisphere as predominated by a particular size range of inclusions, the categorisation was <3µ, 3-6µ, >6µ and a mixed-size group (those that did not fall exclusively under the above three categories).

3.2.3.2 Statistical analysis

For PDF^+ LNv numbers within a regime, a 2-way ANOVA with genotype and age as fixed factors was performed. A two-way ANOVA with regime and age as fixed factors was performed for cell numbers within a genotype. Post-hoc multiple comparisons were conducted using Tukey's Honest Significant Difference test at $\alpha = 0.05$. For comparing the cell number distribution shapes between genotypes for a regime and between regimes for a genotype, the Kolmogorov-Smirnov tests were done with $\alpha = 0.05$. The proportion of hemispheres with PDF^+ DP or CP were compared between genotypes for an age in a regime or between ages for a genotype in a regime or between regimes for a genotype at a specific age using mxn Fisher's Exact tests, followed by pair-wise tests with BH procedure. The inclusion number or size between regimes for an age or between ages for a regime was compared using one-way ANOVA on transformed data followed by Tukey's HSD. To compare the relative proportion of hemispheres predominated by different expHTT forms (or different sized expHTT inclusions) between genotypes for a specific age or between ages for a genotype, mxn Fisher's Exact tests were used. Following this, wherever necessary, multiple specific 2x2 Fisher's Exact test sets with BH procedure on all relevant comparisons were applied (using R).

Other details are described previously in Chapter 2 (2.2.2.1).

3.3 RESULTS

3.3.1 Multiple, complex time cues during pre-adult stages did not prevent the arrhythmic activity of expHTT-expressing adult flies in DD

Given that exposure to time cues during development affects the adult circadian activity rhythms (Sehgal et al., 1992; Matsumoto et al., 1997; Sheeba et al., 2002; Zhao et al., 2019a; Zhao et al., 2019b), I asked whether exposure of *pdf>Q128* flies to specific environments during development modifies the behavioural arrhythmicity of adult flies in DD25. The effect of environmental regimes that modify the circadian rhythms on behavioural arrhythmicity of *pdf>Q128* as adults was tested by exposing flies to either of the four regimes (DD, LD, SN or LL) during the pre-adult stages and monitoring their activity rhythms as adults in DD. DD-reared control flies *pdf>Q0* and *Q128*, like their LD counterparts, were rhythmic (Fig 3.1 first and second rows) with near 100% rhythmicity (Fig 3.2a left, b left) across AWs. DD-reared *pdf>Q128* were arrhythmic like the LD-reared ones (Fig 3.1 first and second rows) with significantly low rhythmicity and poor activity consolidation '*r*' (Fig 3.2a, b) compared to controls across age. Despite being reared under SN, *pdf>Q128* flies were arrhythmic from the start of DD (Fig 3.1 third-row) with lower rhythmicity and activity consolidation compared to controls (Fig 3.2c). LL-reared *pdf>Q128* remained arrhythmic throughout (Figs 3.1 fourth-row and 3.2d). *pdf>Q128* across regimes had similarly low rhythmicity (Fig 3.3a) and activity consolidation (Fig 3.3b). Although LD-reared *pdf>Q128* were significantly more rhythmic than LL-reared flies, the fraction of rhythmic LD flies was low at ~25% (Table 3.1). *pdf>Q128* flies, when rhythmic, had weak rhythms across regimes, though not statistically tested (Table 3.2). While other controls mostly had comparable rhythm robustness across age, LD-and LL-reared *Q128* had relatively weak rhythms in AW2 and AW3 compared to other controls (Table 3.2). The small fraction of rhythmic *pdf>Q128* exhibited a periodicity of around 24h (Table 3.3). *pdf>Q0* had a more extended period than most genotypes across AWs under all regimes reared, partly attributed to the long period of parental *pdfGal* (Table 3.3). Thus, complex, gradually changing cyclic time cues (SN) during development do not mitigate behavioural arrhythmicity in adult *pdf>Q128* flies. In conclusion, complex time cues during development do not affect the breakdown of activity rhythms as adults in DD in expHTT-expressing flies.

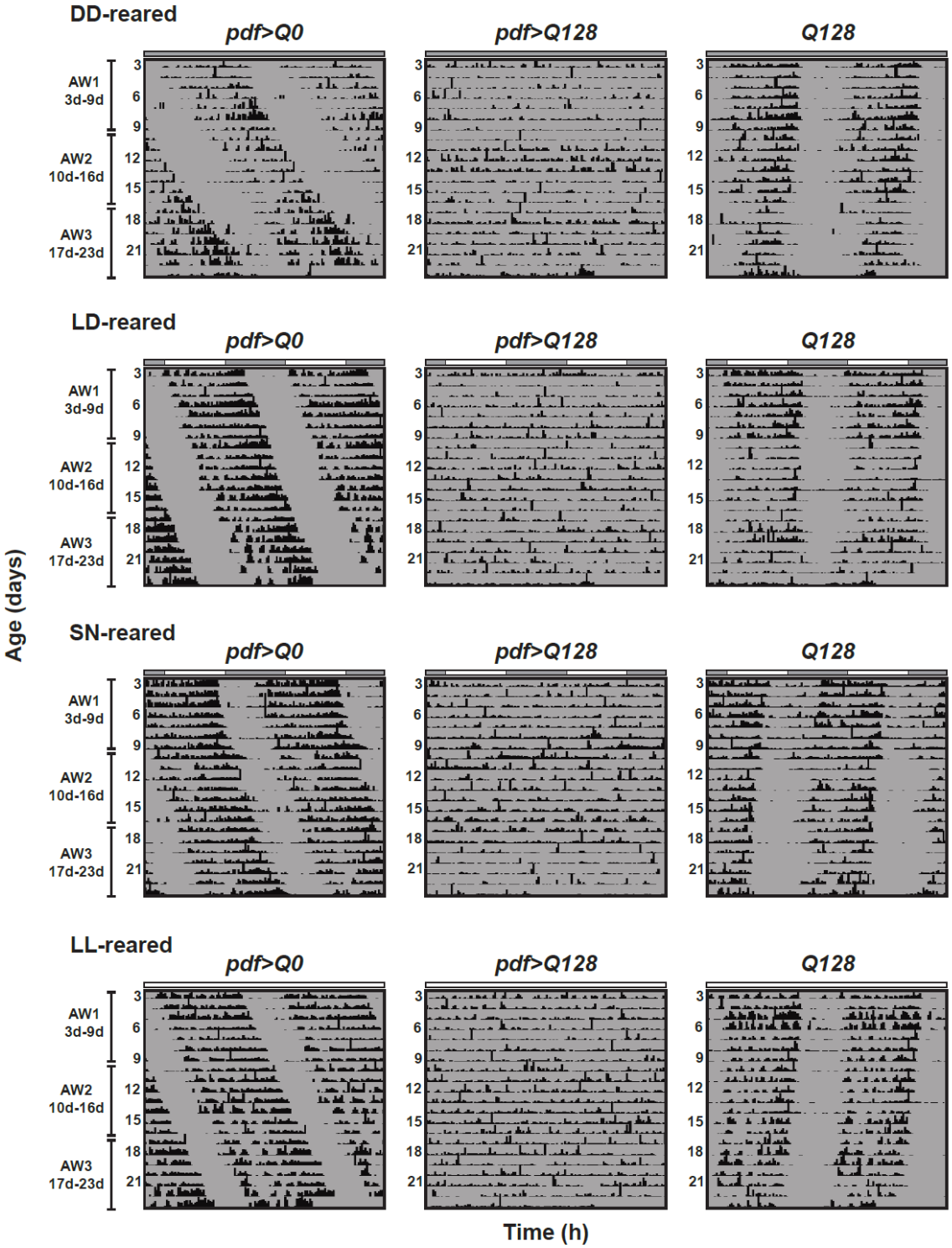

Figure 3.1

Fig 3. 1 Strong light/dark cycles or multiple gradually changing time cues during development do not alter the behavioural arrhythmicity of pdf>Q128 flies as adults in DD.

Representative double-plotted actograms for adult flies of *pdf>Q0*, *pdf>Q128* and *Q128* showing activity data for 21d (age 3d-23d) in DD at 25˚C. All other details are the same as in Fig 2.1. The bars above the actograms represent the regime of rearing, i.e. during development until age 2d (top-row DD, second-row LD, third-row SN and bottom-row LL).

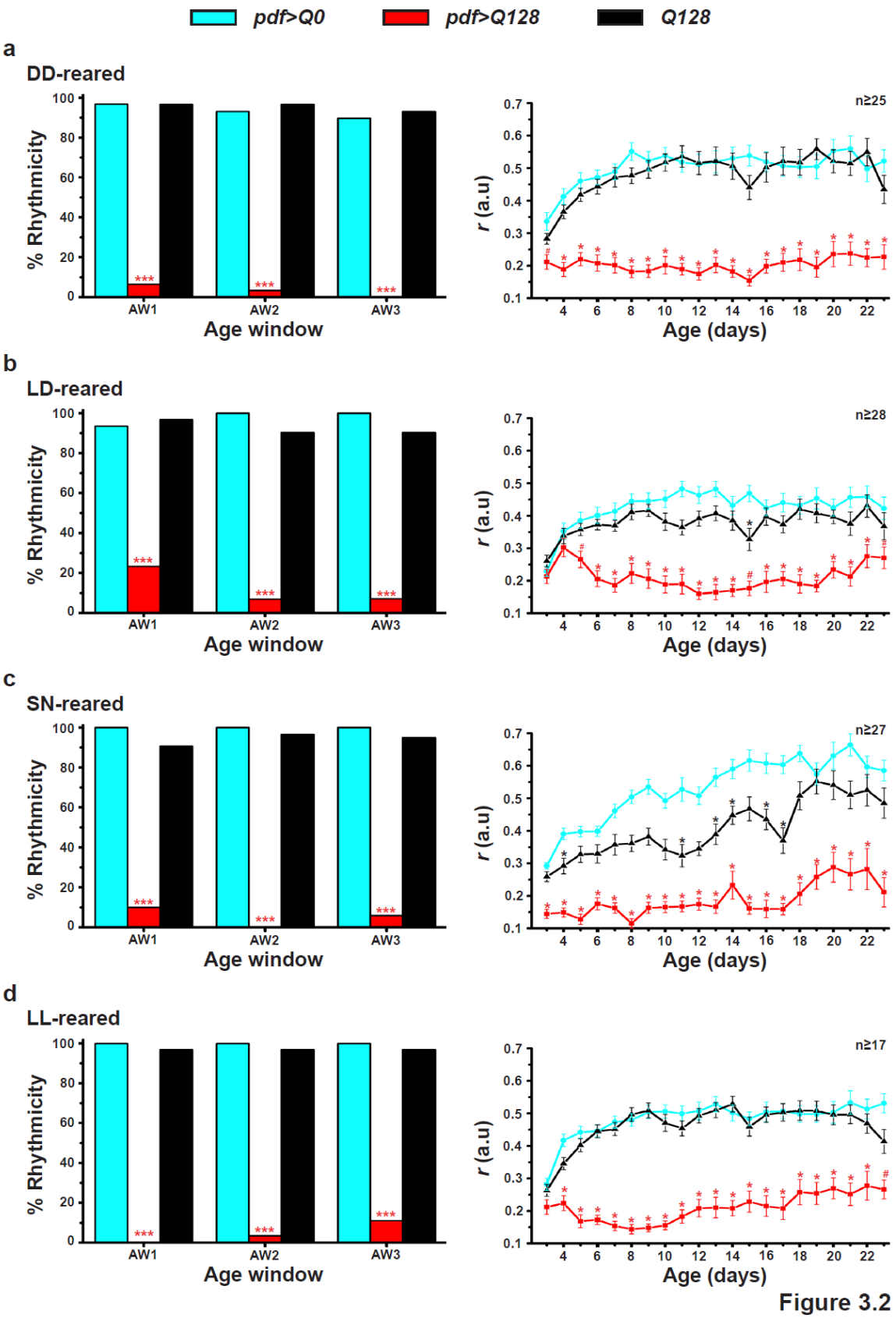

Figure 3.2

Fig 3. 2 Irrespective of the developmental regime, pdf>Q128 flies are mostly arrhythmic with poorly consolidated activity as adults in DD.

Left: The percentage of rhythmic flies in DD is plotted against three AWs for *pdf>Q0*, *pdf>Q128* and*Q128* reared under regimes of DD (a), LD (b), SN (c) and LL (d). Most *pdf>Q128* flies are arrhythmic in DD at all AWs across rearing regimes. *** indicates a significant difference from all controls at $p<0.001$. Right: As adults in DD, '*r*' across age for *pdf>Q128* is lower than controls across all rearing regimes (a-d). Numbers at the top-right indicate the number of flies that survived for 23d. Symbols indicate significant differences at $p<0.05$: red * of *pdf>Q128* from both controls, red # from *pdf>Q0* alone, and black * of *Q128* from the other indicated genotypes. Across panels, the error bars are SEM.

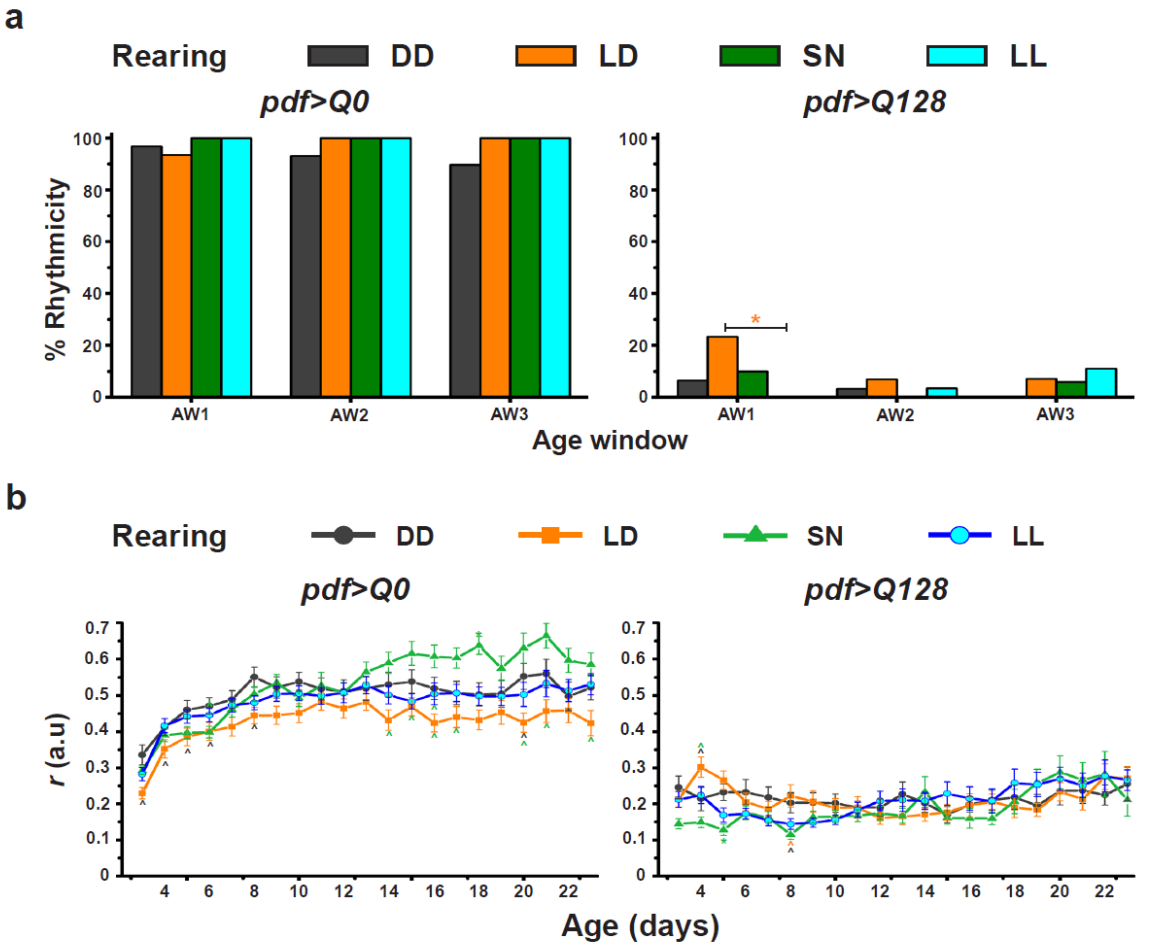

Figure 3.3

Fig 3. 3 The Presence of cyclic light or complex time-cues during development does not improve the activity rhythms of pdf>Q128 as adults in DD.

(a) The percentage of rhythmic flies in DD reared under different regimes across AWs for *pdf>Q0* and *pdf>Q128* plotted against three AWs. * (orange) is at $p<0.05$. (b) Comparison of activity consolidation '*r*' for *pdf>Q0* and *pdf>Q128* flies in DD25 reared in different regimes. Coloured ^ near an error bar of a data point indicates a difference of the respective-coloured regime from the data-point regime at $p<0.05$. Across panels, error bars are SEM.

3.3.2 Arrhythmic conditions during pre-adult stages do not alter the entrainment of activity rhythms of expHTT-expressing flies to LD

Environmental interventions during specific developmental stages affect adult circadian rhythms (Sehgal et al., 1992; Matsumoto et al., 1997; Sheeba et al., 2002; Zhao et al., 2019a; Zhao et al., 2019b). I, therefore, asked whether rendering the circadian clocks arrhythmic during development would impair the ability of *pdf>Q128* flies to entrain to LD as adults. The fly clock can be rendered arrhythmic under the rhythm-disrupting environment of LL. Additionally, flies were maintained in DD, LD or SN during development to assess the effect of the developmental environment on the entrainability of the activity rhythms of *pdf>Q128* flies to LD. An extension of this study has been described as part of Chapter 2 (Figs 2.14 and 2.15). DD-reared and LD-reared *pdf>Q128* flies showed activity profiles dissimilar from their *UAS* controls (Figs 3.4 a and b, top-panels). Their daytime and nighttime activity counts were like at least one relevant background control across AWs, except for DD-reared flies in AW3 where *pdf>Q128* had reduced daytime activity than both controls (Figs 3.4 a and b, bottom-panels, Tables 3.4 and 3.5). The morning and evening AIs of *pdf>Q128* were also different only from *pdfGal* but not *Q128* across AWs (Figs 3.4 a and b bottom-panels, Tables 3.6 and 3.7), suggestive of a background effect. Similarly, SN-reared and LL-reared *pdf>Q128* flies had activity profiles, activity counts, and anticipation indices comparable to at least one of the relevant background controls across most AWs (Figs 3.5 a and b, Tables 3.4-3.7). Comparing across regimes for each AW, *pdf>Q128* flies raised in different regimes, including those raised under arrhythmic LL, share similar activity profiles in LD, like their *Q128* controls (Fig 3.6a). Day activity levels of LD-reared *Q128* were lower than DD-reared and LL-reared flies in AW2 and AW3 (Fig 3.6b left). Night activity levels of both *pdf>Q128* and *Q128* flies reared in SN were lower than those reared in LD in AW2 (Fig 3.6c). *pdf>Q128* reared in SN had a higher M-AI than in DD and LD in AW1 (Fig 3.6 d right). Surprisingly, LL-reared *pdf>Q128* had higher M-AI than LD-reared flies in AW2 and AW3, while such between-regime differences were not seen with *Q128* (Fig 3.6d). Both genotypes had slight between-regime differences in E-AI (Fig 3.6d). Thus, the rearing regime had modest effects on the circadian features of flies in LD. Nevertheless, these might not translate to differences of physiological relevance, given their magnitude. Thus, light regime during development had little effect on the entrainment of *pdf>Q128* activity rhythms to LD as adults. Further, the entrainment of flies as adults to LD does not require functional circadian mechanisms during development.

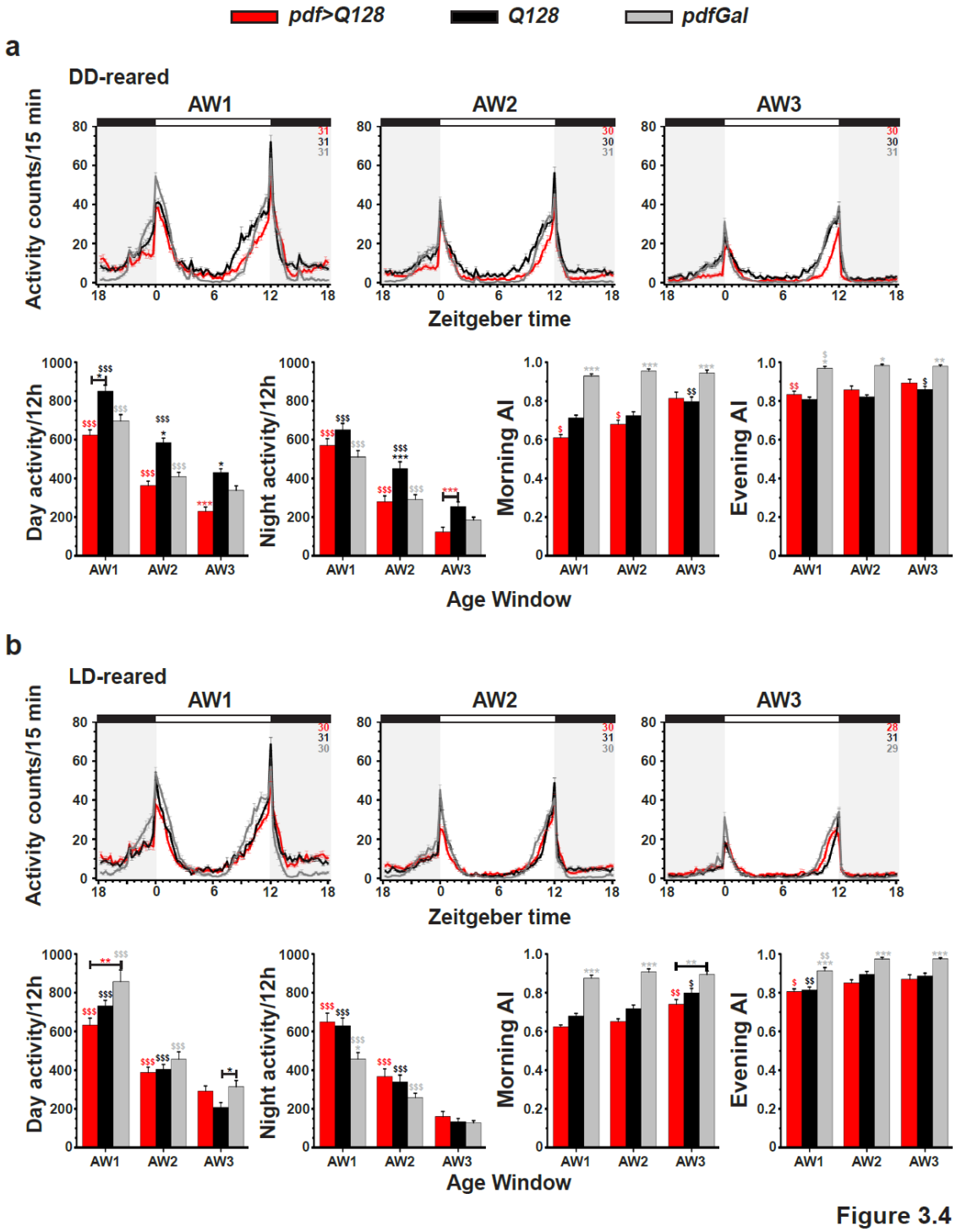

Figure 3.4

Fig 3. 4 pdf>Q128* flies *reared in DD and LD show control-like activity rhythms as adults in LD. (a) Flies reared in DD and as adults in LD. Top: The mean activity counts per 15 minutes in LD are plotted against zeitgeber time for *pdf>Q128* and its relevant controls *Q128* and *pdfGal* for the three AWs. All other details are like Fig 2.9b. Bottom: Mean daytime and nighttime activity levels and morning and evening anticipation indices plotted against AWs. Coloured * indicates significant differences of that genotype from the indicated one or all others for a given AW at * $p<0.05$, ** $p<0.01$ and *** $p<0.001$. Coloured $ indicates significant differences between an AW from the indicated AW or all other AWs for the colour-matched genotype at $ $p<0.05$, $$ $p<0.01$ and $$$ $p<0.001$. Across panels, error bars are SEM. (b) Flies were reared in LD and assayed as adults in LD. All other details are the same as above.

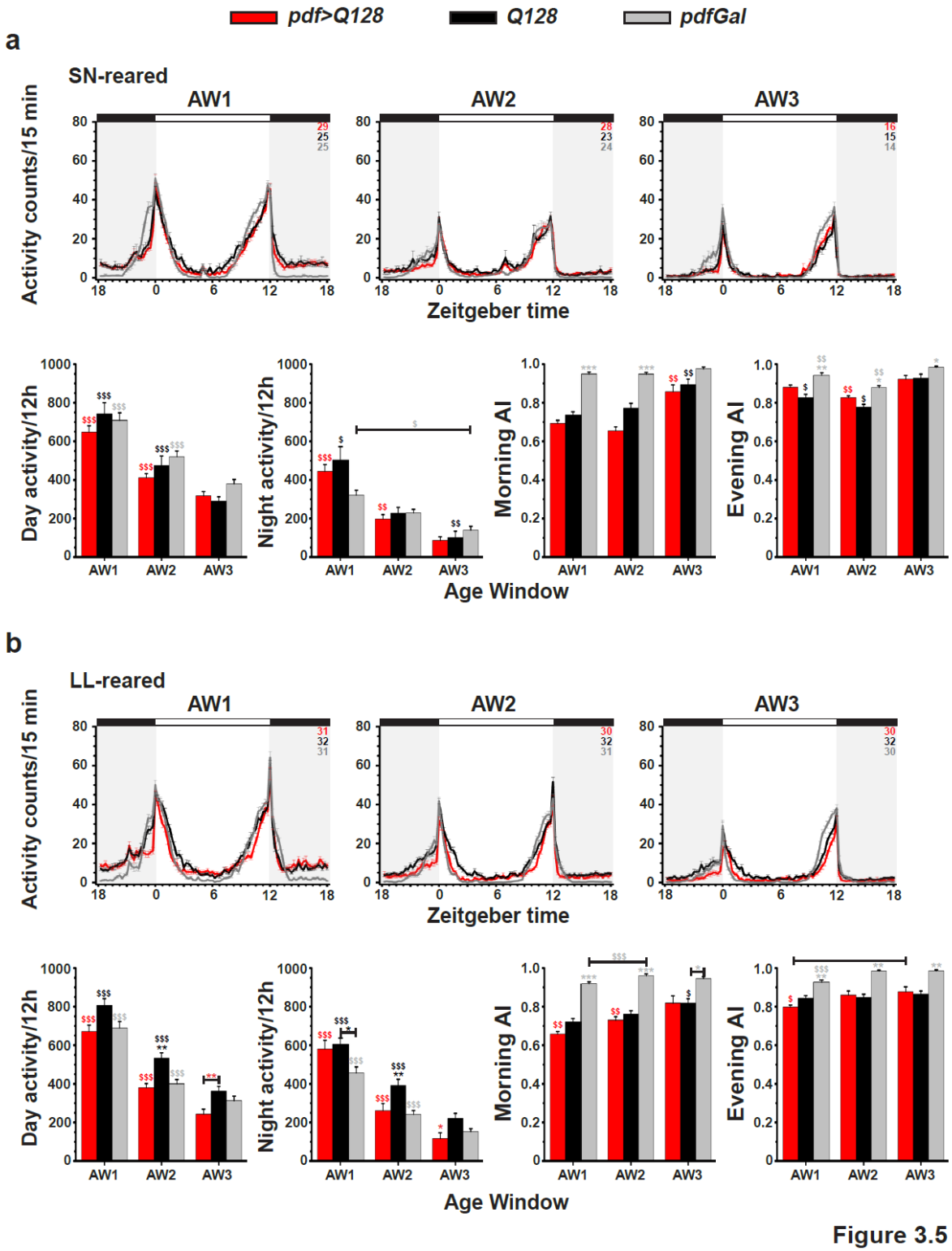

Figure 3.5

Fig 3. 5 pdf>Q128 reared in SN and LL show control-like activity rhythms flies as adults in LD.
(a) Flies were reared in SN and as adults in LD. (b) Flies were reared in LL and assayed as adults in LD. All other details are similar to Fig 3.4.

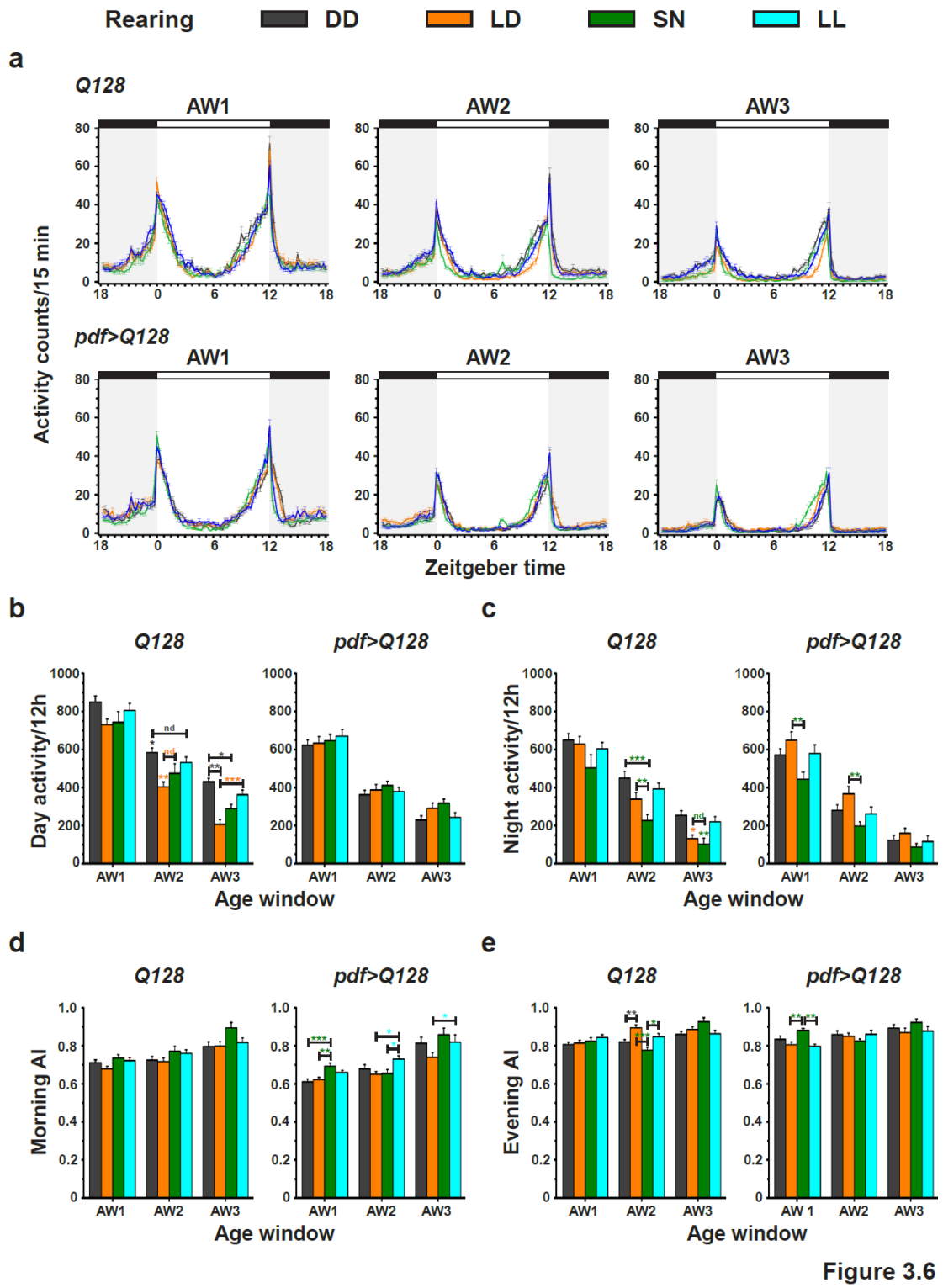

Figure 3.6

Fig 3. 6 pdf>Q128 flies reared under constant or arrhythmic conditions entrain to LD as adults, like those reared under cycling conditions.

(a) Activity profiles under LD of flies reared under different regimes across three AWs showing *Q128* (top) and *pdf>Q128* (bottom). All other details are like Fig 3.4. Age-matched comparisons of the effect of the rearing regime on the mean daytime activity levels (b), mean nighttime activity levels (c), mean morning AIs (d) and mean evening AIs (e) across AWs are plotted for *Q128* and *pdf>Q128*. * indicates significant differences between regimes for specific ages at * $p<0.05$. Across panels, error bars are SEM.

3.3.3 expHTT-expressing flies under different light regimes show progressive loss of PDF$^+$ sLNv, with LL being the most severe and DD being the least

I then asked whether external light conditions known to alter clock properties affect the extent of the cellular neurodegenerative phenotype of *pdf>Q128* flies. I quantified the PDF$^+$ sLNv soma numbers in DD, LD, and LL. *pdf>Q0* flies in DD had close to 4 PDF$^+$ sLNv and lLNv soma across age (Figs 3.7a, b and c). *pdf>Q128* flies had control-like numbers of PDF$^+$ sLNv soma as larvae (Fig 3.7b top and c), which reduced significantly by 1d and remained steadily low after that (Figs 3.7b and c). PDF$^+$ lLNv soma numbers and proportion of hemispheres with PDF$^+$ DP and CP were unaffected in *pdf>Q128* (Figs 3.7d, e and f).

pdf>Q128 flies in LD had control-like PDF$^+$ sLNv soma numbers at L3, which progressively declined with age and compared to *pdf>Q0* (Figs 3.8a-c). PDF$^+$ lLNv soma numbers and proportion of DP and CP were comparable between genotypes (Figs 3.8a,b,d-f).

pdf>Q128 flies in LL had control-like PDF$^+$ sLNv soma numbers at L3, which progressively declined with age and remained significantly lower than *pdf>Q0* (Figs 3.9 a-c). PDF$^+$ lLNv soma numbers and the proportion of hemispheres with PDF$^+$ CP were comparable between genotypes (Figs 3.8d and 3.8f). However, the proportion of hemispheres with PDF$^+$ DP in *pdf>Q128* progressively declined post 7d and was significantly lower than *pdf>Q0* at ages 16d and 23d (Fig 3.9e).

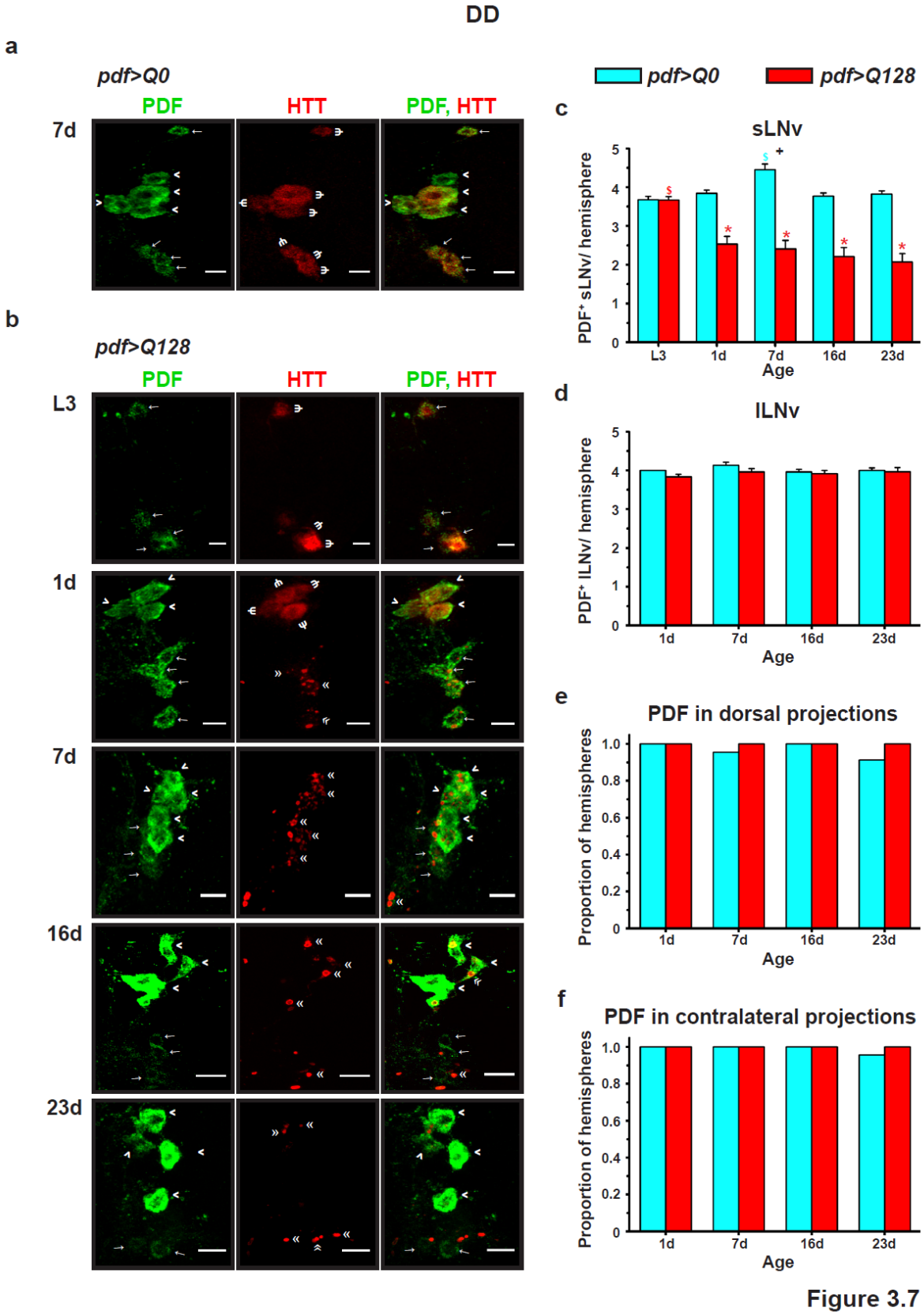

Figure 3.7

Fig 3. 7 pdf>Q128 flies in DD have fewer PDF⁺ sLNv soma than controls; their PDF⁺ lLNv soma numbers are unaffected.

Representative images of brain samples of 7d-old *pdf>Q0* (a) and *pdf>Q128* (b) at life stages of larval L3 and adult at ages 1d,7d,16d and 23d under DD. The samples are stained for PDF (green) and HTT (red), showing sLNv soma (→ arrows), lLNv soma (> arrowheads), diffuse HTT staining (Ψ psi), and inclusions of expHTT (« double arrowheads). Scale bars are 10 µ. (c) Mean PDF^+ sLNv soma numbers per hemisphere across age for *pdf>Q0* and *pdf>Q128*. * indicates a significant difference between genotypes for specific ages at * $p<0.0001$. Coloured $ indicates significant differences between a specific age from the indicated age or all other ages for the colour-matched genotype with $ (cyan) at $p<0.001$ and $ (red) at $p<0.0001$. + at $p<0.001$ indicates that the two distributions differ significantly. (d) Mean PDF^+ lLNv soma numbers per hemisphere across age for *pdf>Q0* and *pdf>Q128*. (e) The proportion of hemispheres showing PDF^+ DP across age for *pdf>Q0* and *pdf>Q128*. (f) The proportion of hemispheres showing PDF^+ CP across age for *pdf>Q0* and *pdf>Q128*. $n \geq 20$ hemispheres/genotype/age. Across panels, error bars are SEM.

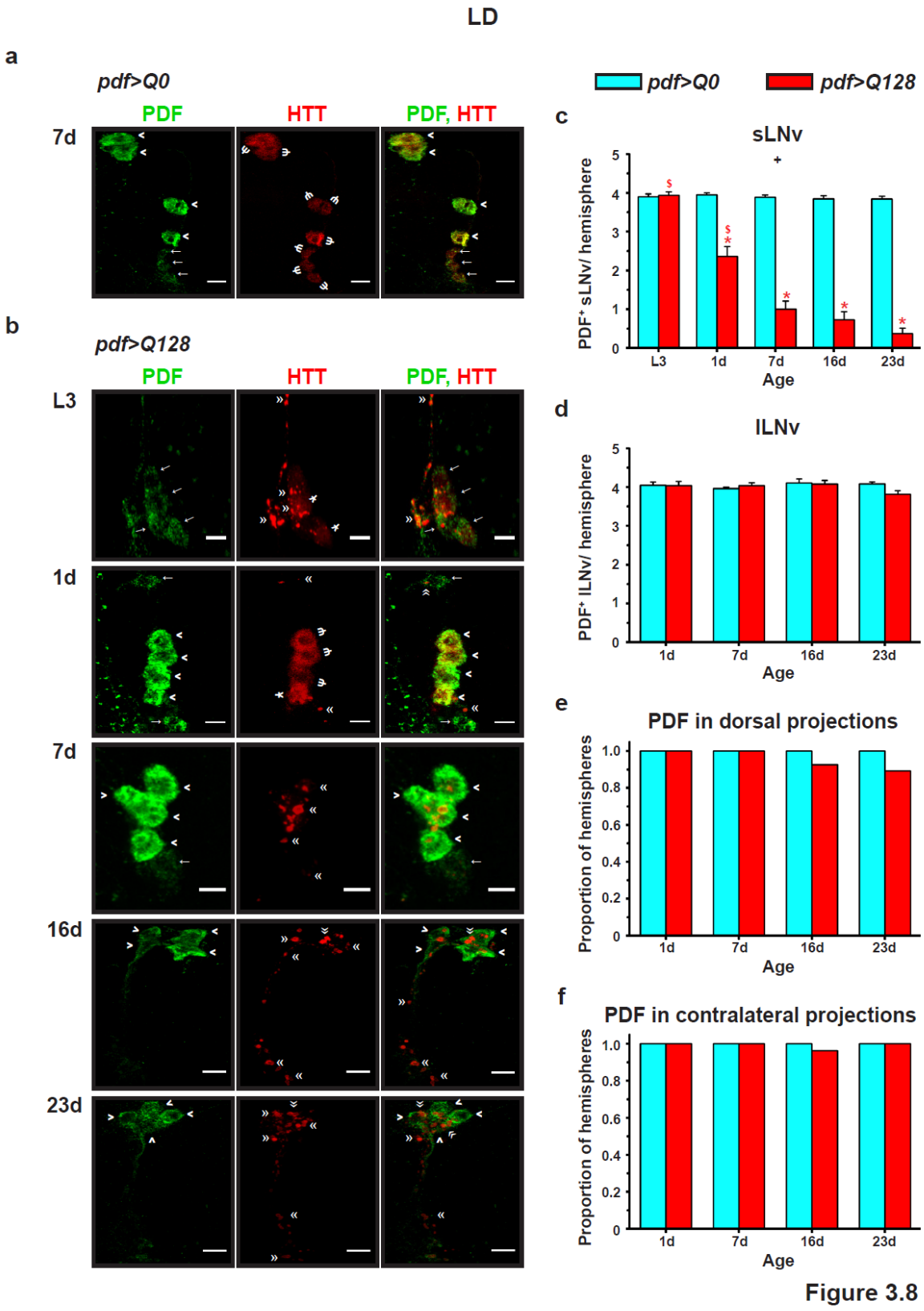

Figure 3.8

Fig 3. 8 pdf>Q128 flies in LD show progressive loss of PDF⁺ sLNv soma.
Representative images of brain samples of flies under LD stained for PDF (green) and HTT (red). Diffuse+inclusion expHTT is also shown (ϒ symbol). All other details are similar to Fig 3.7.

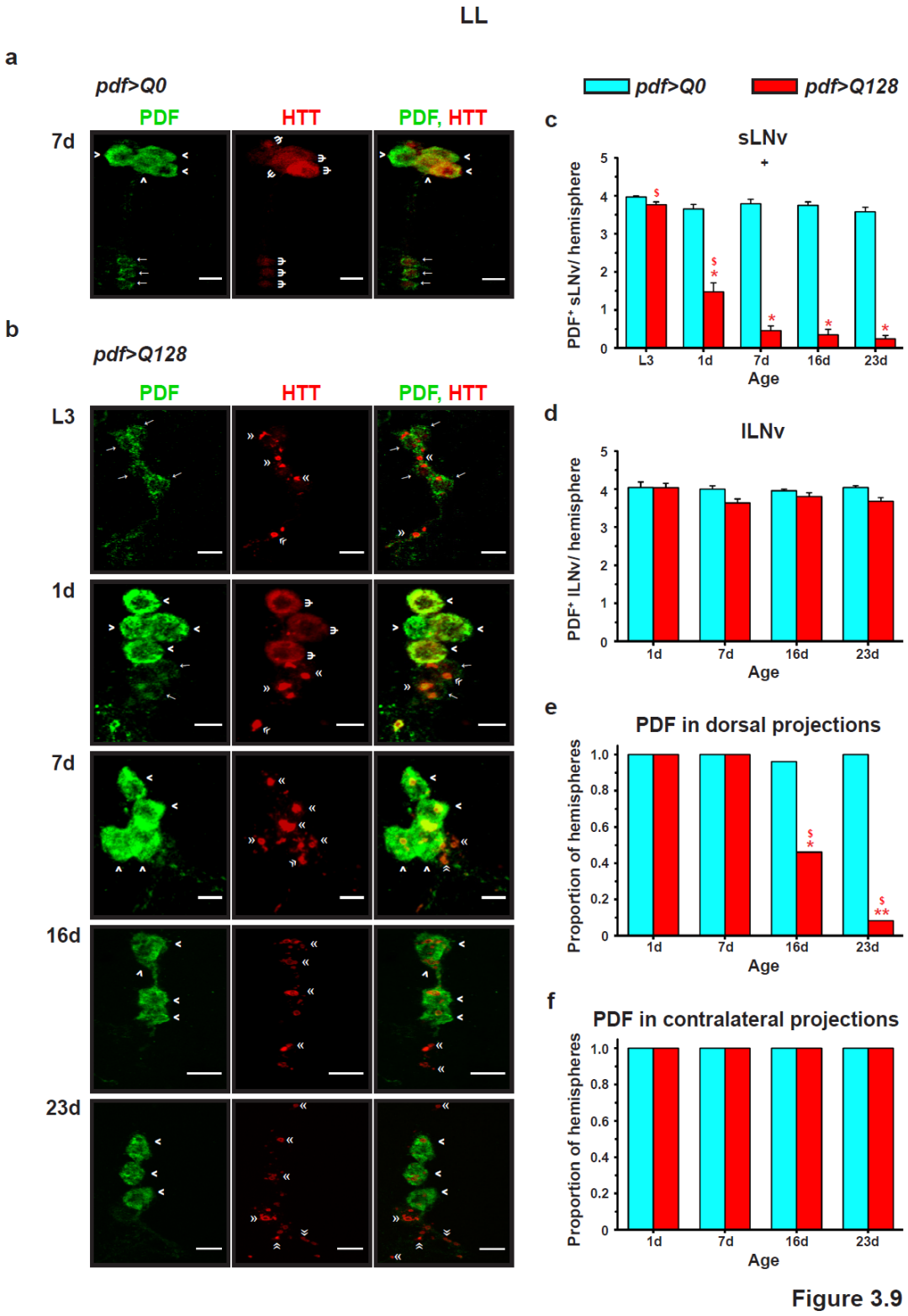

Figure 3.9

Fig 3. 9 pdf>Q128 flies in LL show progressive loss of PDF from the sLNv soma and its DP. Representative images of brain samples of flies under LL stained for PDF (green) and HTT (red). (e) The proportion of hemispheres showing PDF^{+}DP across age for *pdf>Q0* and *pdf>Q128*. * indicates significant differences between genotypes for specific age at * p<0.001 and ** p<00001. Coloured $ indicates a significant age difference from earlier ages for the colour-matched genotype at p<0.01. All other details are similar to Fig 3.7.

Between regimes, *pdf>Q0* was similar in PDF$^+$ LNv soma numbers and proportion of hemispheres with PDF$^+$ DP (Fig 3.10a top). *pdf>Q128* under all three regimes had comparable PDF$^+$ sLNv soma numbers at L3 (Fig 3.10 a bottom-left). At 1d, PDF$^+$ sLNv soma numbers in LL reduced significantly compared to DD and marginally significantly (p=0.051) compared to LD (Fig 3.10 a bottom-left). PDF$^+$ sLNv soma numbers in LD declined at later ages, while DD numbers remained significantly higher than LD and LL (Fig 3.10a bottom-left). In *pdf>Q128*, the PDF$^+$ lLNv soma numbers were comparable across regimes (Fig 3.10a bottom-middle). Thus, LL had the most dramatic effect on PDF$^+$ sLNv numbers, followed by LD and DD.

For a more refined understanding of the effect of light regimes on PDF$^+$ LNv numbers, I compared the shapes of the frequency distributions of PDF$^+$ sLNv soma numbers between regimes across ages. The shapes of the distributions of PDF$^+$ LNv soma numbers (sLNv and lLNv) for *pdf>Q0* and of PDF$^+$ lLNv soma numbers for *pdf>Q128* were comparable between regimes across age (Fig 3.10b first, second and fourth columns). They all showed a left-skewed distribution, with most hemispheres having three to four PDF$^+$ LNv (Fig 3.10b first, second and fourth columns). *pdf*>Q128 at L3 had a left-skewed distribution across regimes, and at 1d, it showed a relatively symmetric distribution (Fig 3.10b, second column). Their distribution appeared to be more right-skewed from 7d onwards in LD and LL; by 23d, the distribution was right-skewed, with most hemispheres showing only one or no PDF$^+$ sLNv (Fig 3.10b, second-column, orange and cyan). On the other hand, in DD, *pdf>Q128* maintained a relatively symmetric distribution across age, with about 70% of the hemispheres showing at least 2 ($\geq 2 \leq 4$) PDF$^+$ sLNv soma (Fig 3.10b, second-column, dark-grey). The shape of the frequency distribution of PDF$^+$ sLNv soma numbers in *pdf>Q128* under LD and LL differed significantly from those in DD at ages 7d, 16d and 23d (Fig 3.10b, second-column), as was also reflected in the mean numbers (Fig 3.10a bottom-left). Only LL affected the PDF in sLNv dorsal projections of *pdf>Q128*. This effect is evident from the significantly lower proportion of hemispheres of *pdf>Q128* in LL showing PDF$^+$ DP compared to those in LD and DD at ages 16d and 23d (Fig 3.10a bottom-right).

In summary, the arrhythmic regime of LL promotes expHTT-induced neurodegenerative features most severely, followed by LD and then DD. Thus, the constant light environment aggravates

the HD neurodegenerative phenotypes of PDF loss from sLNv soma, leading to PDF loss from sLNv DP. The finding that *pdf>Q128* flies under LD had fewer PDF^+ sLNv than those in DD suggests that even cyclic light affects neurodegenerative phenotypes, with the absence of light seeming most beneficial. Even when presented cyclically and for a shorter duration, this negative effect of light confounds any conclusions on the clock-disrupting effects of constant light on the neurodegenerative phenotypes.

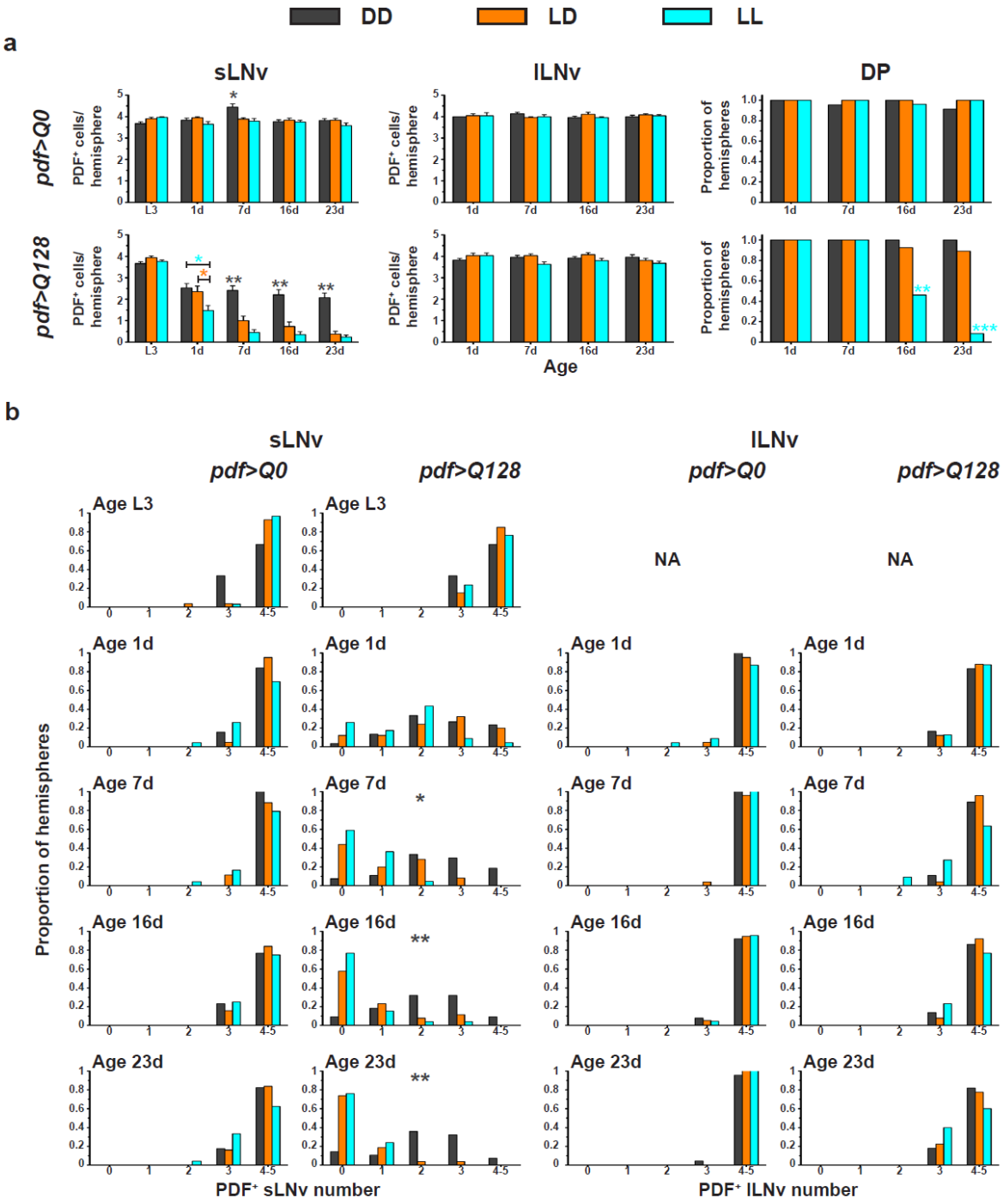

Figure 3.10

Fig 3. 10 pdf>Q128 flies in LL and LD show a rapid decline in PDF⁺ sLNv soma numbers compared to DD.

(a) Mean numbers of PDF⁺ sLNv soma (left) and lLNv soma (middle) per hemisphere and proportion of hemispheres showing PDF⁺ DP (right) in three different light regimes are plotted over age for *pdf>Q0* (top) and *pdf>Q128* (bottom). Symbols indicate age-matched significant differences: * (dark-grey) of DD from other regimes at * $p<0.001$ and ** $p<0.0001$; * (blue) of LL from the indicated regime or other regimes at * $p<0.01$, ** $p<0.001$ and *** $p<0.0001$; and * (orange) at $p=0.051$. + indicates that DD, LD and LL distributions significantly differ at $p<0.001$.

(b) Frequency distribution of the proportion of hemispheres with different numbers of PDF$^+$ sLNv (left pane-sets) or lLNv soma (right-panel sets) for *pdf>Q0* and *pdf>Q128* comparing the three light regimes across various ages. *(dark-grey) indicates significant difference of DD from LD and LL at * $p<0.05$ and ** $p<0.01$. n≥20 hemispheres/genotype/age/regime. Across panels, error bars are SEM.

3.3.4 expHTT-expressing flies under different light regimes show a progressive increase in inclusions, with LL being the most severe

Multiple forms of expHTT, including inclusions, contribute to neurodegeneration by various means, such as sequestering proteins essential for cellular function and physically blocking processes like axonal transport (Nucifora et al., 2001; Donaldson et al., 2003; Gunawardena et al., 2003; Lee et al., 2004; Qin et al., 2004; Schaffar et al., 2004). Given the varying extents of PDF loss from sLNv soma of *pdf>Q128* across the light regimes, I asked whether the light regimes also differentially affected the expHTT forms in the LNv. Across regimes, *pdf>Q0* showed diffuse HTT in the LNv (Figs 3.7a, 3.8a and 3.9a), and the HTT$^+$ sLNv (and lLNv) soma numbers were similar across regimes, an average of ~4 per hemisphere, except for HTT$^+$ sLNv in DD at L3 (Fig 3.11a, left and middle). While nearly every PDF$^+$ sLNv in a hemisphere of *pdf>Q0* was also stained for HTT across age and regimes, the PDF$^+$ sLNv in the third-instar larvae in DD mostly did not show HTT (Fig 3.11a, right).

Across regimes within a hemisphere, Diff expHTT was prevalent in the sLNv of *pdf>Q128* larvae and the lLNv of 1d-old flies, while Inc prevailed at later ages (Fig 3.11b and c). In *pdf>Q128*, in a small proportion of hemispheres, most of the sLNv (or lLNv) soma were without HTT staining across nearly all ages in DD (Fig 3.12a, left, b). In DD, at L3, 50% of the hemispheres had most of their PDF$^+$ sLNv soma without HTT staining, significantly differing from LD and LL, wherein nearly all hemispheres had a majority sLNv with HTT (Fig 3.12b, top-left). A small proportion of hemispheres with most of their sLNv soma without HTT was also prevalent in LD and LL at different ages; however, it is essential to note that at most of these ages, the mean number of PDF$^+$ sLNv is <1 (Fig 3.12a, top-middle and -right, b, top). For further analysis of the prevalence of various expHTT forms across *pdf>Q128*, only those hemispheres were considered where HTT staining was found in most sLNv (or lLNv) somas.

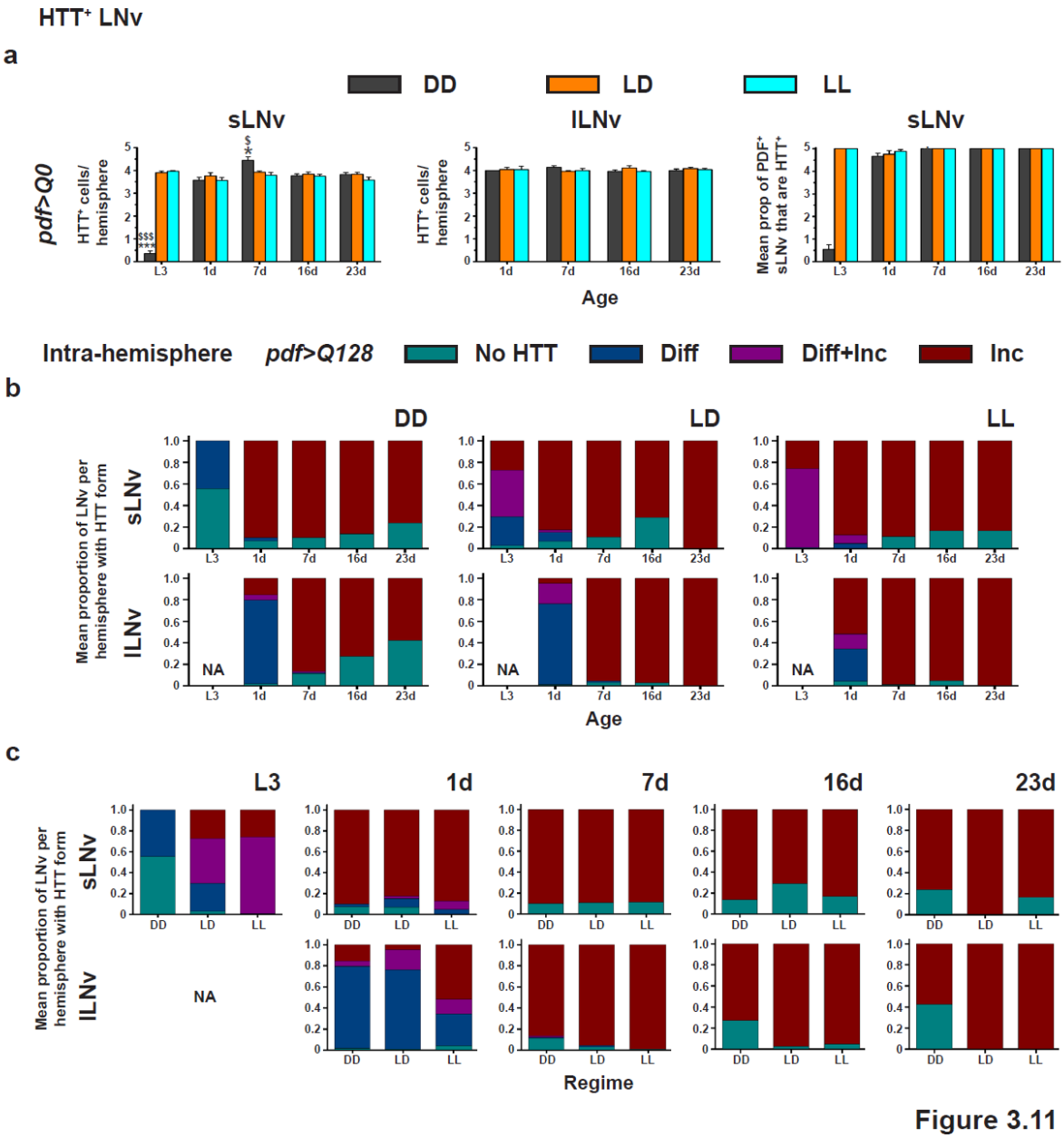

Figure 3.11

Fig 3. 11 Across light regimes, LNv of pdf>Q0 exhibit only the Diff form of HTT, whereas those of pdf>Q128 predominantly exhibit the Inc form.

(a) The Mean number of diffuse-HTT⁺ sLNv soma (left) and lLNv soma (middle) per hemisphere for *pdf>Q0*. * (dark grey) shows an age-matched difference of DD from other regimes at * $p<0.05$ and *** $p<0.001$. $ (dark-grey) indicates significant age differences for DD at $ $p<0.001$ and $$$ $p<0.001$. The mean proportion of PDF⁺ sLNv soma that are also positive for HTT within a hemisphere for the three regimes across age for *pdf>Q0* (right). (b) and (c) The proportions of sLNv (top) or lLNv (bottom) having different expHTT forms per hemisphere (intra-hemisphere) for *pdf>Q128* averaged across hemispheres are plotted for each light regime against age (b) or against regimes for each age (c). NA, not applicable. n ≥ 20 hemispheres/genotype/age/regime. Across panels, error bars are SEM.

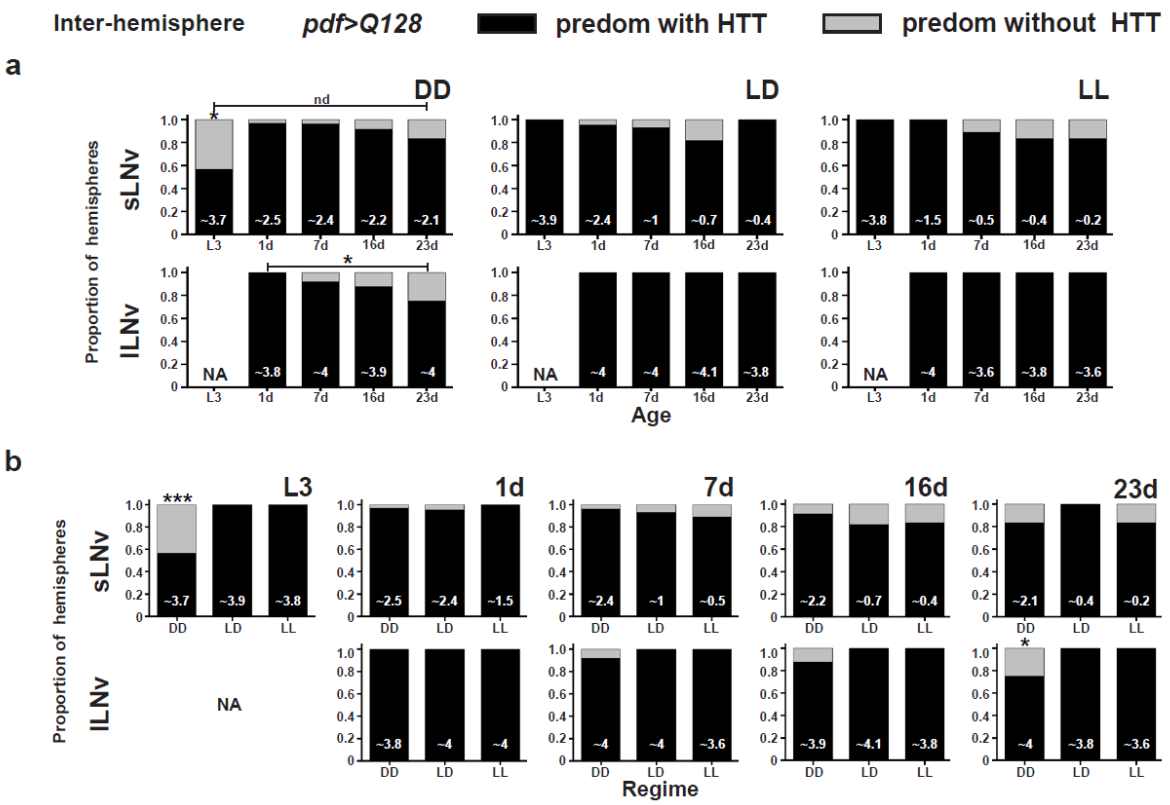

Figure 3.12

Fig 3. 12 expHTT stained LNv dominate most hemispheres of pdf>Q128 across age and light regimes.

(a) and (b) The proportion of hemispheres of *pdf>Q128* dominated by either HTT stained or unstained sLNv (top) or lLNv (bottom) soma for the light regimes plotted against age (a) or between regimes for each age (b). * indicates significant differences between age (a) or of DD from other regimes for a specific age (b) at * $p<0.05$ and *** $p<0.001$. Numbers at the bottom of the bars represent the mean number of PDF^{+} LNv detected in *pdf>Q128* for a regime at an age. NA, not applicable; nd, not different. $n \geq 20$ hemispheres/genotype/age/regime.

The relative proportions of hemispheres dominated by the different expHTT forms in sLNv (or lLNv) differed significantly between ages for a regime (Fig 3.13a). In DD, most hemispheres had Diff expHTT in the sLNv at L3 and in the lLNv at 1d, which significantly changed to most hemispheres with Inc-enriched LNv at subsequent ages (Fig 3.13b, top-left, 3.13c, top-left). A similar trend was seen for the sLNv in LD and LL, with the Diff form seen in DD replaced by Diff+Inc forms (Fig 3.13b, bottom). lLNv in LD also showed a similar trend, with most hemispheres at 1d having Diff expHTT (and some with Diff+Inc) in the lLNv, while older flies had Inc-enriched lLNv (Fig 3.13c, middle). In LL, even though the relative proportions of hemispheres at 1d with Diff-enriched lLNv to that of Inc-enriched lLNv were significantly different from older ages, more than half (~65%) of the hemispheres in the young 1d-old flies already had Inc-enriched lLNv (Fig 3.13a, bottom-right, c, top-right).

The relative proportions of hemispheres dominating different expHTT forms in the sLNv (or lLNv) differed significantly between regimes at L3 for sLNv and 1d for lLNv (Fig 3.14a). At L3, the proportion of hemispheres enriched with Diff-expHTT^{+} sLNv relative to Inc-expHTT^{+} sLNv (or Diff+Inc-expHTT^{+}) in DD differed significantly from LD and LL (Fig 3.14b). Notably, at L3, the proportion of hemispheres enriched with Inc-expHTT^{+} sLNv relative to Diff-expHTT^{+} sLNv (or Diff+Inc-expHTT^{+}) in LL was significantly different from LD as well (Fig 3.14b). At 1d, the proportion of hemispheres enriched with Inc-expHTT^{+} lLNv relative to Diff-expHTT^{+} lLNv in LL differed significantly from DD and LD (Fig 3.14c). Thus, in the relatively low neurotoxic regime of DD (and to some extent LD), young *pdf>Q128* show a predominance of Diff expHTT in the LNv. In contrast, in the circadian arrhythmic and the more neurotoxic regime of LL, there is a predominance of Inc expHTT in the LNv.

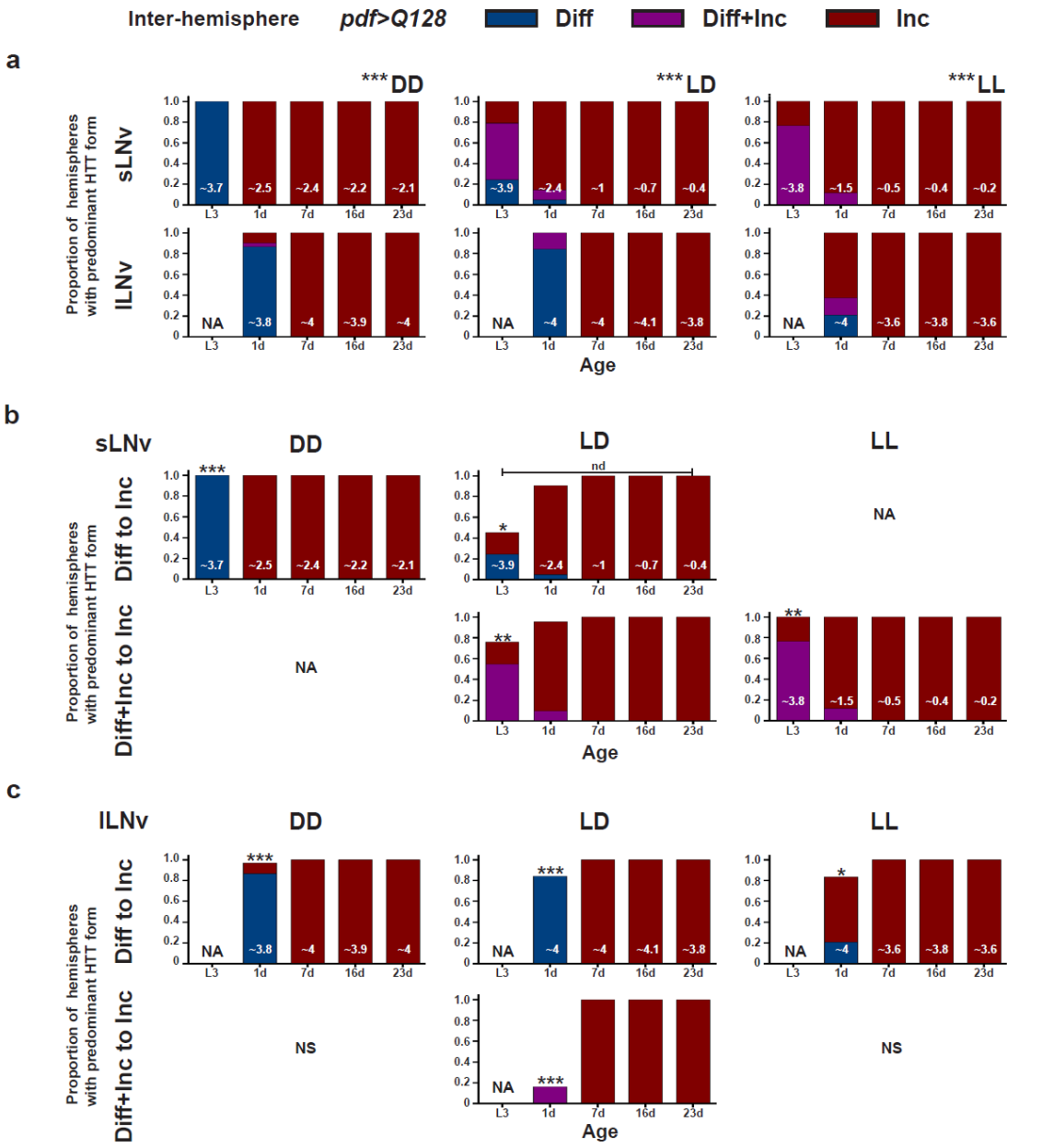

Figure 3.13

Fig 3. 13 In pdf>Q128 flies across light regimes, the relative proportion of hemispheres of inclusion-enriched LNv increases with age.

(a) The proportion of hemispheres of *pdf>Q128* stained with HTT dominated by different expHTT forms in sLNv (top) or lLNv (bottom) is plotted on the *y*-axis to describe the between-hemispheres (inter-hemisphere) distribution of predominant expHTT forms for the three light regimes against age. *** indicates significant changes in relative distributions of expHTT forms between ages for each regime for sLNv and lLNv at $p<0.001$. (b) and (c) The relevant pair-wise comparisons of (a) that are statistically significant or (and) are biologically relevant are plotted for sLNv (b) and lLNv (c). Numbers at the bottom of the bars represent the mean number of PDF$^+$ LNv detected in *pdf>Q128* for a regime at an age. * indicates significant relative changes in pair-wise proportions of hemispheres enriched in expHTT forms of that age from all other ages or indicated age (s) at * $p<0.05$, ** $p<0.01$ and *** $p<0.001$. NA, not applicable; NS, not significant; nd, not different. n ≥ 20 hemispheres/genotype/age/regime.

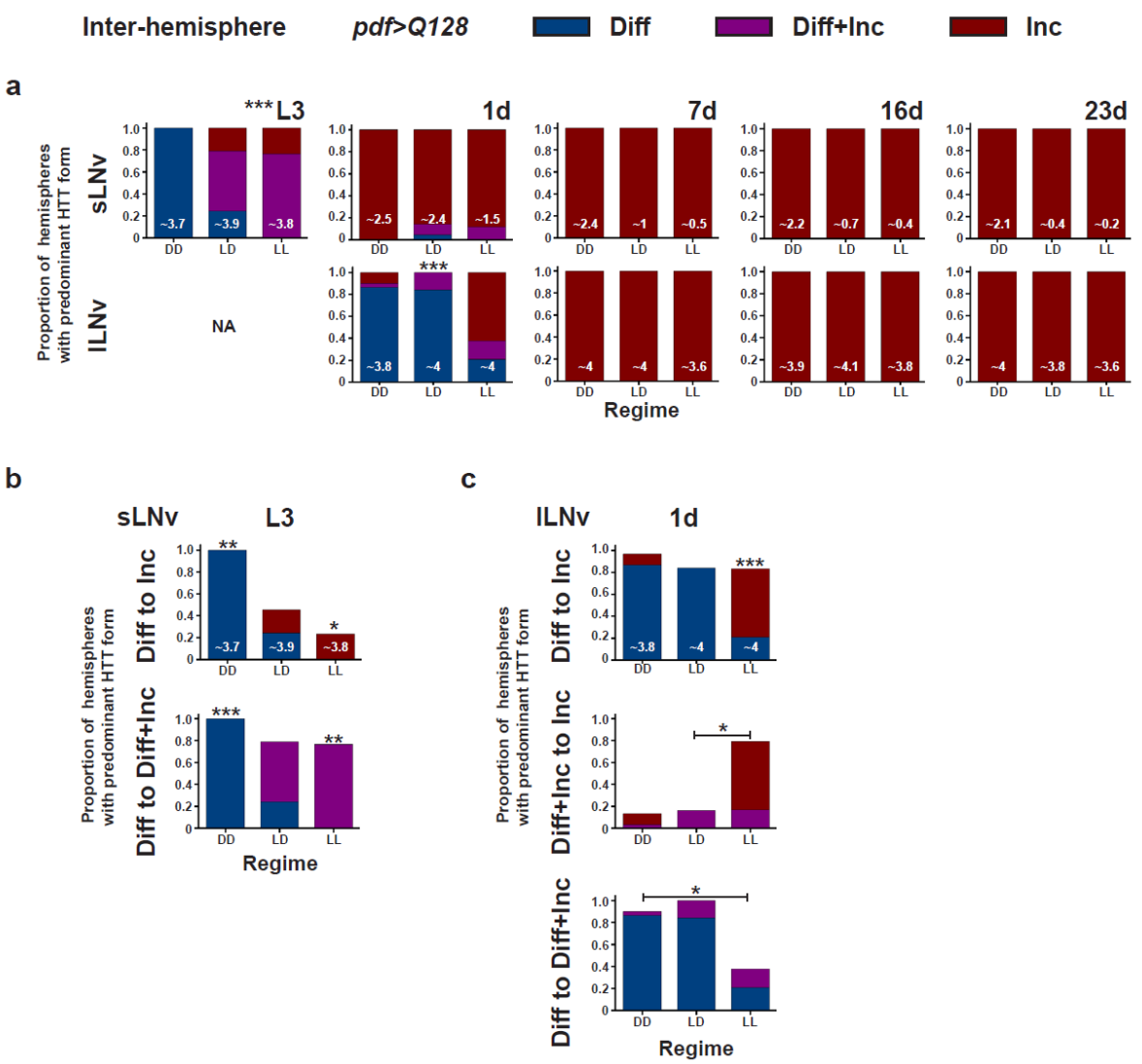

Figure 3.14

Fig 3. 14 In young pdf>Q128, the relative proportion of hemispheres dominated by various expHTT forms in the LNv differs between light regimes, with inclusion-rich hemispheres dominating under LL.

(a) The proportion of hemispheres of *pdf>Q128* stained with HTT dominated by different expHTT forms in sLNv (top) or lLNv (bottom) is plotted on the *y*-axis to describe the inter-hemisphere distribution of predominant expHTT forms against light regimes for each age. *** indicates a significant difference in the relative distributions of expHTT forms between regimes at specific ages at $p<0.001$. (b) and (c) The relevant pair-wise comparisons of (a) that are statistically significant or (and) are biologically relevant are plotted for sLNv (b) and lLNv (c) comparing regimes for an age. All other details are like 3.13b and c, with * indicating differences between regimes at an age.

In DD, *pdf>Q128* larvae did not show expHTT inclusions, but by age 1d, inclusions appeared, and their mean number and size increased with age (Fig 3.15a). In LD, expHTT inclusions were seen as larvae, and the mean inclusion number and size increased significantly at 7d compared to earlier ages and remained high at later ages of 16d and 23d (Fig 3.15a). In LL, HTT inclusions were seen as larvae, their mean numbers increasing significantly by 1d (Fig 3.15a, left). Compared to 1d, the mean inclusion number at older ages was significantly lower in LL while remaining greater than in L3. The mean inclusion size in LL did not change with age (Fig 3.15a, right). At early stages as larvae and at 1d, the mean inclusion number and size were significantly higher in LL than in DD and LD (Fig 3.15a). In contrast, DD showed fewer inclusions across ages than LD and LL. These observations suggest that LL is favourable to inclusions, DD is less favourable, and LD is intermediate.

I also quantified the distribution of various-sized expHTT inclusions. The intra-hemisphere distribution of various-sized expHTT inclusions across ages for the three light regimes is shown (Fig 3.15b). In the inter-hemisphere comparisons, the relative proportion of hemispheres enriched in various sized inclusions differed significantly across age in DD but not LD and LL (Fig 3.15c). Specifically, in DD, on comparing the relative proportion of hemispheres enriched with inclusions of <3µ to mixed sizes, 23d differed from 1d and 16d, with the early ages having predominantly small-sized inclusions (Fig 3.15e, left). The relative proportions differed between regimes at 7d but not at other ages (Fig 3.15d). At 7d, the relative proportion of hemispheres enriched with inclusions of the smaller size range of <3µ to that of mixed sizes differed between DD and LD, with DD having a higher proportion of small-sized Inc (Fig 3.15c).

Overall, across regimes, the proportion of hemispheres having expHTT inclusion enriched LNv increases across ages, as does inclusion number and size. Considering the PDF^{+} sLNv soma numbers, the dominance specific expHTT form in LNv, and the number and size of inclusions in the young *pdf>Q128*, DD emerges as the least neurotoxic regime, followed by LD, while LL is the most neurotoxic. Thus, light worsens neurodegenerative phenotypes.

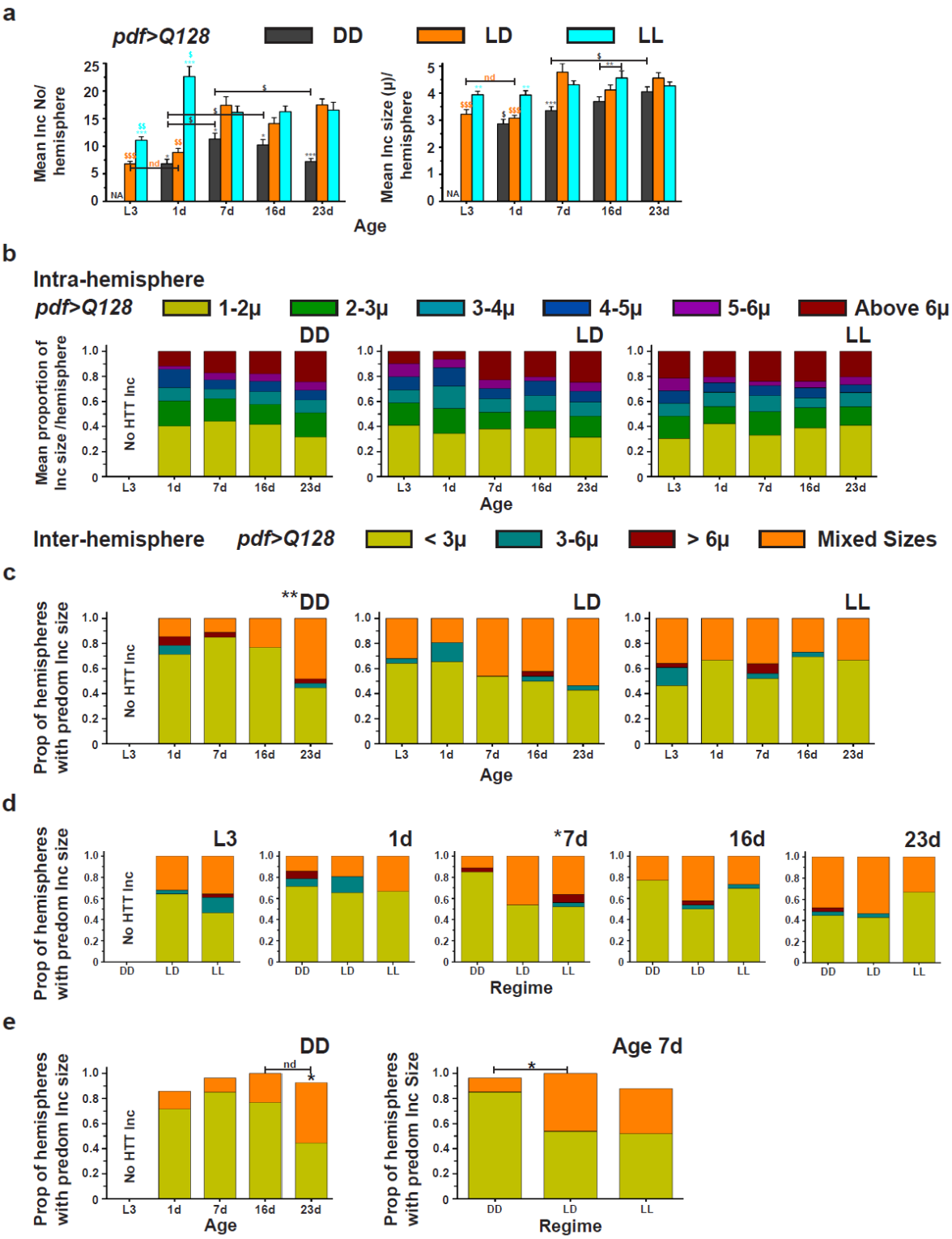

Figure 3.15

Fig 3. 15 Young pdf>Q128 in LL show larger and more expHTT inclusions than those in DD and LL.

(a) Comparison of mean inclusion number per hemisphere (left) and mean inclusion size per hemisphere (right) for *pdf>Q128* under the three light regimes across age.

* indicates significant differences between regimes for a given age: * (dark-grey) from DD, * (orange) from LD and * (blue) from LL at * $p<0.05$, ** $p<0.01$ and *** $p<0.001$. Coloured $ represents differences across age for the respective coloured regime at $ $p<0.05$, $$ $p<0.01$ and $$$ $p<0.0001$. Error bars are SEM. (b) The mean proportion of different-sized expHTT inclusions per hemisphere describing the within-hemisphere size distribution is plotted against age for the three light regimes. (c) and (d) The proportion of hemispheres dominated by different expHTT inclusion size ranges in LNv are plotted on the *y*-axis to describe the between-hemispheres distribution of expHTT inclusion sizes. This proportion is plotted against age for each regime (c) or against regimes for each age (d). The * indicates significant changes in relative distributions of expHTT sizes between ages (c) or between regimes (d) at ** $p<0.01$. (e) Pair-wise comparisons of (c) and (d) that were statistically significant are plotted, with * indicating significant relative changes in pair-wise proportions of hemispheres enriched with differently sized expHTT inclusions between age for DD (left) and between regimes at 7d (right) at $p<0.05$. nd is not different. $n \geq 20$ hemispheres/genotype/age. Error bars are SEM.

3.4 DISCUSSION

3.4.1 Effects of environmental interventions impacting circadian rhythms on HD-induced neuropathology

The case for neurodegeneration leading to circadian disturbances is apparent (Hastings and Goedert, 2013; Musiek, 2015). The converse, however, that circadian dysfunction can amplify neurodegenerative phenotypes is still a nascent idea. Here, I asked whether alterations to circadian rhythms can modify neurodegeneration in a *Drosophila* HD model using environmental conditions that alter circadian function. Some of the neurodegenerative phenotypes of these flies are behavioural arrhythmicity in DD and cellular loss of PDF from sLNv soma and PER from LNv (Chapter 2) (Sheeba et al., 2008a; Prakash et al., 2017). Despite exposure to a rich cyclic environment of SN or a strongly rhythmic environment of LD during development, *pdf>Q128* flies were behaviourally arrhythmic in DD. These observations suggest that specific circadian-rhythm-bolstering environments during development cannot overcome arrhythmicity as adults when such a strongly pathogenic version of HTT is expressed. Also, exposure of *pdf>Q128* to circadian rhythm disrupting the environment of LL during development (or up to age 23d (Chapter 2, Fig 2.14)) did not affect their ability to entrain LD. PER, a core molecular clock component, and PDF, the circadian neuronal output, are affected in the sLNv, giving rise to arrhythmicity in these flies. During development, cycling light or gradually cycling multiple time cues cannot reverse these phenotypes. Thus, specific environmental regimes during development do not seem to modify activity rhythms of expHTT-expressing flies as adults in DD25 or LD25. Also, given that flies reared under LL during development were rhythmic in DD and entrained to LD as adults, this suggests that functional developmental clocks are not necessary for adult activity rhythms.

Regarding cellular markers, across regimes of DD, LD and LL, there is a loss of PDF from sLNv soma, and this loss worsens with age in LD and LL. In all the regimes, the proportion of hemispheres with LNv was dominated by inclusions; the mean inclusion number and mean inclusion size (except in LL) increased with age. This progressive worsening of features is a

characteristic of HD, recapitulated in this *Drosophila* circadian HD model. The arrhythmic clock-disrupting regime of LL aggravated cellular neurotoxicity the most, followed by LD, while DD was relatively neuroprotective.

The continuous presence of light or LL exacerbated neurotoxic phenotypes. *pdf>Q128* under LL had a precocious and more drastic loss of PDF from sLNv, with the dominance of hemispheres with expHTT inclusion-rich LNv and more numerous and more enormous inclusions very early on than LD or DD. Also, most *pdf>Q128* flies under LL lack PDF^+ DP at later ages while present in LD and DD, further attributing more significant neurotoxicity to LL. Thus, LL, which abolishes circadian rhythms, also hastens neurodegenerative features and aggravates them. However, one cannot conclude whether these LL effects solely stem from its clock-disrupting effects, given the detrimental effect of light *per* se. These findings, nevertheless, highlight the importance of lighting conditions, which can translate into good circadian hygiene in combating neurodegenerative symptoms. There is evidence for LL worsening neuropathology in the literature. Aβ expressing flies in LL had a shorter lifespan than LD (Chen et al., 2014). Sub-pathological Aβ rats in LL also showed accelerated aggregation of exogenous Aβ42 (Sharma and Goyal, 2020a). Another study showed that heterozygous CLK^{jrk} flies under LL exhibit retinal degeneration, while those in LD did not (Yu, 2012).

Circadian disruption by LL is known to be detrimental to overall organismal health (Coomans et al., 2013; Lucassen et al., 2016; Chalfant et al., 2020; Rumanova et al., 2020; Yang et al., 2020). Flies in LL have shortened lifespans (Pittendrigh and Minis, 1972; Sheeba et al., 2000; Chen et al., 2014; Vaccaro et al., 2017). Mice exposed chronically to LL had reduced central clock protein oscillations in the SCN, skeletal muscle and innate immune functions and compromised bone structure (Lucassen et al., 2016). Exposure of rats to LL induced oxidative stress, cognitive issues, anxiety and depressive symptoms (Tapia-Osorio et al., 2013; Sharma and Goyal, 2020a). LL affects rhythms in melatonin and corticosterone, disrupts peripheral rhythms, predisposes the organism to metabolic diseases and exacerbates atherosclerosis (Chalfant et al., 2020; Rumanova et al., 2020). Circadian disruption could contribute to neurodegeneration potentially by promoting pro-neurodegenerative processes or impeding neuroprotective processes. For instance,

there is considerable circadian influence on pathways involved in neuronal proteostasis and metabolism, synaptic homeostasis, immune and inflammatory response, oxidative damage, mitochondrial function and DNA repair and maintenance (Musiek et al., 2013; Leng et al., 2019; Lananna and Musiek, 2020; Carter et al., 2021). Sleep timing is under circadian control, and sleep is essential for clearing neurotoxic metabolites from the brain and neuronal homeostasis (Xie et al., 2013; Wu et al., 2019). *pdf>Q128* flies, however, do not exhibit sleep defects (Chapter 2). Circadian disruption by LL could also disrupt the neuroprotective functions of specific clock genes. *pdf>Q128* flies show loss of PER from LNv (Chapter 2) (Prakash et al., 2017) and loss of *Drosophila Per* and mice *Bmal1* results in neuronal damage (Krishnan et al., 2009; Musiek et al., 2013), suggesting a direct role for these genes in neuroprotection. CLK is an anti-ageing factor as CLK mutants show accelerated age-dependent locomotor decline under LL (Vaccaro et al., 2017). Conversely, Clk^{Jrk} mutation suppressed expHTT-induced effects on PDF^{+} sLNv soma numbers and expHTT inclusions in a fly model (Xu et al., 2019a). Under DD, circadian photoreceptor Cryptochrome (CRY) is reported to have an anti-ageing role, promoting robust circadian rhythms and improving lifespan (Rakshit and Giebultowicz, 2013). Under LL, constant light activation of CRY and its degradation could bring down CRY levels, reducing neuroprotection. A previous study has suggested that prolonged light exposure may trigger caspase-mediated degradative pathways dependent on PDF and its receptor PDFR (Means et al., 2015). Excitotoxicity significantly contributes to neuropathology (Salinska et al., 2005; Dong et al., 2009). Continuous activation of the phototransduction pathway leads to retinal degeneration (Dolph et al., 1993). lLNv receiving excitatory visual circuit inputs (Muraro and Ceriani, 2015; Schlichting et al., 2016) could be downstream targets to such prolonged retinal hyper-excitation. *pdf>Q128* flies under light/dark cycles also had a greater extent of PDF loss from sLNv soma and more expHTT inclusions than those in DD across age. At L3, Diff+Inc expHTT enriched sLNv hemispheres dominated LD instead of DD's Diff-enriched sLNv. These observations suggest that light might enhance the neurodegenerative phenotypes. This negative effect of light on the expHTT-induced phenotypes is reflected by improved phenotype in its absence, i.e. in DD, where *pdf>Q128* continues to have, on average, ~2 PDF^{+} sLNv soma for up to three weeks. Another

interesting observation in DD is that at L3, most hemispheres of *pdf>Q0* and nearly 50% of the hemispheres of *pdf>Q128* had the most PDF^+ sLNv without HTT staining. The lack of HTT staining at L3 in both genotypes under DD suggests that lack of light might reduce the Gal4-mediated HTT expression. Further, with age, *pdf>Q128* flies in DD, but not *pdf>Q0*, have a considerable proportion of hemispheres where HTT does not stain most of the LNv, which becomes significant by 23d. So, it seems that in DD, the expHTT expression levels might be low, and with age, its clearance might be higher, giving rise to the absence of HTT staining in LNv. Reducing expHTT levels in LNv could dilute the toxicity, rendering DD neuroprotective. *pdf>Q128* larvae with expHTT stained sLNv show the diffused form or an absence of expHTT inclusions, indicating that the expHTT levels are probably not high enough to form inclusions. The presence of light seems to compound inclusions. Thus, in addition to LL being a regime of circadian dysfunction, the presence of light itself could be an additional factor contributing to neuropathology. Given that Cry^{01} are rhythmic in LL (Emery et al., 2000a; Helfrich-Forster et al., 2001; Klarsfeld et al., 2004), the effect of the continuous presence of light on HD cellular phenotypes, independent of its clock-disrupting effects can be studied using HD flies in a *Cry* mutant background.

Considering the robust circadian rhythms under rhythmic environments such as cyclic light, the LD *vs* DD results are challenging to explain. Some of the adverse effects of light on the HD cellular phenotypes can be attributed to the spectral composition of white light used in these experiments, light intensity, duration and maybe even exposure time.

There is precedence for downsides to light exposure in flies. White light LD shortened lifespan and decreased climbing ability in flies than DD (Nash et al., 2019). This decline was primarily due to the blue light component of white light. The blue light caused retinal damage, brain vacuolisation and locomotion defects and induced stress response genes in old flies (including *Hsps* and *lactate dehydrogenase*), suggesting cumulative light exposure could be a stressor and accelerate ageing (Nash et al., 2019). Chronic exposure of flies to blue light (430nm-500nm), which constitutes a significant portion of artificial illumination, resulted in changes to their energy metabolism, neurotransmitter levels, and age-dependent accelerated brain vacuolization, which is

a marker of neurodegeneration via a decline in mitochondrial respiration independent of light (Song et al., 2022; Yang et al., 2022). Moreover, blue light affects the intrinsically photosensitive retinal ganglion cells, the human photoreceptor. It inhibits the release of melatonin, a chemical the body uses to signal when it is time to go to bed, changing biological cycles (West et al., 2011). A study with *Caenorhabditis elegans* showed that worm lifespan was inversely proportional to the photoperiod, with DD being the most favourable. The visible light effects on lifespan were photooxidative stress, an unfolded protein response and mitochondrial damage (De Magalhaes Filho et al., 2018). Another study also showed that the lifespan advantage conferred by DD (over LD and LL) was reversed in flies defective in DNA repair and replication, suggesting that such repair processes are involved in slowing down cellular ageing in DD (Moskalev and Malysheva, 2009). The authors also showed that mutation in FOXO, a TF mediating oxidative stress, HSP70, a central chaperone, and dSirt2, differentially affected the mean lifespan under varying lighting conditions and attributed them to the damaging effects of additional lighting (Moskalev and Malysheva, 2010; Shostal and Moskalev, 2012). The authors proposed that light could affect lifespan via two independent mechanisms involving neuroendocrine networks: a beneficial effect of decreasing photoperiod by stimulating a stress response and a detrimental effect of photoperiod by enhancing metabolism and oxidative stress. An organism could perceive a decrease in photoperiod (constant dark = 0h photoperiod) as deteriorating external conditions and respond by inhibiting growth and reproduction and activating stress response genes. The improved stress resistance slows ageing and extends lifespan (Shostal and Moskalev, 2012). *Drosophila* HD flies in a shorter 10h:10h photoperiod had better PDF^{+} sLNv numbers and fewer expHTT inclusions than those in a 12h:12h LD (Xu et al., 2019a). Damage by light includes oxidative damage to lipids and proteins, DNA damage, and retinal degeneration, leading to a decline in neuronal excitability and synaptic transmission (Shen and Tower, 2019). A study shows that the blue-light-activated CRY photocycle generates intracellular reactive oxygen species in *Drosophila* (Arthaut et al., 2017).

In DD, sLNv is critical for activity rhythms (Grima et al., 2004a; Stoleru et al., 2004; Shafer and Taghert, 2009). At age 1d, *pdf>Q128* flies under DD, LD, and LL show the presence of PDF^{+}

sLNv soma, albeit reduced numbers from controls. With age, LD and LL show a progressive loss of PDF^+ sLNv soma to a near-complete loss, while those in DD have ~2 PDF^+ sLNv for up to 3 weeks. Nevertheless, behaviourally, flies reared in either of the three regimes during development are arrhythmic as adults from the first day of DD. Despite having non-zero PDF^+ sLNv soma, DD-reared flies are arrhythmic, suggesting that their sLNv are likely dysfunctional. In the absence of light, even though there is mitigation of early-age inclusions and later ages show some LNv without HTT, sLNv seems to require further re-enforcements to be functional and bring about behavioural rhythmicity.

3.4.2 Expanded Huntingtin inclusions and cellular dysfunction

The role of expHTT aggregation in HD pathogenicity is not clearly understood. Some studies suggest a neuro-toxic role for polyQ-protein aggregates in disease pathology, with specific aggregates interacting and sequestering proteins essential for cellular function (McCampbell et al., 2000; Nucifora et al., 2001; Donaldson et al., 2003; Qin et al., 2004) or physically blocking axonal transport (Gunawardena et al., 2003; Lee et al., 2004) or impairing proteasomal function (Bence et al., 2001), thus, affecting neuronal function. Other studies show a dissociation between aggregates and neurodegenerative phenotypes (Saudou et al., 1998; Gutekunst et al., 1999; Kim et al., 1999; Kuemmerle et al., 1999; Slow et al., 2005; Romero et al., 2008), while others show that certain aggregate forms sequester the toxic forms from the cellular milieu and facilitating their clearance, thus playing a protective role (Taylor et al., 2003a; Arrasate et al., 2004; Miller et al., 2010a; Miller et al., 2011). LL shows the greatest extent of inclusion formation early on, accompanied by accelerated loss of PDF from sLNv soma and PDF^+ sLNv DP as flies age. Furthermore, in DD, lack of expHTT inclusions during the developmental L3 stage, fewer inclusions at an early age and a significant proportion of LNv without expHTT at later ages are accompanied by at least ~two PDF^+ sLNv soma till three weeks of age. Though there is no clear evidence for apoptosis of the sLNv, there is a definite sLNv dysfunction as evidenced by loss of PDF and PER from sLNv soma *in vivo*, amounting to a physiological consequence of behavioural

arrhythmicity in DD. Nevertheless, there is a close association between the extent of cellular dysfunction with the presence of inclusions and the inclusion load in this study. Thus, in this *Drosophila* circadian HD model, inclusions serve as markers and potential predictors of cellular dysfunction.

expHTT adopts multiple conformations and follows different trajectories of inclusion formation (Legleiter et al., 2009; Margulis et al., 2013; Hoffner and Djian, 2015). The monomeric polypeptide goes through a multistep process to aggregation (Hatters, 2012; Hoffner and Djian, 2014). Studies suggest that monomeric and oligomeric intermediates contribute to pathogenicity and are likely more toxic than mature HTT fibrils (Sanchez et al., 2003; Ross and Poirier, 2004; Nagai et al., 2007; Takahashi et al., 2008; Kim et al., 2016). Recent evidence shows that the same chaperone-based disaggregase machinery has vastly different outcomes when disaggregating amorphous aggregates *vs* amyloid fibrils: while the former gets solubilised, the disaggregation of the latter gives rise to potentially reactive seeding-competent species (Nachman et al., 2020; Tittelmeier et al., 2020a; Tittelmeier et al., 2020b). Therefore, uncovering the nature of expHTT forms to understand the aggregation process's contribution to neuropathology will be essential.

The current study shows that light aggravates HD-associated neurotoxicity in flies in a quality- and duration/dosage-dependent manner. However, these findings also confound any circadian clock-disrupting effects that the LL regime might have had and make the conclusion regarding the effects of clock disruptions on neurotoxicity difficult. Other avenues of circadian clock disruptions, like disruptive feeding regimes or clock mutants, can be used to address some of those questions. Since sleep and circadian disturbances are some of the early symptoms of HD, which further aggravate the pathophysiology, it is essential to have therapeutic interventions for HD patients that are inclusive of improving their circadian health. Identifying checkpoints of circadian control of critical neuropathological events such as aggregation and cellular damage would slow disease progression. While developing palliative care and treatment regimens for patients, it is vital to consider the light environment, as highlighted in this study.

CHAPTER 4

Effects of Temperature Regimes on the Circadian Dysfunction and Neurotoxicity in HD flies

4.1 INTRODUCTION

The circadian period is relatively stable over a range of physiological temperatures, i.e., the circadian clocks are temperature compensated (Sawyer et al., 1997; Rensing and Ruoff, 2002; Kidd et al., 2015). However, environmental temperature affects the phasing of circadian clocks and is a potent zeitgeber for circadian rhythms across taxa (Rensing and Ruoff, 2002; Someren and JW, 2003; Refinetti, 2020). In *Drosophila*, external temperature cycles synchronise the activity rhythms and molecular oscillations not only in DD but also in the arrhythmic environment of LL; the temperature-mediated entrainment is under clock control (Tomioka et al., 1998a; Yoshii et al., 2002; Glaser and Stanewsky, 2005; Yoshii et al., 2005; Currie et al., 2009). In mammals, ambient temperature cycles entrain circadian rhythms, and their daily body temperature rhythms act as an internal synchroniser that strongly resets peripheral rhythms (Buhr et al., 2010; Refinetti, 2010; Farsi et al., 2020; Hart et al., 2021). Oscillating temperatures also offer health benefits: improvements in lifespan in flies and worms (Economos and Lints, 1986b; Cardoso et al., 2002; Galbadage and Hartman, 2008), enhancement of performance and thermal tolerance in insects (Colinet et al., 2015; Manenti et al., 2018; Salachan and Sørensen, 2022) and mitigation of oxidative damage and cytotoxicity induced by Aβ in human neural cells (Chen et al., 2020). Exposure to stressors in small doses like mild temperature challenges can be beneficial (hormesis), improving the organisms' health, lifespan, and performance; they are also more effective when implemented at an early age as environmentally mediated epigenetic adaptations often occur at specific developmental stages (Vaiserman, 2010; Li et al., 2019a; Agathokleous and Calabrese, 2020; Berry and López-Martínez, 2020; Rossnerova et al., 2020). Further, in *Drosophila*, developmental temperature affects the spontaneous activity of adults (Cavieres et al., 2016; MacLean et al., 2017; Klepsatel and Gáliková, 2022), and cyclic temperature during development affects the circadian activity rhythms of adults (Malpel et al., 2004; Picot et al., 2009). Since expHTT induces immediate-early circadian behavioural and neuronal dysfunction in *Drosophila* adults, the first question was whether providing time cues as thermophase/cryophase temperature cycles during development can affect these phenotypes.

Extreme external temperatures (hypo or hyperthermia) and long-term thermal stress harm organismal health and exacerbate NDs (Walter and Carraretto, 2016; Bongioanni et al., 2021; Zammit et al., 2021). However, mild temperature stress induces adaptive response having positive effects, especially on the lifespan in both poikilotherms and homeotherms, including humans (Holloszy and Smith, 1986; Rattan, 1998; Rattan, 2006; Le Bourg and Rattan, 2008; Rattan et al., 2009; Le Bourg, 2011; Calabrese, 2016; Yi et al., 2017; Brunt et al., 2018; Mane et al., 2018; Berry and López-Martínez, 2020). Exposure to a low level of one stressor is often associated with increased tolerance to another stressor as various stresses share common underlying protective mechanisms (Mattson, 2008; Vaiserman, 2010; Milisav et al., 2012; Horowitz, 2017; Li et al., 2019a; Berry and López-Martínez, 2020; Rodgers and Gomez Isaza, 2021). Neurodegenerative proteins like expanded polyQ HTT tax cellular proteostasis and are considered stressors (Merienne et al., 2003a; Bettencourt et al., 2008; Berendzen et al., 2016). The question was whether exposure to another stressor, like mild thermal stress, can result in adaptation or improved tolerance to neurodegenerative stress. To address these questions, I tested whether temperature changes could alter the course of circadian dysfunction and neurotoxicity in HD flies.

4.1.1 Temperature and Neurodegeneration

Recent studies allude to the possibility of using temperature-based therapies to treat NDs (Hunt et al., 2019; Sun et al., 2019; Kamash and Ding, 2021; Patrick and Johnson, 2021). However, the literature on thermo-modulation of neurodegeneration and circadian dysfunction, especially using mild heat therapy, is scarce. Mild heat-stress-induced HSF-1 reduced polyQ aggregation and extended the lifespan of *C elegans* in an autophagy-dependent way (Kumsta et al., 2017). Hypothermia improved symptoms in *Drosophila* models of autosomal-dominant hereditary spastic paraplegia (Baxter et al., 2014) and traumatic brain injury (Lateef et al., 2019). Exposure of HD mice to cold accelerated HD phenotypes, while the elevation of ambient temperature to 30C (thermoneutral range for rodents) improved their survival (Weydt et al., 2006; Chaturvedi et al., 2010). In contrast, in prion-infected mice, cooling enhanced the expression of RNA-binding

motif protein 3, RMB3, suppressed behavioural deficits and was neuroprotective (Peretti et al., 2015). Sauna-like conditions of mild hyperthermia lowered tau phosphorylation in AD mice models (Guisle et al., 2022). Studies in healthy middle-aged humans show that regular passive heating via sauna baths reduces the risk of developing dementia and AD (Laukkanen et al., 2017; Heinonen and Laukkanen, 2018; Knekt et al., 2020). Thus, there is substantial evidence for the prophylactic effects of transient or mild hyperthermia or passive body heating for various other disease conditions. Such treatments mediate clinically relevant anti-depressive effects, possibly by modifying mitochondrial function and immune system effects and activating brainstem serotonergic neurons (Berk et al., 2016; Janssen et al., 2016; Hanusch and Janssen, 2019; Naumann et al., 2020). They also improve mood and quality of life in cancer and diabetic patients, respectively (Koltyn et al., 1992; Beever, 2010), sleep quality in elderly insomniac patients (Dorsey et al., 1999; Mishima et al., 2005) and women with fibromyalgia (Silva et al., 2013). Furthermore, thermoregulation and circadian body temperature rhythms are compromised in many NDs (Harper et al., 2005; Raupach et al., 2020). HD mice exhibit deficiencies in thermoregulation and adaptive thermogenesis and develop hypothermia (body temperature drops <30°C) (Weydt et al., 2006; Chaturvedi et al., 2010) and circadian body temperature rhythms (Kudo et al., 2011; Fisher et al., 2013). There are conflicting reports for AD, with some studies reporting that low body temperature promotes Tau phosphorylation in AD mice (Carrettiero et al., 2015; Tournissac et al., 2017). Mild hyperthermia reduces it (Guisle et al., 2022), while other studies report that AD rats and patients exhibit hyperthermia (Klegeris et al., 2007; Motzko-Soares et al., 2018). Chronic warm temperatures enhance phosphorylation and toxicity in AD mice (Jung et al., 2022). However, human studies on thermoregulatory defects in HD are sparse and largely anecdotal (Weydt et al., 2018). A recent case study, the first in humans, describes hypothermia in a late-stage HD patient (Altıner et al., 2020). In older healthy adults, lower core body temperature was associated with increased Tau phosphorylation, neurofibrillary tangles, and pathology (Blessing et al., 2022).

4.1.2 Temperature-based interventions as HD modifiers: Specific questions

Different kinds of temperature regimes were used to investigate the effects of temperature on expHTT-induced circadian phenotypes. They broadly fell under two categories: oscillating temperatures or temperature cycles and constant ambient temperature. I specifically asked whether developmental warm/cold or thermo/cryo (TC) temperature cycles alter the expHTT-induced arrhythmic adult activity rhythms in DD and the cellular phenotypes (4.3.1, 4.3.3-4.3.7). I also asked whether slightly lower (cool) or relatively higher temperatures (warm) affect behavioural arrhythmias and neurotoxicity in *pdf>Q128* (4.3.8-4.3.12). Under the constant ambient temperature regime, I tested the effects of changing temperature post-eclosion on HD flies by either providing an adult-restricted warm temperature (upshift) or an adult-restricted cool temperature (downshift) (4.3.13-4.3.16, 4.3.18-20). Under all the categories, the effect of developmental light was also investigated (4.3.2, 4.3.13, 4.3.17). I then compared the phenotypes of *pdf>Q128* raised under developmental temperature cycles and adult-restricted warm temperatures (4.3.21). I also investigated the role of *Hsp70* in the adult-restricted warm-temperature-mediated behavioural rhythmicity of *pdf>Q128* (4.3.22). The following scheme has been employed to describe the circadian neurodegenerative phenotypes of *pdf>Q128* under the various regimes. First are the within-regime comparisons, followed by the relevant between-regime comparisons. The behavioural rhythms of activity/rest are described first, followed by LNv cellular phenotypes (wherever warranted) of PDF^+ LNv numbers, PER^+ LNv numbers, PER cycling (if relevant) and expHTT form and inclusion features.

Broadly, I find that both categories of temperature regimes postpone the behavioural arrhythmicity and PDF loss from the sLNv of *pdf>Q128*, but to different extents and varying in the associated cellular mechanisms. The adult-restricted upshift to warm temperatures provides slightly more substantial neuroprotection to the HD flies than developmental temperature cycles. These results prove that environmental treatments like modifying temperature (cycling and warming) can alleviate circadian defects associated with a neurodegenerative disease and set encouraging precedence for research on alternative therapeutic approaches via environmental modulation.

4.2 MATERIALS AND METHODS

4.2.1 Fly lines

Chapter 2 (section 2.2.1) already describes the transgenic fly lines and the genotype notations. The fly stocks were typically maintained under 12h:12h LD at 25°C with a relative humidity of 70-80%. All fly lines and crosses were maintained on a standard cornmeal medium. The various experiments' light regimes and temperatures during development and adulthood are indicated in Tables 4.1 and 4.2. The flies were transferred to a different temperature (as necessary) at the end of the second-day post-eclosion, immediately after what would be real-time lights-off. This time of transfer was chosen for two reasons. The first was for practical purposes, as collecting freshly eclosed flies at the same temperature as their pre-adult temperatures is more feasible without subjecting the pupated vials to environmental light and temperature changes. Secondly, the developmental temperature (oviposition to eclosion) and acclimation temperature (pre-testing to testing, i.e., as adults from eclosion to testing) were matched right up till the start of the locomotor activity testing since both temperatures affect many phenotypic traits of adult *Drosophila* (Dillon et al., 2009). So, essentially, in all the experiments, **development-specific temperature** refers to **temperature experienced as pre-adults plus 2d as adults**, and **adult-restricted temperature** refers to **temperature experienced from the third day of adulthood** (i.e., excluding the first two days after eclosion, eclosion being 0d).

Table 4.1 Temperature cycles related regimes.

Regime	Development		Adults			
			0-2d		3d onwards	
	Light	Temp (˚C)	Light	Temp (°C)	Light	Temp (˚C)
Cyclic temperature						
DDTCtoDD25	DD	TC	DD	TC	DD	25
DDTCtoDD21	DD	TC	DD	TC	DD	21
DDTCtoDD29	DD	TC	DD	TC	DD	29
LDTCtoDD25	LD	TC	LD	TC	DD	25
LLTCtoDD25	LL	TC	LL	TC	DD	25
Constant temperature						
DD25toDD25 (DD25)	DD	25	DD	25	DD	25
LD25toDD25 (LDtoDD25)	LD	25	LD	25	DD	25
Temperature upshift						
DD21toDD25	DD	21	DD	21	DD	25
Temperature downshift						
DD29toDD25	DD	29	DD	29	DD	25

Development stage-specific TC	Development				Adults			
	Egg to L3		Pupal stages		0-2d		3d onwards	
	Light	Temp (°C)	Light	Temp (°C)	Light	Temp (°C)	Light	Temp (°C)
DDTC upto L3	DD	TC	DD	25	DD	25	DD	25
DDTC as Pupa-2d	DD	25	DD	TC	DD	TC	DD	25

DD, constant darkness. **LD**, 12h:12h **L**ight:**D**ark cycles (light cycles). **LL**, constant light.

TC, 12h:12h: 21°C:29°C **T**hermophase:**C**ryophase cycles (temperature cycles)

Table 4.2 Ambient constant temperature regimes.

Regime	Development		Adults			
			0-2d		3d onwards	
	Light	Temp (°C)	Light	Temp (°C)	Light	Temp (°C)
Constant optimal temperature						
DD25toDD25 (DD25)	DD	25	DD	25	DD	25
LD25toDD25 (LDtoDD25)	LD	25	LD	25	DD	25
Constant low temperature						
DD23toDD23 (DD23)	DD	23	DD	23	DD	23
LD23toDD23 (LDtoDD23)	LD	23	LD	23	DD	23
Constant high temperature						
DD29toDD29 (DD29)	DD	29	DD	29	DD	29
LD29toDD29 (LDtoDD29)	LD	29	LD	29	DD	29
Temperature upshift						
DD23toDD29	DD	23	DD	23	DD	29
DD21toDD25	DD	21	DD	21	DD	25
DD25toDD29	DD	25	DD	25	DD	29
LD23toDD29	LD	23	LD	23	DD	29
LL23toDD29	LL	23	LL	23	DD	29
Temperature downshift						
DD29toDD23	DD	29	DD	29	DD	23

Age-specific acute high temp exposure	Development		Adults				
	Light	Temp (˚C)	0-1d	2-3d (48h)	5-6d	7-8d (48h)	9d onwards
Acute DD29 at 2-3d	DD	23	DD23	DD29	DD23	DD23	DD23
Acute DD29at 7-8d	DD	23	DD23	DD23	DD23	DD29	DD23

For the investigation on whether the heat-inducible stress chaperones, the Hsps, are involved in the adult-restricted warm-temperature-mediated early-age behavioural rhythm rescue of *pdf>Q128*, the free-running activity/rest rhythms of these flies were tested in several *Hsp70* deficiency backgrounds or upon downregulation of Hsps or Hsfs in the LNvs using RNAi. The various lines used for this mini screen, their source repository and the rhythmic percentages of the progeny resulting from the crosses are detailed in Table 4.3.

For the Hsp70 deficiency lines, virgin females of *w;pdfGal4;DfHsp70* were crossed with males of *w;UAS-HTTQ128;DfHsp70* to obtain the progeny *w;pdfGAl4/UAS-HTTQ128;DfHsp70*. *Drosophila melanogaster* has six nearly identical copies of the *Hsp70* gene (Gong and Golic, 2004). Five different *Hsp70* deficiency lines with varying copies of *Hsp70* deletions were used to achieve different levels of *Hsp70* deficiency. *w;+;DfHsp70Ba* with one copy deleted (BL8845), *w;+;DfHsp70A* with two copies deleted (Bl8842), *w;+;DfHsp70A,Hsp70Ba* with three copies deleted (BL8844), *w;+;DfHsp70B* with four copies deleted (BL8843), and *w;+;DfHsp70A,Hsp70B* with all six copies of HSP70 deleted (BL8841) (Gong and Golic, 2004; Gong and Golic, 2006; Bettencourt et al., 2008). The resulting experimental lines are designated *pdf>Q128;DfHsp70* (*pdf>Q128;DfHsp70Ba*, *pdf>Q128,DfHsp70A* and so on). The non-expanded HTT controls are designated *pdf>Q0,DfHsp70* and the *UAS* controls as *Q128,DfHsp70* and *Q0,DfHsp70*. The crosses were maintained in DD at 23°C, virgin male flies were collected under a microscope in the dark with the help of a safe red light and 2d-old virgin male flies were transferred into activity tubes exposed to warm temperatures of 29°C in DD from 3d. The experiments with these *Hsp70* deficiency lines in DD23toDD29 were carried out thrice, with at least one relevant set of controls in each experiment. Since the rhythm rescue of *pdf>Q128* in DD23toDD29 was mainly observed in AW1, the experiments were restricted to seven days (3d-9d, AW1), except for the first experimental set run for 14d. In the first and second sets of *Q128;DfHsp70* lines served as controls. In the third set, *pdf>Q0;DfHsp70*, *Q0;DfHsp70* and *Q128;DfHsp70* lines served as controls. However, due to the high number of fly deaths in the third set, only the *UAS* controls, namely *Q128;DfHsp70* controls, were used for statistical analyses. The few flies of the *pdf>Q0;DfHsp70* genotypes that were alive for 7d were mostly

rhythmic and did not differ from *pdf>Q0* (except for *pdf>Q0;DfHsp70A,70B*) (Table 4.3). This observation shows that the *pdf-driven* transgene expression in a *DfHSP70* background mostly does not affect the free-running behavioural rhythmicity in DD23toDD29.

Similarly, the *pdf>Q128;Hsp-RNAi/Dcr* and *pdf>Q128;Hsf-RNAi/Dcr* lines were obtained by crossing virgin females of *w;pdfGal4;UAS-Dcr* with males of *w;UAS-HTTQ128;Hsp(f)-RNAi*. For the experiments with *Hsp-RNAi* in DD23toDD29, two independent experiments were carried out. However, in both the experimental sets, contrary to nearly all *pdf>Q128* in DD23toDD29 being rhythmic in AW1, >50% of the *pdf>Q128;Dcr/+* flies (progeny of the cross *w;pdfGal4;UAS-Dcr* with *w;UAS-HTTQ128;+*) were arrhythmic (Table 4.3). This increased arrhythmicity of the *pdf>Q128* in a *Dcr* background might be contributing to the reduced rhythmicity (≤50%) of the various *RNAi* expressing experimental fly lines: the *pdf>Q128;Hsp-RNAi,Dcr* (namely, *pdf>Q128;Hsp70Aa-RNAi,Dcr*, *pdf>Q128;Hsp70Bb-RNAi,Dcr*, *pdf>Q128;Hdj1-RNAi,Dcr,* i.e. *Hsp40-RNAi*) and the *pdf>Q128;Hsf-RNAi;Dcr*. The only exception was *pdf>Q128;Iap2-RNAi;Dcr* flies, most of which were rhythmic. Due to the confounding arrhythmicity of the background *pdf>Q128;Dcr* in DD23toDD29, the *pdf>Q128* flies with downregulated *Hsp* or *Hsf* in their LNv have not been considered further. However, *pdf>Q128;Dcr* flies obtained from a different cross of *w;pdfGal4;+* with *w;UAS-HTTQ128;UAS-Dcr* were nearly all rhythmic in DD23toDD29 (Table 4.3). However, since *pdf>Q128;Dcr* of this latter cross is not the appropriate background control for the *pdf>Q128;Hsp(f)RNAi/Dcr* experimental flies, these experiments have not been considered for further analyses.

4.2.2 Behavioural assays

For the assessment of locomotor activity/rest rhythms, 3d-old virgin flies were recorded as described in section 2.2.2. The light and temperature regimes during recording from 3d adulthood and the various environmental regimes used in this study and their notations are indicated in Tables 4.1 and 4.2. The sample sizes are given in Table 4.4.

Most of the details of quantifying rhythm features are described in section 2.2.2. The extent of activity consolidation '*r*', which aids in tracking daily variations in activity/rest rhythms, was

determined using a modified version of the MATLAB method previously reported (2.2.2). '*r*' represents the extent to which activity data points are consolidated over a circadian cycle of activity. The activity time series for a genotype was obtained at a resolution of 20 min bins. This time series was divided into cycles of length determined by the period (*T*) of that genotype, thereby identifying each circadian cycle in the time series. Thus, each 'day' used to calculate 'daily' '*r*' was obtained as a modulo *T* value. On each 'day', activity counts were imagined as unit vectors for which direction represented the timepoint (*t*) at which the count occurred within the cycle. Because counts were clustered into 20-minute intervals, the data can be represented as vectors with a constant angular separation of $20*2\pi/T$ radians and magnitudes corresponding to the activity count in each interval. *R* was calculated as the magnitude of the mean of these activity vectors. The rectangular coordinates of the mean vector were obtained (Zar, 2010) using $X=\Sigma A_t.\cos\theta_t/\Sigma A_t$ and $Y=\Sigma A_t \sin\theta_t / \Sigma A_t$, where A_t represents activity counts at a given time point *t* and θ_t represents the vector angle associated with the time point. The magnitude of this vector '*r*' was calculated as $\sqrt{X^2+Y^2}$. The greater the magnitude of '*r*', the better the degree of consolidation, with most activity occurring over a few closely spaced time points. The lower the magnitude of '*r*', the poorer the consolidation, with activity spread over time. Given that sometimes period changes were observed across age for a fly, daily cycles were identified separately for each 7d AW using the mean period values for the corresponding AW. For arrhythmic flies, the cycle length was determined using the mean period of all surviving flies of the genotype for that AW. The period of the fly in the previous AW (if any) was utilised to calculate the cycle length for a fly that passed away in the middle of an AW. The daily '*r*' was averaged across flies to obtain the mean daily '*r*'.

4.2.2.1 Criteria for inclusion of genotypes and AWs in the statistical analyses, figures, and tables

Most of the differences between regimes were observed in AW1 and some in AW2. So, unless otherwise demonstrated or mentioned, statistical analyses have been limited to AW1 and AW2 for a significant amount of this work. Across all runs, genotypes where fly numbers were <10 have been excluded from statistical analyses (mainly due to deaths in AW3 or arrhythmicity in the case of *pdf>Q128*). *pdf>Q128* is included in the statistical analysis of period and robustness within- and between-regimes if ≥10 flies were rhythmic. Such exclusions are indicated in the right-most column of Tables 4.5 (within-regime) and 4.6 (between-regime). In many within-regime, between-genotype plots for '*r*', only the genotypes *pdf>Q0*, *pdf>Q128*, *Q128*, and *pdfGal* are plotted to ease visualisation. However, all the control genotypes were run, and the relevant statistical comparisons were carried out. The plots for robustness are shown for regimes where ≥10 rhythmic *pdf>Q128* are rhythmic. Otherwise, rhythm robustness and period values for most other consequential runs are plotted in Tables 4.7 and 4.8, respectively, and all relevant between-genotype statistical differences are indicated. Statistical comparisons across AWs for a genotype for robustness and period are carried out only for essential regimes, indicated in the plots by the presence of '$' symbols. Whenever multiple runs were carried out, the statistical analyses for robustness, period and '*r*' were done for a representative run with a reasonable sample size. This run is represented as experiment 1 in Table 4.4.

For many between-regime comparisons, statistical tests were carried out for AW1 and AW2 (3d-16d of age) unless otherwise specified or indicated because, by AW2, most flies of *pdf>Q128* are rendered arrhythmic. In some control genotypes, <10 flies survived during AW3. Unless unique differences occur due to other background genetic influences, which are then shown on a case-by-case basis, *pdf>Q128* and two of its controls (*Q128* and *pdf>Q0*) are given for the plots of between-regime comparisons of activity rhythms. Also, in most cases, *pdf>Q0* mirrors *pdfGal* in most of the rhythm features and therefore, the *pdfGal* controls are not plotted unless they are significantly dissimilar from *pdf>Q0*. Also, since most of the temperature-influenced rhythm rescue of *pdf>Q128* was restricted to AW1, between-regime robustness comparisons are plotted

only for AW1. For the temperature regimes that provided rhythm rescue of *pdf>Q128*, the between-regime period comparisons during AW1 for *pdf>Q0*, *pdf>Q128* and *Q128* are shown in Table 4.9.

The rhythmicity of *pdf>Q128* varied significantly between tests in the TCtoDD25 studies, particularly with the LDTCtoDD25 runs. For each of the TCto25 runs, at least four independent experiments with all the controls and a fifth trial using only *pdf>Q0* and *pdf>Q128* were carried out to increase the confidence in our inferences. The '*r*' of *pdf>Q128* for DDTCtoDD25 also showed considerable variation between experiments. *r*-values from three different sets of experiments are plotted for the between-genotype comparisons to illustrate this difference. The DDTCtoDD25 experiment with the highest duration of improvement in activity consolidation of *pdf>Q128* was used for the corresponding between-regime comparisons of '*r*'.

4.2.2.2 Statistical analyses

Shapiro-test Wilk's was used to check the normality of the data sets, followed by Levene's test for variance homogeneity and Mauchly's test for sphericity. The data set comprised period or robustness values across three 7d AWs (AW1, AW2, AW3) or *r*-values for 21d (age 3d-23d, day being circadian day). The genotypes were *pdf>Q0*, *pdf>Q128*, *Q0*, *Q128*, *pdfGal* and w^{1118}. The values were compared across genotypes in a particular regime across AWs (or age in circadian days for '*r*') and between regimes for a genotype at an AW (or age in circadian days for '*r*').

Where the data (untransformed or transformed) were normal, their variances homogenous, and the assumption of sphericity was met, a repeated measures ANOVA with age window (AW) as the repeating measure, followed by Unequal N HSD was conducted for within-regime comparisons between age-matched genotypes. Where the repeated measures ANOVA's assumptions were not met, the within-regime comparisons were conducted independently between genotypes for an AW (or age) and as a repeated measure between AWs (or ages) for a genotype. Each AW data set was tested separately for normality and variance homogeneity for within-regime and between-genotype comparisons. If the data sets were normal and their variances homogenous (on untransformed or transformed data), a one-way ANOVA was carried

out, followed by Tukey's HSD (or Unequal N HSD). A Welch's ANOVA and Games-Howell test were conducted if the data were normal, but their variances were not homogeneous despite transformations. Where the data were not normal despite transformations, the Kruskal-Wallis test followed by multiple comparisons of mean ranks were conducted. For within-regime comparison of repeated values across AWs for a genotype, Friedman's test followed by multiple pair-wise Wilcoxon matched-pairs tests with Bonferroni correction were applied for period and robustness values.

Another data set was the percentage of rhythmic flies in the three AWs for the six genotypes in each regime. The mean percentages of rhythmic flies between genotypes (or between regimes) were compared using repeated measures ANOVAs with AW as the repeating factor, followed by Tukey's HSD (or unequal N HSD) tests, wherever at least three separate experiments per regime were conducted. It is important to note that in most of these situations, the Repeated Measures ANOVA assumptions of normality, sphericity, and, in some cases, variance homogeneity were broken, increasing the likelihood of making a Type I error, mistakenly rejecting the null hypothesis, and consequently identifying false positives. Since the significance level is indicated in all the plots of mean rhythmicity, one can minimise the chances of making Type I errors by using a lower *p*-value as the alpha value while interpreting the results. Also, these rhythmic percentages were obtained from at least three independent runs that showed trends in similar directions. The power of these tests is anticipated to be low, meaning that the likelihood of making a Type II error is likely to be high, given that replication is at the level of experiments and results in small sample sizes. Thus, repeated Measures ANOVA on these data sets reduces the chances of falsely rejecting a null hypothesis. If only one run was performed, the proportion of rhythmic to arrhythmic flies between genotypes for an AW was compared using a 6x2 Fisher's Exact test, followed by numerous pertinent 2x2 Fisher's Exact tests. The false discovery rate (FDR) was then decreased by applying a Benjamini-Hochberg (BH) procedure to the pair-wise *p*-values (with the FDR set to 5%). The comparisons of rhythmicity between AWs for a genotype were carried out using the Cochran Q test followed by pairwise McNemar's test with Bonferroni correction.

The specific tests used for each within-regime and between-regime comparison of rhythmicity, '*r*', robustness, and period are given in Tables 4.5 and 4.6, respectively.

For the experiment using *Hsp70* deficiency lines in DD23toDD29, the number of rhythmic and arrhythmic flies in AW1 were pooled across experiments for computing the rhythmicity values shown in Table 4.3. For statistical analyses of rhythmicity and *r*-values, the *pdf>Q128,DfHsp70* were compared with their respective *UAS* controls *Q128;DfHsp70* and with *pdf>Q128* in DD23toDD29 and *pdf>Q128* in DD23 was used as the negative/baseline control. The various *pdf>Q128,DfHsp70* lines were also contrasted to determine whether the dosage of the Hsp70 gene impacted the rhythms. The rhythmicity of the surviving *pdf>Q0;DfHsp70* was compared with *pdf>Q0*. The proportion of rhythmic flies was compared between genotypes using mxn Fisher's Exact test, followed by multiple 2x2 Fisher's Exact tests and BH procedure on the pair-wise *p*-values. For the plots of percentage rhythmicity and *r*-value, the first experimental set run for 14d was used. The *r*-values were averaged for each fly over eight days and then averaged across flies to obtain the mean '*r*'. '*r*' was compared between genotypes using one-way ANOVA followed by unequal N HSD. The robustness was compared using one-way ANOVA followed by Unequal N HSD.

4.2.3 Immunocytochemistry and image analysis

Most of the details of the dissections, immunocytochemical protocols, detection and image analysis methods are described in sections 2.2.3 and 3.2.3. For staining with antibodies against PDF and HTT, *pdf>Q0* and *pdf>Q128* flies placed under various temperature regimes (DD23, DD29, DD23toDD29, DDTCtoDD25) were dissected at various ages. For the DD23toDD29 regime, flies reared in DD23 were transferred to DD29 at 3d of age. So, flies in DD23, DD29 and DDTCtoDD25 were dissected at L3 and ages 1d, 3d, 5d, 7d, 9d, 16d and 23d, whereas those in DD23toDD29 were dissected at 3d, 5d, 7d, 9d, 16d and 23d. Flies in DDTCtoDD25 were compared to flies in DD25 (described in Chapter 3 as DD-reared flies) at L3 and ages 1d, 3d, 7d, 9d, 16d and 23d. Flies in DD29toDD25 were dissected at 7d and compared with age-matched flies in DD5 and DDTCtoDD25. All age-matched dissections and immunocytochemical assays

were carried out simultaneously except for those in DD29toDD25, which were dissected later. These control flies were dissected at L3 and ages 1d, 3d, 5d, 7d, 16d, and 23d because the PDF^+ LNv counts of *pdf>Q0* do not change significantly with age. Also, the immunostaining with anti-PDF of 5d flies in DD25 was very faint, and the PDF^+ LNv were difficult to discern from the background and eliminated from the analyses.

For PER cycling, 7d-old flies maintained in different regimes were dissected at CT23 and CT11. The regimes were DDTCtoDD25, DD29toDD25, DD23, and DD23toDD29. The PER^+ LNv numbers were calculated for CT23.

Each hemisphere was classified as either having ≥3 PDF^+ LNv soma (3 to 5 sLNv or lLNv) or ≤2 PDF^+ LNv soma (0 to 2 sLNv or lLNv) to compare the proportion of hemispheres having ≥3 PDF^+ LNv (or PER^+ LNv) between genotypes for age or between ages or regimes for a genotype.

The sample sizes for immunocytochemical studies are provided in Table 4.10.

4.2.3.1 Statistical analyses

4.2.3.1.1 PDF^+ LNv numbers

PDF^+ LNv numbers (sLNv or lLNv) were compared between ages for a genotype using Kruskal-Wallis tests. PDF^+ LNv numbers (sLNv or lLNv) were compared between age-matched genotypes *pdf>Q0* and *pdf>Q128* for a regime using Mann-Whitney U tests. For between-regime comparisons of a genotype, depending on the number of independent samples, either a Mann-Whitney U test or a Kruskal-Wallis test was carried out for each age. The shape of the frequency distribution of PDF^+ LNv numbers was compared between age-matched genotypes for a regime or between regimes for a genotype at each age using the Kolmogrov-Smirnov tests, followed by the Benjamini-Hochberg procedure. mxn Fisher's Exact test, followed by multiple 2x2 Fisher's tests with BH procedure on pair-wise *p*-values, were used to compare the proportion of hemispheres with ≥3 PDF^+ LNv (or PER^+ LNv) between genotypes for a regime at an age or between ages or regimes for a genotype. The categories were ≥3 PDF^+ LNv soma (3 to 5 sLNv or lLNv) and ≤2 PDF^+ LNv soma (0 to 2 sLNv or lLNv).

4.2.3.1.2 PER$^+$ LNv numbers

Mann-Whitney U tests were used to compare PER$^+$ LNv numbers (sLNv or lLNv) between age-matched genotypes *pdf>Q0* and *pdf>Q128* for a regime. The shape of the frequency distribution of PDF$^+$ LNv numbers was compared between genotypes for a regime or between regimes for a genotype using the Kolmogrov-Smirnov tests, followed by the Benjamini-Hochberg procedure. For between-regime comparison of a genotype, either a Mann-Whitney U test (For DD25 *vs* DD23 or DD23 *vs* DD23toDD29 or DDTCtoDD25 *vs* DD23toDD29) or a Kruskal-Wallis test (for DD25 *vs* DDTCtoDD25 *vs* DD29toDD25) was carried out. As described above for PDF, the proportion of hemispheres with ≥3 PER$^+$ LNv soma were compared between genotypes for a regime at an age or between ages or regimes for a genotype.

4.2.3.1.3 PER cycling

The data sets were assessed for normality using Shapiro-Wilk's test, and their variance homogeneity was assessed using Levene's test. The data sets comprised of PER staining intensity in sLNv or lLNv at CT23 or CT11 for the genotype's *pdf>Q0* and *pdf>Q128* in various regimes (DDTCtoDD25, DD29toDD25, DD23, and DD23toDD29). For within-regime comparisons of intensity with genotype and time points as fixed factors, if the data (untransformed or transformed) was normal and variances homogenous, then a factorial ANOVA was carried out, followed by Tukey's HSD. If the assumptions of ANOVA were not satisfied, the within-regime comparisons were carried out separately between time points for a genotype and between genotypes for a time point. A one-way ANOVA was carried out if the data was normal and their variances homogenous (on untransformed or transformed data). If the data was normal, but their variances were not homogenous despite the transformation, then a Welch's ANOVA was carried out. If the data was not normal, then the Mann-Whitney U test was carried out. For sLNv PER intensity under DDTCtoDD25, Mann-Whitney U tests were carried out for between-timepoint comparison for a genotype or between-genotype comparison. For lLNv PER intensity under DDTCtoDD25, one-way ANOVA was carried out for the above comparisons. Mann-Whitney U tests were carried out for the between-timepoint comparisons of PER in the lLNv of *pdf>Q128* under DDTCtoDD25 and DD23toDD29. For DD23toDD29, for the above comparisons of PER

intensities in sLNv and lLNv, one-way ANOVAs on transformed datasets were carried out with either time points or genotypes as independent variables. For sLNv PER intensity in DD23 and DD29toDD25, one-way ANOVAs on transformed datasets were carried out for between-timepoint comparisons for a genotype. Mann-Whitney U tests were carried out for between-genotype comparisons of sLNv PER intensity for a time point for the two regimes. For lLNv PER intensity in DD23toDD23, a two-way ANOVA was carried out, followed by Tukey's HSD. PER was considered oscillating if the PER intensity in the LNv soma at CT23 significantly differed from CT11. The oscillations were considered anti-phasic if the PER intensity at CT11 was significantly higher than at CT23 for a genotype. If the PER intensity in the LNv soma was significantly lower in the *pdf>Q128* than *pdf>Q0* at either time point, especially CT23, then the oscillations in *pdf>Q128* were said to be of low amplitude or dampened.

4.2.3.1.4 Inclusion numbers and size

The data sets were assessed for normality using Shapiro-Wilk's test and variance homogeneity using Levene's test. The data set comprised expHTT inclusion features (number and size) for *pdf>Q128* across ages in various regimes.(DD25, DDTCtoDD25, D29toDD25, DD23, DD29 and DD23toDD29). For comparisons of inclusion number and size across ages within a regime, one-way ANOVA on transformed data, followed by Unequal N HSD, was largely used. Only for inclusion size comparisons with age in DD23, a Welch's ANOVA, followed by the Games-Howell test, was used. For between-regime comparisons of inclusion number (or size) across age, if the data (untransformed or transformed) was normal and variances homogenous, then a factorial ANOVA with age and regime as fixed factors was carried out, followed by Unequal N HSD. If the assumptions of ANOVA were not met, then the between-regime comparisons for each age were carried out separately. If the data was normal and their variances homogenous (on untransformed or transformed data), then a one-way ANOVA was carried out, followed by post-hoc testing via Unequal N HSD. If the data was normal, but their variances were not homogenous despite the transformation, then a Welch's ANOVA, followed by the Games-Howell test, was performed. For comparing the inclusion number or size between DDTCtoDD25 with DD25

across age, a two-way ANOVA, followed by an Unequal N HSD test, was carried out. Inclusion numbers were compared at each age between DD25, DD23 and DD29 using one-way ANOVAs and Unequal N HSDs. A Welch's ANOVA was conducted to compare inclusion sizes between DD25, DD23 and DD29 or DD23, DD29 and DD23toDD29 at each age, followed by Games-Howell tests. A two-way ANOVA was used to compare inclusion numbers between DD23, DD29 and DD23toDD29 across ages, followed by an Unequal N HSD test. For comparing inclusion numbers and sizes between DDTCtoDD25 and DD23toDD29, a one-way ANOVA, followed by Unequal N HSD, was used. A one-way ANOVA was used to compare inclusion numbers (or sizes) between DD25toDD25, DDTCtoDD25 and DD29toDD25 at 7d. Since most of the sLNv had diffuse expHTT as larvae, the analysis for expHTT inclusion number and size have been carried out from 1d onwards.

4.2.3.1.5 expHTT forms in the LNv

By 7d of age, across all the regimes, most of the hemispheres of *pdf>Q128* are dominated by inclusion-enriched LNv. Hence, for between-regime comparisons of the relative proportion of hemispheres enriched in different expHTT forms in LNv, the figures are comparisons up to 7d (for sLNv) and up to 9d (for lLNv).

As described previously (Section 3.2.3.2), mxn Fisher's Exact tests were used, followed by multiple 2x2 tests and then the Benjamini-Hochberg procedure applied to the pair-wise *p*-value sets of each relative pair of expHTT forms to compare the relative proportion of *pdf>Q128* hemispheres dominated by various expHTT forms in the LNv between ages for a regime or between regimes for an age.

4.3 RESULTS

4.3.1 Provision of temperature cycles during pre-adult developmental stages postpones behavioural arrhythmicity and PDF loss from the sLNv of *pdf>Q128* flies

Temperature cycles are potent zeitgebers that synchronise circadian molecular and behavioural rhythms and override the arrhythmicity imposed by LL (Tomioka et al., 1998a; Yoshii et al., 2002; Glaser and Stanewsky, 2005). Time cues provided during development are known to modify adult circadian rhythms (Sehgal et al., 1992; Matsumoto et al., 1997; Kaneko et al., 2000; Sheeba et al., 2002; Malpel et al., 2004; Zhao et al., 2019b). Further, TCs can entrain developmental clocks, as evidenced by synchronised free-running activity of completely blind adult flies whose larvae experience TCs. In larvae lacking PDF or the LNv, the CRY-negative DN2s are synchronised by TCs, and the phase of PDF^{+} LNv molecular oscillations follows that of the DN2s (Malpel et al., 2004; Picot et al., 2009). Therefore, I asked whether providing temperature cycles during development helps improve free-running activity rhythms of adult *pdf>Q128* at DD25.

Warm/cold temperature cycles of 12h:12h::29°C:21°C were used in the studies. Studies from the lab have shown that such an 8°C amplitude TC strongly synchronised activity/rest rhythms of *D.melanogaster* (Prabhakaran and Sheeba, 2014). Further, this range of temperatures is also symmetric with a mean of 25°C at which most other experiments have been done; hence, this regime was adopted.

Most of the *pdf>Q128* flies in DDTCtoDD25 across experiments were rhythmic in AW1, and their mean percentage rhythmicity was comparable to controls (Fig 4.1a top-middle, b). By AW2, the rhythmicity of *pdf>Q128* declined significantly compared to AW1 and from their age-matched controls, and they continued to be poorly rhythmic in AW3 (Fig 4.1b). The activity consolidation '*r*' of these flies showed considerable experiment-to-experiment variation. Thus, '*r*' from three different experiments is plotted. In the first one, even though '*r*' of *pdf>Q128* was comparable to *Q128* up to 11d, they still were lower than *pdf>Q0* and *pdfGal* (Fig 4.1c top). In the second experiment, '*r*' of *pdf>Q128* was like controls up to 10d, which intermittently declined

from some controls (Fig 4.1c middle). In the third experiment, '*r*' of *pdf>Q128* was control-like briefly (4d-6d), beyond which it was lower than most controls (Fig 4.1c bottom). Since *pdf>Q128* showed early-age rhythmicity rescue in AW1 across experiments, '*r*' from the second experiment, which shows improved activity consolidation in *pdf>Q128* till 10d, are considered for following between-regime comparisons. The rhythmic *pdf>Q128* had rhythms of lower robustness than controls in AW1 and AW2 (Fig 4.1d), indicating a moderate rescue of rhythms. Further, rhythmic *pdf.Q128* in AW1 had a longer period than some controls and was longer than 24h (Fig 4.1 e). Considering that *pdf>Q128* experienced TCs of 24h before being recorded, the >24h period shown by adults in DD25 indicates that the rhythm restoration is not a mere after-effect of the previous entraining cycles. Overall, development-specific temperature cycles delay arrhythmicity in the free-running activity rhythms of flies expressing expHTT in LNv.

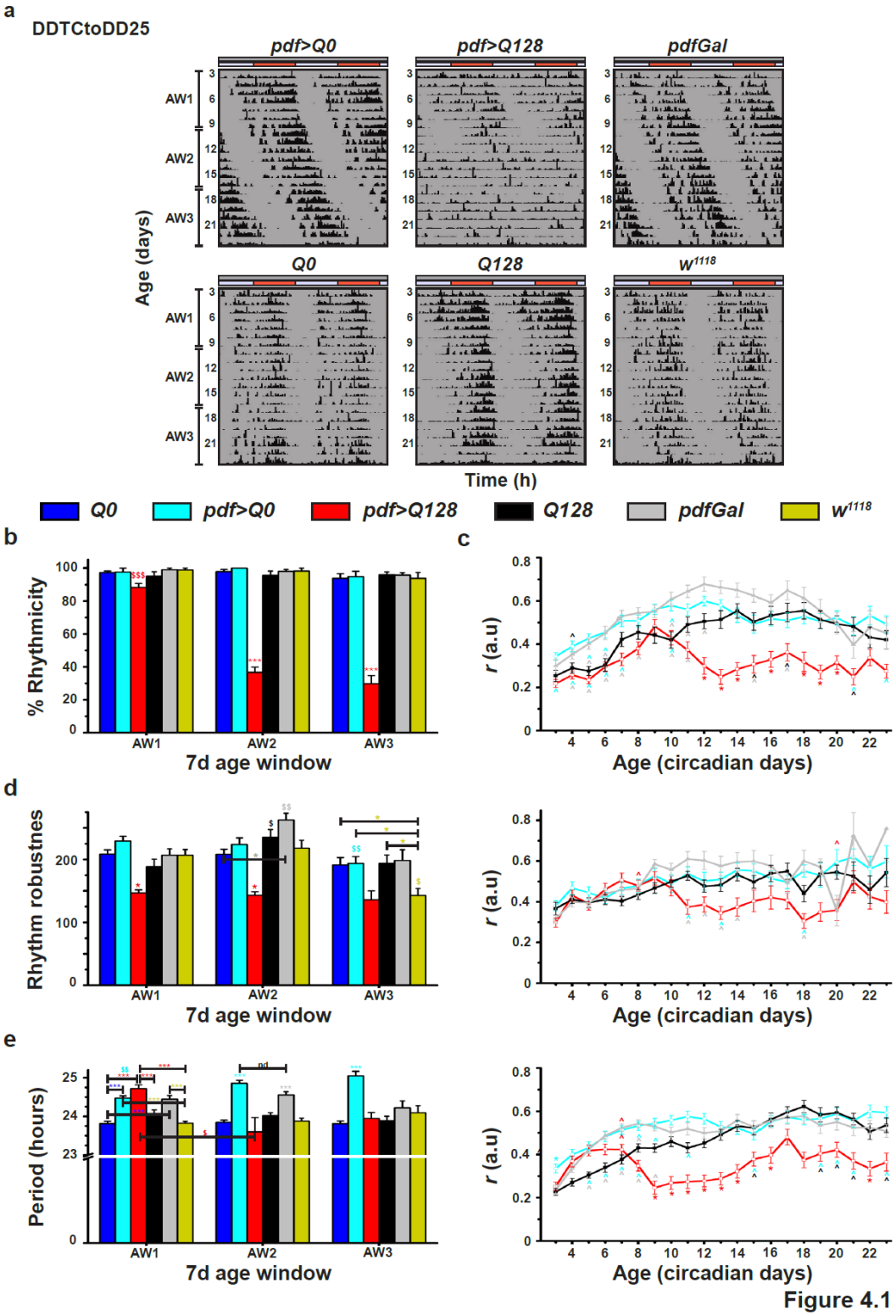

Figure 4.1

Fig 4. 1 pdf>Q128 experiencing developmental temperature cycles show early-age behavioural rhythms as adults in DD25.

(a) Representative double-plotted actograms for adult flies in DDTCtoDD25 showing activity data for 21d (age 3d-23d). The bars at the top of the actograms represent the developmental rearing condition: grey bars for DD and the lavender and rust-coloured bars for the cryophase (21°C) and thermophase (29°C), respectively, of the 12h:12h temperature cycles.

All other details are the same as in Fig 2.1. (b-e) The percentage rhythmicity (b), the extent of activity consolidation '*r*' (c), the mean rhythm robustness (d) and the mean period (e) for various genotypes plotted against AWs (or age for '*r*'). The three rows of *r*-values (c) are from three different experiments. a.u, arbitrary units. Symbols represent statistically significant differences: coloured * of that coloured genotype from all others or indicated ones and coloured $ between AWs for that coloured genotype. For '*r*', coloured ^ near an error bar of a data point indicates a difference between the respective-coloured genotype and the data-point genotype. The number of symbols represents statistical significance: single $p<0.05$, double $p<0.01$ and triple $p<0.001$. Error bars are SEM.

Since there was an early age rescue of activity rhythms upon developmental exposure of *pdf>Q128* to temperature cycles, I asked whether circadian neurodegenerative cellular features like PDF and PER in the LNv and expHTT form and inclusion characteristics are also affected. *pdf>Q128* flies in DDTCtoDD25 had an average of ~3 PDF^+ sLNv soma up to 5d that is nearly comparable to *pdf>Q0* (Fig 4.2 a, b left). Although *pdf>Q128* at 1d showed statistically reduced numbers than controls, the mean was ~3, and there was no difference at 3d (Fig 4.2b left). Similarly, the shape of the frequency distributions also differed significantly between the genotypes at 1d but not 3d (Fig 4.3 left). However, despite the differing distribution shapes between genotypes at 1d, ~77% of *pdf>Q128* hemispheres still had ≥3 PDF^+ sLNv soma. The statistical difference seen at 1d may not be biologically significant in terms of impairing rhythmic function, based on comparisons between the percentage of hemispheres with ≥3 PDF^+ sLNv soma at 1d (77%) with that of later ages of 7d (58%), 16d (25%) ($p<0.001$, Fisher's Exact test) and 23d (0%) ($p<0.001$, Fisher's Exact test), which also revealed significantly different distribution shapes between genotypes (Fig. 4.3a left). This conclusion is also substantiated by the finding that younger *pdf>Q128* flies (L3 to 5d) showed a significantly higher proportion of hemispheres (>75%) with ≥3 PDF^+ sLNv soma than older flies (7d, 16d and 23d) (Fig 4.3b) ($p<0.05$, Fisher's Exact test). From 7d onwards, the PDF^+ sLNv soma numbers declined significantly in *pdf>Q128* compared to *pdf>Q0* (Fig 4.2b left). The numbers at 16d- and 23d-old *pdf>Q128* were significantly lower than most earlier ages, falling to ~1 by age 23d. The frequency distribution of PDF^+ sLNv soma numbers in *pdf>Q128* is like that of the left-skewed *pdf>Q0* at L3, 3d and 5d (Fig 4.3a left). With age, the shapes of the distributions change significantly between genotypes, with *pdf>Q128* tending to a right skew, which is obvious by 23d (Fig 4.3a left). The PDF^+ lLNv soma numbers and the shape of their frequency distributions were comparable across age between *pdf>Q0* and *pdf>Q128* (Figs 4.2a, b right, 4.3 right). Thus, exposure of *pdf>Q128* to temperature cycles during development postpones the loss of PDF from sLNv soma.

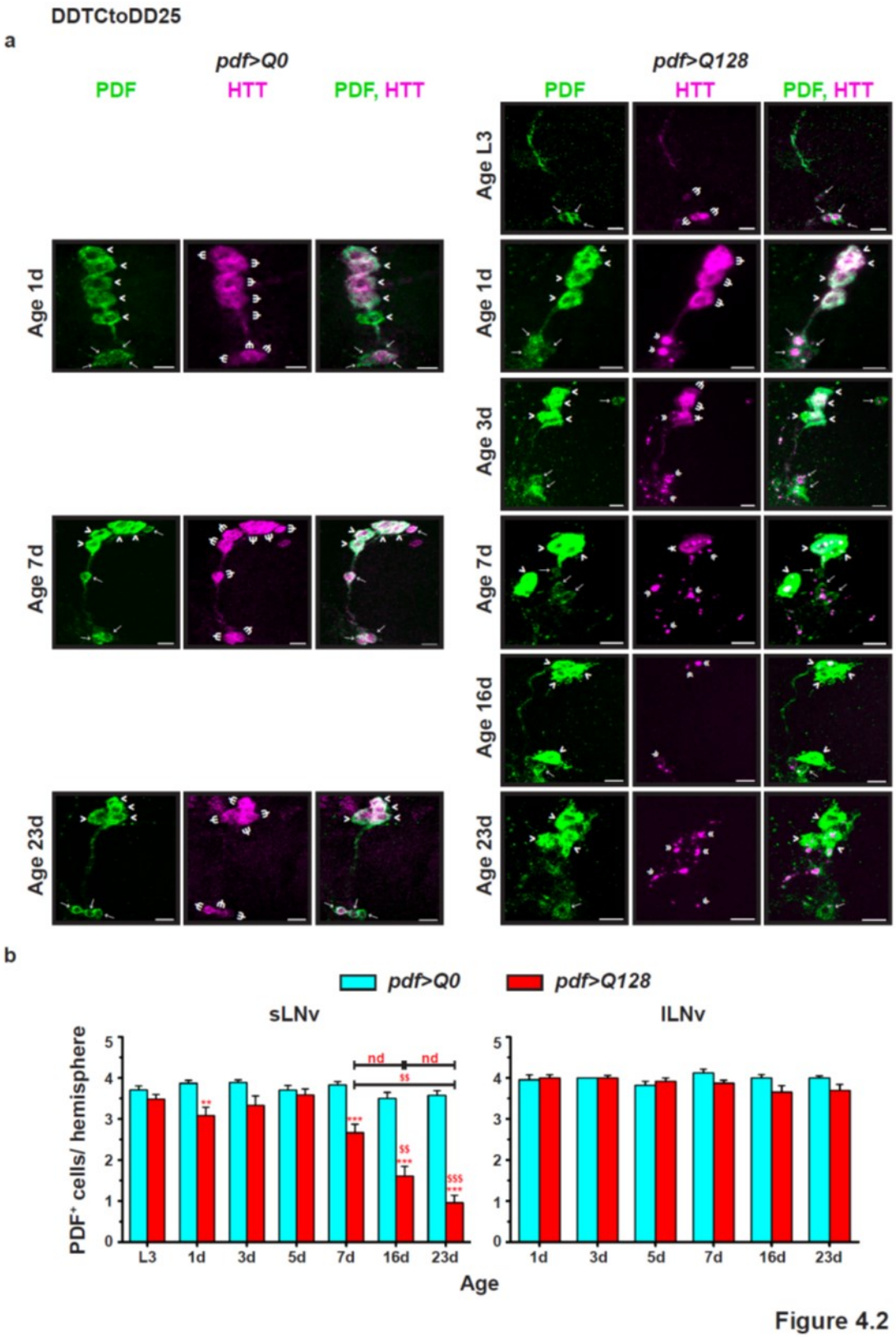

Fig 4. 2 Exposure of pdf>Q128 to DDTC during development restores the early-age PDF$^+$ sLNv soma numbers of adults in DD25.

(a) Representative images of the adult fly brains under DDTCtoDD25 stained for PDF (green) and HTT (magenta) in LNv at 1d, 7d and 23d for *pdf>Q0* (left panel sets) and at L3, 1d, 3d, 7d, 16d and 23d

for *pdf>Q128* (right panel sets). Indicated in the images are sLNv soma (→ arrows), lLNv soma (> arrowhead), diffuse expHTT (Ψ psi), diffuse+inclusions expHTT (Ɏ straight U with stroke), and expHTT inclusions (« double arrowheads). Scale bars are 10 µm. (b) The mean number of PDF^+ sLNv soma (left) and lLNv soma (right) across age. Coloured symbols indicate significant differences, * for age-matched, inter-genotype differences and $ for differences between ages of the corresponding-coloured genotype at * $p<0.05$, ** $p<0.01$, *** $p<0.001$. nd, not different. Error bars are SEM.

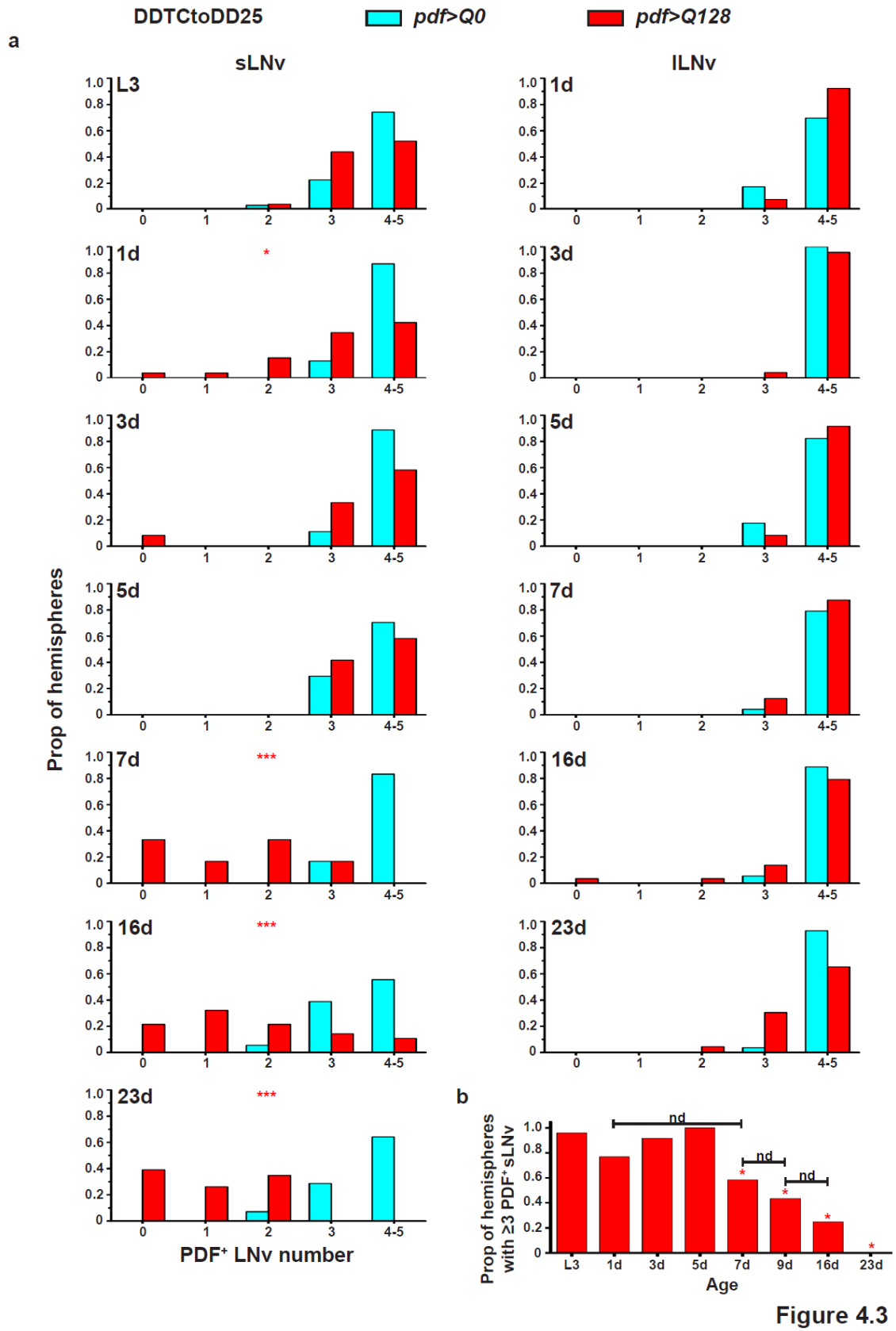

Figure 4.3

Fig 4. 3 The distribution of PDF⁺ sLNv soma numbers of pdf>Q128 diverges from that of pdf>Q0 with age under DDTCtoDD25.

(a) Frequency distribution of the proportion of hemispheres of *pdf>Q0* and *pdf>Q128* in DDTCtoDD25 with 0 to 5 PDF^+ LNv soma numbers (sLNv - left and lLNv - right). Coloured * indicates significantly different distribution shapes between age-matched genotypes at $p<0.05$. NA, not applicable. (b) The proportion of pdf>Q128 hemispheres having ≥3 PDF^+ sLNv across age. * indicates statistically different proportions between ages at $p<0.05$. .nd, not different.

pdf>Q128 in DDTCtoDD25 showed significantly reduced PER^+ sLNv (~1.3) and lLNv (~2.3) soma numbers than *pdf>Q0* at 7d (Fig 4.4b). This difference was also reflected in the shapes of their frequency distributions, with *pdf>Q128* differing significantly from the left-skewed *pdf>Q0* and nearly 83% of *pdf>Q128* hemispheres having ≤2 PER^+ sLNv soma (Fig 4.4c). sLNv soma of 7d *pdf>Q128* showed a significant oscillation of lowered amplitude and anti-phasic to control *pdf>Q0* oscillation (Fig 4.4d top). There was no PER oscillation in the lLNv of both genotypes at 7d (Fig 4.4d bottom). PER intensity in sLNv and lLNv of *pdf>Q128* at CT23 was significantly lower than *pdf>Q0* (Fig 4.4d). Thus, temperature cycles during development induced low amplitude PER oscillation in the sLNv of *pdf>Q128* without improving PER^+ LNv numbers or PER intensity in the LNv, suggesting a functional, albeit weak LNv clock with developmental TCs.

I then assessed the expHTT form in the LNv and expHTT inclusion features. The relative proportions of hemispheres dominated by different expHTT forms in LNv of *pdf>Q128* in DDTCtoDD25 changed significantly with age (Fig 4.5a top). The proportion of hemispheres dominated by Diff-enriched relative to Inc-enriched sLNv was significantly higher at L3 than as adults (Fig 4.5a left, second-row). Similarly, for expHTT in lLNv, 1d significantly differed from older ages (Fig 4.5a right, second-row). The proportion of hemispheres dominated by Diff+Inc-enriched relative to Inc-enriched lLNv was significantly higher at 1d than most older ages (Fig 4.5a right, third-row). Overall, the proportion of hemispheres predominated by Inc-enriched LNv increased with age and post-3d, most hemispheres had Inc-enriched LNv. The number of expHTT inclusions was significantly lower at ages 1d than at older ages (Fig 4.5b top). Unexpectedly, 3d had more inclusion, albeit smaller in size than most older ages (Fig 4.5b).

A summary of HD flies' behavioural and cellular phenotypes in the different temperature regimes is shown in Table 4.11.

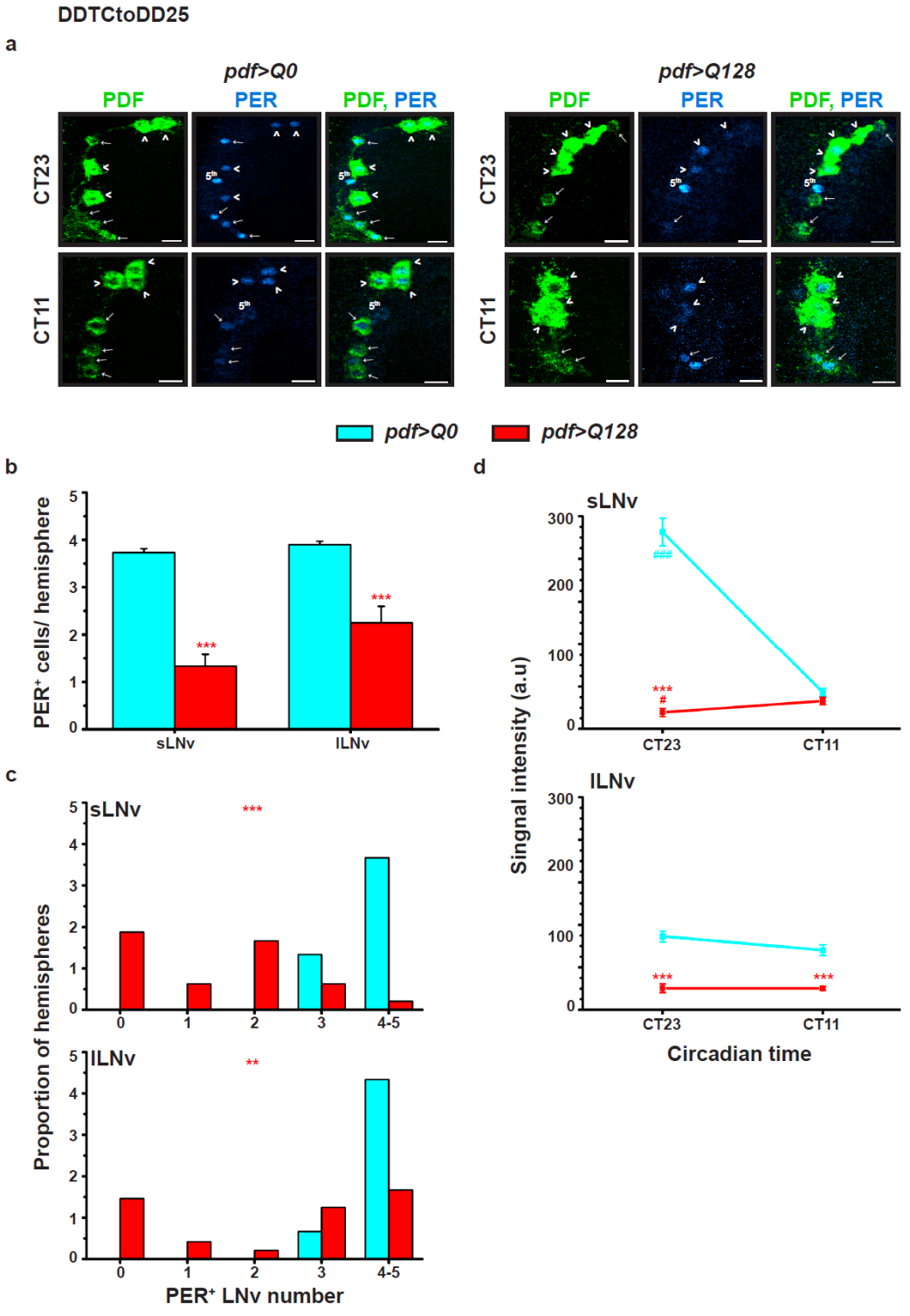

Figure 4.4

Fig 4. 4 pdf>Q128 flies in DDTC show fewer PER$^+$ LNv and exhibit low-amplitude PER oscillations in the sLNv, anti-phasic to controls.

(a) Representative images of 7d-old adult fly brains of *pdf>Q0* (left) and *pdf>Q128* (right) in DDTCtoDD25 stained for PER (cyan hot) and PDF (green) in LNv at CT23 (top) and CT11 (bottom). sLNv soma (→ arrows), lLNv soma (> arrowheads) and PDF$^-$ PER$^+$ 5th sLNv are indicated. Scale bars are 10 µm. (b) The mean number of PER$^+$ sLNv soma and lLNv soma at

CT23. * indicates age-matched differences between genotypes. (c) Frequency distribution of the proportion of hemispheres having 0 to 5 PER^+ LNv soma: sLNv soma (top) and lLNv soma (bottom) in 7d-old flies at CT23. * indicates significantly differing shapes of distribution between genotypes. (d) For the two genotypes, the quantification of PER intensity at CT23 and CT11 in sLNv (top) and lLNv (bottom). Differences between time points CT23 and CT11 are represented by # (cyan) for *pdf>Q0* and # (red) for *pdf>Q128*. Coloured * represents the difference between genotypes at that time point. Statistical significance is at single-symbol $p<0.05$, double-symbol $p<0.01$, triple-symbol $p<0.001$. Error bars are SEM.

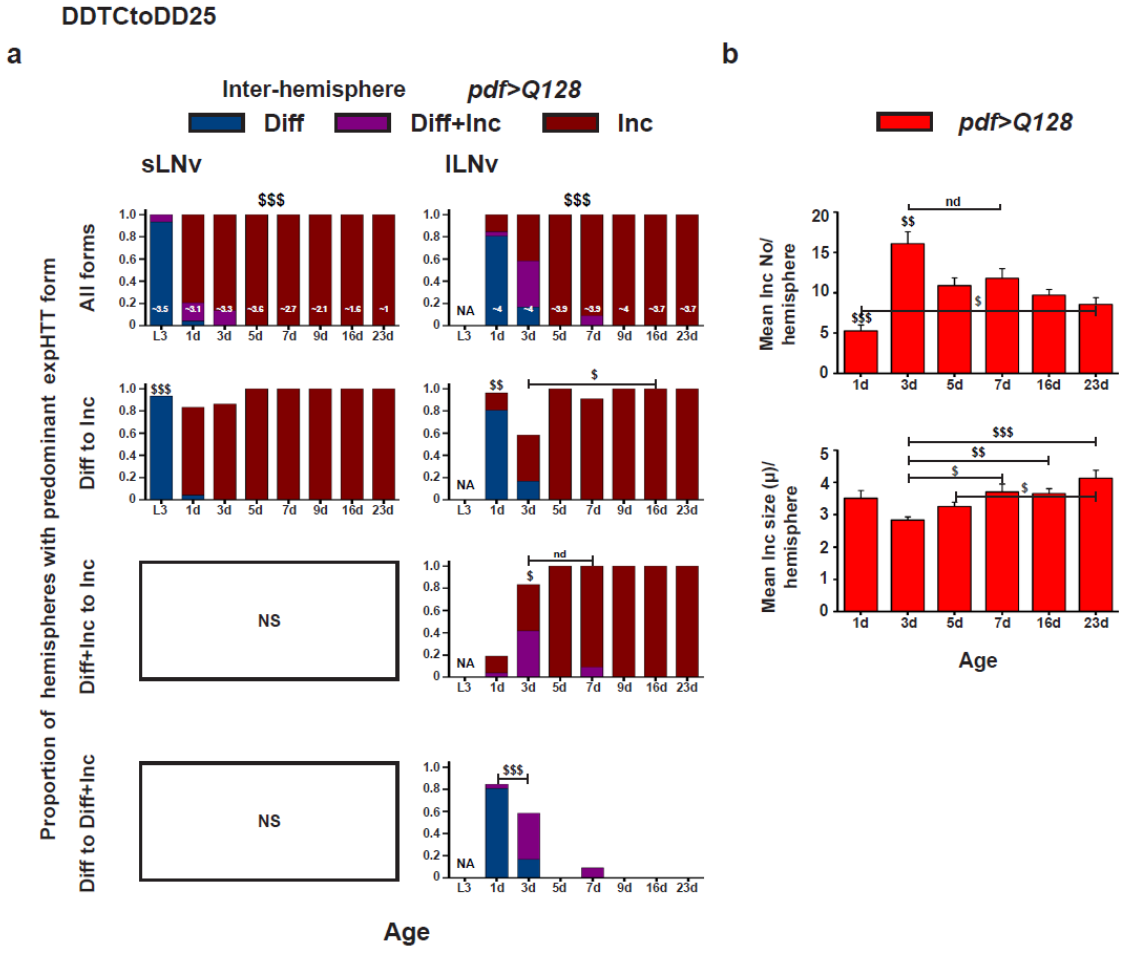

Figure 4.5

Fig 4. 5 Under DDTCtoDD25, diffuse-expHTT-enriched-LNvs dominate hemispheres of very young pdf>Q128, whereas, with age, inclusion-enriched-LNv solely dominate.

(a) The proportion of hemispheres dominated by different expHTT forms in sLNv (left) or lLNv (right) is plotted against age for *pdf>Q128* in DDTCtoDD25 to describe the between-hemispheres distribution of predominant expHTT forms. These are plotted for all expHTT forms (top) or significantly different pair-wise comparisons (second, third, and bottom rows). $ indicates significant changes in the relative proportions of hemispheres across age for all expHTT forms (top) or pair-wise expHTT forms between specific ages (second, third, bottom rows). NA, not applicable and NS, not significant. At the bottom of some bars, numbers represent the mean number of PDF^+ LNv detected at that age. (b) Comparison of mean inclusion number per hemisphere (top) and mean inclusion size per hemisphere (bottom) for *pdf>Q128* in DDTCtoDD25 across age. Significant differences between ages are $ $p<0.05$, $$ at $p<0.01$ and $$$ $p<0.001$. nd, not different. Error bars are SEM.

4.3.2 Light during development counters the rescue of early-age activity rhythms of *pdf>Q128* adults by developmental temperature cycles

Fly activity rhythms and in-phase molecular rhythms in clock neurons are more robust when a combination of light and temperature is provided than alone (Yoshii et al., 2010). Also, coupling temperature cycles with light cycles improved the consolidation of activity rhythms and sleep in ageing flies (Luo et al., 2012). LD cycles were provided in phase with developmental warm/cold temperature cycles to determine if developmental-LD+TC had a more significant effect on the activity rhythms of *pdf>Q128* as adults in DD25 than -DDTC. *pdf>Q128* flies in LDTCtoDD25 were arrhythmic from the beginning of the free-running conditions (Fig 4.6a top), with their rhythmicities and activity consolidation being significantly lower than controls across age (Fig 4.6b, c). Thus, the presence of LD during development with TC antagonises the TC-mediated rhythm restoration in young *pdf>Q128* adults. Developmental cyclic light counteracting the protective effect of developmental-TC to *pdf>Q128* suggests that light cues during development are detrimental to *pdf>Q128* adult rhythms.

I then investigated whether developmental clocks are essential for the developmental-TC-mediated rescue of activity rhythms in young *pdf>Q128* by providing constant light during development along with the TCs to weaken the molecular clockwork. *pdf>Q128* flies in LLTCtoDD25 were arrhythmic (Fig 4.6a bottom) with significantly decreased rhythmicities and '*r*' than controls across age (Fig 4.6d, e). Thus, functional clocks during development seem necessary for developmental-TC-mediated early-age rhythms rescue of *pdf>Q128* adults. However, this conclusion is complicated by the initial discovery of arrhythmicity of *pdf>Q128* adults even under LDTCtoDD25, under which the clocks are expected to be robust and functional during development.

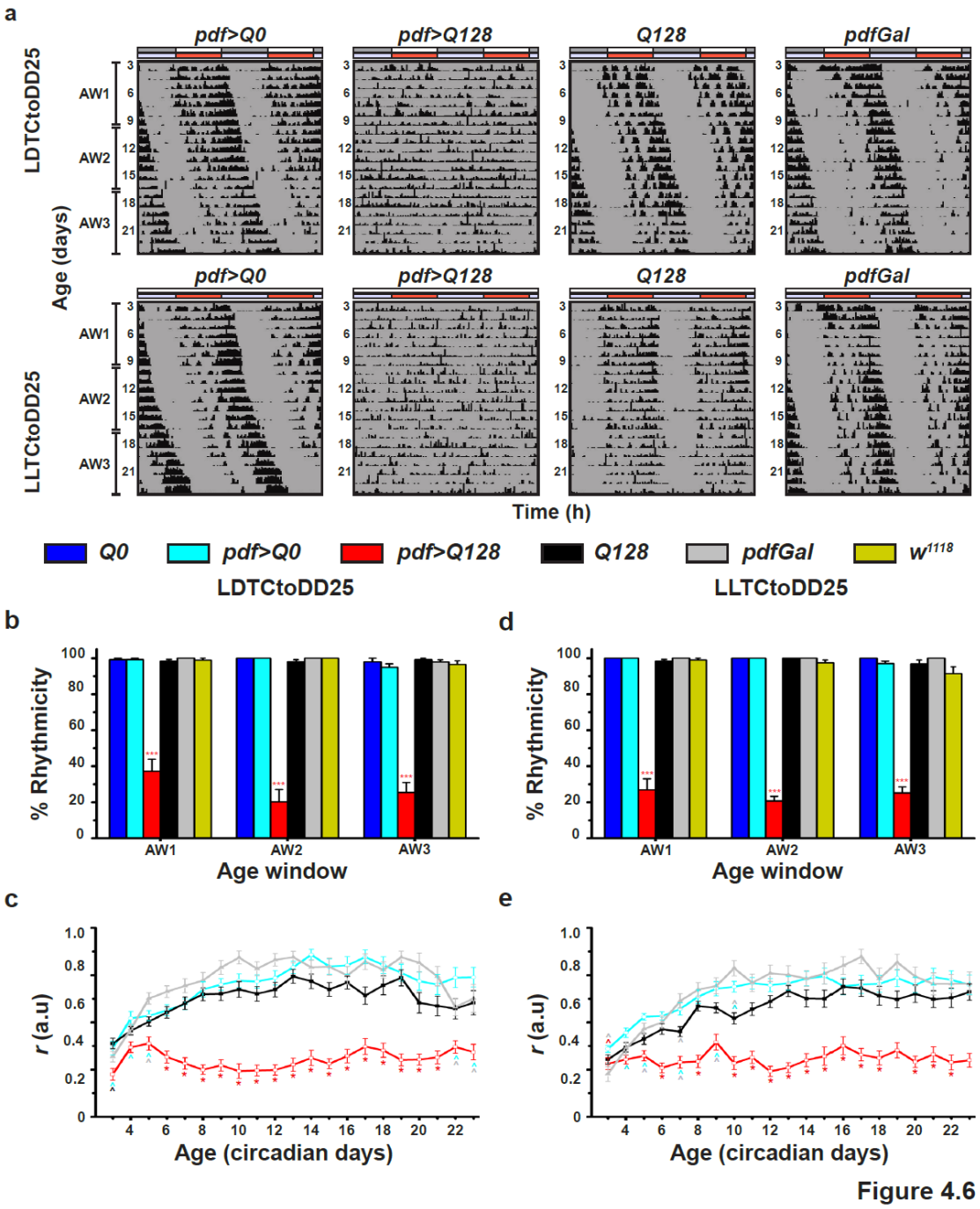

Figure 4.6

Fig 4. 6 pdf>Q128 flies in LDTCtoDD25 or LLTCtoDD25 are arrhythmic as adults in DD25.
(a) Representative double-plotted actograms for adult flies in LDTCtoDD25 (top) and those in LLTCtoDD25 (bottom) showing activity data for 21d (age 3d-23d). The bars at the top of the actograms represent the developmental rearing condition: white and grey bars for 12h:12h LD, the rust and lavender coloured bars for 12h:12h warm (29°C) cold (21°C) temperature cycles and white bars for LL. All other details are the same as in Fig 2.1. (b-g) Plots for mean rhythmicity (b, d) and activity consolidation '*r*' (c, e) for flies in LDTCtoDD25 (b, c) and those in LLTCtoDD25 (d, e). All other details are like Fig 4.1.

Comparing the rhythms across the various developmental-TC regimes with those under DD25, *pdf>Q128* flies in DDTCtoDD25 had significantly more significant rhythmicity than those in the other regimes in AW1 (Fig 4.7a middle). Despite a significant fall of *pdf>Q128* rhythmicity in DDTCtoDD25 in AW2 compared to AW1, they still had higher rhythmicity than those in DD25 at AW2. At AW3, *pdf>Q128* in DD25 had the least rhythmicity than in the other regimes. This trend was also reflected in the significantly higher activity consolidation of *pdf>Q128* in DDTCtoDD25 than other regimes at most early ages (Fig 4.7b middle). However, *pdf>Q128* across regimes had similarly weak rhythms (Fig 4.7c). The controls had nearly 100% rhythmicities across regimes and nearly comparable *r*-values, except those in DD25 with lower '*r*' than those under other regimes at a few ages (Fig 4.7 a,b). Thus, exposure to only temperature cycles during development rescues early-age rhythms of *pdf>Q128*, but the rhythmicity is abolished in the presence of light during development. This result suggests a detrimental effect of the presence of light during development on the temperature cycle-mediated early-age rhythm rescue of *pdf>Q128*. Further, a complete absence of external time cues during development exacerbates the loss of rhythmicity of *pdf>Q128,* as seen with those experiencing DD25, as does the presence of light as a developmental time cue (LD25toDD25, see LD-reared flies in Chapter 3). So overall, the presence of temperature as a time cue during development, but not light, has a positive effect on the adult activity rhythms of HD flies.

A summary of the between-regime comparisons of the free-running activity rhythm features of HD flies is shown in Table 4.12.

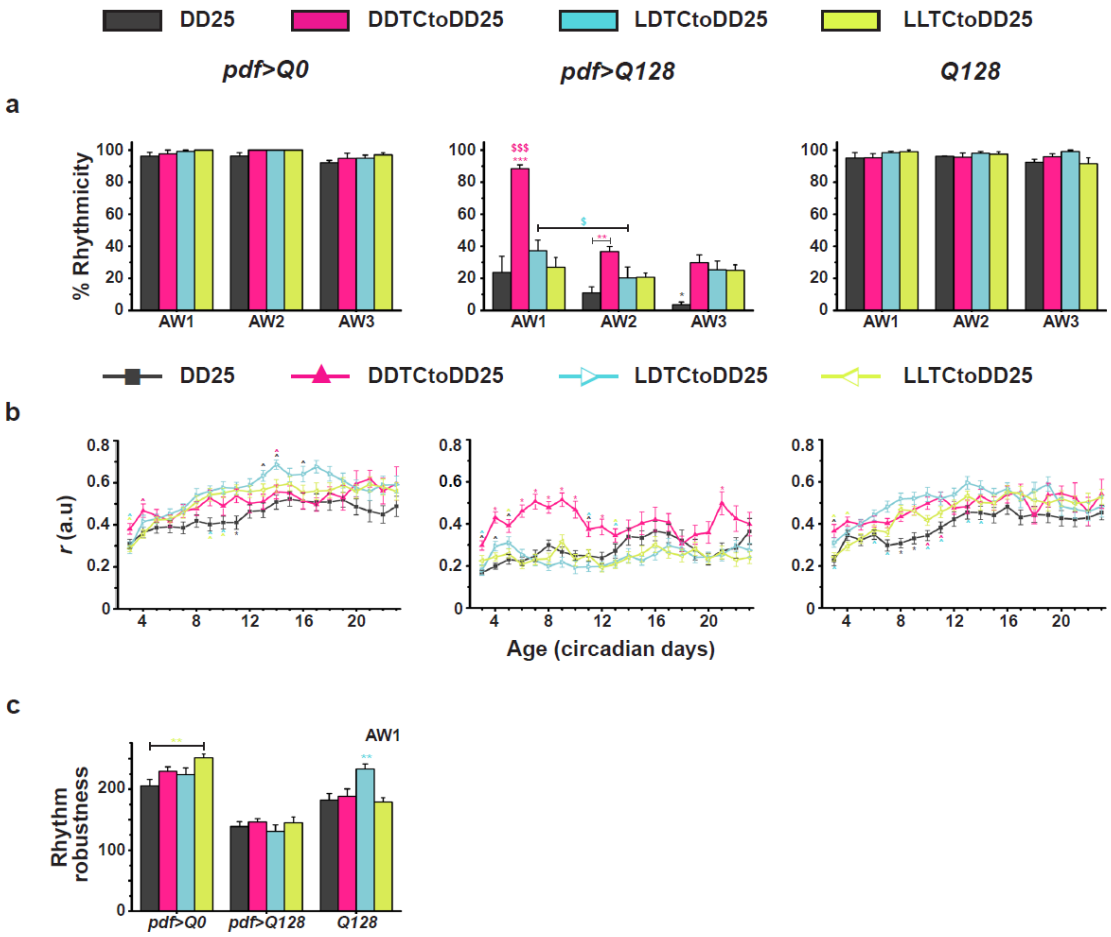

Figure 4.7

Fig 4. 7 Exposure of pdf>Q128 to LDTC or LLTC during development does not rescue behavioural arrhythmicity in adults under DD25.

(a-c) The between-regime comparisons of the mean percentage rhythmicity (a), the mean activity consolidation '*r*' (b), and the mean rhythm robustness in AW1(c) plotted against AWs (or age) (in a and b) for each genotype. Symbols represent statistically significant differences: coloured * of that coloured regime from all others or indicated ones for a genotype and coloured $ of between-AW comparisons of a genotype for that regime. For '*r*', coloured ^ near an error bar of a data point indicates a difference of the respective-coloured regime from the data-point regime. Regime colour codes: dark grey, DD25; pink, DDTCtoDD25; cyan, LDTCtoDD25; lime green, LLTCtoDD25. The number of symbols represents statistical significance: single $p<0.05$, double $p<0.01$ and triple $p<0.001$. Error bars are SEM.

4.3.3 Exposure of *pdf>Q128* to temperature cycles throughout development is necessary for the behavioural rhythmicity as adults

The next step was determining if specific development stages must be exposed to temperature cycles to rescue early-age rhythms in *pdf>Q128*, as ectotherms with distinct life stages differ in their microhabitats and thermal sensitivities (Kingsolver et al., 2011). TC was either provided from the egg to the third instar larva (L3) stage and then placed in DD25, termed "DDTC up to L3", or TC was provided from early pupal stages up to 2d post-eclosion, followed by DD25, termed "DDTC as Pupa-2d". *pdf>Q128* flies in both these regimes had very low rhythmicity (Fig 4.8a-c) and '*r*' than their regime-matched controls (Fig 4.8d-e). The rhythmicity of *pdf>Q128* in these two regimes was significantly lower than those in DDTCtoDD25 at AW1 (Fig 4.8f), as was the case with early age '*r*' (till 10d) (Fig 4.8g middle). The controls were similar between regimes (Fig 4.8f, g). Thus, exposing *pdf>Q128* at specific developmental stages to DDTC is not beneficial in the rhythm rescue as adults, indicating that these flies need chronic exposure to temperature cycles throughout development for free-running behavioural rhythms.

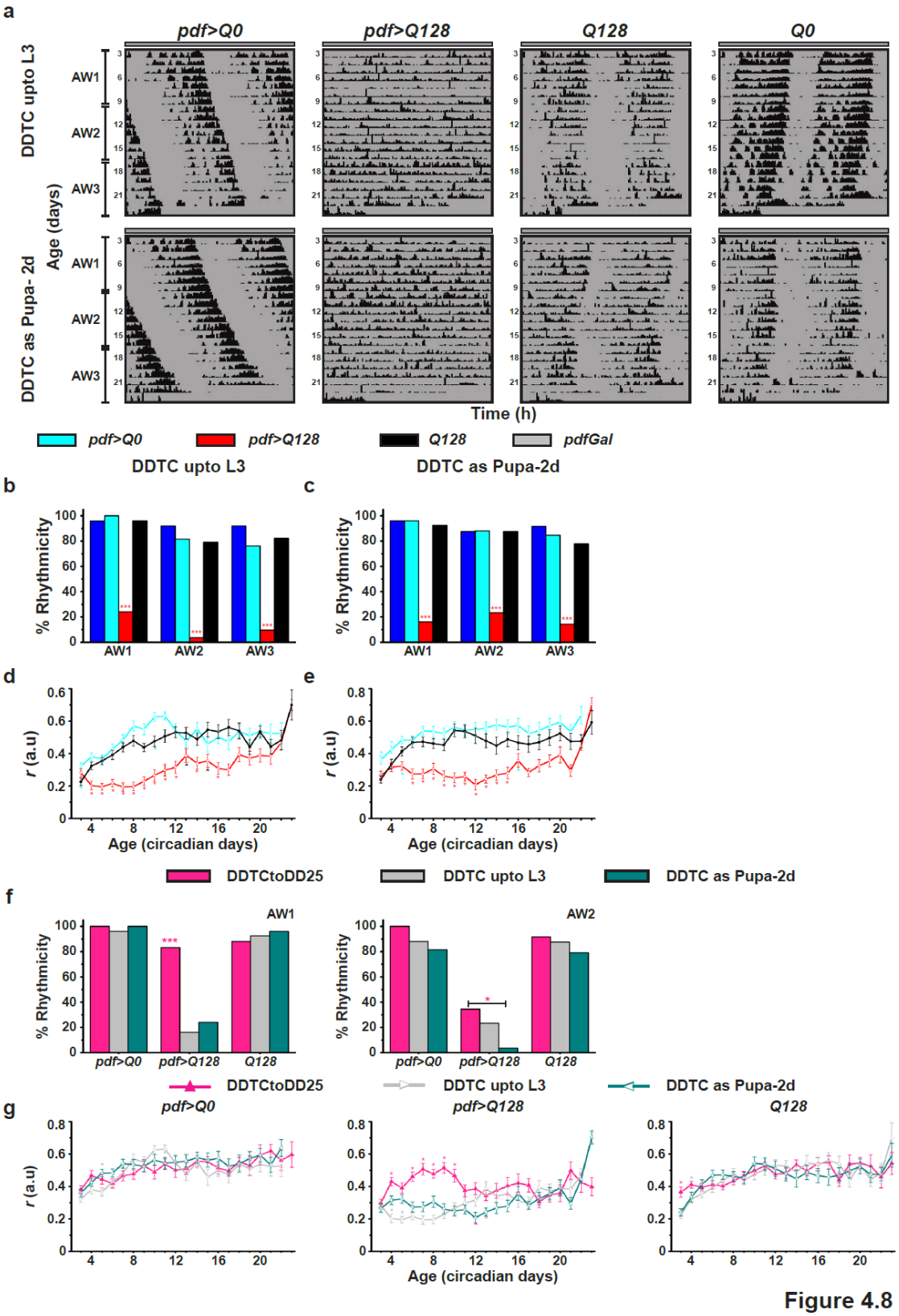

Figure 4.8

Fig 4. 8 Exposure of pdf>Q128 to DDTC either during egg to larvae or pupae to post-eclosion does not rescue behavioural arrhythmicity during adulthood.

(a) Representative double-plotted actograms for adult flies in DDTCasL3 (top) and DDTCaspupa-2d (bottom) showing activity data for 21d (age 3d-23d). (b-e) Plots for rhythmicity (b, c)

and activity consolidation '*r*' (d, e) for the within-regime comparisons in acute DDTCasL3 (left) and DDTCaspupa-2d (right). Symbols represent statistically significant differences: coloured * of that coloured genotype from all others or indicated ones in an AW, and coloured $ between AWs for a genotype. Coloured ^ near an error bar of a data point indicates a difference between the respective-coloured genotype and the data-point genotype. All other details are the same as in Fig 4.1. (f-g) The between-regime comparisons of the percentage rhythmicity (f) in AW1 and AW2 and the mean activity consolidation '*r*' (g) across age for each of the three genotypes. All other details are like Fig 4.7. Regime colour codes: pink, DDTCtoDD25; light grey, DDTCasL3; dark cyan, DDTCaspupa-2d.

4.3.4 Exposure of *pdf>Q128* to constant warm temperatures during development improves LNv-PER without affecting the behavioural arrhythmicity of adults in DD25

Exposure of *pdf>Q128* to 12h:12h::29°C:21°C warm/cold temperature cycles in DD during development and then to constant ambient 25°C in DD during adulthood resulted in rhythmic activity rhythms in the early ages (Fig 4.1). I asked whether the cycling aspect of temperature during development was necessary for this rescue or if it could be just an effect of the change in temperature from development to adulthood. So, instead of developmental TCs, flies were reared in chronic cool (21°C) or chronic warm (29°C) temperatures and then moved to DD25 as adults. *pdf>Q128* in both the DD21toDD25 and DD29toDD25 regimes were mostly arrhythmic (Fig 4.9a middle), and their percentage rhythmicities and *r*-values differed from their regime-matched controls across age (Fig 4.9b-e). Such contrasts were also evident between regimes: *pdf>Q128* in DDTCtoDD25, which exhibited rhythmicity in AW1 and even AW2, which was much higher than those in DD21toDD25 and DD29toDD25 (Fig 4.9e). The '*r*' of young *pdf>Q128* in DDTCtoDD25 was also higher than those in the other regimes, while controls had comparable between-regime rhythmicities and '*r*' (4.9f). Thus, the presentation of developmental temperature as warm/cold cycles is crucial for the early-age rhythms of *pdf>Q128* as adults in DD25 rather than a change in the constant ambient temperatures experienced upon transitioning from development to adulthood.

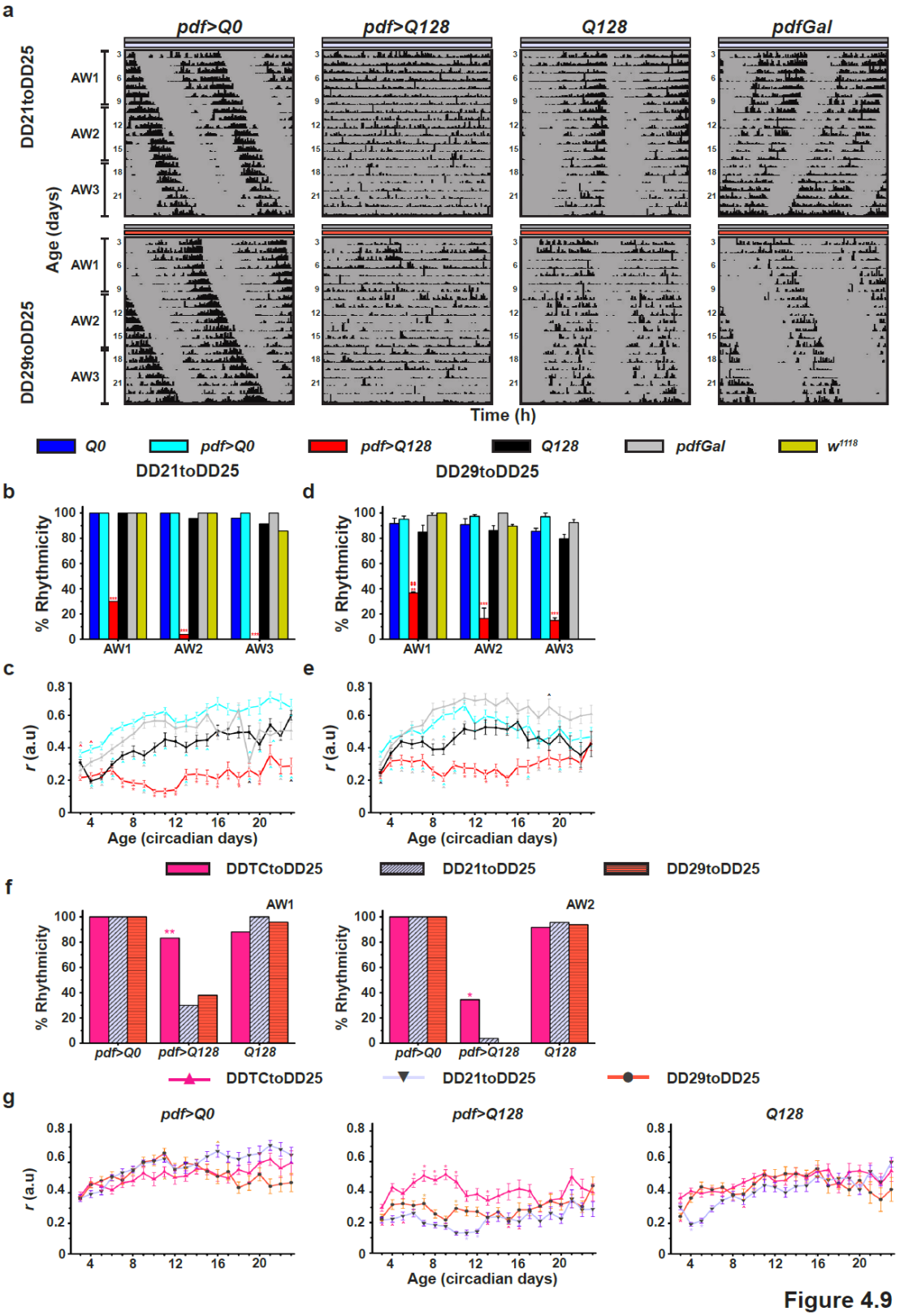

Figure 4.9

Fig 4. 9 pdf>Q128 exposed to chronic cool or warm temperatures during development are behaviourally arrhythmic as adults in DD25.

(a) Representative double-plotted actograms for adult flies in DD21toDD25 (top) and DD29toDD5 (bottom) showing activity data for 21d (age 3d-23d). (b-e) Plots for rhythmicity (b, d) and activity consolidation '*r*' (c, e) for the within regime comparisons in DD21toDD25 (left) and

DD29toDD25 (right). All other details are the same as in Fig 4.1. (f-g) The between-regime comparisons of the percentage rhythmicity (f) in AW1 and AW2 and the mean activity consolidation '*r*' (g) across age for each of the three genotypes. All other details are like Fig 4.7. Regime colour codes: pink, DDTCtoDD25; lavender, DD21toDD25; orange, DD29toDD25.

The cellular features of *pdf>Q128* flies in DD29toDD25 were also examined. *pdf>Q128* in DD29toDD25 at 7d showed a significant reduction in the PDF^+ sLNv soma numbers compared to *pdf>Q0* (Fig 10a, b), also reflected in the different shapes of their frequency distributions (Fig 4.10c top). However, the distribution of *pdf>Q128* was still left-skewed, with 65% of hemispheres showing ≥3 PDF^+ sLNv soma, and both the median and mode of this dataset were 3. These observations suggest that DD29toDD25 may partially improve PDF expression in the sLNv. The PDF^+ lLNv soma numbers of *pdf>Q128* at 7d were higher than *pdf>Q0* (Fig 4.10a, b), while their distribution shapes were comparable (Fig 4.10c bottom).

PER^+ sLNv soma numbers of *pdf>Q128* in DD29toDD25 at 7d were significantly lower than *pdf>Q0*, albeit *pdf>Q128* having a mean of ~ 2.7 (Fig 4.11a, b). This trend was also reflected in 58% of *pdf>Q128's* hemispheres showing ≥3 PER^+ sLNv soma, despite its frequency distribution shape differing significantly from *pdf>Q0* (Fig 4.11c top). Interestingly, unlike the loss of PER from lLNv of *pdf>Q128* in other regimes, *pdf>Q128* in DD29toDD25 exhibited control-like PDF^+ lLNv soma numbers and distribution shapes (Fig 4.11a, b, c bottom). PER in lLNv soma of *pdf>Q128* in DD29toDD25 showed a dampened oscillation; PER in the sLNv was non-oscillatory (Fig 4.11a, d). The PER LNv oscillations of *pdf>Q128* were also anti-phasic to *pdf>Q0*. Thus, exposure of *pdf>Q128* to DD29toDD25 rescues loss of PER from lLNv, partially suppresses loss of PER and maybe PDF from sLNv and induces low amplitude lLNv PER oscillations.

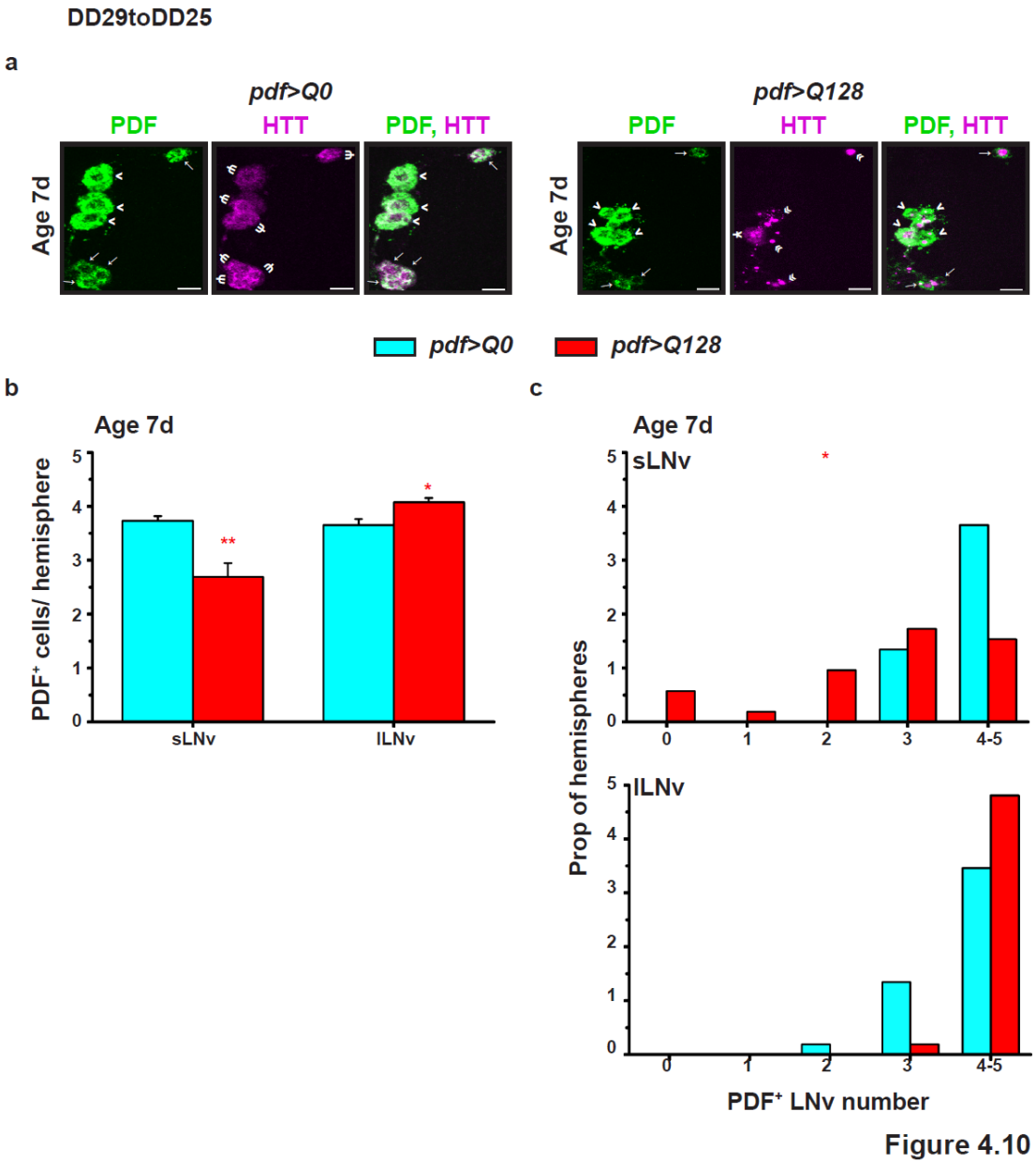

Figure 4.10

Fig 4. 10 pdf>Q128 under DD29toDD25 show a decrease in PDF⁺ sLNv soma numbers.
(a) Representative images of 7d adult fly brains under DD29toDD25 stained for PDF (green) and HTT (magenta) in the LNv of *pdf>Q0* (left panels) and *pdf>Q128* (right panels). Indicated in the images are sLNv soma (→ arrows), lLNv soma (> arrowheads), diffuse expHTT (Ψ psi), diffuse+inclusions expHTT (Ɣ), and expHTT inclusions (« double arrowheads). Scale bars are 10 µm. (b) The mean number of PDF⁺ sLNv soma and lLNv soma at 7d. Coloured * indicates significant age-matched inter-genotype differences at * $p<0.05$, ** $p<0.01$, *** $p<0.001$. (c) Frequency distribution of the proportion of hemispheres with 0 to 5 PDF⁺ LNv soma numbers (sLNv - top and lLNv - bottom) comparing *pdf>Q0* and *pdf>Q128* at 7d. Coloured * indicates significantly different distribution shapes between genotypes at $p<0.05$. Error bars are SEM.

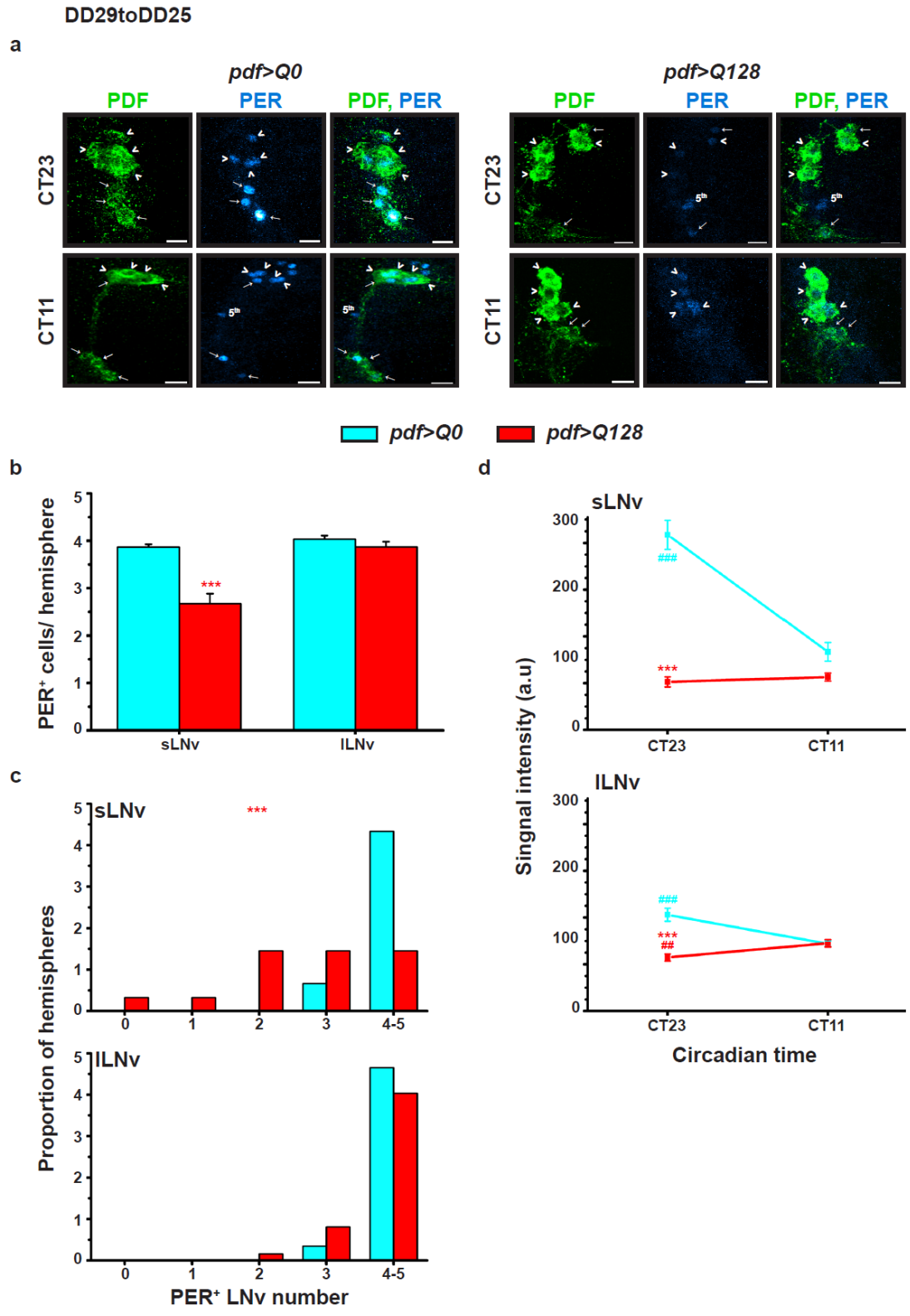

Figure 4.11

Fig 4. 11 pdf>Q128 flies in DD29toDD25 show a loss of PER from the sLNv, but not the lLNv; exhibit low-amplitude PER oscillations in the lLNv.

(a) Representative images of 7d-old adult fly brains of *pdf>Q0* (left) and *pdf>Q128* (right) in DD29toDD25 stained for PER (cyan hot) and PDF (green) in LNv at CT23 (top) and CT11 (bottom). sLNv soma (→ arrows), lLNv soma (> arrowheads) and PDF^{-} PER^{+} 5th sLNv are indicated.

Scale bars are 10 µm. (b) The mean number of PER^+ sLNv soma and lLNv soma at CT23. * indicates age-matched differences between genotypes. (c) Frequency distribution of the proportion of hemispheres having 0 to 5 PER^+ LNv soma: sLNv soma (top) and lLNv soma (bottom) in 7d-old flies at CT23. * indicates significantly differing shapes of distribution between genotypes. (d) For the two genotypes, the quantification of PER intensity at CT23 and CT11 in sLNv (top) and lLNv (bottom). Differences between time points CT23 and CT11 are represented by # (cyan) for *pdf>Q0* and # (red) for *pdf>Q128*. Coloured * represents the difference between genotypes at that time point. Statistical significance is at single-symbol $p<0.05$, double-symbol $p<0.01$, and triple-symbol $p<0.001$. Error bars are SEM.

4.3.5 The early-age rhythm rescue of *pdf>Q128* by developmental temperature cycles is altered by the temperature experienced as adults

After examining the effects of developmental temperatures in the developmental-TC-mediated behavioural rhythm rescue of young *pdf>Q128*, I investigated the effect of the temperature experienced as adults. Flies reared under TC two days after eclosion were either exposed to 21°C or 29°C in DD. *pdf>Q128* flies in DDTCtoDD21 were arrhythmic across age with poor activity consolidation than controls (Fig 4.12a-d). In contrast, most of the *pdf>Q128* flies in DDTCtoDD29 were rhythmic, like controls (Fig 4.12a bottom, e) and showed '*r*' comparable to controls *pdf*>Q0 and *pdfGal* up to 8d (Fig 4.12f). They, however, had poorer robustness than the said controls in AW1 (Fig 4.12g).

Comparing the regimes, *pdf>Q128* experiencing cooler temperatures of 21°C as adults had very low rhythmicity than those experiencing relatively warmer temperatures of 25°C and warm temperatures of 29°C, which had ≥80% rhythmicity in AW1 (Fig 4.12h). This difference was also reflected in *pdf>Q128* flies in DDTCtoDD21 having lower '*r*' than those in DDTCtoDD25 and DDTCtoDD29 till 8d (Fig 4.12j, middle). Thus, post-developmental-TC, the temperature experienced as adults also determines the behavioural rhythmicity of *pdf>Q128*: relatively optimal or warm ambient temperatures as adults are rhythm-promoting but not cooler. The rhythm robustness of *pdf>Q128* in DDTCtoDD29 was more remarkable than those in DDTCtoDD25 (Fig 4.12i). The rhythm robustness of controls in DDTCtoDD21 was poorer than those in the other two regimes (Fig 4.12i), indicating that low temperatures as adults during recording weaken fly activity rhythms. Young *pdf>Q0* in DDTCtoDD29 had higher '*r*' than those in the other regimes, and *Q128* in DDTCtoDD21 had lower '*r*' than those in DDTCtoDD29, suggesting an effect of ambient temperature during recording on the extent of activity consolidation. Overall, both the developmental temperature cycles and the temperature experienced by the flies in adulthood contribute to the early age rhythmicity of *pdf>Q128* adults under DDTCtoDD25.

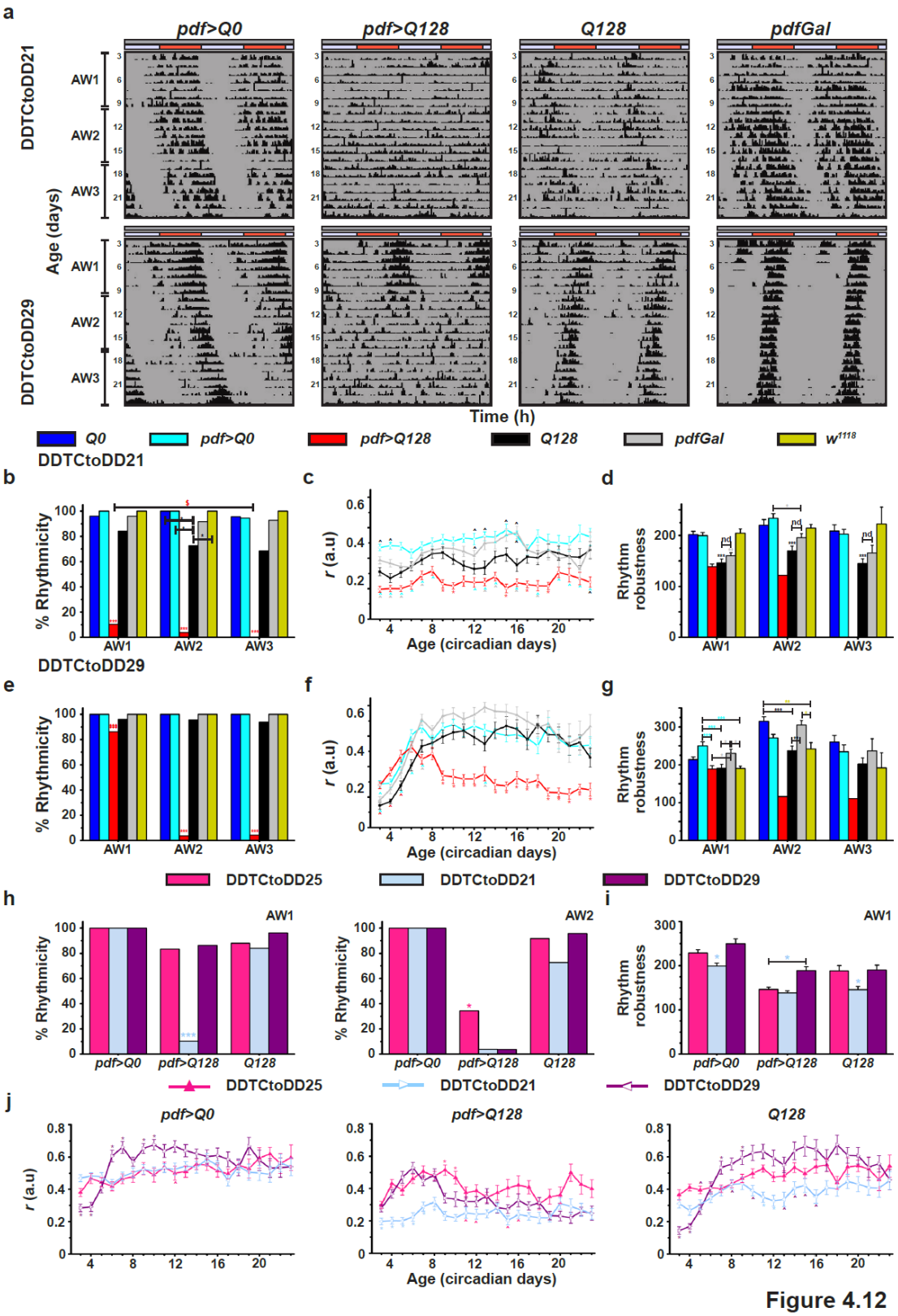

Fig 4. 12 pdf>Q128 in DDTCtoDD29 show early-age activity rhythms but not those in DDTCtoDD21.

(a) Representative double-plotted actograms for adult flies in DDTCtoDD21 (top) and DDTCtoDD29 (bottom) showing activity data for 21d (age 3d-23d). (b-e) Plots for rhythmicity (b, e),

mean activity consolidation '*r*' (c, f) and mean rhythm robustness (d, g) for the within-regime comparisons in DDTCtoDD21 (b-d) and DDTCtoDD29 (e-g). All other details are the same as in Fig 4.1. (h-j) The between-regime comparisons of the percentage rhythmicity (h) in AW1 and AW2, the mean robustness in AW1 (i) and the mean activity consolidation '*r*' (j) for each of the three genotypes. All other details are like Fig 4.7. Regime colour codes: pink, DDTCtoDD25; light blue, DDTtoDD21; dark purple, DDTCtoDD29.

4.3.6 Developmental temperature cycles delay the loss of PDF from the sLNv of *pdf>Q128* without affecting the expHTT inclusion load

Further, the cellular features are compared between the DDTCtoDD25 and DD25. Even though the PDF^+ sLNv soma numbers in DD25 and DDTCtoDD25 started similarly at L3, as young adults (at 1d and 3d), those in DDTCtoDD25 had noticeably greater numbers than those in DD25 (Fig 4.13a left). Post-3d, the numbers fell for those in DDTCtoDD25 and became comparable to those in DD25 up to 16d, following which, at 23d, those in DDTCtoDD25 had fewer PDF^+ sLNv soma than those in DD25. The PDF^+ lLNv soma numbers of *pdf>Q128* remain comparable between regimes across age (Fig 4.13a middle). The shapes of the frequency distributions of PDF^+ sLNv soma were comparable across age, except at 3d and 23d (Fig 4.13b). Even though the distribution shapes were not different between regimes at 1d, ~77% of hemispheres in DDTCtoDD25 had 3 to 4 PDF^+ sLNv (~23% had 0-2 sLNv), which was significantly higher compared to the ~47% of hemispheres in DD25 ($p = 0.02902$, Fisher's Exact test). Thus, exposure of *pdf>Q128* to temperature cycles during development improves PDF^+ sLNv soma numbers in the very young, i.e., for **enhancing PDF^+ sLNv soma numbers**, **DDTCtoDD25>DD25.**

The mean PER^+ LNv soma numbers of *pdf>Q128* were similarly low under DD25 and DDTCtoDD25 (Fig 4.13c). The shape of the PER^+ LNv frequency distributions under DDTCtoDD25 was similar to those under DD25 (Fig 4.13d). Thus, the mean PER^+ LNv numbers and their relative distributions were similar between DDTCtoDD25 and DD25. However, a key difference was that DDTCtoDD25 restored low amplitude PER oscillations in the sLNv of *pdf>Q128* (Fig 4.4), which are absent in DD25. These observations suggest that PER oscillations in the LNv of *pdf>Q128* in DDTCtoDD25 are better protected than those in DD25. Therefore, overall, for **PER in the LNv**, **DDTCtoDD25>DD25.**

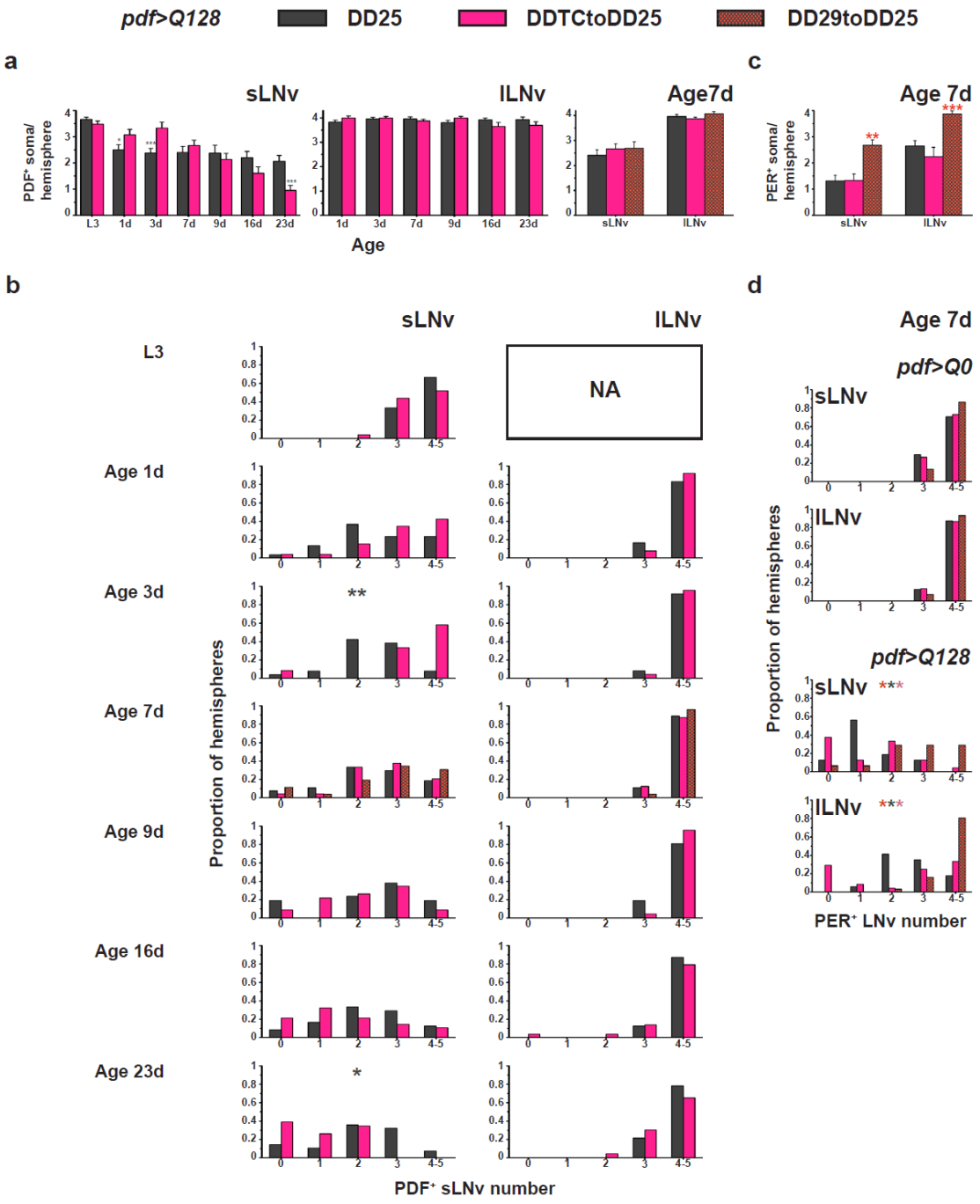

Figure 4.13

Fig 4. 13 DDTCtoDD25 slows down PDF loss from the sLNv soma of pdf>Q128, while DD29toDD25 mitigates PER loss from the LNv.

(a) The Mean number of PDF$^+$ sLNv soma (left) or lLNv soma (middle) across age comparing *pdf>Q128* maintained in the DD25 with DDTCtoDD25. Mean PDF$^+$ LNv soma numbers comparing 7d *pdf>Q128* in DD25, DDTCtoDD25 and DD29toDD25 (right). (b) Frequency distribution of the proportion of hemispheres of *pdf>Q128* with 0 to 5 PDF$^+$ LNv soma numbers (sLNv - left and lLNv - right) in DD25 and DDTCtoDD25 across age. NA, not applicable. * indicates significantly different distribution shapes. (c) The mean PER$^+$ LNv soma numbers in 7d-old *pdf>Q128* in DD23 and DD25. (d) Frequency distribution of the proportion of hemispheres of *pdf>Q0* (top-sets) or

pdf>Q128 (bottom-sets) with 0 to 5 PDF^+ LNv soma numbers (sLNv - top and lLNv - bottom) in the three regimes. Coloured multiple * indicates significantly different distribution shapes between regimes, with the first colour of the reference regime and the subsequent colours of regimes differing from the reference at $p<0.05$. Significant differences are at * $p<0.05$, ** at $p<0.01$ and *** $p<0.001$. Error bars are SEM.

Comparing *pdf>Q128* in DDTCtoDD25 with those in DD25, the relative proportions of hemispheres dominated by different expHTT forms in LNv were nearly similar across age with domination by Diff-enriched LNv very early-on and near-exclusive domination by Inc-enriched LNv as the flies aged (Fig 4.14a, top, b top). However, between-regime differences were seen for sLNv at 1d and lLNv at 3d. Although most of the hemispheres in both the regimes had Inc-enriched sLNv, at 1d, those in DDDTCtoDD25 had considerably lower proportions of Inc-enriched sLNv relative to the Diff+Inc-enriched sLNv than those in DD25 (Fig 4.14a bottom). Conversely, the proportion of hemispheres dominated by Diff-enriched relative to Inc-enriched lLNv or Diff+Inc-enriched lLNv was significantly lower for those in DDTCtoDD25 than those in DD25 at 3d. Thus, *pdf>Q128* in DDTCtoDD25 differs from those in DD25 in that, in the former, Diff+Inc is present for a longer duration in the sLNv, and Diff expHTT decreases in favour of Diff+Inc and Inc expHTT in the lLNv at 3d.

The inclusion number and size were comparable between *pdf>Q128* in the two regimes across most ages, except those in DDTC at 3d that had significantly more inclusions than other ages and from those in DD25 at 3d (Fig 4.14c). So, by and large, DDTCtoDD25 did not affect *pdf>Q128*'s expHTT forms in LNv, or inclusion features differentially from that of DD25, i.e., for **effect on inclusion load**, **DDTCtoDD25=DD25**. Thus, *pdf>Q128*'s early-age rhythm rescue and delay in the PDF loss from sLNv imparted by developmental exposure to temperature cycles occur without altering the expHTT inclusion load.

In summary, in terms of **hindering expHTT-induced neurotoxicity** like delaying arrhythmicity in activity rhythms and PDF loss from sLNv and moderately rescuing the LNv PER oscillations in the *pdf>Q128* young, **DDTCtoDD25>DD25.** Thus, the development-specific exposure of *pdf>Q128* to temperature cycles slows down the circadian neurodegenerative phenotypes as adults, indicating that circadian bolstering environmental interventions (during development) mitigate circadian impairments (as adults).

A summary of the between-regime comparisons of the behavioural and cellular phenotypes of HD flies is shown in Table 4.13

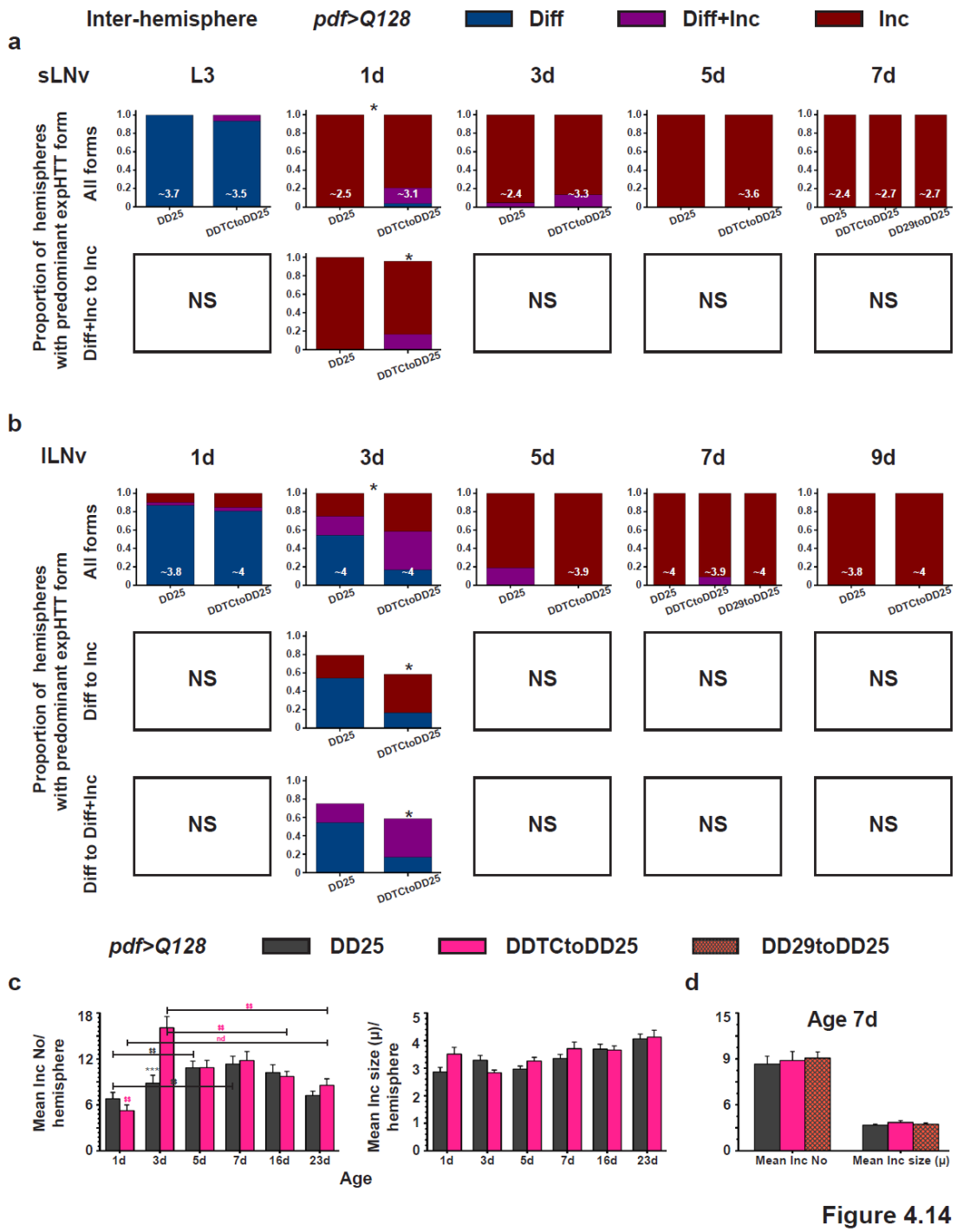

Figure 4.14

Fig 4. 14 pdf>Q128 in DDTCtoDD25 and DD25 are comparable in the relative proportions of hemispheres of different expHTT forms enriching LNv and inclusion features across age.

(a) and (b) The proportion of hemispheres dominated by different expHTT forms in sLNv (a) or lLNv (b) is plotted for *pdf>Q128* comparing DD25 and DDTCtoDD25 at various ages and with DD29toDD25 (at 7d). These are plotted for all expHTT forms (top) or significantly different pair-wise comparisons (a – bottom, b - middle and bottom). * indicates significant changes in the relative proportions of hemispheres for all expHTT forms between regimes for an age (top) or pair-wise expHTT forms between regimes for a particular age (a – bottom, b - middle and bottom). NS, not significant.

At the bottom of some bars, numbers represent the mean number of PDF^+ LNv detected for that regime at that age. (c) Comparison of mean inclusion number per hemisphere (left) and mean inclusion size per hemisphere (right) between DD25 and DDTCtoDD25 across age for *pdf>Q128*. (d) Comparison of mean inclusion number and size between the three regimes for 7d-old *pdf>Q128*. Coloured * indicates a significant age-matched difference between that regime and other regimes or indicated regimes, and coloured $ indicates differences between those regimes' ages. Symbols represent statistical differences: single $p<0.05$, double $p<0.01$ and triple $p<0.001$. nd, not different. Error bars are SEM.

4.3.7 Development-specific warm temperatures improve PER in the LNv of *pdf>Q128* without altering sLNv PDF loss or expHTT features

I asked whether the differential effects of development-specific-temperature-cycles versus -constant-temperature on the activity rhythms of adult *pdf>Q128* flies in DD25 also extend to the cellular features of the LNv. *pdf>Q128* exposed to development-specific temperature cycles were compared against those exposed to constant warm temperatures. PDF^+ LNv soma numbers and their distributions' shapes were similar to those in DD25, DDTCtoDD25 and DD29toDD25 at 7d (Fig 4.13a right and b fourth-row). *pdf>Q128* in DD29toDD25, despite being behaviourally arrhythmic, had significantly higher number of PER^+ LNv soma at 7d than those in DD25 and DDTCtoDD25 (Fig 4.13c). The distribution shapes of PER^+ LNv also differed significantly (Fig 4.13d). Thus, in terms of **improving PER^+ LNv, DD29toDD25>DD25=DDTCtoDD25**. However**,** PER oscillations were absent from the sLNv of *pdf>Q128* in DD29toDD25, like those in DD25 (Fig 4.11d), but under DDTCtoDD25, were restored to a low amplitude (Fig 4.4d). Thus, concerning promoting clock function for which **PER oscillations in the sLNv** is a proxy, **DDTCtoDD25>DD29toDD25**.

At 7d, like *pdf>Q128* in DD25 and DDTCtoDD25, nearly all hemispheres of *pdf>Q128* in DD29toDD25 had Inc-enriched LNv (Fig 4.14a top, b top). Their inclusion number and size were also not different between regimes at 7d (Fig 4.14d).

Thus, mere exposure of *pdf>Q128* to constant warm temperatures during development improves PER in the LNv but is insufficient to overcome most other expHTT-induced circadian neurodegenerative phenotypes. However, a caveat to this inference is that DD29toDD25 could modify expHTT forms and PDF in LNv of *pdf>Q128* differentially from that of DD25 at the very early ages, which have not been examined in this study, due to the absence of a behavioural rescue. Nonetheless, based on PER restoration in the LNv, DD29toDD25>DDTCtoDD25=DD25; based on PER oscillations in the sLNv, DDTCtoDD25>DD29toDD25=DD25; and based on delaying

behavioural arrhythmicity, DDTCtoDD25>DD25 and DDTCtoDD25>DD29toDD25 and PDF loss from sLNv, DDTCtoDD25>DD25. Thus, the order of **neuroprotection against expHTT-induced circadian deficits** is **DDTCtoDD5>DD29toDD25>DD25**. In conclusion, temperature as an external time-giver during development in the form of cycles of warm and cold and not merely development-specific constant high temperature improves the adult circadian function of HD flies in DD25.

4.3.8 Exposure of *pdf>Q128* to constant cool temperatures restores low amplitude PER oscillations in the LNv without altering arrhythmic activity rhythms

So far, I have found early-age activity rhythm improvements with development-specific temperature cycles. The *Gal4-UAS*-based tissue-specific expression system used here for targeting human expHTT to the circadian pacemaker LNvs is sensitive to temperature, with transgene expression increasing with temperature and cooler temperatures having the opposite effect (Brand and Perrimon, 1993). Exposing the flies to warm and cold temperatures would help achieve differential expHTT expression levels and serve as a proxy to test the dosage effects of expHTT. This line of reasoning prompted me to investigate further the differential effects of relatively warm and cooler temperatures on activity rhythms of *pdf>Q128* in DD. When I tested the effect of cool temperatures, namely 19°C, 21°C and 23°C on activity rhythms of the flies used in this study, I found that at both 19°C and 21°C, even controls like *pdfGal* and w^{1118} exhibited weak rhythms of low robustness. Thus, 23°C was chosen as the relatively cool temperature for further investigations. Since 29°C is warm enough to alter the activity distribution and remain within the physiological range (Majercak et al., 1999; Low et al., 2008; Menegazzi et al., 2012b), it was chosen as the warm temperature. A concern here is that temperature affects development time, with lower temperature increasing development time (~12d at 23°C). In contrast, higher temperature decreases it (8-9d at 29°C). Some of the effects seen could result from temperature effects on the development time.

pdf>Q128 experienced a relatively cooler temperature of 23°C in DD during development and as adults were arrhythmic across AWs (Fig 4.15a,b). They also showed poor activity consolidation across ages (Fig 4.15c). Most controls were rhythmic and had significantly higher '*r*' than *pdf>Q128* across age, except *Q128*, which showed lowered activity consolidation than some controls (Fig 4.15c).

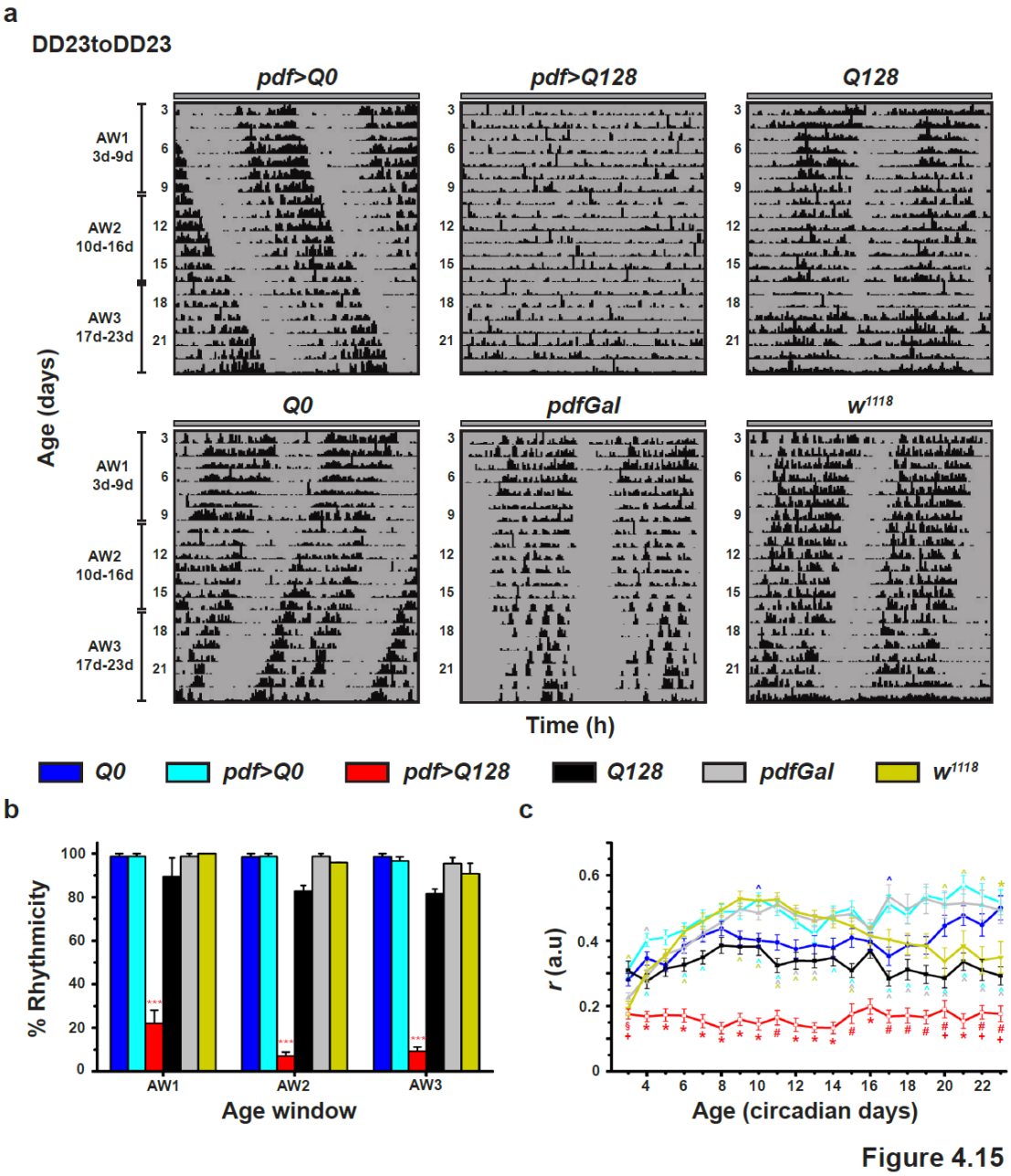

Figure 4.15

Fig 4. 15 pdf>Q128 flies in DD23 are arrhythmic and show poor activity consolidation.

(a) Representative double-plotted actograms for adult flies in DD23 showing activity data for 21d (age 3d-23d). The grey bars at the top of the actograms represent the developmental rearing condition, which in this regime is DD23. All other details are the same as in Fig 2.1. (b-c) The percentage rhythmicity (b) and the extent of activity consolidation '*r*' (c) are plotted against age (or AWs). a.u is arbitrary units. Symbols represent statistically significant differences: coloured * of that coloured genotype from all others, coloured # of that genotype from all others except *Q128*, coloured § from all others except *pdfGal* and coloured + from all others except w^{1118}. Coloured ^ near an error bar of a data point indicates a difference between the respective-coloured genotype and the data-point genotype. The number of symbols represents statistical significance: single $p<0.05$, double $p<0.01$ and triple $p<0.001$. Error bars are SEM.

I then assessed the LNv cellular features and expHTT forms of HD flies in DD23. The number of PDF$^+$ sLNv soma was comparable between *pdf>Q128* and *pdf>Q0* up to 3d, following which *pdf>Q128* had a significant reduction in numbers compared to control and earlier ages (Fig 4.16a, b left). Even though the mean PDF$^+$ sLNv numbers differed between genotypes at 5d, the shapes of their frequency distributions were left-skewed up to 9d and different between genotypes only from 7d onwards (Figs 4.16b left and 4.17 left). The PDF$^+$ lLNv soma numbers and their distribution shapes were comparable between genotypes across age (Figs 4.16a, b right, 4.17 right). Thus, exposure of *pdf>Q128* to a modestly cool temperature of 23°C delays the loss of PDF from sLNv soma.

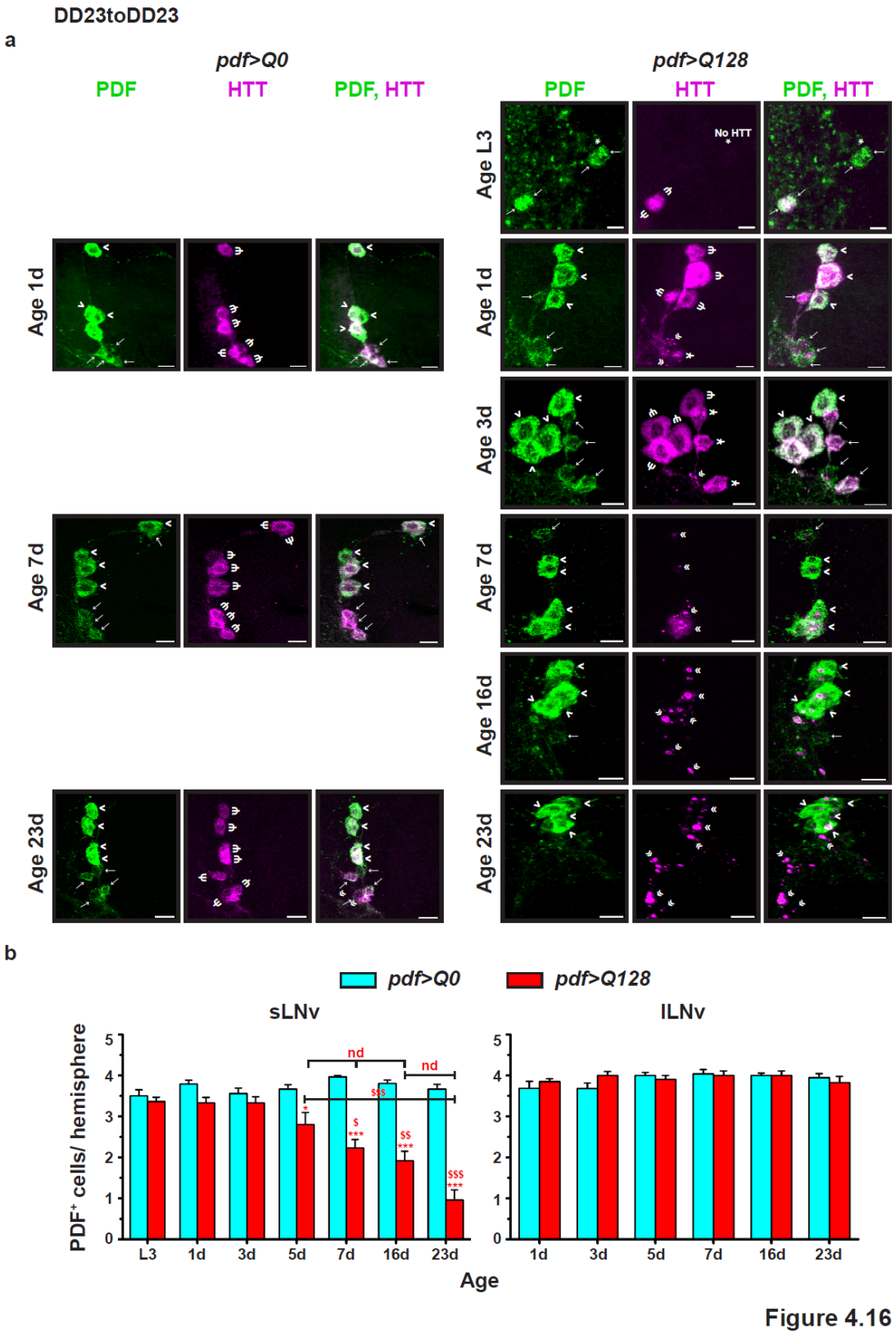

Figure 4.16

Fig 4. 16 Exposure of pdf>Q128 to DD23 delays the loss of PDF from sLNv soma.

(a) Representative images of the adult fly brains under DD23toDD23 stained for PDF (green) and HTT (magenta) in LNv at 1d, 7d and 23d for *pdf>Q0* (left panel-sets) and at L3, 1d, 3d, 7d, 16d and 23d for *pdf>Q128* (right panel-sets). Indicated in the images are sLNv soma (→ arrows),

lLNv soma (> arrowheads), diffuse expHTT (Ψ psi), diffuse+inclusions expHTT (Ɣ), and expHTT inclusions (« double arrowheads). Scale bars are 10 µm. (b) The mean number of PDF$^+$ sLNv soma (left) and lLNv soma (right) across age. Coloured symbols indicate significant differences, * for age-matched, inter-genotype differences and $ for differences between ages of the corresponding-coloured genotype at * p<0.05, ** p<0.01, *** p<0.001. nd, not different. Error bars are SEM.

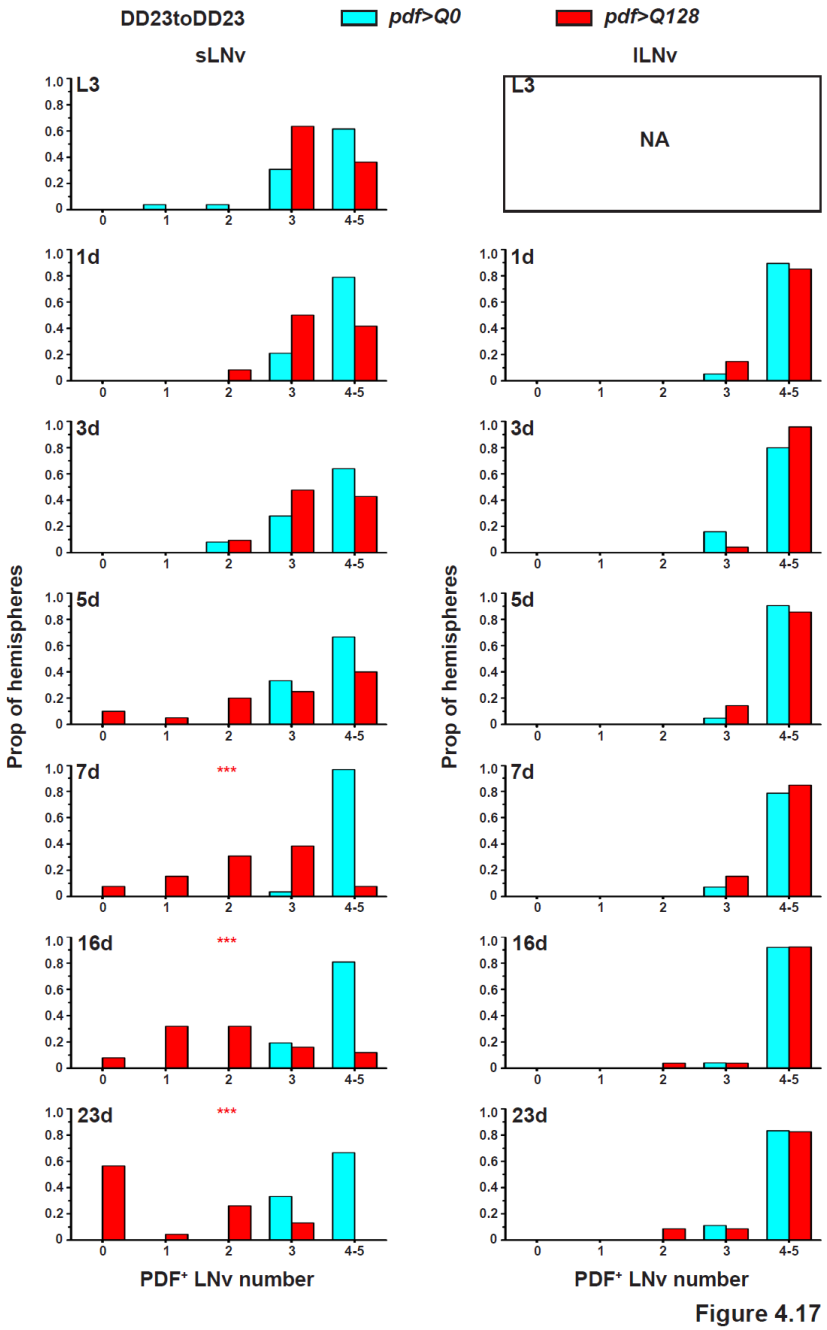

Fig 4. 17 The early-age frequency distribution of PDF$^+$ sLNv soma numbers is similar between genotypes under DD23.

Frequency distribution of the proportion of hemispheres of *pdf>Q0* and *pdf>Q128* in DD23toDD23 with 0 to 5 PDF$^+$ LNv soma numbers (sLNv - left and lLNv - right). Coloured * indicates significantly different distribution shapes between age-matched genotypes at p<0.05. NA, not applicable.

PER$^+$ sLNv soma numbers in 7d *pdf>Q128* in DD23 were significantly reduced than *pdf>Q0* (Fig 4.18a top, b). This reduction was also mimicked by the differing shapes of their distributions, with ~77% of the hemispheres of *pdf*>Q128 having fewer (0, 1 or 2) PER$^+$ sLNv (Fig 4.18c top). Even though the PER$^+$ lLNv soma numbers and their distribution shapes also differed between genotypes (Fig 4.18a top, b, c bottom), ~85% of the hemispheres of *pdf>Q128* had ≥3 PER$^+$ lLNv (Fig 4.18c bottom). PER in both the LNv of *pdf>Q128* oscillated, albeit with lower amplitude and in-phase than PER LNv oscillations of *pdf>Q0* (Fig 4.18a, d). Thus, exposure of *pdf>Q128* to DD23 improves PER in lLNv and restores its oscillations in the LNv of *pdf>Q128*.

The proportions of hemisphere dominated by various expHTT forms in LNv changes significantly with age for *pdf>Q128* in DD23 (Fig 4.19a top). For both the LNv, there is a domination of hemispheres enriched with Diff and Diff+Inc forms at early ages, while Inc-enriched ones dominate completely at later ages. There were significantly higher hemisphere proportions of Diff-enriched and Diff+Inc-enriched sLNv relative to Inc-enriched sLNv at early ages (L3 and 1d for Diff and 1d and 3d for Diff+Inc) than at later ages (Fig 4.19a left, second- and third-rows). A similar trend is seen for Diff-enriched lLNv relative to Inc-enriched lLNv at ages 1d and 3d compared to ages 7d upwards (Fig 4.19a right, second row). The Diff-enriched lLNv dominate hemispheres at ages 1d and 3d, giving way to Diff+Inc- and Inc-enriched lLNv domination at subsequent ages (Fig 4.19a, top-right). The hemisphere proportion of Diff+Inc-enriched relative to Diff-enriched lLNv is significantly higher at 5d, 7d and 9d than 1d and 3d (Fig 4.19a right, bottom). The Inc-enriched lLNv relative to Diff+Inc-enriched lLNv almost exclusively dominates the hemispheres at later ages of 16 and 23d (Fig 4.19a right, third-row).

The expHTT inclusion numbers of *pdf>Q128* in DD23 at 1d were significantly lower than subsequent ages and those at 3d compared to 5d and 7d (Fig 4.19b top). The inclusion sizes were comparable across most ages (Fig 4.19b bottom).

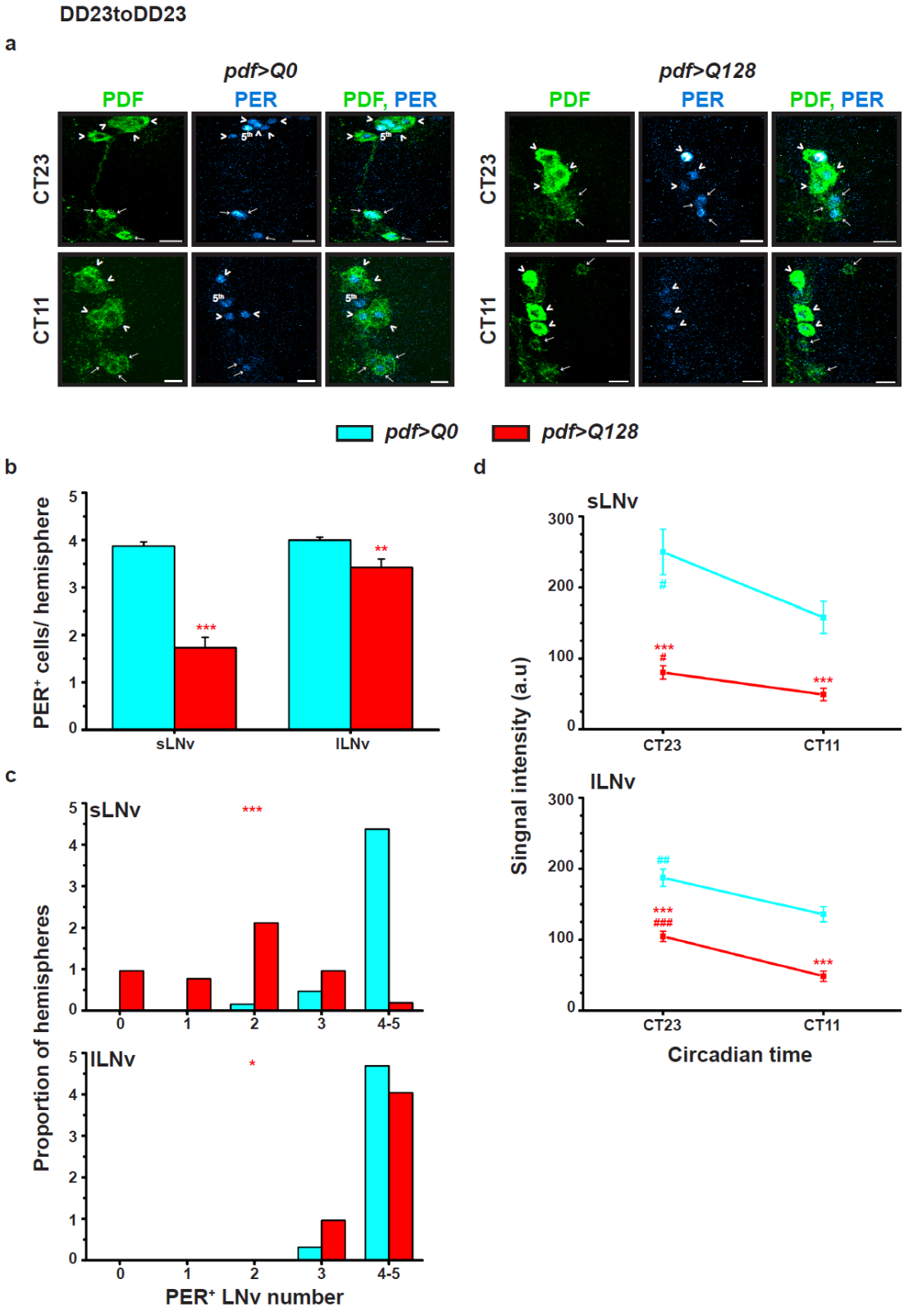

Figure 4.18

Fig 4. 18 The few PER⁺ sLNv soma of pdf>Q128 in DD23 exhibit low-amplitude PER oscillations.

(a) Representative images of 7d-old adult fly brains of *pdf>Q0* (left) and *pdf*>Q128 (right) in DD23 stained for PER (cyan hot) and PDF (green) in LNv at CT23 (top) and CT11 (bottom). sLNv soma (→ arrows), lLNv soma (> arrowheads) and PDF$^-$ PER$^+$ 5th sLNv are indicated. Scale bars are 10 µm. (b) The mean number of PER$^+$ sLNv soma and lLNv soma at CT23. * indicates age-matched differences between genotypes. (c) Frequency distribution of the proportion of hemispheres having 0 to 5 PER$^+$ LNv soma: sLNv soma (top) and lLNv soma (bottom) in 7d-old flies at CT23. * indicates significantly differing shapes of distribution between genotypes. (d) For the two genotypes, the quantification of PER intensity at CT23 and CT11 in sLNv (top) and lLNv (bottom). Differences between time points CT23 and CT11 are represented by # (cyan) for *pdf>Q0* and # (red) for *pdf>Q128*. Coloured * represents the difference between genotypes at that time point. Statistical significance is at single-symbol $p<0.05$, double-symbol $p<0.01$, triple-symbol $p<0.001$. Error bars are SEM.

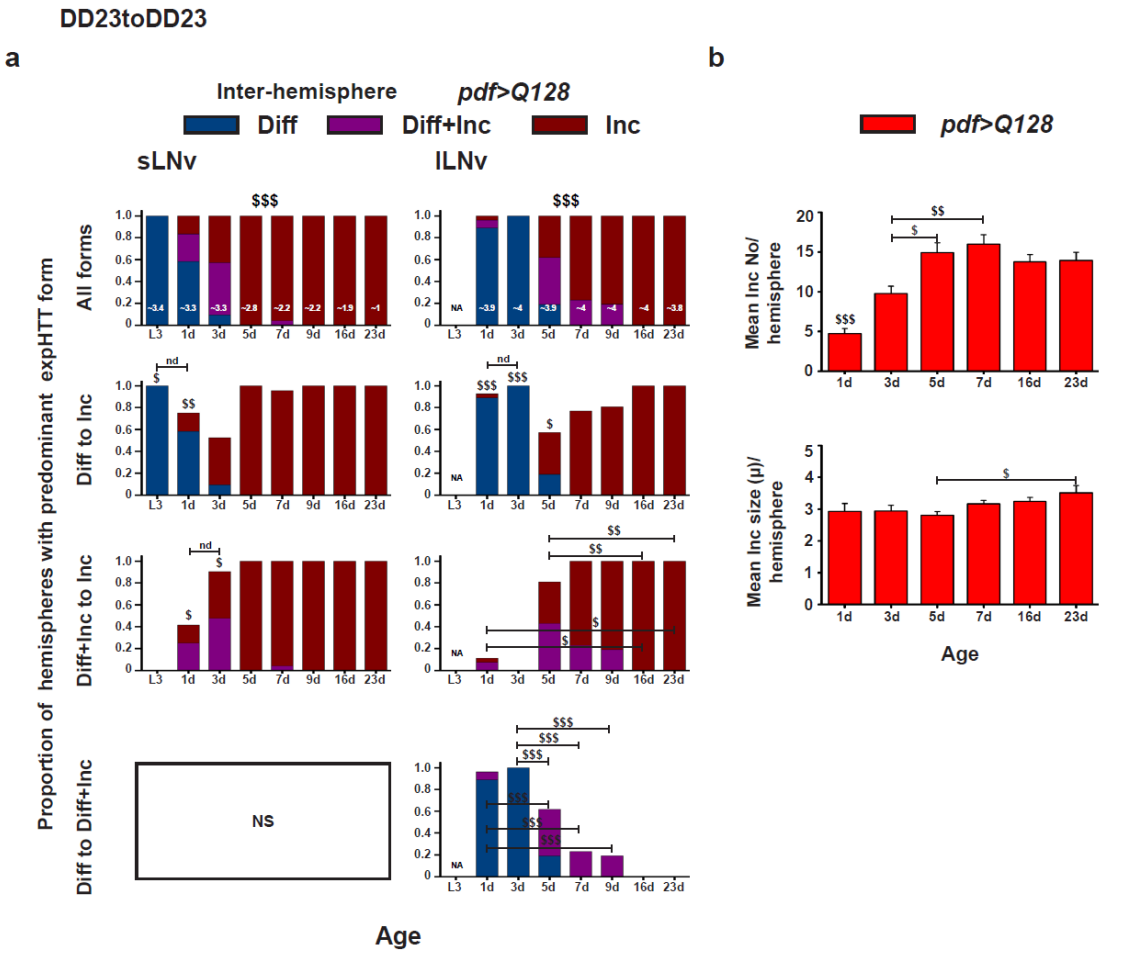

Figure 4.19

Fig 4. 19 Hemispheres of young pdf>Q128 are dominated by diff-enriched LNvs, which also have fewer inclusions than older flies.

(a) The proportion of hemispheres dominated by different expHTT forms in sLNv (left) or lLNv (right) is plotted against age for *pdf>Q128* in DD23toDD23 to describe the between-hemispheres distribution of predominant expHTT forms. These are plotted for all expHTT forms (top) or significantly different pair-wise comparisons (second, third, and bottom rows). $ indicates significant changes in the relative proportions of hemispheres across age for all expHTT forms (top) or pair-wise expHTT forms between specific ages (second, third, bottom rows). NA, not applicable; NS, not significant; nd, not different.

At the bottom of some bars, numbers represent the mean number of PDF^+ LNv detected at that age. (b) Comparison of mean inclusion number per hemisphere (top) and mean inclusion size per hemisphere (bottom) for *pdf>Q128* in DD23 across age. Significant differences between ages are $ $p<0.05$, $$ at $p<0.01$ and $$$ $p<0.001$. Error bars are SEM.

4.3.9 Exposure of *pdf>Q128* to constant warm temperatures rescues early-age behavioural arrhythmicity and PDF loss from the sLNv and improves activity consolidation over an extended duration

pdf>Q128 experiencing relatively warm constant temperature of 29°C in DD during development and as adults were rhythmic in AW1 and comparable to all controls (Fig 4.20 a, b). However, in the successive AWs, they had lower rhythmicity than controls, and their rhythmicity decline considerably decreased compared to AW1. A significant improvement in the extent of activity consolidation of *pdf>Q128* across age, like most controls (Fig 4.20 c), is also evidence for DD29-moderated enhancement of *pdf>Q128*'s activity rhythms. However, the rhythmic *pdf>Q128* flies still had weaker rhythms than at least one relevant control across AWs (Fig 4.20 d) and near 24h periods like most controls (Fig 4.20 e). Thus, exposure to warm temperatures restores early-age rhythmicity and improves activity consolidation over longer durations without improving rhythm robustness.

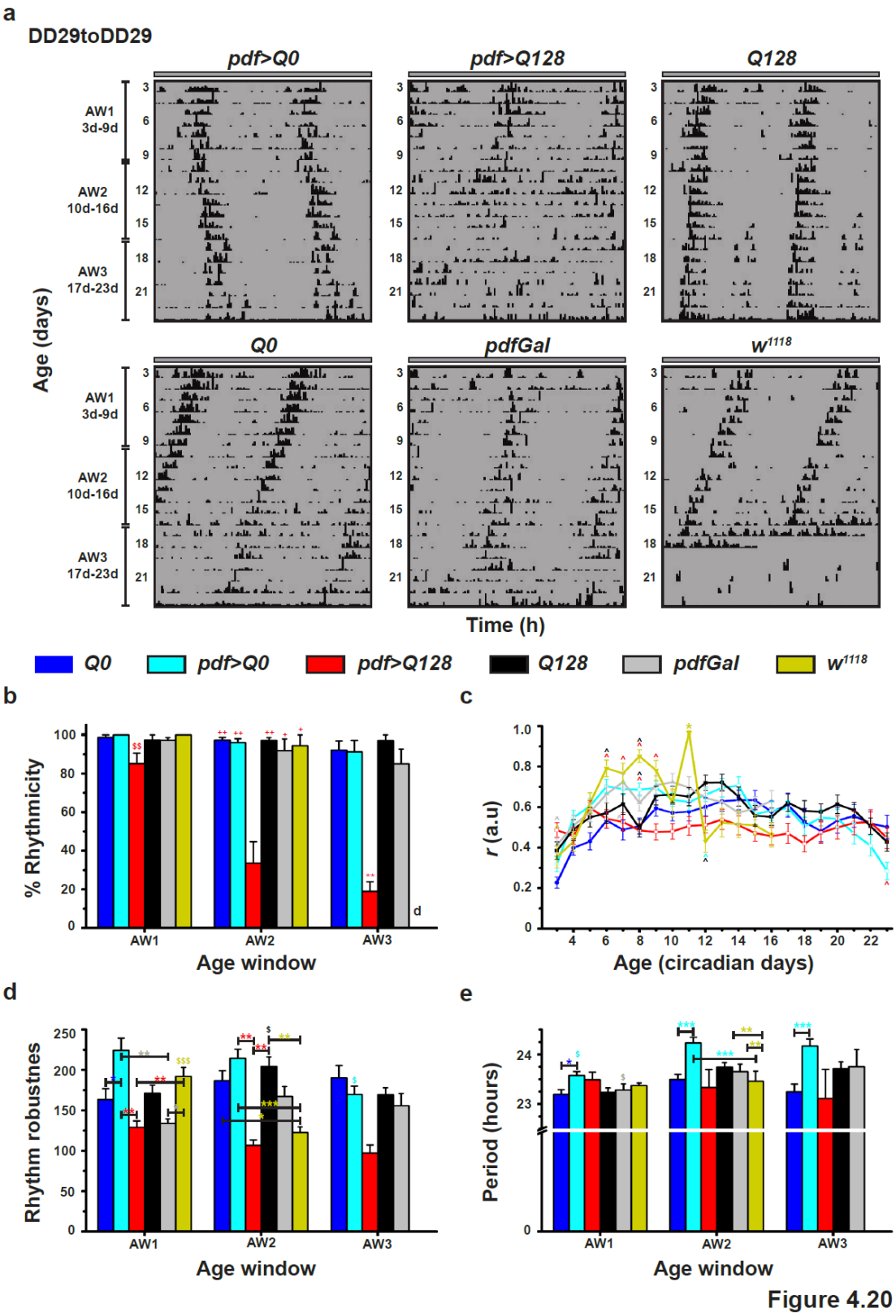

Figure 4.20

Fig 4. 20 pdf>Q128 flies in DD29 are rhythmic during the early age window and show improved activity consolidation across AWs.

(a) Representative double-plotted actograms for adult flies in DD29 showing activity data for 21d (age 3d-23d). All other details are the same as in Fig 4.1. (b-c) The percentage rhythmicity (b), the extent of activity consolidation '*r*' (c), the mean rhythm robustness (d) and the mean period (e) are plotted against AWs (or age for '*r*'). Symbols represent statistically significant differences: coloured * of that coloured genotype from all others or indicated ones and coloured $ differences between AWs for that coloured genotype at single $p<0.05$, double $p<0.01$ and triple $p<0.001$. Only in the rhythmicity plot (b) does the red + near the error bars of genotypes in AW2 indicate that those genotypes differ significantly from *pdf>Q128*. Coloured ^ near an error bar of a data point indicates a difference between the respective-coloured genotype and the data-point genotype. d represents that most flies are dead. Since very few *pdfGal* and w^{1118} survived in AW3, these are not included in the AW3 statistical analyses and are absent in the '*r*' representation between 17d and 23d. Most *pdf>Q128* flies in AW3 were arrhythmic, and the genotype is excluded from the robustness and period statistics for AW3. Error bars are SEM.

pdf>Q128 in DD29 exhibited *control-like* PDF^+ sLNv soma numbers at L3 and 1d, post-which the numbers between genotypes differed significantly (Fig 4.21a, b left). The numbers at 16d and 23d were significantly lower than L3 and 1d (Fig 4.21b left). Notably, though the shapes of the PDF^+ sLNv soma frequency distribution differed between genotypes in most older flies: *pdf>Q128* distribution was left-skewed up to 9d with ~ ≥85% of the hemispheres having ≥ 3 PDF^+ sLNv soma (Fig 4.22 left), differing significantly from those at later ages (≥ 3 PDF^+ sLNv: ~54% at 16d and 33% at 23d, $p<0.05$, Fisher's exact tests with BH procedure; distribution right-skewed at 23d). The PDF^+ lLNv numbers and shapes of their distributions were comparable between genotypes at most ages (Figs 4.21a, b right, 4.22 right). Thus, exposure of *pdf>Q128* to DD29 restores PDF in the sLNv of the young.

The proportion of *pdf>Q128* hemispheres in DD29 dominated by an expHTT form in LNv changes significantly from Diff and Diff+Inc enriched to exclusively Inc enriched with age (Fig 4.23a top). The hemispheres have predominantly Diff-enriched LNv up to 1d, decreasing significantly with age with a concomitant increase in Inc-enriched LNv (Fig 4.23a middle). The proportion of hemispheres with Diff+Inc-enriched relative to Inc-enriched sLNv also decreased at 3d compared to 1d (Fig 4.23a bottom).

The expHTT inclusions of *pdf>Q128* in DD29 at 16d and 23d were significantly higher than 1d, 3d, and 5d (Fig 4.23b top). The inclusion sizes did not vary with age (Fig 4.23b bottom).

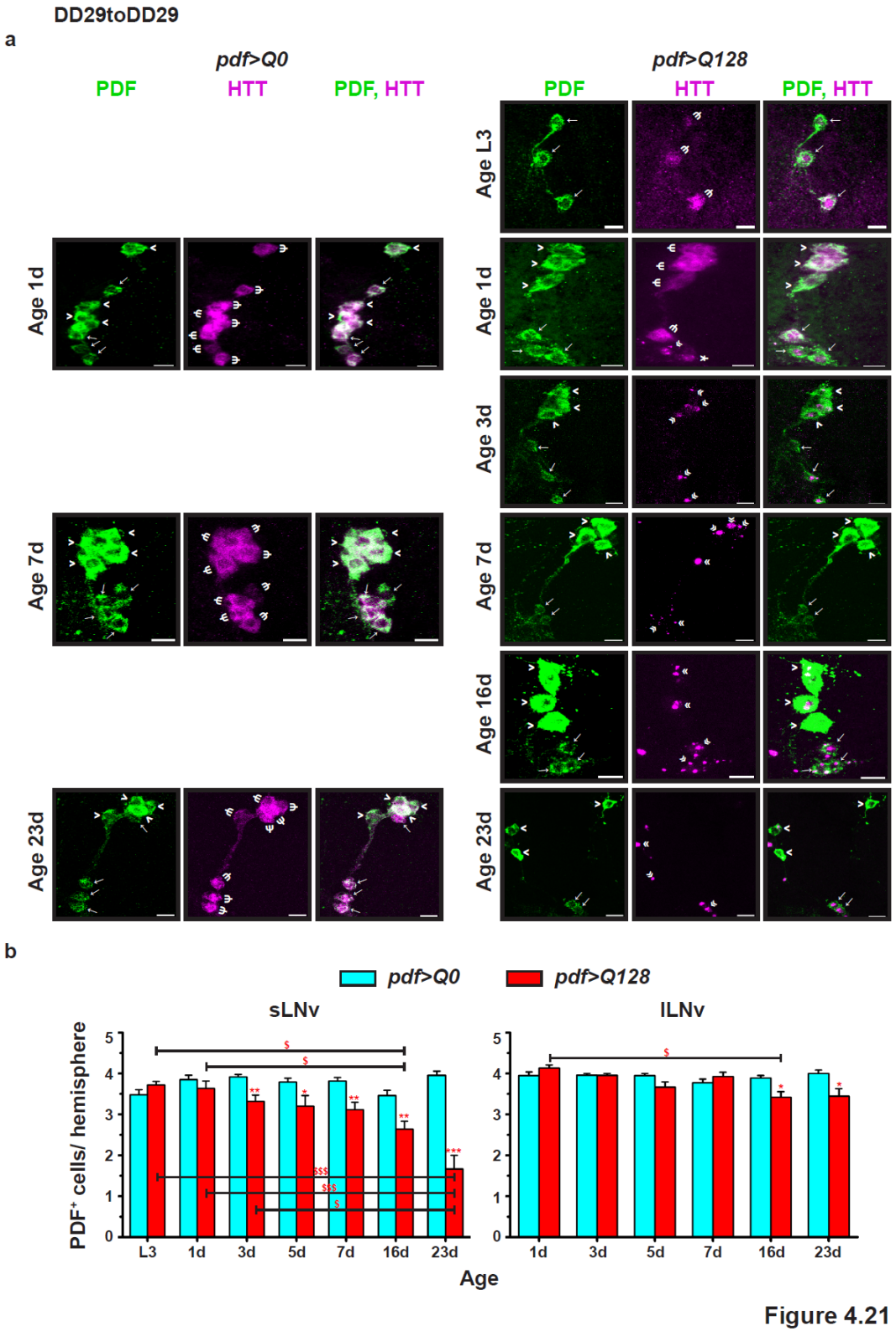

Figure 4.21

Fig 4. 21 Exposure of pdf>Q128 to DD29 slows the loss of PDF from the sLNv soma.

(a) Representative images of the adult fly brains under DD29toDD29 stained for PDF (green) and HTT (magenta) in LNv at 1d, 7d and 23d for *pdf>Q0* (left panel-sets) and at L3, 1d, 3d, 7d, 16d and 23d for *pdf>Q128* (right panel-sets). Indicated in the images are sLNv soma (→ arrows), lLNv soma (> arrowheads), diffuse expHTT (Ψ psi), diffuse+inclusions expHTT (Ɏ), and expHTT inclusions (« double arrowheads). Scale bars are 10 µm. (b) The mean number of PDF^{+} sLNv soma

(left) and lLNv soma (right) across age. Coloured symbols indicate significant differences, * for age-matched, inter-genotype differences and $ for differences between ages of the corresponding-coloured genotype at * $p<0.05$, ** $p<0.01$, *** $p<0.001$. nd, not different. Error bars are SEM.

Fig 4. 22 The distribution of PDF$^+$ sLNv soma numbers of pdf>Q128 differs from that of pdf>Q0

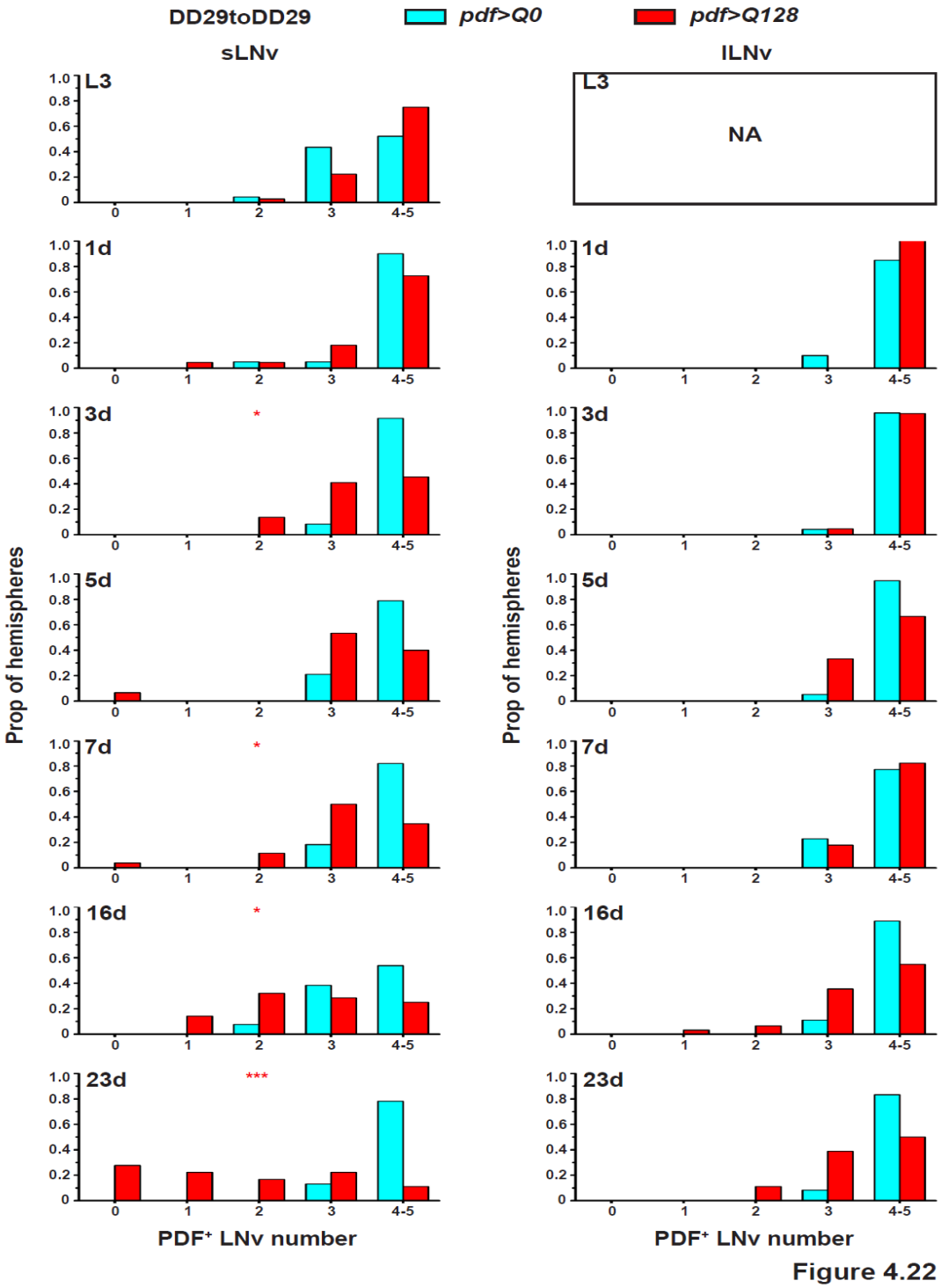

Figure 4.22

only at later ages under DD29.

Frequency distribution of the proportion of hemispheres of *pdf>Q0* and *pdf>Q128* in DD29toDD29 with 0 to 5 PDF$^+$ LNv soma numbers (sLNv - left and lLNv - right). Coloured * indicates significantly different distribution shapes between age-matched genotypes at $p<0.05$. NA, not applicable.

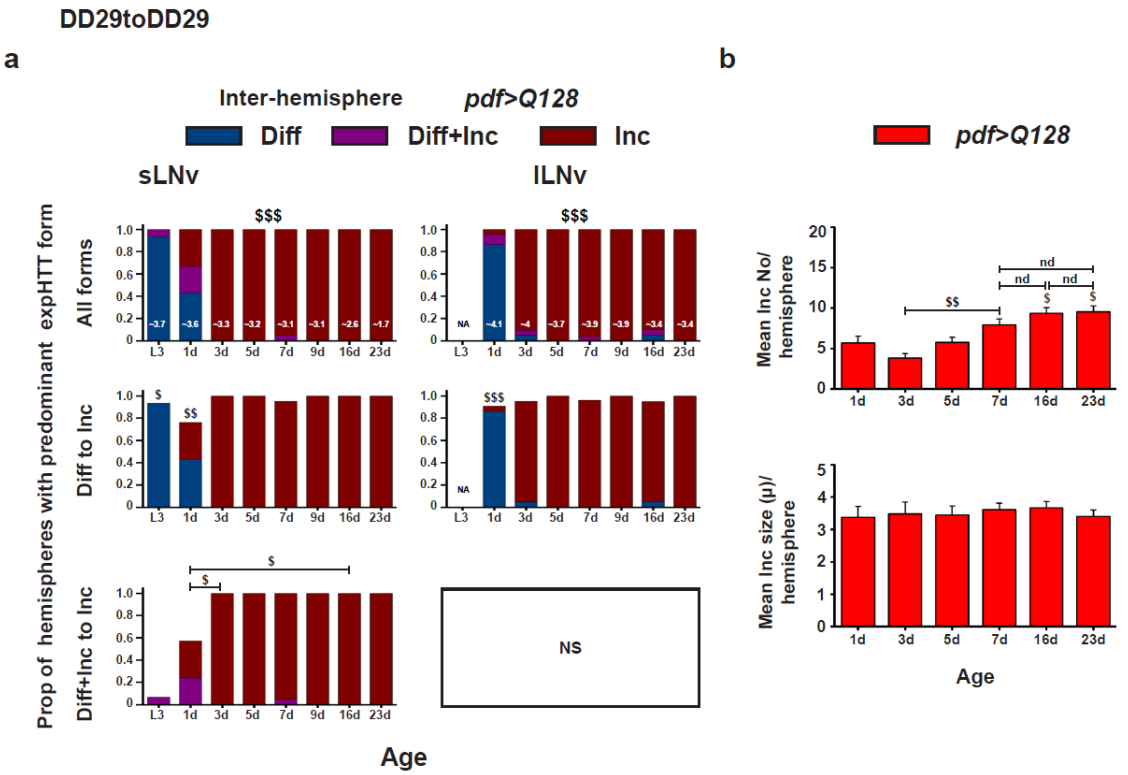

Figure 4.23

Fig 4. 23 Hemispheres of pdf>Q128 in DD29 are entirely dominated by inclusion-enriched LNv from age 3d and show increased inclusions with age.

(a) The proportion of hemispheres dominated by different expHTT forms in sLNv (left) or lLNv (right) is plotted against age for *pdf>Q128* in DD29toDD29 to describe the between-hemispheres distribution of predominant expHTT forms. These are plotted for all expHTT forms (top) or significantly different pair-wise comparisons (middle and bottom). $ indicates significant changes in the relative proportions of hemispheres across age for all expHTT forms (top) or pair-wise expHTT forms between specific ages (middle and bottom). NA, not applicable; NS, not significant. At the bottom of some bars, numbers represent the mean number of PDF$^+$ LNv detected at that age. (b) Comparison of mean inclusion number per hemisphere (top) and mean inclusion size per hemisphere (bottom) for *pdf>Q128* in DD29 across age. Significant differences between ages are $ $p<0.05$, $$ at $p<0.01$ and $$$ $p<0.001$. nd, not different. Error bars are SEM.

4.3.10 Warm temperatures improve the early-age rhythmicity of *pdf>Q128* by enabling a large proportion of the daily activity within a limited time window.

The rhythm characteristics of flies in DD23, DD25, and DD29 were studied to evaluate the impact of constant ambient temperatures on expHTT-induced changes in activity rhythms. During AW1, the rhythmicity of *pdf>Q128* in DD29 was noticeably higher than in DD23 and DD25 (Fig 4.24a middle). However, their rhythmicity declined significantly in AW2, becoming comparable to those in DD23 and DD25. The controls had comparable rhythmicities and rhythm robustness between regimes (Fig 4.24a, c). *pdf>Q128* in DD29 also had significantly higher activity consolidation than those in DD23 and DD25 across age. The improved '*r*' of *pdf>Q128* can be primarily attributed to warm temperatures improving the activity consolidation across the board since even controls in DD29 showed more significant activity consolidation than their counterparts in DD23 and DD25 (Fig 4.24b). Also, *pdf>Q128* in DD23 showed even poorer activity consolidation than those in DD25 between 8d-17d (Fig 4.24b middle), suggesting that **in terms of activity rhythms, the effect of temperature in mitigating expHTT-induced neurotoxicity is DD29>DD25>DD23.** The period of control flies in AW1 was significantly shorter in DD29 than in DD23 and DD25 (Fig 4.24d). This observation suggests an under-compensation of the free-running period to temperature changes.

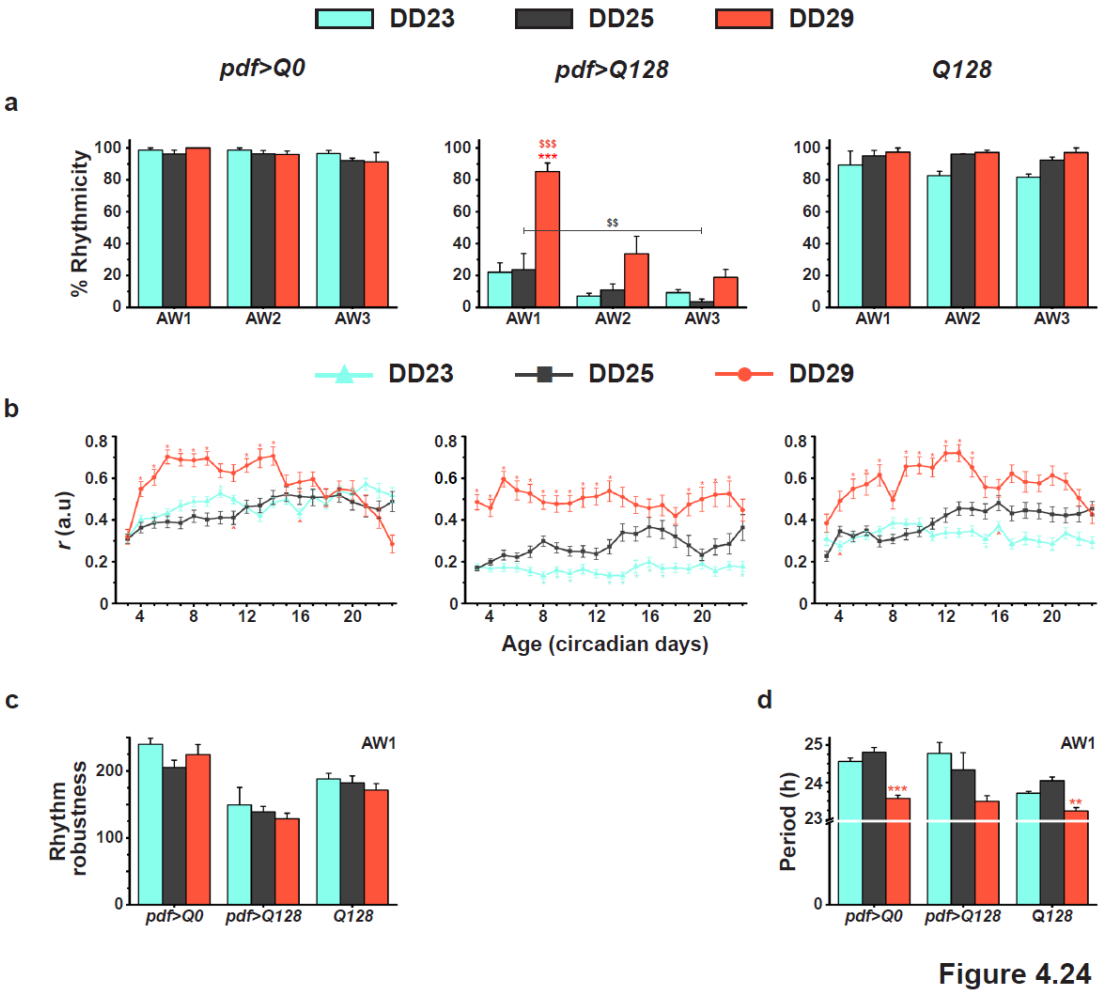

Figure 4.24

Fig 4. 24 pdf>Q128 in warm temperatures shows improved early-age rhythmicity and activity consolidation than at lower temperatures.

(a-c) The between-regime comparisons of the mean percentage rhythmicity (a), the mean activity consolidation '*r*' (b), the mean rhythm robustness in AW1(c) and the mean period in AW1 (d) plotted against AWs (or age). Symbols represent statistically significant differences: coloured * of that coloured regime from all others or indicated ones for a genotype and coloured $ for between-AW comparisons of a genotype for that regime. For '*r*', coloured ^ near an error bar of a data point indicates a difference of the respective-coloured regime from the data-point regime. Regime colour codes: cyan, DD23; dark grey, DD25; rust, DD29. The number of symbols represents statistical significance: single $p<0.05$, double $p<0.01$ and triple $p<0.001$. Error bars are SEM.

4.3.11 Constant warm or cool temperatures offer better protection against loss of circadian proteins from the LNv of *pdf>Q128* than the constant ambient temperatures of 25°C

Next, the LNv cellular features of *pdf>Q128* in the three constant temperature regimes were compared. *pdf>Q128* in DD25 had significantly fewer PDF$^+$ sLNv soma than those in DD23 and DD29 at 1d and 3d (Fig 4.25a left). Those in DD29 had significantly higher numbers than DD23 at 7d and 9d. Importantly, DD23 and DD25 differed at 1d, 3d and 23d, with fewer numbers in DD23 at 1d and 3d and greater at 23d. In the shapes of the distribution of PDF$^+$ sLNv soma numbers also, DD25 differed from both DD23 and DD29 at 1d and 3d (Fig 4.25b right), with ~50% of hemispheres of *pdf>Q128* in DD25 having 0-2 PDF$^+$ sLNv, contrasting from ~10% significantly in DD23 and DD29 (p<0.01, Fisher's exact tests and BH procedure). Thus, neuroprotection by the rescue of **PDF in sLNv soma** follows the order **DD29>DD23>DD25**. The PDF$^+$ lLNv soma numbers and their distribution shapes are comparable across regimes (Fig 4.25a right, b right).

The PER$^+$ sLNv soma numbers of *pdf>Q128* in DD23 were similar to those in DD25 (Fig 4.25c). However, *pdf>Q128* in DD23 had higher PER$^+$ lLNv soma numbers than in DD25. The shapes of the PER$^+$ LNv distributions did not differ between DD23 and DD25 (Fig 4.25d, bottom sets). Thus, for PER$^+$ sLNv DD23=DD25, while concerning PER$^+$ lLNv DD23>DD25. Considering that PER in LNv of *pdf>Q128* in DD23 oscillated (Fig 4.18), but not of those in DD25, overall, for **PER sustenance in the LNv**, **DD23>DD25**.

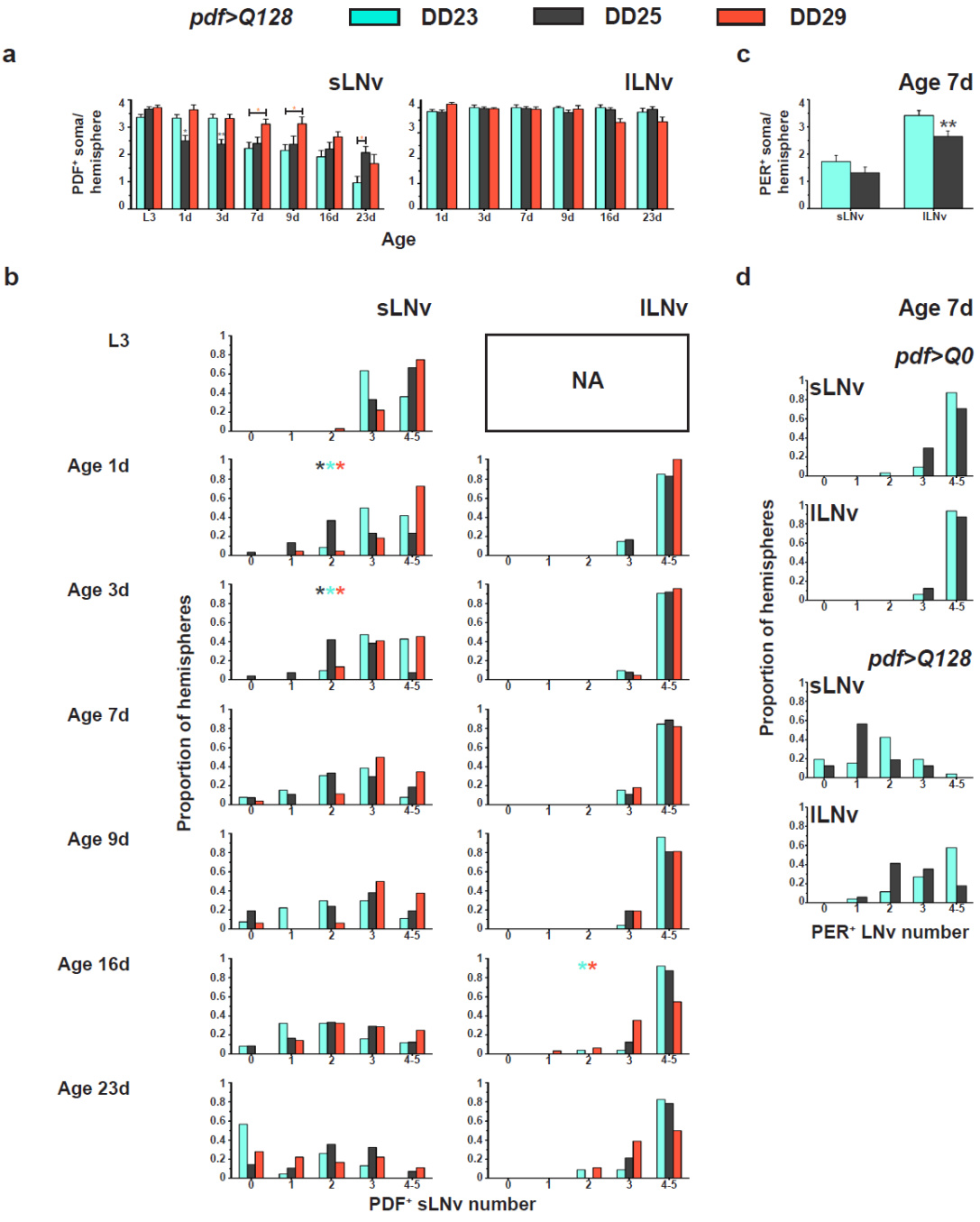

Figure 4.25

Fig 4. 25 pdf>Q128 in relatively warm or cooler temperatures show improvements in PDF⁺ and PER⁺ LNv numbers.

(a) The mean number of PDF⁺ sLNv soma (left) or lLNv soma (right) across age comparing *pdf>Q128* maintained in the constant temperature regimes of DD23, DD25 and DD29. (b) Frequency distribution of the proportion of hemispheres of *pdf>Q128* with 0 to 5 PDF⁺ LNv soma numbers (sLNv - left and lLNv - right) in the three regimes across age. NA, not applicable. Coloured multiple * indicates significantly different distribution shapes between regimes, with the first colour of the reference regime and the subsequent colours of regimes differing from the reference at $p<0.05$.

(c) The mean number of PER^+ LNv soma numbers in 7d-old *pdf>Q128* in DD23 and DD25. (d) Frequency distribution of the proportion of hemispheres of *pdf>Q0* (top-sets) or *pdf>Q128* (bottom-sets) with 0 to 5 PDF^+ LNv soma numbers (sLNv - top and lLNv - bottom) in DD23 and DD25. * indicates significantly differing distribution shapes at ** at $p<0.01$ and *** $p<0.001$. Coloured * indicates a significant difference between that regime and all other regimes or indicated regimes at * $p<0.05$, ** at $p<0.01$ and *** $p<0.001$. Error bars are SEM.

4.3.12 *pdf>Q128* show a temperature-dependent decrease in the expHTT inclusion load

The expHTT forms and includes features of *pdf>Q128* under the three constant temperature regimes were also compared. Diff-enriched LNv dominated most hemispheres of *pdf>Q128* across regimes DD23, DD25 and DD29 at L3 (for sLNv) (Fig 4.26a top-left) and at 1d (for lLNv) (Fig 4.26b top-left). The proportion of hemispheres dominating different expHTT forms in LNv differed significantly between regimes at 1d and 3d for sLNv and 3d and 5d for lLNv (Fig 4.26a top, b top).

pdf>Q128 in DD23 and DD29 had a greater proportion of Diff-enriched sLNv relative to Inc-enriched than those in DD25 at 1d (Fig 4.26a middle). ~20% of the hemispheres in DD23 and DD29 also had Diff+Inc-enriched sLNv at 1d which was absent from those under DD25, where all hemispheres were dominated by Inc-rich sLNvs (Fig 4.26a bottom). DD23 also ensured a longer presence of hemispheres with Diff+Inc-enriched sLNv, and their proportion relative to the hemispheres of Inc-enriched sLNv was different from the completely Inc-rich DD25 and DD29 at 3d (Fig 4.26a bottom).

In contrast to the domination by Diff and Diff+Inc expHTT forms in the sLNv of 1d *pdf>Q128* flies in DD29, the lLNv of 3d flies in DD29 were dominated by Inc (Fig 4.26a top-second panel, b top-second panel). The proportion of hemispheres of Inc-enriched lLNv relative to Diff-enriched (or Diff+Inc-enriched lLNv) in DD29 was significantly higher than those in DD23 and DD25 at 3d (Fig 4.26b second-column). DD23, on the other hand, still favoured Diff-enriched lLNv at 3d, with its hemisphere proportions relative to hemispheres of Inc-enriched lLNv (or Diff+Inc-enriched lLNv) being more remarkable than those in DD25 (Fig 4.26b second-column). Even at 5d, the proportion of hemispheres of Inc-enriched lLNv relative to Diff-enriched lLNv was significantly lower in DD23 than those in DD25 and DD29, the latter being similar (Fig 4.26b

third-column). The trend seen at DD23 with expHTT forms in sLNv was also seen with lLNv with a prolonged presence of Diff+Inc form (Fig 4.26b top), the proportion of their hemispheres relative to hemispheres of Inc-enriched lLNv in DD23 being significantly greater than those in DD29 at 5d (Fig 4.26b third row). DD25 was placed intermediary to DD23 and DD29 with the proportion of hemispheres of Diff-enriched lLNv relative to Diff+Inc-enriched lLNv being significantly lower than DD23 at 3d (Fig 4.26b second-column bottom), and the proportion of hemispheres of Inc-enriched lLNv relative to Diff+Inc-enriched lLNv being significantly lower than DD29 at 3d and comparable at 5d (Fig 4.26b third-column third-row).

Regarding the predomination of the three expHTT forms in the LNv (Diff *vs* Diff+Inc *vs* Inc), since DD25 and DD29 have slightly contrasting effects on sLNv versus lLNv at 3d, the regime effects on prolonging Diff form is DD23>DD25=DD29.

The expHTT inclusion numbers were significantly higher in *pdf>Q128* in DD23 than those in DD25 and DD29 from 5d upwards (Fig 4.26c left). In contrast, DD29 had fewer inclusions than those in DD25 from 3d to 7d. Inclusion sizes were nearly similar between regimes across ages (Fig 4.26c right). Thus, regarding decreasing inclusion numbers, DD29>DD25>DD23.

Even though Diff- and Diff+Inc-enriched LNv dominated the hemispheres of young *pdf>Q128* in DD23, the few LNv and the area near the LNv seem to have enough inclusions contributing to the significantly higher inclusion numbers in those under DD23 than those in other regimes. The enhanced numbers persist in older flies in DD23 (Fig 4.26c left). In contrast, despite the hemispheres of 3d *pdf>Q128* having almost entirely Inc-rich lLNv, across most ages, these flies had overall fewer inclusions than those in DD23 and even compared to those in DD25 till 7d of age. In summary, these observations suggest that, for **reducing the expHTT inclusion load**, **DD29>DD25>DD23**.

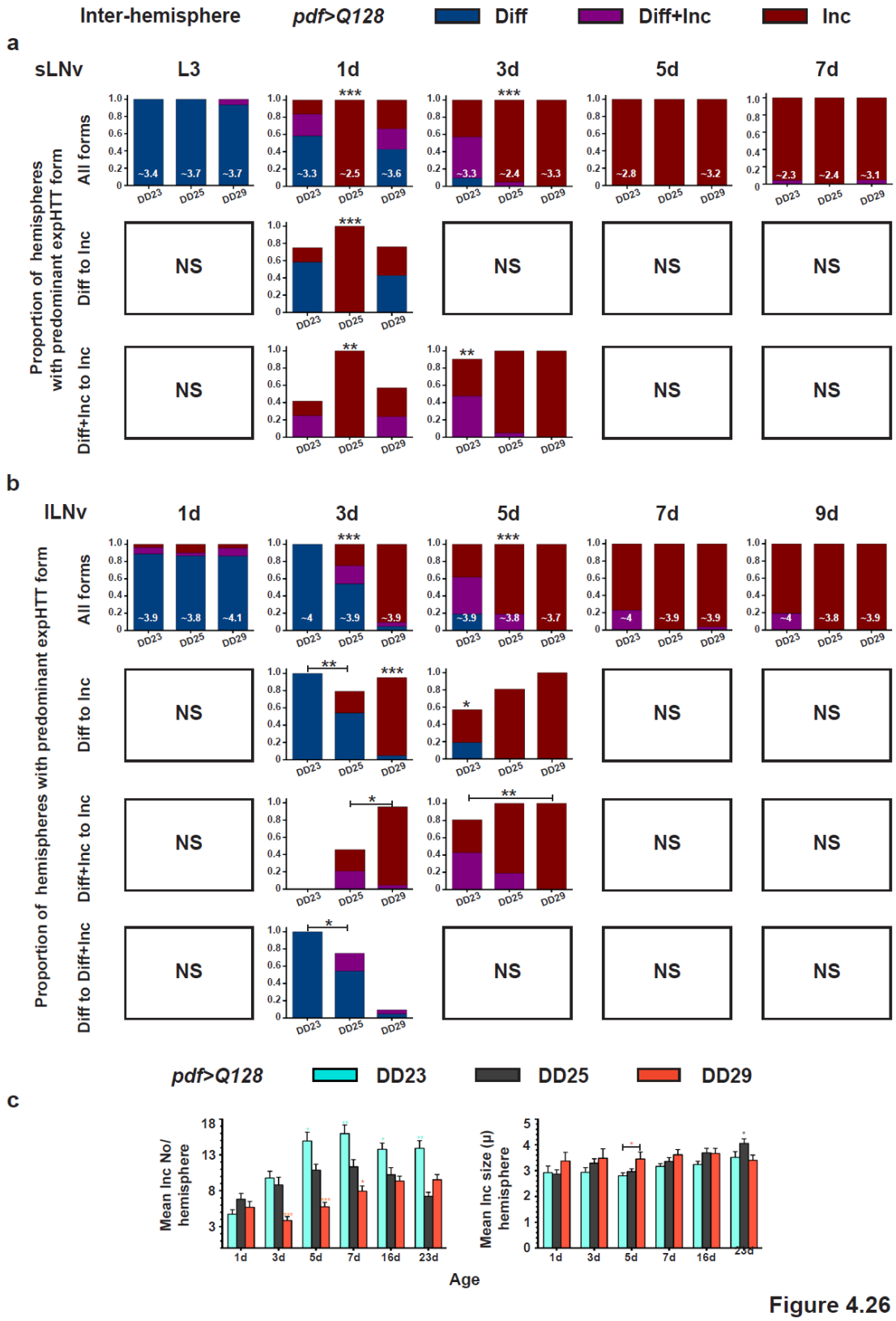

Figure 4.26

Fig 4. 26 pdf>Q128 shows a temperature-dependent gradation in the relative proportion of hemispheres enriched with different expHTT forms in the lLNv and inclusion numbers, but in opposite directions.

(a) and (b) The proportion of hemispheres dominated by different expHTT forms in sLNv (a) or lLNv (b) is plotted for *pdf>Q128* comparing constant temperature regimes DD23, DD25 and DD295 at various ages. These are plotted for all expHTT forms (top) or significantly different pair-wise comparisons (a - middle and bottom, b - second, third and bottom rows). * indicates significant changes in the relative proportions of hemispheres for all expHTT forms between regimes for an age (top) or pair-wise expHTT forms between regimes for an age (a - middle and bottom, b - second, third and bottom rows). NS, not significant. At the bottom of some bars, numbers represent the mean number of PDF^+ LNv detected for that regime at that age. (c) Comparison of mean inclusion number per hemisphere (left) and mean inclusion size per hemisphere (right) between the three regimes across age for *pdf>Q128*. Significant differences between regimes for each age are at * $p<0.05$, ** at $p<0.01$ and *** $p<0.001$. Error bars are SEM.

4.3.13 Light/dark cycles during development intensify the effects of constant temperatures on the activity rhythms of *pdf>Q128* adults

I then asked whether developmental exposure to light/dark cycles affects the activity rhythms of *pdf>Q128* flies as adults in DD under constant temperatures (cool, 23°C and warm, 29°C). Despite LD during development, *pdf>Q128* flies experiencing cooler temperatures of 23°C were arrhythmic across AWs (Fig 4.27a top, b), and their activity consolidation was significantly lower than most controls, except *Q128*, which also had significantly lower '*r*' than controls (Fig 4.27c). *Q128* also had weaker rhythms than controls (Fig 4.27d).

Like their DD-counterparts, *pdf>Q128* in LD29toDD29 showed control-like high rhythmicity in AW1 (Fig 4.27a bottom, e), and their activity consolidation was also comparable to controls up to 7d of age (Fig 4.27f). However, the rhythmic *pdf>Q128* flies had reduced rhythm robustness compared to controls (Fig 4.27g). The rhythmicity (and '*r*') of *pdf>Q128* dropped significantly compared to controls in later AWs (and 8d upwards).

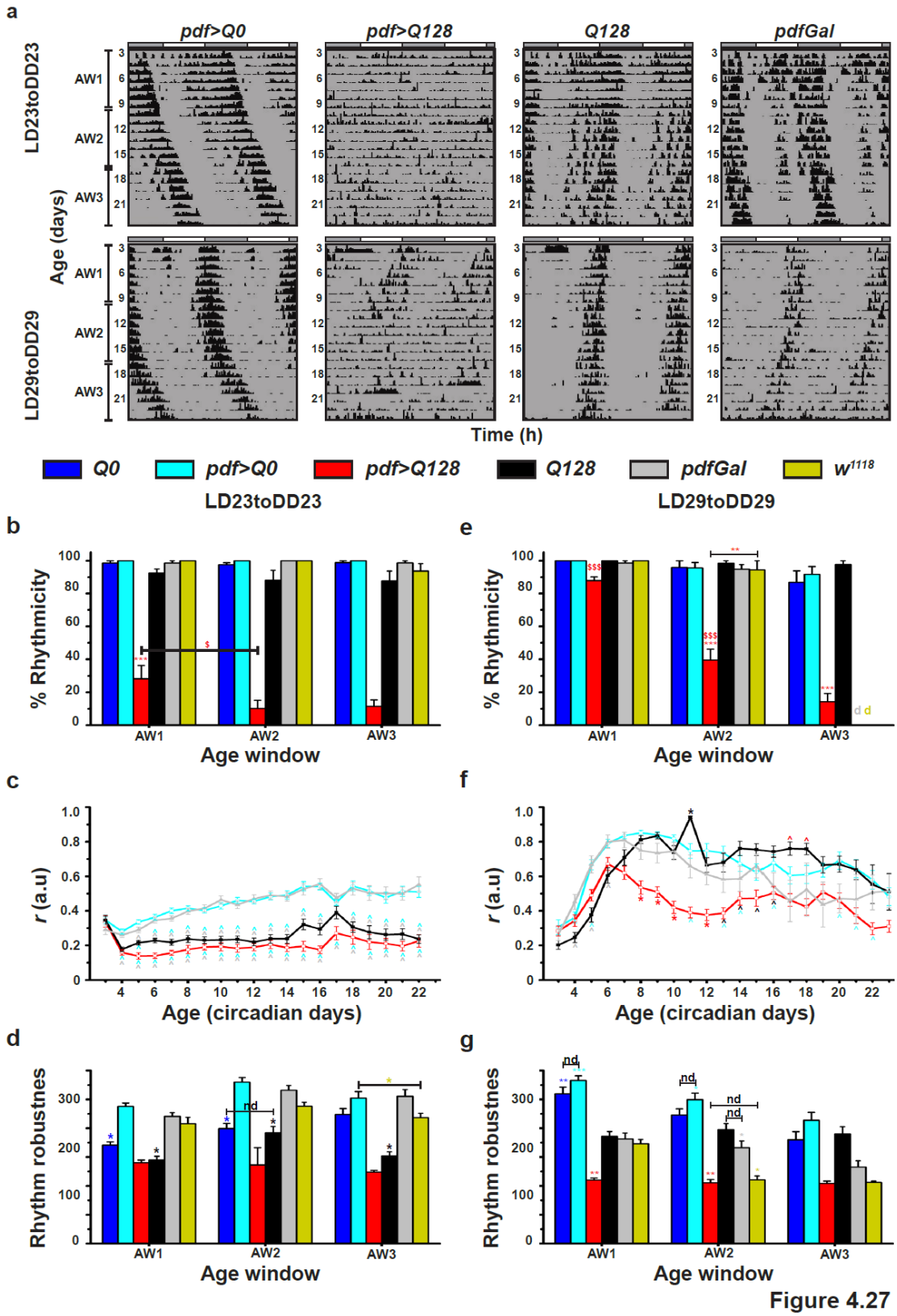

Fig 4. 27 pdf>Q128 flies in LD29toDD29 are rhythmic during the early age window but not those in LD23toDD23.

(a) Representative double-plotted actograms for adult flies in LD23toDD23 (top) and those in LD29toDD29 (bottom) showing activity data for 21d (age 3d-23d). Placed above the actograms are

grey and white bars depicting light/dark cycles during development. (b-g) Plots for mean rhythmicity (b, e), activity consolidation '*r*' (c, f), and mean robustness (d, g) for flies in LD23toDD23 (b, c, d) and those in LD29toDD29 (e, f, g). *pdf>Q128* across AWs in LD23toDD23, *pdf>Q128* at AW3 in LD29toDD29, and *pdfGal* and w^{1118} are not included in statistical analyses of period and robustness. *pdfGal* and w^{1118} in AW3 (or ages 17-23d) are not included in the statistical analysis for DD29toDD29 due to most flies not surviving; d (in plot e) indicates that there are no surviving flies from the two genotypes in AW3 across experiments. All other details are like Fig 4.1 and 4.6.

Comparing *pdf>Q128* in DD with those in LD, those in DD23 and DD29 were nearly indistinguishable from those in LD23toDD23 and LD29toDD29, respectively, in terms of rhythmicity (Fig 4.28a middle, d middle), similar to how their controls behave between regimes (Fig 4.28a, d). The rhythmic *pdf>Q128* flies and controls *pdf>Q0* also had comparable robustness between regimes (for *pdf>Q128*, only between DD29 and LD29toDD29), while that of *Q128* was lower in LD23toDD23 than that of those in DD23 (Fig 4.28b, d). The activity consolidations of *pdf>Q128* between regimes were also comparable to a large extent (Fig 4.28c middle, f middle). Thus, under constant ambient temperatures, developmental LD does not affect the activity rhythms of *pdf>Q128* differentially. However, developmental exposure to LD for controls under cool temperatures resulted in poorer activity consolidation than those in darkness and vice-versa under warm temperatures (Fig 4.28c, f) (also the case with *pdfGal*). So, on the one hand, developmental LD further weakened the poor activity consolidation under cooler temperatures of 23°C. On the other hand, developmental LD further strengthened the high activity consolidation under warmer temperatures of 29°C. These observations suggest that developmental light augments the effects of constant temperatures on activity consolidation, furthering the cool-temperature-mediated diminishment of consolidation or the warm-temperature-mediated enhancement.

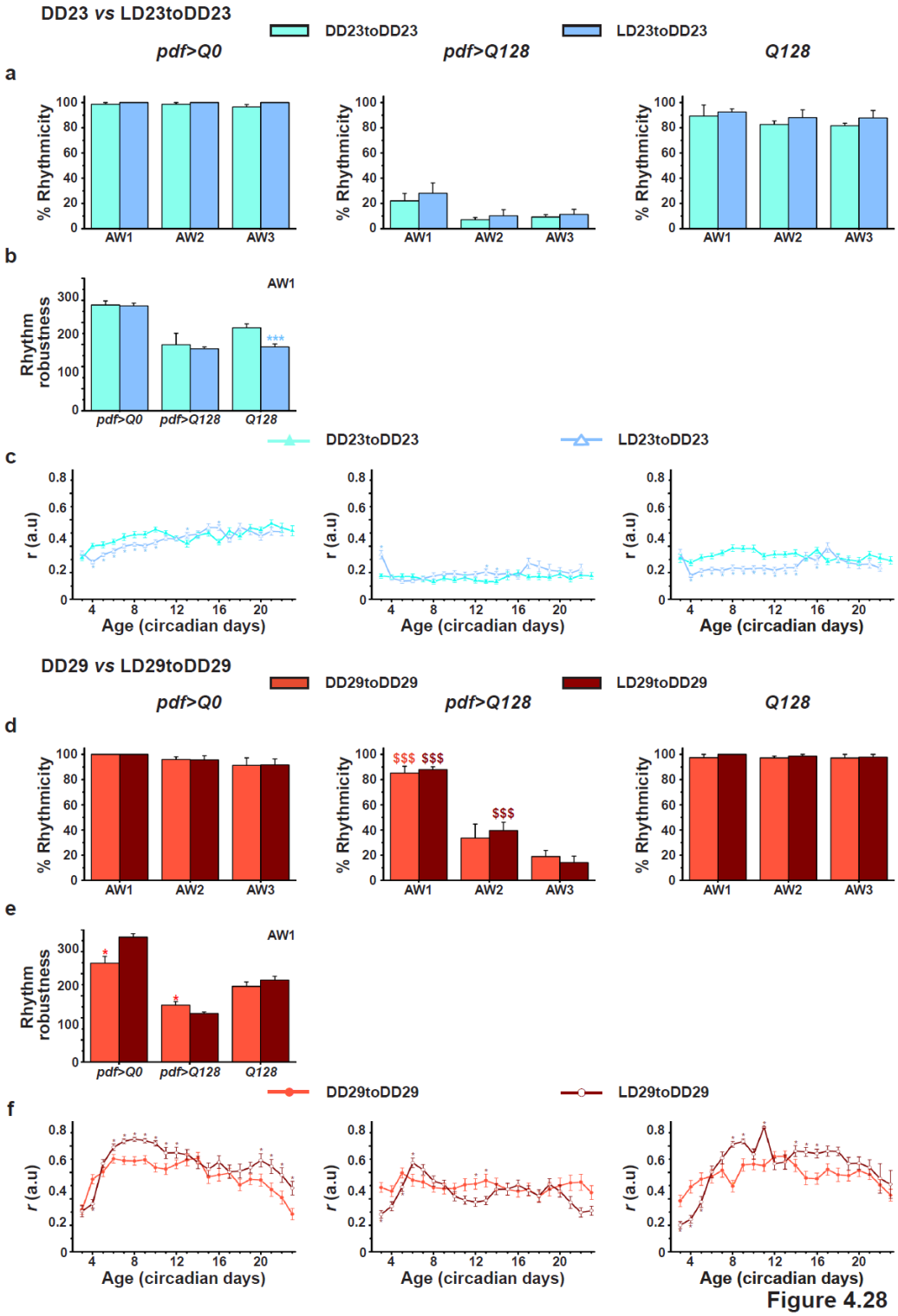

Figure 4.28

Fig 4. 28 Exposure of pdf>Q128 to light/dark cycles during development heightens the effects of constant warm or cool temperatures on its activity consolidation.

(a-f) The between-regime comparisons of the mean percentage rhythmicity across AWs (a, d), the mean rhythm robustness in AW1 (b, e) and the mean activity consolidation '*r*' across age (c, f) comparing DD23toDD23 with LD23toDD23 (a-c) and DD29toDD29 with LD29toDD29 (d - f). All other details are like Fig 4.7 and 4.24. Regime colour codes: cyan, DD23; blue, LD23toDD23; rust, DD29; brown, LD29toDD29.

4.3.14 Exposure of *pdf>Q128* to adult-specific, but not development-restricted constant warm temperatures restores the early-age activity rhythms and improves sLNv PDF

So far, we have seen that exposure of *pdf>Q128* to constant warm temperatures rescues early-age behavioural rhythmicity. Since the life stages of holometabolous insects are differentially sensitive to temperature, determine the degree of temperature acclimation response and affects the spontaneous activity levels (Kingsolver et al., 2011; MacLean et al., 2017), I investigated whether this rescue is dependent on the time at which flies experience warm temperatures. Specifically, I asked whether development-specific or adult-restricted warm temperature exposure is sufficient to rescue the activity rhythms of *pdf>Q128*.

pdf>Q128 flies in DD29toDD23 showed arrhythmic activity/rest across AWs (Fig 4.29a), with rhythmicity and activity consolidation being significantly lower than most controls (Fig 4.29b, c). Thus, development-specific exposure of *pdf>Q128* to warm temperatures does not rescue its arrhythmic activity rhythms as adults in DD23.

pdf>Q128 experiencing relatively warm constant temperature of 29°C in DD only as adults were rhythmic in AW1, like controls (Fig 4.30a,b). This rhythmicity was not sustained over later ages, where it declined significantly compared to AW1 and when compared to age-matched controls. For about 16d, *pdf>Q128* also showed activity consolidation like most controls (Fig 4.30c). At certain ages during AW2, w^{1118} and *pdfGal* showed significantly better consolidation than *pdf>Q128* and controls *Q128* and *Q0*. However, the rhythmic *pdf>Q128* flies in AW1 still had weaker rhythms than *pdf>Q0* and w^{1118} and those in AW2 than all controls (Fig 4.30d). Rhythmic *pdf>Q128* flies in AW1 had >24h periods, significantly longer than *Q128* and w^{1118} (Fig 4.30e). Thus, exposure to warm temperatures only as adults rescues free-running activity rhythms of *pdf>Q128* by restoring its early-age rhythmicity and activity consolidation (over a prolonged duration), but not rhythm robustness.

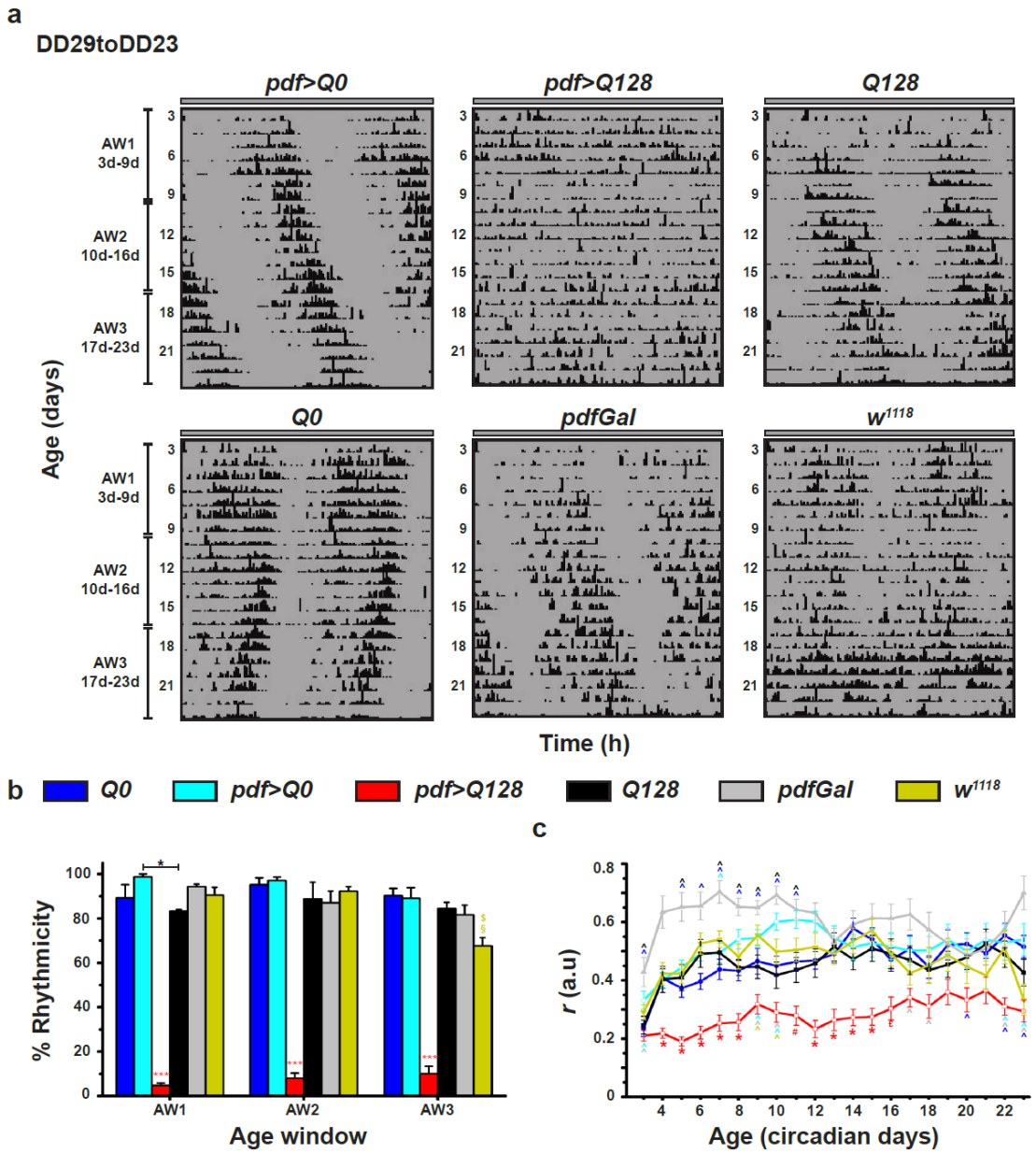

Figure 4.29

Fig 4. 29 pdf>Q128 flies in DD29to23 are arrhythmic and show poor activity consolidation.
(a) Representative double-plotted actograms for adult flies in DD23 showing activity data for 21d (age 3d-23d). All other details are the same as in Fig 4.1. Symbols represent statistically significant differences: coloured * of that coloured genotype from all others, coloured # of that genotype from all others except *Q128*, coloured £ from other genotypes except *Q0*, coloured § from all others except *pdfGal*, and coloured $ between AWs for a genotype. Coloured ^ near an error bar of a data point indicates a difference between the respective-coloured genotype and the data-point genotype. The number of symbols represents statistical significance: single $p<0.05$, double $p<0.01$ and triple $p<0.001$. Error bars are SEM.

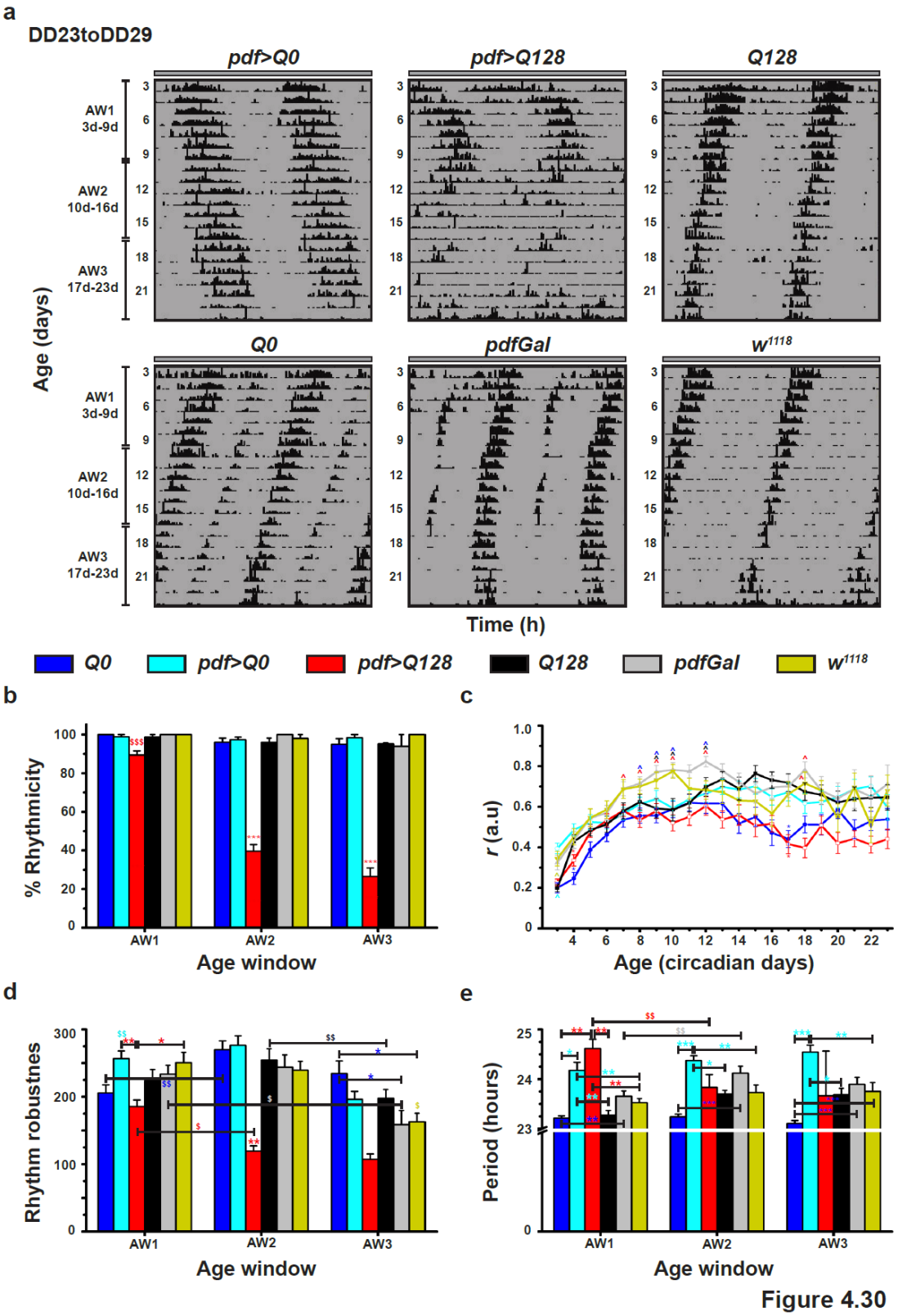

Figure 4.30

Fig 4. 30 pdf>Q128 flies in DD23to29 are rhythmic during the early age window with control-like activity consolidation.

(a) Representative double-plotted actograms for adult flies in DD29 showing activity data for 21d (age 3d-23d). All other details are the same as in Fig 4.1. Symbols represent statistically significant

difference: coloured * of that coloured genotype from all others or indicated ones and coloured $ differences between AWs for that coloured genotype at single $p<0.05$, double $p<0.01$ and triple $p<0.001$. Coloured ^ near an error bar of a data point indicates a difference between the respective-coloured genotype and the data-point genotype. Most *pdf>Q128* flies in AW3 were arrhythmic, and the genotype is excluded from the robustness (d) and period (e) statistics for AW3. Error bars are SEM.

Like *pdf>Q128* in DD29, those in DD23toDD29 had significantly reduced PDF^+ sLNv soma numbers than *pdf>Q0* from 3d upwards, but the mean was around three till 7d (Fig 4.31a, b left). The numbers at 16d and 23d were significantly diminished than earlier ages (Fig 4.31b left). The between-genotype differences were also observed in the shapes of PDF^+ sLNv distribution from 3d onwards (Fig 4.32 left). Like the *pdf>Q128* in DD29 (Fig 4.22), many hemispheres of those in DD23toDD29 also exhibited ≥3 PDF^+ sLNv up to 9d (>90% at 3d and 5d and ≥80% at 7d and 9d) (Fig 4.32left), which was different from the 25% hemispheres at 16d and 23d ($p<0.001$, Fisher's exact tests and BH procedure). The PDF^+ lLNv soma numbers and their distribution shapes were similar between genotypes across age (Figs 4.31a, b right, 4.32 right). Thus, adult-restricted exposure to high temperatures, following low developmental temperatures, suppresses PDF loss from the sLNv soma in young flies.

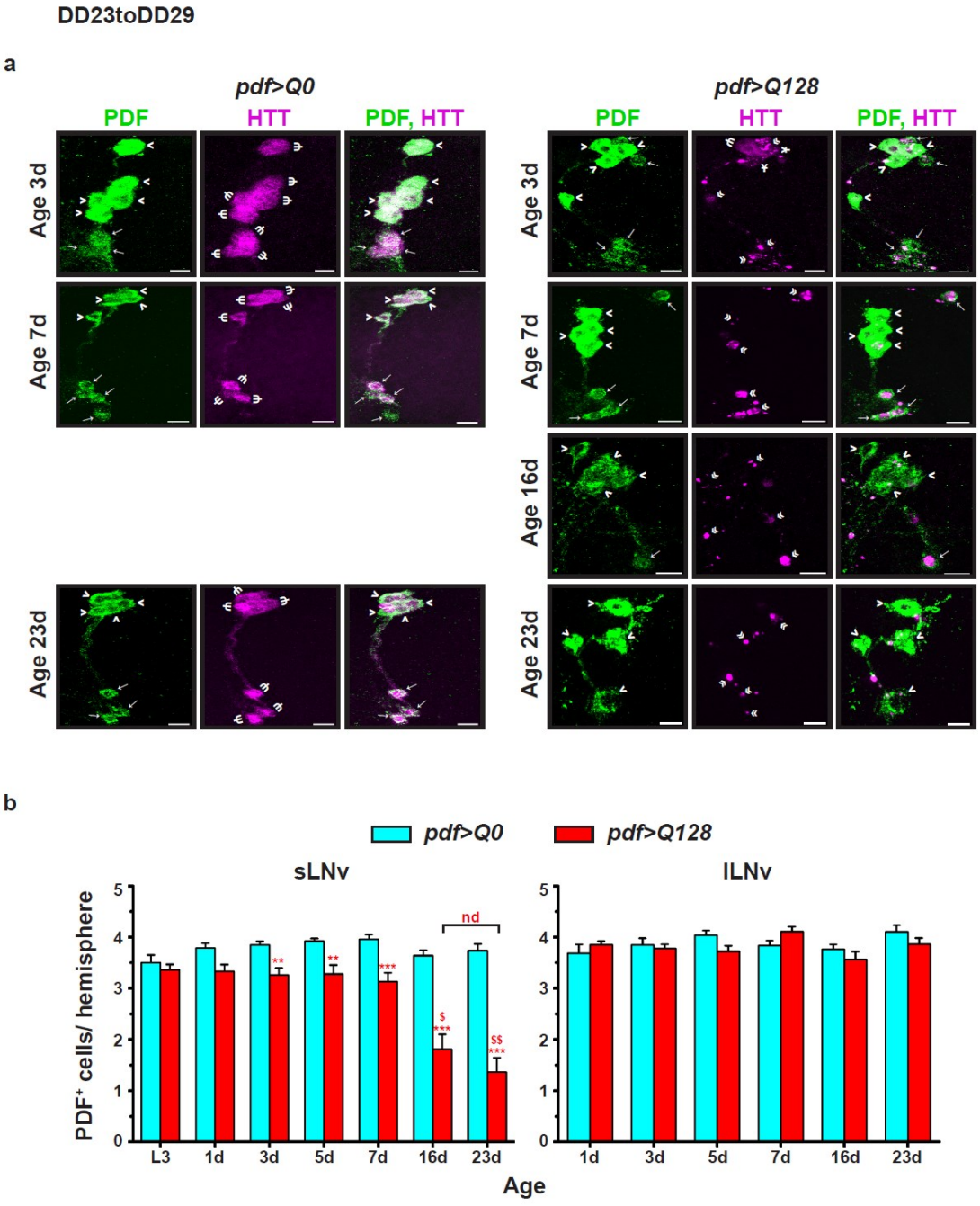

Figure 4.31

Fig 4. 31 pdf>Q128 under DD23toDD29 show enhancement in PDF⁺ sLNv soma numbers.
(a) Representative images of the adult fly brains under DD23toDD29 stained for PDF (green) and HTT (magenta) in LNv at 3d, 7d and 23d for *pdf>Q0* (left panel-sets) and at 3d, 7d, 16d and 23d for *pdf>Q128* (right panel-sets). Indicated in the images are sLNv soma (→ arrows), lLNv soma (> arrowheads), diffuse expHTT (Ψ psi), diffuse+inclusions expHTT (Ɣ), and expHTT inclusions (« double arrowheads). Scale bars are 10 µm. (b) The mean number of PDF⁺ sLNv soma (left) and lLNv soma (right) across age. Coloured symbols indicate significant differences, * for age-matched, inter-genotype differences and $ for differences between ages of the corresponding-coloured genotype at * $p<0.05$, ** $p<0.01$, *** $p<0.001$. nd, not different. Error bars are SEM.

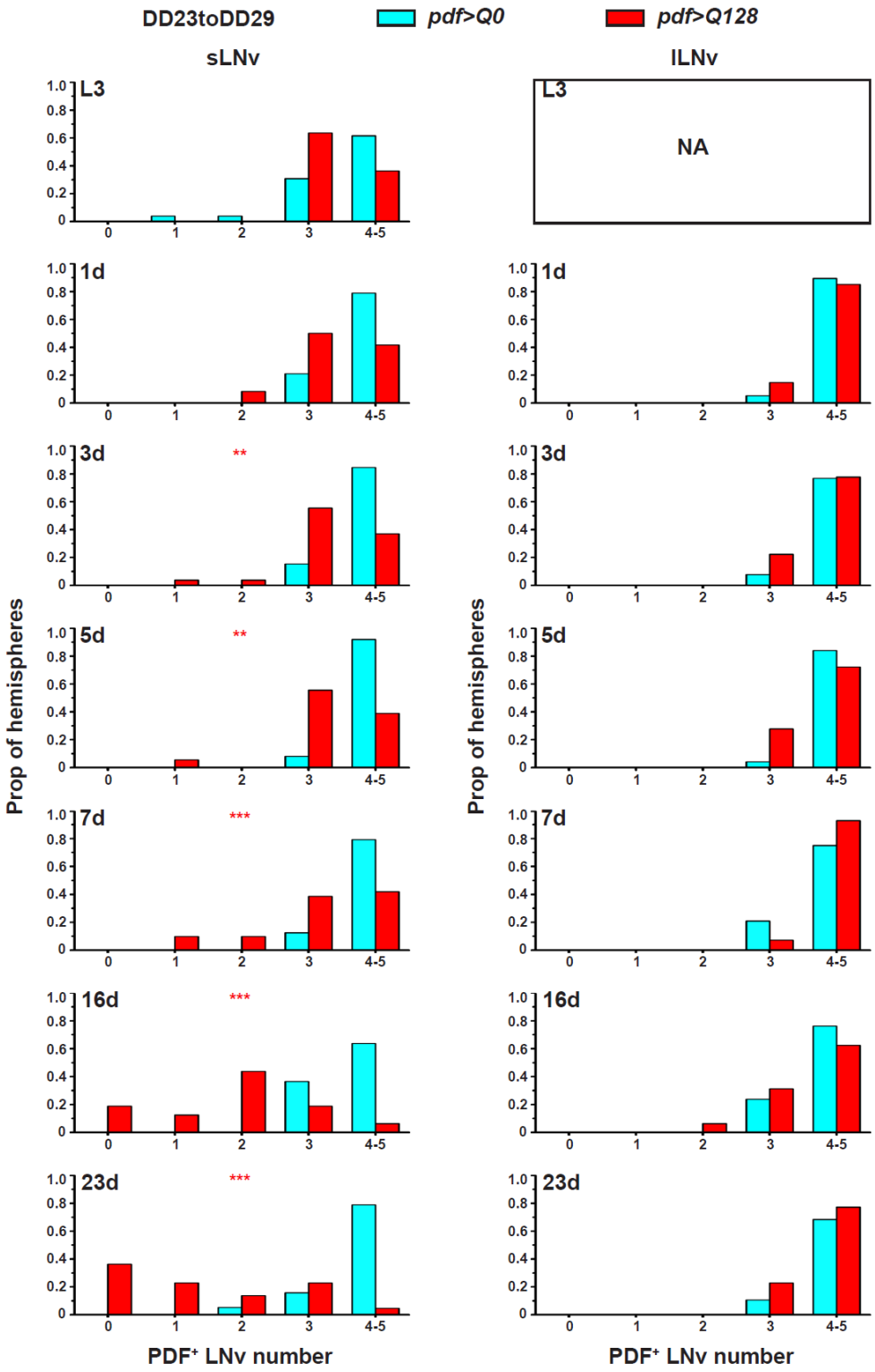

Figure 4.32

Fig 4. 32 The frequency distribution of PDF$^+$ sLNv soma numbers are similar between genotypes only up to 1d under DD23toDD29.

Frequency distribution of the proportion of hemispheres of *pdf>Q0* and *pdf>Q128* in DD23toDD29 with 0 to 5 PDF$^+$ LNv soma numbers (sLNv - left and lLNv - right). Coloured * indicates significantly different distribution shapes between age-matched genotypes at $p<0.05$. NA, not applicable.

PER$^+$ sLNv and lLNv soma numbers were significantly reduced in 7d *pdf>Q128* compared to *pdf>Q0* in DD23toDD29 (Fig 4.33a top, b). This decline was also mimicked by the significantly differing shapes of the distributions between the two genotypes (Fig 4.33c). ~42% of *pdf>Q128* hemispheres had ≥3 PER$^+$ sLNv, while ~65% had ≥3 PER$^+$ lLNv (Fig 4.33c). Further, 7d *pdf>Q128* showed no oscillation in the sLNv PER intensity, while controls showed a clear oscillation (Fig d top). However, PER in the lLNv of *pdf>Q128* showed a low amplitude oscillation (Fig d bottom). Thus, exposure of *pdf>Q128* to DD23 during development did not restore PER oscillations in the sLNv of young adults in DD29.

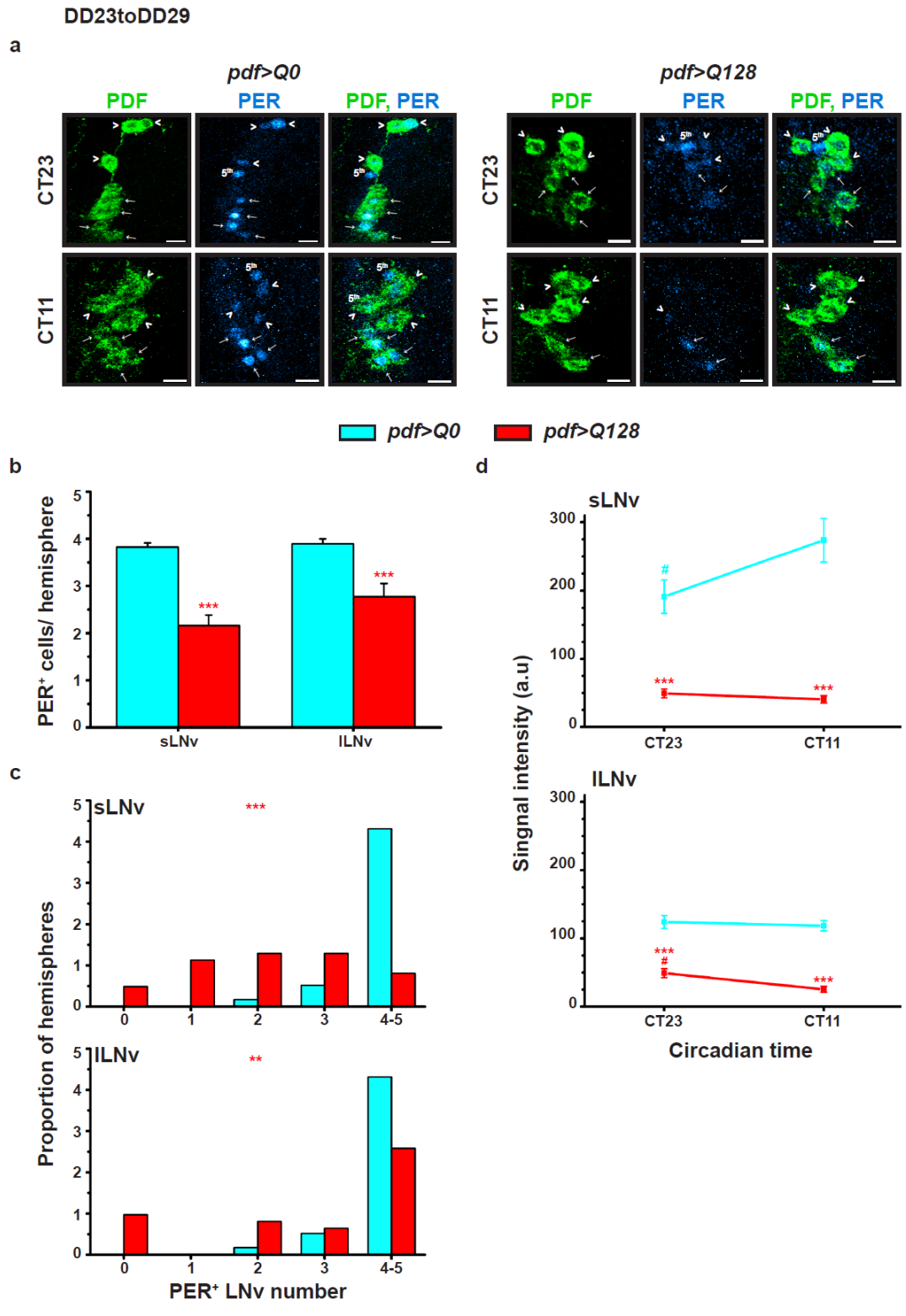

Figure 4.33

Fig 4. 33 pdf>Q128 flies in DD23toDD29 show loss of both PER and its oscillations from the sLNv. (a) Representative images of 7d-old adult fly brains of *pdf*>Q0 (left) and *pdf*>Q128 (right) in DD23toDD29 stained for PER (cyan hot) and PDF (green) in LNv at CT23 (top) and CT11 (bottom). sLNv soma (→ arrows), lLNv soma (> arrowheads) and PDF^{-} PER^{+} 5th sLNv are

indicated. Scale bars are 10 µm. (b) The mean number of PER^+ sLNv soma and lLNv soma at CT23. * indicates age-matched differences between genotypes. (c) Frequency distribution of the proportion of hemispheres having 0 to 5 PER^+ LNv soma: sLNv soma (top) and lLNv soma (bottom) in 7d-old flies at CT23. * indicates significantly differing shapes of distribution between genotypes. (d) For the two genotypes, the quantification of PER intensity at CT23 and CT11 in sLNv (top) and lLNv (bottom). Differences between time points CT23 and CT11 are represented by # (cyan) for *pdf>Q0* and # (red) for *pdf>Q128*. Coloured * represents the difference between genotypes at that time point. Statistical significance is at single-symbol $p<0.05$, double-symbol $p<0.01$, and triple-symbol $p<0.001$. Error bars are SEM.

The proportion of hemispheres with different expHTT forms in LNv changed significantly with age, with a predomination of Diff- and Diff+Inc-enriched LNv at early ages and a near complete domination of Inc-enriched LNv at later ages (Fig 4.34a top). Proportions of hemispheres dominated by Diff-enriched LNv relative to Inc-enriched LNv were significantly higher at young ages (L3, 1d for sLNv and 1d, 3d for lLNv) than subsequent ages where nearly all the hemispheres had Inc-enriched LNv (Fig 4.34a middle). The hemisphere proportions with Diff+Inc-enriched LNv relative to Inc-enriched LNv also declined significantly with age (after 1d for sLNv and after 3d for lLNv) (Fig 4.34a bottom). Both expHTT inclusion numbers and size were generally comparable across age for *pdf>Q128* in DD23toDD29 (Fig 4.34b).

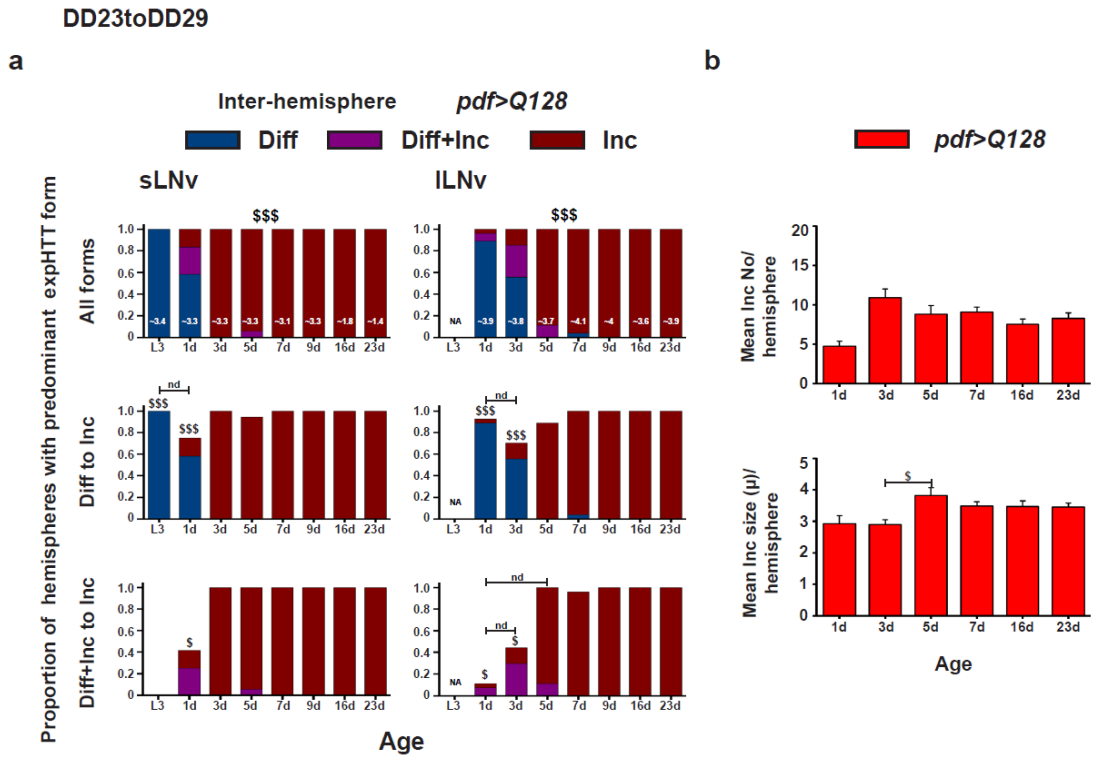

Figure 4.34

Fig 4. 34 The proportion of hemispheres dominant in an expHTT form in the LNv of pdf>Q128 under DD23toDD29 changes from diffuse-rich to inclusion-rich with age.

(a) The proportion of hemispheres dominated by different expHTT forms in sLNv (left) or lLNv (right) is plotted against age for *pdf>Q128* in DD23toDD29 to describe the between-hemispheres distribution of predominant expHTT forms. These are plotted for all expHTT forms (top) or significantly different pair-wise comparisons (middle and bottom). $ indicates significant changes in the relative proportions of hemispheres across age for all expHTT forms (top) or pair-wise expHTT forms between specific ages (middle and bottom). NA, not applicable; nd, not different. At the bottom of some bars, numbers represent the mean number of PDF^+ LNv detected at that age. (b) Comparison of mean inclusion number per hemisphere (top) and mean inclusion size per hemisphere (bottom) for *pdf>Q128* in DD23toDD29 across age. Significant differences between ages are $ $p<0.05$, $$ at $p<0.01$ and $$$ $p<0.001$. Error bars are SEM.

4.3.15 Adult-restricted upshift to warm temperatures rescues early-age rhythms of *pdf>Q128* only when the temperature experienced as adults is a warm 29°C

I then asked whether the magnitude of the upshift and the lower- and upper limits of the temperature upshift influence the early-age rhythm rescue of *pdf>Q128* seen under exposure to adult-restricted warm temperatures. As seen earlier, exposure of *pdf>Q128* to DD21toDD25 did not rescue activity rhythms (Fig 4.9 a-c). However, with the same 4°C magnitude of temperature difference, but with the warm temperatures upon upshift being 29°C, most of the *pdf>Q128* flies in DD25toDD29 were rhythmic in AW1 and comparable to controls (Fig 4.35a, b). Their rhythmicity declined dramatically in the subsequent AWs. Nevertheless, this improvement in rhythmicity of *pdf>Q128* did not translate to robustness and '*r*', which were significantly lower than most controls (Fig 4.35c, d). Thus, the early-age rhythm rescue of *pdf>Q128* upon temperature upshift depends on the upper limit rather than the magnitude of the upshift.

Comparing the three upshift regimes where flies were exposed to higher temperatures as adults relative to what they experience during development, *pdf>Q128* adults experiencing an upshift to warm temperatures of 29°C (DD25toDD29 and DD23toDD29) showed higher rhythmicity than those experiencing an upshift to ambient temperatures of 25°C (DD21toDD25) in AW1 (Fig 4.35e middle). In AW2, though the rhythmicity declined, there were still significantly more rhythmic *pdf>Q128* flies in DD23toDD29 than those in DD21toDD25 or DD25toDD29 (Fig 4.35e middle). Rhythmic *pdf>Q128* flies in DD23toDD29 also had more robust rhythms than those in DD25toDD29 (Fig 4.35g). These observations suggest that the magnitude of temperature upshift also determines the extent of rescue: the more significant the magnitude, the greater the rhythm's power and the longer the rhythmicity duration. The activity consolidation of *pdf>Q128* in DD25toDD29 and DD23toDD29 was also significantly higher than in DD21toDD25 (Fig 4.35f middle). Controls had comparable rhythmicity and nearly similar robustness between regimes (Fig 4.35e, g). However, their *r*-values differed between regimes; flies in DD21toDD25 had lower '*r*' than those in DD25toDD29 and DD23toDD29 for *Q128* and *pdfGal.* For *pdf>Q0* and *pdfGal* flies, '*r*' in DD25toDD29 was more significant than in DD23toDD29 at a few ages (Fig 4.35e). So, the improved rhythmicity of *pdf>Q128* upon adult-restricted exposure to 29°C is an

effect of warm temperatures during recording consolidating the flies' activity, irrespective of the genotype. Despite both regimes having a 4°C temperature upshift, the rhythmicities of *pdf>Q128* in DD25toDD29 differed from those in DD21toDD25, suggesting that the flies must be exposed to warm temperatures as adults during recording for the temperature upshift to restore *pdf>Q128*'s activity rhythms. As a result, the degree to which the temperature upshifts facilitate the rhythmicity of *pdf>Q128* depends on both the magnitude and the upper bound of the upshift.

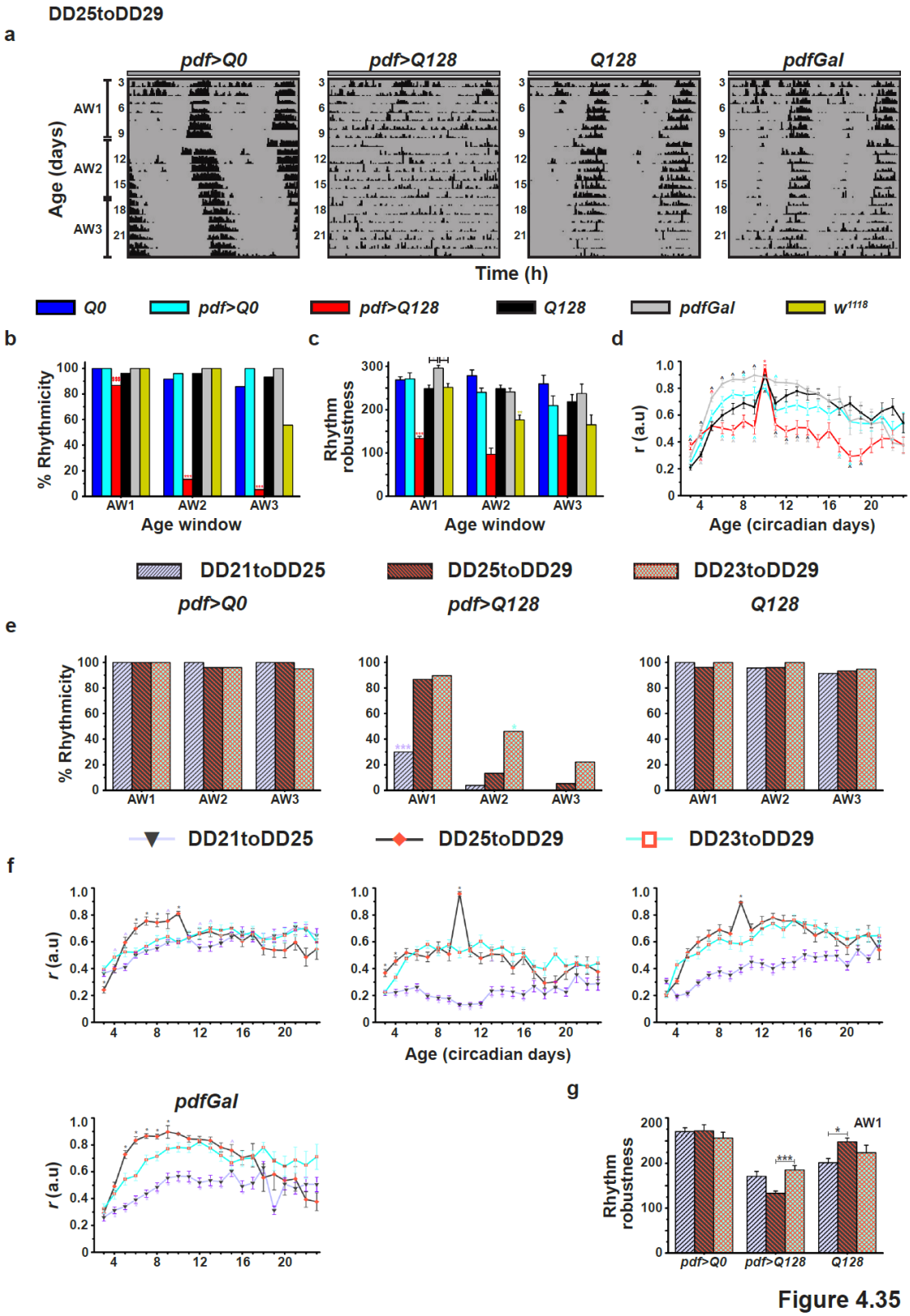

Figure 4.35

Fig 4. 35 pdf>Q128 exposed to temperature upshifts as adults show early-age rhythms with well-consolidated activity only when the adults experience warm temperatures during recording.

(a) Representative double-plotted actograms for adult flies in DD25toDD29 showing activity data for 21d (age 3d-23d). (b-d) Plots for rhythmicity (b), activity consolidation '*r*' (c) and

mean robustness (d). Symbols represent statistically significant differences: coloured * of that coloured genotype from all others or indicated ones in an AW, and coloured $ between AWs for a genotype. Coloured ^ near an error bar of a data point indicates a difference between the respective-coloured genotype and the data-point genotype. All other details are the same as in Fig 4.1. (e-g) The between-regime comparisons of the percentage rhythmicity (e) and the mean activity consolidation '*r*' (f) plotted against AWs (or age) and the mean rhythm robustness at AW1 (g) for *pdf>Q0*, *pdf>Q128* and *Q128*. An additional genotype *pdfGal* is shown for '*r*' (f). All other details are like Fig 4.7. Regime colour codes: light purple, DD21toDD25; dark grey, DD25toDD29; cyan, DD23to29.

4.3.16 Acute exposure to warm temperatures as adults is not sufficient to rescue activity rhythms of *pdf>Q128*

I wanted to know whether the duration of constant warm temperatures as adults is vital for the early-age rhythm rescue of *pdf>Q128* seen upon adult-restricted temperature upshift. Instead of the adult-restricted chronic warm temperature exposure, flies in DD23 were exposed to a short burst (48h) of warm temperatures termed 'acute DD29' either during 2d-3d or 7d-8d of age. Most of these *pdf>Q128* were, however, arrhythmic across AWs and regimes (Fig 4.36a- c) and had low '*r*' than all controls barring *Q128* (Fig 4.36d-e), which also showed lower rhythmicity and '*r*' than most controls across age (Fig 4.36b-e). Consequently, *pdf>Q128* and control flies that experienced acute DD29 did not differ from their counterparts in DD23 in rhythmicity or activity consolidation (Fig 4.36 f, g). The lack of rhythm rescue upon acute exposure to warm temperatures as adults indicate that the rescue of early-age activity rhythms of *pdf>Q128* on upshift to warm temperatures requires long-term or chronic exposure to warm temperatures as adults.

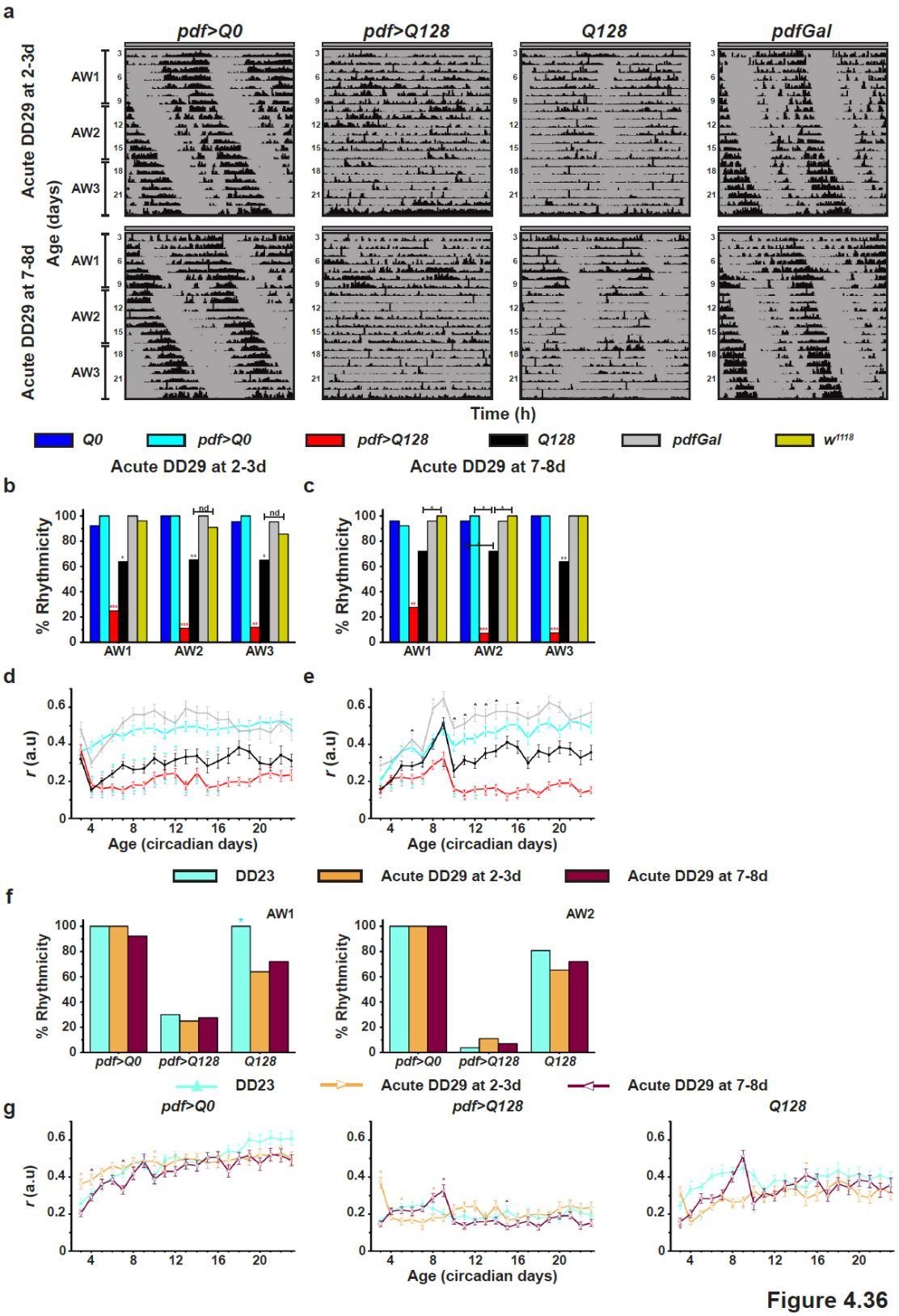

Figure 4.36

Fig 4. 36 Exposure of pdf>Q128 to short durations of warm temperatures as adults does not rescue behavioural rhythms.

(a) Representative double-plotted actograms for adult flies in acute DD29 at 2-3d (top) and 7-8d (bottom) showing activity data for 21d (age 3d-23d). (b-e) Plots for rhythmicity (b, c) and

activity consolidation '*r*' (d, e) for the within-regime comparisons in acute DD29 at 2-3d (left) and acute DD29 at 7-8d (right). Symbols represent statistically significant differences: coloured * of that coloured genotype from all others or indicated ones in an AW, and coloured $ between AWs for a genotype. Coloured ^ near an error bar of a data point indicates a difference between the respective-coloured genotype and the data-point genotype. All other details are the same as in Fig 4.1. (f-g) The between-regime comparisons of the percentage rhythmicity (f) in AW1 and AW2 and the mean activity consolidation '*r*' (g) across age for each of the three genotypes. All other details are like Fig 4.7. Regime colour codes: cyan, DD23; orange, acute DD29 at 2-3d; purple, acute DD29 at 7-8d.

4.3.17 The rescue of early-age activity rhythms of *pdf>Q128* by adult-restricted upshift to warm temperatures is not countered by cyclic light or constant light during development

Considering the differential effect of light on circadian neurodegenerative features (documented in Chapter 3), I investigated if developmental light exposure modifies the early-age rhythm rescue in adult *pdf>Q128* seen upon adult-restricted upshift to warm temperatures. Flies experienced LD23 or LL23 during development and then DD29 as adults. The LL23toDD29 experiment also tests whether developmental clocks are required for the adult-restricted warm-temperature-mediated rescue of behavioural rhythms in the *pdf>Q128* young. *pdf>Q128* in LD23toDD29 and LL23toDD29 were rhythmic like their within-regime controls in AW1 (Fig 4.37a, b, e). The mean rhythmicity of *pdf>Q128* declined in AW2 and was significantly lower than that of controls in both regimes (Fig 4.37b, e). Though rhythmicity of *pdf>Q128* in LD23toDD29 was control-like, its activity consolidation was lower compared to at least one relevant control from 6d onwards (Fig 4.37c) and robustness less than all controls in AW1 (Fig 4.37d). *pdf>Q128* in LL23toDD29 showed improved activity consolidation like controls *pdf>Q0* and w^{1118} up to 9d, beyond which it declined from only *pdf>Q0* (Fig 4.37f). *Q128* control showed a decline in activity consolidation till 8d than other controls and even from *pdf>Q128* up to 7d. However, *pdf>Q128* in LL23toDD29 also showed weaker rhythms than most controls in AW1 (Fig 4.37g).

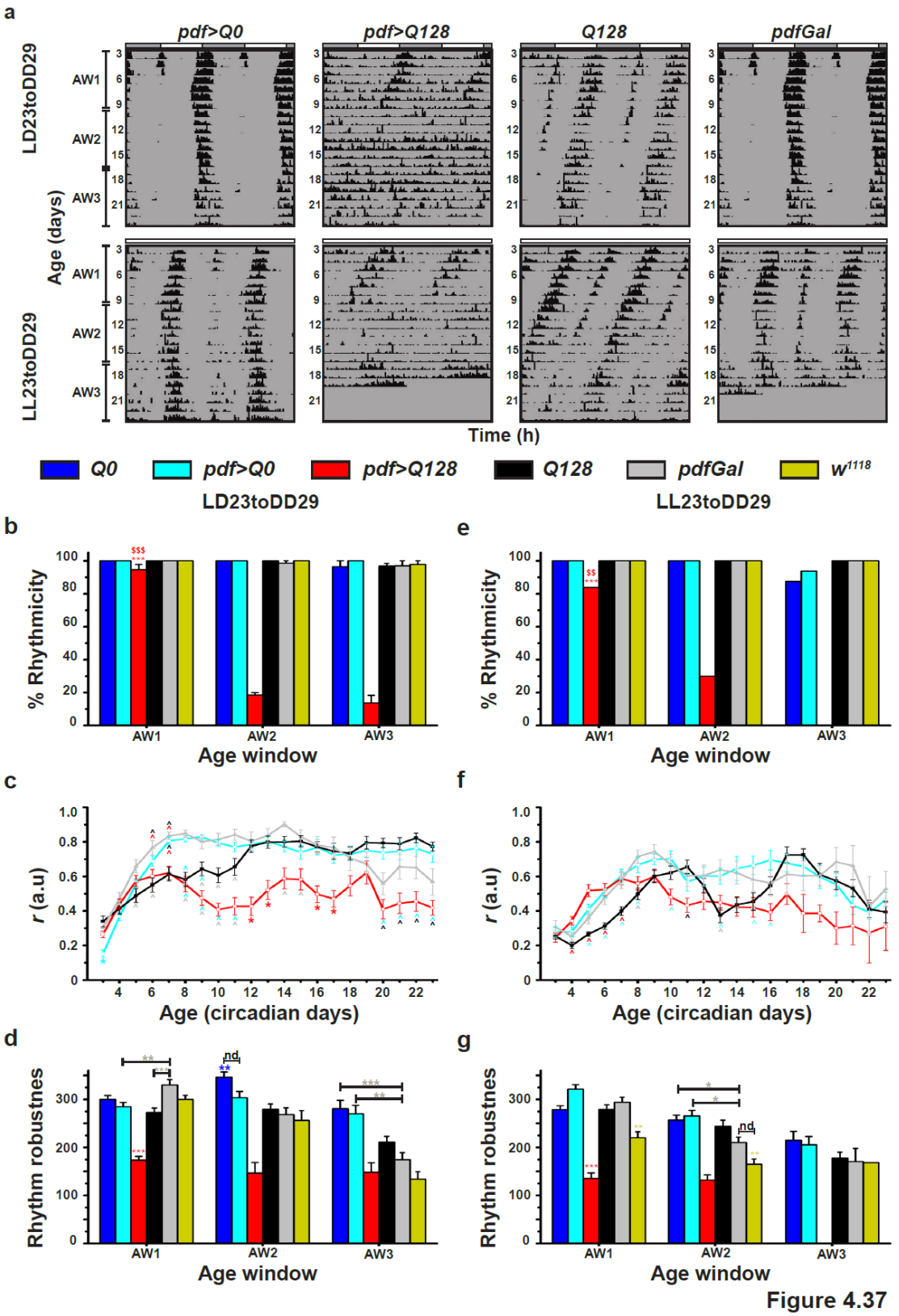

Figure 4.37

Fig 4. 37 pdf>Q128 flies in LD23toDD29 and LL23toDD29 are rhythmic at the early age window. (a) Representative double-plotted actograms for adult flies in LD23toDD29 (top) and those in LL23toDD29 (bottom) showing activity data for 21d (age 3d-23d). Placed above the actograms are

grey and white bars (top) and white bars (bottom) depicting the light regimes during development, light/dark cycles (top) and constant light (bottom), respectively. (b-g) Plots for mean rhythmicity (b, e), activity consolidation '*r*' (c, f), and mean robustness (d, g) for flies in LD23toDD29 (b, c, d) and those in LL23toDD29 (e, f, g). AW3 (or ages 17-23d) are not included in the statistical analysis for LL23toDD29 due to very few surviving flies; fly deaths by AW3 are also cause for gaps in the LL actograms (a bottom). All other details are like Fig 4.1.

Comparing between regimes, the rhythmicity of *pdf>Q128* in different regimes was similar across AWs, with most of the flies in AW1 being rhythmic in all three regimes (Fig 4.38b middle). However, their mean rhythmicities averaged over three experiments were significantly higher in DD23toDD29 than LD23toDD29 in AW2 and AW3 (Fig 4.38a middle). Nevertheless, considering that only ~40% and ~27% of *pdf>Q128* in DD23toDD29 were rhythmic in AW2 and AW3, respectively, and the margin of difference in the rhythmicities between the regimes were 20% and 13% in the respective AWs, such statistical differences might not be of biological significance. Controls *pdf>Q0* and *Q128* also were indistinguishable between regimes in their rhythmicities across AWs (Fig 4.38a, b). The rhythm robustness of *pdf>Q128* in LL23toDD29 was lower than DD23toDD29 and LD23toDD29 in AW1; its control controls showed the opposite trend of having higher robustness in LL23toDD29 (Fig 4.38c). Also, whether this slight difference in robustness of *pdf>Q128* between regimes is of physiological consequence is debatable. *pdf>Q128* across age had comparable between-regime activity consolidation (Fig 4.38d middle). *pdf>Q0* in LD23toDD29 had significantly better consolidation than its counterparts in other regimes at early ages (Fig 4.38d left) (*pdfGal* also shows a similar significant trend). This higher '*r*' of controls in LD23toDD29 can partly explain the significant difference of *pdf>Q128*'s '*r*' from controls observed in LD23toDD29 (Fig 4.37c). *Q128* in LL23toDD29 had poorer consolidation than other regimes (Fig 4.38d right), also reflected in the within-regime, between-genotype comparisons (Fig 4.37f). Consequently, light exposure (cyclic or continuous) throughout development has minimal distinctive effects on the behavioural rhythmicity of *pdf>Q128* young conferred by adult-specific warm temperatures. Further, this restoration of early-age rhythms of *pdf>Q128* does not seem to require functional circadian mechanisms during development, as evidenced by a rescue with LL23toDD29. Unlike the absence of early-age rhythmicity seen with *pdf>Q128* in LDTCtoDD25, those in LD23toDD29 show a rhythm rescue, suggesting different underlying mechanisms mediating the early-age rhythm restoration in these two regimes, the former being sensitive to light and the latter being relatively less sensitive to light.

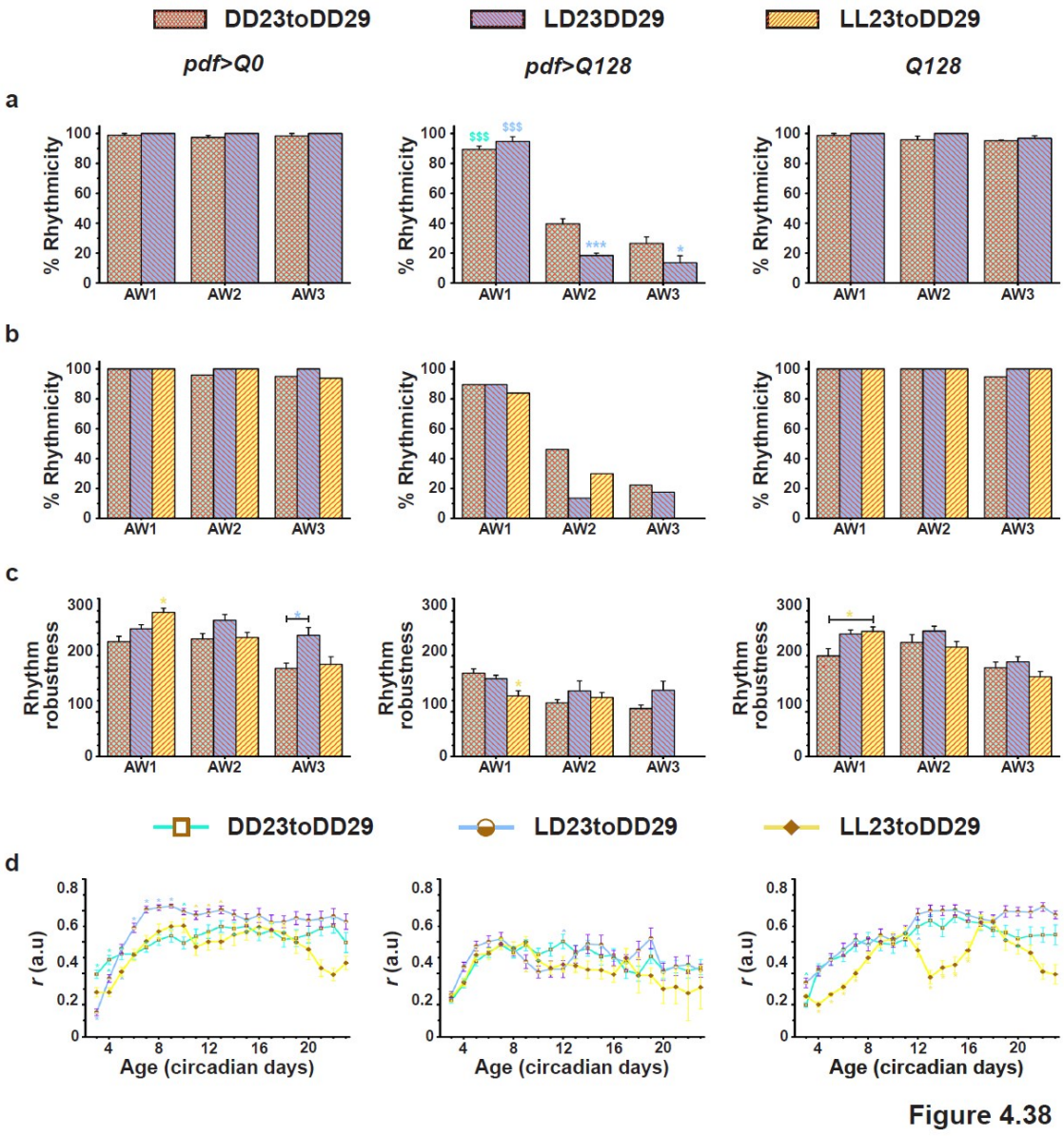

Fig 4. 38 pdf>Q128 experiencing warm temperatures during recording shows early-age rhythms, irrespective of the light conditions during development.

(a-d) The between-regime comparisons of the mean percentage rhythmicity (a), percentage rhythmicity (b), the mean rhythm robustness (c) and the mean activity consolidation '*r*' (d) plotted against AWs (or age) for *pdf>Q0* (left), *pdf>Q128* (middle) and *Q128* (right). The mean percentage rhythmicities are obtained by averaging over three experiments for DD23toDD29 and LD23toDD29 (a). The percentage rhythmicities of individual runs comparing the three regimes are plotted (b). All other details are like Fig 4.7. Regime colour codes: cyan, DD23toDD29; blue, LD23toDD29; yellow, LL23toDD29.

4.3.18 Exposure of *pdf>Q128* to warm temperatures as adults are sufficient to delay arrhythmicity and improve activity consolidation

I then compared the activity rhythms of flies in the four constant temperature regimes, constant cool or warm temperatures through all life stages and the temperature upshift or downshift as adults: constant cool (DD23), constant warm (DD29), temperature upshift as adults or adult-restricted warm (DD23toDD29) and temperature downshift as adults or development-specific warm (DD29toDD23). *pdf>Q128* in both DD29 and DD23toDD29 showed significantly greater rhythmicity than those in DD23 and DD29toDD23 in AW1 (Fig 4.39a, middle). In AW2, though the rhythmicities of *pdf>Q128* in DD29 and DD23toDD29 decline compared to AW1, they still were higher than those in DD23, and those in DD23toDD29 were also higher than those in DD29toDD23. Across AWs, the controls *pdf>Q0* and *Q128* in different regimes showed comparable rhythmicities between regimes. (Fig 4.39a). The robustness of rhythms for all three genotypes differed in a certain manner between regimes: in AW1, *pdf>Q128* in DD23toDD29 had stronger rhythms than those in DD29 (Fig 4.39b middle), and controls in DD23toDD29 exhibited more robust rhythms than those in at least one of the other regimes at AW1 and AW2 (Fig 4.39b). *pdf>Q128* in DD23 and DD29toDD23 also showed poorer activity consolidation than those in DD29 and DD23toDD29 across most circadian ages (Fig 4.39c, middle). Interestingly, even controls in DD23, and to a lesser extent, those in DD29toDD23 showed lower activity consolidation than their counterparts in other regimes (Fig 4.39c top, bottom). Such a temperature-dependent effect on the activity consolidation was evident with the *Q128* background in DD23 across age, but to a lesser extent with those in DD29toDD23: from 8d to 19d (Fig 4.39c right). Thus, overall, the experience of warm temperatures during development and as adults or only as adults improves the flies' ability to consolidate their activity. A point of note here is that though exposure to DD29 or DD23toDD29 improved '*r*' across genotypes, this effect seems even more pronounced with *pdf>Q128* for them to reach control-like levels of consolidation (Figs 4.20c, 4.30c). Another interesting finding is that the rhythmicity or '*r*' of *pdf>Q128* in DD29 did not differ from those in DD23toDD29, indicating that adult-restricted warm temperature exposure is adequate to delay *pdf>Q128* behavioural arrhythmia. Conversely, rhythm features did not

differ between *pdf>Q128* in DD23 and those in DD29toDD23, whereas DD29 provided them with a significant rhythm rescue over DD29toDD23, suggesting that **relatively cooler temperature as adults is detrimental to activity rhythms of *pdf>Q128*. Further, the recording temperature experienced by adult *pdf>Q128* flies determines rhythmicity, where adult-restricted warm temperatures favour rhythms, whereas adult-restricted relatively cooler temperatures do not. Crucially, warm temperatures experienced by adult *pdf>Q128* flies improve their activity rhythms by increasing their ability to consolidate daily locomotor activity.** Since the young *pdf>Q128* in DD23toDD29 had more robust rhythms than those in DD29, in terms of **restoration of early-age activity rhythms**, **DD23toDD29≥DD29> DD29toD23=DD23**.

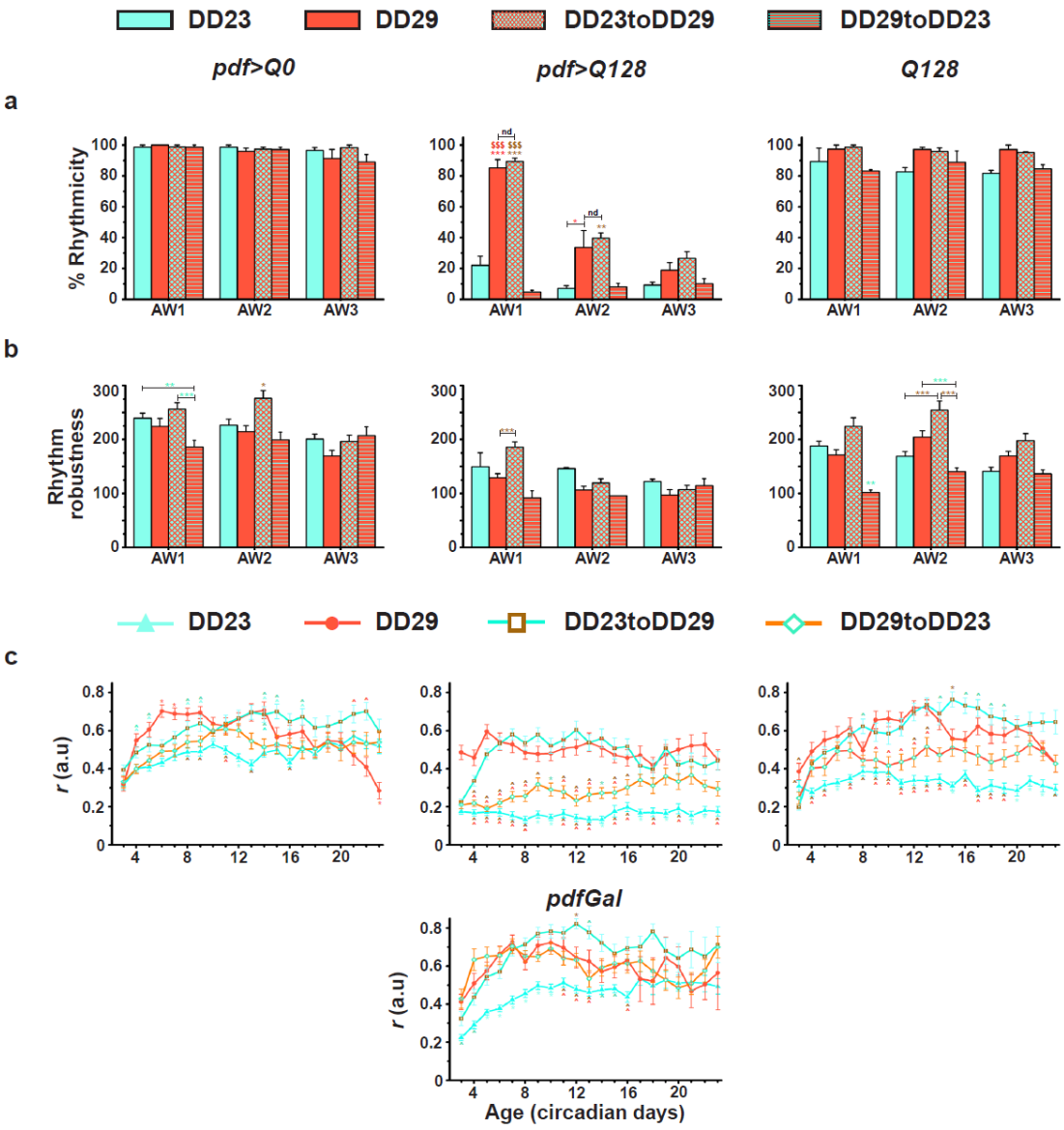

Figure 4.39

Fig 4. 39 pdf>Q128 that experience warm temperatures as adults show early-age rhythms with well-consolidated activity across age.

(a-c) The between-regime comparisons of the mean percentage rhythmicity (a), the mean rhythm robustness (b), and the mean activity consolidation '*r*' (c) plotted against AWs (or age) for *pdf>Q0* (left), *pdf>Q128* (middle) and *Q128* (right). An additional genotype *pdfGal* is shown for '*r*' (c). Symbols represent statistically significant differences: coloured * of that coloured regime from all others or indicated ones and coloured $ of between-AW comparisons for that regime. For '*r*', coloured ^ near an error bar of a data point indicates a difference of the respective-coloured regime from the data-point regime. Regime colour codes: cyan, DD23; rust, DD29, brown, DD23toDD29 and green, DD29toDD23. The number of symbols represents statistical significance: single $p<0.05$, double $p<0.01$ and triple $p<0.001$. Error bars are SEM.

4.3.19 Exposure to warm temperatures rescues PDF loss from sLNv soma in young *pdf>Q128*

The circadian proteins PDF and PER in the LNv of *pdf>Q128* were then compared between those in a regime that lacked rhythmic activity, namely, DD23 and those in regimes that provided early-age rhythm rescue, namely, DD29 and DD23toDD29. *pdf>Q128* as larvae showed on an average ~4 PDF^+ sLNv soma when reared in either DD23 or DD29 (Fig 4.40a left). However, their mean numbers and distributions at L3 differed significantly (Fig 4.40a left, 4.40b left). PDF^+ sLNv soma numbers of *pdf>Q128* in different regimes were comparable between regimes up to 5d into adulthood (Fig 4.40a middle). Beyond 5d, those in DD23 declined, becoming significantly lower than those in DD29 and DD23toDD29 at 7d and 9d (Fig 4.40a middle). This decline was reflected in the differing distribution shapes of *pdf>Q128* in the three regimes, but only at 9d (Fig 4.40b left). Nevertheless, at 7d and 9d, only ~45% of the hemispheres in DD23 had ≥3 PDF^+ sLNv, contrasting from ~85% of those in DD29 and DD23toDD29 ($p<0.05$ at 7d and $p<0.01$ at 9d, Fisher's exact tests and BH procedure) significantly. By 16d, the PDF^+ sLNv numbers had declined in those in DD29 and DD23toDD29, like those in DD23 (Fig 4.40a middle). *pdf>Q128*'s PDF^+ lLNv soma numbers and the shape of their distributions were largely comparable between regimes across age (Fig 4.40a right, b right). So, relatively warm temperatures delay the loss of PDF from sLNv.

PER loss in the LNv of *pdf>Q128* was similar between DD23 and DD23toDD29 (Fig 4.40c, d). Thus, rearing and maintaining *pdf>Q128* in relatively warm temperatures or exposing them to high temperatures only as adults rescues early-age behavioural arrhythmicity and slows down the loss of PDF from the sLNv, without retarding PER loss. In terms of PDF preservation in the sLNv, DD29=DD23toDD29>DD23. And, regarding the preservation of PER, DD23toDD29=DD23. Although *pdf>Q128* in DD23 did show a dampened PER oscillation in the sLNv (Fig 4.18d top), and those in DD23toDD29 did not (Fig 4.33d top), this low-amplitude LNv PER oscillation in DD23 may not amount to be of physiological consequence to sLNv functionality as the behavioural rhythms of *pdf>Q128* were not restored in DD23. Thus, based on the finding that DD23 does not rescue early age rhythmicity of *pdf>Q128* and hastens the loss of PDF from sLNv relative to DD29 and DD23toDD29, it seems to offer the least neuroprotection.

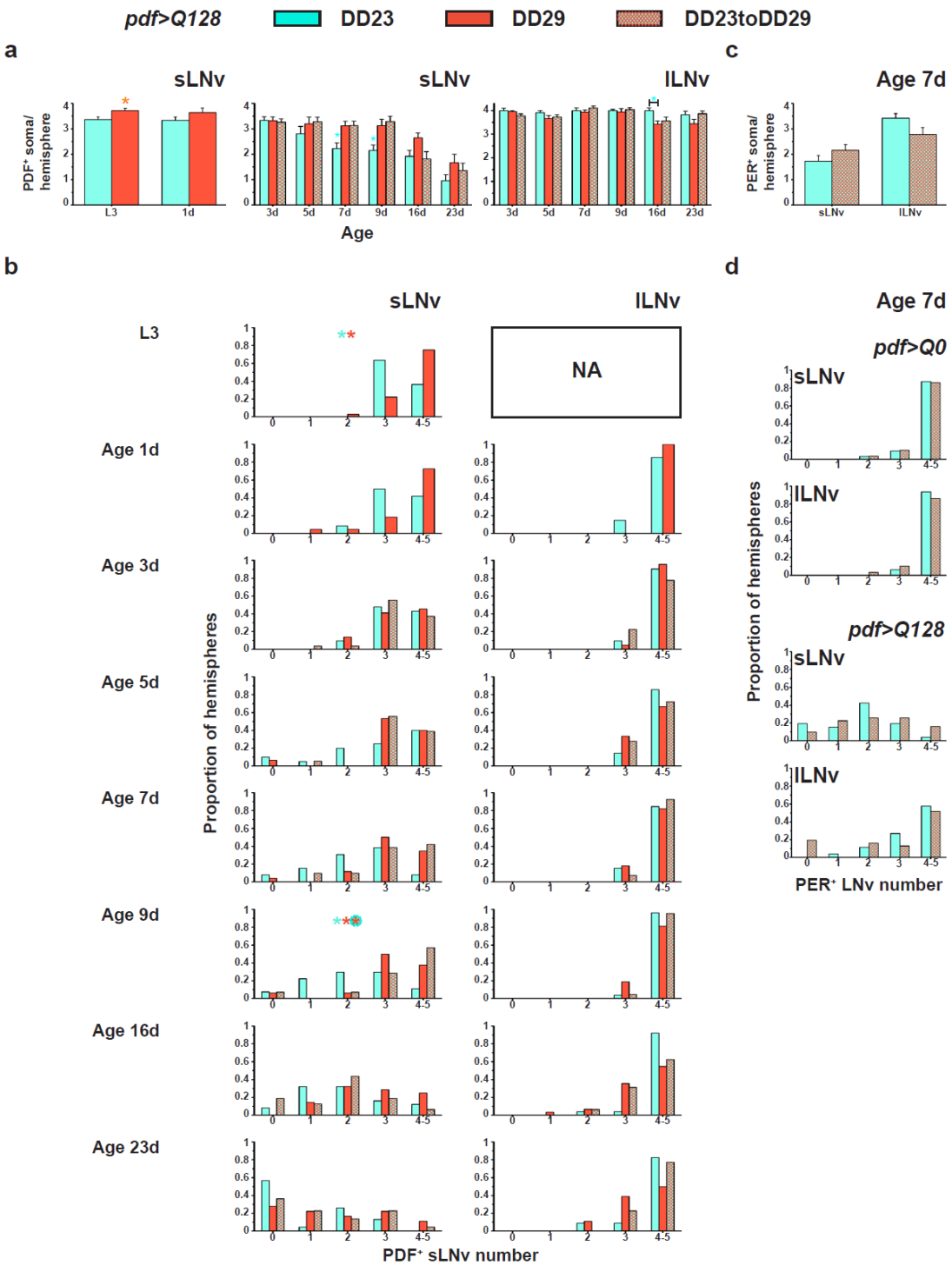

Figure 4.40

Fig 4. 40 Warm temperatures slow down PDF loss, but not PER loss, from the sLNv of pdf>Q128. (a) Mean PDF$^+$ sLNv soma numbers in *pdf>Q128* in DD23 and in DD29 at L3 and 1d (left). The mean number of PDF$^+$ sLNv soma (middle) or lLNv soma (right) in *pdf>Q128* across age maintained in DD23, DD29 and DD23toDD29. (b) Frequency distribution of the proportion of hemispheres of *pdf>Q128* with 0 to 5 PDF$^+$ LNv soma numbers (sLNv - left and lLNv - right) in the three regimes across age. NA, not applicable. Coloured multiple * indicates a significantly different distribution

shapes between regimes, with the first colour of the reference regime and the subsequent colours of regimes differing from the reference at $p<0.05$. (c) The mean PER^+ LNv soma numbers in 7d-old *pdf>Q128* in DD23 and DD23toDD29. (d) Frequency distribution of the proportion of hemispheres of *pdf>Q0* (top-sets) or *pdf>Q128* (bottom-sets) with 0 to 5 PDF^+ LNv soma numbers (sLNv - top and lLNv - bottom) in the two regimes. * indicates significantly different distribution shapes. Significant differences are at * $p<0.05$, ** at $p<0.01$ and *** $p<0.001$. Error bars are SEM.

4.3.20 Adult-restricted exposure of *pdf>Q128* to warm temperatures dramatically reduces the expHTT inclusion load and is the most neuroprotective

I then asked if the expHTT forms in LNv of *pdf>Q128* differed between the regimes DD23, DD29 and DD23toDD29. The trend of hemispheres dominated by Diff-enriched LNv at a very early age and near-complete domination by Inc-enriched LNv at subsequent ages was a common observation across regimes (Fig 4.41a top, b top). The relative proportions of hemispheres of *pdf>Q128* enriched with different expHTT forms in the sLNv were also similar between regimes across most ages, except at 3d (Fig 4.41a top). Specifically, at 3d, while all the hemispheres in DD29 and DD23toDD29 had Inc-enriched sLNv, only ~43% of the hemispheres in DD23 had Inc-enriched sLNv, whereas the other 48% had Diff+Inc enriched sLNv (Fig 4.41a top, third-panel). Those in DD23 had significantly fewer hemispheres of Inc-enriched sLNv relative to Diff+Inc-enriched sLNv than those in DD29 and DD23toDD29 (Fig 4.1a bottom). Thus, unlike the other two regimes, DD23 allowed for a more prolonged presence of hemispheres with Diff+Inc-enriched sLNv, thereby putting off the dominance of hemispheres with Inc-enriched sLNv.

Contrary to the sLNv, the relative proportions of *pdf>Q128* hemispheres enriched with different expHTT forms in lLNv differed significantly across most ages, except 1d (Fig 4.41b top). However, the pair-wise comparisons showed significant between-regime differences only at 3d and 5d (Fig 4.41b, second-, third-, bottom-rows). A significantly higher proportion of *pdf>Q128* hemispheres in DD23 and DD23toDD29 were dominated by Diff-enriched lLNv relative to Inc-enriched lLNv than those in DD29 (Fig 4.41b second-row). Further, the proportion of *pdf>Q128* hemispheres with Inc-enriched lLNv relative to the Diff+Inc-enriched lLNv was more significant in DD29 than those in DD23toDD29 (Fig 4.41b, third-row, second-panel). The above observations posit DD23 and DD23toDD29 as regimes that promote Diff-enriched lLNv at early ages when DD29 substantially promotes Inc. However, the proportion of hemispheres of Diff-

enriched lLNv relative to Diff+Inc-enriched lLNv was higher in DD23 than in DD23toDD29 at 3d (Fig 4.41b bottom). This finding suggests that DD23 favours Diff-enriched lLNv to a greater extent than DD23toDD29. Also, like in the case of sLNv, hemispheres in DD23 showed an extended presence of Diff+Inc-enriched lLNv compared to those in DD29 and DD23toDD29 (Fig 4.41b top). There was a significantly higher proportion of hemispheres of Diff+Inc-enriched lLNv relative to the Inc-enriched lLNv in DD23 at 5d compared to those in DD29 and DD23toDD29 (Fig 4.41b, third-row, third-panel). Thus, concerning expHTT forms in the LNv at early ages, DD23 seems to favour significantly Diff, DD29 favours Inc, while DD23toD29 seems intermedial. Thus, a possible ranking order for promoting domination by hemispheres of Inc-enriched LNv is DD29>DD23toDD29>DD23.

Both inclusion numbers and sizes were comparable between *pdf>Q128* in DD23 and those in DD29 at 1d (Fig 4.41c). Intriguingly, those in DD23 showed more inclusions than those in other regimes across most ages. The inclusion numbers for those in DD23 and, to a limited extent, for those in DD29 (3d versus subsequent ages) also increased significantly with age (Fig 4.41d left). For *pdf>Q128* in DD23toDD29, the inclusion numbers did not change with age. Even for aged flies at 23d, those in DD23toDD29 still had fewer inclusions (Fig 4.41d left). Thus, regarding reducing the number of inclusions, DD23toDD29=DD29>DD23. The inclusion sizes were mostly comparable between *pdf>Q128* in different regimes across age; those in DD23 had more minor inclusions from those in other regimes only at 5d (Fig 4.41d, right).

Based on the **ability to decrease the number of inclusions**, **DD23toD29=DD29>DD23**. However, based on the **ability to suppress the early-age dominance by hemispheres having Inc-rich LNv**, **DD23>DD23toDD29>DD29**, with DD23 largely favouring Diff forms. However, *pdf>Q128* in DD23 also had the most significant number of inclusions across age, suggesting that the few LNv that are Inc-enriched (especially at the early ages) are sufficiently dense with numerous Inc, and along with the inclusions found in the vicinity of the LNv, contribute to *pdf>Q128*'s enhanced inclusion numbers in DD23. Thus, regarding diminishing the **inclusion load**, **DD23toDD29>DD29>DD23**. Further, the warm-temperature-mediated suppression of PDF loss from the sLNv of young HD flies compared to cooler temperatures is associated with fewer inclusions, suggesting that sLNv functionality is inversely proportional to inclusion numbers.

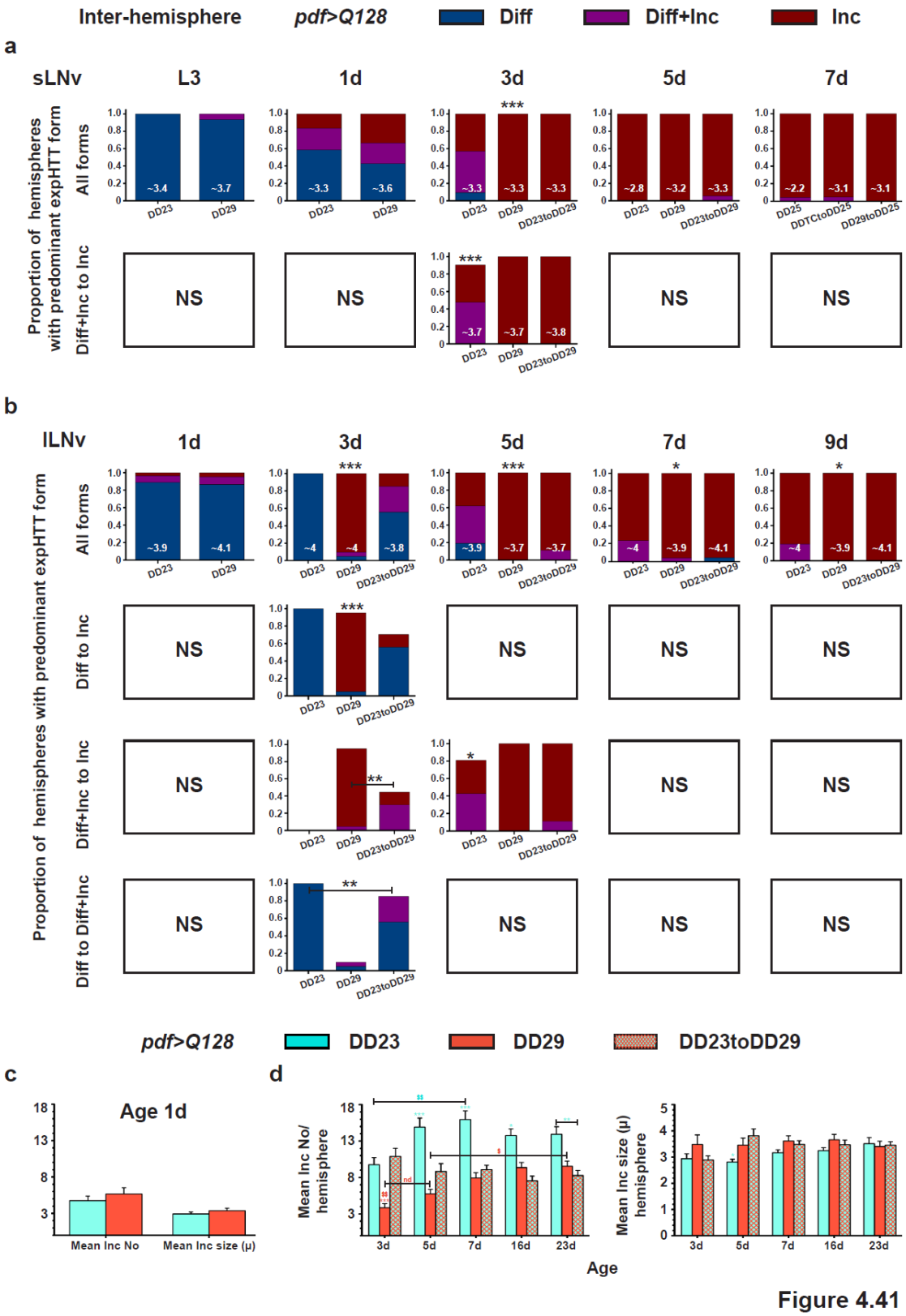

Figure 4.41

Fig 4. 41 pdf>Q128 in DD23 show greater domination by hemispheres with diffuse forms enriching LNv at early ages and higher inclusion numbers across ages than those in DD29 and DD23toDD29.

(a) and (b) The proportion of hemispheres dominated by different expHTT forms in sLNv (a) or lLNv (b) is plotted for *pdf>Q128* comparing DD23 and DD29 at various ages (L3,1d) and with DD23toDD29 (at 3d, 5d, 7d for sLNv and lLNv and 9d for lLNv). These are plotted for all expHTT forms (top) or significantly different pair-wise comparisons (a - bottom, b - second, third and bottom rows). * indicates significant changes in the relative proportions of hemispheres for all expHTT forms between regimes for an age (top) or pair-wise expHTT forms between regimes for an age (a - bottom, b - second, third and third and bottom rows). NS, not significant. At the bottom of some bars, numbers represent the mean number of PDF^+ LNv detected for that regime at that age. (c) Comparison of mean inclusion number and size between DD23 and DD29 for 1d-old *pdf>Q128*. (d) Comparison of mean inclusion number per hemisphere (left) and mean inclusion size per hemisphere (right) between DD23, DD29 and DD23toDD29 across age for *pdf>Q128*. Coloured * indicates a significant age-matched difference between that regime and other regimes or indicated regime, and coloured $ indicates differences between that regime from indicated age(s) or all other ages. Symbols represent statistical differences: single $p<0.05$, double $p<0.01$ and triple $p<0.001$. Error bars are SEM.

In summary, DD23 does not rescue early-age rhythmicity and hastens the loss of PDF from the sLNv, suggesting that it is the least neuroprotective. DD29 and DD23toDD29 confer early-age rhythms, delay loss of PDF^+ sLNv and reduce expHTT inclusions better than DD23, thus, supporting DD29=DD23toDD29>DD23 in neuroprotection. Nevertheless, DD23toDD29 has a more significant impact than DD29 on the strength of the activity rhythms and the inclusion load of *pdf>Q128*, hence offering better suppression of neurotoxicity. Accordingly, on the **capacity for circadian neuroprotection**, **DD23toDD29>DD29>DD23**. Thus, adult-restricted warm temperatures are sufficient to delay most circadian neurodegenerative symptoms of *pdf>Q128*. In conclusion, temperature-based environmental interventions moderate the severity of HD-induced circadian deficits.

4.3.21 Adult-restricted warm temperatures confer greater neuroprotection to HD flies than developmental temperature cycles

I then compared the potency of the two differently acting temperature regimes, the developmental-TC and the adult-restricted warm temperature upshift, to relieve expHTT-perpetrated pathogenicity. Both regimes were comparable in the extent of rhythmicity restored in *pdf>Q128* (Fig 4.42a). Both regimes improved the activity consolidation of *pdf>Q128* compared to its controls in the respective temperature regimes (Figs 4.7b and 4.39c). Since warm temperatures enhanced activity consolidation even in control genotypes across age (Fig 4.42b), it is not surprising to find that *pdf>Q128* in DD23toDD29 showed significantly more consolidated activity than those in DDTCtoDD25 up to 16d (Fig 4.42b top-middle). Further, in AW1, rhythmic *pdf>Q128* in DD23toDD29 had significantly more resilient rhythms than those in DDTCtoDD25 (Fig 4.42c). Although both regimes delayed the loss of PDF from the sLNv soma of *pdf>Q128* compared to their control regimes (Figs 4.13a and 4.40a), those in DD23toDD29 had significantly more PDF^+ sLNv soma than those in DDTCtoDD25 at 9d (Fig 4.43a top), suggesting a more enduring neuroprotection under DD23toDD29. DDTCtoDD25 did modestly restore molecular clock PER oscillations to the sLNv of *pdf>Q128* (Fig 4.4d), whereas DD23toDD29 did not (Fig 4.33d), suggesting that early-age rhythm rescue in the latter occurs independent of PER-driven sLNv clocks. However, PER^+ sLNv soma numbers in *pdf>Q128* under DD23toDD29 were significantly higher than those under DDTCtoDD25 at 7d (Fig 4.43b). The frequency distributions of PER^+ sLNv or the PDF^+ sLNv of *pdf>Q128* in the two regimes were comparable across age (Fig 4.43 c and d), except at 9d, when those in DD23toDD29 had significantly more hemispheres with ≥3 PDF^+ sLNv relative to 0-2 PDF^+ sLNv soma than those in DDTCtoDD25 ($p<0.01$, Fisher's Exact test) (Fig 4.43c). Finally, *pdf>Q128* under DD23toDD29 showed a slightly longer presence of hemispheres dominated by Diff- or Diff+Inc-enriched LNv relative to Inc-enriched LNv than those under DDTCtoDD25 (Fig 4.43e, see sLNv at 1d and lLNv at 3d). However, *pdf>Q128* in DD23toDD29 had generally similar expHTT inclusion numbers (except at 3d) and sizes (except at 1d and 23d) compared to those in DDTCtoDD25 (Fig 4.43f). Thus, DD23toDD29 delays the appearance of inclusions in the LNv of *pdf>Q128* but does not dramatically alter inclusion features compared to DDTCtoDD25. Overall, DD23toDD29 confers slightly longer and better neuroprotection than DDTCtoDD25 in combating expHTT-induced cellular toxicity and circadian dysfunction.

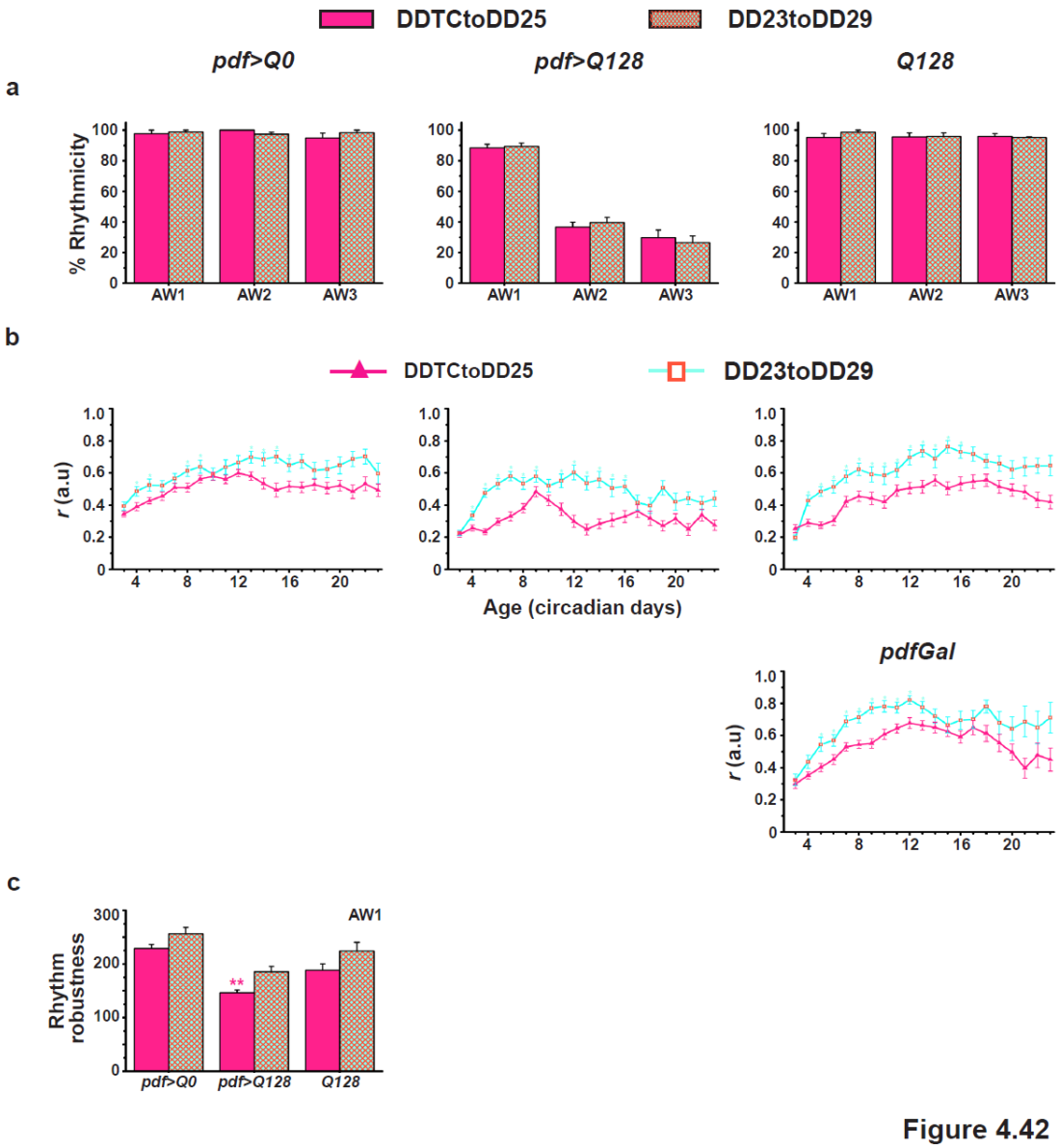

Figure 4.42

Fig 4. 42 pdf>Q128 in DD23toDD29 exhibit higher activity consolidation than in DDTCtoDD25. (a-c) The between-regime comparisons of the mean percentage rhythmicity (a), the mean activity consolidation '*r*' (b), and the mean rhythm robustness in AW1 (c) plotted against AWs (or age) (a and b) for each genotype. Regime colour codes: pink, DDTCtoDD25; cyan, DD23toDD29. All other details are the same as in Fig 4.7.

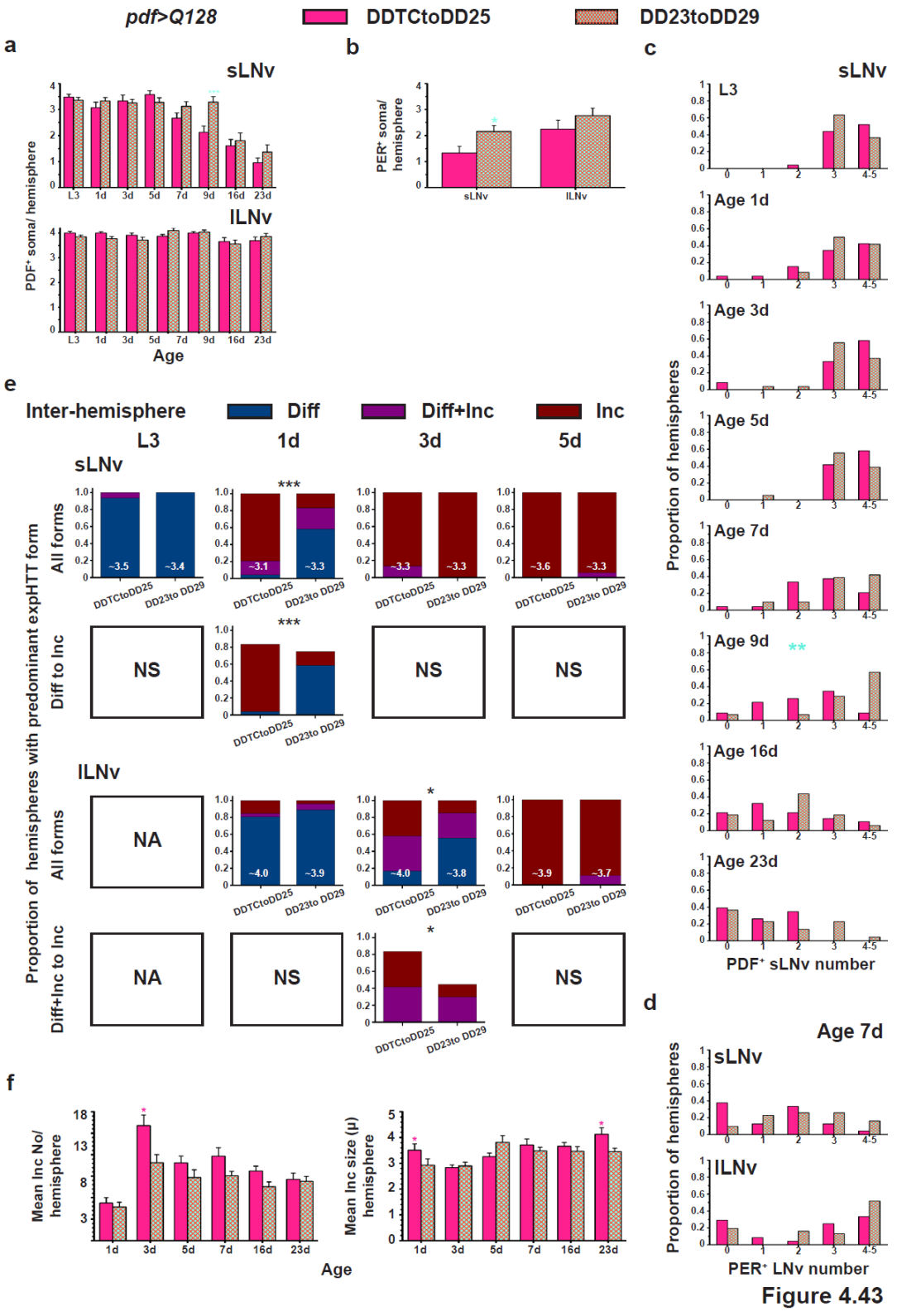

Figure 4.43

Fig 4. 43 Exposure of pdf>Q128 to DD23toDD29 retarded neurotoxicity better than exposure to DDTCtoDD25.

(a) Mean number of PDF$^+$ sLNv soma (top) or lLNv soma (bottom) across age comparing *pdf>Q128* maintained in the DDTCtoDD25 with those in DD23toDD29. (b) Mean PER$^+$ sLNv soma and lLNv soma at 7d. (c) Frequency distribution of the proportion of hemispheres of *pdf>Q128* with 0 to 5

PDF$^+$ sLNv soma numbers in the two regimes across age. (d) Frequency distribution of the proportion of hemispheres of *pdf>Q128* with 0 to 5 PER$^+$ LNv soma numbers in the two regimes at 7d. (e) The proportion of hemispheres dominated by different expHTT forms in sLNv (top panel sets) or lLNv (bottom panel sets) is plotted for *pdf>Q128* comparing the two regimes at various ages. The significantly different pair-wise comparisons are also shown. NS, not significant; NA, not applicable. (f) The mean inclusion number per hemisphere (left) and mean inclusion size per hemisphere (right) of *pdf>Q128* under the two regimes across age. Regime colour codes: pink, DDTCtoDD25; cyan, DD23toDD29. * indicates significant age-matched difference between the regimes at * $p<0.05$, ** $p<0.01$ and *** $p<0.001$. Error bars are SEM.

4.3.22 Remarks on the expHTT forms and their plausible range of toxicity

In *pdf>Q128* under standard conditions of DD25, the Diff form of expHTT appears early-on (L3, and dominates at 1d for sLNv and till 3d for lLNv), followed by Diff+Inc and Inc forms (at 3d for lLNv) and then near exclusively-Inc form (1d onwards for sLNv and 5d onwards for lLNv). Young *pdf>Q128* flies have greater PDF$^+$ and PER$^+$ LNv soma (particularly sLNv) compared to older flies, which coincides with the lower proportions of Inc-enriched LNv. Thus, age similarly affects the expHTT forms and sLNv circadian proteins of *pdf>Q128*: inclusions and loss of circadian proteins from the sLNv increase with age. In most rescue regimes, the early-age rhythms are restored, which in many instances also accompanied a substantial enhancement of PDF$^+$ (and PER$^+$) sLNv soma numbers and dominance of non-Inc forms at early ages, thereby delaying Inc dominance. These observations allude to two inferences. First, the early ages are more amenable and responsive to neuroprotective strategies than the later ages. Furthermore, more importantly, in most of the rescue regimes, the circadian improvements are accompanied by a delay in inclusion dominance concomitant with a prolonged presence and dominance by Diff form (and to a limited extent Diff+inc form) and a decline in Inc numbers, indicating that apart from age, a reduction in the Inc expHTT contributes to abating neurotoxicity. Thus, Diff expHTT seems relatively more benign than Inc expHTT, and the above findings can be approximated onto the following **toxicity scale**: **Diff <Diff+Inc<Inc**.

4.3.23 *Hsp70* is involved in the early-age rhythm rescue of *pdf>Q128* by the adult-restricted warm temperatures

Adult-restricted warm temperatures emerged as the regime that provided the strongest alleviation of expHTT-induced circadian neurodegenerative features. I questioned whether the rescue of the early-age rescue behavioural rhythms of *pdf>Q128* upon upshift to warm temperatures entails Hsp70 because it is upregulated under heat stress, is essential for thermotolerance, and opposes neurodegenerative effects of expanded polyQ proteins (Gong and Golic, 2006; Bettencourt et al., 2008). Since the rhythm rescue was confined to AW1, the statistical analyses of rhythmicity were restricted to AW1, and the daily '*r*' of each fly was averaged across eight days and then across flies to obtain an 8d mean or 'pooled *r*'. In DD23toDD29, as expected, *pdf>Q128* had high rhythmicity (Figs 4.44 top, 4.45a top); both its rhythmicity in AW1and mean 'pooled *r*' were significantly higher than those in DD23 (Fig 4.45a top left and middle). *pdf>Q128* flies deficient in *Hsp70*, be it 1 copy (*Hsp70Ba*) or 2 copies (*Hsp70A*) or 3 copies (*Hsp70A,70Ba*) or 4 copies (*Hsp70B*) or all 6 copies (*Hsp70A,70B*) were arrhythmic (Fig 4.44) with a significantly lower rhythmicity (Fig 4.45a left) and 'pooled *r*' (Fig 4.45a middle) than *pdf>Q128* in DD23toDD29 and also from their respective background controls, the *Q128DfHsp70*s (except *DfHsp70Ba*, for which 'pooled *r*' of control *Q128,DfHsp70Ba* was comparable to that of *pdf>Q128,DfHsp70Ba* and lower than that of *pdf>Q128* in DD23toDD29). This finding suggests that *Hsp70* contributes to the early-age rhythms of *pdf>Q128* in DD23toDD29 since in the partial or complete absence of *Hsp70*, the early-age rhythm rescue of *pdf>Q128* was abrogated. Further, the observation that most of the control *Q128,DfHsp70* genotypes were rhythmic (Fig 4.45a left) and their robustness in AW1 was higher than that of *pdf>Q128* in DD23toDD29 (except for that of *Q128;DfHsp70*) (Fig 4.45a right), indicates that the loss of *Hsp70* by itself does not overtly affect the free-running rhythms.

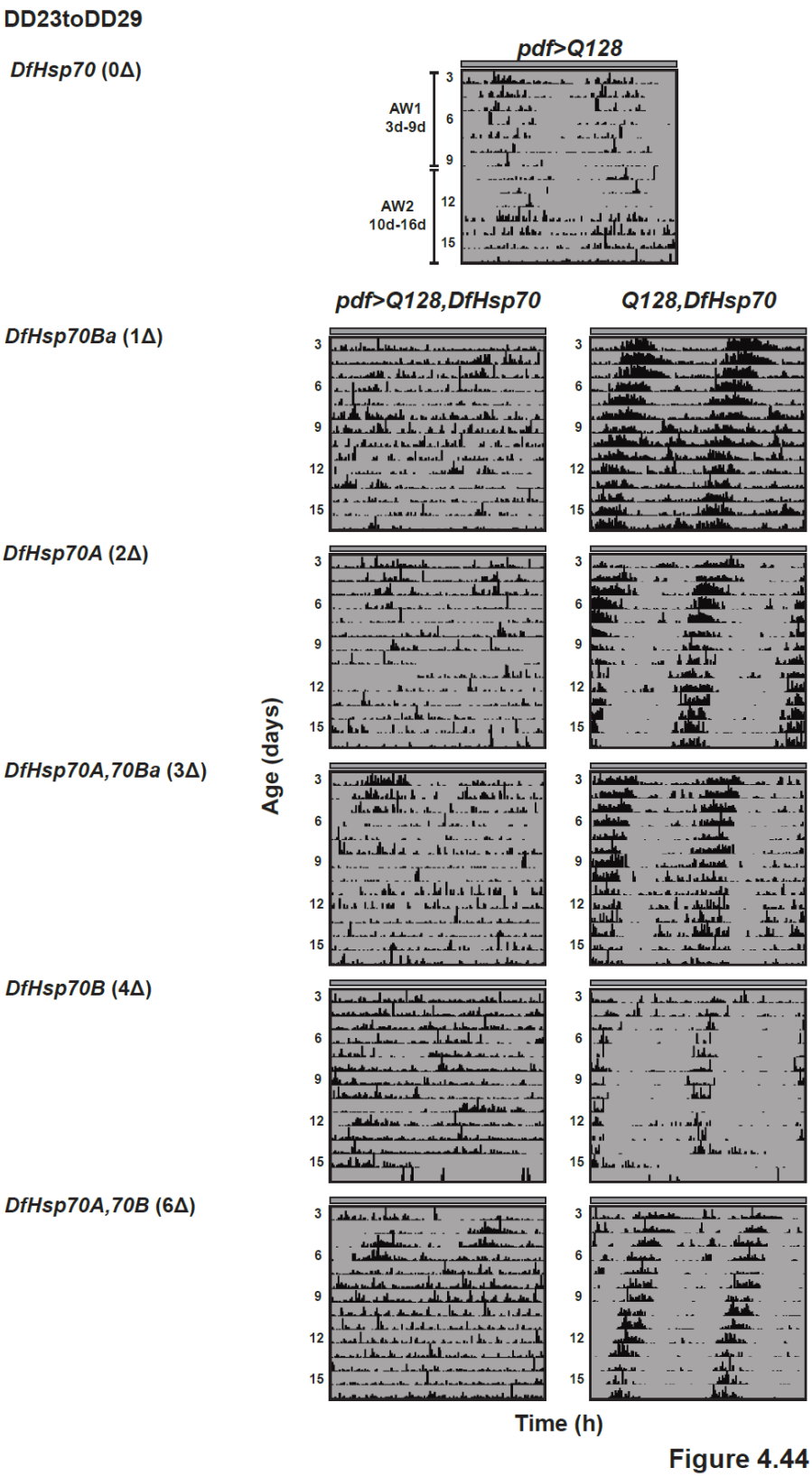

Fig 4. 44 pdf>Q128 in DD23toDD29 are arrhythmic without Hsp70.

Representative double-plotted actograms for adult flies reared in DD23 and recorded in DD29 as adults for 21d (age 3d-23d). Since many fly deaths were beyond 10d, many actograms show missing data or blanks. All other details are the same as in Fig 4.1.

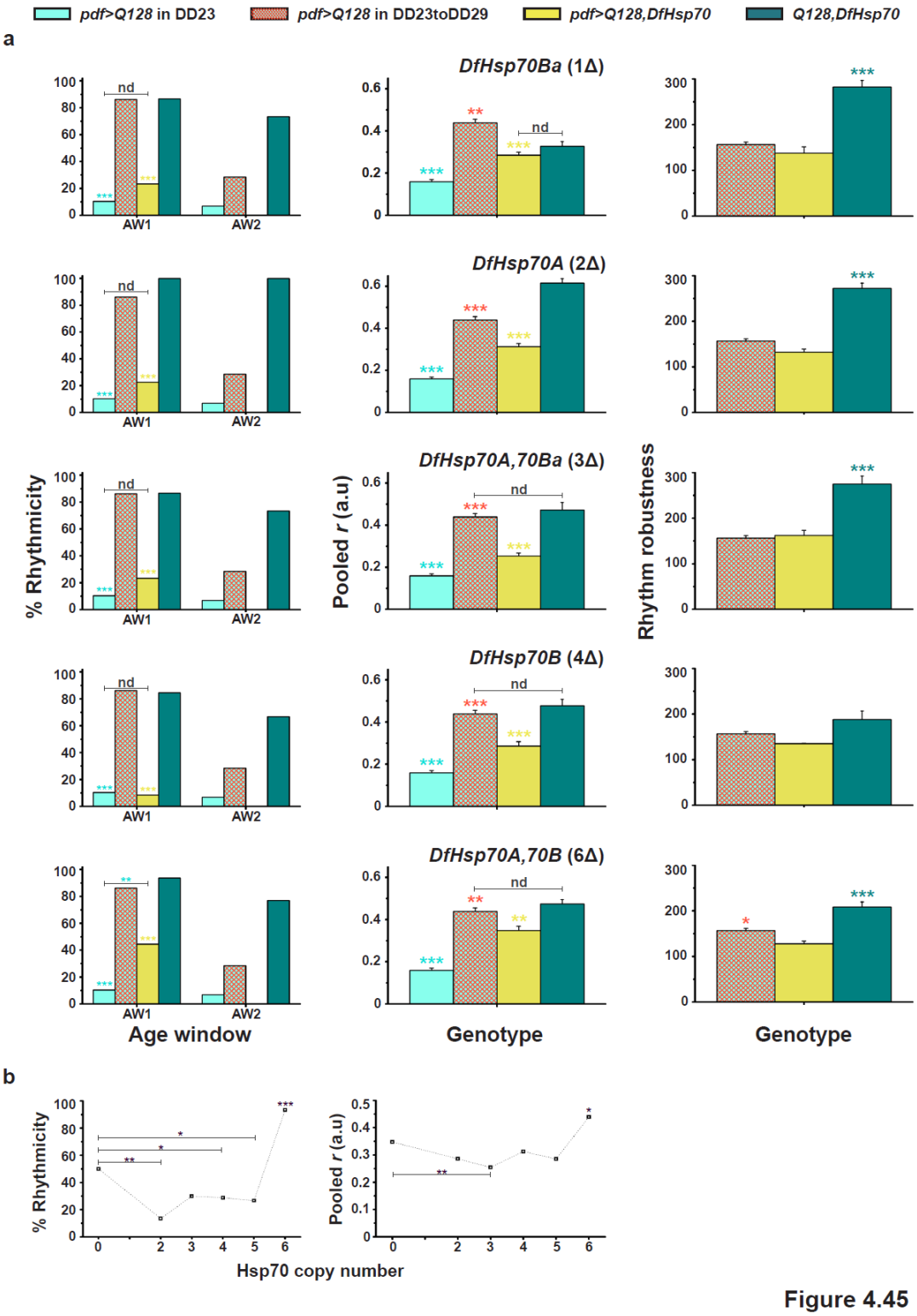

Figure 4.45

Fig 4. 45 Most pdf>Q128 flies lacking Hsp70 do not show rhythmic activity and have poor activity consolidation in DD23toDD29.

(a) Percentage rhythmicity (left), mean activity consolidation '*r*' over eight days (middle) and rhythm robustness (right) in DD23toDD29 for *pdf>Q128* with *DfHsp70* arranged in the ascending order of the number of *Hsp70* copies deleted, their respective *Q128DfHsp70* controls and *pdf>Q128* in DD23toDD29. *pdf>Q128* in DD23 serves as a negative baseline control. The statistical analyses are restricted to AW1 for rhythmicity and robustness. (b) The percentage rhythmicity obtained by pooling samples across three

different experiments (left) and the mean '*r*' (right) plotted against the *Hsp70* copy number. nd, not different, a.u, arbitrary unit. * indicates statistically significant differences between genotypes at * $p<0.05$, ** $p<0.01$ and *** $p<0.001$. Error bars are SEM.

pdf>Q128 in DD23 was taken as a negative control due to their near-complete lack of rhythmicity, and DD23 is also the appropriate temperature-regime control. The percentage rhythmicities of most of the *pdf>Q128,Hsp70* genotypes were similar to *pdf>Q128* in DD23 (Fig 4.45a left), further supporting a role for *Hsp70* in early age rhythmicity of *pdf>Q128*. The only surprising exception was *pdf>Q128,DfHsp70A,70B* with a complete deletion of *Hsp70,* which showed higher rhythmicity than *pdf>Q128* in DD23. The 'pooled *r*' of the various *pdf>Q128,DfHsp70* genotypes, while being lower than *pdf>Q128* in DD23toDD29, was still higher than *pdf>Q128* in DD23 (Fig 4.45a middle). This observation that the *Hsp70* deficient *pdf>Q128* flies, which are poorly rhythmic in DD23toDD29 have a higher 'pooled *r*' than *pdf>Q128* in DD23 (with intact *Hsp70*), again alludes to a consolidating effect of warm temperatures on the fly locomotor activity. However, the persistence of this effect even in the *Hsp70* deficient flies indicates that the synchronizing effect of warm temperatures on fly activity does not require *Hsp70*. Overall, the involvement of heat-stress-inducible Hsp70 in the rescue of early-age behavioural rhythms of HD flies by adult-restricted warm temperatures suggests that Hsp70-mediated heat shock response (and enhancement of proteostatic mechanisms) may underly the rescue.

Comparing the rhythm parameters against the *Hsp70* copy number reveals an interesting pattern. *pdf>Q128* with all 6 copies of the *Hsp70* intact and those with complete deletion of *Hsp70*, both have better rhythmicity and 'pooled *r*' than many of their counterparts with intermediate copy numbers (Fig 4.45b). *pdf>Q128* having all 6 copies of *Hsp70* (i.e. *pdf>Q128* in DD23toDD29 without any deficiencies) had significantly higher rhythmicity and 'pooled *r*' than its counterparts with *Hsp70* deficiencies, regardless of the number of deletions. *pdf>Q128* lacking all 6 copies of *Hsp70* had higher rhythmicity than those with 2, 4 and 5 copies of *Hsp70* and higher 'pooled *r*' than those with 3 copies of *Hsp70*. Thus, the free-running activity rhythm parameters show a somewhat J-shaped curve concerning the *Hsp70* copy number. A low copy number is mildly rhythm-promoting, and a high copy number is strongly rhythm-promoting, while intermediate copy numbers have the least positive effects. Such a J-shaped dose-response curve with low-dose reduction and high-dose enhancement of effects (Cook and Calabrese, 2006) is an example of a hormetic curve. However, it is most often reported in the context of adverse effects of a stressor/hormetic agent.

4.4 DISCUSSION

4.4.1 Mechanisms of temperature-mediated retardation of expHTT-induced circadian dysfunction and neurotoxicity

The key finding of this study that mild heating delays the neurotoxic effects of expHTT in flies strongly suggests that exposure to a stressor like heat may indeed improve flies' ability to withstand and respond to a neurodegenerative stressor. This study shows that temperature affects expHTT-induced cellular and behavioural circadian neurodegenerative properties in different ways and directions using combinations of environmental modulations: cycling and constant temperatures, developmental stage and (or) adult exposure, and developmental light presentation or deprivation. These differences likely reflect the complex interplay of temperature, its nature of change (non-cyclic *vs.* cyclic, constant across development and adulthood *vs.* changing post-eclosion, and the magnitude and direction of change), life stages, presence of light, physiology, and the specific phenotypic trait. In the following sections, I will primarily discuss the phenotypes of the genotype *pdf>Q128* under various environmental regimes. So, unless otherwise specified, most discussion sections pertain to *pdf>Q128*.

4.4.1.1 Developmental temperature cycles

The exposure of *pdf>Q128* to cycling temperatures of 12h:12h 29°C:21°C (warm/cold cycles in the absence of light) during development, followed by DD25 during adulthood, but not developmental constant warm (29°C) or constant cold (21°C) followed by DD25 as adults, rescues the early-age adult free-running rhythms. This finding suggests that the developmental presence of temperature as an oscillating circadian signal (zeitgeber) is an essential aspect of the rescue. The restoration of early-age adult activity rhythms on developmental exposure of *pdf>Q128* to temperature cycles was accompanied by low-amplitude LNv PER oscillations with modest delay in loss of PDF from sLNv, suggesting a robust circadian component to the rescue. Furthermore, since LNv PER is known to be essential for rhythm strength (Delventhal et al., 2019; Schlichting et al., 2019b), under DDTCtoDD25, the restoration of early-age activity rhythms,

albeit of low robustness accompanied by low PER in the LNv also supports a circadian mechanism of rescue. The effects of developmental TC on activity rhythms in adults were counteracted by constant light during development, again suggesting an underlying circadian rhythm. Developmental-TC did not improve LNv PER levels or PER^{+} LNv numbers nor affect the expHTT forms in the LNv or inclusion features, suggesting that the LNv cellular health is not effectively revived. With a weakly functioning sLNv, the central pacemakers of free-running rhythms and the early-age behavioural rhythms evoked by developmental TC suggest a circadian neuronal network-level reinforcement by cycling temperatures. Thus, the developmental-TC mediated adult rhythm rescue seems driven by circadian mechanisms at the neuronal and circuit levels, depends on the temperature experienced as adults, and is opposed by light during development. Additionally, temperature cycles must be present over the entire duration of development for early-age rhythmicity.

The observation that the early-age adult activity rhythms of *pdf>Q128* under developmental-TC also depend on the temperature experienced as an adult, with the experience of relatively optimal or warm temperatures as adults a requisite for rhythmicity, indicates that rhythmicity is also -dependent on the temperature experienced as adults, in the direction of an upshift. Since changing temperatures can activate the temperature stress response (Colinet et al., 2015; Manenti et al., 2018), the above finding also suggests that a minimum temperature of 25 °C, which the flies prefer, is necessary for these cytoprotective mechanisms to work in adults.

The developmental time under temperature cycles (12h:12 29°C:21°C) is like that under 25°C, i.e. 9-10d. So, HD flies in DDTCtoDD25 (TC during development) do not exhibit differential developmental time. However, the effect of such a fluctuating temperature on the Gal4-driven protein expression levels, cellular kinetics and Hsp expression is unknown.

4.4.1.2 Constant temperatures during development and adulthood

In regimes where ambient temperatures were held constant during development and adulthood, *pdf>Q128* phenotypes had a complex relationship with temperature: temperature had a directly proportional effect on improving activity rhythms and reducing inclusion load (DD29>DD25>DD23), a somewhat U-shaped effect on PDF preservation in the sLNv (DD29>DD23>DD25) and a similar trend of DD23>DD25 in LNv PER preservation. The constant warm temperatures are the most neuroprotective for most of the features.

4.4.1.3 Change in temperature as adults (upshifts and downshifts)

Exposure of adults to warm temperatures was sufficient in slowing down circadian HD progression, suggesting that warm temperatures during development were unnecessary for the deceleration. The adult-restricted warm temperatures were even better in diminishing the inclusion load and enhancing activity rhythm robustness than warm temperatures throughout development and adulthood, indicating that the former regime is more neuroprotective than the latter. Adult exposure to *pdf>Q128* to warm temperatures resulted in the restoration of early adult activity rhythms and a delayed loss of PDF and PER from sLNv without restoration of PER oscillation, i.e., restoration of circadian proteins, not PER-controlled molecular clocks. This finding suggests that the activity rhythm rescue is via a *per*-less clock mechanism or has limited contribution from the LNv clocks. Improved activity consolidation in all genotypes under warm temperatures, i.e., most flies restricting their activity to specific time points, suggests a time-of-day dependent clock contribution. The decline in expHTT inclusion load and the requirement of *Hsp70* for the exhibition of well consolidated activity rhythms upon adult-restricted warm temperature exposure also suggests that this regime improves cellular proteostasis, a proxy for healthier neurons. Thus, warm temperatures do not restore the individual neuronal clocks (*per-driven*); however, upregulating the heat shock proteins/response could boost cellular proteostasis and neuronal pacemaker health, strengthening the overall network functioning and contributing to rhythmicity.

The warm-temperature-mediated rhythm rescue was directional since the exposure of *pdf>Q128* to development-specific warm temperatures did not overcome adult behavioural arrhythmicity, indicating that warm developmental temperature is unnecessary. These results reveal that the

adult-restricted temperature is critical in determining the rescue and must be sufficiently warm. Overall, adult-restricted warm temperatures are necessary and sufficient to mitigate the expHTT-induced behavioural arrhythmicity. Not only are the warm-temperature-mediated improvements in the locomotor activity rhythm parameters of *pdf>Q128* directional (upshift), but they are also influenced by the upshift temperature, the duration of warm temperature exposure, and the magnitude of upshift: early-age rhythm rescue was only possible at warm enough adult temperatures of 29°C, under chronic exposure and a 6°C upshift had a more significant effect on activity rhythms than a 4°C upshift (DD25toDD29 vsDD23toDD29). The requirement for the sufficiently high and chronic presence of warmth as adults suggests that rescue processes are not limited to an immediate stress response to the temperature hike but might also involve long-acting adaptive responses.

4.4.1.4 Development-specific temperature cycles *vs.* adult-restricted upshift to warm temperatures

The two critical regimes that mitigated the expHTT-indued phenotypes were the developmental temperature cycles (DDTCtoDD25) and adult-restricted upshift to warm temperatures (DD23toDD29). Though these two regimes shared a few commonalities of delaying phenotypes and cellular underpinnings of the rescue, they differed in their potency and rescue mechanisms. In both the regimes, developmental and adult stages experienced different temperatures. However, on the one hand, with development-specific TC, the ambient environmental conditions predominantly during development and the temperature experienced as adults determined the activity rhythm rescue to a limited extent. In contrast, rescue by adult-restricted warm temperatures was solely determined by the temperature experienced during adulthood.

Both the regimes rescued early-age behavioural rhythms of *pdf>Q128*, and the rescue also depended on the temperature experienced as adults. Even though for the development-specific, an ambient temperature of 25°C as adults were sufficient (DDTCtoDD21 *vs* DDTCtoDD25 and DDTCtoDD29, see Fig 4.12), for the upshift regime, a warm temperature of 29°C as adults were significant (DD21toDD25 *vs* DD25toDD29 and DD23toDD29, see Fig 4.35). These contrasting findings indicate a divergence in the mechanism of rescue by the two regimes, the former manifesting effects at 25°C, which is the preferred temperature of adult *Drosophila (*Kaneko et

al., 2012; Goda and Hamada, 2019) and the mean temperature of the TC, while the latter manifesting effects only at 29°C, which is a mild heat stress to the flies. Though both regimes improved activity consolidation and delayed the loss of PDF from the sLNv soma, the warm-temperature-mediated effects were more pronounced and slightly prolonged. Better preservation of PER^{+} sLNv and a reduction in the inclusion load under DD23toDD29 indicate that the regime is more facilitative of neuroprotective mechanisms than DDTCtoDD25. DDTC-mediated rhythm rescue is accompanied by partial restoration of PER-driven sLNv clocks, whereas DD23toDD29 rescue is independent. Interestingly, unlike development-specific TC wherein *pdf>Q128* in LDTCtoDD25 or LLTCtoDD25 were arrhythmic as adults, adult-restricted upshift to warm temperatures resulted in early-age rhythm rescue despite the presentation of LD or LL during development (LD23toDD29 and LL23toDD29). This result suggests that the warm-temperature-mediated delay in the breakdown of behavioural rhythms is mainly a temperature effect, essentially light-independent and does not require functional developmental clocks. This finding also emphasises a significant distinction between the developmental-TC- and the warm-temperature-mediated early-age rhythmicity of *pdf>Q128*: whereas the latter is relatively light-insensitive and does not require developmental clocks, the former is light-sensitive (inhibited by light) and may require functioning clocks. Thus, this study uncovers two different mechanisms of temperature-mediated suppression of expHTT-induced neurotoxicity and circadian dysfunction (Fig 4.46). One via developmental temperature cycles that is largely clock-dependent, sensitive to developmental light, may require functional clocks during development and is independent of expHTT inclusion load. The other is via upshift to warm temperatures as an adult is partially clock-dependent, insensitive to developmental light, independent of developmental clocks, reduces the expHTT inclusion load and requires Hsp70. The second mechanism mediated by warm temperatures is more potent in mitigating neurotoxicity and likely so because it more strongly impacts pathways of neuronal proteostasis, as evidenced by a pronounced effect of inclusions and the involvement of *Hsp70*. In flies, the temperature has been shown to elicit two distinct responses on the genome-wide transcriptional profiles: a clock-dependent circadian response and a clock-independent, temperature-driven response (Boothroyd et al., 2007).

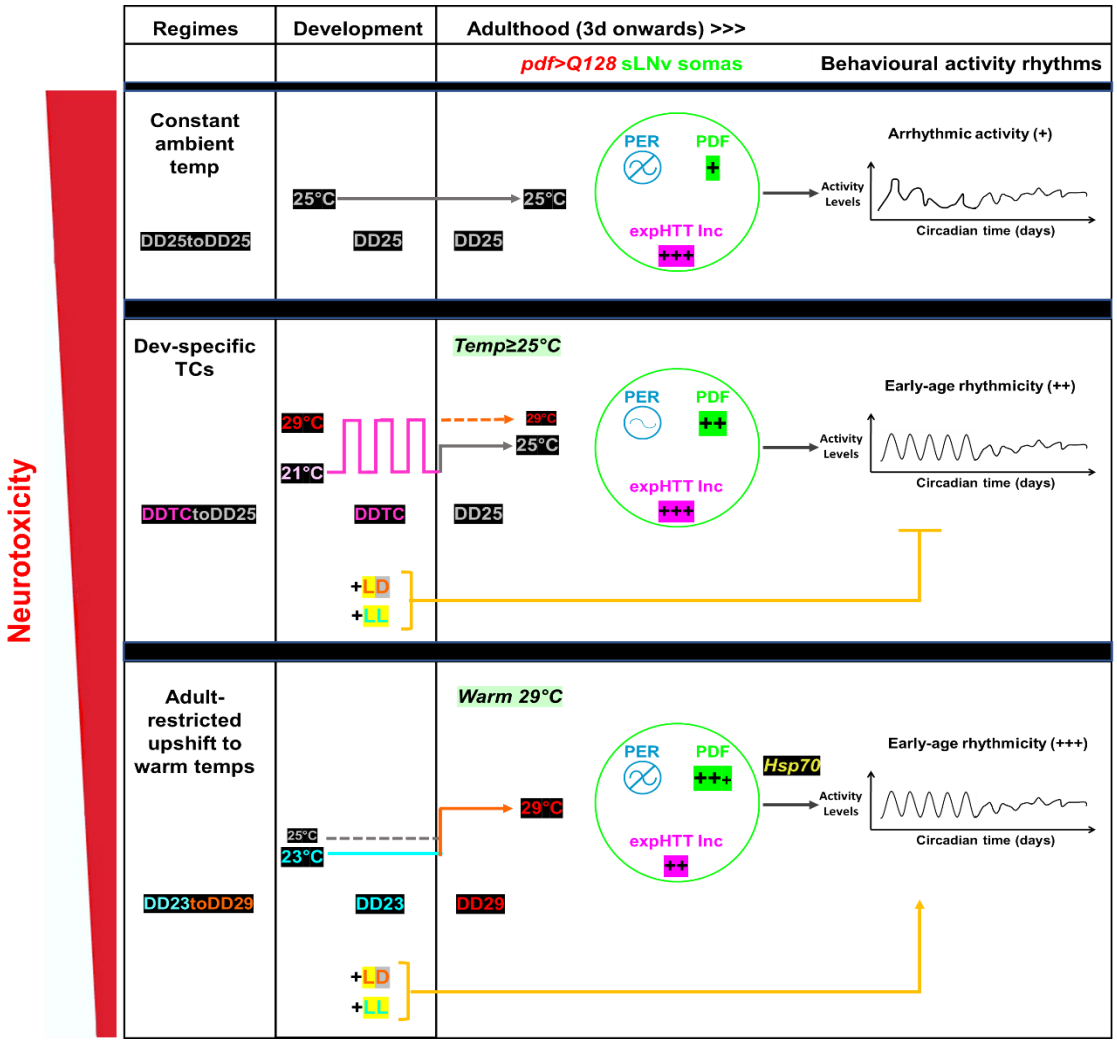

Fig 4.46

Fig 4. 46 An illustration summarising the mechanisms involved in ameliorating circadian dysfunction and neurotoxicity in HD flies by two different temperature regimes.

The pathogenic *pdf>Q128* expressing expanded HTT in the circadian pacemaker LNv neurons of *Drosophila*, reared under free-running conditions of DD25 during development and maintained in DD25 as adults, show a loss of molecular clock protein PER oscillations in the sLNv soma, a reduction in the PDF^{+} sLNv soma numbers, presence of expHTT inclusions and a concomitant loss of behavioural locomotor activity/rest rhythms (top). Two temperature-dependent mechanisms significantly delay these phenotypes: development-specific temperature cycles (centre) and adult-restricted upshift to warm temperatures (bottom). Both regimes restore early-age circadian activity rhythms and improve circadian output peptide PDF in the sLNv, with the latter having a more substantial effect. The restoration of activity rhythms under both regimes is contingent on the temperature experienced during adulthood: the former requiring ≥25°C, the latter requiring warm temperatures of 29°C. The former's reinstitution of early-age behavioural rhythms is sensitive to light (cyclic or constant) during development, wherein light opposes the rescue. In contrast, those established by the latter regime are primarily unaffected by developmental light and require *Hsp70*. Developmental temperature cycles also modestly restore PER oscillations to the sLNv, whereas adult-restricted upshift to warm temperatures does not. The former does not affect the expHTT inclusion load, whereas the latter diminishes it. Altogether, adult-restricted warm temperatures offer more significant relief from neurotoxicity and circadian decline to HD flies than development-restricted temperature cycles.

4.4.2 Temperature, *Drosophila* circadian neuronal network, and activity rhythms

External temperatures directly influence the relative allocation of circadian activity across a day: warm temperatures suppress daytime activity, phase advance morning activity and phase delay evening activity (Majercak et al., 1999; Low et al., 2008; Das et al., 2016; Iyengar et al., 2022), while cooler temperatures suppress morning activity and phase advance and suppresses evening activity (Alpert et al., 2020). They also influence sleep levels and onset in a time-specific manner, which involves the DN1(p) neuronal cluster (Ishimoto et al., 2012; Guo et al., 2016; Parisky et al., 2016; Lamaze et al., 2018; Beckwith and French, 2019; Jin et al., 2021). The circadian DN1ps directly respond to temperature: inhibited by heating and activated by cooling (Yadlapalli et al., 2018). Not only are the fly neuronal circuits sensitive to changes in temperature, but even complete temperature information is also encoded and relayed. Two recent studies in the fly showed that parallel pathways convey constant warm and cold temperature information from the thermosensors to different clock neuronal subsets (LPN activation and DN2 inhibition, respectively) via parallel pathways to restructure sleep (Alpert et al., 2020; Alpert et al., 2022). Thus, constant ambient temperatures also affect a behaviour like sleep by directly and differentially impacting the circadian neuronal subgroups in a time-of-day- and absolute-temperature-dependent manner. Therefore, it is strongly conceivable that similar network-level pathways and responses exist that mediate the differential effects of constant warm and cool temperatures on the adult circadian activity rhythms.

4.4.2.1 Warm temperatures and activity consolidation

Adult flies prefer a temperature of 25°C (Sayeed and Benzer, 1996; Hamada et al., 2008; Dillon et al., 2009) and tend to avoid harsh environments, including warm temperatures, using behavioural strategies like seeking shaded microhabitats to avoid direct exposure to extreme heat and decreasing their daytime activity (and sleeping more) to reduce the foraging and other critical activities to lower the desiccation risk (Hoffmann, 2010; Ishimoto et al., 2012; Harvey et al., 2020; Ma et al., 2021a). Even the pattern of their circadian activity rhythms is modified to avoid warm temperatures: under LD29 or LD30, flies reduce their daytime activity by shifting most of

their activity to the dark phase by advancing their morning activity and delaying their evening activity (Majercak et al., 1999; Low et al., 2008; Das et al., 2016; Iyengar et al., 2022). In LD29, flies sleep more during the day and less at night, and in DD29, they show an increase in sleep during the subjective day (Ishimoto et al., 2012; Parisky et al., 2016). Now, my studies show an effect of temperature on activity consolidation with a contribution from the presence of light during development (the effect of light is discussed in 4.4.2.3.1). Support for temperature affecting the activity consolidation comes not only from warm temperatures enhancing activity consolidation across genotypes but also from control flies reared and recorded at lower temperatures having poor activity consolidation than their counterparts in ambient or warm temperatures (comparing flies in DD23, DD25 and DD29). The increase in activity consolidation in DD29 seen across genotypes indicates that flies are highly active during a specific time window, thus shrinking the duration of activity. Time-restricted consolidation of activity might be yet another behavioural strategy to regulate body temperature in these ectotherms because locomotor activity rhythm is a thermogenic process (Block, 1994; Loli and Bicudo, 2005; Refinetti, 2020), which will further increase the body temperature of these ectotherms who are already experiencing warm temperatures of 29°C, which is 4-5°C above their preferred temperature. There is evidence from *Drosophila* for an association between activity, metabolic rate and temperature sensitivity mediated by dopamine: *fumin* flies defective in a dopamine transporter are hyperactive and short on sleep, also exhibited higher metabolic rate and were thermophobic, preferring lower temperatures (Kume et al., 2005; Kume, 2006; Ueno et al., 2012). Even though high temperatures (31°C) during development reduce spontaneous activity as adults (activity over 12h), adult-restricted upshift to warm temperatures (19°C to 31°C) increases spontaneous adult activity (MacLean et al., 2017; Klepsatel and Gáliková, 2022). However, for inbred and outbred *Drosophila melanogaster* under LD and in DD, circadian daily activity levels averaged over longer durations (≥3d) are not different across a range of constant temperatures (Prabhakaran and Sheeba, 2014; Ito and Awasaki, 2022) demonstrating that the total activity levels *per se* are unaffected over a range of constant external temperatures. Considering this information, the activity levels under different temperature regimes were not quantified.

4.4.2.2 Understanding the effects of development-specific temperature cycles on the circadian neuronal network of HD flies

In my experiments, exposure of *Drosophila* clocks to cyclic time cues mainly targeted the pre-adult stages. Hence, it is vital to restrict the inferences regarding zeitgeber effects to the developmental stages. However, there are limited studies on the developmental clock perception of circadian inputs affecting adult activity rhythms, and most of them have been carried out in larvae. Given that the adult circadian network has been extensively studied, the larval and adult stages can serve as two points of reference and using the data on the developmental timing of the various circadian neuronal subsets, one can make a few logical predictions about the relative roles of circadian neurons in light and temperature entrainment during development. The larval circadian clock comprises nine clock neurons per hemisphere: the four PDF^{+} sLNv, the PDF^{-} 5^{th} sLNv, two DN1s and two DN2s, and light input to the larval clock is via CRY in the sLNvs and the DN1s and the larval visual system (Helfrich-Förster, 1997; Kaneko et al., 1997b; Kaneko and Hall, 2000; Klarsfeld et al., 2004; Malpel et al., 2004; Keene et al., 2011; Klarsfeld et al., 2011). Though the other pacemakers, including the LNds, appear at L3, they exhibit molecular clock oscillations only in the late pupal stages; the lLNvs develop around the mid-pupal stage (Kaneko et al., 1997b; Kaneko and Hall, 2000; Helfrich-Förster et al., 2007; Liu et al., 2015b). During pupal development, the H-B eyelets replace the BOs (Malpel et al., 2002).

In adult flies, the LPNs and DNs, particularly the CRY^{-} LPNs, DN1ps and DN2s, are shown to be more temperature-sensitive, and they are preferentially entrained by temperature-when conflicting light and temperature cues are provided (Busza et al., 2007; Miyasako et al., 2007; Yoshii et al., 2010; Harper et al., 2016). Additionally, DN1p clocks regulate temperature entrainment because, in per^{01} flies, PER expression in the DN1ps was sufficient to rescue synchronisation to TCs (Zhang et al., 2010c). Moreover, DN1ps are modulated by ambient temperature cues via chordotonal organs (Chen et al., 2015a; Chen et al., 2018; Lamaze and Stanewsky, 2019; Roessingh et al., 2019) receive temperature inputs from the warmth-sensing ACs (Hamada et al., 2008; Jin et al., 2021) and are acutely inhibited on heating and excited on

cooling (Yadlapalli et al., 2018). The DN1as are inhibited by absolute cold temperatures (Alpert et al., 2020), and the LPNs are excited by absolute warm temperatures (Alpert et al., 2022). The DN2s, the DN1as and DN1ps are necessary for another independent circadian behaviour, the temperature preference rhythm, a time-of-day-dependent preference of optimal ambient temperature over a temperature gradient (Kaneko et al., 2012; Chen et al., 2022). These studies posit the LPNs and the DNs, predominantly the CRY^- subsets, as the temperature-sensitive clock neurons. My findings demonstrate that TC during larval or pupal stages alone is insufficient for adult activity rhythms of *pdf>Q128* and can be attributed to the emergence of different subsets of temperature-sensitive clock neurons at various developmental stages (Yoshii et al., 2005; Helfrich-Förster et al., 2007; Picot et al., 2009; Liu et al., 2015b) and it may be essential to expose the subsets to TC throughout each stage of their development to achieve rhythmicity as adults.

The observation that developmental DDTC, but not LDTC or LLTC, rescues circadian behavioural free-running rhythms of young *pdf>Q128* adults in DD25 gives rise to several conclusions.

1) To a certain degree, the rhythm rescue is mediated by the clock neurons that are more sensitive to temperature than light (and possibly intrinsically light-insensitive, i.e., CRY^-, see 5 below), the non-LNv circadian neuronal subsets. Since PDF and sLNv are vital for mediating free-running activity rhythms (Renn et al., 1999; Grima et al., 2004b; Stoleru et al., 2004; Shafer and Taghert, 2009), and they are required for circadian behavioural rhythmicity after exposure to TC (Busza et al., 2007), the relatively longer presence of PDF^+ sLNv in *pdf>Q128* under DDTCtoDD25 as compared to those in DD25 can partly explain the improved early-age rhythmicity. However, by 7d, PDF^+ sLNv numbers of *pdf*>Q128 in DDTCtoDD25 are comparable to those in DD25. In contrast, behaviourally, *pdf>Q128* in DDTCtoDD25 show control-like activity consolidation that is significantly better than those in DD25 up to 11d (Figs 4.1c, 4.13a, 4.7b). As PER levels are significantly lower in the LNv of *pdf>Q128* under DDTCtoDD25, there is a modest PER oscillation in their sLNv anti-phasic to controls and the entraining TC; the persistent behavioural rhythmicity also cannot be explained entirely by

the LNv clock functions (Fig 4.4d). A factor contributing to the extended rhythmicity of *pdf>Q128* under DDTCtoDD25 could be the sLNv dorsal termini, which are unaffected in the *pdf>Q128* flies in DD (Prakash et al., 2017) and present as larvae. These dorsal termini are required for entertainment to gradually ramped temperature cycles and the following free-running rhythms (Fernandez et al., 2020). LNv functioning under DDTCtoDD25 is likely limited and transient and does not fully explain the extended rhythmicity of *pdf>Q128*. To fully explain the rhythmic activity of these flies under DDTCtoDD2, the non-PDF$^+$LNv clock neurons, many of which are temperature sensitive (as explained below), are invoked. These circadian neurons of *pdf>Q128* have functional clocks in them, as proven by the synchronous clock protein PER oscillations in them (LNds and DNs) under DD (Prakash et al., 2017). Although a functional clock in the PDF$^+$ LNv neurons is required for the synchronisation of morning activity under 25°C:16°C DDTC (Lorber et al., 2022), there is increased synchronisation of activity rhythms by temperature in flies with dysfunctional or ablated LNv, and the clocks in the non-PDF$^+$LNv are sufficient for the synchronised activity under high-temperature TCs (Yoshii et al., 2005; Busza et al., 2007; Zhang et al., 2010c; Gentile et al., 2013). Notably, the entrainment of larval LNs to temperature cycles requires DN2 clocks (Picot et al., 2009). These data strongly indicate that the non-LNv clock neurons mediate synchronous circadian activity rhythms under TCs, even without the LNv. Some of these mechanisms are established as early as the larval stages. Further, DN1s communicate to the output centres that control behaviour (Cavanaugh et al., 2014; Guo et al., 2018a; Lamaze et al., 2018; Barber et al., 2021; Jin et al., 2021; Zhang et al., 2021a). Thus, the DN1s can directly be synchronised by temperature and receive timing information from other clock neurons, particularly the (Zhang et al., 2021a) weakening sLNv, and integrate and communicate them to the locomotor regions to mediate rhythmic behaviour. The DN1s also form reciprocal connections with the LNs, which can impact pacemaker function (Collins et al., 2012; Collins et al., 2014; Guo et al., 2016; Fujiwara et al., 2018; Díaz et al., 2019; Fernandez et al., 2020) and synchrony between the DN1 and LN clocks are essential for the synchrony of activity rhythms (Yao et al., 2016). Thus, temperature synchronisation of the

DN1s can in-turn also influence the LNs and impose temporal information on the circuit. In light of earlier research, the current study suggests that in conditions of compromised LNv function, such as in the *pdf>Q128*, even though developmental 29°C:21°C TCs only partially rescue LNv PER and PDF, they may be able to synchronise temperature-sensitive non-LNv circadian neurons and (or) transmit temporal information to the locomotor output networks that contribute to rhythmic activity in the young adults in the DD25 post-TC.

2) The above discussion also suggests that whole-organismal interventions like temperature impinge on the entirety of the circadian network to bring about rhythmic behaviour. Environmental signals like temperature regulate organismal physiology through non-autonomous cellular mechanisms (Vakkayil and Hoppe, 2022). Temperature signals could strengthen downstream, compensatory, or alternate mechanisms to re-establish network functioning and improve robustness. A recent study in-fact suggests that though the DN1s are not necessary for generating circadian behavioural rhythms *per se*, they could serve as a parallel, albeit redundant pathway for the control of output circuits that regulate activity/rest rhythms and might become relevant in specific environmental contexts (Nettnin et al., 2021).

3) The finding that though developmental-TC improves early-age activity rhythms of *pdf>Q128* adults, the effects are not long-lasting could be because, as adults, after removal of the cycling temperature signals, its entraining effects on the temperature-sensitive neurons, especially the DN1s, likely wane. DN1s are non-autonomous circadian oscillators that depend on peptidergic inputs from other lateral clock neurons, such as PDF from the sLNv, to maintain free-running rhythms in molecular clocks and electrical activity (Klarsfeld et al., 2004; Yoshii et al., 2009; Seluzicki et al., 2014; Liang et al., 2017; Lamaze and Stanewsky, 2019). As adults, in the continued absence of temperature cues and gradually weakening sLNvs, the DN clocks might weaken in the long run and not be able to sustain rhythmic activity.

4) The temperature-sensitive developmental clocks are functional in *pdf>Q128*. This conclusion is consistent with our empirical observation that PER is present in the larval DN2s, and the larval DN2 clocks are essential for entraining larval LNs to TCs (Picot et al., 2009).

The findings also provide proof-of-concept evidence that the developmental clocks are temperature-sensitive and temperature-entrained. Their temperature synchronisation can alter adult circadian rhythms, as has previously been reported for the synchronisation of free-running adult activity rhythms in entirely blind flies (Malpel et al., 2004). Our previous finding of in-sync molecular clock cycling in the DNs (Prakash et al., 2017), which are strongly responsive to temperature and the finding here of sustained early-age free-running adult activity rhythms driven by developmental-TCs, also suggest that the temperature-sensitive clocks continue to be functional as adults. The entrainment of adult *pdf>Q128* flies to temperature cycles with activity levels and morning and evening AIs comparable to at least one background control and free running rhythms from the phase of entrainment when released into constant conditions (data not shown) provide further evidence for unaffected temperature-sensitive activity clocks in these flies.

5) The presence of light inhibits the effectiveness of TCs during development in rescuing the early-age adult activity rhythms of *pdf>Q128*. There are a few possible explanations for why developmental-TC restores adult activity rhythms in the young *pdf>Q128* at DD25 but not developmental LD+TC. Cooperative synchronisation by light and temperature likely requires temperature changes in advance of light changes as observed in nature (Boothroyd et al., 2007). However, my finding that exposing *pdf>Q128* flies to naturally gradually changing time cues under semi-natural conditions during development does not overcome the arrhythmic behaviour of adults in DD25 (Chapter 3) refutes this explanation. The activity rhythms of flies with dysfunctional or absent LNvs show more excellent responsiveness to temperature inputs (Busza et al., 2007). CRY antagonises the ability of TCs to synchronise activity rhythms and dampens the PER oscillations in the LNds and the DNs, the temperature-sensitive clock neurons (Miyasako et al., 2007; Yoshii et al., 2010; Zhang et al., 2010c; Gentile et al., 2013; Harper et al., 2016; Yadlapalli et al., 2018). In *pdf>Q128*, given that behavioural and molecular clock entrainment to light is unaffected (Sheeba et al., 2010; Prakash et al., 2017), it is likely that the cyclic accumulation of CRY in the CRY^{+} clock

neurons under LD is intact. The TC-mediated temperature input to the clock during development could be diminished by light input pathways through the compound eye and accumulating CRY, effectively making light the only significant clock input during development. However, as shown previously (Chapters 2 and 3) and as will be discussed later, developmental light cycles are ineffective at bringing about rhythmic activity in *pdf>Q128* adults. Thus, in the LDTCtoDD25 regime, light, albeit cyclic, might dominate over temperature as the clock input, thereby interfering with the synchronising and rhythm-promoting effects of TC during development. In adult flies, the output of the temperature-sensitive DN1ps and their capacity to synchronise distinct components of activity behaviour under different environmental conditions are both affected by light intensity (Zhang et al., 2010c). Such integration may even start to take place in the pre-adult stages. Additionally, the ecological constraints on different developmental stages as opposed to adulthood, such as oviposition sites, burrowing and feeding in the larvae, and pupation height, among others, may shift the relative strengths of zeitgebers, their cooperation in entertainment and their influence on adult rhythms, necessitating careful study.

6) Though TCs synchronise molecular and behavioural rhythms in LL (Matsumoto et al., 1998; Yoshii et al., 2005), in the circadian neurodegenerative context, developmental-LLTC could not rescue adult behavioural rhythms in DD25. This result can be attributed to a reduction of PER in the LNv of *pdf>Q128* because, in per^{01} flies, high-temperature TC (20°C / 29°C) in LL was unable to synchronise activity, and this was true even when PER was restored in either the LNv or a subset of LNd and DNs or the DN1ps, indicating that in the absence of PER in some of the subsets (or in the presence of PER only in a few of the subsets), TC cannot synchronise activity under LL (Zhang et al., 2010c; Gentile et al., 2013).

4.4.2.3 Differential effects of light on the temperature-mediated impediment of behavioural arrhythmicity

4.4.2.3.1 In the presence of developmental light: Developmental temperature cycles *vs.* constant temperatures and temperature upshifts

Developmental light has differential effects on the temperature-mediated activity rhythms of *pdf>Q128*. Cyclic or constant light during development obstructs the rhythm-improving effects of developmental TC. On the contrary, they do not affect the rhythm-improving effects of adult-restricted warm temperatures. These opposing effects suggest different mechanisms of rescue by the two temperature regimes. The light-inhibitory effect on developmental TC is probably caused by features of light and temperature entrainment of the *Drosophila* developmental circadian neuronal network, discussed in the previous section. The developmental lightproof effects of adult-specific upshift to warm temperatures upshift on the behavioural rhythms of *pdf>Q128* suggests a light-insensitive, developmental-clock-independent mechanism. These are likely warm-temperature-activated stress responses and adaptive homeostatic mechanisms that improve adult clock neuronal health and function. However, one may note that under conditions of constant temperatures during both development and adulthood, the presence of cyclic light during development accentuates the effects of temperature on the activity consolidation of *pdf>Q128* adults. The accompanying constant temperature determines the direction of the effect, whereas LD during development merely heightens the temperature effects, weakening the consolidation at 23°C and strengthening it at 29°C. This differential sensitivity of *pdf>Q128* clocks to developmental light under upshift and constant warm temperature regimes again allude to subtle differences in the underlying circadian rescue mechanisms reflecting interactions of life stages, the magnitude of temperature, its constancy and fluctuations, the direction of temperature change and the presence of light.

4.4.2.3.2 Developmental-TC (TCtoDD25) *vs* Developmental-LD (LDtoDD25)

In the neurodegeneration-driven circadian context, the findings that during development, cycling temperatures but not cycling light is adequate in mediating adult activity rhythms, whereas, during adulthood, both light and temperature are independently capable of entraining the activity

rhythms of *pdf>Q128* suggests that the circadian neuronal network of *pdf>Q128* is amenable to temperature entrainment during pre-adult as well as adult stages, but to light entrainment only as adults. Despite light being the stronger zeitgeber for fly circadian rhythms than temperature (Yoshii et al., 2010; Harper et al., 2016), the result that developmental-TC but not developmental LD (see LDtoDD in chapter 3) restores adult activity rhythms in the *pdf>Q128* young at DD25 is tricky to explain. It could be a direct consequence of the light-sensitive pacemakers, the PDF^{+} LNv, targeted by expHTT. However, this line of reasoning conflicts with the findings that in adult *pdf>Q128*, light and temperature entrainment are unaffected (Sheeba et al., 2010; Prakash et al., 2017) (unpublished data regarding temperature entrainment). Nevertheless, suppose one restricts the interpretations to the developmental stages. Apart from the sLNv and the two DN2s, the other crucial clock neurons essential for light entrainment are functional only at the later developmental stages. In that case, one can attempt an alternate explanation. Circadian light perception and pathways of conveyance of light information to the circadian neurons emerge early during *Drosophila* development (Kaneko et al., 1997b; Kaneko et al., 2000; Malpel et al., 2004). Since lLNv and LNd differentiate only at mid-pupal stages (Helfrich-Förster, 1997; Helfrich-Förster, 1998; Helfrich-Förster et al., 2007), and the molecular clock of CRY^{-} DN2 (and those of CRY^{+} DN1s in the absence of CRY activation) are dependent on PDF for light entrainment (Picot et al., 2009), the critical pre-adult light-sensitive clock neurons are the CRY^{+} sLNvs that perceive light information cell autonomously via CRY and also via a direct connection to the visual system (Klarsfeld et al., 2011). However, in the pdf^{01} larvae, the molecular oscillations in most clock neuronal groups are entrained and in-phase, suggesting that PDF might not be critical for larval light entrainment of molecular rhythms in most clock neurons (Picot et al., 2009). In *pdf>Q128*, PDF and PER are intact in the sLNv of *pdf>Q128* in the third instar larvae; their status in the pupal stages have not been examined. Nevertheless, post-eclosion, the PDF and PER are affected in the sLNv of very young adult flies. Thus, it is reasonable to assume that the effects of expHTT on the sLNv may have set in at the pre-adult stages. Throughout development, despite the presence of light-sensitive 5^{th} sLNv and DN2s, a gradual decline in the health and functioning of the sLNv of the *pdf>Q128* can weaken the entrainment of the developmental clock network by

light. However, as adults, *pdf>Q128* flies have functional lLNv (Sheeba et al., 2008a; Sheeba et al., 2010) and PDF in the lLNv, the other functional light-sensitive CRY^{+} circadian neurons like the LNds and DN1s and a well-developed visual system, will orchestrate light entrainment of these flies. On the other hand, in the case of temperature inputs, as discussed in 1-3, the temperature-sensitive pacemakers can mediate temperature entrainment both during development and adulthood, even with a weakening sLNv and reduction of PDF (larval PDF is not necessary for entrainment of molecular rhythms in clock neurons by temperature (Picot et al., 2009). These results also emphasise that zeitgeber strength and dominance are context-dependent, as was shown previously (Harper et al., 2016). A deeper understanding of the mechanisms underlying the failure of cyclic light during development to evoke rhythmicity in *pdf>Q128* adults can be gained by expanding the explanation beyond the entraining effects of light. White light, particularly the blue light component, may negatively affect the circadian neurodegenerative symptoms of *pdf>Q128*, as seen and discussed earlier (Chapter 3), which can contribute to the lack of behavioural rhythmicity under LD25toDD25 and LDTCtoDD25.

4.4.3 Warm-temperature-mediated effects

4.4.3.1 Benefits of heat acclimation, hormesis and passive heat therapy

One of the objectives of this study was to see the effect of expHTT dosage on the HD phenotypes using temperature to tweak the *Gal4-driven* expHTT expression levels. The premise was that warm temperatures speed up cellular physiology, including increasing protein production and aggregation, and the expectation was that *pdf>Q128* in DD29 would have exaggerated phenotypes than those in DD25. However, the results obtained across nearly most phenotypic markers are opposite. Despite the expectation that warm temperatures will increase Gal4-mediated expHTT expression and aggregation, the toxicity associated at 23°C and 25°C is more than that at 29°C. This finding suggests that at 29°C, the speeding of cellular activities and Hsp activation overrides any effect of increased expHTT expression levels. Also, the observation that HD flies under DD23toDD29 (23°C during development) are like those under DD29toDD29

(29°C during development) suggests that the differences in development time due to temperature differences during development do not contribute to the abrogation of HD circadian phenotypes of adults experiencing warm temperatures. Furthermore, given that DD29toDD23 (29°C during development) does not rescue circadian behavioural rhythms of HD flies, whereas DD23toDD29 (23°C during development) does, it suggests that it is the warm temperatures as adults that drives the rescue rather than the developmental temperatures.

At first, the findings seem counterintuitive with adult-restricted or pre-adult and adult exposure of *pdf>Q128* to warm temperatures, which can potentially increase expHTT expression, delaying the circadian neurodegenerative phenotypes. In the following section, I describe some of the cellular mechanisms evoked by the warm temperatures that, in turn, can prove beneficial in combating neurotoxicity associated with expHTT. These broadly fall under heat acclimation and hormesis and expound on passive heat therapy as a potential therapeutic avenue for NDs. First and foremost, warm-temperature-mediated delay of circadian neurodegenerative phenotypes in *Drosophila* expressing expHTT in the pacemaker LNv suggests that any effects of increased expHTT transgene expression on increasing the ambient temperatures are negligible and outweighed by the immediate benefits arising from exposure to relatively warm temperatures, leading to delayed HD impairments.

Acclimation is a form of within-lifetime phenotypic plasticity triggered by exposure to specific environments or stressors within the viable range of an organism (mild and long-term lasting days or weeks, or extreme and short-term lasting hours) that improves the organism's ability to tolerate the stress, and reduces damage due to the stressor (Horowitz, 2001; Hoffmann et al., 2003; Bowler, 2005; Loeschcke and Sørensen, 2005; Angilletta Jr, 2009). Thermal acclimation improves thermal tolerance and overall performance and plausibly enhances fitness (Angilletta Jr, 2009; Klepsatel and Gáliková, 2022). Acclimation response, including thermal acclimation to mild heat stress, is also dose-dependent, showing **hormesis**: stressor at low levels is beneficial but detrimental at higher levels (Kristensen et al., 2003; Berry and López-Martínez, 2020). For example, in *Drosophila*, mild thermal pre-treatment is beneficial in combating severe secondary

stress and improving longevity (Khazaeli et al., 1997; Kristensen et al., 2003; Sarup et al., 2014; Berry and López-Martínez, 2020). In humans, heat acclimation (HA) manifests as a physiological adaptation in response to the elevation of core body temperature or due to exercise in hot conditions (Nava and Zuhl, 2020). HA in humans serves a similar function to other animals, such as managing core body temperature and protecting against the ill effects of heat stress. HA is often recommended to soldiers, firefighters, field workers and endurance athletes (Carter et al., 2005; Garrett et al., 2011). Because it boosts stress-resistance mechanisms like heat shock, anti-oxidant and detoxification pathways, epigenetic transcriptional reorganisation, increases neurotrophic factors, and enhances general performance and life history traits, HA can protect against neurodegenerative diseases (Mattson, 2008; Vaiserman, 2008; Calabrese et al., 2012; Calabrese, 2013; Sarup et al., 2014; Dattilo et al., 2015; Rix and Cutler, 2022). Hormetic response promotes neuronal survival and synaptogenesis (Mattson et al., 2002). Passive heat treatments improve health indicators like cardiovascular markers, metabolic regulation and glycaemic control (Brunt et al., 2016; Janssen et al., 2016; Kimball et al., 2018; Ely et al., 2019; Maley et al., 2019). Mild heat stress is neuroprotective in a mice model of traumatic brain injury (Umscheif et al., 2010; Umschweif et al., 2014), stimulates autophagic pathways (Kumsta et al., 2017; McCormick et al., 2021; Amirkavei et al., 2022), reduces ageing related neuropathology, amyloid beta aggregation and improved neuronal survival *in vitro* (Mane et al., 2020). In humans, ambient temperature also affects sleep (Haskell et al., 1981; Okamoto-Mizuno et al., 2003; Buguet, 2007; Togo et al., 2007; Lack et al., 2008), and moderate passive heating promotes slow sleep wave the following night (Horne and Reid, 1985; Bunnell et al., 1988).

When treating ND pathology with warm temperatures, caution must be taken. There are fitness and metabolic costs associated with warm temperatures, vastly investigated in ectotherms (Le Bourg and Rattan, 2014; McClure et al., 2014; González-Tokman et al., 2020). Increasing the growing temperature of Q35 nematodes beyond 20°C led to accelerated polyQ aggregation and toxicity (Haldimann et al., 2011). Lower core body temperature was associated with a longer lifespan in mice (Conti et al., 2006). Long-term warm ambient temperature, which results in high body temperature, exacerbates cognitive dysfunction and ND pathophysiology (Noorani et al.,

2020; Jung et al., 2022). Thus, it will be crucial to investigate and optimise the modality, site, dosage/magnitude/intensity, duration, frequency, site of application, age of intervention, the effect of gender, and pre-existing conditions, in combination with other treatment modalities, and to study the short- and long-term advantages, as well as to test in clinically relevant mammalian models.

A way of circumventing the thermal damage due to continuous heating is to use thermal cycles of warm/cold. Studies have shown that fluctuating temperatures activate stress response and, within the permissive thermal range, improve performance, thermal tolerance, and lifespan and mitigate temperature stress in insects and worms (Economos and Lints, 1986a; Cardoso et al., 2002; Galbadage and Hartman, 2008; Colinet et al., 2015; Gomez et al., 2016; Manenti et al., 2018; Goh et al., 2021; Salachan and Sørensen, 2022). Through the stimulation of pro-survival Akt-dependent pathways, cycling hyperthermia enhanced the anti-cancer effects of several medications and reduced oxidative damage and cytotoxicity brought on by hydrogen peroxide and Abeta in human brain cells (Chen et al., 2019; Chen et al., 2020). Further, cyclic temperatures affect the circadian clocks and can orchestrate clock-dependent neuroprotective mechanisms, as is supported by the findings of this study. In further support, a recent study showed that cycling temperature rescued the clock gene oscillatory amplitude decline upon ageing in male flies (Goh et al., 2021). In the present study, adult-restricted constant warm seems better in *Drosophila* HD flies than oscillating warm; however, the trade-offs associated with warming are not addressed. Nevertheless, the background from other studies and the current findings strongly endorse exploring the middle ground of intermittently warm or fluctuating warm temperature effects on HD circadian neuropathology.

4.4.3.1.1 Translational impact of temperature-based interventional studies in *Drosophila*

Drosophila exhibit rhythms of temperature preference where flies choose or prefer relatively warm temperatures during the day and cooler temperatures at night (Hamada et al., 2008; Kaneko et al., 2012; Goda et al., 2014). Since *Drosophila* are ectotherms wherein their body temperature matches that of the environmental temperature (Stevenson, 1985; Refinetti and Menaker, 1992;

Dillon et al., 2009; Garrity et al., 2010), their temperature preference rhythm (TPR) translates to a daily body temperature rhythm (BTR) (Goda and Hamada, 2019). Humans and other homeothermic mammals display clock-controlled BTR and circadian oscillations in body temperature in the 1°C range, which decrease during sleep and increase during wakefulness (Aschoff, 1983; Duffy et al., 1998; Kräuchi, 2002). These temperature rhythms serve as an internal time cue to synchronise peripheral rhythms (Brown et al., 2002; Schibler, 2009; Buhr et al., 2010). The BTR in rodents and humans share many similarities with *Drosophila* TPR, including a circadian clock control and a functionally conserved underlying mechanism that is distinct from the control centre for locomotor activity rhythms (Duffy et al., 1998; Saper et al., 2005; Morrison et al., 2008; Kaneko et al., 2012; Goda et al., 2014; Goda et al., 2016; Tang et al., 2017; Goda et al., 2018; Goda and Hamada, 2019).

Humans are homeothermic, meaning their core body temperature is kept within a specific range, unlike the poikilothermic *Drosophila* (Schlader and Vargas, 2019). However, the core body temperature is influenced by external temperatures (Dewasmes et al., 1994; Dewasmes et al., 1996; Teramoto et al., 1998; Wakamura and Tokura, 2002), and passive exposure to warm temperatures elicits mild hyperthermia (Patrick and Johnson, 2021). Moreover, regularly challenging the thermal equilibrium via moderate thermal stress also has positive effects in mammals even under disease conditions like cardiovascular diseases, diabetes, and depression (Hooper, 1999; Kihara et al., 2002; Janssen et al., 2016; Tyler et al., 2016; Brunt and Minson, 2021).

Overall, though the core body temperature in humans is relatively protected against perturbations of external temperatures, it is affected by it and manifests physiological consequences. Moreover, temperature affects cellular physiology similarly across taxa, such as eliciting stress responses like heat shock. Finally, temperature rhythms synchronise circadian rhythms in both flies and mammals. Thus, understanding how temperature affects neurodegeneration and circadian rhythms in *Drosophila* under the settings of circadian rhythm-disrupting illnesses has implications for human body thermoregulation and temperature cycles and their impact on physiology and pathophysiology.

Thus, the outcome of understanding how temperature affects neurodegeneration and circadian rhythms, especially in the context of circadian rhythm-disrupting diseases in *Drosophila,* has consequences for human body thermo-modulation and temperature rhythms and their effect on physiology and pathophysiology.

4.4.3.2 Effect of temperature on circadian protein expression

Temperature, constant and fluctuating, affects organisms' transcriptomic, proteomic, and epigenetic profiles. These involve mechanisms such as alternative splicing, alternative promoter and translational start site usage, differential small RNA structural composition and abundance, RNA editing, and kinase activation, with effects on genes involved in circadian regulation (Liu et al., 1997a; Boothroyd et al., 2007; van der Linden et al., 2010; Rieder et al., 2015; Gotic et al., 2016; Sørensen et al., 2016; Buchumenski et al., 2017; Fast et al., 2017; Preußner et al., 2017; Martin Anduaga et al., 2019; Haltenhof et al., 2020; Zhou et al., 2021). This broad-spectrum effect of temperature on the protein expression possibly prolongs PDF and PER in the sLNv under warm temperatures and induces low amplitude PER oscillations under developmental TC. The effect of cycling temperature on the temperature-sensitive DN1 clocks and their connection and communication with the LNs (Collins et al., 2012; Collins et al., 2014; Guo et al., 2016; Fujiwara et al., 2018; Díaz et al., 2019; Fernandez et al., 2020) can also aid in the restoration of PER oscillations in the of sLNv under developmental-TCs. In *Drosophila*, both *per* and *tim* mRNAs are subject to temperature-specific alternate splicing events that, in turn, bring about circadian and sleep behavioural adaptations (Majercak et al., 1999; Majercak et al., 2004; Shakhmantsir et al., 2018; Foley et al., 2019; Martin Anduaga et al., 2019; Shakhmantsir and Sehgal, 2019). In *Drosophila*, at a warm temperature of 29°C, genes involved in transcription, chromatin organisation, histone modification, protein folding, and metabolism were upregulated (Fast et al., 2017; Martin Anduaga et al., 2019), and development-specific warm temperatures in addition also upregulated cell cycle and DNA repair genes (Chen et al., 2015a). At warm temperatures, accessibility to chromatin and RNA secondary structures is also enhanced (Chereji et al., 2016; Fast et al., 2017).

4.4.3.3 Warm temperatures, Hsp70 and expHTT inclusion load

Hsps: In flies, though *Hsp* genes show a temperature-dependent change, the change direction differs between studies, especially for *Hsp70* (Colinet et al., 2013; Chen et al., 2015a). A mild heat stress of 29°C or 30°C induces *Hsp70* and Hsp70 expression in *Drosophila* (Wheeler et al., 1995; Jedlicka et al., 1997; Chen et al., 2018). High temperatures elevated mice's core body temperature and cortical HSPs (Jung et al., 2022). In a few instances, benefits from mild heat stress did not involve increased Hsp70 in cultured neurons (Snider and Choi, 1996; Batulan et al., 2003). In humans, HA increases basal intracellular Hsp70 levels (Yamada et al., 2007; Magalhães Fde et al., 2010; Amorim et al., 2011; Nava and Zuhl, 2020), which then suppresses the inflammatory response and maintains cell integrity (Chen et al., 2005; Dokladny et al., 2010; Bittencourt and Porto, 2017). HSp70 activation in humans is protective against heat stress (Amorim et al., 2015; Zuhl et al., 2015), HSP suppression prevents the protective effect of HA (Kuennen et al., 2011) and individuals vulnerable to heat stress versus those resistant to it show differential basal HSP70 levels (Xiao et al., 2003). Healthy human volunteers showed increased Hsp70 and Hsp90 mRNA levels with passive heating (Kuhlenhoelter et al., 2016). Although some human research reveals the effects of both active and passive heat treatments without changes in HSP (Morton et al., 2007; Hom et al., 2012; Hoekstra et al., 2018), other studies demonstrate that heat treatments raise intracellular and extracellular Hsp70 levels (Oehler et al., 2001; Yamada et al., 2007; McClung et al., 2008; Magalhães Fde et al., 2010; Amorim et al., 2011; Faulkner et al., 2017; Nava and Zuhl, 2020). The heat-shock-induced TF *Hsf1* is also a circadian transcription factor involved in synchronising the peripheral clocks to body temperature rhythms (Reinke et al., 2008; Buhr et al., 2010; Saini et al., 2012; Kovács et al., 2019).

In this study, adult-restricted upshift to warm temperatures emerged as the most neuroprotective regime among those tested. This regime's ability to mediate behavioural rhythmicity involved Hsp70 to a certain degree, indicating that the circadian rhythm rescue by warm temperatures likely involves Hsp70-mediated responses such as the heat shock response. The degree of rhythmicity had a rather J-shaped relationship to the number of *Hsp70* copies, with both high and low copy

numbers being more rhythm-promoting than intermediate copy numbers. In this regard, the observation that *pdf>Q128* flies lacking all 6 copies of *Hsp70* had better rhythmicity than those lacking fewer copies is intriguing. It suggests that in the complete absence of *Hsp70*, other *Hsps* or compensatory mechanisms come into play that can improve cellular health and circadian function. The presence of *Hsp70*-independent compensatory stress response mechanisms is suggested by the fact that *Drosophila* lacking inducible *Hsp70* maintain significant thermotolerance under mild heat shock and have upregulated expression of other inducible *Hsps* (e.g. *sHsps*, *Hsp40*) and constitutive stress-response genes (e.g. *Hsc70*-2, *GstE1*) under severe heat shock (Gong and Golic, 2006; Neal et al., 2006; Bettencourt et al., 2008). Further proof for the possible involvement of *Hsps* in the warm-temperature mediated rescue is the lowered expHTT inclusion load. Experiments are ongoing to determine whether the levels of Hsp70 in the LNv differ between the temperature regimes.

Flies lacking varying copy numbers of Hsp70 show a dose-dependent decrease in thermotolerance: flies lacking fewer copies have better thermotolerance than those lacking more. In contrast, both have poorer thermotolerance than WT (Gong and Golic, 2006). Similarly, the enhancement of eye neurodegeneration on expressing expanded MJD was roughly proportional to the number of deleted copies. In my experiments, I do not observe such dose-dependent phenomena regarding loss of rhythmicity or activity consolidation. One possible explanation for the abrogation of the positive effects of the warm temperature on the expHTT-induced behavioural deficits on removing even a single copy of the six *Drosophila* Hsp70 genes can be the increased sensitivity of expHTT-stressed-sLNv to cellular proteostatic demands in the face of warm temperatures. The sLNv of HD flies are stressed to begin with, as evidenced by the detection of Hsp70-stained sLNv (more significant in number than $Hsp70^{+}$ lLNv), as early as 1d in *pdf>Q128*, even at 25°C, that is wholly undetected in the LNv of controls *pdf>Q0* (Sharma et al., 2023). Such sLNv-stressed HD flies, on exposure to prolonged warm temperatures, are likely to experience heat stress, with an increased demand for proteostatic components like molecular chaperones, rendering these circadian neurons particularly sensitive to even the slightest of

proteostatic perturbations. Under such conditions, losing even a single copy of the central chaperone, *Hsp70,* probably renders the sLNv dysfunctional and the HD flies arrhythmic.

Inclusions: In general, under most conditions, with increases in temperature, aggregation kinetics, inclusion body formation, and amyloid fibrillation processes increased and facilitated the α-to-β transition, including that of polyQ proteins (Shehi et al., 2003; Bulone et al., 2006; Haldimann et al., 2011; Moronetti Mazzeo et al., 2012; Ghavami et al., 2013). However, in my study, there was a decrease in inclusion numbers with an increase in temperature. Nevertheless, in flies at an early age, there was a predominance of hemispheres with Diff-enriched LNv at DD23 as opposed to Inc-enriched LNv at DD29 (Fig 4.26b, c). The decreased inclusion number with temperature in this *in vivo Drosophila* model could be due to an induction of Hsps that are known to interfere with aggregation. Under developmental temperature cycles, the inclusion load was not affected, suggesting that fluctuations in temperature could cancel out the effects of warm and cool temperatures on aggregation. These results indicate that under *in vivo* conditions, the temperature effects on aggregation are not straightforward and confounded by other physiological processes that also affect aggregation. However, there were general trends across the various temperature regimes concerning age: the dominance of hemispheres with Diff-enriched LNv, followed by Diff+Inc (or mixed Diff+Inc and Inc) at early ages and exclusively Inc-enriched at later ages, an increase of inclusion number, and size mostly remaining constant. The duration of domination of hemispheres of Diff and Diff+Inc varied between regimes.

The above studies also support environmental factors like temperature being disease modifiers and polyQ proteins being sensitive to temperature and sensitising organisms to environmental stresses. In nematodes grown at temperature <20°C, temperature-sensitive mutant proteins do not themselves induce a phenotype, but when co-expressed with intermediate-length polyQs, the worms are paralysed at those temperatures (Gidalevitz et al., 2006). Increasing the growing temperature of Q35 nematodes beyond 20°C led to accelerated polyQ aggregation and toxicity (Haldimann et al., 2011), providing evidence that environmental factors contribute to variability in the age-of-onset and severity of polyQ diseases.

4.4.4 Temperature-based interventions for NDs

Thermal therapies can be broadly classified into two categories (Habash, 2018; Lowry et al., 2018; Hunt et al., 2019; Sun et al., 2019; Brunt and Minson, 2021). They can internally generate metabolic heat, called active heat therapies, like exercise or modify the external environmental temperatures that warm or cool the body (though altering the core body temperature is not a requisite). The latter category includes passive heat treatments (e.g. saunas, hot water immersions, warming blankets, infrared heating) and therapeutic hypothermia (e.g. cold rooms, cooling blankets). Thermal therapies can be applied locally, regionally, or to the entire body and mimicked pharmacologically. Habitual activity and exercise-heat stress, a common lifestyle intervention to improve brain health for aged members and patients of NDs, can be challenging to implement in clinical populations; their noncompliance to exercise or limited mobility also minimises their experience of physiological stressors (Hunt et al., 2019; Schulz et al., 2020). Heat therapy is a feasible alternative to achieve various health benefits in people deprived of sufficient exposure to bright light and experiencing motor difficulties: the institutionalised healthy, elderly, neurodegenerative patients, and blind people. Also, under compromised circadian conditions, temperature cues can serve as a masking stimulus and, if provided in alignment with natural cycles, can strengthen daily patterns and benefit organismal health (Gall and Shuboni-Mulligan, 2022).

Body warming modulates thermoregulatory mechanisms through autonomic responses like increasing the cardiac output, and heart rate, activating skin vasodilation and blood flow and promoting evaporative heat loss via sweating (Madden and Morrison, 2019; Brunt and Minson, 2021), activating adaptive stress response pathways like the upregulation of HSPs (Faulkner et al., 2017; Brunt et al., 2018), and improving cellular respiration, circulating factors like irisin and BDNF, vascular function, muscle strength and motor skill and metabolic health (Racinais et al., 2017; Brunt et al., 2018; Hafen et al., 2018; Kojima et al., 2018; Ely et al., 2019; Hunt et al., 2019; Brunt and Minson, 2021; Glazachev et al., 2021). Given the metabolic imbalances(Wang et al., 2014; Handley et al., 2016), decreased cerebral blood flow (Harris et al., 1999; de la Torre, 2004; Ma and Eidelberg, 2007; Rocha et al., 2022), and skeletal muscle atrophy (Zielonka et al., 2014)

are present in many NDs, including HD, heat therapy and heat acclimation offer an additional benefit of enhancing these faculties. Since several of these characteristics, such as circadian and sleep disruptions, are already present in ND at an early stage, heat therapy may be not only palliative, but when incorporated at early stages, can delay symptoms, decrease the disease's course, and maybe even lessen the disease severity. Heat therapy can also complement conventional treatments by augmenting and accelerating clinical improvements. Thus, heat therapy to evoke positive adaptations and improve health span is gaining traction as a possible therapeutic means that can influence neurodegenerative disease outcomes (Hunt et al., 2019). The results presented here further support the use of mild heat stress as a therapeutic means for neurodegenerative conditions and associated circadian rhythm disruptions.

Heat therapy may offer a relatively safe, inexpensive, non-invasive, and practical way to reap several health benefits, including boosting HSPs and restoring proteostasis, even though research into how temperature modulates neurodegenerative pathways and hyperthermia as a therapeutic intervention for neurodegenerative conditions is still in its infancy. The findings from this study illustrate thermotherapy as a potential treatment for neurodegenerative symptoms of cellular toxicity and circadian disruption. Agents that promote thermogenesis and mimic mild heat therapy can be tested. For instance, serotonergic neuronal stimulation and serotonin release were sufficient to induce HSR and reduce the misfolded protein burden in *C.elegans* (Tatum et al., 2015), and topical menthol treatment mirrored hyperthermic effects of reducing tau phosphorylation in AD animals (Guisle et al., 2022).

Caution must be exercised while using environmental interventions like heat treatments with ND patients and the elderly. Their thermoregulatory systems and cardiovascular regulation might be compromised, affecting their ability to withstand these treatments (Hunt et al., 2019). There is a paucity of studies looking at the direct effects of passive heating on neurodegenerative diseases. Most of the studies conducted focus on the therapeutic effects of exercise interventions, and not necessarily on body warming by exercise in mitigating symptoms of neurodegenerative diseases such as improvements in motor and cognitive symptoms (Loprinzi et al., 2013; Paillard et al., 2015; Hou et al., 2017; Liu et al., 2019a; Mueller et al., 2019). A few studies show that regular

passive heating via sauna baths reduces the risk of developing dementia and AD in the healthy middle-aged (Laukkanen et al., 2017; Heinonen and Laukkanen, 2018; Knekt et al., 2020). In addition, most research findings on the effectiveness of heat therapy are associative and circumstantial, and the underlying mechanisms are not fully understood (Hunt et al., 2019). Thus, there is a pressing need to focus future research on the modalities of heat therapy and their effects on NDs and circadian disruptions in NDs for effectively implementing them in treatment regimens. Understanding the effects of temperature changes on neurodegenerative diseases is crucial and urgent, bearing in mind the rising global temperatures, increasing frequency and severity of heat waves, and temperature elevations posing the risk of worsening neurological symptoms (Bongioanni et al., 2021; Zammit et al., 2021).

CHAPTER 5

Impact of Heat Shock Protein Overexpression on the Circadian Dysfunction and Neurotoxicity in HD flies

Work from this chapter has been published as "Prakash P, Pradhan AK, Sheeba V. Hsp40 overexpression in pacemaker neurons delays circadian dysfunction in a Drosophila model of Huntington's disease. Dis Model Mech. 2022 Jun 1;15(6):dmm049447."

https://doi.org/10.1242/dmm.049447

5.1 INTRODUCTION

5.1.1 A Screen for modifiers of expHTT-induced disruption of activity rhythms

Circadian and sleep disruptions are now recognised as early symptoms of many NDs, including HD (Goodman et al., 2011; Morton et al., 2014; Lebreton et al., 2015; Bellosta Diago et al., 2017). The mammalian clock centre suprachiasmatic nucleus (SCN) is affected in HD mice, including molecular clock disruptions and reduction in the Vasoactive Intestinal Peptide, a clock output neuropeptide (Morton et al., 2005; Maywood et al., 2010; Kudo et al., 2011; van Wamelen et al., 2013). Emerging evidence supports bi-directional crosstalk between the circadian and neurodegenerative axes, with circadian function impacting the aetiology and progression of NDs (Hood and Amir, 2017a; Leng et al., 2019; Carter et al., 2021; Voysey et al., 2021a). Studies show that treatments imposing sleep cycles and (or) synchronising circadian rhythms also improve neurodegenerative phenotypes such as cognitive decline, motor performance and survival of HD mice (Pallier et al., 2007; Pallier and Morton, 2009; Maywood et al., 2010; Aungier et al., 2012b; Skillings et al., 2014; Ouk et al., 2017; Wang et al., 2017; Whittaker et al., 2018; Cabanas et al., 2019). These treatments include pharmacological interventions, timed light exposure, restricted food cycles, daily scheduled voluntary exercise, and environmental enrichment. On the other hand, clock disruptions worsen ND (Krishnan et al., 2012; Lauretti et al., 2017a; Kim et al., 2018; Sharma and Goyal, 2020a). Given the beneficial effects of circadian improvement on neurodegeneration, I aimed to uncover modifiers of expHTT-induced circadian arrhythmicity. In the *pdf>Q128* flies, I carried out a screen of genetic modifiers of cellular toxicity of HD for their ability to suppress circadian behavioural arrhythmicity. These genes are grouped under different categories based on function (Table 5.1), and the expressed proteins assist in neuronal function and are modifiers of neurodegeneration (Steffan et al., 2001; Singaraja et al., 2002; Gunawardena et al., 2003; Shulman and Feany, 2003; Cozzolino et al., 2004; Sang et al., 2005; Mugat et al., 2008; Wyttenbach and Arrigo, 2009; Zhang et al., 2009; Singaraja et al., 2011; Turturici et al., 2011; Sutton et al., 2013; Karunanithi and Brown, 2015; Kampinga and Bergink, 2016; Menzies et al., 2017; Metaxakis et

al., 2018; Alcalà-Vida et al., 2021; Wang et al., 2021). Co-expression of expHTT in the LNv with candidates from the Heat Shock Protein (Hsp) or autophagy group significantly improved flies' rhythmicity compared to their expHTT-only expressing counterparts (Table 5.1). In the Hsp group, these included *Hsp23*, *Hsp40* and *HSP70* homologs. A mutated form of *Hsc70-4* also showed a highly significant rescue. A significantly higher proportion of *tim>Q128,HSP70* flies were also rhythmic than *tim>Q128* flies. Overexpressing autophagy genes *atg5* or *atg8a* in *pdf>Q128* also rescued activity rhythms in DD, which is being pursued by others in our group. The central chaperone HSP70 and co-chaperone Hsp40 were chosen for further analysis.

5.1.2 Hsps: Function and Role in neurodegenerative diseases

Hsps serve diverse cellular functions both in housekeeping and stress-induced capacities. They play a central role in cellular proteostasis by aiding in protein folding, preventing aberrant inter-and intra-protein interactions, protein trafficking, targeting of organelles, protein translocation across membranes, protein degradation, exocytosis, vesicular trafficking and disaggregation, among others (Hartl and Hayer-Hartl, 2009; Kim et al., 2013; Mannini and Chiti, 2017; Nillegoda et al., 2018). In several protein-aggregation diseases like the polyQ diseases, components of chaperone machinery such as Hsp40 and HSP70 co-localise with mutant protein aggregates (Cummings et al., 1998; Chai et al., 1999; Jana, 2000; Muchowski et al., 2000; Kim et al., 2002; Shimura et al., 2004a; Wyttenbach, 2004a; Dedmon et al., 2005; Muchowski and Wacker, 2005; Scior et al., 2018). The levels of many Hsps, particularly the ATP-dependent ones and the cellular proteostasis capacity, reduce with age, and these contribute to the middle-age onset of NDs like HD (Taylor and Dillin, 2011; Brehme et al., 2014b; Yerbury et al., 2016; Hipp et al., 2019b; Margulis et al., 2020). In HD, many essential chaperones decline with age, especially HSP70, possibly by getting trapped in aggregates or due to reduced gene expression or increased turnover, thereby titrating chaperones away from client proteins, further taxing global proteostasis (Helmlinger, 2002; Kim et al., 2002; Merienne et al., 2003b; Hay, 2004; Yamanaka et al., 2008; Hipp et al., 2012b; Park et al., 2013; Yu et al., 2014). This phenomenon is often called the chaperone competition or depletion hypothesis

(Labbadia and Morimoto, 2015). The upregulation of Hsps, thus, alleviates proteotoxic stress and HD symptoms. In support of this, multiple studies across animal models of yeast, worms, flies and mice show that up-regulating Hsps such as HSP70 and Hsp40 suppress neurodegenerative phenotypes of HD in motor and cognitive performances, lifespan, neuronal degeneration, cell death and expHTT aggregation (Muchowski and Wacker, 2005; Duncan et al., 2015b; Pratt et al., 2015; Brehme and Voisine, 2016a; Reis et al., 2016; Harding and Tong, 2018a; Chaari, 2019; Soares et al., 2019; Davis et al., 2020). Reduction of Hsps also aggravates neurodegenerative phenotypes in several NDs, including HD, in cell cultures and animal models (Tagawa et al., 2007; Wacker et al., 2009; Hageman et al., 2010; Jiang et al., 2012; Scior et al., 2018). In some cases, the depletion of chaperone levels directly results in neurodegenerative phenotypes (Elefant and Palter, 1999; Bonini, 2002). Mutations in chaperones and co-chaperones are also known to cause neuromyopathies and neurodegeneration (Bonifati et al., 2003; Magnoni et al., 2013; Shi et al., 2013; Lin and Farrer, 2014; Vilarino-Guell et al., 2014; Ruggieri et al., 2016; Davis et al., 2020; Sarparanta et al., 2020; Vendredy et al., 2020). Therefore, the emergence of Hsps as modifiers in this screen is unsurprising. However, the role of Hsps in circadian rehabilitation is relatively unexplored.

5.1.3 Hsps as modifiers of expHTT-induced circadian decline

In this study, I investigated the role of Hsp40 and HSP70 as modifiers of expHTT-induced circadian neurodegenerative phenotypes in *Drosophila*. Most flies expressing expHTT in the PDF^+ LNv (*pdf>Q128*) had disrupted behavioural activity rhythms in DD, a loss of PDF from sLNv soma, loss of PER and its oscillations from LNv and the presence of expHTT inclusions. (Chapters 2 and 3) (Prakash et al., 2017). The issues addressed in this chapter are the effects of Hsp40 or HSP70 overexpression in *pdf>Q128* flies on the circadian free-running activity rhythms (5.3.1), PDF^+ sLNv soma numbers (5.3.2), the forms of expHTT in LNv (5.3.3), expHTT inclusion features (5.3.4) and LNv PER and its oscillations (5.3.5).

I investigated the role of Hsp40 and HSP70 as modifiers of expHTT-induced circadian neurodegenerative phenotypes in *Drosophila*. Of the two Hsps, Hsp40 emerged as the more

potent modifier of expHTT-induced phenotypes. It has postponed the loss of rhythmic locomotion over a substantial duration and the loss of PER and its oscillations from sLNv. Notably, there was a rescue of PDF loss from sLNv and a decrease in the visible expHTT inclusion load favouring a new feature - a spot-like form of expHTT. HSP70 overexpression rescued rhythmicity and lowered expHTT inclusion numbers early, without rescuing PDF or PER in the sLNv or affecting inclusions as the predominant form of expHTT in the LNv. Co-expression of Hsp40 and HSP70 in *pdf>Q128* led to a synergistic improvement in the consolidation of activity rhythms. The present study establishes a role for Hsps as suppressors of expHTT-induced circadian impairments in a *Drosophila* circadian HD model. It also suggests that proteostasis disruptions contribute to the circadian disruptions associated with HD.

5.2 MATERIALS AND METHODS

5.2.1 Fly lines

Some of the transgenic fly lines used here are described in Chapter 2 (Section 2.2.1). For the genetic screen, the fly lines used are listed in Table 5.1. The genes were either overexpressed or downregulated in the *pdf>Q128* background (and, in a few cases, *tim>Q128* background) (Table 5.1). A recombinant line of *w;pdfGal4;+* and *w;UAS-HTTQ128/+;+* was generated, denoted by *w;pdf-Q128;+* and used for the screen. The sample size for the screen varied between 16 to 32 flies per genotype.

For most of this study, the fly lines of focus were generated using the two Hsp *UAS* lines, namely *w;+;UAS-DnaJ1k* (Bl 30553) and *w;+;UAS-HSPA1L* (Bl 7054). The human HSP70 homolog used in this study was HSPA1L (Bl 7454) (https://flybase.org/reports/FBgn0029163.html), as a recent analysis revealed that among the various chaperone families, the Hsp70 family most frequently provided considerable proteotoxic relief in a variety of protein misfolding diseases (Brehme and Voisine, 2016a). The next potent proteotoxic suppressor was the Hsp40 family, among which DNAJB4 and DNAJB6 were the most potent polyQ disease modifiers (Brehme and Voisine, 2016a). The dHDJ1 (DnaJ1k or CG10578 or DnaJ-1 or Dm Hsp40) (Bl 30553) used in this study is a *Drosophila* ortholog of members of the human Hsp40 Class B family with varying degrees of homology (DNAJB5, DNAJB4 and DNAJB1) (https://flybase.org/reports/FBgn0263106.html).

The *UAS-Hsp* lines generated the *w;pdfGal4/UAS-Q128;UAS-DnaJ1k/+* or *w;pdfGal4/UAS-Q128;HSPA1L/+* lines which would respectively overexpress Hsp40 or HSP70 in the PDF^{+} LNv neurons, also expressing HTT-Q128. The above-generated lines are called *pdf>Q128,Hsp40* and *pdf>Q128,HSP70* throughout the text. Their *UAS* control lines are *Q128,Hsp40* and *Q128,HSP70,* and their *driver* control lines are as *pdf>Hsp40* and *pdf>HSP70*. Their corresponding *Q0* lines are *pdf>Q0,Hsp40* and *pdf>Q0,HSP70*. All other relevant background controls were also used. Due to space constraints, in some figures (Figs 5.7a, c, e, 5.8, 5.7a and 5.10b, d and f), *pdf>Q128*, *pdf>Q128,Hsp40* and *pdf>Q128,HSP70* are abbreviated as *Q128*,

H40 and *H70*, respectively. Flies co-expressing both Hsp40 and HSP70 and HTT-Q128 in the LNv are referred to as *pdf>Q128,Hsp40,HSP70* and their Q0 counterparts *pdf>Q0,Hsp40,HSP70*. Crosses were maintained under 12h:12h light: dark cycles (LD), with ~200 lux intensity of light phase, at 25°C. Flies were moved to DD 25°C after two days post-eclosion for behavioural and immunocytochemical assays. All flies and crosses were maintained on a standard cornmeal medium.

5.2.2 Behavioural assays

Most of the locomotor activity setup, assay conditions and analyses performed are described in Chapter 2 (Sections 2.2.2 and 4.2.2). At least three independent activity runs were carried out for overexpression of Hsp40 with its *Q0* and *UAS* controls, all giving similar results. For overexpression of HSP70, three independent activity runs were carried out with its *Q0* controls, giving similar results. At least one experiment was conducted with all possible genetic controls for Hsp40 and HSP70 overexpression experiments. No statistical tests were carried out to determine the minimum required sample sizes. However, as recommended (Kostadinov et al., 2021), one full DAM2 monitor accommodating 32 flies per genotype was set up at the start of the experiment. The average percentage rhythmicity across multiple runs is plotted for Hsp40 and HSP70 overexpression experiments. In addition, the percentage rhythmicity, period, robustness, and extent of activity consolidation *r*-values of a representative run with all relevant controls for the above overexpression experiments are plotted. For synergistic effects, a single run was carried out. There were fly deaths in AW3; therefore, AW3 analyses had fewer samples. When the fly numbers went below 10 (e.g., in a few instances in AW3), those genotypes were excluded from statistical analyses for that AW. In cases where very few flies (n<10) were rhythmic like *pdf>Q128* number across AWs in the HSP70 overexpression and synergistic effect experiments and during AW3 in Hsp40 overexpression experiment or *pdf>Q128,Hsp40* during AW3 in the Hsp40 overexpression experiment or most of the experimental genotypes during AW3 in the synergistic effect experiment, those genotypes were excluded from the between-genotype

statistical analyses of period and rhythm robustness for that AW. Indicated in Table 5.2 are the numbers of surviving flies in AW2 and AW3 across experiments.

5.2.2.1 Statistical analysis

Data sets were first tested for normality using Shapiro-Wilk's test and then for variance homogeneity using Levene's test. Across experiments, the data comparing period or activity consolidation '*r*' between genotypes for an AW or age did not satisfy the ANOVA assumption of normality despite transformations. So was the case for rhythm robustness in the Hsp40 overexpression experiment. Therefore, the non-parametric Kruskal-Wallis test of ranks followed by multiple comparisons of mean ranks was used. For the HSP70 overexpression experiment, datasets comparing rhythm robustness between genotypes for an AW were normally distributed post-transformation, but variances were not always homogenous. Hence, Welch's ANOVA was used, followed by the Games-Howell post-hoc test. For the synergistic effect experiment, the data comparing robustness between genotypes for an AW was normally distributed, and their variances were homogenous. A one-way ANOVA followed by unequal N HSD tests were carried out. Friedman's test for repeated measures was used to compare robustness, period and '*r*' between AWs or ages for a genotype. Then Wilcoxon matched-pairs tests (or Conover Test for '*r*') with Bonferroni correction (or Benjamini-Hochberg (BH) procedure to decrease the False Discovery Rate (FDR) for '*r*'; FDR set at 5%) on the pair-wise *p*-values were used. A m x n Fisher's Exact test and multiple 2x2 Fisher's Exact tests with BH procedure on all relevant comparisons were used (using R) to compare the proportions of rhythmic flies between genotypes for an AW. Cochran Q test on the dichotomous variable rhythmicity (rhythmic and arrhythmic categories) was used to compare the proportion of rhythmic flies between AWs for a genotype, followed by multiple 2x2 McNemar's tests on the dependent samples and Bonferroni correction on the pair-wise *p*-values. For comparing the mean rhythmicity of multiple independent runs between genotypes or between ages, a repeated-measures ANOVA followed by Tukey's HSD was performed post-arcsine conversion of the square-root transformed data. Other details are described previously in Chapter 2 (Section 2.2.2.1).

5.2.3 Immunocytochemistry and image analysis

The dissections, immunocytochemistry and image analysis procedures performed are described in Chapter 2 (Section 2.2.3). Briefly, the adult flies' brain tissue was dissected at different ages, fixed with 4% PFA and stained with the appropriate antibodies: double staining, anti-HTT mouse (1:500) and anti-PDF rabbit (1:30,000) and triple staining, anti-PER rabbit (1:20,000), anti-HTT mouse (1:500) and anti-PDF rat (1:1000). Anti-PDF rat was a generous gift from Jae Park, Vanderbilt University. For PER oscillations, flies were dissected at CT23-24 (CT23) and CT11-12 (CT11). These samples were co-stained with anti-PDF to enable the identification of LNv.

For characterising the PER^+ and PDF^+ LNv soma numbers, the adult flies brain dissections were carried out in parallel at different ages. Since, with *pdf>Q128,Hsp40*, a sustained rescue for two AWs were seen in behaviour, dissections were carried out in 3d-, 9d-, and 16d-old flies corresponding to the beginning of AW1, the transition of AW1-AW2 and end of AW2, respectively. With *pdf>Q128,HSP70*, rhythm rescue was restricted to AW1. Hence, dissections were carried out at 3d and 9d, corresponding to the beginning and end of AW1, respectively. For characterising HTT status in LNv, the adult fly brain dissections were carried out in parallel for the five genotypes (*pdf>Q128*, *pdf>Q0,Hsp40*, *pdf>Q128,Hsp40*, *pdf>Q0,HSP70* and *pdf>Q128,HSP70*) at 3d and 9d. Many of the Hsp-expressing flies had periods longer than 24h. Therefore, the mean period values of the respective genotypes were considered to calculate the circadian time (CT) for dissections to detect PER oscillations in the LNv. For quantifying PER oscillations in DD, LD-reared flies were dissected at CT23-24 (CT23) and CT11-12 (CT11) at different ages: all the five genotypes at 3d and *pdf>Q0,Hsp40* and *pdf>Q128,Hsp40* also at 9d. These samples were co-stained with anti-PDF to aid in identifying LNv and anti-HTT. The sample sizes were determined empirically (Table 5.3). There was no blinding during sample preparation.

5.2.3.1 Image acquisition and analysis

The number of PDF^+ and PER^+ LNv and the form of expHTT in the LNv were noted on manual observation of the samples using a Zeiss Axio Observer Z1 epifluorescence microscope with the

63X/oil 1.4NA objective and without blinding. The collected data were then cross-verified with images captured using a 40X/oil 1.3NA objective as a *z*-stack of 1µm interval. The PDF-stained sLNv and lLNv were distinguished based on their anatomical location, size, and staining pattern. For quantification of PER intensity and expHTT inclusions, the lamp intensity and exposure time were kept constant across samples for an experiment. The PER intensity was calculated from the obtained images as described previously in a single-anonymized manner (Sections 2.2.3.1 and 3.2.3.1). NIH imaging software ImageJ was used for analysis and quantification. Confocal *z*-stacks were captured using Zeiss LSM 880 for representative images, keeping the PMT gain, offset and laser power below saturating pixels. In the representative images, brightness/contrast adjustments have been applied to the whole image to better visualise the LNv, especially the sLNv, as they show less intense and sparser PDF staining than the lLNv. The inclusion quantifications (number and size) were described in section 3.2.3.1.

5.2.3.1.1 Categorisation and quantification of expHTT forms

Based on the predominant expHTT form present in the LNv, each LNv (intra-hemisphere) or each hemisphere (inter-hemisphere) was divided into various categories, as described in section 3.2.3.1.1. In addition to expHTT appearing with a uniform diffuse expHTT staining (Diff), appearing as puncta-like shiny specks of varying sizes named inclusions (Inc), diffuse expHTT with a few puncta-like inclusions (Diff+Inc) and without expHTT staining (No HTT) (Fig 5.1a, top-panels), with overexpression of Hsp40, a new form of expHTT was seen. This hitherto unreported form of expHTT was oval with a compact appearance, henceforth referred to as expHTT spot or spot-like expHTT (Spot) (Fig 5.1a, second-row). Also observed less frequently was an LNv with an expHTT Spot and the canonical inclusions, giving the Spot a distorted appearance. Hence, such forms of expHTT were included under the Inc category. If the spot appeared amidst a diffused expHTT distribution, primarily seen in lLNv of young flies, it was designated as Diff+Spot (Fig 5.1a, second-row). Each hemisphere was allotted a particular category depending on the most predominant expHTT form found sLNv (or lLNv) (Fig 5.1b). The hemisphere categorisation (inter-hemisphere) based on the predominant expHTT form in

LNv (sLNv or lLNv) was as follows: predominantly diffuse distribution (Fig 5.1b top-left), an equal distribution of diffused and inclusions (Diff+Inc) (Fig 5.1b top, middle and right), predominantly had Diff+Spot (Fig 5.1b, second-row, left), predominantly had spots (Spot) (Fig 5.1b, second row, middle and right), a near mix of diffuse, inclusions and spots (Diff+Spot+Inc) (Fig 5.1b third row, left), an equal distribution of spot and inclusions (Spot+Inc) (Fig 5.1b, third row, middle and right), or predominantly had inclusions (Inc) (Fig 5.1b, fourth row, middle and right). Upon such a hemisphere-level categorisation, hemispheres in which sLNv or lLNv were without expHTT never dominated, so the NoHTT category does not exist. The arrangement order used in the figures describing various expHTT forms is based on post-hoc observations regarding the appearance and predominance of various expHTT forms in LNv over time (Fig 5.1c). For example, in most *pdf>Q128* samples, sLNv shows Diff expHTT as larvae and young adults mostly exhibit Diff+Inc in lLNv, followed by Inc as they age. *pdf>Q128,Hsp40* flies mostly show Diff expHTT in the young. With age, different combinations of Diff, Spot, and some Inc appear and dominate (mostly non-Inc forms), and Inc-exclusive becomes more prominent only in much older flies.

5.2.3.1.2 Quantification of expHTT inclusions

The quantification of expHTT inclusion numbers and size and the proportion of hemispheres enriched in different-sized inclusions were described in section 3.2.3.1.2. However, the quantification method did not distinguish between expHTT Inc and Spots, resulting in Spots being included in the inclusion number and size quantifications.

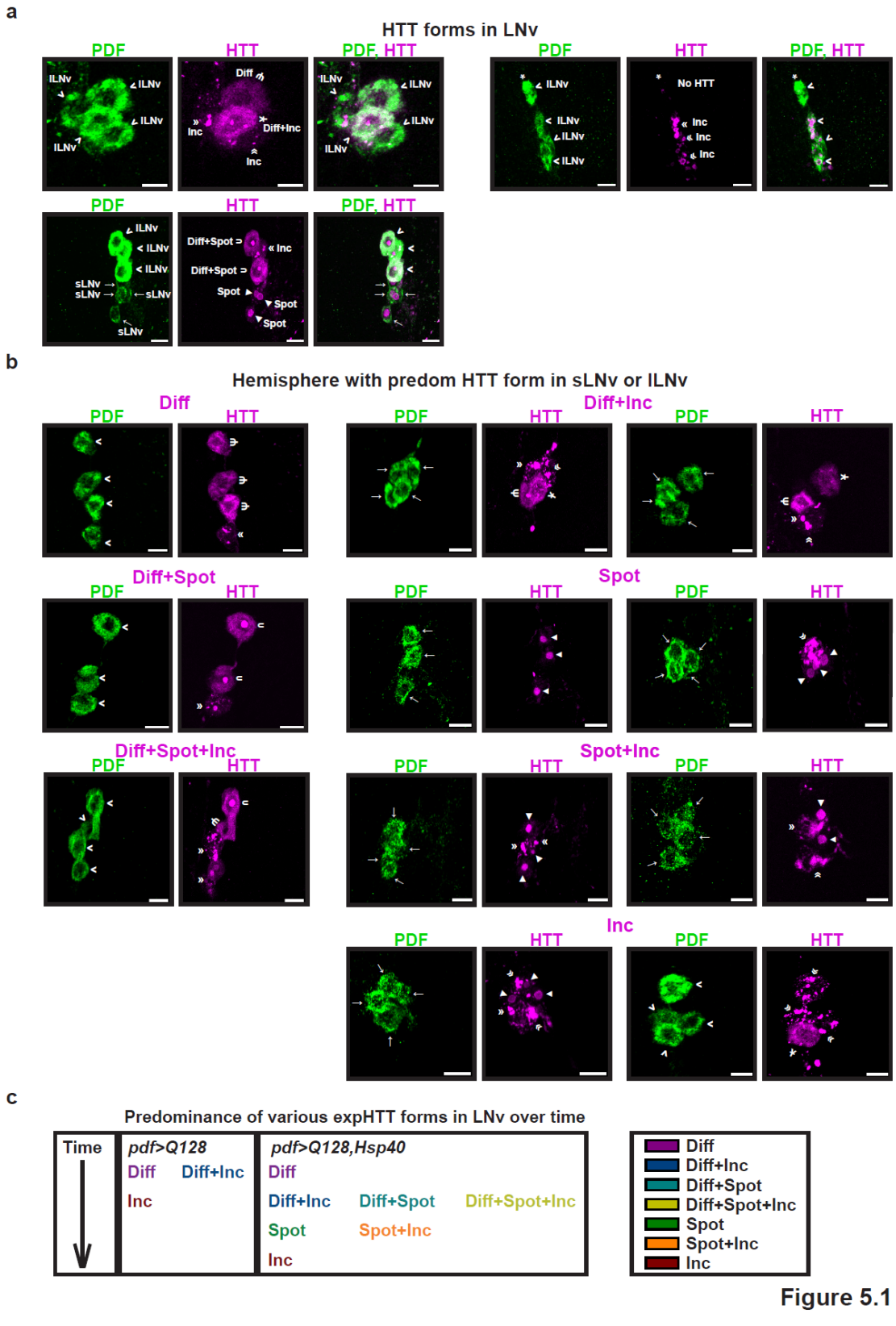

Figure 5.1

Fig 5. 1 An illustration of the different forms of expHTT detected in LNv.

Representative images of the adult fly brains stained for PDF (green) and HTT (magenta) in LNv soma. sLNv soma is indicated by arrows (→) and lLNv soma by arrowheads (>). (a) The various forms of expHTT detected in LNv are shown, namely, diffuse expHTT or Diff (Ψ psi),

diffuse+inclusions expHTT or Diff+Inc (Ɣ symbol), diffuse+spot expHTT or Diff+Spot (ᴜ upsilon), spot expHTT or Spot (◄ triangles) and expHTT inclusions or Inc (« double arrowheads). The * represents an lLNv without expHTT (top-right panels) indicated as NoHTT. (b) The categorisation of hemispheres into seven categories is based on the most predominant form of expHTT in sLNv (or lLNv). The hemispheres are categorised as Diff, Diff+Inc, Diff+Spot, Spot, Diff+Spot+Inc, Spot+Inc and Inc. (c) The predominance of various expHTT forms in LNv over time, based on empirical observations for *pdf>Q128* and *pdf>Q128,Hsp40*. The order of appearance and predominance depicted here are for ease of reading and are not to scale are not age-matched events in time across *pdf>Q128* and *pdf>Q128,Hsp40*. Scale bars are 10 µm.

5.2.3.2 Statistical analysis

For comparing PDF^+ or PER^+ LNv numbers between genotypes or between ages, the Kruskal-Wallis test of ranks, followed by multiple comparisons of mean ranks, was used. The change in the distribution shapes of PDF^+ and PER^+ LNv numbers between genotypes was assessed using Kolmogorov-Smirnov tests with $\alpha = 0.05$, followed by Bonferroni correction on pair-wise *p*-values. Multi-factor ANOVA followed by Tukey's HSD post-hoc test was used on transformed data to compare inclusion numbers between genotypes or across ages. Since the variances were not homogenous for inclusion size comparisons, the transformed data sets, primarily normal, were subjected to Welch's ANOVAs, followed by Games-Howell post-hoc tests (McDonald, 2014). The data sets were either transformed (where required) to analyse the status of PER oscillations between the time points CT23 and CT11 for a genotype or the PER intensities at a time point between genotypes or directly analysed using One-Way ANOVA, followed by Tukey's HSD wherever necessary. To compare the proportion of hemispheres predominated by different expHTT forms (or different expHTT Inc sizes) between genotypes for age or ages for a genotype, m x n Fisher's exact tests were used. Following this, wherever necessary, multiple specific 2x2 Fisher's Exact test sets with BH procedure on all relevant comparisons were applied (using R). The proportion of hemispheres with $Spot^+$ LNv between ages was compared using multiple 2x2 Fisher's exact tests followed by Bonferroni corrections. Spot sizes between ages for sLNv or lLNv were analysed by one-way ANOVA (on transformed data, if required), followed by Tukey's HSD tests; for Spot sizes between sLNv and lLNv, a factorial ANOVA with LNv and age as fixed factors was carried out on transformed data, followed by Tukey's HSD. Other details are described previously in Chapter 2 (2.2.2.1).

5.3 RESULTS

5.3.1 Overexpression of Hsp40 or HSP70 delays arrhythmicity in flies expressing expHTT in the LNv

Flies expressing expHTT in LNv are arrhythmic immediately upon entering DD25 (Fig 5.2 second-row, left) (Prakash et al., 2017). Overexpressing heat shock proteins Hsp40 or HSP70 in *pdf>Q128* flies delayed the onset of this arrhythmicity (Fig 5.2 second-row, centre-panels). Most flies co-expressing HTT-Q128 with Hsp40 were rhythmic during the early AW1 and mid-AW2, their mean rhythmicities being comparable to those of controls expressing HTT-Q0 and significantly higher than those of *pdf>Q128* (Fig 5.3a). However, the rhythmicity of *pdf>Q128,Hsp40* declined significantly during the later age AW3 than during the earlier AWs and compared to their age-matched controls and was like that of *pdf>Q128*. Despite a drop in rhythmicity compared to AW1, most *pdf>Q128,Hsp40* flies remained rhythmic during AW2. *pdf>Q128,HSP70,* had significantly higher rhythmicity than *pdf>Q128* in AW1 and AW2 (Fig 5.3a). However, it was like controls only in AW1, beyond which it declined. Notably, in AW2, while about 50% of *pdf>Q128,HSP70* remained rhythmic, their rhythmicity was significantly lower than that of *pdf>Q128,Hsp40*. In AW3, like *pdf>Q128,Hsp40* and *pdf>Q128, pdf>Q128,HSP70* also had poor rhythmicity. Whereas the rhythmicity of *pdf>Q128,Hsp40* was like that of background controls across AW1 and AW2 (Figs 5.2a, middle-column, 5.3b, top), that of *pdf>Q128,HSP70* was control-like only during AW1 (Figs 5.2a, third-column, 5.3c, top). Unlike the sharp fall in rhythmicity of *pdf>Q128,HSP70* in AW2, *pdf>Q128,Hsp40*, despite having a progressive reduction in rhythmicity with age, showed a significant fall in mean rhythmicity only in AW3 (Fig 5.3a,b, top,c, top). Thus, the rescue of rhythmicity by Hsp40 lasted longer than that by HSP70.

In AW1, the rhythmic flies of *pdf>Q128,Hsp40* had robust rhythms comparable to most controls and significantly higher robustness than *pdf>Q128* (Fig 5.3b, second-panel). In AW2, the robustness of rhythmicity of *pdf>Q128,Hsp40* dropped lower than that of both parental controls and was comparable to that of *pdf>Q128*. Overall, the overexpression of Hsp40 in *pdf>Q128* flies rescued both rhythmicity and rhythm robustness in AW1. In AW1, the rhythmic

pdf>Q128,Hsp40 and *pdf>Q0,Hsp40* flies had longer periods than other controls (Figs 5.2, second-column, 5.3b, third-panel). The *pdf>Q128,Hsp40* flies showed significantly better activity consolidation than *pdf>Q128* flies across ages 5d-8d and 11-14d (Fig 5.3b, bottom). However, this improved consolidation was comparable to controls at 6-7d and 12-15d. Thus, overexpression of Hsp40 in *pdf>Q128* flies rescues both rhythmicity and rhythm strength at an early age. Activity rhythms persist until the middle-age, postponing arrhythmicity onset by over two weeks. These results indicate that Hsp40 is a potent suppressor of expHTT-induced circadian behavioural arrhythmicity.

The rhythmic flies of *pdf>Q128,HSP70* exhibited weaker rhythms than controls across AWs, and robustness in older AWs was lower than in AW1 (Fig 5.3c, second-panel). Controls *pdf>Q0,HSP70* and *pdf>HSP70* mostly had longer periods than rhythmic *pdf>Q128,HSP70* and *Q128,HSP70* across AWs (Figs 5.2, third-column, 5.3c, third-panel). The activity consolidation of *pdf>Q128,HSP70* was significantly better than that of *pdf>Q128* across 4d-5d and 6d-13d and was comparable to controls at most ages (Fig 5.3c, bottom). Thus, the overexpression of HSP70 in *pdf>Q128* flies improves their early-age rhythmicity and activity consolidation. In contrast to the rescue with Hsp40 overexpression, rhythm rescue with HSP70 overexpression at an early age did not extend to middle age. Hence, HSP70 partially suppresses expHTT-induced circadian behavioural arrhythmicity and is less efficient than Hsp40.

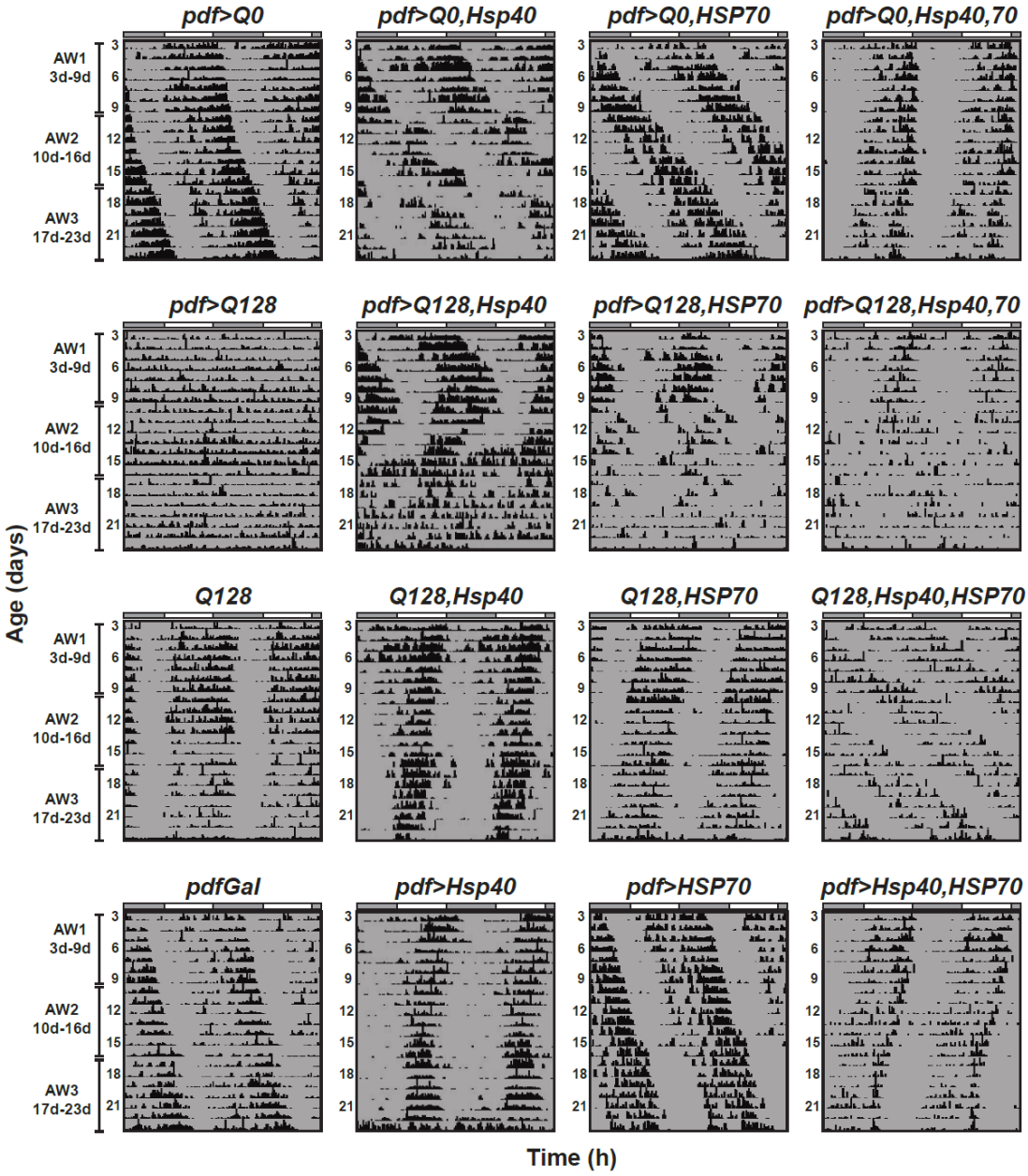

Figure 5.2

Fig 5. 2 pdf>Q128 flies overexpressing Hsp40 or HSP70 show early-age behavioural activity/rest rhythms.

Representative double-plotted actograms for flies showing activity data for 21d (age 3d-23d) in DD at 25 ºC for 16 genotypes. As shown to the left, the 21d data has been divided into three 7d age windows (AWs). The white and grey bars above the actograms represent the light and dark phases of the previous LD.

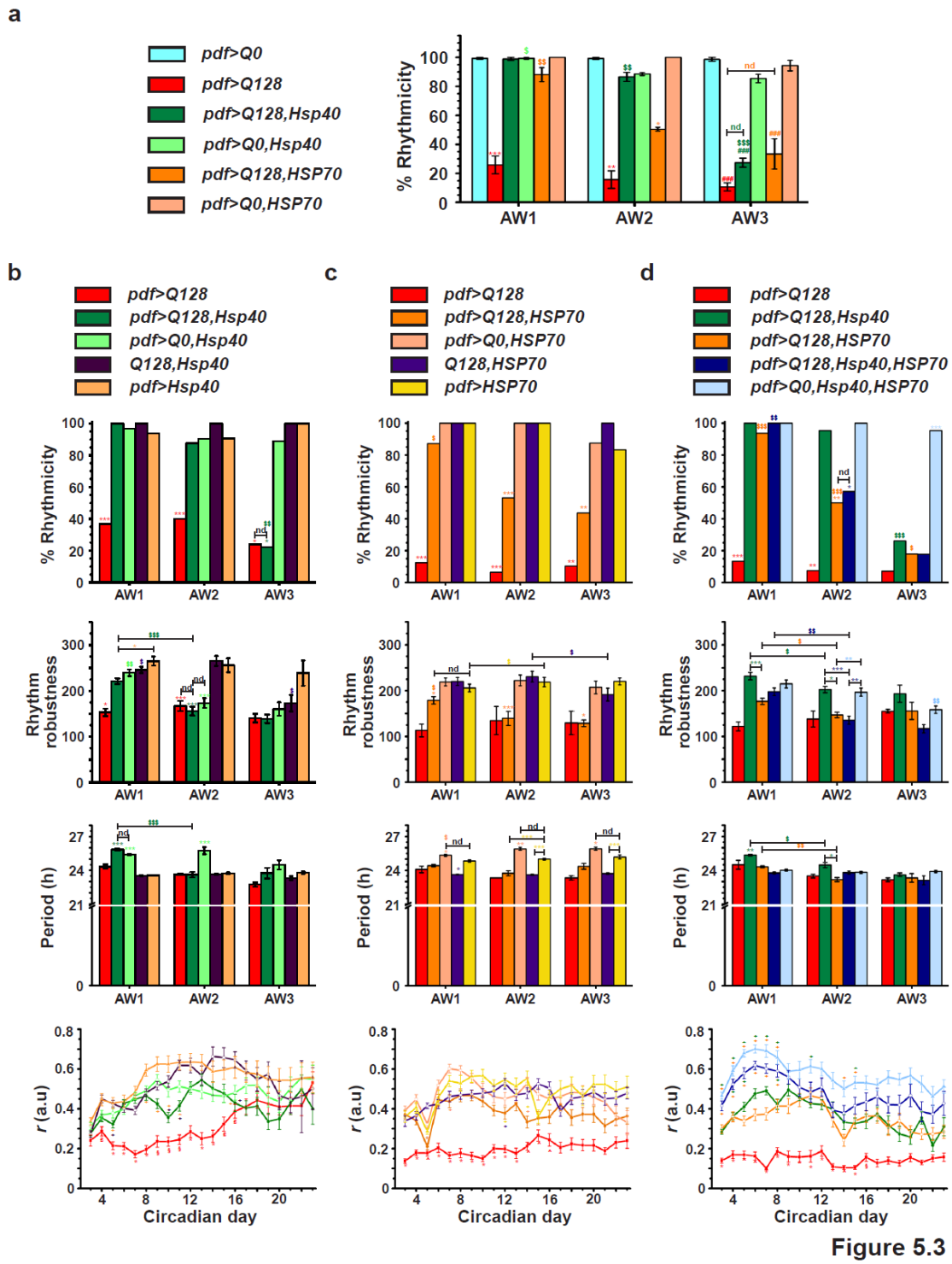

Figure 5.3

Fig 5. 3 In pdf>Q128 flies, Hsp40 overexpression leads to sustained behavioural rhythms, while HSP70 overexpression leads to early-age rhythmicity.

(a) The percentage of rhythmic flies averaged over at least three independent runs plotted across age windows. (b) (c) (d) For three different activity runs with the primary experimental genotype being *pdf>Q128,Hsp40* (b), *pdf>Q128,HSP70* (c) and *pdf>Q128,Hsp40,HSP70* (d), comparisons across AWs of percentage rhythmicity (top-panel), mean rhythm robustness (second-panel), mean period (third-panel) and mean *r*-value (bottom-panel). *pdf>Q128* has not been considered for between-genotype statistical comparisons of robustness and period across AWs in the HSP70 overexpression

and synergistic effect experiments (c and d, second and third panels) and during AW3 in the Hsp40 overexpression experiment (b, second and third panels), as very few flies were rhythmic. Also, for AW3, *pdf>Q128,Hsp40* in the Hsp40 overexpression experiment (b, second and third panels) or most of the experimental genotypes in the synergistic effect experiment (d, second and third panels) are not considered for statistical analysis of period and robustness. Across all panels, coloured symbols represent statistically significant differences: coloured * indicates age-matched differences of the respective-coloured genotype from all other genotypes or indicated genotype, coloured # indicates age-matched differences of the respective-coloured genotype from all *Q0*-containing controls and coloured $ indicates differences across age for the respective-coloured genotype. Statistical significance at single-symbol $p<0.05$, dual-symbol $p<0.01$ and triple-symbol $p<0.001$. nd indicates not different. For the bottom-panels of *r*-values, red-coloured symbols indicate significant differences at $p<0.05$ of *pdf>Q128* from * all other genotypes, § from all genotypes except *pdf>Q128,Hsp40*, ^ from all genotypes except *pdf>Q128,HSP70*, £ from all non-expanded controls and * (orange) of *pdf>Q128,HSP70* from all other genotypes. Coloured + near an error bar of a data point indicates significant differences at $p<0.05$ of the respective-coloured genotype from the data-point genotype. Error bars are SEM.

5.3.2 Co-expression of Hsp40 and HSP70 synergistically improves the consolidation of activity rhythms in flies expressing expHTT in the LNv

Previous studies show that co-expression of Hsp40 and HSP70 has a synergistic effect of providing a more significant effect on neurodegenerative features than expressing Hsp40 or HSP70 individually (Chan et al., 2000; Jana, 2000; Kobayashi et al., 2000; Muchowski et al., 2000; Sittler et al., 2001; Bailey et al., 2002; Bonini, 2002; Rujano et al., 2007). Therefore, I asked whether overexpression of both the Hsps provides a greater rescue (e.g. sustained robust rhythms across AWs) than expressing each alone. In AW1, flies expressing both Hsps in the presence of expHTT, i.e. *pdf>Q128,Hsp40,HSP70*, were mostly rhythmic, comparable to *pdf>Q128,Hsp40*, *pdf>Q128,HSP70* and control *pdf>Q0,Hsp40,HSP70* and significantly better than *pdf>Q128* (Figs 5.2, second-row, 5.3d, top-panel). However, in AW2, the percentage rhythmicity of *pdf>Q128,Hsp40,HSP70*, like that of *pdf>Q128,HSP70*, dropped significantly compared to AW1 while remaining higher than that of *pdf>Q128* but lower than that of *pdf>Q128,Hsp40* and *pdf>Q0,Hsp40,HSP70* (Fig 5.3d, top-panel). In AW3, the rhythmicity percentage of *pdf>Q128,Hsp40,HSP70* declined further and, like for single Hsp overexpression, was comparable to that of *pdf>Q128*.

In AW1, the rhythmic *pdf>Q128,Hsp40,HSP70* flies exhibited robust rhythms comparable to those of control *pdf>Q0,Hsp40,HSP70* and the single rescue *pdf>Q128,HSP70* (Fig 5.3d second-panel). Its period was similar to most other genotypes across age (Figs 5.2 and 5.3d third-panel).

Both *pdf>Q128,Hsp40,HSP70* and *pdf>Q128,HSP70* had weaker rhythms than that of *pdf>Q128,Hsp40* in AW1 and AW2 and than *pdf>Q0,Hsp40,HSP70* in AW2 (Fig 5.3d second-panel). Interestingly, the extent of activity consolidation '*r*' of *pdf>Q128,Hsp40,HSP70* was significantly greater than that of *pdf>Q128* and both *pdf>Q128,Hsp40* and *pdf>Q128,HSP70* during most of the early age, while remaining comparable to that of *pdf>Q0,Hsp40,HSP70* and *pdf>Hsp40,HSP70* (Fig 5.3d, bottom). Overexpression of both Hsp40 and HSP70 (*pdf>Hsp40,HSP70*) leads to a higher '*r*' and, by extension, better-consolidated activity rhythms than those of experimental genotypes *pdf>Q128*, *pdf>Q128,Hsp40* and *pdf>Q128,HSP70* in early and middle ages, and also from control *Q128,Hsp40,HSP70* at early ages (Fig S1). This enhanced consolidation upon expressing both the HSPs in the LNv is also reflected in the significantly higher '*r*' of *pdf>Q0,Hsp40,HSP70* and *pdf>Q128,Hsp40,HSP70* than that of the other experimental genotypes. Thus, although overexpression of both Hsp40 and HSP70 in *pdf>Q128* did not have a synergistic effect on percentage rhythmicity *per se*, there was a synergistic improvement in early-age activity consolidation.

5.3.3 Hsp40 overexpression in flies expressing expHTT in the LNv rescues PDF$^+$ sLNv soma numbers

I then investigated whether overexpression of Hsp40 or HSP70 in *pdf>Q128* also rescues LNv cellular features. As described previously (Sheeba et al., 2010; Prakash et al., 2017) and as is also shown here, *pdf>Q128* flies had a loss of PDF from the sLNv soma from an early age, while PDF in lLNv soma was unaltered (Figs 5.4, top, 5.5a). In contrast, flies overexpressing Hsp40, the *pdf>Q128,Hsp40*, showed significantly higher PDF$^+$ sLNv soma numbers than *pdf>Q128* and were indistinguishable from control *pdf>Q0,Hsp40* across ages (Figs 5.4, middle panel-sets, 5.5a, left). The shapes of the frequency distributions of PDF$^+$ sLNv numbers for *pdf>Q128,Hsp40* across age were left-skewed, like those of controls, with most hemispheres having 4-5 sLNvs, and differed significantly from the right-skewed distribution of *pdf>Q128* (Fig 5.5b). In contrast, at 3d and 9d, the PDF$^+$ sLNv soma numbers of *pdf>Q128,HSP70* were diminished, like those of *pdf>Q128* and significantly lower than those of control *pdf>Q0,HSP70* and *pdf>Q128,Hsp40* (Figs 5.4, bottom panel-sets, 5.5a, left). Mirroring the mean PDF$^+$ sLNv soma numbers was the shape of their distributions at both ages: *pdf>Q128,HSP70* was like *pdf>Q128* and different from controls (Fig 5.5c). The PDF$^+$ lLNv soma numbers were comparable for all the genotypes across

age (Figs 5.4, '>', 5.5a, right). Thus, overexpression of Hsp40, but not HSP70, completely rescues PDF^+ sLNv numbers. The sustained circadian rhythm rescue in *pdf>Q128,Hsp40* accompanied by the circadian output neuropeptide PDF rescue in the soma of pacemaker neurons sLNv suggest Hsp40 as a disease-modifier effective in restoring cellular function as well as associated behaviour. Despite the persistence of circadian activity rhythms, the lack of rescue of PDF+ sLNv soma in *pdf>Q128,HSP70* at an early age suggests an unconventional mode of rhythm restoration by HSP70 in the absence of somal PDF in the sLNv.

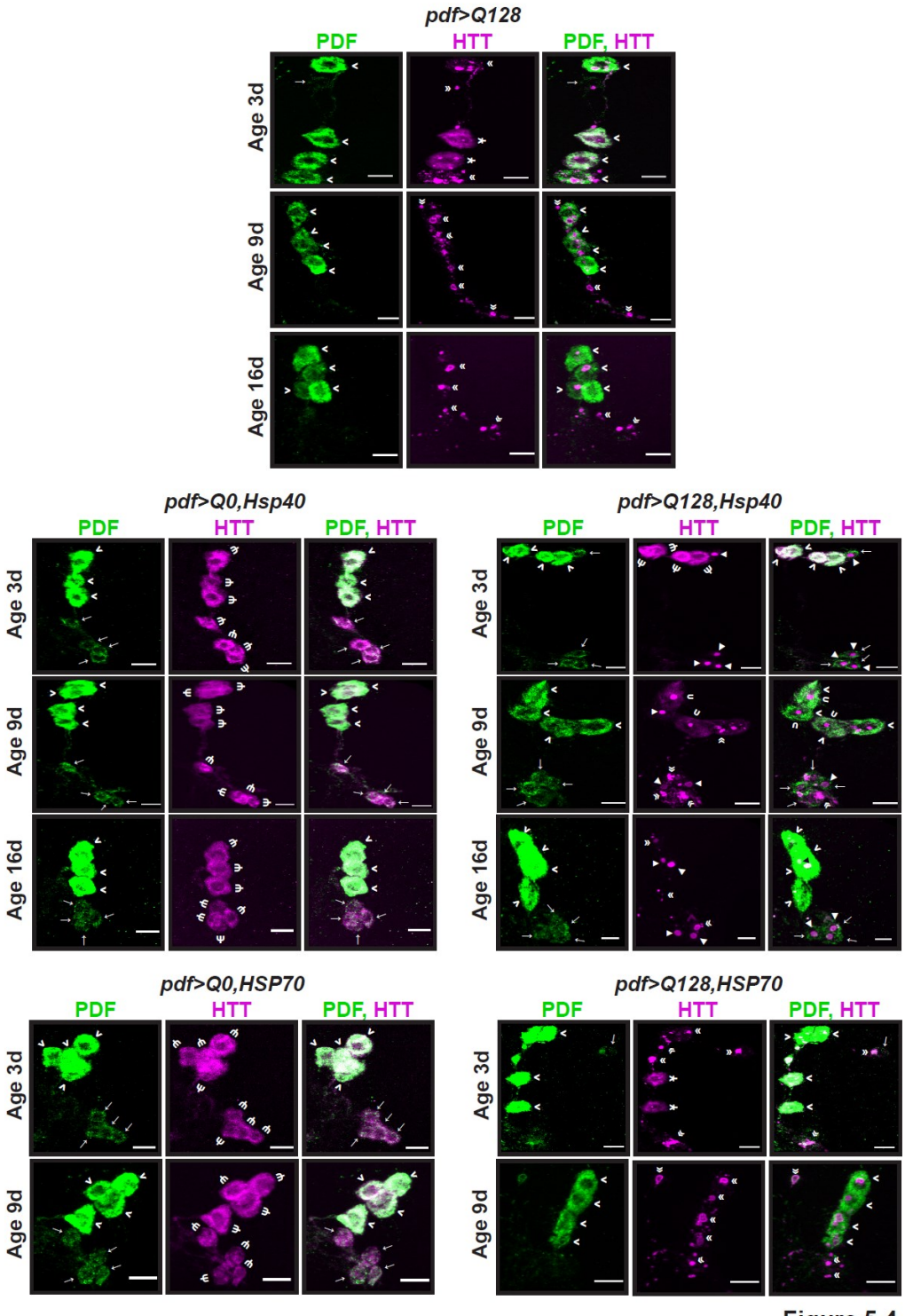

Figure 5.4

Fig 5. 4 pdf>Q128 flies overexpressing Hsp40 retain PDF^{+} sLNv soma across age.
Representative images of adult fly brains stained for PDF (green) and HTT (magenta) in LNv at 3d, 9d and 16d for *pdf>Q128* (top panel-sets), *pdf>Q0,Hsp40* (middle-left panel-sets), *pdf>Q128,Hsp40* (middle-right panel-sets), and at 3d and 9d for *pdf>Q0,HSP70* (bottom-left panel-sets) and *pdf>Q128,HSP70* (bottom-right panel-sets). Indicated in the images are sLNv soma (→ arrows), lLNv soma (> arrowheads), diffuse expHTT (Ψ psi), diffuse+inclusions expHTT (Ɏ), diffuse+spot expHTT (υ upsilon), spot expHTT (◄ triangles) and expHTT inclusions (« double arrowheads) for the five genotypes. Scale bars are 10 µm.

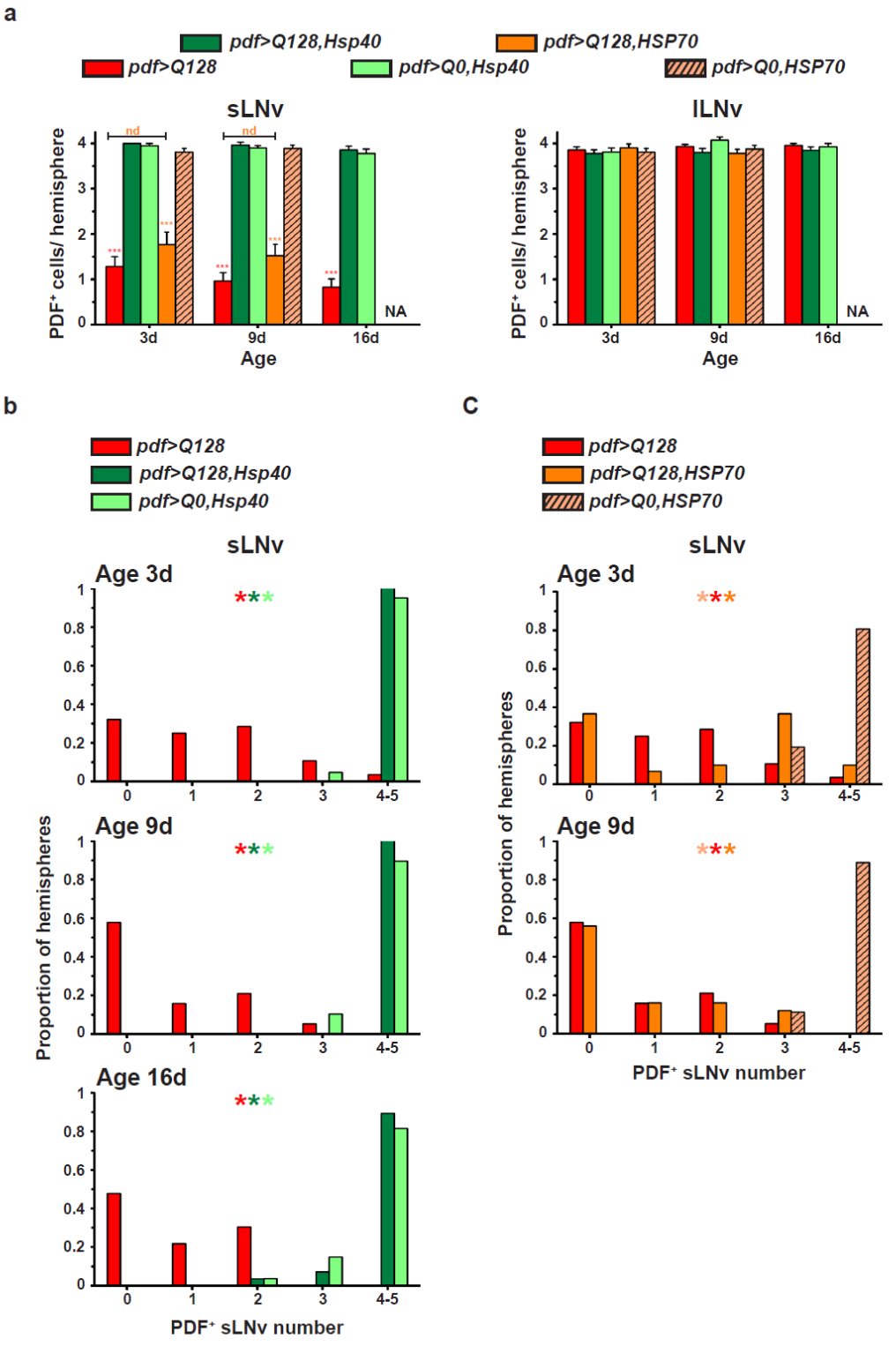

Figure 5.5

Fig 5. 5 pdf>Q128 flies overexpressing Hsp40 have control-like PDF⁺ sLNv soma numbers.

(a) The Mean number of PDF⁺ sLNv soma (left) and lLNv soma (right) across three ages. Symbols indicate significant differences, * for age-matched, inter-genotype differences and $ for differences between ages for each genotype: * (red) of *pdf>Q128* from all other genotypes except *pdf>Q128,HSP70* and * (orange) of *pdf>Q128,HSP70* from other genotypes except *pdf>Q128* at * $p<0.05$, ** $p<0.01$, *** $p<0.001$. NA is not applicable since early-age-rescue of PDF⁺ LNv was not

seen in *pdf>Q128,HSP70*, 16d dissections were not done. (b) and (c) Frequency distribution of the proportion of hemispheres with 0 to 5 PDF^+ sLNv soma numbers comparing *pdf>Q128* with *pdf>Q128,Hsp40* and *pdf>Q0,Hsp40* at 3d, 9d and 16d (b) and with *pdf>Q128,HSP70* and *pdf>Q0,HSP70* at 3d and 9d (c). Coloured multiple * indicates significantly different distribution shapes between genotypes, with the first colour of the reference genotype and the subsequent colours of genotypes differing from the reference at $p<0.01$. nd, not different. Error bars are SEM.

5.3.4 Hsp40 overexpression in *pdf>Q128* flies reduces the inclusion form of expHTT in favour of a new form

Hsps are molecular chaperones that interfere with various stages of aggregation and modify the nature, conformation, and solubility of expHTT inclusions (Barral et al., 2004; Wyttenbach and Arrigo, 2009; Lotz et al., 2010; Arrasate and Finkbeiner, 2012). I used immunocytochemistry and light microscopy to determine whether Hsp overexpression modifies the expHTT forms detected in the LNv of *pdf>Q128*. As detailed in the Materials and Methods section, the expHTT forms in each sLNv or lLNv were categorised based on appearance. Interestingly, *pdf>Q128* with overexpressed Hsp40 had an additional expHTT form that has not been observed in these flies and instances of which seem unreported in the literature. Visually and qualitatively, this form of HTT-Q128 appeared as a compact oval and was excluded from the cytoplasmic PDF staining (Figs 5.4, middle row, right panel-sets, see '◀', 5.6a, b). I refer to this as the "Spot" form of expHTT. PER at CT23 was mainly nuclear, and the compact Spot expHTT form appeared to overlap with nuclear PER and might be peri-nuclear (Fig 5.6a, b). The Spot form was also restricted to a single structure per LNv. Further, the spots appeared to be present throughout the circadian cycle, and when PER oscillations were examined, a similar number of expHTT spots were observed at both CT23 and CT11.

Only the *pdf>Q128,Hsp40* showed the presence of expHTT spots (Fig 5.4). Within each hemisphere, Spot expHTT was present in ~75% sLNv (three of four) at 3d and ~50% sLNv (two of four) at 9d and 16d (Fig 5.9a, top). At 3d and 9d, nearly every hemisphere of *pdf>Q128, Hsp40* had at least one sLNv with Spot expHTT, which decreased to ~ 75% at 16d (Fig 5.6c, left). In lLNv of *pdf>Q128,Hsp40*, Spot expHTT was absent at 3d, detected in ~60% lLNv per hemisphere (two to three of four) at 9d as Diff+Spot and in ~50% lLNv at 16d as a distinct Spot (Fig 5.9a, bottom). Across samples of *pdf>Q128,Hsp40*, most of the hemispheres showed the presence of

Spot in at least one lLNv (as Diff+Spot or Spot) at 9d and 16d (Fig 5.6c, left). On average, sLNv of older flies had significantly bigger spots (~25 μ) than those of 3d flies (~17 μ), and in lLNv, a similar trend was seen, with bigger spots at 16d (~20μ) than at 9d (~12μ) (Fig 5.6c right). The spots in the sLNv were larger than those in age-matched lLNv (Fig 5.6c, right).

Comparing the within-hemisphere distribution of predominant expHTT forms in LNv, it is apparent that at 3d and 9d, expHTT inclusions dominated both the sLNvs and lLNvs of *pdf>Q128* and *pdf>Q128,HSP70* (Fig 5.7a, b). In contrast, in the LNv of *pdf>Q128,Hsp40*, expHTT Spot dominated at 3d and continued to be present at 9d and in lLNv, expHTT was mostly diffuse at 3d, giving way to Diff+Spot and Inc expHTT at 9d (Fig 5.7 a, b). These intra-hemisphere differences were reflected in the inter-hemisphere comparisons (Fig 5.7a-d). Comparing the between-hemisphere distribution of predominant expHTT forms in LNv, it is apparent that at 3d and 9d, inclusions dominated in both the sLNvs and lLNvs of *pdf>Q128* and *pdf>Q128,HSP70* (Figs 5.4, 5.7c, d). In contrast, in the LNv of *pdf>Q128,Hsp40*, non-inclusion forms of expHTT like Diff and Spot dominated over exclusively-Inc (Fig 5.7c, d). At both ages, the overall distributions of expHTT forms in sLNv and lLNv of *pdf>Q128,Hsp40* differed significantly from those of *pdf>Q128* and *pdf>Q128,HSP70* (Fig 5.7c). We then compared the relative proportion of hemispheres in various pair-wise-category combinations. Specifically, at 3d, the proportion of hemispheres dominated by Inc expHTT in sLNv relative to Spot forms was significantly higher in *pdf>Q128* and *pdf>Q128,HSP70* than that in *pdf>Q128,Hsp40*, which mostly had hemispheres dominated by Spot expHTT and to a lesser extent Spot+Inc in the sLNv (Fig 5.8a, top). At 9d, nearly 50% of *pdf>Q128,Hsp40* hemispheres still had Spot-enriched sLNv either as Spot or Spot+Inc expHTT, while a similar proportion of hemispheres also had Inc-enriched sLNv (Fig 5.8a, bottom). It is of note that, by 9d, more than 50% of *pdf>Q128* and *pdf>Q128,HSP70* had no PDF^+ sLNv, with a mean number of ~1, whereas nearly all *pdf>Q128,Hsp40* had 4 PDF^+ sLNv (Fig 5.8a - mean PDF^+ LNv numbers are indicated at the bottom of ear bar).

The proportion of hemispheres with Inc-enriched lLNv relative to other forms of expHTT was significantly higher in *pdf>Q128* and *pdf>Q128,HSP70* than *pdf>Q128,Hsp40* at both 3d and 9d (Fig 5.8b, top-left and bottom). *pdf>Q128,Hsp40* at these ages mostly favoured hemispheres

dominated by non-Inc-enriched lLNv. At 3d, most of the hemispheres of *pdf>Q128,Hsp40* had Diff expHTT in lLNv, and by 9d, Spot expHTT appeared, giving rise to hemispheres predominated by mostly non-Inc expHTT forms in lLNv, namely Diff+Spot and Diff+Spot+Inc (Fig 5.8b). Thus, the inclusion form of expHTT predominates over other forms in LNv across age in *pdf>Q128* and *pdf>Q128, HSP70*, whereas, in *pdf>Q128,Hsp40* diffuse and spot forms are prevalent.

To track the progress of these distinct forms of expHTT over a more extended duration in the presence of Hsp40, in a separate experiment with *pdf>Q128* and *pdf>Q128,Hsp40*, we quantified cellular phenotypes up to 16d. Like the previous experimental results (Fig 5.7c, d), across age, the relative proportions of hemispheres with different expHTT forms in sLNv and lLNv differed significantly between genotypes (Fig 5.7e, f). Most of the *pdf>Q128* hemispheres had Inc-enriched sLNv across age and Inc-enriched lLNv at 9d and 16d, while in *pdf>Q128,Hsp40*, Spot expHTT in various combinations dominated the LNv (Fig 5.7e, f). In *pdf>Q128*, as the flies aged, there was a significant reduction in the proportion of hemispheres predominating in Diff or Diff+Inc expHTT in lLNv relative to those predominating in Inc expHTT (Fig 5.9b). In hemispheres of *pdf>Q128,Hsp40*, Spot-enriched sLNv were present across age (Fig 5.9c), and with age, the proportion of hemispheres with predominantly Spot-enriched sLNv relative to Inc-enriched diminished (Fig 5.9c, left). *pdf>Q128,Hsp40* showed a significant change across age in the proportion of hemispheres dominated by Diff-enriched lLNv relative to lLNv enriched by other expHTT forms (Fig 5.9d, top-row). Post 3d, Diff expHTT steeply declined in lLNv, making way for Diff+Spot, Diff+Spot+Inc and Inc at 9d and Spot, Spot+Inc and Inc at 16d (Fig 5.9d, top-row). From 9d to 16d, the relative proportions of hemispheres of Diff+Spot- (and Diff+Spot+Inc)- enriched lLNv to that of Inc enriched lLNv decreased significantly (Fig 5.9d, middle row, first and second panels). Concomitantly, the relative proportions of hemispheres of Spot- (and Spot+Inc)-enriched lLNv to that of Inc-enriched lLNv increased significantly (Fig 5.9d, middle-row, third and fourth panels). Thus, the overexpression of Hsp40 in *pdf>Q128* flies decreases the expHTT inclusions in LNv and facilitates expHTT spots. HSP70 overexpression, on the other hand, did not decrease expHTT inclusions in LNv.

In summary, Hsp40 overexpression improves LNv health by reducing inclusions of expHTT in favour of a new form of expHTT, the "Spot", and preserving PDF^+ sLNv. The Spot expHTT might be a relatively less toxic form of expHTT, given the control-like PDF^+ sLNv numbers of *pdf>Q128,Hsp40*. Also, *pdf>Q128,HSP70* and *pdf>Q128* were nearly indistinguishable in the dominance of expHTT inclusions in LNv, suggesting that mechanisms mediating the early-age rhythms upon HSP70 overexpression might not involve mitigation of visible inclusions.

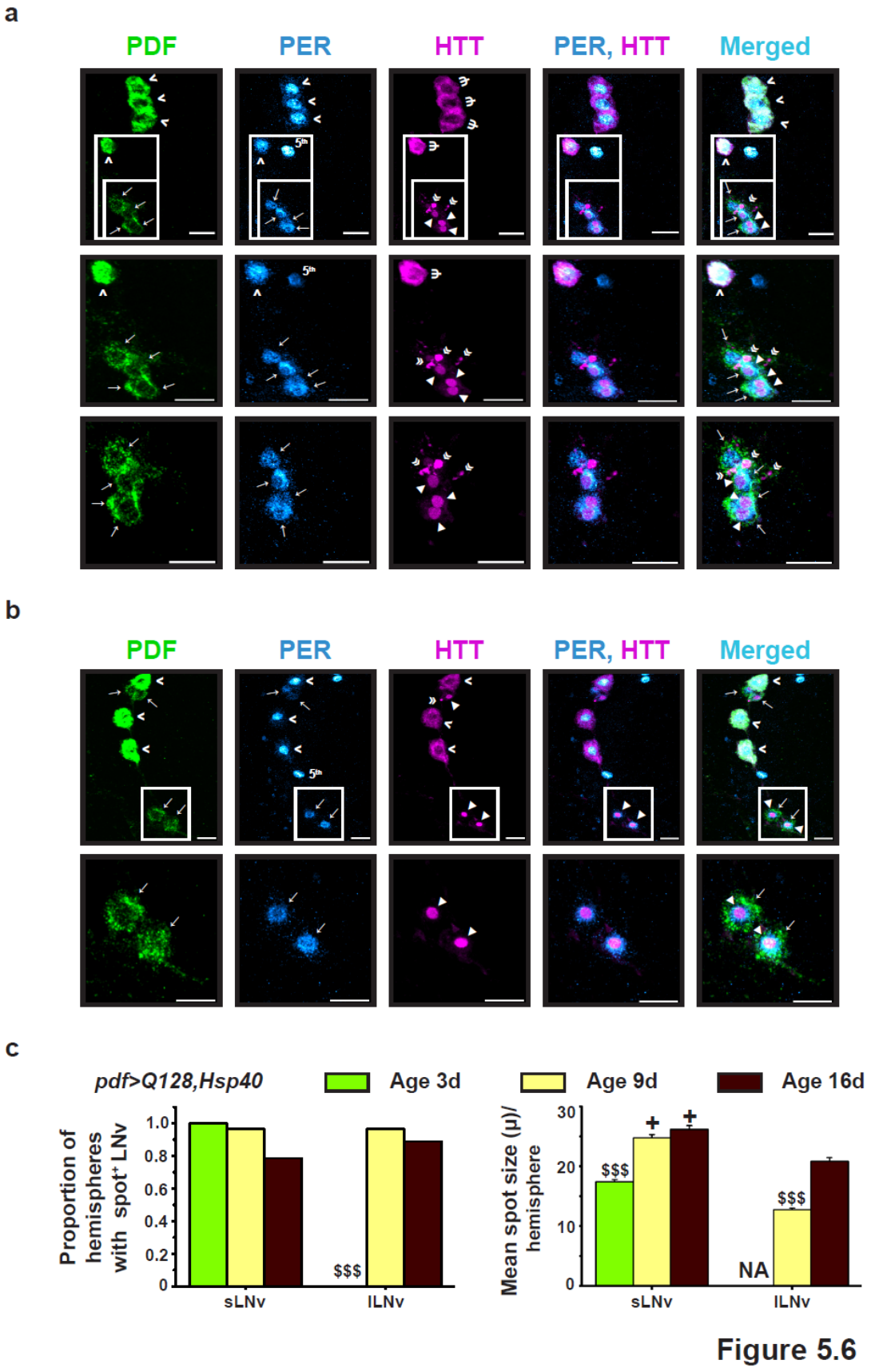

Figure 5.6

Fig 5. 6 pdf>Q128 flies overexpressing Hsp40 show the presence of a novel expHTT form, the 'Spot'.

(a) and (b) Two sets of representative images of 3d adult brains of *pdf>Q128,Hsp40* stained for PDF (green), PER (cyan hot) and expHTT (magenta) showing better resolved expHTT spots, where marked rectangles in each panel are enlarged in the subsequent panels below. Indicated in the images are sLNv soma (→ arrows), lLNv soma (> arrow-heads), diffuse expHTT (Ψ psi), spot expHTT (◄ triangles), expHTT inclusions (« double arrow-heads) and the PDF^{-}, PER^{+} 5^{th} sLNv. (c) Across three ages, the proportion of hemispheres with spots in sLNv or lLNv (left) and the mean spot sizes in sLNv and lLNv (right) are compared. $ depicts the difference of one age from other ages at $$$ $p<0.001$, and + indicates age-matched differences between sLNv and lLNv at $p<0.0001$. NA is not applicable. Error bars are SEM. Scale bars are 10 µm.

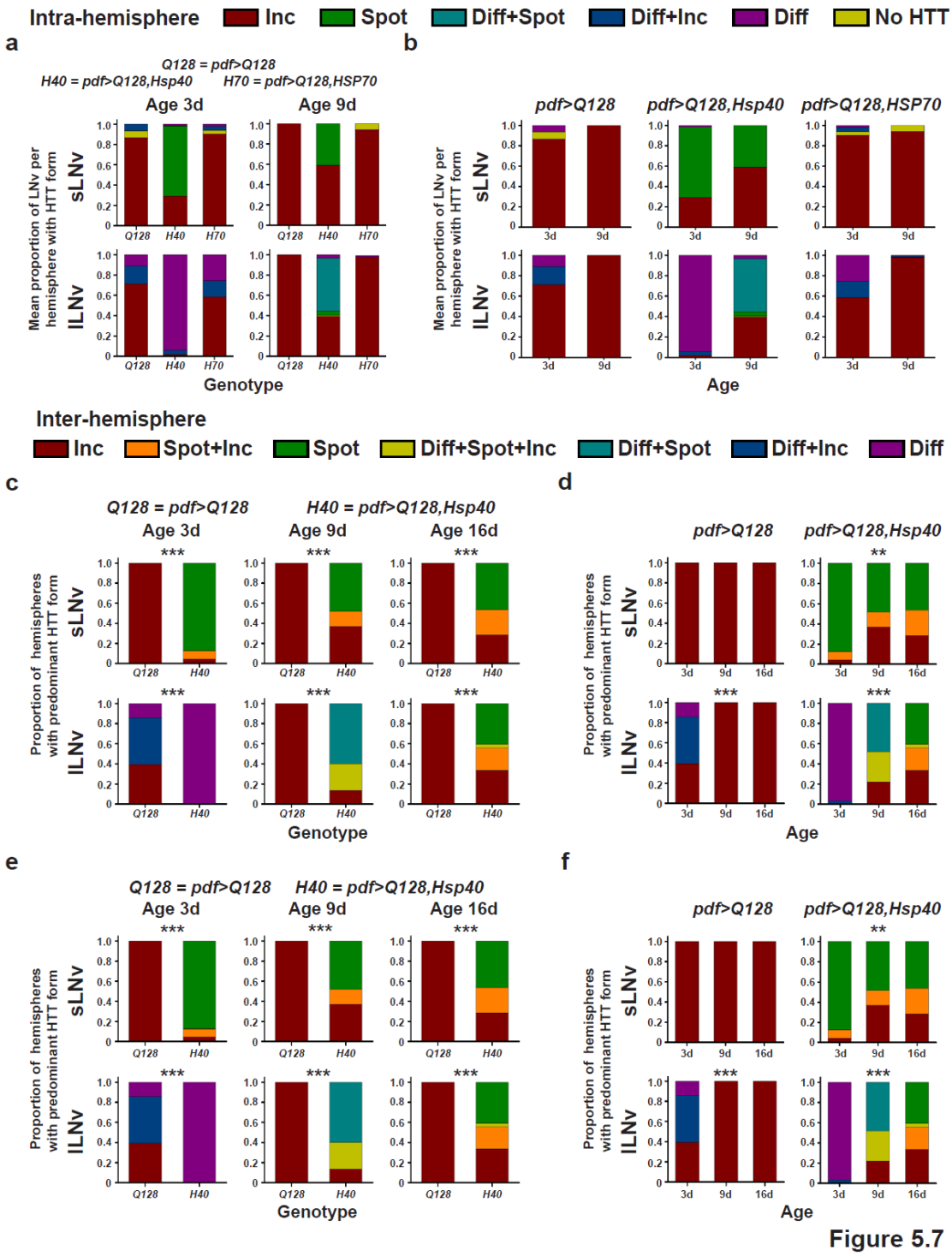

Figure 5.7

Fig 5. 7 pdf>Q128 flies overexpressing Hsp40 have fewer hemispheres with expHTT-inclusion-enriched LNv.

(a) and (b) The proportion of sLNv (top) or lLNv (bottom) having different expHTT forms in a hemisphere (intra-hemisphere) averaged across hemispheres are plotted against three genotypes for each age (a) or against two ages for each of the three genotypes (b). (c) and (d) The proportion of hemispheres dominated by different expHTT forms in sLNv (top) or lLNv (bottom) is plotted on the *y*-axis to describe the between-hemispheres (inter-hemisphere) distribution of predominant expHTT forms. This proportion is plotted at 3d and 9d against three genotypes (a) or for each genotype against ages 3d and 9d (b). * indicates significant changes in relative distributions of expHTT forms between

genotypes (c) or between ages (d) at ** p<0.01 and *** p<0.0001. The relevant pair-wise comparisons of (c) are plotted in Fig 5.8a, b. (e) and (f) are like (c) and (d), comparing the three ages, 3d, 9d, and 16d, for *pdf>Q128* and *pdf>Q128,Hsp40*. The relevant pair-wise comparisons of (d) are plotted in Fig 5.9a-c.

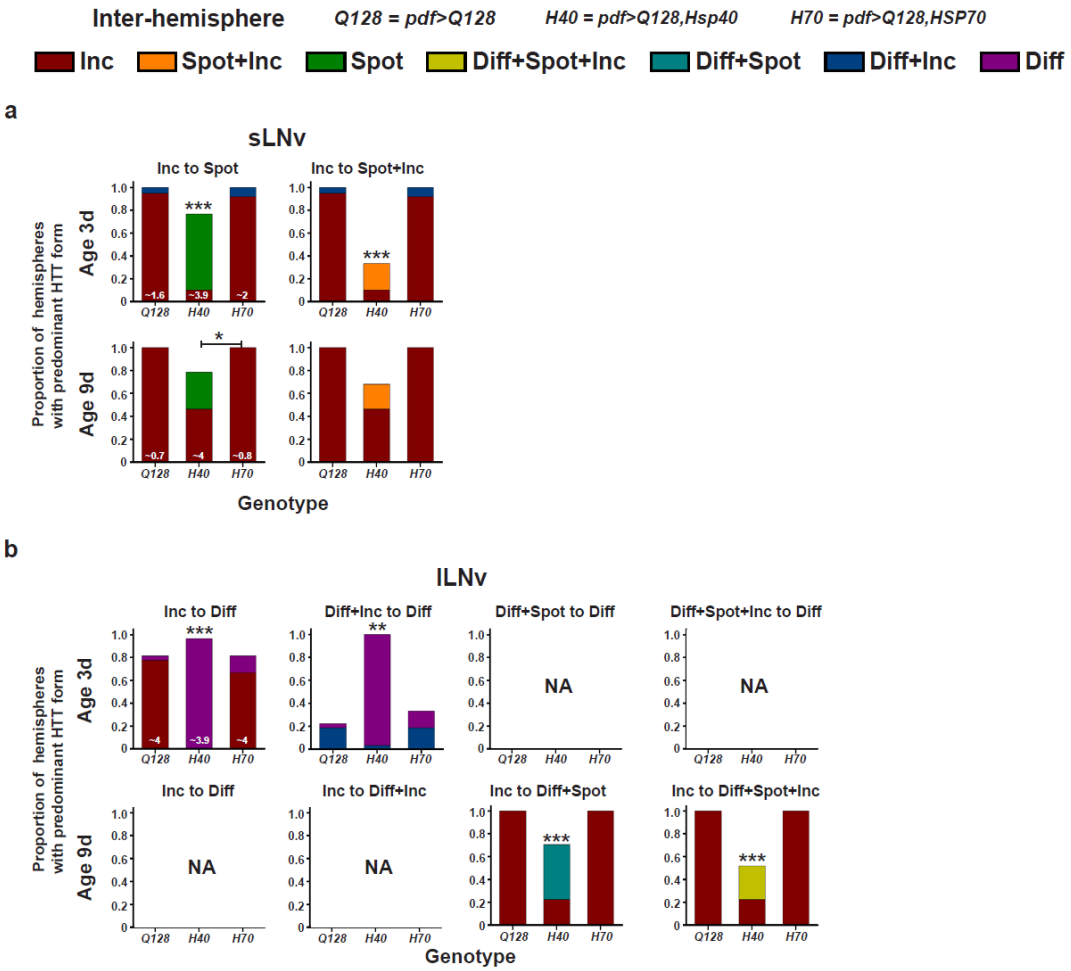

Figure 5.8

Fig 5. 8 Hemispheres dominated by expHTT inclusion enriched LNv were reduced in favour of diffuse and spot enriched LNv in pdf>Q128 flies overexpressing Hsp40.

(a) and (b) From the entire set in Fig 5.7c, various pair-wise relative hemisphere proportions enriched with expHTT forms in sLNv (b) and lLNv (c) that are statistically significant or (and) are biologically relevant are plotted against the three genotypes for 3d (top) and 9d (bottom). At the bottom of some bars, numbers represent the mean number of PDF^{+} LNv detected for that genotype at that age. * indicates significant relative changes in pair-wise proportions of hemispheres enriched in expHTT forms between genotypes at * p<0.05, ** p<0.01 and *** p<0.001. NA, not applicable.

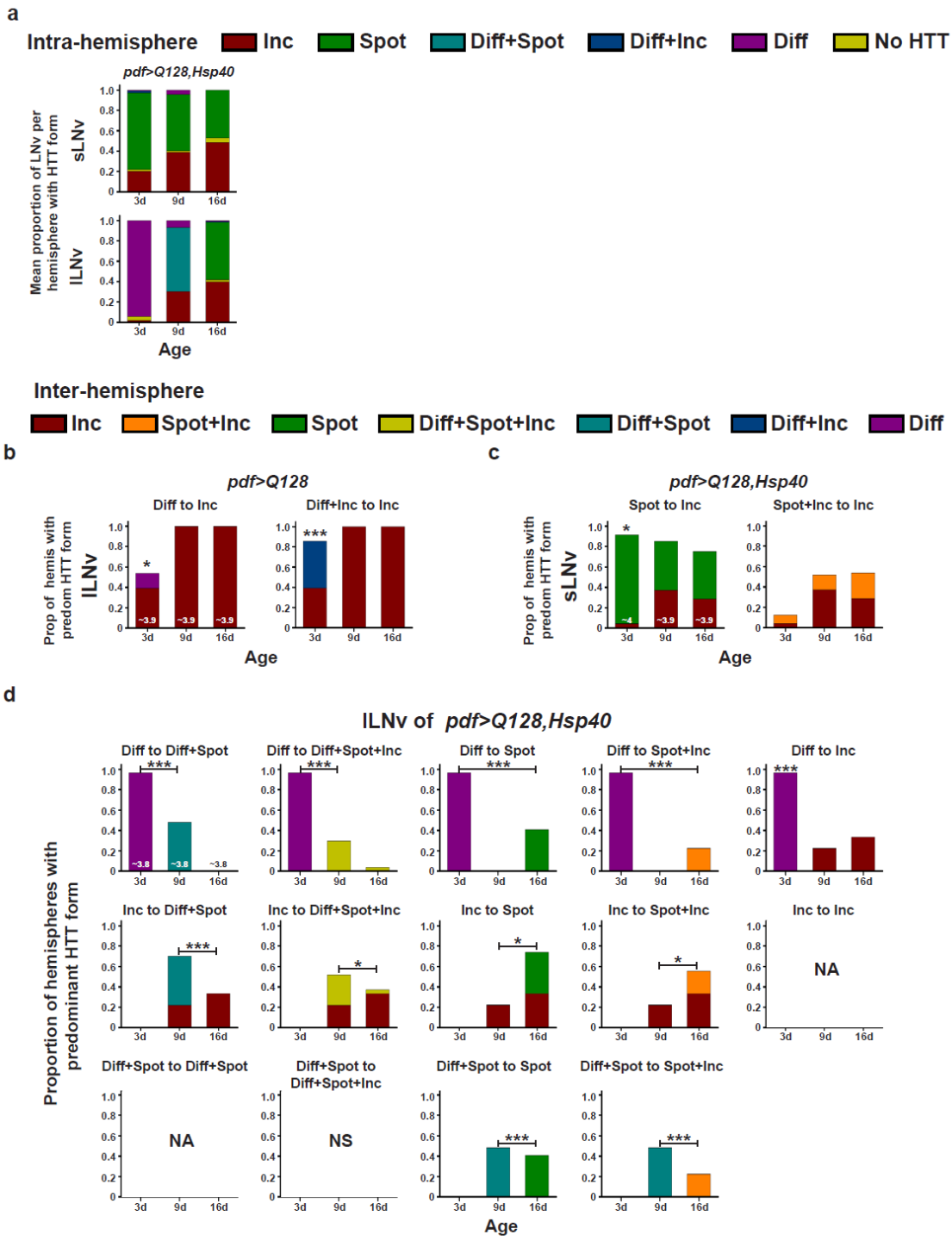

Fig 5. 9 Most pdf>Q128 flies overexpressing Hsp40 possess hemispheres with expHTT spot form enriched LNv.

(a) The proportion of sLNv (top) or lLNv (bottom) having different expHTT forms in a hemisphere (intra-hemisphere) averaged across hemispheres are plotted against three ages of *pdf>Q128,Hsp40* showing the within-hemisphere distribution of expHTT forms. (b) - (d) From the entire set in Fig 5.7e, various pair-wise relative hemisphere proportions enriched with expHTT forms in lLNv (b and d) and sLNv (c) that are statistically significant or (and) are biologically relevant are plotted against age for the genotypes *pdf>Q128* (b) and *pdf>Q128,Hsp40* (c and d). At the bottom of some bars, numbers represent the mean number of PDF^{+} LNv detected for that genotype at that age. * indicates significant relative changes in pair-wise proportions of hemispheres enriched in expHTT

forms between genotypes at * $p<0.05$, ** $p<0.01$ and *** $p<0.001$. NA, not applicable; NS, not significant.

5.3.5 Hsp40 overexpression in *pdf>Q128* flies reduces the number of expHTT inclusions

I quantified the number and size of expHTT inclusions in and around the LNv. At both 3d and 9d, *pdf>Q128,Hsp40* had significantly fewer inclusions than that of *pdf>Q128* and *pdf>Q128,HSP70* (Fig 5.10a, left). At 3d, *pdf>Q128,HSP70* also had fewer inclusions than *pdf>Q128*, but not at 9d. Both *pdf>Q128,Hsp40* and *pdf>Q128,HSP70* exhibited increased inclusion numbers with age. Altogether, these results indicate that overexpression of Hsp40 or HSP70 in *pdf>Q128* reduces expHTT inclusion numbers, with Hsp40 having lasting effects.

The mean inclusion size of *pdf>Q128,Hsp40* was higher than that of *pdf>Q128* and *pdf>Q128,HSP70* at 3d, which is likely a reflection of including the relatively large-sized expHTT spots among inclusions during quantification (Fig 5.10a, right). Surprisingly, at 9d, *pdf>Q128* had smaller inclusions than *pdf>Q128,Hsp40* and *pdf>Q128,HSP70*. Inclusion size of *pdf>Q128* and *pdf>Q128,HSP70* increased with age.

Qualitatively, at 3d, *pdf>Q128* and *pdf>Q128,HSP70* had a relatively higher prevalence of smaller-sized Inc in the intra-hemisphere distribution. At the same time, the bigger-sized Inc prevailed in *pdf>Q128,Hsp40*, likely a reflection of Spot presence (Fig 5.10b, c). The relative proportions of hemispheres enriched in various-sized inclusions changed significantly between the three genotypes at 3d but not 9d (Fig 5.8d). The relative proportions of hemispheres enriched in various-sized inclusions did not change with age for the genotypes (Fig 5.8e). At 3d, the relative proportions of hemispheres enriched in <3µ-sized inclusions to those enriched in bigger-sized inclusions (3-6µ or >6µ) changed significantly between *pdf>Q128* and *pdf>Q128,Hsp40*, with the former mainly exhibiting <3µ-sized inclusions (Fig 5.8f, left and middle panels). Such a prevalence of hemispheres rich in smaller-sized inclusions in *pdf>Q128* is interesting.

In summary, co-expression of expHTT with Hsp40 in the LNv decreases the proportion of hemispheres with inclusion-enriched LNv across age, with a concomitant increase in the proportion of hemispheres enriched in a hitherto unreported Spot form of expHTT in LNv and a decrease in the expHTT inclusion numbers. All the above observations, taken together, will be henceforth referred to as a decrease in the 'inclusion load'. Thus, Hsp40 overexpression in *pdf>Q128* flies reduces the inclusion load of the LNv.

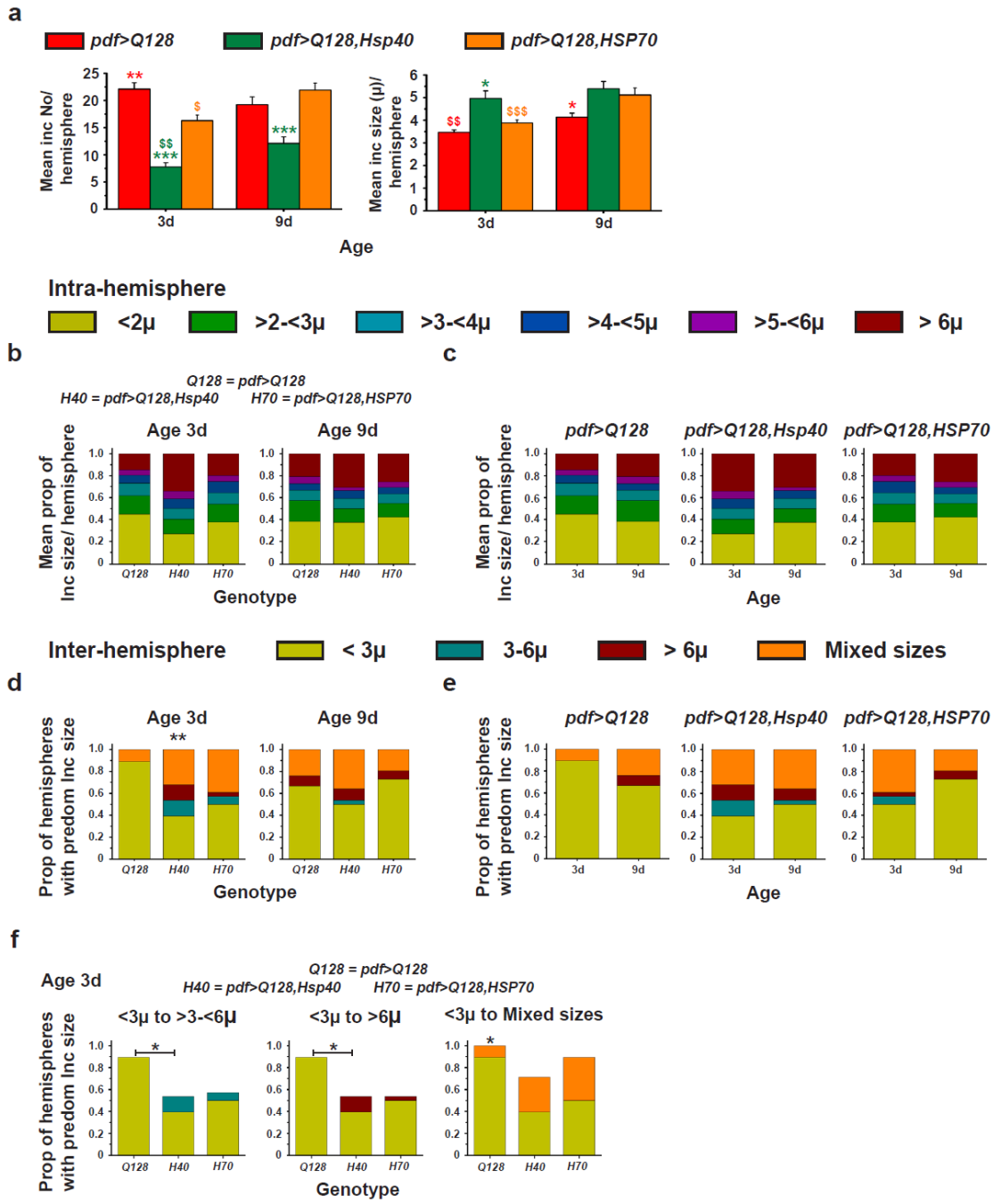

Figure 5.10

Fig 5. 10 Young pdf>Q128 flies overexpressing Hsp40 or HSP70 have reduced expHTT inclusions numbers.

(a) Comparison of mean inclusion number per hemisphere (left) and mean inclusion size per hemisphere (right) for three genotypes at 3d and 9d. Coloured * indicates statistically significant age-matched differences between genotypes: * (olive-green) from *pdf>Q128,Hsp40* and * (red) from *pdf>Q128*, coloured $ represent differences across age for the respective-coloured genotype. Statistical significance is at single-symbol $p<0.05$, dual-symbol $p<0.01$ and triple-symbol $p<0.001$. Error bars are s.e.m. (b) and (c) The mean proportion of expHTT inclusions of different size ranges in the vicinity of LNv in a hemisphere describing the within-hemisphere expHTT inclusion size distribution is plotted against genotypes for ages 3d and 9d (b) or against age for each genotype (c).

The proportion of different-sized expHTT inclusions for each hemisphere is plotted for three genotypes comparing across ages. (d) and (e) The proportion of hemispheres dominated by different expHTT inclusion size ranges in LNv describing the between-hemispheres distribution of expHTT inclusion sizes are plotted against genotypes for ages 3d and 9d (d) or against age for each genotype (e). The * indicates significant changes in relative distributions of expHTT sizes between genotypes at ** $p<0.01$. From the entire set in (d), three pair-wise relative hemisphere proportions enriched with specified inclusion sizes that were statistically significant are plotted against the three genotypes for age 3d (f). The * indicates significant relative changes in pair-wise proportions of hemispheres enriched with differently sized expHTT inclusions between genotypes at * $p<0.05$.

5.3.6 Hsp40 overexpression rescues early-age sLNv PER oscillations in the expHTT-expressing flies

PER, a central clock protein, is lost from the soma of LNv in *pdf>Q128* flies (Chapter 2) (Prakash et al., 2017), also seen here, with *pdf>Q128* having significantly fewer PER$^+$ sLNv soma at 3d and 9d and almost none at 16d (Figs 5.11a, left, bottom-right, b, top). I addressed whether the neuroprotective effect of Hsp40 overexpression on *pdf>Q128* flies extends to the loss of PER and its oscillations in the LNv. *pdf>Q128,Hsp40* showed the presence of PER$^+$ sLNv and lLNv soma at 3d and 9d, with control-like numbers (Fig 5.11a, left panel-sets, b), and their frequency distributions were left-skewed like that of *pdf>Q0,Hsp40* and differed from that of *pdf>Q128* (Fig 5.11c, first and second columns, top and middle rows). However, unlike the rescue of PDF in sLNv soma, PER rescue in the LNv soma was not sustained up to 16d, by which time, *pdf>Q128,Hsp40* had significantly fewer PER$^+$ sLNv and lLNv than those of controls and was comparable to *pdf>Q128* (Fig 5.11a, right, bottom panel-sets, b). The shape of the frequency distribution of PER$^+$ sLNv and lLNv soma numbers in *pdf>Q128,Hsp40* changed from a control-like left-skew at 9d to a *pdf>Q128*-like shape at 16d (Fig 5.11c, first and second columns, middle and bottom rows). *pdf>Q128,HSP70*, did not show rescue of PER$^+$ sLNv soma across age. Its mean numbers and frequency distribution shapes were comparable to those of *pdf>Q128* and significantly differed from those of *pdf>Q0,HSP70* and *pdf>Q128,Hsp40* (Fig 5.11a, right panel-sets, b, top, c, right column, top and middle rows). PER$^+$ lLNv soma numbers of *pdf>Q128,HSP70* were comparable to *pdf>Q128* at 3d and 9d, control-like at 3d and significantly reduced at 9d (Fig 5.11b, bottom). The shape of the PER$^+$ lLNv soma distribution of 9d-old

pdf>Q128,HSP70, like that *of pdf>Q128*, differed from the left-skewed distribution of *pdf>Q0,HSP70* (Fig 5.11c, bottom-right).

Because *pdf>Q128,Hsp40* showed control-like PER$^+$ sLNv soma numbers at 3d and 9d, PER oscillations in LNv were assessed at these ages. At 3d, *pdf>Q128* did not show PER oscillations in sLNv; *pdf>Q128,Hsp40* showed a significant oscillation in PER levels like *pdf>Q0,Hsp40* (Fig 5.11a, top-left panel-sets, d, top-left). The PER intensity in sLNv of *pdf>Q128* was significantly lower than for the other two genotypes at CT23. However, at 9d, despite having control-like sLNv numbers and PER in the sLNv, PER oscillation was absent in sLNv of *pdf>Q128,Hsp40*, with intensity at CT23 being significantly diminished compared to that of *pdfQ0Hsp40* (Fig 5.11a, bottom-left panel-sets, d, top-middle). At 3d, PER oscillation was seen in lLNv of *pdf>Q128*, *pdf>Q128,Hsp40* and *pdf>Q0,Hsp40* (Fig 5.11a, top-left panel-sets, d, bottom-left). At 9d, PER oscillations were absent from lLNv of both *pdf>Q128,Hsp40* and control *pdf>Q0,Hsp40* (Fig 5.11a, bottom-left panel-sets, d, bottom-middle), as is reported for wildtype flies (Shafer et al., 2002; Veleri et al., 2003). PER oscillations in LNv of *pdf>Q128,HSP70* were like *pdf>Q128*, with no PER oscillation in sLNv at 3d, and a significant oscillation in lLNv (Fig 5.11a, top-right panel-sets, d, right). HSP70 overexpression did not rescue PER in the sLNv, even in young *pdf>Q128* flies. Thus, in young expHTT-expressing flies, Hsp40 overexpression restores both PER$^+$ sLNv numbers and PER oscillations in the sLNv. This study is the first thus far to report rescue in circadian molecular oscillations accompanying the restoration of behavioural rhythms observed in these flies, underscoring the effectiveness of Hsp40 as a potent circadian modifier in HD.

Hsp40 overexpression in LNv of expHTT flies leads to the rescue of sLNv circadian clock output, molecular oscillations, and their associated behavioural rhythms in young flies. The rescue in behaviour and the clock output PDF is long-lasting. There is also a considerable reduction in the expHTT inclusion load. This sustained rescue at multiple levels posits Hsp40 as a potential therapeutic candidate in improving circadian health under neurodegenerative conditions.

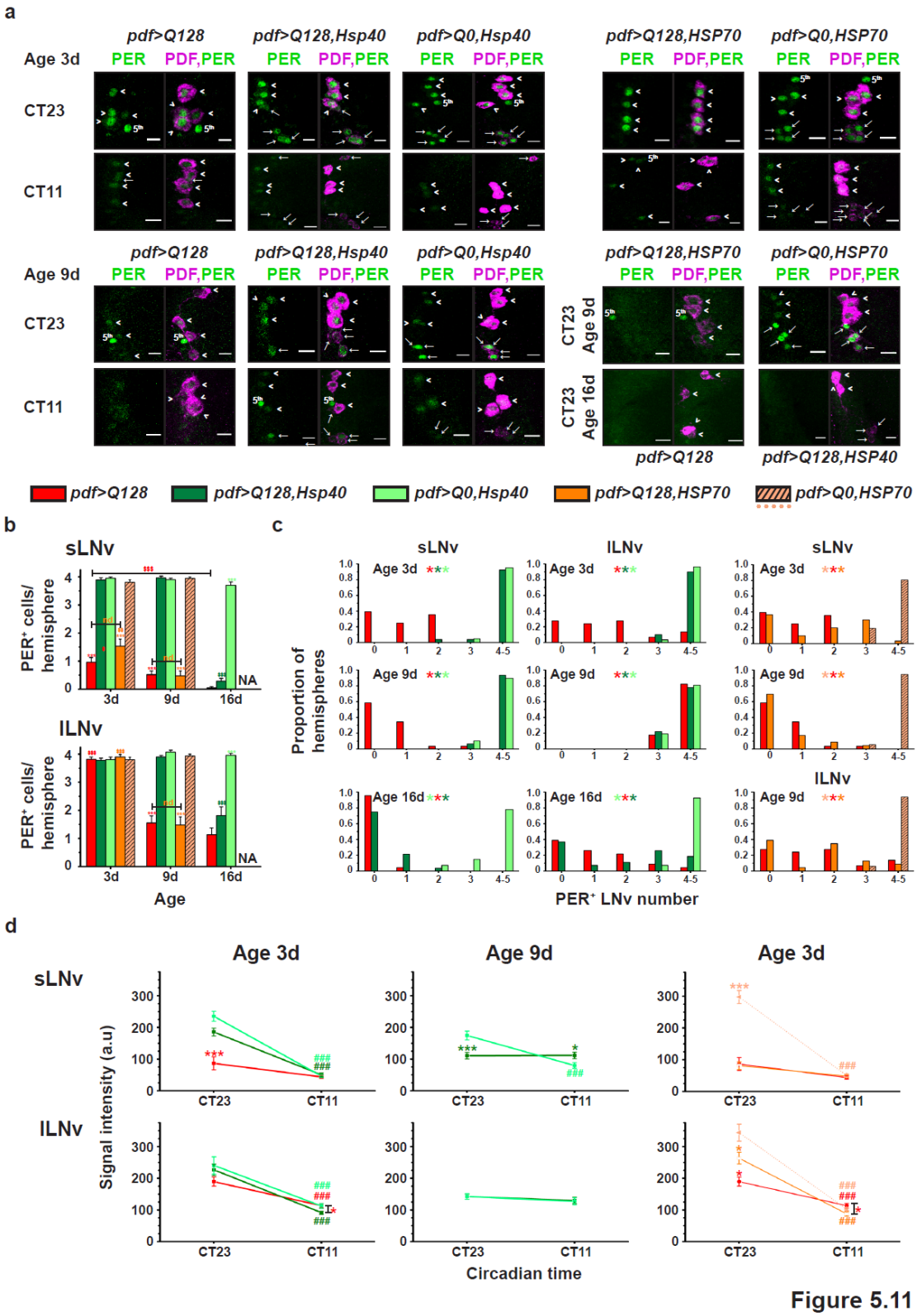

Figure 5.11

Fig 5. 11 Young pdf>Q128 flies co-expressing Hsp40 show PER oscillations in sLNv.

(a) Representative images of the adult fly brains stained for PER (green) and PDF (magenta) in LNv at CT23 and CT11. sLNv soma (→ arrows), lLNv soma (> arrowheads) and PDF^{-} PER^{+} 5th sLNv are indicated. Top panel-sets: 3d-old flies of five genotypes. Bottom panel-sets: first three panel-sets are of 9d-old flies of *pdf>Q128*, *pdf>Q128,Hsp40* and *pdf>Q0,Hsp40* at CT23 and CT11; fourth- and fifth panel-sets: top of 9d-old *pdf>Q128,HSP70* and *pdf>Q0,HSP70* at CT23 and bottom of 16d-old

pdf>Q128 and *pdf>Q128,Hsp40* at CT23. Scale bars are 10 µm. (b) At three ages, the mean number of PER^+ sLNv soma (top) and lLNv soma (bottom) at CT23. Symbols indicate significant differences, * for age-matched, inter-genotype differences and $ for differences between ages for each genotype: * (red) of *pdf>Q128* from all other genotypes except *pdf>Q128,HSP70* and * (orange) of *pdf>Q128,HSP70* from other genotypes except *pdf>Q128*. NA, not applicable; nd, not different. (c) Frequency distribution of the proportion of hemispheres having 0 to 5 PER^+ LNv soma: of sLNv soma (left) and lLNv soma (middle) in *pdf>Q128,Hsp40*, *pdf>Q128* and *pdf>Q0,Hsp40* at 3d, 9d and 16d, of sLNv soma at 3d (right-top) and 9d (right-middle) and lLNv soma at 9d (right-bottom) in *pdf>Q128,HSP70*, *pdf>Q128* and *pdf>Q0,HSP70*. Coloured multiple * indicates significantly different distribution shapes between genotypes, with the first colour of the reference genotype and the subsequent colours of genotypes differing from the reference at $p<0.01$. (d) Quantification of PER intensity at CT23 and CT11 in sLNv (top) and lLNv (bottom) comparing *pdf>Q128* with *pdf>Q128,Hsp40* and *pdf>Q0,Hsp40* at 3d (left) and 9d (middle) and comparing *pdf>Q128* with *pdf>Q128,HSP70* and *pdf>Q0,HSP70* at 3d (right). Differences between time points CT23 and CT11 are represented by # (red) *pdf>Q128*, # (olive-green) *pdf>Q128,Hsp40*, # (pale-green) *pdf>Q0,Hsp40*, # (orange) *pdf>Q128,HSP70* and # (pale-orange) *pdf>Q0,HSP70*. Coloured * represents age-matched differences of respective-coloured genotypes from the indicated one or all others. Statistical significance at single-symbol $p<0.05$, double-symbol $p<0.01$, triple-symbol $p<0.001$. Error bars are SEM.

5.4 DISCUSSION

5.4.1 Hsps as modifiers of HD-induced circadian dysfunction

The role of Hsps, known modifiers of neurodegeneration, in HD-associated circadian disturbances is relatively unexplored. In this study, we show that the overexpression of the co-chaperone Hsp40 in circadian pacemaker neurons of *Drosophila* delays expHTT-induced circadian behavioural arrhythmicity over extended durations and suppresses circadian neurotoxicity. Overexpression of the central chaperone HSP70 mitigates expHTT-induced circadian behavioural rhythm disruptions in young flies but does not rescue cellular phenotypes. The rescue upon Hsp40 overexpression was more robust, pronounced and sustained. In young flies, Hsp40 overexpression seemed to restore the functionality of LNv, particularly the central pacemaker sLNv. Evidence for sLNv functionality is the restoration of circadian proteins, the core-clock protein PER, its oscillations and the output neuropeptide PDF in the sLNv soma, and lowered expHTT inclusion load, leading to an overall improvement in the LNv-circuit associated behavioural rhythms. These flies continued to be behaviourally rhythmic up to 16d but with lowered robustness, with the presence of PER in LNv and control-like PDF^+ sLNv soma numbers and diminished inclusion load, but without PER oscillations. The persistence of activity rhythms without PER oscillations in sLNv suggests two conclusions. First, Hsp40-mediated rescue at the circadian output level seems sufficient for behavioural rhythm rescue. Second, the PER oscillations in the sLNv might be dispensable for rhythm sustenance. Two recent studies that support this reasoning show that PER in LNv does not seem necessary for the persistence of free-running activity rhythms but is vital for rhythm strength (Delventhal et al., 2019; Schlichting et al., 2019b). In relatively older flies, despite the presence of nearly 4 PDF^+ sLNv soma (16d) and reduction in the inclusion load (aggregate numbers of 16d-old *pdf>Q128,Hsp40* flies were comparable to 9d; quantification not shown), the flies were arrhythmic during AW3 (16d-23d). Thus, the Hsp40 neuroprotection does not seem sufficient as the flies age, contributing to a deterioration of LNv health. The inadequacy of Hsp40 expression to extend protection to LNv over prolonged durations suggests two conclusions. First, restoring PDF^+ sLNv does not

guarantee sustained free-running rhythms without PER. Our previous results show that about 20% of 7d-old arrhythmic *pdf>Q128* flies had at least 1-2 PDF$^+$ sLNv. Also, the PDF levels in the sLNv dorsal projections were oscillating and functional in synchronising downstream circadian neurons (Prakash et al., 2017). The previous results and present observations of behavioural arrhythmicity in older flies despite PDF rescue in sLNv indicate that sLNv PDF, in the absence of PER, is insufficient for rhythmic activity. Secondly, over time, neuroprotective benefits offered by Hsp40 can be overwhelmed upon HD progression, probably by the age-related burden on LNv proteostasis, rendering the cells vulnerable to expHTT toxicity. Therefore, sustained rhythm rescue might require supplementing Hsps with further enhancement of proteostasis via proteasomal or autophagic upregulation.

HSP70 overexpression, in contrast, showed a rescue in only early-age rhythms and activity consolidation, albeit of lowered robustness, a decrease in early-age inclusion number, without the rescue of PDF$^+$ sLNv numbers or PER oscillations in sLNv or alterations to inclusions being the prevalent form of expHTT in LNv. The rhythmic flies of *pdf>Q128,HSP70* have poor rhythm robustness and can be attributed to the absence of PER rescue in the LNv. However, the persistence of behavioural rhythms on HSP70 overexpression in the absence of PDF rescue in the sLNv soma is intriguing. It suggests that the presence of PDF in sLNv is unnecessary for behavioural rhythm restoration. Other studies in *pdf>Q128* have reported rhythm rescue with only marginal PDF restoration in sLNv soma upon ATX2 or HOP down-regulation (Xu et al., 2019a; Xu et al., 2019b). Together with ours, these reports suggest that other mechanisms might drive circadian behavioural rhythms without canonical circadian cellular proteins. Possible intersections of Hsp onto improving the LNv function and output in orchestrating rhythmicity are circadian oscillations in arborisations of the sLNv termini and secondary molecular loop components, non-PER driven clocks, LNv membrane properties, neuronal firing, synaptic strength and network-level communication (Edgar et al., 2012; Beckwith and Ceriani, 2015b; Yao et al., 2016; Rey et al., 2018; Bulthuis et al., 2019). Enhancing central proteostasis players, the Hsps suppresses HD-induced circadian dysfunction, suggesting that **mechanisms that maintain cellular proteostasis are compromised in the LNv, and proteostasis perturbations underly circadian disruptions**.

A limitation of the methodology of expressing more than one transgene used in this study is the effect of the competition of multiple UAS promoters for the GAL4 factor, leading to attenuated expression of expHTT. Such a situation is revealed in a study on fly lifespan where, on expressing two UAS promoters, the presence of one attenuates the activation of the reduced-lifespan gene, leading to improved lifespan (Nakayama et al., 2014). This factor could have been addressed by quantifying the levels of non-expanded HTT-Q0 expressed in the controls upon expression of two transgenes (HTT and Hsp40 or HTT and HSP70) or three transgenes (HTT, Hsp40 and HSP70). Such an experiment has been done for the expression of two transgenes (HTT and Atg8a) in the recent paper from the lab (Sharma et al., 2023), where the authors do not find any dilution effects on HTT-Q0 levels upon expression of both the transgenes in the LNv compared to HTT-Q0 alone. They find an increase in HTT-Q0 expression upon dual transgene expression. In addition, Sharma et al. show that the co-expression of HTT-Q128 with GFP (which is expected to be benign but could potentially result in dilution effects) in the LNv does not improve behavioural arrhythmicity. Further, in the mini screen carried out in this study, even though there are several scenarios where an additional transgene is expressed along with HTT-Q128 in the LNv, only a particular set of genes involved in proteostasis gave a behavioural rescue, arguing against a general dilution of expHTT expression in the presence of another *UAS* construct. Thus, evidence from both immunocytochemical and behavioural experiments show that on the expression of an additional *UAS-transgene* with *UAS-HTT*, competition for the GAL4 factor, if any, does not result in a reduction of HTT protein or non-specific alterations of the activity rhythms, suggesting that the rescue on co-expression of Hsp40 with HTT-Q128 is unlikely due to dilution of expHTT expression. However, HTT-Q0 levels in flies co-expressing HTT-Q0 with Hsp40 or HSP70 can be performed for confirmation. A similar quantification will help address competition effects on expHTT expression levels from expressing three transgenes. For example, findings from such an experiment can likely explain the overall poor synergy in % rhythmicity and the fall of rhythmicity in AW2 on the co-expression of both the HSPs with expHTT.

Circadian disturbances in HD stem from perturbations to the circadian organisation's input, molecular oscillator and output components (Fifel and Videnovic, 2020; Colwell, 2021). In the R6/2 HD mice, free-running activity rhythms are disrupted, and the SCN molecular oscillations are impaired *in vivo* while persisting in its organotypic slices, suggesting that the inputs to and outputs from the central clock are affected rather than the molecular clock itself (Morton et al., 2005; Pallier et al., 2007). Dysfunctional intrinsically photosensitive retinal ganglion cells, reduction of VIP immunostaining in the SCN, and disrupted rhythms in SCN electrophysiology, cortisol, melatonin, body temperature, heart rate and metabolic outputs (Smarr et al., 2019; Fifel and Videnovic, 2020; Colwell, 2021) provide evidence for circadian disturbances in HD mice at levels of clock input and output, thus also affecting molecular clockwork *in vivo*, resulting in overt behavioural and peripheral rhythm disturbances. Although the HD flies used in this study had only a subset of their clock neurons targeted, they exhibited a definite circadian disturbance in the overt behavioural rhythms, molecular oscillations, and circadian output neuropeptide PDF, recapitulating central clock and output impairments seen *in vivo* in HD mice. Such parallels between model systems suggest the possibility of finding mammalian counterparts to the Hsp40-mediated rescue of circadian disturbances. Whether the benefits of Hsp40 treatment extend to other circadian rhythms remains to be elucidated.

5.4.2 Impact of Hsp overexpression on the visible inclusions of expHTT

Hsps dilute the presence of aggregate-prone proteins by interfering with the aggregation pathway by delaying nucleation, fibril elongation or redirecting the pathway towards less-toxic versions, sequestrating intermediates into cellular compartments or organelles and targeting for degradation (Kampinga and Bergink, 2016; Mannini and Chiti, 2017; Hipp et al., 2019b). The effect of Hsps on aggregation varies, depending on a host of factors like the definition of aggregates, their nature and conformation, the cellular context, the stage of aggregation, age and disease stage, quantification method and model system. Indeed, with up-regulation of Hsps (Hsp40 and Hsp70) in HD models, there is evidence for differential effects: many show a decline in aggregation (Jana,

2000; Zhou et al., 2001; Hay, 2004; Guzhova et al., 2011; Labbadia et al., 2012; Popiel et al., 2012; Maheshwari et al., 2014; Scior et al., 2018), some show no effect (Kazemi-Esfarjani and Benzer, 2000; Wyttenbach et al., 2000; Karpuj et al., 2002; Borrell-Pages et al., 2006; McLear et al., 2008), and one study shows an increase in aggregation (Wyttenbach et al., 2000).

The present study defines the visible puncta-like clumped appearance of HTT-Q128, as detected under a fluorescence light microscope using immunocytochemistry, as an inclusion. This definition excludes detecting many species below the resolution limit and does not distinguish based on solubility and other biochemical features. Hence, the inferences are limited to particle size range and gross features detected via an epifluorescence scope. However, this does not take away the validity of the effect of Hsp40 overexpression on expHTT inclusions and its impact on LNv function at the cellular and behavioural stages. In *pdf>Q128* flies, Hsp40 overexpression in the LNv leads to a reduction in the number of visible expHTT inclusions, a decline in the dominance of inclusion form of expHTT, and the appearance and dominance of expHTT spots. Accompanying them are improvements in LNv pacemaker function, as evidenced by the re-establishment of circadian molecular and behavioural rhythms. Thus, a decreased inclusion load and the dominance of expHTT spots could lead to enhanced functionality of the LNv. The reduction of expHTT inclusions upon Hsp40 overexpression also suggests improvements in the cellular proteostasis capacity.

A pictorial representation of the locomotor behaviour and the LNv cellular phenotypes comparing *pdf>Q128* with *pdf>Q128,Hsp40* is shown (Fig 5.12). A clear pattern for expHTT forms in LNv with age emerges. For the toxic *pdf>Q128* and relatively less-toxic *pdf>Q128,HSP70*, Diff+Inc expHTT in lLNv at an early age gives way to exclusively Inc at later ages. In the neuroprotective *pdf>Q128,Hsp40*, across age, Spots are present in the sLNv, dominating over Inc at 3d, whereas Inc dominates at later ages. In the lLNv of *pdf>Q128,Hsp40*, Diff expHTT dominates at 3d, giving way to a combination of diffuse, spot and inclusion at 9d and then to non-diffuse expHTT (Spot and Spot+Inc) at 16d. In *pdf>Q128,Hsp40*, the continued presence and domination of expHTT Spot in LNv is associated with intact PDF^{+} sLNv and behavioural rhythmicity of most of the *pdf>Q128,Hsp40* flies up to 16d. Together, these results indicate an association between specific expHTT forms predominating in the LNv and LNv health, namely, diffuse and spot forms

with healthy LNv and rhythmic activity, while inclusions with poor LNv function and arrhythmicity.

HSP70 overexpression in *pdf>Q128* flies rescues early-age rhythms and reduces expHTT inclusion numbers, but with the dominance of inclusion as the main expHTT form in the LNv, suggesting that HSP70-mediated improvements to LNv health are via inclusion-independent mechanisms. HSP70 serves aggregation-independent neuroprotective roles like inhibiting apoptosis (Beere, 2004; Kennedy et al., 2014), combating inflammation (Borges et al., 2012; Dukay et al., 2019), reducing ROS and oxidative stress (Kalmar and Greensmith, 2009; Wyttenbach and Arrigo, 2009) and supporting synaptic function (Deane and Brown, 2016; Gorenberg and Chandra, 2017). Studies supporting such aggregation-independent neuroprotection by Hsp40 and Hsp70 in HD are reported (Zhou et al., 2001; Wyttenbach, 2002; Borrell-Pages et al., 2006; Wacker et al., 2009). HSP70's versatility in enhancing neuronal health and function can be attributed to circadian rhythm improvements in the absence of an effect on inclusion load and PDF restoration in the sLNv.

The prevalence of more minor-sized inclusions (<3µ) in young *pdf>Q128* flies is interesting. The arrhythmicity of most of these flies and the absence of PER and PDF in their sLNv soma suggests that these relatively smaller-sized inclusions might be cytotoxic.

5.4.2.1 The spot form of expHTT

Upon overexpression of Hsp40 in *pdf>Q128* flies, a new form of expHTT with a spot-like appearance close to the nucleus and seemingly overlapping with the nuclear PER was observed. This study is the first to report a "Spot" form of expHTT. The appearance of the Spot and a reduction in the inclusion load accompanying the suppression of circadian dysfunction suggests that a reduction of inclusions is associated with a suppression of neurotoxicity or expHTT. Spots are probably benign and may even be protective or both of the above. Upon Hsp40 overexpression, the appearance of Spot expHTT coincides with a reduction of inclusions and an improved LNv function, suggesting that its formation could be another mechanism to reduce the cellular proteostatic burden. We discuss the possible significance of the Spot expHTT. In eukaryotes, aggregate-prone proteins are often sequestered into specialised cellular compartments

thought to be neuroprotective and are typically membrane-less, sometimes referred to as sequestrosomes or into membrane-bound membrane organelles (Sontag et al., 2014; Tan and Wong, 2017; Johnston and Samant, 2021). A few examples of such spatially-sequestered quality control sites are the cytoplasmic Q-bodies or stress foci, cytoplasmic p62 bodies or aggresome-like induced structures (ALIS), peri-nuclear juxta-nuclear quality control compartment (JUNQ), intranuclear quality control compartment (INQ), peri-nuclear aggresomes and peri-vacuolar insoluble protein deposit (IPOD) (Tan and Wong, 2017; Johnston and Samant, 2021). Hsps participate in such compartmentalisations (Nollen et al., 2001; Specht et al., 2011; Escusa-Toret et al., 2013; Miller et al., 2015). The aggresomes are mostly juxta-nuclear, membrane-free inclusions carrying ubiquitinated misfolded proteins formed at the microtubule organising centre (MTOC) (Johnston et al., 1998; Kopito, 2000; Johnston and Samant, 2021). There is evidence for the colocalization of Hsp40 and Hsp70 colocalise with aggresomes (Garcia-Mata et al., 1999; Junn et al., 2002; Gamerdinger et al., 2011; Zhang and Qian, 2011). A recent study shows that overexpression of Sis1, a yeast homolog of Hsp40 or mammalian DnaJB6, but not DnaJB1 in HTTQ97 expressing yeast cells modifies the morphology of aggregates into a single large diffuse cloud-like cytoplasmic condensate per cell, a less dense aggregated state with lowered HttQ97 concentration that behaved like an immobile mesh (Klaips et al., 2020). Sis1 interacted with soluble polyQ oligomers, promoting their coalescence into the condensate in an Hsp70-dependent manner.

Another observation is that the average size of an expHTT Spot in the small LNv is significantly larger than in the large LNv. `This sizeable expHTT Spot in the sLNv could reflect a more significant expHTT burden and toxicity in the vulnerable sLNv or a longer HTT and Hsp40 expression duration owing to their earlier appearance than lLNv during development (Helfrich-Förster, 1997). The presence of three to four PDF^+ sLNv in nearly every hemisphere of *pdf>Q128,Hsp40* across age parallels with the presence of at least one sLNv per hemisphere having Spot expHTT (proportion of hemisphere with at least one $Spot^+$ sLNv: 3d, 100%; 9d, ~ 97%; 16d, ~79%). Such co-occurrences indicate that the appearance of expHTT spots might be protective. Thus, Hsp40 might modify the nature of expHTT inclusions, and the spots could

represent a less reactive and relatively benign form of expHTT, contributing to an enhancement in LNv health and function.

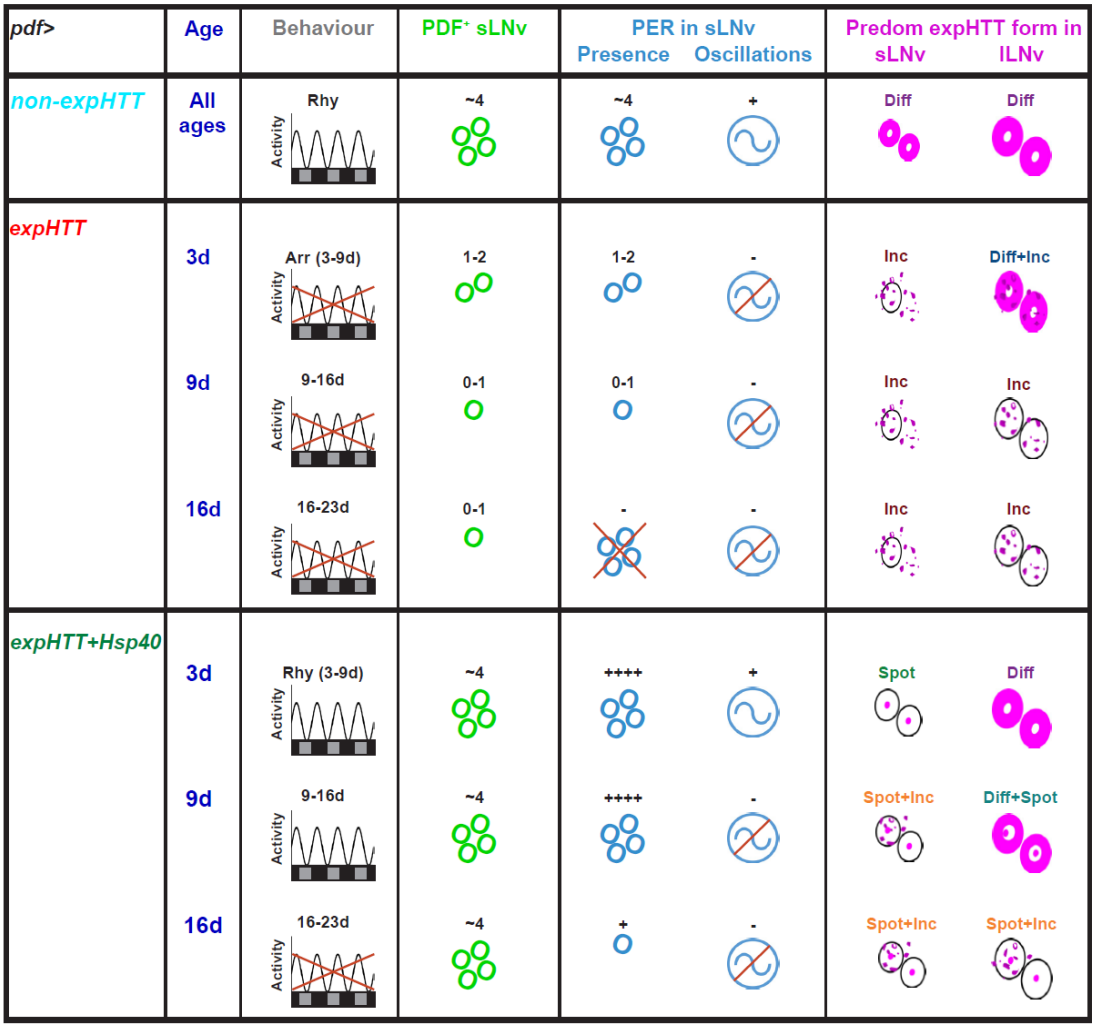

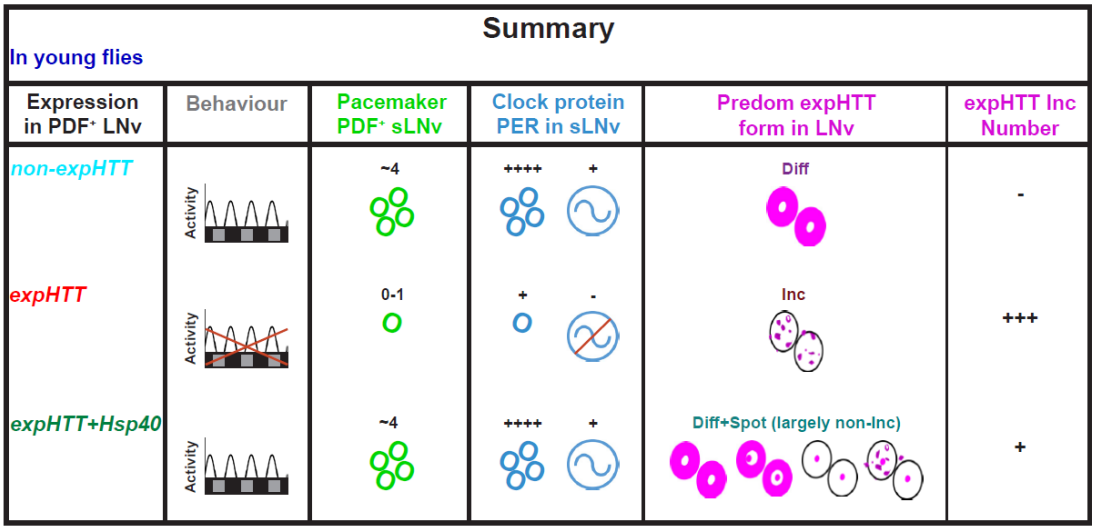

Figure 5.12

Fig 5. 12 Hsp40 is neuroprotective and delays circadian dysfunction in HD: A graphical summary. Top table: A pictorial representation of the effect of expressing expHTT alone and with Hsp40 in the LNv of *Drosophila* on circadian neurodegenerative phenotypes across age. The control phenotype on expressing non-expanded HTT (Q0) in LNv is shown at the top.

The effects on the circadian behavioural activity/rest rhythms, PDF^+ and PER^+ sLNv soma numbers, PER oscillations in sLNv, and the predominant form of expHTT in sLNv and lLNv are shown across age. The behavioural rhythms are represented for three 7d age windows, whereas the cellular phenotypes are for specific ages. Arr stands for arrhythmic, and Rhy for rhythmic. Bottom table: A summary of the key findings. Co-expressing Hsp40 with expHTT in the LNv reverses the expHTT-induced circadian phenotypes of behavioural arrhythmicity, PDF loss from sLNv soma and loss of PER oscillations and PER in sLNv of young flies. Also, the expHTT inclusions, a characteristic neurodegenerative phenotype, and the predominant expHTT form observed in the LNv of *pdf>Q128* flies are replaced by mainly non-inclusion forms: diffuse, spots and a combination. The prevalence of non-Inc expHTT forms is also reflected as a decrease in expHTT inclusions. In summary, Hsp40 is an effective suppressor of HD-induced circadian disruptions.

5.4.4 Effects of co-expressing Hsp40 and HSP70

Many studies in polyQ models have described a synergistic effect upon co-expression of Hsp40 and Hsp70 on the toxicity: expression of both offered better protection than either alone (Chan et al., 2000; Jana, 2000; Kobayashi et al., 2000; Muchowski et al., 2000; Sittler et al., 2001; Bailey et al., 2002; Bonini, 2002; Rujano et al., 2007). The current study shows a synergistic improvement in young HD flies' circadian rhythms in daily activity consolidation but not in their rhythmic percentages or robustness. The synergistic effect seems subtle, evident with a daily readout like '*r*', but not with a 7d-overt-readout of rhythmicity. Over time, there was a decline in rhythm robustness of *pdf>Q128* flies expressing both Hsps than those expressing Hsp40 alone, suggesting that co-expression of multiple Hsps could become detrimental. One study shows an absence of synergy or protective effect upon co-expression in a SCA7 mice model (Helmlinger et al., 2004). In another study, such co-expression eliminated the survival benefit of HSP70-only expression, enhancing cell death (Ormsby et al., 2013). Additionally, HSC70 antagonised the Hsp40 (DNAJA1) activity, and their co-expression prevented clearance of Tau in an Alzheimer's disease cellular model (Abisambra et al., 2012).

Some drawbacks of Hsp co-expression and Hsp overexpression, like their pro-carcinogenic effects and generation of seeding-competent nuclei, call for caution when targeting central Hsps for therapy (Jaattela, 1995; Nylandsted et al., 2002; Tittelmeier et al., 2020b). Therefore, in some instances, researchers have proposed that targeting specific chaperones is more beneficial and could minimise network adaptations, improve effectiveness, and reduce side effects, rather than targeting the entire network or central chaperones like HSP70 and HSP90 (Mendillo et al., 2012;

Kakkar et al., 2016). Further research on testing combinations of specific- and network-wide strategies in a conditional, time-specific manner, supplemented by other proteostasis modifying treatments, would help realise a safer and more practical therapeutic strategy.

5.4.5 Hsp40 *vs* HSP70: Hsp40, a superior suppressor of HD neurotoxicity

In our study, Hsp40 emerges as a superior suppressor of most expHTT-induced phenotypes examined and in terms of duration of rescue. However, the differences in the efficiency of *Drosophila* Hsp40 and human HSP70 in mitigating expHTT toxicity in flies could arise due to the different species origin of the two transgenes with different temperatures of maximal activation and codon bias, leading to different levels of expression and activity. Local genomic position effects owing to different chromosomal loci of insertion of the two *UAS* constructs are an additional factor influencing expression and rescue efficiency. An additional experiment using UAS constructs of Hsp40 and Hsp70, both sourced from *Drosophila* and with similar chromosomal insertions, would have been helpful to compare and clarify the effects of the two Hsps on the expHTT-induced circadian neurodegenerative phenotypes.

Nevertheless, there is substantial support for Hsp40 being a more effective HD neurotoxic modifier. Among the Hsp40, HSP70 and HSP110 chaperone families, the DNAJB class of Hsp40 emerged as the most potent protector against polyQ toxicity (Hageman et al., 2010), and in R6/2 mice, Hsp70 suppressed HD only moderately (Hansson et al., 2003; Hay, 2004; Popiel et al., 2012), while Hsp40 members had better success (Labbadia et al., 2012; Kakkar et al., 2016). Hsp40 also prevented the secretion of expanded polyQ proteins from cultured cells (Popiel et al., 2012), thus likely preventing cell-to-cell transmission, an emerging concern in NDs. Findings from the present study and other studies (Chai et al., 1999; Zhou et al., 2001; Rujano et al., 2007; Ormsby et al., 2013) show that Hsp40 reduces aggregation more often than HSP70. Hsp40 is rate-limiting in the suppression and reversal of expHTT aggregation by disaggregases (Rujano et al., 2007; Scior et al., 2018), and some members can act without requiring HSP70 (Hageman et al., 2010; Kuo et al., 2013b; Månsson et al., 2013; Kakkar et al., 2016). A study of genetic

modifiers of different NDs, including HD in different model organisms, revealed *Drosophila* DnaJ1 (and its mammalian ortholog DNAJB4) as a modifier across many NDs (Na et al., 2013). The significant role of the DNAJB protein family in synaptic health and neuronal proteostasis and their diversity in function, distribution and substrate specificity underscore their usefulness in directed therapy while minimising the side effects (Chuang et al., 2002; Westhoff et al., 2005; Gibbs et al., 2009; Kampinga and Craig, 2010; Gao et al., 2015; Nillegoda et al., 2018; Kampinga et al., 2019; Tittelmeier et al., 2020a).

5.4.6 A need for screening circadian-specific neurotoxic modulators

In an *in vivo* system, I have shown the neuroprotective role of chaperone Hsp40 in rescuing HD-induced circadian deficits and neurotoxicity at multiple levels and across the temporal scale. Such a multi-level associated functional rescue offers an edge over conventional non-associated cellular and behavioural rescues to make better cause-effect inferences due to reduced off-target effects, test the modifying treatment's robustness and versatility, and serve as proof-of-principle evaluations. Also, although most candidates screened are known modulators of HD cellular neurotoxicity, only two groups of proteins emerged as potent suppressors of circadian disruptions, indicating that only a subset of the cellular pathophysiological mechanisms contributing to HD is involved in circadian disruptions. These findings also uncover a gap in establishing circadian-specific neuroprotective agents and exemplify a need for screens specifically targeting circadian dysfunction.

5.4.7 Hsps, circadian health and neurodegenerative diseases

There is ample evidence for clock control of the regulation of proteostasis components, including chaperones (Desvergne and Friguet, 2017; Ryzhikov et al., 2019; Wang et al., 2020), with both Hsp40 and Hsp70 isoforms, showing rhythmic gene expression across taxa (Li et al., 2017). In the *Drosophila* LNv, mRNA transcripts of the Hsp40 isoforms, DnaJ-1 and DnaJ-H, are present,

and in the lLNv, *DnaJ-H* gene expression is cyclic (Kula-Eversole et al., 2010; Ma et al., 2021b), while *Hsp70* transcripts cycle in the LNv (Abruzzi et al., 2017; Ma et al., 2021b). Further, *Hsp40* gene transcripts have been classified under the experimentally identified circadian genes (Li et al., 2017). The converse, i.e. proteostasis affecting molecular clock via post-translational modifications and autophagy, is also prevalent (Mehra et al., 2009; Stojkovic et al., 2014; Toledo et al., 2018; Juste et al., 2021). However, very few studies have assessed the role of Hsps in circadian maintenance and its deterioration in NDs, especially in animals. In *Drosophila*, the Hsp70/Hsp90-organizing protein (HOP) improved rhythmicity in an HD model (Xu et al., 2019a), Hsp70 expression overcame arrhythmicity due to Gal4-overexpression in the LNv (Rezaval et al., 2007), Hsp90 disruptions led to the loss of activity rhythms without affecting molecular oscillations (Hung et al., 2009) and the Hsps were indirectly implicated in circadian behaviour (Benbahouche Nel et al., 2014; Means et al., 2015). In mouse fibroblasts, Hsp90 is required for circadian rhythmicity, while Hsf1 and endoplasmic reticulum Hsp70 strengthen rhythms post-stress (Tamaru et al., 2011; Schneider et al., 2014; Pickard et al., 2019). The present findings of a relatively novel role for the Hsps in protecting against ND-induced circadian dysfunction and the above studies encourage further research on Hsps in circadian function. Given that circadian and sleep disturbances occur early and are pre-manifest in HD (Soneson et al., 2010; Morton et al., 2014; Lazar et al., 2015; Bellosta Diago et al., 2017), treatments targeting Hsps could impact HD's early stages in postponing symptoms and provide a meaningful therapeutic impact. An ageing population worldwide has increased the prevalence of NDs (Gitler et al., 2017; Lassonde, 2017; Bejot and Yaffe, 2019). Given the pivotal roles of proteostasis and circadian health in NDs, studying the involvement of molecular chaperones in circadian maintenance will significantly improve our understanding of ND progression and treatment.

CHAPTER 6

The Effects of *Drosophila* HTT and the Protein Context of the Polyglutamine Repeats on the Circadian Activity Rhythms

6.1 INTRODUCTION

It is well documented that the cellular context in which the expanded polyglutamine tracts are expressed leads to the variation in the extent of its toxicity, amply demonstrated by the differential vulnerability of neuronal groups and brain regions and the heterogeneity in the timing and severity of dysfunction exhibited by various tissues affected (Ghosh and Feany, 2004; Duennwald et al., 2006a; Shelbourne et al., 2007b; Caron et al., 2014; Sala et al., 2017; Fu et al., 2018; Creus-Muncunill and Ehrlich, 2019). Furthermore, we know that differences in the protein context of the polyQ tracts can drastically alter their pathogenicity (Morley et al., 2002; La Spada and Taylor, 2003; Duennwald et al., 2006b; Robertson and Bottomley, 2010; Adegbuyiro et al., 2017; Kuiper et al., 2017; Silva et al., 2018). Throughout my studies, I have examined various aspects of the protein context of expanded polyQ tracts in the human Htt protein (6.3.2, 6.3.3, 6.3.4). I also examined the importance of the native *Drosophila melanogaster dhtt* gene in normal circadian activity rhythms (6.3.1). I also examined the effect of another distinct polyQ protein, Ataxin 3, where expanded glutamine tracts are associated with a neurodegenerative condition, Spinocerebellar ataxia 3 or SCA3, in the same neuronal circuit (6.3.5). I collate my findings on these somewhat disparate questions in this last chapter of my thesis.

6.2 MATERIALS AND METHODS

6.2.1 Fly lines

The UAS fly lines w*[1118]; +; P{w[+mC]=UAS-HTT.128Q.FL}f27b* (BL 33808) and *w[1118]; +; P{w[+mC]=UAS-HTT.16Q.FL}F24/CyO* (BL33810) were back-crossed for 5 generations onto a w^{1118} (BL 5905) background. For most experiments, virgin females of the driver lines (*w;pdfGAL4;+* or *w;timGal4;UAS-CD8::GFP*) were crossed with males of UAS lines. The UAS lines of eGFP-tagged N-terminal Htt exon 1 with and without a C-terminal NLS *w;+;UAS-18 Q EGFP-NLS T4-2/TM6b*, *w;+;UAS-18 Q EGFP T3-2 U-13/TM6b*, *w;+;UAS-152 Q EGFP-NLS T6-2U-12/TM6b* and *w;+;UAS-152 Q EGFP T1 U-09/TM6b*, are from Dr Nobuyuki Nukina, RIKEN Brain Science Institute, Japan (Doumanis et al., 2009). The eGFP-tagged Httex1 UAS lines *w;+;UAS-Httex1 QP25 EGFP, w;+;UAS-Httex1 QP46 EGFP*, *w;+;UAS-Httex1 QP72 EGFP* and *w;+;UAS-Httex1 QP103 EGFP* are from Dr Nobert Perrimon, Harvard Medical School, USA (Zhang et al., 2010b). The other UAS lines used are *w[*];+;P{w[+mC]=UAS-hATXN3.tr-Q27}N18.3d* (BL 8149), *w[*];P{w[+mC]=UAS-hATXN3.tr-Q78}c211.2;+* (Bl 8150), *w[1118];+;P{w[+mC]=UAS-Zzzz\CAG.20Q}3* (BL 30549), *w[1118];P{w[+mC]=UAS-Zzzz\CAG.63Q}2;+* (BL 30544), *w;dhttRNAi:+* (VDRC GD 14339) and *w;dhttRNAi;+* (VDRC KK 107149). The *dhtt* mutant line is *w[1118];+;Mi{ET1}htt[MB03997]* (BL 24665).

6.2.2 Locomotor assays

Most of the assay set-up and analysis details are described in Chapter 2 (Section 2.2.1). 3-4-day-old virgin males were assayed in DD at 25 °C. The experiments on dhtt had 16 flies at the beginning of the assay, while other experiments had >25 flies. For the MJD run, three independent experiments were done. The average percentage rhythmicity across the three experiments and the robustness and period are plotted for a representative run.

6.2.3 Immunocytochemistry and image analysis

The dissections, immunocytochemistry and image analysis procedures performed are described in Chapter 2 (Section 2.2.3). 12d-old flies of *pdf>MJDQ27* and *pdf>MJDQ78* were dissected

and stained with ant-PDF rabbit (1:30,000), and anti-HA mouse and secondary antibodies Alexa fluors anti-rabbit 488 and anti-mouse 546 were used.

6.2.4 Statistical analyses

Those genotypes where <10 flies were rhythmic or alive were eliminated from statistical analysis of robustness and period. For most comparisons between genotypes for an AW of rhythm robustness and period, the Kruskal-Wallis test of ranks followed by multiple comparisons of mean ranks were used. For comparing rhythmicity proportion between genotypes for an AW, m x n Fisher's Exact test, followed by multiple 2x2 Fisher's Exact tests with BH procedure on all relevant comparisons, were used. For a comparison of mean rhythmicity between genotypes for an AW in the MJD experiment, a one-way ANOVA followed by Tukey's HSD was used. For comparisons of robustness or period between AWs for a genotype, Friedman's test for repeated measures was followed by multiple Wilcoxon matched-pairs tests (or Conover Test for 'r') with the Bonferroni procedure used. For comparing the proportion of rhythmic flies between AWs for a genotype, the Cochran Q test, followed by multiple 2x2 McNemar's tests on the dependent samples and the BH procedure on all relevant comparisons, were used. Mann-Whitney U tests compared robustness and period between an AW's pdf-driven and tim-driven Q (or MJD) lines. For a comparison of rhythmicity between the *pdf-driven* and *tim-driven* Q (or MJD) lines for an AW, a 2x2 Fisher's Exact test was used. Mann-Whitney U tests were used to compare PDF^+ or MJD^+ LNv numbers between genotypes of *pdf>MJD*. All other details are described in Chapter 2 (Section 2.2.2.1).

6.3 RATIONALE, RESULTS AND CONCLUSIONS

6.3.1 The effect of *Drosophila* Huntingtin on the circadian free-running activity rhythms and the expHTT-induced disruption of those rhythms

6.3.1.1 Rationale

Endogenous *Drosophila* Huntingtin or dhtt is a single ortholog of the human Huntingtin (hHTT) (Li et al., 1999). dhtt shows five areas of high evolutionary conservation: three relatively large and two smaller segments. These homologous regions, comprising about 1200 a.a. residues in dhtt, share around 24% identity and 49% similarity at the amino acid level with human sequences and may represent functional domains. The *dhtt* transcript is widely expressed from embryogenesis through all the developmental stages and in adulthood. The dhtt protein comprises 3583 amino acids.

Interestingly, the *Drosophila* HD gene product does not contain the polyglutamine and polyproline tracts, nor are any consensus caspase cleavage sites found in the N-terminal. dhtt contains 28 consensus HEAT repeats. dhtt is mainly a cytoplasmic protein, unlike its human ortholog.

dhtt serves several roles. Neuronal downregulation of dhtt caused axonal transport defects (Gunawardena et al., 2003). dhtt is involved in fast axonal transport (Zala et al., 2013a; Weiss and Littleton, 2016). dhtt is essential for Rab11 vesicle transport within axons (Power et al., 2012) and crucial for neuronal development and function (Richards et al., 2011; Steinert et al., 2012). dhtt is required for the retrograde transport of dense-core vesicles and is a potential regulator of synaptic capture and neuropeptide storage (Bulgari et al., 2017). *dhtt* knockout is not embryonic lethal, does not cause developmental defects or rough eye phenotype and is not essential for synapse formation and organization at NMJs (Zhang et al., 2010b). However, *dhtt-ko* flies display an age-dependent decline in mobility and survival compared to WT flies (Zhang et al., 2010b).

dhtt is involved in mitotic spindle orientation, essential for mitosis (Godin et al., 2010), and influences chromatin organization (Dietz et al., 2015). dhtt is crucial for selective autophagy, possibly as a scaffold protein (Ochaba et al., 2014; Rui et al., 2015). dhtt represses the activity of the tyrosine kinase Abl, thereby maintaining the appropriate levels required for axonal growth (Marquilly et al., 2021). Notably, dhtt can restore mammalian HTT spindle orientation function in mouse cells (Godin et al., 2010). hHTT can rescue neuropathology caused by dhtt knockdown (Mugat et al., 2008) and mobility, lifespan and autophagic defects of *dhtt* knockout flies (Rui et al., 2015). These studies illustrate the conservation of biological properties and functions of HTT across taxa.

There is evidence for dhtt as a neuroprotector. *dhtt* reduction in the eye leads to a progressive rough eye phenotype, and its tissue-specific reduction results in organelle accumulation in larval neurons, characteristic of axonal transport defects (Gunawardena et al., 2003). In a *Drosophila* HD model, overexpression of the N-terminal of dhtt prevented expHTT aggregation, while dhtt downregulation worsened aggregation (Mugat et al., 2008). Also, *dhtt-ko* exacerbated neurodegenerative phenotypes of HD flies (Zhang et al., 2010b) and Tau-expressing flies (Rui et al., 2015).

Given the diverse cellular roles of dhtt and its neuroprotective ability, I investigated its effect on fly circadian rhythms *per se* and expHTT-induced behavioural arrhythmicity in HD flies.

6.3.1.2 Results and Conclusions

6.3.1.2.1 *dhtt* does not contribute to the sustenance of activity rhythms in DD

I asked whether dhtt has a role to play in circadian rhythms. The activity rhythms in DD were assessed for *Drosophila* mutants of *dhtt* and flies with dhtt downregulated only in circadian pacemaker LNv. All the experimental flies were like control w^{1118} in their rhythmicity and robustness and had ~24h periods (Fig 6.1). Thus, dhtt is not essential for circadian locomotor activity rhythms. On the other hand, dhtt is essential for sleep as pan-neuronal downregulation of dhtt leads to nighttime sleep deficits and fragmentation (Gonzales and Yin, 2010).

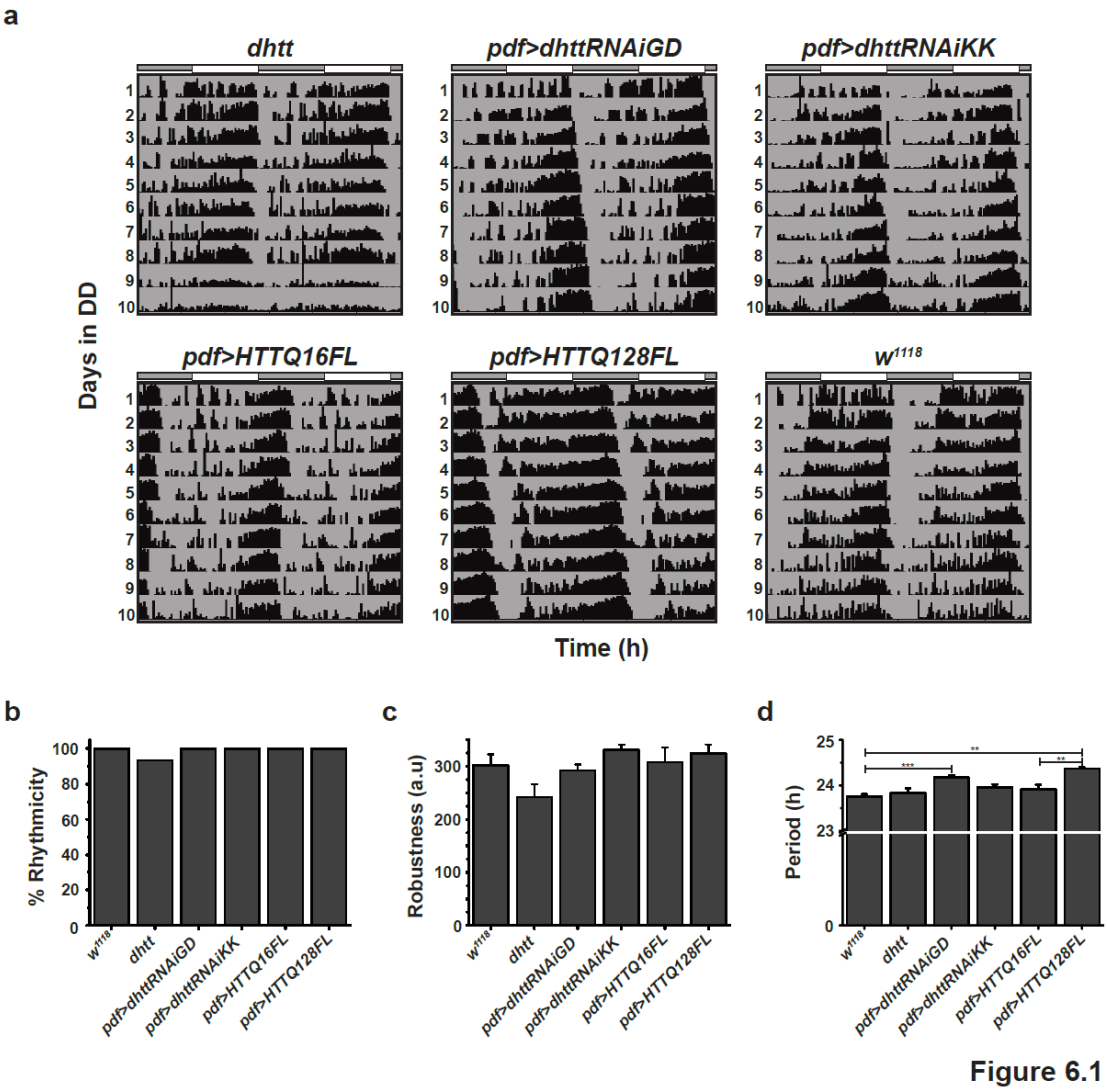

Fig 6. 1 dhtt mutants and flies expressing full-length expanded HTT in the LNv are rhythmic in DD25.

(a) Representative double-plotted actograms for flies showing activity data for 10d (age 3d-12d) in DD at 25 ºC of for *dhtt* mutants, flies with down-regulated *dhtt* in LNv (*pdf>dHttRNAiGD* and *pdf>dHttRNAiKK*) and expressing FLHTT in LNv (*pdf>HTTQ16FL* and *pdf>HTTQ128FL*), compared against w^{1118} controls. The white and grey bars above actograms represent light and dark phases of the previous LD. (b-d) Percentage rhythmicity (b), the robustness of rhythm (c) and period (d) for the above genotypes. ** is at p <0.01 and *** at p <0.001. Across all panels, error bars are SEM.

6.3.1.2.2 *dhtt* overexpression in the LNv does not rescue the disruption of free-running rhythms in HD flies

Since dhtt is neuroprotective across animal models, I asked whether its overexpression in *pdf>Q128* flies rescues behavioural arrhythmicity. My studies show that co-expressing dhtt of different fragment lengths in the LNv could not overcome expHTT-induced rhythm impairment in DD (Table 5.1), suggesting that in the circadian context of flies, dhtt is not neuroprotective. Further, I find that dhtt is dispensable to circadian activity rhythms and is non-essential to the functioning of LNv.

6.3.2 The effect of expressing full-length HTT in the LNv pacemakers on the free-running activity rhythms

6.3.2.1 Rationale

Expression of full-length (FL) expanded HTT protein in neurons leads to increased synaptic transmission in the NMJ of *Drosophila* larvae. Altered intracellular $Ca2^{+}$ levels in neurons increase neurotransmitter release probability and neuronal degeneration (Romero et al., 2008). The full-length HTT staining is diffuse, and flies expressing FL expHTT did not show axonal transport defects, unlike those expressing truncated HTTs (Steffan et al., 2000; Gunawardena et al., 2003; Lee et al., 2011). Expression of FL expHTT in the eye causes progressive ommatidia loss, neuronal expression reduces lifespan and mobility, while glial expression leads to reversed electroretinogram polarity (Romero et al., 2008; Burr et al., 2014; Yeh et al., 2018). Leg-specific expression resulted in cell loss and affected mitochondrial distribution and numbers (Fernius et al., 2017). Several regions in the HTT protein, like the caspase-6 site (586aa), cleavage which is required for neuronal dysfunction (Graham et al., 2006; Warby et al., 2008), NES and the glutamic acid, serine and proline-rich regions at the C-terminal, additional HEAT repeats and protease cleavage sites that get differentially cleaved in the cerebral cortex and striatum are absent from the long N-terminal truncated form but are intact in the FL protein. As a result, several characteristics of the FL HTT, such as tissue-specific proteolytic processing, various conformations, subcellular localisation, post-translational modifications, and interactions with cellular proteins via HEAT repeats, might not be captured in animal models that use truncated versions of hHTT. I, therefore, wanted to assess the effect of expressing full-length hHTT in the LNv on circadian behavioural rhythms.

6.3.2.2 Results and Conclusions

6.3.2.2.1 Expression of full-length expHTT in the LNv does not alter free-running activity rhythms

Flies expressing full-length expHTT (with 128Q repeats) in the LNv showed rhythmic robust activity rhythms like their counterparts with non-expanded full-length HTT (with 16Q repeats)

and controlled w^{1118} (Fig 6.1a, bottom, b and c). The full-length expHTT-expressing flies had slightly lengthened periods than controls (Fig. 6.1d). Thus, although the flies expressing the truncated version of expanded hHTT with the first 548aa in LNv show immediate behavioural arrhythmicity in DD, the rhythms of expanded FL hHTT expressing flies were relatively unaffected, suggesting weaker toxicity of the full-length protein. These findings suggest that full-length expHTT might be less cytotoxic in HD-associated circadian dysfunction than the truncated versions. Indeed, in both *in vitro* and *in vivo* models, truncated forms of HTT are more toxic than full-length models: more severe and early-onset symptoms, more aggregates present both in the nucleus and cytoplasm and rapid aggregate formation and cell death (Slow et al., 2005; Cisbani and Cicchetti, 2012; Farshim and Bates, 2018; Kosior and Leavitt, 2018; Kaye et al., 2021). These studies also reinforce the role of proteolytic cleavage of expHTT in HD toxicity. Evidence suggests that full-length HTT predominates during the early disease stages that do not require nuclear accumulation of HTT in detectable amounts (Romero et al., 2008). With disease progression, cleavage of HTT might tilt the balance in favour of the truncated fragments, especially the toxic polyQ-containing N-terminal fragment, which then shapes the course of the disease. Thus, as the disease advances, the truncated versions are more prevalent than full-length, and the more toxic expHTT species show early discernible effects on LNv function and circadian behaviour. Some studies show that murine HD models of truncated expHTT exhibit more severe and early-onset symptoms than full-length HD models (Slow et al., 2005; Farshim and Bates, 2018; Kosior and Leavitt, 2018; Kaye et al., 2021). The finding that in the circadian neurons, FL HTT is benign, whereas exon1 or 548aa N-terminal fragments are not, as seen previously, and cause circadian behavioural arrhythmicity (Chapter 2), indicates that the protein-context around polyQ stretch also determines neurotoxicity. Pan-neuronal expression of the FL expHTT in *Drosophila* leads to deficits in sleep: impaired sleep initiation, fragmented and diminished sleep, and nighttime hyperactivity (Gonzales and Yin, 2010; Gonzales et al., 2016). So, one could look at the effect of FL expHTT on circadian neurons by expressing them using a widespread circadian driver.

6.3.3 The effect of expressing GFP-tagged-HTT of varying polyQ lengths in the LNv pacemakers on the activity rhythms

6.3.3.1 Rationale

GFP-tagged HTT polyQ lines ease the visualisation of HTT, aggregation, and interactions. Therefore, I tested whether the expression of GFP-tagged expHTT in the LNv alters activity rhythms in DD. Two different sets of GFP-tagged lines were tested. The first was a gift from Dr Norbert Perrimon, Harvard Medical School, USA (Zhang et al., 2010b), namely UAS-Httex1-Q_neGFP with different polyQ repeat lengths (Q25, Q46, Q72, and Q103). The second was a gift from Dr Nobuyuki Nukina, RIKEN Brain Science Institute, Japan (Doumanis et al., 2009), namely N-terminal Htt exon 1 with varying Q lengths (Q18 and Q152) as fusions with EGFP either lacking or containing a nuclear localization signal (NLS).

Httex1-Q_neGFP with expanded HTT (Q46, Q72 and Q103) was demonstrated to be toxic in various fly models. For example, their expression in neurons showed a polyQ-length- and age-dependent reduction of fly lifespan, eye degeneration, mobility issues and increased aggregation (Zhang et al., 2010b; Kim et al., 2017). Q25 was diffuse, while Q103 exclusively formed aggregates, and Q46 and Q72 were intermediate, with Q72 showing accelerated aggregation than Q46 (Zhang et al., 2010b). PolyQ-length-dependent cardiac defects were also observed in flies expressing expHTT using a heart-specific driver (Melkani et al., 2013). Also, various modifiers of neurotoxicity show an effect on neuropathology in flies expressing GFP-tagged expHTT, such as aggregation (Xiao et al., 2013; Jimenez-Sanchez et al., 2015; Menzies et al., 2015; Yue et al., 2015; Xu et al., 2019a; Xu et al., 2019b), autophagic flux (Yue et al., 2015), and circadian activity rhythms (Xu et al., 2019a; Xu et al., 2019b). Expression of HTTQ103-eGFP in LNv reduced the number of PDF^+ sLNv and decreased PER levels in the LNv while moderately weakening locomotor rhythms (Xu et al., 2019a; Xu et al., 2019b). Expression of the Nhtt(Q152)EGFP results in a degenerative eye phenotype along with inclusions while its Q18 controls (Nhtt(Q18)EGFP and Nhtt(Q18)$EGFP^{NLS}$) were unaffected (Doumanis et al., 2009).

6.3.3.2 Results and Conclusions

6.3.3.2.1 Expression of expanded Httex1-QneGFP in the LNv does not alter free-running activity rhythms

Most flies expressing Httex1-QneGFP with expanded HTT (Q46, Q72 and Q103) in LNv were rhythmic in DD (9 days of recording), their robustness comparable to controls (except *pdf>HTTQ46*), with periods longer than most controls (Fig 6.2 a-d). However, unlike the *pdf-driven UAS-HTTQ103-eGFP* expression leading to a reduction in rhythmicity (~75%) and rhythm robustness than controls around 10-16d in DD (Xu et al., 2019b), in my experiments, most of the *pdf>HTTQ103* were rhythmic (~85%) even in AW2 (age 10d-16d) and had more robust rhythms and a more extended period than control *Q103* (Fig 6.2 e-g). Verifying these results would be a logical next step, given the discrepancy between my findings from other studies.

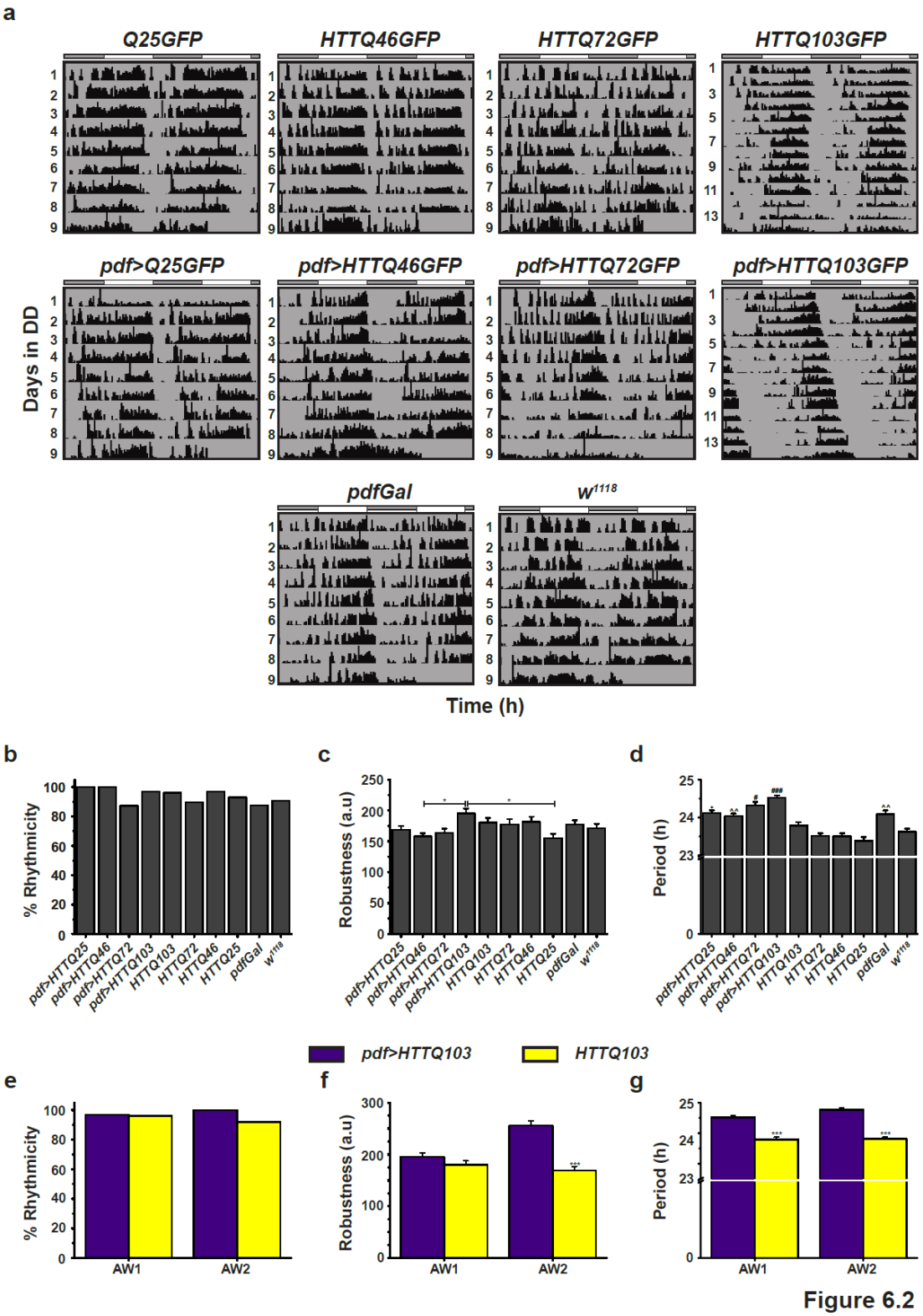

Figure 6.2

Fig 6. 2 Flies expressing GFP-tagged expanded HTT of various polyQ lengths are rhythmic in DD25.

(a) Representative double-plotted actograms for flies showing activity data for 9d (age 3d-11d) in DD at 25 ºC for flies expressing GFP-tagged HTT of varying polyQ lengths in LNv and their controls. The significantly expanded polyQ stretch of Q103 has been recorded for 14d (age 3d-16d). The white and grey bars above the actograms represent the light and dark phases of the previous LD.

Percentage rhythmicity (b), the robustness of rhythm (c) and period (d) for the above genotypes. 14d recorded *pdf>HTTQ103,* and *Q103* are compared across AWs 1 and 2 in terms of percentage rhythmicity (e), rhythm robustness (f) and period (g). Significant differences in period (d) of indicated genotype are as follows: # from all controls except *pdfGal*, + from *Q25*, *Q46*, *Q72* and *w1118*, ^ from *Q25*, *Q46* and *Q72* at single-symbol at $p < 0.05$, double-symbol at $p < 0.01$ and triple-symbol at $p < 0.001$. Across panels, error bars are SEM.

6.3.3.2.2 Expression of expanded HTTQ152eGFP in the LNv progressively impairs the free-running activity rhythms

With the second set of GFP-tagged flies, in AW1, most flies expressing expHTT were rhythmic with robustness comparable to controls (Fig 6.3 a-c). In AW2, nearly 50% of *pdf>Q152eGFP* flies and *pdf>Q1252eGFPNLS* were arrhythmic, but so were ~65% of *Q18eGFPNLS* controls, with rhythmic *pdf>Q152eGFPNLS* also having weak rhythms (Fig 6.3 b, c). In AW3, only ~ 40% of *Q18eGFPNLS* flies were rhythmic, while none of *pdf>Q152eGFP* or *pdf>Q152eGFPNLS* were rhythmic, and their percentage rhythmicity differed from most controls (Fig 6.3b). Rhythmic *pdf>Q152eGFP* had a longer period than controls in AW1, while rhythmic *pdf>Q152eGFPNLS* had a longer period than controls in AW1 and AW2 (Fig 6.3d). Thus, flies expressing HTTQ152eGFP in the LNv showed a progressive decline in activity rhythms with age. It will be crucial to verify the status of circadian proteins PDF and PER and expHTT inclusions in their LNv. 4d-old flies of all four experimental genotypes showed the presence of ~3-4 PDF^+ sLNv and lLNv and GFP^+ LNv with intact dorsal and contralateral sLNv projections (data not shown). The *pdf>Q152eGFP* also showed the presence of inclusions as seen via GFP staining (data not shown). Even though *pdf>Q152eGFPNLS* showed progressive arrhythmicity, so did one of its controls *Q18eGFPNLS*. So, it would be prudent not to use these NLS-tagged genotypes in future experiments.

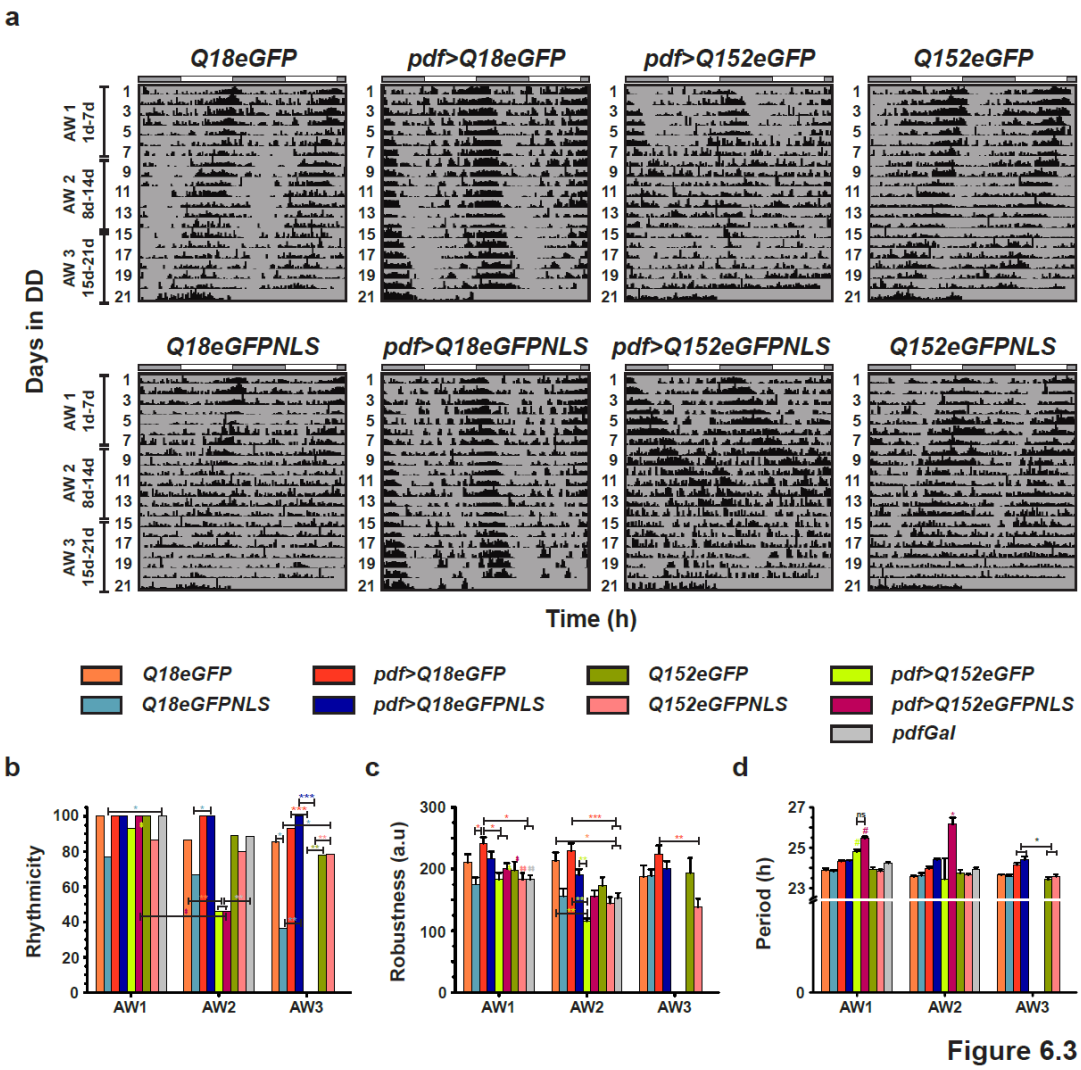

Figure 6.3

Fig 6. 3 Expression of GFP-tagged or NLS-GFP-tagged HTTQ103 in LNv leads to progressively weak rhythms and arrhythmicity post-AW1 in DD25.

(a) Representative double-plotted actograms for flies showing activity data for 21d (age 3d-23d) in DD at 25 ºC for flies expressing GFP-tagged HTT of varying polyQ lengths in LNv and their controls. The other details are the same as in Fig 5.2. (b-d) Percentage rhythmicity (b), the robustness of rhythm (c) and period (d) for the above genotypes. Symbols represent significant differences: * between indicated age-matched genotypes, $ between AWs for a genotype at * or $ at $p<0.05$ ** or $$ at $p<0.01$ and *** or $$$ at $p<0.001$. Across panels, error bars are SEM.

6.3.4 The effect of expressing expanded-polyQ-peptides in the circadian neurons on the activity rhythms

6.3.4.1 Rationale

Flies expressing expanded polyQ peptides alone, even without a protein context, are known to be neurotoxic. In *Drosophila*, their tissue-specific expression (Q127, Q63) leads to the formation of inclusions, retinal and photoreceptor degeneration, and reduced lifespan, and many of these features are susceptible to modifiers (Kazemi-Esfarjani and Benzer, 2000; Marek et al., 2000; Kazemi-Esfarjani, 2002; Taylor et al., 2003b; Ghosh and Feany, 2004; Kim et al., 2005; Fayazi et al., 2006a; Burnett et al., 2008; Kuo et al., 2013a; Yadav and Tapadia, 2013; Nelson et al., 2016). So, I asked whether the expression of expanded polyQ peptide in the LNv disrupts circadian rhythms.

6.3.4.2 Results and Conclusions

6.3.4.2.1 Expression of expanded polyQ in the PDF$^+$ LNv did not affect free-running rhythms

Most flies expressing only the polyQ peptide of varying lengths (Q20 and Q63) in the LNv were rhythmic across age, like their controls (Fig 6.4a and b). The robustness of *pdf>Q63* was comparable to most controls across ages (Fig 6.4c). Both *pdf>Q20* and *pdf>Q63* had more extended periods than their *UAS* controls but were comparable to *pdfGal* across age (Fig 6.4d). Thus, the mere expression of expanded polyQ repeats in LNv cannot induce behavioural arrhythmicity.

6.3.4.2.2 Expression of expanded polyQ in the TIM$^+$ circadian neurons leads to weakening of free-running rhythms

tim>Q63 flies, like all their controls, are mostly rhythmic across ages (Fig 6.4a and e). However, their rhythms are not as robust as most controls in AW1 and AW2 (Fig 6.4f). Both *tim>Q20* and *tim>Q63* had more extended periods than their *UAS* controls but were comparable to *pdfGal* across age (Fig 6.4g). Thus, widespread circadian expression of CAG-Q63 peptide does not lead to complete rhythm breakdown, but the robustness of rhythm is reduced. The results suggest that,

unlike the expanded polyQ in the context of HD (or MJD, see next section), the mere presence of expanded polyQ peptide in circadian neurons is seemingly less neurotoxic. Additionally, most free-running rhythm features are comparable between polyQ expression in PDF^+ and TIM^+ circadian neurons across ages (Fig 6.6a and b). Thus, even widespread expression of polyQ63 not dramatically impairing the free-running rhythms suggests a relatively benign effect of expanded Q63 in the circadian context. Experiments with longer polyQ lengths, such as Q108 or Q127, could yield further insights into the importance of protein and cellular contexts on polyQ disease progression.

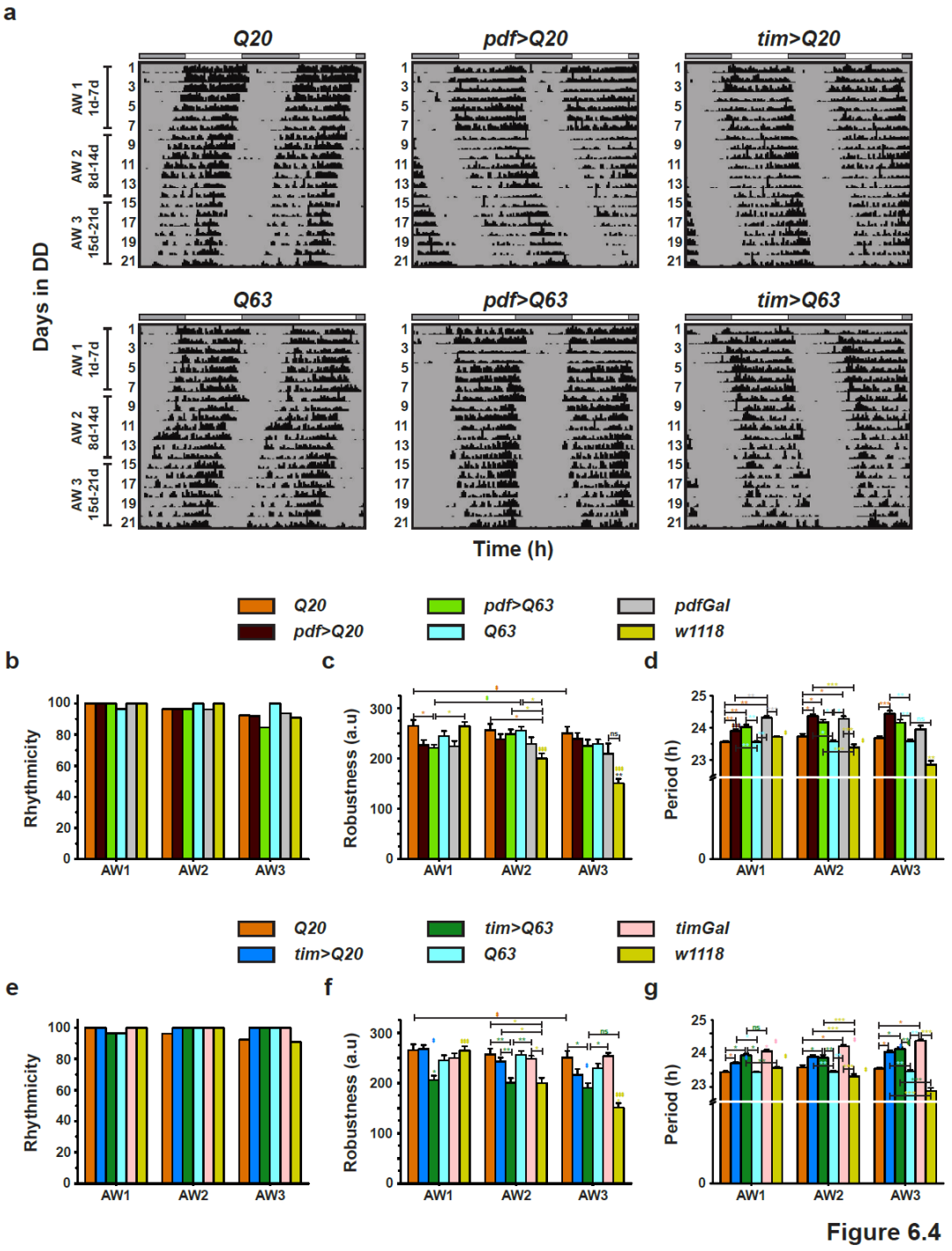

Fig 6. 4 Flies expressing expanded polyQ in a broad group of circadian neurons show weak rhythms in DD25.

(a) Representative double-plotted actograms for flies showing activity data for 21d (age 3d-23d) in DD at 25 ºC for flies expressing non-expanded (Q20) and expanded polyQ protein in either the *pdf-driven* LNv subset or *tim-driven* broad circadian neuronal group and their controls. The other details are the same as in Fig 5.2. (b- d) Percentage rhythmicity (b), the robustness of rhythm (c) and period (d) for the *pdf-driven* flies and their controls. (e-g) Percentage rhythmicity (e), the robustness of rhythm (f) and period (g) for the *tim-driven* flies and their controls. Symbols represent significant differences: * between indicated age-matched genotypes, $ between AWs for a genotype at * or $ at $p<0.05$ ** or $$ at $p<0.01$ and *** or $$$ at $p<0.001$. Across panels, error bars are SEM.

6.3.5 The effect of expressing expanded MJD protein in the circadian neurons on the activity rhythms

6.3.5.1 Rationale

HD is a member of the polyQ disease family characterised by expanding the CAG repeats (or glutamine amino acid repeats in the protein) past a certain threshold. Middle-age onset, progressive worsening with age, longer Q repeats showing earlier age-of-onset and greater severity, repeat expansion with subsequent generations and earlier onset (genetic anticipation), a toxic gain-of-function by the mutant protein and the presence of expanded protein aggregates, and selectivity in brain regions affected are common pathological features shared by these diseases (Fan et al., 2014; Lieberman et al., 2019). Spinocerebellar Ataxia Type 3 (SCA3), or Machado Joseph disease (SCA3/MJD), is a polyQ disease. It is caused by abnormal expansion of CAG repeats (>50) in the MJD-1 gene, encoding ATXN3 protein, which contrasts with other polyQ diseases with a Q length threshold of <40 (Bichelmeier et al., 2007; Alves et al., 2008; Costa Mdo and Paulson, 2012). The clinical hallmark of MJD is progressive ataxia, i.e. dysfunction of motor coordination that can affect gaze, speech, gait, balance, muscular atrophy, dystonia and spasticity. Even though the Ataxin3 protein is expressed ubiquitously, there is selective loss of neurons in non-cortical cerebellar systems (particularly the dentate nucleus and pontine neurons), cranial nerve motor nuclei, substantia nigra and spinal cord. Ataxin3 is a deubiquitinating enzyme participating in ubiquitin-dependent proteasomal degradation and helps regulate the stability or activity of many proteins implicated in proteotoxic stress response, ageing, and cell differentiation (Warrick et al., 2005; Costa Mdo and Paulson, 2012). The expanded ATXN3 protein triggers interconnected pathogenic cascades that cause cellular dysfunction and selective neuronal death (Warrick et al., 2005).

Multiple studies in *Drosophila* have shown the neurodegenerative effects of expanded MJD protein. In flies, tissue-specific expression of expanded truncated MJDQ78 causes retinal degeneration, cell loss, decrease in longevity and climbing ability, decrease in mating behaviour, increase in inclusions and oxidative stress, changes in autophagy, and mitochondrial and dendritic

defects (Warrick et al., 1998; Warrick et al., 2005; Kadener et al., 2006; Bilen and Bonini, 2007; Lessing and Bonini, 2008; Lee et al., 2011; Park et al., 2011; Cushman-Nick et al., 2013; Jia et al., 2013; Long et al., 2014b; Lin et al., 2015; Wu et al., 2018; Baumgartner et al., 2021; Nan et al., 2021). In contrast to MJDQ78, there were no deficits in expressing the non-expanded MJDQ27, which shows diffuse staining (Warrick et al., 1998; Warrick et al., 2005; Bilen and Bonini, 2007; Li et al., 2008a; Lee et al., 2011; Park et al., 2011; Cushman-Nick et al., 2013; Jia et al., 2013; Lin et al., 2015; Zhang et al., 2016; Wu et al., 2018; Baumgartner et al., 2021; Nan et al., 2021).

HD and MJD share several salient features of pathology, such as the middle age onset, progressive neurodegeneration, protein aggregation, reduced lifespan, and the length of the polyQ repeat correlating inversely with the age of disease onset and directly with disease severity (Cummings and Zoghbi, 2000; Takahashi et al., 2010; Bunting et al., 2021). Sleep disorders like restless legs syndrome and REM sleep disorder are seen in MJD (Pedroso et al., 2016; Huebra et al., 2019). I asked whether the shared pathogenicity between HD and MJD extends to circadian disturbances, as seen with the fly HD model.

6.3.5.2 Results and Conclusions

6.3.5.2.1 Expression of either MJDQ27 or MJDQ78 in the LNv renders flies behaviourally arrhythmic upon ageing

In AW1, *pdf>MJDQ27* and *pdf>MJDQ78* are rhythmic, like other controls (Fig 6.5a and b). In AW2 and AW3, the rhythmicity of both the genotypes falls to about 50%, differing significantly from other controls. The rhythm robustness of *pdf>MJDQ78* is lower than at least one of the controls across AWs and comparable to *pdf>MJDQ27* (Fig 6.5c). The period of *pdf>MJDQ78* is longer than other genotypes at AW1 (Fig 6.5d). The arrhythmicity and weak rhythms of *pdf>MJDQ27* are unexpected as these flies express the non-pathogenic, wild-type (WT) form of MJD. These results indicate that the expression of MJD protein (both WT and expanded versions) is intermediate toxic, leading to loss of behavioural rhythmicity as the flies age.

6.3.5.2.2 Flies expressing MJDQ78 in the TIM$^+$ circadian neurons are arrhythmic from the beginning, whereas those expressing MJDQ27 become arrhythmic at a later age

Nearly all *tim>MJDQ78* expressing flies are arrhythmic as soon as they enter DD, whereas most *tim>MJDQ27* flies are rhythmic up to at least nine days of age and become arrhythmic from AW2 onwards (Fig 6.5a and e). The rhythmic *pdf>MJDQ27* flies have weak and longer rhythms than some of the controls in AW1 (Fig 6.5f and g). Thus, expression of the expanded and WT forms of MJD in circadian neurons disrupts free-running rhythms, suggesting that activity rhythms are sensitive to the levels of WT MJD. In AW1, the finding that *tim>MJDQ27* mainly was rhythmic, albeit of poor robustness, compared to the arrhythmic *tim>MJDQ78*, suggests that expanded MJD has an exaggerated effect on rhythmicity than the WT MJD.

Comparing *pdf-driven* MJD expression with *tim-driven* MJD, the *tim-driven* MJD was more aggressive in activity rhythm breakdown. Most *tim>MJDQ27* flies were arrhythmic in AW2 and AW3, compared to ~50% arrhythmicity of *pdf>MJDQ27* (Fig 6.6c). Similarly, across AWs, a significantly more significant proportion of *tim>MJDQ78* flies were arrhythmic than *pdf>MJDQ78* (Fig 6.6d). The more significant toxicity associated with the *tim-driver* is not surprising given the widespread neuronal expression of TIM compared to the narrow expression of PDF (16-18 cells).

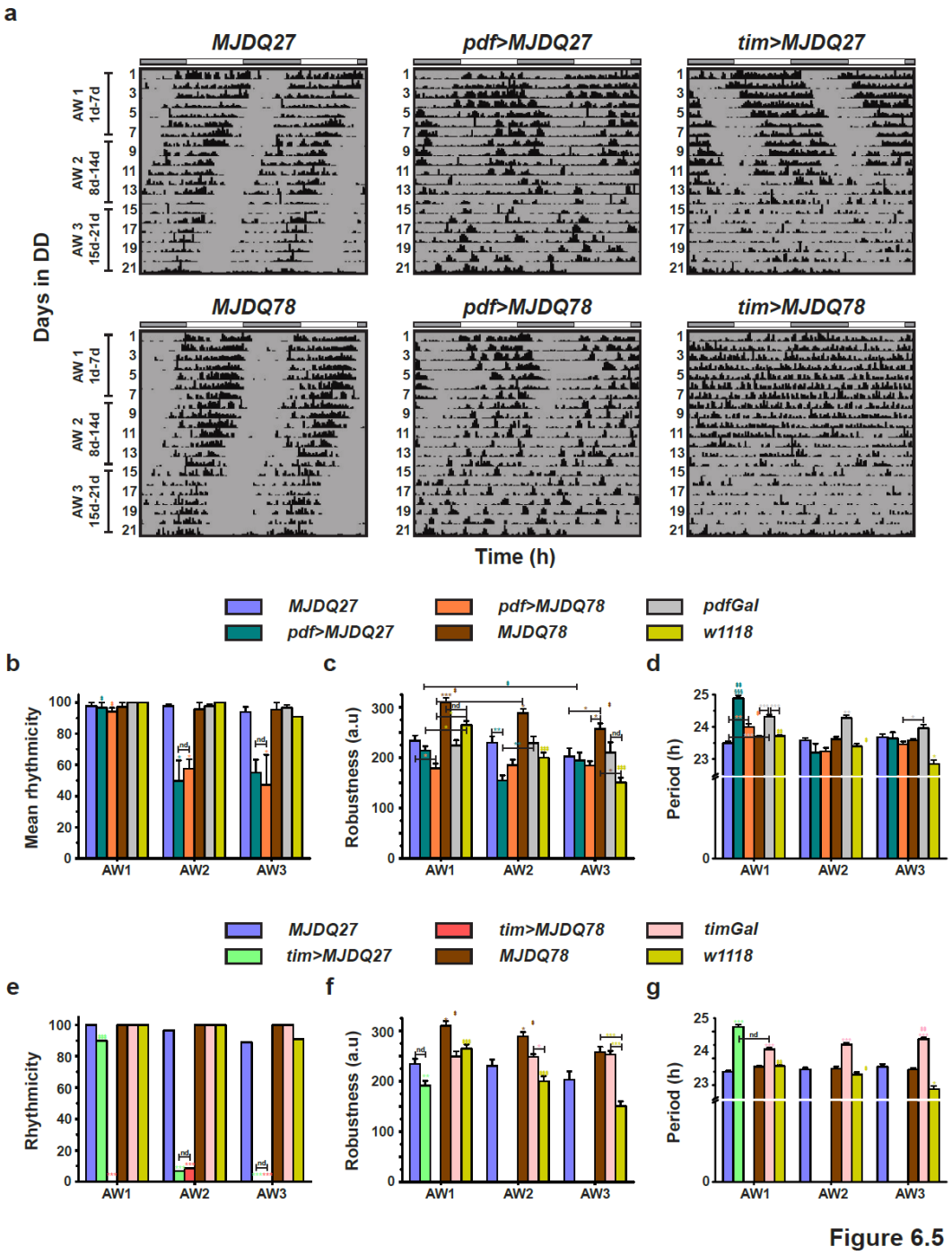

Fig 6. 5 Expression of MJD protein in circadian neurons leads to arrhythmicity and weak rhythms in DD25.

(a) Representative double-plotted actograms for flies showing activity data for 21d (age 3d-23d) in DD at 25 ºC for flies expressing non-expanded (Q27) or expanded (Q78) MJD protein in either the *pdf-diven* LNv subset or *tim-driven* broad circadian neuronal group and their controls. The other details are the same as in Fig 5.2. (b) Mean percentage rhythmicity averaged over three independent experiments for the *pdf-driven* flies and their controls. (c-d) The mean robustness of rhythm (c) and the mean period (d) for the *pdf-driven* flies and their controls for a representative run. (e-g) Percentage rhythmicity (e), the robustness of rhythm (f) and period (g) for the *tim-driven* flies and their controls. Symbols represent significant differences: * between indicated age-matched genotypes, $ between AWs for a genotype at * or $ at $p<0.05$ ** or $$ at $p<0.01$ and *** or $$$ at $p<0.001$. Across panels, error bars are SEM.

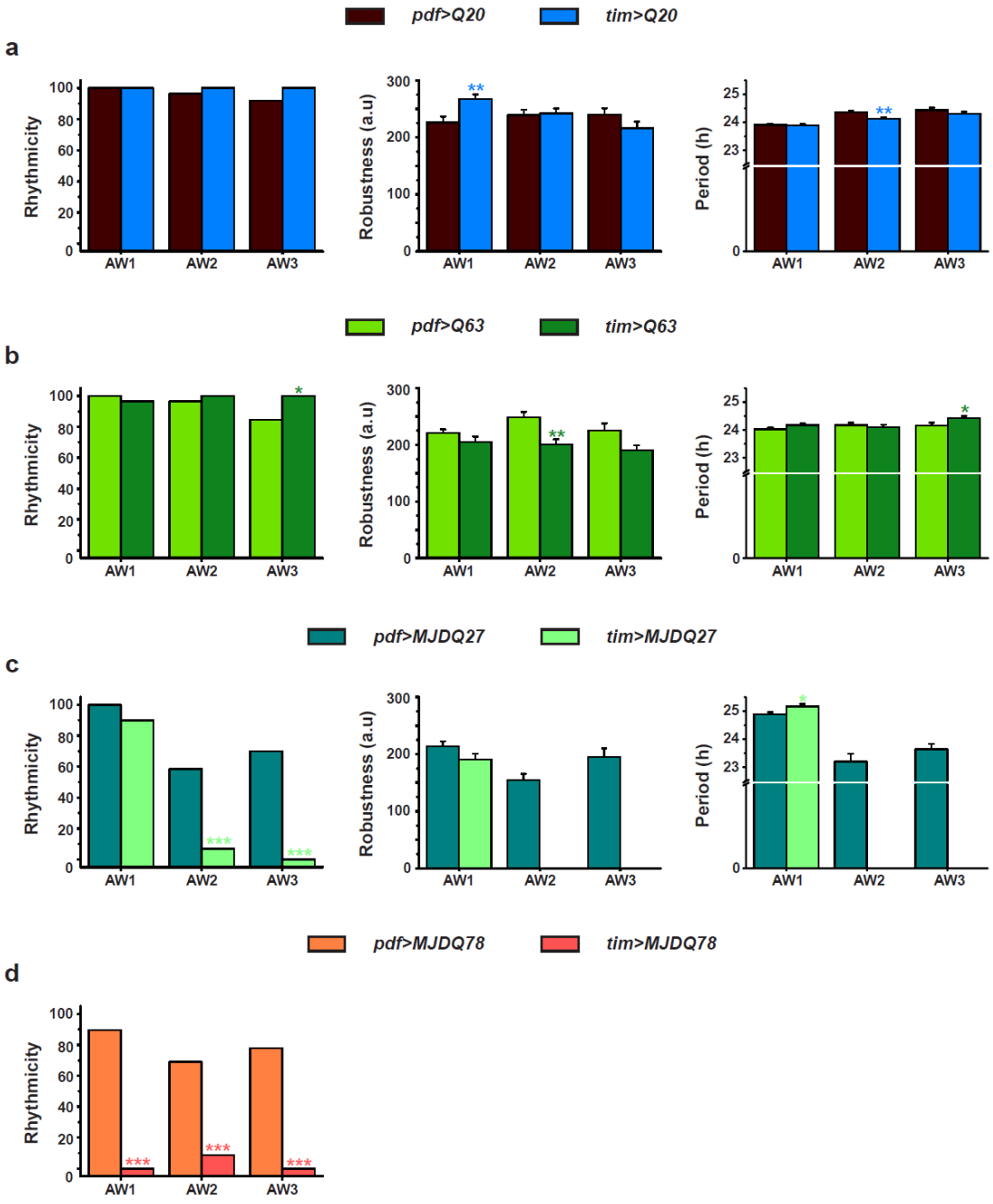

Figure 6.6

Fig 6. 6 Expression of MJD protein in a broad circadian neuronal group affects rhythmicity more severely than expression in the LNv subgroup alone.

(a-d) Comparison of rhythmicity (left), robustness (middle) and period (right) between *pdf-driven* and *tim-driven* expression of *Q20* (a), *Q63* (b), *MJDQ27* (c) and *MJDQ78* (d) across AWs. Symbols represent significant differences: * between indicated age-matched genotypes at * at $p<0.05$ ** at $p<0.01$ and *** at $p<0.001$. Across panels, error bars are SEM.

6.3.5.2.3 The PDF$^+$ LNv soma numbers are unaffected in flies expressing MJD in the LNv

The behavioural arrhythmicity associated with MJD expression in LNv prompted me to assess the status of PDF in these flies. Both *pdf>MJDQ27* and *pdf>MJDQ78* showed ~4 PDF$^+$ sLNv and lLNv soma stained with the HA-tagged MJD at 12d (Fig 6.7). 12d falls in AW2 when ~50% of these flies are arrhythmic. Thus, the arrhythmicity of *pdf>MJD* might not stem from their effect on PDF. However, the PDF levels in these flies have not been assessed and could contribute to arrhythmicity.

Only two other studies have targeted MJD-polyQ expression in circadian neurons. In the first, MJDQ78 was expressed in a broad group of circadian neurons using the *timGal4* driver (Kadener et al., 2006). Flies were arrhythmic in DD, had disrupted LD activity profiles, and showed a loss of *tim* mRNA and PER protein in clock neurons and reduced PDF$^+$ sLNv numbers. Expression of MJDQ78 in the PDF$^+$ LNv also disrupted free-running rhythms (Xu et al., 2019b). Like the above studies, the flies expressing MJDQ78 in circadian neurons (TIM$^+$ or PDF$^+$) showed different extents of behavioural arrhythmicities in the present study. However, the non-expanded MJQ27 expressing flies were also arrhythmic, like the expanded MJDQ78 expressing flies. In both the previous studies targeting MJD to clock neurons, the non-expanded control genotype with the expression of MJDQ27 in Tim$^+$ or PDF$^+$ neurons is missing (without any mention of their adverse effects) (Kadener et al., 2006; Xu et al., 2019b).

Hence, so far, there is no precedence for ill effects on expressing MJDQ27 in any of the *Drosophila* models using different tissue-specific expressions (Warrick et al., 1998; Warrick et al., 2005; Bilen and Bonini, 2007; Li et al., 2008a; Lee et al., 2011; Park et al., 2011; Cushman-Nick et al., 2013; Jia et al., 2013; Lin et al., 2015; Zhang et al., 2016; Wu et al., 2018; Baumgartner et al., 2021; Nan et al., 2021). On the contrary, the pan-glial expression of MJDQ27 alone extended the fly's lifespan (Yeh et al., 2018). Additionally, MJDQ27 Ataxin-3 protein, when co-expressed with MJDQ78, suppressed the rough eye phenotype, improved lifespan, and reduced inclusions and, when co-expressed with MJDQ84 in the glia, protected the Blood-Brain Barrier/Blood Retinal Barrier integrity, reflecting that MJDQ27 retains the normal function of

Ataxin-3 and is neuro and glia protective (Warrick et al., 2005; Jung et al., 2009; Vinatier et al., 2015; Yeh et al., 2018). Co-expression of MJDQ27 with HTTQ120 or with SCA1-Q82 or with Atx7Q102tr also suppressed exp-polyQ protein-induced retinal degeneration, indicating the neuroprotective function of Ataxin-3 protein is not specific to MJD but works broadly against pathogenic polyQ proteins (Warrick et al., 2005; Vinatier et al., 2015). The ubiquitin protease function of Ataxin-3 was required for its neuroprotective activity (Warrick et al., 2005). Despite the WT Ataxin-3 function of MJDQ27 and its neuroprotective effects, its expression in the circadian neurons impaired the free-running activity rhythms, suggesting that WT MJD protein levels are crucial for circadian function and an increase in its levels is detrimental to activity rhythms. It also highlights the cell-specific effects of a WT protein and the importance of cellular and protein contexts in influencing neurotoxicity. Given that PDF in LNv seems unaffected in *pdf>MJDQ27* flies up to 12d of age, the cellular basis for arrhythmicity and weak activity rhythms in these flies is unclear. However, some inclusions were seen in the LNv, which has not been quantified. It will be essential to verify the effect of expressing MJD proteins in the circadian neurons on the cellular phenotypes, such as the status of PER, PDF levels and MJD forms, including inclusions, to understand and explain the observations in behavioural rhythms.

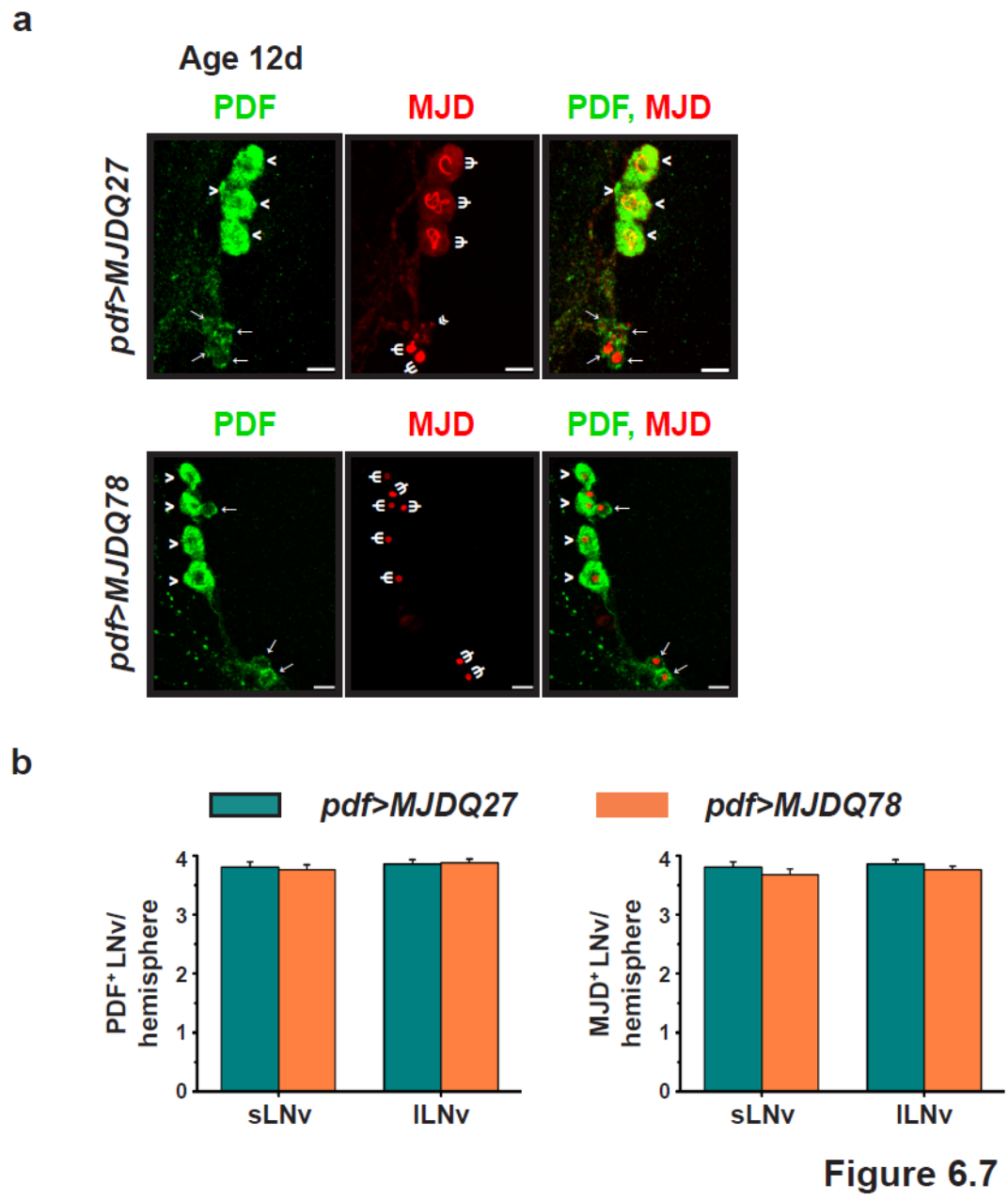

Fig 6. 7 LNv expression of MJD proteins does not affect PDF in LNv soma.
(a) Representative images of a 12d adult fly brain stained for PDF (green) and HTT (red) showing sLNv soma (arrows), lLNv soma (arrow-heads), diffused MJD (via anti-HA) staining (Ψ psi symbol) and MJD inclusions (« double arrowheads). (b) The mean number of PDF^+ LNv soma (left) and MJD^+ LNv soma (right) per hemisphere. Error bars are SEM.

6.4 FINAL REMARKS

6.4.1 Protein- and cellular-contexts in mediating polyQ effects on the circadian activity rhythms

So far, expanded polyQs of varying lengths and disease contexts (HTT with the first 548aa: $HTT^{548aa}Q0$ and $HTT^{548aa}Q128$, HTT with exon1: $HTT^{Ex1}Q20$, $HTT^{Ex1}Q50$, $HTT^{Ex1}Q93$, HTT full-length: $HTTQ16^{FL}$ and $HTTQ128^{FL}$, GFP-tagged Ex1HTT: HTTQ25, HTTQ46, HTTQ72 and HTTQ103, eGFP-tagged Ex1HTT: HTTQ18, HTTQ18NLS, HTTQ152 and HTTQ152NLS, expanded polyQs: Q20 and Q63 and truncated MJD: $MJD^{tr}Q27$ and $MJD^{tr}Q78$) have been expressed in the circadian pacemaker neurons in *Drosophila* (Chapters 2 and 6). Even though, as described earlier, the expanded versions are shown to be neurotoxic in various cellular contexts, targeting them to circadian neurons has variable effects on activity rhythms in DD. Some show an immediate severe effect of complete loss of rhythmicity, others show a delayed loss, some show marginal effects of weak rhythms, and others show no alteration in the rhythm features. The range of effects of expanded polyQs with and without flanking sequences in the circadian context brings to the fore the influence of the protein and cellular contexts in mediating the toxicity of polyQs.

The polyQ-length dependence for disease thresholds, penetrance, severity, and age-of-onset in diseases due to polyQ expansion, despite lack of sequence similarity outside the polyQ domain, suggests expanded polyQ as the primary driver of neurodegeneration among polyQ expansion diseases. However, despite broad underlying commonality in disease manifestation and underlying pathophysiology (Adegbuyiro et al., 2017; Paulson et al., 2017; Stoyas and La Spada, 2018a), each of the diseases has a relatively distinct clinical presentation, unique region-specificity of neurodegeneration, differing disease threshold and notably very different affected proteins, differing in their flanking sequences, endogenous expression, native function, interactome and post-translational modifications (Lieberman et al., 2019; Johnson et al., 2022). The contribution of the context of polyQ and its flanking regions and the cellular milieu to the differential dynamic properties in different polyQ disease proteins is significant (Chai et al., 2002;

Morley et al., 2002; Duennwald et al., 2006a; Gidalevitz et al., 2006; Calamini et al., 2013; Kuiper et al., 2017). These varying contexts also influence the polyQ-proteins' biophysical and biochemical properties like conformation, aggregation kinetics and solubility, post-translational modifications, proteolysis, its interactions (both homotypic and heterotypic), stability, quality control mechanisms, cellular localization and thereby, its toxicity, thus, introducing heterogeneity to disease pathology and progression (La Spada and Taylor, 2003; Ghosh and Feany, 2004; Tam et al., 2009; Robertson and Bottomley, 2010; Caron et al., 2014; Adegbuyiro et al., 2017; Silva et al., 2018). Thus, while interpreting results from various studies in the context of model systems, disease proteins, tissue-specificity, and phenotypic toxicity readouts must be considered.

CHAPTER 7

Summary, Conclusions, and Future Studies

7.1 SUMMARY, CONCLUSIONS, AND SIGNIFICANCE

In this study, I have characterised a circadian model of HD in *Drosophila*. This discussion focuses on *Drosophila* expressing expHTT in their circadian pacemaker neurons (the PDF^{+} LNv) or *pdf>Q128* flies (HD flies) unless otherwise specified.

Statement of significance: This study describes a *Drosophila* model that allows researchers to examine HD-related neurotoxicity and circadian disruptions at the cellular and behavioural levels. It then investigates strategies to modify these disease outcomes and uncovers several avenues for delaying expHTT-induced circadian neurodegenerative phenotypes like temperature cycles, warm temperatures and Hsps. Furthermore, there is evidence that expHTT inclusions serve as proxies for neurotoxicity and that HD-induced circadian dysfunction may be caused by disruption of cellular proteostasis. It also shows that the rescue of circadian behavioural outputs under neurodegenerative conditions can occur via different combinations of cellular rescue. Mechanisms underlying neuronal function, neurodegeneration, and circadian rhythms are conserved between flies and mammals. Hence, it is feasible to test the therapeutic approaches established here in clinically relevant mammalian systems that will help inform advances towards improving the life quality of HD patients and carers. Since several NDs share symptoms of circadian and sleep disruptions, which are often affected before the manifestation of clinical symptoms, the lessons from this study are also relevant for other NDs. They can inform targeting early disease stages and stall disease manifestation. Vitally, the findings of this study support two-way interactions between circadian and neurodegenerative networks and bring to light the effects of the external environment and cellular proteostasis on the outcomes of such interactions. This study supports the need to investigate and establish neuroprotective interventions that are also chronotherapeutic and provides evidence-based arguments for integrating circadian medicine into neuromedicine.

7.1.1 Common themes of neurodegeneration and the associated circadian alterations

In this fly model, several characteristics of HD, a polyQ-expansion neurodegenerative disease, have been recapitulated. These include age-dependent increase in symptom severity (progressive decline in activity rhythms and PDF loss from LNv), differential neuronal susceptibility (sLNv more susceptible than lLNv), increasing severity and lower age-of-onset with increasing polyQ-repeat-length (comparing HTTQ20, Q50, and Q93), middle-age onset (with HTTQ50), and the presence of inclusions of expHTT, a critical hallmark of protein-aggregation diseases. The progressing worsening with age also extends to HD-associated circadian disruptions like loss of core clock protein PER oscillation and circadian output PDF from the soma of the sLNv circadian pacemakers and a reduction in the extent of activity consolidation, similar to the loss of molecular oscillations in SCN *in vivo* and circadian output VIP neurons in the SCN of HD mice (Morton et al., 2005; Fahrenkrug et al., 2007; Maywood et al., 2010; van Wamelen et al., 2013). Some differential results include unaffected lifespan, entrainment of behavioural rhythms to LD cycles and sleep. However, the former two are likely owing to the small numbers of circadian neurons targeted and how they affect behaviour under LD. The latter can be attributed to the lack of replication of sleep studies, as sleep is very sensitive to experimental conditions, and more recent lab studies show a sleep disruption in HD flies in DD (Sharma et al., 2023). Though I do not find evidence of cell death of the LNv, the loss of cellular markers like PDF, PER and GFP from the soma and associated functional loss in behavioural rhythmicity are strong evidence for neuronal dysfunction. Also, in young HD flies, $Hsp70^{+}PDF^{-}$ sLNv soma are observed (Sharma et al., 2023), indicating that the sLNv is not lost and the PDF loss from sLNv soma does not amount to neuronal loss in the young. The neuronal death might be slow and may be captured in much older flies, as indicated by the reduction of $Hsp70^{+}$ sLNv soma with age (Sharma et al., 2023). The presence of sLNv axonal projections detected by PDF and GFP staining in the absence of sLNv somal staining is puzzling and is currently under investigation in the laboratory. This finding argues against an axonal die-back mechanism often observed in NDs (Benarroch, 2015;

Salvadores et al., 2017). Differential susceptibility of specific neuronal groups is captured in the form of sLNv affected more significantly than lLNv, which presents a fertile ground to investigate the mechanisms underlying the greater susceptibility of the sLNvs versus the relative protection offered by the lLNvs. A recent study from the lab supports the lLNv being more stress-resistant than the sLNv, given the fewer Hsp70-stained lLNv than sLNv (Sharma et al., 2023). Thus, this circadian HD model captures several salient characteristics of HD and its associated circadian disturbances. It must be noted that since a highly long polyQ stretch (128Qs) has been used in this study, the results presented here are more representative of a severe form of HD, like juvenile HD. This feature is reflected in the development of most circadian neurodegenerative phenotypes described above within the first seven to nine days of eclosion or in young flies.

7.1.2 Disease-modifying strategies

My studies have unveiled an environmental impact in delaying HD circadian and neurodegenerative outcomes mediated via clock and non-clock mechanisms in modifying disease progression.

7.1.2.1 Environmental modifiers

Light

This study shows light exacerbates neurotoxic cellular attributes, whether provided cyclically or continuously. Constant light was the most cytotoxic, hastening PDF loss from LNv and inclusion load. As the flies aged under constant light, it culminated in a complete loss of PDF from the whole of the sLNv, including its axons. Such a worsening of neurodegeneration has not been previously seen with any other regime. Following LL in neurotoxicity was LD, and DD was the least neurotoxic (Fig 7.1). Given that light is amongst the most potent synchronising stimuli for circadian rhythms, the observation that the absence of light (DD) offers better circadian neuroprotection than cyclic light (LD) seems counterintuitive. Further, the lack of proper lighting, like dim lighting and DD, harms mood and cognition and induces depression-like behaviour in rodents (LeGates et al., 2014; González, 2018; Kim et al., 2021b). Recent studies highlight the

significance of developmental light on *Drosophila* CNS development (larval neuroblast and adult mushroom body size reduced in DD-reared flies) and sleep where some pathways regulating wakefulness were enhanced (higher activity levels, lower nighttime sleep levels, increased dopamine receptor Dop1R1 expression in DD-reared flies), but not circadian clocks (comparable free-running rhythmicity, period and phasing of M-and E-peak between LD-reared and DD-reared flies, but decrease in expression of *pdf* and *pdfr* in DD-reared) (González, 2018; Dapergola et al., 2021; Damulewicz et al., 2022b). The adverse effects of LD (discussed in Chapter 3) can be attributed to the toxic effects of blue light or blue-enriched white light, which have not only chronobiological impacts but also affect visual performance, cause retinal damage, impair mitochondrial function and energy metabolism, cause oxidative damage, and affect neurotransmitter levels (Chen et al., 2017; De Magalhaes Filho et al., 2018; Nash et al., 2019; Shen et al., 2019; Liu et al., 2020; Ouyang et al., 2020; Kam et al., 2021; Krittika and Yadav, 2022; Song et al., 2022; Wong and Bahmani, 2022; Yang et al., 2022). The finding that cycling and constant light had aggravating effects on neurodegenerative features lends credibility to the criticality of environment and circadian hygiene in managing NDs. They also indicate that simple environmental changes like the extent and type of light exposure can significantly modify disease processes. So, it will be imperative to optimise various qualities of light like spectral composition, intensity, duration, and timing of application to reap the benefits of cyclic light as a robust circadian-rhythm-synchronising signal while minimising the adverse effects of light on neurodegeneration.

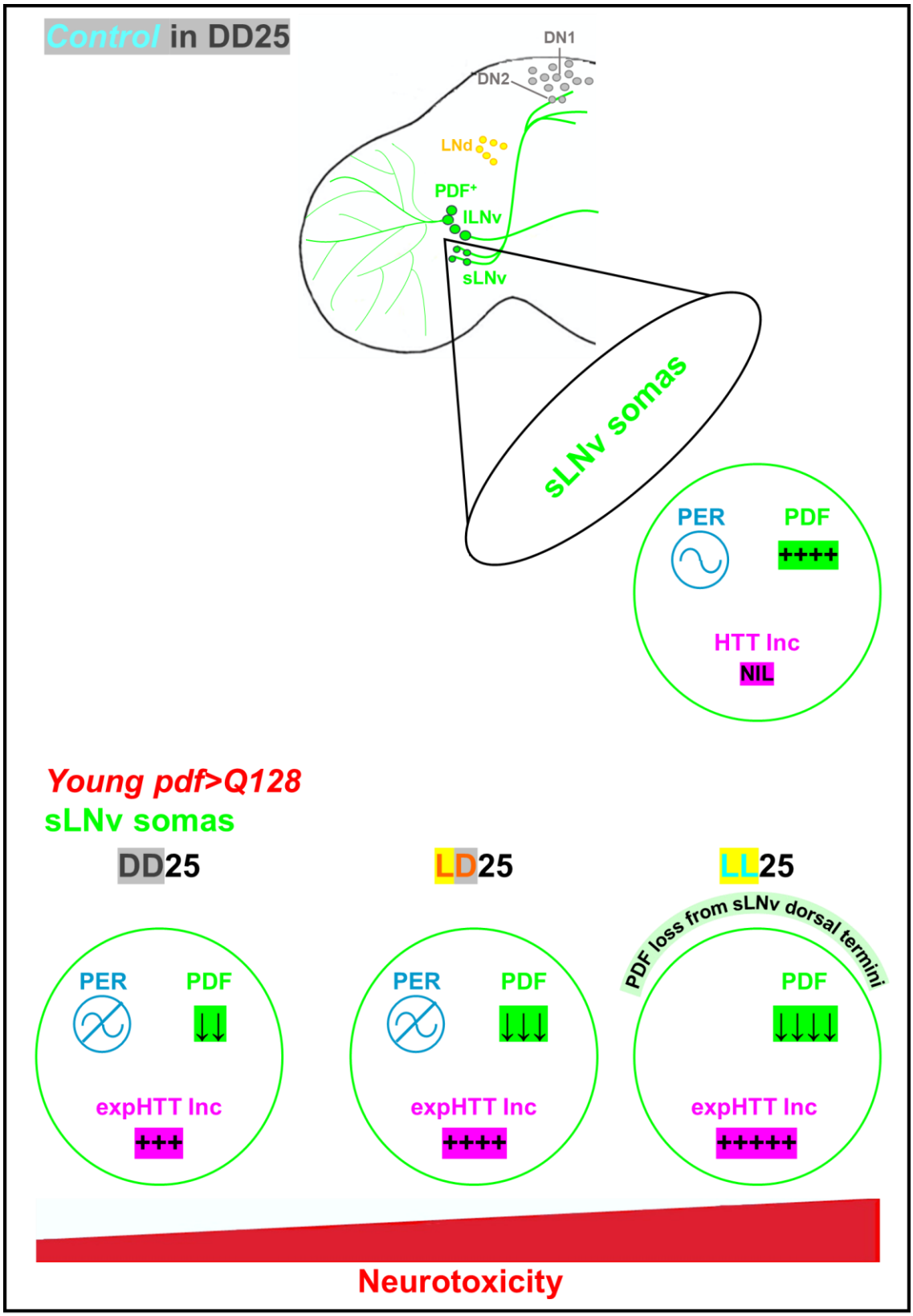

Fig 7.1

Fig 7. 1 A summary of the effect of lights on circadian cellular neurotoxicity in pdf>Q128 flies: constant light exacerbates toxicity, whereas the absence of light is the least toxic.

The top panel is a schematic of a hemisphere of a control *Drosophila* brain showing the critical circadian neurons. The cellular features of sLNv soma in *control* flies (top), and young *pdf>Q128* flies under three light regimes (DD25, LD25, and LL25) (bottom) are depicted. The cellular features studied are indicators of LNv functionality and health: oscillations in PER levels (a marker for the molecular clock), the status of PDF (a marker for circadian output) and expHTT inclusions (a proxy for the effectiveness of cellular proteostasis). The magnitude of neurotoxicity for the cellular features PDF and expHTT Inc in *pdf>Q128* is assigned based on comparing the three regimes. The ~ against PER represents the presence of oscillations in PER levels. The ++++ against PDF represents the presence of nearly four PDF^+ sLNv in controls, whereas ↓ against PDF is an overall representation of the loss of PDF from sLNv soma, which is primarily a decrease in the PDF^+ sLNv soma numbers (or decrease in PDF intensity in the sLNv below detection levels) and in the case of LL also signifies the loss of PDF from sLNv dorsal termini, thereby, a near complete sLNv PDF loss. The greater the number of ↓, the more severe (magnitude and speed - earlier) is the loss of PDF. The +s against expHTT inclusion indicates the extent of inclusion load considering the number of inclusions and the proportion of hemispheres dominated by Inc-enriched LNv relative to other expHTT forms. The approximate weightage of values shown here are representative of the overall sLNv somal status till 7d of age (and holds till the end of assay duration (23d) for PDF and expHTT inclusion number comparisons of *pdf>Q128* in DD against those in the other light regimes).

Temperature

Evidence-based studies on the impact of temperature on neurodegenerative outcomes are scarce. This study demonstrates that temperature-based approaches can delay the progression of HD. It offers some insight into the mechanisms underlying the processes mediating temperature-based restoration of early-age activity rhythms, which have some features in common but also differ from one another. Improvements in activity rhythm observed under both the regimes, the development-specific TCs and the adult-restricted warm temperatures, are contingent upon the temperature experienced as adults and are associated with a delay in PDF loss from the sLNv to varying degrees. In contrast to the former regime, which improves only behavioural rhythmicity and sLNv PER oscillations without affecting expHTT inclusions, the latter improves rhythmicity, and activity consolidation reduces inclusion load without restoring PER oscillations. Another prominent contrasting feature is the effect of light during development, which abolishes DDTCtoDD25-mediated early-age activity rhythm restoration but has minimal effect on the DD23toDD29-mediated behavioural rhythmicity. Of the two regimes, adult-restricted warm temperatures were modestly better in alleviating neurotoxicity. *Hsp70* contributes to the behavioural rhythm improvements mediated by adult-restricted warm temperatures in a dose-

dependent manner that seems to follow a J-shaped curve. These findings also imply that HD flies experience proteostasis stress and that warm temperatures facilitate rescue by reinforcing or enhancing cellular proteostasis. The involvement of *Hsp* in this rescue ties up neatly with *Hsps* emerging as potent suppressors of circadian neurodegenerative phenotypes in HD, discussed in the next section.

Even though the SCN *per se* seems resistant to temperature effects, circadian rhythms and peripheral clocks can be phase-shifted by temperature (Brown et al., 2002; Buhr et al., 2010; Tamaru et al., 2011; Saini et al., 2012). The finding that development-specific warm/cold temperature cycles can delay HD-induced circadian neurodegenerative phenotypes via largely clock-centric mechanisms is encouraging for using temperature as an entraining time cue and even as a masking agent, serving as an alternative to other zeitgebers like light, food, and social schedules. Using fluctuating/ oscillatory temperatures also circumvents some of the ill effects of using chronic warm temperatures. The finding that warm temperatures, particularly adult-restricted warm temperatures, can delay HD circadian outcomes is proof of the potential for the positive effects of heat acclimation on neurodegeneration. In other words, this study demonstrates the effectiveness of cross-modal hormesis in neurodegeneration: one stressor, like mild heat, can mitigate the effect of another stressor, like aggregation-prone protein. These findings also make a case for testing and optimising heat treatments like whole-body hyperthermia and passive heat therapy as treatment modalities.

Previous studies have shown the effectiveness of non-pharmacological interventions known to improve circadian function, like timed light therapy, time-restricted feeding, scheduled physical exercise and social settings, in improving circadian parameters, cognitive performance and metabolic functions alleviating HD symptoms in animal models (Pallier et al., 2007; Pallier and Morton, 2009; Maywood et al., 2010; Aungier et al., 2012b; Skillings et al., 2014; Ouk et al., 2017; Wang et al., 2017; Whittaker et al., 2018; Cabanas et al., 2019). Using *Drosophila,* this study underscores the potential for temperature-based intervention in mitigating HD-associated circadian dysfunction via at least two different approaches. Temperature-based interventions like saunas and hot tubs have a long history of traditional use and have now been shown to have

several health benefits (Brunt and Minson, 2021; Patrick and Johnson, 2021), setting encouraging precedence for the findings of this study in *Drosophila*. Temperature-based strategies will be particularly useful in the treatment of circadian rhythm disruptions (CRDs) in people with limited mobility, those deprived of ample bright light exposure or unable to avail themselves of the benefits of other complementary treatments like bright light and physical therapy: the institutionalised healthy, elderly, neurodegenerative patients, blind people and (or) people with poor light perception or decreased photosensitivity. Also, as a therapeutic modality, heat (temperature-based interventions) is cheap, convenient, widely accessible, non-invasive, and relatively easy to incorporate as part of lifestyle (Chen et al., 2020).

7.1.2.2 Genetic modifiers

Hsps

Using a screen for known cellular neurotoxic modifiers of HD, I have uncovered Hsps (Hsp40 and Hsp70) as suppressors of HD-associated circadian behavioural arrhythmia. Hsp40 emerged as the more potent mitigator of HD-induced deficits. Upon Hsp40 overexpression in the LNv, the behavioural rhythm rescue was associated with the restoration of PER and its oscillations in the LNv of young flies and a long-lasting rescue of PDF in sLNv soma. Significantly, there was a reduction in the expanded Huntingtin inclusion load, concomitant with the appearance of a hitherto novel expHTT form, spot-like. Surprisingly, early-age rhythm rescue upon Hsp70 overexpression did not see improvements in any of the LNv cellular features.

Throughout my research, two independent studies have established a role for Hsps in circadian rehabilitation in the context of NDs. The improvement of ND-induced circadian dysfunction at both the cellular and behavioural levels due to the involvement of a known proteostasis influencer with a long history of protecting against neurodegeneration highlights intersections between the circadian and neurodegeneration axes. It strengthens the emerging theory of a bi-directional relationship between the two. Given the importance of protein homeostasis and circadian health in brain and protein aggregation diseases, the involvement of molecular chaperones in circadian maintenance has broader therapeutic implications for several other neurodegenerative diseases

like Parkinson's and Alzheimer's. Circadian and sleep disturbances occur early and are pre-manifest in many NDs. Therefore, treatments targeting HSPs could impact the early stages of the disease, delay symptoms and aid in therapy. The findings on chaperones' role in circadian rehabilitation pave the way for exploring the relatively uncharted area of HSP and the molecular clockwork interactions. This study also reveals a need to explore and establish nodal molecules that affect several pathways compromised in ND and develop chronotherapeutic neuroprotective agents.

7.1.3 Trajectories of circadian rhythm rescue in HD: Mechanistic insights

There has been intense debate on the toxic form of expHTT conformer in HD. In this study, the puncta-like appearance of expHTT in the LNv visible via fluorescence light microscopy has been termed "inclusions". No assumptions about its solubility, polymeric state, or ultrastructure have been made. The uniform distribution of expHTT appearance that often mimics the PDF distribution is termed "diffuse". Furthermore, if an LNv expHTT staining appears diffuse with a few inclusions, the staining is said to be "Diff+Inc". In most experiments across various regimes and genetic backgrounds, a few trends were observed regarding the expHTT forms in LNv of *pdf>Q128*. Most of these observations are limited to the first seven days post-eclosion. First, the expHTT form changes from Diff to Diff+Inc to Inc as the flies age. The lower proportions of Inc-enriched LNvs in young *pdf>Q128* flies coincide with more PDF^+ and PER^+ LNv soma (particularly the sLNv). In regimes (DD23toDD29, DD29toDD29) and genetic backgrounds (Hsp40 overexpression) that show early-age rhythm rescue (in AW1), the delay in loss of PDF from sLNv also coincides with a decrease in expHTT inclusion load (see exceptions below) and a more extended presence of Diff-enriched LNv. However, there are certain exceptions, such as DDTCtoDD25 and HSP70 overexpression, where a decrease in inclusion load did not follow the early-age restoration of behavioural rhythms; however, the latter did not demonstrate rescue of PDF or PER in the sLNv. Conversely, exacerbation of PDF loss from sLNv by clock-disrupting constant light LL was associated with an increased inclusion load. So, by and large, in these flies,

expHTT inclusions are often predictors of LNv dysfunction and **neurotoxicity**. This result that polyQ aggregation propensity is a reliable predictor of HD-related pathology is supported by a recent study (Drombosky et al., 2018). Furthermore, in this discussion, a reduction in expHTT inclusion load (which in my studies is more often associated with improved LNv functionality) is considered a surrogate marker for improved overall cellular health and a proxy for bolstered cellular proteostasis (Duncan et al., 2015a).

This study shows that a composite set of cellular mechanisms can restore circadian behavioural rhythms in *pdf>Q128,* as shown in Fig 7.2. Restoration of LNv circadian output (PDF in sLNv soma), molecular clock component (PER in the LNv), molecular clock oscillations (PER oscillations in sLNv), and an overall improvement in cellular proteostasis (reduction in inclusion load), as in the case of Hsp40 overexpression, can all contribute to the recovery of early-age circadian activity rhythms. However, it can also happen with the improvement of LNv clock output and proteostasis, but in the absence of a ticking molecular clock as in the case of adult-specific upshift to warm temperatures (DD23toDD29). It can also happen with improvements to LNv clock output and molecular clocks but without improving proteostasis, as in the case of development-specific temperature cycles (DDTCtoDD25). Lastly, behavioural rhythms can surprisingly manifest without rescuing LNv circadian output, molecular clocks, or even likely effects on proteostasis evidenced by marginal effects on expHTT inclusion load (Hsp70 overexpression). However, it should be noted that activity rhythm rescue of *pdf>Q128* by Hsp40, which was more pronounced and long-lasting than all the other strategies, was associated with the most significant improvements of underlying cellular phenotypes, showing that the extent of behavioural rescue depends on the degree of cellular rescue. Ranking next were flies under DD23toDD29, better protected than those under DDTCtoDD25, indicating that a decrease in expHTT inclusion load probably benefits cellular health. Thus, multiple pathways of varying potency can exist to improve circadian rhythm disruptions in neurodegeneration.

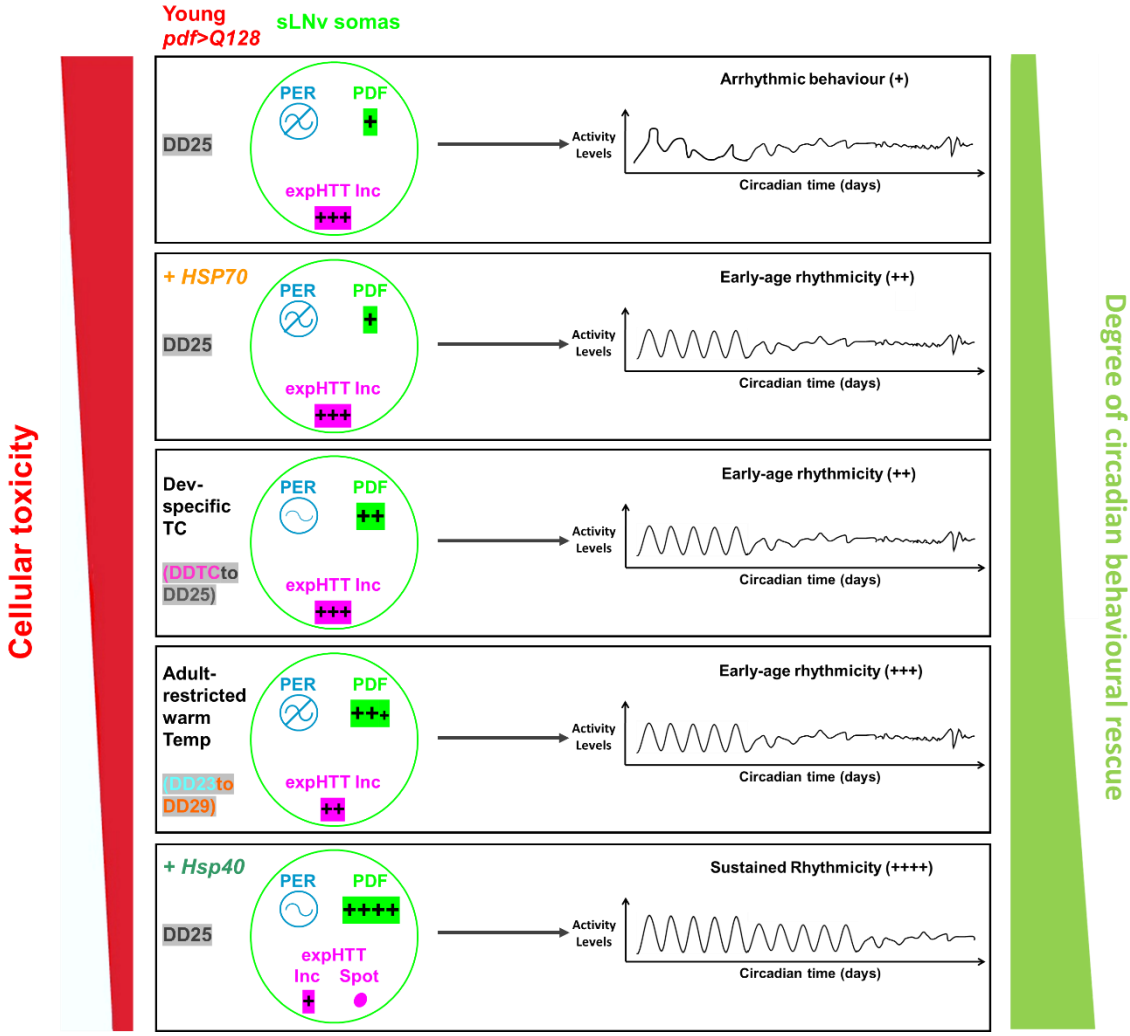

Fig 7. 2 A pictorial representation of the various disease-alleviating strategies established in this study in the increasing order of their ability to provide circadian neuroprotection.

Depicted here are the cellular characteristics of the sLNv soma (left) and the rhythmicity status of locomotor activity behaviour (right) of *pdf>Q128* flies under three different temperature regimes (DD25, DDTCtoDD25, and DD23toDD29) (environmental regimens), as well as the effects of overexpressing Hsp40 or HSP70 in these flies under DD25 (genetic approach). These are arranged in the ascending order of the strategies' effectiveness: in exerting neuroprotection or suppressing neurotoxicity (descending order of neurotoxicity) (red on the left) and in improving behavioural rhythms (green on the right). Most of the details are like in Fig 7.1. The magnitude of + against PDF is based on the mean number of PDF^{+} sLNv soma till 7d of age and its frequency distribution. The behavioural rhythm depictions are approximately based on the percentage rhythmicities across multiple experiments, the extent of activity consolidation and rhythm robustness (for reference, *WT* flies will have a rhythm score of ++++++). The early-age PER oscillations in the sLNv, the complete rescue of PDF in the sLNv, the reduction in inclusion load, and the appearance of a Spot form of expHTT and free-running rhythmic activity that was sustained for an extended duration were evidence of the most effective suppression of expHTT-induced circadian dysfunction and neurotoxicity caused by the overexpression of Hsp40. As is evident here, although several strategies rescue early-age activity rhythms to varying extents, they do so by altering the underlying circadian neuronal features differentially in terms of which features are affected (if any) and the magnitude and duration of effect. These findings suggest overlapping, albeit divergent, mechanisms of circadian rescue.

7.1.4 *Drosophila* Huntingtin, protein context of the polyQ peptide and cellular context in mediating polyQ-induced circadian dysfunction

Other preliminary studies in this thesis have given rise to the following conclusions. *Drosophila* Huntingtin does not mediate circadian activity rhythms or offer neuroprotection to the circadian neurons expressing expHTT. Expression of full-length expanded human HTT or only expanded polyQ peptides in the LNv did not alter free-running rhythms, showing that the protein context around the polyQ and the expHTT protein length influence the extent of circadian alterations in HD. The expression of either polyQ-unexpanded or -expanded MJD protein in the circadian neurons causes behavioural arrhythmicity to varying degrees without changing the number of PDF^{+} LNvs, indicating that cellular settings influence the toxicity of polyQ proteins.

7.1.5 Conclusions on the *Drosophila* circadian neuronal network

The present study also adds nuances to our understanding of the role of LNv and PDF in mediating activity rhythms under DD (free-running condition) and LD. The sLNv are considered, for the most part, the central pacemakers mediating free-running behavioural rhythms (Renn et al., 1999; Grima et al., 2004a; Stoleru et al., 2004; Shafer and Taghert, 2009). This role is orchestrated mainly by PDF in the sLNv. Previous research supported the idea that the rhythm-driving effects of the sLNv via PDF are restricted to sLNv output in the form of oscillations in PDF levels at the sLNv dorsal termini (that likely reflects rhythmic PDF release) and the downstream effect of synchronising other pacemaker neurons to evoke a network-level rhythmic effect on the locomotor behaviour (Nitabach et al., 2006; Fernández et al., 2007a; Wu et al., 2008a; Wu et al., 2008b; Depetris-Chauvin et al., 2011; Gunawardhana and Hardin, 2017). However, later studies challenged this notion (Muraro et al., 2013; Depetris-Chauvin et al., 2014; Gorostiza et al., 2014). In this direction, the current study, using the neurodegenerative expHTT to render sLNv dysfunctional selectively, shows that the rhythm-evoking ability of the sLNv via PDF is disrupted even in the face of sustained PDF oscillations in the dorsal termini and its downstream

synchronising effects. The breakdown of LNv molecular clocks and the loss of PDF from sLNv cell bodies are plausible explanations for why sLNv PDF oscillations are insufficient in inducing behavioural rhythmicity. This study proposes a PDF-oscillation-independent component (POIC) in the sLNv to drive behavioural rhythms. In support of this idea, other studies show the existence of many parallel and compensatory mechanisms (within and outside of the sLNv) involved in eliciting activity rhythms in DD (Gorostiza et al., 2014; Frenkel et al., 2017; Sabado et al., 2017; Bulthuis et al., 2019; Fernandez et al., 2020; Jaumouillé et al., 2021; Nettnin et al., 2021). This study also furnishes evidence for the sufficiency of lLNv PDF in modulating the entrainment of activity rhythms to LD and M-activity and the non-requirement of PER-driven molecular clocks for this behaviour.

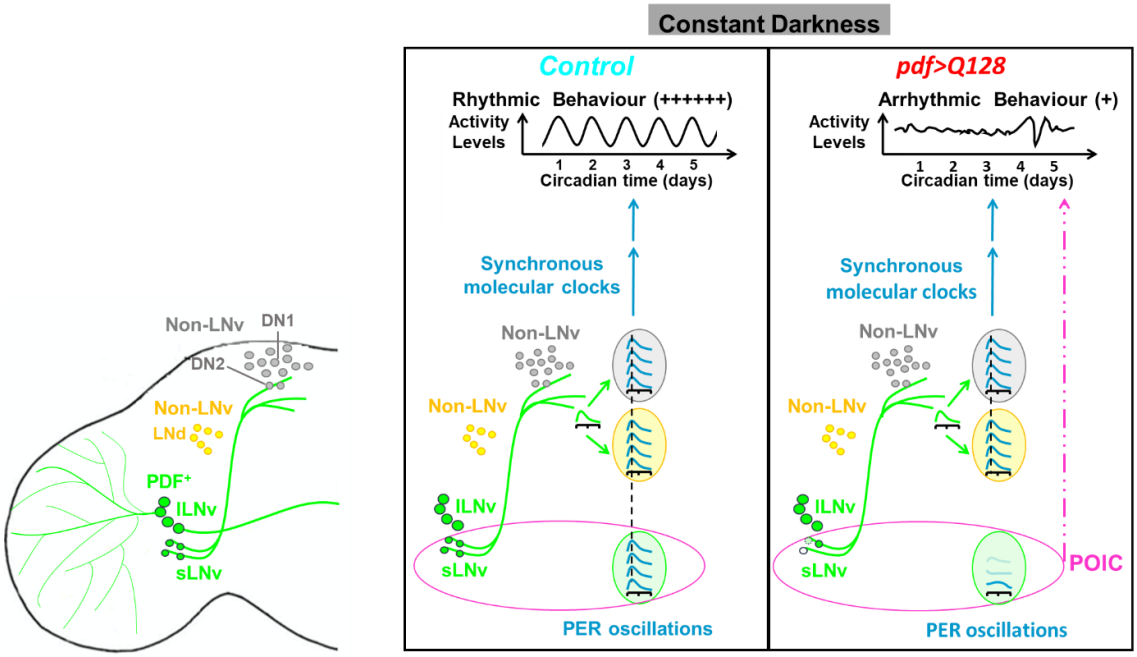

Fig 7.3

Fig 7. 3 A refined understanding of the role of sLNv in driving free-running rhythms: oscillations in PDF levels at the sLNv dorsal projections are insufficient.

A schematic of a hemisphere of the *Drosophila* brain showing the PDF$^+$ LNv and the non-LNv subsets (the LNds, DN1s and DN2s). Green is PDF; blue is PER, and ~ depicts oscillations in their levels over a circadian cycle (PER in the soma of sLNv and non-LNv subsets, PDF in sLNv dorsal projections). Earlier studies concluded that sLNv's rhythm eliciting capacity via PDF was mainly via cyclic accumulation and release of PDF at its termini that then synchronises the downstream non-LNv neurons (*Control*, middle). Even after rendering sLNv dysfunctional (diminished PDF and abolishment of PER oscillations in the sLNv soma) using expHTT (HTT-Q128) (*pdf>Q128*, right), the PDF in the sLNv termini continues to not only accumulate rhythmically in DD but also synchronise

the molecular clock oscillations between the non-LNvs. Despite this functional transmission, the *pdf>Q128* flies were behaviourally arrhythmic, leading to the proposal of an alternate pathway for communicating time information from the sLNv to motor centres via PDF: a PDF-oscillation independent component (POIC).

This study also challenges the centrality of PER-driven molecular clocks in mediating free-running behavioural rhythms as there are instances of restoration of behavioural rhythmicity in DD in the absence of PER oscillations in the LNv (*pdf>Q128* in DD23toDD29, *pdf>Q128* overexpressing HSP70 and middle-ages of *pdf>Q128* overexpressing Hsp40). The study also shows that the mere presence of PDF (arrhythmic *pdf>Q128*) or oscillating PER in the sLNv (*pdf>Q128* in DD23) does not guarantee behavioural rhythmicity, signifying the overall health and LNv functionality, not restricted to PDF and PER, in mediating activity rhythms. Even more startling is the result of early-age rhythm restoration on overexpressing HSP70 in *pdf>Q128* without the rescue of LNv PDF or PER. These findings question the centrality of canonical molecular clocks and PDF in the sLNv mediating free-running rhythms and suggest other compensatory clock mechanisms in play (see Chapter 2, Discussion). This study's results support the consensus that the circadian clock neuronal network is a distributed network of mutually coupled multiple oscillators. In the face of impairment of the canonical PDF^{+} LNv pacemakers, other pacemakers compensate for driving free-running rhythms, at least for a limited duration (Top and Young, 2018).

The results from the various development-specific temperature cycles suggest that an intervention like temperature with cell-autonomous, global, organismal effects can mediate free-running rhythms post-removal of the time cue by potentially impacting the entire circadian clock network. Depending on the temperature modality, LD during development has different effects on the activity rhythms in adults: under developmental temperature cycles, it opposes rhythm rescue (arrhythmicity under LDTCtoDD25); under constant temperature, adult-restricted temperature downshift and adult-restricted temperature upshift, it follows temperature effects (absence of rhythms in LD23toDD23, LD25toDD25, and LD29toDD23; rhythm rescue in LD29toDD29 and

LD23toDD29). These results raise several questions about context-dependent light and temperature interactions in the *Drosophila* circadian system.

7.1.6 Benefits and limitations of using a *Drosophila* model

Given that HD is monogenic, it has been reasonably straightforward to model across various systems. The versatility and genetic tools in *Drosophila*, ease of use for genetic screens, and well-studied and conserved circadian system make the fly system an obvious choice to screen for modifiers of HD-induced circadian arrhythmia. The fly's short lifespan also allowed us to track pathological changes with age, a key feature in the study of progressive neurodegenerative diseases. A significant advantage of targeting a neuronal circuit *in vivo* that controls an organismal behaviour like the activity/rest rhythms is the ability to probe and intervene at various levels of regulation: molecular, cellular, neuronal circuitry and behavioural. Since the levels are functionally associated, better cause-effect inferences, rigorous testing of the modifying treatment and proof-of-principle evaluations can be made.

Our assays were confined to a subset of critical circadian neurons, cellular markers, and circadian activity/rest behaviour. Studying other circadian physiological rhythms, health markers, and the biochemistry of mutant HTT in the circadian context would help get a broader understanding of disease pathology. There is variability in the extent of circadian disturbance in HD mice models, and chaperone treatments have differential effects on mice HD pathology, making the study of the effect of chaperones on the mammalian clockwork in neurodegeneration a worthwhile endeavour. Further, since *Drosophila* are endotherms, while humans are poikilothermic mammals, a detailed study of the short-term and long-term effects of temperature-based interventions while minimising the side effects in mammalian models will be helpful. Considering the fly system's relative simplicity and low redundancy, investigating environment-based and chaperone interventions on HD-induced circadian dysfunction in mammalian systems like rodents and sheep will provide more excellent clinical traction.

7.2 SCOPE FOR FUTURE WORK

This is a study of the circadian disturbances and associated neurodegenerative phenotypes due to the expression of expanded *Huntingtin*, the causative gene for Huntington's Disease, in a subset of the *Drosophila* circadian neurons. Many meaningful, engaging, and valuable findings have been made throughout this study that open much potential for further research. These can be divided into those to address immediate and more proximate questions and those in the broader context of circadian function in neurodegenerative diseases. The *Drosophila* circadian model described here can address several other neurodegenerative disease-relevant questions. The environmental and genetic modifiers of HD-associated circadian dysfunction and neurotoxicity emerging from this study are translationally relevant to test in clinically relevant models and explore chronotherapeutics in the larger context for NDs and circadian rhythm disruptions.

For starters, more experiments could assist in validating some of the findings from this study and address the mechanistic specifics. Here are a few exciting leads to pursue to resolution. The mechanisms of PER and PDF loss in sLNv by expHTT expression, the status of rhythms in sLNv DP arbours in the *pdf>Q128* flies, the biochemical nature of expHTT inclusions, the detrimental effects of light *per se* exacerbating the cellular neurotoxic phenotypes, the effect of light duration, particularly continuous light, independent of its clock-disrupting effects on the HD cellular features, developmental light's differential effect on the rhythm rescue with developmental temperature cycles, but not temperature upshift, the role of CRY in interfering with developmental TCs and contributing to developmental LD's countering of rhythm rescue by TCtoDD25, the contribution of blue light to the detrimental effects of light (e.g. use of filters to block or enhance blue light component, or genetic perturbation of pathways mediating response to blue light) (Hall et al., 2018; Escobedo et al., 2022; Jauregui-Lozano et al., 2022; Vandenberghe et al., 2022), test the role of Hsps and autophagy in the developmental-TC-mediated rhythm rescue, the mechanism of warm-temperature mediated activity consolidation, whether it is genuinely circadian and involves activity levels and (or) metabolic alterations, test the differential effect of adult-specific warm temperatures *vs.* developmental temperature cycles on *Drosophila* circadian network coupling and responses, assess the relative contributions of clock-mechanisms and 12 hours of

warm temperatures in the developmental TC's rescue by using low amplitude TCs of cool/ambient temperature cycles, combining developmental TCs and adult-restricted warm temperatures to see if a longer-lasting rescue can be obtained, spot-like expHTT's localisation, biochemical constituents and role in conferring cellular protection, and pathways and partners of Hsp40 in mediating circadian recovery like autophagy and proteasomal pathways and whether the circadian rescue by Hsp40 is dependent on HSP70 and whether circadian protection by Hsp40 also extends to other circadian rhythms like feeding and metabolic rhythms. Exploring the effects of light intensity, duration, frequency, and spectral composition on circadian neurodegenerative phenotypes, and for temperature-based interventions, the modality, site, dosage/magnitude/intensity, duration, frequency, and site of application, age of intervention, the effect of gender, and pre-existing conditions, in combination with other treatment modalities, while minimising the side effects will aid in their optimisation. The other aspect is to investigate possible strategies to achieve an enhanced circadian rescue that is long-lasting (over time), stronger (in terms of intensity, e.g., rhythm robustness) and at multiple levels of organisation (molecular, neuronal, circuit and behavioural levels). To do this, one may investigate combinatorial techniques such as Hsp40 overexpression with adult-specific temperature upshift or either of the two with upregulation of proteasomal or autophagic pathways. One could also test the ability of pharmacological mimics of Hsps or warm temperatures in mediating circadian rescue, as this will have a faster translational potential. The potential of the circadian *Drosophila* model described here to screen for pharmacological agents and small molecules that modify circadian dysfunction is immense and unexplored. In neurodegenerative disorders, other circadian-modifying therapies such as time-restricted meals, sleep disruptions caused by somniferous and stimulant drugs, physical activity, various phototherapy modalities, and photobiomodulation can be investigated.

This study has uncovered Hsps as a potential intermediator between the circadian and neurodegenerative axes. Though other proteostasis players directly influence circadian clocks, the role of Hsps in circadian function is relatively unexplored. There could also exist other intermediate crosstalk partners between Hsps and circadian clock components. One could also

investigate other potential pathways involved in the circadian-neurodegenerative interface, like the redox pathway, mitochondrial function, energy metabolism, autophagy, and transcription.

The result of the greater vulnerability of sLNv to expHTT than lLNv also provides an excellent system to investigate the possible reasons for differential susceptibility in HD, a pressing question in the field. Studies from the lab suggest that lLNvs are more competent in tackling stressors like aggregate-prone proteins (Sharma et al., 2023) and that the ~7d developmental time difference between the sLNv and the lLNv or the developmental stage from which expHTT expression begins, do not contribute to their differential susceptibility to the neurotoxic effects of expHTT (Ganguly, 2015). The presence of sLNv dorsal projections, despite the absence of PDF^+ sLNv cell bodies, challenges the axonal dying back mechanism, and this disease-relevant process can be pursued. Another extremely intriguing discovery is the presence of expHTT spots upon Hsp40 overexpression in the LNv, which offers an excellent opportunity to investigate the potential presence and involvement of protein sequestrosomes or other such spatially sequestered quality control sites in *Drosophila* as a cellular strategy to isolate aggregate-prone proteins and decide their fate towards the restoration of proteostasis. The emerging role of non-cell autonomous mechanisms, like glial function and cell-to-cell transmission of aggregate-prone proteins, can be investigated in this system to glean mechanistic insights. Also, given that glial dysfunction is integral to HD (Liévens et al., 2008; Tamura et al., 2009; Besson et al., 2010; Wilton and Stevens, 2020), and in flies, glial cells physiologically modulate circadian neuronal circuitry and behaviour (Ng et al., 2011; Ng et al., 2013; Jackson et al., 2015), clocks in the glia are essential for the circadian structural plasticity of the sLNv terminals (Herrero et al., 2017; Damulewicz et al., 2022a) and those in the epithelial glia regulate amplitude of the circadian remodelling (Damulewicz et al., 2022a), it would be interesting to see the effect of glial expression of expHTT on the circadian behaviour.

The findings here also raise broader issues about *Drosophila* circadian biology, such as how the pacemaker sLNv DP's PDF level circadian oscillations are controlled in the absence of known central clock protein PER (e.g. local translation, non-canonical clocks and glial clocks), the mechanisms underlying activity rhythms in the absence of core circadian proteins (restoration of

activity rhythms in the absence of PER and PDF in sLNv soma upon co-expression of HSP70 with HTT-Q128 in the LNv), how warm temperatures affect the activity consolidation of rhythms, and why adult-specific temperatures are critical for rhythm improvements. They also highlight the necessity to assess other markers of LNv circadian health and functionality, like rhythms in sLNv axonal complexity, synaptic connections and other neurotransmitters and neuropeptides involved in this system and the circadian field. Considering the temperature-regime-dependent differential effects of lighting conditions during development upon the activity rhythms as adults, it is crucial to investigate light and temperature interactions in varying environmental, genetic, and developmental-stage-specific contexts, evaluate the relative strengths of zeitgebers and determine how these factors affect circadian neuronal outputs and rhythmicity. There is also scope for expanding the relevance of these studies to a broader range of health markers and a more comprehensive array of clinically relevant organismal circadian phenotypes like metabolic and feeding rhythms, sleep, redox cycles, and inflammatory response. Scouting and optimising a few other neuronal health markers to expand the range of neurodegenerative outputs affected would improve the versatility of this system and answer a broader range of questions. For example, this expansion would be helpful to assess the damaging effects of white light and its blue light component on cellular parameters like mitochondrial function, redox stress, bioenergetics, and inflammatory response. The findings here also point to the potential of this model as a testing ground for the hormetic and cross-protective properties of various modalities (stressors) in disease therapeutics, whose effects extend beyond neurodegenerative progression to a wide range of diseases and circadian alterations therein.

Some of the common overlapping molecular and cellular mechanisms of many NDs, including the polyQ family of diseases to which HD belongs, include mitochondrial dysfunction, oxidative stress, transcriptional dysregulation, overwhelmed proteostasis, impairments to the proteasomal and autophagic degradation pathways, excitotoxicity, neuroinflammation, and the presence of protein aggregates (Argueti-Ostrovsky et al., 2021). These diseases also share similarities in their manifestation and progression: greater susceptibility of select brain regions/ neuronal subsets, typical middle-age onset, worsening of symptoms with age, and circadian and sleep disorders,

often early symptoms. Given this convergence, the findings of this study about circadian dysfunction and neurotoxicity in HD are relevant in improving our understanding of circadian disturbances in NDs in general. The mitigators of circadian neurodegenerative symptoms of HD discovered in this study, Hsp40, warm temperatures, development-restricted temperature cycles, and their aggravator, light, may also affect other NDs. However, given the role of cellular and protein context in disease manifestation and severity in ND-induced circadian arrhythmicity (as seen in Chapter 6), such predictions need to be tested case by case. The findings of this study will have better clinical traction if their mammalian counterparts are tested for circadian rehabilitation in HD models of mice, sheep, or pigs. For example, the possibility that the finding of warm temperatures being beneficial to *Drosophila* circadian rhythms translates to improving sleep and circadian dysfunction upon timed exposure to warm sauna in mammals could be explored. Alternatively, whether avoiding constant illumination or timed-light exposure by filtering out the blue light improves neurodegenerative phenotypes in mammals. Eventually, testing if mammalian HSPs can improve ND-induced circadian deficits will be crucial. The HD circadian model developed here replicates the *in vivo* impaired central clock and circadian outputs and behavioural arrhythmicity found in HD mice. Such parallels between the model systems suggest the possibility of finding genetic counterparts and environmental interventions that could alter circadian disturbances in mammals, including human primates.

This study's scope is considerably widened by the model developed here, which offers a broad framework for investigating the general relationship between circadian function and neurodegeneration and addressing pressing problems concerning a sizable family of neurodegenerative diseases that share a common underlying pathology. These could include proof-of-concept studies, disease modifier screens (genetic, pharmacological, environmental), identifying ways to improve circadian function that also improve neurodegeneration and candidates involved in the crosstalk between the two systems, examining the differential susceptibility of neurons (sLNv over lLNv), the cell-to-cell transmission of mutant proteins, an emerging concern in NDs, investigating combinatorial therapy, and addressing neuro-developmental aspects of NDs, among others.

7.2.1 Circadian rhythm disruptions and treatments

Several physiological, social, and environmental scenarios lead to CRDs (Eisenstein, 2013; Baron and Reid, 2014; Roenneberg and Merrow, 2016; Sletten et al., 2020; Vetter, 2020). Physiological factors include clock gene mutations, disease conditions and ageing. Social and occupational factors include transmeridian travel, shift work and meal timings. Human circadian physiology is particularly sensitive to short-wavelength-enriched light from light-emitting electronic devices like cell phones, tablets, and laptops. Environmental conditions can be natural, like short day length, or artificial, like artificial light in the evening and at night (ALAN) (especially blue light), continuous bright light exposure, particularly at the wrong time, and constant/untimely exposure to these lights (Hatori et al., 2017; Wahl et al., 2019). The latter category of exposure to aberrant lighting and other rhythm-disturbing habits like irregular meal timings and sleep/wake timings often accompany contemporary lifestyles and are emerging as frontrunners to poor circadian hygiene. Light during the day, remarkably blue light and preferably sunlight, is essential and improves alertness, mood, and cognitive function (Vetter et al., 2019; Wirz-Justice et al., 2021; Fernandez, 2022; Wong and Bahmani, 2022). However, aberrant lighting, like ALAN, suppresses the production and release of the darkness hormone melatonin in humans and rodents, disrupts clock gene expression and affects cellular homeostasis. Blue light reduces melanopsin expression in ipRGCs; chronic light exposure phase shifts circadian rhythms, increasing screen time results in shorter sleep duration and poor sleep efficiency; e-book reading before bedtime increases sleep latency (the time to fall asleep) and delays the circadian clock; the overall acute effects of circadian misalignment are suppressing melatonin levels at night, altered phasing of circadian rhythms, poor sleep levels and quality, increased daytime sleepiness, reduced alertness and performance, hypertension and altered inflammatory response (Blume et al., 2019; Wahl et al., 2019; Caliandro et al., 2021; Ziólkowska et al., 2022; Verma et al., 2023). These lifestyle habits leading to misalignment between internal circadian rhythms and external light/dark and feeding cycles not only lead to sleep and circadian rhythm disruptions (SCRDs) but are also directly and indirectly (via CRDs) detrimental to healthspan, increasing the risk of premature ageing, metabolic syndromes, auto-immunity, tumorigenesis, cancer, cognitive impairment, and

psychiatric illness (Xie et al., 2019; Woller and Gonze, 2021; Roenneberg et al., 2022). Thus, there is a pressing need to address CRDs and implement strategies and systems to streamline lifestyle habits and maintain good circadian hygiene. Further, given the pivotal role of circadian health in influencing ND progression and outcomes, it is prudent to integrate and implement circadian-maintaining regimens in treating NDs. Suppressing circadian and sleep disruptions would be not only helpful to the patients by serving in a palliative capacity and in slowing down NDs (or at least suppressing their escalation) but also bring much-needed relief to caregivers, especially where restoration of circadian rhythms like sleep/wake cycles are concerned.

Non-invasive, non-pharmacological interventions to enhance circadian hygiene include bright light therapy (timed exposure to bright light: full spectrum or blue-enriched), avoidance of light at inappropriate times, scheduled sleep/wake times and meal times, time-restricted feeding (restricting food intake to a small window of time) and cognitive behavioural therapies (CBT) like scheduled exercise, scheduled outdoor exercise that strengthens natural zeitgebers, stimulus control and relaxation techniques (Schroeder and Colwell, 2013; Zee et al., 2013; Ballesta et al., 2017; Lee et al., 2021; Ruan et al., 2021; Voysey et al., 2021b). Pharmacological interventions can achieve circadian realignment by entrainment/correct phasing of circadian rhythms and management of sleep/wake timing and efficiency. Medications include timed low-dose melatonin and melatonin agonists, medications targeting CK1δ, REV-ERBs, RORs, CRY, glycogen synthase kinase 3 (GSK3) and Sirtuin1, and natural compounds modulating clock function (drugging the clock) like resveratrol, nobiletin, and curcumin, drugs that promote alertness, such as caffeine, modafinil, and armodafinil, as well as drugs that promote sleep, such as GABA-modulators (benzodiazepines, Z-drugs), sedating antihistamines (diphenhydramine, hydroxyzine), antidepressants (amitryptiline, trazodone, mirtazapine), and orexin antagonists (Schroeder and Colwell, 2013; Zee et al., 2013; Chang and Kim, 2020; Lee et al., 2021; Ruan et al., 2021; Voysey et al., 2021b).

Preliminary studies with chronotherapy in patients of ND have shown promising results, a few examples of which are provided here. Phototherapy improved cognitive and noncognitive symptoms and sleep in dementia, AD and PD patients (Liu et al., 2020; Zhu et al., 2022). In PD

patients, a 1h light bright light pulse before bedtime improved both motor and non-motor symptoms like insomnia, anxiety, and depression (Willis et al., 2012; Martino et al., 2018; Fifel and Videnovic, 2019). In AD patients, too, 1h of blue-enriched light therapy in the morning positively affected sleep and cognition (Kim et al., 2021b). Stimulant modafinil improved daytime sleepiness in HD and PD patients and cognitive function only in PD (Adler et al., 2003; Blackwell et al., 2008; Kim et al., 2021b). Melatonin improves sleep quality in AD and PD patients (Dowling et al., 2005; Mayo et al., 2005; Sumsuzzman et al., 2021); however, it adversely affects mood, which can be counteracted when administered with bright-light therapy (Riemersma-van der Lek et al., 2008). The use of sedative antidepressant doxepin along with CBT improved cognitive and sleep outcomes in a PD cohort (Rios Romenets et al., 2013). Physical exercise, specifically aerobic, mitigates neuropsychiatric symptoms in the elderly with AD (Fukushima et al., 2016; Mendonça et al., 2021). New methods of non-invasive brain stimulation techniques are being developed: repetitive transcranial magnetic stimulation (rTMS), transcranial direct-current stimulation (TDCS) and acoustic stimulation to improve sleep (Voysey et al., 2021b; Shen et al., 2023). Photobiomodulation (PBM), which uses red to infrared light energy from a laser or LED to control biological effects when given directly to the neurons (e.g., transcranial) or indirectly to distant body areas (e.g., thigh or abdomen), is another therapy approach being researched against NDs (Hamblin, 2016; Hong, 2019; Bathini et al., 2022; Moro et al., 2022).

In this direction, the present study shows the effectiveness of temperature regimes in improving circadian dysfunction and neurotoxicity in an HD fly model. These results strongly support the addition of temperature-based modalities to the arsenal of environmental interventions as a complementary strategy to mainstream healthcare in combating neurodegeneration and associated CRDs. Some advantages of environment-based interventions are their relative ease of adapting to daily lifestyle, cost-effectiveness, minimal side-effects, relative safety, and ease of individual-centric customisation. Optimisation of environmental interventions to complement conventional therapeutics will facilitate the development of a multimodal approach to accelerate circadian

realignment under various pathologies. As uncovered in this study, the potential for Hsps as circadian-rhythm-bolstering agents is promising for future research.

7.2.2 Time will tell: Chronotherapy in mainstream healthcare

These are exciting times for chronotherapy because of the growing interest in how circadian health affects the aetiology of diseases and general well-being. However, efforts must be made to optimise chronotherapy and integrate it with mainstream medicine. One has to start at the grassroots with a clear definition of terms in the field. For example, circadian disruption is an umbrella term. It could broadly signify a loss of rhythms, a decline in rhythm amplitude, internal desynchronisation between different body clocks, or circadian misalignment arising from a mismatch between the internal biological clock and external clocks due to personal, social, or professional demands (Kramer et al., 2022). As well-highlighted in the excellent review by Céline Vetter (Vetter, 2020), in order for circadian research to advance as translational science, we need to differentiate between circadian rhythms from daily physiological and behavioural patterns (Broussard et al., 2017b), understand the interactions between various external and internal time cues that bring about organismal synchronisation, choose appropriate metrics to systematically monitor and address the varied facets of circadian disruption, capture the disruption at all levels under the varying zeitgeber landscape, carry out evidence-based classification of the CRDs, have comprehensive and scalable quantifications of circadian disruptions under various settings graduating to randomised clinical trials, carry out long-term studies with repeated assessments, identify predictive biomarkers of CRDs and have a consensus in the field to define a set of measures to study CRDs and their acute and chronic effects on healthspan.

Further, there is a requirement for evidence-based guidelines and recommendations for pathology and symptom-specific circadian medicine, for which research elucidating circadian function and dysfunction in disease and mechanisms to circadian rescue, followed by randomised controlled clinical trials, are necessary (Kramer et al., 2022). Optimising existing non-pharmacological and pharmacological therapies and research into novel therapeutic strategies will prove beneficial

against circadian dysfunction in patients with NDs. The long-term goal is to strive for person-centric precision circadian medicine, considering individual chronotypes.

Chronotherapy is beneficial not only for CRDs and NDs but also in mainstream healthcare, as it is also essential for enhancing drug efficacy and lowering drug toxicity by figuring out the best time to administer the drugs (clocking the drugs), as many drugs exhibit time-of-day effects or toxicity (Ballesta et al., 2017; Ruben et al., 2019; Bicker et al., 2020; Lee et al., 2021; Walton et al., 2021). Chronopharmacology for precision and personalised medicine is now exploring various treatments like treatment of neuropsychiatric, cardiovascular, and metabolic disorders, inflammation and auto-immune diseases, COVID-19, vaccination and chemotherapy. Further bringing awareness to circadian-disrupting practices in various settings like healthcare (hospitals, clinics, ICUs and care homes), professional (classrooms, offices, industry), social (hotels, shopping centres) and domestic venues (homes) (Houser and Esposito, 2021) will help re-think standard lighting practices and move towards a more human-centric lighting concept (Houser and Esposito, 2021; Stefani and Cajochen, 2021). In healthcare settings, for example, addressing poor circadian practises like irregular lighting (inadequate lighting during the day or light at night), medication at any time of day or night, waking up for medication and tests, nighttime noise, enforced continuous activity 24 hours a day, and non-optimal time of surgery and drug administration (Cederroth et al., 2019; Vandenberghe et al., 2022) will minimise damages from such avoidable practises, benefiting the patients, their families, and the healthcare system. Given a world of increasing light pollution, rampant screen time, and irregular meal timings, an awareness of our circadian rhythms, the effects of contemporary lifestyle in disrupting rhythms and health spans and adapting strategies to minimise them is the need of the hour. Similarly, people are losing sleep in the current climate of intense competition, social media exposure, screen time, school, work and other social pressures. Hence, as a society, we must prioritise and encourage improved sleep and circadian hygiene in the here and now and emphasise and invest sufficiently in chronotherapy and sleep research.

APPENDIX A: Table for Chapter 2

Table 2. 1 The extent of variation in PER intensity within a neuronal group in expHTT-expressing flies is not greater than controls.

	pdf>Q0	*pdf>Q128*
LNd		
CT23	102.81±28.21	132.15±16.6**
CT5	80.6±7.44	116.91±9.26**
CT11	34.41±8.73***	0
CT17	113.45±12.9	124.26±10.69
DN1		
CT23	79.93±7.13	99.98±9.08*
CT5	58.85±3.04	55.97±3.77
CT11	40.58±3.73	44.76±3.46
CT17	56.38±5.81	57.93±3.4

The table shows the within-neuronal group mean ± standard deviation in PER intensity for LNd and DN1 across time points in DD for *pdf>Q128* and its control *pdf>Q0*. Standard deviation within LNd for *pdf>Q128* is significantly lower than control at CT23, CT5 and higher only at CT11 when in *pdf>Q0*, PER is undetectable. The standard deviation within DN1 for *pdf>Q128* is significantly lower than *pdf>Q0* at CT23. *p<0.05, **p<0.01, ***p<0.001.

APPENDIX B: Tables for Chapter 3

Appendix B

Table 3. 1 Percentage of rhythmic flies in DD for all the genotypes raised in four regimes across AWs.

% Rhythmicity						
	DD-reared			LD-reared		
	AW1	AW2	AW3	AW1	AW2	AW3
pdf>Q0	96.78	93.103	89.66	93.55	93.55	100
pdf>Q128	6.45***	3.33***	0*	24.24***	6.7***	2***
Q0	93.55	96.77	93.1	100	100	96.77
Q128	96.67	96.67	93.1	96.77	90.32	90.32
pdfGal	100	83.87 $	77.78	100	100	100
w1118	100	96.55	76	100	100	100
	SN-reared			LL-reared		
	AW1	AW2	AW3	AW1	AW2	AW3
pdf>Q0	100	100	100	100	100	100
pdf>Q128	10***	0***	5.88***	0***	1***	11.11***
Q0	100	100	100	100	100	96.77
Q128	90.63	96.55	95	96.88	96.88	96.88
pdfGal	100	100	100	100	100	100
w1118	100	100	100	100	100	100

* indicates a significant difference of *pdf>Q128* from other genotypes: * at $p<0.05$ and *** at $p<0.001$.
$ indicates a difference between AWs for a genotype at $p<0.05$.

Appendix B

Table 3. 2 Mean robustness of activity rhythms (±SEM) in DD for all the genotypes raised in four regimes across AWs.

	Robustness of rhythm (a.u)					
	DD-reared			LD-reared		
	AW1	AW2	AW3	AW1	AW2	AW3
pdf>Q0	210.9±10.2^{a}	202.74±9.5^{ac}	183.46±10.7^{ab}	208.86±7.2^{b}	225.92±8.9^{b}	190.95±9.4^{b}
pdf>Q128	133.39±3.4	103.73	NA	127.58±9.8	118.63	114.37±15.8
Q0	254.13±7.9^{b}	240.76±10.2^{b}	$ 200.47±11.9^{a}	$ 219.57±7.6^{a}	$ 231.39±7.3^{b}	191.6±9^{b}
Q128	190.62±8.3^{a}	$ 171.3±8.4^{ac}	161.08±7.5^{ab}	191.52±7.16^{b}	184.24±8.5^{a}	$ 156.06±6^{a}
pdfGal	190.4±8.1^{a}	189.41±9.5^{bc}	178.97±12.4^{ab}	205.24±6.8^{b}	226.53±8.3^{b}	191.73±9.9^{a}
w1118	185.01±8.9^{a}	182.86±10.7^{ac}	$ 144.56±9.4^{b}	250.44±9.3^{a}	$ 230.55±7.7^{b}	$ 172.99±8.5^{a}
	SN-reared			LL-reared		
	AW1	AW2	AW3	AW1	AW2	AW3
pdf>Q0	271.71±7.1	249±7.8	279.1±13.4	223.74±6.4^{a}	$ 232.44±7.4^{b}	204.17±8.3^{b}
pdf>Q128	149.91±14.5	NA	111.41	NA	120.76	121.73±18.9
Q0	289.29±8.7	261±9.5	259.8±20	$ 248.01±10.2^{a}	228.82±8.9^{a}	199.27±8.6^{a}
Q128	205.22±9.9	183.83±8	194.99±13.1	$ 187.08±5.6^{b}	174.65±6.9^{b}	143.87±5.5^{b}
pdfGal	238.93±8.1	224.04±8.7	250.7±13.6	184.45±6.4^{b}	208.48±8.1^{b}	187.61±7.2^{bc}
w1118	273.74±13.9	225.14±10.6	207.5±19	$ 239.91±7.5^{a}	$ 216.62±7.3^{b}	170.12±6.3^{ac}

Different letters indicate statistically significant age-matched differences between genotypes at $p<0.05$. $ indicates significant differences of a given AW from indicated ones or all other AWs for a genotype at $p<0.05$. *pdf>Q128* was not included for statistical tests as most were arrhythmic. NA, not applicable, as all flies were arrhythmic; au, arbitrary units.

Table 3. 3 Mean activity rhythms periods (±SEM) in DD for all the genotypes raised in four regimes across AWs.

	Period (h)					
	DD-reared			LD-reared		
	AW1	AW2	AW3	AW1	AW2	AW3
pdf>Q0	24.64±0.1^{a}	24.83±0.12^{a}	24.9±0.11^{a}	24.77±0.07^{a}	24.71±0.07^{a}	24.81±0.07^{a}
pdf>Q128	24.67±2	23.67	NA	24.24±0.4	23.67	24±0.33
Q0	23.85±0.05^{bc}	23.8±0.09^{bc}	23.74±0.09^{bd}	$ 24.06±0.06^{be}	$ 23.66±0.04^{ce}	23.47±0.07^{ce}
Q128	23.85±0.06^{bc}	24.17±0.21^{bc}	23.94±0.12^{bc}	23.85±0.05^{ce}	23.86±0.08^{bde}	23.91±0.09^{bde}
pdfGal	24.06±0.15^{c}	24.18±0.11^{c}	24.35±0.12^{ac}	24.25±0.05^{bd}	24.11±0.06^{bd}	24.41±0.11^{abd}
w1118	23.7±0.1^{b}	23.6±0.1^{b}	23.29±0.14^{bd}	$ 23.78±0.04^{c}	$ 23.4±0.05^{c}	23.2±0.05^{c}
	SN-reared			LL-reared		
	AW1	AW2	AW3	AW1	AW2	AW3
pdf>Q0	24.27±0.05^{a}	24.2±0.07^{b}	24.65±0.07^{a}	25.01±0.09^{a}	24.98±0.07^{a}	25.15±0.08^{a}
pdf>Q128	24.11±0.22	NA	23.33	NA	23.67	24.5±0.59
Q0	23.67±0.02^{b}	23.63±0.04^{a}	23.67±0.1^{bd}	23.63±0.04^{b}	23.63±0.05^{b}	23.69±0.07^{b}
Q128	23.81±0.05^{b}	23.98±0.08^{b}	23.95±0.11^{bc}	23.81±0.05^{b}	23.74±0.05^{bc}	23.72±0.06^{b}
pdfGal	24.23±0.04^{a}	$ 23.94±0.06^{b}	24.39±0.08^{ac}	24.41±0.06^{a}	$ 24.05±0.07^{c}	24.51±0.1^{a}
w1118	23.68±0.05^{b}	23.5±0.06^{a}	23.52±0.07^{bd}	23.73±0.04^{b}	$ 23.57±0.06^{b}	23.48±0.06^{b}

Different letters indicate statistically significant age-matched differences between genotypes at $p<0.05$. $ indicates significant differences of a given AW from indicated ones or all other AWs for a genotype at $p<0.05$. *pdf>Q128* was not included for statistical tests as most were arrhythmic. NA, not applicable, as all flies were arrhythmic.

Appendix B

Table 3. 4 Mean daytime activity levels (±SEM) under LD for all the genotypes raised in four regimes across AWs.

Daytime activity counts						
	DD-reared			LD-reared		
	AW1	AW2	AW3	AW1	AW2	AW3
pdf>Q0	$ 800.5±42.9^{b}	$ 557±27.8^{b}	405.36±25.3^{b}	$ 696.58±42.7	$ 436.97±27.7	341.51±25.1^{a}
pdf>Q128	$ 623.12±27.5	$ 362.56±23.1^{a}	229.84±21.9^{a}	$ 633.45±34.8	$ 387.94±28.1	291.41±27^{a}
Q0	$ 713.88±35.3	$ 505.1±22.2^{b}	412.44±19.7^{b}	$ 790.93±37.5	$ 527.41±31.6	396.62±25.7^{a}
Q128	$ 850.4±31.4	$ 584.8±23.3^{b}	430.25±18.9^{b}	$ 730.63±29.9	$ 403.88±25.6	207.09±25.3^{b}
pdfGal	$ 696.22±33.2	$ 409.22±22.3^{a}	337.29±23.5^{a}	$ 857.88±60.1	$ 456.41±38.1	314.38±32.7^{a}
w1118	$ 901.04±48.7	$ 578.9±33.9^{b}	444.04±26.9^{b}	$ 609.87±37.3	$ 315.39±23	239.76±22.9^{a}
	SN-reared			LL-reared		
	AW1	AW2	AW3	AW1	AW2	AW3
pdf>Q0	$ 568.51±29.1	$ 426.12±27.2	243.01±23	$ 688.43±38	$ 424.98±28.5	350.12±24.8
pdf>Q128	$ 647.19±33.1	$ 411.74±21.5	317.89±21.7	$ 670.98±34.1	$ 379.47±22.2	243.7±25.4
Q0	$ 810.14±46.5	$ 549.72±29.5	335.53±19.9	$ 717.5±31.9	$ 477.28±31.1	382.19±28.9
Q128	$ 743.25±56.3	$ 475.25±49.6	288.99±23.6	$ 806.7±35.5	$ 532.35±28.7	362.56±24.2
pdfGal	$ 709.19±38.4	$ 520.66±30.1	379.63±23.7	$ 688.52±35.1	$ 400.4±22	313.06±23.2
w1118	$ 806.2±48.5	$ 695.91±44.3	521.75±33.6	$ 696.33±31.7	$ 420.2±22.4	369.9±44.8

Different letters indicate statistically significant age-matched differences between genotypes at $p<0.05$. $ indicates significant differences of a given AW from indicated ones or all other AWs for a genotype at $p<0.05$.

Appendix B

Table 3. 5 Mean nighttime activity levels (±SEM) under LD for all the genotypes raised in four regimes across AWs.

Nighttime activity counts						
	DD-reared			**LD-reared**		
	AW1	**AW2**	**AW3**	**AW1**	**AW2**	**AW3**
pdf>Q0	$ 466.09±34.4	$ 317.95±28.5	207.28±18.3	$ 586.05±43.9^{abc}	$ 348.53±28.8^{ab}	256.68±27.7^{a}
pdf>Q128	$ 571.42±33.1	$ 280.01±29.5	123.74±24.8	$ 648.98±45.1^{c}	$ 367.34±38.9^{ab}	160.15±26^{ab}
Q0	$ 656.54±37.2	$ 429.67±25.5	284.06±19.3	$ 575.33±36.8^{abc}	$ 376.31±30.9^{b}	260.91±28.6^{ac}
Q128	$ 650.67±33.3	$ 450.81±35.1	254±24.5	$ 629.42±39.7^{a}	$ 338.84±35.5^{ab}	132.24±18.7^{b}
pdfGal	$ 511.01±32.9	$ 290.4±25.2	184.14±15.4	$ 458.18±32.1^{b}	$ 257.71±23.6^{a}	128.58±10.5^{b}
w1118	$ 551.97±36.9	$ 355.43±29.4	234.66±25.1	$ 465.09±29.7^{bc}	$ 281.17±20.7^{ab}	153.2±10.44^{b}
	SN-reared			**LL-reared**		
	AW1	**AW2**	**AW3**	**AW1**	**AW2**	**AW3**
pdf>Q0	302.14±26.8	252.21±25	165.13±27.9	$ 648.2±22.7	$ 449.71±36	306.46±27.2^{b}
pdf>Q128	$ 443.61±36.6	$ 198.21±22	87.84±18.2	$ 580.11±45.1	$ 261.62±36.1	115.86±30.5^{a}
Q0	396.41±35.9	248.09±27.2	124.77±18.7	$ 549.31±37.7	$ 358.79±34.4	227.24±23.3^{b}
Q128	$ 503.86±68.9	$ 226.99±30.8	101.55±33	$ 604.6±32.9	$ 392.52±31.5	220.53±26.7^{ab}
pdfGal	320.79±26.1	$ 228.22±19.7	139.13±20.9	$ 456.47±31.5	$ 241.56±20.6	153.56±14.3^{ab}
w1118	361.6±33.5	$ 285.4±32.2	242.98±36.1	$ 431.95±24.8	$ 275.07±21.9	198.71±23.8^{ab}

Different letters indicate statistically significant age-matched differences between genotypes at $p<0.05$. $ indicates significant differences of a given AW from indicated ones or all other AWs for a genotype at $p<0.05$.

Table 3. 6 Mean morning anticipation index (±SEM) under LD for all the genotypes raised in four regimes across AWs.

Morning anticipation indices						
	DD-reared			**LD-reared**		
	AW1	**AW2**	**AW3**	**AW1**	**AW2**	**AW3**
pdf>Q0	$ 0.833±0.03^{bc}	0.887±0.03^{b}	0.939±0.01^{bc}	$ 0.799±0.02^{c}	$ 0.888±0.02^{b}	0.933±0.02^{b}
pdf>Q128	$ 0.61±0.02^{a}	0.680±0.02^{a}	$ 0.814±0.03^{ac}	0.623±0.01^{a}	0.651±0.01^{a}	$ 0.74±0.03^{a}
Q0	$ 0.803±0.02^{c}	0.917±0.02^{b}	0.963±0.01^{bd}	$ 0.845±0.02^{bc}	$ 0.906±0.02^{b}	0.947±0.01^{b}
Q128	0.712±0.02^{a}	0.725±0.02^{a}	$ 0.796±0.03^{a}	0.68±0.01^{a}	0.717±0.02^{a}	$ 0.798±0.02^{ac}
pdfGal	0.929±0.01^{b}	0.954±0.01^{b}	0.945±0.02^{bd}	0.876±0.02^{bc}	0.906±0.02^{b}	0.894±0.02^{bc}
w1118	0.913±0.01^{b}	0.938±0.01^{b}	0.909±0.02^{bc}	0.913±0.02^{b}	$ 0.944±0.01^{b}	0.879±0.02^{bc}
	SN-reared			**LL-reared**		
	AW1	**AW2**	**AW3**	**AW1**	**AW2**	**AW3**
pdf>Q0	0.94±0.01^{b}	0.897±0.02^{bd}	0.972±0.02	$ 0.818±0.02^{bc}	$ 0.888±0.02^{b}	0.932±0.02^{b}
pdf>Q128	0.693±0.02^{a}	0.655±0.02^{a}	$ 0.858±0.04	$ 0.659±0.01^{a}	$ 0.73±0.02^{a}	$ 0.847±0.03^{ab}
Q0	0.889±0.02^{b}	$ 0.852±0.02^{bc}	0.95±0.03	$ 0.831±0.02^{be}	0.91±0.01^{b}	0.922±0.023^{b}
Q128	a 0.736±0.02^{a}	0.772±0.03^{ac}	$ 0.894±0.03	$ 0.722±0.02^{ac}	$ 0.761±0.02^{a}	a 0.818±0.02^{a}
pdfGal	0.95±0.01^{b}	0.948±0.01^{d}	0.976±0.01	$ 0.919±0.01^{de}	0.96±0.01^{b}	0.946±0.01^{b}
w1118	0.889±0.02^{b}	0.914±0.01^{bd}	0.953±0.02	$ 0.94±0.01^{d}	$ 0.962±0.01^{b}	0.936±0.01^{b}

Different letters indicate statistically significant age-matched differences between genotypes at $p<0.05$. $ indicates significant differences of a given AW from indicated ones or all other AWs for a genotype at $p<0.05$.

Appendix B

Table 3. 7 Mean evening anticipation index (±SEM) under LD for all the genotypes raised in four regimes across AWs.

Evening anticipation indices						
	DD-reared			**LD-reared**		
	AW1	**AW2**	**AW3**	**AW1**	**AW2**	**AW3**
pdf>Q0	$ 0.858±0.02^{bc}	0.898±0.02^{cd}	0.935±0.01^{bc}	$ 0.867±0.02^{ab}	0.945±0.01^{bc}	0.94±0.02^{bc}
pdf>Q128	$ 0.834±0.02^{bd}	0.858±0.02^{ad}	0.893±0.02^{bc}	$ 0.806±0.01^{a}	0.851±0.02^{a}	0.870±0.02^{c}
Q0	0.894±0.01^{cd}	0.939±0.01^{c}	$ 0.968±0.01^{ac}	$ 0.889±0.01^{bcd}	0.957±0.01^{bd}	0.976±0.01^{b}
Q128	b 0.808±0.01^{b}	a 0.820±0.01^{a}	$ 0.860±0.02^{b}	$ 0.815±0.02^{ac}	0.895±0.02^{ac}	0.886±0.02^{ac}
pdfGal	$ 0.969±0.01^{a}	$ 0.983±0.01^{b}	0.979±0.01^{a}	$ 0.913±0.02^{bd}	0.974±0.01^{bd}	0.975±0.01^{b}
w1118	$ 0.907±0.01^{c}	$ 0.953±0.01^{bc}	0.968±0.01^{ac}	$ 0.944±0.01^{d}	0.991±0.01^{d}	0.981±0.01^{b}
	SN-reared			**LL-reared**		
	AW1	**AW2**	**AW3**	**AW1**	**AW2**	**AW3**
pdf>Q0	$ 0.925±0.02^{acd}	$ 0.818±0.01^{bc}	0.978±0.01^{b}	$ 0.841±0.02^{b}	$ 0.91±0.02^{b}	0.941±0.01^{bc}
pdf>Q128	0.881±0.01^{bd}	$ 0.826±0.01^{bc}	0.923±0.02^{a}	$ 0.797±0.01^{b}	0.861±0.02^{b}	0.878±0.03^{bd}
Q0	$ 0.86±0.02^{b}	$ 0.819±0.01^{bc}	0.95±0.03^{ab}	$ 0.843±0.02^{b}	0.933±0.01^{b}	0.952±0.01^{cd}
Q128	$ 0.826±0.02^{b}	$ 0.777±0.02^{c}	0.927±0.02^{a}	0.843±0.02^{b}	0.848±0.02^{b}	0.864±0.02^{b}
pdfGal	$ 0.943±0.01^{a}	$ 0.879±0.01^{a}	0.984±0.01^{b}	$ 0.927±0.01^{a}	0.985±0.01^{a}	0.986±0.01^{a}
w1118	$ 0.932±0.01^{acd}	$ 0.842±0.01^{ab}	0.981±0.01^{ab}	$ 0.934±0.02^{a}	0.979±0.01^{a}	0.974±0.01^{ac}

Different letters indicate statistically significant age-matched differences between genotypes at $p<0.05$. $ indicates significant differences of a given AW from indicated ones or all other AWs for a genotype at $p<0.05$.

APPENDIX C: Tables for Chapter 4

Table 4. 1 Temperature cycles related regimes.

Regime	Development		Adults			
			0-2d		3d onwards	
	Light	Temp (˚C)	Light	Temp (°C)	Light	Temp (˚C)
Cyclic temperature						
DDTCtoDD25	DD	TC	DD	TC	DD	25
DDTCtoDD21	DD	TC	DD	TC	DD	21
DDTCtoDD29	DD	TC	DD	TC	DD	29
LDTCtoDD25	LD	TC	LD	TC	DD	25
LLTCtoDD25	LL	TC	LL	TC	DD	25
Constant temperature						
DD25toDD25 (DD25)	DD	25	DD	25	DD	25
LD25toDD25 (LDtoDD25)	LD	25	LD	25	DD	25
Temperature upshift						
DD21toDD25	DD	21	DD	21	DD	25
Temperature downshift						
DD29toDD25	DD	29	DD	29	DD	25

Development stage-specific TC	Development				Adults			
	Egg to L3		Pupal stages		0-2d		3d onwards	
	Light	Temp (°C)	Light	Temp (°C)	Light	Temp (°C)	Light	Temp (°C)
DDTC upto L3	DD	TC	DD	25	DD	25	DD	25
DDTC as Pupa-2d	DD	25	DD	TC	DD	TC	DD	25

DD, constant darkness. **LD**, 12h:12h **L**ight:**D**ark cycles (light cycles). **LL**, constant light.
TC, 12h:12h: 21°C:29°C **T**hermophase:**C**ryophase cycles (temperature cycles).

Table 4. 2 Ambient constant temperature regimes.

Regime	Development		Adults			
			0-2d		3d onwards	
	Light	Temp (°C)	Light	Temp (°C)	Light	Temp (°C)
Constant optimal temperature						
DD25toDD25 (DD25)	DD	25	DD	25	DD	25
LD25toDD25 (LDtoDD25)	LD	25	LD	25	DD	25
Constant low temperature						
DD23toDD23 (DD23)	DD	23	DD	23	DD	23
LD23toDD23 (LDtoDD23)	LD	23	LD	23	DD	23
Constant high temperature						
DD29toDD29 (DD29)	DD	29	DD	29	DD	29
LD29toDD29 (LDtoDD29)	LD	29	LD	29	DD	29
Temperature upshift						
DD23toDD29	DD	23	DD	23	DD	29
DD21toDD25	DD	21	DD	21	DD	25
DD25toDD29	DD	25	DD	25	DD	29
LD23toDD29	LD	23	LD	23	DD	29
LL23toDD29	LL	23	LL	23	DD	29
Temperature downshift						
DD29toDD23	DD	29	DD	29	DD	23

Age-specific acute high temp exposure	Development		Adults				
	Light	Temp (˚C)	0-1d	2-3d (48h)	5-6d	7-8d (48h)	9d onwards
Acute DD29 at 2-3d	DD	23	DD23	DD29	DD23	DD23	DD23
Acute DD29 at 7-8d	DD	23	DD23	DD23	DD23	DD29	DD23

Table 4. 3 Percentage rhythmicity in AW1 for various genotypes in DD23toDD29.

Gene	Fly line source	Genotype			
		% Rhythmicity (n)			
hHTT	Lee et al., 2004	***w;pdfGal/Q128;+*** **(in DD23toDD29)**	***w;pdfGal/Q128;+*** **(in DD23)**	***w;pdfGal/Q0;+*** **(in DD23toDD29)**	
		93.5 (92)	**22.22** (90)	**100** (26)	
***DfHSP70* lines**					
		pdf>Q128; DfHsp70	***Q128; DfHsp70***	***pdf>Q0; DfHsp70***	***Q0; DfHsp70***
DfHsp70Ba **(1 copy of *Hsp70* deleted)**	BL 8845	*w;pdfGal/Q128; DfHsp70Ba*	*w;Q128/+; DfHsp70Ba*	*w;pdfGal/Q0; DfHsp70Ba*	*w;Q0/+; DfHsp70Ba*
		26.7 (75)	**94.5 (44)**	**80 (10)**	**100 (16)**
DfHsp70A **(2 copies of *Hsp70* deleted)**	BL 8842	*w;pdfGal/Q128; DfHsp70A*	*w;Q128/+; DfHsp70A*	*w;pdfGal/Q0; DfHsp70A*	*w;Q0/+; DfHsp70A*
		28.8 (66)	**93.8** (48)	**81.8** (11)	**100** (11)
DfHsp70A,70Ba **(3 copies of *Hsp70* deleted)**	BL 8844	*w;pdfGal/Q128; DfHsp70A,70Ba*	*w;Q128/+; DfHsp70A,70Ba*	*w;pdfGal/Q0; DfHsp70A,70Ba*	*w;Q0/+; DfHsp70A,70Ba*
		29.8 (57)	**85** (40)	**100** (16)	Very few alive
DfHsp70B **(4 copies of *Hsp70* deleted)**	BL 8843	*w;pdfGal/Q128; DfHsp70B*	*w;Q128/+; DfHsp70B*	*w;pdfGal/Q0; DfHsp70B*	*w;Q0/+; DfHsp70B*
		13.5 (37)	**86.4** (44)	**83.3** (6)	**100** (13)
DfHsp70A,70B **(All 6 copies of *Hsp70* deleted)**	BL 8841	*w;pdfGal/Q128; DfHsp70A,70B*	*w;Q128/+; DfHsp70A,70B*	*w;pdfGal/Q0; DfHsp70A,70B*	*w;Q0/+; DfHsp70A,70B*
		50 (50)	**87** (46)	**60*** (10)	**100** (14)

Various genes used in the mini screen, their Bloomington or VDRC source IDs, the fly genotypes where they are used and their respective percentage rhythmicities are shown. The *w;pdfGal4/Q128;DfHSP70* lines are compared statistically with their respective control *w;Q128/+;DfHSP* lines and *w;pdfGal4/Q128;+* in DD23toDD29 and DD23, while the *w;pdfGal4/Q0;DfHSP70* are compared with *pdf>Q0* in DD23toDD29. # indicates significant difference of a *w;pdfGal4/Q128;DfHSP70* line from its respective *w;Q128/+;DfHSP* line, * of a *w;pdfGal4/Q128;DfHSP70* line (or *w;pdfGal4/Q0;DfHSP70*) from *pdf>Q128* in DD23toDD29 (or *pdf>Q0* in DD23toDD29) and + from *pdf>Q128* in DD23 at single symbol, $p<0.05$; double $p<0.01$; triple $p<0.001$.

Table 4.3 Percentage rhythmicity in AW1 for various genotypes in DD23toDD29.

Gene	Fly line source	Genotype		
		% Rhythmicity (n)		
hHTT	Lee et al., 2004	***w;pdfGal/Q128; Dcr/+*** (Parental cross: *w;pdfGal4;UAS-Dcr* with *w;UAS-HTTQ128;+*)	***w;pdfGal/Q128; Dcr/+*** (Parental cross: *w;pdfGal4;+* with *w;UAS-HTTQ128; UAS-Dcr*)	***w;pdfGal/Q0; Dcr/+***
		46.6 (88)	93.33 (30)	**88.9** (27)
***RNAi* lines**				
		pdf>Q128; RNAi/Dcr	***Q128; RNAi/Dcr***	***pdf>Q0; RNAi/Dcr***
Hsp70Aa	GD 41718	*w;pdfGal/Q128; Hsp70AaRNAi/Dcr*	*w;Q128/+; Hsp70AaRNA/Dcri*	*w;pdfGal/Q0; Hsp70AaRNAi/Dcr*
		72.1 (43)	**92.9** (14)	**80** (15)
Hsp70Bb	GD 36640	*w;pdfGal/Q128; Hsp70BbRNAi/Dcr*	*w;Q128/+; Hsp70BbRNAi/Dcr*	*w;pdfGal/Q0; Hsp70BbRNAi/Dcr*
		46.1 (76)	**100** (29)	**93.3** (15)
Hdj1 or Hsp40	GD 31271	*w;pdfGal/Q128; Hdj1-RNAi/Dcr*	*w;Q128/+; Hdj1-RNAi/Dcr*	*w;pdfGal/Q0; Hdj1-RNAi/Dcr*
		61 (41)	**100** (15)	**85.7** (7)
Hsf	GD 48692	*w;pdfGal/Q128; Hsf-RNAi/Dcr*	*w;Q128/+; Hsf-RNAi/Dcr*	*w;pdfGal/Q0; Hsf-RNAi/Dcr*
		48.9 (45)	**93.8** (16)	**100** (7)
Hsf	BL 27070	*w;pdfGal/Q128; Hsf-RNAi/Dcr*	*w;Q128/+; Hsf-RNAi/Dcr*	*w;pdfGal/Q0; Hsf-RNAi/Dcr*
		61.1 (54)	**92.3** (13)	**100** (17)
Iap2	BL 34776	*w;pdfGal/Q128; Iap2-RNAi/Dcr*	*w;Q128/+; Iap2-RNAi/Dcr*	*w;pdfGal/Q0; Iap2-RNAi/Dcr*
		93.75 (32)		

Table 4. 4 Sample sizes for behavioural experiments.

Regime	*Experiment*	*Age*	*pdf>Q0*	*pdf>Q128*	*Q0*	*Q128*	*pdfGal*	*w^{1118}*
		AW1	**26**	**30**	**26**	**26**	**26**	**26**
	1-PP79	**AW2**	**26**	**27**	**26**	**26**	**26**	**23**
		AW3	**25**	**20**	**23**	**25**	**24**	**15**
		AW1	31	31	31	30	32	31
DD25toDD25	2-PP34	AW2	29	30	31	30	31	29
		AW3	29	25	29	29	27	25
		AW1	26	29	26	26	26	26
	3-PP74a	AW2	25	27	24	25	18	21
		AW3	19	18	16	23	13	16
		AW1	**26**	**30**	**26**	**25**	**25**	**26**
	1-PP79a	**AW2**	**26**	**29**	**26**	**24**	**24**	**25**
		AW3	**26**	**26**	**23**	**22**	**19**	**16**
		AW1	32	32	32	32	32	32
	2-PP40	AW2	32	32	32	32	29	31
		AW3	30	32	30	30	20	16
		AW1	32	32	32	32	31	32
DDTCtoDD25	3-PP38	AW2	32	32	31	32	31	26
		AW3	24	30	27	27	30	16
		AW1	25	29	26	24	24	22
	4-PP65	AW2	15	25	18	22	21	14
		AW3	11	18	8	12	6	3
		AW1	31	31				
	5-PP79b	AW2	29	31				
		AW3	28	29				
		AW1	**24**	**29**	**26**	**24**	**25**	**25**
	1-PP43	AW2	**23**	**27**	**24**	**16**	**23**	**17**
		AW3	**14**	**24**	**20**	**14**	**21**	**3**
		AW1	27	30	24	26		
DD29toDD25	2-PP102.1	AW2	26	27	20	24		
		AW3	24	23	16	24		
		AW1	26	31	24	27		
	3-PP102.2	AW2	24	30	24	27		
		AW3	22	29	21	23		
		AW1	**25**	**30**	**26**	**24**	**26**	**25**
DD21toDD25	**PP43**	**AW2**	**25**	**26**	**26**	**23**	**25**	**22**
		AW3	**18**	**18**	**24**	**23**	**20**	**14**

Table 4.4 Sample sizes for behavioural experiments.

Regime	*Experiment*	*Age*	*pdf>Q0*	*pdf>Q128*	*Q0*	*Q128*	*pdfGal*	*w^{1118}*
DDTC upto L3	**PP58**	**AW1**	**26**	**31**	**26**	**27**		
		AW2	**25**	**30**	**24**	**24**		
		AW3	**13**	**28**	**12**	**18**		
DDTC as Pupa-2d	**PP58**	**AW1**	**27**	**29**	**25**	**26**		
		AW2	**27**	**28**	**25**	**24**		
		AW3	**21**	**21**	**25**	**17**		
DDTCtoDD29	**PP68**	**AW1**	**24**	**29**	**26**	**26**	**26**	**25**
		AW2	**21**	**27**	**22**	**23**	**20**	**22**
		AW3	**17**	**23**	**22**	**16**	**8**	**4**
DDTCtoDD21	**PP68**	**AW1**	**25**	**29**	**26**	**25**	**25**	**26**
		AW2	**22**	**26**	**26**	**22**	**24**	**23**
		AW3	**18**	**24**	**23**	**19**	**14**	**5**
LDTCtoDD25	**1-PP79a**	**AW1**	**26**	**30**	**25**	**26**	**26**	**26**
		AW2	**26**	**29**	**25**	**25**	**26**	**24**
		AW3	**25**	**29**	**25**	**21**	**24**	**12**
	2-PP40	AW1	32	32	31	32	32	32
		AW2	32	32	30	32	32	31
		AW3	30	25	30	31	31	28
	3-PP38	AW1	32	32	32	31	32	31
		AW2	31	29	31	30	28	28
		AW3	31	28	31	30	23	16
	4-PP65	AW1	26	30	24	23	24	25
		AW2	18	25	22	23	18	8
		AW3	3	9	5	9	3	2
	5-PP79b	AW1	30	32				
		AW2	30	30				
		AW3	27	26				
LLTCtoDD25	**1-PP79a**	**AW1**	**25**	**29**	**25**	**26**	**26**	**25**
		AW2	**25**	**28**	**25**	**25**	**26**	**25**
		AW3	**25**	**27**	**24**	**25**	**20**	**20**
	2-PP40	AW1	31	31	32	31	31	32
		AW2	31	31	32	31	31	32
		AW3	28	29	16	29	31	25
	3-PP38	AW1	31	32	31	32	31	27
		AW2	30	30	30	31	29	26
		AW3	26	32	28	27	24	22
	4-PP65	AW1	26	30	26	25	25	26
		AW2	22	29	23	22	14	10
		AW3	8	18	13	11	6	0
	5-PP79b	AW1	31	32				
		AW2	30	32				
		AW3	28	32				

Table 4.4 Sample sizes for behavioural experiments.

Regime	*Experiment*	*Age*	*pdf>Q0*	*pdf>Q128*	*Q0*	*Q128*	*pdfGal*	*w^{1118}*
DD23toDD23	**1-PP48**	**AW1**	**26**	**29**	**25**	**25**	**26**	**25**
		AW2	**26**	**29**	**25**	**25**	**26**	**25**
		AW3	**26**	**28**	**23**	**24**	**24**	**19**
	2-PP73	AW1	26	30	26	26	26	26
		AW2	26	26	25	26	26	25
		AW3	26	23	22	25	21	17
	3-PP74a	AW1	26	31	24	25	25	26
		AW2	25	29	22	24	25	24
		AW3	16	26	20	14	22	16
DD29toDD29	**1-PP75**	**AW1**	**28**	**32**	**25**	**26**	**27**	**28**
		AW2	**28**	**29**	**24**	**24**	**22**	**18**
		AW3	**25**	**19**	**18**	**23**	**5**	**1**
	2-PP51	AW1	26	28	26	25	22	25
		AW2	20	27	26	24	15	18
		AW3	16	16	15	12	8	1
	3-PP49b	AW1	26	27	24	25	24	25
		AW2	21	18	20	16	16	16
		AW3	17	10	9	10	4	8
DD29toDD23	**1-PP51**	**AW1**	**25**	**29**	**26**	**24**	**25**	**25**
		AW2	**25**	**28**	**26**	**24**	**24**	**25**
		AW3	**22**	**28**	**25**	**24**	**19**	**19**
	2-PP49a	AW1	26	26	23	22	19	23
		AW2	22	20	19	16	9	9
		AW3	19	17	18	14	7	6
	3-PP49b	AW1	26	28	24	26	25	26
		AW2	26	28	22	24	24	24
		AW3	24	27	22	22	17	18
DD23toDD29	**1-PP76**	**AW1**	**25**	**29**	**23**	**23**	**25**	**26**
		AW2	**25**	**27**	**23**	**19**	**25**	**24**
		AW3	**20**	**27**	**19**	**19**	**13**	**15**
	2-PP48	AW1	28	28	26	26	24	22
		AW2	27	26	26	26	18	17
		AW3	22	18	20	26	11	6
	3-PP77	AW1	24	28	26	25	24	26
		AW2	18	21	26	22	22	15
		AW3	17	17	20	19	13	5
DD25toDD29	1-PP51	**AW1**	25	30	25	26	26	26
		AW2	25	30	24	25	25	23
		AW3	15	19	21	15	10	9

Table 4.4 Sample sizes for behavioural experiments.

Regime	*Experiment*	*Age*	*pdf>Q0*	*pdf>Q128*	*Q0*	*Q128*	*pdfGal*	*w^{1118}*
Acute DD29 at 2-3d	PP73	**AW1**	25	28	26	25	25	26
		AW2	25	27	24	23	25	22
		AW3	25	25	22	20	21	14
Acute DD29 at 7-8d	PP73	**AW1**	26	29	26	25	25	25
		AW2	26	28	26	25	24	25
		AW3	26	27	25	25	24	19
LD23toDD23	**1-PP74b**	**AW1**	**26**	**29**	**26**	**26**	**26**	**26**
		AW2	**26**	**25**	**26**	**25**	**26**	**24**
		AW3	**26**	**20**	**24**	**25**	**26**	**23**
	2-PP73	AW1	26	30	26	26	25	26
		AW2	26	28	25	24	22	22
		AW3	24	19	19	21	15	13
	3-PP24	AW1	30	31	32	32	31	32
		AW2	30	29	31	25	30	30
LD29toDD29	**1-PP75b**	**AW1**	**28**	**32**	**26**	**19**	**23**	**26**
		AW2	**28**	**31**	**25**	**18**	**18**	**10**
		AW3	**17**	**26**	**22**	**11**	**6**	**4**
	2-PP51	AW1	24	30	26	25	25	
		AW2	22	26	26	24	10	
		AW3	12	14	17	15	4	
	3-PP49b	AW1	26	29	26	23	25	22
		AW2	23	20	20	17	20	4
		AW3	16	14	14	11	10	3
	4-PP75a	AW1	29	32				
		AW2	29	29				
		AW3	29	22				
LD23toDD29	**1-PP77**	**AW1**	**26**	**29**	**25**	**24**	**24**	**26**
		AW2	**23**	**22**	**22**	**23**	**21**	**13**
		AW3	**18**	**17**	**22**	**21**	**16**	**5**
	2-PP76a	AW1	25	30	26	26	26	26
		AW2	22	20	23	25	24	24
		AW3	21	10	19	18	11	15
	3-PP23	AW1	28	27	32	31	31	31
		AW2	24	25	29	20	25	19
		AW3	20	19	22	25	15	17
	4-PP76b	AW1	29	28				
		AW2	23	20				
		AW3	21	19				
LL23toDD29	1-PP101	**AW1**	**25**	**31**	**25**	**26**	**25**	**28**
		AW2	**20**	**20**	**23**	**22**	**18**	**10**
		AW3	**16**	**6**	**16**	**17**	**6**	**1**

Table 4.4 Sample sizes for behavioural experiments.

DD23toDD29	AW1
pdf>Q128	29
pdf>Q128;DfHsp70Ba	32
Q128;DfHsp70Ba	15
pdf>Q128;DfHsp70A	31
Q128;DfHsp70A	16
pdf>Q128;DfHsp70A,70Ba	32
Q128;DfHsp70A,70Ba	16
pdf>Q128;DfHsp70B	24
Q128;DfHsp70B	13
pdf>Q128;DfHsp70A,70B	27
Q128;DfHsp70A,70B	16

Table 4. 5 Statistical tests used for within-regime comparisons of behaviour.

Within-regime comparisons				
Regime	**Comparison of**	**Between geno**	**Between AWs (or age)**	**Exclusion from statistical analyses** (<10 surviving rhythmic flies)
DDTCtoDD25	**Rhythmicity** ***r*** **Robustness** **Period**	*RMA + THSD* *KW + MCMR* *WA +GHT* *KW + MCMR*	 *FT + WT + Bon* *FT + WT + Bon*	*pdf>Q128* from between-genotype analyses of robustness and period in AW3.
DD29toDD25	Rhythmicity *r* Robustness Period	*RMA + THSD* *KW + MCMR* *1A + THSD* *KW + MCMR*		*pdf>Q128* from between-genotype statistical analysis of robustness and period in AW2 and AW3 and w^{1118} in AW3.
DD21toDD25	Rhythmicity *r* Robustness Period	*6x2FET+2x2FET+BH* *KW + MCMR* *1A + THSD* *KW + MCMR*	*CQT+MNT+Bon*	*pdf>Q128* from between-genotype statistical analysis of robustness and period in AW2 and AW3.
DDTC upto L3	Rhythmicity *r*	*6x2FET+2x2FET+BH* *KW+MCMR*	*CQT+MNT+Bon*	'*r*' post-16d
DDTC as Pupa-2d	Rhythmicity *r*	*6x2FET+2x2FET+BH* *KW+MCMR*	*CQT+MNT+Bon*	'*r*' post-16d
DDTCtoDD29	Rhythmicity *r* Robustness Period	*6x2FET+2x2FET+BH* *KW+MCMR* *1A + THSD* *KW + MCMR*	*CQT+MNT+Bon*	*pdf>Q128* from between-genotype statistical analysis of robustness and period in AW2 and AW3, *pdfGal* and w^{1118} from AW3 (16d-23d) statistical analyses.
DDTCtoDD21	Rhythmicity *r* Robustness Period	*6x2FET+2x2FET+BH* *KW+MCMR* *1A + THSD* *KW + MCMR*	*CQT+MNT+Bon*	*pdf>Q128* from between-genotype analyses of robustness and period across AWs. w^{1118} from AW3 statistical analyses.
	r Robustness	*1A+UNHSD* *1A+UNHSD*		

Appendix C

Table Key

RMA, Repeated Measures ANOVA

1A, One-way ANOVA

THSD, Tukey's Honest Significant Test

UNHSD, Unequal N Honest Significant Test

KW, Kruskal Wallis Test

MCMR, Multiple Comparisons of Mean Ranks

MWU, Mann-Whitney U Test

WA, Welch's ANOVA

GHT, Games-Howell Test

FT, Friedman's Test

WT, Wilcoxon matched-pairs Test

CT, Conover Test

Bon, Bonferroni Correction

BH, Benjamini-Hochberg procedure

FET, Fisher's Exact Test

CQT, Cochran Q Test

MNT, McNemar's Test

Table 4.5 Statistical tests used for within-regime comparisons of behaviour.

Regime	Comparison of	Between geno	Between AWs (or age)	Exclusion from statistical analyses (<10 surviving rhythmic flies)
LDTCtoDD25	Rhythmicity	*RMA + THSD*		*pdf>Q128* from between-genotype analyses of robustness and period in AW2 and AW3.
	r	*KW + MCMR*		
	Robustness	*1A + THSD*		
	Period	*KW + MCMR*		
LLTCtoDD25	Rhythmicity	*RMA + THSD*		*pdf>Q128* from between-genotype analyses of robustness and period in AW2 and AW3.
	r	*KW + MCMR*		
	Robustness	*1A + THSD*		
	Period	*KW + MCMR*		
DD23toDD23	Rhythmicity	*RMA + THSD*		*pdf>Q128* from between-genotype analyses of robustness and period across AWs.
	r	*KW+MCMR*		
	Robustness	*1A + THSD*	*FT + WT + Bon*	
	Period	*KW + MCMR*	*FT + WT + Bon*	
DD29toDD29	Rhythmicity	*RMA + THSD (All genotypes for AW1 and AW2)*		*pdf>Q128* from between-genotype analyses of robustness and period in AW3. *pdfGal* and w^{1118} from AW3 statistical analyses.
		1A+UNHSD between pdf>Q0, Q0, Q128 for AW3	*FT + WT + Bon for pdf>Q0, Q0, Q128 between AWs*	
	r	*KW+MCMR*		
		RMA+UNHSD for all genotypes for AW1 and AW2		
	Robustness	*1A+UNHSD between genotypes for AW3*	*FT + WT + Bon for pdfGal and w^{1118} between AW1 and AW2*	
	Period	*KW + MCMR*	*FT + WT + Bon*	
DD29toDD23	Rhythmicity	*RMA + THSD*		*pdf>Q128* from between-genotype analyses of robustness and period across AWs.
	r	*KW+MCMR*		
	Robustness	*1A+UNHSD*	*FT + WT + Bon*	
	Period	*KW + MCMR*	*FT + WT + Bon*	
DD23toDD29	Rhythmicity	*RMA + THSD*		*pdf>Q128* from between-genotype analyses of robustness and period in AW3.
	r	*KW+MCMR*		
	Robustness	*KW + MCMR*	*FT + WT + Bon*	
	Period	*KW + MCMR*	*FT + WT + Bon*	

Table 4.5 Statistical tests used for within-regime comparisons of behaviour.

Regime	Comparison of	Between geno	Between AWs (or age)	Exclusion from statistical analyses (<10 surviving rhythmic flies)
DD25toDD29	Rhythmicity *r* Robustness Period	*6x2FET+2x2FET+BH* *KW+MCMR* *1A+UNHSD* *KW + MCMR*	*CQT+MNT+Bon*	*pdf>Q128* from between-genotype analyses of robustness and period in AW2 and AW3. w^{1118} from AW3 (17-23d) statistical analyses.
Acute DD29 at 2-3 d	Rhythmicity *r*	*6x2FET+2x2FET+BH* *KW+MCMR*	*CQT+MNT+Bon*	'*r*' post-16d
Acute DD29 at 7-8 d	Rhythmicity *r*	*6x2FET+2x2FET+BH* *KW+MCMR*	*CQT+MNT+Bon*	'*r*' post-16d
LD23toDD23	Rhythmicity *r* Robustness Period	*RMA + THSD* *KW+MCMR* *WA+GHT* *KW + MCMR*		*pdf>Q128* from between-genotype analyses of robustness and period across AWs.
LD29toDD29	Rhythmicity *r* Robustness Period	*RMA + THSD* *KW+MCMR* *KW+MCMR* *KW + MCMR*		*pdfGal* and w^{1118} from AW3 (17-23d) statistical analyses. *pdf>Q128* from between-genotype analyses of robustness and period in AW3.
LD23toDD29	Rhythmicity *r* Robustness Period	*RMA + THSD* *KW+MCMR* *1A+UNHSD* *KW + MCMR*		*pdf>Q128* from between-genotype statistical analysis of robustness and period in AW2 and AW3 and w^{1118} in AW3.
LL23toDD29	Rhythmicity *r* Robustness Period	*6x2 FET+* *2x2 FET+BH* *KW+MCMR* *1A+UNHSD* *KW + MCMR*	*CQT+MNT+Bon*	*pdf>Q128* from AW2 analyses of period and robustness, AW3 (17-23d) from statistical analysis (for *pdf>Q128, pdfGal* and w^{1118})
***Hsp70* Deficiency lines in DD23toDD29**	Rhythmicity *r* Robustness	*mxn FET+* *2x2 FET+BH* *1A+UNHSD* *1A+UNHSD*		Analyses of rhythmicity restricted to AW1 and those of '*r*' to 8 days in DD (age 3d-10d)

Table 4. 6 Statistical tests used for between-regime comparisons of behaviour.

Between-regime comparisons			
Regimes compared	**Comparison of**	**Between regimes for an AW**	**Exclusion from statistical analyses**
DD25toDD25 **DDTCtoDD25** **LDTCtoDD25** **LLTCtoDD25**	Rhythmicity *r* Robustness Period	*RMA + THSD* *KW + MCMR* *1A + UNHSD* *KW + MCMR*	*pdf>Q128* from between-regime analyses of robustness and period in AW2 and AW3
DDTCtoDD25 **DD29toDD25** **DD21toDD25**	Rhythmicity *r* Robustness Period	*3x2 FET+* *2x2 FET+Bon* *KW + MCMR* *1A + UNHSD* *KW + MCMR*	
DDTCtoDD25 **DDTCuptoL3** **DDTC as Pupa-2d**	Rhythmicity *r*	*3x2 FET+* *2x2 FET+Bon* *KW + MCMR*	
DDTCtoDD25 **DDTCtoDD29** **DDTCtoDD21**	Rhythmicity *r* Robustness Period	*3x2 FET+* *2x2 FET+Bon/BH* *KW + MCMR* *1A + UNHSD* *KW + MCMR,* *MWU for pdf>Q128*	*pdf>Q128* in DDTCtoDD21 from between-regime analyses of robustness and period.
DD25 **DDTCtoDD25** **LDTCtoDD25** **LLTCtoDD25**	Rhythmicity *r* Robustness Period	*RMA + THSD* *KW + MCMR* *1A + UNHSD* *KW + MCMR*	*pdf>Q128* from between-regime analyses of robustness and period in AW2 and AW3.

Table key: RMA, Repeated Measures ANOVA; **1A,** One-way ANOVA; **THSD,** Tukey's Honest Significant Test; **UNHSD,** Unequal N Honest Significant Test; **KW,** Kruskal Wallis Test; **MCMR,** Multiple Comparisons of Mean Ranks; **MWU,** Mann-Whitney U Test; **WA,** Welch's ANOVA; **GHT,** Games-Howell Test; **FT,** Friedman's Test.

Table 4.6 Statistical tests used for between-regime comparisons of behaviour.

Regimes compared	Comparison of	Between regimes for an AW	Exclusion from statistical analyses
DD23 **DD25** **DD29**	Rhythmicity *r* Robustness Period	*RMA + THSD* *KW + MCMR* *1A + UNHSD* *KW + MCMR,* *MWU for pdf>Q128*	*pdf>Q128* in DD23 from between-regime analyses of robustness and period in AW1.
DD23toDD23 **LD23toDD23**	Rhythmicity *r* Robustness Period	*RMA + THSD* *MWU* *1A + UNHSD* *MWU*	*pdf>Q128* from between-regime analyses of robustness and period across AWs.
DD29toDD29 **LD29toDD29**	Rhythmicity *r* Robustness Period	*RMA + THSD* *MWU* *1A + UNHSD* *MWU*	*pdf>Q128* from between-regime analyses of robustness and period in AW3.
DD23 **DD29** **DD23toDD29** **DD29toDD23**	Rhythmicity *r* Robustness Period	*RMA + THSD* *KW + MCMR* *1A + UNHSD* *KW + MCMR*	*pdf>Q128* in DD23 and DD29toDD23 excluded from between-regime statistical analyses.
DD23toDD29 **DD21toDD25** **DD25toDD29**	Rhythmicity *r* Robustness Period	*3x2 FET+* *2x2 FET+Bon* *KW + MCMR* *1A + UNHSD,* *For Q128 and pdfGal WA+GHT* *KW + MCMR*	*pdf>Q128* from between-regime analyses of robustness and period in AW2 and AW3.
DD23 **Acute DD29 at 2-3d** **Acute DD29 at 7-8d**	Rhythmicity *r*	*4x2 FET+* *2x2 FET+Bon* *KW + MCMR*	
DD23toDD29 **LD23toDD29**	Rhythmicity	*RMA + THSD*	
DD23toDD29 **LD23toDD29** **LL23toDD29**	Rhythmicity *r* Robustness Period	*3x2 FET+* *2x2 FET+ Bon* *KW + MCMR* *1A + UNHSD* *KW + MCMR*	*pdf>Q128* from between-regime analyses of robustness and period in AW2.
DDTCtoDD25 **DD23toDD29**	Rhythmicity *r* Robustness Period	*RMA + THSD* *MWU* *1A + UNHSD* *MWU*	*pdf>Q128* from between-regime analyses of robustness and period in AW3.

Table 4. 7 Within-regime mean robustness (± SEM) [significant differences].

Regime	Expt code	Age	*pdf>Q0*	*pdf>Q128*	*Q0*	*Q128*	*pdfGal*	*w*^{1118}
DD29toDD25	PP43	**AW1**	**258.3** (10.2) [a]	**148.95** (11.2) [b]	**239.8** (6.8) [a]	**167.6** (8.7) [b]	**166.2** (7.97) [b]	**156.7** (6.3) [b]
		AW2	255.2 (15.7) [a]	NA	220.03 (12.2) [ac]	175.3 (11.8) [bc]	169.95 (11.3) [b]	135.3 (8.3) [b]
		AW3	225.9 (15.4) [a]	121.8 (7.3)	189.7 (16.5) [ac]	143.6 (9.7) [bc]	155.7 (8.8) [bc]	88.4 (14.8) [ac]
DD21toDD25	PP43	**AW1**	**269.6** (8.5) [bc]	**171.3** (10.9) [a]	**286.6** (10.4) [b]	**201.73** (9.5) [a]	**232.3** (9.1) [ac]	**259.1** (9.7) [bc]
		AW2	280.3 (12.02) [b]	140.1	288.2 (11.5) [b]	220.5 (13.4) [ac]	261.9 (10.8) [bc]	219.6 (11.6) [ac]
		AW3	252.8 (14.7) [a]	NA	222.4 (13.9) [ac]	196.9 (13.1) [bc]	229.2 (11.7) [ac]	184.1 (15.2) [bc]
DD23toDD23	PP48	**AW1**	**239.8** (9.1) [a]	**149.5** (25.96)	**223** (7.7) [ac]	**188.2** (8.6) [b]	**196.4** (6.3) [bc]	**200** (8.4) [bc]
		AW2	226.6 (11.4) [bc]	146.2 (1.8)	214 (10.4) [bc]	169 (8.7) [a]	203.3 (6.95) [bc]	224.6 (8.1) [ac]
		AW3	200.9 (9.3) [bc]	122.2 (4.5)	187.3 (11.2) [bc]	141 (7.4) [a]	192.8 (9.8) [bc]	178 (9.5) [ac]
DD29toDD23	PP51	**AW1**	**185.99 (12.7)** [a]	**91.8 (13.4)**	**136.4 (6.6)** [b]	**101.6 (5.1)** [c]	**116.2 (4.5)** [bc]	**125.7 (5.6)** [b]
		AW2	199.6 (13.89) [a]	95.9	159.1 (8.8) [b]	140.5 (6.8)	148.7 (5.7)	140.5 (4.98) [b]
		AW3	207.3 (16.18) [a]	114.7 (12.9) [b]	144.9 (6.8) [b]	136.6 (7.6) [b]	145.4 (8.4) [b]	121.3 (9.5) [b]

Different letters indicate statistically significant age-matched differences between genotypes at $p<0.05$.

Table 4. 8 Within-regime mean period (± SEM) [significant differences].

Regime	Expt code	Age	*pdf>Q0*	*pdf>Q128*	*Q0*	*Q128*	*pdfGal*	*w*^{1118}
DD29toDD25	PP43	**AW1**	**24.5** (0.04) [a]	**24.2** (0.07)	**24.01** (0.08) [b]	**24.3** (0.08) [ab]	**24.6** (0.07) [a]	**23.9** (0.07) [b]
		AW2	24.8 (0.08) [a]	NA	23.7 (0.08) [bd]	24.1 (0.07) [bc]	24.2 (0.12) [c]	23.3 (0.12) [d]
		AW3	24.9 (0.11) [b]	23.5 (0.1)	23.5 (0.07) [a]	24.2 (0.1) [bc]	24.2 (0.13) [c]	24
DD21toDD25	PP43	**AW1**	**24.7** (0.06) [a]	**24.9** (0.16) [a]	**23.7** (0.04) bcd	**24.1** (0.06) [b]	**24.4** (0.06) [ac]	**23.7** (0.04) [d]
		AW2	25 (0.05) [c]	24.33	23.6 (0.06) [a]	24.1 (0.06) [b]	24.4 (0.05) [bc]	23.6 (0.07) [a]
		AW3	25 (0.09) [d]	NA	23.4 (0.06) [a]	24 (0.09) [bc]	24.6 (0.1) [bd]	23.5 (0.11) [ac]
DDTCtoDD29	PP68	**AW1**	**24.2** (0.06) [d]	**24.1** (0.14) [bd]	**23.3** (0.04) [a]	**23.6** (0.07) [bc]	**23.8** (0.06) bcd	**23.6** (0.07) ac
		AW2	24.5 (0.1) [a]	26.33	23.5 (0.04) [b]	23.6 (0.04) [b]	24.2 (0.73) [b]	23.6 (0.06) [a]
		AW3	24.5 (0.1) [a]	21.67	23.4 (0.08) [b]	23.7 (0.06) [b]	23.9 (0.21)	23.2 (0.1)
DDTCtoDD21	PP68	**AW1**	**24.1** (0.09) [a]	**24.4** (0.29)	**23.6** (0.06) [b]	**23.7** (0.08) [b]	**23.97** (0.09) [ab]	**23.8** (0.08) ab
		AW2	24.4 (0.11) [b]	23.67	23.7 (0.05) [a]	23.9 (0.1) [ab]	24.3 (0.09) [b]	24.3 (0.11) [b]
		AW3	24.95 (0.18) [a]	NA	23.6 (0.06) [b]	23.9 (0.15) [b]	24.4 (0.13) [b]	24 (0.26) ab

Different letters indicate statistically significant age-matched differences between genotypes at $p<0.05$.

Table 4.8 Within-regime mean period (± SEM) [significant differences].

Regime	Expt code	Age	*pdf>Q0*	*pdf>Q128*	*Q0*	*Q128*	*pdfGal*	w^{1118}
LDTCtoDD25	PP79a	**AW1**	**24.6** (0.05) [a]	**23.9** (0.18) [bc]	**23.8** (0.06) [b]	**24.5** (0.08) [a]	**24.4** (0.05) [ac]	**23.9** (0.07) [b]
		AW2	24.7 (0.06) [b]	23 (0.59)	24.1 (0.1) [ac]	24.4 (0.09) [bc]	24.5 (0.07) [b]	23.9 (0.07) [a]
		AW3	24.7 (0.09) [a]	23.7 (0.14)	23.9 (0.08) [b]	24.2 (0.13) [ab]	24.3 (0.13) [ab]	23.8 (0.14) [b]
LLTCtoDD25	PP79a	**AW1**	**24.6** (0.05) [ac]	**24.4** (0.17) [c]	**23.7** (0.05) [b]	**24.03** (0.07) [bc]	**24.5** (0.08) [ac]	**23.95** (0.07) [bc]
		AW2	24.7 (0.07) [a]	23.7 (0.16)	23.8 (0.06) [b]	24.02 (0.08) [b]	24.5 (0.06) [a]	23.8 (0.07) [b]
		AW3	24.8 (0.07) [a]	23.9 (0.19)	23.8 (0.07) [b]	23.95 (0.06) [b]	24.5 (0.07) [a]	23.7 (0.07) [b]
DD23toDD23	PP48	**AW1**	**24.6** (0.09) [a]	**24.8** (0.29)	**23.7** (0.05) [b]	**23.7** (0.05) [b]	**24.1** (0.7) [b]	**23.7** (0.5) [b]
		AW2	24.7 (0.07) [a]	23.2 (0.17)	23.5 (0.07) [b]	23.9 (0.1) [bc]	24.2 (0.7) [ac]	23.7 (0.06) [b]
		AW3	24.8 (0.09) [a]	23.5 (0.83)	23.5 (0.08) [b]	23.9 (0.09) [bc]	24.3 (0.1) [ac]	23.6 (0.06) [b]
DD29toDD23	PP51	**AW1**	**24.4** (0.1) [a]	**23.8** (0.17)	**23.7** (0.05) [b]	**23.95** (0.13)	**24.3** (0.15) [ac]	**23.8** (0.11) [bc]
		AW2	24.6 (0.12) [b]	23	23.7 (0.07) [a]	24.2 (0.11) [bc]	24.5 (0.12) [b]	23.7 (0.11) [ac]
		AW3	24.7 (0.13) [b]	24.7 (0.53)	23.7 (0.08) [a]	24.4 (0.13) [bc]	24.4 (0.16) [b]	23.6 (0.19) [ac]

Different letters indicate statistically significant age-matched differences between genotypes at $p<0.05$.

Table 4.8 Within-regime mean period (± SEM) [significant differences]**.**

Regime	Expt code	Age	*pdf>Q0*	*pdf>Q128*	*Q0*	*Q128*	*pdfGal*	w^{1118}
DD25toDD29	PP51	**AW1**	**23.8** (0.06) [b]	**22.8** (0.13) [a]	**23.5** (0.04) [b]	**23.6** (0.03) [b]	**23.7** (0.23) [b]	**23.4** (0.05) [ab]
		AW2	24.5 (0.09) [a]	23.3 (0.25)	23.6 (0.05) [bc]	23.7 (0.05) [b]	23.9 (0.06) [ab]	23.2 (0.09) [c]
		AW3	24.2 (0.15) [b]	23.3	23.3 (0.08) [a]	23.8 (0.1) [b]	23.96 (0.19) [b]	23.1 (0.17)
LD23toDD23	PP74b	**AW1**	**24.4** (0.05) [a]	**24.3** (0.23)	**23.8** (0.06) [c]	**23.9** (0.07) [bc]	**24.2** (0.06) [ab]	**23.7** (0.05) [c]
		AW2	24.6 (0.05) [a]	23.5 (0.134)	23.8 (0.05) [b]	23.9 (0.07) [b]	24.5 (0.06) [a]	23.6 (0.05) [b]
		AW3	24.9 (0.09) [a]	24 (0.19)	23.7 (0.04) [b]	23.8 (0.05) [b]	24.6 (0.08) [a]	23.7 (0.07) [b]
LD29toDD29	PP75b	**AW1**	**23.9** (0.06) [a]	**22.8** (0.2)	**23.5** (0.04) [b]	**23.5** (0.04) [b]	**23.6** (0.07) [ab]	23.3 (0.05) [b]
		AW2	24.2 (0.07) [a]	23.5 (0.19)	23.5 (0.05) [bc]	23.7 (0.04) [c]	23.7 (0.1) [c]	23.7 (0.39) [b]
		AW3	24.2 (0.12)	24.8 (0.17)	23.8 (0.1)	23.8 (0.15)	23.7 (0.32)	23.3 (0.38)

Different letters indicate statistically significant age-matched differences between genotypes at $p<0.05$.

Table 4.8 Within-regime mean period (± SEM) [significant differences].

Regime	Expt code	Age	*pdf>Q0*	*pdf>Q128*	*Q0*	*Q128*	*pdfGal*	w^{1118}
LD23toDD29	PP77	**AW1**	**23.9** (0.06) [ac]	**23.1** (0.1) [d]	**23.5** (0.03) [bcd]	**23.6** (0.03) [bc]	**23.7** (0.03) [c]	**23.6** (0.03) [bc]
		AW2	24.2 (0.08) [a]	22.4 (0.29) [b]	23.4 (0.04) [b]	23.7 (0.04) [b]	24.1 (0.08) [a]	23.3 (0.06) [b]
		AW3	24.2 (0.09) [b]	23.5 (0.22)	23.3 (0.04) [a]	23.8 (0.06) [b]	23.9 (0.11) [b]	23.1 (0.12) [b]
LL23toDD29	PP101	**AW1**	**23.7** (0.03) [a]	**22.6** (0.18)	**23.1** (0.33) [b]	**23.1** (0.4) [b]	**23.6** (0.04) [a]	**23.3** (0.05) [b]
		AW2	24 (0.09) [a]	23.1 (0.57)	23.1 (0.05) [b]	23.4 (0.05) [b]	23.95 (0.08) [a]	23.3 (0.08) [b]
		AW3	24.2 (0.1) [a]	NA	23.1 (0.1) [b]	23.6 (0.15) [b]	23.8 (0.21)	23.3

Different letters indicate statistically significant age-matched differences between genotypes at $p<0.05$.

Appendix C

Table 4. 9 Between-regimes rhythm features in AW1 showing mean (± SEM) [significant differences]***.***

Rhythm feature	Genotype	Between-regime comparisons			
		DD25to DD25	**DDTCto DD25**	**LDTCto DD25**	**LLTCto DD25**
Period	***pdf>Q0***	24.8 (0.13) [a]	24.5 (0.06) [b]	24.6 (0.05) [ab]	24.6 (0.05) [ab]
	pdf>Q128	**24.3** (0.47) [ab]	**24.7** (0.1) [a]	**23.9** (0.18) [b]	**24.4** (0.17) [ab]
	Q128	24.1 (0.1) [b]	24.1 (0.1) [b]	24.5 (0.08) [a]	24.03 (0.07) [b]
		DDTCto DD25	**DD29to DD25**	**DD21to DD25**	
Robust-ness	***pdf>Q0***	229.2 (7.4) [a]	258.3 (10.2) [ab]	269.6 (8.5) [b]	
	pdf>Q128	**146.6** (5.2)	**148.95** (11.2)	**171.3** (10.9)	
	Q128	188.4 (12.1)	167.6 (8.7)	201.7 (9.5)	
		DDTCto DD25	**DD29to DD25**	**DD21to DD25**	
Period	***pdf>Q0***	24.5 (0.06) [a]	24.5 (0.04) [a]	24.7 (0.06) [b]	
	pdf>Q128	**24.7** (0.1) [a]	**24.2** (0.07) [b]	**24.9** (0.16) [a]	
	Q128	24.1 (0.1)	24.3 (0.08)	24.1 (0.06)	
		DDTCto DD25	**DDTCto DD29**	**DDTCto DD21**	
Period	***pdf>Q0***	24.5 (0.06) [a]	24.2 (0.06) [ab]	24.1 (0.09) [b]	
	pdf>Q128	**24.7** (0.1) [a]	**24.1** (0.14) [b]	**24.4** (0.29) [ab]	
	Q128	24.1 (0.1) [a]	23.6 (0.07) [b]	23.7 (0.08) [b]	

Different letters indicate statistically significant age-matched differences between genotypes at $p<0.05$.

Table 4.9 Between-regimes rhythm features in AW1 showing mean (± SEM) [significant differences]***.***

Rhythm feature	Genotype	Between-regime comparisons				
Period		**DD23**	**LD23to DD23**		**DD29**	**LD29to DD29**
	pdf>Q0	24.6 (0.09)	24.4 (0.05)		23.6 (0.08) [a]	23.9 (0.06) [b]
	pdf>Q128	**24.8** (0.3)	**24.3** (0.23)		**23.5** (0.15)	**22.8** (0.22)
	Q128	23.7 (0.05) [a]	24 (0.07) [b]		23.2 (0.09) [a]	23.5 (0.04) [b]
Period		**DD23**	**DD29**	**DD23to DD29**	**DD29to DD23**	
	pdf>Q0	24.6 (0.09) [b]	23.6 (0.08) [a]	24.2 (0.16) [b]	24.4 (0.1) [b]	
	pdf>Q128	**24.8** (0.29)	**23.5** (0.15) [a]	**24.6** (0.19) [b]	**23.8** (0.17)	
	Q128	23.7 (0.05) [a]	23.2 (0.09) [b]	23.3 (0.09) [b]	23.95 (0.13) [a]	
Period		**DD23to DD29**	**DD21to DD25**	**DD25to DD29**		
	pdf>Q0	24.2 (0.16) [a]	24.7 (0.06) [b]	23.8 (0.06) [c]		
	pdf>Q128	**24.86** (0.19) [a]	**24.9** (0.16) [a]	**22.8** (0.13) [b]		
	Q128	23.3 (0.09) [a]	24.1 (0.06) [b]	23.6 (0.03) [c]		
Period		**DD23to DD29**	**LD23to DD29**	**LL23to DD29**		
	pdf>Q0	24.2 (0.16) [a]	23.9 (0.06) [ac]	23.7 (0.03) [bc]		
	pdf>Q128	**24.86** (0.19) [a]	**23.1** (0.1) [b]	**22.6** (0.18) [b]		
	Q128	23.3 (0.09) [a]	23.6 (0.02) [b]	23.1 (0.04) [c]		

Table 4. 10 Sample sizes for immunocytochemical experiments.

Regime	Genotype	L3	1d	3d	5d	7d	9d	16d	23d
DD25	***pdf>Q0***	31	19	22	Not clear	22	Not done	26	23
	pdf>Q128	30	30	26	Not clear	27	21	24	28
DDTC toDD25	***pdf>Q0***	31	23	27	17	24	Not done	18	28
	pdf>Q128	25	26	24	12	24	23	28	23
DD29to DD25	***pdf>Q0***						26		
	pdf>Q128						26		
DD23	***pdf>Q0***	26	19	25	21	28	Not done	26	18
	pdf>Q128	22	24	21	20	26	27	25	23
DD29	***pdf>Q0***	23	20	24	19	22	Not done	26	23
	pdf>Q128	36	22	22	15	26	16	28	18
DD23to DD29	***pdf>Q0***	Same as DD23	Same as DD23	26	25	24	Not done	22	19
	pdf>Q128	Same as DD23	Same as DD23	27	18	31	28	16	22

Regime	Genotype	Age 6d	
		CT23	CT11
DD25	***pdf>Q0***	17	
	pdf>Q128	17	
DDTCtoDD25	***pdf>Q0***	30	26
	pdf>Q128	24	31
DD29toDD25	***pdf>Q0***	29	28
	pdf>Q128	29	33
DD23	***pdf>Q0***	32	29
	pdf>Q128	24	30
DD23toDD29	***pdf>Q0***	29	26
	pdf>Q128	31	25

Table 4. 11 Regime-wise behavioural and cellular data for pdf>Q128.

Regime	Age	Behav (% Rhy)	PDF in sLNv (~mean)	PER in LNv (~mean)		PER oscillations in LNv		expHTT form in LNv dominating the Hemis		Change of Inc feature with age	
				sLNv	lLNv	sLNv	lLNv	sLNv	lLNv	Inc No.	Inc Size
DD25	L3		3.7					Diff	NA		
	1d	Arr (23.7)	2.5					Inc	Diff	Slight ↑ with age	↑ with age
	3d		2.4					Inc	Diff + Inc		
	5d		NTA*					Inc	Inc		
	7d		2.4	1.3	2.7	Nil	Nil	Inc	Inc		
	9d		2.4					Inc	Inc		
	AW2	Arr (11)	2.2					Inc	Inc		
	AW3	Arr (3.5)	2.1					Inc	Inc		
DDTC toDD25	L3		3.5					Diff	NA		
	1d	**Rhy (88.4)**	**3.1**					Inc	Diff	Slight ↑ with age	↑ with age
	3d		**3.3**					Inc	Diff, Diff + Inc		
	5d		**3.6**					Inc	Inc		
	7d		2.7	1.3	2.3	**Low amp, anti-phase**	Nil	Inc	Inc		
	9d		2.1					Inc	Inc		
	AW2	Arr (36.7)	1.6					Inc	Inc		
	AW3	Arr (29.7)	1					Inc	Inc		
DD29to DD25	AW1 7d	Arr (36.7)	2.7	**2.7**	**3.8**	Nil	**Low amp, anti-phase**	Inc	Inc	**NTA**	**NTA**
	AW2	Arr (16.5)									
	AW3	Arr (14.8)									

***** Very faint PDF staining at 5d, therefore, the PDF^{+} LNv numbers not clear. NTA, not available. NA, not applicable. Improvement/rescue is indicated by lilac shading.

Table 4.11 Regime-wise behavioural and cellular data for pdf>Q128.

Regime	Age	Behav (% Rhy)	PDF in sLNv (~mean)	PER in LNv (~mean)		PER oscillations in LNv		expHTT form in LNv dominating the Hemis		Change of Inc feature with age	
				sLNv	lLNv	sLNv	lLNv	sLNv	lLNv	Inc No.	Inc Size
DD23	L3		3.4					Diff	NA		
	1d	Arr (22.1)	**3.3**					Diff, Diff + Inc	Diff	Slight ↑ with age	No
	3d		**3.3**					Diff + Inc	Diff		
	5d		2.8					Inc	Diff, Diff + Inc		
	7d		2.2	**1.7**	**3.4**	**Low amp**	**Low amp**	Inc	Inc		
	9d		2.2					Inc	Inc		
	AW2	Arr (7)	1.9					Inc	Inc		
	AW3	Arr (9.3)	1					Inc	Inc		
DD29	L3		3.7					Diff	NA		
	1d	**Rhy (85.2)**	**3.6**					Diff, Diff + Inc	Diff		No
	3d		**3.3**					Inc	Inc		
	5d		**3.2**					Inc	Inc		
	7d		**3.1**	NTA	NTA	NTA	NTA	Inc	Inc		
	9d		**3.1**					Inc	Inc		
	AW2	Arr (33.7)	2.7					Inc	Inc	↑ with age	
	AW3	Arr (19)	1.7					Inc	Inc		
DD23to DD29	L3		3.4					Diff	NA		
	1d	**Rhy (89.4)**	**3.3**					Diff	Diff	No	No
	3d		**3.3**					Inc	Diff, Diff + Inc		
	5d		**3.3**					Inc	Inc		
	7d		**3.1**	**2.2**	**2.8**	Nil	**Low amp**	Inc	Inc		
	9d		**3.3**					Inc	Inc		
	AW2	Arr (39.6)	1.8					Inc	Inc		
	AW3	Arr (26.6)	1.4					Inc	Inc		

***** The PDF staining at 5d was faint; therefore, the PDF^{+} LNv numbers could not be discerned. NTA, not available. NA, not applicable. Improvement/rescue is indicated by lilac shading.

Appendix C

Table 4. 12 Between-regime comparisons of activity rhythms of pdf>Q128 in AW1.

Regimes compared	Behaviour in AW1						Overall activity rhythm improvements
	% Rhythmicity			Rhythmicity	'r' improvements	Robustness	
	Robustness						
DDTCtoDD25-related regimes							
DDTCto DD25	**DDTC**	**DD25**		DDTC> DD25	DDTC> DD25	Poor robustness under both regimes	**DDTC> DD25**
DD25	**88.4** 147	23.7 138					
DDTCtoDD25 *vs* constant high (29°C) or low (21°C) temperatures during development to DD25							
DDTCto DD25	**DDTC**	**DD29to DD25**	**DD21to DD25**	DDTCto DD25> DD29to DD25 =DD21to DD25	DDTCto DD25> DD29to DD25 =DD21to DD25		**DDTCto DD25> DD29to DD25 =DD21to DD25**
DD29to DD25	**83.33** 147	36.7 149	30 171				
DD21toDD25							
DDTCtoDD25 *vs.* DDTC to either DD29 or DD21							
DDTCto DD25	**DDTCto DD25**	**DDTCto DD29**	**DDTCto DD21**	DDTCto DD25= DDTCto DD29> DDTCto DD21	DDTCto DD25= DDTCto DD29> DDTCto DD21	DDTCto DD29> DDTCto DD25	**DDTCto DD25= DDTCto DD29> DDTCto DD21**
DDTCto DD29	**83.33** 147	**86.2 189**	10.4 139				
DDTCto DD21							
DDTCtoDD25 *vs* DDTC from egg to L3 *vs* DDTC as pupa to 2d adults							
DDTCto DD25	**DDTC through dev**	**DDTC upto L3**	**DDTC as Pupa-2d**	DDTC> DDTC upto L3 = DDTC as pupa-2d	DDTC> DDTC upto L3 = DDTC as pupa-2d		**DDTC> DDTC from egg to L3= DDTC as pupa to 2d**
DDTC up to L3 to DD25							
DD25 to DDTC from pupa to 2d adult to DD25	**83.33** 147	16 173	24 130				

Rhythm rescue is indicated by lilac shading.

Table 4.12 Between-regime comparisons of activity rhythms of pdf>Q128 in AW1.

Regimes compared	Behaviour in AW1					Overall activity rhythm improvements
	% Rhythmicity / Robustness		Rhythmicity	'r' improvements	Robustness	
Effect of cycling light and temperature and essentiality of functional clocks during development (DDTCtoDD25 *vs* LDTCtoDD25 *vs* LLTCtoDD25)						
DDTCto DD25 **LDTCto DD25** **LLTCto DD25**	**DDTC**	**LDTC**	**LLTC**	DDTCto DD25> LDTCto DD25= LLTCto DD25	DDTCto DD25> LDTCto DD25= LLTCto DD25	Poor robustness under all regimes	**DDTCto DD25> LDTCto DD25 =LLTCto DD25**
	88.4 146	37.3 130	26.9 145				
Constant temperature regimes						
DD23 *vs* DD25 *vs* DD29						
DD23 **DD25** **DD29**	**DD23**	**DD25**	**DD29**	DD29> DD23= DD25	**DD29> DD25> DD23** (For controls *pdf*>Q0 and *Q128*, DD29> DD25= DD23)	Poor robustness under all regimes	**DD29> DD25> DD23**
	22.1 149	23.7 138	**85.2** 141				
Upshift temperature regimes						
Different degrees of upshift						
DD23to DD29 **DD21to DD25** **DD25to DD29**	**DD23to DD29**	**DD21to DD25**	**DD25to DD29**	DD23to DD29= DD25to DD29> DD21to DD25	DD23to DD29= DD25to DD29> DD21to DD25 (even for controls)	DD23to DD29> DD25to DD29	**DD23to DD29> DD25to DD29> DD21to DD25**
	89.7 **185**	30 171	**86.7** 133				

Rhythm rescue is indicated by lilac shading.

Table 4.12 Between regime comparisons of activity rhythms of pdf>Q128 in AW1.

Regimes compared	Behaviour in AW1						Overall activity rhythm improvements
	% Rhythmicity		Rhythmicity	'r' improvements	Robustness		
	Robustness						
DD23toDD29-related temperature regimes							
DD23 *vs* DD29 *vs* DD23toDD29 *vs* DD29toDD23							
DD23to DD23 **DD29to DD29**	**DD23**	**DD29**	**DD23to DD29**	**DD29to DD23**	DD23to DD29= DD29> DD23= DD29to DD23	DD23to DD29= DD29> DD29to DD23> DD23 (Even for control *Q128*)	DD23to DD29> DD29	**DD23to DD29> DD29> DD29to DD23> DD23**
DD23to DD29 **DD29to DD23**	22.1 149	**85.2** 128	**89.4** **185**	4.8 91				
Adult-restricted warm temperatures- Chronic exposure *vs.* short duration (48h of 29°C) exposure								
DD23to DD23 **DD23to DD29** **DD23to 48hof DD29@3d toDD23** **DD23to 48hof DD29@6d toDD23**	**DD23to DD23**	**DD23to DD29**	**DD23+ 48h29 at 3d**	**DD23+ 48h29 at 6d**	DD23to DD29> DD23= DD23to48h29at3d = DD23to48h29at9d	DD23to DD29> DD23= DD23to 48h29@ 3d= DD23to 48h29@ 9d		**DD23to DD29> DD23= DD23to 48h29@3d = DD23to 48h29@9d**
22.1 149	**89.4** 185	25 129	27 146					
Effect of cycling light or lack of functional clocks during development on DD23toDD29 rescue (DD23toDD29 *vs* LD23toDD29 *vs* LL23toDD29)								
DD23to DD29 **LD23to DD29** **LL23to DD29**	**DD23to DD29**	**LD23to DD29**	**LL23to DD29**		DD23to DD29= LD23to DD29= LL23to DD29	DD23to DD29= LD23to DD29= LL23to DD29	DD23to DD29= LD23to DD29> LL23to DD29	**DD23to DD29= LD23to DD29> LL23to DD29**
89.4 185	**94.6** 173	**83.9** 135						

Rhythm rescue is indicated by lilac shading.

Table 4.12 Between regime comparisons of activity rhythms of pdf>Q128 in AW1.

Regimes compared	Behaviour in AW1					Overall activity rhythm improvements
	% Rhythmicity / Robustness		Rhythmicity	'r' improvements	Robust-ness	
Effect of cyclic light during development: DDtoDD *vs* LDtoDD						
	TCtoDD25					
DDTCtoDD25	**DDTC**	**LDTC**	DDTCtoDD25> LDTCtoDD25	DDTCtoDD25> LDTCtoDD25	DDTCtoDD25= LDTCtoDD25	**DDTCtoDD25> LDTCtoDD25**
LDTCtoDD25	**88.4** 147	37.3 130				
	Constant cool temperatures (23°C)					
DD23toDD23	**DD23toDD23**	**LD23toDD23**	DD23toDD23= LD23toDD23	DD23toDD23= LD23toDD23		**DD23toDD23= LD23toDD23**
LD23toDD23	22.1 149	28.2 140				
	Constant warm temperatures (29°C)					
DD29toDD29	**DD29toDD29**	**LD29toDD29**	DD29toDD29= LD29toDD29	DD29toDD29= LD29toDD29	DD29toDD29= LD29toDD29	**DD29toDD29= LD29toDD29**
LD29toDD29	**85.2** 128	**87.9** 110				
	Temperature upshift (23°Cto29°C)					
DD23toDD29	**DD23toDD29**	**LD23toDD29**	DD23toDD29= LD23toDD29	DD23toDD29= LD23toDD29	DD23toDD29= LD23toDD29	**DD23toDD29= LD23toDD29**
LD23toDD29	**89.7** 185	**94.6** 174				
	Temperature downshift (29°Cto23°C)					
DD29toDD23	**DD29toDD23**	**LD29toDD23**	DD29toDD23= LD29toDD23	DD29toDD23= LD29toDD23		**DD29toDD23= LD29toDD23**
LD29toDD23	4.8 91	2.2 NA				

Rhythm rescue is indicated by lilac shading.

Table 4. 13 Between-regime comparisons of behaviour and cellular phenotypes of pdf>Q128.

Regi-mes comp-ared	Behaviour in AW1		PDF rescue in sLNv	PER^{+} LNv	PER oscillations in LNv	expHTT form in LNv (Diff> Diff+ Inc> Inc)	↓ Inc No.	↓ Inc load	Circadian function and neuro-protection
	Rhythmicity	'r' improvement							
DDTCtoDD25-related regimes									
DD25 **DDTCto DD25**	DDTC> DD25	DDTC> DD25	DDTC> DD25	DDTC> DD25	DDTC> DD25	DDTC= DD25	DDTC= DD25	**DDTC= DD25**	**DDTC> DD25**
DD25 **DDTCto DD25** **DD29to DD25**	**DDTC> DD25= DD29to DD25**	DDTC> DD29to DD25	**DDTC> DD25= DD29to DD25**	DD29to DD25> DDTC= DD25	DDTC> DD25= DD29to DD25	DDTC= DD25 (=DD29 to DD25, maybe)	DDTC= DD25 (=DD29 to DD25, maybe)	**DDTC= DD25 (=DD29 to DD25, maybe)**	**DDTC> DD29to DD25> DD25**
Constant temperature-related regimes									
DD23 **DD25** **DD29**	DD29> DD25= DD23	**DD29> DD25> DD23**	DD29> DD23> DD25	DD23> DD25	DD23> DD25	DD23> DD23= DD29	DD29> DD25> DD23	**DD29> DD25> DD23**	**DD29> DD23> DD25**
Temperature upshift-related regimes									
DD23 **DD29** **DD23to 29**	DD23to DD29= DD29> DD23	DD23to DD29= DD29> DD23	DD23to DD29= DD29> DD23	DD23to DD29= DD23	DD23> DD23to DD29	DD23> DD23to DD29> DD29	DD23to DD29> DD29 >DD23	**DD23to DD29> DD29 >DD23**	**DD23to DD29> DD29> DD23**

APPENDIX D: Tables and Supplementary Figure for Chapter 5

Appendix D

Table 5. 1 A genetic screen for modifiers of arrhythmicity of expHTT-expressing flies.

Gene	Description	Modification	Modifier line source	Genotype (s)	% Rhythmicity
	Huntingtin				
hHTT	Human huntingtin with 548aa containing 128 Q repeats.		Lee et al., 2000	***w;pdf-Q128/+;+***	**54.84**
				w;pdfGal4/Q128;+	**20**
				w;timGal4/Q128;+	**0**
dhtt	*D.melanogaster* huntingtin	OE	Zhang et al., 2009	***w;pdf-Q128/UAS-dhtt;+***	**50**
dhtt	*D.melanogaster* huntingtin with 82aa	OE	Mugat et al., 2008	***w;pdf-Q128/+;UAS-dhtt82aa/+***	**60**
				w;pdfGal4/Q128;UAS-dhtt82aa/+	**6.25**
				w;timGal4/Q128;UAS-dhtt82aa/+	**0**
dhtt	*D.melanogaster* huntingtin with 620aa	OE	Mugat et al., 2008	***w;pdf-Q128/+;UAS-dhtt620aa/+***	**31.25**
				w;pdfGal4/Q128;UAS-dhtt620aa/+	**12.5**
				w;timGal4/Q128;UAS-dhtt620aa/+	**0**
dhtt	*D.melanogaster* huntingtin	DR	GD 36204	***w;pdf-Q128/UAS-dhtt-RNAi/+;+***	**62.5**
dhtt	*D.melanogaster* huntingtin	DR	GD29532	***w;pdf-Q128/+;UAS-dhtt-RNAi/+***	**53.33**
				w;pdfGal4/Q128;UAS-dhtt-RNAi/+	**12.5**
				w;timGal4/Q128;UAS-dhtt-RNAi/+	**6.25**
Hip14	*D.melanogaster* Huntingtin interacting protein	OE	Bl 17109	***w;pdf-Q128/+;UAS-Hip14/+***	**73.33**

The genetic modifiers are grouped according to their most well-known function or protein family. OE is overexpressed, and DR is down-regulated. Each modifier genotype is compared against its respective *circadian driver-Q128* genotype (placed at the top of the table), i.e., the recombinant *w;pdfGal4-Q128/+* (denoted as *w;pdf-Q128/+;+*) or *w;pdfGal4/Q128;+* or *w;timGal4/Q128;+*. Asterisks indicate significant differences from respective controls at * $p<0.05$, ** $p<0.01$, *** $p<0.001$.

Table 5.1 A genetic screen for modifiers of arrhythmicity of expHTT-expressing flies.

Gene	Description	Modification	Modifier line source	Genotype (s)	% Rhythmicity
	Heat shock proteins (HSPs)				
Hsp23	*D.melanogaster* Hsp23	OE	Bl 30541	***w;pdf-Q128/ UAS-Hsp23;+***	**86.67***
Hsap/ JB1/ DnaJB1	Human DNAJB1 (Hsp40 homolog, sub-family B, member 1)	OE	Bl 53730	***w;pdf-Q128/ UAS-DnaJB1;+***	**93.75****
DnaJ1k/ dhdJ1	*D.melanogaster* DnaJ- like-1 or Hsp40, droj1 (member of J/Hsp40 co-chaperone family; provides specificity to HSP70 chaperones)	OE	Bl 30553	***w;pdf-Q128/+; UAS-DnaJ1k/+***	**93.75****
HSPA1L/ HSP70/ HSAP	Human heat shock 70kDa protein 1-like or HSP70	OE	Bl7454	***w;pdf-Q128/+; UAS- HSPA1L/+*** ***w;pdfGal4/Q128; UAS- HSPA1L/+*** ***w;timGal4/Q128; UAS- HSPA1L/+***	**93.75*** **100***** **43.75****
Hsc70-3	*D.melanogaster* heat shock 70-kDa protein cognate 3 or BiP or Hsc3 or Grp78	OE	Bl 5843	***w;pdf-Q128/+; UAS-Hsc70-3WT/+***	**43.75**
Hsc70-3	Expresses Hsc70-3 with a disrupted ATP binding site	DR	Bl 5842	***w;pdf-Q128/+; UAS-HSc70-3.K97S/+***	**80**
Hsc70-4	*D.melanogaster* Heat shock protein cognate 4 or Hsc4 or BAP74 or scattered	DR	Bl 7453	***w;pdf-Q128/+; UAS-Hsc70-4K71S/+***	**100****
Hsf	*D.melanogaster* Heat shock Factor or Hsf1 or Dm-Hsf	DR	Bl 27070	***w;pdf-Q128/+; UAS-Hsf-RNAi/+***	**58.33**
Hsf	*D.melanogaster* Heat shock Factor or HSF1 or Dm-Hsf	DR	GD 48692	***w;pdf-Q128/ UAS-Hsf-RNAi/+***	**62.5**
HDJ1/ Hsp40	*D.melanogaster* dHdj1/ Hsp40	DR	GD 31271	***w;pdf-Q128/+; UAS-Hdj1-RNAi/+***	**60**
Hsp70Aa	*D.melanogaster* Heat shock protein-70Aa	DR	GD 41748	***w;pdf-Q128/+; UAS- Hsp70Aa-RNAi/+***	**68.75**
Hsp70Bb	*D.melanogaster* Heat shock protein-70Bb	DR	GD 36640	***w;pdf-Q128/+; UAS- Hsp70Bb-RNAi/+***	**75**

Table 5.1 A genetic screen for modifiers of arrhythmicity of expHTT-expressing flies.

Gene	Description	Modification	Modifier line source	Genotype (s)	% Rhythmicity
	Histone deacetylases				
Hdac3	*D.melanogaster* histone deacetylase involved in chromatin silencing	OE	Bl 32248	***w;pdf-Q128/UAS-Hdac3;+***	**31.25**
Hdac6	*D.melanogaster* cytosolic deacetylase functions as a key modulator of proteostasis	OE	Bl 51181	***w;pdf-Q128/+;UAS-Hdac6/+***	**56.25**
Hdac3	*D.melanogaster* histone deacetylase	DR	Bl 34778	***w;pdf-Q128/+; UAS-Hdac3-RNAi/+***	**50**
	Autophagy				
atg1/ unc- 51/ DK-4	*D.melanogaster* Autophagy-related 1; a protein kinase, functions in the regulation of autophagy	OE	Bl 51654	***w;pdf-Q128/UAS-atg1;+***	**60**
			Bl 51655	***w;pdf-Q128/+;UAS-atg1/+***	**43.75**
atg5	*D.melanogaster* Autophagy-related 5; has Atg8 ligase activity	OE	Bl 59848	***w;pdf-Q128/+;UAS-atg5/+***	**87.5 ***
atg8a/ LC3	*D.melanogaster* Autophagy-related 8a; has roles in autophagosome formation, maintenance of neuro-muscular function and average lifespan	OE	Bl 52005	***w;pdf-Q128/UAS-atg8a;+***	**88.24 ***
			Bl 51656	***w;pdf-Q128/+;UAS-atg8a/+***	**87.5 ***
	Apoptosis				
Iap2/ Diap-2/ Diha	*D.melanogaster* Death-associated inhibitor of apoptosis 2; ubiquitin E3-ligase activity	DR	Bl 34776	***w;pdf-Q128/+; UAS-Iap2-RNAi/+***	**62.5**
dark/ ark/ hac-1/ Apaf-1	*D.melanogaster* Death-associated APAF1-related killer (Dark), an essential component of the apoptosome	DR	KK 104215	***w;pdf-Q128/UAS-dark-RNAi;+***	**35.71**

Table 5. 2 The number of surviving flies for comparisons in AW2 and AW3 for the locomotor activity experiments.

Sample sizes							
Genotype	**Exper-iment**	**AW2**	**AW3**	**Genotype**	**Exper-iment**	**AW2**	**AW3**
pdf>Q0,Hsp40	1	**31**	**18**	***pdf>Q128,Hsp40***	1	**32**	**18**
	2	**30**	**24**		2	**32**	**31**
	3	**27**	**22**		3	**32**	**29**
	4	**31**	**31**		4	**32**	**31**
	5	**31**	**28**		5	**31**	**30**
pdf>Q0	1	**29**	**9**	***pdf>Q128***	1	**30**	**21**
	2	**31**	**30**		2	**31**	**31**
	3	**24**	**24**		3	**28**	**26**
	4	**30**	**30**		4	**31**	**29**
	5	**16**	**12**		5	**27**	**23**
Q0,Hsp40	1	**25**	**4**	***Q128,Hsp40***	1	**29**	**11**
	2	**30**	**26**		2	**32**	**31**
	3	**15**	**0**		3	**13**	**0**
pdf>Q0,HSP70	1	**28**	**24**	***pdf>Q128,HSP70***	1	**32**	**32**
	2	**29**	**23**		2	**29**	**26**
	3	**23**	**17**		3	**32**	**28**
Q0,HSP70	1	**22**	**21**	***Q128,HSP70***	1	**27**	**25**
pdf>Hsp40	1	**32**	**13**	***pdf>HSP70***	1	**28**	**23**
	2	**30**	**29**				
Synergistic effect experiment							
pdf>Q128,Hsp40,HSP70		**22**	**17**	***pdf>Q128***		**27**	**28**
pdf>Q0,Hsp40,HSP70		**26**	**21**	***pdf>Q128,Hsp40***		**21**	**21**
pdf>Hsp40,HSP70		**22**	**19**	***pdf>Q128,HSP70***		**30**	**28**
Q128,Hsp40,HSP70		**28**	**24**				

Table 5. 3 The number of hemispheres per genotype per age to quantify the cellular features.

Number of hemispheres/genotype/time-point/age					
	CT23			CT11	
Genotype	**3d**	**9d**	**16d**	**3 d**	**9d**
pdf>Q128	28	29	23	30	
pdf>Q0,Hsp40	21	26	27	27	27
pdf>Q128,Hsp40	26	29	28	25	25
pdf>Q0,HSP70	26	18		31	
pdf>Q128,HSP70	30	23		27	

expHTT inclusions		
Genotype	**3d**	**9d**
pdf>Q128	27	20
pdf>Q128,Hsp40	30	30
pdf>Q128,HSP70	27	25

Top: For PER oscillations, flies were dissected around CT23 and CT11 at different ages: all the five genotypes at 3d and *pdf>Q0,Hsp40* and *pdf>Q128,Hsp40* also at 9d (n for Fig 5.11d). For PDF^{+} and PER^{+} LNv numbers, CT23 (top-left) samples were used (n for Figs 5.5 and 5.11b, c). Bottom: For quantification of expHTT inclusions and expHTT forms in *pdf>Q128*, *pdf>Q128,Hsp40* and *pdf>Q128,HSP70* across 3d and 9d (n for Figs 5.7 a-d, 5.8, 5.10). For comparisons of expHTT forms across 3d, 9d and 16d for in *pdf>Q128* and *pdf>Q128,Hsp40*, samples at CT23 (top-left) were used (n for Figs 5.6c, 5.7e, f, 5.9).

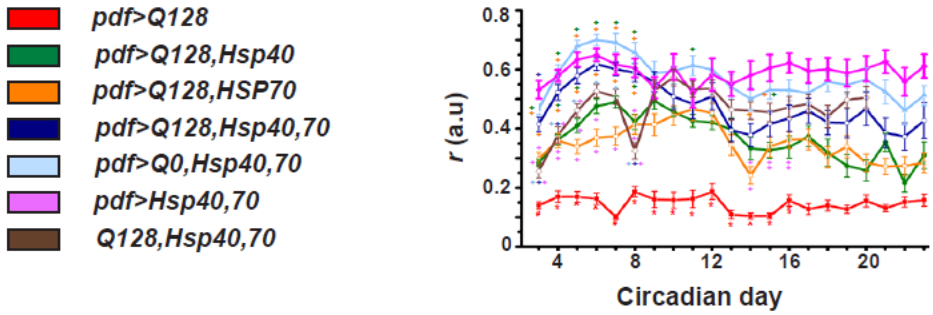

Figure S1

Fig S 1 Mean r-value comparing genotypes across age for testing the synergistic effect of co-expression on Hsp40 and HSP70 in pdf>Q128 flies.

Data Post-16 d is omitted from between-genotype statistical tests due to few surviving flies. The blank in the *Q128,Hsp40,HSP70* line graph between ages 21-23 d is due to the division of the 21 d data based on a circadian day with a periodicity of ~27 h. Across all panels, coloured symbols represent statistically significant differences: red-coloured symbols indicate significant differences at $p<0.05$ of *pdf>Q128* from '*' all other genotypes, '#' from all genotypes except *Q128,Hsp40,HSP70*, '§' from all genotypes except *pdf>Q128,Hsp40*, '^' from all genotypes except *pdf>Q128,HSP70*, and orange '*' of *pdf>Q128,HSP70* from all other genotypes. Coloured '+' near the error bar of a data point indicates significant differences at $p<0.05$ of the respective-coloured genotype from the data-point genotype. Error bars are SEM. *n* for these analyses is shown in Table 5.2 as the synergistic effect experiment.

REFERENCES

Abisambra, J. F., Jinwal, U. K., Suntharalingam, A., Arulselvam, K., Brady, S., Cockman, M., Jin, Y., Zhang, B. and Dickey, C. A. (2012). DnaJA1 antagonizes constitutive Hsp70-mediated stabilization of Tau. *J Mol Biol* **421**, 653-661. https://doi.org/10.1016/j.jmb.2012.02.003.

Abraham, U., Granada, A. E., Westermark, P. O., Heine, M., Kramer, A. and Herzel, H. (2010). Coupling governs entrainment range of circadian clocks. *Mol Syst Biol* **6**, 438. https://doi.org/10.1038/msb.2010.92.

Abruzzi, K. C., Zadina, A., Luo, W., Wiyanto, E., Rahman, R., Guo, F., Shafer, O. and Rosbash, M. (2017). RNA-seq analysis of *Drosophila* clock and non-clock neurons reveals neuron-specific cycling and novel candidate neuropeptides. *PLoS Genet* **13**, e1006613. https://doi.org/10.1371/journal.pgen.1006613.

ACMG/ASHG. (1998). ACMG/ASHG statement. Laboratory guidelines for Huntington disease genetic testing. The American College of Medical Genetics/American Society of Human Genetics Huntington Disease Genetic Testing Working Group. *Am J Hum Genet* **62**, 1243-7.

Adachi, H., Waza, M., Tokui, K., Katsuno, M., Minamiyama, M., Tanaka, F., Doyu, M. and Sobue, G. (2007). CHIP overexpression reduces mutant androgen receptor protein and ameliorates phenotypes of the spinal and bulbar muscular atrophy transgenic mouse model. *J Neurosci* **27**, 5115-26. https://doi.org/10.1523/jneurosci.1242-07.2007.

Adamczak-Ratajczak, A., Kupsz, J., Owecki, M., Zielonka, D., Sowinska, A., Checinska-Maciejewska, Z., Krauss, H., Michalak, S. and Gibas-Dorna, M. (2017). Circadian rhythms of melatonin and cortisol in manifest Huntington's disease and in acute cortical ischemic stroke. *J Physiol Pharmacol* **68**, 539-546.

Adams, M. D. Celniker, S. E. Holt, R. A. Evans, C. A. Gocayne, J. D. Amanatides, P. G. Scherer, S. E. Li, P. W. Hoskins, R. A. Galle, R. F. et al. (2000). The genome sequence of *Drosophila melanogaster*. *Science* **287**, 2185-95. https://doi.org/10.1126/science.287.5461.2185.

Adegbuyiro, A., Sedighi, F., Pilkington, A. W. t., Groover, S. and Legleiter, J. (2017). Proteins containing expanded polyglutamine tracts and neurodegenerative disease. *Biochemistry* **56**, 1199-1217. https://doi.org/10.1021/acs.biochem.6b00936.

Adler, C. H., Caviness, J. N., Hentz, J. G., Lind, M. and Tiede, J. (2003). Randomized trial of modafinil for treating subjective daytime sleepiness in patients with Parkinson's disease. *Mov Disord* **18**, 287-293. https://doi.org/10.1002/mds.10390.

AdobeIndesignCS. Version 3.0. Adobe Systems Incorporated. San Jose, California, USA.

Agathokleous, E. and Calabrese, E. J. (2020). A global environmental health perspective and optimisation of stress. *Sci Total Environ* **704**, 135263. https://doi.org/10.1016/j.scitotenv.2019.135263.

Agrawal, N., Pallos, J., Slepko, N., Apostol, B. L., Bodai, L., Chang, L. W., Chiang, A. S., Thompson, L. M. and Marsh, J. L. (2005). Identification of combinatorial drug regimens for treatment of Huntington's disease using *Drosophila*. *Proc Natl Acad Sci U S A* **102**, 3777-81. https://doi.org/10.1073/pnas.0500055102.

Agrawal, P. and Hardin, P. E. (2016). The *Drosophila* receptor protein tyrosine phosphatase LAR is required for development of circadian pacemaker neuron processes that support rhythmic activity

in constant darkness but not during light/dark cycles. *J Neurosci* **36**, 3860-70. https://doi.org/10.1523/JNEUROSCI.4523-15.2016.

Ahmad, M., Li, W. and Top, D. (2021). Integration of circadian clock information in the *Drosophila* circadian neuronal network. *J Biol Rhythms* **36**, 203-220. https://doi.org/10.1177/0748730421993953.

Akbergenova, Y. and Littleton, J. T. (2017). Pathogenic Huntington alters BMP signaling and synaptic growth through local disruptions of endosomal compartments. *J Neurosci* **37**, 3425-3439. https://doi.org/10.1523/JNEUROSCI.2752-16.2017.

Akerfelt, M., Morimoto, R. I. and Sistonen, L. (2010). Heat shock factors: integrators of cell stress, development and lifespan. *Nat Rev Mol Cell Biol* **11**, 545-55. https://doi.org/10.1038/nrm2938.

Al-Ramahi, I., Lam, Y. C., Chen, H. K., de Gouyon, B., Zhang, M., Pérez, A. M., Branco, J., de Haro, M., Patterson, C., Zoghbi, H. Y. et al. (2006). CHIP protects from the neurotoxicity of expanded and wild-type ataxin-1 and promotes their ubiquitination and degradation. *J Biol Chem* **281**, 26714-24. https://doi.org/10.1074/jbc.M601603200.

Alberti, S., Esser, C. and Höhfeld, J. (2003). BAG-1--a nucleotide exchange factor of Hsc70 with multiple cellular functions. *Cell Stress Chaperones* **8**, 225-31. https://doi.org/10.1379/1466-1268(2003)008<0225:bnefoh>2.0.co;2.

Alcalà-Vida, R., Awada, A., Boutillier, A.-L. and Merienne, K. (2021). Epigenetic mechanisms underlying enhancer modulation of neuronal identity, neuronal activity and neurodegeneration. *Neurobiology of Disease* **147**. https://doi.org/10.1016/j.nbd.2020.105155.

Alders, J., Smits, M., Kremer, B. and Naarding, P. (2009). The role of melatonin in sleep disturbances in end-stage Huntington's disease. *J Neuropsychiatry Clin Neurosci* **21**, 226-7. https://doi.org/10.1176/jnp.2009.21.2.226.

Ali, Y. O., Kitay, B. M. and Zhai, R. G. (2010). Dealing with misfolded proteins: examining the neuroprotective role of molecular chaperones in neurodegeneration. *Molecules* **15**, 6859-87. https://doi.org/10.3390/molecules15106859.

Allemand, R., Cohet, Y. and David, J. (1973). Increase in the longevity of adult *Drosophila melanogaster* kept in permanent darkness. *Exp Gerontol* **8**, 279-83. https://doi.org/10.1016/0531-5565(73)90040-5.

Almqvist, E. W., Elterman, D. S., MacLeod, P. M. and Hayden, M. R. (2001). High incidence rate and absent family histories in one quarter of patients newly diagnosed with Huntington disease in British Columbia. *Clin Genet* **60**, 198-205. https://doi.org/10.1034/j.1399-0004.2001.600305.x.

Alonso, M. E., Yescas, P., Rasmussen, A., Ochoa, A., Macías, R., Ruiz, I. and Suástegui, R. (2002). Homozygosity in Huntington's disease: new ethical dilemma caused by molecular diagnosis. *Clin Genet* **61**, 437-42. https://doi.org/10.1034/j.1399-0004.2002.610607.x.

Alpert, M. H., Frank, D. D., Kaspi, E., Flourakis, M., Zaharieva, E. E., Allada, R., Para, A. and Gallio, M. (2020). A circuit encoding absolute cold temperature in *Drosophila*. *Curr Biol* **30**, 2275-2288.e5. https://doi.org/10.1016/j.cub.2020.04.038.

References

Alpert, M. H., Gil, H., Para, A. and Gallio, M. (2022). A thermometer circuit for hot temperature adjusts *Drosophila* behavior to persistent heat. *Curr Biol* **32**, 4079-4087.e4. https://doi.org/10.1016/j.cub.2022.07.060.

Altar, C. A., Cai, N., Bliven, T., Juhasz, M., Conner, J. M., Acheson, A. L., Lindsay, R. M. and Wiegand, S. J. (1997). Anterograde transport of brain-derived neurotrophic factor and its role in the brain. *Nature* **389**, 856-60. https://doi.org/10.1038/39885.

Altıner, Ş., Ardic, S. and Çebi, A. H. (2020). Extending the phenotypic spectrum of Huntington disease: Hypothermia. *Mol Syndromol* **11**, 56-58. https://doi.org/10.1159/000505887.

Alves, S., Regulier, E., Nascimento-Ferreira, I., Hassig, R., Dufour, N., Koeppen, A., Carvalho, A. L., Simoes, S., de Lima, M. C., Brouillet, E. et al. (2008). Striatal and nigral pathology in a lentiviral rat model of Machado-Joseph disease. *Hum Mol Genet* **17**, 2071-83. https://doi.org/10.1093/hmg/ddn106.

Amaro, I. A. and Henderson, L. A. (2016). An Intrabody Drug (rAAV6-INT41) Reduces the Binding of N-Terminal Huntingtin Fragment(s) to DNA to Basal Levels in PC12 Cells and Delays Cognitive Loss in the R6/2 Animal Model. *J Neurodegener Dis* **2016**, 7120753. https://doi.org/10.1155/2016/7120753.

Ambegaokar, S. S., Roy, B. and Jackson, G. R. (2010). Neurodegenerative models in *Drosophila:* Polyglutamine disorders, Parkinson disease, and amyotrophic lateral sclerosis. *Neurobiol Dis* **40**, 29-39. https://doi.org/10.1016/j.nbd.2010.05.026.

Ambrose, C. M., Duyao, M. P., Barnes, G., Bates, G. P., Lin, C. S., Srinidhi, J., Baxendale, S., Hummerich, H., Lehrach, H., Altherr, M. et al. (1994). Structure and expression of the Huntington's disease gene: Evidence against simple inactivation due to an expanded CAG repeat. *Somat Cell Mol Genet* **20**, 27-38. https://doi.org/10.1007/bf02257483.

Amirkavei, M., Plastino, F., Kvanta, A., Kaarniranta, K., Andre, H. and Koskelainen, A. (2022). Hormetic heat shock enhances autophagy through HSF1 in retinal pigment epithelium cells. *Cells* **11**. https://doi.org/10.3390/cells11111778.

Amorim, F., Yamada, P., Robergs, R., Schneider, S. and Moseley, P. (2011). Effects of whole-body heat acclimation on cell injury and cytokine responses in peripheral blood mononuclear cells. *Eur J Appl Physiol* **111**, 1609-18. https://doi.org/10.1007/s00421-010-1780-4.

Amorim, F. T., Fonseca, I. T., Machado-Moreira, C. A. and Magalhães Fde, C. (2015). Insights into the role of heat shock protein 72 to whole-body heat acclimation in humans. *Temperature (Austin)* **2**, 499-505. https://doi.org/10.1080/23328940.2015.1110655.

Anca, M. H., Gazit, E., Loewenthal, R., Ostrovsky, O., Frydman, M. and Giladi, N. (2004). Different phenotypic expression in monozygotic twins with Huntington disease. *Am J Med Genet A* **124a**, 89-91. https://doi.org/10.1002/ajmg.a.20328.

Anckar, J. and Sistonen, L. (2011). Regulation of HSF1 function in the heat stress response: implications in aging and disease. *Annu Rev Biochem* **80**, 1089-115. https://doi.org/10.1146/annurev-biochem-060809-095203.

Andrade, M. A. and Bork, P. (1995). HEAT repeats in the Huntington's disease protein. *Nat Genet* **11**, 115-6. https://doi.org/10.1038/ng1095-115.

References

André, W., Sandt, C., Dumas, P., Djian, P. and Hoffner, G. (2013). Structure of inclusions of Huntington's disease brain revealed by synchrotron infrared microspectroscopy: polymorphism and relevance to cytotoxicity. *Anal Chem* **85**, 3765-73. https://doi.org/10.1021/ac400038b.

Andrew, S. E., Goldberg, Y. P., Kremer, B., Telenius, H., Theilmann, J., Adam, S., Starr, E., Squitieri, F., Lin, B., Kalchman, M. A. et al. (1993). The relationship between trinucleotide (CAG) repeat length and clinical features of Huntington's disease. *Nat Genet* **4**, 398-403. https://doi.org/10.1038/ng0893-398.

Angilletta Jr, M. (2009). Looking for answers to questions about heat stress: researchers are getting warmer. *J Functional Ecology* **23**, 231-232. https://doi.org/10.1111/j.1365-2435.2009.01548.x.

Argueti-Ostrovsky, S., Alfahel, L., Kahn, J. and Israelson, A. (2021). All roads lead to Rome: Different molecular players converge to common toxic pathways in neurodegeneration. *Cells* **10**. https://doi.org/10.3390/cells10092438.

Arndt, J. R., Chaibva, M. and Legleiter, J. (2015). The emerging role of the first 17 amino acids of huntingtin in Huntington's disease. *Biomol Concepts* **6**, 33-46. https://doi.org/10.1515/bmc-2015-0001.

Arnes, M., Alaniz, M. E., Karam, C. S., Cho, J. D., Lopez, G., Javitch, J. A. and Santa-Maria, I. (2019). Role of Tau protein in remodeling of circadian neuronal circuits and sleep. *Front Aging Neurosci* **11**, 320. https://doi.org/10.3389/fnagi.2019.00320.

Arnulf, I., Nielsen, J., Lohmann, E., Schiefer, J., Wild, E., Jennum, P., Konofal, E., Walker, M., Oudiette, D., Tabrizi, S. et al. (2008). Rapid eye movement sleep disturbances in Huntington disease. *Arch Neurol* **65**, 482-8. https://doi.org/10.1001/archneur.65.4.482.

Aron, R., Pellegrini, P., Green, E. W., Maddison, D. C., Opoku-Nsiah, K., Oliveira, A. O., Wong, J. S., Daub, A. C., Giorgini, F., Muchowski, P. et al. (2018). Deubiquitinase Usp12 functions noncatalytically to induce autophagy and confer neuroprotection in models of Huntington's disease. *Nat Commun* **9**, 3191. https://doi.org/10.1038/s41467-018-05653-z.

Aronin, N., Chase, K., Young, C., Sapp, E., Schwarz, C., Matta, N., Kornreich, R., Landwehrmeyer, B., Bird, E., Beal, M. F. et al. (1995). CAG expansion affects the expression of mutant huntingtin in the Huntington's disease brain. *Neuron* **15**, 1193-201. https://doi.org/10.1016/0896-6273(95)90106-x.

Arrasate, M. and Finkbeiner, S. (2012). Protein aggregates in Huntington's disease. *Exp Neurol* **238**, 1-11. https://doi.org/10.1016/j.expneurol.2011.12.013.

Arrasate, M., Mitra, S., Schweitzer, E. S., Segal, M. R. and Finkbeiner, S. (2004). Inclusion body formation reduces levels of mutant huntingtin and the risk of neuronal death. *Nature* **431**, 805-10. https://doi.org/10.1038/nature02998.

Arribat, Y., Bonneaud, N., Talmat-Amar, Y., Layalle, S., Parmentier, M. L. and Maschat, F. (2013). A huntingtin peptide inhibits polyQ-huntingtin associated defects. *PLoS One* **8**, e68775. https://doi.org/10.1371/journal.pone.0068775.

Arteaga-Bracho, E. E., Gulinello, M., Winchester, M. L., Pichamoorthy, N., Petronglo, J. R., Zambrano, A. D., Inocencio, J., De Jesus, C. D., Louie, J. O., Gokhan, S. et al. (2016). Postnatal and adult consequences of loss of huntingtin during development: Implications for Huntington's disease. *Neurobiol Dis* **96**, 144-155. https://doi.org/10.1016/j.nbd.2016.09.006.

References

Arthaut, L. D., Jourdan, N., Mteyrek, A., Procopio, M., El-Esawi, M., d'Harlingue, A., Bouchet, P. E., Witczak, J., Ritz, T., Klarsfeld, A. et al. (2017). Blue-light induced accumulation of reactive oxygen species is a consequence of the *Drosophila* cryptochrome photocycle. *PLoS One* **12**, e0171836. https://doi.org/10.1371/journal.pone.0171836.

Arundine, M. and Tymianski, M. (2003). Molecular mechanisms of calcium-dependent neurodegeneration in excitotoxicity. *Cell Calcium* **34**, 325-37. https://doi.org/10.1016/s0143-4160(03)00141-6.

Aschoff, J. (1983). Circadian control of body temperature. *J Therm Biol* **8**, 143-147. https://doi.org/10.1016/0306-4565(83)90094-3.

Ashkenazi, A., Bento, C. F., Ricketts, T., Vicinanza, M., Siddiqi, F., Pavel, M., Squitieri, F., Hardenberg, M. C., Imarisio, S., Menzies, F. M. et al. (2017). Polyglutamine tracts regulate beclin 1-dependent autophagy. *Nature* **545**, 108-111. https://doi.org/10.1038/nature22078.

Ashton, A., Foster, R. G. and Jagannath, A. (2022). Photic entrainment of the circadian system. *Int J Mol Sci* **23**. https://doi.org/10.3390/ijms23020729.

Ast, A., Buntru, A., Schindler, F., Hasenkopf, R., Schulz, A., Brusendorf, L., Klockmeier, K., Grelle, G., McMahon, B., Niederlechner, H. et al. (2018). mHTT seeding activity: A marker of disease progression and neurotoxicity in models of Huntington's disease. *Mol Cell* **71**, 675-688.e6. https://doi.org/10.1016/j.molcel.2018.07.032.

ASTATSA. Friedman test for correlated multiple samples with follow-up post-hoc multiple comparison tests by the (1) Conover and (2) Nemenyi methods.: https://astatsa.com/FriedmanTest/.

Aton, S. J., Colwell, C. S., Harmar, A. J., Waschek, J. and Herzog, E. D. (2005). Vasoactive intestinal polypeptide mediates circadian rhythmicity and synchrony in mammalian clock neurons. *Nat Neurosci* **8**, 476-83. https://doi.org/10.1038/nn1419.

Aton, S. J. and Herzog, E. D. (2005). Come together, right...now: Synchronization of rhythms in a mammalian circadian clock. *Neuron* **48**, 531-4. https://doi.org/10.1016/j.neuron.2005.11.001.

Auerbach, W., Hurlbert, M. S., Hilditch-Maguire, P., Wadghiri, Y. Z., Wheeler, V. C., Cohen, S. I., Joyner, A. L., MacDonald, M. E. and Turnbull, D. H. (2001). The HD mutation causes progressive lethal neurological disease in mice expressing reduced levels of huntingtin. *Hum Mol Genet* **10**, 2515-23. https://doi.org/10.1093/hmg/10.22.2515.

Aungier, J., Cuesta, M. and Morton, A. (2012a). B29 voluntary exercise improves circadian function in a mouse model of Huntington's disease. In *Journal of Neurology, Neurosurgery & Psychiatry 2012;83:A14.*, vol. 83, pp. A14-A14. https://doi.org/10.1136/jnnp-2012-303524.45.

Aungier, J., Cuesta, M. and Morton, A. (2012b). B29 Voluntary exercise improves circadian function in a mouse model of Huntington's disease. *Journal of Neurology, Neurosurgery & Psychiatry* **83**, A14-A14. https://doi.org/10.1136/jnnp-2012-303524.45.

Aziz, A., Fronczek, R., Maat-Schieman, M., Unmehopa, U., Roelandse, F., Overeem, S., van Duinen, S., Lammers, G. J., Swaab, D. and Roos, R. (2008). Hypocretin and melanin-concentrating hormone in patients with Huntington disease. *Brain Pathol* **18**, 474-83. https://doi.org/10.1111/j.1750-3639.2008.00135.x.

References

Aziz, N. A., Anguelova, G. V., Marinus, J., Lammers, G. J. and Roos, R. A. (2010). Sleep and circadian rhythm alterations correlate with depression and cognitive impairment in Huntington's disease. *Parkinsonism Relat Disord* **16**, 345-50. https://doi.org/10.1016/j.parkreldis.2010.02.009.

Aziz, N. A., Pijl, H., Frolich, M., Schroder-van der Elst, J. P., van der Bent, C., Roelfsema, F. and Roos, R. A. (2009a). Delayed onset of the diurnal melatonin rise in patients with Huntington's disease. *J Neurol* **256**, 1961-5. https://doi.org/10.1007/s00415-009-5196-1.

Aziz, N. A., Pijl, H., Frölich, M., Schröder-van der Elst, J. P., van der Bent, C., Roelfsema, F. and Roos, R. A. (2009b). Delayed onset of the diurnal melatonin rise in patients with Huntington's disease. *J Neurol* **256**, 1961-5. https://doi.org/10.1007/s00415-009-5196-1.

Aziz, N. A., Pijl, H., Frölich, M., van der Graaf, A. W., Roelfsema, F. and Roos, R. A. (2009c). Increased hypothalamic-pituitary-adrenal axis activity in Huntington's disease. *J Clin Endocrinol Metab* **94**, 1223-8. https://doi.org/10.1210/jc.2008-2543.

Aziz, N. A., Swaab, D. F., Pijl, H. and Roos, R. A. (2007). Hypothalamic dysfunction and neuroendocrine and metabolic alterations in Huntington's disease: clinical consequences and therapeutic implications. *Rev Neurosci* **18**, 223-51. https://doi.org/10.1515/revneuro.2007.18.3-4.223.

Babcock, D. T. and Ganetzky, B. (2015). Transcellular spreading of huntingtin aggregates in the *Drosophila* brain. *Proc Natl Acad Sci U S A* **112**, E5427-33. https://doi.org/10.1073/pnas.1516217112.

Bae, B. I., Xu, H., Igarashi, S., Fujimuro, M., Agrawal, N., Taya, Y., Hayward, S. D., Moran, T. H., Montell, C., Ross, C. A. et al. (2005). p53 mediates cellular dysfunction and behavioral abnormalities in Huntington's disease. *Neuron* **47**, 29-41. https://doi.org/10.1016/j.neuron.2005.06.005.

Bai, L., Lee, Y., Hsu, C. T., Williams, J. A., Cavanaugh, D., Zheng, X., Stein, C., Haynes, P., Wang, H., Gutmann, D. H. et al. (2018). A conserved circadian function for the neurofibromatosis 1 gene. *Cell Rep* **22**, 3416-3426. https://doi.org/10.1016/j.celrep.2018.03.014.

Baias, M., Smith, P. E., Shen, K., Joachimiak, L. A., Żerko, S., Koźmiński, W., Frydman, J. and Frydman, L. (2017). Structure and Dynamics of the huntingtin exon-1 N-Terminus: A Solution NMR Perspective. *J Am Chem Soc* **139**, 1168-1176. https://doi.org/10.1021/jacs.6b10893.

Bailey, C. K., Andriola, I. F., Kampinga, H. H. and Merry, D. E. (2002). Molecular chaperones enhance the degradation of expanded polyglutamine repeat androgen receptor in a cellular model of spinal and bulbar muscular atrophy. *Hum Mol Genet* **11**, 515-23. https://doi.org/10.1093/hmg/11.5.515.

Baker, C. R., Domínguez, D. J., Stout, J. C., Gabery, S., Churchyard, A., Chua, P., Egan, G. F., Petersén, Å., Georgiou-Karistianis, N. and Poudel, G. R. (2016). Subjective sleep problems in Huntington's disease: A pilot investigation of the relationship to brain structure, neurocognitive, and neuropsychiatric function. *J Neurol Sci* **364**, 148-53. https://doi.org/10.1016/j.jns.2016.03.021.

Balch, W. E., Morimoto, R. I., Dillin, A. and Kelly, J. W. (2008). Adapting proteostasis for disease intervention. *Science* **319**, 916-9. https://doi.org/10.1126/science.1141448.

Balchin, D., Hayer-Hartl, M. and Hartl, F. U. (2016). In vivo aspects of protein folding and quality control. *Science* **353**, aac4354. https://doi.org/10.1126/science.aac4354.

Baldo, B., Weiss, A., Parker, C. N., Bibel, M., Paganetti, P. and Kaupmann, K. (2012). A screen for enhancers of clearance identifies huntingtin as a heat shock protein 90 (Hsp90) client protein. *J Biol Chem* **287**, 1406-14. https://doi.org/10.1074/jbc.M111.294801.

References

Ballesta, A., Innominato, P. F., Dallmann, R., Rand, D. A. and Lévi, F. A. (2017). Systems chronotherapeutics. *Pharmacol Rev* **69**, 161-199. https://doi.org/10.1124/pr.116.013441.

Balsalobre, A., Damiola, F. and Schibler, U. (1998). A serum shock induces circadian gene expression in mammalian tissue culture cells. *Cell* **93**, 929-37. https://doi.org/10.1016/s0092-8674(00)81199-x.

Bañez-Coronel, M., Ayhan, F., Tarabochia, A. D., Zu, T., Perez, B. A., Tusi, S. K., Pletnikova, O., Borchelt, D. R., Ross, C. A., Margolis, R. L. et al. (2015). RAN translation in Huntington disease. *Neuron* **88**, 667-77. https://doi.org/10.1016/j.neuron.2015.10.038.

Bano-Otalora, B., Moye, M. J., Brown, T., Lucas, R. J., Diekman, C. O. and Belle, M. D. (2021). Daily electrical activity in the master circadian clock of a diurnal mammal. *Elife* **10**. https://doi.org/10.7554/eLife.68179.

Baquet, Z. C., Gorski, J. A. and Jones, K. R. (2004). Early striatal dendrite deficits followed by neuron loss with advanced age in the absence of anterograde cortical brain-derived neurotrophic factor. *J Neurosci* **24**, 4250-8. https://doi.org/10.1523/jneurosci.3920-03.2004.

Barbaro, B. A., Lukacsovich, T., Agrawal, N., Burke, J., Bornemann, D. J., Purcell, J. M., Worthge, S. A., Caricasole, A., Weiss, A., Song, W. et al. (2015). Comparative study of naturally occurring huntingtin fragments in *Drosophila* points to exon 1 as the most pathogenic species in Huntington's disease. *Hum Mol Genet* **24**, 913-25. https://doi.org/10.1093/hmg/ddu504.

Barbé, L. and Finkbeiner, S. (2022). Genetic and epigenetic interplay define disease onset and severity in repeat diseases. *Front Aging Neurosci* **14**, 750629. https://doi.org/10.3389/fnagi.2022.750629.

Barber, A. F., Erion, R., Holmes, T. C. and Sehgal, A. (2016). Circadian and feeding cues integrate to drive rhythms of physiology in *Drosophila* insulin-producing cells. *Genes Dev* **30**, 2596-2606. https://doi.org/10.1101/gad.288258.116.

Barber, A. F., Fong, S. Y., Kolesnik, A., Fetchko, M. and Sehgal, A. (2021). *Drosophila* clock cells use multiple mechanisms to transmit time-of-day signals in the brain. *Proc Natl Acad Sci U S A* **118**. https://doi.org/10.1073/pnas.2019826118.

Bardet, P. L., Kolahgar, G., Mynett, A., Miguel-Aliaga, I., Briscoe, J., Meier, P. and Vincent, J. P. (2008). A fluorescent reporter of caspase activity for live imaging. *Proc Natl Acad Sci U S A* **105**, 13901-5. https://doi.org/10.1073/pnas.0806983105.

Barker, R. A., Fujimaki, M., Rogers, P. and Rubinsztein, D. C. (2020). Huntingtin-lowering strategies for Huntington's disease. *Expert Opin Investig Drugs* **29**, 1125-1132. https://doi.org/10.1080/13543784.2020.1804552.

Baron, K. G. and Reid, K. J. (2014). Circadian misalignment and health. *Int Rev Psychiatry* **26**, 139-54. https://doi.org/10.3109/09540261.2014.911149.

Barone, P., Antonini, A., Colosimo, C., Marconi, R., Morgante, L., Avarello, T. P., Bottacchi, E., Cannas, A., Ceravolo, G., Ceravolo, R. et al. (2009). The PRIAMO study: A multicenter assessment of nonmotor symptoms and their impact on quality of life in Parkinson's disease. *Mov Disord* **24**, 1641-9. https://doi.org/10.1002/mds.22643.

References

Barral, J. M., Broadley, S. A., Schaffar, G. and Hartl, F. U. (2004). Roles of molecular chaperones in protein misfolding diseases. *Semin Cell Dev Biol* **15**, 17-29. https://doi.org/10.1016/j.semcdb.2003.12.010.

Barron, J. C., Hurley, E. P. and Parsons, M. P. (2021). Huntingtin and the synapse. *Front Cell Neurosci* **15**, 689332. https://doi.org/10.3389/fncel.2021.689332.

Batcha, A. H., Greferath, U., Jobling, A. I., Vessey, K. A., Ward, M. M., Nithianantharajah, J., Hannan, A. J., Kalloniatis, M. and Fletcher, E. L. (2012). Retinal dysfunction, photoreceptor protein dysregulation and neuronal remodelling in the R6/1 mouse model of Huntington's disease. *Neurobiol Dis* **45**, 887-96. https://doi.org/10.1016/j.nbd.2011.12.004.

Bates, G., Tabrizi, S. and Jones, L. (2014). Huntington's Disease. https://doi.org/10.1093/med/9780199929146.001.0001.

Bates, G. P., Dorsey, R., Gusella, J. F., Hayden, M. R., Kay, C., Leavitt, B. R., Nance, M., Ross, C. A., Scahill, R. I., Wetzel, R. et al. (2015). Huntington disease. *Nat Rev Dis Primers* **1**, 15005. https://doi.org/10.1038/nrdp.2015.5.

Bathini, M., Raghushaker, C. R. and Mahato, K. K. (2022). The molecular mechanisms of action of photobiomodulation against neurodegenerative diseases: A systematic review. *Cell Mol Neurobiol* **42**, 955-971. https://doi.org/10.1007/s10571-020-01016-9.

Batulan, Z., Shinder, G. A., Minotti, S., He, B. P., Doroudchi, M. M., Nalbantoglu, J., Strong, M. J. and Durham, H. D. (2003). High threshold for induction of the stress response in motor neurons is associated with failure to activate HSF1. *J Neurosci* **23**, 5789-98. https://doi.org/10.1523/jneurosci.23-13-05789.2003.

Bauer, P. O., Goswami, A., Wong, H. K., Okuno, M., Kurosawa, M., Yamada, M., Miyazaki, H., Matsumoto, G., Kino, Y., Nagai, Y. et al. (2010). Harnessing chaperone-mediated autophagy for the selective degradation of mutant huntingtin protein. *Nat Biotechnol* **28**, 256-63. https://doi.org/10.1038/nbt.1608.

Bäuerlein, F. J. B., Fernández-Busnadiego, R. and Baumeister, W. (2020). Investigating the structure of neurotoxic protein aggregates inside cells. *Trends Cell Biol* **30**, 951-966. https://doi.org/10.1016/j.tcb.2020.08.007.

Bäuerlein, F. J. B., Saha, I., Mishra, A., Kalemanov, M., Martínez-Sánchez, A., Klein, R., Dudanova, I., Hipp, M. S., Hartl, F. U., Baumeister, W. et al. (2017). In situ architecture and cellular interactions of polyq inclusions. *Cell* **171**, 179-187.e10. https://doi.org/10.1016/j.cell.2017.08.009.

Baumgartner, M. E., Dinan, M. P., Langton, P. F., Kucinski, I. and Piddini, E. (2021). Proteotoxic stress is a driver of the loser status and cell competition. *Nat Cell Biol* **23**, 136-146. https://doi.org/10.1038/s41556-020-00627-0.

Baxter, S. L., Allard, D. E., Crowl, C. and Sherwood, N. T. (2014). Cold temperature improves mobility and survival in *Drosophila* models of autosomal-dominant hereditary spastic paraplegia (AD-HSP). *Dis Model Mech* **7**, 1005-12. https://doi.org/10.1242/dmm.013987.

Baydyuk, M. and Xu, B. (2014). BDNF signaling and survival of striatal neurons. *Front Cell Neurosci* **8**, 254. https://doi.org/10.3389/fncel.2014.00254.

References

Beaver, L. M., Gvakharia, B. O., Vollintine, T. S., Hege, D. M., Stanewsky, R. and Giebultowicz, J. M. (2002). Loss of circadian clock function decreases reproductive fitness in males of *Drosophila melanogaster*. *Proc Natl Acad Sci U S A* **99**, 2134-9. https://doi.org/10.1073/pnas.032426699.

Beckwith, E. J. and Ceriani, M. F. (2015a). Communication between circadian clusters: The key to a plastic network. *FEBS Lett* **589**, 3336-42. https://doi.org/10.1016/j.febslet.2015.08.017.

Beckwith, E. J. and Ceriani, M. F. (2015b). Experimental assessment of the network properties of the *Drosophila* circadian clock. *J Comp Neurol* **523**, 982-96. https://doi.org/10.1002/cne.23728.

Beckwith, E. J. and French, A. S. (2019). Sleep in *Drosophila* and Its context. *Front Physiol* **10**, 1167. https://doi.org/10.3389/fphys.2019.01167.

Beere, H. M. (2004). "The stress of dying": the role of heat shock proteins in the regulation of apoptosis. *J Cell Sci* **117**, 2641-51. https://doi.org/10.1242/jcs.01284.

Beever, R. (2010). The effects of repeated thermal therapy on quality of life in patients with type II diabetes mellitus. *J Altern Complement Med* **16**, 677-81. https://doi.org/10.1089/acm.2009.0358.

Behl, C. (2011). BAG3 and friends: co-chaperones in selective autophagy during aging and disease. *Autophagy* **7**, 795-8. https://doi.org/10.4161/auto.7.7.15844.

Behrends, C., Langer, C. A., Boteva, R., Böttcher, U. M., Stemp, M. J., Schaffar, G., Rao, B. V., Giese, A., Kretzschmar, H., Siegers, K. et al. (2006). Chaperonin TRiC promotes the assembly of polyQ expansion proteins into nontoxic oligomers. *Mol Cell* **23**, 887-97. https://doi.org/10.1016/j.molcel.2006.08.017.

Bejot, Y. and Yaffe, K. (2019). Ageing Population: A Neurological Challenge. *Neuroepidemiology* **52**, 76-77. https://doi.org/10.1159/000495813.

Bélanger, V., Picard, N. and Cermakian, N. (2006). The circadian regulation of Presenilin-2 gene expression. *Chronobiol Int* **23**, 747-66. https://doi.org/10.1080/07420520600827087.

Belfer, S. J., Bashaw, A. G., Perlis, M. L. and Kayser, M. S. (2021). A *Drosophila* model of sleep restriction therapy for insomnia. *Mol Psychiatry* **26**, 492-507. https://doi.org/10.1038/s41380-019-0376-6.

Bellosta Diago, E., Perez Perez, J., Santos Lasaosa, S., Viloria Alebesque, A., Martinez Horta, S., Kulisevsky, J. and Lopez Del Val, J. (2017). Circadian rhythm and autonomic dysfunction in presymptomatic and early Huntington's disease. *Parkinsonism Relat Disord* **44**, 95-100. https://doi.org/10.1016/j.parkreldis.2017.09.013.

Benarroch, E. E. (2015). Acquired axonal degeneration and regeneration: Recent insights and clinical correlations. *Neurology* **84**, 2076-85. https://doi.org/10.1212/wnl.0000000000001601.

Benbahouche Nel, H., Iliopoulos, I., Torok, I., Marhold, J., Henri, J., Kajava, A. V., Farkas, R., Kempf, T., Schnolzer, M., Meyer, P. et al. (2014). *Drosophila* Spag is the homolog of RNA polymerase II-associated protein 3 (RPAP3) and recruits the heat shock proteins 70 and 90 (Hsp70 and Hsp90) during the assembly of cellular machineries. *J Biol Chem* **289**, 6236-47. https://doi.org/10.1074/jbc.M113.499608.

Benca, R., Duncan, M. J., Frank, E., McClung, C., Nelson, R. J. and Vicentic, A. (2009). Biological rhythms, higher brain function, and behavior: Gaps, opportunities, and challenges. *Brain Res Rev* **62**, 57-70. https://doi.org/10.1016/j.brainresrev.2009.09.005.

References

Bence, N. F., Sampat, R. M. and Kopito, R. R. (2001). Impairment of the ubiquitin-proteasome system by protein aggregation. *Science* **292**, 1552-5. https://doi.org/10.1126/science.292.5521.1552.

Benito, J., Houl, J. H., Roman, G. W. and Hardin, P. E. (2008). The blue-light photoreceptor CRYPTOCHROME is expressed in a subset of circadian oscillator neurons in the *Drosophila* CNS. *J Biol Rhythms* **23**, 296-307. https://doi.org/10.1177/0748730408318588.

Benito, J., Zheng, H., Ng, F. S. and Hardin, P. E. (2007). Transcriptional feedback loop regulation, function, and ontogeny in *Drosophila*. *Cold Spring Harb Symp Quant Biol* **72**, 437-44. https://doi.org/10.1101/sqb.2007.72.009.

Benn, C. L., Landles, C., Li, H., Strand, A. D., Woodman, B., Sathasivam, K., Li, S. H., Ghazi-Noori, S., Hockly, E., Faruque, S. M. et al. (2005). Contribution of nuclear and extranuclear polyQ to neurological phenotypes in mouse models of Huntington's disease. *Hum Mol Genet* **14**, 3065-78. https://doi.org/10.1093/hmg/ddi340.

Bennett, E. J., Bence, N. F., Jayakumar, R. and Kopito, R. R. (2005). Global impairment of the ubiquitin-proteasome system by nuclear or cytoplasmic protein aggregates precedes inclusion body formation. *Mol Cell* **17**, 351-65. https://doi.org/10.1016/j.molcel.2004.12.021.

Berendzen, K. M., Durieux, J., Shao, L. W., Tian, Y., Kim, H. E., Wolff, S., Liu, Y. and Dillin, A. (2016). Neuroendocrine coordination of mitochondrial stress signaling and proteostasis. *Cell* **166**, 1553-1563.e10. https://doi.org/10.1016/j.cell.2016.08.042.

Berger, Z., Ttofi, E. K., Michel, C. H., Pasco, M. Y., Tenant, S., Rubinsztein, D. C. and O'Kane, C. J. (2005). Lithium rescues toxicity of aggregate-prone proteins in *Drosophila* by perturbing Wnt pathway. *Hum Mol Genet* **14**, 3003-11. https://doi.org/10.1093/hmg/ddi331.

Berk, M., Tye, S., Walder, K. and McGee, S. (2016). Hyperthermia for major depressive disorder? *JAMA Psychiatry* **73**, 1095-1096. https://doi.org/10.1001/jamapsychiatry.2016.1532.

Berlandi, J., Lin, F. J., Ambrée, O., Rieger, D., Paulus, W. and Jeibmann, A. (2017). Swing boat: Inducing and recording locomotor activity in a *Drosophila melanogaster* model of Alzheimer's disease. *Front Behav Neurosci* **11**, 159. https://doi.org/10.3389/fnbeh.2017.00159.

Berry, R., 3rd and López-Martínez, G. (2020). A dose of experimental hormesis: When mild stress protects and improves animal performance. *Comp Biochem Physiol A Mol Integr Physiol* **242**, 110658. https://doi.org/10.1016/j.cbpa.2020.110658.

Bersuker, K., Brandeis, M. and Kopito, R. R. (2016). Protein misfolding specifies recruitment to cytoplasmic inclusion bodies. *J Cell Biol* **213**, 229-41. https://doi.org/10.1083/jcb.201511024.

Besson, M. T., Dupont, P., Fridell, Y. W. and Lievens, J. C. (2010). Increased energy metabolism rescues glia-induced pathology in a *Drosophila* model of Huntington's disease. *Hum Mol Genet* **19**, 3372-82. https://doi.org/10.1093/hmg/ddq249.

Bett, J. S., Goellner, G. M., Woodman, B., Pratt, G., Rechsteiner, M. and Bates, G. P. (2006). Proteasome impairment does not contribute to pathogenesis in R6/2 Huntington's disease mice: Exclusion of proteasome activator REGgamma as a therapeutic target. *Hum Mol Genet* **15**, 33-44. https://doi.org/10.1093/hmg/ddi423.

Bettencourt, B. R., Hogan, C. C., Nimali, M. and Drohan, B. W. (2008). Inducible and constitutive heat shock gene expression responds to modification of Hsp70 copy number in *Drosophila*

melanogaster but does not compensate for loss of thermotolerance in Hsp70 null flies. *BMC Biol* **6**, 5. https://doi.org/10.1186/1741-7007-6-5.

Bhattacharyya, A., Thakur, A. K., Chellgren, V. M., Thiagarajan, G., Williams, A. D., Chellgren, B. W., Creamer, T. P. and Wetzel, R. (2006). Oligoproline effects on polyglutamine conformation and aggregation. *J Mol Biol* **355**, 524-35. https://doi.org/10.1016/j.jmb.2005.10.053.

Bhattacharyya, A., Trotta, C. R., Narasimhan, J., Wiedinger, K. J., Li, W., Effenberger, K. A., Woll, M. G., Jani, M. B., Risher, N., Yeh, S. et al. (2021). Small molecule splicing modifiers with systemic HTT-lowering activity. *Nat Commun* **12**, 7299. https://doi.org/10.1038/s41467-021-27157-z.

Biagioli, M., Ferrari, F., Mendenhall, E. M., Zhang, Y., Erdin, S., Vijayvargia, R., Vallabh, S. M., Solomos, N., Manavalan, P., Ragavendran, A. et al. (2015). Htt CAG repeat expansion confers pleiotropic gains of mutant huntingtin function in chromatin regulation. *Hum Mol Genet* **24**, 2442-57. https://doi.org/10.1093/hmg/ddv006.

Bianchetti, A., Scuratti, A., Zanetti, O., Binetti, G., Frisoni, G. B., Magni, E. and Trabucchi, M. (1995). Predictors of mortality and institutionalization in Alzheimer disease patients 1 year after discharge from an Alzheimer dementia unit. *Dementia* **6**, 108-12. https://doi.org/10.1159/000106930.

Bichelmeier, U., Schmidt, T., Hubener, J., Boy, J., Ruttiger, L., Habig, K., Poths, S., Bonin, M., Knipper, M., Schmidt, W. J. et al. (2007). Nuclear localization of ataxin-3 is required for the manifestation of symptoms in SCA3: in vivo evidence. *J Neurosci* **27**, 7418-28. https://doi.org/10.1523/JNEUROSCI.4540-06.2007.

Bicker, J., Alves, G., Falcão, A. and Fortuna, A. (2020). Timing in drug absorption and disposition: The past, present, and future of chronopharmacokinetics. *Br J Pharmacol* **177**, 2215-2239. https://doi.org/10.1111/bph.15017.

Bier, E. (2005). *Drosophila,* the golden bug, emerges as a tool for human genetics. *Nat Rev Genet* **6**, 9-23. https://doi.org/10.1038/nrg1503.

Bilen, J. and Bonini, N. M. (2007). Genome-wide screen for modifiers of ataxin-3 neurodegeneration in *Drosophila*. *PLoS Genet* **3**, 1950-64. https://doi.org/10.1371/journal.pgen.0030177.

Bittencourt, A. and Porto, R. R. (2017). eHSP70/iHSP70 and divergent functions on the challenge: effect of exercise and tissue specificity in response to stress. *Clin Physiol Funct Imaging* **37**, 99-105. https://doi.org/10.1111/cpf.12273.

Björklund, A. and Parmar, M. (2020). Neuronal replacement as a tool for basal ganglia circuitry repair: 40 years in perspective. *Front Cell Neurosci* **14**, 146. https://doi.org/10.3389/fncel.2020.00146.

Bjørkøy, G., Lamark, T., Brech, A., Outzen, H., Perander, M., Overvatn, A., Stenmark, H. and Johansen, T. (2005). p62/SQSTM1 forms protein aggregates degraded by autophagy and has a protective effect on huntingtin-induced cell death. *J Cell Biol* **171**, 603-14. https://doi.org/10.1083/jcb.200507002.

Blackwell, A. D., Paterson, N. S., Barker, R. A., Robbins, T. W. and Sahakian, B. J. (2008). The effects of modafinil on mood and cognition in Huntington's disease. *Psychopharmacology (Berl)* **199**, 29-36. https://doi.org/10.1007/s00213-008-1068-0.

References

Blake, M. R., Holbrook, S. D., Kotwica-Rolinska, J., Chow, E. S., Kretzschmar, D. and Giebultowicz, J. M. (2015). Manipulations of amyloid precursor protein cleavage disrupt the circadian clock in aging *Drosophila*. *Neurobiol Dis* **77**, 117-26. https://doi.org/10.1016/j.nbd.2015.02.012.

Blau, J. and Young, M. W. (1999). Cycling vrille expression is required for a functional *Drosophila* clock. *Cell* **99**, 661-71. https://doi.org/10.1016/s0092-8674(00)81554-8.

Blessing, E. M., Parekh, A., Betensky, R. A., Babb, J., Saba, N., Debure, L., Varga, A. W., Ayappa, I., Rapoport, D. M., Butler, T. A. et al. (2022). Association between lower body temperature and increased tau pathology in cognitively normal older adults. *Neurobiol Dis* **171**, 105748. https://doi.org/10.1016/j.nbd.2022.105748.

Block-Galarza, J., Chase, K. O., Sapp, E., Vaughn, K. T., Vallee, R. B., DiFiglia, M. and Aronin, N. (1997). Fast transport and retrograde movement of huntingtin and HAP 1 in axons. *Neuroreport* **8**, 2247-51. https://doi.org/10.1097/00001756-199707070-00031.

Block, B. A. (1994). Thermogenesis in muscle. *Annu Rev Physiol* **56**, 535-77. https://doi.org/10.1146/annurev.ph.56.030194.002535.

Blume, C., Garbazza, C. and Spitschan, M. (2019). Effects of light on human circadian rhythms, sleep and mood. *Somnologie (Berl)* **23**, 147-156. https://doi.org/10.1007/s11818-019-00215-x.

Boatz, J. C., Piretra, T., Lasorsa, A., Matlahov, I., Conway, J. F. and van der Wel, P. C. A. (2020). Protofilament structure and supramolecular polymorphism of aggregated mutant huntingtin exon 1. *J Mol Biol* **432**, 4722-4744. https://doi.org/10.1016/j.jmb.2020.06.021.

Bodai, L., Pallos, J., Thompson, L. M. and Marsh, J. L. (2012). Pcaf modulates polyglutamine pathology in a *Drosophila* model of Huntington's disease. *Neurodegener Dis* **9**, 104-6. https://doi.org/10.1159/000330505.

Bodner, R. A., Outeiro, T. F., Altmann, S., Maxwell, M. M., Cho, S. H., Hyman, B. T., McLean, P. J., Young, A. B., Housman, D. E. and Kazantsev, A. G. (2006). Pharmacological promotion of inclusion formation: A therapeutic approach for Huntington's and Parkinson's diseases. *Proc Natl Acad Sci U S A* **103**, 4246-51. https://doi.org/10.1073/pnas.0511256103.

Bolus, H., Crocker, K., Boekhoff-Falk, G. and Chtarbanova, S. (2020). Modeling neurodegenerative disorders in *Drosophila* melanogaster. *Int J Mol Sci* **21**. https://doi.org/10.3390/ijms21093055.

Bongioanni, P., Del Carratore, R., Corbianco, S., Diana, A., Cavallini, G., Masciandaro, S. M., Dini, M. and Buizza, R. (2021). Climate change and neurodegenerative diseases. *Environ Res* **201**, 111511. https://doi.org/10.1016/j.envres.2021.111511.

Bonifati, V., Rizzu, P., van Baren, M. J., Schaap, O., Breedveld, G. J., Krieger, E., Dekker, M. C., Squitieri, F., Ibanez, P., Joosse, M. et al. (2003). Mutations in the DJ-1 gene associated with autosomal recessive early-onset parkinsonism. *Science* **299**, 256-9. https://doi.org/10.1126/science.1077209.

Bonini, N. M. (2002). Chaperoning brain degeneration. *Proc Natl Acad Sci U S A* **99 Suppl 4**, 16407-11. https://doi.org/10.1073/pnas.152330499.

References

Boothroyd, C. E., Wijnen, H., Naef, F., Saez, L. and Young, M. W. (2007). Integration of light and temperature in the regulation of circadian gene expression in *Drosophila*. *PLoS Genet* **3**, e54. https://doi.org/10.1371/journal.pgen.0030054.

Borges, T. J., Wieten, L., van Herwijnen, M. J., Broere, F., van der Zee, R., Bonorino, C. and van Eden, W. (2012). The anti-inflammatory mechanisms of Hsp70. *Front Immunol* **3**, 95. https://doi.org/10.3389/fimmu.2012.00095.

Borrell-Pages, M., Canals, J. M., Cordelieres, F. P., Parker, J. A., Pineda, J. R., Grange, G., Bryson, E. A., Guillermier, M., Hirsch, E., Hantraye, P. et al. (2006). Cystamine and cysteamine increase brain levels of BDNF in Huntington disease via HSJ1b and transglutaminase. *J Clin Invest* **116**, 1410-24. https://doi.org/10.1172/JCI27607.

Bortvedt, S. F., McLear, J. A., Messer, A., Ahern-Rindell, A. J. and Wolfgang, W. J. (2010). Cystamine and intrabody co-treatment confers additional benefits in a fly model of Huntington's disease. *Neurobiol Dis* **40**, 130-4. https://doi.org/10.1016/j.nbd.2010.04.007.

Bouchecareilh, M. and Balch, W. E. (2011). Proteostasis: a new therapeutic paradigm for pulmonary disease. *Proc Am Thorac Soc* **8**, 189-95. https://doi.org/10.1513/pats.201008-055MS.

Bowler, K. (2005). Acclimation, heat shock and hardening. *Journal of Thermal Biology* **30**, 125-130. https://doi.org/10.1016/j.jtherbio.2004.09.001.

Bowman, A. B., Yoo, S. Y., Dantuma, N. P. and Zoghbi, H. Y. (2005). Neuronal dysfunction in a polyglutamine disease model occurs in the absence of ubiquitin-proteasome system impairment and inversely correlates with the degree of nuclear inclusion formation. *Hum Mol Genet* **14**, 679-91. https://doi.org/10.1093/hmg/ddi064.

Branco-Santos, J., Herrera, F., Poças, G. M., Pires-Afonso, Y., Giorgini, F., Domingos, P. M. and Outeiro, T. F. (2017). Protein phosphatase 1 regulates huntingtin exon 1 aggregation and toxicity. *Hum Mol Genet* **26**, 3763-3775. https://doi.org/10.1093/hmg/ddx260.

Branco, J., Al-Ramahi, I., Ukani, L., Perez, A. M., Fernandez-Funez, P., Rincon-Limas, D. and Botas, J. (2008). Comparative analysis of genetic modifiers in *Drosophila* points to common and distinct mechanisms of pathogenesis among polyglutamine diseases. *Hum Mol Genet* **17**, 376-90. https://doi.org/10.1093/hmg/ddm315.

Brand, A. H. and Perrimon, N. (1993). Targeted gene expression as a means of altering cell fates and generating dominant phenotypes. *Development* **118**, 401-15. https://doi.org/10.1242/dev.118.2.401.

Brandstaetter, H., Kruppa, A. J. and Buss, F. (2014). Huntingtin is required for ER-to-Golgi transport and for secretory vesicle fusion at the plasma membrane. *Dis Model Mech* **7**, 1335-40. https://doi.org/10.1242/dmm.017368.

Brandt, J., Bylsma, F. W., Gross, R., Stine, O. C., Ranen, N. and Ross, C. A. (1996). Trinucleotide repeat length and clinical progression in Huntington's disease. *Neurology* **46**, 527-31. https://doi.org/10.1212/wnl.46.2.527.

Bravo-Arredondo, J. M., Kegulian, N. C., Schmidt, T., Pandey, N. K., Situ, A. J., Ulmer, T. S. and Langen, R. (2018). The folding equilibrium of huntingtin exon 1 monomer depends on its polyglutamine tract. *J Biol Chem* **293**, 19613-19623. https://doi.org/10.1074/jbc.RA118.004808.

References

Brehme, M. and Voisine, C. (2016a). Model systems of protein-misfolding diseases reveal chaperone modifiers of proteotoxicity. *Disease Models & Mechanisms* **9**, 823-838. 10.1242/dmm.024703.

Brehme, M. and Voisine, C. (2016b). Model systems of protein-misfolding diseases reveal chaperone modifiers of proteotoxicity. *Dis Model Mech* **9**, 823-38. https://doi.org/10.1242/dmm.024703.

Brehme, M., Voisine, C., Rolland, T., Wachi, S., Soper, J. H., Zhu, Y., Orton, K., Villella, A., Garza, D., Vidal, M. et al. (2014a). A chaperome subnetwork safeguards proteostasis in aging and neurodegenerative disease. *Cell Rep* **9**, 1135-50. https://doi.org/10.1016/j.celrep.2014.09.042.

Brehme, M., Voisine, C., Rolland, T., Wachi, S., Soper, James H., Zhu, Y., Orton, K., Villella, A., Garza, D., Vidal, M. et al. (2014b). A chaperome subnetwork safeguards proteostasis in aging and neurodegenerative disease. *Cell Reports* **9**, 1135-1150. 10.1016/j.celrep.2014.09.042.

Brettschneider, J., Del Tredici, K., Lee, V. M. and Trojanowski, J. Q. (2015). Spreading of pathology in neurodegenerative diseases: A focus on human studies. *Nat Rev Neurosci* **16**, 109-20. https://doi.org/10.1038/nrn3887.

Broadley, S. A. and Hartl, F. U. (2009). The role of molecular chaperones in human misfolding diseases. *FEBS Lett* **583**, 2647-53. https://doi.org/10.1016/j.febslet.2009.04.029.

Broussard, J. L., Reynolds, A. C., Depner, C. M., Ferguson, S. A., Dawson, D. and Wright, K. P. (2017a). Circadian rhythms versus daily patterns in human physiology and behavior. In *Biological timekeeping: Clocks, rhythms and behaviour*, (ed. V. Kumar), pp. 279-295: Springer. https://doi.org/10.1007/978-81-322-3688-7_13.

Broussard, J. L., Reynolds, A. C., Depner, C. M., Ferguson, S. A., Dawson, D. and Wright, K. P. (2017b). Circadian rhythms versus daily patterns in human physiology and behavior. *Biological timekeeping: Clocks, rhythms*, 279-295. https://doi.org/10.1007/978-81-322-3688-7_13.

Brown, S. A., Zumbrunn, G., Fleury-Olela, F., Preitner, N. and Schibler, U. (2002). Rhythms of mammalian body temperature can sustain peripheral circadian clocks. *Curr Biol* **12**, 1574-83. https://doi.org/10.1016/s0960-9822(02)01145-4.

Brown, T. M., Colwell, C. S., Waschek, J. A. and Piggins, H. D. (2007). Disrupted neuronal activity rhythms in the suprachiasmatic nuclei of vasoactive intestinal polypeptide-deficient mice. *J Neurophysiol* **97**, 2553-8. https://doi.org/10.1152/jn.01206.2006.

Browne, S. E. and Beal, M. F. (2006). Oxidative damage in Huntington's disease pathogenesis. *Antioxid Redox Signal* **8**, 2061-73. https://doi.org/10.1089/ars.2006.8.2061.

Brunt, V. E., Howard, M. J., Francisco, M. A., Ely, B. R. and Minson, C. T. (2016). Passive heat therapy improves endothelial function, arterial stiffness and blood pressure in sedentary humans. *J Physiol* **594**, 5329-42. https://doi.org/10.1113/jp272453.

Brunt, V. E. and Minson, C. T. (2021). Heat therapy: Mechanistic underpinnings and applications to cardiovascular health. *J Appl Physiol (1985)* **130**, 1684-1704. https://doi.org/10.1152/japplphysiol.00141.2020.

Brunt, V. E., Wiedenfeld-Needham, K., Comrada, L. N. and Minson, C. T. (2018). Passive heat therapy protects against endothelial cell hypoxia-reoxygenation via effects of elevations in temperature and circulating factors. *J Physiol* **596**, 4831-4845. https://doi.org/10.1113/jp276559.

References

Brustovetsky, N. (2016). Mutant Huntingtin and Elusive Defects in Oxidative Metabolism and Mitochondrial Calcium Handling. *Mol Neurobiol* **53**, 2944-2953. https://doi.org/10.1007/s12035-015-9188-0.

Buchumenski, I., Bartok, O., Ashwal-Fluss, R., Pandey, V., Porath, H. T., Levanon, E. Y. and Kadener, S. (2017). Dynamic hyper-editing underlies temperature adaptation in *Drosophila*. *PLoS Genet* **13**, e1006931. https://doi.org/10.1371/journal.pgen.1006931.

Buguet, A. (2007). Sleep under extreme environments: effects of heat and cold exposure, altitude, hyperbaric pressure and microgravity in space. *J Neurol Sci* **262**, 145-52. https://doi.org/10.1016/j.jns.2007.06.040.

Buhl, E., Higham, J. P. and Hodge, J. J. L. (2019). Alzheimer's disease-associated tau alters *Drosophila* circadian activity, sleep and clock neuron electrophysiology. *Neurobiol Dis* **130**, 104507. https://doi.org/10.1016/j.nbd.2019.104507.

Buhr, E. D., Yoo, S. H. and Takahashi, J. S. (2010). Temperature as a universal resetting cue for mammalian circadian oscillators. *Science* **330**, 379-85. https://doi.org/10.1126/science.1195262.

Bulgari, D., Deitcher, D. L. and Levitan, E. S. (2017). Loss of Huntingtin stimulates capture of retrograde dense-core vesicles to increase synaptic neuropeptide stores. *Eur J Cell Biol* **96**, 402-406. https://doi.org/10.1016/j.ejcb.2017.01.001.

Bulone, D., Masino, L., Thomas, D. J., San Biagio, P. L. and Pastore, A. (2006). The interplay between polyQ and protein context delays aggregation by forming a reservoir of protofibrils. *PLoS One* **1**, e111. https://doi.org/10.1371/journal.pone.0000111.

Bulthuis, N., Spontak, K. R., Kleeman, B. and Cavanaugh, D. J. (2019). Neuronal activity in non-LNv clock cells is required to produce free-running rest:activity rhythms in *Drosophila*. *J Biol Rhythms* **34**, 249-271. https://doi.org/10.1177/0748730419841468.

Bunnell, D. E., Agnew, J. A., Horvath, S. M., Jopson, L. and Wills, M. (1988). Passive body heating and sleep: influence of proximity to sleep. *Sleep* **11**, 210-9. https://doi.org/10.1093/sleep/11.2.210.

Bunting, E. L., Hamilton, J. and Tabrizi, S. J. (2021). Polyglutamine diseases. *Curr Opin Neurobiol* **72**, 39-47. https://doi.org/10.1016/j.conb.2021.07.001.

Bunting, E. L., Hamilton, J. and Tabrizi, S. J. (2022). Polyglutamine diseases. *Curr Opin Neurobiol* **72**, 39-47. https://doi.org/10.1016/j.conb.2021.07.001.

Burke, K. A., Hensal, K. M., Umbaugh, C. S., Chaibva, M. and Legleiter, J. (2013a). Huntingtin disrupts lipid bilayers in a polyQ-length dependent manner. *Biochim Biophys Acta* **1828**, 1953-61. https://doi.org/10.1016/j.bbamem.2013.04.025.

Burke, K. A., Yates, E. A. and Legleiter, J. (2013b). Amyloid-forming proteins alter the local mechanical properties of lipid membranes. *Biochemistry* **52**, 808-17. https://doi.org/10.1021/bi301070v.

Burnett, B. G., Andrews, J., Ranganathan, S., Fischbeck, K. H. and Di Prospero, N. A. (2008). Expression of expanded polyglutamine targets profilin for degradation and alters actin dynamics. *Neurobiol Dis* **30**, 365-374. https://doi.org/10.1016/j.nbd.2008.02.007.

Burr, A. A., Tsou, W. L., Ristic, G. and Todi, S. V. (2014). Using membrane-targeted green fluorescent protein to monitor neurotoxic protein-dependent degeneration of *Drosophila* eyes. *J Neurosci Res* **92**, 1100-9. https://doi.org/10.1002/jnr.23395.

References

Busse, M., Quinn, L., Debono, K., Jones, K., Collett, J., Playle, R., Kelly, M., Simpson, S., Backx, K., Wasley, D. et al. (2013). A randomized feasibility study of a 12-week community-based exercise program for people with Huntington's disease. *J Neurol Phys Ther* **37**, 149-58. https://doi.org/10.1097/npt.0000000000000016.

Busza, A., Emery-Le, M., Rosbash, M. and Emery, P. (2004). Roles of the two *Drosophila* CRYPTOCHROME structural domains in circadian photoreception. *Science* **304**, 1503-6. https://doi.org/10.1126/science.1096973.

Busza, A., Murad, A. and Emery, P. (2007). Interactions between circadian neurons control temperature synchronization of *Drosophila* behavior. *J Neurosci* **27**, 10722-33. https://doi.org/10.1523/jneurosci.2479-07.2007.

Cabanas, M., Pistono, C., Puygrenier, L., Rakesh, D., Jeantet, Y., Garret, M. and Cho, Y. H. (2019). Neurophysiological and behavioral effects of anti-orexinergic treatments in a mouse model of Huntington's disease. *Neurotherapeutics* **16**, 784-796. https://doi.org/10.1007/s13311-019-00726-3.

Calabrese, E. J. (2013). Hormetic mechanisms. *Crit Rev Toxicol* **43**, 580-606. https://doi.org/10.3109/10408444.2013.808172.

Calabrese, E. J. (2016). Preconditioning is hormesis part I: Documentation, dose-response features and mechanistic foundations. *Pharmacol Res* **110**, 242-264. https://doi.org/10.1016/j.phrs.2015.12.021.

Calabrese, E. J., Iavicoli, I. and Calabrese, V. (2012). Hormesis: Why it is important to biogerontologists. *Biogerontology* **13**, 215-35. https://doi.org/10.1007/s10522-012-9374-7.

Calamini, B., Lo, D. C. and Kaltenbach, L. S. (2013). Experimental models for identifying modifiers of polyglutamine-induced aggregation and neurodegeneration. *Neurotherapeutics* **10**, 400-15. https://doi.org/10.1007/s13311-013-0195-4.

Caliandro, R., Streng, A. A., van Kerkhof, L. W. M., van der Horst, G. T. J. and Chaves, I. (2021). Social jetlag and related risks for human health: A timely review. *Nutrients* **13**. https://doi.org/10.3390/nu13124543.

Campesan, S., Del Popolo, I., Marcou, K., Straatman-Iwanowska, A., Repici, M., Boytcheva, K. V., Cotton, V. E., Allcock, N., Rosato, E., Kyriacou, C. P. et al. (2023). Bypassing mitochondrial defects rescues Huntington's phenotypes in *Drosophila*. *Neurobiol Dis* **185**, 106236. https://doi.org/10.1016/j.nbd.2023.106236.

Campesan, S., Green, E. W., Breda, C., Sathyasaikumar, K. V., Muchowski, P. J., Schwarcz, R., Kyriacou, C. P. and Giorgini, F. (2011). The kynurenine pathway modulates neurodegeneration in a *Drosophila* model of Huntington's disease. *Curr Biol* **21**, 961-6. https://doi.org/10.1016/j.cub.2011.04.028.

Cao, G. and Nitabach, M. N. (2008). Circadian control of membrane excitability in *Drosophila melanogaster* lateral ventral clock neurons. *J Neurosci* **28**, 6493-501. https://doi.org/10.1523/jneurosci.1503-08.2008.

Cardoso, V. V., Ferreira, M. P., Montagner, J. M., Fernandez, C. G., Moreira, J. C. and Oliveira, A. K. (2002). The effects of constant and alternating temperatures on the reproductive potential, life span, and life expectancy of Anastrepha fraterculus (Wiedemann) (Diptera: Tephritidae). *Braz J Biol* **62**, 775-86. https://doi.org/10.1590/s1519-69842002000500006.

References

Carmo, C., Naia, L., Lopes, C. and Rego, A. C. (2018). Mitochondrial dysfunction in Huntington's disease. *Adv Exp Med Biol* **1049**, 59-83. https://doi.org/10.1007/978-3-319-71779-1_3.

Caron, N. S., Desmond, C. R., Xia, J. and Truant, R. (2013). Polyglutamine domain flexibility mediates the proximity between flanking sequences in huntingtin. *Proc Natl Acad Sci U S A* **110**, 14610-5. https://doi.org/10.1073/pnas.1301342110.

Caron, N. S., Hung, C. L., Atwal, R. S. and Truant, R. (2014). Live cell imaging and biophotonic methods reveal two types of mutant huntingtin inclusions. *Hum Mol Genet* **23**, 2324-38. https://doi.org/10.1093/hmg/ddt625.

Carra, S., Seguin, S. J., Lambert, H. and Landry, J. (2008). HspB8 chaperone activity toward poly(Q)-containing proteins depends on its association with Bag3, a stimulator of macroautophagy. *J Biol Chem* **283**, 1437-1444. https://doi.org/10.1074/jbc.M706304200.

Carra, S., Sivilotti, M., Chávez Zobel, A. T., Lambert, H. and Landry, J. (2005). HspB8, a small heat shock protein mutated in human neuromuscular disorders, has in vivo chaperone activity in cultured cells. *Hum Mol Genet* **14**, 1659-69. https://doi.org/10.1093/hmg/ddi174.

Carrettiero, D. C., Santiago, F. E., Motzko-Soares, A. C. and Almeida, M. C. (2015). Temperature and toxic Tau in Alzheimer's disease: New insights. *Temperature (Austin)* **2**, 491-8. https://doi.org/10.1080/23328940.2015.1096438.

Carter, B., Justin, H. S., Gulick, D. and Gamsby, J. J. (2021). The molecular clock and neurodegenerative disease: A stressful time. *Front Mol Biosci* **8**, 644747. https://doi.org/10.3389/fmolb.2021.644747.

Carter, R., 3rd, Cheuvront, S. N., Williams, J. O., Kolka, M. A., Stephenson, L. A., Sawka, M. N. and Amoroso, P. J. (2005). Epidemiology of hospitalizations and deaths from heat illness in soldiers. *Med Sci Sports Exerc* **37**, 1338-44. https://doi.org/10.1249/01.mss.0000174895.19639.ed.

Carter, R. J., Hunt, M. J. and Morton, A. J. (2000). Environmental stimulation increases survival in mice transgenic for exon 1 of the Huntington's disease gene. *Mov Disord* **15**, 925-37. https://doi.org/10.1002/1531-8257(200009)15:5<925::aid-mds1025>3.0.co;2-z.

Cassar, M., Law, A. D., Chow, E. S., Giebultowicz, J. M. and Kretzschmar, D. (2020). Disease-associated mutant Tau prevents circadian changes in the cytoskeleton of central pacemaker neurons. *Front Neurosci* **14**, 232. https://doi.org/10.3389/fnins.2020.00232.

Caterino, M., Squillaro, T., Montesarchio, D., Giordano, A., Giancola, C. and Melone, M. A. B. (2018). Huntingtin protein: A new option for fixing the Huntington's disease countdown clock. *Neuropharmacology* **135**, 126-138. https://doi.org/10.1016/j.neuropharm.2018.03.009.

Cattaneo, E., Zuccato, C. and Tartari, M. (2005). Normal huntingtin function: An alternative approach to Huntington's disease. *Nat Rev Neurosci* **6**, 919-30. https://doi.org/10.1038/nrn1806.

Caulkins, B. G., Cervantes, S. A., Isas, J. M. and Siemer, A. B. (2018). Dynamics of the Proline-Rich C-Terminus of huntingtin exon-1 fibrils. *J Phys Chem B* **122**, 9507-9515. https://doi.org/10.1021/acs.jpcb.8b09213.

Cavanaugh, D. J., Geratowski, J. D., Wooltorton, J. R., Spaethling, J. M., Hector, C. E., Zheng, X., Johnson, E. C., Eberwine, J. H. and Sehgal, A. (2014). Identification of a circadian output

circuit for rest:Activity rhythms in *Drosophila*. *Cell* **157**, 689-701. https://doi.org/10.1016/j.cell.2014.02.024.

Cavey, M., Collins, B., Bertet, C. and Blau, J. (2016). Circadian rhythms in neuronal activity propagate through output circuits. *Nat Neurosci* **19**, 587-95. https://doi.org/10.1038/nn.4263.

Cavieres, G., Bogdanovich, J. M. and Bozinovic, F. (2016). Ontogenetic thermal tolerance and performance of ectotherms at variable temperatures. *J Evol Biol* **29**, 1462-8. https://doi.org/10.1111/jeb.12886.

Caviston, J. P., Ross, J. L., Antony, S. M., Tokito, M. and Holzbaur, E. L. (2007). Huntingtin facilitates dynein/dynactin-mediated vesicle transport. *Proc Natl Acad Sci U S A* **104**, 10045-50. https://doi.org/10.1073/pnas.0610628104.

Cederroth, C. R., Albrecht, U., Bass, J., Brown, S. A., Dyhrfjeld-Johnsen, J., Gachon, F., Green, C. B., Hastings, M. H., Helfrich-Förster, C., Hogenesch, J. B. et al. (2019). Medicine in the fourth dimension. *Cell Metab* **30**, 238-250. https://doi.org/10.1016/j.cmet.2019.06.019.

Cepeda, C., Wu, N., André, V. M., Cummings, D. M. and Levine, M. S. (2007). The corticostriatal pathway in Huntington's disease. *Prog Neurobiol* **81**, 253-71. https://doi.org/10.1016/j.pneurobio.2006.11.001.

Ceriani, M. F., Darlington, T. K., Staknis, D., Más, P., Petti, A. A., Weitz, C. J. and Kay, S. A. (1999). Light-dependent sequestration of TIMELESS by CRYPTOCHROME. *Science* **285**, 553-6. https://doi.org/10.1126/science.285.5427.553.

Chaari, A. (2019). Molecular chaperones biochemistry and role in neurodegenerative diseases. *Int J Biol Macromol* **131**, 396-411. https://doi.org/10.1016/j.ijbiomac.2019.02.148.

Chai, Y., Koppenhafer, S. L., Bonini, N. M. and Paulson, H. L. (1999). Analysis of the role of Heat Shock Protein (Hsp) molecular chaperones in polyglutamine disease. *The Journal of Neuroscience* **19**, 10338-10347. https://doi.org/10.1523/jneurosci.19-23-10338.1999.

Chai, Y., Shao, J., Miller, V. M., Williams, A. and Paulson, H. L. (2002). Live-cell imaging reveals divergent intracellular dynamics of polyglutamine disease proteins and supports a sequestration model of pathogenesis. *Proc Natl Acad Sci U S A* **99**, 9310-5. https://doi.org/10.1073/pnas.152101299.

Chalfant, J. M., Howatt, D. A., Tannock, L. R., Daugherty, A. and Pendergast, J. S. (2020). Circadian disruption with constant light exposure exacerbates atherosclerosis in male ApolipoproteinE-deficient mice. *Sci Rep* **10**, 9920. https://doi.org/10.1038/s41598-020-66834-9.

Chan, H. Y., Warrick, J. M., Andriola, I., Merry, D. and Bonini, N. M. (2002). Genetic modulation of polyglutamine toxicity by protein conjugation pathways in *Drosophila*. *Hum Mol Genet* **11**, 2895-904. https://doi.org/10.1093/hmg/11.23.2895.

Chan, H. Y., Warrick, J. M., Gray-Board, G. L., Paulson, H. L. and Bonini, N. M. (2000). Mechanisms of chaperone suppression of polyglutamine disease: selectivity, synergy and modulation of protein solubility in *Drosophila*. *Hum Mol Genet* **9**, 2811-20. https://doi.org/10.1093/hmg/9.19.2811.

Chang, Y. C. and Kim, J. Y. (2020). Therapeutic implications of circadian clocks in neurodegenerative diseases. *J Neurosci Res* **98**, 1095-1113. https://doi.org/10.1002/jnr.24572.

References

Chatterjee, A., Lamaze, A., De, J., Mena, W., Chelot, E., Martin, B., Hardin, P., Kadener, S., Emery, P. and Rouyer, F. (2018a). Reconfiguration of a multi-oscillator network by light in the *Drosophila* circadian clock. *Curr Biol* **28**, 2007-2017 e4. https://doi.org/10.1016/j.cub.2018.04.064.

Chatterjee, A., Lamaze, A., De, J., Mena, W., Chélot, E., Martin, B., Hardin, P., Kadener, S., Emery, P. and Rouyer, F. (2018b). Reconfiguration of a multi-oscillator network by light in the *Drosophila* circadian clock. *Curr Biol* **28**, 2007-2017.e4. https://doi.org/10.1016/j.cub.2018.04.064.

Chaturvedi, R. K., Calingasan, N. Y., Yang, L., Hennessey, T., Johri, A. and Beal, M. F. (2010). Impairment of PGC-1alpha expression, neuropathology and hepatic steatosis in a transgenic mouse model of Huntington's disease following chronic energy deprivation. *Hum Mol Genet* **19**, 3190-205. https://doi.org/10.1093/hmg/ddq229.

Chen, C., Buhl, E., Xu, M., Croset, V., Rees, J. S., Lilley, K. S., Benton, R., Hodge, J. J. and Stanewsky, R. (2015a). *Drosophila* ionotropic receptor 25a mediates circadian clock resetting by temperature. *Nature* **527**, 516-20. https://doi.org/10.1038/nature16148.

Chen, C., Xu, M., Anantaprakorn, Y., Rosing, M. and Stanewsky, R. (2018). nocte Is Required for Integrating Light and Temperature Inputs in Circadian Clock Neurons of *Drosophila*. *Curr Biol* **28**, 1595-1605 e3. https://doi.org/10.1016/j.cub.2018.04.001.

Chen, H. F., Huang, C. Q., You, C., Wang, Z. R. and Si-qing, H. (2013). Polymorphism of CLOCK gene rs 4580704 C > G is associated with susceptibility of Alzheimer's disease in a Chinese population. *Arch Med Res* **44**, 203-7. https://doi.org/10.1016/j.arcmed.2013.01.002.

Chen, H. W., Kuo, H. T., Wang, S. J., Lu, T. S. and Yang, R. C. (2005). In vivo heat shock protein assembles with septic liver NF-kappaB/I-kappaB complex regulating NF-kappaB activity. *Shock* **24**, 232-8. https://doi.org/10.1097/01.shk.0000174020.87439.f2.

Chen, K. F., Possidente, B., Lomas, D. A. and Crowther, D. C. (2014). The central molecular clock is robust in the face of behavioural arrhythmia in a *Drosophila* model of Alzheimer's disease. *Dis Model Mech* **7**, 445-58. https://doi.org/10.1242/dmm.014134.

Chen, Q., Peng, X. D., Huang, C. Q., Hu, X. Y. and Zhang, X. M. (2015b). Association between ARNTL (BMAL1) rs2278749 polymorphism T >C and susceptibility to Alzheimer disease in a Chinese population. *Genet Mol Res* **14**, 18515-22. https://doi.org/10.4238/2015.December.23.39.

Chen, S., Berthelier, V., Yang, W. and Wetzel, R. (2001). Polyglutamine aggregation behavior in vitro supports a recruitment mechanism of cytotoxicity. *J Mol Biol* **311**, 173-82. https://doi.org/10.1006/jmbi.2001.4850.

Chen, S. C., Tang, X., Goda, T., Umezaki, Y., Riley, A. C., Sekiguchi, M., Yoshii, T. and Hamada, F. N. (2022). Dorsal clock networks drive temperature preference rhythms in *Drosophila*. *Cell Rep* **39**, 110668. https://doi.org/10.1016/j.celrep.2022.110668.

Chen, W. T., Kuo, Y. Y., Lin, G. B., Lu, C. H., Hsu, H. P., Sun, Y. K. and Chao, C. Y. (2020). Thermal cycling protects SH-SY5Y cells against hydrogen peroxide and β-amyloid-induced cell injury through stress response mechanisms involving Akt pathway. *PLoS One* **15**, e0240022. https://doi.org/10.1371/journal.pone.0240022.

References

Chen, W. T., Sun, Y. K., Lu, C. H. and Chao, C. Y. (2019). Thermal cycling as a novel thermal therapy to synergistically enhance the anticancer effect of propolis on PANC-1 cells. *Int J Oncol* **55**, 617-628. https://doi.org/10.3892/ijo.2019.4844.

Chen, X., Hall, H., Simpson, J. P., Leon-Salas, W. D., Ready, D. F. and Weake, V. M. (2017). Cytochrome b5 protects photoreceptors from light stress-induced lipid peroxidation and retinal degeneration. *NPJ Aging Mech Dis* **3**, 18. https://doi.org/10.1038/s41514-017-0019-6.

Chereji, R. V., Kan, T. W., Grudniewska, M. K., Romashchenko, A. V., Berezikov, E., Zhimulev, I. F., Guryev, V., Morozov, A. V. and Moshkin, Y. M. (2016). Genome-wide profiling of nucleosome sensitivity and chromatin accessibility in *Drosophila melanogaster*. *Nucleic Acids Res* **44**, 1036-51. https://doi.org/10.1093/nar/gkv978.

Chiti, F. and Dobson, C. M. (2017). Protein misfolding, amyloid formation, and human disease: A summary of progress over the last decade. *Annu Rev Biochem* **86**, 27-68. https://doi.org/10.1146/annurev-biochem-061516-045115.

Chiu, J. C., Ko, H. W. and Edery, I. (2011). NEMO/NLK phosphorylates PERIOD to initiate a time-delay phosphorylation circuit that sets circadian clock speed. *Cell* **145**, 357-70. https://doi.org/10.1016/j.cell.2011.04.002.

Cho, K. (2001). Chronic 'jet lag' produces temporal lobe atrophy and spatial cognitive deficits. *Nat Neurosci* **4**, 567-8. https://doi.org/10.1038/88384.

Cho, Y., Ryu, S. H., Lee, B. R., Kim, K. H., Lee, E. and Choi, J. (2015). Effects of artificial light at night on human health: A literature review of observational and experimental studies applied to exposure assessment. *Chronobiol Int* **32**, 1294-310. https://doi.org/10.3109/07420528.2015.1073158.

Choi, C., Cao, G., Tanenhaus, A. K., McCarthy, E. V., Jung, M., Schleyer, W., Shang, Y., Rosbash, M., Yin, J. C. and Nitabach, M. N. (2012). Autoreceptor control of peptide/neurotransmitter corelease from PDF neurons determines allocation of circadian activity in *Drosophila*. *Cell Rep* **2**, 332-44. https://doi.org/10.1016/j.celrep.2012.06.021.

Choi, J. Y., Ryu, J. H., Kim, H. S., Park, S. G., Bae, K. H., Kang, S., Myung, P. K., Cho, S., Park, B. C. and Lee, D. H. (2007). Co-chaperone CHIP promotes aggregation of ataxin-1. *Mol Cell Neurosci* **34**, 69-79. https://doi.org/10.1016/j.mcn.2006.10.002.

Choi, Y. B., Kadakkuzha, B. M., Liu, X. A., Akhmedov, K., Kandel, E. R. and Puthanveettil, S. V. (2014). Huntingtin is critical both pre- and postsynaptically for long-term learning-related synaptic plasticity in Aplysia. *PLoS One* **9**, e103004. https://doi.org/10.1371/journal.pone.0103004.

Choi, Y. S., Lee, B., Cho, H. Y., Reyes, I. B., Pu, X. A., Saido, T. C., Hoyt, K. R. and Obrietan, K. (2009). CREB is a key regulator of striatal vulnerability in chemical and genetic models of Huntington's disease. *Neurobiol Dis* **36**, 259-68. https://doi.org/10.1016/j.nbd.2009.07.014.

Chongtham, A. and Agrawal, N. (2016). Curcumin modulates cell death and is protective in Huntington's disease model. *Sci Rep* **6**, 18736. https://doi.org/10.1038/srep18736.

Chopra, G., Shabir, S., Yousuf, S., Kauts, S., Bhat, S. A., Mir, A. H. and Singh, M. P. (2022). Proteinopathies: Deciphering physiology and mechanisms to develop effective therapies for neurodegenerative diseases. *Mol Neurobiol* **59**, 7513-7540. https://doi.org/10.1007/s12035-022-03042-8.

References

Chuang, D. M., Leng, Y., Marinova, Z., Kim, H. J. and Chiu, C. T. (2009). Multiple roles of HDAC inhibition in neurodegenerative conditions. *Trends Neurosci* **32**, 591-601. https://doi.org/10.1016/j.tins.2009.06.002.

Chuang, J. Z., Zhou, H., Zhu, M., Li, S. H., Li, X. J. and Sung, C. H. (2002). Characterization of a brain-enriched chaperone, MRJ, that inhibits Huntingtin aggregation and toxicity independently. *J Biol Chem* **277**, 19831-8. https://doi.org/10.1074/jbc.M109613200.

Ciarleglio, C. M., Gamble, K. L., Axley, J. C., Strauss, B. R., Cohen, J. Y., Colwell, C. S. and McMahon, D. G. (2009). Population encoding by circadian clock neurons organizes circadian behavior. *J Neurosci* **29**, 1670-6. https://doi.org/10.1523/jneurosci.3801-08.2009.

Ciechanover, A. and Kwon, Y. T. (2017). Protein Quality Control by Molecular Chaperones in Neurodegeneration. *Front Neurosci* **11**, 185. https://doi.org/10.3389/fnins.2017.00185.

Cisbani, G. and Cicchetti, F. (2012). An in vitro perspective on the molecular mechanisms underlying mutant huntingtin protein toxicity. *Cell Death Dis* **3**, e382. https://doi.org/10.1038/cddis.2012.121.

Clift, D., McEwan, W. A., Labzin, L. I., Konieczny, V., Mogessie, B., James, L. C. and Schuh, M. (2017). A method for the acute and rapid degradation of endogenous proteins. *Cell* **171**, 1692-1706.e18. https://doi.org/10.1016/j.cell.2017.10.033.

Cohen, M. S., Bas Orth, C., Kim, H. J., Jeon, N. L. and Jaffrey, S. R. (2011). Neurotrophin-mediated dendrite-to-nucleus signaling revealed by microfluidic compartmentalization of dendrites. *Proc Natl Acad Sci U S A* **108**, 11246-51. https://doi.org/10.1073/pnas.1012401108.

Colin, E., Zala, D., Liot, G., Rangone, H., Borrell-Pagès, M., Li, X. J., Saudou, F. and Humbert, S. (2008). Huntingtin phosphorylation acts as a molecular switch for anterograde/retrograde transport in neurons. *Embo j* **27**, 2124-34. https://doi.org/10.1038/emboj.2008.133.

Colinet, H., Overgaard, J., Com, E. and Sørensen, J. G. (2013). Proteomic profiling of thermal acclimation in *Drosophila melanogaster*. *Insect Biochem Mol Biol* **43**, 352-65. https://doi.org/10.1016/j.ibmb.2013.01.006.

Colinet, H., Sinclair, B. J., Vernon, P. and Renault, D. (2015). Insects in fluctuating thermal environments. *Annu Rev Entomol* **60**, 123-40. https://doi.org/10.1146/annurev-ento-010814-021017.

Collins, B., Kane, E. A., Reeves, D. C., Akabas, M. H. and Blau, J. (2012). Balance of activity between LN(v)s and glutamatergic dorsal clock neurons promotes robust circadian rhythms in *Drosophila*. *Neuron* **74**, 706-18. https://doi.org/10.1016/j.neuron.2012.02.034.

Collins, B., Kaplan, H. S., Cavey, M., Lelito, K. R., Bahle, A. H., Zhu, Z., Macara, A. M., Roman, G., Shafer, O. T. and Blau, J. (2014). Differentially timed extracellular signals synchronize pacemaker neuron clocks. *PLoS Biol* **12**, e1001959. https://doi.org/10.1371/journal.pbio.1001959.

Colwell, C. S. (2021). Defining circadian disruption in neurodegenerative disorders. *J Clin Invest* **131**. https://doi.org/10.1172/jci148288.

Conti, B., Sanchez-Alavez, M., Winsky-Sommerer, R., Morale, M. C., Lucero, J., Brownell, S., Fabre, V., Huitron-Resendiz, S., Henriksen, S., Zorrilla, E. P. et al. (2006). Transgenic mice with a reduced core body temperature have an increased life span. *Science* **314**, 825-8. https://doi.org/10.1126/science.1132191.

References

Cook, R. and Calabrese, E. J. (2006). The importance of hormesis to public health. *J Environmental Health Perspectives* **114**, 1631-1635. https://doi.org/10.1289/ehp.8606.

Coomans, C. P., van den Berg, S. A., Houben, T., van Klinken, J. B., van den Berg, R., Pronk, A. C., Havekes, L. M., Romijn, J. A., van Dijk, K. W., Biermasz, N. R. et al. (2013). Detrimental effects of constant light exposure and high-fat diet on circadian energy metabolism and insulin sensitivity. *FASEB J* **27**, 1721-32. https://doi.org/10.1096/fj.12-210898.

Costa, M. D. and Maciel, P. (2022). Modifier pathways in polyglutamine (PolyQ) diseases: From genetic screens to drug targets. *Cell Mol Life Sci* **79**, 274. https://doi.org/10.1007/s00018-022-04280-8.

Costa Mdo, C. and Paulson, H. L. (2012). Toward understanding Machado-Joseph disease. *Prog Neurobiol* **97**, 239-57. https://doi.org/10.1016/j.pneurobio.2011.11.006.

Costanzo, M., Abounit, S., Marzo, L., Danckaert, A., Chamoun, Z., Roux, P. and Zurzolo, C. (2013). Transfer of polyglutamine aggregates in neuronal cells occurs in tunneling nanotubes. *J Cell Sci* **126**, 3678-85. https://doi.org/10.1242/jcs.126086.

Cox, D. B., Platt, R. J. and Zhang, F. (2015). Therapeutic genome editing: Prospects and challenges. *Nat Med* **21**, 121-31. https://doi.org/10.1038/nm.3793.

Cozzolino, M., Ferraro, E., Ferri, A., Rigamonti, D., Quondamatteo, F., Ding, H., Xu, Z. S., Ferrari, F., Angelini, D. F., Rotilio, G. et al. (2004). Apoptosome inactivation rescues proneural and neural cells from neurodegeneration. *Cell Death Differ* **11**, 1179-91. https://doi.org/10.1038/sj.cdd.4401476.

Creus-Muncunill, J. and Ehrlich, M. E. (2019). Cell-autonomous and non-cell-autonomous pathogenic mechanisms in Huntington's disease: Insights from in vitro and in vivo models. *Neurotherapeutics* **16**, 957-978. https://doi.org/10.1007/s13311-019-00782-9.

Crick, S. L., Ruff, K. M., Garai, K., Frieden, C. and Pappu, R. V. (2013). Unmasking the roles of N- and C-terminal flanking sequences from exon 1 of huntingtin as modulators of polyglutamine aggregation. *Proc Natl Acad Sci U S A* **110**, 20075-80. https://doi.org/10.1073/pnas.1320626110.

Croce, K. R. and Yamamoto, A. (2019). A role for autophagy in Huntington's disease. *Neurobiol Dis* **122**, 16-22. https://doi.org/10.1016/j.nbd.2018.08.010.

Cuesta, M., Aungier, J. and Morton, A. J. (2014). Behavioral therapy reverses circadian deficits in a transgenic mouse model of Huntington's disease. *Neurobiol Dis* **63**, 85-91. https://doi.org/10.1016/j.nbd.2013.11.008.

Culver, B. P., Savas, J. N., Park, S. K., Choi, J. H., Zheng, S., Zeitlin, S. O., Yates, J. R., 3rd and Tanese, N. (2012). Proteomic analysis of wild-type and mutant huntingtin-associated proteins in mouse brains identifies unique interactions and involvement in protein synthesis. *J Biol Chem* **287**, 21599-614. https://doi.org/10.1074/jbc.M112.359307.

Cummings, C. J., Mancini, M. A., Antalffy, B., DeFranco, D. B., Orr, H. T. and Zoghbi, H. Y. (1998). Chaperone suppression of aggregation and altered subcellular proteasome localization imply protein misfolding in SCA1. *Nat Genet* **19**, 148-154. https://doi.org/10.1038/502.

Cummings, C. J. and Zoghbi, H. Y. (2000). Trinucleotide repeats: mechanisms and pathophysiology. *Annu Rev Genomics Hum Genet* **1**, 281-328. https://doi.org/10.1146/annurev.genom.1.1.281.

References

Currie, J., Goda, T. and Wijnen, H. (2009). Selective entrainment of the *Drosophila* circadian clock to daily gradients in environmental temperature. *BMC Biol* **7**, 49. https://doi.org/10.1186/1741-7007-7-49.

Cushman-Nick, M., Bonini, N. M. and Shorter, J. (2013). Hsp104 suppresses polyglutamine-induced degeneration post onset in a *Drosophila* MJD/SCA3 model. *PLoS Genet* **9**, e1003781. https://doi.org/10.1371/journal.pgen.1003781.

Cusumano, P., Klarsfeld, A., Chélot, E., Picot, M., Richier, B. and Rouyer, F. (2009). PDF-modulated visual inputs and cryptochrome define diurnal behavior in *Drosophila*. *Nat Neurosci* **12**, 1431-7. https://doi.org/10.1038/nn.2429.

Daan, S., Spoelstra, K., Albrecht, U., Schmutz, I., Daan, M., Daan, B., Rienks, F., Poletaeva, I., Dell'Omo, G., Vyssotski, A. et al. (2011). Lab mice in the field: unorthodox daily activity and effects of a dysfunctional circadian clock allele. *J Biol Rhythms* **26**, 118-29. https://doi.org/10.1177/0748730410397645.

Daldin, M., Fodale, V., Cariulo, C., Azzollini, L., Verani, M., Martufi, P., Spiezia, M. C., Deguire, S. M., Cherubini, M., Macdonald, D. et al. (2017). Polyglutamine expansion affects huntingtin conformation in multiple Huntington's disease models. *Sci Rep* **7**, 5070. https://doi.org/10.1038/s41598-017-05336-7.

Damiola, F., Le Minh, N., Preitner, N., Kornmann, B., Fleury-Olela, F. and Schibler, U. (2000). Restricted feeding uncouples circadian oscillators in peripheral tissues from the central pacemaker in the suprachiasmatic nucleus. *Genes Dev* **14**, 2950-61. https://doi.org/10.1101/gad.183500.

Damulewicz, M., Doktor, B., Baster, Z. and Pyza, E. (2022a). The role of glia clocks in the regulation of sleep in *Drosophila melanogaster*. *J Neurosci* **42**, 6848-60. https://doi.org/10.1523/JNEUROSCI.2340-21.2022.

Damulewicz, M., Tyszka, A. and Pyza, E. (2022b). Light exposure during development affects physiology of adults in *Drosophila melanogaster*. *Front Physiol* **13**, 1008154. https://doi.org/10.3389/fphys.2022.1008154.

Dapergola, E., Menegazzi, P., Raabe, T. and Hovhanyan, A. (2021). Light stimuli and circadian clock affect neural development in *Drosophila melanogaster*. *Front Cell Dev Biol* **9**, 595754. https://doi.org/10.3389/fcell.2021.595754.

Darrow, M. C., Sergeeva, O. A., Isas, J. M., Galaz-Montoya, J. G., King, J. A., Langen, R., Schmid, M. F. and Chiu, W. (2015). Structural Mechanisms of Mutant Huntingtin Aggregation Suppression by the Synthetic Chaperonin-like CCT5 Complex Explained by Cryoelectron Tomography. *J Biol Chem* **290**, 17451-61. https://doi.org/10.1074/jbc.M115.655373.

Das, A., Holmes, T. C. and Sheeba, V. (2016). dTRPA1 in non-circadian neurons modulates temperature-dependent rhythmic activity in *Drosophila melanogaster*. *J Biol Rhythms* **31**, 272-88. https://doi.org/10.1177/0748730415627037.

Dash, D. and Mestre, T. A. (2020). Therapeutic update on Huntington's disease: Symptomatic treatments and emerging disease-modifying therapies. *Neurotherapeutics* **17**, 1645-1659. https://doi.org/10.1007/s13311-020-00891-w.

References

Dattilo, S., Mancuso, C., Koverech, G., Di Mauro, P., Ontario, M. L., Petralia, C. C., Petralia, A., Maiolino, L., Serra, A., Calabrese, E. J. et al. (2015). Heat shock proteins and hormesis in the diagnosis and treatment of neurodegenerative diseases. *Immun Ageing* **12**, 20. https://doi.org/10.1186/s12979-015-0046-8.

Davis, A. A., Leyns, C. E. G. and Holtzman, D. M. (2018). Intercellular spread of protein aggregates in neurodegenerative disease. *Annu Rev Cell Dev Biol* **34**, 545-568. https://doi.org/10.1146/annurev-cellbio-100617-062636.

Davis, A. K., Pratt, W. B., Lieberman, A. P. and Osawa, Y. (2020). Targeting Hsp70 facilitated protein quality control for treatment of polyglutamine diseases. *Cell Mol Life Sci* **77**, 977-996. https://doi.org/10.1007/s00018-019-03302-2.

Davis, M. B., Bateman, D., Quinn, N. P., Marsden, C. D. and Harding, A. E. (1994). Mutation analysis in patients with possible but apparently sporadic Huntington's disease. *Lancet* **344**, 714-7. https://doi.org/10.1016/s0140-6736(94)92208-x.

De, J., Varma, V., Saha, S., Sheeba, V. and Sharma, V. K. (2013). Significance of activity peaks in fruit flies, *Drosophila melanogaste*r, under seminatural conditions. *Proc Natl Acad Sci U S A* **110**, 8984-9. https://doi.org/10.1073/pnas.1220960110.

de la Torre, J. C. (2004). Is Alzheimer's disease a neurodegenerative or a vascular disorder? Data, dogma, and dialectics. *Lancet Neurol* **3**, 184-90. https://doi.org/10.1016/s1474-4422(04)00683-0.

De Magalhaes Filho, C. D., Henriquez, B., Seah, N. E., Evans, R. M., Lapierre, L. R. and Dillin, A. (2018). Visible light reduces *C. elegans* longevity. *Nat Commun* **9**, 927. https://doi.org/10.1038/s41467-018-02934-5.

De Rooij, K. E., De Koning Gans, P. A., Roos, R. A., Van Ommen, G. J. and Den Dunnen, J. T. (1995). Somatic expansion of the (CAG)n repeat in Huntington disease brains. *Hum Genet* **95**, 270-4. https://doi.org/10.1007/bf00225192.

Deane, C. A. S. and Brown, I. R. (2016). Induction of heat shock proteins in differentiated human neuronal cells following co-application of celastrol and arimoclomol. *Cell Stress and Chaperones* **21**, 837-848. https://doi.org/10.1007/s12192-016-0708-2.

Dedmon, M. M., Christodoulou, J., Wilson, M. R. and Dobson, C. M. (2005). Heat shock protein 70 inhibits α-Synuclein fibril formation via preferential binding to prefibrillar species. *Journal of Biological Chemistry* **280**, 14733-14740. https://doi.org/10.1074/jbc.M413024200.

Déglon, N. (2017). From huntingtin gene to Huntington's disease-altering strategies. In *Disease-Modifying Targets in Neurodegenerative Disorders*, (ed. E. L. Veerle Baekelandt), pp. 251-276: Elsevier. https://doi.org/10.1016/b978-0-12-805120-7.00010-5.

Dehay, B. and Bertolotti, A. (2006). Critical role of the proline-rich region in huntingtin for aggregation and cytotoxicity in yeast. *J Biol Chem* **281**, 35608-15. https://doi.org/10.1074/jbc.M605558200.

Delfino, L., Mason, R. P., Kyriacou, C. P., Giorgini, F. and Rosato, E. (2020). Rab8 Promotes mutant HTT aggregation, reduces neurodegeneration, and ameliorates behavioural alterations in a *Drosophila* model of Huntington's disease. *J Huntingtons Dis* **9**, 253-263. https://doi.org/10.3233/jhd-200411.

References

Delventhal, R., O'Connor, R. M., Pantalia, M. M., Ulgherait, M., Kim, H. X., Basturk, M. K., Canman, J. C. and Shirasu-Hiza, M. (2019). Dissection of central clock function in *Drosophila* through cell-specific CRISPR-mediated clock gene disruption. *Elife* **8**. https://doi.org/10.7554/eLife.48308.

Denis, H. L., David, L. S. and Cicchetti, F. (2019). Antibody-based therapies for Huntington's disease: Current status and future directions. *Neurobiol Dis* **132**, 104569. https://doi.org/10.1016/j.nbd.2019.104569.

Depetris-Chauvin, A., Berni, J., Aranovich, E. J., Muraro, N. I., Beckwith, E. J. and Ceriani, M. F. (2011). Adult-specific electrical silencing of pacemaker neurons uncouples molecular clock from circadian outputs. *Curr Biol* **21**, 1783-93. https://doi.org/10.1016/j.cub.2011.09.027.

Depetris-Chauvin, A., Fernandez-Gamba, A., Gorostiza, E. A., Herrero, A., Castano, E. M. and Ceriani, M. F. (2014). Mmp1 processing of the PDF neuropeptide regulates circadian structural plasticity of pacemaker neurons. *PLoS Genet* **10**, e1004700. https://doi.org/10.1371/journal.pgen.1004700.

Desmond, C. R., Atwal, R. S., Xia, J. and Truant, R. (2012). Identification of a karyopherin β1/β2 proline-tyrosine nuclear localization signal in huntingtin protein. *J Biol Chem* **287**, 39626-33. https://doi.org/10.1074/jbc.M112.412379.

Desvergne, A. and Friguet, B. (2017). Circadian rhythms and proteostasis in aging. In *Circadian rhythms and their impact on aging*, pp. 163-191. https://doi.org/10.1007/978-3-319-64543-8_8.

Dewasmes, G., Nicolas, A., Rodriguez, D., Salame, P., Eschenlauer, R., Joly, D. and Muzet, A. (1994). Human core temperature minimum can be modified by ambient thermal transients. *Neurosci Lett* **173**, 151-4. https://doi.org/10.1016/0304-3940(94)90171-6.

Dewasmes, G., Signoret, P., Nicolas, A., Ehrhart, J. and Muzet, A. (1996). Advances of human core temperature minimum and maximal paradoxical sleep propensity by ambient thermal transients. *Neurosci Lett* **215**, 25-8. https://doi.org/10.1016/s0304-3940(96)12936-0.

Diaz-Hernandez, M., Valera, A. G., Moran, M. A., Gomez-Ramos, P., Alvarez-Castelao, B., Castano, J. G., Hernandez, F. and Lucas, J. J. (2006). Inhibition of 26S proteasome activity by huntingtin filaments but not inclusion bodies isolated from mouse and human brain. *J Neurochem* **98**, 1585-96. https://doi.org/10.1111/j.1471-4159.2006.03968.x.

Díaz, M. M., Schlichting, M., Abruzzi, K. C., Long, X. and Rosbash, M. (2019). Allatostatin-C/AstC-R2 Is a novel pathway to modulate the circadian activity pattern in *Drosophila*. *Curr Biol* **29**, 13-22.e3. https://doi.org/10.1016/j.cub.2018.11.005.

Dibner, C., Schibler, U. and Albrecht, U. (2010). The mammalian circadian timing system: Organization and coordination of central and peripheral clocks. *Annu Rev Physiol* **72**, 517-49. https://doi.org/10.1146/annurev-physiol-021909-135821.

Dickey, A. S. and La Spada, A. R. (2018). Therapy development in Huntington disease: From current strategies to emerging opportunities. *Am J Med Genet A* **176**, 842-861. https://doi.org/10.1002/ajmg.a.38494.

Dietz, K. N., Di Stefano, L., Maher, R. C., Zhu, H., Macdonald, M. E., Gusella, J. F. and Walker, J. A. (2015). The *Drosophila* Huntington's disease gene ortholog dhtt influences chromatin regulation during development. *Hum Mol Genet* **24**, 330-45. https://doi.org/10.1093/hmg/ddu446.

References

DiFiglia, M., Sapp, E., Chase, K., Schwarz, C., Meloni, A., Young, C., Martin, E., Vonsattel, J. P., Carraway, R., Reeves, S. A. et al. (1995). Huntingtin is a cytoplasmic protein associated with vesicles in human and rat brain neurons. *Neuron* **14**, 1075-81. https://doi.org/10.1016/0896-6273(95)90346-1.

DiFiglia, M., Sapp, E., Chase, K. O., Davies, S. W., Bates, G. P., Vonsattel, J. P. and Aronin, N. (1997). Aggregation of huntingtin in neuronal intranuclear inclusions and dystrophic neurites in brain. *Science* **277**, 1990-3. https://doi.org/10.1126/science.277.5334.1990.

DiGiovanni, L. F., Mocle, A. J., Xia, J. and Truant, R. (2016). Huntingtin N17 domain is a reactive oxygen species sensor regulating huntingtin phosphorylation and localization. *Hum Mol Genet* **25**, 3937-3945. https://doi.org/10.1093/hmg/ddw234.

Dillon, M. E., Wang, G., Garrity, P. A. and Huey, R. B. (2009). Review: Thermal preference in *Drosophila*. *J Therm Biol* **34**, 109-119. https://doi.org/10.1016/j.jtherbio.2008.11.007.

Dissel, S., Angadi, V., Kirszenblat, L., Suzuki, Y., Donlea, J., Klose, M., Koch, Z., English, D., Winsky-Sommerer, R., van Swinderen, B. et al. (2015). Sleep restores behavioral plasticity to *Drosophila* mutants. *Curr Biol* **25**, 1270-81. https://doi.org/10.1016/j.cub.2015.03.027.

Dissel, S., Hansen, C. N., Özkaya, Ö., Hemsley, M., Kyriacou, C. P. and Rosato, E. (2014). The logic of circadian organization in *Drosophila*. *Curr Biol* **24**, 2257-66. https://doi.org/10.1016/j.cub.2014.08.023.

Dissel, S., Klose, M., Donlea, J., Cao, L., English, D., Winsky-Sommerer, R., van Swinderen, B. and Shaw, P. J. (2017). Enhanced sleep reverses memory deficits and underlying pathology in *Drosophila* models of Alzheimer's disease. *Neurobiol Sleep Circadian Rhythms* **2**, 15-26. https://doi.org/10.1016/j.nbscr.2016.09.001.

Dockendorff, T. C., Su, H. S., McBride, S. M., Yang, Z., Choi, C. H., Siwicki, K. K., Sehgal, A. and Jongens, T. A. (2002). *Drosophila* lacking dfmr1 activity show defects in circadian output and fail to maintain courtship interest. *Neuron* **34**, 973-84. https://doi.org/10.1016/s0896-6273(02)00724-9.

Dodd, A. N., Salathia, N., Hall, A., Kévei, E., Tóth, R., Nagy, F., Hibberd, J. M., Millar, A. J. and Webb, A. A. (2005). Plant circadian clocks increase photosynthesis, growth, survival, and competitive advantage. *Science* **309**, 630-3. https://doi.org/10.1126/science.1115581.

Dokladny, K., Lobb, R., Wharton, W., Ma, T. Y. and Moseley, P. L. (2010). LPS-induced cytokine levels are repressed by elevated expression of HSP70 in rats: possible role of NF-kappaB. *Cell Stress Chaperones* **15**, 153-63. https://doi.org/10.1007/s12192-009-0129-6.

Doktór, B., Damulewicz, M. and Pyza, E. (2019). Effects of MUL1 and PARKIN on the circadian clock, brain and behaviour in *Drosophila* Parkinson's disease models. *BMC Neurosci* **20**, 24. https://doi.org/10.1186/s12868-019-0506-8.

Dolph, P. J., Ranganathan, R., Colley, N. J., Hardy, R. W., Socolich, M. and Zuker, C. S. (1993). Arrestin function in inactivation of G protein-coupled receptor rhodopsin *in vivo*. *Science* **260**, 1910-6. https://doi.org/10.1126/science.8316831.

Donaldson, K. M., Li, W., Ching, K. A., Batalov, S., Tsai, C. C. and Joazeiro, C. A. (2003). Ubiquitin-mediated sequestration of normal cellular proteins into polyglutamine aggregates. *Proc Natl Acad Sci U S A* **100**, 8892-7. https://doi.org/10.1073/pnas.1530212100.

References

Dong, X. and Cong, S. (2021). The emerging roles of long non-coding RNAs in polyglutamine diseases. *J Cell Mol Med* **25**, 8095-8102. https://doi.org/10.1111/jcmm.16808.

Dong, X. X., Wang, Y. and Qin, Z. H. (2009). Molecular mechanisms of excitotoxicity and their relevance to pathogenesis of neurodegenerative diseases. *Acta Pharmacol Sin* **30**, 379-87. https://doi.org/10.1038/aps.2009.24.

Dong, Y., Cheng, L. and Zhao, Y. (2022). Resetting the circadian clock of Alzheimer's mice via GLP-1 injection combined with time-restricted feeding. *Front Physiol* **13**, 911437. https://doi.org/10.3389/fphys.2022.911437.

Donnelly, K. M., Coleman, C. M., Fuller, M. L., Reed, V. L., Smerina, D., Tomlinson, D. S. and Pearce, M. M. P. (2022). Hunting for the cause: Evidence for prion-like mechanisms in Huntington's disease. *Front Neurosci* **16**, 946822. https://doi.org/10.3389/fnins.2022.946822.

Donnelly, K. M., DeLorenzo, O. R., Zaya, A. D., Pisano, G. E., Thu, W. M., Luo, L., Kopito, R. R. and Panning Pearce, M. M. (2020). Phagocytic glia are obligatory intermediates in transmission of mutant huntingtin aggregates across neuronal synapses. *Elife* **9**. https://doi.org/10.7554/eLife.58499.

Dorsey, C. M., Teicher, M. H., Cohen-Zion, M., Stefanovic, L., Satlin, A., Tartarini, W., Harper, D. and Lukas, S. E. (1999). Core body temperature and sleep of older female insomniacs before and after passive body heating. *Sleep* **22**, 891-8. https://doi.org/10.1093/sleep/22.7.891.

Doumanis, J., Wada, K., Kino, Y., Moore, A. W. and Nukina, N. (2009). RNAi screening in *Drosophila* cells identifies new modifiers of mutant huntingtin aggregation. *PLoS One* **4**, e7275. https://doi.org/10.1371/journal.pone.0007275.

Dowling, G. A., Mastick, J., Colling, E., Carter, J. H., Singer, C. M. and Aminoff, M. J. (2005). Melatonin for sleep disturbances in Parkinson's disease. *Sleep Med* **6**, 459-66. https://doi.org/10.1016/j.sleep.2005.04.004.

Dragatsis, I., Efstratiadis, A. and Zeitlin, S. (1998). Mouse mutant embryos lacking huntingtin are rescued from lethality by wild-type extraembryonic tissues. *Development* **125**, 1529-39. https://doi.org/10.1242/dev.125.8.1529.

Dragatsis, I., Levine, M. S. and Zeitlin, S. (2000). Inactivation of Hdh in the brain and testis results in progressive neurodegeneration and sterility in mice. *Nat Genet* **26**, 300-6. https://doi.org/10.1038/81593.

Drombosky, K. W., Rode, S., Kodali, R., Jacob, T. C., Palladino, M. J. and Wetzel, R. (2018). Mutational analysis implicates the amyloid fibril as the toxic entity in Huntington's disease. *Neurobiol Dis* **120**, 126-138. https://doi.org/10.1016/j.nbd.2018.08.019.

Dubois, C., Kong, G., Tran, H., Li, S., Pang, T. Y., Hannan, A. J. and Renoir, T. (2021). Small non-coding RNAs are dysregulated in Huntington's disease transgenic mice independently of the therapeutic effects of an environmental intervention. *Mol Neurobiol* **58**, 3308-3318. https://doi.org/10.1007/s12035-021-02342-9.

Duennwald, M. L., Jagadish, S., Giorgini, F., Muchowski, P. J. and Lindquist, S. (2006a). A network of protein interactions determines polyglutamine toxicity. *Proc Natl Acad Sci U S A* **103**, 11051-6. https://doi.org/10.1073/pnas.0604548103.

References

Duennwald, M. L., Jagadish, S., Muchowski, P. J. and Lindquist, S. (2006b). Flanking sequences profoundly alter polyglutamine toxicity in yeast. *Proc Natl Acad Sci U S A* **103**, 11045-50. https://doi.org/10.1073/pnas.0604547103.

Duffy, J. F., Dijk, D. J., Klerman, E. B. and Czeisler, C. A. (1998). Later endogenous circadian temperature nadir relative to an earlier wake time in older people. *Am J Physiol* **275**, R1478-87. https://doi.org/10.1152/ajpregu.1998.275.5.r1478.

Dugger, B. N. and Dickson, D. W. (2017). Pathology of Neurodegenerative Diseases. *Cold Spring Harb Perspect Biol* **9**. https://doi.org/10.1101/cshperspect.a028035.

Duim, W. C., Jiang, Y., Shen, K., Frydman, J. and Moerner, W. E. (2014). Super-resolution fluorescence of huntingtin reveals growth of globular species into short fibers and coexistence of distinct aggregates. *ACS Chem Biol* **9**, 2767-78. https://doi.org/10.1021/cb500335w.

Dukay, B., Csoboz, B. and Toth, M. E. (2019). Heat-Shock proteins in neuroinflammation. *Front Pharmacol* **10**, 920. https://doi.org/10.3389/fphar.2019.00920.

Duncan, E. J., Cheetham, M. E., Chapple, J. P. and van der Spuy, J. (2015a). The role of HSP70 and its co-chaperones in protein misfolding, aggregation and disease. *Subcell Biochem* **78**, 243-73. https://doi.org/10.1007/978-3-319-11731-7_12.

Duncan, E. J., Cheetham, M. E., Chapple, J. P. and van der Spuy, J. (2015b). The role of HSP70 and its co-chaperones in protein misfolding, aggregation and disease. In *The Networking of Chaperones by Co-chaperones*, pp. 243-273. https://doi.org/10.1007/978-3-319-11731-7_12.

Dürr, A., Dodé, C., Hahn, V., Pêcheux, C., Pillon, B., Feingold, J., Kaplan, J. C., Agid, Y. and Brice, A. (1995). Diagnosis of "sporadic" Huntington's disease. *J Neurol Sci* **129**, 51-5. https://doi.org/10.1016/0022-510x(94)00250-r.

Duyao, M., Ambrose, C., Myers, R., Novelletto, A., Persichetti, F., Frontali, M., Folstein, S., Ross, C., Franz, M., Abbott, M. et al. (1993). Trinucleotide repeat length instability and age of onset in Huntington's disease. *Nat Genet* **4**, 387-92. https://doi.org/10.1038/ng0893-387.

Duyao, M. P., Auerbach, A. B., Ryan, A., Persichetti, F., Barnes, G. T., McNeil, S. M., Ge, P., Vonsattel, J. P., Gusella, J. F., Joyner, A. L. et al. (1995). Inactivation of the mouse Huntington's disease gene homolog Hdh. *Science* **269**, 407-10. https://doi.org/10.1126/science.7618107.

Economos, A. C. and Lints, F. A. (1986a). Developmental temperature and life span in *Drosophila melanogaster*. I. Constant developmental temperature: evidence for physiological adaptation in a wide temperature range. *Gerontology* **32**, 18-27. https://doi.org/10.1159/000212761.

Economos, A. C. and Lints, F. A. (1986b). Developmental temperature and life span in *Drosophila melanogaster.* II. Oscillating temperature. *Gerontology* **32**, 28-36. https://doi.org/10.1159/000212762.

Edgar, R. S., Green, E. W., Zhao, Y., van Ooijen, G., Olmedo, M., Qin, X., Xu, Y., Pan, M., Valekunja, U. K., Feeney, K. A. et al. (2012). Peroxiredoxins are conserved markers of circadian rhythms. *Nature* **485**, 459-64. https://doi.org/10.1038/nature11088.

Ehrnhoefer, D. E., Duennwald, M., Markovic, P., Wacker, J. L., Engemann, S., Roark, M., Legleiter, J., Marsh, J. L., Thompson, L. M., Lindquist, S. et al. (2006). Green tea (-)-epigallocatechin-

gallate modulates early events in huntingtin misfolding and reduces toxicity in Huntington's disease models. *Hum Mol Genet* **15**, 2743-51. https://doi.org/10.1093/hmg/ddl210.

Ehrnhoefer, D. E., Sutton, L. and Hayden, M. R. (2011). Small changes, big impact: Posttranslational modifications and function of huntingtin in Huntington disease. *Neuroscientist* **17**, 475-92. https://doi.org/10.1177/1073858410390378.

Eisenstein, M. (2013). Chronobiology: Stepping out of time. *Nature* **497**, S10-2. https://doi.org/10.1038/497S10a.

El-Daher, M. T., Hangen, E., Bruyère, J., Poizat, G., Al-Ramahi, I., Pardo, R., Bourg, N., Souquere, S., Mayet, C., Pierron, G. et al. (2015). Huntingtin proteolysis releases non-polyQ fragments that cause toxicity through dynamin 1 dysregulation. *Embo j* **34**, 2255-71. https://doi.org/10.15252/embj.201490808.

Elefant, F. and Palter, K. B. (1999). Tissue-specific expression of dominant negative mutant *Drosophila* HSC70 causes developmental defects and lethality. *Mol Biol Cell* **10**, 2101-17. https://doi.org/10.1091/mbc.10.7.2101.

Elias, S., McGuire, J. R., Yu, H. and Humbert, S. (2015). Huntingtin Is required for epithelial polarity through RAB11A-mediated apical trafficking of PAR3-aPKC. *PLoS Biol* **13**, e1002142. https://doi.org/10.1371/journal.pbio.1002142.

Ely, B. R., Clayton, Z. S., McCurdy, C. E., Pfeiffer, J., Needham, K. W., Comrada, L. N. and Minson, C. T. (2019). Heat therapy improves glucose tolerance and adipose tissue insulin signaling in polycystic ovary syndrome. *Am J Physiol Endocrinol Metab* **317**, E172-e182. https://doi.org/10.1152/ajpendo.00549.2018.

Emerson, K. J., Bradshaw, W. E. and Holzapfel, C. M. (2008). Concordance of the circadian clock with the environment is necessary to maximize fitness in natural populations. *Evolution* **62**, 979-83. https://doi.org/10.1111/j.1558-5646.2008.00324.x.

Emery, P., So, W. V., Kaneko, M., Hall, J. C. and Rosbash, M. (1998). CRY, a *Drosophila* clock and light-regulated cryptochrome, is a major contributor to circadian rhythm resetting and photosensitivity. *Cell* **95**, 669-79. https://doi.org/10.1016/s0092-8674(00)81637-2.

Emery, P., Stanewsky, R., Hall, J. C. and Rosbash, M. (2000a). A unique circadian-rhythm photoreceptor. *Nature* **404**, 456-7. https://doi.org/10.1038/35006558.

Emery, P., Stanewsky, R., Helfrich-Förster, C., Emery-Le, M., Hall, J. C. and Rosbash, M. (2000b). *Drosophila* CRY is a deep brain circadian photoreceptor. *Neuron* **26**, 493-504. https://doi.org/10.1016/s0896-6273(00)81181-2.

Engelender, S., Sharp, A. H., Colomer, V., Tokito, M. K., Lanahan, A., Worley, P., Holzbaur, E. L. and Ross, C. A. (1997). Huntingtin-associated protein 1 (HAP1) interacts with the p150Glued subunit of dynactin. *Hum Mol Genet* **6**, 2205-12. https://doi.org/10.1093/hmg/6.13.2205.

Escobedo, S. E., Stanhope, S. C., Dong, Z. and Weake, V. M. (2022). Aging and light stress result in overlapping and unique gene expression changes in photoreceptors. *Genes (Basel)* **13**. https://doi.org/10.3390/genes13020264.

References

Escusa-Toret, S., Vonk, W. I. and Frydman, J. (2013). Spatial sequestration of misfolded proteins by a dynamic chaperone pathway enhances cellular fitness during stress. *Nat Cell Biol* **15**, 1231-43. https://doi.org/10.1038/ncb2838.

Esler, W. P. and Wolfe, M. S. (2001). A portrait of Alzheimer secretases--new features and familiar faces. *Science* **293**, 1449-54. https://doi.org/10.1126/science.1064638.

Esser, C., Alberti, S. and Höhfeld, J. (2004). Cooperation of molecular chaperones with the ubiquitin/proteasome system. *Biochim Biophys Acta* **1695**, 171-88. https://doi.org/10.1016/j.bbamcr.2004.09.020.

Evans, J. A. (2016). Collective timekeeping among cells of the master circadian clock. *J Endocrinol* **230**, R27-49. https://doi.org/10.1530/JOE-16-0054.

Evans, J. A. and Davidson, A. J. (2013). Health consequences of circadian disruption in humans and animal models. *Prog Mol Biol Transl Sci* **119**, 283-323. https://doi.org/10.1016/b978-0-12-396971-2.00010-5.

Evans, J. A., Leise, T. L., Castanon-Cervantes, O. and Davidson, A. J. (2011). Intrinsic regulation of spatiotemporal organization within the suprachiasmatic nucleus. *PLoS One* **6**, e15869. https://doi.org/10.1371/journal.pone.0015869.

Evans, J. A., Pan, H., Liu, A. C. and Welsh, D. K. (2012). Cry1-/- circadian rhythmicity depends on SCN intercellular coupling. *J Biol Rhythms* **27**, 443-52. https://doi.org/10.1177/0748730412461246.

Fahrenkrug, J., Popovic, N., Georg, B., Brundin, P. and Hannibal, J. (2007). Decreased VIP and VPAC2 receptor expression in the biological clock of the R6/2 Huntington's disease mouse. *J Mol Neurosci* **31**, 139-48. https://doi.org/10.1385/jmn/31:02:139.

Falcon, J., Torriglia, A., Attia, D., Vienot, F., Gronfier, C., Behar-Cohen, F., Martinsons, C. and Hicks, D. (2020). Exposure to artificial light at night and the consequences for flora, fauna, and ecosystems. *Front Neurosci* **14**, 602796. https://doi.org/10.3389/fnins.2020.602796.

Fan, H. C., Ho, L. I., Chi, C. S., Chen, S. J., Peng, G. S., Chan, T. M., Lin, S. Z. and Harn, H. J. (2014). Polyglutamine (PolyQ) diseases: genetics to treatments. *Cell Transplant* **23**, 441-58. https://doi.org/10.3727/096368914X678454.

Fão, L. and Rego, A. C. (2021). Mitochondrial and redox-based therapeutic strategies in Huntington's disease. *Antioxid Redox Signal* **34**, 650-673. https://doi.org/10.1089/ars.2019.8004.

Farago, A., Zsindely, N. and Bodai, L. (2019). Mutant huntingtin disturbs circadian clock gene expression and sleep patterns in *Drosophila*. *Sci Rep* **9**, 7174. 10.1038/s41598-019-43612-w.

Faragó, A., Zsindely, N. and Bodai, L. (2019). Mutant huntingtin disturbs circadian clock gene expression and sleep patterns in *Drosophila*. *Sci Rep* **9**, 7174. https://doi.org/10.1038/s41598-019-43612-w.

Farshim, P. P. and Bates, G. P. (2018). Mouse Models of Huntington's Disease. *Methods Mol Biol* **1780**, 97-120. https://doi.org/10.1007/978-1-4939-7825-0_6.

Farsi, H., Achaâban, M. R., Piro, M., Bothorel, B., Ouassat, M., Challet, E., Pévet, P. and El Allali, K. (2020). Entrainment of circadian rhythms of locomotor activity by ambient temperature cycles in the dromedary camel. *Sci Rep* **10**, 19515. https://doi.org/10.1038/s41598-020-76535-y.

References

Fast, I., Hewel, C., Wester, L., Schumacher, J., Gebert, D., Zischler, H., Berger, C. and Rosenkranz, D. (2017). Temperature-responsive miRNAs in *Drosophila* orchestrate adaptation to different ambient temperatures. *Rna* **23**, 1352-1364. https://doi.org/10.1261/rna.061119.117.

Faulkner, S. H., Jackson, S., Fatania, G. and Leicht, C. A. (2017). The effect of passive heating on heat shock protein 70 and interleukin-6: A possible treatment tool for metabolic diseases? *Temperature (Austin)* **4**, 292-304. https://doi.org/10.1080/23328940.2017.1288688.

Fayazi, Z., Ghosh, S., Marion, S., Bao, X., Shero, M. and Kazemi-Esfarjani, P. (2006a). A Drosophila ortholog of the human MRJ modulates polyglutamine toxicity and aggregation. *Neurobiology of Disease* **24**, 226-244. 10.1016/j.nbd.2006.06.015.

Fayazi, Z., Ghosh, S., Marion, S., Bao, X., Shero, M. and Kazemi-Esfarjani, P. (2006b). A *Drosophila* ortholog of the human MRJ modulates polyglutamine toxicity and aggregation. *Neurobiol Dis* **24**, 226-44. https://doi.org/10.1016/j.nbd.2006.06.015.

Ferguson, M. W., Kennedy, C. J., Palpagama, T. H., Waldvogel, H. J., Faull, R. L. M. and Kwakowsky, A. (2022). Current and possible future therapeutic options for huntington's disease. *J Cent Nerv Syst Dis* **14**, 11795735221092517. https://doi.org/10.1177/11795735221092517.

Fernández-Fernández, M. R. and Valpuesta, J. M. (2018). Hsp70 chaperone: a master player in protein homeostasis. *F1000Res* **7**. https://doi.org/10.12688/f1000research.15528.1.

Fernandez, F. X. (2022). Current insights into optimal lighting for promoting sleep and circadian health: Brighter days and the importance of sunlight in the built environment. *Nat Sci Sleep* **14**, 25-39. https://doi.org/10.2147/NSS.S251712.

Fernandez, M. P., Berni, J. and Ceriani, M. F. (2008). Circadian remodeling of neuronal circuits involved in rhythmic behavior. *PLoS Biol* **6**, e69. https://doi.org/10.1371/journal.pbio.0060069.

Fernández, M. P., Berni, J. and Ceriani, M. F. (2008). Circadian remodeling of neuronal circuits involved in rhythmic behavior. *PLoS Biol* **6**, e69. https://doi.org/10.1371/journal.pbio.0060069.

Fernández, M. P., Chu, J., Villella, A., Atkinson, N., Kay, S. A. and Ceriani, M. F. (2007a). Impaired clock output by altered connectivity in the circadian network. *Proc Natl Acad Sci U S A* **104**, 5650-5. https://doi.org/10.1073/pnas.0608260104.

Fernández, M. P., Chu, J., Villella, A., Atkinson, N., Kay, S. A. and Ceriani, M. F. (2007b). Impaired clock output by altered connectivity in the circadian network. In *Proc Natl Acad Sci U S A*, vol. 104, pp. 5650-5. https://doi.org/10.1073/pnas.0608260104.

Fernandez, M. P., Pettibone, H. L., Bogart, J. T., Roell, C. J., Davey, C. E., Pranevicius, A., Huynh, K. V., Lennox, S. M., Kostadinov, B. S. and Shafer, O. T. (2020). Sites of circadian clock neuron plasticity mediate sensory integration and entrainment. *Curr Biol* **30**, 2225-2237 e5. https://doi.org/10.1016/j.cub.2020.04.025.

Fernius, J., Starkenberg, A. and Thor, S. (2017). Bar-coding neurodegeneration: identifying subcellular effects of human neurodegenerative disease proteins using *Drosophila* leg neurons. *Dis Model Mech* **10**, 1027-1038. https://doi.org/10.1242/dmm.029637.

Fifel, K. and Videnovic, A. (2019). Chronotherapies for Parkinson's disease. *Prog Neurobiol* **174**, 16-27. https://doi.org/10.1016/j.pneurobio.2019.01.002.

References

Fifel, K. and Videnovic, A. (2020). Circadian alterations in patients with neurodegenerative diseases: Neuropathological basis of underlying network mechanisms. *Neurobiol Dis* **144**, 105029. https://doi.org/10.1016/j.nbd.2020.105029.

Finkbeiner, S. (2011). Huntington's disease. *Cold Spring Harb Perspect Biol* **3**. https://doi.org/10.1101/cshperspect.a007476.

Fisher, S. P., Black, S. W., Schwartz, M. D., Wilk, A. J., Chen, T. M., Lincoln, W. U., Liu, H. W., Kilduff, T. S. and Morairty, S. R. (2013). Longitudinal analysis of the electroencephalogram and sleep phenotype in the R6/2 mouse model of Huntington's disease. *Brain* **136**, 2159-72. https://doi.org/10.1093/brain/awt132.

Fisher, S. P., Schwartz, M. D., Wurts-Black, S., Thomas, A. M., Chen, T. M., Miller, M. A., Palmerston, J. B., Kilduff, T. S. and Morairty, S. R. (2016). Quantitative electroencephalographic analysis provides an early-stage indicator of disease onset and progression in the zQ175 knock-in mouse model of Huntington's disease. *Sleep* **39**, 379-91. https://doi.org/10.5665/sleep.5448.

Fiumara, F., Fioriti, L., Kandel, E. R. and Hendrickson, W. A. (2010). Essential role of coiled coils for aggregation and activity of Q/N-rich prions and PolyQ proteins. *Cell* **143**, 1121-35. https://doi.org/10.1016/j.cell.2010.11.042.

Flourakis, M., Kula-Eversole, E., Hutchison, A. L., Han, T. H., Aranda, K., Moose, D. L., White, K. P., Dinner, A. R., Lear, B. C., Ren, D. et al. (2015). A conserved bicycle model for circadian clock control of membrane excitability. *Cell* **162**, 836-48. https://doi.org/10.1016/j.cell.2015.07.036.

Foley, L. E. and Emery, P. (2020). *Drosophila* cryptochrome: Variations in blue. *J Biol Rhythms* **35**, 16-27. https://doi.org/10.1177/0748730419878290.

Foley, L. E., Ling, J., Joshi, R., Evantal, N., Kadener, S. and Emery, P. (2019). *Drosophila* PSI controls circadian period and the phase of circadian behavior under temperature cycle via tim splicing. *Elife* **8**. https://doi.org/10.7554/eLife.50063.

Fonken, L. K. and Nelson, R. J. (2011). Illuminating the deleterious effects of light at night. *F1000 Med Rep* **3**, 18. https://doi.org/10.3410/M3-18.

Fox, J. H., Kama, J. A., Lieberman, G., Chopra, R., Dorsey, K., Chopra, V., Volitakis, I., Cherny, R. A., Bush, A. I. and Hersch, S. (2007). Mechanisms of copper ion mediated Huntington's disease progression. *PLoS One* **2**, e334. https://doi.org/10.1371/journal.pone.0000334.

Francelle, L., Lotz, C., Outeiro, T., Brouillet, E. and Merienne, K. (2017). Contribution of neuroepigenetics to Huntington's disease. *Front Hum Neurosci* **11**, 17. https://doi.org/10.3389/fnhum.2017.00017.

Franco-Iborra, S., Vila, M. and Perier, C. (2018). Mitochondrial quality control in neurodegenerative diseases: Focus on Parkinson's disease and Huntington's disease. *Front Neurosci* **12**, 342. https://doi.org/10.3389/fnins.2018.00342.

Frenkel, L. and Ceriani, M. F. (2011). Circadian plasticity: from structure to behavior. *Int Rev Neurobiol* **99**, 107-38. https://doi.org/10.1016/b978-0-12-387003-2.00005-7.

Frenkel, L., Muraro, N. I., Beltran Gonzalez, A. N., Marcora, M. S., Bernabo, G., Hermann-Luibl, C., Romero, J. I., Helfrich-Forster, C., Castano, E. M., Marino-Busjle, C. et al. (2017).

References

Organization of circadian behavior relies on Glycinergic transmission. *Cell Rep* **19**, 72-85. https://doi.org/10.1016/j.celrep.2017.03.034.

Friedman, J. H., Trieschmann, M. E., Myers, R. H. and Fernandez, H. H. (2005). Monozygotic twins discordant for Huntington disease after 7 years. *Arch Neurol* **62**, 995-7. https://doi.org/10.1001/archneur.62.6.995.

Fu, H., Hardy, J. and Duff, K. E. (2018). Selective vulnerability in neurodegenerative diseases. *Nat Neurosci* **21**, 1350-1358. https://doi.org/10.1038/s41593-018-0221-2.

Fuchs, M., Poirier, D. J., Seguin, S. J., Lambert, H., Carra, S., Charette, S. J. and Landry, J. (2009). Identification of the key structural motifs involved in HspB8/HspB6-Bag3 interaction. *Biochem J* **425**, 245-55. https://doi.org/10.1042/bj20090907.

Fujikake, N., Nagai, Y., Popiel, H. A., Okamoto, Y., Yamaguchi, M. and Toda, T. (2008). Heat shock transcription factor 1-activating compounds suppress polyglutamine-induced neurodegeneration through induction of multiple molecular chaperones. *J Biol Chem* **283**, 26188-97. https://doi.org/10.1074/jbc.M710521200.

Fujiwara, Y., Hermann-Luibl, C., Katsura, M., Sekiguchi, M., Ida, T., Helfrich-Förster, C. and Yoshii, T. (2018). The CCHamide1 neuropeptide expressed in the anterior dorsal neuron 1 conveys a circadian signal to the ventral lateral neurons in *Drosophila melanogaster*. *Front Physiol* **9**, 1276. https://doi.org/10.3389/fphys.2018.01276.

Fukushima, R. L. M., do Carmo, E. G., Pedroso, R. D. V., Micali, P. N., Donadelli, P. S., Fuzaro, G. J., Venancio, R. C. P., Viola, J. and Costa, J. L. R. (2016). Effects of cognitive stimulation on neuropsychiatric symptoms in elderly with Alzheimer's disease: A systematic review. *Dement Neuropsychol* **10**, 178-184. https://doi.org/10.1590/s1980-5764-2016dn1003003.

Fusco, F. R., Chen, Q., Lamoreaux, W. J., Figueredo-Cardenas, G., Jiao, Y., Coffman, J. A., Surmeier, D. J., Honig, M. G., Carlock, L. R. and Reiner, A. (1999). Cellular localization of huntingtin in striatal and cortical neurons in rats: lack of correlation with neuronal vulnerability in Huntington's disease. *J Neurosci* **19**, 1189-202. https://doi.org/10.1523/jneurosci.19-04-01189.1999.

Futter, M., Diekmann, H., Schoenmakers, E., Sadiq, O., Chatterjee, K. and Rubinsztein, D. C. (2009). Wild-type but not mutant huntingtin modulates the transcriptional activity of liver X receptors. *J Med Genet* **46**, 438-46. https://doi.org/10.1136/jmg.2009.066399.

Gabery, S., Murphy, K., Schultz, K., Loy, C. T., McCusker, E., Kirik, D., Halliday, G. and Petersén, A. (2010). Changes in key hypothalamic neuropeptide populations in Huntington disease revealed by neuropathological analyses. *Acta Neuropathol* **120**, 777-88. https://doi.org/10.1007/s00401-010-0742-6.

Gajula Balija, M. B., Griesinger, C., Herzig, A., Zweckstetter, M. and Jäckle, H. (2011). Pre-fibrillar α-synuclein mutants cause Parkinson's disease-like non-motor symptoms in *Drosophila*. *PLoS One* **6**, e24701. https://doi.org/10.1371/journal.pone.0024701.

Galbadage, T. and Hartman, P. S. (2008). Repeated temperature fluctuation extends the life span of *Caenorhabditis elegans* in a daf-16-dependent fashion. *Mech Ageing Dev* **129**, 507-14. https://doi.org/10.1016/j.mad.2008.04.012.

References

Gall, A. J. and Shuboni-Mulligan, D. D. (2022). Keep your mask on: The benefits of masking for behavior and the contributions of aging and disease on dysfunctional masking pathways. *Front Neurosci* **16**, 911153. https://doi.org/10.3389/fnins.2022.911153.

Gamerdinger, M., Kaya, A. M., Wolfrum, U., Clement, A. M. and Behl, C. (2011). BAG3 mediates chaperone-based aggresome-targeting and selective autophagy of misfolded proteins. *EMBO Rep* **12**, 149-56. https://doi.org/10.1038/embor.2010.203.

Gan, L., Cookson, M. R., Petrucelli, L. and La Spada, A. R. (2018). Converging pathways in neurodegeneration, from genetics to mechanisms. *Nat Neurosci* **21**, 1300-1309. https://doi.org/10.1038/s41593-018-0237-7.

Ganguly, P. (2015). Effects of temporally controlled Huntingtin expression and autophagy upregulation in *Drosophila melanogaster*. In *MS Thesis, EOBU*: Jawaharlal Nehru Centre for Advanced Scientific Research, Bangalore, India. https://libjncir.jncasr.ac.in/jspui/handle/10572/2628.

Gao, X., Carroni, M., Nussbaum-Krammer, C., Mogk, A., Nillegoda, Nadinath B., Szlachcic, A., Guilbride, D. L., Saibil, Helen R., Mayer, Matthias P. and Bukau, B. (2015). Human Hsp70 disaggregase reverses Parkinson's-linked α-Synuclein amyloid fibrils. *Mol Cell* **59**, 781-793. https://doi.org/10.1016/j.molcel.2015.07.012.

Gao, Y. G., Yan, X. Z., Song, A. X., Chang, Y. G., Gao, X. C., Jiang, N., Zhang, Q. and Hu, H. Y. (2006). Structural insights into the specific binding of huntingtin proline-rich region with the SH3 and WW domains. *Structure* **14**, 1755-65. https://doi.org/10.1016/j.str.2006.09.014.

Garcia-Mata, R., Bebok, Z., Sorscher, E. J. and Sztul, E. S. (1999). Characterization and dynamics of aggresome formation by a cytosolic GFP-chimera. *J Cell Biol* **146**, 1239-54. https://doi.org/10.1083/jcb.146.6.1239.

Garrett, A. T., Rehrer, N. J. and Patterson, M. J. (2011). Induction and decay of short-term heat acclimation in moderately and highly trained athletes. *Sports Med* **41**, 757-71. https://doi.org/10.2165/11587320-000000000-00000.

Garriga-Canut, M., Agustín-Pavón, C., Herrmann, F., Sánchez, A., Dierssen, M., Fillat, C. and Isalan, M. (2012). Synthetic zinc finger repressors reduce mutant huntingtin expression in the brain of R6/2 mice. *Proceedings of the National Academy of Sciences* **109**, E3136-E3145. https://doi.org/10.1073/pnas.1206506109.

Garrity, P. A., Goodman, M. B., Samuel, A. D. and Sengupta, P. (2010). Running hot and cold: behavioral strategies, neural circuits, and the molecular machinery for thermotaxis in *C. elegans* and *Drosophila*. *Genes Dev* **24**, 2365-82. https://doi.org/10.1101/gad.1953710.

Gasset-Rosa, F., Chillon-Marinas, C., Goginashvili, A., Atwal, R. S., Artates, J. W., Tabet, R., Wheeler, V. C., Bang, A. G., Cleveland, D. W. and Lagier-Tourenne, C. (2017). Polyglutamine-expanded huntingtin exacerbates age-related disruption of nuclear integrity and nucleocytoplasmic transport. *Neuron* **94**, 48-57.e4. https://doi.org/10.1016/j.neuron.2017.03.027.

Gatchel, J. R. and Zoghbi, H. Y. (2005). Diseases of unstable repeat expansion: mechanisms and common principles. *Nat Rev Genet* **6**, 743-55. https://doi.org/10.1038/nrg1691.

References

Gatto, E. M., Rojas, N. G., Persi, G., Etcheverry, J. L., Cesarini, M. E. and Perandones, C. (2020). Huntington disease: Advances in the understanding of its mechanisms. *Clin Park Relat Disord* **3**, 100056. https://doi.org/10.1016/j.prdoa.2020.100056.

Gauthier, L. R., Charrin, B. C., Borrell-Pagès, M., Dompierre, J. P., Rangone, H., Cordelières, F. P., De Mey, J., MacDonald, M. E., Lessmann, V., Humbert, S. et al. (2004). Huntingtin controls neurotrophic support and survival of neurons by enhancing BDNF vesicular transport along microtubules. *Cell* **118**, 127-38. https://doi.org/10.1016/j.cell.2004.06.018.

Gekakis, N., Saez, L., Delahaye-Brown, A. M., Myers, M. P., Sehgal, A., Young, M. W. and Weitz, C. J. (1995). Isolation of timeless by PER protein interaction: defective interaction between timeless protein and long-period mutant PERL. *Science* **270**, 811-5. https://doi.org/10.1126/science.270.5237.811.

Gentile, C., Sehadova, H., Simoni, A., Chen, C. and Stanewsky, R. (2013). Cryptochrome antagonizes synchronization of *Drosophila's* circadian clock to temperature cycles. *Curr Biol* **23**, 185-95. https://doi.org/10.1016/j.cub.2012.12.023.

Georgiou, N., Bradshaw, J. L., Chiu, E., Tudor, A., O'Gorman, L. and Phillips, J. G. (1999). Differential clinical and motor control function in a pair of monozygotic twins with Huntington's disease. *Mov Disord* **14**, 320-5. https://doi.org/10.1002/1531-8257(199903)14:2<320::aid-mds1018>3.0.co;2-z.

Gervais, F. G., Singaraja, R., Xanthoudakis, S., Gutekunst, C. A., Leavitt, B. R., Metzler, M., Hackam, A. S., Tam, J., Vaillancourt, J. P., Houtzager, V. et al. (2002). Recruitment and activation of caspase-8 by the huntingtin-interacting protein Hip-1 and a novel partner Hippi. *Nat Cell Biol* **4**, 95-105. https://doi.org/10.1038/ncb735.

Ghavami, M., Rezaei, M., Ejtehadi, R., Lotfi, M., Shokrgozar, M. A., Abd Emamy, B., Raush, J. and Mahmoudi, M. (2013). Physiological temperature has a crucial role in amyloid β in the absence and presence of hydrophobic and hydrophilic nanoparticles. *ACS Chem Neurosci* **4**, 375-8. https://doi.org/10.1021/cn300205g.

Ghosh, R. and Tabrizi, S. J. (2018a). Clinical Features of Huntington's Disease. *Adv Exp Med Biol* **1049**, 1-28. https://doi.org/10.1007/978-3-319-71779-1_1.

Ghosh, R. and Tabrizi, S. J. (2018b). Huntington disease: Elsevier. https://doi.org/10.1016/b978-0-444-63233-3.00017-8.

Ghosh, S. and Feany, M. B. (2004). Comparison of pathways controlling toxicity in the eye and brain in *Drosophila* models of human neurodegenerative diseases. *Hum Mol Genet* **13**, 2011-8. https://doi.org/10.1093/hmg/ddh214.

Giacomello, M., Oliveros, J. C., Naranjo, J. R. and Carafoli, E. (2013). Neuronal Ca(2+) dyshomeostasis in Huntington disease. *Prion* **7**, 76-84. https://doi.org/10.4161/pri.23581.

Gibbs, S. J., Barren, B., Beck, K. E., Proft, J., Zhao, X., Noskova, T., Braun, A. P., Artemyev, N. O. and Braun, J. E. (2009). Hsp40 couples with the CSPalpha chaperone complex upon induction of the heat shock response. *PLoS One* **4**, e4595. https://doi.org/10.1371/journal.pone.0004595.

Gibson, E. M., Wang, C., Tjho, S., Khattar, N. and Kriegsfeld, L. J. (2010). Experimental 'jet lag' inhibits adult neurogenesis and produces long-term cognitive deficits in female hamsters. *PLoS One* **5**, e15267. https://doi.org/10.1371/journal.pone.0015267.

References

Gidalevitz, T., Ben-Zvi, A., Ho, K. H., Brignull, H. R. and Morimoto, R. I. (2006). Progressive disruption of cellular protein folding in models of polyglutamine diseases. *Science* **311**, 1471-4. https://doi.org/10.1126/science.1124514.

Giebultowicz, J. M. (2018). Circadian regulation of metabolism and healthspan in *Drosophila*. *Free Radic Biol Med* **119**, 62-68. https://doi.org/10.1016/j.freeradbiomed.2017.12.025.

Gilestro, G. F. and Cirelli, C. (2009). pySolo: a complete suite for sleep analysis in *Drosophila*. *Bioinformatics* **25**, 1466-7. https://doi.org/10.1093/bioinformatics/btp237.

Giorgini, F. (2013). A flexible polyglutamine hinge opens new doors for understanding huntingtin function. *Proc Natl Acad Sci U S A* **110**, 14516-7. https://doi.org/10.1073/pnas.1313668110.

Gitler, A. D., Dhillon, P. and Shorter, J. (2017). Neurodegenerative disease: models, mechanisms, and a new hope. *Dis Model Mech* **10**, 499-502. https://doi.org/10.1242/dmm.030205.

Glaser, F. T. and Stanewsky, R. (2005). Temperature synchronization of the *Drosophila* circadian clock. *Curr Biol* **15**, 1352-63. https://doi.org/10.1016/j.cub.2005.06.056.

Glazachev, O. S., Zapara, M. A., Kryzhanovskaya, S. Y., Dudnik, E. N., Yumatov, E. A. and Susta, D. (2021). Whole-body repeated hyperthermia increases irisin and brain-derived neurotrophic factor: A randomized controlled trial. *J Therm Biol* **101**, 103067. https://doi.org/10.1016/j.jtherbio.2021.103067.

Goda, T., Doi, M., Umezaki, Y., Murai, I., Shimatani, H., Chu, M. L., Nguyen, V. H., Okamura, H. and Hamada, F. N. (2018). Calcitonin receptors are ancient modulators for rhythms of preferential temperature in insects and body temperature in mammals. *Genes Dev* **32**, 140-155. https://doi.org/10.1101/gad.307884.117.

Goda, T. and Hamada, F. N. (2019). *Drosophila* Temperature preference rhythms: An innovative model to understand body temperature rhythms. *Int J Mol Sci* **20**. https://doi.org/10.3390/ijms20081988.

Goda, T., Leslie, J. R. and Hamada, F. N. (2014). Design and analysis of temperature preference behavior and its circadian rhythm in *Drosophila*. *J Vis Exp*, e51097. https://doi.org/10.3791/51097.

Goda, T., Tang, X., Umezaki, Y., Chu, M. L., Kunst, M., Nitabach, M. N. N. and Hamada, F. N. (2016). *Drosophila* DH31 neuropeptide and pdf receptor regulate night-onset temperature preference. *J Neurosci* **36**, 11739-11754. https://doi.org/10.1523/jneurosci.0964-16.2016.

Godin, J. D., Colombo, K., Molina-Calavita, M., Keryer, G., Zala, D., Charrin, B. C., Dietrich, P., Volvert, M. L., Guillemot, F., Dragatsis, I. et al. (2010). Huntingtin is required for mitotic spindle orientation and mammalian neurogenesis. *Neuron* **67**, 392-406. https://doi.org/10.1016/j.neuron.2010.06.027.

Godin, J. D. and Humbert, S. (2011). Mitotic spindle: focus on the function of huntingtin. *Int J Biochem Cell Biol* **43**, 852-6. https://doi.org/10.1016/j.biocel.2011.03.009.

Goh, G. H., Blache, D., Mark, P. J., Kennington, W. J. and Maloney, S. K. (2021). Daily temperature cycles prolong lifespan and have sex-specific effects on peripheral clock gene expression in *Drosophila melanogaster*. *J Exp Biol* **224**. https://doi.org/10.1242/jeb.233213.

Gohil, V. M., Offner, N., Walker, J. A., Sheth, S. A., Fossale, E., Gusella, J. F., MacDonald, M. E., Neri, C. and Mootha, V. K. (2011). Meclizine is neuroprotective in models of Huntington's disease. *Hum Mol Genet* **20**, 294-300. https://doi.org/10.1093/hmg/ddq464.

References

Goldberg, Y. P., Kremer, B., Andrew, S. E., Theilmann, J., Graham, R. K., Squitieri, F., Telenius, H., Adam, S., Sajoo, A., Starr, E. et al. (1993). Molecular analysis of new mutations for Huntington's disease: intermediate alleles and sex of origin effects. *Nat Genet* **5**, 174-9. https://doi.org/10.1038/ng1093-174.

Goldberg, Y. P., Nicholson, D. W., Rasper, D. M., Kalchman, M. A., Koide, H. B., Graham, R. K., Bromm, M., Kazemi-Esfarjani, P., Thornberry, N. A., Vaillancourt, J. P. et al. (1996). Cleavage of huntingtin by apopain, a proapoptotic cysteine protease, is modulated by the polyglutamine tract. *Nat Genet* **13**, 442-9. https://doi.org/10.1038/ng0896-442.

Gómez-Esteban, J. C., Lezcano, E., Zarranz, J. J., Velasco, F., Garamendi, I., Pérez, T. and Tijero, B. (2007). Monozygotic twins suffering from Huntington's disease show different cognitive and behavioural symptoms. *Eur Neurol* **57**, 26-30. https://doi.org/10.1159/000097006.

Gómez-Jaramillo, L., Cano-Cano, F., González-Montelongo, M. D. C., Campos-Caro, A., Aguilar-Diosdado, M. and Arroba, A. I. (2022). A new perspective on Huntington's disease: How a neurological disorder influences the peripheral tissues. *Int J Mol Sci* **23**. https://doi.org/10.3390/ijms23116089.

Gomez, F. H., Sambucetti, P. and Norry, F. M. (2016). Elevated extension of longevity by cyclically heat stressing a set of recombinant inbred lines of *Drosophila melanogaster* throughout their adult life. *Biogerontology* **17**, 883-892. https://doi.org/10.1007/s10522-016-9658-4.

Gong, W. J. and Golic, K. G. (2004). Genomic deletions of the *Drosophila melanogaster* Hsp70 genes. *Genetics* **168**, 1467-76. https://doi.org/10.1534/genetics.104.030874.

Gong, W. J. and Golic, K. G. (2006). Loss of Hsp70 in *Drosophila* is pleiotropic, with effects on thermotolerance, recovery from heat shock and neurodegeneration. *Genetics* **172**, 275-86. https://doi.org/10.1534/genetics.105.048793.

Gonitel, R., Moffitt, H., Sathasivam, K., Woodman, B., Detloff, P. J., Faull, R. L. and Bates, G. P. (2008). DNA instability in postmitotic neurons. *Proc Natl Acad Sci U S A* **105**, 3467-72. https://doi.org/10.1073/pnas.0800048105.

Gonzales, E. and Yin, J. (2010). *Drosophila* Models of Huntington's Disease exhibit sleep abnormalities. *PLoS Curr* **2**. https://doi.org/10.1371/currents.RRN1185.

Gonzales, E. D., Tanenhaus, A. K., Zhang, J., Chaffee, R. P. and Yin, J. C. (2016). Early-onset sleep defects in *Drosophila* models of Huntington's disease reflect alterations of PKA/CREB signaling. *Hum Mol Genet* **25**, 837-52. https://doi.org/10.1093/hmg/ddv482.

González-Tokman, D., Córdoba-Aguilar, A., Dáttilo, W., Lira-Noriega, A., Sánchez-Guillén, R. A. and Villalobos, F. (2020). Insect responses to heat: Physiological mechanisms, evolution and ecological implications in a warming world. *Biol Rev Camb Philos Soc* **95**, 802-821. https://doi.org/10.1111/brv.12588.

González, M. M. C. (2018). Dim light at night and constant darkness: Two frequently used lighting conditions that jeopardize the health and well-being of laboratory rodents. *Front Neurol* **9**, 609. https://doi.org/10.3389/fneur.2018.00609.

Goodman, A. O. and Barker, R. A. (2010). How vital is sleep in Huntington's disease? *J Neurol* **257**, 882-97. https://doi.org/10.1007/s00415-010-5517-4.

References

Goodman, A. O., Rogers, L., Pilsworth, S., McAllister, C. J., Shneerson, J. M., Morton, A. J. and Barker, R. A. (2011). Asymptomatic sleep abnormalities are a common early feature in patients with Huntington's disease. *Curr Neurol Neurosci Rep* **11**, 211-7. https://doi.org/10.1007/s11910-010-0163-x.

Gorenberg, E. L. and Chandra, S. S. (2017). The role of co-chaperones in synaptic proteostasis and neurodegenerative disease. *Front Neurosci* **11**. https://doi.org/10.3389/fnins.2017.00248.

Gorostiza, E. A. and Ceriani, M. F. (2013). Retrograde Bone Morphogenetic Protein signaling shapes a key circadian pacemaker circuit. *J Neurosci* **33**, 687-96. https://doi.org/10.1523/JNEUROSCI.3448-12.2013.

Gorostiza, E. A., Depetris-Chauvin, A., Frenkel, L., Pírez, N. and Ceriani, M. F. (2014). Circadian pacemaker neurons change synaptic contacts across the day. *Curr Biol* **24**, 2161-2167. https://doi.org/10.1016/j.cub.2014.07.063.

Gotic, I., Omidi, S., Fleury-Olela, F., Molina, N., Naef, F. and Schibler, U. (2016). Temperature regulates splicing efficiency of the cold-inducible RNA-binding protein gene Cirbp. *Genes Dev* **30**, 2005-17. https://doi.org/10.1101/gad.287094.116.

Graham, R. K., Deng, Y., Slow, E. J., Haigh, B., Bissada, N., Lu, G., Pearson, J., Shehadeh, J., Bertram, L., Murphy, Z. et al. (2006). Cleavage at the caspase-6 site is required for neuronal dysfunction and degeneration due to mutant huntingtin. *Cell* **125**, 1179-91. https://doi.org/10.1016/j.cell.2006.04.026.

Greco, T. M., Secker, C., Ramos, E. S., Federspiel, J. D., Liu, J. P., Perez, A. M., Al-Ramahi, I., Cantle, J. P., Carroll, J. B., Botas, J. et al. (2022). Dynamics of huntingtin protein interactions in the striatum identifies candidate modifiers of Huntington disease. *Cell Syst* **13**, 304-320.e5. https://doi.org/10.1016/j.cels.2022.01.005.

Green, E. W. and Giorgini, F. (2012). Choosing and using *Drosophila* models to characterize modifiers of Huntington's disease. *Biochem Soc Trans* **40**, 739-45. https://doi.org/10.1042/BST20120072.

Green, R. M., Tingay, S., Wang, Z. Y. and Tobin, E. M. (2002). Circadian rhythms confer a higher level of fitness to arabidopsis plants. *Plant Physiol* **129**, 576-84. https://doi.org/10.1104/pp.004374.

Grima, B., Chelot, E., Xia, R. and Rouyer, F. (2004a). Morning and evening peaks of activity rely on different clock neurons of the *Drosophila* brain. *Nature* **431**, 869-73. 10.1038/nature02935.

Grima, B., Chélot, E., Xia, R. and Rouyer, F. (2004b). Morning and evening peaks of activity rely on different clock neurons of the *Drosophila* brain. *Nature* **431**, 869-73. https://doi.org/10.1038/nature02935.

Grima, J. C., Daigle, J. G., Arbez, N., Cunningham, K. C., Zhang, K., Ochaba, J., Geater, C., Morozko, E., Stocksdale, J., Glatzer, J. C. et al. (2017). Mutant huntingtin disrupts the nuclear pore complex. *Neuron* **94**, 93-107.e6. https://doi.org/10.1016/j.neuron.2017.03.023.

Gruber, A., Hornburg, D., Antonin, M., Krahmer, N., Collado, J., Schaffer, M., Zubaite, G., Lüchtenborg, C., Sachsenheimer, T., Brügger, B. et al. (2018). Molecular and structural architecture of polyQ aggregates in yeast. *Proc Natl Acad Sci U S A* **115**, E3446-e3453. https://doi.org/10.1073/pnas.1717978115.

References

Gu, Z., Wang, B., Zhang, Y. B., Ding, H., Zhang, Y., Yu, J., Gu, M., Chan, P. and Cai, Y. (2015). Association of ARNTL and PER1 genes with Parkinson's disease: A case-control study of Han Chinese. *Sci Rep* **5**, 15891. https://doi.org/10.1038/srep15891.

Guiretti, D., Sempere, A., Lopez-Atalaya, J. P., Ferrer-Montiel, A., Barco, A. and Valor, L. M. (2016). Specific promoter deacetylation of histone H3 is conserved across mouse models of Huntington's disease in the absence of bulk changes. *Neurobiol Dis* **89**, 190-201. https://doi.org/10.1016/j.nbd.2016.02.004.

Guisle, I., Canet, G., Pétry, S., Fereydouni-Forouzandeh, P., Morin, F., Kérauden, R., Whittington, R. A., Calon, F., Hébert, S. S. and Planel, E. (2022). Sauna-like conditions or menthol treatment reduce tau phosphorylation through mild hyperthermia. *Neurobiol Aging* **113**, 118-130. https://doi.org/10.1016/j.neurobiolaging.2022.02.011.

Gunawardena, S., Her, L. S., Brusch, R. G., Laymon, R. A., Niesman, I. R., Gordesky-Gold, B., Sintasath, L., Bonini, N. M. and Goldstein, L. S. (2003). Disruption of axonal transport by loss of huntingtin or expression of pathogenic polyQ proteins in *Drosophila*. *Neuron* **40**, 25-40. https://doi.org/10.1016/s0896-6273(03)00594-4.

Gunawardhana, K. L. and Hardin, P. E. (2017). VRILLE controls PDF neuropeptide accumulation and arborization rhythms in Small Ventrolateral Neurons to drive rhythmic behavior in *Drosophila*. *Curr Biol* **27**, 3442-3453 e4. https://doi.org/10.1016/j.cub.2017.10.010.

Guo, C., Pan, Y. and Gong, Z. (2019). Recent advances in the genetic dissection of neural circuits in *Drosophila*. *Neurosci Bull* **35**, 1058-1072. https://doi.org/10.1007/s12264-019-00390-9.

Guo, F., Cerullo, I., Chen, X. and Rosbash, M. (2014). PDF neuron firing phase-shifts key circadian activity neurons in *Drosophila*. *Elife* **3**. https://doi.org/10.7554/eLife.02780.

Guo, F., Holla, M., Díaz, M. M. and Rosbash, M. (2018a). A circadian output circuit controls sleep-wake arousal in *Drosophila*. *Neuron* **100**, 624-635.e4. https://doi.org/10.1016/j.neuron.2018.09.002.

Guo, F., Yu, J., Jung, H. J., Abruzzi, K. C., Luo, W., Griffith, L. C. and Rosbash, M. (2016). Circadian neuron feedback controls the *Drosophila* sleep--activity profile. *Nature* **536**, 292-7. https://doi.org/10.1038/nature19097.

Guo, Q., Bin, H., Cheng, J., Seefelder, M., Engler, T., Pfeifer, G., Oeckl, P., Otto, M., Moser, F., Maurer, M. et al. (2018b). The cryo-electron microscopy structure of huntingtin. *Nature* **555**, 117-120. https://doi.org/10.1038/nature25502.

Gusella, J. F. and MacDonald, M. E. (1995). Huntington's disease. *Semin Cell Biol* **6**, 21-8. https://doi.org/10.1016/1043-4682(95)90011-x.

Gusella, J. F. and MacDonald, M. E. (2006). Huntington's disease: seeing the pathogenic process through a genetic lens. *Trends Biochem Sci* **31**, 533-40. https://doi.org/10.1016/j.tibs.2006.06.009.

Gusella, J. F., Wexler, N. S., Conneally, P. M., Naylor, S. L., Anderson, M. A., Tanzi, R. E., Watkins, P. C., Ottina, K., Wallace, M. R., Sakaguchi, A. Y. et al. (1983). A polymorphic DNA marker genetically linked to Huntington's disease. *Nature* **306**, 234-8. https://doi.org/10.1038/306234a0.

Gutekunst, C. A., Levey, A. I., Heilman, C. J., Whaley, W. L., Yi, H., Nash, N. R., Rees, H. D., Madden, J. J. and Hersch, S. M. (1995). Identification and localization of huntingtin in brain and

human lymphoblastoid cell lines with anti-fusion protein antibodies. *Proc Natl Acad Sci U S A* **92**, 8710-4. https://doi.org/10.1073/pnas.92.19.8710.

Gutekunst, C. A., Li, S. H., Yi, H., Ferrante, R. J., Li, X. J. and Hersch, S. M. (1998). The cellular and subcellular localization of huntingtin-associated protein 1 (HAP1): comparison with huntingtin in rat and human. *J Neurosci* **18**, 7674-86. https://doi.org/10.1523/jneurosci.18-19-07674.1998.

Gutekunst, C. A., Li, S. H., Yi, H., Mulroy, J. S., Kuemmerle, S., Jones, R., Rye, D., Ferrante, R. J., Hersch, S. M. and Li, X. J. (1999). Nuclear and neuropil aggregates in Huntington's disease: Relationship to neuropathology. *J Neurosci* **19**, 2522-34. https://doi.org/10.1523/jneurosci.19-07-02522.1999.

Guzhova, I. V., Lazarev, V. F., Kaznacheeva, A. V., Ippolitova, M. V., Muronetz, V. I., Kinev, A. V. and Margulis, B. A. (2011). Novel mechanism of Hsp70 chaperone-mediated prevention of polyglutamine aggregates in a cellular model of Huntington disease. *Hum Mol Genet* **20**, 3953-63. https://doi.org/10.1093/hmg/ddr314.

Habash, R. W. Y. (2018). Therapeutic hyperthermia. *Handb Clin Neurol* **157**, 853-868. https://doi.org/10.1016/b978-0-444-64074-1.00053-7.

Hackam, A. S., Singaraja, R., Zhang, T., Gan, L. and Hayden, M. R. (1999). In vitro evidence for both the nucleus and cytoplasm as subcellular sites of pathogenesis in Huntington's disease. *Hum Mol Genet* **8**, 25-33. https://doi.org/10.1093/hmg/8.1.25.

Hafen, P. S., Preece, C. N., Sorensen, J. R., Hancock, C. R. and Hyldahl, R. D. (2018). Repeated exposure to heat stress induces mitochondrial adaptation in human skeletal muscle. *J Appl Physiol (1985)* **125**, 1447-1455. https://doi.org/10.1152/japplphysiol.00383.2018.

Hageman, J., Rujano, M. A., van Waarde, M. A., Kakkar, V., Dirks, R. P., Govorukhina, N., Oosterveld-Hut, H. M., Lubsen, N. H. and Kampinga, H. H. (2010). A DNAJB chaperone subfamily with HDAC-dependent activities suppresses toxic protein aggregation. *Mol Cell* **37**, 355-69. https://doi.org/10.1016/j.molcel.2010.01.001.

Haldimann, P., Muriset, M., Vígh, L. and Goloubinoff, P. (2011). The novel hydroxylamine derivative NG-094 suppresses polyglutamine protein toxicity in *Caenorhabditis elegans*. *J Biol Chem* **286**, 18784-94. https://doi.org/10.1074/jbc.M111.234773.

Hall, H., Ma, J., Shekhar, S., Leon-Salas, W. D. and Weake, V. M. (2018). Blue light induces a neuroprotective gene expression program in *Drosophila* photoreceptors. *BMC Neurosci* **19**, 43. https://doi.org/10.1186/s12868-018-0443-y.

Haltenhof, T., Kotte, A., De Bortoli, F., Schiefer, S., Meinke, S., Emmerichs, A. K., Petermann, K. K., Timmermann, B., Imhof, P., Franz, A. et al. (2020). A conserved kinase-based body-temperature sensor globally controls alternative splicing and gene expression. *Mol Cell* **78**, 57-69.e4. https://doi.org/10.1016/j.molcel.2020.01.028.

Hamada, F. N., Rosenzweig, M., Kang, K., Pulver, S. R., Ghezzi, A., Jegla, T. J. and Garrity, P. A. (2008). An internal thermal sensor controlling temperature preference in *Drosophila*. *Nature* **454**, 217-20. https://doi.org/10.1038/nature07001.

Hamblin, M. R. (2016). Shining light on the head: Photobiomodulation for brain disorders. *BBA Clin* **6**, 113-124. https://doi.org/10.1016/j.bbacli.2016.09.002.

References

Han, I., You, Y., Kordower, J. H., Brady, S. T. and Morfini, G. A. (2010). Differential vulnerability of neurons in Huntington's disease: The role of cell type-specific features. *J Neurochem* **113**, 1073-91. https://doi.org/10.1111/j.1471-4159.2010.06672.x.

Handley, R. R., Reid, S. J., Patassini, S., Rudiger, S. R., Obolonkin, V., McLaughlan, C. J., Jacobsen, J. C., Gusella, J. F., MacDonald, M. E., Waldvogel, H. J. et al. (2016). Metabolic disruption identified in the Huntington's disease transgenic sheep model. *Sci Rep* **6**, 20681. https://doi.org/10.1038/srep20681.

Hansson, O., Nylandsted, J., Castilho, R. F., Leist, M., Jäättelä, M. and Brundin, P. (2003). Overexpression of heat shock protein 70 in R6/2 Huntington's disease mice has only modest effects on disease progression. *Brain Research* **970**, 47-57. https://doi.org/10.1016/s0006-8993(02)04275-0.

Hanusch, K. U. and Janssen, C. W. (2019). The impact of whole-body hyperthermia interventions on mood and depression - are we ready for recommendations for clinical application? *Int J Hyperthermia* **36**, 573-581. https://doi.org/10.1080/02656736.2019.1612103.

Happe, S., Berger, K. and Investigators, F. S. (2002). The association between caregiver burden and sleep disturbances in partners of patients with Parkinson's disease. *Age Ageing* **31**, 349-54. https://doi.org/10.1093/ageing/31.5.349.

Hardin, P. E. (2006). Essential and expendable features of the circadian timekeeping mechanism. *Curr Opin Neurobiol* **16**, 686-92. https://doi.org/10.1016/j.conb.2006.09.001.

Hardin, P. E. (2011). Molecular genetic analysis of circadian timekeeping in *Drosophila*. *Adv Genet* **74**, 141-73. https://doi.org/10.1016/b978-0-12-387690-4.00005-2.

Harding, R. J. and Tong, Y.-f. (2018a). Proteostasis in Huntington's disease: disease mechanisms and therapeutic opportunities. *Acta Pharmacol Sin* **39**, 754-769. https://doi.org/10.1038/aps.2018.11.

Harding, R. J. and Tong, Y. F. (2018b). Proteostasis in Huntington's disease: Disease mechanisms and therapeutic opportunities. *Acta Pharmacol Sin* **39**, 754-769. https://doi.org/10.1038/aps.2018.11.

Haremaki, T., Deglincerti, A. and Brivanlou, A. H. (2015). Huntingtin is required for ciliogenesis and neurogenesis during early Xenopus development. *Dev Biol* **408**, 305-15. https://doi.org/10.1016/j.ydbio.2015.07.013.

Harjes, P. and Wanker, E. E. (2003). The hunt for huntingtin function: Interaction partners tell many different stories. *Trends Biochem Sci* **28**, 425-33. https://doi.org/10.1016/s0968-0004(03)00168-3.

Harper, D. G., Volicer, L., Stopa, E. G., McKee, A. C., Nitta, M. and Satlin, A. (2005). Disturbance of endogenous circadian rhythm in aging and Alzheimer disease. *Am J Geriatr Psychiatry* **13**, 359-68. https://doi.org/10.1176/appi.ajgp.13.5.359.

Harper, R. E. F., Dayan, P., Albert, J. T. and Stanewsky, R. (2016). Sensory conflict disrupts activity of the *Drosophila* circadian network. *Cell Rep* **17**, 1711-1718. https://doi.org/10.1016/j.celrep.2016.10.029.

Harris, G. J., Codori, A. M., Lewis, R. F., Schmidt, E., Bedi, A. and Brandt, J. (1999). Reduced basal ganglia blood flow and volume in pre-symptomatic, gene-tested persons at-risk for Huntington's disease. *Brain* **122 (Pt 9)**, 1667-78. https://doi.org/10.1093/brain/122.9.1667.

References

Harrisingh, M. C., Wu, Y., Lnenicka, G. A. and Nitabach, M. N. (2007). Intracellular Ca^{2+} regulates free-running circadian clock oscillation *in vivo*. *J Neurosci* **27**, 12489-99. https://doi.org/10.1523/JNEUROSCI.3680-07.2007.

Hart, D. W., van Jaarsveld, B., Lasch, K. G., Grenfell, K. L., Oosthuizen, M. K. and Bennett, N. C. (2021). Ambient temperature as a strong zeitgeber of circadian rhythms in response to temperature sensitivity and poor heat dissipation abilities in subterranean african mole-rats. *J Biol Rhythms* **36**, 461-469. https://doi.org/10.1177/07487304211034287.

Hartl, F. U., Bracher, A. and Hayer-Hartl, M. (2011). Molecular chaperones in protein folding and proteostasis. *Nature* **475**, 324-32. https://doi.org/10.1038/nature10317.

Hartl, F. U. and Hayer-Hartl, M. (2009). Converging concepts of protein folding in vitro and in vivo. *Nature Structural & Molecular Biology* **16**, 574-581. https://doi.org/10.1038/nsmb.1591.

Harvey, J. A., Heinen, R., Gols, R. and Thakur, M. P. (2020). Climate change-mediated temperature extremes and insects: From outbreaks to breakdowns. *Glob Chang Biol* **26**, 6685-6701. https://doi.org/10.1111/gcb.15377.

Haskell, E. H., Palca, J. W., Walker, J. M., Berger, R. J. and Heller, H. C. (1981). The effects of high and low ambient temperatures on human sleep stages. *Electroencephalogr Clin Neurophysiol* **51**, 494-501. https://doi.org/10.1016/0013-4694(81)90226-1.

Hastings, M., O'Neill, J. S. and Maywood, E. S. (2007). Circadian clocks: regulators of endocrine and metabolic rhythms. *J Endocrinol* **195**, 187-98. https://doi.org/10.1677/joe-07-0378.

Hastings, M. H. and Goedert, M. (2013). Circadian clocks and neurodegenerative diseases: time to aggregate? *Curr Opin Neurobiol* **23**, 880-7. https://doi.org/10.1016/j.conb.2013.05.004.

Hastings, M. H., Maywood, E. S. and Brancaccio, M. (2018). Generation of circadian rhythms in the suprachiasmatic nucleus. *Nat Rev Neurosci* **19**, 453-469. https://doi.org/10.1038/s41583-018-0026-z.

Hastings, M. H., Maywood, E. S. and Brancaccio, M. (2019). The mammalian circadian timing system and the suprachiasmatic nucleus as its pacemaker. *Biology (Basel)* **8**. https://doi.org/10.3390/biology8010013.

Hastings, M. H., Reddy, A. B. and Maywood, E. S. (2003). A clockwork web: Circadian timing in brain and periphery, in health and disease. *Nat Rev Neurosci* **4**, 649-61. https://doi.org/10.1038/nrn1177.

Hatori, M., Gronfier, C., Van Gelder, R. N., Bernstein, P. S., Carreras, J., Panda, S., Marks, F., Sliney, D., Hunt, C. E., Hirota, T. et al. (2017). Global rise of potential health hazards caused by blue light-induced circadian disruption in modern aging societies. *NPJ Aging Mech Dis* **3**, 9. https://doi.org/10.1038/s41514-017-0010-2.

Hatters, D. M. (2012). Putting huntingtin "aggregation" in view with windows into the cellular milieu. *Curr Top Med Chem* **12**, 2611-22. https://doi.org/10.2174/1568026611212220013.

Hay, D. G. (2004). Progressive decrease in chaperone protein levels in a mouse model of Huntington's disease and induction of stress proteins as a therapeutic approach. *Human Molecular Genetics* **13**, 1389-1405. https://doi.org/10.1093/hmg/ddh144.

References

HDCRG. (1993). A novel gene containing a trinucleotide repeat that is expanded and unstable on Huntington's disease chromosomes. The Huntington's Disease Collaborative Research Group. *Cell* **72**, 971-83. https://doi.org/10.1016/0092-8674(93)90585-e.

He, W. T., Xue, W., Gao, Y. G., Hong, J. Y., Yue, H. W., Jiang, L. L. and Hu, H. Y. (2017). HSP90 recognizes the N-terminus of huntingtin involved in regulation of huntingtin aggregation by USP19. *Sci Rep* **7**, 14797. https://doi.org/10.1038/s41598-017-13711-7.

Hegazi, S., Lowden, C., Rios Garcia, J., Cheng, A. H., Obrietan, K., Levine, J. D. and Cheng, H. M. (2019). A Symphony of Signals: Intercellular and Intracellular Signaling Mechanisms Underlying Circadian Timekeeping in Mice and Flies. *Int J Mol Sci* **20**. https://doi.org/10.3390/ijms20092363.

Heinonen, I. and Laukkanen, J. A. (2018). Effects of heat and cold on health, with special reference to Finnish sauna bathing. *Am J Physiol Regul Integr Comp Physiol* **314**, R629-r638. https://doi.org/10.1152/ajpregu.00115.2017.

Helfrich-Forster, C. (1997). Development of pigment-dispersing hormone-immunoreactive neurons in the nervous system of *Drosophila melanogaster*. *J Comp Neurol* **380**, 335-54. https://doi.org/10.1002/(SICI)1096-9861(19970414)380:3<335::AID-CNE4>3.0.CO;2-3.

Helfrich-Förster, C. (1995). The period clock gene is expressed in central nervous system neurons which also produce a neuropeptide that reveals the projections of circadian pacemaker cells within the brain of *Drosophila melanogaster*. *Proc Natl Acad Sci U S A* **92**, 612-6. https://doi.org/10.1073/pnas.92.2.612.

Helfrich-Förster, C. (1997). Development of pigment-dispersing hormone-immunoreactive neurons in the nervous system of *Drosophila melanogaster*. *J Comp Neurol* **380**, 335-54. 10.1002/(sici)1096-9861(19970414)380:3<335::aid-cne4>3.0.co;2-3.

Helfrich-Förster, C. (1998). Robust circadian rhythmicity of *Drosophila melanogaster* requires the presence of lateral neurons: a brain-behavioral study of *disconnected* mutants. *J Comp Physiol A* **182**, 435-53. https://doi.org/10.1007/s003590050192.

Helfrich-Förster, C. (2009). Neuropeptide PDF plays multiple roles in the circadian clock of *Drosophila melanogaster*. *Sleep and Biological Rhythms* **7**, 130-143. https://doi.org/10.1111/j.1479-8425.2009.00408.x.

Helfrich-Förster, C. (2017). The *Drosophila* clock system. New Delhi: Springer. https://doi.org/10.1007/978-81-322-3688-7.

Helfrich-Förster, C. (2020). Light input pathways to the circadian clock of insects with an emphasis on the fruit fly *Drosophila melanogaste*r. *J Comp Physiol A Neuroethol Sens Neural Behav Physiol* **206**, 259-272. https://doi.org/10.1007/s00359-019-01379-5.

Helfrich-Forster, C., Shafer, O. T., Wulbeck, C., Grieshaber, E., Rieger, D. and Taghert, P. (2007). Development and morphology of the clock-gene-expressing lateral neurons of *Drosophila melanogaster*. *J Comp Neurol* **500**, 47-70. https://doi.org/10.1002/cne.21146.

Helfrich-Förster, C., Shafer, O. T., Wülbeck, C., Grieshaber, E., Rieger, D. and Taghert, P. (2007). Development and morphology of the clock-gene-expressing lateral neurons of *Drosophila melanogaster*. *J Comp Neurol* **500**, 47-70. https://doi.org/10.1002/cne.21146.

References

Helfrich-Förster, C., Täuber, M., Park, J. H., Mühlig-Versen, M., Schneuwly, S. and Hofbauer, A. (2000). Ectopic expression of the neuropeptide pigment-dispersing factor alters behavioral rhythms in *Drosophila melanogaster*. *J Neurosci* **20**, 3339-53. https://doi.org/10.1523/JNEUROSCI.20-09-03339.2000.

Helfrich-Forster, C., Winter, C., Hofbauer, A., Hall, J. C. and Stanewsky, R. (2001). The circadian clock of fruit flies is blind after elimination of all known photoreceptors. *Neuron* **30**, 249-61. https://doi.org/10.1016/s0896-6273(01)00277-x.

Helfrich-Förster, C., Wulf, J. and de Belle, J. S. (2002). Mushroom body influence on locomotor activity and circadian rhythms in *Drosophila melanogaster*. *J Neurogenet* **16**, 73-109. https://doi.org/10.1080/01677060213158.

Helmlinger, D. (2002). Progressive retinal degeneration and dysfunction in R6 Huntington's disease mice. *Human Molecular Genetics* **11**, 3351-3359. https://doi.org/10.1093/hmg/11.26.3351.

Helmlinger, D., Bonnet, J., Mandel, J.-L., Trottier, Y. and Devys, D. (2004). Hsp70 and Hsp40 chaperones do not modulate retinal phenotype in SCA7 mice. *Journal of Biological Chemistry* **279**, 55969-55977. https://doi.org/10.1074/jbc.M409062200.

Herbst, M. and Wanker, E. E. (2007). Small molecule inducers of heat-shock response reduce polyQ-mediated huntingtin aggregation. A possible therapeutic strategy. *Neurodegener Dis* **4**, 254-60. https://doi.org/10.1159/000101849.

Hermann-Luibl, C. and Helfrich-Forster, C. (2015). Clock network in *Drosophila*. *Curr Opin Insect Sci* **7**, 65-70. https://doi.org/10.1016/j.cois.2014.11.003.

Herrero, A., Duhart, J. M. and Ceriani, M. F. (2017). Neuronal and glial clocks underlying structural remodeling of pacemaker neurons in *Drosophila*. *Front Physiol* **8**, 918. https://doi.org/10.3389/fphys.2017.00918.

Herrero, A., Yoshii, T., Ispizua, J. I., Colque, C., Veenstra, J. A., Muraro, N. I. and Ceriani, M. F. (2020). Coupling neuropeptide levels to structural plasticity in *Drosophila* clock neurons. *Curr Biol* **30**, 3154-3166 e4. https://doi.org/10.1016/j.cub.2020.06.009.

Herzog-Krzywoszanska, R. and Krzywoszanski, L. (2019). Sleep disorders in Huntington's disease. *Front Psychiatry* **10**, 221. https://doi.org/10.3389/fpsyt.2019.00221.

Herzog, E. D. (2007). Neurons and networks in daily rhythms. *Nat Rev Neurosci* **8**, 790-802. https://doi.org/10.1038/nrn2215.

Herzog, E. D., Aton, S. J., Numano, R., Sakaki, Y. and Tei, H. (2004). Temporal precision in the mammalian circadian system: A reliable clock from less reliable neurons. *J Biol Rhythms* **19**, 35-46. https://doi.org/10.1177/0748730403260776.

Herzog, E. D. and Huckfeldt, R. M. (2003). Circadian entrainment to temperature, but not light, in the isolated suprachiasmatic nucleus. *J Neurophysiol* **90**, 763-70. https://doi.org/10.1152/jn.00129.2003.

Herzog, E. D., Kiss, I. Z. and Mazuski, C. (2015). Measuring synchrony in the mammalian central circadian circuit. *Methods Enzymol* **552**, 3-22. https://doi.org/10.1016/bs.mie.2014.10.042.

Hipp, M. S., Kasturi, P. and Hartl, F. U. (2019a). The proteostasis network and its decline in ageing. *Nat Rev Mol Cell Biol* **20**, 421-435. https://doi.org/10.1038/s41580-019-0101-y.

References

Hipp, M. S., Kasturi, P. and Hartl, F. U. (2019b). The proteostasis network and its decline in ageing. *Nature Reviews Molecular Cell Biology* **20**, 421-435. 10.1038/s41580-019-0101-y.

Hipp, M. S., Park, S. H. and Hartl, F. U. (2014). Proteostasis impairment in protein-misfolding and -aggregation diseases. *Trends Cell Biol* **24**, 506-14. https://doi.org/10.1016/j.tcb.2014.05.003.

Hipp, M. S., Patel, C. N., Bersuker, K., Riley, B. E., Kaiser, S. E., Shaler, T. A., Brandeis, M. and Kopito, R. R. (2012a). Indirect inhibition of 26S proteasome activity in a cellular model of Huntington's disease. *J Cell Biol* **196**, 573-87. https://doi.org/10.1083/jcb.201110093.

Hipp, M. S., Patel, C. N., Bersuker, K., Riley, B. E., Kaiser, S. E., Shaler, T. A., Brandeis, M. and Kopito, R. R. (2012b). Indirect inhibition of 26S proteasome activity in a cellular model of Huntington's disease. *Journal of Cell Biology* **196**, 573-587. 10.1083/jcb.201110093.

Hirth, F. (2010). *Drosophila melanogaster* in the study of human neurodegeneration. *CNS Neurol Disord Drug Targets* **9**, 504-23. https://doi.org/10.2174/187152710791556104.

Hjerpe, R., Bett, J. S., Keuss, M. J., Solovyova, A., McWilliams, T. G., Johnson, C., Sahu, I., Varghese, J., Wood, N., Wightman, M. et al. (2016). UBQLN2 Mediates Autophagy-Independent Protein Aggregate Clearance by the Proteasome. *Cell* **166**, 935-949. https://doi.org/10.1016/j.cell.2016.07.001.

Hoekstra, S. P., Bishop, N. C., Faulkner, S. H., Bailey, S. J. and Leicht, C. A. (2018). Acute and chronic effects of hot water immersion on inflammation and metabolism in sedentary, overweight adults. *J Appl Physiol (1985)* **125**, 2008-2018. https://doi.org/10.1152/japplphysiol.00407.2018.

Hoffmann, A. A. (2010). Physiological climatic limits in *Drosophila*: Patterns and implications. *J Exp Biol* **213**, 870-80. https://doi.org/10.1242/jeb.037630.

Hoffmann, A. A., Sørensen, J. G. and Loeschcke, V. (2003). Adaptation of *Drosophila* to temperature extremes: Bringing together quantitative and molecular approaches. *J Therm Biol* **28**, 175-216. https://doi.org/10.1016/S0306-4565(02)00057-8.

Hoffner, G. and Djian, P. (2014). Monomeric, oligomeric and polymeric proteins in Huntington disease and other diseases of polyglutamine expansion. *Brain Sci* **4**, 91-122. https://doi.org/10.3390/brainsci4010091.

Hoffner, G. and Djian, P. (2015). Polyglutamine aggregation in Huntington disease: Does structure determine toxicity? *Mol Neurobiol* **52**, 1297-1314. https://doi.org/10.1007/s12035-014-8932-1.

Hoffner, G., Kahlem, P. and Djian, P. (2002). Perinuclear localization of huntingtin as a consequence of its binding to microtubules through an interaction with beta-tubulin: relevance to Huntington's disease. *J Cell Sci* **115**, 941-8. https://doi.org/10.1242/jcs.115.5.941.

Holbert, S., Denghien, I., Kiechle, T., Rosenblatt, A., Wellington, C., Hayden, M. R., Margolis, R. L., Ross, C. A., Dausset, J., Ferrante, R. J. et al. (2001). The Gln-Ala repeat transcriptional activator CA150 interacts with huntingtin: neuropathologic and genetic evidence for a role in Huntington's disease pathogenesis. *Proc Natl Acad Sci U S A* **98**, 1811-6. https://doi.org/10.1073/pnas.98.4.1811.

Holloszy, J. O. and Smith, E. K. (1986). Longevity of cold-exposed rats: a reevaluation of the "rate-of-living theory". *J Appl Physiol (1985)* **61**, 1656-60. https://doi.org/10.1152/jappl.1986.61.5.1656.

Holmberg, C. I., Staniszewski, K. E., Mensah, K. N., Matouschek, A. and Morimoto, R. I. (2004). Inefficient degradation of truncated polyglutamine proteins by the proteasome. *Embo j* **23**, 4307-18. https://doi.org/10.1038/sj.emboj.7600426.

References

Hom, L. L., Lee, E. C., Apicella, J. M., Wallace, S. D., Emmanuel, H., Klau, J. F., Poh, P. Y., Marzano, S., Armstrong, L. E., Casa, D. J. et al. (2012). Eleven days of moderate exercise and heat exposure induces acclimation without significant HSP70 and apoptosis responses of lymphocytes in college-aged males. *Cell Stress Chaperones* **17**, 29-39. https://doi.org/10.1007/s12192-011-0283-5.

Hong, N. (2019). Photobiomodulation as a treatment for neurodegenerative disorders: Current and future trends. *Biomed Eng Lett* **9**, 359-366. https://doi.org/10.1007/s13534-019-00115-x.

Honma, S., Nakamura, W., Shirakawa, T. and Honma, K. (2004). Diversity in the circadian periods of single neurons of the rat suprachiasmatic nucleus depends on nuclear structure and intrinsic period. *Neurosci Lett* **358**, 173-6. https://doi.org/10.1016/j.neulet.2004.01.022.

Honma, S., Shirakawa, T., Katsuno, Y., Namihira, M. and Honma, K. (1998). Circadian periods of single suprachiasmatic neurons in rats. *Neurosci Lett* **250**, 157-60. https://doi.org/10.1016/s0304-3940(98)00464-9.

Hood, S. and Amir, S. (2017a). Neurodegeneration and the circadian clock. *Frontiers in Aging Neuroscience* **9**. https://doi.org/10.3389/fnagi.2017.00170.

Hood, S. and Amir, S. (2017b). Neurodegeneration and the circadian clock. *Front Aging Neurosci* **9**, 170. 10.3389/fnagi.2017.00170.

Hoogeveen, A. T., Willemsen, R., Meyer, N., de Rooij, K. E., Roos, R. A., van Ommen, G. J. and Galjaard, H. (1993). Characterization and localization of the Huntington disease gene product. *Hum Mol Genet* **2**, 2069-73. https://doi.org/10.1093/hmg/2.12.2069.

Hoop, C. L., Lin, H. K., Kar, K., Magyarfalvi, G., Lamley, J. M., Boatz, J. C., Mandal, A., Lewandowski, J. R., Wetzel, R. and van der Wel, P. C. (2016). Huntingtin exon 1 fibrils feature an interdigitated β-hairpin-based polyglutamine core. *Proc Natl Acad Sci U S A* **113**, 1546-51. https://doi.org/10.1073/pnas.1521933113.

Hooper, P. L. (1999). Hot-tub therapy for type 2 diabetes mellitus. *N Engl J Med* **341**, 924-5. https://doi.org/10.1056/nejm199909163411216.

Horn, M., Mitesser, O., Hovestadt, T., Yoshii, T., Rieger, D. and Helfrich-Förster, C. (2019). The circadian clock improves fitness in the fruit fly, *Drosophila melanogaster*. *Front Physiol* **10**, 1374. https://doi.org/10.3389/fphys.2019.01374.

Horne, J. A. and Reid, A. J. (1985). Night-time sleep EEG changes following body heating in a warm bath. *Electroencephalogr Clin Neurophysiol* **60**, 154-7. https://doi.org/10.1016/0013-4694(85)90022-7.

Horowitz, M. (2001). Heat acclimation: phenotypic plasticity and cues to the underlying molecular mechanisms. *Journal of Thermal Biology* **26**, 357-363. https://doi.org/10.1016/S0306-4565(01)00044-4.

Horowitz, M. (2017). Heat acclimation-mediated cross-tolerance: origins in within-life epigenetics? *Front Physiol* **8**, 548. https://doi.org/10.3389/fphys.2017.00548.

Hosp, F., Gutiérrez-Ángel, S., Schaefer, M. H., Cox, J., Meissner, F., Hipp, M. S., Hartl, F. U., Klein, R., Dudanova, I. and Mann, M. (2017). Spatiotemporal proteomic profiling of Huntington's disease inclusions reveals widespread loss of protein function. *Cell Rep* **21**, 2291-2303. https://doi.org/10.1016/j.celrep.2017.10.097.

References

Hou, L., Chen, W., Liu, X., Qiao, D. and Zhou, F. M. (2017). Exercise-induced neuroprotection of the nigrostriatal dopamine system in Parkinson's disease. *Front Aging Neurosci* **9**, 358. https://doi.org/10.3389/fnagi.2017.00358.

Houser, K. W. and Esposito, T. (2021). Human-centric lighting: Foundational considerations and a five-step design process. *Front Neurol* **12**, 630553. https://doi.org/10.3389/fneur.2021.630553.

Huang, B., Guo, Q., Niedermeier, M. L., Cheng, J., Engler, T., Maurer, M., Pautsch, A., Baumeister, W., Stengel, F., Kochanek, S. et al. (2021). Pathological polyQ expansion does not alter the conformation of the huntingtin-HAP40 complex. *Structure* **29**, 804-809.e5. https://doi.org/10.1016/j.str.2021.04.003.

Huebra, L., Coelho, F. M., Filho, F. M. R., Barsottini, O. G. and Pedroso, J. L. (2019). Sleep Disorders in Hereditary Ataxias. *Current Neurology and Neuroscience Reports* **19**. https://doi.org/10.1007/s11910-019-0968-1.

Hughes, A. C., Mort, M., Elliston, L., Thomas, R. M., Brooks, S. P., Dunnett, S. B. and Jones, L. (2014). Identification of novel alternative splicing events in the huntingtin gene and assessment of the functional consequences using structural protein homology modelling. *J Mol Biol* **426**, 1428-38. https://doi.org/10.1016/j.jmb.2013.12.028.

Hughes, A. T., Guilding, C., Lennox, L., Samuels, R. E., McMahon, D. G. and Piggins, H. D. (2008). Live imaging of altered period1 expression in the suprachiasmatic nuclei of Vipr2-/- mice. *J Neurochem* **106**, 1646-57. https://doi.org/10.1111/j.1471-4159.2008.05520.x.

Hung, H. C., Kay, S. A. and Weber, F. (2009). HSP90, a capacitor of behavioral variation. *J Biol Rhythms* **24**, 183-92. https://doi.org/10.1177/0748730409333171.

Hunt, A. P., Minett, G. M., Gibson, O. R., Kerr, G. K. and Stewart, I. B. (2019). Could heat therapy be an effective treatment for Alzheimer's and Parkinson's diseases? A narrative review. *Front Physiol* **10**, 1556. https://doi.org/10.3389/fphys.2019.01556.

Huntington, G. (1872). On Chorea. *Medical Surgical Reporter*, 317-321.

Hyun, S., Lee, Y., Hong, S. T., Bang, S., Paik, D., Kang, J., Shin, J., Lee, J., Jeon, K., Hwang, S. et al. (2005). *Drosophila* GPCR Han is a receptor for the circadian clock neuropeptide PDF. *Neuron* **48**, 267-78. https://doi.org/10.1016/j.neuron.2005.08.025.

Ide, K., Nukina, N., Masuda, N., Goto, J. and Kanazawa, I. (1995). Abnormal gene product identified in Huntington's disease lymphocytes and brain. *Biochem Biophys Res Commun* **209**, 1119-25. https://doi.org/10.1006/bbrc.1995.1613.

Igarashi, S., Morita, H., Bennett, K. M., Tanaka, Y., Engelender, S., Peters, M. F., Cooper, J. K., Wood, J. D., Sawa, A. and Ross, C. A. (2003). Inducible PC12 cell model of Huntington's disease shows toxicity and decreased histone acetylation. *Neuroreport* **14**, 565-8. https://doi.org/10.1097/00001756-200303240-00007.

Iijima-Ando, K., Wu, P., Drier, E. A., Iijima, K. and Yin, J. C. (2005). cAMP-response element-binding protein and heat-shock protein 70 additively suppress polyglutamine-mediated toxicity in *Drosophila*. *Proc Natl Acad Sci U S A* **102**, 10261-6. https://doi.org/10.1073/pnas.0503937102.

References

Ikeda, H., Yamaguchi, M., Sugai, S., Aze, Y., Narumiya, S. and Kakizuka, A. (1996). Expanded polyglutamine in the Machado-Joseph disease protein induces cell death in vitro and in vivo. *Nat Genet* **13**, 196-202. https://doi.org/10.1038/ng0696-196.

Illarioshkin, S. N., Igarashi, S., Onodera, O., Markova, E. D., Nikolskaya, N. N., Tanaka, H., Chabrashwili, T. Z., Insarova, N. G., Endo, K., Ivanova-Smolenskaya, I. A. et al. (1994). Trinucleotide repeat length and rate of progression of Huntington's disease. *Ann Neurol* **36**, 630-5. https://doi.org/10.1002/ana.410360412.

Illarioshkin, S. N., Klyushnikov, S. A., Vigont, V. A., Seliverstov, Y. A. and Kaznacheyeva, E. V. (2018). Molecular pathogenesis in Huntington's disease. *Biochemistry (Mosc)* **83**, 1030-1039. https://doi.org/10.1134/s0006297918090043.

Imarisio, S., Carmichael, J., Korolchuk, V., Chen, C. W., Saiki, S., Rose, C., Krishna, G., Davies, J. E., Ttofi, E., Underwood, B. R. et al. (2008). Huntington's disease: From pathology and genetics to potential therapies. *Biochem J* **412**, 191-209. https://doi.org/10.1042/bj20071619.

Isas, J. M., Langen, A., Isas, M. C., Pandey, N. K. and Siemer, A. B. (2017). Formation and structure of wild type huntingtin exon-1 fibrils. *Biochemistry* **56**, 3579-3586. https://doi.org/10.1021/acs.biochem.7b00138.

Ishimoto, H., Lark, A. and Kitamoto, T. (2012). Factors that differentially affect daytime and nighttime sleep in *Drosophila melanogaster*. *Front Neurol* **3**, 24. https://doi.org/10.3389/fneur.2012.00024.

Ito, F. and Awasaki, T. (2022). Comparative analysis of temperature preference behavior and effects of temperature on daily behavior in 11 *Drosophil*a species. *Sci Rep* **12**, 12692. https://doi.org/10.1038/s41598-022-16897-7.

Iwata, A., Riley, B. E., Johnston, J. A. and Kopito, R. R. (2005). HDAC6 and microtubules are required for autophagic degradation of aggregated huntingtin. *J Biol Chem* **280**, 40282-92. https://doi.org/10.1074/jbc.M508786200.

Iyengar, A. S., Kulkarni, R. and Sheeba, V. (2022). Under warm ambient conditions, *Drosophila melanogaster* suppresses nighttime activity via the neuropeptide pigment dispersing factor. *Genes Brain Behav* **21**, e12802. https://doi.org/10.1111/gbb.12802.

Iyer, R. R. and Pluciennik, A. (2021). DNA mismatch repair and its role in Huntington's disease. *J Huntingtons Dis* **10**, 75-94. https://doi.org/10.3233/jhd-200438.

Jaattela, M. (1995). Over-expression of hsp70 confers tumorigenicity to mouse fibrosarcoma cells. *Int J Cancer* **60**, 689-93. https://doi.org/10.1002/ijc.2910600520.

Jackson, F. R., Ng, F. S., Sengupta, S., You, S. and Huang, Y. (2015). Glial cell regulation of rhythmic behavior. *Methods Enzymol* **552**, 45-73. https://doi.org/10.1016/bs.mie.2014.10.016.

Jackson, G. R., Salecker, I., Dong, X., Yao, X., Arnheim, N., Faber, P. W., MacDonald, M. E. and Zipursky, S. L. (1998). Polyglutamine-expanded human huntingtin transgenes induce degeneration of *Drosophila* photoreceptor neurons. *Neuron* **21**, 633-42. https://doi.org/10.1016/s0896-6273(00)80573-5.

Jacomin, A. C. and Nezis, I. P. (2019). Assays to monitor aggrephagy in *Drosophila* brain. *Methods Mol Biol* **1854**, 147-157. https://doi.org/10.1007/7651_2018_157.

References

Jana, N. R. (2000). Polyglutamine length-dependent interaction of Hsp40 and Hsp70 family chaperones with truncated N-terminal huntingtin: their role in suppression of aggregation and cellular toxicity. *Human Molecular Genetics* **9**, 2009-2018. https://doi.org/10.1093/hmg/9.13.2009.

Jana, N. R., Dikshit, P., Goswami, A., Kotliarova, S., Murata, S., Tanaka, K. and Nukina, N. (2005). Co-chaperone CHIP associates with expanded polyglutamine protein and promotes their degradation by proteasomes. *J Biol Chem* **280**, 11635-40. https://doi.org/10.1074/jbc.M412042200.

Jana, N. R. and Nukina, N. (2005). BAG-1 associates with the polyglutamine-expanded huntingtin aggregates. *Neurosci Lett* **378**, 171-5. https://doi.org/10.1016/j.neulet.2004.12.031.

Jana, N. R., Zemskov, E. A., Wang, G. and Nukina, N. (2001). Altered proteasomal function due to the expression of polyglutamine-expanded truncated N-terminal huntingtin induces apoptosis by caspase activation through mitochondrial cytochrome c release. *Hum Mol Genet* **10**, 1049-59. https://doi.org/10.1093/hmg/10.10.1049.

Janssen, C. W., Lowry, C. A., Mehl, M. R., Allen, J. J., Kelly, K. L., Gartner, D. E., Medrano, A., Begay, T. K., Rentscher, K., White, J. J. et al. (2016). Whole-body hyperthermia for the treatment of major depressive disorder: A randomized clinical trial. *JAMA Psychiatry* **73**, 789-95. https://doi.org/10.1001/jamapsychiatry.2016.1031.

Jarabo, P., Barredo, C. G., de Pablo, C., Casas-Tinto, S. and Martin, F. A. (2022). Alignment between glioblastoma internal clock and environmental cues ameliorates survival in *Drosophila*. *Commun Biol* **5**, 644. https://doi.org/10.1038/s42003-022-03600-9.

Jarosińska, O. D. and Rüdiger, S. G. D. (2021). Molecular strategies to target protein aggregation in Huntington's disease. *Front Mol Biosci* **8**, 769184. https://doi.org/10.3389/fmolb.2021.769184.

Jauhari, A., Baranov, S. V., Suofu, Y., Kim, J., Singh, T., Yablonska, S., Li, F., Wang, X., Oberly, P., Minnigh, M. B. et al. (2020). Melatonin inhibits cytosolic mitochondrial DNA-induced neuroinflammatory signaling in accelerated aging and neurodegeneration. *J Clin Invest* **130**, 3124-3136. https://doi.org/10.1172/jci135026.

Jaumouille, E., Koch, R. and Nagoshi, E. (2021). Uncovering the Roles of Clocks and Neural Transmission in the Resilience of Drosophila Circadian Network. *Front Physiol* **12**, 663339. 10.3389/fphys.2021.663339.

Jaumouillé, E., Koch, R. and Nagoshi, E. (2021). Uncovering the roles of clocks and neural transmission in the resilience of *Drosophila* circadian network. *Front Physiol* **12**, 663339. 10.3389/fphys.2021.663339.

Jauregui-Lozano, J., Hall, H., Stanhope, S. C., Bakhle, K., Marlin, M. M. and Weake, V. M. (2022). The Clock:Cycle complex is a major transcriptional regulator of *Drosophila* photoreceptors that protects the eye from retinal degeneration and oxidative stress. *PLoS Genet* **18**, e1010021. https://doi.org/10.1371/journal.pgen.1010021.

Jedlicka, P., Mortin, M. A. and Wu, C. (1997). Multiple functions of *Drosophila* heat shock transcription factor in vivo. *Embo j* **16**, 2452-62. https://doi.org/10.1093/emboj/16.9.2452.

Jelgersma, G. (1908). Neue anatomische befunde bei paralysis agitans und bei chronischer chorea. *Neurol. Centralbl* **27**, 995.

References

Jeong, E. M., Kwon, M., Cho, E., Lee, S. H., Kim, H., Kim, E. Y. and Kim, J. K. (2022). Systematic modeling-driven experiments identify distinct molecular clockworks underlying hierarchically organized pacemaker neurons. *Proc Natl Acad Sci U S A* **119**. https://doi.org/10.1073/pnas.2113403119.

Jeong, H., Then, F., Melia, T. J., Jr., Mazzulli, J. R., Cui, L., Savas, J. N., Voisine, C., Paganetti, P., Tanese, N., Hart, A. C. et al. (2009). Acetylation targets mutant huntingtin to autophagosomes for degradation. *Cell* **137**, 60-72. https://doi.org/10.1016/j.cell.2009.03.018.

Jha, M., Kamble, N., Lenka, A., Yadav, R., Purushottam, M., Jain, S. and Pal, P. K. (2019). Sleep disturbances in patients with Huntington's disease: A questionnaire-based study. *Annals of Movement Disorders* **2**, 9. https://doi.org/10.4103/AOMD.AOMD_1_19.

Jia, D. D., Zhang, L., Chen, Z., Wang, C. R., Huang, F. Z., Duan, R. H., Xia, K., Tang, B. S. and Jiang, H. (2013). Lithium chloride alleviates neurodegeneration partly by inhibiting activity of GSK3beta in a SCA3 *Drosophila* model. *Cerebellum* **12**, 892-901. https://doi.org/10.1007/s12311-013-0498-3.

Jiang, M., Wang, J., Fu, J., Du, L., Jeong, H., West, T., Xiang, L., Peng, Q., Hou, Z., Cai, H. et al. (2011). Neuroprotective role of Sirt1 in mammalian models of Huntington's disease through activation of multiple Sirt1 targets. *Nat Med* **18**, 153-8. https://doi.org/10.1038/nm.2558.

Jiang, M., Zhang, X., Liu, H., LeBron, J., Alexandris, A., Peng, Q., Gu, H., Yang, F., Li, Y., Wang, R. et al. (2020). Nemo-like kinase reduces mutant huntingtin levels and mitigates Huntington's disease. *Hum Mol Genet* **29**, 1340-1352. https://doi.org/10.1093/hmg/ddaa061.

Jiang, Y., Lv, H., Liao, M., Xu, X., Huang, S., Tan, H., Peng, T., Zhang, Y. and Li, H. (2012). GRP78 counteracts cell death and protein aggregation caused by mutant huntingtin proteins. *Neurosci Lett* **516**, 182-7. https://doi.org/10.1016/j.neulet.2012.03.074.

Jimenez-Sanchez, M., Lam, W., Hannus, M., Sonnichsen, B., Imarisio, S., Fleming, A., Tarditi, A., Menzies, F., Dami, T. E., Xu, C. et al. (2015). siRNA screen identifies QPCT as a druggable target for Huntington's disease. *Nat Chem Biol* **11**, 347-354. https://doi.org/10.1038/nchembio.1790.

Jimenez-Sanchez, M., Licitra, F., Underwood, B. R. and Rubinsztein, D. C. (2017). Huntington's disease: Mechanisms of pathogenesis and therapeutic strategies. *Cold Spring Harb Perspect Med* **7**. https://doi.org/10.1101/cshperspect.a024240.

Jin, X., Tian, Y., Zhang, Z. C., Gu, P., Liu, C. and Han, J. (2021). A subset of DN1p neurons integrates thermosensory inputs to promote wakefulness via CNMa signaling. *Curr Biol* **31**, 2075-2087.e6. https://doi.org/10.1016/j.cub.2021.02.048.

Johnson, R. (2012). Long non-coding RNAs in Huntington's disease neurodegeneration. *Neurobiol Dis* **46**, 245-54. https://doi.org/10.1016/j.nbd.2011.12.006.

Johnson, R., Zuccato, C., Belyaev, N. D., Guest, D. J., Cattaneo, E. and Buckley, N. J. (2008). A microRNA-based gene dysregulation pathway in Huntington's disease. *Neurobiol Dis* **29**, 438-45. https://doi.org/10.1016/j.nbd.2007.11.001.

Johnson, S. L., Tsou, W. L., Prifti, M. V., Harris, A. L. and Todi, S. V. (2022). A survey of protein interactions and posttranslational modifications that influence the polyglutamine diseases. *Front Mol Neurosci* **15**, 974167. https://doi.org/10.3389/fnmol.2022.974167.

Johnston, H. E. and Samant, R. S. (2021). Alternative systems for misfolded protein clearance: life beyond the proteasome. *Febs j* **288**, 4464-4487. https://doi.org/10.1111/febs.15617.

Johnston, J. A., Ward, C. L. and Kopito, R. R. (1998). Aggresomes: a cellular response to misfolded proteins. *J Cell Biol* **143**, 1883-98. https://doi.org/10.1083/jcb.143.7.1883.

Jucker, M. and Walker, L. C. (2018). Propagation and spread of pathogenic protein assemblies in neurodegenerative diseases. *Nat Neurosci* **21**, 1341-1349. https://doi.org/10.1038/s41593-018-0238-6.

Juenemann, K., Schipper-Krom, S., Wiemhoefer, A., Kloss, A., Sanz Sanz, A. and Reits, E. A. J. (2013). Expanded polyglutamine-containing N-terminal huntingtin fragments are entirely degraded by mammalian proteasomes. *J Biol Chem* **288**, 27068-27084. https://doi.org/10.1074/jbc.M113.486076.

Julienne, H., Buhl, E., Leslie, D. S. and Hodge, J. J. L. (2017). *Drosophila* PINK1 and parkin loss-of-function mutants display a range of non-motor Parkinson's disease phenotypes. *Neurobiol Dis* **104**, 15-23. https://doi.org/10.1016/j.nbd.2017.04.014.

Jung, C. G., Kato, R., Zhou, C., Abdelhamid, M., Shaaban, E. I. A., Yamashita, H. and Michikawa, M. (2022). Sustained high body temperature exacerbates cognitive function and Alzheimer's disease-related pathologies. *Sci Rep* **12**, 12273. https://doi.org/10.1038/s41598-022-16626-0.

Jung, J., Xu, K., Lessing, D. and Bonini, N. M. (2009). Preventing Ataxin-3 protein cleavage mitigates degeneration in a *Drosophila* model of SCA3. *Hum Mol Genet* **18**, 4843-52. https://doi.org/10.1093/hmg/ddp456.

Junn, E., Lee, S. S., Suhr, U. T. and Mouradian, M. M. (2002). Parkin accumulation in aggresomes due to proteasome impairment. *J Biol Chem* **277**, 47870-7. https://doi.org/10.1074/jbc.M203159200.

Jurcau, A. (2022). Molecular pathophysiological mechanisms in Huntington's disease. *Biomedicines* **10**. https://doi.org/10.3390/biomedicines10061432.

Jurcau, A. and Jurcau, M. C. (2022). Therapeutic strategies in Huntington's disease: From genetic defect to gene therapy. *Biomedicines* **10**. https://doi.org/10.3390/biomedicines10081895.

Juste, Y. R., Kaushik, S., Bourdenx, M., Aflakpui, R., Bandyopadhyay, S., Garcia, F., Diaz, A., Lindenau, K., Tu, V., Krause, G. J. et al. (2021). Reciprocal regulation of chaperone-mediated autophagy and the circadian clock. *Nat Cell Biol*. https://doi.org/10.1038/s41556-021-00800-z.

Kadener, S., Stoleru, D., McDonald, M., Nawathean, P. and Rosbash, M. (2007). Clockwork Orange is a transcriptional repressor and a new *Drosophila* circadian pacemaker component. *Genes Dev* **21**, 1675-86. https://doi.org/10.1101/gad.1552607.

Kadener, S., Villella, A., Kula, E., Palm, K., Pyza, E., Botas, J., Hall, J. C. and Rosbash, M. (2006). Neurotoxic protein expression reveals connections between the circadian clock and mating behavior in *Drosophila*. *Proc Natl Acad Sci U S A* **103**, 13537-42. https://doi.org/10.1073/pnas.0605962103.

Kakkar, V., Mansson, C., de Mattos, E. P., Bergink, S., van der Zwaag, M., van Waarde, M., Kloosterhuis, N. J., Melki, R., van Cruchten, R. T. P., Al-Karadaghi, S. et al. (2016). The S/T-rich motif in the DNAJB6 chaperone delays polyglutamine aggregation and the onset of disease in a mouse model. *Mol Cell* **62**, 272-283. https://doi.org/10.1016/j.molcel.2016.03.017.

Kalchman, M. A., Graham, R. K., Xia, G., Koide, H. B., Hodgson, J. G., Graham, K. C., Goldberg, Y. P., Gietz, R. D., Pickart, C. M. and Hayden, M. R. (1996). Huntingtin is ubiquitinated and

interacts with a specific ubiquitin-conjugating enzyme. *J Biol Chem* **271**, 19385-94. https://doi.org/10.1074/jbc.271.32.19385.

Kalkhoven, C., Sennef, C., Peeters, A. and van den Bos, R. (2014). Risk-taking and pathological gambling behavior in Huntington's disease. *Front Behav Neurosci* **8**, 103. https://doi.org/10.3389/fnbeh.2014.00103.

Kalliolia, E., Silajdžić, E., Nambron, R., Hill, N. R., Doshi, A., Frost, C., Watt, H., Hindmarsh, P., Björkqvist, M. and Warner, T. T. (2014). Plasma melatonin is reduced in Huntington's disease. *Mov Disord* **29**, 1511-5. https://doi.org/10.1002/mds.26003.

Kalmar, B. and Greensmith, L. (2009). Induction of heat shock proteins for protection against oxidative stress. *Adv Drug Deliv Rev* **61**, 310-8. https://doi.org/10.1016/j.addr.2009.02.003.

Kaltenbach, L. S., Romero, E., Becklin, R. R., Chettier, R., Bell, R., Phansalkar, A., Strand, A., Torcassi, C., Savage, J., Hurlburt, A. et al. (2007). Huntingtin interacting proteins are genetic modifiers of neurodegeneration. *PLoS Genet* **3**, e82. https://doi.org/10.1371/journal.pgen.0030082.

Kam, J. H., Hogg, C., Fosbury, R., Shinhmar, H. and Jeffery, G. (2021). Mitochondria are specifically vulnerable to 420nm light in *Drosophila* which undermines their function and is associated with reduced fly mobility. *PLoS One* **16**, e0257149. https://doi.org/10.1371/journal.pone.0257149.

Kamash, P. and Ding, Y. (2021). Hypothermia promotes synaptic plasticity and protective effects in neurological diseases. *Brain Circ* **7**, 294-297. https://doi.org/10.4103/bc.bc_28_21.

Kampinga, H. H., Andreasson, C., Barducci, A., Cheetham, M. E., Cyr, D., Emanuelsson, C., Genevaux, P., Gestwicki, J. E., Goloubinoff, P., Huerta-Cepas, J. et al. (2019). Function, evolution, and structure of J-domain proteins. *Cell Stress Chaperones* **24**, 7-15. https://doi.org/10.1007/s12192-018-0948-4.

Kampinga, H. H. and Bergink, S. (2016). Heat shock proteins as potential targets for protective strategies in neurodegeneration. *The Lancet Neurology* **15**, 748-759. https://doi.org/10.1016/s1474-4422(16)00099-5.

Kampinga, H. H. and Craig, E. A. (2010). The HSP70 chaperone machinery: J proteins as drivers of functional specificity. *Nat Rev Mol Cell Biol* **11**, 579-92. https://doi.org/10.1038/nrm2941.

Kaneko, H., Head, L. M., Ling, J., Tang, X., Liu, Y., Hardin, P. E., Emery, P. and Hamada, F. N. (2012). Circadian rhythm of temperature preference and its neural control in *Drosophila*. *Curr Biol* **22**, 1851-7. https://doi.org/10.1016/j.cub.2012.08.006.

Kaneko, M. and Hall, J. C. (2000). Neuroanatomy of cells expressing clock genes in *Drosophila*: Transgenic manipulation of the period and timeless genes to mark the perikarya of circadian pacemaker neurons and their projections. *J Comp Neurol* **422**, 66-94. https://doi.org/10.1002/(sici)1096-9861(20000619)422:1<66::aid-cne5>3.0.co;2-2.

Kaneko, M., Hamblen, M. J. and Hall, J. C. (2000). Involvement of the period gene in developmental time-memory: Effect of the perShort mutation on phase shifts induced by light pulses delivered to *Drosophila* larvae. *J Biol Rhythms* **15**, 13-30. https://doi.org/10.1177/074873040001500103.

Kaneko, M., Helfrich-Forster, C. and Hall, J. C. (1997a). Spatial and temporal expression of the period and timeless genes in the developing nervous system of *Drosophila*: newly identified pacemaker

candidates and novel features of clock gene product cycling. *J Neurosci* **17**, 6745-60. https://doi.org/10.1523/JNEUROSCI.17-17-06745.1997.

Kaneko, M., Helfrich-Förster, C. and Hall, J. C. (1997b). Spatial and temporal expression of the period and timeless genes in the developing nervous system of *Drosophila*: Newly identified pacemaker candidates and novel features of clock gene product cycling. *J Neurosci* **17**, 6745-60. 10.1523/jneurosci.17-17-06745.1997.

Kang, H., Vázquez, F. X., Zhang, L., Das, P., Toledo-Sherman, L., Luan, B., Levitt, M. and Zhou, R. (2017). Emerging β-sheet rich conformations in supercompact huntingtin exon-1 mutant structures. *J Am Chem Soc* **139**, 8820-8827. https://doi.org/10.1021/jacs.7b00838.

Kang, J. E., Lim, M. M., Bateman, R. J., Lee, J. J., Smyth, L. P., Cirrito, J. R., Fujiki, N., Nishino, S. and Holtzman, D. M. (2009). Amyloid-beta dynamics are regulated by orexin and the sleep-wake cycle. *Science* **326**, 1005-7. https://doi.org/10.1126/science.1180962.

Kantor, S., Szabo, L., Varga, J., Cuesta, M. and Morton, A. J. (2013). Progressive sleep and electroencephalogram changes in mice carrying the Huntington's disease mutation. *Brain* **136**, 2147-58. https://doi.org/10.1093/brain/awt128.

Kar, K., Hoop, C. L., Drombosky, K. W., Baker, M. A., Kodali, R., Arduini, I., van der Wel, P. C., Horne, W. S. and Wetzel, R. (2013). β-hairpin-mediated nucleation of polyglutamine amyloid formation. *J Mol Biol* **425**, 1183-97. https://doi.org/10.1016/j.jmb.2013.01.016.

Kar, K., Jayaraman, M., Sahoo, B., Kodali, R. and Wetzel, R. (2011). Critical nucleus size for disease-related polyglutamine aggregation is repeat-length dependent. *Nat Struct Mol Biol* **18**, 328-36. https://doi.org/10.1038/nsmb.1992.

Karatsoreos, I. N., Bhagat, S., Bloss, E. B., Morrison, J. H. and McEwen, B. S. (2011). Disruption of circadian clocks has ramifications for metabolism, brain, and behavior. *Proc Natl Acad Sci U S A* **108**, 1657-62. https://doi.org/10.1073/pnas.1018375108.

Karpuj, M. V., Becher, M. W., Springer, J. E., Chabas, D., Youssef, S., Pedotti, R., Mitchell, D. and Steinman, L. (2002). Prolonged survival and decreased abnormal movements in transgenic model of Huntington disease, with administration of the transglutaminase inhibitor cystamine. *Nat Med* **8**, 143-9. https://doi.org/10.1038/nm0202-143.

Karunanithi, S. and Brown, I. R. (2015). Heat shock response and homeostatic plasticity. *Front Cell Neurosci* **9**. https://doi.org/10.3389/fncel.2015.00068.

Kassubek, J., Juengling, F. D., Kioschies, T., Henkel, K., Karitzky, J., Kramer, B., Ecker, D., Andrich, J., Saft, C., Kraus, P. et al. (2004). Topography of cerebral atrophy in early Huntington's disease: a voxel based morphometric MRI study. *J Neurol Neurosurg Psychiatry* **75**, 213-20. http://doi.org/10.1136/jnnp.2002.009019.

Kaushik, S. and Cuervo, A. M. (2012). Chaperone-mediated autophagy: a unique way to enter the lysosome world. *Trends Cell Biol* **22**, 407-17. http://doi.org/10.1016/j.tcb.2012.05.006.

Kaye, J., Reisine, T. and Finkbeiner, S. (2021). Huntington's disease mouse models: unraveling the pathology caused by CAG repeat expansion. *Fac Rev* **10**, 77. http://doi.org/10.12703/r/10-77.

References

Kazemi-Esfarjani, P. (2002). Suppression of polyglutamine toxicity by a *Drosophila* homolog of myeloid leukemia factor 1. *Human Molecular Genetics* **11**, 2657-2672. http://doi.org/10.1093/hmg/11.21.2657.

Kazemi-Esfarjani, P. and Benzer, S. (2000). Genetic suppression of polyglutamine toxicity in *Drosophila*. *Science* **287**, 1837-40. http://doi.org/10.1126/science.287.5459.1837.

Keene, A. C., Mazzoni, E. O., Zhen, J., Younger, M. A., Yamaguchi, S., Blau, J., Desplan, C. and Sprecher, S. G. (2011). Distinct visual pathways mediate *Drosophila* larval light avoidance and circadian clock entrainment. *J Neurosci* **31**, 6527-34. http://doi.org/10.1523/jneurosci.6165-10.2011.

Kegel, K. B., Meloni, A. R., Yi, Y., Kim, Y. J., Doyle, E., Cuiffo, B. G., Sapp, E., Wang, Y., Qin, Z. H., Chen, J. D. et al. (2002). Huntingtin is present in the nucleus, interacts with the transcriptional corepressor C-terminal binding protein, and represses transcription. *J Biol Chem* **277**, 7466-76. http://doi.org/10.1074/jbc.M103946200.

Kegel, K. B., Sapp, E., Yoder, J., Cuiffo, B., Sobin, L., Kim, Y. J., Qin, Z. H., Hayden, M. R., Aronin, N., Scott, D. L. et al. (2005). Huntingtin associates with acidic phospholipids at the plasma membrane. *J Biol Chem* **280**, 36464-73. http://doi.org/10.1074/jbc.M503672200.

Keller, C. G., Shin, Y., Monteys, A. M., Renaud, N., Beibel, M., Teider, N., Peters, T., Faller, T., St-Cyr, S., Knehr, J. et al. (2022). An orally available, brain penetrant, small molecule lowers huntingtin levels by enhancing pseudoexon inclusion. *Nat Commun* **13**, 1150. http://doi.org/10.1038/s41467-022-28653-6.

Kennedy, D., Jager, R., Mosser, D. D. and Samali, A. (2014). Regulation of apoptosis by heat shock proteins. *IUBMB Life* **66**, 327-38. http://doi.org/10.1002/iub.1274.

Kennedy, L., Evans, E., Chen, C. M., Craven, L., Detloff, P. J., Ennis, M. and Shelbourne, P. F. (2003). Dramatic tissue-specific mutation length increases are an early molecular event in Huntington disease pathogenesis. *Hum Mol Genet* **12**, 3359-67. http://doi.org/10.1093/hmg/ddg352.

Kennedy, L. and Shelbourne, P. F. (2000). Dramatic mutation instability in HD mouse striatum: does polyglutamine load contribute to cell-specific vulnerability in Huntington's disease? *Hum Mol Genet* **9**, 2539-44. http://doi.org/10.1093/hmg/9.17.2539.

Kennedy, M. A., Greco, T. M., Song, B. and Cristea, I. M. (2022). HTT-OMNI: A web-based platform for huntingtin interaction exploration and multi-omics data integration. *Mol Cell Proteomics* **21**, 100275. http://doi.org/10.1016/j.mcpro.2022.100275.

Kerschbamer, E. and Biagioli, M. (2015). Huntington's disease as neurodevelopmental disorder: Altered chromatin regulation, coding, and non-coding RNA transcription. *Front Neurosci* **9**, 509. http://doi.org/10.3389/fnins.2015.00509.

Keryer, G., Pineda, J. R., Liot, G., Kim, J., Dietrich, P., Benstaali, C., Smith, K., Cordelières, F. P., Spassky, N., Ferrante, R. J. et al. (2011). Ciliogenesis is regulated by a huntingtin-HAP1-PCM1 pathway and is altered in Huntington disease. *J Clin Invest* **121**, 4372-82. http://doi.org/10.1172/jci57552.

Kettern, N., Dreiseidler, M., Tawo, R. and Hohfeld, J. (2010). Chaperone-assisted degradation: multiple paths to destruction. *Biol Chem* **391**, 481-9. http://doi.org/10.1515/BC.2010.058.

Keum, J. W., Shin, A., Gillis, T., Mysore, J. S., Abu Elneel, K., Lucente, D., Hadzi, T., Holmans, P., Jones, L., Orth, M. et al. (2016). The HTT CAG-expansion mutation determines age at

death but not disease duration in Huntington disease. *Am J Hum Genet* **98**, 287-98. http://doi.org/10.1016/j.ajhg.2015.12.018.

Khalil, H., Quinn, L., van Deursen, R., Dawes, H., Playle, R., Rosser, A. and Busse, M. (2013). What effect does a structured home-based exercise programme have on people with Huntington's disease? A randomized, controlled pilot study. *Clin Rehabil* **27**, 646-58. http://doi.org/10.1177/0269215512473762.

Khan, S., Nabi, G., Yao, L., Siddique, R., Sajjad, W., Kumar, S., Duan, P. and Hou, H. (2018). Health risks associated with genetic alterations in internal clock system by external factors. *Int J Biol Sci* **14**, 791-798. http://doi.org/10.7150/ijbs.23744.

Khazaeli, A. A., Tatar, M., Pletcher, S. D. and Curtsinger, J. W. (1997). Heat-induced longevity extension in *Drosophila*. I. Heat treatment, mortality, and thermotolerance. *J Gerontol A Biol Sci Med Sci* **52**, B48-52. http://doi.org/10.1093/gerona/52a.1.b48.

Khyati, Malik, I., Agrawal, N. and Kumar, V. (2021). Melatonin and curcumin reestablish disturbed circadian gene expressions and restore locomotion ability and eclosion behavior in *Drosophila* model of Huntington's disease. *Chronobiol Int* **38**, 61-78. http://doi.org/10.1080/07420528.2020.1842752.

Ki, Y., Ri, H., Lee, H., Yoo, E., Choe, J. and Lim, C. (2015). Warming up your tick-tock: Temperature-dependent regulation of circadian clocks. *Neuroscientist* **21**, 503-18. http://doi.org/10.1177/1073858415577083.

Kidd, P. B., Young, M. W. and Siggia, E. D. (2015). Temperature compensation and temperature sensation in the circadian clock. *Proc Natl Acad Sci U S A* **112**, E6284-92. http://doi.org/10.1073/pnas.1511215112.

Kihara, T., Biro, S., Imamura, M., Yoshifuku, S., Takasaki, K., Ikeda, Y., Otuji, Y., Minagoe, S., Toyama, Y. and Tei, C. (2002). Repeated sauna treatment improves vascular endothelial and cardiac function in patients with chronic heart failure. *J Am Coll Cardiol* **39**, 754-9. http://doi.org/10.1016/s0735-1097(01)01824-1.

Killoran, A., Biglan, K. M., Jankovic, J., Eberly, S., Kayson, E., Oakes, D., Young, A. B. and Shoulson, I. (2013). Characterization of the Huntington intermediate CAG repeat expansion phenotype in PHAROS. *Neurology* **80**, 2022-7. http://doi.org/10.1212/WNL.0b013e318294b304.

Kim, A., Lalonde, K., Truesdell, A., Gomes Welter, P., Brocardo, P. S., Rosenstock, T. R. and Gil-Mohapel, J. (2021a). New avenues for the treatment of Huntington's disease. *Int J Mol Sci* **22**. http://doi.org/10.3390/ijms22168363.

Kim, M., Lee, H. S., LaForet, G., McIntyre, C., Martin, E. J., Chang, P., Kim, T. W., Williams, M., Reddy, P. H., Tagle, D. et al. (1999). Mutant huntingtin expression in clonal striatal cells: dissociation of inclusion formation and neuronal survival by caspase inhibition. *J Neurosci* **19**, 964-73. http://doi.org/10.1523/JNEUROSCI.19-03-00964.1999.

Kim, M., Subramanian, M., Cho, Y. H., Kim, G. H., Lee, E. and Park, J. J. (2018). Short-term exposure to dim light at night disrupts rhythmic behaviors and causes neurodegeneration in fly models of tauopathy and Alzheimer's disease. *Biochem Biophys Res Commun* **495**, 1722-1729. http://doi.org/10.1016/j.bbrc.2017.12.021.

References

Kim, M. W., Chelliah, Y., Kim, S. W., Otwinowski, Z. and Bezprozvanny, I. (2009). Secondary structure of Huntingtin amino-terminal region. *Structure* **17**, 1205-12. http://doi.org/10.1016/j.str.2009.08.002.

Kim, S., Nollen, E. A. A., Kitagawa, K., Bindokas, V. P. and Morimoto, R. I. (2002). Polyglutamine protein aggregates are dynamic. *Nat Cell Biol* **4**, 826-831. http://doi.org/10.1038/ncb863.

Kim, S. A., D'Acunto, V. F., Kokona, B., Hofmann, J., Cunningham, N. R., Bistline, E. M., Garcia, F. J., Akhtar, N. M., Hoffman, S. H., Doshi, S. H. et al. (2017). Sedimentation velocity analysis with fluorescence detection of mutant Huntingtin exon 1 aggregation in *Drosophila melanogaster* and *Caenorhabditis elegans*. *Biochemistry* **56**, 4676-4688. http://doi.org/10.1021/acs.biochem.7b00518.

Kim, S. J., Lee, S. H., Suh, I. B., Jang, J. W., Jhoo, J. H. and Lee, J. H. (2021b). Positive effect of timed blue-enriched white light on sleep and cognition in patients with mild and moderate Alzheimer's disease. *Sci Rep* **11**, 10174. http://doi.org/10.1038/s41598-021-89521-9.

Kim, W. Y., Fayazi, Z., Bao, X., Higgins, D. and Kazemi-Esfarjani, P. (2005). Evidence for sequestration of polyglutamine inclusions by *Drosophila* myeloid leukemia factor. *Mol Cell Neurosci* **29**, 536-44. http://doi.org/10.1016/j.mcn.2005.04.005.

Kim, Y. E., Hipp, M. S., Bracher, A., Hayer-Hartl, M. and Ulrich Hartl, F. (2013). Molecular chaperone functions in protein folding and proteostasis. *Annu Rev Biochem* **82**, 323-355. http://doi.org/10.1146/annurev-biochem-060208-092442.

Kim, Y. E., Hosp, F., Frottin, F., Ge, H., Mann, M., Hayer-Hartl, M. and Hartl, F. U. (2016). Soluble oligomers of polyq-expanded huntingtin target a multiplicity of key cellular factors. *Mol Cell* **63**, 951-64. http://doi.org/10.1016/j.molcel.2016.07.022.

Kimball, A. L., McCue, P. M., Petrie, M. A. and Shields, R. K. (2018). Whole body heat exposure modulates acute glucose metabolism. *Int J Hyperthermia* **35**, 644-651. http://doi.org/10.1080/02656736.2018.1516303.

King, A. N., Barber, A. F., Smith, A. E., Dreyer, A. P., Sitaraman, D., Nitabach, M. N., Cavanaugh, D. J. and Sehgal, A. (2017). A peptidergic circuit links the circadian clock to locomotor activity. *Curr Biol* **27**, 1915-1927.e5. http://doi.org/10.1016/j.cub.2017.05.089.

King, A. N. and Sehgal, A. (2020). Molecular and circuit mechanisms mediating circadian clock output in the *Drosophila* brain. *Eur J Neurosci* **51**, 268-281. http://doi.org/10.1111/ejn.14092.

Kingsolver, J. G., Woods, H. A., Buckley, L. B., Potter, K. A., MacLean, H. J. and Higgins, J. K. (2011). Complex life cycles and the responses of insects to climate change. *Integr Comp Biol* **51**, 719-32. http://doi.org/10.1093/icb/icr015.

Kingwell, K. (2021). Double setback for ASO trials in Huntington disease. *Nat Rev Drug Discov* **20**, 412-413. http://doi.org/10.1038/d41573-021-00088-6.

Klaips, C. L., Gropp, M. H. M., Hipp, M. S. and Hartl, F. U. (2020). Sis1 potentiates the stress response to protein aggregation and elevated temperature. *Nat Commun* **11**, 6271. http://doi.org/10.1038/s41467-020-20000-x.

Klaips, C. L., Jayaraj, G. G. and Hartl, F. U. (2018). Pathways of cellular proteostasis in aging and disease. *J Cell Biol* **217**, 51-63. http://doi.org/10.1083/jcb.201709072.

References

Klarsfeld, A., Malpel, S., Michard-Vanhée, C., Picot, M., Chélot, E. and Rouyer, F. (2004). Novel features of cryptochrome-mediated photoreception in the brain circadian clock of *Drosophila*. *J Neurosci* **24**, 1468-77. http://doi.org/10.1523/jneurosci.3661-03.2004.

Klarsfeld, A., Picot, M., Vias, C., Chélot, E. and Rouyer, F. (2011). Identifying specific light inputs for each subgroup of brain clock neurons in *Drosophila* larvae. *J Neurosci* **31**, 17406-15. http://doi.org/10.1523/jneurosci.5159-10.2011.

Klarsfeld, A. and Rouyer, F. (1998). Effects of circadian mutations and LD periodicity on the life span of *Drosophila melanogaster*. *J Biol Rhythms* **13**, 471-8. http://doi.org/10.1177/074873098129000309.

Klegeris, A., Schulzer, M., Harper, D. G. and McGeer, P. L. (2007). Increase in core body temperature of Alzheimer's disease patients as a possible indicator of chronic neuroinflammation: a meta-analysis. *Gerontology* **53**, 7-11. http://doi.org/10.1159/000095386.

Klein, F. A., Pastore, A., Masino, L., Zeder-Lutz, G., Nierengarten, H., Oulad-Abdelghani, M., Altschuh, D., Mandel, J. L. and Trottier, Y. (2007). Pathogenic and non-pathogenic polyglutamine tracts have similar structural properties: towards a length-dependent toxicity gradient. *J Mol Biol* **371**, 235-44. http://doi.org/10.1016/j.jmb.2007.05.028.

Klepsatel, P. and Gáliková, M. (2022). Developmental temperature affects thermal dependence of locomotor activity in *Drosophila*. *J Therm Biol* **103**, 103153. http://doi.org/10.1016/j.jtherbio.2021.103153.

Klose, M., Duvall, L., Li, W., Liang, X., Ren, C., Steinbach, J. H. and Taghert, P. H. (2016). Functional PDF signaling in the *Drosophila* Circadian neural circuit is gated by Ral A-dependent modulation. *Neuron* **90**, 781-794. http://doi.org/10.1016/j.neuron.2016.04.002.

Klug, A. (2010). The discovery of zinc fingers and their applications in gene regulation and genome manipulation. *Annu Rev Biochem* **79**, 213-31. http://doi.org/10.1146/annurev-biochem-010909-095056.

Knekt, P., Järvinen, R., Rissanen, H., Heliövaara, M. and Aromaa, A. (2020). Does sauna bathing protect against dementia? *Prev Med Rep* **20**, 101221. http://doi.org/10.1016/j.pmedr.2020.101221.

Ko, H. W., Kim, E. Y., Chiu, J., Vanselow, J. T., Kramer, A. and Edery, I. (2010). A hierarchical phosphorylation cascade that regulates the timing of PERIOD nuclear entry reveals novel roles for proline-directed kinases and GSK-3beta/SGG in circadian clocks. *J Neurosci* **30**, 12664-75. http://doi.org/10.1523/jneurosci.1586-10.2010.

Ko, J., Ou, S. and Patterson, P. H. (2001). New anti-huntingtin monoclonal antibodies: Implications for huntingtin conformation and its binding proteins. *Brain Res Bull* **56**, 319-29. http://doi.org/10.1016/s0361-9230(01)00599-8.

Kobayashi, Y., Kume, A., Li, M., Doyu, M., Hata, M., Ohtsuka, K. and Sobue, G. (2000). Chaperones Hsp70 and Hsp40 suppress aggregate formation and apoptosis in cultured neuronal cells expressing truncated androgen receptor protein with expanded polyglutamine tract. *J Biol Chem* **275**, 8772-8. http://doi.org/10.1074/jbc.275.12.8772.

References

Koga, H., Martinez-Vicente, M., Arias, E., Kaushik, S., Sulzer, D. and Cuervo, A. M. (2011). Constitutive upregulation of chaperone-mediated autophagy in Huntington's disease. *J Neurosci* **31**, 18492-505. http://doi.org/10.1523/jneurosci.3219-11.2011.

Koh, K., Evans, J. M., Hendricks, J. C. and Sehgal, A. (2006). A *Drosophila* model for age-associated changes in sleep:wake cycles. *Proc Natl Acad Sci U S A* **103**, 13843-7. http://doi.org/10.1073/pnas.0605903103.

Kojima, D., Nakamura, T., Banno, M., Umemoto, Y., Kinoshita, T., Ishida, Y. and Tajima, F. (2018). Head-out immersion in hot water increases serum BDNF in healthy males. *Int J Hyperthermia* **34**, 834-839. http://doi.org/10.1080/02656736.2017.1394502.

Kolobkova, Y. A., Vigont, V. A., Shalygin, A. V. and Kaznacheyeva, E. V. (2017). Huntington's disease: Calcium dyshomeostasis and pathology models. *Acta Naturae* **9**, 34-46. https://doi.org/10.32607/20758251-2017-9-2-34-46.

Koltyn, K. F., Robins, H. I., Schmitt, C. L., Cohen, J. D. and Morgan, W. P. (1992). Changes in mood state following whole-body hyperthermia. *Int J Hyperthermia* **8**, 305-7. https://doi.org/10.3109/02656739209021785.

Kondratova, A. A. and Kondratov, R. V. (2012). The circadian clock and pathology of the ageing brain. *Nat Rev Neurosci* **13**, 325-35. https://doi.org/10.1038/nrn3208.

Konopka, R. J., Pittendrigh, C. and Orr, D. (1989). Reciprocal behaviour associated with altered homeostasis and photosensitivity of *Drosophila* clock mutants. *J Neurogenet* **6**, 1-10. https://doi.org/10.3109/01677068909107096.

Kopito, R. R. (2000). Aggresomes, inclusion bodies and protein aggregation. *Trends Cell Biol* **10**, 524-30. https://doi.org/10.1016/s0962-8924(00)01852-3.

Kosior, N. and Leavitt, B. R. (2018). Murine Models of Huntington's Disease for Evaluating Therapeutics. *Methods Mol Biol* **1780**, 179-207. https://doi.org/10.1007/978-1-4939-7825-0_10.

Kostadinov, B., Lee Pettibone, H., Bell, E. V., Zhou, X., Pranevicius, A., Shafer, O. T. and Fernandez, M. P. (2021). Open-source computational framework for studying *Drosophila* behavioral phase. *STAR Protoc* **2**, 100285. https://doi.org/10.1016/j.xpro.2020.100285.

Kotler, S. A., Tugarinov, V., Schmidt, T., Ceccon, A., Libich, D. S., Ghirlando, R., Schwieters, C. D. and Clore, G. M. (2019). Probing initial transient oligomerization events facilitating Huntingtin fibril nucleation at atomic resolution by relaxation-based NMR. *Proc Natl Acad Sci U S A* **116**, 3562-3571. https://doi.org/10.1073/pnas.1821216116.

Kott, J., Leach, G. and Yan, L. (2012). Direction-dependent effects of chronic "jet-lag" on hippocampal neurogenesis. *Neurosci Lett* **515**, 177-80. https://doi.org/10.1016/j.neulet.2012.03.048.

Kovács, D., Sigmond, T., Hotzi, B., Bohár, B., Fazekas, D., Deák, V., Vellai, T. and Barna, J. (2019). HSF1Base: A comprehensive database of HSF1 (Heat Shock Factor 1) target genes. *Int J Mol Sci* **20**. https://doi.org/10.3390/ijms20225815.

Kovalenko, M., Dragileva, E., St Claire, J., Gillis, T., Guide, J. R., New, J., Dong, H., Kucherlapati, R., Kucherlapati, M. H., Ehrlich, M. E. et al. (2012). Msh2 acts in medium-spiny striatal neurons as an enhancer of CAG instability and mutant huntingtin phenotypes in Huntington's disease knock-in mice. *PLoS One* **7**, e44273. https://doi.org/10.1371/journal.pone.0044273.

References

Koyuncu, S., Fatima, A., Gutierrez-Garcia, R. and Vilchez, D. (2017). Proteostasis of Huntingtin in health and disease. *Int J Mol Sci* **18**. https://doi.org/10.3390/ijms18071568.

Kramer, A., Lange, T., Spies, C., Finger, A. M., Berg, D. and Oster, H. (2022). Foundations of circadian medicine. *PLoS Biol* **20**, e3001567. https://doi.org/10.1371/journal.pbio.3001567.

Kräuchi, K. (2002). How is the circadian rhythm of core body temperature regulated? *Clin Auton Res* **12**, 147-9. https://doi.org/10.1007/s10286-002-0043-9.

Kremer, B. (2002). Clinical neurology of Huntington's disease: Diversity in unity, unity in diversity: Oxford University Press.

Kremer, B., Almqvist, E., Theilmann, J., Spence, N., Telenius, H., Goldberg, Y. P. and Hayden, M. R. (1995). Sex-dependent mechanisms for expansions and contractions of the CAG repeat on affected Huntington disease chromosomes. *Am J Hum Genet* **57**, 343-50.

Krench, M. and Littleton, J. T. (2017). Neurotoxicity pathways in *Drosophila* models of the polyglutamine disorders. *Curr Top Dev Biol* **121**, 201-223. https://doi.org/10.1016/bs.ctdb.2016.07.006.

Kress, G. J., Liao, F., Dimitry, J., Cedeno, M. R., FitzGerald, G. A., Holtzman, D. M. and Musiek, E. S. (2018). Regulation of amyloid-β dynamics and pathology by the circadian clock. *J Exp Med* **215**, 1059-1068. https://doi.org/10.1084/jem.20172347.

Krishnan, N., Davis, A. J. and Giebultowicz, J. M. (2008). Circadian regulation of response to oxidative stress in *Drosophila melanogaster*. *Biochem Biophys Res Commun* **374**, 299-303. https://doi.org/10.1016/j.bbrc.2008.07.011.

Krishnan, N., Kretzschmar, D., Rakshit, K., Chow, E. and Giebultowicz, J. M. (2009). The circadian clock gene period extends healthspan in aging *Drosophila melanogaster*. *Aging (Albany NY)* **1**, 937-48. https://doi.org/10.18632/aging.100103.

Krishnan, N., Rakshit, K., Chow, E. S., Wentzell, J. S., Kretzschmar, D. and Giebultowicz, J. M. (2012). Loss of circadian clock accelerates aging in neurodegeneration-prone mutants. *Neurobiol Dis* **45**, 1129-35. https://doi.org/10.1016/j.nbd.2011.12.034.

Kristensen, T. N., Sørensen, J. G. and Loeschcke, V. (2003). Mild heat stress at a young age in *Drosophila melanogaster* leads to increased Hsp70 synthesis after stress exposure later in life. *J Genet* **82**, 89-94. https://doi.org/10.1007/bf02715811.

Krittika, S. and Yadav, P. (2022). Alterations in lifespan and sleep:wake duration under selective monochromes of visible light in *Drosophila melanogaster*. *Biol Open* **11**. https://doi.org/10.1242/bio.059273.

Krupp, J. J., Billeter, J. C., Wong, A., Choi, C., Nitabach, M. N. and Levine, J. D. (2013). Pigment-dispersing factor modulates pheromone production in clock cells that influence mating in *Drosophila*. *Neuron* **79**, 54-68. https://doi.org/10.1016/j.neuron.2013.05.019.

Kudo, T., Schroeder, A., Loh, D. H., Kuljis, D., Jordan, M. C., Roos, K. P. and Colwell, C. S. (2011). Dysfunctions in circadian behavior and physiology in mouse models of Huntington's disease. *Exp Neurol* **228**, 80-90. https://doi.org/10.1016/j.expneurol.2010.12.011.

Kuemmerle, S., Gutekunst, C. A., Klein, A. M., Li, X. J., Li, S. H., Beal, M. F., Hersch, S. M. and Ferrante, R. J. (1999). Huntington aggregates may not predict neuronal death in Huntington's disease. *Ann Neurol* **46**, 842-9. https://doi.org/10.1002/1531-8249(199912)46:6<842::AID-ANA6>3.3.CO;2-F.

References

Kuennen, M., Gillum, T., Dokladny, K., Bedrick, E., Schneider, S. and Moseley, P. (2011). Thermotolerance and heat acclimation may share a common mechanism in humans. *Am J Physiol Regul Integr Comp Physiol* **301**, R524-33. https://doi.org/10.1152/ajpregu.00039.2011.

Kuhlenhoelter, A. M., Kim, K., Neff, D., Nie, Y., Blaize, A. N., Wong, B. J., Kuang, S., Stout, J., Song, Q., Gavin, T. P. et al. (2016). Heat therapy promotes the expression of angiogenic regulators in human skeletal muscle. *Am J Physiol Regul Integr Comp Physiol* **311**, R377-91. https://doi.org/10.1152/ajpregu.00134.2016.

Kuiper, E. F., de Mattos, E. P., Jardim, L. B., Kampinga, H. H. and Bergink, S. (2017). Chaperones in Polyglutamine Aggregation: Beyond the Q-Stretch. *Front Neurosci* **11**, 145. https://doi.org/10.3389/fnins.2017.00145.

Kula-Eversole, E., Nagoshi, E., Shang, Y., Rodriguez, J., Allada, R. and Rosbash, M. (2010). Surprising gene expression patterns within and between PDF-containing circadian neurons in *Drosophila*. *Proc Natl Acad Sci U S A* **107**, 13497-502. https://doi.org/10.1073/pnas.1002081107.

Kula, E., Levitan, E. S., Pyza, E. and Rosbash, M. (2006). PDF cycling in the dorsal protocerebrum of the *Drosophila* brain is not necessary for circadian clock function. *J Biol Rhythms* **21**, 104-17. https://doi.org/10.1177/0748730405285715.

Kuljis, D., Kudo, T., Tahara, Y., Ghiani, C. A. and Colwell, C. S. (2018). Pathophysiology in the suprachiasmatic nucleus in mouse models of Huntington's disease. *J Neurosci Res* **96**, 1862-1875. https://doi.org/10.1002/jnr.24320.

Kumar, A. and Ratan, R. R. (2016). Oxidative stress and Huntington's disease: The good, the bad, and the ugly. *J Huntingtons Dis* **5**, 217-237. https://doi.org/10.3233/jhd-160205.

Kumar, A., Vaish, M. and Ratan, R. R. (2014). Transcriptional dysregulation in Huntington's disease: a failure of adaptive transcriptional homeostasis. *Drug Discov Today* **19**, 956-62. https://doi.org/10.1016/j.drudis.2014.03.016.

Kumar, S., Mohan, A. and Sharma, V. K. (2005). Circadian dysfunction reduces lifespan in *Drosophila melanogaster*. *Chronobiol Int* **22**, 641-53. https://doi.org/10.1080/07420520500179423.

Kume, K. (2006). A *Drosophila* dopamine transporter mutant, fumin (fmn), is defective in arousal regulation. *Sleep and Biological Rhythms* **4**, 263-273. https://doi.org/10.1111/j.1479-8425.2006.00225.x.

Kume, K., Kume, S., Park, S. K., Hirsh, J. and Jackson, F. R. (2005). Dopamine is a regulator of arousal in the fruit fly. *J Neurosci* **25**, 7377-84. https://doi.org/10.1523/jneurosci.2048-05.2005.

Kumsta, C., Chang, J. T., Schmalz, J. and Hansen, M. (2017). Hormetic heat stress and HSF-1 induce autophagy to improve survival and proteostasis in *C. elegans*. *Nat Commun* **8**, 14337. https://doi.org/10.1038/ncomms14337.

Kuo, Y., Ren, S., Lao, U., Edgar, B. A. and Wang, T. (2013a). Suppression of polyglutamine protein toxicity by co-expression of a heat-shock protein 40 and a heat-shock protein 110. *Cell Death Dis* **4**, e833. 10.1038/cddis.2013.351.

Kuo, Y., Ren, S., Lao, U., Edgar, B. A. and Wang, T. (2013b). Suppression of polyglutamine protein toxicity by co-expression of a heat-shock protein 40 and a heat-shock protein 110. *Cell Death & Disease* **4**, e833-e833. https://doi.org/10.1038/cddis.2013.351.

References

La Spada, A. R. and Taylor, J. P. (2003). Polyglutamines placed into context. *Neuron* **38**, 681-4. https://doi.org/10.1016/s0896-6273(03)00328-3.

Labbadia, J., Cunliffe, H., Weiss, A., Katsyuba, E., Sathasivam, K., Seredenina, T., Woodman, B., Moussaoui, S., Frentzel, S., Luthi-Carter, R. et al. (2011). Altered chromatin architecture underlies progressive impairment of the heat shock response in mouse models of Huntington disease. *J Clin Invest* **121**, 3306-19. https://doi.org/10.1172/jci57413.

Labbadia, J. and Morimoto, R. I. (2013). Huntington's disease: Underlying molecular mechanisms and emerging concepts. *Trends Biochem Sci* **38**, 378-85. https://doi.org/10.1016/j.tibs.2013.05.003.

Labbadia, J. and Morimoto, R. I. (2015). The biology of proteostasis in aging and disease. *Annu Rev Biochem* **84**, 435-464. https://doi.org/10.1146/annurev-biochem-060614-033955.

Labbadia, J., Novoselov, S. S., Bett, J. S., Weiss, A., Paganetti, P., Bates, G. P. and Cheetham, M. E. (2012). Suppression of protein aggregation by chaperone modification of high molecular weight complexes. *Brain* **135**, 1180-96. https://doi.org/10.1093/brain/aws022.

Lack, L. C., Gradisar, M., Van Someren, E. J., Wright, H. R. and Lushington, K. (2008). The relationship between insomnia and body temperatures. *Sleep Med Rev* **12**, 307-17. https://doi.org/10.1016/j.smrv.2008.02.003.

Lamark, T. and Johansen, T. (2012). Aggrephagy: selective disposal of protein aggregates by macroautophagy. *Int J Cell Biol* **2012**, 736905. https://doi.org/10.1155/2012/736905.

Lamaze, A., Krätschmer, P., Chen, K. F., Lowe, S. and Jepson, J. E. C. (2018). A wake-promoting circadian output circuit in *Drosophila*. *Curr Biol* **28**, 3098-3105.e3. https://doi.org/10.1016/j.cub.2018.07.024.

Lamaze, A. and Stanewsky, R. (2019). DN1p or the "Fluffy" cerberus of clock outputs. *Front Physiol* **10**, 1540. https://doi.org/10.3389/fphys.2019.01540.

Lananna, B. V. and Musiek, E. S. (2020). The wrinkling of time: Aging, inflammation, oxidative stress, and the circadian clock in neurodegeneration. *Neurobiol Dis* **139**, 104832. https://doi.org/10.1016/j.nbd.2020.104832.

Landles, C., Sathasivam, K., Weiss, A., Woodman, B., Moffitt, H., Finkbeiner, S., Sun, B., Gafni, J., Ellerby, L. M., Trottier, Y. et al. (2010). Proteolysis of mutant huntingtin produces an exon 1 fragment that accumulates as an aggregated protein in neuronal nuclei in Huntington disease. *J Biol Chem* **285**, 8808-23. https://doi.org/10.1074/jbc.M109.075028.

Landwehrmeyer, G. B., McNeil, S. M., Dure, L. S. t., Ge, P., Aizawa, H., Huang, Q., Ambrose, C. M., Duyao, M. P., Bird, E. D., Bonilla, E. et al. (1995). Huntington's disease gene: Regional and cellular expression in brain of normal and affected individuals. *Ann Neurol* **37**, 218-30. https://doi.org/10.1002/ana.410370213.

Lanska, D. J., Lanska, M. J., Lavine, L. and Schoenberg, B. S. (1988a). Conditions associated with Huntington's disease at death. A case-control study. *Arch Neurol* **45**, 878-80. https://doi.org/10.1001/archneur.1988.00520320068017.

Lanska, D. J., Lavine, L., Lanska, M. J. and Schoenberg, B. S. (1988b). Huntington's disease mortality in the United States. *Neurology* **38**, 769-72. https://doi.org/10.1212/wnl.38.5.769.

References

Lassonde, M., Candel, S. , Hacker, J. , Quadrio-Curzio, A. , Onishi, T. , Ramakrishnan, V. , and McNutt, M. (2017). The Challenge of Neurodegenerative Diseases in an Aging Population. *TRENDS IN THE SCIENCES* **22**, 6_92-6_93. https://doi.org/10.5363/tits.22.6_92.

Lateef, S., Holman, A., Carpenter, J. and James, J. (2019). Can therapeutic hypothermia diminish the impact of traumatic brain injury in *Drosophila melanogaster*? *J Exp Neurosci* **13**, 1179069518824852. https://doi.org/10.1177/1179069518824852.

Laukkanen, T., Kunutsor, S., Kauhanen, J. and Laukkanen, J. A. (2017). Sauna bathing is inversely associated with dementia and Alzheimer's disease in middle-aged Finnish men. *Age Ageing* **46**, 245-249. https://doi.org/10.1093/ageing/afw212.

Lauretti, E., Di Meco, A., Merali, S. and Pratico, D. (2017a). Circadian rhythm dysfunction: a novel environmental risk factor for Parkinson's disease. *Mol Psychiatry* **22**, 280-286. https://doi.org/10.1038/mp.2016.47.

Lauretti, E., Di Meco, A., Merali, S. and Praticò, D. (2017b). Circadian rhythm dysfunction: A novel environmental risk factor for Parkinson's disease. *Mol Psychiatry* **22**, 280-286. https://doi.org/10.1038/mp.2016.47.

Lazar, A. S., Panin, F., Goodman, A. O., Lazic, S. E., Lazar, Z. I., Mason, S. L., Rogers, L., Murgatroyd, P. R., Watson, L. P., Singh, P. et al. (2015). Sleep deficits but no metabolic deficits in premanifest Huntington's disease. *Ann Neurol* **78**, 630-48. https://doi.org/10.1002/ana.24495.

Le Bourg, E. (2011). Using *Drosophila melanogaster* to study the positive effects of mild stress on aging. *Exp Gerontol* **46**, 345-8. https://doi.org/10.1016/j.exger.2010.08.003.

Le Bourg, É. and Rattan, S. I. (2008). Mild stress and healthy aging: applying hormesis in aging research and interventions. Dordrecht: Springer. https://doi.org/10.1007/978-1-4020-6869-0.

Le Bourg, É. and Rattan, S. I. (2014). Hormesis and trade-offs: a comment. *Dose Response* **12**, 522-4. https://doi.org/10.2203/dose-response.14-054.LeBourg.

Lear, B. C., Merrill, C. E., Lin, J. M., Schroeder, A., Zhang, L. and Allada, R. (2005). A G protein-coupled receptor, *groom-of-PDF*, is required for PDF neuron action in circadian behavior. *Neuron* **48**, 221-7. https://doi.org/10.1016/j.neuron.2005.09.008.

Lear, B. C., Zhang, L. and Allada, R. (2009). The neuropeptide PDF acts directly on evening pacemaker neurons to regulate multiple features of circadian behavior. *PLoS Biol* **7**, e1000154. https://doi.org/10.1371/journal.pbio.1000154.

Leavitt, B. R., Guttman, J. A., Hodgson, J. G., Kimel, G. H., Singaraja, R., Vogl, A. W. and Hayden, M. R. (2001). Wild-type huntingtin reduces the cellular toxicity of mutant huntingtin in vivo. *Am J Hum Genet* **68**, 313-24. https://doi.org/10.1086/318207.

Lebreton, F., Cayzac, S., Pietropaolo, S., Jeantet, Y. and Cho, Y. H. (2015). Sleep physiology alterations precede plethoric phenotypic changes in R6/1 Huntington's disease mice. *PLoS One* **10**, e0126972. https://doi.org/10.1371/journal.pone.0126972.

Lee, C., Parikh, V., Itsukaichi, T., Bae, K. and Edery, I. (1996). Resetting the *Drosophila* clock by photic regulation of PER and a PER-TIM complex. *Science* **271**, 1740-4. https://doi.org/10.1126/science.271.5256.1740.

References

Lee, D., Zheng, X., Shigemori, K., Krasniak, C., Bin Liu, J., Tang, C., Kavaler, J. and Ahmad, S. T. (2019). Expression of mutant CHMP2B linked to neurodegeneration in humans disrupts circadian rhythms in *Drosophila*. *FASEB Bioadv* **1**, 511-520. https://doi.org/10.1096/fba.2019-00042.

Lee, J., Moulik, M., Fang, Z., Saha, P., Zou, F., Xu, Y., Nelson, D. L., Ma, K., Moore, D. D. and Yechoor, V. K. (2013). Bmal1 and β-cell clock are required for adaptation to circadian disruption, and their loss of function leads to oxidative stress-induced β-cell failure in mice. *Mol Cell Biol* **33**, 2327-38. https://doi.org/10.1128/mcb.01421-12.

Lee, S. B., Bagley, J. A., Lee, H. Y., Jan, L. Y. and Jan, Y. N. (2011). Pathogenic polyglutamine proteins cause dendrite defects associated with specific actin cytoskeletal alterations in *Drosophila*. *Proc Natl Acad Sci U S A* **108**, 16795-800. https://doi.org/10.1073/pnas.1113573108.

Lee, W. C., Yoshihara, M. and Littleton, J. T. (2004). Cytoplasmic aggregates trap polyglutamine-containing proteins and block axonal transport in a *Drosophila* model of Huntington's disease. *Proc Natl Acad Sci U S A* **101**, 3224-9. https://doi.org/10.1073/pnas.0400243101.

Lee, Y., Field, J. M. and Sehgal, A. (2021). Circadian rhythms, disease and chronotherapy. *J Biol Rhythms* **36**, 503-531. https://doi.org/10.1177/07487304211044301.

LeGates, T. A., Fernandez, D. C. and Hattar, S. (2014). Light as a central modulator of circadian rhythms, sleep and affect. *Nat Rev Neurosci* **15**, 443-54. https://doi.org/10.1038/nrn3743.

Legleiter, J., Lotz, G. P., Miller, J., Ko, J., Ng, C., Williams, G. L., Finkbeiner, S., Patterson, P. H. and Muchowski, P. J. (2009). Monoclonal antibodies recognize distinct conformational epitopes formed by polyglutamine in a mutant huntingtin fragment. *J Biol Chem* **284**, 21647-58. https://doi.org/10.1074/jbc.M109.016923.

Leitman, J., Ulrich Hartl, F. and Lederkremer, G. Z. (2013). Soluble forms of polyQ-expanded huntingtin rather than large aggregates cause endoplasmic reticulum stress. *Nat Commun* **4**, 2753. https://doi.org/10.1038/ncomms3753.

Leng, Y., Musiek, E. S., Hu, K., Cappuccio, F. P. and Yaffe, K. (2019). Association between circadian rhythms and neurodegenerative diseases. *Lancet Neurol* **18**, 307-318. https://doi.org/10.1016/S1474-4422(18)30461-7.

Lenz, S., Karsten, P., Schulz, J. B. and Voigt, A. (2013). *Drosophila* as a screening tool to study human neurodegenerative diseases. *J Neurochem* **127**, 453-60. https://doi.org/10.1111/jnc.12446.

Lessing, D. and Bonini, N. M. (2008). Polyglutamine genes interact to modulate the severity and progression of neurodegeneration in *Drosophila*. *PLoS Biol* **6**, e29. https://doi.org/10.1371/journal.pbio.0060029.

Levitan, E. S., Lanni, F. and Shakiryanova, D. (2007). *In vivo* imaging of vesicle motion and release at the *Drosophila* neuromuscular junction. *Nat Protoc* **2**, 1117-25. https://doi.org/10.1038/nprot.2007.142.

Lewis, E. A. and Smith, G. A. (2016). Using *Drosophila* models of Huntington's disease as a translatable tool. *J Neurosci Methods* **265**, 89-98. https://doi.org/10.1016/j.jneumeth.2015.07.026.

Leyssen, M., Ayaz, D., Hébert, S. S., Reeve, S., De Strooper, B. and Hassan, B. A. (2005). Amyloid precursor protein promotes post-developmental neurite arborization in the *Drosophila* brain. *Embo j* **24**, 2944-55. https://doi.org/10.1038/sj.emboj.7600757.

References

Li, H., Li, S. H., Yu, Z. X., Shelbourne, P. and Li, X. J. (2001). Huntingtin aggregate-associated axonal degeneration is an early pathological event in Huntington's disease mice. *J Neurosci* **21**, 8473-81. https://doi.org/10.1523/jneurosci.21-21-08473.2001.

Li, J. Y., Plomann, M. and Brundin, P. (2003). Huntington's disease: A synaptopathy? *Trends Mol Med* **9**, 414-20. https://doi.org/10.1016/j.molmed.2003.08.006.

Li, L., Liu, H., Dong, P., Li, D., Legant, W. R., Grimm, J. B., Lavis, L. D., Betzig, E., Tjian, R. and Liu, Z. (2016). Real-time imaging of huntingtin aggregates diverting target search and gene transcription. *Elife* **5**. https://doi.org/10.7554/eLife.17056.

Li, L. B., Yu, Z., Teng, X. and Bonini, N. M. (2008a). RNA toxicity is a component of ataxin-3 degeneration in *Drosophila*. *Nature* **453**, 1107-11. https://doi.org/10.1038/nature06909.

Li, S., Shui, K., Zhang, Y., Lv, Y., Deng, W., Ullah, S., Zhang, L. and Xue, Y. (2017). CGDB: a database of circadian genes in eukaryotes. *Nucleic Acids Res* **45**, D397-D403. https://doi.org/10.1093/nar/gkw1028.

Li, S. H., Schilling, G., Young, W. S., 3rd, Li, X. J., Margolis, R. L., Stine, O. C., Wagster, M. V., Abbott, M. H., Franz, M. L., Ranen, N. G. et al. (1993). Huntington's disease gene (IT15) is widely expressed in human and rat tissues. *Neuron* **11**, 985-93. https://doi.org/10.1016/0896-6273(93)90127-d.

Li, W., Serpell, L. C., Carter, W. J., Rubinsztein, D. C. and Huntington, J. A. (2006). Expression and characterization of full-length human huntingtin, an elongated HEAT repeat protein. *J Biol Chem* **281**, 15916-22. https://doi.org/10.1074/jbc.M511007200.

Li, X., Sapp, E., Valencia, A., Kegel, K. B., Qin, Z. H., Alexander, J., Masso, N., Reeves, P., Ritch, J. J., Zeitlin, S. et al. (2008b). A function of huntingtin in guanine nucleotide exchange on Rab11. *Neuroreport* **19**, 1643-7. https://doi.org/10.1097/WNR.0b013e328315cd4c.

Li, X., Wang, C. E., Huang, S., Xu, X., Li, X. J., Li, H. and Li, S. (2010). Inhibiting the ubiquitin-proteasome system leads to preferential accumulation of toxic N-terminal mutant huntingtin fragments. *Hum Mol Genet* **19**, 2445-55. https://doi.org/10.1093/hmg/ddq127.

Li, X., Yang, T. and Sun, Z. (2019a). Hormesis in health and chronic diseases. *Trends Endocrinol Metab* **30**, 944-958. https://doi.org/10.1016/j.tem.2019.08.007.

Li, X. J., Li, S. H., Sharp, A. H., Nucifora, F. C., Jr., Schilling, G., Lanahan, A., Worley, P., Snyder, S. H. and Ross, C. A. (1995). A huntingtin-associated protein enriched in brain with implications for pathology. *Nature* **378**, 398-402. https://doi.org/10.1038/378398a0.

Li, Z., Karlovich, C. A., Fish, M. P., Scott, M. P. and Myers, R. M. (1999). A putative *Drosophila* homolog of the Huntington's disease gene. *Hum Mol Genet* **8**, 1807-15. https://doi.org/10.1093/hmg/8.9.1807.

Li, Z., Wang, C., Wang, Z., Zhu, C., Li, J., Sha, T., Ma, L., Gao, C., Yang, Y., Sun, Y. et al. (2019b). Allele-selective lowering of mutant HTT protein by HTT-LC3 linker compounds. *Nature* **575**, 203-209. https://doi.org/10.1038/s41586-019-1722-1.

Liang, X., Ho, M. C. W., Zhang, Y., Li, Y., Wu, M. N., Holy, T. E. and Taghert, P. H. (2019). Morning and Evening Circadian Pacemakers Independently Drive Premotor Centers via a Specific Dopamine Relay. *Neuron* **102**, 843-857 e4. https://doi.org/10.1016/j.neuron.2019.03.028.

References

Liang, X., Holy, T. E. and Taghert, P. H. (2016). Synchronous *Drosophila* circadian pacemakers display nonsynchronous Ca^{2+} rhythms in vivo. *Science* **351**, 976-81. https://doi.org/10.1126/science.aad3997.

Liang, X., Holy, T. E. and Taghert, P. H. (2017). A series of suppressive signals within the *Drosophila* circadian neural circuit generates sequential daily outputs. *Neuron* **94**, 1173-1189.e4. https://doi.org/10.1016/j.neuron.2017.05.007.

Lieberman, A. P., Shakkottai, V. G. and Albin, R. L. (2019). Polyglutamine Repeats in Neurodegenerative Diseases. *Annu Rev Pathol* **14**, 1-27. https://doi.org/10.1146/annurev-pathmechdis-012418-012857.

Liévens, J. C., Iché, M., Laval, M., Faivre-Sarrailh, C. and Birman, S. (2008). AKT-sensitive or insensitive pathways of toxicity in glial cells and neurons in *Drosophila* models of Huntington's disease. *Hum Mol Genet* **17**, 882-94. https://doi.org/10.1093/hmg/ddm360.

Lievens, J. C., Rival, T., Iche, M., Chneiweiss, H. and Birman, S. (2005). Expanded polyglutamine peptides disrupt EGF receptor signaling and glutamate transporter expression in *Drosophila*. *Hum Mol Genet* **14**, 713-24. https://doi.org/10.1093/hmg/ddi067.

Lim, A. S., Kowgier, M., Yu, L., Buchman, A. S. and Bennett, D. A. (2013). Sleep fragmentation and the risk of incident Alzheimer's disease and cognitive decline in older persons. *Sleep* **36**, 1027-1032. https://doi.org/10.5665/sleep.2802.

Lim, Y. J. and Lee, S. J. (2017). Are exosomes the vehicle for protein aggregate propagation in neurodegenerative diseases? *Acta Neuropathol Commun* **5**, 64. https://doi.org/10.1186/s40478-017-0467-z.

Lin, B., Rommens, J. M., Graham, R. K., Kalchman, M., MacDonald, H., Nasir, J., Delaney, A., Goldberg, Y. P. and Hayden, M. R. (1993). Differential 3' polyadenylation of the Huntington disease gene results in two mRNA species with variable tissue expression. *Hum Mol Genet* **2**, 1541-5. https://doi.org/10.1093/hmg/2.10.1541.

Lin, L., Park, J. W., Ramachandran, S., Zhang, Y., Tseng, Y. T., Shen, S., Waldvogel, H. J., Curtis, M. A., Faull, R. L., Troncoso, J. C. et al. (2016). Transcriptome sequencing reveals aberrant alternative splicing in Huntington's disease. *Hum Mol Genet* **25**, 3454-3466. https://doi.org/10.1093/hmg/ddw187.

Lin, M. K. and Farrer, M. J. (2014). Genetics and genomics of Parkinson's disease. *Genome Med* **6**, 48. https://doi.org/10.1186/gm566.

Lin, M. S., Liao, P. Y., Chen, H. M., Chang, C. P., Chen, S. K. and Chern, Y. (2019a). Degeneration of ipRGCs in Mouse Models of Huntington's Disease Disrupts Non-Image-Forming Behaviors Before Motor Impairment. *J Neurosci* **39**, 1505-1524. https://doi.org/10.1523/JNEUROSCI.0571-18.2018.

Lin, Y., He, H., Luo, Y., Zhu, T. and Duan, R. (2015). Inhibition of transglutaminase exacerbates polyglutamine-induced neurotoxicity by increasing the aggregation of mutant ataxin-3 in an SCA3 *Drosophila* model. *Neurotox Res* **27**, 259-67. https://doi.org/10.1007/s12640-014-9506-8.

References

Lin, Y., Stormo, G. D. and Taghert, P. H. (2004). The neuropeptide pigment-dispersing factor coordinates pacemaker interactions in the *Drosophila* circadian system. *J Neurosci* **24**, 7951-7. https://doi.org/10.1523/JNEUROSCI.2370-04.2004.

Lin, Y. H., Maaroufi, H. O., Ibrahim, E., Kucerova, L. and Zurovec, M. (2019b). Expression of human mutant Huntingtin protein in *Drosophila* hemocytes impairs immune responses. *Front Immunol* **10**, 2405. https://doi.org/10.3389/fimmu.2019.02405.

Lingor, P., Koch, J. C., Tonges, L. and Bähr, M. (2012). Axonal degeneration as a therapeutic target in the CNS. *Cell Tissue Res* **349**, 289-311. https://doi.org/10.1007/s00441-012-1362-3.

Liot, G., Zala, D., Pla, P., Mottet, G., Piel, M. and Saudou, F. (2013). Mutant huntingtin alters retrograde transport of TrkB receptors in striatal dendrites. *J Neurosci* **33**, 6298-309. https://doi.org/10.1523/jneurosci.2033-12.2013.

Liu, A. C., Welsh, D. K., Ko, C. H., Tran, H. G., Zhang, E. E., Priest, A. A., Buhr, E. D., Singer, O., Meeker, K., Verma, I. M. et al. (2007). Intercellular coupling confers robustness against mutations in the SCN circadian clock network. *Cell* **129**, 605-16. https://doi.org/10.1016/j.cell.2007.02.047.

Liu, J. P. and Zeitlin, S. O. (2017). Is Huntingtin Dispensable in the Adult Brain? *J Huntingtons Dis* **6**, 1-17. https://doi.org/10.3233/JHD-170235.

Liu, K. Y., Shyu, Y. C., Barbaro, B. A., Lin, Y. T., Chern, Y., Thompson, L. M., James Shen, C. K. and Marsh, J. L. (2015a). Disruption of the nuclear membrane by perinuclear inclusions of mutant huntingtin causes cell-cycle re-entry and striatal cell death in mouse and cell models of Huntington's disease. *Hum Mol Genet* **24**, 1602-16. https://doi.org/10.1093/hmg/ddu574.

Liu, T., Mahesh, G., Houl, J. H. and Hardin, P. E. (2015b). Circadian activators are expressed days before they initiate clock function in late pacemaker neurons from *Drosophila*. *J Neurosci* **35**, 8662-71. https://doi.org/10.1523/JNEUROSCI.0250-15.2015.

Liu, Y., Garceau, N. Y., Loros, J. J. and Dunlap, J. C. (1997a). Thermally regulated translational control of FRQ mediates aspects of temperature responses in the neurospora circadian clock. *Cell* **89**, 477-86. https://doi.org/10.1016/s0092-8674(00)80228-7.

Liu, Y., Hu, W., Murakawa, Y., Yin, J., Wang, G., Landthaler, M. and Yan, J. (2013). Cold-induced RNA-binding proteins regulate circadian gene expression by controlling alternative polyadenylation. *Sci Rep* **3**, 2054. https://doi.org/10.1038/srep02054.

Liu, Y., Yan, T., Chu, J. M., Chen, Y., Dunnett, S., Ho, Y. S., Wong, G. T. and Chang, R. C. (2019a). The beneficial effects of physical exercise in the brain and related pathophysiological mechanisms in neurodegenerative diseases. *Lab Invest* **99**, 943-957. https://doi.org/10.1038/s41374-019-0232-y.

Liu, Y. F., Deth, R. C. and Devys, D. (1997b). SH3 domain-dependent association of huntingtin with epidermal growth factor receptor signaling complexes. *J Biol Chem* **272**, 8121-4. https://doi.org/10.1074/jbc.272.13.8121.

Liu, Y. L., Gong, S. Y., Xia, S. T., Wang, Y. L., Peng, H., Shen, Y. and Liu, C. F. (2020). Light therapy: A new option for neurodegenerative diseases. *Chin Med J (Engl)* **134**, 634-645. https://doi.org/10.1097/cm9.0000000000001301.

References

Liu, Z., Tabuloc, C. A., Xue, Y., Cai, Y., McIntire, P., Niu, Y., Lam, V. H., Chiu, J. C. and Zhang, Y. (2019b). Splice variants of DOMINO control *Drosophila* circadian behavior and pacemaker neuron maintenance. *PLoS Genet* **15**, e1008474. https://doi.org/10.1371/journal.pgen.1008474.

Loeschcke, V. and Sørensen, J. (2005). Acclimation, heat shock and hardening—a response from evolutionary biology. *J Therm Biol* **3**, 255-257. https://doi.org/10.1016/j.jtherbio.2004.12.005.

Logan, R. W. and McClung, C. A. (2019). Rhythms of life: Circadian disruption and brain disorders across the lifespan. *Nat Rev Neurosci* **20**, 49-65. https://doi.org/10.1016/j.jtherbio.2004.12.00510.1038/s41583-018-0088-y.

Logan, R. W., Williams, W. P., 3rd and McClung, C. A. (2014). Circadian rhythms and addiction: Mechanistic insights and future directions. *Behav Neurosci* **128**, 387-412. https://doi.org/10.1037/a0036268.

Loh, D. H., Kudo, T., Truong, D., Wu, Y. and Colwell, C. S. (2013). The Q175 mouse model of Huntington's disease shows gene dosage- and age-related decline in circadian rhythms of activity and sleep. *PLoS One* **8**, e69993. https://doi.org/10.1371/journal.pone.0069993.

Loli, D. and Bicudo, J. E. (2005). Control and regulatory mechanisms associated with thermogenesis in flying insects and birds. *Biosci Rep* **25**, 149-80. https://doi.org/10.1007/s10540-005-2883-8.

Lone, S. R., Ilangovan, V., Murugan, M. and Sharma, V. K. (2010). Circadian resonance in the development of two sympatric species of camponotus ants. *J Insect Physiol* **56**, 1611-6. https://doi.org/10.1016/j.jinsphys.2010.05.023.

Long, D. M., Blake, M. R., Dutta, S., Holbrook, S. D., Kotwica-Rolinska, J., Kretzschmar, D. and Giebultowicz, J. M. (2014a). Relationships between the circadian system and Alzheimer's disease-like symptoms in *Drosophila*. *PLoS One* **9**, e106068. https://doi.org/10.1371/journal.pone.0106068.

Long, Z., Tang, B. and Jiang, H. (2014b). Alleviating neurodegeneration in *Drosophila* models of PolyQ diseases. *Cerebellum Ataxias* **1**, 9. https://doi.org/10.1186/2053-8871-1-9.

Lontay, B., Kiss, A., Virág, L. and Tar, K. (2020). How do post-translational modifications influence the pathomechanistic landscape of Huntington's disease? A comprehensive review. *Int J Mol Sci* **21**. https://doi.org/10.3390/ijms21124282.

Loprinzi, P. D., Herod, S. M., Cardinal, B. J. and Noakes, T. D. (2013). Physical activity and the brain: a review of this dynamic, bi-directional relationship. *Brain Res* **1539**, 95-104. https://doi.org/10.1016/j.brainres.2013.10.004.

Lorber, C., Leleux, S., Stanewsky, R. and Lamaze, A. (2022). Light triggers a network switch between circadian morning and evening oscillators controlling behaviour during daily temperature cycles. *PLoS Genet* **18**, e1010487. https://doi.org/10.1371/journal.pgen.1010487.

Lotz, G. P., Legleiter, J., Aron, R., Mitchell, E. J., Huang, S. Y., Ng, C., Glabe, C., Thompson, L. M. and Muchowski, P. J. (2010). Hsp70 and Hsp40 functionally interact with soluble mutant huntingtin oligomers in a classic ATP-dependent reaction cycle. *J Biol Chem* **285**, 38183-93. https://doi.org/10.1074/jbc.M110.160218.

References

Low, K. H., Lim, C., Ko, H. W. and Edery, I. (2008). Natural variation in the splice site strength of a clock gene and species-specific thermal adaptation. *Neuron* **60**, 1054-67. https://doi.org/10.1016/j.neuron.2008.10.048.

Lowrey, P. L. and Takahashi, J. S. (2004). Mammalian circadian biology: Elucidating genome-wide levels of temporal organization. *Annu Rev Genomics Hum Genet* **5**, 407-41. https://doi.org/10.1146/annurev.genom.5.061903.175925.

Lowrey, P. L. and Takahashi, J. S. (2011). Genetics of circadian rhythms in mammalian model organisms. *Adv Genet* **74**, 175-230. https://doi.org/10.1016/b978-0-12-387690-4.00006-4.

Lowry, C., Flux, M. and Raison, C. (2018). Whole-body heating: An emerging therapeutic approach to treatment of major depressive disorder. *Focus (Am Psychiatr Publ)* **16**, 259-265. https://doi.org/10.1176/appi.focus.20180009.

Lu, B., Al-Ramahi, I., Valencia, A., Wang, Q., Berenshteyn, F., Yang, H., Gallego-Flores, T., Ichcho, S., Lacoste, A., Hild, M. et al. (2013). Identification of NUB1 as a suppressor of mutant Huntington toxicity via enhanced protein clearance. *Nat Neurosci* **16**, 562-70. https://doi.org/10.1038/nn.3367.

Lu, B. and Vogel, H. (2009). *Drosophila* models of neurodegenerative diseases. *Annu Rev Pathol* **4**, 315-42. https://doi.org/10.1146/annurev.pathol.3.121806.151529.

Luan, H., Diao, F., Scott, R. L. and White, B. H. (2020). The *Drosophila* split Gal4 system for neural circuit mapping. *Front Neural Circuits* **14**, 603397. https://doi.org/10.3389/fncir.2020.603397.

Lucassen, E. A., Coomans, C. P., van Putten, M., de Kreij, S. R., van Genugten, J. H., Sutorius, R. P., de Rooij, K. E., van der Velde, M., Verhoeve, S. L., Smit, J. W. et al. (2016). Environmental 24-hr cycles are essential for health. *Curr Biol* **26**, 1843-53. https://doi.org/10.1016/j.cub.2016.05.038.

Lüders, J., Demand, J. and Höhfeld, J. (2000). The ubiquitin-related BAG-1 provides a link between the molecular chaperones Hsc70/Hsp70 and the proteasome. *J Biol Chem* **275**, 4613-7. https://doi.org/10.1074/jbc.275.7.4613.

Lunkes, A. and Mandel, J. L. (1998). A cellular model that recapitulates major pathogenic steps of Huntington's disease. *Hum Mol Genet* **7**, 1355-61. https://doi.org/10.1093/hmg/7.9.1355.

Luo, W., Chen, W. F., Yue, Z., Chen, D., Sowcik, M., Sehgal, A. and Zheng, X. (2012). Old flies have a robust central oscillator but weaker behavioral rhythms that can be improved by genetic and environmental manipulations. *Aging Cell* **11**, 428-38. https://doi.org/10.1111/j.1474-9726.2012.00800.x.

Luthi-Carter, R., Hanson, S. A., Strand, A. D., Bergstrom, D. A., Chun, W., Peters, N. L., Woods, A. M., Chan, E. Y., Kooperberg, C., Krainc, D. et al. (2002). Dysregulation of gene expression in the R6/2 model of polyglutamine disease: parallel changes in muscle and brain. *Hum Mol Genet* **11**, 1911-26. https://doi.org/10.1093/hmg/11.17.1911.

Luthi-Carter, R., Strand, A., Peters, N. L., Solano, S. M., Hollingsworth, Z. R., Menon, A. S., Frey, A. S., Spektor, B. S., Penney, E. B., Schilling, G. et al. (2000). Decreased expression of striatal signaling genes in a mouse model of Huntington's disease. *Hum Mol Genet* **9**, 1259-71. https://doi.org/10.1093/hmg/9.9.1259.

References

Ma, C. S., Ma, G. and Pincebourde, S. (2021a). Survive a warming climate: Insect responses to extreme high temperatures. *Annu Rev Entomol* **66**, 163-184. https://doi.org/10.1146/annurev-ento-041520-074454.

Ma, D., Przybylski, D., Abruzzi, K. C., Schlichting, M., Li, Q., Long, X. and Rosbash, M. (2021b). A transcriptomic taxonomy of *Drosophila* circadian neurons around the clock. *Elife* **10**. https://doi.org/10.7554/eLife.63056.

Ma, Y. and Eidelberg, D. (2007). Functional imaging of cerebral blood flow and glucose metabolism in Parkinson's disease and Huntington's disease. *Mol Imaging Biol* **9**, 223-33. https://doi.org/10.1007/s11307-007-0085-4.

Mabuchi, I., Shimada, N., Sato, S., Ienaga, K., Inami, S. and Sakai, T. (2016). Mushroom body signaling is required for locomotor activity rhythms in *Drosophila*. *Neurosci Res* **111**, 25-33. https://doi.org/10.1016/j.neures.2016.04.005.

MacDonald, M. E., Barnes, G., Srinidhi, J., Duyao, M. P., Ambrose, C. M., Myers, R. H., Gray, J., Conneally, P. M., Young, A., Penney, J. et al. (1993). Gametic but not somatic instability of CAG repeat length in Huntington's disease. *J Med Genet* **30**, 982-6. https://doi.org/10.1136/jmg.30.12.982.

Maciotta, S., Meregalli, M. and Torrente, Y. (2013). The involvement of microRNAs in neurodegenerative diseases. *Front Cell Neurosci* **7**, 265. https://doi.org/10.3389/fncel.2013.00265.

Mackay, J. P., Nassrallah, W. B. and Raymond, L. A. (2018). Cause or compensation?-Altered neuronal Ca(2+) handling in Huntington's disease. *CNS Neurosci Ther* **24**, 301-310. https://doi.org/10.1111/cns.12817.

MacLean, H. J., Kristensen, T. N., Overgaard, J., Sørensen, J. G. and Bahrndorff, S. (2017). Acclimation responses to short-term temperature treatments during early life stages causes long lasting changes in spontaneous activity of adult *Drosophila melanogaster*. *Physiological Entomology* **42**, 404-411. https://doi.org/10.1111/phen.12212.

Madden, C. J. and Morrison, S. F. (2019). Central nervous system circuits that control body temperature. *Neurosci Lett* **696**, 225-232. https://doi.org/10.1016/j.neulet.2018.11.027.

Magalhães Fde, C., Amorim, F. T., Passos, R. L., Fonseca, M. A., Oliveira, K. P., Lima, M. R., Guimarães, J. B., Ferreira-Júnior, J. B., Martini, A. R., Lima, N. R. et al. (2010). Heat and exercise acclimation increases intracellular levels of Hsp72 and inhibits exercise-induced increase in intracellular and plasma Hsp72 in humans. *Cell Stress Chaperones* **15**, 885-95. https://doi.org/10.1007/s12192-010-0197-7.

Magnoni, R., Palmfeldt, J., Christensen, J. H., Sand, M., Maltecca, F., Corydon, T. J., West, M., Casari, G. and Bross, P. (2013). Late onset motoneuron disorder caused by mitochondrial Hsp60 chaperone deficiency in mice. *Neurobiol Dis* **54**, 12-23. https://doi.org/10.1016/j.nbd.2013.02.012.

Maheshwari, M., Bhutani, S., Das, A., Mukherjee, R., Sharma, A., Kino, Y., Nukina, N. and Jana, N. R. (2014). Dexamethasone induces heat shock response and slows down disease progression in mouse and fly models of Huntington's disease. *Hum Mol Genet* **23**, 2737-51. https://doi.org/10.1093/hmg/ddt667.

References

Maiuri, T., Mocle, A. J., Hung, C. L., Xia, J., van Roon-Mom, W. M. and Truant, R. (2017). Huntingtin is a scaffolding protein in the ATM oxidative DNA damage response complex. *Hum Mol Genet* **26**, 395-406. https://doi.org/10.1093/hmg/ddw395.

Maiuri, T., Woloshansky, T., Xia, J. and Truant, R. (2013). The huntingtin N17 domain is a multifunctional CRM1 and Ran-dependent nuclear and cilial export signal. *Hum Mol Genet* **22**, 1383-94. https://doi.org/10.1093/hmg/dds554.

Majercak, J., Chen, W. F. and Edery, I. (2004). Splicing of the period gene 3'-terminal intron is regulated by light, circadian clock factors, and phospholipase C. *Mol Cell Biol* **24**, 3359-72. https://doi.org/10.1128/mcb.24.8.3359-3372.2004.

Majercak, J., Sidote, D., Hardin, P. E. and Edery, I. (1999). How a circadian clock adapts to seasonal decreases in temperature and day length. *Neuron* **24**, 219-30. https://doi.org/10.1016/s0896-6273(00)80834-x.

Maley, M. J., Hunt, A. P., Stewart, I. B., Faulkner, S. H. and Minett, G. M. (2019). Passive heating and glycaemic control in non-diabetic and diabetic individuals: A systematic review and meta-analysis. *PLoS One* **14**, e0214223. https://doi.org/10.1371/journal.pone.0214223.

Mallik, M. and Lakhotia, S. C. (2009). RNAi for the large non-coding hsromega transcripts suppresses polyglutamine pathogenesis in *Drosophila* models. *RNA Biol* **6**, 464-78. https://doi.org/10.4161/rna.6.4.9268.

Malpel, S., Klarsfeld, A. and Rouyer, F. (2002). Larval optic nerve and adult extra-retinal photoreceptors sequentially associate with clock neurons during *Drosophila* brain development. *Development* **129**, 1443-53. https://doi.org/10.1242/dev.129.6.1443.

Malpel, S., Klarsfeld, A. and Rouyer, F. (2004). Circadian synchronization and rhythmicity in larval photoperception-defective mutants of *Drosophila*. *J Biol Rhythms* **19**, 10-21. https://doi.org/10.1177/0748730403260621.

Mane, N. R., Gajare, K. A. and Deshmukh, A. A. (2018). Mild heat stress induces hormetic effects in protecting the primary culture of mouse prefrontal cerebrocortical neurons from neuropathological alterations. *IBRO Rep* **5**, 110-115. https://doi.org/10.1016/j.ibror.2018.11.002.

Mane, N. R., Gajare, K. A. and Deshmukh, A. A. (2020). Hormetic effects of mild heat stress on the primary culture of mouse prefrontal cerebrocortical neurons. *The Journal of Basic and Applied Zoology* **81**, 1-6. https://doi.org/10.1186/s41936-020-00158-y.

Manenti, T., Loeschcke, V. and Sørensen, J. G. (2018). Constitutive up-regulation of Turandot genes rather than changes in acclimation ability is associated with the evolutionary adaptation to temperature fluctuations in *Drosophila* simulans. *J Insect Physiol* **104**, 40-47. https://doi.org/10.1016/j.jinsphys.2017.11.008.

Mangiarini, L., Sathasivam, K., Seller, M., Cozens, B., Harper, A., Hetherington, C., Lawton, M., Trottier, Y., Lehrach, H., Davies, S. W. et al. (1996). Exon 1 of the HD gene with an expanded CAG repeat is sufficient to cause a progressive neurological phenotype in transgenic mice. *Cell* **87**, 493-506. https://doi.org/10.1016/s0092-8674(00)81369-0.

Mannini, B. and Chiti, F. (2017). Chaperones as suppressors of protein misfolded oligomer toxicity. *Front Mol Neurosci* **10**. https://doi.org/10.3389/fnmol.2017.00098.

References

Månsson, C., Kakkar, V., Monsellier, E., Sourigues, Y., Härmark, J., Kampinga, H. H., Melki, R. and Emanuelsson, C. (2013). DNAJB6 is a peptide-binding chaperone which can suppress amyloid fibrillation of polyglutamine peptides at substoichiometric molar ratios. *Cell Stress and Chaperones* **19**, 227-239. https://doi.org/10.1007/s12192-013-0448-5.

Marder, K., Zhao, H., Myers, R. H., Cudkowicz, M., Kayson, E., Kieburtz, K., Orme, C., Paulsen, J., Penney, J. B., Jr., Siemers, E. et al. (2000). Rate of functional decline in Huntington's disease. Huntington study group. *Neurology* **54**, 452-8. https://doi.org/10.1212/wnl.54.2.452.

Marek, K. W., Ng, N., Fetter, R., Smolik, S., Goodman, C. S. and Davis, G. W. (2000). A Genetic Analysis of Synaptic Development. *Neuron* **25**, 537-547. https://doi.org/10.1016/s0896-6273(00)81058-2.

Margulis, B., Tsimokha, A., Zubova, S. and Guzhova, I. (2020). Molecular chaperones and proteolytic machineries regulate protein homeostasis in aging cells. *Cells* **9**. https://doi.org/10.3390/cells9051308.

Margulis, B. A., Vigont, V., Lazarev, V. F., Kaznacheyeva, E. V. and Guzhova, I. V. (2013). Pharmacological protein targets in polyglutamine diseases: mutant polypeptides and their interactors. *FEBS Lett* **587**, 1997-2007. https://doi.org/10.1016/j.febslet.2013.05.022.

Margulis, J. and Finkbeiner, S. (2014). Proteostasis in striatal cells and selective neurodegeneration in Huntington's disease. *Front Cell Neurosci* **8**, 218. https://doi.org/10.3389/fncel.2014.00218.

Marquilly, C., Busto, G. U., Leger, B. S., Boulanger, A., Giniger, E., Walker, J. A., Fradkin, L. G. and Dura, J. M. (2021). Htt is a repressor of Abl activity required for APP-induced axonal growth. *PLoS Genet* **17**, e1009287. https://doi.org/10.1371/journal.pgen.1009287.

Marrus, S. B., Zeng, H. and Rosbash, M. (1996). Effect of constant light and circadian entrainment of *per*^{S} flies: evidence for light-mediated delay of the negative feedback loop in *Drosophila*. *Embo j* **15**, 6877-86. https://doi.org/10.1002/j.1460-2075.1996.tb01080.x.

Marsh, J. L. and Thompson, L. M. (2004). Can flies help humans treat neurodegenerative diseases? *Bioessays* **26**, 485-96. https://doi.org/10.1002/bies.20029.

Martin Anduaga, A., Evantal, N., Patop, I. L., Bartok, O., Weiss, R. and Kadener, S. (2019). Thermosensitive alternative splicing senses and mediates temperature adaptation in *Drosophila*. *Elife* **8**. https://doi.org/10.7554/eLife.44642.

Martin, D. D., Heit, R. J., Yap, M. C., Davidson, M. W., Hayden, M. R. and Berthiaume, L. G. (2014). Identification of a post-translationally myristoylated autophagy-inducing domain released by caspase cleavage of huntingtin. *Hum Mol Genet* **23**, 3166-79. https://doi.org/10.1093/hmg/ddu027.

Martin, D. D., Ladha, S., Ehrnhoefer, D. E. and Hayden, M. R. (2015). Autophagy in Huntington disease and huntingtin in autophagy. *Trends Neurosci* **38**, 26-35. https://doi.org/10.1016/j.tins.2014.09.003.

Martin, E., Heidari, R., Monnier, V. and Tricoire, H. (2021). Genetic screen in adult *Drosophila* reveals that dCBP depletion in glial cells mitigates Huntington disease pathology through a Foxo-dependent pathway. *Int J Mol Sci* **22**. https://doi.org/10.3390/ijms22083884.

References

Martín, F. and Alcorta, E. (2017). Novel genetic approaches to behavior in *Drosophila*. *J Neurogenet* **31**, 288-299. https://doi.org/10.1080/01677063.2017.1395875.

Martinez-Vicente, M., Talloczy, Z., Wong, E., Tang, G., Koga, H., Kaushik, S., de Vries, R., Arias, E., Harris, S., Sulzer, D. et al. (2010). Cargo recognition failure is responsible for inefficient autophagy in Huntington's disease. *Nat Neurosci* **13**, 567-76. https://doi.org/10.1038/nn.2528.

Martino, J. K., Freelance, C. B. and Willis, G. L. (2018). The effect of light exposure on insomnia and nocturnal movement in Parkinson's disease: An open label, retrospective, longitudinal study. *Sleep Med* **44**, 24-31. https://doi.org/10.1016/j.sleep.2018.01.001.

Masnata, M., Sciacca, G., Maxan, A., Bousset, L., Denis, H. L., Lauruol, F., David, L., Saint-Pierre, M., Kordower, J. H., Melki, R. et al. (2019). Demonstration of prion-like properties of mutant huntingtin fibrils in both in vitro and in vivo paradigms. *Acta Neuropathol* **137**, 981-1001. https://doi.org/10.1007/s00401-019-01973-6.

Mason, R. P., Casu, M., Butler, N., Breda, C., Campesan, S., Clapp, J., Green, E. W., Dhulkhed, D., Kyriacou, C. P. and Giorgini, F. (2013). Glutathione peroxidase activity is neuroprotective in models of Huntington's disease. *Nat Genet* **45**, 1249-54. https://doi.org/10.1038/ng.2732.

Matsumoto, A., Matsumoto, N., Harui, Y., Sakamoto, M. and Tomioka, K. (1998). Light and temperature cooperate to regulate the circadian locomotor rhythm of wild type and period mutants of *Drosophila melanogaster*. *J Insect Physiol* **44**, 587-596. https://doi.org/10.1016/s0022-1910(98)00046-8.

Matsumoto, N., Uwozumi, K. and Tomioka, K. (1997). Light cycles given during development affect freerunning period of circadian locomotor rhythm of period mutants in *Drosophila melanogaster*. *J Insect Physiol* **43**, 297-305. https://doi.org/10.1016/s0022-1910(96)00075-3.

Mattoo, R. U. and Goloubinoff, P. (2014). Molecular chaperones are nanomachines that catalytically unfold misfolded and alternatively folded proteins. *Cell Mol Life Sci* **71**, 3311-25. https://doi.org/10.1007/s00018-014-1627-y.

Mattson, M. P. (2008). Hormesis defined. *Ageing Res Rev* **7**, 1-7. https://doi.org/10.1016/j.arr.2007.08.007.

Mattson, M. P., Chan, S. L. and Duan, W. (2002). Modification of brain aging and neurodegenerative disorders by genes, diet, and behavior. *Physiol Rev* **82**, 637-72. https://doi.org/10.1152/physrev.00004.2002.

Mayer, M. P. and Gierasch, L. M. (2019). Recent advances in the structural and mechanistic aspects of Hsp70 molecular chaperones. *J Biol Chem* **294**, 2085-2097. https://doi.org/10.1074/jbc.REV118.002810.

Maynard, C. J., Böttcher, C., Ortega, Z., Smith, R., Florea, B. I., Díaz-Hernández, M., Brundin, P., Overkleeft, H. S., Li, J. Y., Lucas, J. J. et al. (2009). Accumulation of ubiquitin conjugates in a polyglutamine disease model occurs without global ubiquitin/proteasome system impairment. *Proc Natl Acad Sci U S A* **106**, 13986-91. https://doi.org/10.1073/pnas.0906463106.

Mayo, J. C., Sainz, R. M., Tan, D. X., Antolín, I., Rodríguez, C. and Reiter, R. J. (2005). Melatonin and Parkinson's disease. *Endocrine* **27**, 169-78. https://doi.org/10.1385/endo:27:2:169.

Maywood, E. S., Fraenkel, E., McAllister, C. J., Wood, N., Reddy, A. B., Hastings, M. H. and Morton, A. J. (2010). Disruption of peripheral circadian timekeeping in a mouse model of Huntington's

disease and its restoration by temporally scheduled feeding. *J Neurosci* **30**, 10199-204. https://doi.org/10.1523/jneurosci.1694-10.2010.

McBride, S. M., Choi, C. H., Schoenfeld, B. P., Bell, A. J., Liebelt, D. A., Ferreiro, D., Choi, R. J., Hinchey, P., Kollaros, M., Terlizzi, A. M. et al. (2010). Pharmacological and genetic reversal of age-dependent cognitive deficits attributable to decreased presenilin function. *J Neurosci* **30**, 9510-22. https://doi.org/10.1523/jneurosci.1017-10.2010.

McCampbell, A., Taylor, J. P., Taye, A. A., Robitschek, J., Li, M., Walcott, J., Merry, D., Chai, Y., Paulson, H., Sobue, G. et al. (2000). CREB-binding protein sequestration by expanded polyglutamine. *Hum Mol Genet* **9**, 2197-202. https://doi.org/10.1093/hmg/9.14.2197.

McClung, J. P., Hasday, J. D., He, J. R., Montain, S. J., Cheuvront, S. N., Sawka, M. N. and Singh, I. S. (2008). Exercise-heat acclimation in humans alters baseline levels and ex vivo heat inducibility of HSP72 and HSP90 in peripheral blood mononuclear cells. *Am J Physiol Regul Integr Comp Physiol* **294**, R185-91. https://doi.org/10.1152/ajpregu.00532.2007.

McClure, C. D., Zhong, W., Hunt, V. L., Chapman, F. M., Hill, F. V. and Priest, N. K. (2014). Hormesis results in trade-offs with immunity. *Evolution* **68**, 2225-33. https://doi.org/10.1111/evo.12453.

McConoughey, S. J., Basso, M., Niatsetskaya, Z. V., Sleiman, S. F., Smirnova, N. A., Langley, B. C., Mahishi, L., Cooper, A. J., Antonyak, M. A., Cerione, R. A. et al. (2010). Inhibition of transglutaminase 2 mitigates transcriptional dysregulation in models of Huntington disease. *EMBO Mol Med* **2**, 349-70. https://doi.org/10.1002/emmm.201000084.

McCormick, J. J., Dokladny, K., Moseley, P. L. and Kenny, G. P. (2021). Autophagy and heat: a potential role for heat therapy to improve autophagic function in health and disease. *J Appl Physiol (1985)* **130**, 1-9. https://doi.org/10.1152/japplphysiol.00542.2020.

McDonald, J. H. (2014). Handbook of Biological Statistics. Baltimore, Maryland: Sparky House Publishing.

McFarland, K. N., Das, S., Sun, T. T., Leyfer, D., Xia, E., Sangrey, G. R., Kuhn, A., Luthi-Carter, R., Clark, T. W., Sadri-Vakili, G. et al. (2012). Genome-wide histone acetylation is altered in a transgenic mouse model of Huntington's disease. *PLoS One* **7**, e41423. https://doi.org/10.1371/journal.pone.0041423.

McGuire, J. R., Rong, J., Li, S. H. and Li, X. J. (2006). Interaction of huntingtin-associated protein-1 with kinesin light chain: Implications in intracellular trafficking in neurons. *J Biol Chem* **281**, 3552-9. https://doi.org/10.1074/jbc.M509806200.

McGurk, L., Berson, A. and Bonini, N. M. (2015). *Drosophila* as an in vivo model for human neurodegenerative disease. *Genetics* **201**, 377-402. https://doi.org/10.1534/genetics.115.179457.

McKee, C. A., Lee, J., Cai, Y., Saito, T., Saido, T. and Musiek, E. S. (2022). Astrocytes deficient in circadian clock gene Bmal1 show enhanced activation responses to amyloid-beta pathology without changing plaque burden. *Sci Rep* **12**, 1796. https://doi.org/10.1038/s41598-022-05862-z.

McKinstry, S. U., Karadeniz, Y. B., Worthington, A. K., Hayrapetyan, V. Y., Ozlu, M. I., Serafin-Molina, K., Risher, W. C., Ustunkaya, T., Dragatsis, I., Zeitlin, S. et al. (2014). Huntingtin is required for normal excitatory synapse development in cortical and striatal circuits. *J Neurosci* **34**, 9455-72. https://doi.org/10.1523/jneurosci.4699-13.2014.

References

McLear, J. A., Lebrecht, D., Messer, A. and Wolfgang, W. J. (2008). Combinational approach of intrabody with enhanced Hsp70 expression addresses multiple pathologies in a fly model of Huntington's disease. *FASEB J* **22**, 2003-11. https://doi.org/10.1096/fj.07-099689.

McMurray, C. T. (2010). Mechanisms of trinucleotide repeat instability during human development. *Nat Rev Genet* **11**, 786-99. https://doi.org/10.1038/nrg2828.

McNeil, S. M., Novelletto, A., Srinidhi, J., Barnes, G., Kornbluth, I., Altherr, M. R., Wasmuth, J. J., Gusella, J. F., MacDonald, M. E. and Myers, R. H. (1997). Reduced penetrance of the Huntington's disease mutation. *Hum Mol Genet* **6**, 775-9. https://doi.org/10.1093/hmg/6.5.775.

Mealer, R. G., Murray, A. J., Shahani, N., Subramaniam, S. and Snyder, S. H. (2014). Rhes, a striatal-selective protein implicated in Huntington disease, binds beclin-1 and activates autophagy. *J Biol Chem* **289**, 3547-54. https://doi.org/10.1074/jbc.M113.536912.

Means, J. C., Venkatesan, A., Gerdes, B., Fan, J. Y., Bjes, E. S. and Price, J. L. (2015). *Drosophila* spaghetti and doubletime link the circadian clock and light to caspases, apoptosis and tauopathy. *PLoS Genet* **11**, e1005171. https://doi.org/10.1371/journal.pgen.1005171.

Mehler, M. F., Petronglo, J. R., Arteaga-Bracho, E. E., Gulinello, M. E., Winchester, M. L., Pichamoorthy, N., Young, S. K., DeJesus, C. D., Ishtiaq, H., Gokhan, S. et al. (2019). Loss-of-huntingtin in medial and lateral ganglionic lineages differentially disrupts regional interneuron and projection neuron subtypes and promotes Huntington's disease-associated behavioral, cellular, and pathological hallmarks. *J Neurosci* **39**, 1892-1909. https://doi.org/10.1523/jneurosci.2443-18.2018.

Mehra, A., Baker, C. L., Loros, J. J. and Dunlap, J. C. (2009). Post-translational modifications in circadian rhythms. *Trends Biochem Sci* **34**, 483-90. https://doi.org/10.1016/j.tibs.2009.06.006.

Melentijevic, I., Toth, M. L., Arnold, M. L., Guasp, R. J., Harinath, G., Nguyen, K. C., Taub, D., Parker, J. A., Neri, C., Gabel, C. V. et al. (2017). *C. elegans* neurons jettison protein aggregates and mitochondria under neurotoxic stress. *Nature* **542**, 367-371. https://doi.org/10.1038/nature21362.

Melkani, G. C., Trujillo, A. S., Ramos, R., Bodmer, R., Bernstein, S. I. and Ocorr, K. (2013). Huntington's disease induced cardiac amyloidosis is reversed by modulating protein folding and oxidative stress pathways in the *Drosophila* heart. *PLoS Genet* **9**, e1004024. https://doi.org/10.1371/journal.pgen.1004024.

Mendillo, Marc L., Santagata, S., Koeva, M., Bell, George W., Hu, R., Tamimi, Rulla M., Fraenkel, E., Ince, Tan A., Whitesell, L. and Lindquist, S. (2012). HSF1 drives a transcriptional program distinct from heat shock to support highly malignant human cancers. *Cell* **150**, 549-562. https://doi.org/10.1016/j.cell.2012.06.031.

Mendonça, D. C. B., Fernandes, D. R., Hernandez, S. S., Soares, F. D. G., Figueiredo, K. and Coelho, F. G. M. (2021). Physical exercise is effective for neuropsychiatric symptoms in Alzheimer's disease: A systematic review. *Arq Neuropsiquiatr* **79**, 447-456. https://doi.org/10.1590/0004-282x-anp-2020-0284.

Mendoza-Viveros, L., Bouchard-Cannon, P., Hegazi, S., Cheng, A. H., Pastore, S. and Cheng, H. M. (2017). Molecular modulators of the circadian clock: Lessons from flies and mice. *Cell Mol Life Sci* **74**, 1035-1059. https://doi.org/10.1007/s00018-016-2378-8.

References

Menegazzi, P., Yoshii, T. and Helfrich-Forster, C. (2012a). Laboratory versus nature: the two sides of the *Drosophila* circadian clock. *J Biol Rhythms* **27**, 433-42. https://doi.org/10.1177/0748730412463181.

Menegazzi, P., Yoshii, T. and Helfrich-Förster, C. (2012b). Laboratory versus nature: the two sides of the *Drosophila* circadian clock. *J Biol Rhythms* **27**, 433-42. https://doi.org/10.1177/0748730412463181.

Menzies, F. M., Fleming, A., Caricasole, A., Bento, C. F., Andrews, S. P., Ashkenazi, A., Füllgrabe, J., Jackson, A., Jimenez Sanchez, M., Karabiyik, C. et al. (2017). Autophagy and neurodegeneration: Pathogenic mechanisms and therapeutic opportunities. *Neuron* **93**, 1015-1034. https://doi.org/10.1016/j.neuron.2017.01.022.

Menzies, F. M., Garcia-Arencibia, M., Imarisio, S., O'Sullivan, N. C., Ricketts, T., Kent, B. A., Rao, M. V., Lam, W., Green-Thompson, Z. W., Nixon, R. A. et al. (2015). Calpain inhibition mediates autophagy-dependent protection against polyglutamine toxicity. *Cell Death Differ* **22**, 433-44. https://doi.org/10.1038/cdd.2014.151.

Menzies, F. M., Hourez, R., Imarisio, S., Raspe, M., Sadiq, O., Chandraratna, D., O'Kane, C., Rock, K. L., Reits, E., Goldberg, A. L. et al. (2010). Puromycin-sensitive aminopeptidase protects against aggregation-prone proteins via autophagy. *Hum Mol Genet* **19**, 4573-86. https://doi.org/10.1093/hmg/ddq385.

Merienne, K., Helmlinger, D., Perkin, G. R., Devys, D. and Trottier, Y. (2003a). Polyglutamine expansion induces a protein-damaging stress connecting heat shock protein 70 to the JNK pathway. *J Biol Chem* **278**, 16957-67. https://doi.org/10.1074/jbc.M212049200.

Merienne, K., Helmlinger, D., Perkin, G. R., Devys, D. and Trottier, Y. (2003b). Polyglutamine expansion induces a protein-damaging stress connecting heat shock protein 70 to the JNK Pathway. *Journal of Biological Chemistry* **278**, 16957-16967. 10.1074/jbc.M212049200.

Mertens, I., Vandingenen, A., Johnson, E. C., Shafer, O. T., Li, W., Trigg, J. S., De Loof, A., Schoofs, L. and Taghert, P. H. (2005). PDF receptor signaling in *Drosophila* contributes to both circadian and geotactic behaviors. *Neuron* **48**, 213-9. https://doi.org/10.1016/j.neuron.2005.09.009.

Metaxakis, A., Ploumi, C. and Tavernarakis, N. (2018). Autophagy in age-associated neurodegeneration. *Cells* **7**. https://doi.org/10.3390/cells7050037.

Metzler, M., Gan, L., Mazarei, G., Graham, R. K., Liu, L., Bissada, N., Lu, G., Leavitt, B. R. and Hayden, M. R. (2010). Phosphorylation of huntingtin at Ser421 in YAC128 neurons is associated with protection of YAC128 neurons from NMDA-mediated excitotoxicity and is modulated by PP1 and PP2A. *J Neurosci* **30**, 14318-29. https://doi.org/10.1523/jneurosci.1589-10.2010.

Mezan, S., Feuz, J. D., Deplancke, B. and Kadener, S. (2016). PDF signaling Is an Integral part of the *Drosophila* circadian molecular oscillator. *Cell Rep* **17**, 708-719. https://doi.org/10.1016/j.celrep.2016.09.048.

Michalik, A. and Van Broeckhoven, C. (2004). Proteasome degrades soluble expanded polyglutamine completely and efficiently. *Neurobiol Dis* **16**, 202-11. https://doi.org/10.1016/j.nbd.2003.12.020.

References

Michel, S. and Meijer, J. H. (2020). From clock to functional pacemaker. *Eur J Neurosci* **51**, 482-493. https://doi.org/10.1111/ejn.14388.

Milisav, I., Poljsak, B. and Šuput, D. (2012). Adaptive response, evidence of cross-resistance and its potential clinical use. *Int J Mol Sci* **13**, 10771-10806. https://doi.org/10.3390/ijms130910771.

Miller, C. B., Espie, C. A., Epstein, D. R., Friedman, L., Morin, C. M., Pigeon, W. R., Spielman, A. J. and Kyle, S. D. (2014). The evidence base of sleep restriction therapy for treating insomnia disorder. *Sleep Med Rev* **18**, 415-24. https://doi.org/10.1016/j.smrv.2014.01.006.

Miller, J., Arrasate, M., Brooks, E., Libeu, C. P., Legleiter, J., Hatters, D., Curtis, J., Cheung, K., Krishnan, P., Mitra, S. et al. (2011). Identifying polyglutamine protein species in situ that best predict neurodegeneration. *Nat Chem Biol* **7**, 925-34. https://doi.org/10.1038/nchembio.694.

Miller, J., Arrasate, M., Shaby, B. A., Mitra, S., Masliah, E. and Finkbeiner, S. (2010a). Quantitative relationships between huntingtin levels, polyglutamine length, inclusion body formation, and neuronal death provide novel insight into Huntington's disease molecular pathogenesis. *J Neurosci* **30**, 10541-50. https://doi.org/10.1523/jneurosci.0146-10.2010.

Miller, J. P., Holcomb, J., Al-Ramahi, I., de Haro, M., Gafni, J., Zhang, N., Kim, E., Sanhueza, M., Torcassi, C., Kwak, S. et al. (2010b). Matrix metalloproteinases are modifiers of huntingtin proteolysis and toxicity in Huntington's disease. *Neuron* **67**, 199-212. https://doi.org/10.1016/j.neuron.2010.06.021.

Miller, J. P., Yates, B. E., Al-Ramahi, I., Berman, A. E., Sanhueza, M., Kim, E., de Haro, M., DeGiacomo, F., Torcassi, C., Holcomb, J. et al. (2012). A genome-scale RNA-interference screen identifies RRAS signaling as a pathologic feature of Huntington's disease. *PLoS Genet* **8**, e1003042. https://doi.org/10.1371/journal.pgen.1003042.

Miller, S. B., Ho, C. T., Winkler, J., Khokhrina, M., Neuner, A., Mohamed, M. Y., Guilbride, D. L., Richter, K., Lisby, M., Schiebel, E. et al. (2015). Compartment-specific aggregases direct distinct nuclear and cytoplasmic aggregate deposition. *Embo j* **34**, 778-97. https://doi.org/10.15252/embj.201489524.

Miller, V. M., Nelson, R. F., Gouvion, C. M., Williams, A., Rodriguez-Lebron, E., Harper, S. Q., Davidson, B. L., Rebagliati, M. R. and Paulson, H. L. (2005). CHIP suppresses polyglutamine aggregation and toxicity in vitro and in vivo. *J Neurosci* **25**, 9152-61. https://doi.org/10.1523/jneurosci.3001-05.2005.

Mills, P. J., Ancoli-Israel, S., von Kanel, R., Mausbach, B. T., Aschbacher, K., Patterson, T. L., Ziegler, M. G., Dimsdale, J. E. and Grant, I. (2009). Effects of gender and dementia severity on Alzheimer's disease caregivers' sleep and biomarkers of coagulation and inflammation. *Brain Behav Immun* **23**, 605-10. https://doi.org/10.1016/j.bbi.2008.09.014.

Minakawa, E. N. and Nagai, Y. (2021). Protein aggregation inhibitors as disease-modifying therapies for polyglutamine diseases. *Front Neurosci* **15**, 621996. https://doi.org/10.3389/fnins.2021.621996.

Mishima, Y., Hozumi, S., Shimizu, T., Hishikawa, Y. and Mishima, K. (2005). Passive body heating ameliorates sleep disturbances in patients with vascular dementia without circadian phase-shifting. *Am J Geriatr Psychiatry* **13**, 369-76. https://doi.org/10.1176/appi.ajgp.13.5.369.

References

Mitra, S., Tsvetkov, A. S. and Finkbeiner, S. (2009). Single neuron ubiquitin-proteasome dynamics accompanying inclusion body formation in Huntington disease. *J Biol Chem* **284**, 4398-403. https://doi.org/10.1074/jbc.M806269200.

Miyasako, Y., Umezaki, Y. and Tomioka, K. (2007). Separate sets of cerebral clock neurons are responsible for light and temperature entrainment of *Drosophila* circadian locomotor rhythms. *J Biol Rhythms* **22**, 115-26. https://doi.org/10.1177/0748730407299344.

Mochel, F. and Haller, R. G. (2011). Energy deficit in Huntington disease: Why it matters. *J Clin Invest* **121**, 493-9. https://doi.org/10.1172/jci45691.

Mogk, A., Bukau, B. and Kampinga, H. H. (2018). Cellular handling of protein aggregates by disaggregation machines. *Mol Cell* **69**, 214-226. https://doi.org/10.1016/j.molcel.2018.01.004.

Mohawk, J. A., Green, C. B. and Takahashi, J. S. (2012). Central and peripheral circadian clocks in mammals. *Annu Rev Neurosci* **35**, 445-62. https://doi.org/10.1146/annurev-neuro-060909-153128.

Mohawk, J. A. and Takahashi, J. S. (2011). Cell autonomy and synchrony of suprachiasmatic nucleus circadian oscillators. *Trends Neurosci* **34**, 349-58. https://doi.org/10.1016/j.tins.2011.05.003.

Moily, N. S., Kota, L. N., Anjanappa, R. M., Venugopal, S., Vaidyanathan, R., Pal, P., Purushottam, M., Jain, S. and Kandasamy, M. (2014). Trinucleotide repeats and haplotypes at the huntingtin locus in an Indian sample overlaps with European haplogroup a. *PLoS Curr* **6**. https://doi.org/10.1371/currents.hd.a3ad1a381ab1eed1176751453l8c9a80.

Moily, N. S., Ormsby, A. R., Stojilovic, A., Ramdzan, Y. M., Diesch, J., Hannan, R. D., Zajac, M. S., Hannan, A. J., Oshlack, A. and Hatters, D. M. (2017). Transcriptional profiles for distinct aggregation states of mutant huntingtin exon 1 protein unmask new Huntington's disease pathways. *Mol Cell Neurosci* **83**, 103-112. https://doi.org/10.1016/j.mcn.2017.07.004.

Monsellier, E., Redeker, V., Ruiz-Arlandis, G., Bousset, L. and Melki, R. (2015). Molecular interaction between the chaperone Hsc70 and the N-terminal flank of huntingtin exon 1 modulates aggregation. *J Biol Chem* **290**, 2560-76. https://doi.org/10.1074/jbc.M114.603332.

Moore, R. Y. and Klein, D. C. (1974). Visual pathways and the central neural control of a circadian rhythm in pineal serotonin N-acetyltransferase activity. *Brain Res* **71**, 17-33. https://doi.org/10.1016/0006-8993(74)90188-7.

Morales, J., Hiesinger, P. R., Schroeder, A. J., Kume, K., Verstreken, P., Jackson, F. R., Nelson, D. L. and Hassan, B. A. (2002). *Drosophila* fragile X protein, DFXR, regulates neuronal morphology and function in the brain. *Neuron* **34**, 961-72. https://doi.org/10.1016/s0896-6273(02)00731-6.

Morf, J., Rey, G., Schneider, K., Stratmann, M., Fujita, J., Naef, F. and Schibler, U. (2012). Cold-inducible RNA-binding protein modulates circadian gene expression posttranscriptionally. *Science* **338**, 379-83. https://doi.org/10.1126/science.1217726.

Morigaki, R. and Goto, S. (2017). Striatal vulnerability in Huntington's disease: Neuroprotection versus neurotoxicity. *Brain Sci* **7**. https://doi.org/10.3390/brainsci7060063.

Morishima, Y., Wang, A. M., Yu, Z., Pratt, W. B., Osawa, Y. and Lieberman, A. P. (2008). CHIP deletion reveals functional redundancy of E3 ligases in promoting degradation of both signaling

proteins and expanded glutamine proteins. *Hum Mol Genet* **17**, 3942-52. https://doi.org/10.1093/hmg/ddn296.

Morley, J. F., Brignull, H. R., Weyers, J. J. and Morimoto, R. I. (2002). The threshold for polyglutamine-expansion protein aggregation and cellular toxicity is dynamic and influenced by aging in *Caenorhabditis elegans*. *Proc Natl Acad Sci U S A* **99**, 10417-22. https://doi.org/10.1073/pnas.152161099.

Moro, C., Valverde, A., Dole, M., Hoh Kam, J., Hamilton, C., Liebert, A., Bicknell, B., Benabid, A. L., Magistretti, P. and Mitrofanis, J. (2022). The effect of photobiomodulation on the brain during wakefulness and sleep. *Front Neurosci* **16**, 942536. https://doi.org/10.3389/fnins.2022.942536.

Moronetti Mazzeo, L. E., Dersh, D., Boccitto, M., Kalb, R. G. and Lamitina, T. (2012). Stress and aging induce distinct polyQ protein aggregation states. *Proc Natl Acad Sci U S A* **109**, 10587-92. https://doi.org/10.1073/pnas.1108766109.

Morrison, S. F., Nakamura, K. and Madden, C. J. (2008). Central control of thermogenesis in mammals. *Exp Physiol* **93**, 773-97. https://doi.org/10.1113/expphysiol.2007.041848.

Morton, A. J. (2013). Circadian and sleep disorder in Huntington's disease. *Exp Neurol* **243**, 34-44. https://doi.org/10.1016/j.expneurol.2012.10.014.

Morton, A. J., Rudiger, S. R., Wood, N. I., Sawiak, S. J., Brown, G. C., McLaughlan, C. J., Kuchel, T. R., Snell, R. G., Faull, R. L. and Bawden, C. S. (2014). Early and progressive circadian abnormalities in Huntington's disease sheep are unmasked by social environment. *Hum Mol Genet* **23**, 3375-83. https://doi.org/10.1093/hmg/ddu047.

Morton, A. J., Wood, N. I., Hastings, M. H., Hurelbrink, C., Barker, R. A. and Maywood, E. S. (2005). Disintegration of the sleep-wake cycle and circadian timing in Huntington's disease. *J Neurosci* **25**, 157-63. https://doi.org/10.1523/jneurosci.3842-04.2005.

Morton, J. P., Maclaren, D. P., Cable, N. T., Campbell, I. T., Evans, L., Bongers, T., Griffiths, R. D., Kayani, A. C., McArdle, A. and Drust, B. (2007). Elevated core and muscle temperature to levels comparable to exercise do not increase heat shock protein content of skeletal muscle of physically active men. *Acta Physiol (Oxf)* **190**, 319-27. https://doi.org/10.1111/j.1748-1716.2007.01711.x.

Moskalev, A. A. and Malysheva, O. A. (2009). Effect of illumination regime on life span in *Drosophila melanogaster*. *Russian Journal of Ecology* **40**, 206-212. https://doi.org/10.1134/s1067413609030102.

Moskalev, A. A. and Malysheva, O. A. (2010). The role of transcription factors Dfoxo, Dsir2 and Hsp70 in lifespan alteration of *Drosophila melanogaster* in different light conditions. *Ecological genetics* **8**, 67-80. https://doi.org/10.17816/ecogen8367-80.

Moss, D. J. H., Pardiñas, A. F., Langbehn, D., Lo, K., Leavitt, B. R., Roos, R., Durr, A., Mead, S., Holmans, P., Jones, L. et al. (2017). Identification of genetic variants associated with Huntington's disease progression: A genome-wide association study. *Lancet Neurol* **16**, 701-711. https://doi.org/10.1016/s1474-4422(17)30161-8.

Motzko-Soares, A. C. P., Vizin, R. C. L., Martins, T. M. S., Hungaro, A. R. O., Sato, J. R., Almeida, M. C. and Carrettiero, D. C. (2018). Thermoregulatory profile of neurodegeneration-induced dementia of the Alzheimer's type using intracerebroventricular streptozotocin in rats. *Acta Physiol (Oxf)* **224**, e13084. https://doi.org/10.1111/apha.13084.

References

Muchowski, P. J., Schaffar, G., Sittler, A., Wanker, E. E., Hayer-Hartl, M. K. and Hartl, F. U. (2000). Hsp70 and Hsp40 chaperones can inhibit self-assembly of polyglutamine proteins into amyloid-like fibrils. *Proceedings of the National Academy of Sciences* **97**, 7841-7846. https://doi.org/10.1073/pnas.140202897.

Muchowski, P. J. and Wacker, J. L. (2005). Modulation of neurodegeneration by molecular chaperones. *Nature Reviews Neuroscience* **6**, 11-22. https://doi.org/10.1038/nrn1587.

Mueller, S. M., Petersen, J. A. and Jung, H. H. (2019). Exercise in Huntington's disease: Current state and clinical significance. *Tremor Other Hyperkinet Mov (N Y)* **9**, 601. https://doi.org/10.7916/tm9j-f874.

Mugat, B., Parmentier, M. L., Bonneaud, N., Chan, H. Y. and Maschat, F. (2008). Protective role of Engrailed in a *Drosophila* model of Huntington's disease. *Hum Mol Genet* **17**, 3601-16. https://doi.org/10.1093/hmg/ddn255.

Muller, M. and Leavitt, B. R. (2014). Iron dysregulation in Huntington's disease. *J Neurochem* **130**, 328-50. https://doi.org/10.1111/jnc.12739.

Munsie, L. N. and Truant, R. (2012). The role of the cofilin-actin rod stress response in neurodegenerative diseases uncovers potential new drug targets. *Bioarchitecture* **2**, 204-8. https://doi.org/10.4161/bioa.22549.

Muraro, N. I. and Ceriani, M. F. (2015). Acetylcholine from visual circuits modulates the activity of arousal neurons in *Drosophila*. *J Neurosci* **35**, 16315-27. https://doi.org/10.1523/JNEUROSCI.1571-15.2015.

Muraro, N. I., Pírez, N. and Ceriani, M. F. (2013). The circadian system: Plasticity at many levels. *Neuroscience* **247**, 280-93. https://doi.org/10.1016/j.neuroscience.2013.05.036.

Musiek, E. S. (2015). Circadian clock disruption in neurodegenerative diseases: cause and effect? *Front Pharmacol* **6**, 29. https://doi.org/10.3389/fphar.2015.00029.

Musiek, E. S., Lim, M. M., Yang, G., Bauer, A. Q., Qi, L., Lee, Y., Roh, J. H., Ortiz-Gonzalez, X., Dearborn, J. T., Culver, J. P. et al. (2013). Circadian clock proteins regulate neuronal redox homeostasis and neurodegeneration. *J Clin Invest* **123**, 5389-400. https://doi.org/10.1172/jci70317.

Myers, M. P., Wager-Smith, K., Rothenfluh-Hilfiker, A. and Young, M. W. (1996). Light-induced degradation of TIMELESS and entrainment of the *Drosophila* circadian clock. *Science* **271**, 1736-40. https://doi.org/10.1126/science.271.5256.1736.

Myers, R. H., Leavitt, J., Farrer, L. A., Jagadeesh, J., McFarlane, H., Mastromauro, C. A., Mark, R. J. and Gusella, J. F. (1989). Homozygote for Huntington disease. *Am J Hum Genet* **45**, 615-8.

Myers, R. H., MacDonald, M. E., Koroshetz, W. J., Duyao, M. P., Ambrose, C. M., Taylor, S. A., Barnes, G., Srinidhi, J., Lin, C. S., Whaley, W. L. et al. (1993). De novo expansion of a (CAG)n repeat in sporadic Huntington's disease. *Nat Genet* **5**, 168-73. https://doi.org/10.1038/ng1093-168.

Na, D., Rouf, M., O'Kane, C. J., Rubinsztein, D. C. and Gsponer, J. (2013). NeuroGeM, a knowledgebase of genetic modifiers in neurodegenerative diseases. *BMC Med Genomics* **6**, 52. https://doi.org/10.1186/1755-8794-6-52.

Nachman, E., Wentink, A. S., Madiona, K., Bousset, L., Katsinelos, T., Allinson, K., Kampinga, H., McEwan, W. A., Jahn, T. R., Melki, R. et al. (2020). Disassembly of Tau fibrils by the

human Hsp70 disaggregation machinery generates small seeding-competent species. *J Biol Chem* **295**, 9676-9690. https://doi.org/10.1074/jbc.RA120.013478.

Nagai, Y., Fujikake, N., Ohno, K., Higashiyama, H., Popiel, H. A., Rahadian, J., Yamaguchi, M., Strittmatter, W. J., Burke, J. R. and Toda, T. (2003). Prevention of polyglutamine oligomerization and neurodegeneration by the peptide inhibitor QBP1 in *Drosophila*. *Hum Mol Genet* **12**, 1253-9. https://doi.org/10.1093/hmg/ddg144.

Nagai, Y., Inui, T., Popiel, H. A., Fujikake, N., Hasegawa, K., Urade, Y., Goto, Y., Naiki, H. and Toda, T. (2007). A toxic monomeric conformer of the polyglutamine protein. *Nat Struct Mol Biol* **14**, 332-40. https://doi.org/10.1038/nsmb1215.

Nakamura, W., Honma, S., Shirakawa, T. and Honma, K. (2002). Clock mutation lengthens the circadian period without damping rhythms in individual SCN neurons. *Nat Neurosci* **5**, 399-400. https://doi.org/10.1038/nn843.

Nakayama, M., Ishibashi, T., Ishikawa, H. O., Sato, H., Usui, T., Okuda, T., Yashiro, H., Ishikawa, H., Taikou, Y., Minami, A. et al. (2014). A gain-of-function screen to identify genes that reduce lifespan in the adult of *Drosophila melanogaster*. *BMC Genet* **15**, 46. https://doi.org/10.1186/1471-2156-15-46.

Nan, Y., Lin, J., Cui, Y., Yao, J., Yang, Y. and Li, Q. (2021). Protective role of vitamin B6 against mitochondria damage in *Drosophila* models of SCA3. *Neurochem Int* **144**, 104979. https://doi.org/10.1016/j.neuint.2021.104979.

Nance, M. A. and Myers, R. H. (2001). Juvenile onset Huntington's disease--clinical and research perspectives. *Ment Retard Dev Disabil Res Rev* **7**, 153-7. https://doi.org/10.1002/mrdd.1022.

Nash, T. R., Chow, E. S., Law, A. D., Fu, S. D., Fuszara, E., Bilska, A., Bebas, P., Kretzschmar, D. and Giebultowicz, J. M. (2019). Daily blue-light exposure shortens lifespan and causes brain neurodegeneration in *Drosophila*. *NPJ Aging Mech Dis* **5**, 8. https://doi.org/10.1038/s41514-019-0038-6.

Nasir, J., Floresco, S. B., O'Kusky, J. R., Diewert, V. M., Richman, J. M., Zeisler, J., Borowski, A., Marth, J. D., Phillips, A. G. and Hayden, M. R. (1995). Targeted disruption of the Huntington's disease gene results in embryonic lethality and behavioral and morphological changes in heterozygotes. *Cell* **81**, 811-23. https://doi.org/10.1016/0092-8674(95)90542-1.

Nassel, D. R. and Winther, A. M. (2010). *Drosophila* neuropeptides in regulation of physiology and behavior. *Prog Neurobiol* **92**, 42-104. https://doi.org/10.1016/j.pneurobio.2010.04.010.

Nässel, D. R. and Zandawala, M. (2022). Endocrine cybernetics: neuropeptides as molecular switches in behavioural decisions. *Open Biol* **12**, 220174. https://doi.org/10.1098/rsob.220174.

Nath, S., Munsie, L. N. and Truant, R. (2015). A huntingtin-mediated fast stress response halting endosomal trafficking is defective in Huntington's disease. *Hum Mol Genet* **24**, 450-62. https://doi.org/10.1093/hmg/ddu460.

Naumann, J., Kruza, I., Denkel, L., Kienle, G. and Huber, R. (2020). Effects and feasibility of hyperthermic baths in comparison to exercise as add-on treatment to usual care in depression: a randomised, controlled pilot study. *BMC Psychiatry* **20**, 536. https://doi.org/10.1186/s12888-020-02941-1.

References

Nava, R. and Zuhl, M. N. (2020). Heat acclimation-induced intracellular HSP70 in humans: A meta-analysis. *Cell Stress Chaperones* **25**, 35-45. https://doi.org/10.1007/s12192-019-01059-y.

Neal, S. J., Karunanithi, S., Best, A., So, A. K., Tanguay, R. M., Atwood, H. L. and Westwood, J. T. (2006). Thermoprotection of synaptic transmission in a *Drosophila* heat shock factor mutant is accompanied by increased expression of Hsp83 and DnaJ-1. *Physiol Genomics* **25**, 493-501. https://doi.org/10.1152/physiolgenomics.00195.2005.

Nedergaard, M. and Goldman, S. A. (2020). Glymphatic failure as a final common pathway to dementia. *Science* **370**, 50-56. https://doi.org/10.1126/science.abb8739.

Neef, D. W., Jaeger, A. M. and Thiele, D. J. (2011). Heat shock transcription factor 1 as a therapeutic target in neurodegenerative diseases. *Nature Reviews Drug Discovery* **10**, 930-944. https://doi.org/10.1038/nrd3453.

Nekooki-Machida, Y., Kurosawa, M., Nukina, N., Ito, K., Oda, T. and Tanaka, M. (2009). Distinct conformations of in vitro and in vivo amyloids of huntingtin-exon1 show different cytotoxicity. *Proc Natl Acad Sci U S A* **106**, 9679-84. https://doi.org/10.1073/pnas.0812083106.

Nelson, V. K., Ali, A., Dutta, N., Ghosh, S., Jana, M., Ganguli, A., Komarov, A., Paul, S., Dwivedi, V., Chatterjee, S. et al. (2016). Azadiradione ameliorates polyglutamine expansion disease in *Drosophila* by potentiating DNA binding activity of heat shock factor 1. *Oncotarget* **7**, 78281-78296. https://doi.org/10.18632/oncotarget.12930.

Nettnin, E. A., Sallese, T. R., Nasseri, A., Saurabh, S. and Cavanaugh, D. J. (2021). Dorsal clock neurons in *Drosophila* sculpt locomotor outputs but are dispensable for circadian activity rhythms. *iScience* **24**, 103001. https://doi.org/10.1016/j.isci.2021.103001.

Neueder, A., Landles, C., Ghosh, R., Howland, D., Myers, R. H., Faull, R. L. M., Tabrizi, S. J. and Bates, G. P. (2017). The pathogenic exon 1 HTT protein is produced by incomplete splicing in Huntington's disease patients. *Sci Rep* **7**, 1307. https://doi.org/10.1038/s41598-017-01510-z.

Neuwald, A. F. and Hirano, T. (2000). HEAT repeats associated with condensins, cohesins, and other complexes involved in chromosome-related functions. *Genome Res* **10**, 1445-52. https://doi.org/10.1101/gr.147400.

Newcombe, E. A., Ruff, K. M., Sethi, A., Ormsby, A. R., Ramdzan, Y. M., Fox, A., Purcell, A. W., Gooley, P. R., Pappu, R. V. and Hatters, D. M. (2018). Tadpole-like conformations of huntingtin exon 1 are characterized by conformational heterogeneity that persists regardless of polyglutamine length. *J Mol Biol* **430**, 1442-1458. https://doi.org/10.1016/j.jmb.2018.03.031.

Ng, C. W., Yildirim, F., Yap, Y. S., Dalin, S., Matthews, B. J., Velez, P. J., Labadorf, A., Housman, D. E. and Fraenkel, E. (2013). Extensive changes in DNA methylation are associated with expression of mutant huntingtin. *Proc Natl Acad Sci U S A* **110**, 2354-9. https://doi.org/10.1073/pnas.1221292110.

Ng, F. S., Tangredi, M. M. and Jackson, F. R. (2011). Glial cells physiologically modulate clock neurons and circadian behavior in a calcium-dependent manner. *Curr Biol* **21**, 625-34. https://doi.org/10.1016/j.cub.2011.03.027.

References

Nikhil, K. and Sharma, V. K. (2017). On the origin and implications of circadian timekeeping: An evolutionary perspective. In *Biological timekeeping: Clocks, rhythms and behaviour*, (ed. V. Kumar), pp. 81-129: Springer. https://doi.org/10.1007/978-81-322-3688-7_5.

Nillegoda, N. B. and Bukau, B. (2015). Metazoan Hsp70-based protein disaggregases: emergence and mechanisms. *Front Mol Biosci* **2**, 57. https://doi.org/10.3389/fmolb.2015.00057.

Nillegoda, N. B., Wentink, A. S. and Bukau, B. (2018). Protein disaggregation in multicellular organisms. *Trends in Biochemical Sciences* **43**, 285-300. https://doi.org/10.1016/j.tibs.2018.02.003.

Nishimura, Y., Yalgin, C., Akimoto, S., Doumanis, J., Sasajima, R., Nukina, N., Miyakawa, H., Moore, A. W. and Morimoto, T. (2010). Selection of behaviors and segmental coordination during larval locomotion is disrupted by nuclear polyglutamine inclusions in a new *Drosophila* Huntington's disease-like model. *J Neurogenet* **24**, 194-206. https://doi.org/10.3109/01677063.2010.514367.

Nitabach, M. N., Blau, J. and Holmes, T. C. (2002). Electrical silencing of *Drosophila* pacemaker neurons stops the free-running circadian clock. *Cell* **109**, 485-95. https://doi.org/10.1016/s0092-8674(02)00737-7.

Nitabach, M. N. and Taghert, P. H. (2008). Organization of the *Drosophila* circadian control circuit. *Curr Biol* **18**, R84-93. https://doi.org/10.1016/j.cub.2007.11.061.

Nitabach, M. N., Wu, Y., Sheeba, V., Lemon, W. C., Strumbos, J., Zelensky, P. K., White, B. H. and Holmes, T. C. (2006). Electrical hyperexcitation of lateral ventral pacemaker neurons desynchronizes downstream circadian oscillators in the fly circadian circuit and induces multiple behavioral periods. *J Neurosci* **26**, 479-89. https://doi.org/10.1523/JNEUROSCI.3915-05.2006.

Niu, L., Zhang, F., Xu, X., Yang, Y., Li, S., Liu, H. and Le, W. (2022). Chronic sleep deprivation altered the expression of circadian clock genes and aggravated Alzheimer's disease neuropathology. *Brain Pathol* **32**, e13028. https://doi.org/10.1111/bpa.13028.

Nollen, E. A., Salomons, F. A., Brunsting, J. F., van der Want, J. J., Sibon, O. C. and Kampinga, H. H. (2001). Dynamic changes in the localization of thermally unfolded nuclear proteins associated with chaperone-dependent protection. *Proc Natl Acad Sci U S A* **98**, 12038-43. https://doi.org/10.1073/pnas.201112398.

Noorani, A. A., Yamashita, H., Gao, Y., Islam, S., Sun, Y., Nakamura, T., Enomoto, H., Zou, K. and Michikawa, M. (2020). High temperature promotes amyloid β-protein production and γ-secretase complex formation via Hsp90. *J Biol Chem* **295**, 18010-18022. https://doi.org/10.1074/jbc.RA120.013845.

Novak, M. J. and Tabrizi, S. J. (2010). Huntington's disease. *Bmj* **340**, c3109. https://doi.org/10.1136/bmj.c3109.

Novak, M. J. and Tabrizi, S. J. (2011). Huntington's disease: Clinical presentation and treatment. *Int Rev Neurobiol* **98**, 297-323. https://doi.org/10.1016/b978-0-12-381328-2.00013-4.

Nucifora, F. C., Jr., Sasaki, M., Peters, M. F., Huang, H., Cooper, J. K., Yamada, M., Takahashi, H., Tsuji, S., Troncoso, J., Dawson, V. L. et al. (2001). Interference by huntingtin and atrophin-1 with cbp-mediated transcription leading to cellular toxicity. *Science* **291**, 2423-8. https://doi.org/10.1126/science.1056784.

References

Nylandsted, J., Wick, W., Hirt, U. A., Brand, K., Rohde, M., Leist, M., Weller, M. and Jaattela, M. (2002). Eradication of glioblastoma, and breast and colon carcinoma xenografts by Hsp70 depletion. *Cancer Res* **62**, 7139-42.

Oakeshott, S., Balci, F., Filippov, I., Murphy, C., Port, R., Connor, D., Paintdakhi, A., Lesauter, J., Menalled, L., Ramboz, S. et al. (2011). Circadian abnormalities in motor activity in a BAC transgenic mouse model of Huntington's disease. *PLoS Curr* **3**, Rrn1225. https://doi.org/10.1371/currents.RRN1225.

Ochaba, J., Lukacsovich, T., Csikos, G., Zheng, S., Margulis, J., Salazar, L., Mao, K., Lau, A. L., Yeung, S. Y., Humbert, S. et al. (2014). Potential function for the huntingtin protein as a scaffold for selective autophagy. *Proc Natl Acad Sci U S A* **111**, 16889-94. https://doi.org/10.1073/pnas.1420103111.

Oehler, R., Pusch, E., Zellner, M., Dungel, P., Hergovics, N., Homoncik, M., Eliasen, M. M., Brabec, M. and Roth, E. (2001). Cell type-specific variations in the induction of hsp70 in human leukocytes by feverlike whole body hyperthermia. *Cell Stress Chaperones* **6**, 306-15. https://doi.org/10.1379/1466-1268(2001)006<0306:ctsvit>2.0.co;2.

Okamoto-Mizuno, K., Nagai, Y. and Iizuka, S. (2003). The effect of ambient temperature change on the covered area of the body during sleep. *Journal of home economics of Japan* **54**, 1025-1030. https://doi.org/10.11428/jhej1987.54.1025.

Okray, Z., de Esch, C. E., Van Esch, H., Devriendt, K., Claeys, A., Yan, J., Verbeeck, J., Froyen, G., Willemsen, R., de Vrij, F. M. et al. (2015). A novel Fragile X Syndrome mutation reveals a conserved role for the carboxy-terminus in FMRP localization and function. *EMBO Mol Med* **7**, 423-37. https://doi.org/10.15252/emmm.201404576.

Oliveira, A. O., Osmand, A., Outeiro, T. F., Muchowski, P. J. and Finkbeiner, S. (2016). αB-Crystallin overexpression in astrocytes modulates the phenotype of the BACHD mouse model of Huntington's disease. *Hum Mol Genet* **25**, 1677-89. https://doi.org/10.1093/hmg/ddw028.

Onat, O. E., Kars, M. E., Gül, Ş., Bilguvar, K., Wu, Y., Özhan, A., Aydın, C., Başak, A. N., Trusso, M. A., Goracci, A. et al. (2020). Human CRY1 variants associate with attention deficit/hyperactivity disorder. *J Clin Invest* **130**, 3885-3900. https://doi.org/10.1172/jci135500.

Ordway, J. M., Tallaksen-Greene, S., Gutekunst, C. A., Bernstein, E. M., Cearley, J. A., Wiener, H. W., Dure, L. S. t., Lindsey, R., Hersch, S. M., Jope, R. S. et al. (1997). Ectopically expressed CAG repeats cause intranuclear inclusions and a progressive late onset neurological phenotype in the mouse. *Cell* **91**, 753-63. https://doi.org/10.1016/s0092-8674(00)80464-x.

Origin(Pro). Version 8. OriginLab Corporation. Northampton, MA, USA.

Ormsby, A. R., Ramdzan, Y. M., Mok, Y. F., Jovanoski, K. D. and Hatters, D. M. (2013). A platform to view huntingtin exon 1 aggregation flux in the cell reveals divergent influences from chaperones hsp40 and hsp70. *J Biol Chem* **288**, 37192-203. https://doi.org/10.1074/jbc.M113.486944.

Orr, H. T. and Zoghbi, H. Y. (2007). Trinucleotide repeat disorders. *Annu Rev Neurosci* **30**, 575-621. https://doi.org/10.1146/annurev.neuro.29.051605.113042.

Ortega, Z., Díaz-Hernández, M., Maynard, C. J., Hernández, F., Dantuma, N. P. and Lucas, J. J. (2010). Acute polyglutamine expression in inducible mouse model unravels ubiquitin/proteasome

system impairment and permanent recovery attributable to aggregate formation. *J Neurosci* **30**, 3675-88. https://doi.org/10.1523/jneurosci.5673-09.2010.

Ouk, K., Aungier, J. and Morton, A. J. (2017). Prolonged day length exposure improves circadian deficits and survival in a transgenic mouse model of Huntington's disease. *Neurobiol Sleep Circadian Rhythms* **2**, 27-38. https://doi.org/10.1016/j.nbscr.2016.11.004.

Ouk, K., Aungier, J., Ware, M. and Morton, A. J. (2019). Abnormal Photic Entrainment to Phase-Delaying Stimuli in the R6/2 Mouse Model of Huntington's Disease, despite Retinal Responsiveness to Light. *eNeuro* **6**. https://doi.org/10.1523/ENEURO.0088-19.2019.

Ouk, K., Hughes, S., Pothecary, C. A., Peirson, S. N. and Morton, A. J. (2016). Attenuated pupillary light responses and downregulation of opsin expression parallel decline in circadian disruption in two different mouse models of Huntington's disease. *Hum Mol Genet* **25**, 5418-32. https://doi.org/10.1093/hmg/ddw359.

Ouyang, X., Yang, J., Hong, Z., Wu, Y., Xie, Y. and Wang, G. (2020). Mechanisms of blue light-induced eye hazard and protective measures: A review. *Biomed Pharmacother* **130**, 110577. https://doi.org/10.1016/j.biopha.2020.110577.

Ouyang, Y., Andersson, C. R., Kondo, T., Golden, S. S. and Johnson, C. H. (1998). Resonating circadian clocks enhance fitness in cyanobacteria. *Proc Natl Acad Sci U S A* **95**, 8660-4. https://doi.org/10.1073/pnas.95.15.8660.

Paillard, T., Rolland, Y. and de Souto Barreto, P. (2015). Protective effects of physical exercise in Alzheimer's disease and Parkinson's disease: A narrative review. *J Clin Neurol* **11**, 212-9. https://doi.org/10.3988/jcn.2015.11.3.212.

Pal, A., Severin, F., Lommer, B., Shevchenko, A. and Zerial, M. (2006). Huntingtin-HAP40 complex is a novel Rab5 effector that regulates early endosome motility and is up-regulated in Huntington's disease. *J Cell Biol* **172**, 605-18. https://doi.org/10.1083/jcb.200509091.

Palaiogeorgou, A. M., Papakonstantinou, E., Golfinopoulou, R., Sigala, M., Mitsis, T., Papageorgiou, L., Diakou, I., Pierouli, K., Dragoumani, K., Spandidos, D. A. et al. (2023). Recent approaches on Huntington's disease (Review). *Biomed Rep* **18**, 5. https://doi.org/10.3892/br.2022.1587.

Palidwor, G. A., Shcherbinin, S., Huska, M. R., Rasko, T., Stelzl, U., Arumughan, A., Foulle, R., Porras, P., Sanchez-Pulido, L., Wanker, E. E. et al. (2009). Detection of alpha-rod protein repeats using a neural network and application to huntingtin. *PLoS Comput Biol* **5**, e1000304. https://doi.org/10.1371/journal.pcbi.1000304.

Pallier, P. N., Maywood, E. S., Zheng, Z., Chesham, J. E., Inyushkin, A. N., Dyball, R., Hastings, M. H. and Morton, A. J. (2007). Pharmacological imposition of sleep slows cognitive decline and reverses dysregulation of circadian gene expression in a transgenic mouse model of Huntington's disease. *J Neurosci* **27**, 7869-78. https://doi.org/10.1523/jneurosci.0649-07.2007.

Pallier, P. N. and Morton, A. J. (2009). Management of sleep/wake cycles improves cognitive function in a transgenic mouse model of Huntington's disease. *Brain Res* **1279**, 90-8. https://doi.org/10.1016/j.brainres.2009.03.072.

References

Pallos, J., Bodai, L., Lukacsovich, T., Purcell, J. M., Steffan, J. S., Thompson, L. M. and Marsh, J. L. (2008). Inhibition of specific HDACs and sirtuins suppresses pathogenesis in a *Drosophila* model of Huntington's disease. *Hum Mol Genet* **17**, 3767-75. https://doi.org/10.1093/hmg/ddn273.

Palpagama, T. H., Waldvogel, H. J., Faull, R. L. M. and Kwakowsky, A. (2019). The role of microglia and astrocytes in Huntington's disease. *Front Mol Neurosci* **12**, 258. https://doi.org/10.3389/fnmol.2019.00258.

Panda, S., Antoch, M. P., Miller, B. H., Su, A. I., Schook, A. B., Straume, M., Schultz, P. G., Kay, S. A., Takahashi, J. S. and Hogenesch, J. B. (2002). Coordinated transcription of key pathways in the mouse by the circadian clock. *Cell* **109**, 307-20. https://doi.org/10.1016/s0092-8674(02)00722-5.

Pandey, N. K., Isas, J. M., Rawat, A., Lee, R. V., Langen, J., Pandey, P. and Langen, R. (2018). The 17-residue-long N terminus in huntingtin controls stepwise aggregation in solution and on membranes via different mechanisms. *J Biol Chem* **293**, 2597-2605. https://doi.org/10.1074/jbc.M117.813667.

Panov, A. V., Gutekunst, C. A., Leavitt, B. R., Hayden, M. R., Burke, J. R., Strittmatter, W. J. and Greenamyre, J. T. (2002). Early mitochondrial calcium defects in Huntington's disease are a direct effect of polyglutamines. *Nat Neurosci* **5**, 731-6. https://doi.org/10.1038/nn884.

Parisky, K. M., Agosto Rivera, J. L., Donelson, N. C., Kotecha, S. and Griffith, L. C. (2016). Reorganization of sleep by temperature in *Drosophila* requires light, the homeostat, and the circadian clock. *Curr Biol* **26**, 882-92. https://doi.org/10.1016/j.cub.2016.02.011.

Park, J. H. and Hall, J. C. (1998). Isolation and chronobiological analysis of a neuropeptide pigment-dispersing factor gene in *Drosophila melanogaster*. *J Biol Rhythms* **13**, 219-28. https://doi.org/10.1177/074873098129000066.

Park, J. H., Helfrich-Förster, C., Lee, G., Liu, L., Rosbash, M. and Hall, J. C. (2000). Differential regulation of circadian pacemaker output by separate clock genes in *Drosophila*. *Proc Natl Acad Sci U S A* **97**, 3608-13. https://doi.org/10.1073/pnas.070036197.

Park, S.-H., Kukushkin, Y., Gupta, R., Chen, T., Konagai, A., Hipp, Mark S., Hayer-Hartl, M. and Hartl, F. U. (2013). PolyQ proteins interfere with nuclear degradation of cytosolic proteins by sequestering the Sis1p chaperone. *Cell* **154**, 134-145. https://doi.org/10.1016/j.cell.2013.06.003.

Park, S. and Colwell, C. S. (2019). Do disruptions in the circadian timing system contribute to autonomic dysfunction in Huntington's disease? *Yale J Biol Med* **92**, 291-303.

Park, Y., Kim, W., Kim, A. Y., Choi, H. J., Choi, J. K., Park, N., Koh, E. K., Seo, J. and Koh, Y. H. (2011). Normal prion protein in *Drosophila* enhances the toxicity of pathogenic polyglutamine proteins and alters susceptibility to oxidative and autophagy signaling modulators. *Biochem Biophys Res Commun* **404**, 638-45. https://doi.org/10.1016/j.bbrc.2010.12.030.

Patke, A., Young, M. W. and Axelrod, S. (2020). Molecular mechanisms and physiological importance of circadian rhythms. *Nat Rev Mol Cell Biol* **21**, 67-84. https://doi.org/10.1038/s41580-019-0179-2.

Patrick, R. P. and Johnson, T. L. (2021). Sauna use as a lifestyle practice to extend healthspan. *Exp Gerontol* **154**, 111509. https://doi.org/10.1016/j.exger.2021.111509.

References

Paul, B. D. and Snyder, S. H. (2019). Impaired redox signaling in Huntington's disease: Therapeutic implications. *Front Mol Neurosci* **12**, 68. https://doi.org/10.3389/fnmol.2019.00068.

Paulsen, J. S. (2010). Early detection of Huntington disease. *Future Neurol* **5**. https://doi.org/10.2217/fnl.09.78.

Paulson, H. (2018). Repeat expansion diseases: Elsevier. https://doi.org/10.1016/b978-0-444-63233-3.00009-9.

Paulson, H. L., Perez, M. K., Trottier, Y., Trojanowski, J. Q., Subramony, S. H., Das, S. S., Vig, P., Mandel, J. L., Fischbeck, K. H. and Pittman, R. N. (1997). Intranuclear inclusions of expanded polyglutamine protein in spinocerebellar ataxia type 3. *Neuron* **19**, 333-44. https://doi.org/10.1016/s0896-6273(00)80943-5.

Paulson, H. L., Shakkottai, V. G., Clark, H. B. and Orr, H. T. (2017). Polyglutamine spinocerebellar ataxias - from genes to potential treatments. *Nat Rev Neurosci* **18**, 613-626. https://doi.org/10.1038/nrn.2017.92.

Pavel, M., Imarisio, S., Menzies, F. M., Jimenez-Sanchez, M., Siddiqi, F. H., Wu, X., Renna, M., O'Kane, C. J., Crowther, D. C. and Rubinsztein, D. C. (2016). CCT complex restricts neuropathogenic protein aggregation via autophagy. *Nat Commun* **7**, 13821. https://doi.org/10.1038/ncomms13821.

Pchitskaya, E., Popugaeva, E. and Bezprozvanny, I. (2018). Calcium signaling and molecular mechanisms underlying neurodegenerative diseases. *Cell Calcium* **70**, 87-94. https://doi.org/10.1016/j.ceca.2017.06.008.

Pecho-Vrieseling, E., Rieker, C., Fuchs, S., Bleckmann, D., Esposito, M. S., Botta, P., Goldstein, C., Bernhard, M., Galimberti, I., Müller, M. et al. (2014). Transneuronal propagation of mutant huntingtin contributes to non-cell autonomous pathology in neurons. *Nat Neurosci* **17**, 1064-72. https://doi.org/10.1038/nn.3761.

Pedroso, J. L., Braga-Neto, P., Martinez, A. R. M., Martins, C. R., Rezende Filho, F. M., Sobreira-Neto, M. A., Prado, L. B. F., do Prado, G. F., França, M. C. and Barsottini, O. G. P. (2016). Sleep disorders in Machado–Joseph disease. *Current Opinion in Psychiatry* **29**, 402-408. https://doi.org/10.1097/yco.0000000000000287.

Peng, Y., Stoleru, D., Levine, J. D., Hall, J. C. and Rosbash, M. (2003). *Drosophila* free-running rhythms require intercellular communication. *PLoS Biol* **1**, E13. https://doi.org/10.1371/journal.pbio.0000013.

Peretti, D., Bastide, A., Radford, H., Verity, N., Molloy, C., Martin, M. G., Moreno, J. A., Steinert, J. R., Smith, T., Dinsdale, D. et al. (2015). RBM3 mediates structural plasticity and protective effects of cooling in neurodegeneration. *Nature* **518**, 236-9. https://doi.org/10.1038/nature14142.

Perevozchikova, T., Stanley, C. B., McWilliams-Koeppen, H. P., Rowe, E. L. and Berthelier, V. (2014). Investigating the structural impact of the glutamine repeat in huntingtin assembly. *Biophys J* **107**, 411-421. https://doi.org/10.1016/j.bpj.2014.06.002.

Pérez-Navarro, E., Canals, J. M., Ginés, S. and Alberch, J. (2006). Cellular and molecular mechanisms involved in the selective vulnerability of striatal projection neurons in Huntington's disease. *Histol Histopathol* **21**, 1217-32. https://doi.org/10.14670/hh-21.1217.

References

Persichetti, F., Ambrose, C. M., Ge, P., McNeil, S. M., Srinidhi, J., Anderson, M. A., Jenkins, B., Barnes, G. T., Duyao, M. P., Kanaley, L. et al. (1995). Normal and expanded Huntington's disease gene alleles produce distinguishable proteins due to translation across the CAG repeat. *Mol Med* **1**, 374-83.

Peschel, N., Chen, K. F., Szabo, G. and Stanewsky, R. (2009). Light-dependent interactions between the *Drosophila* circadian clock factors cryptochrome, jetlag, and timeless. *Curr Biol* **19**, 241-7. https://doi.org/10.1016/j.cub.2008.12.042.

Peschel, N. and Helfrich-Förster, C. (2011). Setting the clock--by nature: circadian rhythm in the fruitfly *Drosophila melanogaster*. *FEBS Lett* **585**, 1435-42. https://doi.org/10.1016/j.febslet.2011.02.028.

Peters-Libeu, C., Miller, J., Rutenber, E., Newhouse, Y., Krishnan, P., Cheung, K., Hatters, D., Brooks, E., Widjaja, K., Tran, T. et al. (2012). Disease-associated polyglutamine stretches in monomeric huntingtin adopt a compact structure. *J Mol Biol* **421**, 587-600. https://doi.org/10.1016/j.jmb.2012.01.034.

Petersén, A. and Gabery, S. (2012). Hypothalamic and limbic system changes in Huntington's disease. *J Huntingtons Dis* **1**, 5-16. https://doi.org/10.3233/jhd-2012-120006.

Petsakou, A., Sapsis, T. P. and Blau, J. (2015). Circadian rhythms in Rho1 activity regulate neuronal plasticity and network hierarchy. *Cell* **162**, 823-35. https://doi.org/10.1016/j.cell.2015.07.010.

Pfeiffenberger, C., Lear, B. C., Keegan, K. P. and Allada, R. (2010). Processing circadian data collected from the *Drosophila* Activity Monitoring (DAM) System. *Cold Spring Harb Protoc* **2010**, pdb prot5519. https://doi.org/10.1101/pdb.prot5519.

Pfeiffer, B. D., Truman, J. W. and Rubin, G. M. (2012). Using translational enhancers to increase transgene expression in *Drosophila*. *Proc Natl Acad Sci U S A* **109**, 6626-31. https://doi.org/10.1073/pnas.1204520109.

Piano, C., Losurdo, A., Della Marca, G., Solito, M., Calandra-Buonaura, G., Provini, F., Bentivoglio, A. R. and Cortelli, P. (2015). Polysomnographic findings and clinical correlates in Huntington disease: A cross-sectional cohort study. *Sleep* **38**, 1489-95. https://doi.org/10.5665/sleep.4996.

Pickard, A., Chang, J., Alachkar, N., Calverley, B., Garva, R., Arvan, P., Meng, Q. J. and Kadler, K. E. (2019). Preservation of circadian rhythms by the protein folding chaperone, BiP. *FASEB J* **33**, 7479-7489. https://doi.org/10.1096/fj.201802366RR.

Picot, M., Klarsfeld, A., Chélot, E., Malpel, S. and Rouyer, F. (2009). A role for blind DN2 clock neurons in temperature entrainment of the *Drosophila* larval brain. *J Neurosci* **29**, 8312-20. https://doi.org/10.1523/jneurosci.0279-08.2009.

Pieri, L., Madiona, K., Bousset, L. and Melki, R. (2012). Fibrillar α-synuclein and huntingtin exon 1 assemblies are toxic to the cells. *Biophys J* **102**, 2894-905. https://doi.org/10.1016/j.bpj.2012.04.050.

Pirez, N., Bernabei-Cornejo, S. G., Fernandez-Acosta, M., Duhart, J. M. and Ceriani, M. F. (2019). Contribution of non-circadian neurons to the temporal organization of locomotor activity. *Biol Open* **8**. https://doi.org/10.1242/bio.039628.

References

Pittendrigh, C. S. (1954). On temperature independence in the clock system controlling emergence time in *Drosophila*. *Proc Natl Acad Sci U S A* **40**, 1018-29. https://doi.org/10.1073/pnas.40.10.1018.

Pittendrigh, C. S. (1960). Circadian rhythms and the circadian organization of living systems. *Cold Spring Harb Symp Quant Biol* **25**, 159-84. https://doi.org/10.1101/sqb.1960.025.01.015.

Pittendrigh, C. S. and Daan, S. (1976). A functional analysis of circadian pacemakers in nocturnal rodents: IV. Entrainment: Pacemaker as clock. *Journal of comparative physiology* **106**, 291-331. https://doi.org/10.1007/BF01417859.

Pittendrigh, C. S. and Minis, D. H. (1972). Circadian systems: longevity as a function of circadian resonance in *Drosophila melanogaster*. *Proc Natl Acad Sci U S A* **69**, 1537-9. https://doi.org/10.1073/pnas.69.6.1537.

Podvin, S., Reardon, H. T., Yin, K., Mosier, C. and Hook, V. (2019). Multiple clinical features of Huntington's disease correlate with mutant HTT gene CAG repeat lengths and neurodegeneration. *J Neurol* **266**, 551-564. https://doi.org/10.1007/s00415-018-8940-6.

Podvin, S., Rosenthal, S. B., Poon, W., Wei, E., Fisch, K. M. and Hook, V. (2022). Mutant huntingtin protein interaction map implicates dysregulation of multiple cellular pathways in neurodegeneration of Huntington's disease. *J Huntingtons Dis* **11**, 243-267. https://doi.org/10.3233/jhd-220538.

Poirier, M. A., Li, H., Macosko, J., Cai, S., Amzel, M. and Ross, C. A. (2002). Huntingtin spheroids and protofibrils as precursors in polyglutamine fibrilization. *J Biol Chem* **277**, 41032-7. https://doi.org/10.1074/jbc.M205809200.

Politis, M., Pavese, N., Tai, Y. F., Tabrizi, S. J., Barker, R. A. and Piccini, P. (2008). Hypothalamic involvement in Huntington's disease: an in vivo PET study. *Brain* **131**, 2860-9. https://doi.org/10.1093/brain/awn244.

Pollak, C. P. and Perlick, D. (1991). Sleep problems and institutionalization of the elderly. *J Geriatr Psychiatry Neurol* **4**, 204-10. https://doi.org/10.1177/089198879100400405.

Popiel, H. A., Takeuchi, T., Fujita, H., Yamamoto, K., Ito, C., Yamane, H., Muramatsu, S., Toda, T., Wada, K. and Nagai, Y. (2012). Hsp40 gene therapy exerts therapeutic effects on polyglutamine disease mice via a non-cell autonomous mechanism. *PLoS One* **7**, e51069. https://doi.org/10.1371/journal.pone.0051069.

Potdar, S. and Sheeba, V. (2012). Large ventral lateral neurons determine the phase of evening activity peak across photoperiods in *Drosophila melanogaster*. *J Biol Rhythms* **27**, 267-79. https://doi.org/10.1177/0748730412449820.

Potter, G. D., Skene, D. J., Arendt, J., Cade, J. E., Grant, P. J. and Hardie, L. J. (2016). Circadian rhythm and sleep disruption: Causes, metabolic consequences, and countermeasures. *Endocr Rev* **37**, 584-608. https://doi.org/10.1210/er.2016-1083.

Power, D., Srinivasan, S. and Gunawardena, S. (2012). In-vivo evidence for the disruption of Rab11 vesicle transport by loss of huntingtin. *Neuroreport* **23**, 970-7. https://doi.org/10.1097/WNR.0b013e328359d990.

References

Prabhakaran, P. M. and Sheeba, V. (2013). Insights into differential activity patterns of *Drosophilids* under semi-natural conditions. *J Exp Biol* **216**, 4691-702. https://doi.org/10.1242/jeb.092270.

Prabhakaran, P. M. and Sheeba, V. (2014). Temperature sensitivity of circadian clocks is conserved across *Drosophila* species *melanogaster*, *malerkotliana* and *ananassae*. *Chronobiol Int* **31**, 1008-16. https://doi.org/10.3109/07420528.2014.941471.

Prakash, P., Nambiar, A. and Sheeba, V. (2017). Oscillating PDF in termini of circadian pacemaker neurons and synchronous molecular clocks in downstream neurons are not sufficient for sustenance of activity rhythms in constant darkness. *PLoS One* **12**, e0175073. https://doi.org/10.1371/journal.pone.0175073.

Prakash, P., Pradhan, A. K. and Sheeba, V. (2022). Hsp40 overexpression in pacemaker neurons delays circadian dysfunction in a *Drosophila* model of Huntington's disease. *Dis Model Mech* **15**. https://doi.org/10.1242/dmm.049447.

Pramanik, S., Basu, P., Gangopadhaya, P. K., Sinha, K. K., Jha, D. K., Sinha, S., Das, S. K., Maity, B. K., Mukherjee, S. C., Roychoudhuri, S. et al. (2000). Analysis of CAG and CCG repeats in huntingtin gene among HD patients and normal populations of India. *Eur J Hum Genet* **8**, 678-82. https://doi.org/10.1038/sj.ejhg.5200515.

Pratt, W. B., Gestwicki, J. E., Osawa, Y. and Lieberman, A. P. (2015). Targeting Hsp90/Hsp70-based protein quality control for treatment of adult onset neurodegenerative diseases. *Annual Review of Pharmacology and Toxicology* **55**, 353-371. https://doi.org/10.1146/annurev-pharmtox-010814-124332.

Preußner, M., Goldammer, G., Neumann, A., Haltenhof, T., Rautenstrauch, P., Müller-McNicoll, M. and Heyd, F. (2017). Body Temperature cycles control rhythmic alternative splicing in mammals. *Mol Cell* **67**, 433-446.e4. https://doi.org/10.1016/j.molcel.2017.06.006.

Price, J. L., Dembinska, M. E., Young, M. W. and Rosbash, M. (1995). Suppression of PERIOD protein abundance and circadian cycling by the *Drosophila* clock mutation timeless. *Embo j* **14**, 4044-9. https://doi.org/10.1002/j.1460-2075.1995.tb00075.x.

Pringsheim, T., Wiltshire, K., Day, L., Dykeman, J., Steeves, T. and Jette, N. (2012). The incidence and prevalence of Huntington's disease: a systematic review and meta-analysis. *Mov Disord* **27**, 1083-91. https://doi.org/10.1002/mds.25075.

Priya, S. B. and Gromiha, M. M. (2019). Structural insights into the aggregation mechanism of huntingtin exon 1 protein fragment with different polyQ-lengths. *J Cell Biochem* **120**, 10519-10529. https://doi.org/10.1002/jcb.28338.

Qi, L. and Zhang, X. D. (2014). Role of chaperone-mediated autophagy in degrading Huntington's disease-associated huntingtin protein. *Acta Biochim Biophys Sin (Shanghai)* **46**, 83-91. https://doi.org/10.1093/abbs/gmt133.

Qi, L., Zhang, X. D., Wu, J. C., Lin, F., Wang, J., DiFiglia, M. and Qin, Z. H. (2012). The role of chaperone-mediated autophagy in huntingtin degradation. *PLoS One* **7**, e46834. https://doi.org/10.1371/journal.pone.0046834.

References

Qin, Z. H., Wang, Y., Kegel, K. B., Kazantsev, A., Apostol, B. L., Thompson, L. M., Yoder, J., Aronin, N. and DiFiglia, M. (2003). Autophagy regulates the processing of amino terminal huntingtin fragments. *Hum Mol Genet* **12**, 3231-44. https://doi.org/10.1093/hmg/ddg346.

Qin, Z. H., Wang, Y., Sapp, E., Cuiffo, B., Wanker, E., Hayden, M. R., Kegel, K. B., Aronin, N. and DiFiglia, M. (2004). Huntingtin bodies sequester vesicle-associated proteins by a polyproline-dependent interaction. *J Neurosci* **24**, 269-81. https://doi.org/10.1523/JNEUROSCI.1409-03.2004.

Racinais, S., Wilson, M. G. and Périard, J. D. (2017). Passive heat acclimation improves skeletal muscle contractility in humans. *Am J Physiol Regul Integr Comp Physiol* **312**, R101-r107. https://doi.org/10.1152/ajpregu.00431.2016.

Radons, J. (2016). The human HSP70 family of chaperones: where do we stand? *Cell Stress Chaperones* **21**, 379-404. https://doi.org/10.1007/s12192-016-0676-6.

Rai, S. N., Singh, B. K., Rathore, A. S., Zahra, W., Keswani, C., Birla, H., Singh, S. S., Dilnashin, H. and Singh, S. P. (2019). Quality control in Huntington's disease: A therapeutic target. *Neurotox Res* **36**, 612-626. https://doi.org/10.1007/s12640-019-00087-x.

Raj, K. and Sarkar, S. (2017). Transactivation domain of human c-Myc is essential to alleviate poly(Q)-mediated neurotoxicity in *Drosophila* disease models. *J Mol Neurosci* **62**, 55-66. https://doi.org/10.1007/s12031-017-0910-4.

Rakshit, K. and Giebultowicz, J. M. (2013). Cryptochrome restores dampened circadian rhythms and promotes healthspan in aging *Drosophila*. *Aging Cell* **12**, 752-62. https://doi.org/10.1111/acel.12100.

Ramdzan, Y. M., Trubetskov, M. M., Ormsby, A. R., Newcombe, E. A., Sui, X., Tobin, M. J., Bongiovanni, M. N., Gras, S. L., Dewson, G., Miller, J. M. L. et al. (2017). Huntingtin inclusions trigger cellular quiescence, deactivate apoptosis, and lead to delayed necrosis. *Cell Rep* **19**, 919-927. https://doi.org/10.1016/j.celrep.2017.04.029.

Ramírez-Jarquín, U. N., Sharma, M., Shahani, N., Li, Y., Boregowda, S. and Subramaniam, S. (2022). Rhes protein transits from neuron to neuron and facilitates mutant huntingtin spreading in the brain. *Sci Adv* **8**, eabm3877. https://doi.org/10.1126/sciadv.abm3877.

Rampelt, H., Kirstein-Miles, J., Nillegoda, N. B., Chi, K., Scholz, S. R., Morimoto, R. I. and Bukau, B. (2012). Metazoan Hsp70 machines use Hsp110 to power protein disaggregation. *Embo j* **31**, 4221-35. https://doi.org/10.1038/emboj.2012.264.

Rao, D. S., Chang, J. C., Kumar, P. D., Mizukami, I., Smithson, G. M., Bradley, S. V., Parlow, A. F. and Ross, T. S. (2001). Huntingtin interacting protein 1 Is a clathrin coat binding protein required for differentiation of late spermatogenic progenitors. *Mol Cell Biol* **21**, 7796-806. https://doi.org/10.1128/mcb.21.22.7796-7806.2001.

Raspe, M., Gillis, J., Krol, H., Krom, S., Bosch, K., van Veen, H. and Reits, E. (2009). Mimicking proteasomal release of polyglutamine peptides initiates aggregation and toxicity. *J Cell Sci* **122**, 3262-71. https://doi.org/10.1242/jcs.045567.

Ratovitski, T., Chighladze, E., Arbez, N., Boronina, T., Herbrich, S., Cole, R. N. and Ross, C. A. (2012). Huntingtin protein interactions altered by polyglutamine expansion as determined by quantitative proteomic analysis. *Cell Cycle* **11**, 2006-21. https://doi.org/10.4161/cc.20423.

References

Rattan, S. I. (1998). Repeated mild heat shock delays ageing in cultured human skin fibroblasts. *Biochem Mol Biol Int* **45**, 753-9. https://doi.org/10.1080/15216549800203162.

Rattan, S. I. (2006). Hormetic modulation of aging and longevity by mild heat stress. *Dose Response* **3**, 533-46. https://doi.org/10.2203/dose-response.003.04.008.

Rattan, S. I., Fernandes, R. A., Demirovic, D., Dymek, B. and Lima, C. F. (2009). Heat stress and hormetin-induced hormesis in human cells: effects on aging, wound healing, angiogenesis, and differentiation. *Dose Response* **7**, 90-103. https://doi.org/10.2203/dose-response.08-014.Rattan.

Raupach, A. K., Ehgoetz Martens, K. A., Memarian, N., Zhong, G., Matar, E., Halliday, G. M., Grunstein, R. and Lewis, S. J. G. (2020). Assessing the role of nocturnal core body temperature dysregulation as a biomarker of neurodegeneration. *J Sleep Res* **29**, e12939. https://doi.org/10.1111/jsr.12939.

Ravikumar, B., Berger, Z., Vacher, C., O'Kane, C. J. and Rubinsztein, D. C. (2006). Rapamycin pre-treatment protects against apoptosis. *Hum Mol Genet* **15**, 1209-16. https://doi.org/10.1093/hmg/ddl036.

Ravikumar, B., Duden, R. and Rubinsztein, D. C. (2002). Aggregate-prone proteins with polyglutamine and polyalanine expansions are degraded by autophagy. *Hum Mol Genet* **11**, 1107-17. https://doi.org/10.1093/hmg/11.9.1107.

Ravikumar, B., Imarisio, S., Sarkar, S., O'Kane, C. J. and Rubinsztein, D. C. (2008). Rab5 modulates aggregation and toxicity of mutant huntingtin through macroautophagy in cell and fly models of Huntington disease. *J Cell Sci* **121**, 1649-60. https://doi.org/10.1242/jcs.025726.

Ravikumar, B., Vacher, C., Berger, Z., Davies, J. E., Luo, S., Oroz, L. G., Scaravilli, F., Easton, D. F., Duden, R., O'Kane, C. J. et al. (2004). Inhibition of mTOR induces autophagy and reduces toxicity of polyglutamine expansions in fly and mouse models of Huntington disease. *Nat Genet* **36**, 585-95. https://doi.org/10.1038/ng1362.

Ravina, B., Romer, M., Constantinescu, R., Biglan, K., Brocht, A., Kieburtz, K., Shoulson, I. and McDermott, M. P. (2008). The relationship between CAG repeat length and clinical progression in Huntington's disease. *Mov Disord* **23**, 1223-7. https://doi.org/10.1002/mds.21988.

Raymond, L. A., André, V. M., Cepeda, C., Gladding, C. M., Milnerwood, A. J. and Levine, M. S. (2011). Pathophysiology of Huntington's disease: Time-dependent alterations in synaptic and receptor function. *Neuroscience* **198**, 252-73. https://doi.org/10.1016/j.neuroscience.2011.08.052.

RCoreTeam. (2013). R: A language and environment for statistical computing. Vienna, Austria: http://www.R-project.org/.

Refinetti, R. (2010). Entrainment of circadian rhythm by ambient temperature cycles in mice. *J Biol Rhythms* **25**, 247-56. https://doi.org/10.1177/0748730410372074.

Refinetti, R. (2015). Comparison of light, food, and temperature as environmental synchronizers of the circadian rhythm of activity in mice. *J Physiol Sci* **65**, 359-66. https://doi.org/10.1007/s12576-015-0374-7.

Refinetti, R. (2020). Circadian rhythmicity of body temperature and metabolism. *Temperature (Austin)* **7**, 321-362. https://doi.org/10.1080/23328940.2020.1743605.

References

Refinetti, R. and Menaker, M. (1992). The circadian rhythm of body temperature. *Physiol Behav* **51**, 613-37. https://doi.org/10.1016/0031-9384(92)90188-8.

Reiner, A. and Deng, Y. P. (2018). Disrupted striatal neuron inputs and outputs in Huntington's disease. *CNS Neurosci Ther* **24**, 250-280. https://doi.org/10.1111/cns.12844.

Reiner, A., Dragatsis, I. and Dietrich, P. (2011). Genetics and neuropathology of Huntington's disease. *Int Rev Neurobiol* **98**, 325-72. https://doi.org/10.1016/b978-0-12-381328-2.00014-6.

Reiner, A., Dragatsis, I., Zeitlin, S. and Goldowitz, D. (2003). Wild-type huntingtin plays a role in brain development and neuronal survival. *Mol Neurobiol* **28**, 259-76. https://doi.org/10.1385/mn:28:3:259.

Reinhard, N., Bertolini, E., Saito, A., Sekiguchi, M., Yoshii, T., Rieger, D. and Helfrich-Förster, C. (2022). The lateral posterior clock neurons of *Drosophila melanogaster* express three neuropeptides and have multiple connections within the circadian clock network and beyond. *J Comp Neurol* **530**, 1507-1529. https://doi.org/10.1002/cne.25294.

Reinke, H., Saini, C., Fleury-Olela, F., Dibner, C., Benjamin, I. J. and Schibler, U. (2008). Differential display of DNA-binding proteins reveals heat-shock factor 1 as a circadian transcription factor. *Genes Dev* **22**, 331-45. https://doi.org/10.1101/gad.453808.

Reis, S. D., Pinho, B. R. and Oliveira, J. M. A. (2016). Modulation of molecular chaperones in Huntington's disease and other polyglutamine disorders. *Mol Neurobiol* **54**, 5829-5854. https://doi.org/10.1007/s12035-016-0120-z.

Reiter, L. T., Potocki, L., Chien, S., Gribskov, M. and Bier, E. (2001a). A systematic analysis of human disease-associated gene sequences in *Drosophila melanogaster*. *Genome Res* **11**, 1114-25. https://doi.org/10.1101/gr.169101.

Reiter, R. J., Acuna-Castroviejo, D., Tan, D. X. and Burkhardt, S. (2001b). Free radical-mediated molecular damage. Mechanisms for the protective actions of melatonin in the central nervous system. *Ann N Y Acad Sci* **939**, 200-15. https://doi.org/10.1111/j.1749-6632.2001.tb03627.x.

Renn, S. C., Park, J. H., Rosbash, M., Hall, J. C. and Taghert, P. H. (1999). A *pdf* neuropeptide gene mutation and ablation of PDF neurons each cause severe abnormalities of behavioral circadian rhythms in *Drosophila*. *Cell* **99**, 791-802. https://doi.org/10.1016/S0092-8674(00)81676-1.

Rensing, L. and Ruoff, P. (2002). Temperature effect on entrainment, phase shifting, and amplitude of circadian clocks and its molecular bases. *Chronobiol Int* **19**, 807-64. https://doi.org/10.1081/cbi-120014569.

Reppert, S. M. and Weaver, D. R. (2002). Coordination of circadian timing in mammals. *Nature* **418**, 935-41. https://doi.org/10.1038/nature00965.

Rey, G., Milev, N. B., Valekunja, U. K., Ch, R., Ray, S., Silva Dos Santos, M., Nagy, A. D., Antrobus, R., MacRae, J. I. and Reddy, A. B. (2018). Metabolic oscillations on the circadian time scale in *Drosophila* cells lacking clock genes. *Mol Syst Biol* **14**, e8376. https://doi.org/10.15252/msb.20188376.

Rezaval, C. (2015). 'The greatness of the smallest ones': The most valuable attributes of flies and worms for the study of neurodegeneration. In *Young perspectives for old diseases*, (ed. G. N. M. Hajj), pp. 49-84: Bentham Science Publishers. https://doi.org/10.2174/97816080599281150101.

References

Rezaval, C., Berni, J., Gorostiza, E. A., Werbajh, S., Fagilde, M. M., Fernandez, M. P., Beckwith, E. J., Aranovich, E. J., Sabio y Garcia, C. A. and Ceriani, M. F. (2008). A functional misexpression screen uncovers a role for *enabled* in progressive neurodegeneration. *PLoS One* **3**, e3332. https://doi.org/10.1371/journal.pone.0003332.

Rezaval, C., Werbajh, S. and Ceriani, M. F. (2007). Neuronal death in *Drosophila* triggered by GAL4 accumulation. *Eur J Neurosci* **25**, 683-94. https://doi.org/10.1111/j.1460-9568.2007.05317.x.

Richards, P., Didszun, C., Campesan, S., Simpson, A., Horley, B., Young, K. W., Glynn, P., Cain, K., Kyriacou, C. P., Giorgini, F. et al. (2011). Dendritic spine loss and neurodegeneration is rescued by Rab11 in models of Huntington's disease. *Cell Death Differ* **18**, 191-200. https://doi.org/10.1038/cdd.2010.127.

Rieder, L. E., Savva, Y. A., Reyna, M. A., Chang, Y. J., Dorsky, J. S., Rezaei, A. and Reenan, R. A. (2015). Dynamic response of RNA editing to temperature in *Drosophila*. *BMC Biol* **13**, 1. https://doi.org/10.1186/s12915-014-0111-3.

Rieger, D., Shafer, O. T., Tomioka, K. and Helfrich-Förster, C. (2006). Functional analysis of circadian pacemaker neurons in *Drosophila melanogaster*. *J Neurosci* **26**, 2531-43. https://doi.org/10.1523/jneurosci.1234-05.2006.

Riemersma-van der Lek, R. F., Swaab, D. F., Twisk, J., Hol, E. M., Hoogendijk, W. J. and Van Someren, E. J. (2008). Effect of bright light and melatonin on cognitive and noncognitive function in elderly residents of group care facilities: a randomized controlled trial. *Jama* **299**, 2642-55. https://doi.org/10.1001/jama.299.22.2642.

Rigamonti, D., Bauer, J. H., De-Fraja, C., Conti, L., Sipione, S., Sciorati, C., Clementi, E., Hackam, A., Hayden, M. R., Li, Y. et al. (2000). Wild-type huntingtin protects from apoptosis upstream of caspase-3. *J Neurosci* **20**, 3705-13. https://doi.org/10.1523/jneurosci.20-10-03705.2000.

Rigamonti, D., Sipione, S., Goffredo, D., Zuccato, C., Fossale, E. and Cattaneo, E. (2001). Huntingtin's neuroprotective activity occurs via inhibition of procaspase-9 processing. *J Biol Chem* **276**, 14545-8. https://doi.org/10.1074/jbc.C100044200.

Riguet, N., Mahul-Mellier, A. L., Maharjan, N., Burtscher, J., Croisier, M., Knott, G., Hastings, J., Patin, A., Reiterer, V., Farhan, H. et al. (2021). Nuclear and cytoplasmic huntingtin inclusions exhibit distinct biochemical composition, interactome and ultrastructural properties. *Nat Commun* **12**, 6579. https://doi.org/10.1038/s41467-021-26684-z.

Rios Romenets, S., Creti, L., Fichten, C., Bailes, S., Libman, E., Pelletier, A. and Postuma, R. B. (2013). Doxepin and cognitive behavioural therapy for insomnia in patients with Parkinson's disease -- a randomized study. *Parkinsonism Relat Disord* **19**, 670-5. https://doi.org/10.1016/j.parkreldis.2013.03.003.

Rix, R. R. and Cutler, G. C. (2022). Review of molecular and biochemical responses during stress induced stimulation and hormesis in insects. *Sci Total Environ* **827**, 154085. https://doi.org/10.1016/j.scitotenv.2022.154085.

Robertson, A. L. and Bottomley, S. P. (2010). Towards the treatment of polyglutamine diseases: the modulatory role of protein context. *Curr Med Chem* **17**, 3058-68. https://doi.org/10.2174/092986710791959800.

References

Roby, D. A., Ruiz, F., Kermath, B. A., Voorhees, J. R., Niehoff, M., Zhang, J., Morley, J. E., Musiek, E. S., Farr, S. A. and Burris, T. P. (2019). Pharmacological activation of the nuclear receptor REV-ERB reverses cognitive deficits and reduces amyloid-β burden in a mouse model of Alzheimer's disease. *PLoS One* **14**, e0215004. https://doi.org/10.1371/journal.pone.0215004.

Rocha, N. P., Charron, O., Colpo, G. D., Latham, L. B., Patino, J. E., Stimming, E. F., Freeman, L. and Teixeira, A. L. (2022). Cerebral blood flow is associated with markers of neurodegeneration in Huntington's disease. *Parkinsonism Relat Disord* **102**, 79-85. https://doi.org/10.1016/j.parkreldis.2022.07.024.

Rodgers, E. M. and Gomez Isaza, D. F. (2021). Harnessing the potential of cross-protection stressor interactions for conservation: A review. *Conserv Physiol* **9**, coab037. https://doi.org/10.1093/conphys/coab037.

Rodrigues, F. B., Abreu, D., Damásio, J., Goncalves, N., Correia-Guedes, L., Coelho, M. and Ferreira, J. J. (2017). Survival, mortality, causes and places of death in a European Huntington's disease prospective cohort. *Mov Disord Clin Pract* **4**, 737-742. https://doi.org/10.1002/mdc3.12502.

Roenneberg, T., Foster, R. G. and Klerman, E. B. (2022). The circadian system, sleep, and the health/disease balance: A conceptual review. *J Sleep Res* **31**, e13621. https://doi.org/10.1111/jsr.13621.

Roenneberg, T. and Merrow, M. (2016). The circadian clock and human health. *Curr Biol* **26**, R432-43. https://doi.org/10.1016/j.cub.2016.04.011.

Roessingh, S., Rosing, M., Marunova, M., Ogueta, M., George, R., Lamaze, A. and Stanewsky, R. (2019). Temperature synchronization of the *Drosophila* circadian clock protein PERIOD is controlled by the TRPA channel PYREXIA. *Commun Biol* **2**, 246. https://doi.org/10.1038/s42003-019-0497-0.

Roessingh, S., Wolfgang, W. and Stanewsky, R. (2015). Loss of *Drosophila melanogaster* TRPA1 function affects "Siesta" behavior but not synchronization to temperature cycles. *J Biol Rhythms* **30**, 492-505. https://doi.org/10.1177/0748730415605633.

Romeo, S., Viaggi, C., Di Camillo, D., Willis, A. W., Lozzi, L., Rocchi, C., Capannolo, M., Aloisi, G., Vaglini, F., Maccarone, R. et al. (2013). Bright light exposure reduces TH-positive dopamine neurons: Implications of light pollution in Parkinson's disease epidemiology. *Sci Rep* **3**, 1395. https://doi.org/10.1038/srep01395.

Romero, E., Cha, G. H., Verstreken, P., Ly, C. V., Hughes, R. E., Bellen, H. J. and Botas, J. (2008). Suppression of neurodegeneration and increased neurotransmission caused by expanded full-length huntingtin accumulating in the cytoplasm. *Neuron* **57**, 27-40. https://doi.org/10.1016/j.neuron.2007.11.025.

Romo, L., Mohn, E. S. and Aronin, N. (2018). A Fresh Look at Huntingtin mRNA Processing in Huntington's Disease. *J Huntingtons Dis* **7**, 101-108. https://doi.org/10.3233/JHD-180292.

Roos, R. A. (2010). Huntington's disease: A clinical review. *Orphanet J Rare Dis* **5**, 40. https://doi.org/10.1186/1750-1172-5-40.

Rosas-Arellano, A., Estrada-Mondragon, A., Pina, R., Mantellero, C. A. and Castro, M. A. (2018). The tiny *Drosophila melanogaster* for the biggest answers in Huntington's disease. *Int J Mol Sci* **19**. https://doi.org/10.3390/ijms19082398.

References

Rosas, H. D., Koroshetz, W. J., Chen, Y. I., Skeuse, C., Vangel, M., Cudkowicz, M. E., Caplan, K., Marek, K., Seidman, L. J., Makris, N. et al. (2003). Evidence for more widespread cerebral pathology in early HD: An MRI-based morphometric analysis. *Neurology* **60**, 1615-20. https://doi.org/10.1212/01.wnl.0000065888.88988.6e.

Roselli, F. and Caroni, P. (2015). From intrinsic firing properties to selective neuronal vulnerability in neurodegenerative diseases. *Neuron* **85**, 901-10. https://doi.org/10.1016/j.neuron.2014.12.063.

Rosenblatt, A., Kumar, B. V., Mo, A., Welsh, C. S., Margolis, R. L. and Ross, C. A. (2012). Age, CAG repeat length, and clinical progression in Huntington's disease. *Mov Disord* **27**, 272-6. https://doi.org/10.1002/mds.24024.

Ross, C. A. and Poirier, M. A. (2004). Protein aggregation and neurodegenerative disease. *Nat Med* **10 Suppl**, S10-7. https://doi.org/10.1038/nm1066.

Ross, C. A. and Tabrizi, S. J. (2011). Huntington's disease: From molecular pathogenesis to clinical treatment. *Lancet Neurol* **10**, 83-98. https://doi.org/10.1016/s1474-4422(10)70245-3.

Rossetti, G., Magistrato, A., Pastore, A., Persichetti, F. and Carloni, P. (2008). Structural properties of polyglutamine aggregates investigated via molecular dynamics simulations. *J Phys Chem B* **112**, 16843-50. https://doi.org/10.1021/jp806548p.

Rossnerova, A., Izzotti, A., Pulliero, A., Bast, A., Rattan, S. I. S. and Rossner, P. (2020). The molecular mechanisms of adaptive response related to environmental stress. *Int J Mol Sci* **21**. https://doi.org/10.3390/ijms21197053.

Roth, D. M., Hutt, D. M., Tong, J., Bouchecareilh, M., Wang, N., Seeley, T., Dekkers, J. F., Beekman, J. M., Garza, D., Drew, L. et al. (2014). Modulation of the maladaptive stress response to manage diseases of protein folding. *PLoS Biol* **12**, e1001998. https://doi.org/10.1371/journal.pbio.1001998.

Ruan, W., Yuan, X. and Eltzschig, H. K. (2021). Circadian rhythm as a therapeutic target. *Nat Rev Drug Discov* **20**, 287-307. https://doi.org/10.1038/s41573-020-00109-w.

Rüb, U., Vonsattel, J. P. G., Heinsen, H. and Korf, H.-W. (2015). The neuropathology of Huntington's disease: classical findings, recent developments and correlation to functional neuroanatomy: Springer Cham. https://doi.org/10.1007/978-3-319-19285-7.

Ruben, M. D., Smith, D. F., FitzGerald, G. A. and Hogenesch, J. B. (2019). Dosing time matters. *Science* **365**, 547-549. https://doi.org/10.1126/science.aax7621.

Rubin, G. M., Yandell, M. D., Wortman, J. R., Gabor Miklos, G. L., Nelson, C. R., Hariharan, I. K., Fortini, M. E., Li, P. W., Apweiler, R., Fleischmann, W. et al. (2000). Comparative genomics of the eukaryotes. *Science* **287**, 2204-15. https://doi.org/10.1126/science.287.5461.2204.

Rubinsztein, D. C., Leggo, J., Coles, R., Almqvist, E., Biancalana, V., Cassiman, J. J., Chotai, K., Connarty, M., Crauford, D., Curtis, A. et al. (1996). Phenotypic characterization of individuals with 30-40 CAG repeats in the Huntington disease (HD) gene reveals HD cases with 36 repeats and apparently normal elderly individuals with 36-39 repeats. *Am J Hum Genet* **59**, 16-22.

Ruby, N. F., Burns, D. E. and Heller, H. C. (1999). Circadian rhythms in the suprachiasmatic nucleus are temperature-compensated and phase-shifted by heat pulses in vitro. *J Neurosci* **19**, 8630-6. https://doi.org/10.1523/jneurosci.19-19-08630.1999.

References

Ruffini, N., Klingenberg, S., Schweiger, S. and Gerber, S. (2020). Common factors in Neurodegeneration: A meta-study revealing shared patterns on a multi-omics scale. *Cells* **9**. https://doi.org/10.3390/cells9122642.

Ruggieri, A., Saredi, S., Zanotti, S., Pasanisi, M. B., Maggi, L. and Mora, M. (2016). DNAJB6 myopathies: Focused review on an emerging and expanding group of myopathies. *Front Mol Biosci* **3**, 63. https://doi.org/10.3389/fmolb.2016.00063.

Rui, Y. N., Xu, Z., Patel, B., Chen, Z., Chen, D., Tito, A., David, G., Sun, Y., Stimming, E. F., Bellen, H. J. et al. (2015). Huntingtin functions as a scaffold for selective macroautophagy. *Nat Cell Biol* **17**, 262-75. https://doi.org/10.1038/ncb3101.

Rujano, M. A., Kampinga, H. H. and Salomons, F. A. (2007). Modulation of polyglutamine inclusion formation by the Hsp70 chaperone machine. *Exp Cell Res* **313**, 3568-78. https://doi.org/10.1016/j.yexcr.2007.07.034.

Rumanova, V. S., Okuliarova, M. and Zeman, M. (2020). Differential effects of constant light and dim light at night on the circadian control of metabolism and behavior. *Int J Mol Sci* **21**. https://doi.org/10.3390/ijms21155478.

Ruzo, A., Ismailoglu, I., Popowski, M., Haremaki, T., Croft, G. F., Deglincerti, A. and Brivanlou, A. H. (2015). Discovery of novel isoforms of huntingtin reveals a new hominid-specific exon. *PLoS One* **10**, e0127687. https://doi.org/10.1371/journal.pone.0127687.

Ryu, H., Lee, J., Hagerty, S. W., Soh, B. Y., McAlpin, S. E., Cormier, K. A., Smith, K. M. and Ferrante, R. J. (2006). ESET/SETDB1 gene expression and histone H3 (K9) trimethylation in Huntington's disease. *Proc Natl Acad Sci U S A* **103**, 19176-81. https://doi.org/10.1073/pnas.0606373103.

Ryzhikov, M., Ehlers, A., Steinberg, D., Xie, W., Oberlander, E., Brown, S., Gilmore, P. E., Townsend, R. R., Lane, W. S., Dolinay, T. et al. (2019). Diurnal rhythms spatially and temporally organize autophagy. *Cell Rep* **26**, 1880-1892.e6. https://doi.org/10.1016/j.celrep.2019.01.072.

Sabado, V., Vienne, L., Nunes, J. M., Rosbash, M. and Nagoshi, E. (2017). Fluorescence circadian imaging reveals a PDF-dependent transcriptional regulation of the *Drosophila* molecular clock. *Sci Rep* **7**, 41560. https://doi.org/10.1038/srep41560.

Sadri-Vakili, G., Bouzou, B., Benn, C. L., Kim, M. O., Chawla, P., Overland, R. P., Glajch, K. E., Xia, E., Qiu, Z., Hersch, S. M. et al. (2007). Histones associated with downregulated genes are hypo-acetylated in Huntington's disease models. *Hum Mol Genet* **16**, 1293-306. https://doi.org/10.1093/hmg/ddm078.

Sahl, S. J., Lau, L., Vonk, W. I., Weiss, L. E., Frydman, J. and Moerner, W. E. (2016). Delayed emergence of subdiffraction-sized mutant huntingtin fibrils following inclusion body formation. *Q Rev Biophys* **49**, e2. https://doi.org/10.1017/s0033583515000219.

Sahl, S. J., Weiss, L. E., Duim, W. C., Frydman, J. and Moerner, W. E. (2012). Cellular inclusion bodies of mutant huntingtin exon 1 obscure small fibrillar aggregate species. *Sci Rep* **2**, 895. https://doi.org/10.1038/srep00895.

Sahoo, B., Arduini, I., Drombosky, K. W., Kodali, R., Sanders, L. H., Greenamyre, J. T. and Wetzel, R. (2016). Folding landscape of mutant huntingtin exon1: Diffusible multimers, oligomers and

fibrils, and no detectable monomer. *PLoS One* **11**, e0155747. https://doi.org/10.1371/journal.pone.0155747.

Saini, C., Morf, J., Stratmann, M., Gos, P. and Schibler, U. (2012). Simulated body temperature rhythms reveal the phase-shifting behavior and plasticity of mammalian circadian oscillators. *Genes Dev* **26**, 567-80. https://doi.org/10.1101/gad.183251.111.

Sajjad, M. U., Green, E. W., Miller-Fleming, L., Hands, S., Herrera, F., Campesan, S., Khoshnan, A., Outeiro, T. F., Giorgini, F. and Wyttenbach, A. (2014). DJ-1 modulates aggregation and pathogenesis in models of Huntington's disease. *Hum Mol Genet* **23**, 755-66. https://doi.org/10.1093/hmg/ddt466.

Sakamoto, K. M., Kim, K. B., Kumagai, A., Mercurio, F., Crews, C. M. and Deshaies, R. J. (2001). Protacs: Chimeric molecules that target proteins to the Skp1-Cullin-F box complex for ubiquitination and degradation. *Proc Natl Acad Sci U S A* **98**, 8554-9. https://doi.org/10.1073/pnas.141230798.

Sala, A. J., Bott, L. C. and Morimoto, R. I. (2017). Shaping proteostasis at the cellular, tissue, and organismal level. *J Cell Biol* **216**, 1231-1241. https://doi.org/10.1083/jcb.201612111.

Salachan, P. V. and Sørensen, J. G. (2022). Molecular mechanisms underlying plasticity in a thermally varying environment. *Mol Ecol* **31**, 3174-3191. https://doi.org/10.1111/mec.16463.

Salinska, E., Danysz, W. and Lazarewicz, J. W. (2005). The role of excitotoxicity in neurodegeneration. *Folia Neuropathol* **43**, 322-39.

Salta, E. and De Strooper, B. (2017). Noncoding RNAs in neurodegeneration. *Nat Rev Neurosci* **18**, 627-640. https://doi.org/10.1038/nrn.2017.90.

Salvadores, N., Sanhueza, M., Manque, P. and Court, F. A. (2017). Axonal degeneration during aging and its functional role in neurodegenerative disorders. *Front Neurosci* **11**, 451. https://doi.org/10.3389/fnins.2017.00451.

Sameni, S., Zhang, R. and Digman, M. A. (2020). Number and molecular brightness analysis reveals Htt25Q protein aggregation upon the uptake of Htt97Q aggregates. *Biochem Biophys Res Commun* **522**, 133-137. https://doi.org/10.1016/j.bbrc.2019.10.041.

Sanchez, I., Mahlke, C. and Yuan, J. (2003). Pivotal role of oligomerization in expanded polyglutamine neurodegenerative disorders. *Nature* **421**, 373-9. https://doi.org/10.1038/nature01301.

Sang, T. K., Li, C., Liu, W., Rodriguez, A., Abrams, J. M., Zipursky, S. L. and Jackson, G. R. (2005). Inactivation of *Drosophila* Apaf-1 related killer suppresses formation of polyglutamine aggregates and blocks polyglutamine pathogenesis. *Hum Mol Genet* **14**, 357-72. https://doi.org/10.1093/hmg/ddi032.

Sap, K. A., Guler, A. T., Bury, A., Dekkers, D., Demmers, J. A. A. and Reits, E. A. (2021). Identification of full-length wild-type and mutant huntingtin interacting proteins by crosslinking immunoprecipitation in mice brain cortex. *J Huntingtons Dis* **10**, 335-347. https://doi.org/10.3233/jhd-210476.

Saper, C. B., Lu, J., Chou, T. C. and Gooley, J. (2005). The hypothalamic integrator for circadian rhythms. *Trends Neurosci* **28**, 152-7. https://doi.org/10.1016/j.tins.2004.12.009.

References

Sapp, E., Schwarz, C., Chase, K., Bhide, P. G., Young, A. B., Penney, J., Vonsattel, J. P., Aronin, N. and DiFiglia, M. (1997). Huntingtin localization in brains of normal and Huntington's disease patients. *Ann Neurol* **42**, 604-12. https://doi.org/10.1002/ana.410420411.

Sarkar, S. and Rubinsztein, D. C. (2008). Huntington's disease: Degradation of mutant huntingtin by autophagy. *Febs j* **275**, 4263-70. https://doi.org/10.1111/j.1742-4658.2008.06562.x.

Sarparanta, J., Jonson, P. H., Kawan, S. and Udd, B. (2020). Neuromuscular diseases due to chaperone mutations: A review and some new results. *Int J Mol Sci* **21**. https://doi.org/10.3390/ijms21041409.

Sarup, P., Sørensen, P. and Loeschcke, V. (2014). The long-term effects of a life-prolonging heat treatment on the *Drosophila melanogaster* transcriptome suggest that heat shock proteins extend lifespan. *Exp Gerontol* **50**, 34-9. https://doi.org/10.1016/j.exger.2013.11.017.

Sathasivam, K., Lane, A., Legleiter, J., Warley, A., Woodman, B., Finkbeiner, S., Paganetti, P., Muchowski, P. J., Wilson, S. and Bates, G. P. (2010). Identical oligomeric and fibrillar structures captured from the brains of R6/2 and knock-in mouse models of Huntington's disease. *Hum Mol Genet* **19**, 65-78. https://doi.org/10.1093/hmg/ddp467.

Sathasivam, K., Neueder, A., Gipson, T. A., Landles, C., Benjamin, A. C., Bondulich, M. K., Smith, D. L., Faull, R. L., Roos, R. A., Howland, D. et al. (2013). Aberrant splicing of HTT generates the pathogenic exon 1 protein in Huntington disease. *Proc Natl Acad Sci U S A* **110**, 2366-70. https://doi.org/10.1073/pnas.1221891110.

Saudou, F., Finkbeiner, S., Devys, D. and Greenberg, M. E. (1998). Huntingtin acts in the nucleus to induce apoptosis but death does not correlate with the formation of intranuclear inclusions. *Cell* **95**, 55-66. https://doi.org/10.1016/s0092-8674(00)81782-1.

Saudou, F. and Humbert, S. (2016). The Biology of Huntingtin. *Neuron* **89**, 910-26. https://doi.org/10.1016/j.neuron.2016.02.003.

Savas, J. N., Makusky, A., Ottosen, S., Baillat, D., Then, F., Krainc, D., Shiekhattar, R., Markey, S. P. and Tanese, N. (2008). Huntington's disease protein contributes to RNA-mediated gene silencing through association with Argonaute and P bodies. *Proc Natl Acad Sci U S A* **105**, 10820-5. https://doi.org/10.1073/pnas.0800658105.

Sawyer, L. A., Hennessy, J. M., Peixoto, A. A., Rosato, E., Parkinson, H., Costa, R. and Kyriacou, C. P. (1997). Natural variation in a *Drosophila* clock gene and temperature compensation. *Science* **278**, 2117-20. https://doi.org/10.1126/science.278.5346.2117.

Sayeed, O. and Benzer, S. (1996). Behavioral genetics of thermosensation and hygrosensation in *Drosophila*. *Proc Natl Acad Sci U S A* **93**, 6079-84. https://doi.org/10.1073/pnas.93.12.6079.

Scappini, E., Koh, T. W., Martin, N. P. and O'Bryan, J. P. (2007). Intersectin enhances huntingtin aggregation and neurodegeneration through activation of c-Jun-NH2-terminal kinase. *Hum Mol Genet* **16**, 1862-71. https://doi.org/10.1093/hmg/ddm134.

Schaffar, G., Breuer, P., Boteva, R., Behrends, C., Tzvetkov, N., Strippel, N., Sakahira, H., Siegers, K., Hayer-Hartl, M. and Hartl, F. U. (2004). Cellular toxicity of polyglutamine expansion proteins: Mechanism of transcription factor deactivation. *Mol Cell* **15**, 95-105. https://doi.org/10.1016/j.molcel.2004.06.029.

References

Schaffer, R., Ramsay, N., Samach, A., Corden, S., Putterill, J., Carré, I. A. and Coupland, G. (1998). The late elongated hypocotyl mutation of arabidopsis disrupts circadian rhythms and the photoperiodic control of flowering. *Cell* **93**, 1219-29. https://doi.org/10.1016/s0092-8674(00)81465-8.

Schaffert, L. N. and Carter, W. G. (2020). Do post-translational modifications influence protein aggregation in neurodegenerative diseases: A systematic review. *Brain Sci* **10**. https://doi.org/10.3390/brainsci10040232.

Scherzinger, E., Lurz, R., Turmaine, M., Mangiarini, L., Hollenbach, B., Hasenbank, R., Bates, G. P., Davies, S. W., Lehrach, H. and Wanker, E. E. (1997). Huntingtin-encoded polyglutamine expansions form amyloid-like protein aggregates in vitro and in vivo. *Cell* **90**, 549-58. https://doi.org/10.1016/s0092-8674(00)80514-0.

Schibler, U. (2009). The 2008 Pittendrigh/Aschoff lecture: peripheral phase coordination in the mammalian circadian timing system. *J Biol Rhythms* **24**, 3-15. https://doi.org/10.1177/0748730408329383.

Schibler, U., Gotic, I., Saini, C., Gos, P., Curie, T., Emmenegger, Y., Sinturel, F., Gosselin, P., Gerber, A., Fleury-Olela, F. et al. (2015). Clock-Talk: Interactions between Central and Peripheral Circadian Oscillators in Mammals. *Cold Spring Harb Symp Quant Biol* **80**, 223-32. https://doi.org/10.1101/sqb.2015.80.027490.

Schilling, G., Sharp, A. H., Loev, S. J., Wagster, M. V., Li, S. H., Stine, O. C. and Ross, C. A. (1995). Expression of the Huntington's disease (IT15) protein product in HD patients. *Hum Mol Genet* **4**, 1365-71. https://doi.org/10.1093/hmg/4.8.1365.

Schilling, J., Broemer, M., Atanassov, I., Duernberger, Y., Vorberg, I., Dieterich, C., Dagane, A., Dittmar, G., Wanker, E., van Roon-Mom, W. et al. (2019). Deregulated splicing is a major mechanism of RNA-induced toxicity in Huntington's disease. *J Mol Biol* **431**, 1869-1877. https://doi.org/10.1016/j.jmb.2019.01.034.

Schipper-Krom, S., Juenemann, K., Jansen, A. H., Wiemhoefer, A., van den Nieuwendijk, R., Smith, D. L., Hink, M. A., Bates, G. P., Overkleeft, H., Ovaa, H. et al. (2014). Dynamic recruitment of active proteasomes into polyglutamine initiated inclusion bodies. *FEBS Lett* **588**, 151-9. https://doi.org/10.1016/j.febslet.2013.11.023.

Schlader, Z. J. and Vargas, N. T. (2019). Regulation of body temperature by autonomic and behavioral thermoeffectors. *Exerc Sport Sci Rev* **47**, 116-126. https://doi.org/10.1249/jes.0000000000000180.

Schlichting, M., Diaz, M. M., Xin, J. and Rosbash, M. (2019a). Neuron-specific knockouts indicate the importance of network communication to *Drosophila* rhythmicity. *Elife* **8**. https://doi.org/10.7554/eLife.48301.

Schlichting, M., Díaz, M. M., Xin, J. and Rosbash, M. (2019b). Neuron-specific knockouts indicate the importance of network communication to *Drosophila* rhythmicity. *Elife* **8**. 10.7554/eLife.48301.

Schlichting, M., Menegazzi, P., Lelito, K. R., Yao, Z., Buhl, E., Dalla Benetta, E., Bahle, A., Denike, J., Hodge, J. J., Helfrich-Förster, C. et al. (2016). A neural network underlying circadian entrainment and photoperiodic adjustment of sleep and activity in *Drosophila*. *J Neurosci* **36**, 9084-96. https://doi.org/10.1523/JNEUROSCI.0992-16.2016.

References

Schlichting, M., Weidner, P., Diaz, M., Menegazzi, P., Dalla Benetta, E., Helfrich-Forster, C. and Rosbash, M. (2019c). Light-mediated circuit switching in the *Drosophila* neuronal clock network. *Curr Biol* **29**, 3266-3276 e3. 10.1016/j.cub.2019.08.033.

Schlichting, M., Weidner, P., Diaz, M., Menegazzi, P., Dalla Benetta, E., Helfrich-Förster, C. and Rosbash, M. (2019d). Light-mediated circuit switching in the *Drosophila* neuronal clock network. *Curr Biol* **29**, 3266-3276.e3. https://doi.org/10.1016/j.cub.2019.08.033.

Schneider, C. A., Rasband, W. S. and Eliceiri, K. W. (2012). NIH Image to ImageJ: 25 years of image analysis. *Nat Methods* **9**, 671-5. https://doi.org/10.1038/nmeth.2089.

Schneider, R., Linka, R. M. and Reinke, H. (2014). HSP90 affects the stability of BMAL1 and circadian gene expression. *J Biol Rhythms* **29**, 87-96. https://doi.org/10.1177/0748730414523559.

Schroeder, A. M. and Colwell, C. S. (2013). How to fix a broken clock. *Trends Pharmacol Sci* **34**, 605-19. https://doi.org/10.1016/j.tips.2013.09.002.

Schulte, J. and Littleton, J. T. (2011). The biological function of the huntingtin protein and its relevance to Huntington's disease pathology. *Curr Trends Neurol* **5**, 65-78.

Schulte, J., Sepp, K. J., Wu, C., Hong, P. and Littleton, J. T. (2011). High-content chemical and RNAi screens for suppressors of neurotoxicity in a Huntington's disease model. *PLoS One* **6**, e23841. https://doi.org/10.1371/journal.pone.0023841.

Schulz, R., Beach, S. R., Czaja, S. J., Martire, L. M. and Monin, J. K. (2020). Family Caregiving for Older Adults. *Annu Rev Psychol* **71**, 635-659. https://doi.org/10.1146/annurev-psych-010419-050754.

Scior, A., Buntru, A., Arnsburg, K., Ast, A., Iburg, M., Juenemann, K., Pigazzini, M. L., Mlody, B., Puchkov, D., Priller, J. et al. (2018). Complete suppression of Htt fibrilization and disaggregation of Htt fibrils by a trimeric chaperone complex. *Embo j* **37**, 282-299. https://doi.org/10.15252/embj.201797212.

SciStatCalc. McNemar's Test Calculator.: https://scistatcalc.blogspot.com/2013/11/mcnemars-test-calculator.html.

Seefelder, M., Klein, F. A. C., Landwehrmeyer, B., Fernández-Busnadiego, R. and Kochanek, S. (2022). Huntingtin and Its partner huntingtin-associated protein 40: Structural and functional considerations in health and disease. *J Huntingtons Dis* **11**, 227-242. https://doi.org/10.3233/jhd-220543.

Seeley, C. and Kegel-Gleason, K. B. (2021). Taming the Huntington's disease proteome: What have we learned? *J Huntingtons Dis* **10**, 239-257. https://doi.org/10.3233/jhd-200465.

Sehadova, H., Glaser, F. T., Gentile, C., Simoni, A., Giesecke, A., Albert, J. T. and Stanewsky, R. (2009). Temperature entrainment of *Drosophila*'s circadian clock involves the gene nocte and signaling from peripheral sensory tissues to the brain. *Neuron* **64**, 251-66. https://doi.org/10.1016/j.neuron.2009.08.026.

Sehgal, A., Price, J. and Young, M. W. (1992). Ontogeny of a biological clock in *Drosophila melanogaster*. *Proc Natl Acad Sci U S A* **89**, 1423-7. https://doi.org/10.1073/pnas.89.4.1423.

Seluzicki, A., Flourakis, M., Kula-Eversole, E., Zhang, L., Kilman, V. and Allada, R. (2014). Dual PDF signaling pathways reset clocks via TIMELESS and acutely excite target neurons to control circadian behavior. *PLoS Biol* **12**, e1001810. https://doi.org/10.1371/journal.pbio.1001810.

References

Semaka, A., Creighton, S., Warby, S. and Hayden, M. R. (2006). Predictive testing for Huntington disease: interpretation and significance of intermediate alleles. *Clin Genet* **70**, 283-94. https://doi.org/10.1111/j.1399-0004.2006.00668.x.

Semaka, A., Kay, C., Doty, C., Collins, J. A., Bijlsma, E. K., Richards, F., Goldberg, Y. P. and Hayden, M. R. (2013). CAG size-specific risk estimates for intermediate allele repeat instability in Huntington disease. *J Med Genet* **50**, 696-703. https://doi.org/10.1136/jmedgenet-2013-101796.

Şentürk, M. and Bellen, H. J. (2018). Genetic strategies to tackle neurological diseases in fruit flies. *Curr Opin Neurobiol* **50**, 24-32. https://doi.org/10.1016/j.conb.2017.10.017.

Seong, I. S., Woda, J. M., Song, J. J., Lloret, A., Abeyrathne, P. D., Woo, C. J., Gregory, G., Lee, J. M., Wheeler, V. C., Walz, T. et al. (2010). Huntingtin facilitates polycomb repressive complex 2. *Hum Mol Genet* **19**, 573-83. https://doi.org/10.1093/hmg/ddp524.

Seredenina, T. and Luthi-Carter, R. (2012). What have we learned from gene expression profiles in Huntington's disease? *Neurobiol Dis* **45**, 83-98. https://doi.org/10.1016/j.nbd.2011.07.001.

Seugnet, L., Galvin, J. E., Suzuki, Y., Gottschalk, L. and Shaw, P. J. (2009). Persistent short-term memory defects following sleep deprivation in a *Drosophila* model of Parkinson disease. *Sleep* **32**, 984-92. https://doi.org/10.1093/sleep/32.8.984.

Shacham, T., Sharma, N. and Lederkremer, G. Z. (2019). Protein Misfolding and ER Stress in Huntington's Disease. *Front Mol Biosci* **6**, 20. https://doi.org/10.3389/fmolb.2019.00020.

Shafer, O. T., Helfrich-Forster, C., Renn, S. C. and Taghert, P. H. (2006). Reevaluation of *Drosophila melanogaster's* neuronal circadian pacemakers reveals new neuronal classes. *J Comp Neurol* **498**, 180-93. https://doi.org/10.1002/cne.21021.

Shafer, O. T., Rosbash, M. and Truman, J. W. (2002). Sequential nuclear accumulation of the clock proteins Period and Timeless in the pacemaker neurons of *Drosophila melanogaster*. *J Neurosci* **22**, 5946-54. https://doi.org/10.1523/JNEUROSCI.22-14-05946.2002.

Shafer, O. T. and Taghert, P. H. (2009). RNA-interference knockdown of *Drosophila* pigment dispersing factor in neuronal subsets: the anatomical basis of a neuropeptide's circadian functions. *PLoS One* **4**, e8298. https://doi.org/10.1371/journal.pone.0008298.

Shahmoradian, S. H., Galaz-Montoya, J. G., Schmid, M. F., Cong, Y., Ma, B., Spiess, C., Frydman, J., Ludtke, S. J. and Chiu, W. (2013). TRiC's tricks inhibit huntingtin aggregation. *Elife* **2**, e00710. https://doi.org/10.7554/eLife.00710.

Shakhmantsir, I., Nayak, S., Grant, G. R. and Sehgal, A. (2018). Spliceosome factors target timeless (tim) mRNA to control clock protein accumulation and circadian behavior in *Drosophila*. *Elife* **7**. https://doi.org/10.7554/eLife.39821.

Shakhmantsir, I. and Sehgal, A. (2019). Splicing the clock to maintain and entrain circadian rhythms. *J Biol Rhythms* **34**, 584-595. https://doi.org/10.1177/0748730419868136.

Sharma, A. and Goyal, R. (2020a). Long-term exposure to constant light induces dementia, oxidative stress and promotes aggregation of sub-pathological Abeta42 in Wistar rats. *Pharmacol Biochem Behav* **192**, 172892. https://doi.org/10.1016/j.pbb.2020.172892.

References

Sharma, A. and Goyal, R. (2020b). Long-term exposure to constant light induces dementia, oxidative stress and promotes aggregation of sub-pathological Aβ(42) in Wistar rats. *Pharmacol Biochem Behav* **192**, 172892. https://doi.org/10.1016/j.pbb.2020.172892.

Sharma, A., Narasimha, K., Manjithaya, R. and Sheeba, V. (2023). Restoration of sleep and circadian behavior by autophagy modulation in Huntington's disease. *J Neurosci* **43**, 4907-4925. https://doi.org/s10.1523/JNEUROSCI.1894-22.2023.

Sharma, D., Shinchuk, L. M., Inouye, H., Wetzel, R. and Kirschner, D. A. (2005). Polyglutamine homopolymers having 8-45 residues form slablike beta-crystallite assemblies. *Proteins* **61**, 398-411. https://doi.org/10.1002/prot.20602.

Sharma, M. and Subramaniam, S. (2019). Rhes travels from cell to cell and transports Huntington disease protein via TNT-like protrusion. *J Cell Biol* **218**, 1972-1993. https://doi.org/10.1083/jcb.201807068.

Sharma, S. K., De los Rios, P., Christen, P., Lustig, A. and Goloubinoff, P. (2010). The kinetic parameters and energy cost of the Hsp70 chaperone as a polypeptide unfoldase. *Nat Chem Biol* **6**, 914-20. https://doi.org/10.1038/nchembio.455.

Sharp, A. H., Loev, S. J., Schilling, G., Li, S. H., Li, X. J., Bao, J., Wagster, M. V., Kotzuk, J. A., Steiner, J. P., Lo, A. et al. (1995). Widespread expression of Huntington's disease gene (IT15) protein product. *Neuron* **14**, 1065-74. https://doi.org/10.1016/0896-6273(95)90345-3.

Sheeba, V., Chandrashekaran, M. K., Joshi, A. and Sharma, V. K. (2002). Developmental plasticity of the locomotor activity rhythm of *Drosophila melanogaster*. *J Insect Physiol* **48**, 25-32. https://doi.org/10.1016/s0022-1910(01)00139-1.

Sheeba, V., Fogle, K. J. and Holmes, T. C. (2010). Persistence of morning anticipation behavior and high amplitude morning startle response following functional loss of small ventral lateral neurons in *Drosophila*. *PLoS One* **5**, e11628. https://doi.org/10.1371/journal.pone.0011628.

Sheeba, V., Fogle, K. J., Kaneko, M., Rashid, S., Chou, Y. T., Sharma, V. K. and Holmes, T. C. (2008a). Large ventral lateral neurons modulate arousal and sleep in *Drosophila*. *Curr Biol* **18**, 1537-45. 10.1016/j.cub.2008.08.033.

Sheeba, V., Fogle, K. J., Kaneko, M., Rashid, S., Chou, Y. T., Sharma, V. K. and Holmes, T. C. (2008b). Large ventral lateral neurons modulate arousal and sleep in *Drosophila*. *Curr Biol* **18**, 1537-45. https://doi.org/10.1016/j.cub.2008.08.033.

Sheeba, V., Gu, H., Sharma, V. K., O'Dowd, D. K. and Holmes, T. C. (2008b). Circadian- and light-dependent regulation of resting membrane potential and spontaneous action potential firing of *Drosophila* circadian pacemaker neurons. *J Neurophysiol* **99**, 976-88. https://doi.org/10.1152/jn.00930.2007.

Sheeba, V., Sharma, V. K., Gu, H., Chou, Y. T., O'Dowd, D. K. and Holmes, T. C. (2008c). Pigment dispersing factor-dependent and -independent circadian locomotor behavioral rhythms. *J Neurosci* **28**, 217-27. https://doi.org/10.1523/JNEUROSCI.4087-07.2008.

Sheeba, V., Sharma, V. K., Shubha, K., Chandrashekaran, M. K. and Joshi, A. (2000). The effect of different light regimes on adult life span in *Drosophila melanogaster* is partly mediated through reproductive output. *J Biol Rhythms* **15**, 380-92. https://doi.org/10.1177/074873000129001477.

References

Shehi, E., Fusi, P., Secundo, F., Pozzuolo, S., Bairati, A. and Tortora, P. (2003). Temperature-dependent, irreversible formation of amyloid fibrils by a soluble human ataxin-3 carrying a moderately expanded polyglutamine stretch (Q36). *Biochemistry* **42**, 14626-32. https://doi.org/10.1021/bi0352825.

Shelbourne, P. F., Keller-McGandy, C., Bi, W. L., Yoon, S. R., Dubeau, L., Veitch, N. J., Vonsattel, J. P., Wexler, N. S., Arnheim, N. and Augood, S. J. (2007a). Triplet repeat mutation length gains correlate with cell-type specific vulnerability in Huntington disease brain. *Hum Mol Genet* **16**, 1133-42. https://doi.org/10.1093/hmg/ddm054.

Shelbourne, P. F., Keller-McGandy, C., Bi, W. L., Yoon, S. R., Dubeau, L., Veitch, N. J., Vonsattel, J. P., Wexler, N. S., Group, U. S.-V. C. R., Arnheim, N. et al. (2007b). Triplet repeat mutation length gains correlate with cell-type specific vulnerability in Huntington disease brain. *Hum Mol Genet* **16**, 1133-42. https://doi.org/10.1093/hmg/ddm054.

Shen, J. and Tower, J. (2019). Effects of light on aging and longevity. *Ageing Res Rev* **53**, 100913. https://doi.org/10.1016/j.arr.2019.100913.

Shen, J., Zhu, X., Gu, Y., Zhang, C., Huang, J. and Xiao, Q. (2019). Toxic effect of visible light on *Drosophila* life span depending on diet protein content. *J Gerontol A Biol Sci Med Sci* **74**, 163-167. https://doi.org/10.1093/gerona/gly042.

Shen, K., Calamini, B., Fauerbach, J. A., Ma, B., Shahmoradian, S. H., Serrano Lachapel, I. L., Chiu, W., Lo, D. C. and Frydman, J. (2016). Control of the structural landscape and neuronal proteotoxicity of mutant huntingtin by domains flanking the polyQ tract. *Elife* **5**. https://doi.org/10.7554/eLife.18065.

Shen, Y., Lv, Q. K., Xie, W. Y., Gong, S. Y., Zhuang, S., Liu, J. Y., Mao, C. J. and Liu, C. F. (2023). Circadian disruption and sleep disorders in neurodegeneration. *Transl Neurodegener* **12**, 8. https://doi.org/10.1186/s40035-023-00340-6.

Sheng, Z. H. (2017). The interplay of axonal energy homeostasis and mitochondrial trafficking and anchoring. *Trends Cell Biol* **27**, 403-416. https://doi.org/10.1016/j.tcb.2017.01.005.

Shi, Y., Wang, J., Li, J. D., Ren, H., Guan, W., He, M., Yan, W., Zhou, Y., Hu, Z., Zhang, J. et al. (2013). Identification of CHIP as a novel causative gene for autosomal recessive cerebellar ataxia. *PLoS One* **8**, e81884. https://doi.org/10.1371/journal.pone.0081884.

Shimura, H., Miura-Shimura, Y. and Kosik, K. S. (2004a). Binding of Tau to heat shock protein 27 leads to decreased concentration of hyperphosphorylated Tau and enhanced cell survival. *Journal of Biological Chemistry* **279**, 17957-17962. 10.1074/jbc.M400351200.

Shimura, H., Miura-Shimura, Y. and Kosik, K. S. (2004b). Binding of tau to heat shock protein 27 leads to decreased concentration of hyperphosphorylated tau and enhanced cell survival. *J Biol Chem* **279**, 17957-62. https://doi.org/10.1074/jbc.M400351200.

Shin, J. W., Kim, K. H., Chao, M. J., Atwal, R. S., Gillis, T., MacDonald, M. E., Gusella, J. F. and Lee, J. M. (2016). Permanent inactivation of Huntington's disease mutation by personalized allele-specific CRISPR/Cas9. *Hum Mol Genet* **25**, 4566-4576. https://doi.org/10.1093/hmg/ddw286.

Shirasaki, D. I., Greiner, E. R., Al-Ramahi, I., Gray, M., Boontheung, P., Geschwind, D. H., Botas, J., Coppola, G., Horvath, S., Loo, J. A. et al. (2012). Network organization of the huntingtin

proteomic interactome in mammalian brain. *Neuron* **75**, 41-57. https://doi.org/10.1016/j.neuron.2012.05.024.

Shokri-Kojori, E., Wang, G. J., Wiers, C. E., Demiral, S. B., Guo, M., Kim, S. W., Lindgren, E., Ramirez, V., Zehra, A., Freeman, C. et al. (2018). β-Amyloid accumulation in the human brain after one night of sleep deprivation. *Proc Natl Acad Sci U S A* **115**, 4483-4488. https://doi.org/10.1073/pnas.1721694115.

Shorter, J. (2011). The mammalian disaggregase machinery: Hsp110 synergizes with Hsp70 and Hsp40 to catalyze protein disaggregation and reactivation in a cell-free system. *PLoS One* **6**, e26319. https://doi.org/10.1371/journal.pone.0026319.

Shostal, O. A. and Moskalev, A. A. (2012). The genetic mechanisms of the influence of the light regime on the lifespan of *Drosophila melanogaster*. *Front Genet* **3**, 325. https://doi.org/10.3389/fgene.2012.00325.

Shulman, J. M. and Feany, M. B. (2003). Genetic modifiers of tauopathy in *Drosophila*. *Genetics* **165**, 1233-42. https://doi.org/10.1093/genetics/165.3.1233.

Siddiqi, F. H., Menzies, F. M., Lopez, A., Stamatakou, E., Karabiyik, C., Ureshino, R., Ricketts, T., Jimenez-Sanchez, M., Esteban, M. A., Lai, L. et al. (2019). Felodipine induces autophagy in mouse brains with pharmacokinetics amenable to repurposing. *Nat Commun* **10**, 1817. https://doi.org/10.1038/s41467-019-09494-2.

Sieradzan, K. A., Mechan, A. O., Jones, L., Wanker, E. E., Nukina, N. and Mann, D. M. (1999). Huntington's disease intranuclear inclusions contain truncated, ubiquitinated huntingtin protein. *Exp Neurol* **156**, 92-9. https://doi.org/10.1006/exnr.1998.7005.

SigmaPlot. Version 11.0, from Systat Software. San Jose California USA.

Silva, A., de Almeida, A. V. and Macedo-Ribeiro, S. (2018). Polyglutamine expansion diseases: More than simple repeats. *J Struct Biol* **201**, 139-154. https://doi.org/10.1016/j.jsb.2017.09.006.

Silva, A., Queiroz, S. S., Andersen, M. L., Mônico-Neto, M., Campos, R. M., Roizenblatt, S., Tufik, S. and Mello, M. T. (2013). Passive body heating improves sleep patterns in female patients with fibromyalgia. *Clinics (Sao Paulo)* **68**, 135-40. https://doi.org/10.6061/clinics/2013(02)oa03.

Simpson, J. H. (2009). Mapping and manipulating neural circuits in the fly brain. *Adv Genet* **65**, 79-143. https://doi.org/10.1016/s0065-2660(09)65003-3.

Sinadinos, C., Burbidge-King, T., Soh, D., Thompson, L. M., Marsh, J. L., Wyttenbach, A. and Mudher, A. K. (2009). Live axonal transport disruption by mutant huntingtin fragments in *Drosophila* motor neuron axons. *Neurobiol Dis* **34**, 389-95. https://doi.org/10.1016/j.nbd.2009.02.012.

Singaraja, R. R., Hadano, S., Metzler, M., Givan, S., Wellington, C. L., Warby, S., Yanai, A., Gutekunst, C. A., Leavitt, B. R., Yi, H. et al. (2002). HIP14, a novel ankyrin domain-containing protein, links huntingtin to intracellular trafficking and endocytosis. *Hum Mol Genet* **11**, 2815-28. https://doi.org/10.1093/hmg/11.23.2815.

Singaraja, R. R., Huang, K., Sanders, S. S., Milnerwood, A. J., Hines, R., Lerch, J. P., Franciosi, S., Drisdel, R. C., Vaid, K., Young, F. B. et al. (2011). Altered palmitoylation and neuropathological deficits in mice lacking HIP14. *Hum Mol Genet* **20**, 3899-909. https://doi.org/10.1093/hmg/ddr308.

References

Singh, A. and Agrawal, N. (2022). Metabolism in Huntington's disease: A major contributor to pathology. *Metab Brain Dis* **37**, 1757-1771. https://doi.org/10.1007/s11011-021-00844-y.

Sinnige, T., Yu, A. and Morimoto, R. I. (2020). Challenging proteostasis: Role of the chaperone network to control aggregation-prone proteins in human disease. *Adv Exp Med Biol* **1243**, 53-68. https://doi.org/10.1007/978-3-030-40204-4_4.

Sipione, S., Rigamonti, D., Valenza, M., Zuccato, C., Conti, L., Pritchard, J., Kooperberg, C., Olson, J. M. and Cattaneo, E. (2002). Early transcriptional profiles in huntingtin-inducible striatal cells by microarray analyses. *Hum Mol Genet* **11**, 1953-65. https://doi.org/10.1093/hmg/11.17.1953.

Sittler, A., Lurz, R., Lueder, G., Priller, J., Lehrach, H., Hayer-Hartl, M. K., Hartl, F. U. and Wanker, E. E. (2001). Geldanamycin activates a heat shock response and inhibits huntingtin aggregation in a cell culture model of Huntington's disease. *Hum Mol Genet* **10**, 1307-15. https://doi.org/10.1093/hmg/10.12.1307.

Sittler, A., Wälter, S., Wedemeyer, N., Hasenbank, R., Scherzinger, E., Eickhoff, H., Bates, G. P., Lehrach, H. and Wanker, E. E. (1998). SH3GL3 associates with the huntingtin exon 1 protein and promotes the formation of polygln-containing protein aggregates. *Mol Cell* **2**, 427-36. https://doi.org/10.1016/s1097-2765(00)80142-2.

Sivanandam, V. N., Jayaraman, M., Hoop, C. L., Kodali, R., Wetzel, R. and van der Wel, P. C. (2011). The aggregation-enhancing huntingtin N-terminus is helical in amyloid fibrils. *J Am Chem Soc* **133**, 4558-66. https://doi.org/10.1021/ja110715f.

Skillings, E. A., Wood, N. I. and Morton, A. J. (2014). Beneficial effects of environmental enrichment and food entrainment in the R6/2 mouse model of Huntington's disease. *Brain Behav* **4**, 675-86. https://doi.org/10.1002/brb3.235.

Skovronsky, D. M., Lee, V. M. and Trojanowski, J. Q. (2006). Neurodegenerative diseases: new concepts of pathogenesis and their therapeutic implications. *Annu Rev Pathol* **1**, 151-70. https://doi.org/10.1146/annurev.pathol.1.110304.100113.

Sletten, T. L., Cappuccio, F. P., Davidson, A. J., Van Cauter, E., Rajaratnam, S. M. W. and Scheer, F. (2020). Health consequences of circadian disruption. *Sleep* **43**. https://doi.org/10.1093/sleep/zsz194.

Slow, E. J., Graham, R. K., Osmand, A. P., Devon, R. S., Lu, G., Deng, Y., Pearson, J., Vaid, K., Bissada, N., Wetzel, R. et al. (2005). Absence of behavioral abnormalities and neurodegeneration in vivo despite widespread neuronal huntingtin inclusions. *Proc Natl Acad Sci U S A* **102**, 11402-7. https://doi.org/10.1073/pnas.0503634102.

Smalley, J. L., Breda, C., Mason, R. P., Kooner, G., Luthi-Carter, R., Gant, T. W. and Giorgini, F. (2016). Connectivity mapping uncovers small molecules that modulate neurodegeneration in Huntington's disease models. *J Mol Med (Berl)* **94**, 235-45. https://doi.org/10.1007/s00109-015-1344-5.

Smarr, B., Cutler, T., Loh, D. H., Kudo, T., Kuljis, D., Kriegsfeld, L., Ghiani, C. A. and Colwell, C. S. (2019). Circadian dysfunction in the Q175 model of Huntington's disease: Network analysis. *J Neurosci Res* **97**, 1606-1623. https://doi.org/10.1002/jnr.24505.

Smith-Dijak, A. I., Sepers, M. D. and Raymond, L. A. (2019). Alterations in synaptic function and plasticity in Huntington disease. *J Neurochem* **150**, 346-365. https://doi.org/10.1111/jnc.14723.

References

Smith, H. L., Li, W. and Cheetham, M. E. (2015). Molecular chaperones and neuronal proteostasis. *Semin Cell Dev Biol* **40**, 142-52. https://doi.org/10.1016/j.semcdb.2015.03.003.

Snell, R. G., MacMillan, J. C., Cheadle, J. P., Fenton, I., Lazarou, L. P., Davies, P., MacDonald, M. E., Gusella, J. F., Harper, P. S. and Shaw, D. J. (1993). Relationship between trinucleotide repeat expansion and phenotypic variation in Huntington's disease. *Nat Genet* **4**, 393-7. https://doi.org/10.1038/ng0893-393.

Snider, B. J. and Choi, D. W. (1996). Heat stress reduces glutamate toxicity in cultured neurons without hsp70 expression. *Brain Res* **729**, 273-6. https://doi.org/10.1016/0006-8993(96)00572-0.

Soares, T. R., Reis, S. D., Pinho, B. R., Duchen, M. R. and Oliveira, J. M. A. (2019). Targeting the proteostasis network in Huntington's disease. *Ageing Res Rev* **49**, 92-103. https://doi.org/10.1016/j.arr.2018.11.006.

Solberg, O. K., Filkuková, P., Frich, J. C. and Feragen, K. J. B. (2018). Age at death and causes of death in patients with Huntington disease in Norway in 1986-2015. *J Huntingtons Dis* **7**, 77-86. https://doi.org/10.3233/jhd-170270.

Solovev, I., Dobrovolskaya, E., Shaposhnikov, M., Sheptyakov, M. and Moskalev, A. (2019). Neuron-specific overexpression of core clock genes improves stress-resistance and extends lifespan of *Drosophila melanogaster*. *Exp Gerontol* **117**, 61-71. https://doi.org/10.1016/j.exger.2018.11.005.

Someren, V. and JW, E. (2003). Thermosensitivity of the circadian timing system. *Sleep and Biological Rhythms* **1**, 55-64. https://doi.org/10.1046/j.1446-9235.2003.00002.x.

Soneson, C., Fontes, M., Zhou, Y., Denisov, V., Paulsen, J. S., Kirik, D., Petersen, A. and Huntington Study Group, P.-H. D. i. (2010). Early changes in the hypothalamic region in prodromal Huntington disease revealed by MRI analysis. *Neurobiol Dis* **40**, 531-43. https://doi.org/10.1016/j.nbd.2010.07.013.

Song, Q., Feng, G., Huang, Z., Chen, X., Chen, Z. and Ping, Y. (2016). Aberrant axonal arborization of PDF neurons induced by Abeta42-mediated JNK activation underlies sleep disturbance in an Alzheimer's Model. *Mol Neurobiol*. https://doi.org/10.1007/s12035-016-0165-z.

Song, Q., Feng, G., Huang, Z., Chen, X., Chen, Z. and Ping, Y. (2017). Aberrant axonal arborization of PDF neurons induced by Aβ42-mediated JNK activation underlies sleep disturbance in an Alzheimer's model. *Mol Neurobiol* **54**, 6317-6328. https://doi.org/10.1007/s12035-016-0165-z.

Song, Y., Yang, J., Law, A. D., Hendrix, D. A., Kretzschmar, D., Robinson, M. and Giebultowicz, J. M. (2022). Age-dependent effects of blue light exposure on lifespan, neurodegeneration, and mitochondria physiology in *Drosophila melanogaster*. *NPJ Aging* **8**, 11. https://doi.org/10.1038/s41514-022-00092-z.

Sontag, E. M., Lotz, G. P., Agrawal, N., Tran, A., Aron, R., Yang, G., Necula, M., Lau, A., Finkbeiner, S., Glabe, C. et al. (2012). Methylene blue modulates huntingtin aggregation intermediates and is protective in Huntington's disease models. *J Neurosci* **32**, 11109-19. https://doi.org/10.1523/JNEUROSCI.0895-12.2012.

Sontag, E. M., Samant, R. S. and Frydman, J. (2017). Mechanisms and Functions of Spatial Protein Quality Control. *Annu Rev Biochem* **86**, 97-122. https://doi.org/10.1146/annurev-biochem-060815-014616.

References

Sontag, E. M., Vonk, W. I. M. and Frydman, J. (2014). Sorting out the trash: the spatial nature of eukaryotic protein quality control. *Curr Opin Cell Biol* **26**, 139-146. https://doi.org/10.1016/j.ceb.2013.12.006.

Sørensen, J. G., Schou, M. F., Kristensen, T. N. and Loeschcke, V. (2016). Thermal fluctuations affect the transcriptome through mechanisms independent of average temperature. *Sci Rep* **6**, 30975. https://doi.org/10.1038/srep30975.

Sørensen, S. A. and Fenger, K. (1992). Causes of death in patients with Huntington's disease and in unaffected first degree relatives. *J Med Genet* **29**, 911-4. https://doi.org/10.1136/jmg.29.12.911.

Sousa, R. and Lafer, E. M. (2019). The Physics of Entropic Pulling: A Novel Model for the Hsp70 Motor Mechanism. *Int J Mol Sci* **20**. https://doi.org/10.3390/ijms20092334.

Southwell, A. L., Khoshnan, A., Dunn, D. E., Bugg, C. W., Lo, D. C. and Patterson, P. H. (2008). Intrabodies binding the proline-rich domains of mutant huntingtin increase its turnover and reduce neurotoxicity. *J Neurosci* **28**, 9013-20. https://doi.org/10.1523/jneurosci.2747-08.2008.

Specht, S., Miller, S. B., Mogk, A. and Bukau, B. (2011). Hsp42 is required for sequestration of protein aggregates into deposition sites in *Saccharomyces cerevisiae*. *J Cell Biol* **195**, 617-29. https://doi.org/10.1083/jcb.201106037.

Squitieri, F., Andrew, S. E., Goldberg, Y. P., Kremer, B., Spence, N., Zeisler, J., Nichol, K., Theilmann, J., Greenberg, J., Goto, J. et al. (1994). DNA haplotype analysis of Huntington disease reveals clues to the origins and mechanisms of CAG expansion and reasons for geographic variations of prevalence. *Hum Mol Genet* **3**, 2103-14. https://doi.org/10.1093/hmg/3.12.2103.

Squitieri, F., Gellera, C., Cannella, M., Mariotti, C., Cislaghi, G., Rubinsztein, D. C., Almqvist, E. W., Turner, D., Bachoud-Lévi, A. C., Simpson, S. A. et al. (2003). Homozygosity for CAG mutation in Huntington disease is associated with a more severe clinical course. *Brain* **126**, 946-55. https://doi.org/10.1093/brain/awg077.

Sroka, K., Voigt, A., Deeg, S., Reed, J. C., Schulz, J. B., Bahr, M. and Kermer, P. (2009). BAG1 modulates huntingtin toxicity, aggregation, degradation, and subcellular distribution. *J Neurochem* **111**, 801-7. https://doi.org/10.1111/j.1471-4159.2009.06363.x.

Stanewsky, R., Kaneko, M., Emery, P., Beretta, B., Wager-Smith, K., Kay, S. A., Rosbash, M. and Hall, J. C. (1998). The cryb mutation identifies cryptochrome as a circadian photoreceptor in *Drosophila*. *Cell* **95**, 681-92. https://doi.org/10.1016/s0092-8674(00)81638-4.

StatSoftInc. (2004). STATISTICA (data analysis software system), version 7. Tulsa, USA: www.statsoft.com.

Stefani, O. and Cajochen, C. (2021). Should we re-think regulations and standards for lighting at workplaces? A practice review on existing lighting recommendations. *Front Psychiatry* **12**, 652161. https://doi.org/10.3389/fpsyt.2021.652161.

Steffan, J. S., Agrawal, N., Pallos, J., Rockabrand, E., Trotman, L. C., Slepko, N., Illes, K., Lukacsovich, T., Zhu, Y. Z., Cattaneo, E. et al. (2004). SUMO modification of huntingtin and Huntington's disease pathology. *Science* **304**, 100-4. https://doi.org/10.1126/science.1092194.

Steffan, J. S., Bodai, L., Pallos, J., Poelman, M., McCampbell, A., Apostol, B. L., Kazantsev, A., Schmidt, E., Zhu, Y. Z., Greenwald, M. et al. (2001). Histone deacetylase inhibitors arrest

polyglutamine-dependent neurodegeneration in *Drosophila*. *Nature* **413**, 739-43. https://doi.org/10.1038/35099568.

Steffan, J. S., Kazantsev, A., Spasic-Boskovic, O., Greenwald, M., Zhu, Y. Z., Gohler, H., Wanker, E. E., Bates, G. P., Housman, D. E. and Thompson, L. M. (2000). The Huntington's disease protein interacts with p53 and CREB-binding protein and represses transcription. *Proc Natl Acad Sci U S A* **97**, 6763-8. https://doi.org/10.1073/pnas.100110097.

Stehle, J. H., von Gall, C. and Korf, H. W. (2001). Analysis of cell signalling in the rodent pineal gland deciphers regulators of dynamic transcription in neural/endocrine cells. *Eur J Neurosci* **14**, 1-9. https://doi.org/10.1046/j.0953-816x.2001.01627.x.

Steinert, J. R., Campesan, S., Richards, P., Kyriacou, C. P., Forsythe, I. D. and Giorgini, F. (2012). Rab11 rescues synaptic dysfunction and behavioural deficits in a *Drosophila* model of Huntington's disease. *Hum Mol Genet* **21**, 2912-22. https://doi.org/10.1093/hmg/dds117.

Stevenson, R. (1985). The relative importance of behavioral and physiological adjustments controlling body temperature in terrestrial ectotherms. *J The American Naturalist* **126**, 362-386. https://doi.org/10.1086/284423.

Stier, E. (1903). Zur pathologischen anatomie der Huntingtonschen Chorea. Berlin: Springers.

Stojkovic, K., Wing, S. S. and Cermakian, N. (2014). A central role for ubiquitination within a circadian clock protein modification code. *Front Mol Neurosci* **7**, 69. https://doi.org/10.3389/fnmol.2014.00069.

Stokkan, K. A., Yamazaki, S., Tei, H., Sakaki, Y. and Menaker, M. (2001). Entrainment of the circadian clock in the liver by feeding. *Science* **291**, 490-3. https://doi.org/10.1126/science.291.5503.490.

Stoleru, D., Peng, Y., Agosto, J. and Rosbash, M. (2004). Coupled oscillators control morning and evening locomotor behaviour of *Drosophila*. *Nature* **431**, 862-8. https://doi.org/10.1038/nature02926.

Stoleru, D., Peng, Y., Nawathean, P. and Rosbash, M. (2005). A resetting signal between *Drosophila* pacemakers synchronizes morning and evening activity. *Nature* **438**, 238-42. https://doi.org/10.1038/nature04192.

Stoyas, C. A. and La Spada, A. R. (2018a). The CAG-polyglutamine repeat diseases: a clinical, molecular, genetic, and pathophysiologic nosology. *Handb Clin Neurol* **147**, 143-170. https://doi.org/10.1016/B978-0-444-63233-3.00011-7.

Stoyas, C. A. and La Spada, A. R. (2018b). The CAG–polyglutamine repeat diseases: a clinical, molecular, genetic, and pathophysiologic nosology: Elsevier. https://doi.org/10.1016/B978-0-444-63233-3.00011-7.

Strong, T. V., Tagle, D. A., Valdes, J. M., Elmer, L. W., Boehm, K., Swaroop, M., Kaatz, K. W., Collins, F. S. and Albin, R. L. (1993). Widespread expression of the human and rat Huntington's disease gene in brain and nonneural tissues. *Nat Genet* **5**, 259-65. https://doi.org/10.1038/ng1193-259.

Stürner, E. and Behl, C. (2017). The Role of the Multifunctional BAG3 Protein in Cellular Protein Quality Control and in Disease. *Front Mol Neurosci* **10**, 177. https://doi.org/10.3389/fnmol.2017.00177.

References

Suhr, S. T., Senut, M. C., Whitelegge, J. P., Faull, K. F., Cuizon, D. B. and Gage, F. H. (2001). Identities of sequestered proteins in aggregates from cells with induced polyglutamine expression. *J Cell Biol* **153**, 283-94. https://doi.org/10.1083/jcb.153.2.283.

Sullivan, F. R., Bird, E. D., Alpay, M. and Cha, J. H. (2001). Remotivation therapy and Huntington's disease. *J Neurosci Nurs* **33**, 136-42. https://doi.org/10.1097/01376517-200106000-00005.

Sumsuzzman, D. M., Choi, J., Jin, Y. and Hong, Y. (2021). Neurocognitive effects of melatonin treatment in healthy adults and individuals with Alzheimer's disease and insomnia: A systematic review and meta-analysis of randomized controlled trials. *Neurosci Biobehav Rev* **127**, 459-473. https://doi.org/10.1016/j.neubiorev.2021.04.034.

Sun, C. S., Lee, C. C., Li, Y. N., Yao-Chen Yang, S., Lin, C. H., Chang, Y. C., Liu, P. F., He, R. Y., Wang, C. H., Chen, W. et al. (2015). Conformational switch of polyglutamine-expanded huntingtin into benign aggregates leads to neuroprotective effect. *Sci Rep* **5**, 14992. https://doi.org/10.1038/srep14992.

Sun, Y. J., Zhang, Z. Y., Fan, B. and Li, G. Y. (2019). Neuroprotection by therapeutic hypothermia. *Front Neurosci* **13**, 586. https://doi.org/10.3389/fnins.2019.00586.

Sutton, L. M., Sanders, S. S., Butland, S. L., Singaraja, R. R., Franciosi, S., Southwell, A. L., Doty, C. N., Schmidt, M. E., Mui, K. K. N., Kovalik, V. et al. (2013). Hip14l-deficient mice develop neuropathological and behavioural features of Huntington disease. *Human Molecular Genetics* **22**, 452-465. https://doi.org/10.1093/hmg/dds441.

Sweeney, P., Park, H., Baumann, M., Dunlop, J., Frydman, J., Kopito, R., McCampbell, A., Leblanc, G., Venkateswaran, A., Nurmi, A. et al. (2017). Protein misfolding in neurodegenerative diseases: implications and strategies. *Transl Neurodegener* **6**, 6. https://doi.org/10.1186/s40035-017-0077-5.

Tabrizi, S. J., Estevez-Fraga, C., van Roon-Mom, W. M. C., Flower, M. D., Scahill, R. I., Wild, E. J., Munoz-Sanjuan, I., Sampaio, C., Rosser, A. E. and Leavitt, B. R. (2022). Potential disease-modifying therapies for Huntington's disease: lessons learned and future opportunities. *Lancet Neurol* **21**, 645-658. https://doi.org/10.1016/S1474-4422(22)00121-1.

Tabrizi, S. J., Ghosh, R. and Leavitt, B. R. (2019). Huntingtin lowering strategies for disease modification in Huntington's disease. *Neuron* **101**, 801-819. https://doi.org/10.1016/j.neuron.2019.01.039.

Tabuchi, M., Lone, S. R., Liu, S., Liu, Q., Zhang, J., Spira, A. P. and Wu, M. N. (2015a). Sleep interacts with abeta to modulate intrinsic neuronal excitability. *Curr Biol* **25**, 702-712. https://doi.org/10.1016/j.cub.2015.01.016.

Tabuchi, M., Lone, S. R., Liu, S., Liu, Q., Zhang, J., Spira, A. P. and Wu, M. N. (2015b). Sleep interacts with aβ to modulate intrinsic neuronal excitability. *Curr Biol* **25**, 702-712. https://doi.org/10.1016/j.cub.2015.01.016.

Tagawa, K., Marubuchi, S., Qi, M. L., Enokido, Y., Tamura, T., Inagaki, R., Murata, M., Kanazawa, I., Wanker, E. E. and Okazawa, H. (2007). The induction levels of heat shock protein 70 differentiate the vulnerabilities to mutant huntingtin among neuronal subtypes. *J Neurosci* **27**, 868-80. https://doi.org/10.1523/JNEUROSCI.4522-06.2007.

Takahashi, J. S. (2017). Transcriptional architecture of the mammalian circadian clock. *Nat Rev Genet* **18**, 164-179. https://doi.org/10.1038/nrg.2016.150.

References

Takahashi, T., Katada, S. and Onodera, O. (2010). Polyglutamine diseases: where does toxicity come from? what is toxicity? where are we going? *J Mol Cell Biol* **2**, 180-91. https://doi.org/10.1093/jmcb/mjq005.

Takahashi, T., Kikuchi, S., Katada, S., Nagai, Y., Nishizawa, M. and Onodera, O. (2008). Soluble polyglutamine oligomers formed prior to inclusion body formation are cytotoxic. *Hum Mol Genet* **17**, 345-56. https://doi.org/10.1093/hmg/ddm311.

Takano, H. and Gusella, J. F. (2002). The predominantly HEAT-like motif structure of huntingtin and its association and coincident nuclear entry with dorsal, an NF-kB/Rel/dorsal family transcription factor. *BMC Neurosci* **3**, 15. https://doi.org/10.1186/1471-2202-3-15.

Talsma, A. D., Christov, C. P., Terriente-Felix, A., Linneweber, G. A., Perea, D., Wayland, M., Shafer, O. T. and Miguel-Aliaga, I. (2012). Remote control of renal physiology by the intestinal neuropeptide pigment-dispersing factor in *Drosophila*. *Proc Natl Acad Sci U S A* **109**, 12177-82. https://doi.org/10.1073/pnas.1200247109.

Tam, S., Geller, R., Spiess, C. and Frydman, J. (2006). The chaperonin TRiC controls polyglutamine aggregation and toxicity through subunit-specific interactions. *Nat Cell Biol* **8**, 1155-62. https://doi.org/10.1038/ncb1477.

Tam, S., Spiess, C., Auyeung, W., Joachimiak, L., Chen, B., Poirier, M. A. and Frydman, J. (2009). The chaperonin TRiC blocks a huntingtin sequence element that promotes the conformational switch to aggregation. *Nat Struct Mol Biol* **16**, 1279-85. https://doi.org/10.1038/nsmb.1700.

Tamaru, T., Hattori, M., Honda, K., Benjamin, I., Ozawa, T. and Takamatsu, K. (2011). Synchronization of circadian Per2 rhythms and HSF1-BMAL1:CLOCK interaction in mouse fibroblasts after short-term heat shock pulse. *PLoS One* **6**, e24521. https://doi.org/10.1371/journal.pone.0024521.

Tamura, T., Sone, M., Yamashita, M., Wanker, E. E. and Okazawa, H. (2009). Glial cell lineage expression of mutant ataxin-1 and huntingtin induces developmental and late-onset neuronal pathologies in *Drosophila* models. *PLoS One* **4**, e4262. https://doi.org/10.1371/journal.pone.0004262.

Tan, S. and Wong, E. (2017). Kinetics of protein aggregates disposal by aggrephagy. *Methods Enzymol* **588**, 245-281. https://doi.org/10.1016/bs.mie.2016.09.084.

Tang, X., Roessingh, S., Hayley, S. E., Chu, M. L., Tanaka, N. K., Wolfgang, W., Song, S., Stanewsky, R. and Hamada, F. N. (2017). The role of PDF neurons in setting the preferred temperature before dawn in *Drosophila*. *Elife* **6**. https://doi.org/10.7554/eLife.23206.

Tapia-Osorio, A., Salgado-Delgado, R., Angeles-Castellanos, M. and Escobar, C. (2013). Disruption of circadian rhythms due to chronic constant light leads to depressive and anxiety-like behaviors in the rat. *Behav Brain Res* **252**, 1-9. https://doi.org/10.1016/j.bbr.2013.05.028.

Tartari, M., Gissi, C., Lo Sardo, V., Zuccato, C., Picardi, E., Pesole, G. and Cattaneo, E. (2008). Phylogenetic comparison of huntingtin homologues reveals the appearance of a primitive polyQ in sea urchin. *Mol Biol Evol* **25**, 330-8. https://doi.org/10.1093/molbev/msm258.

Tataroglu, O. and Emery, P. (2014). Studying circadian rhythms in *Drosophila melanogaster*. *Methods* **68**, 140-50. https://doi.org/10.1016/j.ymeth.2014.01.001.

Tataroglu, O. and Emery, P. (2015). The molecular ticks of the *Drosophila* circadian clock. *Curr Opin Insect Sci* **7**, 51-57. https://doi.org/10.1016/j.cois.2015.01.002.

References

Tatum, M. C., Ooi, F. K., Chikka, M. R., Chauve, L., Martinez-Velazquez, L. A., Steinbusch, H. W. M., Morimoto, R. I. and Prahlad, V. (2015). Neuronal serotonin release triggers the heat shock response in *C. elegans* in the absence of temperature increase. *Curr Biol* **25**, 163-174. https://doi.org/10.1016/j.cub.2014.11.040.

Taylor, J. P., Tanaka, F., Robitschek, J., Sandoval, C. M., Taye, A., Markovic-Plese, S. and Fischbeck, K. H. (2003a). Aggresomes protect cells by enhancing the degradation of toxic polyglutamine-containing protein. *Hum Mol Genet* **12**, 749-57. https://doi.org/10.1093/hmg/ddg074.

Taylor, J. P., Taye, A. A., Campbell, C., Kazemi-Esfarjani, P., Fischbeck, K. H. and Min, K. T. (2003b). Aberrant histone acetylation, altered transcription, and retinal degeneration in a *Drosophila* model of polyglutamine disease are rescued by CREB-binding protein. *Genes Dev* **17**, 1463-8. https://doi.org/10.1101/gad.1087503.

Taylor, N. and Bramble, D. (1997). Sleep disturbance and Huntington's disease. *Br J Psychiatry* **171**, 393. https://doi.org/10.1192/bjp.171.4.393c.

Taylor, R. C. and Dillin, A. (2011). Aging as an event of proteostasis collapse. *Cold Spring Harbor Perspectives in Biology* **3**, a004440-a004440. https://doi.org/10.1101/cshperspect.a004440.

Telenius, H., Kremer, B., Goldberg, Y. P., Theilmann, J., Andrew, S. E., Zeisler, J., Adam, S., Greenberg, C., Ives, E. J., Clarke, L. A. et al. (1994). Somatic and gonadal mosaicism of the Huntington disease gene CAG repeat in brain and sperm. *Nat Genet* **6**, 409-14. https://doi.org/10.1038/ng0494-409.

Telenius, H., Kremer, H. P., Theilmann, J., Andrew, S. E., Almqvist, E., Anvret, M., Greenberg, C., Greenberg, J., Lucotte, G., Squitieri, F. et al. (1993). Molecular analysis of juvenile Huntington disease: the major influence on (CAG)n repeat length is the sex of the affected parent. *Hum Mol Genet* **2**, 1535-40. https://doi.org/10.1093/hmg/2.10.1535.

Tello, J. A., Williams, H. E., Eppler, R. M., Steinhilb, M. L. and Khanna, M. (2022). Animal models of neurodegenerative disease: Recent advances in fly highlight innovative approaches to drug discovery. *Front Mol Neurosci* **15**, 883358. https://doi.org/10.3389/fnmol.2022.883358.

Teramoto, Y., Tokura, H., Ioki, I., Suho, S., Inoshiri, R. and Masuda, M. (1998). The effect of room temperature on rectal temperature during night sleep. *J Therm Biol* **23**, 15-21. https://doi.org/10.1016/S0306-4565(97)00041-7.

Thakur, A. K., Jayaraman, M., Mishra, R., Thakur, M., Chellgren, V. M., Byeon, I. J., Anjum, D. H., Kodali, R., Creamer, T. P., Conway, J. F. et al. (2009). Polyglutamine disruption of the huntingtin exon 1 N terminus triggers a complex aggregation mechanism. *Nat Struct Mol Biol* **16**, 380-9. https://doi.org/10.1038/nsmb.1570.

Thompson, L. M., Aiken, C. T., Kaltenbach, L. S., Agrawal, N., Illes, K., Khoshnan, A., Martinez-Vincente, M., Arrasate, M., O'Rourke, J. G., Khashwji, H. et al. (2009). IKK phosphorylates huntingtin and targets it for degradation by the proteasome and lysosome. *J Cell Biol* **187**, 1083-99. https://doi.org/10.1083/jcb.200909067.

Tittelmeier, J., Nachman, E. and Nussbaum-Krammer, C. (2020a). Molecular chaperones: A double-edged sword in neurodegenerative diseases. *Front Aging Neurosci* **12**, 581374. https://doi.org/10.3389/fnagi.2020.581374.

References

Tittelmeier, J., Sandhof, C. A., Ries, H. M., Druffel-Augustin, S., Mogk, A., Bukau, B. and Nussbaum-Krammer, C. (2020b). The HSP110/HSP70 disaggregation system generates spreading-competent toxic alpha-synuclein species. *Embo j* **39**, e103954. https://doi.org/10.15252/embj.2019103954.

Togo, F., Aizawa, S., Arai, J., Yoshikawa, S., Ishiwata, T., Shephard, R. J. and Aoyagi, Y. (2007). Influence on human sleep patterns of lowering and delaying the minimum core body temperature by slow changes in the thermal environment. *Sleep* **30**, 797-802. https://doi.org/10.1093/sleep/30.6.797.

Toledo, M., Batista-Gonzalez, A., Merheb, E., Aoun, M. L., Tarabra, E., Feng, D., Sarparanta, J., Merlo, P., Botre, F., Schwartz, G. J. et al. (2018). Autophagy regulates the liver clock and glucose metabolism by degrading CRY1. *Cell Metab* **28**, 268-281 e4. https://doi.org/10.1016/j.cmet.2018.05.023.

Tomioka, K., Sakamoto, M., Harui, Y., Matsumoto, N. and Matsumoto, A. (1998a). Light and temperature cooperate to regulate the circadian locomotor rhythm of wild type and period mutants of *Drosophila melanogaster*. *J Insect Physiol* **44**, 587-596. https://doi.org/10.1016/S0022-1910(98)00046-8.

Tomioka, K., Sakamoto, M., Harui, Y., Matsumoto, N. and Matsumoto, A. J. J. o. i. p. (1998b). Light and temperature cooperate to regulate the circadian locomotor rhythm of wild type and period mutants of *Drosophila melanogaster*. **44**, 587-596.

Tomoshige, S., Nomura, S., Ohgane, K., Hashimoto, Y. and Ishikawa, M. (2017). Discovery of small molecules that induce the degradation of huntingtin. *Angew Chem Int Ed Engl* **56**, 11530-11533. https://doi.org/10.1002/anie.201706529.

Top, D. and Young, M. W. (2018). Coordination between Differentially Regulated Circadian Clocks Generates Rhythmic Behavior. *Cold Spring Harb Perspect Biol* **10**. https://doi.org/10.1101/cshperspect.a033589.

Tourette, C., Li, B., Bell, R., O'Hare, S., Kaltenbach, L. S., Mooney, S. D. and Hughes, R. E. (2014). A large scale huntingtin protein interaction network implicates Rho GTPase signaling pathways in Huntington disease. *J Biol Chem* **289**, 6709-6726. https://doi.org/10.1074/jbc.M113.523696.

Tournissac, M., Vandal, M., François, A., Planel, E. and Calon, F. (2017). Old age potentiates cold-induced tau phosphorylation: linking thermoregulatory deficit with Alzheimer's disease. *Neurobiol Aging* **50**, 25-29. https://doi.org/10.1016/j.neurobiolaging.2016.09.024.

Trajkovic, K., Jeong, H. and Krainc, D. (2017). Mutant huntingtin is secreted via a late endosomal/lysosomal unconventional secretory pathway. *J Neurosci* **37**, 9000-9012. https://doi.org/10.1523/jneurosci.0118-17.2017.

Tranah, G. J., Blackwell, T., Stone, K. L., Ancoli-Israel, S., Paudel, M. L., Ensrud, K. E., Cauley, J. A., Redline, S., Hillier, T. A., Cummings, S. R. et al. (2011). Circadian activity rhythms and risk of incident dementia and mild cognitive impairment in older women. *Ann Neurol* **70**, 722-32. https://doi.org/10.1002/ana.22468.

Trembath, M. K., Horton, Z. A., Tippett, L., Hogg, V., Collins, V. R., Churchyard, A., Velakoulis, D., Roxburgh, R. and Delatycki, M. B. (2010). A retrospective study of the impact of lifestyle on age at onset of Huntington disease. *Mov Disord* **25**, 1444-50. https://doi.org/10.1002/mds.23108.

References

Trottier, Y., Biancalana, V. and Mandel, J. L. (1994). Instability of CAG repeats in Huntington's disease: relation to parental transmission and age of onset. *J Med Genet* **31**, 377-82. https://doi.org/10.1136/jmg.31.5.377.

Trottier, Y., Devys, D., Imbert, G., Saudou, F., An, I., Lutz, Y., Weber, C., Agid, Y., Hirsch, E. C. and Mandel, J. L. (1995). Cellular localization of the Huntington's disease protein and discrimination of the normal and mutated form. *Nat Genet* **10**, 104-10. https://doi.org/10.1038/ng0595-104.

Trushina, E., Dyer, R. B., Badger, J. D., 2nd, Ure, D., Eide, L., Tran, D. D., Vrieze, B. T., Legendre-Guillemin, V., McPherson, P. S., Mandavilli, B. S. et al. (2004). Mutant huntingtin impairs axonal trafficking in mammalian neurons in vivo and in vitro. *Mol Cell Biol* **24**, 8195-209. https://doi.org/10.1128/mcb.24.18.8195-8209.2004.

Trushina, E., Heldebrant, M. P., Perez-Terzic, C. M., Bortolon, R., Kovtun, I. V., Badger, J. D., 2nd, Terzic, A., Estévez, A., Windebank, A. J., Dyer, R. B. et al. (2003). Microtubule destabilization and nuclear entry are sequential steps leading to toxicity in Huntington's disease. *Proc Natl Acad Sci U S A* **100**, 12171-6. https://doi.org/10.1073/pnas.2034961100.

Tsvetkov, A. S., Arrasate, M., Barmada, S., Ando, D. M., Sharma, P., Shaby, B. A. and Finkbeiner, S. (2013). Proteostasis of polyglutamine varies among neurons and predicts neurodegeneration. *Nat Chem Biol* **9**, 586-92. https://doi.org/10.1038/nchembio.1308.

Tue, N. T., Shimaji, K., Tanaka, N. and Yamaguchi, M. (2012). Effect of αB-crystallin on protein aggregation in *Drosophila*. *J Biomed Biotechnol* **2012**, 252049. https://doi.org/10.1155/2012/252049.

Turturici, G., Sconzo, G. and Geraci, F. (2011). Hsp70 and its molecular role in nervous system diseases. *Biochemistry Research International* **2011**, 1-18. https://doi.org/10.1155/2011/618127.

Tycko, R. (2015). Amyloid polymorphism: Structural basis and neurobiological relevance. *Neuron* **86**, 632-45. https://doi.org/10.1016/j.neuron.2015.03.017.

Tydlacka, S., Wang, C. E., Wang, X., Li, S. and Li, X. J. (2008). Differential activities of the ubiquitin-proteasome system in neurons versus glia may account for the preferential accumulation of misfolded proteins in neurons. *J Neurosci* **28**, 13285-95. https://doi.org/10.1523/jneurosci.4393-08.2008.

Tyebji, S. and Hannan, A. J. (2017). Synaptopathic mechanisms of neurodegeneration and dementia: Insights from Huntington's disease. *Prog Neurobiol* **153**, 18-45. https://doi.org/10.1016/j.pneurobio.2017.03.008.

Tyler, C. J., Reeve, T., Hodges, G. J. and Cheung, S. S. (2016). The effects of heat adaptation on physiology, perception and exercise performance in the heat: A meta-analysis. *Sports Med* **46**, 1699-1724. https://doi.org/10.1007/s40279-016-0538-5.

Ueda, H. R., Hayashi, S., Chen, W., Sano, M., Machida, M., Shigeyoshi, Y., Iino, M. and Hashimoto, S. (2005). System-level identification of transcriptional circuits underlying mammalian circadian clocks. *Nat Genet* **37**, 187-92. https://doi.org/10.1038/ng1504.

Ueno, T., Tomita, J., Kume, S. and Kume, K. (2012). Dopamine modulates metabolic rate and temperature sensitivity in *Drosophila melanogaster*. *PLoS One* **7**, e31513. https://doi.org/10.1371/journal.pone.0031513.

References

Ugur, B., Chen, K. and Bellen, H. J. (2016). *Drosophila* tools and assays for the study of human diseases. *Dis Model Mech* **9**, 235-44. https://doi.org/10.1242/dmm.023762.

Umezaki, Y., Yoshii, T., Kawaguchi, T., Helfrich-Förster, C. and Tomioka, K. (2012). Pigment-dispersing factor is involved in age-dependent rhythm changes in *Drosophila melanogaster*. *J Biol Rhythms* **27**, 423-32. https://doi.org/10.1177/0748730412462206.

Umscheif, G., Shein, N. A., Alexandrovich, A. G., Trembovler, V., Horowitz, M. and Shohami, E. (2010). Heat acclimation provides sustained improvement in functional recovery and attenuates apoptosis after traumatic brain injury. *J Cereb Blood Flow Metab* **30**, 616-27. https://doi.org/10.1038/jcbfm.2009.234.

Umschweif, G., Shabashov, D., Alexandrovich, A. G., Trembovler, V., Horowitz, M. and Shohami, E. (2014). Neuroprotection after traumatic brain injury in heat-acclimated mice involves induced neurogenesis and activation of angiotensin receptor type 2 signaling. *J Cereb Blood Flow Metab* **34**, 1381-90. https://doi.org/10.1038/jcbfm.2014.93.

Urbanek, A., Popovic, M., Morató, A., Estaña, A., Elena-Real, C. A., Mier, P., Fournet, A., Allemand, F., Delbecq, S., Andrade-Navarro, M. A. et al. (2020). Flanking Regions Determine the Structure of the Poly-Glutamine in Huntingtin through Mechanisms Common among Glutamine-Rich Human Proteins. *Structure* **28**, 733-746.e5. https://doi.org/10.1016/j.str.2020.04.008.

Ureshino, R. P., Erustes, A. G., Bassani, T. B., Wachilewski, P., Guarache, G. C., Nascimento, A. C., Costa, A. J., Smaili, S. S. and Pereira, G. (2019). The interplay between Ca(2+) signaling pathways and neurodegeneration. *Int J Mol Sci* **20**. https://doi.org/10.3390/ijms20236004.

Vaccaro, A., Birman, S. and Klarsfeld, A. (2016). Chronic jet lag impairs startle-induced locomotion in *Drosophila*. *Exp Gerontol* **85**, 24-27. https://doi.org/10.1016/j.exger.2016.09.012.

Vaccaro, A., Issa, A. R., Seugnet, L., Birman, S. and Klarsfeld, A. (2017). *Drosophila* clock is required in brain pacemaker neurons to prevent premature locomotor aging independently of its circadian function. *PLoS Genet* **13**, e1006507. https://doi.org/10.1371/journal.pgen.1006507.

Vaiserman, A. M. (2008). Epigenetic engineering and its possible role in anti-aging intervention. *Rejuvenation Res* **11**, 39-42. https://doi.org/10.1089/rej.2007.0579.

Vaiserman, A. M. (2010). Hormesis, adaptive epigenetic reorganization, and implications for human health and longevity. *Dose Response* **8**, 16-21. https://doi.org/10.2203/dose-response.09-014.Vaiserman.

Vakkayil, K. L. and Hoppe, T. (2022). Temperature-dependent regulation of proteostasis and longevity. *Front Aging* **3**, 853588. https://doi.org/10.3389/fragi.2022.853588.

Valdez, P., Ramírez, C. and García, A. (2012). Circadian rhythms in cognitive performance: implications for neuropsychological assessment. *Chronophysiology and therapy* **2**, 12. https://doi.org/10.2147/CPT.S32586.

Vallone, D., Lahiri, K., Dickmeis, T. and Foulkes, N. S. (2007). Start the clock! Circadian rhythms and development. *Dev Dyn* **236**, 142-55. https://doi.org/10.1002/dvdy.20998.

Valor, L. M. (2015). Transcription, epigenetics and ameliorative strategies in Huntington's disease: A genome-wide perspective. *Mol Neurobiol* **51**, 406-23. https://doi.org/10.1007/s12035-014-8715-8.

References

Valor, L. M. and Guiretti, D. (2014). What's wrong with epigenetics in Huntington's disease? *Neuropharmacology* **80**, 103-14. https://doi.org/10.1016/j.neuropharm.2013.10.025.

Valor, L. M., Guiretti, D., Lopez-Atalaya, J. P. and Barco, A. (2013). Genomic landscape of transcriptional and epigenetic dysregulation in early onset polyglutamine disease. *J Neurosci* **33**, 10471-82. https://doi.org/10.1523/jneurosci.0670-13.2013.

van der Bent, M. L., Evers, M. M. and Vallès, A. (2022). Emerging therapies for Huntington's disease - focus on N-terminal huntingtin and huntingtin exon 1. *Biologics* **16**, 141-160. https://doi.org/10.2147/btt.S270657.

van der Burg, J. M., Björkqvist, M. and Brundin, P. (2009). Beyond the brain: Widespread pathology in Huntington's disease. *Lancet Neurol* **8**, 765-74. https://doi.org/10.1016/s1474-4422(09)70178-4.

van der Linden, A. M., Beverly, M., Kadener, S., Rodriguez, J., Wasserman, S., Rosbash, M. and Sengupta, P. (2010). Genome-wide analysis of light- and temperature-entrained circadian transcripts in *Caenorhabditis elegans*. *PLoS Biol* **8**, e1000503. https://doi.org/10.1371/journal.pbio.1000503.

Van Raamsdonk, J. M., Pearson, J., Rogers, D. A., Bissada, N., Vogl, A. W., Hayden, M. R. and Leavitt, B. R. (2005). Loss of wild-type huntingtin influences motor dysfunction and survival in the YAC128 mouse model of Huntington disease. *Hum Mol Genet* **14**, 1379-92. https://doi.org/10.1093/hmg/ddi147.

van Wamelen, D. J., Aziz, N. A., Anink, J. J., van Steenhoven, R., Angeloni, D., Fraschini, F., Jockers, R., Roos, R. A. and Swaab, D. F. (2013). Suprachiasmatic nucleus neuropeptide expression in patients with Huntington's disease. *Sleep* **36**, 117-25. https://doi.org/10.5665/sleep.2314.

van Wamelen, D. J., Roos, R. A. and Aziz, N. A. (2015). Therapeutic strategies for circadian rhythm and sleep disturbances in Huntington disease. *Neurodegener Dis Manag* **5**, 549-59. https://doi.org/10.2217/nmt.15.45.

Vandenberghe, A., Lefranc, M. and Furlan, A. (2022). An overview of the circadian clock in the frame of chronotherapy: From bench to bedside. *Pharmaceutics* **14**. https://doi.org/10.3390/pharmaceutics14071424.

Vanin, S., Bhutani, S., Montelli, S., Menegazzi, P., Green, E. W., Pegoraro, M., Sandrelli, F., Costa, R. and Kyriacou, C. P. (2012). Unexpected features of *Drosophila* circadian behavioural rhythms under natural conditions. *Nature* **484**, 371-5. https://doi.org/10.1038/nature10991.

Varma, H., Cheng, R., Voisine, C., Hart, A. C. and Stockwell, B. R. (2007). Inhibitors of metabolism rescue cell death in Huntington's disease models. *Proc Natl Acad Sci U S A* **104**, 14525-30. https://doi.org/10.1073/pnas.0704482104.

Vashishtha, M., Ng, C. W., Yildirim, F., Gipson, T. A., Kratter, I. H., Bodai, L., Song, W., Lau, A., Labadorf, A., Vogel-Ciernia, A. et al. (2013). Targeting H3K4 trimethylation in Huntington disease. *Proc Natl Acad Sci U S A* **110**, E3027-36. https://doi.org/10.1073/pnas.1311323110.

Vaze, K. M., Nikhil, K. L. and Sharma, V. K. (2014). Circadian rhythms. *Resonance* **19**, 175-189. https://doi.org/10.1007/s12045-014-0020-3.

References

Veleri, S., Brandes, C., Helfrich-Förster, C., Hall, J. C. and Stanewsky, R. (2003). A self-sustaining, light-entrainable circadian oscillator in the *Drosophila* brain. *Curr Biol* **13**, 1758-67. https://doi.org/10.1016/j.cub.2003.09.030.

Velier, J., Kim, M., Schwarz, C., Kim, T. W., Sapp, E., Chase, K., Aronin, N. and DiFiglia, M. (1998). Wild-type and mutant huntingtins function in vesicle trafficking in the secretory and endocytic pathways. *Exp Neurol* **152**, 34-40. https://doi.org/10.1006/exnr.1998.6832.

Vendredy, L., Adriaenssens, E. and Timmerman, V. (2020). Small heat shock proteins in neurodegenerative diseases. *Cell Stress Chaperones* **25**, 679-699. https://doi.org/10.1007/s12192-020-01101-4.

Venkatraman, P., Wetzel, R., Tanaka, M., Nukina, N. and Goldberg, A. L. (2004). Eukaryotic proteasomes cannot digest polyglutamine sequences and release them during degradation of polyglutamine-containing proteins. *Mol Cell* **14**, 95-104. https://doi.org/10.1016/s1097-2765(04)00151-0.

Venken, K. J., Simpson, J. H. and Bellen, H. J. (2011). Genetic manipulation of genes and cells in the nervous system of the fruit fly. *Neuron* **72**, 202-30. https://doi.org/10.1016/j.neuron.2011.09.021.

Verhoef, L. G., Lindsten, K., Masucci, M. G. and Dantuma, N. P. (2002). Aggregate formation inhibits proteasomal degradation of polyglutamine proteins. *Hum Mol Genet* **11**, 2689-700. https://doi.org/10.1093/hmg/11.22.2689.

Verma, A. K., Singh, S. and Rizvi, S. I. (2023). Aging, circadian disruption and neurodegeneration: Interesting interplay. *Exp Gerontol* **172**, 112076. https://doi.org/10.1016/j.exger.2022.112076.

Vernizzi, L., Paiardi, C., Licata, G., Vitali, T., Santarelli, S., Raneli, M., Manelli, V., Rizzetto, M., Gioria, M., Pasini, M. E. et al. (2020). Glutamine Synthetase 1 increases autophagy lysosomal degradation of mutant Huntingtin aggregates in neurons, ameliorating motility in a *Drosophila* model for Huntington's disease. *Cells* **9**. https://doi.org/10.3390/cells9010196.

Vetter, C. (2020). Circadian disruption: What do we actually mean? *Eur J Neurosci* **51**, 531-550. https://doi.org/10.1111/ejn.14255.

Vetter, C., Phillips, A. J. K., Silva, A., Lockley, S. W. and Glickman, G. (2019). Light me up? Why, when, and how much light we need. *J Biol Rhythms* **34**, 573-575. https://doi.org/10.1177/0748730419892111.

Videnovic, A., Leurgans, S., Fan, W., Jaglin, J. and Shannon, K. M. (2009). Daytime somnolence and nocturnal sleep disturbances in Huntington disease. *Parkinsonism Relat Disord* **15**, 471-4. https://doi.org/10.1016/j.parkreldis.2008.10.002.

Videnovic, A. and Zee, P. C. (2015). Consequences of circadian disruption on neurologic health. *Sleep Med Clin* **10**, 469-80. https://doi.org/10.1016/j.jsmc.2015.08.004.

Vilarino-Guell, C., Rajput, A., Milnerwood, A. J., Shah, B., Szu-Tu, C., Trinh, J., Yu, I., Encarnacion, M., Munsie, L. N., Tapia, L. et al. (2014). DNAJC13 mutations in Parkinson disease. *Hum Mol Genet* **23**, 1794-801. https://doi.org/10.1093/hmg/ddt570.

Villar-Menéndez, I., Blanch, M., Tyebji, S., Pereira-Veiga, T., Albasanz, J. L., Martín, M., Ferrer, I., Pérez-Navarro, E. and Barrachina, M. (2013). Increased 5-methylcytosine and decreased 5-

hydroxymethylcytosine levels are associated with reduced striatal A2AR levels in Huntington's disease. *Neuromolecular Med* **15**, 295-309. https://doi.org/10.1007/s12017-013-8219-0.

Vinatier, G., Corsi, J. M., Mignotte, B. and Gaumer, S. (2015). Quantification of Ataxin-3 and Ataxin-7 aggregates formed in vivo in *Drosophila* reveals a threshold of aggregated polyglutamine proteins associated with cellular toxicity. *Biochem Biophys Res Commun* **464**, 1060-1065. https://doi.org/10.1016/j.bbrc.2015.07.071.

von Saint Paul, U. and Aschoff, J. (1978). Longevity among blowfliesPhormia terraenovae RD kept in non-24-hour light-dark cycles. *Journal of comparative physiology* **127**, 191-195. https://doi.org/10.1007/BF01350109.

Vos, M. J., Zijlstra, M. P., Kanon, B., van Waarde-Verhagen, M. A., Brunt, E. R., Oosterveld-Hut, H. M., Carra, S., Sibon, O. C. and Kampinga, H. H. (2010). HSPB7 is the most potent polyQ aggregation suppressor within the HSPB family of molecular chaperones. *Hum Mol Genet* **19**, 4677-93. https://doi.org/10.1093/hmg/ddq398.

Vosko, A. M., Schroeder, A., Loh, D. H. and Colwell, C. S. (2007). Vasoactive intestinal peptide and the mammalian circadian system. *Gen Comp Endocrinol* **152**, 165-75. https://doi.org/10.1016/j.ygcen.2007.04.018.

Voysey, Z., Fazal, S. V., Lazar, A. S. and Barker, R. A. (2021a). The sleep and circadian problems of Huntington's disease: when, why and their importance. *J Neurol* **268**, 2275-2283. https://doi.org/10.1007/s00415-020-10334-3.

Voysey, Z. J., Barker, R. A. and Lazar, A. S. (2021b). The treatment of sleep dysfunction in neurodegenerative disorders. *Neurotherapeutics* **18**, 202-216. https://doi.org/10.1007/s13311-020-00959-7.

Wacker, J. L., Huang, S. Y., Steele, A. D., Aron, R., Lotz, G. P., Nguyen, Q., Giorgini, F., Roberson, E. D., Lindquist, S., Masliah, E. et al. (2009). Loss of Hsp70 exacerbates pathogenesis but not levels of fibrillar aggregates in a mouse model of Huntington's disease. *J Neurosci* **29**, 9104-14. https://doi.org/10.1523/JNEUROSCI.2250-09.2009.

Waelter, S., Boeddrich, A., Lurz, R., Scherzinger, E., Lueder, G., Lehrach, H. and Wanker, E. E. (2001). Accumulation of mutant huntingtin fragments in aggresome-like inclusion bodies as a result of insufficient protein degradation. *Mol Biol Cell* **12**, 1393-407. https://doi.org/10.1091/mbc.12.5.1393.

Wagner, A. S., Politi, A. Z., Ast, A., Bravo-Rodriguez, K., Baum, K., Buntru, A., Strempel, N. U., Brusendorf, L., Hänig, C., Boeddrich, A. et al. (2018). Self-assembly of mutant huntingtin exon-1 fragments into large complex fibrillar structures involves nucleated branching. *J Mol Biol* **430**, 1725-1744. https://doi.org/10.1016/j.jmb.2018.03.017.

Wahl, S., Engelhardt, M., Schaupp, P., Lappe, C. and Ivanov, I. V. (2019). The inner clock-blue light sets the human rhythm. *J Biophotonics* **12**, e201900102. https://doi.org/10.1002/jbio.201900102.

Wakamura, T. and Tokura, H. (2002). Circadian rhythm of rectal temperature in humans under different ambient temperature cycles. *J Therm Biol* **27**, 439-447. https://doi.org/10.1016/S0306-4565(02)00014-1.

Walker, F. O. (2007). Huntington's disease. *Lancet* **369**, 218-28. https://doi.org/10.1016/s0140-6736(07)60111-1.

References

Walter, E. J. and Carraretto, M. (2016). The neurological and cognitive consequences of hyperthermia. *Crit Care* **20**, 199. https://doi.org/10.1186/s13054-016-1376-4.

Walters, R. H. and Murphy, R. M. (2009). Examining polyglutamine peptide length: A connection between collapsed conformations and increased aggregation. *J Mol Biol* **393**, 978-92. https://doi.org/10.1016/j.jmb.2009.08.034.

Walton, J. C., Walker, W. H., 2nd, Bumgarner, J. R., Meléndez-Fernández, O. H., Liu, J. A., Hughes, H. L., Kaper, A. L. and Nelson, R. J. (2021). Circadian variation in efficacy of medications. *Clin Pharmacol Ther* **109**, 1457-1488. https://doi.org/10.1002/cpt.2073.

Wang, C. E., Tydlacka, S., Orr, A. L., Yang, S. H., Graham, R. K., Hayden, M. R., Li, S., Chan, A. W. and Li, X. J. (2008). Accumulation of N-terminal mutant huntingtin in mouse and monkey models implicated as a pathogenic mechanism in Huntington's disease. *Hum Mol Genet* **17**, 2738-51. https://doi.org/10.1093/hmg/ddn175.

Wang, F., Yang, Y., Lin, X., Wang, J. Q., Wu, Y. S., Xie, W., Wang, D., Zhu, S., Liao, Y. Q., Sun, Q. et al. (2013). Genome-wide loss of 5-hmC is a novel epigenetic feature of Huntington's disease. *Hum Mol Genet* **22**, 3641-53. https://doi.org/10.1093/hmg/ddt214.

Wang, H., Marquilly, C., Busto, G. U., Leger, B. S., Boulanger, A., Giniger, E., Walker, J. A., Fradkin, L. G. and Dura, J.-M. (2021). Htt is a repressor of Abl activity required for APP-induced axonal growth. *PLoS Genet* **17**. https://doi.org/10.1371/journal.pgen.1009287.

Wang, H., Wang, B., Normoyle, K. P., Jackson, K., Spitler, K., Sharrock, M. F., Miller, C. M., Best, C., Llano, D. and Du, R. (2014). Brain temperature and its fundamental properties: a review for clinical neuroscientists. *Front Neurosci* **8**, 307. https://doi.org/10.3389/fnins.2014.00307.

Wang, H. B., Loh, D. H., Whittaker, D. S., Cutler, T., Howland, D. and Colwell, C. S. (2018). Time-restricted feeding improves circadian dysfunction as well as motor symptoms in the Q175 mouse model of Huntington's disease. *eNeuro* **5**. https://doi.org/10.1523/eneuro.0431-17.2017.

Wang, H. B., Whittaker, D. S., Truong, D., Mulji, A. K., Ghiani, C. A., Loh, D. H. and Colwell, C. S. (2017). Blue light therapy improves circadian dysfunction as well as motor symptoms in two mouse models of Huntington's disease. *Neurobiol Sleep Circadian Rhythms* **2**, 39-52. https://doi.org/10.1016/j.nbscr.2016.12.002.

Wang, X., Sirianni, A., Pei, Z., Cormier, K., Smith, K., Jiang, J., Zhou, S., Wang, H., Zhao, R., Yano, H. et al. (2011). The melatonin MT1 receptor axis modulates mutant huntingtin-mediated toxicity. *J Neurosci* **31**, 14496-507. https://doi.org/10.1523/jneurosci.3059-11.2011.

Wang, X., Xu, Z., Cai, Y., Zeng, S., Peng, B., Ren, X., Yan, Y. and Gong, Z. (2020). Rheostatic balance of circadian rhythm and autophagy in metabolism and disease. *Front Cell Dev Biol* **8**, 616434. https://doi.org/10.3389/fcell.2020.616434.

Wang, X. L. and Li, L. (2021). Circadian clock regulates inflammation and the development of neurodegeneration. *Front Cell Infect Microbiol* **11**, 696554. https://doi.org/10.3389/fcimb.2021.696554.

Wanker, E. E., Ast, A., Schindler, F., Trepte, P. and Schnoegl, S. (2019). The pathobiology of perturbed mutant huntingtin protein-protein interactions in Huntington's disease. *J Neurochem* **151**, 507-519. https://doi.org/10.1111/jnc.14853.

References

Warby, S. C., Chan, E. Y., Metzler, M., Gan, L., Singaraja, R. R., Crocker, S. F., Robertson, H. A. and Hayden, M. R. (2005). Huntingtin phosphorylation on serine 421 is significantly reduced in the striatum and by polyglutamine expansion in vivo. *Hum Mol Genet* **14**, 1569-77. https://doi.org/10.1093/hmg/ddi165.

Warby, S. C., Doty, C. N., Graham, R. K., Carroll, J. B., Yang, Y. Z., Singaraja, R. R., Overall, C. M. and Hayden, M. R. (2008). Activated caspase-6 and caspase-6-cleaved fragments of huntingtin specifically colocalize in the nucleus. *Hum Mol Genet* **17**, 2390-404. https://doi.org/10.1093/hmg/ddn139.

Warby, S. C., Montpetit, A., Hayden, A. R., Carroll, J. B., Butland, S. L., Visscher, H., Collins, J. A., Semaka, A., Hudson, T. J. and Hayden, M. R. (2009). CAG expansion in the Huntington disease gene is associated with a specific and targetable predisposing haplogroup. *Am J Hum Genet* **84**, 351-66. https://doi.org/10.1016/j.ajhg.2009.02.003.

Warner, J. B. t., Ruff, K. M., Tan, P. S., Lemke, E. A., Pappu, R. V. and Lashuel, H. A. (2017). Monomeric huntingtin exon 1 has similar overall structural features for wild-type and pathological polyglutamine lengths. *J Am Chem Soc* **139**, 14456-14469. https://doi.org/10.1021/jacs.7b06659.

Warrick, J. M., Morabito, L. M., Bilen, J., Gordesky-Gold, B., Faust, L. Z., Paulson, H. L. and Bonini, N. M. (2005). Ataxin-3 suppresses polyglutamine neurodegeneration in *Drosophila* by a ubiquitin-associated mechanism. *Mol Cell* **18**, 37-48. https://doi.org/10.1016/j.molcel.2005.02.030.

Warrick, J. M., Paulson, H. L., Gray-Board, G. L., Bui, Q. T., Fischbeck, K. H., Pittman, R. N. and Bonini, N. M. (1998). Expanded polyglutamine protein forms nuclear inclusions and causes neural degeneration in *Drosophila*. *Cell* **93**, 939-49. https://doi.org/10.1016/s0092-8674(00)81200-3.

Watson, N. V. and Breedlove, S. M. (2012). The mind's machine: Foundations of brain and behavior. Sunderland, MA, US: Sinauer Associates.

Wear, M. P., Kryndushkin, D., O'Meally, R., Sonnenberg, J. L., Cole, R. N. and Shewmaker, F. P. (2015). Proteins with intrinsically disordered domains are preferentially recruited to polyglutamine aggregates. *PLoS One* **10**, e0136362. https://doi.org/10.1371/journal.pone.0136362.

Webb AB, Angelo N and ED, H. (2008). Individual SCN neurons are weak oscillators with changeable circadian phenotypes (P105). *Soc Res Biol RhythmsSoc Res Biol Rhythms Abstr.* **20**.

Webb, A. B., Angelo, N., Huettner, J. E. and Herzog, E. D. (2009). Intrinsic, nondeterministic circadian rhythm generation in identified mammalian neurons. *Proc Natl Acad Sci U S A* **106**, 16493-8. https://doi.org/10.1073/pnas.0902768106.

Weiss, K. R., Kimura, Y., Lee, W. C. and Littleton, J. T. (2012). Huntingtin aggregation kinetics and their pathological role in a *Drosophila* Huntington's disease model. *Genetics* **190**, 581-600. https://doi.org/10.1534/genetics.111.133710.

Weiss, K. R. and Littleton, J. T. (2016). Characterization of axonal transport defects in *Drosophila* Huntingtin mutants. *J Neurogenet* **30**, 212-221. https://doi.org/10.1080/01677063.2016.1202950.

Wellington, C. L., Ellerby, L. M., Hackam, A. S., Margolis, R. L., Trifiro, M. A., Singaraja, R., McCutcheon, K., Salvesen, G. S., Propp, S. S., Bromm, M. et al. (1998). Caspase cleavage of gene

products associated with triplet expansion disorders generates truncated fragments containing the polyglutamine tract. *J Biol Chem* **273**, 9158-67. https://doi.org/10.1074/jbc.273.15.9158.

Welsh, D. K., Logothetis, D. E., Meister, M. and Reppert, S. M. (1995). Individual neurons dissociated from rat suprachiasmatic nucleus express independently phased circadian firing rhythms. *Neuron* **14**, 697-706. https://doi.org/10.1016/0896-6273(95)90214-7.

Welsh, D. K., Takahashi, J. S. and Kay, S. A. (2010). Suprachiasmatic nucleus: Cell autonomy and network properties. *Annu Rev Physiol* **72**, 551-77. https://doi.org/10.1146/annurev-physiol-021909-135919.

Wentink, A. S., Nillegoda, N. B., Feufel, J., Ubartaitė, G., Schneider, C. P., De Los Rios, P., Hennig, J., Barducci, A. and Bukau, B. (2020). Molecular dissection of amyloid disaggregation by human HSP70. *Nature* **587**, 483-488. https://doi.org/10.1038/s41586-020-2904-6.

West, A. C. and Bechtold, D. A. (2015). The cost of circadian desynchrony: Evidence, insights and open questions. *Bioessays* **37**, 777-88. https://doi.org/10.1002/bies.201400173.

West, K. E., Jablonski, M. R., Warfield, B., Cecil, K. S., James, M., Ayers, M. A., Maida, J., Bowen, C., Sliney, D. H., Rollag, M. D. et al. (2011). Blue light from light-emitting diodes elicits a dose-dependent suppression of melatonin in humans. *J Appl Physiol (1985)* **110**, 619-26. https://doi.org/10.1152/japplphysiol.01413.2009.

Westhoff, B., Chapple, J. P., van der Spuy, J., Hohfeld, J. and Cheetham, M. E. (2005). HSJ1 is a neuronal shuttling factor for the sorting of chaperone clients to the proteasome. *Curr Biol* **15**, 1058-64. https://doi.org/10.1016/j.cub.2005.04.058.

Wetzel, R. (2020). Exploding the repeat length paradigm while exploring amyloid toxicity in Huntington's disease. *Acc Chem Res* **53**, 2347-2357. https://doi.org/10.1021/acs.accounts.0c00450.

Wexler, N. S., Lorimer, J., Porter, J., Gomez, F., Moskowitz, C., Shackell, E., Marder, K., Penchaszadeh, G., Roberts, S. A., Gayán, J. et al. (2004). Venezuelan kindreds reveal that genetic and environmental factors modulate Huntington's disease age of onset. *Proc Natl Acad Sci U S A* **101**, 3498-503. https://doi.org/10.1073/pnas.0308679101.

Wexler, N. S., Young, A. B., Tanzi, R. E., Travers, H., Starosta-Rubinstein, S., Penney, J. B., Snodgrass, S. R., Shoulson, I., Gomez, F., Ramos Arroyo, M. A. et al. (1987). Homozygotes for Huntington's disease. *Nature* **326**, 194-7. https://doi.org/10.1038/326194a0.

Weydt, P., Dupuis, L. and Petersen, Å. (2018). Thermoregulatory disorders in Huntington disease. *Handb Clin Neurol* **157**, 761-775. https://doi.org/10.1016/b978-0-444-64074-1.00047-1.

Weydt, P., Pineda, V. V., Torrence, A. E., Libby, R. T., Satterfield, T. F., Lazarowski, E. R., Gilbert, M. L., Morton, G. J., Bammler, T. K., Strand, A. D. et al. (2006). Thermoregulatory and metabolic defects in Huntington's disease transgenic mice implicate PGC-1alpha in Huntington's disease neurodegeneration. *Cell Metab* **4**, 349-62. https://doi.org/10.1016/j.cmet.2006.10.004.

Wheeler, J. C., Bieschke, E. T. and Tower, J. (1995). Muscle-specific expression of *Drosophila* hsp70 in response to aging and oxidative stress. *Proc Natl Acad Sci U S A* **92**, 10408-12. https://doi.org/10.1073/pnas.92.22.10408.

Wheeler, V. (2021). Dissecting genetic modifiers of HD: Towards understanding mechanism. In *CHDI Foundation Annual Therapeutics Conference* vol. 15, pp. 2015-2024.

References

Wheeler, V. C., Auerbach, W., White, J. K., Srinidhi, J., Auerbach, A., Ryan, A., Duyao, M. P., Vrbanac, V., Weaver, M., Gusella, J. F. et al. (1999). Length-dependent gametic CAG repeat instability in the Huntington's disease knock-in mouse. *Hum Mol Genet* **8**, 115-22. https://doi.org/10.1093/hmg/8.1.115.

White, J. K., Auerbach, W., Duyao, M. P., Vonsattel, J. P., Gusella, J. F., Joyner, A. L. and MacDonald, M. E. (1997). Huntingtin is required for neurogenesis and is not impaired by the Huntington's disease CAG expansion. *Nat Genet* **17**, 404-10. https://doi.org/10.1038/ng1297-404.

Whittaker, D. S., Loh, D. H., Wang, H. B., Tahara, Y., Kuljis, D., Cutler, T., Ghiani, C. A., Shibata, S., Block, G. D. and Colwell, C. S. (2018). Circadian-based treatment strategy effective in the bachd mouse model of Huntington's disease. *J Biol Rhythms* **33**, 535-554. https://doi.org/10.1177/0748730418790401.

Wiggins, R. and Feigin, A. (2021). Emerging therapeutics in Huntington's disease. *Expert Opin Emerg Drugs* **26**, 295-302. https://doi.org/10.1080/14728214.2021.1962285.

Wild, E. J. and Tabrizi, S. J. (2017). Therapies targeting DNA and RNA in Huntington's disease. *Lancet Neurol* **16**, 837-847. https://doi.org/10.1016/s1474-4422(17)30280-6.

Williams, A., Sarkar, S., Cuddon, P., Ttofi, E. K., Saiki, S., Siddiqi, F. H., Jahreiss, L., Fleming, A., Pask, D., Goldsmith, P. et al. (2008). Novel targets for Huntington's disease in an mTOR-independent autophagy pathway. *Nat Chem Biol* **4**, 295-305. https://doi.org/10.1038/nchembio.79.

Williams, A. J., Knutson, T. M., Colomer Gould, V. F. and Paulson, H. L. (2009). In vivo suppression of polyglutamine neurotoxicity by C-terminus of Hsp70-interacting protein (CHIP) supports an aggregation model of pathogenesis. *Neurobiol Dis* **33**, 342-53. https://doi.org/10.1016/j.nbd.2008.10.016.

Willis, G. L., Moore, C. and Armstrong, S. M. (2012). A historical justification for and retrospective analysis of the systematic application of light therapy in Parkinson's disease. *Rev Neurosci* **23**, 199-226. https://doi.org/10.1515/revneuro-2011-0072.

Wilton, D. K. and Stevens, B. (2020). The contribution of glial cells to Huntington's disease pathogenesis. *Neurobiol Dis* **143**, 104963. https://doi.org/10.1016/j.nbd.2020.104963.

Wiprich, M. T. and Bonan, C. D. (2021). Purinergic signaling in the pathophysiology and treatment of Huntington's disease. *Front Neurosci* **15**, 657338. https://doi.org/10.3389/fnins.2021.657338.

Wirz-Justice, A., Skene, D. J. and Münch, M. (2021). The relevance of daylight for humans. *Biochem Pharmacol* **191**, 114304. https://doi.org/10.1016/j.bcp.2020.114304.

Woelfle, M. A., Ouyang, Y., Phanvijhitsiri, K. and Johnson, C. H. (2004). The adaptive value of circadian clocks: an experimental assessment in cyanobacteria. *Curr Biol* **14**, 1481-6. https://doi.org/10.1016/j.cub.2004.08.023.

Woerner, A. C., Frottin, F., Hornburg, D., Feng, L. R., Meissner, F., Patra, M., Tatzelt, J., Mann, M., Winklhofer, K. F., Hartl, F. U. et al. (2016). Cytoplasmic protein aggregates interfere with nucleocytoplasmic transport of protein and RNA. *Science* **351**, 173-6. https://doi.org/10.1126/science.aad2033.

References

Wolfgang, W. J., Miller, T. W., Webster, J. M., Huston, J. S., Thompson, L. M., Marsh, J. L. and Messer, A. (2005). Suppression of Huntington's disease pathology in *Drosophila* by human single-chain Fv antibodies. *Proc Natl Acad Sci U S A* **102**, 11563-8. https://doi.org/10.1073/pnas.0505321102.

Woller, A. and Gonze, D. (2021). Circadian misalignment and metabolic disorders: A story of twisted clocks. *Biology (Basel)* **10**. https://doi.org/10.3390/biology10030207.

Wong, N. A. and Bahmani, H. (2022). A review of the current state of research on artificial blue light safety as it applies to digital devices. *Heliyon* **8**, e10282. https://doi.org/10.1016/j.heliyon.2022.e10282.

Wong, Y. C. and Holzbaur, E. L. (2014). The regulation of autophagosome dynamics by huntingtin and HAP1 is disrupted by expression of mutant huntingtin, leading to defective cargo degradation. *J Neurosci* **34**, 1293-305. https://doi.org/10.1523/jneurosci.1870-13.2014.

Wood, N. I., Carta, V., Milde, S., Skillings, E. A., McAllister, C. J., Ang, Y. L., Duguid, A., Wijesuriya, N., Afzal, S. M., Fernandes, J. X. et al. (2010). Responses to environmental enrichment differ with sex and genotype in a transgenic mouse model of Huntington's disease. *PLoS One* **5**, e9077. https://doi.org/10.1371/journal.pone.0009077.

Wood, N. I., McAllister, C. J., Cuesta, M., Aungier, J., Fraenkel, E. and Morton, A. J. (2013). Adaptation to experimental jet-lag in R6/2 mice despite circadian dysrhythmia. *PLoS One* **8**, e55036. https://doi.org/10.1371/journal.pone.0055036.

Wu, H., Dunnett, S., Ho, Y. S. and Chang, R. C. (2019). The role of sleep deprivation and circadian rhythm disruption as risk factors of Alzheimer's disease. *Front Neuroendocrinol* **54**, 100764. https://doi.org/10.1016/j.yfrne.2019.100764.

Wu, J., Shih, H. P., Vigont, V., Hrdlicka, L., Diggins, L., Singh, C., Mahoney, M., Chesworth, R., Shapiro, G., Zimina, O. et al. (2011). Neuronal store-operated calcium entry pathway as a novel therapeutic target for Huntington's disease treatment. *Chem Biol* **18**, 777-93. https://doi.org/10.1016/j.chembiol.2011.04.012.

Wu, Y., Cao, G. and Nitabach, M. N. (2008a). Electrical silencing of PDF neurons advances the phase of non-PDF clock neurons in *Drosophila*. *J Biol Rhythms* **23**, 117-28. https://doi.org/10.1177/0748730407312984
23/2/117 [pii].

Wu, Y., Cao, G., Pavlicek, B., Luo, X. and Nitabach, M. N. (2008b). Phase coupling of a circadian neuropeptide with rest/activity rhythms detected using a membrane-tethered spider toxin. *PLoS Biol* **6**, e273. https://doi.org/10.1371/journal.pbio.0060273.

Wu, Y. L., Chang, J. C., Lin, W. Y., Li, C. C., Hsieh, M., Chen, H. W., Wang, T. S., Wu, W. T., Liu, C. S. and Liu, K. L. (2018). Caffeic acid and resveratrol ameliorate cellular damage in cell and *Drosophila* models of spinocerebellar ataxia type 3 through upregulation of Nrf2 pathway. *Free Radic Biol Med* **115**, 309-317. https://doi.org/10.1016/j.freeradbiomed.2017.12.011.

Wulbeck, C., Grieshaber, E. and Helfrich-Forster, C. (2008). Pigment-dispersing factor (PDF) has different effects on *Drosophila*'s circadian clocks in the accessory medulla and in the dorsal brain. *J Biol Rhythms* **23**, 409-24. https://doi.org/10.1177/0748730408322699.

References

Wyss-Coray, T. (2016). Ageing, neurodegeneration and brain rejuvenation. *Nature* **539**, 180-186. https://doi.org/10.1038/nature20411.

Wyttenbach, A. (2002). Heat shock protein 27 prevents cellular polyglutamine toxicity and suppresses the increase of reactive oxygen species caused by huntingtin. *Human Molecular Genetics* **11**, 1137-1151. https://doi.org/10.1093/hmg/11.9.1137.

Wyttenbach, A. (2004a). Role of heat shock proteins during polyglutamine neurodegeneration: mechanisms and hypothesis. *Journal of Molecular Neuroscience* **23**, 069-096. 10.1385/jmn:23:1-2:069.

Wyttenbach, A. (2004b). Role of heat shock proteins during polyglutamine neurodegeneration: mechanisms and hypothesis. *J Mol Neurosci* **23**, 69-96. https://doi.org/10.1385/jmn:23:1-2:069.

Wyttenbach, A. and Arrigo, A. P. (2009). The role of Heat shock proteins during neurodegeneration in Alzheimer's, Parkinson's and Huntington's disease. In *Heat Shock Proteins in Neural Cells*, pp. 81-99. https://doi.org/10.1007/978-0-387-39954-6_7.

Wyttenbach, A., Carmichael, J., Swartz, J., Furlong, R. A., Narain, Y., Rankin, J. and Rubinsztein, D. C. (2000). Effects of heat shock, heat shock protein 40 (HDJ-2), and proteasome inhibition on protein aggregation in cellular models of Huntington's disease. *Proc Natl Acad Sci U S A* **97**, 2898-903. https://doi.org/10.1073/pnas.97.6.2898.

Wyttenbach, A., Sauvageot, O., Carmichael, J., Diaz-Latoud, C., Arrigo, A. P. and Rubinsztein, D. C. (2002). Heat shock protein 27 prevents cellular polyglutamine toxicity and suppresses the increase of reactive oxygen species caused by huntingtin. *Hum Mol Genet* **11**, 1137-51. https://doi.org/10.1093/hmg/11.9.1137.

Xia, J., Lee, D. H., Taylor, J., Vandelft, M. and Truant, R. (2003). Huntingtin contains a highly conserved nuclear export signal. *Hum Mol Genet* **12**, 1393-403. https://doi.org/10.1093/hmg/ddg156.

Xiang, C., Zhang, S., Dong, X., Ma, S. and Cong, S. (2018). Transcriptional dysregulation and post-translational modifications in polyglutamine diseases: From pathogenesis to potential therapeutic strategies. *Front Mol Neurosci* **11**, 153. https://doi.org/10.3389/fnmol.2018.00153.

Xiao, C., Wu, T., Ren, A., Pan, Q., Chen, S., Wu, F., Li, X., Wang, R., Hightower, L. E. and Tanguay, R. M. (2003). Basal and inducible levels of Hsp70 in patients with acute heat illness induced during training. *Cell Stress Chaperones* **8**, 86-92. https://doi.org/10.1379/1466-1268(2003)8<86:bailoh>2.0.co;2.

Xiao, G., Fan, Q., Wang, X. and Zhou, B. (2013). Huntington disease arises from a combinatory toxicity of polyglutamine and copper binding. *Proc Natl Acad Sci U S A* **110**, 14995-5000. https://doi.org/10.1073/pnas.1308535110.

Xie, L., Kang, H., Xu, Q., Chen, M. J., Liao, Y., Thiyagarajan, M., O'Donnell, J., Christensen, D. J., Nicholson, C., Iliff, J. J. et al. (2013). Sleep drives metabolite clearance from the adult brain. *Science* **342**, 373-7. https://doi.org/10.1126/science.1241224.

Xie, Y., Tang, Q., Chen, G., Xie, M., Yu, S., Zhao, J. and Chen, L. (2019). New insights into the circadian rhythm and its related diseases. *Front Physiol* **10**, 682. https://doi.org/10.3389/fphys.2019.00682.

Xu, F., Kula-Eversole, E., Iwanaszko, M., Hutchison, A. L., Dinner, A. and Allada, R. (2019a). Circadian clocks function in concert with heat shock organizing protein to modulate mutant huntingtin aggregation and toxicity. *Cell Rep* **27**, 59-70.e4. https://doi.org/10.1016/j.celrep.2019.03.015.

Xu, F., Kula-Eversole, E., Iwanaszko, M., Lim, C. and Allada, R. (2019b). Ataxin2 functions via CrebA to mediate huntingtin toxicity in circadian clock neurons. *PLoS Genet* **15**, e1008356. https://doi.org/10.1371/journal.pgen.1008356.

Xu, H., Bensalel, J., Raju, S., Capobianco, E., Lu, M. L. and Wei, J. (2023). Characterization of huntingtin interactomes and their dynamic responses in living cells by proximity proteomics. *J Neurochem* **164**, 512-528. https://doi.org/10.1111/jnc.15726.

Xu, M. and Wu, Z. Y. (2015). Huntington disease in Asia. *Chin Med J (Engl)* **128**, 1815-9. https://doi.org/10.4103/0366-6999.159359.

Xu, Z., Tito, A. J., Rui, Y. N. and Zhang, S. (2015). Studying polyglutamine diseases in *Drosophila*. *Exp Neurol* **274**, 25-41. https://doi.org/10.1016/j.expneurol.2015.08.002.

Yadav, S. and Tapadia, M. G. (2013). Neurodegeneration caused by polyglutamine expansion is regulated by P-glycoprotein in *Drosophila melanogaster*. *Genetics* **195**, 857-70. https://doi.org/10.1534/genetics.113.155077.

Yadlapalli, S., Jiang, C., Bahle, A., Reddy, P., Meyhofer, E. and Shafer, O. T. (2018). Circadian clock neurons constantly monitor environmental temperature to set sleep timing. *Nature* **555**, 98-102. https://doi.org/10.1038/nature25740.

Yalçin, M., Mundorf, A., Thiel, F., Amatriain-Fernández, S., Kalthoff, I. S., Beucke, J. C., Budde, H., Garthus-Niegel, S., Peterburs, J. and Relógio, A. (2022). It's about time: The circadian network as time-keeper for cognitive functioning, locomotor activity and mental health. *Front Physiol* **13**, 873237. https://doi.org/10.3389/fphys.2022.873237.

Yamada, P. M., Amorim, F. T., Moseley, P., Robergs, R. and Schneider, S. M. (2007). Effect of heat acclimation on heat shock protein 72 and interleukin-10 in humans. *J Appl Physiol (1985)* **103**, 1196-204. https://doi.org/10.1152/japplphysiol.00242.2007.

Yamanaka, T., Miyazaki, H., Oyama, F., Kurosawa, M., Washizu, C., Doi, H. and Nukina, N. (2008). Mutant Huntingtin reduces HSP70 expression through the sequestration of NF-Y transcription factor. *Embo j* **27**, 827-839. https://doi.org/10.1038/emboj.2008.23.

Yamazaki, S., Numano, R., Abe, M., Hida, A., Takahashi, R., Ueda, M., Block, G. D., Sakaki, Y., Menaker, M. and Tei, H. (2000). Resetting central and peripheral circadian oscillators in transgenic rats. *Science* **288**, 682-5. https://doi.org/10.1126/science.288.5466.682.

Yanai, A., Huang, K., Kang, R., Singaraja, R. R., Arstikaitis, P., Gan, L., Orban, P. C., Mullard, A., Cowan, C. M., Raymond, L. A. et al. (2006). Palmitoylation of huntingtin by HIP14 is essential for its trafficking and function. *Nat Neurosci* **9**, 824-31. https://doi.org/10.1038/nn1702.

Yang, C. H., Hwang, C. F., Chuang, J. H., Lian, W. S., Wang, F. S., Huang, E. I. and Yang, M. Y. (2020). Constant light dysregulates cochlear circadian clock and exacerbates noise-induced hearing loss. *Int J Mol Sci* **21**. https://doi.org/10.3390/ijms21207535.

Yang, J., Song, Y., Law, A. D., Rogan, C. J., Shimoda, K., Djukovic, D., Anderson, J. C., Kretzschmar, D., Hendrix, D. A. and Giebultowicz, J. M. (2022). Chronic blue light leads to accelerated

aging in *Drosophila* by impairing energy metabolism and neurotransmitter levels. *Front Aging* **3**, 983373. https://doi.org/10.3389/fragi.2022.983373.

Yang, S., Chang, R., Yang, H., Zhao, T., Hong, Y., Kong, H. E., Sun, X., Qin, Z., Jin, P., Li, S. et al. (2017). CRISPR/Cas9-mediated gene editing ameliorates neurotoxicity in mouse model of Huntington's disease. *J Clin Invest* **127**, 2719-2724. https://doi.org/10.1172/jci92087.

Yao, J., Ong, S. E. and Bajjalieh, S. (2014). Huntingtin is associated with cytomatrix proteins at the presynaptic terminal. *Mol Cell Neurosci* **63**, 96-100. https://doi.org/10.1016/j.mcn.2014.10.003.

Yao, Z., Bennett, A. J., Clem, J. L. and Shafer, O. T. (2016). The *Drosophila* clock neuron network features diverse coupling modes and requires network-wide coherence for robust circadian rhythms. *Cell Rep* **17**, 2873-2881. https://doi.org/10.1016/j.celrep.2016.11.053.

Yao, Z. and Shafer, O. T. (2014). The *Drosophila* circadian clock is a variably coupled network of multiple peptidergic units. *Science* **343**, 1516-20. https://doi.org/10.1126/science.1251285.

Yeh, P. A., Liu, Y. H., Chu, W. C., Liu, J. Y. and Sun, Y. H. (2018). Glial expression of disease-associated poly-glutamine proteins impairs the blood-brain barrier in *Drosophila*. *Hum Mol Genet* **27**, 2546-2562. https://doi.org/10.1093/hmg/ddy160.

Yerbury, J. J., Ooi, L., Dillin, A., Saunders, D. N., Hatters, D. M., Beart, P. M., Cashman, N. R., Wilson, M. R. and Ecroyd, H. (2016). Walking the tightrope: proteostasis and neurodegenerative disease. *J Neurochem* **137**, 489-505. https://doi.org/10.1111/jnc.13575.

Yi, J., He, G., Yang, J., Luo, Z., Yang, X. and Luo, X. (2017). Heat acclimation regulates the autophagy-lysosome function to protect against heat stroke-induced brain injury in mice. *Cell Physiol Biochem* **41**, 101-114. https://doi.org/10.1159/000455979.

Yoo, S. H., Yamazaki, S., Lowrey, P. L., Shimomura, K., Ko, C. H., Buhr, E. D., Siepka, S. M., Hong, H. K., Oh, W. J., Yoo, O. J. et al. (2004). PERIOD2::LUCIFERASE real-time reporting of circadian dynamics reveals persistent circadian oscillations in mouse peripheral tissues. *Proc Natl Acad Sci U S A* **101**, 5339-46. https://doi.org/10.1073/pnas.0308709101.

Yoshii, T., Fujii, K. and Tomioka, K. (2007). Induction of *Drosophila* behavioral and molecular circadian rhythms by temperature steps in constant light. *J Biol Rhythms* **22**, 103-14. https://doi.org/10.1177/0748730406298176.

Yoshii, T., Hermann-Luibl, C., Kistenpfennig, C., Schmid, B., Tomioka, K. and Helfrich-Förster, C. (2015). Cryptochrome-dependent and -independent circadian entrainment circuits in *Drosophila*. *J Neurosci* **35**, 6131-41. https://doi.org/10.1523/jneurosci.0070-15.2015.

Yoshii, T., Hermann, C. and Helfrich-Förster, C. (2010). Cryptochrome-positive and -negative clock neurons in *Drosophila* entrain differentially to light and temperature. *J Biol Rhythms* **25**, 387-98. https://doi.org/10.1177/0748730410381962.

Yoshii, T., Heshiki, Y., Ibuki-Ishibashi, T., Matsumoto, A., Tanimura, T. and Tomioka, K. (2005). Temperature cycles drive *Drosophila* circadian oscillation in constant light that otherwise induces behavioural arrhythmicity. *Eur J Neurosci* **22**, 1176-84. https://doi.org/10.1111/j.1460-9568.2005.04295.x.

Yoshii, T., Rieger, D. and Helfrich-Förster, C. (2012). Two clocks in the brain: An update of the morning and evening oscillator model in *Drosophila*. *Prog Brain Res* **199**, 59-82. https://doi.org/10.1016/b978-0-444-59427-3.00027-7.

References

Yoshii, T., Sakamoto, M. and Tomioka, K. (2002). A temperature-dependent timing mechanism is involved in the circadian system that drives locomotor rhythms in the fruit fly *Drosophila melanogaster*. *Zoolog Sci* **19**, 841-50. https://doi.org/10.2108/zsj.19.841.

Yoshii, T., Todo, T., Wülbeck, C., Stanewsky, R. and Helfrich-Förster, C. (2008). Cryptochrome is present in the compound eyes and a subset of *Drosophila's* clock neurons. *J Comp Neurol* **508**, 952-66. https://doi.org/10.1002/cne.21702.

Yoshii, T., Wülbeck, C., Sehadova, H., Veleri, S., Bichler, D., Stanewsky, R. and Helfrich-Förster, C. (2009). The neuropeptide pigment-dispersing factor adjusts period and phase of *Drosophila*'s clock. *J Neurosci* **29**, 2597-610. https://doi.org/10.1523/JNEUROSCI.5439-08.2009.

Young, M. W. (2018). Time travels: A 40-Year journey from *Drosophila's* clock mutants to human circadian disorders (Nobel Lecture). *Angew Chem Int Ed Engl* **57**, 11532-11539. https://doi.org/10.1002/anie.201803337.

Yu, A., Shibata, Y., Shah, B., Calamini, B., Lo, D. C. and Morimoto, R. I. (2014). Protein aggregation can inhibit clathrin-mediated endocytosis by chaperone competition. *Proceedings of the National Academy of Sciences* **111**, E1481-E1490. https://doi.org/10.1073/pnas.1321811111.

Yu, J. (2012). The role of the clock gene in protection against neural and retinal degeneration.

Yu, W., Houl, J. H. and Hardin, P. E. (2011). NEMO kinase contributes to core period determination by slowing the pace of the *Drosophila* circadian oscillator. *Curr Biol* **21**, 756-61. https://doi.org/10.1016/j.cub.2011.02.037.

Yue, F., Li, W., Zou, J., Chen, Q., Xu, G., Huang, H., Xu, Z., Zhang, S., Gallinari, P., Wang, F. et al. (2015). Blocking the association of HDAC4 with MAP1S accelerates autophagy clearance of mutant Huntingtin. *Aging (Albany NY)* **7**, 839-53. https://doi.org/10.18632/aging.100818.

Zabel, C., Chamrad, D. C., Priller, J., Woodman, B., Meyer, H. E., Bates, G. P. and Klose, J. (2002). Alterations in the mouse and human proteome caused by Huntington's disease. *Mol Cell Proteomics* **1**, 366-75. https://doi.org/10.1074/mcp.m200016-mcp200.

Zala, D., Hinckelmann, M. V. and Saudou, F. (2013a). Huntingtin's function in axonal transport is conserved in *Drosophila melanogaster*. *PLoS One* **8**, e60162. https://doi.org/10.1371/journal.pone.0060162.

Zala, D., Hinckelmann, M. V., Yu, H., Lyra da Cunha, M. M., Liot, G., Cordelières, F. P., Marco, S. and Saudou, F. (2013b). Vesicular glycolysis provides on-board energy for fast axonal transport. *Cell* **152**, 479-91. https://doi.org/10.1016/j.cell.2012.12.029.

Zammit, C., Torzhenskaya, N., Ozarkar, P. D. and Calleja Agius, J. (2021). Neurological disorders vis-à-vis climate change. *Early Hum Dev* **155**, 105217. https://doi.org/10.1016/j.earlhumdev.2020.105217.

Zar, J. H. (2010). Biostatistical analysis Upper Saddle River, N.J: Prentice-Hall/Pearson.

Zarouchlioti, C., Parfitt, D. A., Li, W., Gittings, L. M. and Cheetham, M. E. (2018). DNAJ Proteins in neurodegeneration: essential and protective factors. *Philos Trans R Soc Lond B Biol Sci* **373**. https://doi.org/10.1098/rstb.2016.0534.

Zee, P. C., Attarian, H. and Videnovic, A. (2013). Circadian rhythm abnormalities. *Continuum (Minneap Minn)* **19**, 132-47. https://doi.org/10.1212/01.CON.0000427209.21177.aa.

References

Zeitler, B., Froelich, S., Yu, Q., Pearl, J., Paschon, D. E., Miller, J. C., Li, D., Marlen, K., Guschin, D. and Zhang, L. (2014). Allele-specific repression of mutant huntingtin expression by engineered zinc finger transcriptional repressors as a potential therapy for Huntington's disease. In *Molecular Therapy*, vol. 22, pp. S233-S233: NATURE PUBLISHING GROUP 75 VARICK ST, 9TH FLR, NEW YORK, NY 10013-1917 USA.

Zeitlin, S., Liu, J. P., Chapman, D. L., Papaioannou, V. E. and Efstratiadis, A. (1995). Increased apoptosis and early embryonic lethality in mice nullizygous for the Huntington's disease gene homologue. *Nat Genet* **11**, 155-63. https://doi.org/10.1038/ng1095-155.

Zhang, C., Daubnerova, I., Jang, Y. H., Kondo, S., Žitňan, D. and Kim, Y. J. (2021a). The neuropeptide allatostatin C from clock-associated DN1p neurons generates the circadian rhythm for oogenesis. *Proc Natl Acad Sci U S A* **118**. https://doi.org/10.1073/pnas.2016878118.

Zhang, L., Chung, B. Y., Lear, B. C., Kilman, V. L., Liu, Y., Mahesh, G., Meissner, R. A., Hardin, P. E. and Allada, R. (2010a). DN1(p) circadian neurons coordinate acute light and PDF inputs to produce robust daily behavior in *Drosophila*. *Curr Biol* **20**, 591-9. https://doi.org/10.1016/j.cub.2010.02.056.

Zhang, M. Y., Lear, B. C. and Allada, R. (2021b). The microtubule-associated protein Tau suppresses the axonal distribution of PDF neuropeptide and mitochondria in circadian clock neurons. *Human Molecular Genetics*. 10.1093/hmg/ddab303.

Zhang, M. Y., Lear, B. C. and Allada, R. (2022). The microtubule-associated protein Tau suppresses the axonal distribution of PDF neuropeptide and mitochondria in circadian clock neurons. *Hum Mol Genet* **31**, 1141-1150. https://doi.org/10.1093/hmg/ddab303.

Zhang, Q., Tsoi, H., Peng, S., Li, P. P., Lau, K. F., Rudnicki, D. D., Ngo, J. C. and Chan, H. Y. (2016). Assessing a peptidylic inhibitor-based therapeutic approach that simultaneously suppresses polyglutamine RNA- and protein-mediated toxicities in patient cells and *Drosophila*. *Dis Model Mech* **9**, 321-34. https://doi.org/10.1242/dmm.022350.

Zhang, S., Binari, R., Zhou, R. and Perrimon, N. (2010b). A genomewide RNA interference screen for modifiers of aggregates formation by mutant Huntingtin in *Drosophila*. *Genetics* **184**, 1165-79. https://doi.org/10.1534/genetics.109.112516.

Zhang, S., Feany, M. B., Saraswati, S., Littleton, J. T. and Perrimon, N. (2009). Inactivation of *Drosophila* Huntingtin affects long-term adult functioning and the pathogenesis of a Huntington's disease model. *Dis Model Mech* **2**, 247-66. https://doi.org/10.1242/dmm.000653.

Zhang, X. and Qian, S. B. (2011). Chaperone-mediated hierarchical control in targeting misfolded proteins to aggresomes. *Mol Biol Cell* **22**, 3277-88. https://doi.org/10.1091/mbc.E11-05-0388.

Zhang, X., Smith, D. L., Meriin, A. B., Engemann, S., Russel, D. E., Roark, M., Washington, S. L., Maxwell, M. M., Marsh, J. L., Thompson, L. M. et al. (2005). A potent small molecule inhibits polyglutamine aggregation in Huntington's disease neurons and suppresses neurodegeneration *in vivo*. *Proc Natl Acad Sci U S A* **102**, 892-7. https://doi.org/10.1073/pnas.0408936102.

Zhang, Y., Liu, Y., Bilodeau-Wentworth, D., Hardin, P. E. and Emery, P. (2010c). Light and temperature control the contribution of specific DN1 neurons to *Drosophila* circadian behavior. *Curr Biol* **20**, 600-5. https://doi.org/10.1016/j.cub.2010.02.044.

References

Zhang, Y., Ren, R., Yang, L., Zhou, J., Li, Y., Shi, J., Lu, L., Sanford, L. D. and Tang, X. (2019). Sleep in Huntington's disease: A systematic review and meta-analysis of polysomongraphic findings. *Sleep* **42**. https://doi.org/10.1093/sleep/zsz154.

Zhao, J., Warman, G. and Cheeseman, J. (2019a). The development and decay of the circadian clock in *Drosophila melanogaster*. *Clocks Sleep* **1**, 489-500. https://doi.org/10.3390/clockssleep1040037.

Zhao, J., Warman, G. R., Stanewsky, R. and Cheeseman, J. F. (2019b). Development of the molecular circadian clock and its light sensitivity in *Drosophila melanogaster*. *J Biol Rhythms* **34**, 272-282. https://doi.org/10.1177/0748730419836818.

Zhao, T., Hong, Y., Li, S. and Li, X. J. (2016a). Compartment-dependent degradation of mutant huntingtin accounts for its preferential accumulation in neuronal processes. *J Neurosci* **36**, 8317-28. https://doi.org/10.1523/jneurosci.0806-16.2016.

Zhao, T., Hong, Y., Li, X. J. and Li, S. H. (2016b). Subcellular clearance and accumulation of Huntington Disease protein: A mini-review. *Front Mol Neurosci* **9**, 27. https://doi.org/10.3389/fnmol.2016.00027.

Zheng, J., Winderickx, J., Franssens, V. and Liu, B. (2018). A mitochondria-associated oxidative stress perspective on Huntington's disease. *Front Mol Neurosci* **11**, 329. https://doi.org/10.3389/fnmol.2018.00329.

Zheng, Z. and Diamond, M. I. (2012). Huntington disease and the huntingtin protein. In *Progress in molecular biology translational science*, vol. 107, pp. 189-214. https://doi.org/10.1016/b978-0-12-385883-2.00010-2.

Zheng, Z., Li, A., Holmes, B. B., Marasa, J. C. and Diamond, M. I. (2013). An N-terminal nuclear export signal regulates trafficking and aggregation of huntingtin (Htt) protein exon 1. *J Biol Chem* **288**, 6063-71. https://doi.org/10.1074/jbc.M112.413575.

Zhou, H., Li, S. H. and Li, X. J. (2001). Chaperone suppression of cellular toxicity of huntingtin is independent of polyglutamine aggregation. *J Biol Chem* **276**, 48417-24. https://doi.org/10.1074/jbc.M104140200.

Zhou, L., Miller, C., Miraglia, L. J., Romero, A., Mure, L. S., Panda, S. and Kay, S. A. (2021). A genome-wide microRNA screen identifies the microRNA-183/96/182 cluster as a modulator of circadian rhythms. *Proc Natl Acad Sci U S A* **118**. https://doi.org/10.1073/pnas.2020454118.

Zhu, G., Tong, Q., Ye, X., Li, J., Zhou, L., Sun, P., Liang, F., Zhong, S., Cheng, R. and Zhang, J. (2022). Phototherapy for cognitive function in patients with dementia: A systematic review and meta-analysis. *Front Aging Neurosci* **14**, 936489. https://doi.org/10.3389/fnagi.2022.936489.

Zielonka, D., Piotrowska, I., Marcinkowski, J. T. and Mielcarek, M. (2014). Skeletal muscle pathology in *Huntington's* disease. *Front Physiol* **5**, 380. https://doi.org/10.3389/fphys.2014.00380.

Ziólkowska, N., Chmielewska-Krzesinska, M., Vyniarska, A. and Sienkiewicz, W. (2022). Exposure to blue light reduces melanopsin expression in intrinsically photoreceptive retinal ganglion cells and damages the inner retina in rats. *Invest Ophthalmol Vis Sci* **63**, 26. https://doi.org/10.1167/iovs.63.1.26.

Zuccato, C. and Cattaneo, E. (2009). Brain-derived neurotrophic factor in neurodegenerative diseases. *Nat Rev Neurol* **5**, 311-22. https://doi.org/10.1038/nrneurol.2009.54.

References

Zuccato, C. and Cattaneo, E. (2014). Huntington's disease. Berlin, Heidelberg.: Spriger - Verlag. https://doi.org/10.1007/978-3-642-45106-5_14.

Zuccato, C., Ciammola, A., Rigamonti, D., Leavitt, B. R., Goffredo, D., Conti, L., MacDonald, M. E., Friedlander, R. M., Silani, V., Hayden, M. R. et al. (2001). Loss of huntingtin-mediated BDNF gene transcription in Huntington's disease. *Science* **293**, 493-8. https://doi.org/10.1126/science.1059581.

Zuccato, C., Tartari, M., Crotti, A., Goffredo, D., Valenza, M., Conti, L., Cataudella, T., Leavitt, B. R., Hayden, M. R., Timmusk, T. et al. (2003). Huntingtin interacts with REST/NRSF to modulate the transcription of NRSE-controlled neuronal genes. *Nat Genet* **35**, 76-83. https://doi.org/10.1038/ng1219.

Zuccato, C., Valenza, M. and Cattaneo, E. (2010). Molecular mechanisms and potential therapeutical targets in Huntington's disease. *Physiol Rev* **90**, 905-81. https://doi.org/10.1152/physrev.00041.2009.

Zuhl, M., Dokladny, K., Mermier, C., Schneider, S., Salgado, R. and Moseley, P. (2015). The effects of acute oral glutamine supplementation on exercise-induced gastrointestinal permeability and heat shock protein expression in peripheral blood mononuclear cells. *Cell Stress Chaperones* **20**, 85-93. https://doi.org/10.1007/s12192-014-0528-1.